FY15 ANNUAL PROGRESS REPORT

Laboratory Directed Research and Development

Los Alamos National Laboratory

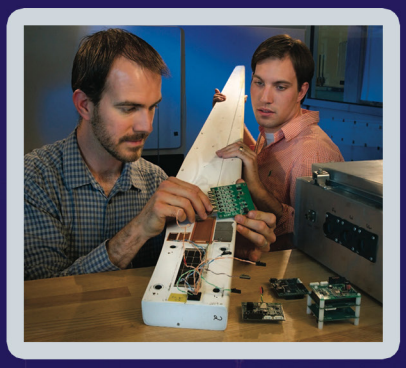

Los Alamos
NATIONAL LABORATORY
EST. 1943

About the Cover

Established in 2003, the Los Alamos Engineering Institute is an ongoing research and education collaboration between the Los Alamos National Laboratory and the University of California San Diego's Jacobs School of Engineering. It promotes mission-relevant engineering research collaborations with UCSD faculty and students and provides the Laboratory with a proactive approach to recruiting, retention and revitalization of its technical staff. Several alumni of the Engineering Institute's Dynamics Summer School were recruited to Los Alamos through LDRD Postdoctoral Research and Development projects; they continue on at the Laboratory today as engineering scientists, some leading LDRD Early Career projects of their own and some contributing to projects as co-Investigators. These early career researchers are featured on the cover.

Los Alamos
NATIONAL LABORATORY
EST.1943

Disclaimer

Issued March 2016
LA-UR-16-21921

Structure of this Report

In accordance with U.S. Department of Energy Order (DOE) 413.2B, the Laboratory Directed Research and Development (LDRD) annual report for fiscal year 2015 (FY15) provides summaries of each LDRD-funded project for the fiscal year, as well as full final reports on completed projects. The report is organized as follows:

Overview: An introduction to the LDRD Program at Los Alamos National Laboratory (LANL), the program's structure and strategic value, the LDRD portfolio management process, and highlights of outstanding accomplishments by LDRD researchers.

Project Summaries: The project summaries are organized first by Focus Areas: Complex Natural and Engineered Systems, Information Science and Technology, Materials for the Future, Nuclear and Particle Futures, and Science of Signatures. Within each category, summaries are organized by LDRD component in the following order: Directed Research (DR, Exploratory Research (ER), Early Career Research (ECR), and Postdoctoral Research and Development (PRD). Annual reports for ongoing projects appear first, followed by full final reports that ended in FY15.

Projects are listed in numerical order according to their project identification number, which consists of three parts. The first is the fiscal year in which the project began; the second is a unique numerical identifier; and the third identifies the project component.

At Los Alamos, postdocs are hired throughout the fiscal year, and at the time this report was published, some PRD projects did not have significant progress to report due to the fact that the postdoc had just been hired. In the first few weeks of a new PRD project, a postdoc will spend time in general employee training, as well as any additional training required for work in a specialized lab or facility. This was the case for the following PRD projects:

20140685PRD4	20150743PRD3	20150708PRD2	20150758PRD3	20150710PRD2
20150711PRD2	20150759PRD3	20150742PRD3	20150702PRD1	20150701PRD1
20150744PRD3	20150712PRD2	20150705PRD2	20150741PRD3	20150717PRD2

Acknowledgements

Technical Review
William Priedhorsky
Jeanne Robinson

Publication Designer
Andrea Maestas

Team Contributors
Lisa Lujan
Debbie Martinez
Stephen Schultz
Epolito Ulibarri
Susan Whittington
Peter Haase

Table of Contents

Information Science and Technology

Materials for the Future

Nuclear and Particle Futures

Science of Signatures

SCIENTIFIC EXCELLENCE

MAKING AN IMPACT ON NATIONAL SECURITY MISSIONS

A Message From William Priedhorsky, Los Alamos LDRD Program Director

The U.S. Department of Energy has charged the Laboratory Directed Research and Development (LDRD) program with supporting high-risk, potentially high-value research at the national laboratories. That LDRD is a proving ground for new concepts in research and development makes its many successes that much more remarkable. Investing in high-risk science and engineering means we may not succeed every time, and yet for more than 25 years, LDRD has supported some of the most impactful technologies to come out of the National Nuclear Security Administration (NNSA) laboratories.

Currently, LDRD is the largest single source of capability investment at Los Alamos, and many key NNSA programs, as well as leading R&D scientists and engineers, trace their roots to research that began under LDRD sponsorship. For example, proton radiography (pRad), whose foundations were developed by LDRD over a decade ago, has made contributions to the nuclear weapons program through more than 500 dynamic experiments. Today pRad influences decisions regarding the reuse of pits from one weapon system to another, and it provides data to help the U.S. Army improve the penetration resistance of armor for our troops on the battlefield.

In the words of Los Alamos Muon Tomography Team Leader Chris Morris, “Early on, LDRD provided the resources to develop the proof of principle that is foundational to pRad. Now a key capability for maintaining the nation’s nuclear stockpile, pRad is the direct result of the synergy between the Laboratory’s defense mission and basic R&D scientists.”

To be sure, there are many technical staff members at the Laboratory who credit LDRD for creating a pathway for their innovative ideas to impact national security missions. In fact, LDRD is a major vehicle for attracting, training, and retaining new technical staff, thus filling the talent pipeline to support the broad generational turnover of national security staff currently underway.

From reducing global nuclear dangers, to improving our energy security, to protecting our service men and women in the field, to assuring the security of our most precious cyber assets, LDRD has made seminal contributions to every facet of national security. ■

Overview

Laboratory Directed Research and Development is the most prestigious source of research and development funding at the Los Alamos National Laboratory. It follows a strategic guidance derived from the missions of the U.S. Department of Energy, the National Nuclear Security Administration, and the Laboratory. To execute that strategy, the Los Alamos LDRD program creates a free market for ideas that draws upon the bottom-up creativity of the Laboratory's best and brightest researchers. The combination of strategic guidance and free-market competition provides a continual stream of capabilities that position the Laboratory to accomplish its missions.

The LDRD program provides the Laboratory Director with the opportunity to strategically invest in forward-thinking, potentially high-payoff research that strengthens the Laboratory's capabilities for national problems. Funded in FY15 with approximately 5.5 percent of the Laboratory's overall budget, the LDRD program makes it possible for researchers to pursue cutting-edge research and development. This in turn enables the Laboratory to anticipate, innovate, and deliver world-class science, technology, and engineering.

Program Structure

The Los Alamos LDRD program is organized into four program components with distinct institutional objectives: Directed Research (DR), flagship investments in mission solutions; Exploratory Research (ER), smaller projects that invest in people and skills that underpin key Laboratory capabilities; Early Career Research (ECR), supporting the development of early-career researchers; and Postdoctoral Research and Development (PRD), recruiting bright, qualified, early-career scientists and engineers. In FY15, the LDRD program funded 278 projects with total costs of $121.5 million. These projects were selected through a rigorous and highly competitive peer review process and are reviewed formally and informally throughout the fiscal year. The LDRD Program Office holds a reserve each year to make modest investments that address new opportunities. In FY15, the reserve budget was approximately $1.0M.

Directed Research

The DR component makes long-range investments in multidisciplinary scientific projects in key competency or technology-development areas vital to LDRD's long-term ability to execute Laboratory missions. In FY15, LDRD funded 46 DR projects, which represents approximately 54% of the program's research funds. Directed Research projects are typically funded up to a maximum of $1.8M per year for three years.

Directed Research is organized around Focus Areas that define key areas of science, technology, and engineering in support of Los Alamos missions and that map directly to the four Los Alamos science pillars, plus an additional multi-disciplinary Focus Area that is not captured by the pillars. Between them, they capture the capabilities that are essential to our Laboratory missions in the long term (3-15 years). For each Focus Area, coordinators led a process to engage broadly with the Lab to set investment priorities for the FY15 Strategic Investment Plan, published labwide.

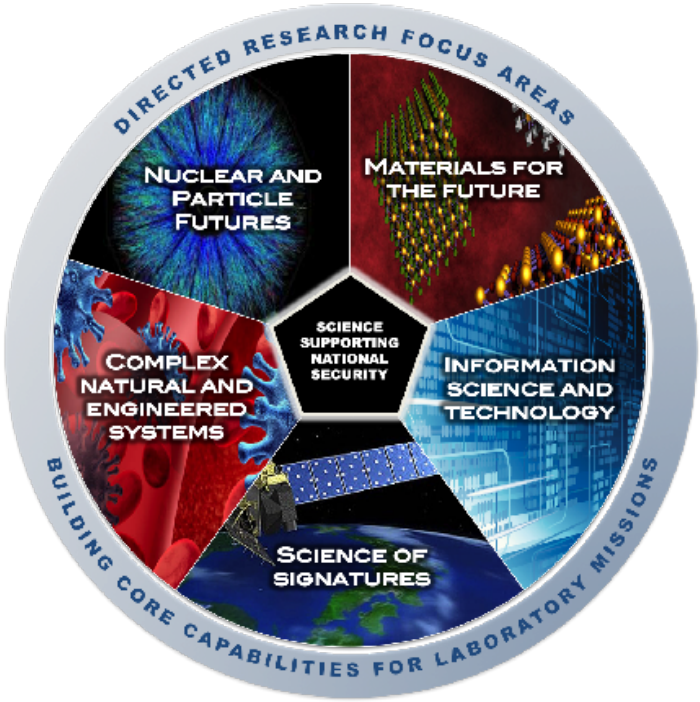

Exploratory Research

The ER component is focused on developing and maintaining technical staff competencies in key strategic disciplines that form the foundation of the Laboratory's readiness for future national missions. Largely focused on a single discipline, ER projects explore highly innovative ideas that underpin Laboratory programs. In FY15, LDRD funded 127 ER projects, which represents approximately 34% of the program's research funds. Exploratory Research projects are funded up to an average maximum of $350K per year for three years.

Unlike DR proposals, division endorsements are not required for ER proposals; instead, this component of the LDRD program is operated as an open and competitive path for every staff member to pursue funding for his/her great idea. The ER component is a critical channel for purely bottom-up creativity at the Laboratory. Nonetheless, it is strongly driven by mission needs via the definition of the 12 ER research categories, and the assignment of investment between them.

Directed Research Focus Areas	Mission Impact
Information Science and Technology	Advance theory, algorithms, and high-performance computing to accelerate the integrative and predictive capability of the scientific method.
Materials for the Future	Rapidly meet mission needs based on a thorough knowledge of materials properties and interactions in relation to composition, structure, and scale.
Science of Signatures	Apply science and technology tools to extremely complex problems in signature, identification, and characterization, understanding, control or mitigation.
Nuclear and Particle Futures	Advance fundamental and applied nuclear science, including accelerator science and technology, in support of all Laboratory missions.
Complex Natural and Engineered Systems	Understand, predict, integrate, design, engineer, and/or control complex systems that significantly impact national security, particularly those involving energy, infrastructure, or societal stainability.

Exploratory Research Technical Categories	Capability
Biological, Biochemical, and Cognitive Sciences	Biosciences
Chemistry and Chemical Sciences	Chemistry
Computational and Numerical Methods	Information and knowledge sciences, computer and computational sciences
Computer Science, Mathematics, and Data Science	High-performance computing, data analysis, and data-driven science
Defects and Interfaces in Materials	Theoretical, computation and modeling, and experimental methods to understand defects and interfaces in materials
Earth and Environmental Sciences and Space Physics	Earth and space sciences
Engineering Applications	Weapons science and engineering, advanced manufacturing, sensors, and remote sensing
Emergent Phenomena in Materials Functionality	Theory, computation and modelling, and experimental methods to understand behavior of materials
High-energy Density, Plasma, and Fluid Physics	High-energy density plasmas and fluids and beams
Measurement Science, Instrumentation, and Diagnostics	Measurement methods that enable new scientific discovery
Nuclear and Particle Physics, Astrophysics, and Cosmology	Nuclear physics, astrophysics, and cosmology
Quantum and Optical Science	Fundamental interactions and excitations in atomic, optical, and molecular systems

Early Career Research

The ECR component of the LDRD program is designed to strengthen the Laboratory's scientific workforce by providing support to exceptional staff members during their crucial early career years. The intent is to aid in the sometimes challenging transition from postdoc to full-time staff member, and to stimulate research in disciplines supported by the LDRD program. In FY15, the LDRD program funded 29 ECR projects, which represents approximately 3% of the program's research funds. Early Career Research projects are funded up to $225K per year for two years, and only up to 60% of their overall funding can be from the LDRD program.

Postdoc Research and Development

The PRD component ensures the vitality of the Laboratory by recruiting outstanding researchers. Through this investment, the LDRD program funds postdoctoral fellows to work under the mentorship of PIs on high-quality projects. The primary criterion for selection of LDRD-supported postdocs is the raw scientific and technical talent of the candidate, with his or her specialty a secondary factor. In FY15, LDRD funded 76 PRD projects, which represents 7% of the program's research funds. These postdocs are supported full-time for two years.

In addition to approximately 62 Director's Postdocs, the LDRD program supported 14 distinguished postdoctoral fellows at a higher salary and for a three-year term. Distinguished postdoctoral fellow candidates typically show evidence of solving a major problem or providing a new approach or insight to a major problem and show evidence of having a major impact in their research field. To recognize their role as future science and technology leaders, these appointments are named after some of the greatest leaders of the Laboratory's past.

More postdocs are hired through DR and ER projects than directly through PRD appointments. Counting both avenues, in FY15 the LDRD program supported 55% of the 488 postdocs at the Laboratory.

Christopher Lee

2015 Early Career Research Program Award
Department of Energy Office of Science

- Joined the Lab in 2012 as a scientist
- 2012 Early Career Researcher project (PI)
- 2014, 2016 Postdoc R&D project (PI)
- Served as chair of the Exploratory Research NPAC review team in FY15

Sarah Hernandez

2015 Best Poster on Plutonium Materials
American Nuclear Society's Plutonium Futures

- Graduate research assistant and PhD candidate at the University of Texas at Arlington
- Co-investigator on 2014 Directed Research project
- Lead author of article published in *Journal of Physics: Condensed Matter*

Project Selection

The LDRD program is the vehicle by which the Laboratory harvests the ideas of some of our best and brightest scientists and engineers to execute DOE/NNSA missions. This bottom-up approach is balanced by a program management strategy in which Senior Laboratory leadership sets science and technology priorities, then opens an LDRD competition for ideas across the breadth of the Laboratory. Panels formed from the Laboratory's intellectual leaders rigorously review proposals. Conflict of interest is carefully regulated, and evaluation criteria include innovation and creativity, potential scientific impact, viability of the research approach, qualifications of the team and leadership, and potential impact on Laboratory missions. The selection processes are modeled on best practices established by the National Science Foundation (NSF) and National Institutes of Health (NIH).

To guarantee fairness and transparency, and to ensure that the strongest proposals are funded, the selection panels include managers and technical staff drawn from the full range of technical divisions. Serving on an LDRD selection panel is often a starting point on the path to leadership roles in the scientific community. Past LDRD panelists have gone on to be Laboratory Fellows, division leaders, program directors, association Fellows, and chief scientists, while others have become leaders in academia.

Benefits of Serving on LDRD Panels

The mission of the Laboratory is to solve the nation's most difficult national security problems. By their nature, these problems lack a well-defined path to solution. In fact, the path is often completely unknown. It is rare that such creative work is done alone; the ideas and results from many colleagues are needed, often drawn out in conferences, hallway conversations, journals, and seminars. LDRD is an internal arena in which Laboratory staff serve as peer reviewers and play a key role of interaction in the scientific process. Proposal selection panelists are chosen for their subject-matter expertise, and the discussions in which they engage are not only critical to the LDRD process, but they also provide an opportunity for panelists to educate themselves on the latest results and practices, and expose themselves to opportunities for collaboration. As noted in an evaluation of peer review conducted by the UK House of Commons, "Peer review is regarded as an integral part of a researcher's professional activity; it helps them become part of the research community."

Annual Project Appraisals

In FY15, the LDRD Program Office conducted an appraisal of every ongoing project it intended to fund in the next fiscal year. The primary objective of a project appraisal is to assess progress and provide peer input to help PIs maintain the highest quality of work. The appraisals also help the LDRD Program Office monitor and manage the program portfolio.

Continuing DR projects are appraised every year of the life of the project, with external reviewers playing an important role in the review that takes place in the project's second year. The internal-external review is open to all Laboratory staff and leaders. Four project appraisers – two internal and two external – are nominated by the PI and approved by the LDRD Program Director. When possible, the appraisal is held as part of a broader workshop hosted by the Laboratory. The Chair of the project appraisal panel is responsible for writing a formal report a formal report of the review that details how well a project is addressing and meeting its goals, as well as documenting any weaknesses the panel may have observed. The PI is then required to respond to the concerns documented in the report with a revised project plan.

Written appraisals, held in the LDRD archives, address: (1) Brief summary of accomplishments; (2) Assessment of quality of science and technology, relevance to Laboratory and national missions, progress toward goals and milestones, project leadership, and the degree to which the project may establish or sustain a position of scientific leadership for the Laboratory; and (3) Recommendations by the committee for changes in the scope or approach of the project. The criteria for the most important point – number (2) above – are derived from criteria developed by the National Academy of Science to assess all federally sponsored research.

In addition to formal project appraisals, which are conducted annually, the LDRD Program Director and Deputy Program Director meet informally with PIs in their labs at least once a year to discuss their projects. The purpose of these one-on-one meetings is to give PIs individualized assistance and to determine what the LDRD Program Office can do to positively impact the success of the project. Every DR project has also been assigned a Program Development Mentor to assist the transition of LDRD successes to mission.

Continuing ER and ECR projects are appraised in their first and second years. The LDRD Deputy Program Director collaborates with the technical divisions to conduct project appraisals. Like DRs, the projects are appraised according to the Federal criteria of quality, performance, leadership, and relevance.

Directed Research Project Appraisals in Depth

The DOE Order (413.2b, CRD) regarding LDRD requires careful evaluation of ongoing LDRD projects in order to assess their scientific quality and mission relevance. The Los Alamos LDRD program doesn't just meet this requirement, it turns the evaluation process into an opportunity to steer its R&D towards ever-increasing excellence and mission impact. For this reason, flagship investments in DR undergo especially rigorous evaluations.

YEAR ONE
New project begins with R&D goals identified at the proposal stage.

YEAR TWO
- 13-16 months into project
- Half-day appraisal
- Panel of four reviewers
- At least two external

YEAR THREE
- 25-28 months into project
- Two-hour appraisal
- Panel of four reviewers
- External reviewers optional

END OF YEAR THREE
Final project appraisal based on full final report.

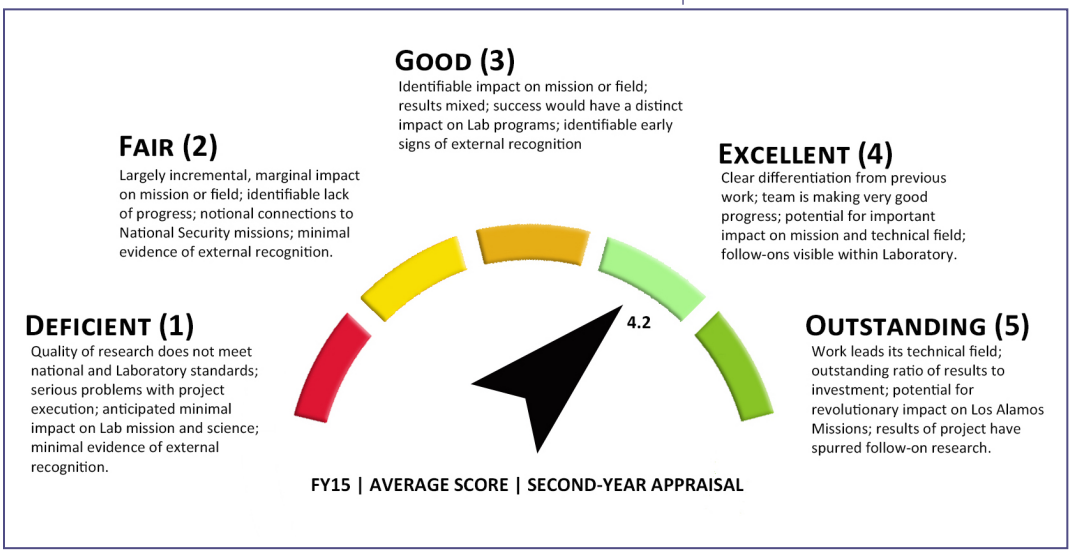

High-quality Reviewers Ensure a Technically Sound DR Project Appraisal

When selecting members of an appraisal panel, a Principal Investigator must seek out individuals with independence, expertise, and stature. All panel members must be *independent* of the project, without management or financial connections, in adherence with the published LDRD Conflict of Interest Policy. Between them, the panelists must have the technical *expertise* required to span the breadth of the project with sound technical review. And finally, while panels often contain members with a mix of seniority, there must be one or two members with *stature*. In the context of a DR appraisal panel, stature is recognized leadership in their field, evidenced by strong professional credentials such as an institute leader, named professorship, society fellowships, and national and/or international prizes. The LDRD Program Director approves all panels well in advance of the appraisal.

Mission Relevance

Mission relevance is one of the most important criteria in the evaluation of a potential LDRD project; it is carefully considered in project selection and tracked annually through the data sheet process. Many of the technologies that put Los Alamos on the map have deep roots in LDRD and are valuable to DOE/NNSA mission areas of nuclear security, energy security, environmental remediation, and scientific discovery and innovation. LDRD work also benefits the national security missions of the Department of Homeland Security, the Department of Defense, and Other Federal Agencies. As a result, the scientific advances and technology innovations from LDRD provide multiple benefits to all Los Alamos stakeholders, consistent with Congressional intent and the Laboratory's scientific strategy.

Enduring Impact on Stockpile Stewardship

A key responsibility of the Stockpile Stewardship program is to assess aging of the nation's stockpile. A 1997 LDRD project established the scientific foundation for accelerated aging of plutonium with experiments that allowed Los Alamos and Lawrence Livermore national laboratories to produce the equivalent of 60-year-old plutonium in a period of only four years. The resulting data were used as a foundation for the 2006 Pit Lifetime Assessment for the nation. The fundamental understanding of plutonium aging continues as a priority for our LDRD portfolio.

"Over the years LDRD helped develop resonant ultrasound spectroscopy from a lab curiosity into a powerful tool for important measurements in condensed matter physics," said Albert Migliori, director of the Los Alamos Seaborg Institute. "In fact, it is the only tool that can track and measure the aging of plutonium in real time."

Today this capability enables new studies of aging in delta-plutonium alloys; advanced experiments to watch aging on a daily basis will form the basis for pit lifetime estimates that are physically sound and advance the understanding of fundamental radiogenic processes in delta-plutonium.

Mission Impact of FY15 LDRD Portfolio ($M)

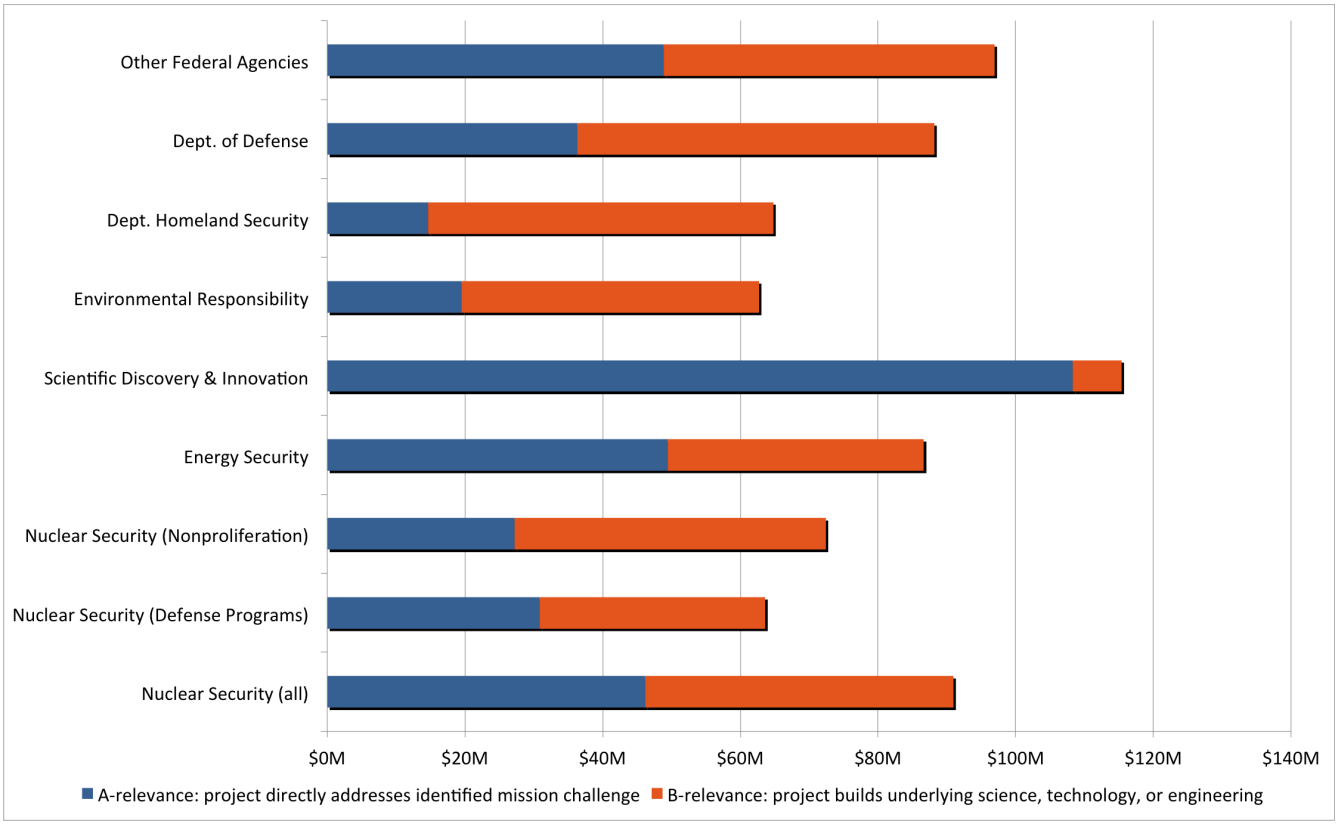

First and foremost, Los Alamos LDRD projects are required to address one or more DOE/NNSA mission areas. Due to the nature of basic R&D, the work may also benefit the mission challenges of other federal agencies. The multi-mission impact of LDRD projects is captured in the chart above, which is why the total expected benefit is approximately double actual costs of the program in FY15.

In partnership with the LDRD program, the Los Alamos Engineering Institute makes investments in multidisciplinary engineering research that integrates advanced modeling and simulations, novel sensing systems, and new developments in information technology.

Investments in Engineering Research and Development:
Capabilities for Mission, Winning Technologies, and Top Talent

Established in 2003, the Engineering Institute is an ongoing research and education collaboration between the Los Alamos National Laboratory and the University of California San Diego's Jacobs School of Engineering. It promotes mission-relevant engineering research collaborations with UCSD faculty and students and provides the Laboratory with a proactive approach to recruiting, retention and revitalization of its technical staff.

The Los Alamos Dynamics Summer School is a very selective summer school in which upper-level US-citizen undergraduate students from universities around the nation attend lectures and work in teams of three with a Los Alamos mentor on research projects related to the Engineering Institute's technology focus. David Mascarenas, Stuart Taylor, and Eric Flynn are examples of top-notch alumni who were recruited to the Laboratory with support from LDRD (through Postdoctoral Research and Development projects) and converted to staff. Their accomplishments are remarkable.

Mascarenas became an R&D Engineer at Los Alamos in 2012 after a Director's Funded fellowship. He currently co-directs the Dynamic Summer School and focuses his research on investigating the application of compressive sensing techniques to structural health monitoring, the deployment of wireless sensor networks from aerial robots, standoff experimental mechanics, and the development of techniques to interface humans to data using vibro-tactile interfaces. He led a 2015 Early Career Research project, and recently received a Presidential Early Career Award.

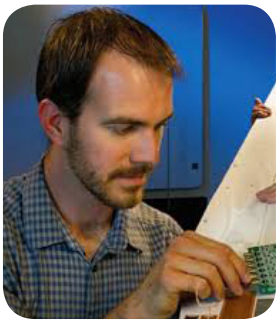

Taylor joined Los Alamos as an R&D Engineer in 2013. As a postdoc he designed and field-tested sensor nodes for structural health monitoring (SHM) on wind turbine rotor blades as part of a 2010 LDRD Directed Research project. Today he applies his expertise in SHM on a project that resulted in a 2015 R&D 100 Award. The award-winning technology, SHMTools, is software that facilitates continuous embedded monitoring and damage detection for new and aging infrastructure. It has aerospace, civil, and mechanical infrastructure applications.

Flynn was converted to an R&D Engineer at Los Alamos in 2013 after joining the Lab as Director's Funded postdoc in 2011. His research focuses on nondestructive testing, signal processing, ultrasonics, applied statistics, optimization and structural dynamics. Flynn won a 2014 R&D 100 Award for the Acoustic Wavenumber Spectrometer (supported by LDRD), leads a 2015 Early Career Project, was recently honored with the Achenbach medal for his contributions in the field of SHM, and was on the team that developed SHMTools.

Performance Metrics

The LDRD program is a key resource for addressing the long-term science and technology goals of the Laboratory, as well as enhancing the scientific capabilities of Laboratory staff. Through careful investment of LDRD funds, the Laboratory builds its reputation, recruits and retains excellent scientists and engineers, and prepares to meet evolving national needs. The impacts of the LDRD program are particularly evident in the number of publications and citations resulting from LDRD-funded research, the number of postdoctoral candidates supported and converted by the program, and the number of awards LDRD researchers received. The following performance metrics are updated annually to reflect the most current data available as more complete information often becomes available well into the next fiscal year.

Intellectual Property

U.S. Patents Issued				
	FY12	FY13	FY14	FY15
LANL Patents	72	77	51	50
LDRD Supported	11	32	14	10
% due to LDRD	15%	42%	27%	20%

Invention Disclosures				
	FY12	FY13	FY14	FY15
LANL Disclosures	129	103	71	71
LDRD Supported	28	34	12	16
% due to LDRD	22%	33%	17%	23%

Science and Engineering Talent Pipeline

Postdoc Support				
	FY12	FY13	FY14	FY15
LANL Postdocs	581	596	508	488
LDRD Supported	349	367	266	266
% due to LDRD	60%	61%	52%	55%

Postdoc Conversions				
	FY12	FY13	FY14	FY15
LANL Conversions	41	57	50	55
LDRD Supported	21	26	29	24
% due to LDRD	51%	46%	58%	44%

Peer-reviewed Publications and Citations

Publications				
	FY12	FY13	FY14	FY15
LANL Pubs	2119	2082	2215	1872
LDRD Supported	458	534	475	392
% due to LDRD	22%	24%	21%	21%

Citations				
	FY12	FY13	FY14	FY15
LANL Citations	33321	22021	9914	3243
LDRD Supported	8146	7620	2182	1175
% due to LDRD	24%	35%	22%	36%

External Collaborations (FY15)

University of California	New Mexico Universities	International	All
48	30	214	902

On the Cover and Beyond

The numerous publications made possible with LDRD funding help Los Alamos maintain a strong presence and scientific reputation in the broader scientific community. Not only does the program support a significant fraction of the Laboratory's publications, it also supports much of the research featured on the covers of peer-reviewed journals. These are just a few examples of the highly visible research and development by LDRD researchers in 2015.

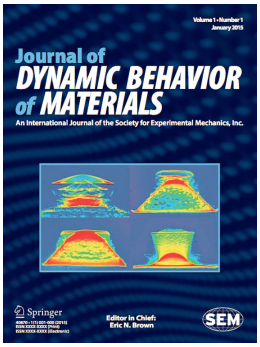

The cover of the first issue of the ***Journal of Dynamic Behavior of Materials*** featured a series of proton radiographs of disks taken by the Los Alamos Proton Radiography Team. The images reveal the internal structure of explosively shocked aluminum, copper, tantalum, and tin. Los Alamos is an international center of excellence for research on the dynamic behavior of materials and materials in extremes. Proton radiography, and much of the R&D that grows out of enduring capability, has roots in the Los Alamos LDRD program.

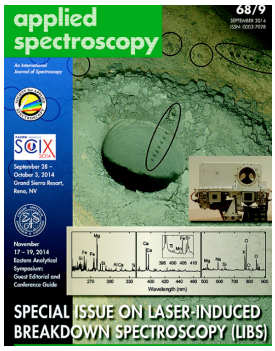

An article by Los Alamos scientists and collaborators in the journal ***Applied Spectroscopy*** describes the feasibility of adding Raman spectrometry to the ChemCam Laser Induced Breakdown Spectrometer (LIBS) instrument used with such great efficacy on NASA's Mars Curiosity Rover. Raman spectroscopy and LIBS are highly synergistic analytical techniques. Raman spectroscopy is sensitive to the sample's molecular structure from which mineralogy is directly determined, and LIBS is an elemental analysis technique that can detect all elements above the detection limit independent of the elemental mass. The new work shows that an integrated Raman spectroscopy and laser-induced breakdown spectroscopy instrument would be a valuable geoanalytical tool for future planetary missions to Mars, Venus, and elsewhere. The cover highlights the many ChemCam LIBS analyses around the "Windjana" drill hole created by the NASA Mars rover, Curiosity. LIBS was developed with support from the Los Alamos LDRD program and has multiple applications, including detecting nuclear and other hazard materials, verifying construction materials, and studying cave environments. In its "backpack" format, LIBS inexpensively takes atomic emission analysis from a traditional laboratory setting into the field.

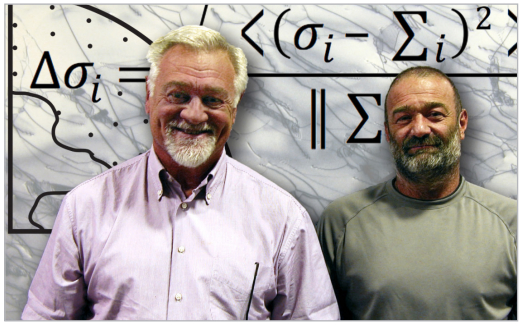

Los Alamos researchers Carolos Tomé and Ricardo Lebensohn (pictured left to right) recently saw their viscoplastic self-consistent code (in background) research reach **1,000 citations in Google Scholar**. Their co-authored 1993 Acta Metallurgica et Materialia paper, "A self-consistent anisotropic approach for the simulation of plastic deformation and texture development of polycrystals: Application to zirconium alloys" was based on their joint work on a computational code to reliably simulate materials behavior. Their viscoplastic self-consistent (VPSC) code has been distributed free of charge to more than 300 external users.

Lebensohn currently leads an LDRD Directed Research project titled "Mesoscale Materials Science of Ductile Damage in 4 Dimensions: Towards the Computational Design of Damage-Tolerant Materials." The project addresses one of the most difficult outstanding problems in materials science: the development of a predictive, microstructure-sensitive ductile failure model. Lebensohn has also contributed to the LDRD peer-review processes for DR and ER proposals.

Awards and Recognitions

In its more than 25 years of existence, the Los Alamos LDRD program has made many significant impacts on national security missions, steadily helping the Laboratory anticipate, innovate, and deliver solutions to some of the nation's toughest challenges. The driving force behind each accomplishment has been the focused initiative of many talented scientists and engineers who choose to apply their knowledge and expertise in service to the nation. The LDRD program is proud to support the work of some of the Laboratory's most accomplished researchers, who in FY15 received many prestigious awards, honors, and recognitions.

Wolfram-Prandl Prize

Marc Janoschek received the 2014 Wolfram-Prandl Prize during the German Conference for Research with Synchrotron Radiation, Neutrons and Ion Beams at Large Facilities in Bonn, Germany. He was honored for "his pioneering studies of the spin dynamics in chiral helimagnets and the development of a cryogen-free apparatus for spherical neutron polarimetry." Janoschek's work on helical magnets has potential for novel memory, computing, and sensing applications continues in a 2015 LDRD Directed Research project. He also serves as co-chair of the Defects and Interfaces in Materials panel for the Exploratory Research peer-review process.

APS Woman Physicist of the Month

The American Physical Society (APS) named **Kathy Prestridge** as the Woman Physicist of the Month for July 2015. Prestridge studies the behavior of materials under high strain conditions, shock-driven instabilities, mixing and turbulence at high resolution. She and her team's research has been highlighted on the cover of *Journal of Fluid Mechanics*. She leads the Professional Skills Development Workshop sessions at various APS meetings, as is serving her second term as Chair of the APS Committee on the Status of Women in Physics. Prestridge has been co-investigator on LDRD projects and currently serves as Chair of the High-Energy Density, Plasma, and Fluid Physics panel for the Exploratory Research peer-review process.

ASME Fellow

The American Society of Mechanical Engineers (ASME) named **Daniel Livescu** a Fellow. The ASME Committee of Past Presidents confers the Fellow grade of membership on worthy candidates to recognize their outstanding engineering achievements. Livescu is an authority in the field of fluid mechanics and has made significant contributions to the LANL/DOE stewardship mission as a Principal Investigator for the NNSA Defense Science Programs. His research focuses on direct-numerical simulation of turbulence and large-scale flow computations is supported by a 2015 LDRD Exploratory Research project. He has also served on the Computational Co-design panel for the Exploratory Research peer-review process.

E.O. Lawrence Award

Two Los Alamos LDRD researchers received Ernest Orlando Lawrence awards from the Department of Energy. The honor is conferred for their contributions in research and development that supports DOE's science, energy and national security missions. Since 1959, the Lawrence Award has recognized mid-career scientists and engineers in the United States who have advanced new research and scientific discovery in the chemical, biological, environmental and computer sciences; condensed matter and materials; fusion and plasma sciences; high energy and nuclear physics; and national security and nonproliferation.

Eric Dors was recognized for his technical leadership and systems engineering integration of next generation satellite-based nuclear explosion sensing and detection systems, and for its impact to the nonproliferation mission. His research focuses on the development of a new generation of exo-atmospheric radiation sensors used to fulfill a critical mission need for satellite-based nuclear explosion monitoring crucial to DOE's nonproliferation mission of global nuclear detonation monitoring and verification of the Limited Test Ban Treaty. Dors received support from LDRD through a 2001 Exploratory Research project. He also serves on the Engineering Applications panel for the Exploratory Research peer-review process. Currently, Dors is program manager for Department of Defense and Intelligence Community space programs within the Lab's Emerging Threats Program Office.

Christopher Fryer was recognized for making seminal advances in theory and modeling answering fundamental questions in astrophysics, for achievement in computational multiphysics, and for contributions impacting high-energy density science. He was honored specifically for his major advances addressing fundamental questions in astrophysics, computational multiphysics, and high-energy density science, and more specifically, for supernova core collapse work using 3-dimensional modeling assimilation to model, explain, and predict astrophysical observations (e.g. from NASA's Swift mission) and phenomena. Fryer's work has deep roots in the LDRD program, most recently through a 2011 Directed Research project focused on building detailed models of supernova. Fryer is an American Physical Society fellow, a former Feynman fellow, and a Los Alamos National Laboratory fellow.

GSA Vice President/President Elect

The Geological Society of America (GSA) elected Claudia Mora as vice president/president elect. Mora is a stable-isotope geochemist whose research spans the traditional fields of geology, soil science and climate science. At Los Alamos, she heads the Earth and Environmental Sciences Division's (EES) largest group, Earth System Observations. This group's research is broad and far-reaching, intersecting geology, ecology and atmospheric sciences. Mora received support from LDRD through a 2009 Postdoctoral Research and Development project, and most recently, an Exploratory Research project. Her LDRD work has been published in the *Journal of Applied Meteorology* and Climatology, and in the *International Journal of Wildland Fire*.

Complex Natural & Engineered Systems

Discovery Science of Hydraulic Fracturing: Innovative Working Fluids and Their Interactions with Rocks, Fractures, and High Value Hydro-carbons

Hari S. Viswanathan
20140002DR

Introduction

Shale gas is an unconventional fossil energy resource that is already having a profound impact on US energy independence and is projected to last for at least 100 years. Production of methane and other hydrocarbons from low permeability shale involves hydrofracturing of rock, establishing fracture connectivity, and multiphase fluid-flow and reaction processes all of which are poorly understood. The result is inefficient extraction with many environmental concerns. These phenomena are part of a broader class of problems involving coupled fluid flow and fractures that are critical to other energy security areas such as shale oil, geothermal, carbon sequestration, and nuclear waste disposal as well as crack propagation in weapons applications. A science-based capability is required to quantify the governing meso-scale fluid-solid interactions, including microstructural control of fracture patterns and the interaction of engineered fluids with hydrocarbon flow. These interactions depend on coupled thermo-hydro-mechanical-chemical (THMC) processes over scales from microns to tens of meters. Determining the key mechanisms in subsurface THMC systems has been impeded due to the lack of sophisticated experimental methods to measure fracture aperture and connectivity, multiphase permeability, and chemical exchange capacities at the high temperature, pressure, and stresses present in the subsurface. Our goal is to use unique LANL microfluidic and triaxial core flood experiments integrated with state-of-the-art numerical simulation to reveal the fundamental dynamics of fracture-fluid interactions to transform fracking from ad hoc to safe and predictable approaches that are based on solid scientific understanding. We will develop CO2-based fracturing fluids and fracturing techniques to enhance production, greatly reduce waste water, while simultaneously sequestering CO2.

Benefit to National Security Missions

Significant R&D is required to increase shale gas production while reducing environmental impacts associated with aqueous hydraulic fracturing. The proposed work could shift the momentum toward greater large scale industry interest in “greener” fracturing fluids leading to greater public acceptance of fracking. Discoveries in fluid properties, rock properties, and their integrated interactions will be required. The proposed study brings together leading scientists from C, EES, MPA and T divisions to develop and apply new experimental methods in observing rock fracturing to efficiently extract hydrocarbons in combination with novel, benchmarked models that will enhance US national and energy security. Success in the proposed work will position LANL at the forefront of shale-gas technology, creating opportunities for significant industrial partnerships, and a leadership role in DOE programs in shale gas. This work also maintains capability for test containment and leakage prediction in the unlikely case of a future US nuclear test, or the more likely case of foreign testing. If the need for resumed testing should ever arise, the capability for understanding underground transport will just as critical as it once was.

Progress

The project received a combination of outstanding and excellent during the midterm review. A summary of the metrics includes:

- 18 publication in high impact peer-reviewed journals, five submitted, and more in preparation
- Organized session/conferences including AGU sessions December 2014, ARMA session June 2015, and a CNLS conference in September 2015
- More than 10 invited talks given by the DR team
- Several follow on projects have been funded including $1.4M representing three successful proposals for unconventional fossil fuels, $200K for a project with Apache and Texas tech to maximize liquid oil production from shale oil and gas, and $600K from UNESE to simulate gas migration from fractures from clandestine nuclear tests (UNESE)

Numerous key capabilities became fully operational in the last year, including:

- Triaxial coreflood with in situ tomagraphy capable of shear, compressive and hydraulic fractures
- Microfluidics with real rock and high temperature and pressure
- Fracture propagation simulation with fluid capability in two dimensions
- High performance computing implementation of discrete fracture network model to simulate hydrocarbon production
- Pore scale models of shale matrix

The midterm review resulted in the DR team coming up with a detailed plan of the remaining 18 months that exists in the form of a presentation. This presentation was submitted to Q.

A quick summary of the overall project is given by: 1) 18 publications in high impact journals, 2) 5 follow on projects funded by DOE, 3) unique LANL experimental and modeling capability aligned with the DOE big ideas SubTER which is focusing controlling fracture propagation and fluid flow in the subsurface and is expected to fully roll out in FY17.

Future Work

Task 1: We will continue to conduct triaxial coreflood experiments to characterize fracture patterns and apertures under different stress conditions as well as using different working fluids (e.g. water and CO2). Have move the triaxial apparatus to AET and have successfully measurement fracture properties under in situ conditions. We have also modified our apparatus to create hydraulic fractures in addition to shear fractures. In FY16, we plan a systematic study of fracture-permeability in shale using these newly developed capabilities.

Task 2: We will continue to develop models of fracture propagation modeling work that are validated by task 1. The focus of fy16 work will be to test our new 3d simulation capability against experiments. We will also continue to develop our integrated solid-fluid solver so that fracture propagation due to fluid pressure can be accurately simulated. The end goal is quantitative simulation of the hydraulic fracture experiments of Task 1.

Task 3: We will continue to conduct microfluidic experiments of sweep efficiency. We have succeeded in conducting microfluidic experiments with real rock (e.g. shale and cement) at high pressure. In the next FY, we will demonstrate how matrix-fracture interactions change simplistic models of hydrocarbon extraction using these new microfluidic capabilities and comparing them to standard glass microfluidic experiments.

Task 4: In the next FY, we focus on 1) comparing lattice Boltzmann simulations to the microfluidics experiments of task 3. In addition, we will continue to study flow and transport in the shale matrix that is not currently observable with our experimental program.

Task 5: We plan to study multiple sites in the next FY. In addition, since we can run larger fracture networks with our high performance computing implementation, we will study infracture variability and reactive transport in a discrete fracture network.

Conclusion

Fracking phenomena involve fluid-solid interactions embedded within coupled thermo-hydro-mechanical-chemical processes over scales from microns to tens of meters. The proposed work is part of a broader class of complex systems involving coupled fluid flow and fractures that are critical to energy security, such as shale oil, geothermal, carbon sequestration, and nuclear waste disposal, as well as, crack propagation in weapons and materials applications. Predicting and controlling fracture propagation due to fluid-solid interaction would be transformative, with significant impact beyond the hydraulic fracturing of rock.

Publications

Aldrich, G., J. D. Hyman, S. Karra, C. W. Gable, N. Makedonska, H. S. Viswanathan, J. Woodring, and B. Hamann. Analysis and visualization of discrete fracture networks using a flow topology graph. To appear in IEEE T Vis Comput Gr..

Bazant, Z., M. Salviato, V. T. Chau, H. S. Viswanathan, and A. Zubelewicz. Why fracking works. 2014. Journal of Applied Mechanics. 81 (10): 101010.

Birdsell, D., H. Rajaram, D. Dempsey, and H. Viswanathan. Hydraulic fracturing fluid migration in the subsurface: A review and modeling results. 2015. Water Resources Research. : 1.

Carey, J. W., H. Mori, D. Brown, and R. Pawar. Geomechanical behavior of caprock and cement: Plasticity in hydrodynamic seals. 2014. Energy Procedia. : 5671.

Carey, J. W., Z. Lei, E. Rougier, H. Mori, and H. S. Viswanathan. Fracture-permeability behavior of shale. 2015. Journal of Unconventional Oil and Gas Resources. : 27.

Chen, L., J. D. Hyman, L. Zhou, T. Min, Q. Kang, E. Rougier, and H. Viswanathan. Effect of fracture density on effective permeability of matrix-fracture system in

shale formations. AGU Books.

Chen, L., L. Zhang, Q. Kang, H. Viswanathan, J. Yao, and W. Tao. Nanoscale simulation of shale transport properties using the lattice Boltzmann method: permeability and diffusivity. 2015. Scientific Reports. : 1.

Chen, L., Q. Kang, B. Carey, and W. Tao. Pore-scale study of diffusion–reaction processes involving dissolution and precipitation using the lattice Boltzmann method. 2014. International Journal of Heat and Mass Transfer. 75: 483.

Chen, L., Q. Kang, H. Deng, J. W. Carey, and W. Tao. Mesoscopic study of the formation of pseudomorphs with presence of chemical fluids. 2014. Geosciences Journal. : 1.

Chen, L., Q. Kang, H. S. Viswanathan, and W. Tao. Pore-scale study of dissolution-induced changes in hydrologic properties of rocks with binary minerals. 2014. Water Resources Research. (50): 1.

Chen, L., Q. Kang, Y. Mu, Y. He, and W. Tao. A critical review of the pseudopotential multiphase lattice Boltzmann model: Methods and applications. 2014. International Journal of Heat and Mass Transfer. 76: 210.

Chen, L., Q. Kang, Z. Dai, H. S. Viswanathan, and W. Tao. Permeability prediction of shale matrix reconstructed using the elementary building block model. 2015. Fuel. : 346.

Chen, L., W. Fang, Q. Kang, J. Hyman, H. S. Viswanathan, and W. Tao. A generalized lattice Boltzmann model for flow through tight porous media with Klinkenberg's effect. 2015. Physical Review E. : 1.

Chen, Y., Q. Kang, Q. Cai, M. Wang, and D. Zhang. Lattice Boltzmann Simulation of Particle Motion in Binary Immiscible Fluids. 2015. Communications in Computational Physics. : 757.

Frash, L., J. W. Carey, E. Rougier, Z. Lei, and H. Viswanathan. Method for in-situ tensile-hydraulic-fracturing in triaxial-coreflood systems. International Journal of Rock Mechanics and Mining Sciences..

Hyman, J. D., A. Guadagnini, and C. L. Winter. Statistical Scaling of Geometric Characteristics in Stochastically Generated Pore Microstructures. 2015. Computational Geosciences. : 1.

Hyman, J. D., S. Karra, N. Makedonska, C. W. Gable, S. L. Painter, and H. S. Viswanathan. dfnWorks: A discrete fracture network framework for modeling subsurface flow and transport. 2015. Computers and Geosciences. 84: 10.

Hyman, J. D., S. L. Painter, H. S. Viswanathan, N. Makedonska, and S. Karra. Influence of Injection Mode in Kilometer Scale Three Dimensional Discrete Fracture Networks. 2015. Water Resources Research. : 1.

Jackson, R. B., A. Vengosh, J. W. Carey, R. Davies, F. O'Sullivan, and G. Petron. The environmental costs and benefits of fracking. 2014. Annual Review of Environment and Resources. : 1.

Jimenez-Martinez, J., M. L. Porter, J. D. Hyman, J. W. Carey, and H. S. Viswanathan. Mixing in a three-phase system: Enhanced production of oil-wet reservoirs by CO2 injection. 2016. Geophysical Research Letters.. : 1.

Kang, Q., L. Chen, A. J. Valocchi, and H. S. Viswanathan. Pore-scale study of dissolution-induced changes in permeability and porosity of porous media. 2014. Journal of Hydrology. 517: 1049.

Karra, S., N. Makedonska, H. S. Viswanathan, S. Painter, and J. Hyman. Effect of advective flow in fractures and matrix diffusion on natural gas production. 2015. Water Resources Research. : 1.

Kelkar, S., K. Lewis, S. Karra, G. Zyvoloski, S. Rapaka, H. S. Viswanathan, P. K. Mishra, S. Chu, D. Coblentz, and R. Pawar. A simulator for modeling coupled thermo-hydro-mechanical processes in subsurface geological media. 2014. International Journal of Rock Mechanics and Mining Sciences. : 569.

Lei, Z., E. Rougier, E. E. Knight, and A. Munjiza. A framework for grand scale parallelization of the combined finite discrete element method in 2D. 2014. Computational Particle Mechanics. : 307.

Lei, Z., E. Rougier, E. Knight, A. Munjiza, and H. Viswanathan. A generalized anisotropic deformation formulation for geomaterials. 2015. Computational Particle Mechanics. : 1.

Lei, Z., E. Rougier, E. Knight, L. Frash, J. W. Carey, and H. Viswanathan. A non-locking composite tetrahedron element for the combined finite discrete element method. To appear in Engineering Computations..

Liu, H., A. J. Valocchi, C. Werth, Q. Kang, and M. Oostrom. Pore-scale simulation of liquid CO< sub> 2</sub> displacement of water using a two-phase lattice Boltzmann model. 2014. Advances in Water Resources. 73: 144.

Liu, H., Q. Kang, C. R. Leonardi, B. D. Jones, S. Schmieschek, A. Narváez, J. R. Williams, A. J. Valocchi, and J. Harting. Multiphase lattice Boltzmann simulations for porous media applications--a review. 2015. Computational Geosciences. : 1.

Makedonska, N., S. L. Painter, Q. M. Bui, C. W. Gable, and

S. Karra. Particle tracking approach for transport in three-dimensional discrete fracture networks. 2015. Computational Geoscience. : 1.

Middleton, R. S., J. S. Levine, J. L. Bielicki, H. S. Viswanathan, J. W. Carey, and P. Stauffer. Jumpstarting commercial-scale CO2 capture and storage with ethylene production and enhanced oil recovery in the US Gulf. 2015. Greenhouse Gases: Science and Technology. : 241.

Middleton, R. S., J. W. Carey, R. Currier, J. D. Hyman, Q. Kang, J. Jimenez-Martinez, M. L. Porter, and H. S. Viswanathan. Shale gas and non-aqueous fracturing fluids: opportunities and challenges for supercritical CO2. 2015. Applied Energy. : 500.

Middleton, R., H. Viswanathan, R. Currier, and R. Gupta. CO2 as a fracturing fluid. 2015. Energy Procedia. : 7780.

O'Malley, D., S. Karra, R. P. Currier, N. Makedonska, J. D. Hyman, and H. Viswanathan. Where does water go during hydraulic fracturing?. 2015. Groundwater. : 1.

Oostrom, M., Y. Mehmani, P. Romero-Gomez, Y. Tang, H. Liu, H. Yoon, Q. Kang, V. Joekar-Niasar, M. Balhoff, and T. Dewers. Pore-scale and continuum simulations of solute transport micromodel benchmark experiments. 2014. Computational Geosciences. 4-0: 1.

Padrino, J. C., B. VanderHeyden, X. Ma, and D. Z. Zhang. A separate phase drag model and a surrogate approximation for simulation of the steam assisted gravity grainage process. To appear in SPE.

Porter, M., J. Jimenez-Martinez, R. Martinez, Q. McCulloch, J. W. Carey, and H. Viswanathan. Geo-material microfluidics at reservoir conditions for subsurface energy resource applications. 2015. Lab on a Chip. : 1.

Summerscales, O. T., B. L. Scott, H. S. Viswanathan, and A. D. Sutton. Synthesis and reactivity of cis-FeH2(dcpe)2 (dcpe = 1,2-bis(dicyclohexylphosphino)ethane). 2016. Inorganic Chemistry Communications. 63: 57.

Viswanathan, H., J. D. Hyman, S. Karra, J. W. Carey, M. L. Porter, E. Rougier, R. P. Currier, Q. Kang, L. Zhou, J. Jimenenz, N. Makedonska, L. Chen, and R. S. Middleton. Using discovery science to increase the efficiency of hydraulic fracturing while reducing water usage. 2015. In Hydraulic Fracturing: Environmental Issues, ACS Symposium Series 1216.. Edited by Drogos, D.. Vol. 1216, p. 71. Laramie, Wyoming: Oxford University Press.

Zhang, L., Q. Kang, J. Yao, Y. Gao, Z. Sun, H. Liu, and A. Valocchi. Pore scale simulation of liquid and gas two-phase flow based on digital core technology. 2015. Science China Technological Sciences. : 1375.

Zhang, L., Q. Kang, L. Chen, and J. Yao. Simulation of flow in multi-scale porous media using the lattice Boltzmann method on quadtree grids. To appear in Communications in Computational Physics..

Zubelewicz, A., E. Rougier, M. Ostoja-Starewski, E. E. Knight, C. Bradley, and H. S. Viswanathan. A mechanisms-based model for dynamic behavior and fracture of geomaterials. 2014. International Journal of Rock Mechanics and Mining Sciences. : 277.

Combating Antibiotic Resistance: Targeting Efflux Pump Systems at Multiple Scales

Sandrasegaram Gnanakaran
20140121DR

Introduction

Multi-drug resistant bacteria such as Staphylococcus aureus and Mycobacterium tuberculosis are emerging at an alarming rate, yet new antibiotics are few and far between. The scarcity of new antibiotics is in part due to a lack of understanding of the mechanisms of multi-drug resistance. Antibiotic efflux is one of the most important mechanisms of bacterial multi-drug resistance. Antibiotics are pumped out of the cell by efflux pumps containing three protein components. We propose to study the highly active efflux pumps in Burkholderia pseudomallei, a high-priority bio-threat agent. X-ray crystallography and molecular dynamics simulation will be valuable for understanding how the efflux pump protein complexes are formed spanning the inner-membrane, periplasm, and outer-membrane, and how the opening-closure dynamics of the complex determines the rate of efflux of an antibiotic. Gene and protein expression studies will be essential to identify how the presence of an antibiotic turns the gene circuits on or off to regulate the expression of the active efflux pumps, thereby determining the net efflux. The same efflux pumps are also responsible for releasing small metabolites, such as quorum-sensing molecules, which act as global regulators of genes belonging to pathways critical to bacterial growth, viability, and morphology. Therefore, gene expression and pathways analyses are essential to determine how the release of these metabolites offers additional fitness to the bacterium in terms of enhanced growth and viability. Integrated modeling of structural, genetic, and cellular processes will provide valuable insight into how these processes are coupled and how this coupling imparts overall bacterial fitness under the selection pressure from antibiotics.

Benefit to National Security Missions

Countermeasure development for treating pathogen infection is central to our project, as efflux pumps are the predominant form of multi-drug efflux, and understanding gained in this project should lead to novel strategies of antibiotic therapy. Because we chose to focus on a biothreat agent (which is also of global public health concern), Burkholderia pseudomallei, this project will be of interest to the biodefense mission of DOE. The multi-scale nature of this work, coupling genetic, regulatory, and biomolecular structure / function aspects in one study will contribute to advances in basic energy science (biofuels) and basic biomedical research.

Progress

Structural and mechanistic studies of efflux pumps. We have obtained synthetic genes for 9 efflux pump proteins from Burkholderia pseudomallei for structure determination. We have purified 5 proteins to high purity and begun crystallization trials for three proteins. Crystals of one outer membrane protein have been obtained. During the next year we plan to optimize the crystallization conditions for the outer membrane protein for which we already have crystals and to determine the structure of this protein, we plan to carry out extensive screening of crystallization conditions for and attempt to determine the structures of the other two proteins for which we have highly purified protein, and we plan to obtain pure protein for an additional two proteins.

To date, the high-resolution structure of an entire efflux pump complex has remained elusive. Our efforts have focused on filling this gap by combining data from various experimental techniques with the available crystal structure and cryo-EM data to develop computational methods to construct atomic-level resolution models of the full efflux pump complex. We have used these models to probe the mechanistic details of drug efflux. Future studies will integrate these molecular level findings into a mechanistic kinetic model of antibiotic efflux.

Gene expression, biochemical, and cellular analysis of

efflux pumps. We first studied the effect of a P. aeruginosa efflux pump, mexAB-oprM, on biofilm formation and related virulence especially in the presence of ciprofloxacin. We performed cellular assays to show that mexAB-oprM facilitates biofilm formation thereby rendering P. aeruginosa impermeable to ciprofolaxin and increasing its survival in the presence of the drug. Second, we performed gene expression by qPCR to identify the genes responsible for biofilm formation and virulence. Finally, we demonstrated by neutrophil lysis assay that efflux-mediated expression of the virulence factors abrogated host innate immune defense in the presence of ciprofloxacin, which is an additional resistance. These studies revealed that mexAB-oprM is more than a pump. It offers additional resistance by facilitating biofilm formation. We also performed genome-wide expression studies on P. aeruginosa in the planktonic state by RNA-seq. Preliminary analysis revealed that the removal of mexAB-oprM induces an adaptive mechanism in the presence of ciprofloxacin, which causes DNA damage leading to an SOS repair response, which is again associated with the release of pyocin and phage proteins that are able to protect the bacteria.

Future studies will determine the effect of the B. thaliandensis efflux pumps in developing resistance against ciprofloxacin both in the planktonic and biofilm stages by combining gene expression, biochemical, and cellular studies. We will apply a reporter assay to measure the release of quorum sensing molecules and correlate biofilm formation vis-a-vis drug resistance. We will initiate collaboration to carry out gene expression and functional studies on BSL-2/3 B. pseudomallei. Finally, we will perform gene expression and cellular studies to determine the effect of abrogating host innate immune defense.

Integrated mathematical models of efflux pump mediated drug resistance. A minimal model of P. aeruginosa response to cipro has been developed. The level of detail of this model is precisely tuned to capture quantitatively the pulsed behavior seen in the measurements. The model was used to predict membrane permeability and efflux from the experimental antibiotic accumulation data. Sensitivity analysis was performed, indicating all parameters of the model contribute substantially to the behavior. A more detailed mechanistic model was developed, which indicates the pulsed behavior can be explained by a delayed influx of antibiotic across the inner membrane plus a cytoplasmic regulation of efflux. Preliminary integration of the model with a model of cellular states was performed. The integrated model indicates that biofilm and efflux synergistically increase resistance, and that the synergy increases at high membrane permeability.

The plan going forward is to develop further the mechanistic model, to integrate further with cell states and structure. The model development will focus on incorporating new antibiotic accumulation data into the P. aeruginosa model, characterizing kinetic parameters of efflux for mutants, and extending the model to B. thailandensis. We will also initiate collaborations to model antibiotic uptake data. The integration will focus on iterating with the cellular task to refine the cell state model, adding known feedback loops, and coupling to the efflux kinetics predicted by the structural task.

Future Work

During the next year, structural biology studies will optimize the crystallization conditions for the outer membrane protein for which we already have crystals and to determine the structure of this protein, we plan to carry out extensive screening of crystallization conditions for and attempt to determine the structures of the other two proteins for which we have highly purified protein, and we plan to obtain pure protein for an additional two proteins. Future theoretical studies will integrate molecular level findings from molecular dynamics simulations study into a mechanistic kinetic model of antibiotic efflux.

Future genetic and cellular studies will determine the effect of the B. thaliandensis efflux pumps in developing resistance against ciprofloxacin both in the planktonic and biofilm stages by combining gene expression, biochemical, and cellular studies. We will apply a reporter assay to measure the release of quorum sensing molecules and correlate biofilm formation vis-a-vis drug resistance. We will initiate collaboration to carry out gene expression and functional studies on BSL-2/3 B. pseudomallei. Finally, we will perform gene expression and cellular studies to determine the effect of abrogating host innate immune defense.

The plan going forward for the integrated mathematical framework is to develop further the mechanistic model, to integrate further with cell states and structure. The model development will focus on incorporating new antibiotic accumulation data into the P. aeruginosa model, characterizing kinetic parameters of efflux for mutants, and extending the model to B. thailandensis. We will also initiate collaborations to model antibiotic update data. The integration will focus on iterating with the cellular task to refine the cell state model, adding known feedback loops, and coupling to the efflux kinetics predicted by the structural task.

Note: Scope of work has changed due to reduced budget.

Conclusion

We will characterize three coupled processes: expulsion of antibiotics from the cell by efflux pumps, stimulation of efflux pump production by antibiotics, and efflux pump-mediated biofilm formation that shields the bacterium from antibiotics. We will combine experimental and theoretical approaches to develop the first predictive model of this system. This model will integrate these molecular, genetic, and cellular processes and will identify critical elements of each process that can inactivate drug resistance. The capability for integrated modeling of a complex adaptive molecular transport system will have broad applications in biosecurity, biofuel production, and microbial clearance of toxic material.

Publications

Ganguly, K., M. Wren, J. Phillips, P. Pardington, H. Schweizer, M. Wall, S. Gnanakaran , and G. Gupta. Interdependence of multi drug efflux pumps and quorum sensing system in Pseudomonas. 2014. In International Congress on Infectious Diseases. (Cape Town, South Africa, 2-6 April). Vol. 21, Suppl 1, Edition, p. 92. International Journal on Infectious Diseases: --.

Hung, L. W., H. B. Kim, S. Murakami, G. Gupta, C. Y. Kim, and T. C. Terwilliger. Crystal structure of AcrB complexed with linezolid at 3.5 Å resolution. . 2014. Journal of Structural and Functional Genomics. . 14 (2): 71.

Phillips, J. L., Ganguly, Wren, Gupta, M. E. Wall, and Gnanakaran. Systems Level Study of Bacterial Multi-Drug Resistance from Efflux Machinery. 2014. BIOPHYSICAL JOURNAL. 106 (2): 791A.

Phillips, J., and S. Gnanakaran. A data-driven approach to modeling the tripartite structure of multidrug resistance efflux pumps. . 2015. Proteins: Structure, Function, and Bioinformatics.. 83: 43.

Zgurskaya, H., S. Gnanakaran, and C. Lopez. The permeability barrier of Gram-negative cell envelopes and approaches to bypass it. To appear in ACS Infectious Diseases.

Quantitative Biology: From Molecules to Cellular Function

Angel E. Garcia
20140566DR

Introduction

Biology is continuously transforming from a qualitative science involving observations and associations to one where quantitative models are necessary for both fundamental understanding and predictive capability. These theoretical and computational models build on methods and concepts in physics, mathematics, and chemistry and are becoming increasingly influential in many areas of biology. LANL has a long tradition in theoretical biology dating back to the 1970s and more recently CNLS has helped establish an international presence in quantitative biology through the q-bio summer school and annual conference and through its continuing emphasis on applying quantitative methodology to challenging biological problems ranging from the structure and dynamics of individual macromolecules, e.g., DNA, RNA, proteins, etc., to the interacting biochemical reactions that drive cellular function. Our research will build bridges at the mesoscale between macromolecular scales and complex cellular function by taking advantage of coarse graining (averaging) over degrees of freedom at microscales that retain the impact on large-scale (cellular) activity. By taking advantage of the quantitative expertise in CNLS and at LANL, we continue to emphasize opportunities with applications to infectious disease mitigation and bio-surveillance, to developing effective algal and cellulosic biofuels, and to develop fundamental understanding of cellular function over the scales from molecules to cells.

Benefit to National Security Missions

The fundamental discovery science associated with the CNLS biology effort has potential applications in energy security via algal and cellulosic biofuels modeling, in biosecurity through understanding and modeling of infectious disease epidemiology and cellular mechanisms, and in health related areas such as the ability to design effective vaccines using biological models of cellular function.

Progress

Biochemical conversion of cellulosic biomass to biofuels can mitigate the negative environmental impacts of the burning of fossil fuels. Thermochemical pretreatments improve enzyme accessibility to embedded cellulose fibers which are then hydrolyzed by enzymes to glucose and converted to biofuels by fermentation or catalysis. The efficiency of these processes is key to the economic viability of cellulosic biofuels and, although several physicochemical aspects of cellulose are readily captured by different experimental approaches, other properties remain elusive and poorly understood. Computational methods offer a complementary approach using, for example, Molecular dynamics (MD) have provided high-resolution data regarding structural, thermodynamic, and mechanical properties of model crystalline cellulose fibers and surfaces. Recent computational studies focusing on cellulose have provided valuable insights into the construction of coarse-grained (CG) models from MD simulations. In principle, CG models preserve the physical and chemical properties of a determined molecular system after averaging key aspects of the atomistic details. Different CG approaches for the simulation of colloidal states are available which allow us access to large-scale biomass systems over extended simulation times. In this study, we introduced a CG model for crystalline cellulose whose parametrization rules are consistent with one modeling framework. We tested the efficacy and versatility of our model on two important cellulosic systems relevant to the biofuel/bioenergy research field. This study is part of a general effort to extend the implementation of the coarse-graining approach to the modeling of large crystalline bio systems.

Bacterial pathogens are developing increasing resistance to antibiotic treatment, motivating a search for next-generation approaches for treating bacterial infections. An Edisonian approach is inadequate implying that a detailed understanding of the molecular basis for antibiotic resistance is needed. Investigations have identified a pri-

mary resistance mechanism in bacteria: the existence and operation of efflux pumps, three part protein complexes that bridge the inner and outer membranes of many bacteria. We developed a fast consistent method for constructing three-part structures that uses existing data-driven models and provides molecular modeling approaches for constructing the structure of efflux pumps. We discovered that conformational changes in the inner membrane component responsible for drug movement have limited impact on conformations of other pump components, and that two distinct models derived from conflicting experimental data are consistent with currently available measurements. These simulations suggest mechanisms for both smaller and larger drugs entering the pump, leading to a better understanding of the role of the efflux pumps in antibiotic drug resistance.

Mitochondria undergo constant remodeling through regulation of two opposing processes, mitochondrial fission and fusion. Although some aspects controlling these processes have been identified, the role of mitochondrial morphology is not determined. We investigated how morphological features extracted from time-lapse live-cell images of mitochondria could be used to predict mitochondrial evolution. A random model was trained to classify mitochondria poised for either fission or fusion based on a series of morphological and positional features. Mitochondrial perimeter positively correlated with a mitochondrial fission event. Similarly mitochondrial solidity (compact shape) positively correlated with mitochondria fusion. Our results indicate that fission and fusion are can be predicted based upon mitochondrial morphological features, implying that mitochondrial fission and fusion may be influenced by mechanical properties of mitochondrial membranes.

Antigen receptors play a central role in adaptive immune responses. Although the molecular networks associated with these receptors have been extensively studied, we lack a systems-level understanding of how combinations of interactions and modifications are regulated during signaling. Thus, we need to piece together information about individual molecular mechanisms to form large-scale computational models of signaling networks. To this end, we developed an interaction library for signaling by a high-affinity receptor. The library, consisting of executable rules for protein–protein and protein–lipid interactions, extends earlier models for receptor signaling and introduces new interactions not previously considered. This interaction library is a toolkit with which existing models can be expanded and from which new models can be built. As an example, we present models of branching pathways from an adaptor protein, which influence production of a phospholipid protein at the plasma membrane and a soluble second messenger protein. We find that inclusion of a positive feedback loop gives rise to a bistable switch, ensuring robust responses to stimulation above a threshold level.

Future Work

Our innovative approach to improve cellulose hydrolysis relies on using liquid ammonia to catalyze a structural crossover between different forms of cellulose where the resultant structure enhances enzymatic hydrolysis rates by a factor of five. We will provide a theoretical rationale for the ongoing work on designer cellulases, improve current kinetic models for enzyme-cellulose interactions, and develop new predictive models based on the ongoing experimental studies. Our results will help improve the efficiency of converting cellulose to biofuels.

HIV evolves rapidly and can escape antibodies produced by the immune system. One prevention strategy is to develop a vaccination schedule that elicits broad antibody response that is effective against multiple HIV strains. By building a model of within-host dynamics that captures the emergence of strain-specific antibody response, we will investigate whether sequential vaccination or single multi-strain vaccination induces stronger and/or broader response. We will also address the evolution of drug resistance in HCV.

Cellular function is built on molecular motion at the smallest scale where full-atom molecular dynamics is an effective tool for characterizing and understanding the physics and biology of those dynamics. Full simulation of even molecular complexes is, however, far beyond current computational capabilities. Thus, one needs a scheme for saving the important degrees of freedom while averaging over other less important motions, a process known as coarse graining. We will develop effective coarse graining strategies for modeling macromolecular complexes in bacteria and introduce advances from computer science to attain more efficient simulations that will provide new insights into mesoscale cellular function.

Conclusion

We will combine experimental probes with simulation/modeling to characterize biomolecular environments that will allow evaluation of potential drug design. We will develop mesoscopic models that bridge scales in biofuel-relevant algae systems and provide a molecular level understanding and design principles for engineering more effective cellulosic biomass. We will develop multiscale models of pathogenesis in bacteria. We will use novel mathematical methods to improve rule-based methodology applied to bio-chemical reaction networks and em-

ploy them to understand and characterize specific cellular mechanisms. We will construct high-level models of infectious diseases including HIV and HCV based on systems-level understanding of immune response.

Publications

Abbink, , L. F. Maxfield, Ng'ang'a, E. N. Borducchi, M. J. Iampietro, C. A. Bricault, J. E. Teigler, Blackmore, Parenteau, Wagh, S. A. Handley, Zhao, H. W. Virgin, Korber, and D. H. Barouch. Construction and Evaluation of Novel Rhesus Monkey Adenovirus Vaccine Vectors. 2015. JOURNAL OF VIROLOGY. 89 (3): 1512.

Chylek, L. A., Akimov, Dengjel, K. T. G. Rigbolt, B. i. n. Hu, W. S. Hlavacek, and Blagoev. Phosphorylation Site Dynamics of Early T-cell Receptor Signaling. 2014. PLOS ONE. 9 (8).

Chylek, L. A., B. S. Wilson, and W. S. Hlavacek. Modeling Biomolecular Site Dynamics in Immunoreceptor Signaling Systems. 2014. SYSTEMS BIOLOGY APPROACH TO BLOOD. 844: 245.

Chylek, L. A., D. A. Holowka, B. A. Baird, and W. S. Hlavacek. An Interaction Library for the FcεRI Signaling Network. 2014. Frontiers in Immunology. 5: 172.

Chylek, L. A., D. A. Holowka, B. A. Baird, and W. S. Hlavacek. An interaction library for Vie Fc epsilon RI signaling network. 2014. FRONTIERS IN IMMUNOLOGY. 5.

Chylek, L. A., L. A. Harris, C. Tung, J. R. Faeder, C. F. Lopez, and W. S. Hlavacek. Rule-based modeling: a computational approach for studying biomolecular site dynamics in cell signaling systems. 2014. Wiley Interdisciplinary Reviews: Systems Biology and Medicine. 6 (1): 13.

Chylek, L. A., L. A. Harris, J. R. Faeder, and W. S. Hlavacek. Modeling for (physical) biologists: an introduction to the rule-based approach. 2015. PHYSICAL BIOLOGY. 12 (4).

Chylek, L. A., L. A. Harris, Tung, J. R. Faeder, C. F. Lopez, and W. S. Hlavacek. Rule-based modeling: a computational approach for studying biomolecular site dynamics in cell signaling systems. 2014. WILEY INTERDISCIPLINARY REVIEWS-SYSTEMS BIOLOGY AND MEDICINE. 6 (1): 13.

Chylek, L. A., V. Akimov, J. Dengiel, K. T. G. Rigbolt, B. Hu, W. S. Hlavacek, and B. Blagoev. Phosphorylation site dynamics of early T-cell receptor signaling. 2014. PLoS One. 9: e104240.

Cooper, C. S., Eeles, D. C. Wedge, Van Loo, Gundem, L. B. Alexandrov, Kremeyer, Butler, A. G. Lynch, Camacho, C. E. Massie, Kay, H. J. Lmcton, Edwards, Kote-Jarai, Dennis, S. u. e. Merson, Leongamornlert, Zamora, Corbishley, Thomas, Nik-Zainal, Ramakrishna, O'Meara, Matthews, Clark, Hurst, Mithen, R. G. Bristow, P. C. Boutros, Fraser, Cooke, Raine, Jones, Menzies, Stebbings, J. o. n. Hinton, J. o. n. Teague, McLaren, Mudie, Hardy, Anderson, Joseph, Goody, B. e. n. Robinson, Maddison, Gamble, Greenman, D. a. n. Berney, Hazell, Livni, Fisher, Ogden, Kumar, Thompson, Woodhouse, Nicol, Mayer, T. i. m. Dudderidge, N. C. Shah, Gnanapragasam, Voet, Campbell, Futreal, Easton, A. Y. Warren, C. S. Foster, M. R. Stratton, H. C. Whitaker, McDermott, D. S. Brewer, and D. E. Neal. Analysis of the genetic phylogeny of multifocal prostate cancer identifies multiple independent clonal expansions in neoplastic and morphologically normal prostate tissue (vol 47, pg 367, 2015). 2015. NATURE GENETICS. 47 (6): 689.

Cooper, C. S., Eeles, D. C. Wedge, Van Loo, Gundem, L. B. Alexandrov, Kremeyer, Butler, A. G. Lynch, Camacho, C. E. Massie, Kay, H. J. Luxton, Edwards, Kote-Jarai, Dennis, S. u. e. Merson, Leongamornlert, Zamora, Corbishley, Thomas, Nik-Zainal, O'Meara, Matthews, Clark, Hurst, Mithen, R. G. Bristow, P. C. Boutros, Fraser, Cooke, Raine, Jones, Menzies, Stebbings, J. o. n. Hinton, J. o. n. Teague, McLaren, Mudie, Hardy, Anderson, Joseph, Goody, B. e. n. Robinson, Maddison, Gamble, Greenman, D. a. n. Berney, Hazell, Livni, Fisher, Ogden, Kumar, Thompson, Woodhouse, Nicol, Mayer, T. i. m. Dudderidge, N. C. Shah, Gnanapragasam, Voet, Campbell, Futreal, Easton, A. Y. Warren, C. S. Foster, M. R. Stratton, H. C. Whitaker, McDermott, D. S. Brewer, and D. E. Neal. Analysis of the genetic phylogeny of multifocal prostate cancer identifies multiple independent clonal expansions in neoplastic and morphologically normal prostate tissue. 2015. NATURE GENETICS. 47 (4): 367.

Giorgi, E. E., D. O. Stram, D. Taverna, S. D. Turner, F. Schumacher, C. A. Haiman, A. Lum-Jones, M. Tirikainen, C. Caberto, D. Duggan, B. E. Henderson, L. Le Marchand, and I. Cheng. Fine-Mapping IGF1 and Prostate Cancer Risk in African Americans: The Multiethnic Cohort Study. 2014. Cancer Epidemiology, Biomarkers & Prevention: A Publication of the American Association for Cancer Research, Cosponsored by the American Society of Preventive Oncology. 23 (9): 1928.

Gottardo, R., R. T. Baller, B. T. Korber, S. Gnanakaran, J. Phillips, X. Shen, G. D. Tomaras, E. Turk, G. Imholte, L. Eckler, H. Wenschuh, J. Zerweck, K. Greene, H. Gao, P. W. Berman, D. Francis, F. Sinangil, C. Lee, S. Nitayaphan, S. Rerks-Ngarm, J. Kaewjungawal, P. Pitsuttithum, J. Tartaglia, M. L. Robb, N. L. Michael, J. H. Kim, S. Zolla-Pazner, B. F. Haynes, J. R. Mascola, S. Self, P. Gilbert, and D. C. Montefiori. Plasma IgG to linear epitopes in the V2 and V3 regions of HIV-1 gp120 correlate with a reduced risk of infection in the RV144 vaccine efficacy trial. 2013. PLoS One. : e75665.

Gundem, , Van Loo, Kremeyer, L. B. Alexandrov, J. M. C. Tubio, Papaemmanuil, D. S. Brewer, H. M. L. Kallio, Hoegnas, Annala, Kivinummi, Goody, Latimer, O'Meara, K. J. Dawson, Isaacs, M. R. Emmert-Buck, Nykter, Foster, Kote-Jarai, Easton, H. C. Whitaker, D. E. Neal, C. S. Cooper, R. A. Eeles, Visakorpi, P. J. Campbell, McDermott, D. C. Wedge, and G. S. Bova. The evolutionary history of lethal metastatic prostate cancer. 2015. NATURE. 520 (7547): 353.

Hong, M. K. H., Macintyre, D. C. Wedge, Van Loo, Lunke, L. B. Alexandrov, Sloggett, Cmero, Mangiola, Lonie, Naeem, Sapre, Phal, Chin, Kerger, J. S. Pedersen, Ryan, Waring, Haviv, A. J. Costello, N. M. Corcoran, and C. M. Hovens. Unexpected complexity in the origins of prostate cancer metastases. 2015. BJU INTERNATIONAL. 115: 92.

Hong, M. K. H., Macintyre, D. C. Wedge, Van Loo, Patel, Lunke, L. B. Alexandrov, Sloggett, Cmero, Marass, Tsui, Mangiola, Lonie, Naeem, Sapre, P. M. Phal, Kurganovs, Chin, Kerger, A. Y. Warren, Neal, Gnanapragasam, Rosenfeld, J. S. Pedersen, Ryan, Haviv, A. J. Costello, N. M. Corcoran, and C. M. Hovens. Tracking the origins and drivers of subclonal metastatic expansion in prostate cancer. 2015. NATURE COMMUNICATIONS. 6.

Hovens, , Hong, Macintyre, Wedge, Van Loo, Lunke, Alexandrov, Slogget, Cmero, Mangiola, Lonie, Naeem, Sapre, Phal, Kerger, Pedersen, Ryan, Haviv, Costello, and Corcoran. Tracking clonal diversity in metastatic prostate cancer progression. 2015. JOURNAL OF CLINICAL ONCOLOGY. 33 (7).

Kong, R. u. i., M. K. Louder, Wagh, R. T. Bailer, deCamp, Greene, Gao, J. D. Taft, Gazumyan, Liu, M. C. Nussenzweig, Korber, D. C. Montefiori, and J. R. Mascola. Improving Neutralization Potency and Breadth by Combining Broadly Reactive HIV-1 Antibodies Targeting Major Neutralization Epitopes. 2015. JOURNAL OF VIROLOGY. 89 (5): 2659.

Kozer, , Barua, Henderson, E. C. Nice, A. W. Burgess, W. S. Hlavacek, and A. H. A. Clayton. Recruitment of the Adaptor Protein Grb2 to EGFR Tetramers. 2014. BIOCHEMISTRY. 53 (16): 2594.

Langan, , Petridis, H. M. O'Neill, S. V. Pingali, Foston, Nishiyama, Schulz, Lindner, B. L. Hanson, Harton, W. T. Heller, Urban, B. R. Evans, Gnanakaran, A. J. Ragauskas, J. C. Smith, and B. H. Davison. Common processes drive the thermochemical pretreatment of lignocellulosic biomass. 2014. GREEN CHEMISTRY. 16 (1): 63.

Lopatina, L. M., and J. V. Selinger. Polymer-disordered liquid crystals: Susceptibility to an electric field. 2013. Physical Review E. 88: 062510.

Lopez, C. A., Bellesia, Redondo, Langan, S. P. S. Chundawat, B. E. Dale, S. J. Marrink, and Gnanakaran. MARTINI Coarse-Grained Model for Crystalline Cellulose Microfibers. 2015. JOURNAL OF PHYSICAL CHEMISTRY B. 119 (2): 465.

Lopez, C. A., Sethi, Goldstein, B. S. Wilson, and Gnanakaran. Membrane-Mediated Regulation of the Intrinsically Disordered CD3 epsilon Cytoplasmic Tail of the TCR. 2015. BIOPHYSICAL JOURNAL. 108 (10): 2481.

Martincorena, , Roshan, Gerstung, Ellis, Van Loo, McLaren, D. C. Wedge, Fullam, L. B. Alexandrov, J. M. Tubio, Stebbings, Menzies, Widaa, M. R. Stratton, P. H. Jones, and P. J. Campbell. High burden and pervasive positive selection of somatic mutations in normal human skin. 2015. SCIENCE. 348 (6237): 880.

Mayes, H. B., Tian, M. W. Nolte, B. H. Shanks, G. T. Beckham, Gnanakaran, and L. J. Broadbelt. Sodium Ion Interactions with Aqueous Glucose: Insights from Quantum Mechanics, Molecular Dynamics, and Experiment. 2014. JOURNAL OF PHYSICAL CHEMISTRY B. 118 (8): 1990.

Nemenman, , J. R. Faeder, Gnanakaran, W. S. Hlavacek, Munsky, M. E. Wall, and Y. i. Jiang. The Seventh q-bio Conference: meeting report and preface. 2014. PHYSICAL BIOLOGY. 11 (4).

Phillips, J. L., and Gnanakaran. A data-driven approach to modeling the tripartite structure of multidrug resistance efflux pumps. 2015. PROTEINS-STRUCTURE FUNCTION AND BIOINFORMATICS. 83 (1): 46.

Russell, C. A., P. M. Kasson, R. O. Donis, Riley, Dunbar, Rambaut, Asher, Burke, C. T. Davis, R. J. Garten, Gnanakaran, S. I. Hay, Herfst, N. S. Lewis, J. O. Lloyd-Smith, C. A. Macken, Maurer-Stroh, Neuhaus, C. R. Parrish, K. M. Pepin, S. S. Shepard, D. L. Smith, D. L. Suarez, S. C. Trock, Widdowson, D. B. George, Lipsitch, and J. D. Bloom. Improving pandemic influenza risk assessment. 2014. ELIFE. 3.

Schulze, , Imbeaud, Letouze, L. B. Alexandrov, Calderaro, Rebouissou, Couchy, Meiller, Shinde, Soysouvanh, Calatayud, Pinyol, Pelletier, Balabaud, Laurent, Blanc, Mazzaferro, Calvo, Villanueva, Nault, Bioulac-Sage, M. R. Stratton, J. M. Llovet, and Zucman-Rossi. Exome sequencing of hepatocellular carcinomas identifies new mutational signatures and potential therapeutic targets. 2015. NATURE GENETICS. 47 (5): 505.

Shlien, , B. B. Campbell, de Borja, L. B. Alexandrov, D. M. Merino, Remke, Bakry, Dirks, Huang, R. G. Grundy, Durno, Aronson, M. D. Taylor, Z. F. Pursell, C. E. Pearson, Malkin, Bouffet, Hawkins, P. J. Campbell, and U. r. i. Tabori. COMBINED HEREDITARY AND SOMATIC MUTATIONS OF REPLICATION ERROR REPAIR GENES RESULT IN RAPID ONSET OF ULTRA-HYPERMUTATED

MALIGNANT BRAIN TUMORS IN CHILDREN. 2015. NEURO-ONCOLOGY. 17: 9.

Shlien, , B. B. Campbell, de Borja, L. B. Alexandrov, Merico, Wedge, Van Loo, P. S. Tarpey, Coupland, S. a. m. Behjati, Pollett, Lipman, Heidari, Deshmukh, Avitzur, Meier, Gerstung, Y. e. Hong, D. M. Merino, Ramakrishna, Remke, Arnold, G. B. Panigrahi, N. P. Thakkar, K. P. Hodel, E. E. Henninger, A. Y. Goeksenin, Bakry, G. S. Charames, Druker, Lerner-Ellis, Mistry, Dvir, Grant, Elhasid, Farah, G. P. Taylor, P. C. Nathan, Alexander, Ben-Shachar, S. C. Ling, Gallinger, Constantini, Dirks, Huang, S. W. Scherer, R. G. Grundy, Durno, Aronson, Gartner, M. S. Meyn, M. D. Taylor, Z. F. Pursell, C. E. Pearson, Malkin, P. A. Futreal, M. R. Stratton, Bouffet, Hawkins, P. J. Campbell, and U. r. i. Tabori. Combined hereditary and somatic mutations of replication error repair genes result in rapid onset of ultra-hypermutated cancers. 2015. NATURE GENETICS. 47 (3): 257.

Stieh, D. J., J. L. Phillips, P. M. Rogers, D. F. King, G. C. Cianci, S. A. Jeffs, S. Gnanakaran, and R. J. Shattock. Dynamic electrophoretic fingerprinting of the HIV-1 envelope glycoprotein. 2013. Retrovirology. 10 (1): 33.

Veelen, V., Matthijs, S. Luo, and B. Simon. A Simple Model of Group Selection that Cannot Be Analyzed with Inclusive Fitness. 2014. Social Science Research Network.

Wagener, , L. B. Alexandrov, Montesinos-Rongen, Schlesner, Haake, H. G. Drexler, Richter, G. R. Bignell, McDermott, and Siebert. Analysis of mutational signatures in exomes from B-cell lymphoma cell lines suggest APOBEC3 family members to be involved in the pathogenesis of primary effusion lymphoma. 2015. LEUKEMIA. 29 (7): 1612.

Westrate, L. M., J. A. Drocco, K. R. Martin, W. S. Hlavacek, and J. P. MacKeigan. Mitochondrial Morphological Features are Associated with Fission and Fusion Events. 2014. PLoS ONE. 9 (4): e95265.

Westrate, L. M., J. A. Drocco, K. R. Martin, W. S. Hlavacek, and J. P. MacKeigan. Mitochondrial Morphological Features Are Associated with Fission and Fusion Events. 2014. PLOS ONE. 9 (4).

Yates, L. R., Gerstung, Knappskog, Desmedt, Gundem, Van Loo, Aas, L. B. Alexandrov, Larsimont, Davies, Li, Y. S. Ju, Ramakrishna, H. K. Haugland, P. K. Lilleng, Nik-Zainal, McLaren, Butler, Martin, Glodzik, Menzies, Raine, Hinton, Jones, L. J. Mudie, Jiang, Vincent, Greene-Colozzi, Adnet, Fatima, Maetens, Ignatiadis, M. R. Stratton, Sotiriou, A. L. Richardson, P. E. Lonning, D. C. Wedge, and P. J. Campbell. Subclonal diversification of primary breast cancer revealed by multiregion sequencing. 2015. NATURE MEDICINE. 21 (7): 751.

SHIELDS: Space Hazards Induced Near Earth by Large Dynamic Storms - Understanding, Modeling, Predicting

Vania K. Jordanova
20150033DR

Introduction

Our society is increasingly dependent on technologies susceptible to harmful conditions in space, e.g., Galaxy 15, a $250M telecommunication satellite in geosynchronous orbit, failed to operate in 2010 due to a space storm, and its recovery operation cost was ~$3.5M. Predicting space weather hazards remains a big space physics challenge due to the complex multi-scale nature of the magnetosphere. This project will address this challenge using a cross-Laboratory team, LANL state-of-the-art models, computational facilities, and data from national security payloads.

This project will develop a new capability, the SHIELDS framework, to understand, model, and predict one of the most important space weather hazards, the spacecraft Surface Charging Environment (SCE), i.e. the hot (less than few 100 keV) electron fluxes whose enhancement can lead to satellite failures during disturbed conditions. This project aims at addressing two mechanisms that may be crucial for the increase of the SCE, but are not included in any existing global model: a) particle injection during geomagnetic substorms (magnetospheric reconfiguration events), and b) scattering by plasma waves. Substorms may contribute significantly to the plasma pressure increase, causing sudden enhancements of the ring current (keV) fluxes.

Plasma waves redistribute energy throughout the collisionless magnetospheric environment; wave-particle interactions can serve as a dominant mechanism for energy diffusion and particle loss. Including these processes requires models that are targeted at key regions/physics regimes, however, the coupling of these models across multiple spatial and temporal scales remains an extreme challenge. Guided by theory and observations, the goal of this project is to bridge macro- and microscopic computational models, allowing for the first time to study the SCE consequences on a global scale. New data assimilation techniques employing data from LANL instruments on Van Allen Probes and geosynchronous satellites will be applied for the first time to the global model.

Benefit to National Security Missions

Our national efforts in nuclear nonproliferation depend in many ways on our satellite sensing systems. Many of the nation's civilian and military space assets operate in the inner magnetosphere, an extremely hazardous region of space causing satellite failures and anomalies. The ability to reliably distinguish between various modes of failure is very important in anomaly resolution and forensics and may be used in decision-making exercises at the highest levels. The crucial national security need to maximize the safety of civilian and military satellites requires a capability to predict dynamic conditions in space, as called out in national studies supporting the National Space Weather Program by DOE, DOD, NOAA, NASA, and NSF. This is especially needed during solar maximum (in ~2015) with its expected high storm occurrence.

Our SHIELDS framework will address the ubiquitous threats posed by surface charging and will specify the fast-changing Surface Charging Environment (SCE) which represents a seed population for the harmful radiation belts. SHIELDS utilizes unique data from DOE/LANL geosynchronous spacecraft, which are operational national security payloads that additionally provide scientific data at critical locations in the magnetosphere. SHIELDS is directly relevant to the Lab's Global Security Space Situational Awareness (SSA) and Energy Security missions and the "Complex Natural and Engineered Systems" priority area to understand key drivers of the radiation belts (e.g., seed populations, plasma waves) and advance toward prediction of the space environment. Being sought both nationally and internationally, such unique LANL capability will position us at the forefront of space science exploration.

Progress

The particle tracing model (PTM) has been ported to both C and FORTRAN 90 and the field interpolation algorithms have been tested and updated to produce more physical results (preserving higher order spatial derivatives across grid cells). The new code has been coupled with the global MHD BATS-R-US model from the Space Weather Modeling Framework (SWMF) and we have begun tracing equatorially mirroring particles in these MHD fields. We have also begun modifying the coupling between BATS-R-US and the inner magnetospheric RAM-SCB module. Currently, the electric field is communicated to RAM-SCB from the rest of the SWMF by mapping only the potential electric field out from the ionosphere into the RAM-SCB domain. While this accounts for much of the convective electric fields associated with storms, it neglects the inductive electric fields produced during very dynamic events like substorms. The electric field coupling has been modified so that the inductive fields can be communicated directly with RAM-SCB.

The coupling between the MHD code BATS-R-US and the Particle-in-Cell (PIC) code iPIC3D has been completely rewritten. The original coupling was through flat files, which was simple to implement but was only intended as a temporary solution. Once the MHD-EPIC algorithm was proven to work, a general parallel coupler was implemented since the existing SWMF couplers were not suitable for passing large amount of data between massively parallel models. The new coupler keeps the grid description and interpolation methods private for the models. This eliminates the need to describe the grid in an abstract manner and pass this information to the SWMF or the coupled model. The coupling between BATS-R-US and iPIC3D now works in 3D, and the two grids don't need to be aligned. We also allow multiple PIC regions to be used. This new efficient and flexible coupler was used to model Ganymede's magnetosphere in 3D with 4 PIC regions. The results gave excellent agreement with Galileo measurements, much better than with Hall MHD, showing that the MHD-EPIC algorithm provides a better description of reconnection than the fluid models can. The results of this work are being prepared for publication in the Journal of Geophysical Research.

We have successfully implemented a data assimilation method into RAM-SCB to properly simulate particle injections. The assimilation method applied was the localized ensemble Kalman filter, which uses an ensemble of model simulations, along with observational data, to calibrate the model. The assimilation is able to nudge the RAM-SCB electron flux so that it's in better agreement with the observed flux. In particular, we successfully simulated the effects of particle injections during an isolated substorm that took place on July 18 2013 by assimilating electron fluxes from the Van-Allen Probe B valid for the substorm date. The results showed a significant improvement in the estimation of the ring current pressure, in agreement with observations from the Van Allen Probe A. These results have been written in a paper submitted to the Geophysical Research Letters. We have also worked on estimating appropriate spatial correlations within RAM-SCB to regularize the covariance matrix, which is an important element for the success of the assimilation.

The first requisite of efficient interfacing between the multiple disparate codes that this project involves was the migration of existing projects to a unified yet distributed version control system. This was achieved in part through the creation and integration into a GIT repository. This facilitated efficient contributions of our external collaborators who subsequently brought the BATS-R-US/RAM-SCB coupled code into parity with the latest SWMF release. This parity can be maintained with little overhead moving forward, allowing SHIELDS to benefit from the latest SWMF optimizations and features. The performance of various components of the code has been examined and we found that the PIC codes are the most significant computational components. We are addressing this for the Curvilinear PIC code by identifying the key computational kernels and regions with potential for shared memory parallelization; these options are currently being explored.

Finally, we organized a SHIELDS kick-off workshop in February 23-25, 2015, attended by both external and internal LANL collaborators. The workshop consisted of introductory talks given by SHIELDS team members, followed by general discussions, and provided a broad forum for interactions on space weather topics.

Future Work

- Expand the coupling of the particle tracing model (PTM) with BATS-R-US and RAM-SCB to off-equatorially mirroring particles and investigate the formation of injection boundaries. Complete the electric field coupling so that inductive fields are passed to RAM-SCB. Perform testing and validation, comparing results with Van Allen Probes and geosynchronous satellite observations.
- Develop further the coupling of BATS-R-US and the iPIC3D code by extending the coupling for electron pressure and multi-ion plasma, and developing direct coupling between separate iPIC3D regions within the SWMF. Improve the efficiency of the coupling and apply it to simulate the magnetosphere of the Earth and Mercury.
- Implement a novel data assimilation scheme, based on the ensemble Kalman filter, to better nudge the

coupled RAM-SCB and BATS-R-US system into reproducing substorm injections. We have developed this scheme theoretically, showing that it captures the most relevant correlations between the models, which is crucial for the propagation of information in the coupled system.

- Incorporate wave-particle interactions in RAM-SCB using quasi-linear theory and event-specific diffusion coefficients. To calculate the necessary cold plasma density, couple RAM-SCB with a 2D plasmasphere model. Perform initial calculations of transport coefficients with the wave PIC code using RAM-SCB input.
- Develop further the SHIELDS distributed version control system, incorporating dependency relationships between the components to facilitate large scale development and build towards production use. Incorporate unit tests and begin the development of workflow tools that allow coherent execution of the many successive components of the SHIELDS framework.
- Upgrade the Curvilinear PIC code (CPIC) from single-block grid geometry to multi-block pursuing three approaches: (1) overlapping grid patches, (2) non-overlapping grid patches, and (3) the immersed boundary method. Upgrade the particle mover and the field solver to the new grid configuration. Evaluate the robustness, simplicity and computational performance of these approaches.

Conclusion

Using a new, system-level approach, we will provide the transformative understanding of mechanisms driving disturbed geomagnetic conditions, critically needed for their accurate prediction and to prevent damages to technological systems in space. We will obtain, for the first time, a realistic description of the magnetosphere, resolving short timescales of substorm dynamics and enabling a better prediction of the spacecraft Surface Charging Environment (SCE). We will examine, for the first time self-consistently on a global scale, the fundamental generation of plasma waves and their feedback on particle dynamics. We expect this to lead to new discoveries and high-impact innovative publications.

Publications

Birn, J., A. Runov, and M. Hesse. Energetic electrons in dipolarization events: Spatial properties and anisotropy. 2014. Journal of Geophysical Research - Space Physics. 119 (5): 3604.

Birn, J., A. Runov, and M. Hesse. Energetic ions in dipolarization events. 2015. Journal of Geophysical Research - Space Physics. doi:10.1002/2015JA021372 (120): 1.

Daldorff, L., G. Toth, T. I. Gombosy, G. Lapenta, J. Amaya, S. Markidis, and J. U. Brackbill. Two-way coupling of a global Hall magnetohydrodynamics model with a local implicit Particle-in-Cell model. 2014. Journal of Computational Physics. 268: 236.

Denton, M. H., M. F. Thomsen, V. K. Jordanova, M. G. Henderson, J. E. Borovsky, J. S. Denton, Pitchford, and D. P. Hartley. An empirical model of electron and ion fluxes derived from observations at geosynchronous orbit. 2015. SPACE WEATHER-THE INTERNATIONAL JOURNAL OF RESEARCH AND APPLICATIONS. 13 (4): 233.

Godinez, H. C., Y. Yu, M. G. Henderson, B. Larsen, and V. K. Jordanova. Ring current pressure estimation with RAM-SCB using data assimilation and Van Allen Probe flux data. Geophysical Research Letters.

Jordanova, V. K.. Global modeling of wave generation processes in the inner magnetosphere. To appear in Magnetosphere-Ionosphere Coupling in the Solar System. Edited by Chappell, R., and R. Thorne.

Peng, I. B., S. Markidis, E. Laure, A. Johlander, A. Vaivads, Y. Khotyaintsev, P. Henri, and G. Lapenta. Kinetic structures of quasi-perpendicular shocks in global particle-in-cell simulations. 2015. Physics of Plasmas. doi: 10.1063/1.4930212 (22): 1.

Welling, D. T., V. K. Jordanova, Glocer, Toth, M. W. Liemohn, and D. R. Weimer. The two-way relationship between ionospheric outflow and the ring current. 2015. JOURNAL OF GEOPHYSICAL RESEARCH-SPACE PHYSICS. 120 (6): 4338.

Yu, Y., V. Jordanova, D. Welling, Larsen, S. G. Claudepierre, and Kletzing. The role of ring current particle injections: Global simulations and Van Allen Probes observations during 17 March 2013 storm. 2014. Geophysical Research Letters. 41 (4): 1126.

Yu, Y., V. K. Jordanova, S. Zou, R. Heelis, M. Ruohoniemi, and J. Wygant. Modeling subauroral polarization streams (SAPS) during the March 17, 2013 storm. 2015. Journal of Geophysical Research - Space Physics. doi:10.1002/2014JA020371 (3): 1738.

Zhao, L., Y. Yu, G. Delzanno, and V. Jordanova. Bounce- and MLT-averaged diffusion coefficients in a physics-based magnetic field geometry obtained from RAM-SCB for the March 17 2013 storm. 2015. Journal of Geophysical Research - Space Physics. doi:10.1002/2014JA020858 (4): 2616.

Critical Watersheds: Climate Change, Tipping Points, and Water Security Impacts

Richard S. Middleton
20150397DR

Introduction

Water is critical for domestic health, wealth, and security. Our changing climate will have a significant and detrimental impact on terrestrial ecosystems and subsequent water supply for the energy-water nexus (EWN). Currently, we do not understand the interactions and feedbacks between climate, forest mortality, wildfire, and hydrology. Without this understanding, we cannot predict and plan for climate-induced impacts on society and the EWN.

This project develops the necessary basic science and modeling capabilities to (1) predict, (2) quantify, and (3) mitigate climate-related impacts on our natural ecosystems and the EWN. The project focuses on the novel concept of "critical watersheds", watersheds that are both critical to society and vulnerable to climate change, and climate-induced extreme events. The project is advancing the predictive understanding of integrated watershed hydrology and the role of disruptive events in ecosystems. The project focuses on processes that operate and are manifested on multiple scales, requiring multiple study sites to capture the range of climate-ecosystem-hydrologic interactions. Our study sites range from small-scale ecosystem study plots and hillslopes (< 0.1 km2) and small watersheds (<2 km2) up to mesoscale watersheds and the entire Colorado River basin. The broad project focus will is on the US Southwest though the science, tools, and understanding developed will be broadly applicable to critical domestic and global watersheds. The project will use combination of existing data from LANL and multiple collaborators, new modeling approaches, new model-based data analyses and syntheses, and new experiments. The project will uniquely position LANL to predict, quantify, and mitigate the impacts of climate change on water supply to municipalities and energy producers, with multiple potential sponsors in DOE, state and federal agencies, and private industry.

The project will develop a first-of-a-kind fully-integrated framework to directly address interactions and feedbacks between climate, terrestrial ecosystems, wildfire, and hydrology.

Benefit to National Security Missions

The project directly addresses the energy security and environment missions, with anticipated substantial contributions to the DOE applied energy and science programs.

Environment mission: The project focuses on climate and energy impacts, specifically exploring climate change/extremes and water supply for the energy-water nexus (EWN). This includes all energy production/extraction that requires water including coal-fired and gas plants, nuclear power plants, renewable energy (e.g., hydropower), and conventional and unconventional oil and gas production. The stretch goal of the project is to develop quantitative mitigation plans—including remediation and restoration—that increase ecosystem resiliency (e.g., fire suppression, hydrologic stability) to changing climate and extremes. Science and modeling capabilities developed in this project directly address challenges set out by the DOE-SC including integrating fire behavior, drought mortality, and hydrology into standalone watershed frameworks as well as providing key input for DOE-SC's Accelerated Climate Model for Energy (ACME).

Energy security mission: the EWN is a key focus of the project, understanding how nuclear energy, fossil energy, and renewable energy/power will be impacted by climate change/extremes, particularly in critical watersheds such as the Colorado River.

Agency relevance: Project outcomes are designed to directly address challenges and needs set out by DOE-SC (see above) and DOD (e.g., SERDP). The project addresses applications critical to DOE-EERE (e.g., biomass

and hydropower programs). Long-term, the project could position LANL for non-traditional federal agencies including USDA (food security), EPA (environmental impacts), and Department of State (geopolitically critical watersheds such as the Nile River basin).

Progress

The project has made significant advances in each area described in Year 1 planning. This includes successfully addressing and on-time progress for accomplishments in each FY15 goal, task, and sub-task.

We have developed a scientific manuscript (soon-to-be-submitted) that details challenges and opportunities to understand the interaction between climate change, extreme events, and climate-induced disturbances. This manuscript directly addresses our first year goals. The challenges and opportunities in the paper also will guide key scientific questions and approaches in Year 2 as well as provide the basis for focuses discussion with collaborators and the wider community. And in the longer term (e.g., post-project), we anticipate that the paper will serve as a scientific roadmap and lay the groundwork for a national workshop, potentially funded by DOE Office of Science, that brings together key researchers in this area.

We have developed a preliminary framework that incorporates climate drivers, vegetation responses, offline wildfire behavior, and hydrology. The Advanced Terrestrial Simulator (ATS) framework will undergo testing, validation, and calibration in the remaining four months of the project. We anticipate that ATS will be applied to a key small watershed in the Valles Caldera National Preserve (VCNP) before the end of Year 1, an activity that was not anticipated until Year 2 in original scoping and planning.

In Task 1 we developed specific modeling and experimental research plans for Years 2 and 3 including developing research access and collaboration with the VCNP and identifying an illustrative watershed (Jaramillo River), access to multiple field sites and data with the University of New Mexico (UNM), New Mexico State University (NMSU), Oregon State University (OSU), and Bandelier National Monument (BNM). We have developed a new approach to integrating dynamic vegetation responses and succession into the ATS framework and, ahead of schedule, expect preliminary outcomes by the end of Year 1 (contributing to FY15 Task 2 below). In conjunction with the VCNP, we have identified specific field sites and data to validate and calibrate vegetation dynamics and ATS. We have identified a new approach to upscaling fine-physics wildfire modeling into a reduced model of wildfire ecology called QUICFIRE. The preliminary QUICFIRE model is approaching demonstration, approximately two months ahead of anticipated schedule.

Task 2 involved development of the ATS framework and incorporating key processes critical for understanding interaction between climate, vegetation, fire, and hydrology. Specifically, we have focused on understanding the role of ground cover (e.g., litter, duff layer) in both fire and hydrology and have successfully integrated a unique, novel representation of groundcover into ATS. We expect this to have a transformational impact on ecohydrologic modeling and understanding.

Task 3 has involved collecting and collating large volumes of data to support our science and modeling work at multiple scales and for multiple sites. This includes regional climate data, vegetation disturbances (e.g., infestation, historic wildfire impacts), and historic hydrology. This data collection is currently supporting ongoing research and serve as a critical platform for Years 2 and 3.

Specific accomplishments:

The preliminary QUICFIRE modeling framework has already advanced to a stage where potential sponsors (e.g., DHS) are preparing to send seed money to develop the technology in new direction (i.e., urban fire modeling) not part of this project. We have been selected as primary conveners for an upcoming targeted special session (American Geophysical Union, 2015) that will bring together key domestic and international researchers to better understand critical watersheds in transition. We will us this opportunity as an ad hoc workshop on climate and ecohydrology interactions.

Science and modeling developed in Year 1 has enabled multiple proposals, within and beyond DOE, and collaborations that are advancing the concept of critical watersheds and the impacts of climate change on natural ecosystems and water for the energy-water nexus.

The research team presented multiple talks (5-10) at several national and international conferences. Multiple manuscripts are published, in review, and preparation highlighting new science developed in first eight months of the project, including a significant “roadmapping” manuscript outlining the key scientific challenges and opportunities for understanding critical watersheds.

We formed a reciprocal relationship with USDA’s Southern Research Station (SRS) to develop the QUICFIRE model.

Future Work

Goal 1. Understand climate-ecohydrologic interactions/ processes at small scales (<5 km2). We will incorporate physical representations of vegetation, wildfire, and hydrology into the Advanced Terrestrial Simulator (ATS) ecohydrologic framework. We will move ATS beyond preliminary development (Year 1 goal) and demonstrate ATS on the Jaramillo River watershed (~3 km2) in the Valles Caldera National Preserve (VCNP). Compare and validate ATS with an existing ecohydrologic model (PARFLOW).

Goal 2. Understand climate-ecohydrology interactions at regional scale (1000s km2), and develop a fully calibrated hydrologic model of the Colorado River based on high-resolution multispectral remote sensing, historic natural flows, regional climate drivers, drought mortality, wildfire, extreme climate events, and climate-driven vegetation changes. Analyze multiple coupled climate-ecosystem and energy-water nexus (EWN) scenarios. Compare/validate outputs with existing hydrologic models.

Goal 3. We will deliver 3-5 publications demonstrating the basic science needs and project advancements linking climate change, extreme events, dynamic ecosystems, wildfire, and hydrology. Bring multiple key researchers together for a workshop/special session at a national/international conference.

Conclusion

The overarching goal of this project is to develop the science and modeling capabilities to predict and quantify climate impacts on critical watersheds and water supply. This will have a potentially transformative impact on our understanding of climate change and the energy-water nexus (EWN) and our ability to mitigate and adapt to climate change. Specifically, we are developing a new understanding of the interaction and feedbacks between climate change and extreme events, climate-driven disturbances such as wildfire, drought and forest mortality, hydrology, and water for the EWN.

Publications

Allen, C. D., D. D. Breshears, and N. G. McDowell. On underestimation of global vulnerability to tree mortality and forest die-off from hotter drought in the Anthropocene. 2015. ECOSPHERE. 6 (8).

Fisher, R., S. Muszala, M. Verteinstein, P. Lawrence, C. Xu, N. McDowell, R. Knox, C. Koven, J. Holm, B. Rogers, and others. Taking off the training wheels: the properties of a dynamic vegetation model without climate envelopes. 2015. Geoscientific Model Development Discussions. 8 (4).

Middleton, R. S., J. S. Levine, J. M. Bielicki, H. S. Viswanathan, J. W. Carey, and P. H. Stauffer. Jumpstarting commercial-scale CO2 capture and storage with ethylene production and enhanced oil recovery in the US Gulf. 2015. GREENHOUSE GASES-SCIENCE AND TECHNOLOGY. 5 (3): 241.

Middleton, R. S., J. W. Carey, R. P. Currier, J. D. Hyman, Kang, Karra, Jimenez-Martinez, M. L. Porter, and H. S. Viswanathan. Shale gas and non-aqueous fracturing fluids: Opportunities and challenges for supercritical CO2. 2015. APPLIED ENERGY. 147: 500.

Using Microreactors for Efficient Plutonium Separations (U)

Stephen L. Yarbro
20130003DR

Abstract

Chemical separations, especially difficult separations depend on many factors. Fundamentally, reactions and rates are controlled by the mass and heat transfer characteristics of the equipment. In equipment where the length scales are very large with respect to the boundary layers and turbulent eddies are formed, mass and heat transfer are controlled by the contact area and mixing energy per unit volume. In equipment such as microreactors, where the length scales are small with respect to the boundary layer and the flow is predominantly laminar, heat and mass transfer are controlled by different mechanisms. In this work, plutonium mass transfer was characterized with both neutral and anionic extractants and in channels with diameters from 0.1 mm (micro) to 5 mm (milli). The mass transfer rates were measured and mass transfer models were developed to predict behavior. Also, several different slug-flow and membrane-based microreactor designs were successfully evaluated. It was demonstrated that microchannel contactors are very efficient for Pu separations, with characteristic equilibrium times of <0.5 seconds per stage. Therefore, automated micro- and milli-reactor/contactor systems can be used to reduce footprint and increase the efficiency of plutonium separation processes.

Background and Research Objectives

All industrially significant actinides have hazards associated with their storage and handling. All are radioactive, and fissile actinide isotopes require mass and volume limits to prevent a criticality accident. Typical separation operations use hazardous chemicals, such as concentrated nitric or hydrochloric acid and various organic extractants for separation and purification. To protect workers from the radiation and direct exposure to hazardous materials, processing is done in remote-handling facilities or within engineered barriers like gloveboxes. Such facilities are expensive to build, operate and maintain. Actinides also have high waste-handling, storage and disposal costs due to their radiotoxicity. These processing constraints make actinide processing operations an excellent candidate for microfluidics. Microfluidic systems and microreactors have high mass and heat transfer rates, which reduce stage volume and increase efficiency. Given the exacting requirements for processing actinides, these features are very attractive for reducing footprint and associated handling and disposal costs.

Also, actinide separations continue to be important to the US for national security and energy programs. In this work, mass transfer rates for several design concepts were verified with experimental testing, supported by multiscale modeling including continuum and Lattice-Boltzmann. Fabrication and testing of the equipment under various operating conditions occurred in parallel with refinement of the chemical systems chosen for study. The microfluidic devices were tested with plutonium solutions and parameters were developed for simple mixing, separation and reduction-oxidation methods. This work resulted in the design and fabrication of more complex devices based on the selected chemical system, Aliquat-336 in hydrochloric acid, and scale-up of the preliminary contacting equipment. Hydrochloric acid was selected as the aqueous system for its relevance to pyrochemical residue treatment, and to reduce the complexity of stripping plutonium from the organic phase for purification and waste management.

The goals were the following:

Objective 1: demonstrate that a microreactor/contactor-based liquid-liquid extraction system can provide the necessary mass transfer rates for a compact and efficient separation process;

Objective 2: develop the engineering approach to demonstrate a workable separation apparatus;

Objective 3: demonstrate that the precise control achievable in a microreactor can improve efficiency, selectivity, and control in nuclear material processing.

Scientific Approach and Accomplishments

Enhanced mass transfer is important to improving the efficiency of actinide separation processes. It enables the contacting stage volume and flows to be minimized, reducing the associated processing costs. Therefore, the approach focused on developing milli- and microfluidic contactors of various dimensions and phase contacting methods, then characterizing the mass transfer rate and operation characteristics of each. Mass transfer and operating data was used to develop models for future optimization. Specifically, three main areas of research were pursued.

1. Developing experimental and analytical protocols for characterizing the mass transfer performance of various contactor configurations.

2. Designing and developing fabrication methods for contactor configurations. Two approaches were selected for development. In one approach, contactors were tested that used a micro-mixing "tee"-joint which produced interspersed droplets (slugs) of alternating organic and aqueous solutions in a narrow channel, and then separated the two immiscible phases. In the second approach, contactors were tested that used different configurations of membranes at the interface between two serpentine microchannels in which the organic and aqueous streams flowed countercurrent to each other. Various membrane combinations (thickness, porosity and surface wetting) were tested, and very thin graphene membranes with precise porosity characteristics were developed.

3. Modeling the mass transfer of the various contacting approaches using both continuum and Lattice-Boltzmann methods.

In developing microfluidic contactors for actinide separations, there are several important aspects that impact the design, fabrication and operation. For example, surface roughness and wettability are very important to controlling the droplet generation, separation and flow in membrane contactors. Depending on the direction of mass transfer, a thin film adhering to the surface in a slug-flow contactor can improve the mass transfer in the device. Also, the wetting characteristics of the construction materials influence how well the phases are separated in a slug-flow device, and how well they absorb into the membranes for the membrane contactors.

For modeling, resolving the interface and ensuring conservation of mass is difficult and can prove troublesome to obtaining accurate models. To overcome this problem, a moving-mesh method was used. The moving-mesh method can be effectively applied to model hydrodynamics and mass transfer behavior in complex systems. System variables such as contact angle, which is a measure of wettability, can be examined to predict changes in conversion rates. While model sensitivities may be explored in 2-D, a full 3-D model is needed to capture conversion rates that were observed in the experiment, due to the additional flow pattern induced by the wall.

Also, due to the solvent ability of the organics, it is very important to select chemically-resistant polymer materials for the contactors, to ensure that contaminants and leaks do not affect the operations. At these very small volumes, trace contaminants can influence the operation by altering the wettability or by stripping or plugging the channels.

Overall, the project met the objectives with the various accomplishments outlined below.

Objective 1

- Successfully measured mass transfer coefficients for uranium and plutonium in a single stage with both tributyl phosphate (TBP) and Aliquat-336 (A336) in a hydrochloric acid system, and in multiple stages with A336 in a hydrochloric acid system.
- Successfully measured mass transfer rates for uranium and plutonium in both TBP and A336.

Objective 2

- Fabricated and successfully tested serpentine membrane countercurrent contactors with 60-cm path lengths and ten contact stages.
- Fabricated and successfully tested slug-flow contactors with phase-separators incorporated into the contactor.
- Fabricated graphene membranes on a glass substrate with a microchannel
- Implemented a successful moving mesh 2-D model of micro-channel membrane counter-current flow mass transfer with reaction.
- Initiated Lattice-Boltzmann models and incorporated mass transfer effects at the phase boundary.

Objective 3

- Successfully demonstrated microfluidics for glovebox operations with plutonium.

Patent disclosures

- 13-00193 - Using microchannels to simulate countercurrent contacting columns
- 14-00165 - Laminated thermoplastic film microfluidic device

Impact on National Missions

The U.S. has an ongoing need for efficient actinide separation methods, specifically, developing the ability to deploy advanced separation methods for weapons materials purification, advanced nuclear systems, nuclear forensics, and environmental management. It expands US capabilities in detection, measurement, and analysis of nuclear and radiological materials. In addition, microfluidics provide an ability to conduct small-scale research and development with scarce and unique materials. Multi-stage systems have been developed and demonstrated based on a new understanding of the mass and heat transfer effects at small length and time scales, enabling a robust capability to carry out difficult separations. This results in a processing capability that can meet new programmatic needs in a variety of national security, research, space and nonproliferation programs.

Publications

Boland, K. S., R. M. Chamberlin, G. S. Goff, and S. L. Yarbro. Physical properties of Aliquat 336 loaded with metal (Fe, U) chlorides. Presented at 39th Annual Actinide Separations Conference. (Salt Lake City, UT, 18-21 May, 2015).

Chamberlin, R. M., B. T. Manard, K. J. Spencer, R. E. Keller, D. R. Porterfield, D. L. Decker, and S. L. Yarbro. (U) Plutonium separations by liquid-liquid extraction in microfluidic cells. 2015. Los Alamos Controlled Publication report in preparation.

Chamberlin, R. M., D. L. Decker, D. R. Porterfield, P. T. Martinez, and S. L. Yarbro. Kinetic factors in Aliquat-336 extraction of Pu(IV) from hydrochloric acid solution. 2015. Manuscript in preparation.

Chamberlin, R. M., K. J. Spencer, D. R. Porterfield, R. C. Keller, and S. L. Yarbro. (U) New solvent system for a plutonium separation. 2015. Los Alamos Controlled Publication report in preparation.

Chamberlin, R. M., S. L. Yarbro, A. P. Borrego, D. L. Decker, C. C. Finstad, J. Gao, P. Martinez, Q. McCulloch, D. R. Porterfield, J. Rowley, K. R. Weisbrod, and N. Xu. Microfluidic and micro-engineered separations for actinide processing and analysis. Presented at 38th Actinide Separations Conference. (Albuquerque NM, 20-22 May, 2014).

Chamberlin, R. M., S. L. Yarbro, N. Xu, D. L. Decker, and P. T. Martinez. Microfluidic separations for actinide processing and analysis . Invited presentation at 249th American Chemical Society National Meeting. (Denver, CO, 22-26 March, 2015).

Chamberlin, R. M., S. L. Yarbro, N. Xu, K. J. Spencer, and A. Castro. (U) Using microreactors for efficient plutonium separations: FY13 annual progress report. 2014. Report LA-CP-14-00131.

Dervishi, E.. Graphene as a potential membrane material. 2015. Los Alamos National Laboratory unclassified release (in preparation).

McCulloch, Q., S. L. Yarbro, R. M. Chamberlin, K. R. Weisbrod, and E. Dervishi. Fabrication and testing of countercurrent and quasi-countercurrent microfluidic systems. 2014. Report LA-UR-14-28228.

Roberts, R. M.. FY14 report: Lattice Boltzmann modeling of microreactor systems. 2014. Report LA-UR-14-28228.

Weisbrod, K. R., R. M. Roberts, R. M. Chamberlin, and S. L. Yarbro. Simulation of mass transfer in a microfluidic experiment using the moving mesh method. 2014. In COMSOL User's Conference. (Boston, MA, 8-10 October 2014). , p. 1. Boston : COMSOL.

Xu, N., A. Castro, J. Gao, B. Manard, L. Meyers, R. M. Chamberlin, and L. Tandon. Chemical separation and measurement tool box for bulk SNM analysis. Presented at DHS-DNDO-NTNFC Annual Review. (Chicago IL, 4-7 August 2014).

Maximizing Flux through Engineered Metabolic Pathways

Clifford J. Unkefer
20130091DR

Abstract

The long-term goal of synthetic biology is to engineer microorganisms to produce high-value products for biotechnological applications such as, the carbon neutral production of biofuels or chemicals. To achieve this goal, it will be necessary to engineer functional multi step metabolic pathways in organisms, which will require a new approach to independently regulate the expression of each of the enzymes in the pathway in order to optimize the flux through the pathway. Until recently, engineering strategies for altering gene expression have focused on transcription control using strong inducible promoters. We have developed a new approach for translational control of gene expression involving a class of modular synthetic riboregulator that has the potential to finely tune protein expression and independently control the concentration of each enzyme in an engineered metabolic pathway. This development is important because the most straightforward approach to altering the flux through a particular metabolic step is to increase or decrease the concentration of the enzyme. Our design includes a cis-repressor at the 5' end of the mRNA that suppresses translation by forming a stem-loop helix occluding the ribosomal binding sequence. A trans-expressed activating-RNA frees the ribosomal-binding sequence, turning on translation. Using Watson-Crick base-pairing stability, we designed a cis-repressor that completely shuts off translation of the target gene and a trans-activator that restores translation demonstrating it is possible to achieve translational control of gene expression over a wide dynamic range. We have also found that a targeting sequence can be modified to develop riboregulators that can independently regulate translation of many genes. Finally we demonstrated that by subtly altering the sequence of the trans-activator, it is possible to alter the ratio of the repressed and activated states and achieve intermediate translational control. These riboregulators will find broad application in achieving DOE's goal of carbon neutral renewable production of transportation fuels.

Background and Research Objectives

Maximizing metabolic flux requires finely tuned regulation of individual steps. The long-term goal of synthetic biology is to engineer microorganisms to produce high-value products for medical, pharmaceutical, and biotechnological applications. To achieve this goal, it will be necessary to engineer functional metabolic pathways in organisms. Maximizing flux through metabolic pathways is not simply a matter of over expressing all of the enzymes in the pathway. In living systems, control of function occurs at the cellular (transcription to RNA and translation to protein) and molecular levels (allostery – feedback inhibition or activation). These controls are implemented by regulating the concentrations of the species taking part in biochemical reactions, including the enzymes (e), substrates (s), products (p) and regulatory molecules (r), such that the rate of an enzymatic reaction can be generally expressed as v = v(ce, cs, cp, cr). De Novo design of optimized pathways is not possible because even in model organisms, the cellular concentrations and kinetic coefficients necessary to design a regulated pathway are not known. In addition, cellular metabolism is a complex network of branched and interconnecting pathways. Metabolites may serve several functions. For example, many intermediates in the central metabolism that many organisms use to generate energy also serve as substrates for the biosynthesis of essential cellular components, e.g., amino acids (protein synthesis) and nucleotides (DNA synthesis). Because of this complex metabolic network, engineering an organism to direct a particular metabolite to produce a desired product could have an unanticipated deleterious effect on growth, rendering the de novo design of regulated metabolic pathways extremely complex.

Riboregulators can be used to finely tune gene expression. Because the output of a metabolic reaction is directly proportional to the enzyme concentration (d[cp]/dt ~ kcat[ce]), by far the most straightforward approach to altering the flux through a particular metabolic step

is to increase or decrease the concentration of the enzyme catalyst. Current strategies for engineering gene expression are limited to increasing the expression of a particular gene by placing it under the control of a stronger transcriptional promoter or using one of several strategies to knock down or knock out a wasteful gene. Our overall goal was to develop the molecular biology tools necessary to finely tune the expression of individual enzymes in an engineered metabolic pathway. Specifically our goals were 1) to develop a family of riboregulators that can be used for translational regulation of the expression of each of the enzymes in a complete metabolic pathway and 2) demonstrate a strategy for the simultaneous directed evolution of riboregulators to optimize the expression of the enzymes to maximize flux through a metabolic pathway.

Scientific Approach and Accomplishments

Modular design of riboregulators. In our riboregulator system (Fig. 1), both the cis-repressor (crRNA) and the trans-activator RNAs (taRNA) have modular structures composed of targeting (black) and regulatory (red) sequences. The crRNA is within the 5' untranslated region (UTR) of the mRNA and naturally folds to a structure that sequesters the ribosomal binding sequence (RBS), preventing translation of the downstream gene (Fig. 1a). The taRNA is transcribed in trans and the binding and subsequent structural transition between these two regulatory RNA elements dictates whether or not the transcribed mRNA will be translated into the protein product (Fig. 1b). The targeting sequences are complementary and target a particular taRNA to a specific crRNA (Fig 1c). The stability of the taRNA regulatory element is dictated by the sequence in its variable region. The all ON version of the taRNA has little potential to form secondary structures in its regulatory helix as depicted in Fig. 1d. Depending on the relative stability of the structural elements in the regulatory regions of the crRNA and the taRNA, the complex can rearrange to form the translation-activating extended duplex, freeing the RBS to turn on translation (Fig. 1d). Since the extended duplex between the elements has a much greater potential stability, expression tuning is accomplished by altering the availability of the sequence within the taRNA. Availability is determined by weakening the intramolecular base-pairing of the taRNA helix and adjusting the intermolecular interactions in a common spacer region (Fig.1d). By tuning the relative stability between the regulatory helices of the crRNA and the taRNA and that of the extended crRNA/taRNA duplex, it is possible to alter the ratio between repressed (Fig. 1c) and activated (Fig. 1d) states and to achieve intermediate translational control (Fig.1e).

In our systems, translation of both the crRNA:gene fusion and the taRNA are driven independently by separate copies of the same strong constitutive promoter. To achieve our overall goal of a wide dynamic range of riboregulator control, it was necessary to perform the following tasks: 1) create a modular system with the capacity to regulate multiple genes independently and consistently; 2) design crRNA regulatory sequences that sequester the RBS and completely block translation (crRNA OFF); 3) identify taRNA regulatory elements that free the RBS from the crRNA OFF state and turn back on translation to the fullest extent possible; 4) demonstrate that we can design orthogonal targeting sequences that can be used to direct a taRNA to its specific partner crRNA; 5) demonstrate intermediate levels of translation by altering the regulatory sequence in the taRNA.

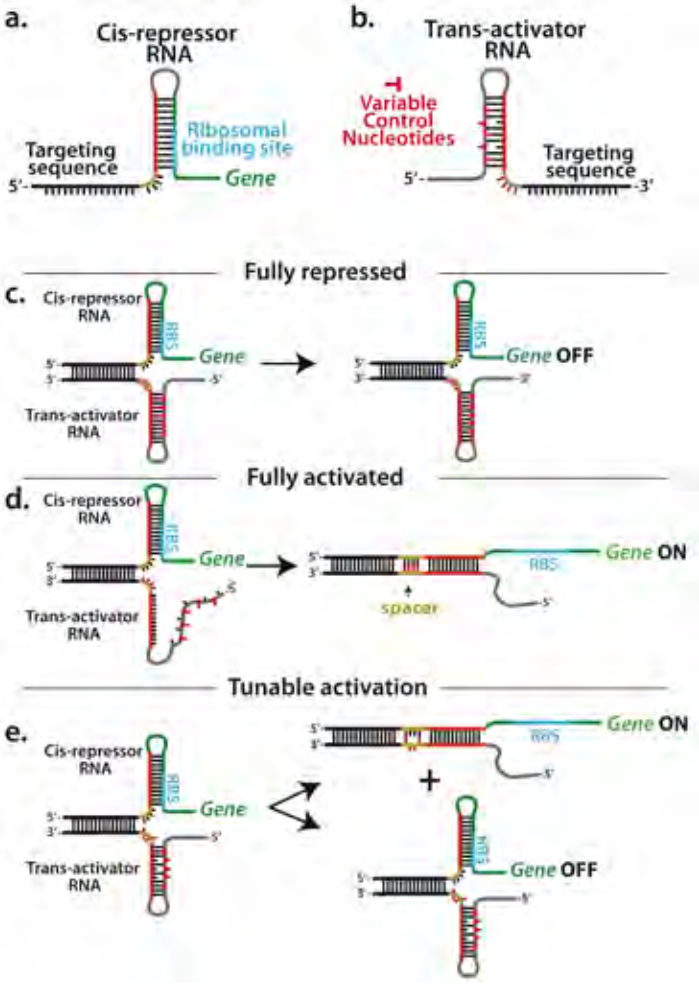

Figure 1. (a) The crRNA has a modular design that includes a targeting sequence (black) and a regulatory sequence (red) that forms a stem-loop structure at the 5'-end of the gene, sequestering the Ribosomal Binding Sequence (RBS) and preventing translation of the mRNA; (b) the taRNA is transcribed in trans and contains modules that are complementary to the targeting and variable regulatory sequences that produce stem-loop structures of differential stability. The all ON version of the taRNA has little potential to form secondary structures as depicted in (d). (c) The targeting sequence binding event results in the formation of

a taRNA:crRNA/mRNA complex. In this complex, translation of the target gene is either repressed or (d) the complex rearranges to free the RBS and activate translation. (e) It is possible to tune the relative stability of the secondary structural elements in the crRNA and taRNA to obtain intermediate levels of translation.

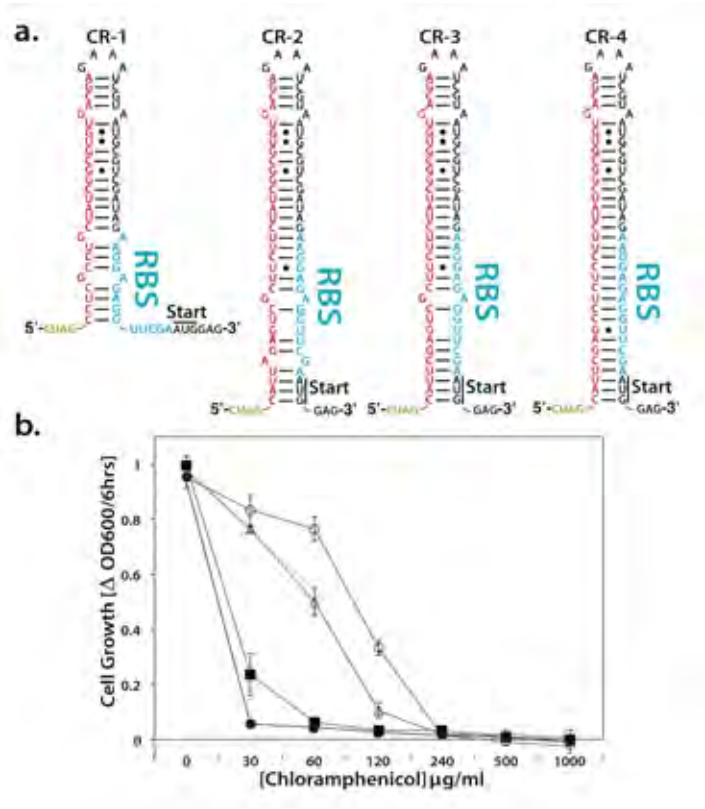

Figure 2. (a) crRNA sequences that occlude the RBS with stem-loop structures of increasing stability. Potential Watson-Crick (−) and wobble base pairs are indicated. (b) Plot of the growth rate of transformants carrying a plasmid encoding a crRNA/ (chloramphenicol resistance) fusion. In every case, translation is driven constitutively by the T7A1 promoter/T7 terminator pair and translation is controlled by CR-1 (O), CR-2 (Δ), CR-3 (), or CR-4.

The cis-Repressor. We initially optimized the cis-repressor element in the absence of a taRNA to determine the sequence and structure of the cis-repressor element required for complete repression of mRNA translation. We transformed E. coli with a plasmid encoding the chloramphenicol antibiotic resistance gene under control CR-1 (Fig 2a) and measured the bacterial growth of the transformants using the antibiotic chloramphenicol as a sensitive, titratable marker for translational leakage (Fig. 2b). Under our experimental conditions, we found that the growth of wild type E. coli was completely inhibited in a culture medium containing 30 µg/mL chloramphenicol. Because our initial sequence, CR-1, showed a significant growth phenotype to chloramphenicol concentrations of 120 µg/ml, we developed cis regulatory elements with the helix extended by eight base pairs (CR-2, Fig. 2a) and then further increased its stability by systematically removing mismatched bulges (CR-3 and CR-4). Based on Watson-Crick base-pairing stabilities, we estimated the thermodynamic stability of each of these stem loop structures as follows: CR-1, -34.3 kcal/mol; CR-2, -40.0 kcal/mol; CR-3, -45.9 kcal/mol; CR-4, -57.5 kcal/mol. As expected, the translation was dependent on the thermodynamic stability of the RBS-occluding helix. Complete occlusion of RBS and minimal leakage of translation were possible only when the cis-repressor was designed to form a stem loop that had a nearly perfect double helical structure (CR-4, Fig. 2b). Significantly, subtle changes in the sequence near the RBS, with single base pair mismatches, resulted in increased translation of the cat gene (as seen for CR-2 and CR-3), indicating that even minimal structural breathing around the RBS allowed ribosome access and translation of cat and imparted chloramphenicol resistance.

Riboregulated translation. We chose CR-4 as the regulatory element for further experiments as this sequence/structure represented the maximal OFF riboregulated state (crRNA OFF) and provided minimal leakage of translation and protein expression. Our next goal was to identify taRNA regulatory elements that free the RBS from the crRNA OFF and turn back on the translation to the fullest extent possible. The taRNA contained a targeting sequence (TS1) that could recognize a specific cis-repressor RNA through Watson-Crick base pairing and a regulatory element that could hybridize with the crRNA regulatory element in a fashion that could expose the RBS, leading to translation (Fig. 1). To test the taRNA, we designed the four constructs diagrammed in Figure 3a. In the Maximum ON construct, expression of cat is driven by the pT7A1 with no translational control. The transcription of the crRNA:cat fusion construct is also driven by pT7A1; however, as described above, translation of cat is fully attenuated by a crRNA with the CR-4 regulatory element. In the Regulated ON construct, transcription of the crRNA:cat fusion and the taRNA are driven independently by identical pT7A1 promoters; taRNA is designed to hybridize with the crRNA in a fashion to free the RBS and modulate the translation of cat (Fig. 1c). The sequence of the taRNA-ON variant provides for minimal structure, facilitating the formation of an extended duplex with the crRNA. In addition, the spacer is fully complementary to the crRNA, facilitating taRNA strand invasion and RBS release (Fig. 1c). In the Regulated OFF construct, the stability of the secondary structure of the taRNA and lack of complementary spacer nucleotides prevents rearrangement of the regulatory complex (Fig. 1b), leaving the RBS occluded and blocking translation.

Cells transformed with the Regulated ON construct grew at chloramphenicol concentrations up to 750 µg/mL, indicating that regulated ON taRNA restored translation to a very

significant extent (Fig 3b). The chloramphenicol-resistant phenotype caused by expression of the Regulated ON taRNA, demonstrated that the taRNA is capable of freeing the RBS on the cis-repressed mRNA, resulting in translation of cat. By contrast, expression of the Regulated OFF taRNA did not activate translation and its phenotype was essentially identical to the Maximum OFF state, indicating that the structure within the taRNA and mismatches in the four nucleotide spacers effectively prevented the formation of a translation-activating extended duplex as diagrammed in Figure 1d.

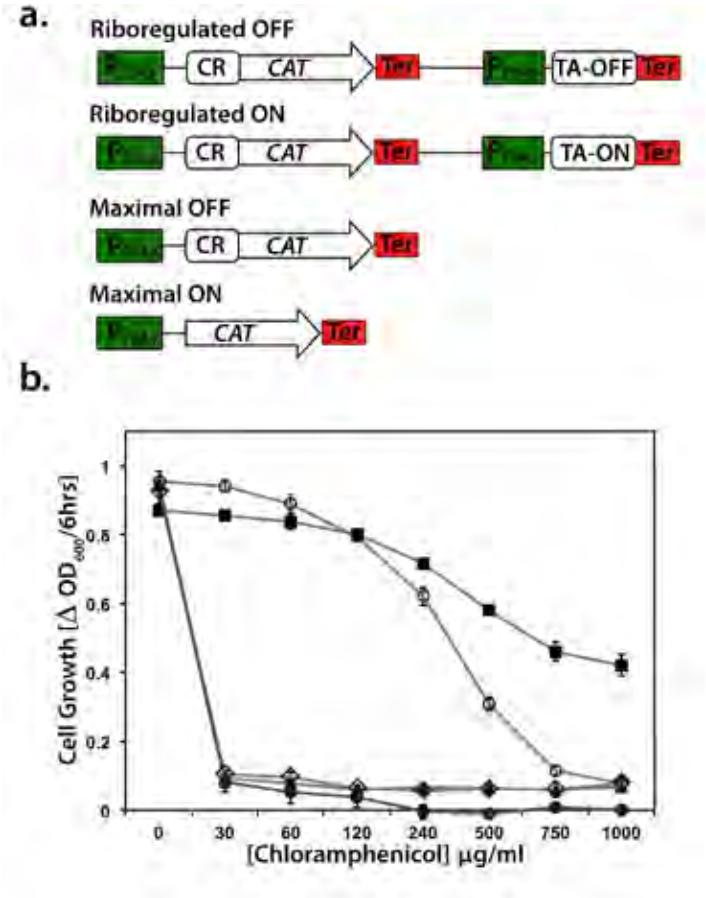

Figure 3. (a) Schematic of the plasmid encoded expression cassettes used to test the efficacy of the riboregulators. In the Maximum ON construct, expression of is driven by the pT7A1 with no translational control. The Maximum OFF construct transcription of the crRNA: fusion is driven by pT7A1; translation of is attenuated by the crRNA. In the Regulated ON construct, transcription of the taRNA is driven independently by pT7A1; taRNA modulates the translation of . In the Regulated OFF construct the stability of the secondary structure of the taRNA prevents rearrangement of the regulatory complex (see); translation remains blocked. (b) Plot of growth rate of transformants as a function of chloramphenicol concentration. The were transformed with the various expression vectors and are plotted as follows: Maximum ON (), Maximum OFF (), Regulated ON (O), Regulated OFF () and wild-type.

Summary of riboregulator properties. To optimize engineered metabolic pathways, it is necessary to tune the level of expression of each enzyme catalyst independently in the pathway. We have shown that riboregulators can achieve translational control of gene expression over a wide dynamic range. In our system, the crRNA is encoded in the 5'-untranslated region of the mRNA and folds to block the ribosome-binding site. We have demonstrated a crRNA regulatory sequence that can completely shut off translation (CR-4, Fig. 2). Expression of a trans-activator RNA (taRNA) initiates a targeted binding event, followed by structural rearrangements between crRNA and taRNA, which dictates whether or not the transcribed mRNA will be translated into the protein product. We have designed a regulatory sequence in the taRNA that can interact with the CR-4 regulatory sequence to turn the translation back on to a high level. In our riboregulator system (Fig. 1) both the cis-repressor and trans-activator RNAs are composed of targeting and regulatory sequences. The targeting sequences on a crRNA/taRNA pair are complementary and formation of the targeting helix is required for taRNA to modulate translation of a crRNA-regulated gene. While we have tested initially only two targeting sequences, our design with 34 nucleotides, in principle, provides ample sequence diversity to design multiple orthogonal targeting sequences. In our modular design, only the targeting sequence is changed to develop riboregulators that can independently regulate translation of many genes. By subtly altering the taRNA's regulatory helix and spacer, we can alter the equilibrium between repressed and activated states and achieve intermediate translational control. We introduced sequence diversity at only five positions in the regulatory region of the taRNA and were able to identify taRNAs that produced intermediate levels of cat expression. We have demonstrated the riboregulators work when engineered cis-RNA regulated genes are encoded in the bacterial chromosome and the taRNA is plasmid encoded. More recently we used have demonstrated the riboregulation of translation of chromosome encoded antibiotic resistance genes in the photosynthetic bacterium Synechococcus elongatus.

Impact on National Missions

The riboregulators described in this report will be valuable for optimizing metabolic flux through engineered metabolic pathways using directed evolution approaches. We envision chromosomal genes encoding each enzyme in the pathway to be placed under independent transcription control using the same strong promoter/terminator pair for each gene. These genes will be translationally repressed by a crRNA consisting of a unique targeting sequence and the Maximum OFF regulatory helix CR-4. Targeting sequences will specifically pair a single crRNA

controlled gene with its taRNA partner. The pathway taRNAs will be plasmid encoded making it straightforward to introduce diversity and generate a library of taRNAs that cover the range of translational activation for each gene. Transformants would include all combinations of TA regulatory sequences, creating a cell population expected to have a range of metabolic fluxes. It will be necessary to develop high-throughput screening or selection methods to identify cells in this population with optimal metabolic flux. Riboregulators will provide the metabolic engineer a new tool to tune the level of expression of each enzyme independently in a pathway. The synthetic biology capability developed in this project and more specifically the riboregulators developed here will play an essential role in engineering organisms optimized for biofuel production and for carbon neutral production of commodity chemical feedstocks that drive U.S. Industry. Developing these synthetic biology approaches will be essential to achieving the Department of Energy's goals of replacing petrochemicals with renewable biological feedstocks.

Publications

Fox, D. T.. Maximization of Isoprenoid Production and Extraction in a Model Organism. Presented at Algae Biomass Summit. (Orlando, FL, 1-3 Oct. 2013).

Fox, D. T.. Biocatalytic Production of Commodity Chemicals. Presented at American Society of Microbiology. (Boston, MA, 17-20 May 2014).

Fox, D. T., M. Krishnamurthy, T. Kern, M. K. DeAguero, S. P. Hennelly, T. Dale, S. N. Twary, S. R. Starkenburg, R. Marti-Arbona, K. Sanbonmatsu, and C. J. Unkefer. Riboregulation of gene expression in Synechococcus elongatus PCC7942. Presented at Pacificahem 2015. (Honolulu HI, 15-20 Dec 2015).

Gonzalez, J. M., R. Marti-Arbona, and C. J. Unkefer. Crystal structure of phosphoenolpyruvate carboxylase from Methylobacterium extorquens. Presented at American Crystallographic Association Annual Meeting. (Albuquerque, NM, 24-28 May 2014).

Gonzalez, J. M., R. Marti-Arbona, and C. J. Unkefer. Crystal structure of Enolase from Synechococcus elongatus. 2014. Protein Data Bank.

Gonzalez, J. M., R. Marti-Arbona, and C. J. Unkefer. Crystal structure of Malyl-CoA lyase from Methylobacterium extorquens. 2015. Protein Data Bank.

Gonzalez, J. M., R. Marti-Arbona, and C. J. Unkefer. Crystal structure of Malyl-CoA lyase from Methylobacterium extorquens. 2015. Protein Data Bank.

Gonzalez, J. M., R. Marti-Arbona, and C. J. Unkefer. Crystal structure of Methylobacterium extorquens malate dehydrogenase complexed with oxaloacetate and adenosine-5-diphosphoribose. 2015. Protein Data Bank.

Hall, R. S., R. Martí-Arbona, S. P. Hennelly, T. S. Maity, F. Mu, J. M. Dunbar, C. J. Unkefer, and P. J. Unkefer. In-vitro Characterization of an L-Kynurenine-Responsive Transcription Regulator of the Oxidative Tryptophan Degradation Pathway in Burkholderia xenovorans. 2013. Journal of Molecular Biology Research. 3 (1): 55.

Hayes, R. L., J. K. Noel, A. Mandic, P. C. Whitford, K. Y. Sanbonmatsu, U. Mohanty, and J. N. Onuchic. Generalized Manning Condensation Model Captures the RNA Ion Atmosphere. 2015. Physical Review Letters. 114: 258015.

Hayes, R. L., J. K. Noel, U. Mohanty, P. C. Whitford, S. P. Hennelly, and K. Y. Sanbonmatsu. Molecular simulation captures free energy stabilization of RNA by Mg2+. 2014. Biophysical Journal. 106 (7): 1508.

Hennelly, S. P., I. V. Novikova, and K. Y. Sanbonmatsu. The expression platform and the aptamer: cooperativity between Mg2+ and ligand in the SAM-I riboswitch. 2013. NUCLEIC ACIDS RESEARCH. 41 (3): 1922.

Hennelly, S. P., I. V. Novikova, and K. Y. Sanbonmatsu. The expression platform and the aptamer: cooperativity between Mg2+ and ligand in the SAM-I riboswitch. 2013. Nucleic Acids Research. 41 (3): 1922.

Jarchow-Choy, S. K., A. T. Koppisch, and D. T. Fox. Synthetic Routes to Methylerythritol Phosphate Pathway Intermediates and Downstream Isoprenoids. 2014. CURRENT ORGANIC CHEMISTRY. 18 (8): 1050.

Jarchow-Choy, S., D. Fox, E. Schmidt, A. Koppisch, R. Marti-Arbona, and C. Unkefer. Monitoring the distribution of isoprenoid products from the MEP pathway in algae and cyanobacteria. 2013. ABSTRACTS OF PAPERS OF THE AMERICAN CHEMICAL SOCIETY. 245: -.

Jha, R. K., T. L. Kern, D. T. Fox, and C. E. M. Strauss. Engineering an Acinetobacter regulon for biosensing and high-throughput enzyme screening in E-coli via flow cytometry. 2014. NUCLEIC ACIDS RESEARCH. 42 (12): 8150.

Kirmizialtin, S., S. P. Hennelly, A. Schug, J. N. Onuchic, and K. Y. Sanbonmatsu. Integrating Molecular Dynamics Simulations with Chemical Probing Experiments Using SHAPE-FIT. 2014. Methods in Enzymology. 553: 215.

Krishnamurthy, M., S. P. Hennelly , K. Y. Sanbonmatsu , and C J. Unkefer . Riboregulators as tunable gene switches for post-transcriptional control of gene expression. 2015. In 249th ACS National Meeting. (Denver, CO, March 22-26). , p. BIOL. Abstracts of Papers 249 ACS National Meeting: ACS.

Krishnamurthy, M., S. P. Hennelly, K. Y. Sanbonmatsu, and C. J. Unkefer. Riboregulators as gene switches for post-transcriptional regulation of gene expression. Presented at Precision Genome Engineering and Synthetic Biology, Keystone Symposia Conference,. (Big Sky, Monanta, 11-16 Jan 2014).

Krishnamurthy, M., S. P. Hennelly, R. Marti-Arbona, J. M. Gonzalez, K. Y. Sanbonmatsu, and C. J. Unkefer. Progress toward tunable riboregulator switches for post-transcriptional control of gene expression and the development of a synthetic pathway for acetyl-CoA biosynthesis . Invited presentation at Asia-Oceania Algae Innovation Summit. (Deajeon, South Korea, 11-17 Nov 2014).

Krishnamurthy, M., S. P. Hennelly, T. Dale, S. R. Starkenburg, R. Marti-Arbona, S. N. Twary, K. Y. Sanbonmatsu, D. T. Fox, and C. J. Unkefer. Tunable riboregulator switches for post-transcriptional control of gene expression. 2015. ACS Synthetic Biology. : 1.

Marti-Arbona, R.. New Advances Toward the Understanding and Manipulation of Metabolic Regulation. Invited presentation at Department of Chemistry, Rice University. (Houston, Texas, 13 April 2014).

Marti-Arbona, R.. New Advances Toward the Understanding and Manipulation of Metabolic Regulation. Invited presentation at University of Puerto Rico, Rio Piedras Campus. (San Juan, Puerto Rico, 30 Oct 2015).

Marti-Arbona, R., F. Mu, F. Nowak-Lovato, M. S. Wren, P. J. Unkefer, and C. J. Unkefer. • "Automated Genomic Context Analysis and Experimental Validation Platform for Discovery of Prokaryote Transcriptional Regulator Functions" . 2014. BMC Genomics. 15: 1.

Martí-Arbona, R., T. S. Maity, J. M. Dunbar, C. J. Unkefer, and P. J. Unkefer. Discovery of a Choline-Responsive Transcriptional Regulator in Burkholderia xenovorans. 2013. Journal of Molecular Biology Research . 3 (1): 91.

Nguyen, T. T., R. Martí-Arbona, R. S. Hall, T. Maity, Y. E. Valdez, J. M. Dunbar, C. J. Unkefer, and P. J. Unkefer. Identification and In-vivo Characterization of a Novel OhrR Transcriptional Regulator in Burkholderia xenovorans LB400. 2013. Journal of Molecular Biology Research. 3 (1): 37.

Novikova, I. V., A. Dharap, S. P. Hennelly, and K. Y. Sanbonmatsu. Shotgun secondary structure determination of long non-coding RNAs. 2013. Methods. 63: 170.

Novikova, I. V., S. P. Hennelly, and K. Y. Sanbonmatsu. Sizing up long non-coding RNAs: Do lncRNAs have secondary and tertiary structure? . 2012. BioArchitecture. 2 (6): 189.

Novikova, I. V., S. P. Hennelly, and K. Y. Sanbonmatsu. . Experimentally determined secondary structures of cancer-related long non-coding RNAs. 013. In 245th ACS National Meeting & Exposition. (New Orleans, 7-11 April, 2013). , p. PHYS. Abstracts of Papers: ACS.

Novikova, I. V., S. P. Hennelly, and K. Y. Sanbonmatsu. Tackling Structures of Long Noncoding RNAs. 2013. INTERNATIONAL JOURNAL OF MOLECULAR SCIENCES. 14 (12): 23672.

Novikova, I. V., S. P. Hennely, C. S. Tung, and K. Y. Sanbonmatsu. Rise of the RNA machines: Exploring the structure of long non-coding RNAs. 2013. Journal of Molecular Biology. 425: 3731.

Sanbonmatsu, K. Y.. Rise of the RNA Machines: Long Non-Coding RNAs. Invited presentation at 10th Horizons in Molecular Biology Conference International . (Max Planck Institute, Gottingen, Germany, Sept 9-12 2013).

Sanbonmatsu, K. Y.. Integrating simulations and experiments of the SAM-I riboswitch. Invited presentation at RNA Dynamics. (Telluride, Colorado, 22-26 July, 2013).

Sanbonmatsu, K. Y.. Large-scale simulations of biomolecular machines. Invited presentation at Biosupercomputing Symposium. (Tokyo Japan, December 2012).

Sanbonmatsu, K. Y.. Understanding the atomistic mechanism of magnesium effects of RNA dynamics. Invited presentation at Mini-symposium on Modeling, Simulation and Function of Biomolecular Assemblies. (Tokyo University, Tokyo Japan, November 2012).

Sanbonmatsu, K. Y.. Computational & Experimental Studies: Ribosomes, Riboswitches & Long non-coding RNAs. Invited presentation at Fourth Annual Summer Symposium on Cellular Dynamics of Macromolecular Complexes. (Montreal, Canada, 3-8 June 2014).

Sanbonmatsu, K. Y.. Structural Studies of Intact LncRNAs in Plants and Mammals. Invited presentation at Keystone Symposium: Long non-coding RNAs: Marching towards Mechanism. (Santa Fe, NM, 2-6 March 2014).

Sanbonmatsu, K. Y.. Dynamics of riboswitches: Molecular simulation. 2014. Biochimica et Biophysica Acta: Gene Regulatory Mechanisms. 1839: 1046.

Sanbonmatsu, K. Y.. Dynamics of riboswitches. Invited presentation at RNA Society. (Madison, WI, 26-31 May 2015).

Sanbonmatsu, K. Y.. Structural architecture of lncRNAs in plants and mammals. Invited presentation at The Royal Society: Long non-coding RNAs: evolution of new epigenetic and post-transcriptional functions. (Kavli Royal Society Centre, Buckinghamshire, 28-29 Sept 2015).

Sanbonmatsu, K. Y.. Integrating Molecular Dynamics Simulations with Chemical Probing Experiments. Invited presentation at Telluride Science Research Center: RNA Dynamics. (Telluride, CO, 20-24 July 2015).

Sanbonmatsu, K. Y.. Dynamics of riboswitches: Molecular simulations. Invited presentation at Wellcome Trust Conference of Computational RNA Biology. (Cambridge UK, 11-13 Nov 2014).

Twary, S. N., S. R. Starkenburg, C. J. Unkefer, and M. A. Alvarez. Comparative transcriptomics across algal species after induced lipid accumulation. Presented at International Conference on Algal Biomass, Biofuels and Bioproducts. (Santa Fe, NM, 15-18 June 2014).

Unkefer, C. J.. Development of a synthetic pathway for acetyl-CoA biosynthesis. Invited presentation at Special Microalgae Workshop at the Korea Advanced Institute of Science and Technology. (Deajeon, South Korea, 21 Nov 2014).

Unkefer, C. J., S. N. Twary, S. R. Starkenburg, M. Teshima, M. A. Alvarez, and P. J. Unkefer. Characterization of Lipid Metabolism in Nannochloropsis salina 1776: Development of a Systems Biology Pipeline and Transcriptome Analysis. Invited presentation at Asia-Oceania Algae Innovation Summit. (Deajeon, South Korea, 17-20 Nov 2014).

Deciphering Nature's Chemical Toolbox: Decoding the Logic of Biosynthetic Assembly Lines

Alexander Koglin
20140624ECR

Introduction

The overarching goal of this project is to support the biosecurity mission of LANL in defeating biothreats due to drug-resistant bacteria and viruses and confront the accelerating development of antibiotic resistance by identifying novel bioactive compounds. This project focuses on the identification of new biosynthetic clusters that produce novel natural products with new chemical properties (chemotypes) to create a compound database for drug development and to decipher the logic of natural product biosynthesis. Those compounds have the potential to be developed into highly effective antibacterial treatments while being immune to current resistance mechanisms, since pathogenic bacterial strains have not been exposed to those compounds.

Genetic and enzymatic studies provide insight of isolated enzymatic functions in natural product biosynthesis, but have not led to new strategies to discover novel natural products biosynthesized by complex enzyme assemblies. Bioinformatics and structural studies are providing insight of three-dimensional folding and selective protein complex formation processes of key enzymes essential for the formation of biosynthetic clusters that produce medically relevant compounds. The unique and not-yet understood spontaneous self-assembly of these enzymes into clusters defines the very selective biosynthesis of all secondary metabolites of which only an estimated 0.1% have been identified so far. Once understood, known biosynthetic complexes can then be engineered to produce new drugs or lead to an efficient identification of new enzymatic assembly lines in vast genome data and isolation of their products that are novel drug leads.

Benefit to National Security Missions

New antibacterial and antiviral treatment options are urgently needed to reduce the threat to public health. The accelerating development of drug resistance in pathogens and its impact on lethality rates is widely discussed by several funding agencies (incl. HHS, DARPA, BARDA, DTRA, DOD), in scientific press releases and among general public press outlets.

This project is directly related to LANL's missions in Global Security, Biothreat Reduction, and in alignment with the National Security goal of LANL's Bioscience Division. It addresses Priority Area 1 of the Complex Natural and Engineered Systems focus area. Specifically, the ability to decode the biosynthetic logic will accelerate the field of synthetic and systems biology and allow for efficient engineering of drug candidates. This project supports LANL public health mission (Homeland Security Act 2002, DOE Strategic Plan 2011, Public Health Security and Bioterrorism Preparedness and Response Act 2002) as well as its mission in global threat reduction. It also has direct appeal to WFO sponsors, as expressed in ongoing interests by DTRA to develop countermeasures for natural and man-made biothreats. It will both leverage and strengthen LANL's capabilities in computing, genomic and biosynthetic research. We will keep program managers in Global Security (Science of Signatures), DTRA and DOE BES programs appraised of the results of our research so that we can develop future funding for this effort.

Progress

For the bioinformatic part of the project, it was proposed to use and develop code that identifies as many new gene clusters encoding for biosynthetic machineries for natural product production as possible in the vast genome space of bacteria, fungi and plants. Within the analyzed 3,000+ genomes of bacterial and fungal strains, more than 16,000 new gene clusters were found. From this vast amount of available strains, five were chosen (Myxococcus xanthus DK 1622, Corallococcus coralloides DSM 2259, Streptosporangium roseum DSM 43021, Catenulispora acidiphila DSM 44928, Herpetosiphon au-

rantiacus DSM 785) in which the biosynthetic clusters are unusual, i.e. not following the classical linear, multi-modular organization (Koglin, Walsh, Nat Prod Rep., 2009, 101; Strieker et al., Curr. Opin. Struct. Biol. 2010, 20, 234). This approach significantly reduces the probability of isolating compounds similar to known or identified natural products. Within these five strains a total of 124 gene clusters have been identified and further characterized.

Initially, the linear EMBL file format was chosen as the data output format. The advantage of this file format is that it is compatible with a wide range of software for data analysis and for genome, gene and peptide sequence alignment. The disadvantages of a linear data depository became obvious as soon as the amount of produced data increased significantly. While the manual comparison of 124 linear data sets can be accomplished, it becomes increasingly harder if not impossible as the number of identified biosynthetic systems reached 2,000 and more. The EMBL file format deposits all identified information for one full genome in a single text file, including all DNA and peptide sequences of all protein with all predicted enzymatic functions and substrates. In cases a strain contains more than 30 biosynthetic systems, the file size is significantly larger than 2MB (output files with up to 35MB have been generated) and cannot be utilized for comparative analysis on gene, peptide or protein function level.

As a consequence, we decided to change the layout of our data depository and the design of our database significantly and currently create an SQL-based database that allows to deposit each biosynthetic system separated in genes, peptide sequence, protein domains, domain and protein function and produced secondary metabolite and independent from the strain. This way, we now enable comparative analyses within one strain family and between all sequenced bacterial strains simultaneously. At the same time, it reduced depository files to manageable sizes and increases the speed for comparative analyses. We can now further include information from existing databases containing information of known bioactive natural products and increase the learning base for the machine learning efforts to reliably predict the chemical composition and structure of a novel secondary metabolite from bacteria and fungi before the compound was first isolated. This SQL database also allows the integration of plant genomes and database that include information of natural products from plants. For instance, with the help of the Bitter Database of the Weizman Institute that connects the chemical structure of bitter tasting natural products with the genome of the producing plant, we can now identify the genes and enzymes that are responsible for the production of this compound. This will help us to gain information to predict natural products in plants. We plan to complete the SQL database by the end of September.

Future Work

Natural products represent the class of small bioactive molecules that are widely applied as antibacterial, antiviral, antitumor, antifungal, immunosuppressant and analgesic drugs. This project focuses on methods to identify genes coding for new biosynthetic enzyme clusters that produce bioactive metabolites with new chemical properties (chemotypes) in genetic information of bacteria, fungi and plants, and to predict the chemical composition or chemical structure of these biosynthesized natural products based on their encoding. This knowledge will allow (1) identification of new drug classes with new physiological properties, and (2) manipulation of these assembly lines to produce specific drugs and/or efficiently manufacture novel and unique metabolites.

In the next funding period, we will continue analyzing vast bacterial and fungal genome data in an automated search algorithm we developed. We will identify and characterize novel natural product assembly lines, continue to complete the database of biosynthetic clusters to allow the identification of common recognition motifs (jigsaw puzzle links). We will continue updating and improving the search algorithm using the new data.

We will also expand the search for relevant biosynthetic clusters and natural products to plant genomes and include those in our created libraries.

We will begin isolation of first, predicted natural products and confirmation of their structure/composition.

Conclusion

This project leads to the identification of biosynthetic clusters in diverse genomes and the informed isolation of novel natural products from strains known to synthesize potent bioactive compounds. We collect and characterize data in a library of diverse biosynthetic clusters and medicinally relevant natural products. This information is the basis to decipher the mechanism of complex self-assembly in natural product biosynthesis, which will reflect in the development of algorithms to predict the chemical structure of natural products based on their genetic encoding.

Toward a Coupled Multi-physics Modeling Framework for Induced Seismicity

Satish Karra
20150693ECR

Introduction

The recent shale-gas revolution, has been accompanied by a five-fold increase in small to moderate magnitude (greater than 3) seismicity in the central and eastern US. It is likely that many of these earthquakes are induced by industry practice of disposing of fracking fluids into deep formations. The issue of induced seismicity presents a significant threat to US energy security, as regulatory barriers could curb the expansion of unconventional shale-gas operations as well as deployment of renewable energy technologies such as carbon sequestration and enhanced geothermal systems.

An induced earthquake occurs when pressurized fluid enters a fault and causes frictional failure. However, induced seismicity does not simply manifest as one single earthquake, but rather as a migrating, sporadic sequence of events. Modeling these sequences requires an understanding of the feedbacks between pressurization and fault rupture, and the ability to capture both small and large space and time-scales.

This project addresses the technology gaps in modeling induced seismicity. We propose a high-performance computing coupled multi-physics framework in which earthquakes alter fluid flow through fault networks, thereby influencing pressure migration and the location, timing and magnitude of subsequent earthquakes.

Benefit to National Security Missions

Shale gas, geothermal energy, carbon sequestration, and enhanced oil and gas recovery have a clear role in the U.S. energy policy, both in securing cost-effective energy and reducing atmospheric CO2. Injection-induced seismicity poses a significant mitigation challenge to the US energy sector, as it is intrinsically linked to the shale-gas fracking revolution, renewable energy technologies such as Carbon Capture and Storage and Enhanced Geothermal Systems, as well as underground waste water disposal. The coupled modeling framework developed in this work will form the basis for future forecasting tools. This will have a direct and immediate impact on policy-making as well as on the DOE's Offices of Fossil Energy (FE) and Energy Efficiency & Renewable Energy (EERE) programs in carbon storage, unconventional fossil fuels, and geothermal energy along with State agencies with regard to waste water disposal. Our research will also place LANL at the forefront when the DOE initiatives such as SubTER and Energy-Water Nexus commence.

Progress

The project had started on June 15, 2015 and there are no accomplishments to report for this period.

Future Work

The main goal of this project is to develop the INDUS framework that is aimed to be built on top of two HPC codes – PFLOTRAN (developed at LANL and other DOE labs) for flow and PyLith for earthquake dynamics. The coupler developed in FY15 will be used in the exchange of fluid pressure and earthquake slip information between PyLith and PFLOTRAN sub-simulations, time-stepping control, and mesh interpolation. Once testing on benchmark problems is complete, the coupler will be used to perform simulations on real datasets.

Conclusion

Our primary goal is development of a new physics-based framework for induced seismicity that couples the traditionally separate fields of geomechanics (earthquakes) and hydrology (fluid injection). The coupling will be achieved through the use of innovative new fracture-permeability damage relationships that describe flow changes by as much four orders of magnitude in the fractured zone around a fault rupture. The framework leverages recent advancements in two high-performance computing open-source simulators – PFLOTRAN for subsurface flow and PyLith for fault dynamics. The meth-

odology will have wide utility for industry, academic and government partners in carbon sequestration, waste water injection and enhanced geothermal systems.

Publications

Chang, J., S. Karra, and K. B. Nakshatrala. Large-scale optimization-based non-negative computational framework for diffusion equations: parallel implementation and performance studies. Journal of Scientific Computing.

Grasinger, M., D. O'Malley, V. Vesselinov, and S. Karra. Decision analysis for robust CO2 injection: application of Bayesian-information-gap decision theory. To appear in International Journal of Greenhouse Gas Control.

The World's First Drought and Insect Caused Global Tree Mortality Monitoring System

Chonggang Xu
20130733ECR

Abstract

The critical urgency of forecasting climate impacts and feedbacks makes understanding, quantifying, and predicting terrestrial carbon balance and subsequent climate impacts one of the greatest science challenges currently facing the world. The real-time monitoring systems for dominant types of disturbances will provide a key foundation for our understanding of global carbon balance. We currently already have a fire-burned area monitoring system and comprehensive land-use change database; however, there is no global monitoring system of drought/insect-caused vegetation mortality, which could be at similar magnitude of fire-caused tree mortality. Armed with the world's leading capability in dynamic vegetation modeling and tree mortality research, we developed the world's first automated global drought/insect-caused tree mortality monitoring system. The mortality monitoring system was developed based on the fusion of different sources of information including real-time mortality signals from remote sensing imagery, vegetation change information simulated from a vegetation dynamics model, radiative transfer and reflectance information from a forest reflectance model, and different sources of background information from forest inventory and remote sensing products. We have successfully tested this system locally at Los Alamos and regionally in NM State.

Background and Research Objectives

Armed with the world's leading research in vegetation mortality and state-of-the-art capability in dynamics vegetation modeling and vegetation anomaly detection, we developed the world's first global monitoring system for drought and insect-caused tree mortality. The developed monitoring system fused real-time mortality signals from MODIS imagery, predicted vegetation dynamics information from an ecosystem demography (ED) model, radiative transfer and reflectance information from a forest canopy reflectance and transmittance (FRT) model, and different sources of background information from forest inventory and remote sensing products. The fusion of different sources of information makes it feasible to accurately quantify tree mortality from MODIS imagery, which has never been possible from image analysis alone. The ED model tracks the growth and mortality for cohorts of plants with similar sizes and we have incorporated the world-leading theory and data on mortality mechanisms into the model, which provides mechanistic accuracy unparalleled in other global vegetation models. The FRT model is a leading model that simulates light reflectance and transmittance for a very heterogeneous canopy represented by different tree cohorts, the same canopy structure representation in the ED model. An automated fitting algorithm based on Ensemble Kalman filter (EnKF) was used to tune the tree mortality parameter in the ED model so that the simulated light reflectance in the FRT model tracks real-time observation from MODIS imagery. Our ultimate goal is to develop an unprecedented capability at LANL to simultaneously monitor global vegetation dynamics and estimate their consequences for global carbon balance and climate feedback; however it will take a very large infrastructure development in terms of computing and basic data handling for real-time global tree mortality monitoring. Thus, although the developed ED-FRT-MODIS system is a global tree mortality monitoring system, we only applied the system to areas where we have already classified high and medium resolution images in New Mexico.

Scientific Approach and Accomplishments

With the support of this project, we have successfully developed a tree mortality detection, attribution and quantification system. Our forest disturbance detection and attribution system used anomaly detection of time series stacks of satellite imagery (Landsat or MODIS) to identify forest mortality events and classify them as fire-, drought-, or insect-caused. The system is divided into three components: Pixel Processing, Disturbance Detection, and Attribution and Evaluations. There are two phases of pixel processing, image selection and calcula-

tion of vegetation indices (VIs). Image selection requires the identification of one image for each year within a specific phonological window that has the least amount of cloud or snow coverage. The ideal time window for conifers in New Mexico is late October/early November. Pixels that are contaminated by clouds or snow can be filled from adjacent time windows if a suitable clear image is unavailable. Images are then opened sequentially, appropriate VIs are calculated, and saved as time series stacks. We use five VIs (Normalized Difference Vegetation Index (NDVI), Normalized Burn Ratio (NBR), Brightness, Greenness, and Wetness) that have been proven to be useful for identifying changes in vegetation. We perform disturbance detection by examining the time series for each pixel independently for dates when the trend deviates by a predetermined amount (2-3σ) for each VI. Specifically, pixels and dates are flagged for potential mortality when NDVI, Greenness, or Wetness decrease or NBR or Brightness increase. Finally, mortality events are identified and attribution is proposed according to combinations of flags and then growth through other pixels for contagious disturbances like fire and insects. Specifically, fire occurs during severe events (NDVI, NBR, Greenness, and Brightness are flagged regardless of Wetness), and grows into adjacent pixels with lower disturbance severity; drought is indicated by increases in Brightness and losses of Wetness in the remaining unburned pixels (this potentially misses drought killed pixels that burn in the same year); finally, pixels with insect mortality are those that have less disturbance (primarily those with a loss of greenness or NDVI). Our system has been tested for the LANDSAT images in Los Alamos (Fig. 1).

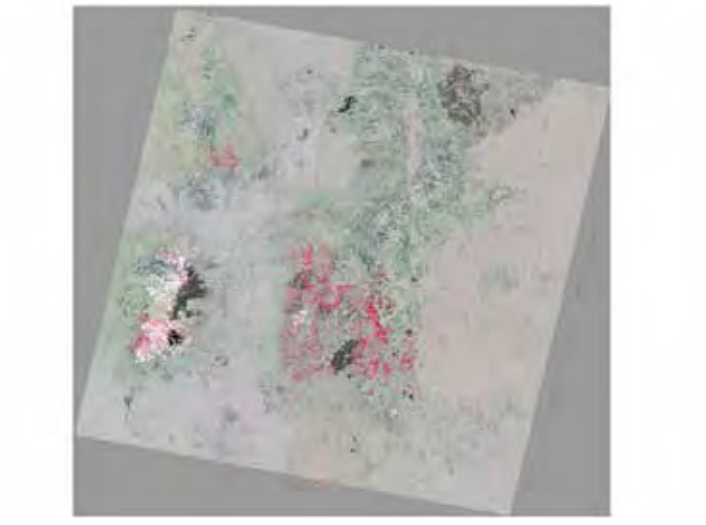

Figure 1. Detection of fire- (1993-2012; shades of gray), drought- (2002-2004; shades of red and 2011-2012; shades of orange), and insect-induced (1993-2012; shades of blue) forest mortality in the Los Alamos/Santa Fe vegetated region (green) using our methodology.

Our ED-FRT-MODIS tree quantification system is built on the fusion of vegetation dynamics from ED and the remote sensing signals. In order to account for the prior knowledge on specie drought tolerance, we have developed a mechanistic hydraulic failure model (Fig. 2 a) and the initial runs showed that it performed relatively well at the site level (Fig. 2b). A sensitivity analysis has been conducted to identify key model parameters for the prediction of hydraulic failure, which is critical for the success of the literature survey and laboratory measurements targeted for the global mortality monitoring. This new model has been used to predict the tree mortality in SW USA for pinion pine (Fig. 3).

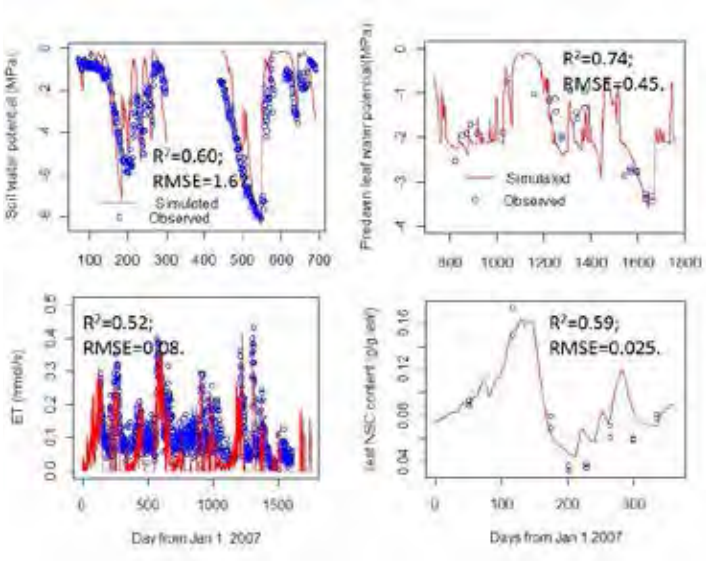

Figure 2. Plant hydraulic failure and evaluation at a LANL measurement site (Sevilleta, NM).

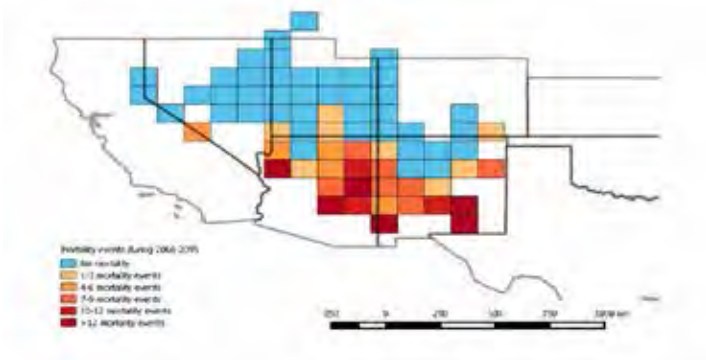

Figure 3. Predictions of piñon pine mortality events using our hydraulic-faiure model in ED using the CMIP5 predictions by CESM under RCP 8.5 (McDowell, William and Xu et al In Review).

With the new hydraulic failure model, we have first tested our ED-FRT system at a 3km by 3 km location in Los Alamos. It shows that the ED-FRT system is able to track the estimation of mortality from the high resolution Quickbird image (Fig. 4). With the local model evaluations, we have

implemented our tree mortality detection, attribution and quantification system for the NM state (Fig. 5).

With the support of this project, we have published 6 papers, with 1 paper in review and 3 papers in preparation. We have also presented our work at AGU, ESA and IURO meetings in 2013 and 2014.

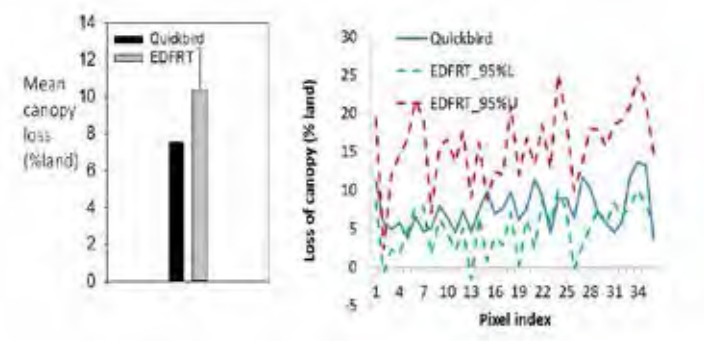

Figure 4. ED-FRT Model Evaluation for the means and individual pixels for an 3km by 3km area in Los Alamos.

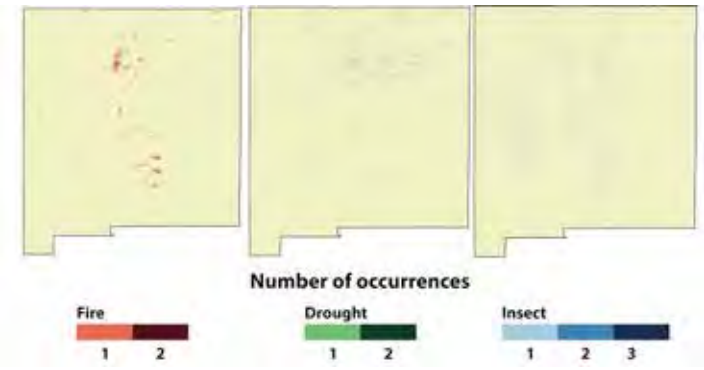

Figure 5. Mortality detection and attribution for fire, drought and insect for NM state.

Impact on National Missions

The development of ED-FRT-MODIS system represented an enormous step forward in our understanding of terrestrial carbon feedback to atmosphere, which is a key area of climatic change research in LANL's mission to mitigate the impacts of global energy demand. With the support of this project, the PI has successfully secured the current follow-on findings:

- Developing Global Simulation of Drought-associated Vegetation Mortality within the Community Land Model, 2015-2017, Role: Co-I. Funding: DOE office of science, $3 million; N. McDowell (PI), C. XU (co-I) , S. Sevanto, M Cai

- Next Generation Ecosystem Experiments in the Tropics, 2014 -2024: Role: Deputy POC. Funding: DOE office of science, $15million (5 million per year for 3 years for Phase I and potential extension with another 7 years of Phase II); PI: Jeff Chamber (LBL)

- Global Tree Mortality Prediction Based on Hydraulic Function Failure, 2015-2017, Role: PI . Funding: LANL LDRD ER, $1.2 million; C Xu (PI), S Sevanto (co-PI)

- Critical Watersheds: Climate Change, Tipping Points, and Water Security Impacts, 2015-2017, Role: co-I. Funding: LANL LDRD ER, $2.7 million; R. Middleton (PI), C. Xu (co-I), R. Linn, N. McDowell

Publications

Adam, H., P. William, C. Xu, S. Rausher, and N. McDowell. Empirical and process-based approaches to climate-induced forest mortality models. 2013. Frontiers in Functional Plant Ecology. : 438.

McDowell, N. G., N. C. Coops, P. S. A. Beck, J. Q. Chambers, Gangodagamage, J. A. Hicke, Huang, Kennedy, D. J. Krofcheck, Litvak, A. J. H. Meddens, Muss, Negron-Juarez, Peng, A. M. Schwantes, J. J. Swenson, L. J. Vernon, A. P. Williams, Xu, Zhao, S. W. Running, and C. D. Allen. Global satellite monitoring of climate-induced vegetation disturbances. 2015. TRENDS IN PLANT SCIENCE. 20 (2): 114.

McDowell, N. G., R. A. Fisher, Xu, J. C. Domec, Holtta, D. S. Mackay, J. S. Sperry, Boutz, L. e. e. Dickman, Gehres, J. M. Limousin, Macalady, Martinez-Vilalta, Mencuccini, J. A. Plaut, Ogee, R. E. Pangle, D. P. Rasse, M. G. Ryan, Sevanto, R. H. Waring, A. P. Williams, E. A. Yepez, and W. T. Pockman. Evaluating theories of drought-induced vegetation mortality using a multimodel-experiment framework. 2013. NEW PHYTOLOGIST. 200 (2): 304.

Muss, J., and C. Xu. Remote Identification and Attribution of Tree Mortality in Northern New Mexico. Remote Sensing of Environment.

XU, C., J. Muss, and N. McDowell. A Tree Mortality Quantification system based on the integration of a dynamic vegetation model and a radiative transfer model. Remote Sensing of Environment.

XU, C., J. Muss, and N. McDowell. A global sensitivity analysis for process-based tree mortality prediction under future climatic change. Ecological Modelling.

Xu, C.. Decoupling correlated and uncorrelated uncertainty contributions for nonlinear models. 2013. Applied Mathematical Modelling. 37: 9950–9969.

Xu, C., J. Muss, and N. McDowell. Uncertainty and Sensitivity Analysis for a tree mortality quantification system. Presented at IUFRO 2014 World congress. (Salt Lake City, 5-11 Oct, 2014).

Xu, C., R. Fisher, J. Muss, and N. McDowell. Uncertainty

and Sensitivity Analysis for Process-based Tree Mortality Modelling. Invited presentation at ECOLOGICAL ASSOCIATION OF AMERICA 2013. (Minneapolis, 8-13 AGU 2013).

Xu, C., R. Fisher, N. McDowell, and S. Sevanto. Our Limited Ability to Predict Vegetation Responses to Water Stress. 2013. New Phytologist. 200 (2): 8.

Xu, C., S. Sevanto, N. McDowell, and J. Muss. Challenges and Solutions for Simulating Drought-Caused Tree Mortality in Earth System Models. Presented at 2014 AGU. (San Francisco, 5-9 Dec, 2014).

Xu, C., and M. Chen. Application of Remote Sensing in Ecosystem and Landscape Modeling. 2013. In Remote Sensing of Natural Resources. Edited by Wang, G.. , p. 173. Florida: CRC Press.

From Troposphere to Ionosphere: How Much Do Thunderstorms Disturb the Total Electron Distribution?

Erin H. Lay
20130737ECR

Abstract

This work addressed the emerging field of coupling between tropospheric and ionospheric phenomena. It was largely an empirical study that bounded the magnitudes and extent of ionospheric disturbances caused by underlying thunderstorms. It also focused on understanding the coupling of energy from the thunderstorm, through the bottomside of the ionosphere, and into the bulk ionospheric plasma, called the F-region. The project was extremely successful with two publications and one submitted paper, several follow-on funding opportunities, including a funded Intelligence Community Postdoc proposal that brought a new postdoc to LANL. The tools developed in this work for analysis of ionospheric data will continue to be used at LANL for many future projects.

Background and Research Objectives

The ionosphere is a high-density layer of plasma through which all satellite-detected natural and man-made electromagnetic signals from the Earth's surface must pass. Similar to dispersion of light by transparent solids, significant perturbations in the ionospheric plasma electrons disrupt electromagnetic signals. Variation in ionospheric plasma has traditionally been attributed to changes in geomagnetic activity (space weather). Only recently, the ionospheric community has begun to realize that tropospheric weather (below ~12 km) could have a significant effect on the ionospheric plasma [1,2]. Thunderstorm-originated atmospheric gravity waves (AGW) with periods longer than ~5 minutes have been observed in the ionospheric F-region (200-400 km) [3,4] and at lower D-layer altitudes (80-100 km) [5-8]. The source of these gravity waves is typically thought to be the pressure force of overshooting of convective thunderstorm plumes [1]. Figure 1 illustrates the thunderstorm/ionosphere system and altitudes of importance at which we have detected ionospheric fluctuations.

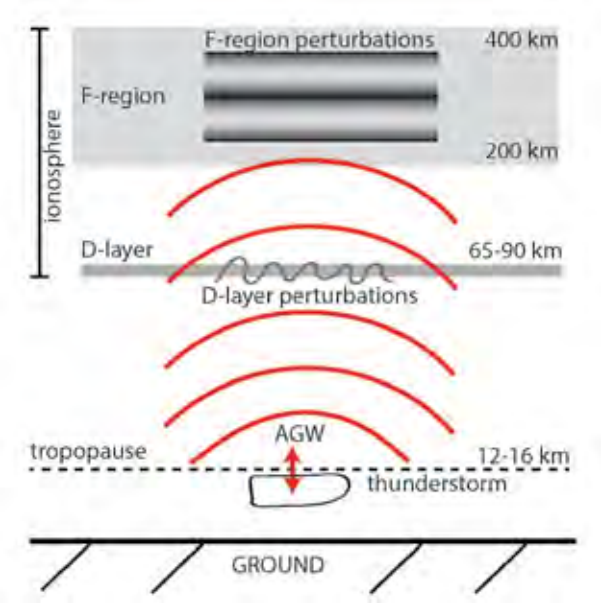

Figure 1. Illustration of the thunderstorm/ionosphere system and altitudes of importance at which ionospheric fluctuations have been detected.

Shorter period (1 – 4.5 min; 3.7 – 16.7 mHz) wave variations associated with severe thunderstorms have also been observed in the F-region [3,9,10] and D-layer [11]. Model results of acoustic wave propagation are consistent with observations, and indicate that such waves originating from thunderstorm heights (< 12 km) should be able to reach 250-350 km altitude within ~250 km horizontally of the source [12,13]. Although propagation and ray tracing models indicate that acoustic waves can reach ionospheric heights, the source for such waves is still unclear. While models typically use thunderstorm convection as the source, such a mechanism has not been confirmed. In addition, the atmospheric cutoff at lower frequencies makes it unclear whether the source is a narrowband emitter, or whether it is a broadband emitter that is filtered as it propagates to the ionosphere.

As these buoyancy and acoustic waves propagate into the plasma of the ionosphere, the motion of the neutral molecules drags the ionospheric ions. Charge separation, in turn, generates electric fields that cause motion of the electrons. Because electrons are bound to the magnetic field lines of the Earth's magnetic field, field-aligned irregularities can occur. While the general physics behind this coupling is understood, there have been very few measurements done to allow an understanding of the expected magnitude and spatial size of the ionospheric response to thunderstorm-produced buoyancy and acoustic waves. In addition, the static and electromagnetic field generated by electric charges in the thunderstorm itself also can introduce instabilities and electron density fluctuations.

The research objectives of this project were 1) to characterize spatial size, magnitude, and temporal evolution of ionospheric perturbations related to nearby thunderstorms on a regional scale, and how they vary with thunderstorm properties (i.e. size, height, lightning activity); and 2) to characterize the magnitude and spatial extent of troposphere/ionosphere coupling on a global scale as a function of geomagnetic latitude.

Objective #1 was addressed in several papers: Lay et al. [3] presented preliminary case studies of ionospheric response in the bulk of the plasma. Lay et al. [14] was a statistical study that characterizes, for the first time, the spatial extent and magnitude of ionospheric buoyancy and acoustic waves response versus thunderstorm size. Lay et al. [15] characterized the bottom of the ionosphere to understand how waves couple from below into the main plasma layer, and it found that the background bottomside ionosphere has a much steeper increase in electron density with altitude than used in most previous models. This has significant implications in future modeling efforts.

Objective #2 was addressed by searching for similar correlations between thunderstorms and ionospheric disturbances in lower latitudes. However, we found that ionospheric dynamics in lower latitudes is dominated by processes other than thunderstorms (equatorial plasma drifts, solar/geomagnetic storms) so much so that effects due to thunderstorms are indistinguishable from the noise. This finding is important in understanding the relative effect of thunderstorms on overall ionospheric fluctuations globally. Because the finding was a null result, this part of the work was not published. However, this work lead to some interesting follow-on proposals addressing ionospheric scintillation at low latitudes (the degradation of an electromagnetic signal as it propagates through a disturbed plasma).

An additional objective developed during the course of the project based on the frequent observation of highly coherent acoustic waves that were closely localized over extremely large thunderstorms. This new objective was to utilize these acoustic signatures to determine a source region in the storm for these waves. We were able to develop a technique that yielded two probable source regions in the thunderstorms: the convective core and the stratiform region. This work will soon be submitted soon to Nature Geoscience. The location technique is also potentially useful in locating other tropospheric sources such as explosions, tsunamis, and earthquakes. We have proposed to several new sources of funding (Underground Nuclear Explosion Signatures Experiment, Space Nuclear Detection Program, LANL LDRD) to aid in locating such events with this technique.

Scientific Approach and Accomplishments

The scientific approach of this study was to correlate ionospheric fluctuations with thunderstorm activity on a regional and global scale to better understand thunderstorm influence on the ionospheric plasma.

Understanding the bottomside ionosphere was important for generating an understanding of coupling processes from below. We used a technique developed previously at LANL to probe the lower ionospheric electron density and fluctuations [6,7,16]. Using this technique, we found that the background quiet-time bottomside electron density profile increased significantly faster in altitude than previously thought. Based on a case study over a thunderstorm, we found that a nighttime profile over a thunderstorm becomes much less steep than in a quiet region, becoming more like a daytime profile. These results were published in Lay et al., [15]. Figure 2 shows our experimentally-determined nighttime profile as a solid line, which increases in electron density with altitude much faster than that of the previously used community model (red dashed line). Above thunderstorms the electron density does not increase as rapidly with altitude (Figure 2, black dashed line).

Next we looked at case studies of F-region (where the main ionospheric plasma resides) perturbations above thunderstorms. We found very good spatial and temporal correlation between thunderstorms and ionospheric gravity waves (periods 6 - 20 minutes) and ionospheric acoustic waves (periods 2 – 4 minutes). Figure 3 shows an example of the results from this study. Two nights with thunderstorm activity are plotted on the two rows. The underlying blue contours show lightning density in the thunderstorm. The left column shows the acoustic waves over the thunderstorm in red. The right column shows the gravity waves in red. Both the left and right columns show that with the larger thunderstorm in the top row, there are more acous-

tic and gravity waves. The smaller thunderstorm still has visible waves, but to a smaller extent.

These results were published in Lay et al., [3] and submitted for publication to Journal of Geophysical Research – Space Physics [14]. In order to analyze these F-region data, we developed data analysis tools for freely-available measurements of total electron content made by Global Positioning System ground receivers. These tools will be useful to the lab for any future ionospheric projects involving total electron content measurements. In fact, they are already being used for follow-on projects and proposals.

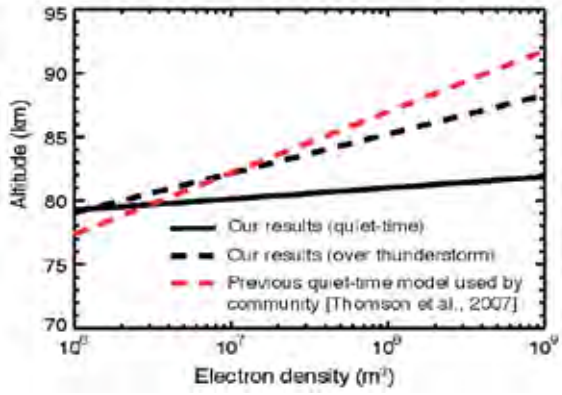

Figure 2. Electron density profile versus altitude. Solid black line shows our experimentally-determined nighttime profile, which increases in electron density with altitude much faster than that of the previously used community model (red dashed line). Above thunderstorms the electron density does not increase as rapidly with altitude (black dashed line).

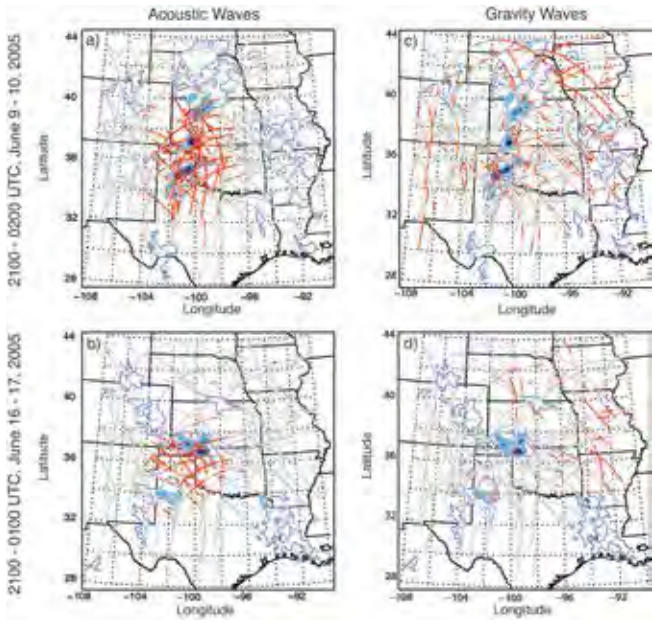

Figure 3. Ionospheric gravity waves (red, right column) and ionospheric acoustic waves (red, left column) over thunderstorms (blue contours) on June 9-10, 2005 (top row) and June 16-17, 2005 (bottom row). Above the larger thunderstorm in the top row, there are more acoustic and gravity waves. The smaller thunderstorm in the bottom row still has visible waves, but to a smaller extent.

With the case studies motivating further investigation, we performed a statistical study of data from May – July 2005 over the U.S. Great Plains. This analysis compared thunderstorm size with the associated area covered by ionospheric perturbations, as well as the magnitude of the perturbations. We found that the ionospheric area covered by gravity waves increased with respect to thunderstorm size, typically covering 10 times the area of the thunderstorm (Figure 4c). The ionospheric area covered by acoustic waves (Figure 4a) and the maximum acoustic wave amplitude (Figure 4b) increase as thunderstorm area increases. However, there seems to be a minimum effect detectable only when thunderstorm size exceeds a threshold of ~30,000 km2. These results have been submitted for publication to Journal of Geophysical Research – Space Physics [14].

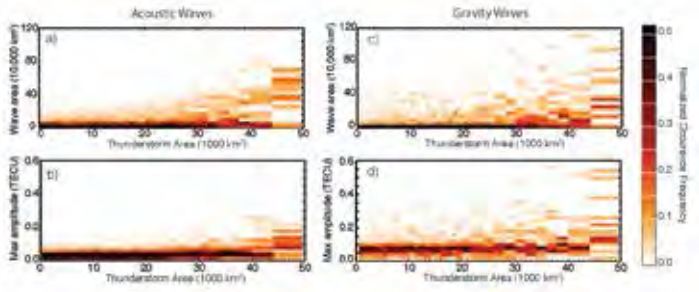

Figure 4. Results of statistical study of data from May – July 2005 over the U.S. Great Plains comparing thunderstorm size with the area of ionospheric acoustic waves (a), the maximum magnitude of the acoustic waves (b), the area of the ionospheric gravity waves (c), and the maximum magnitude of gravity waves (d).

In addition to the peer-reviewed publications above, several notable follow-on projects developed from this project:

The finding of coherent acoustic waves above thunderstorms led to the development of a phase-differential method to trace those waves back to the source. Locating the source can give an understanding of the source mechanism. Preliminary findings suggested an acoustic source from the collapse of a high convective core, as well as a source in the stratiform region of the storm associated with large horizontal “spider” lightning and ionospheric electrical discharges called sprites. These findings will soon be submitted to Nature Geoscience. Further development of this method and investigation of source coupling physics has been submitted to LANL DR (20160065DR). This method can also be used for locating explosions via their ionospheric signatures. Using this method the West, TX

fertilizer plant explosion in 2013 was located amid a front of thunderstorms. A proposal to the Underground Nuclear Explosions Signature Experiment was submitted to exploit this signature, and additional related proposals are in preparation.

A notable cluster of acoustic waves in the statistical data was not associated with any thunderstorms or geomagnetic storms, yet it was associated with a time period with meteor activity. The hypothesis that the cluster was associated with meteor activity led to a funded Intelligence Community Postdoc proposal. We now have a postdoc, Dr. Robert Haaser, working in this position under the mentor supervision of Drs. Erin Lay and William Junor.

The development and availability of ionospheric GPS tools created the opportunity for several new proposals. We are currently submitting proposals to address ionospheric scintillation (degradation of radio signals as they pass through a plasma) using GPS measurements. We have submitted to LANL ER (20160231ER) and plan to submit to the NASA ROSES call.

Impact on National Missions

This study focused on understanding the magnitude and extent of ionospheric perturbations, which is important for predicting ionospheric disruption of satellite communications, GPS geolocation signals, and electromagnetic signals such as EMP that are an important part of the Lab's national security mission. The empirical results from this work gave an estimate of the ionospheric area affected by thunderstorm perturbations and associated magnitudes in mid-latitude regions. These findings also indicated that primary disruptions in the equatorial region are not likely to be associated with thunderstorms, but instead with scintillation. Proposed follow-on work will use the tools developed here to further understand scintillation disruptions.

The empirical findings from this study will be used to test and evaluate existing atmospheric gravity wave models, enabling us to distill and discover the physical processes responsible for energy and mass transport between the bottomside and main plasma layer, and to better nowcast and forecast ionospheric disturbances. More in-depth modeling is required to fully understand atmospheric/ionospheric coupling for forecasting capabilities. The necessary work has been proposed as a LDRD-DR.

The proposed follow-on work for ionospheric signatures detection of explosives directly impacts work on detection and characterization of explosive events. These signatures could be used as a complimentary technique to determining location and yield of explosive events.

This work also brought Dr. Robert Haaser to our team as part of the Intelligence Community Postdoc Program. He is studying ionospheric effects of meteors and bolides using the tools developed from this work. The IC postdoc sponsor, Peter Bythrow, will also be visiting LANL soon as part of the project, and will be renewing contacts in the areas of Space Nuclear Power and National Security.

The results of this study directly impact LANL's on-orbit and ground-based nuclear detection (NUDET) program. The newly-developed understanding of characteristics (magnitude, area) of ionospheric perturbations associated with thunderstorms will impact our interpretation of on-orbit detected signals that passed over thunderstorms. The improved understanding of the bottomside ionosphere will aid in ground-based NUDET detection. Ground-based very-low-frequency (VLF) signals travel in the Earth-Ionosphere waveguide, of which the bottomside ionosphere forms the upper boundary. Thus, the VLF wave attenuation is very sensitive to the bottomside electron density profile, and an accurate location and characterization of an event is therefore also sensitive to that profile. Finally, the results of this study are of interest to external funding agencies that support our work in that understanding thunderstorm-generated wave characteristics helps us to distill thunderstorm-driven waves from other phenomena, such as meteors and explosions. This, in turn, can allow us to better understand ionospheric fluctuations from those other sources.

References

1. Vadas, S. L., and D. C. Fritts. Thermospheric responses to gravity waves arising from mesoscale convective complexes. 2004. JOURNAL OF ATMOSPHERIC AND SOLAR-TERRESTRIAL PHYSICS. 66 (6-9): 781.

2. Immel, T. J., Sagawa, S. L. England, S. B. Henderson, M. E. Hagan, S. B. Mende, H. U. Frey, C. M. Swenson, and L. J. Paxton. Control of equatorial ionospheric morphology by atmospheric tides. 2006. GEOPHYSICAL RESEARCH LETTERS. 33 (15).

3. Lay, E. H., Shao, and C. S. Carrano. Variation in total electron content above large thunderstorms. 2013. GEOPHYSICAL RESEARCH LETTERS. 40 (10): 1945.

4. Vadas, S. L., and H. -. Liu. Numerical modeling of the large-scale neutral and plasma responses to the body forces created by the dissipation of gravity waves from 6 h of deep convection in Brazil. 2013. JOURNAL OF GEOPHYSICAL RESEARCH-SPACE PHYSICS. 118 (5): 2593.

5. Yue, J. i. a., S. L. Vadas, She, Nakamura, S. C. Reising, Liu, Stamus, D. A. Krueger, Lyons, and T. a. o. Li. Con-

centric gravity waves in the mesosphere generated by deep convective plumes in the lower atmosphere near Fort Collins, Colorado. 2009. JOURNAL OF GEOPHYSICAL RESEARCH-ATMOSPHERES. 114.

6. Lay, E. H., and X. -. Shao. Multi-station probing of thunderstorm-generated D-layer fluctuations by using time-domain lightning waveforms. 2011. GEOPHYSICAL RESEARCH LETTERS. 38.

7. Lay, E. H., and Shao. High temporal and spatial-resolution detection of D-layer fluctuations by using time-domain lightning waveforms. 2011. JOURNAL OF GEOPHYSICAL RESEARCH-SPACE PHYSICS. 116.

8. Yue, J. i. a., Hoffmann, and M. J. Alexander. Simultaneous observations of convective gravity waves from a ground-based airglow imager and the AIRS satellite experiment. 2013. JOURNAL OF GEOPHYSICAL RESEARCH-ATMOSPHERES. 118 (8): 3178.

9. GEORGES, T. M.. HF DOPPLER STUDIES OF TRAVELING IONOSPHERIC DISTURBANCES. 1968. JOURNAL OF ATMOSPHERIC AND TERRESTRIAL PHYSICS. 30 (5): 735.

10. BAKER, D. M., and K. DAVIES. F2-REGION ACOUSTIC WAVES FROM SEVERE WEATHER. 1969. JOURNAL OF ATMOSPHERIC AND TERRESTRIAL PHYSICS. 31 (11): 1345.

11. Marshall, R. A., and J. B. Snively. Very low frequency subionospheric remote sensing of thunderstorm-driven acoustic waves in the lower ionosphere. 2014. JOURNAL OF GEOPHYSICAL RESEARCH-ATMOSPHERES. 119 (9): 5037.

12. Walterscheid, R. L., G. Schubert, and D. G. Brinkman. Acoustic waves in the upper mesosphere and lower thermosphere generated by deep tropical convection. 2003. JOURNAL OF GEOPHYSICAL RESEARCH-SPACE PHYSICS. 108 (A11).

13. Zettergren, M. D., and J. B. Snively. Ionospheric signatures of acoustic waves generated by transient tropospheric forcing. 2013. GEOPHYSICAL RESEARCH LETTERS. 40 (20): 5345.

14. Lay, E. H., X. M. Shao, A. K. Kendrick, and C. S. Carrano. Ionospheric acoustic and gravity waves associated with thunderstorms. 2015. Submitted to J. of Geophys. Res. – Space Physics, April 2015, LA-UR-15-22667.

15. Lay, E. H., X. M. Shao, and A. R. Jacobson. D region electron profiles observed with substantial spatial and temporal change near thunderstorms. 2014. Journal of Geophysical Research: Space Physics. 119 (6): 4916.

16. Shao, , E. H. Lay, and A. R. Jacobson. Reduction of electron density in the night-time lower ionosphere in response to a thunderstorm. 2013. NATURE GEOSCIENCE. 6 (1): 29.

Publications

Lay, E. H., X. M. Shao, A. K. Kendrick, and C. S. Carrano. Ionospheric acoustic and gravity waves associated with thunderstorms. 2015. In press, J. of Geophys. Res. – Space Physics, July 2015, LA-UR-15-22667.

Lay, E. H., X. M. Shao, and A. R. Jacobson. D region electron profiles observed with substantial spatial and temporal change near thunderstorms. 2014. Journal of Geophysical Research: Space Physics. 119 (6): 4916.

Lay, E. H., X. M. Shao, and C. S. Carrano. Variation in total electron content above large thunderstorms. 2013. Geophysical Research Letters. 40: 1945.

Shao, X., E. H. Lay, and A. R. Jacobson. Ionospheric variations in response to lightning discharges and their parental thunderstorms. Presented at International Conference on Atmospheric Electricity. (Norman, OK, USA, 15-20 June 2014).

Understanding The Catalytic Conversion of Oligosaccharides to Fuels and Chemical Feedstocks

Andrew Sutton
20130757ECR

Abstract

Our recent work has developed a procedure to produce branched alkanes containing twelve carbon atoms from starch in two steps using mild acidic conditions with lanthanide and palladium catalysts. The reaction proceeds well at 200 oC and 200 psi H2 but the mechanism and reaction intermediates are unknown. If we can fully understand the steps required for this reaction we can develop routes to obviate the need for expensive catalysts and move to ambient reaction conditions.

Background and Research Objectives

We have clearly demonstrated the feasibility of converting oligosaccharides to branched alkanes which helps LANL position itself as a leader in alternative energy fuel production. However, the process uses palladium (Pd) and Lewis acidic lanthanide (Ln) compounds as catalysts. Palladium is an expensive metal (~ $5000/100g) and rare-earth metals have been highlighted by the Department of Energy (DOE) as “Critical Materials” (i.e. materials that are essential to many clean energy technologies but also at significant risk of supply disruption). We are currently unaware as to the mechanism or the key intermediates involved in this transformation and if we could identify these and develop a stepwise understanding of the process, then we believe that we could develop non-precious metal catalysts (NPMC) that could perform both the hydrogenation (palladium catalyzed reaction) and the hydrodeoxygenation reaction (HDO, catalyzed by Pd and Ln). A deeper understanding of how the reaction proceeds could also enable us to perform these transformations under ambient temperatures and pressures which would lead to significant cost benefits on subsequent scale-up of this process to produce fuel or feedstocks on a commercial scale.

The challenge to perform controlled low temperature dehydration and deoxygenation of multifunctional substrates is significant and any advances or insight into this chemistry can be readily applied to polyols, sugars and other biomass derived products which are inherently over-functionalized for use as chemical feedstocks or fuels. Carbohydrates represent an attractive carbon source for conversion to hydrocarbons and chemical feedstocks. Glucose is the most abundant monosaccharide on the planet and its use as a fuel and chemical feedstock precursor represents a worthwhile target, if cost effective chemical transformations can be developed. In contrast to introducing functional groups to crude oil derived substrates, biomass conversion to fuels requires removal of functional groups that represents a complete paradigm shift from traditional catalysis science. Biomass is composed of carbohydrates and aromatics, both of which are chemically linked into large polymers and chemically “over-functionalized”. The primary challenges in biomass conversion are thus depolymerization to monomers and as the resulting intermediates possess an abundance of oxygen, deoxygenation. These two chemical transformations both require the catalytic cleavage of carbon-oxygen bonds, and are the primary thrusts of catalysis science in biomass conversion. This new field presents great opportunities to redefine some areas of modern catalysis science.

Recently, organocatalyzed aldol chemistry has been developed at LANL to extend the chain length of furan aldehydes (5-hydroxymethylfurfural (HMF) R = OH or furfural (FF) R = H) derived from glucose (Figure 1). This method of chain extension (required for resultant fuel energy density) can be performed with a variety of donor molecules to allow molecules with between 8 and 16 carbon atoms to be synthesized. These molecules share common functional group combinations comprised of furans, olefins, carbonyls, and hydroxyl groups. Our recent catalytic HDO approach uses palladium (Pd) with Lewis acidic lanthanide triflate salts (Ln(OTf)3). Sequential hydrogenation of exocyclic substrate unsaturation, then furan ring-opening followed by HDO of the resultant polyketone species produces linear alkanes (Figure 2). Direct hydrogenation of the furan to produce

a tetrahydrofuran (THF) adduct requires a significantly more energy intensive route to ring-open so is a less desirable route. To eliminate the conversion of glucose to HMF of FF and use glucose or starch directly we used an adaptation of Garcia-Gonzalez chemistry. In our approach we converted starch to cyclized tetrahydrofuranylfuran derivatives and even performed the same reaction with starch extracted from a potato. These species share the same functional groups as the aldol products shown in Figure 1, and thus similar reaction conditions can be used to convert these molecules into branched alkanes (Figure 3). Although this conversion of starch to alkanes works well, we currently have no details on the intermediates formed or the mechanism by which alkanes are produced

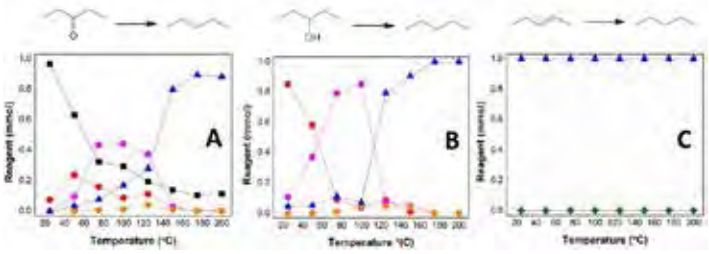

Figure 1. Temperature-dependent product distributions observed when 3-pentanone (A), 3-pentanol (B), and 2-pentene (C) are subjected to standard HDO conditions for 15 hours ([Substrate] = 400 mM, [La(OTf)] = 60 mM, 10 wt% Pd/C relative to substrate, 2.5 mL acetic acid, 200 psi H). Substrate key: 3-pentanone = (black square), 3-pentanol = (red circle), 3-acetoxypentane = (pink circle), 2-acetoxypentane = (orange circle), 2-pentene = (green diamond), pentane = (blue triangle).

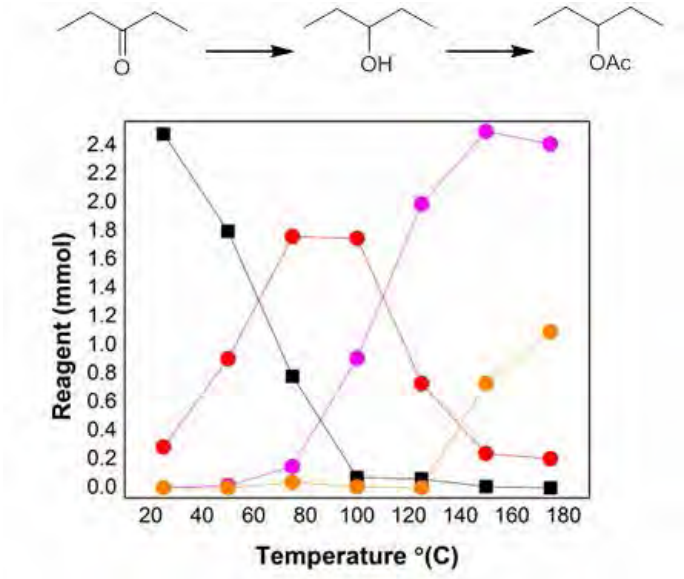

Figure 2. Temperature-dependent product distributions observed during the HDO reaction with La(OTf) absent for 15 hours. ([Substrate] = 1.2 M, 10 wt% Pd/C relative to substrate, 2.5 mL acetic acid, 200 psi H). Substrate key: 3-pentanone = (black square), 3-pentanol = (red circle), 3-acetoxypentane = (pink circle), 2-acetoxypentane = (orange circle).

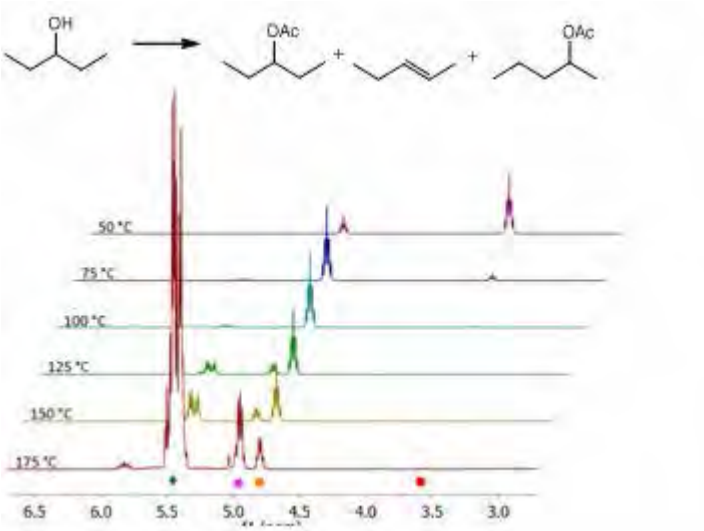

Figure 3. H NMR following the La(OTf) catalyzed dehydration of 3-pentanol in acetic acid. Substrate key: 3-pentanol = (red circle), 3-acetoxypentane = (pink circle), 2-acetoxypentane = (orange circle), 2-pentene = (green diamond).

Scientific Approach and Accomplishments

Non-food based carbohydrates are attractive renewable starting materials for conversion into fuels and feedstocks. Glucose and xylose, as the main building blocks of lignocellulosic biomass, are the most abundant monosaccharides on the planet and their use as precursors for these applications are a worthwhile target. Conversion of these sugars into platform chemicals such as furfural or 5-hydroxymethylfurfural (HMF) provides useful precursor molecules for further chain extension or derivatization in order to add value or energy density. In order for these molecules to be converted into direct drop-in fuel replacements, the abundant functional groups associated with carbohydrates (i.e. oxygen atoms) need to be removed. Recently we developed a route for selective chain extension of furan aldehydes (furfural and HMF) to produce isolable higher order furfuraldehydes containing between 8 and 16 carbon atoms. These can then be selectively converted into linear alkanes in excellent yields using a standard set of catalysts and reaction conditions. The chain extended furfuraldehydes are converted into polyketones via hydrogenation of their exocyclic double bond followed by subsequent acid-catalyzed ring opening.

However, the following hydrodeoxygenation HDO reaction to convert the polyketones into hydrocarbons requires more forcing conditions (200 °C and 200 psi H2). Reducing the energy required for this final step (i.e. via lower temperatures and pressures) should allow for a more economically viable process for potential commercialization. Studying this reaction and understanding the stepwise mechanism would allow us to improve the HDO reaction

by specifically addressing the highest energy transformations. Herein we report the use of a simple model system to probe a stepwise HDO reaction applicable to bio-derived molecules.

Initial mechanistic studies utilizing polyketone substrates were complicated by the presence of multiple reactive centers within the substrates. For example, 2,5,8-nonanetrione could potentially yield 39 possible intermediates. To overcome this complication, 3-pentanone was chosen as a model substrate containing a single functional group that was anticipated to proceed through a pathway that included 3-pentanol and 2-pentene. This allows for rapid and easy identification of intermediates and gives us a model system where we can effectively screen catalysts and reaction conditions to elicit the desired transformations. To test this hypothesis, we subjected each of these compounds to our typical HDO conditions (Pd/C, La(OTf)¬3, acetic acid, 200 psi H¬2, 200 °C, 15 hours) and observed pentane formation in all cases. We also obtained ethyl acetate as a side product from acetic acid reduction under these conditions.

In order to observe the intermediates, we performed the HDO reaction of each substrate as a function of temperature. Our standard reactions involved combining the reactants in a stainless steel reactor and heating for 15 hours at temperatures between 25 and 200 oC (with 200 psi H2 if required). Following cooling of the reactor, the crude reaction mixtures were filtered and yields were obtained by 1H NMR relative to an internal standard. For the HDO reactions of 3-pentanone, 3-pentanol and 2-pentene, the product distributions are shown in Figure 1.

At temperatures above 175 ° C, 3-pentanone forms pentane as sole product at up to 85% yield. At temperatures below 175 ° C, 3-pentanol and the intermediates 2- and 3-acetoxypentane are observed (Figure 1A). The acetoxypentanes prove to be an important intermediate in our process and their importance will be discussed later. Decreasing the temperature results in lower conversions of 3-pentanone and the expected 2-pentene intermediate is not observed under these conditions.

The conversion of 3-pentanol into pentane goes to completion at temperatures above 175 ° C with both 2- and 3-acetoxypentane observed at below this temperature. Below 100 °C, 3-acetoxypentane was the major observed product (Figure 1B) and as the reaction temperature is decreased, lower conversion of 3-pentanol is seen. The lack of observable 2-pentene indicates that the alkene intermediate is readily hydrogenated under these reaction conditions; accordingly, hydrogenation of 2-pentene proved to be facile at all temperatures investigated (Figure 1C).

Employing Pd/C and La(OTf)3 independently rather than in tandem allowed us to isolate intermediates in the HDO process. Subjecting 3-pentanone to HDO conditions (200 o C) in the absence of La(OTf)3 yields only 3-acetoxypentane (Figure 2), confirming that the role of La(OTf)3 is to facilitate C-O bond cleavage. Following this reaction as a function of temperatures shows reduction to the alcohol at 100 o C followed, at higher temperatures, by a conversion into the acetoxypentanes with nearly complete conversion at 180 o C. As expected, heating 3-pentanol in the presence of La(OTf)3 in acetic acid results in efficient production of 3-acetoxypentane at 100 ° C and 2-pentene at 150 ° C; additionally, the 2-acetoxypentane intermediate is also observed at temperatures greater than 100 ° C (Figure 3).

The individual steps comprising the net dehydration reaction were also studied. The esterification of 3-pentanol proceeds to completion at 100 °C in acetic acid, and heating 3-acetoxypentane with La(OTf)3 results in nearly complete conversion into 2-pentene at temperatures greater than 150 oC (Figure 4). The reverse reaction (i.e. the acetoxylation of 2-pentene) does not proceed at 150 oC in acetic acid alone, although a small amount of both 2- and 3-acetoxypentane are observed in the presence of La(OTf)3 and prolonged heating. 2-acetoxypentane can be substituted for 3-acetoxypentane with no change in reactivity observed.

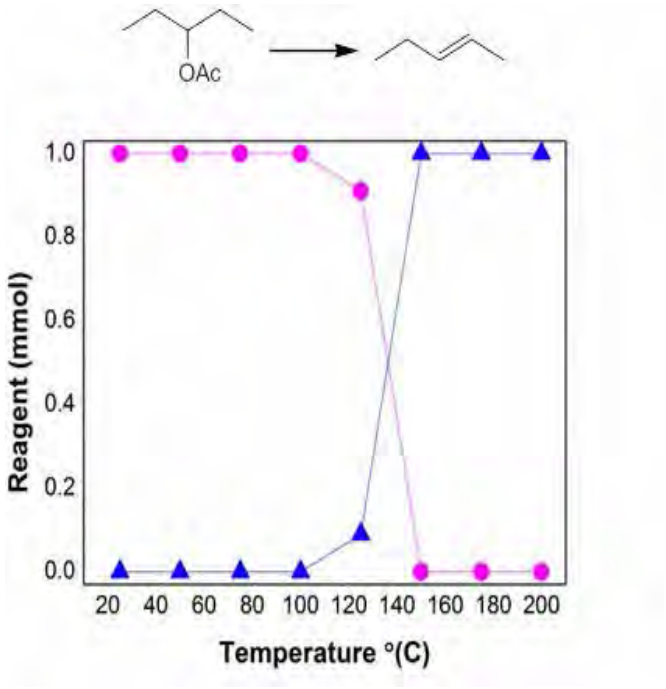

Figure 4. Temperature-dependent product distributions observed during the C-O bond cleavage reaction with La(OTf) in acetic acid. 15 hours. ([Substrate] = 1.2 M, [La(OTf)] = 40 mM, 2.5 mL acetic acid). Substrate key: 3-acetoxypentane = (pink circle), pentane = (blue triangle).

In order to determine the importance of acetoxypentane and whether this is a key intermediate that facilitates facile C-O cleavage, we attempted the dehydration of 3-pentanol and 3-acetoxypentane in sulfolane. In the presence of La(OTf)¬3 excluding acetic acid, 3-pentanol did not undergo C-O cleavage reactions. However, subjecting 3-acetoxypentane to identical conditions yielded complete conversion into the alkene at 150 oC. This result indicates that the acetate moieties are important in enabling more facile C-O bond cleavage and subsequent alkene formation.

This reaction pathway is summarized in Figure 5; palladium reduced the ketone to the alcohol which is converted to the acetoxypentane by acetic acid. The C-O bond cleavage is facilitated by the La(OTf)3 resulting in the alkene which is readily hydrogenated to the alkene. Using acetic acid as a solvent also has the benefit of being able to solubilize all the intermediates which prevents precipitation and char formation upon heating.

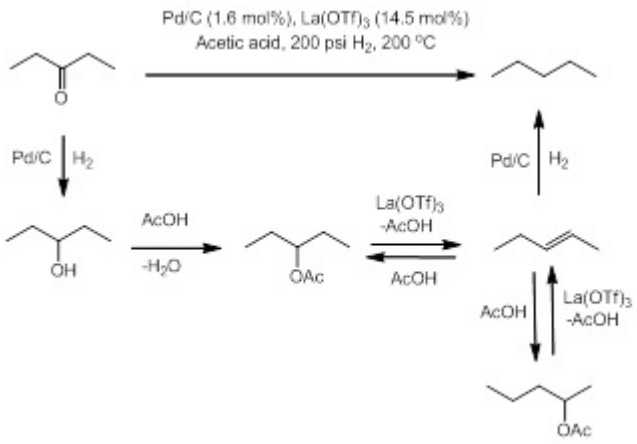

Figure 5. Reaction Pathway and Intermediates Formed in Acetoxy Mediated Hydrodeoxygenation.

We also analyzed this reaction pathway via computational studies applied to reaction free energies for all the intermediate steps in Figure 5. The computed free energy landscape indicates that once the first step (pentanone to pentanol) is accomplished, the rest of the reaction follows in an exergonic fashion (i.e. downhill).

Our calculations did not include the modeling of the Pd/C catalysis within ketone reduction, however we find this reaction to be uphill by only ΔG=+0.4 kcal/mol. From the point of view of the accuracy of Density Functional Theory, these two species are isoenergetic (pentanone+H2 and pentanol). However, Pd/C lowers the H2 dissociation barrier, thus accelerating this reaction. Step 2 consists of the acetoxylation of pentanol. As in all the remaining steps, the reaction free energy can be affected by side reactions in solution; therefore, several possibilities were considered as detailed in the supporting information. The formation of the acetoxypentane is favored by 0.31 kcal/mol. This step is followed by the release of HOAc and formation of pentene and is exergonic, releasing ΔG=6.9 kcal/mol. Again, depending on the different models we studied for coordination of HOAc in solution, the reaction free energy can vary by 0.2 kcal/mol, and in the crudest model by 2.6 kcal/mol. However this does not change the conclusion of the favorability of this step. Finally, reaction with H2 yields pentane in a highly exergonic reaction, with a ΔG=-17.5kcal/mol which supports the experimental data.

The results of this study have important implications for the design of catalysts for the HDO of biomass derived molecules into fuels, especially those that facilitate the removal of a ketone fragment. Our standard HDO reaction conditions permits both ketone reduction and C-O bond cleavage. The latter transformation is a multi-step process that is aided by the formation of the corresponding acetoxy compound. Cleavage of the C-O bond in this intermediate requires lower temperatures than the parent alcohol under the conditions we employ.

While a number of both precious- and non-precious metal catalysts for ketone hydrogenation at temperatures as low as 25 °C are known, to the best of our knowledge very few are stable under the acidic conditions employed in this study. To that end, we are currently developing more effective ketone reduction approaches into our HDO process. By breaking down the HDO reaction into several reaction steps that are easy to study, we can rapidly screen catalysts and conditions in order to develop faster and lower energy routes to bio-derived replacements for fuels and chemical feedstocks. Additionally, by studying this reaction in depth, we have uncovered the importance of acetate esters as intermediates in the cleavage of C-O bonds within our HDO process. This can be applied to other approaches that have also adopted our approach of utilizing acetic acid and could give insight into the mechanism involved in the use of other acid catalysts and the selection of acid used for this purpose. We have achieved this by using a simple commercially available surrogate for this reaction that can be easily and rapidly studied and can be used effectively to screen new catalysts and reaction conditions in the future. By doing this we have revealed an additional component of our initial HDO chemistry using acetic acid for us to consider as we strive to minimize required energy inputs for the conversion of biomass derived substrates into drop-in fuels and feedstocks. Future work is focused on optimizing performance through the use of flow-reactors to capitalize on the insight presented in this manuscript and applying this stepwise approach to polyketone substrates.

Impact on National Missions

The conversion of biomass into fuels and feedstocks is an area of huge growth and has seen considerable investment in the past decade. Success in this arena has the potential to secure a domestic supply of energy (in the form of fossil fuel replacements) and could also provide important routes to chemical feedstocks. LANL has begun to develop a capability to convert biomass into value added chemicals through external research collaborations and internal LDRD funding. In order to continue to be competitive in this bioenergy arena, continued investment is required and this will not only be of great value to the DOE complex but will also allow LANL to become a leader in a developing and promising research area.

Publications

King, A. E., T. J. Brooks, Y. Tian, E. R. Batista, and A. D. Sutton. Understanding Ketone Hydrodeoxygenation for the Production of Fuels and feedstocks From Biomass. 2015. ACS Catalysis. 5 (2): 1223.

Methane Coupling Chemistry Promoted by Catalysts Containing Inexpensive Metals

John C. Gordon
20150454ER

Introduction

Current methodologies for the conversion of methane (CH4) into commodity chemicals or fuels more amenable to transportation, storage and use either depend upon high energy input (Fischer-Tropsch) or on toxic/rare metals (e.g. Ir, Hg). The emerging importance of CH4 with respect to the Nation's energy portfolio makes this an unsatisfactory scenario. To have any hope of wide-spread implementation, any prospective CH4 functionalization catalyst must not require extensive energy input and must not be constructed of elements such that it is prohibitively expensive and/or impossible to obtain in sufficient quantities for Global utilization.

Our specific goal in this project is to prepare molecular systems comprised of inexpensive first row transition metals that can facilitate both C-H and C-C bond coupling chemistries utilizing CH4 to produce ethane (C2H6). C2H6 is itself a precursor to ethylene (C2H4), a valuable chemical feedstock used in the production of important commodity chemicals that include polyethylene, surfactants, detergents, alcohols and others. Annual worldwide production of C2H4 was 120 x 106 tons in 2008.

Benefit to National Security Missions

In direct line with the Chemistry & Chemical Sciences ER category, this project directly addresses how to advance our understanding of the chemistry and chemical methods that directly bear upon energy security, the impact of energy production, and mitigating that impact. In this case, the chemistry focuses on how to effectively upgrade an inert, abundant and cheap molecule in the form of CH4 into a useful C2 chemical feedstock. Moving away from precious metals to first row transition metals will potentially enable us to develop a catalytic system for C-H bond activation (a necessary step in functionalizing CH4) and C-C coupling chemistries that are economically scalable. This effort will capitalize on LANL's considerable expertise in catalysis using earth abundant metals. Success will competitively position LANL for funding from DOE OBES, DOE-FE, ARPA-E, and industry.

Progress

The original proposal highlighted the potential of low-valent Mn compounds supported by phosphine ligands to affect the desired CH4 chemistry. Several methodologies have been employed to access various phosphine containing scaffolds, including chelating phosphines as well as monodentate phosphines containing sterically encumbered groups.

We have had limited success in placing a chelating phosphine onto divalent Mn as a result of competitive binding of the Lewis basic solvent in which the initially chosen Mn starting materials have to be dissolved. We will pursue the use of alternative metal starting materials that have higher solubilities in non-coordinating organic solvents.

One alternative to phosphine based chemistry of Mn is the use of imines as ligands in order to more closely match the polarizability of the ligand to the metal. A second feasible approach is to use charged (i.e. anionic) ligands. These approaches were not explored at first because imines can be more prone to unwanted reactivity and charged ligands also necessitate lower electron density at the metal. Using DFT calculations, we have found that the most promising combination for CH4 activation at Mn (in terms of both thermodynamics and kinetics) occurs when an amide-imine platform with an ethylene bridge is used. Based on these results, a ligand of this type has been synthesized, with current experiments focusing on obtaining good purity and yield so that the metal chemistry can commence in earnest.

Another interest lies in low valent, low coordinate

Fe complexes. Unlike Mn to date, we have found that Fe has a propensity to bind phosphines under all metal oxidation states of interest. Towards the pursuit of sterically encumbered neutral phosphine ligands that will enable Fe to bind and activate methane towards ethane formation, the syntheses of phosphobenzene ligands has also been pursued. The use of very large substituents on the benzene ring appears to complicate the isolation of the desired products. Unsubstituted phenyl substituents have been successfully made, however. These less sterically demanding ligands will be explored in terms of their chemistry with iron and the resulting complexes derived from these ligands will be explored with respect to their propensity to promote both the C-H and C-C activation chemistries that will be required to convert methane into ethane.

Future Work

We will begin the next FY by synthesizing and spectroscopically characterizing initial target phosphine complexes. The structural and magnetic properties of some of these complexes will also be used to benchmark DFT functionals and basis sets in order to determine the combination that most accurately describes the physical and electronic structure of complexes being used in this work without undue computational cost or compromising numerical accuracy.

Conclusion

The primary result from successful completion of this project will be experimental demonstration of each of the steps along the catalyzed pathway for conversion of CH_4 into C_2H_6.

While our ultimate goal is catalytic C_2H_6 production, even stoichiometric conversion of CH_4 to C_2H_6 would be a significant accomplishment.

Fundamental Actinium Science In Search of Radiotherapeutics

Eva R. Birnbaum
20150575ER

Introduction

We propose a multi-disciplinary effort to enable the rational design of actinium-225 complexes for targeted radiotherapy treatment of cancer. Actinium-225 is one of the most promising isotopes identified for use in targeted alpha therapy of cancer, a treatment strategy that utilizes high-energy alpha particles to selectively eradicate malignant tissue. The greater widespread clinical utility of 225Ac is hindered by radiotoxic side effects that result from detachment of the radiometal from its biological delivery vector. The design of ligands that effectively sequester actinium under biological conditions, however, has been impeded by a lack of fundamental knowledge of this rare, highly-radioactive element. The proposed work will launch, for the first time, a comprehensive investigation of the chemical and electronic properties of the element actinium in support of rational design of actinium ligands for medical use. The chemical hardness, coordination number, and covalency of actinium ions in solution will be determined. Preliminary data obtained with the stable analog lanthanum and a heavier actinide (plutonium) reveal that fluorescence spectroscopy and grazing incidence X-ray absorption spectroscopy can probe these important chemical properties while exhibiting high sensitivity for the detection of the extremely low concentrations of actinium available for investigation. In addition, density functional theory (DFT) calculations will be employed to interpret the spectroscopic data. With understanding of the electronic structure and basic chemical properties of actinium, rational ligand design will be pursued in the service of clinical use of 225Ac-containing compounds, which we hope can save lives.

Benefit to National Security Missions

An improved understanding of the fundamental chemistry of actinium is essential to the clinical use of 225Ac for the therapeutic treatment of disease, in particular malignant disease. The nature of the facilities required to produce large amounts of 225Ac ensures that only domestic facilities currently operated by the Department of Energy Office of Science have the capability to meet anticipated research demand for the isotope, if it can be shown functional in viable clinical trials. Among the National Institutes of Health's primary mission is the fight against cancer, and 225Ac's potential to incite a paradigm shift in treatment of this destructive disease in many forms is well recognized by the scientific community. We anticipate that our research into fundamental principles that govern the chemical bonding of actinium to biological vectors will catalyze further biological research, clinical trials supported by DOE isotope production infrastructure, and ultimately widespread, curative use of 225Ac in patients.

Progress

Efforts are underway to understand the chemical properties of actinium (Ac) employing the long-lived isotope, 227Ac (t1/2 = 21.77 years). This knowledge is necessary to design novel ligands that can bind actinium to biological agents, allowing 225Ac to selectively target diseases such as cancer and infectious pathogens after injection into the patient. For this research, we have utilized a supply of 10 mCi of 227Ac, which corresponds to only 0.61 µmol or 140 µg of actinium. The small quantities available, combined with challenges associated with handling this highly radioactive element, necessitate a method of chemical analysis that is sensitive to low concentrations. Fluorescence spectroscopy, a technique commonly used for the detection of sub-micromolar concentrations of analyte, has been explored as a method for probing Ac3+ chemistry. Because Ac3+ is spectroscopically silent, an organic fluorophore with a metal ion-binding unit is needed to relay information. Furthermore, to extract useful data regarding the Ac3+ ion, a fluorescent sensor is required whose response varies along with the bound metal ion. These efforts led to the design and synthesis

of a new ligand, Ds-DOTAM. This ligand bears a macrocyclic metal ion-binding unit and a fluorescent dansyl group. The oxygen atom of the sulfone group of dansyl can interact with a metal ion, perturbing its photophysical properties. The properties of the ligand and baseline fluorescence measurements were first collected using lanthanum (La) as a surrogate. Indeed, addition of La(NO3)3 to Ds-DOTAM leads to a red-shift in the absorbance maximum of the ligand and a quenching of the dansyl emission. Density Functional Theory (DFT) calculations were performed to understand the molecular orbital energies as well as the effect of metal binding. These results indicated that this red-shift arose from a stabilization of the lowest unoccupied molecular orbital (LUMO), primarily due to an electrostatic interaction of the M3+ ion with the dansyl sulfone group. The addition of Ac(NO3)3 resulted in similar but not identical spectroscopic changes as observed with La. The UV-vis absorbance spectrum is also shifted, although interpretation is complicated by signal from an excess of NO3- ion carried over from radiochemical separation procedures. These data, interpreted with the help of theoretical calculations, suggest that the actinium ion is slightly softer than its lanthanum counterpart and may prefer a slightly different coordination environment.

Although the fluorescence spectroscopic results revealed that both La3+ and Ac3+ interact with Ds-DOTAM, the precise nature of that interaction will certainly be different for the two ions, which possess substantially different ionic radii. To ascertain structural aspects of actinium chemistry, we are also performing X-ray absorption near edge spectroscopy (XANES) and extended X-ray absorption fine structure (EXAFS) measurements using high intensity synchrotron sources coupled to fluorescence detection methods. The use of 2 mCi of 227Ac in 0.45 mL (270 µM) gave a spectrum with a sufficiently large signal-to-noise ratio for the XANES and EXAFS measurements. For this particular sample, Ac3+ was dissolved in 0.1 M ammonium acetate pH 5 buffer. These conditions mimic those used to create 225Ac-labeled antibodies for medical use and can therefore shed light on the speciation and nature of Ac3+ prior to conjugation. Preliminary analysis of solutions showed the inflection point for the Ac LIII-edge at ~15,870 eV, which is the first XANES measurement made on the element actinium. Future XANES experiments are underway using Ac's LIII-edge to learn about Ac's electronic structure and chemical bonding tendencies. It is possible that substantial edge-shifts (of 2 to 3 eV) may be observable and used to quantify orbital mixing in the Ac–ligand interaction. The first ever actinium EXAFS spectrum was also collected using our small stock of 227Ac. Preliminary analysis of those data suggested that the major species present in solution was Ac(O2CMe)2(H2O)3. Currently, we are working in close collaboration with theorists conducting DFT and molecular dynamics calculations to confirm this EXAFS interpretation of novel Ac chemical structure. These X-ray absorption spectra of actinium will enable, for the first time, the determination of Ac–ligand interatomic distances and coordination numbers in the solution phase. Our results will find their way into textbooks, as they provide information useful in developing actinide separations schemes and biological delivery agents for alpha radiotherapy.

Future Work

In year two, we will start the second phase of our study using organic fluorophores to bind actinium. We will use the photophysical response of a new set of Ac-chelating ligands, lariat crown ethers, to investigate Ac's preferred electronic structure. These cyclic ligands contain an additional side group (the lariat) to assist with cation binding. They will be additionally modified with a fluorophore-containing group to give an appropriate spectroscopic signal as a probe. Stable, surrogate lanthanum compounds will provide initial insight into analogous lanthanide electronic structure and experimental method development using the necessarily small concentrations of sample Ac. Titrations will be performed to determine the relative thermodynamic stability of novel La and 227Ac compounds we consider for this work. Promising compounds will be modeled with DFT and compared to spectroscopic data, allowing confirmation of electronic structure information, and ultimately to select ligand systems that are most likely to provide clear information on fundamental chemical properties of Ac.

We will also continue to expand the XANES and EXAFS data sets for other simple actinium complexes. We have already validated our ability to analyze extremely low solution concentrations of actinium. Building on the initial acetate data set, we will define the coordination chemistry of 227Ac with foundational ligand sets (e.g. H2O, Cl, Br, I). These measurements will provide a basis for the analyzing more complicated actinium compounds ligated by the lariat crown ethers or other more complex ligands.

Conclusion

The proposed work will elucidate fundamental chemical properties of the element actinium to enable the rational design of actinium-225 complexes for targeted alpha therapy. A better understanding of the element, actinium, will allow application of the specific therapeutic isotope, actinium-225, in medicine for treatment of cancer.

Publications

Wilson, J. J., E. R. Birnbaum, E. R. Batista, R. L. Martin, and K. D. John. Synthesis and Characterization of Nitrogen-Rich Macrocyclic Ligands and an Investigation of Their Coordination Chemistry with Lanthanum(III). 2015. INORGANIC CHEMISTRY. 54 (1): 97.

Wilson, J. J., Ferrier, Radchenko, J. R. Maassen, J. W. Engle, E. R. Batista, R. L. Martin, F. M. Nortier, M. E. Fassbender, K. D. John, and E. R. Birnbaum. Evaluation of nitrogen-rich macrocyclic ligands for the chelation of therapeutic bismuth radioisotopes. 2015. NUCLEAR MEDICINE AND BIOLOGY. 42 (5): 428.

Label-Free Measurement of Single Cells by Impedance Cytometry in a Microfluidic Device

Babetta L. Marrone
20130239ER

Abstract

Microfluidic-based devices have important applications in biomedical diagnostics and bioprocess monitoring, as well as in biotechnology research such as sequencing and protein engineering. The main objective of this project was to design, build, and test a microfluidic sensor device for counting and measuring cells. Cells will be manipulated in the device using Surface Acoustic Wave (SAW) technology. Sensing will be based on single cell impedance cytometry, an emerging technology that simply measures the current displaced by a cell as it flows between two electrodes. The measurements are label-free, and provide accurate information about cell size and direct dielectric properties that are directly related to functional state, such as lipid production or proliferation stage. As part of this research we will determine the underlying cell properties that contribute to acoustic contrast between the cell and medium; and the underlying cell properties that contribute to differences in impedance signals between cells. Model biological systems to be studied will include: sensing and separating red and white blood cells and sensing of algae cells based on lipid content. The measurements made using the sensing devices will be validated using standard flow cytometry methods. The primary application that will be pursued in the future using this technology is monitoring cell growth and lipid content in microalgae during cultivation. The technology will have primary impact on the development of advanced biofuels and bioproducts as supported by the DOE, Office of Energy Efficiency and Renewable Energy, Bioenergy Technologies Office.

Background and Research Objectives

Single cell impedance cytometry is emerging as a leading edge approach for non-destructive, label-free analysis of informative cell features because of its technical simplicity [1] as well as its versatility, i.e. its potential to be applied to a wide range of particle types and a broad set of applications. Impedance cytometry simply measures the current displaced by a single cell as it flows between two electrodes. It has been demonstrated for cell counting, and for discriminating cells on the basis of size, and differences in cell morphology [2]. Cell physical parameters like membrane capacitance can be calculated from impedance measurements. By varying frequencies, information about cell volume, and cytoplasm conductivity and permittivity can be obtained. Single cell impedance analysis has been applied to measurement of cell viability, and cell stage analysis [2-4]. It has also been used for measuring heterogeneity in bacterial populations applied to bioprocess monitoring [5] and to differentiate between normal red blood cells (RBCs) and RBCs infected with a parasite [6] using phase differences. The impedance response of cancer cells and comparable normal cells were found to be different in magnitude and phase [7] and three white blood cell populations were discriminated based on their impedance responses[8]. In some examples, measured differences in impedance response have been directly traced to re-structuring of the cytoskeleton, a process that is associated with disease states [9-16].

Impedance analysis is relatively easy to implement on a microfluidic device, using integrated digital electrodes [1-3]. However, accurate measurement of cell properties in a microfluidic channel depends on consistent positioning of the particle within the channel detection volume [17]. Traditional methods of focusing single cells in a microchannel use hydrodynamic focusing to confine and direct a slower flowing (sample) stream by a faster flowing sheath stream [18]. A newly demonstrated approach to cell focusing in a microfluidic channel is using Surface Acoustic Wave technology (SAW), which propagates a sound wave across the surface of a microchannel. The SAW effect is an immediate and gentle means of manipulating cells to focus them into the measurement volume or to deflect them for sorting. Shi et al. [19] reported using standing SAW as a focusing mechanism in a microfluidic device, using interdigital transducers (IDTs) patterned on a piezoelectric substrate to generate the

acoustic field. In a recent Review by Xuan et al. [20] on different methods of particle focusing in microfluidic devices, the primary advantage of SAW to manipulate particles was that the channel size can be flexible to accommodate a wide range of particle sizes from 1µm (bacteria) to large particles (800µm droplets) or cell clusters (e.g. circulating tumor cell aggregates) or larger organisms in an algae culture, such as rotifers. Another advantage is that by using SAW, sheath fluid is eliminated, thus reducing consumable cost and waste from the device. Cheung et al. [4] report 11 papers on microfluidic particle focusing for impedance sensing flow cytometry, but none use SAWs. This indicates that there is a significant opportunity to optimize microfluidic impedance cytometry by combining this technology with SAW technology for enhanced particle focusing and sorting.

Scientific Approach and Accomplishments

There are three parts to the R&D approach in this project:

- Design/simulate and build a microfluidic device combining SAW (for focusing and sorting) with impedance sensing of cell properties.
- Use the device to study and validate the impedance sensing and develop signatures by attributing the measurements to specific cell properties.
- Demonstrate the approach through application to a relevant model system; we focused on counting and measuring microalgae cells during cultivation.

Figure 1 shows a composite of the project, including the concept of impedance sensing, the expected signals from impedance sensing, the original concept of the impedance sensor combined with acoustic separation in the same microfluidic device; and an impedance spectrum from a single particle in our device.

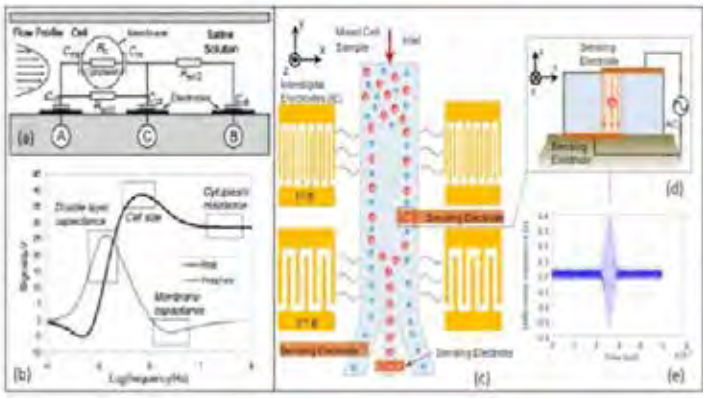

Figure 1. (a) Differential impedance circuit concept, and (b) impedance spectrum [21] (Gawad et al, Lab on a Chip 1 (2001) 76). (c) LANL's SAW concept for cell focusing and separation with impedance measurement. (d) Top/bottom electrode arrangement for accurate impedance measurements. (e) Time resolved differential impedance measurement by this team of a single particle at a single frequency.

Technical milestones

Lab-on-a-Chip Device Development/Demonstration

- Successfully made microfluidics devices using a soft lithography approach with Interdigital Electrodes (IE) via metal deposition and masking, in collaboration with LANL's Center for Integrated NanoTechnology (CINT). We finally settled on a device manufactured commercially and made to our specifications, from Micronit Microfluidics company (http://www.micronit.com/), Figures 2 and 3.
- Used IEs to generate Surface Acoustic Waves (SAWs) for particle/biological cell separation and translocation.
- Measured differential impedance particle/cell signals with and without acoustic focusing for detection based on size.
- Measured impedance spectroscopy for particle/cell property assessment with and without acoustic focusing.
- Integrated the microfluidic device with the CCD camera for full confirmation of measurement integrity.

Figure 2. The microchannel device with impedance electrodes integrated and fabricated by Micronit using our design.

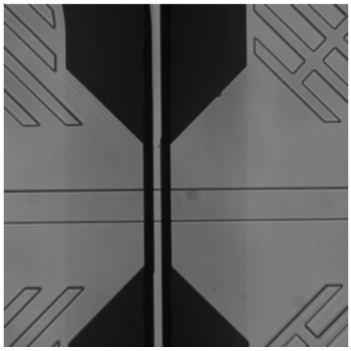

Figure 3. Close-up of an impedance electrode array. The channel is running horizontally in this image. There are 4 electrodes; the two shown above are on top of the channel. The two below are on the bottom surface of the channel. Both sets extend across the channel. The reference electrode is further upstream (out of vision).

Data Analysis

- Developed a MATLAB code to identify single cell spectroscopic absorption/scattering measurements from an imaging flow cytometer as candidates for eliminating the use of chemical labels and tags in measurement of algae lipid accumulation.
- Developed MATLAB and LabView codes to measure differential impedance amplitude at single (and multiple) frequencies, to establish the basis for impedance particle/cell size and property measurements in our microfluidic devices.
- Modeling: Constructed a COMSOL model of the electrical field in a fluid-filled channel between two electrodes.

Applications

- Demonstrated 1-D particle/cell focusing in a microchannel by surface acoustic waves generated from straight interdigital transducers (SIDT)
- Demonstrated bacteria/blood cell separation in a microfluidic device by surface acoustic waves generated from SIDTs.
- Developed particle/biological cell detection and size measurements by single-frequency impedance measurement in a microfluidics device.
- Investigated impedance spectroscopy (multi-frequency) on a particle/cell in a microfluidic device.

Impact on National Missions

This script imports flow cytometry data and searches this data to discover label-free signatures. The script takes as an input two sets of training data: one with fluorescent labels for a chemical of interest (protein, RNA, lipids, etc.) and one without any labels. The script then searches for a linear or quadratic combination of the label free measurements that can reproduce the intensity distribution for the labeled target in the labeled cells. Once the script has learned the combination of features that predict the target features for the unlabeled cells, this prediction power is tested on additional data sets that the user can provide. The analysis to discover signatures in labels-free measurements is based upon simple and well known linear regression approaches. The script can utilize a Genetic Algorithm (provided by MathWork's MATLAB) to automatically remove features that are not informative or misleading for the prediction of the target feature in the unlabeled cells. The script provides a Graphical User Interface for the user to manually add and remove features to be used in the label-free parameter identification. The script allows the user to change the file name for the inputs to the training and testing data. The script works in its most basic functionality, and an example data set is included which utilizes algae cells that increase their lipid content during nitrogen starvation. The script is not stand-alone. It requires Mathwork's Matlab and several routines in the Matlab Global Search Toolbox, Parallel Processing Toolbox, and Optimization Toolbox.

The code is highly preliminary, and a users manual and several other functions need to be added.

The outcome of this project is highly relevant to both the Energy Security and National Security missions of the Laboratory. We developed a new measurement modality and new set of signatures for investigating and identifying biological particles in real time for high-impact applications in biofuel production, as well as medical diagnostics, drug discovery and screening, toxicology testing, and biomedical research. The greatest impact of this simple, label-free, nondestructive approach is that it can be implemented on small, low cost platforms, thus enabling introduction of real-time sensing and measurement technologies into new fields of bioenergy and medical diagnostics.

The research supports LANL's Signature of Science pillar by developing new signatures of cell phenotypes based on their intrinsic physical properties. The project has helped to build a new capability at LANL in Bioengineering and Microengineering. The capability to design and test lab-on-chip devices is crucial for increasing our competitiveness for external funding opportunities from DOE, Bioenergy Technologies Office (for algae cultivation monitoring); and the National Institutes of Health and the Department of Defense, who are actively seeking to develop miniaturized sensor devices for biomedical and biosecurity applications

in support of National and Global Security mission challenges.

The team has relevant intellectual property under development. We will actively pursue technology transfer to industry, working with the Feynman Center for Innovation and directed to both the biofuel and medical diagnostic industries.

References

1. Capua, R. Di. Towards the realization of label-free biosensors through impedance spectroscopy integrated with IDES technology. 2012. Eur. Biophys. J.. 41: 249.

2. Sun, T., and H. Morgan. Single-cell microfluidic impedance cytometry: A review. 2010. Microfluid. Nanofluid.. 8: 423.

3. Gou, H. L.. Label-free electrical discrimination of cells at normal, apoptotic, and necrotic status with a microfluidic device. 2011. J Chromatography A . 1218: 5727.

4. Cheung, K.. Microfluidic impedance-based flow cytometry. 2010. Cytometry Part A . 77A: 648.

5. David, F.. Viability and membrane potential analysis of Bacillus megaterium cells by impedance flow cytometry. 2011. Biotechnology and Bioengineering . 10: 483.

6. Kuttel, C.. Label-free detection of Babesia bovis infected red blood cells using impedance spectroscopy on a microfabricated flow cytometer. 2007. Acta Tropica. 102: 63.

7. Han, A.. Quantification of the heterogeneity in breast cancer cell lines using whole-cell impedance spectroscopy. 2007. Clin. Cancer Res.. 13: 139.

8. Holmes, D.. Leukocyte analysis and differentiation using high speed microfluidic single cell impedance cytometry. 2009. Lab on a Chip. 9: 2881.

9. Lincoln, B.. Deformability-based flow cytometry. 2004. Cytometry Part A . 59A: 203.

10. Suresh, S.. Connections between single-cell biomechanics and human disease states: Gastrointestinal cancer and malaria. 2005. Acta Biomaterialia . 1: 15.

11. Suresh, S.. Mechanical response of human red blood cells in health and disease: Some structure-property-function relationships. 2006. J. Mater. Res. . 21: 1871.

12. Suresh, S.. Biomechanics and biophysics of cancer cells. 2007. Acta Biomaterialia . 3: 413.

13. Rosenbluth, M. J.. Analyzing cell mechanics in hematologic diseases with microfluidic biophysical flow cytometry. 2008. Lab on a Chip. 8: 1062.

14. Moutzouri, A. G.. Severe sepsis and diabetes mellitus have additive effects on red blood cell deformability. 2008. J. Infection. 57: 147.

15. Khismatullin, D. B.. The cytoskeleton and deformability of white blood cells. 2009. Current Topics in Membranes. 64: 47.

16. Diez-Silva, M.. Shape and biomechanical characteristics of human red blood cells in health and disease. 2010. MRS Bulletin. 35: 382.

17. Spencer, D., and H. Morgan. Positional dependence of particles in microfluidic impedance cytometry. 2011. Lab on a Chip. 11: 1234.

18. Golden, J. P.. Hydrodynamic focusing-A versatile tool. 2012. Anal. Bioanal. Chem.. 402: 325.

19. Shi, J. D.. Acoustic tweezers: Patterning cells and microparticles using standing surface acoustic waves (SSAW). 2009. Lab on a Chip. 9: 2890.

20. Xuan, X.. Particle focusing in microfluidic devices. 2010. Microfluid. Nanofluid.. 9: 1.

Publications

Ai, Y. e., and B. L. Marrone. Droplet translocation by focused surface acoustic waves. 2012. MICROFLUIDICS AND NANOFLUIDICS. 13 (5): 715.

Ai, Y. e., and B. L. Marrone. Separation of Biological Cells in a Microfluidic Device Using Surface Acoustic Waves (SAWs). 2014. MICROFLUIDICS, BIOMEMS, AND MEDICAL MICROSYSTEMS XII. 8976.

Ai, Y., C. K. Sanders, and B. L. Marrone. Separation of Escherichia coli bacteria from Peripheral Blood Mononuclear Cells (PBMC) using Standing Surface Acoustic Waves (SSAW). 2013. Analytical Chemistry. 85 (19): 9126.

Marrone, B. L.. Flow cytometry in algae biofuels and byproducts research. Invited presentation at 4th International Conference on Algal Biomass, Biofuels and Bioproducts. (Santa Fe, NM, 15-18 June, 2014).

Marrone, B. L., Y. Ai, and J. E. Coons. Cyto-AMP Cell Acoustic Manipulation Platform. 2014. R&D 100 Award, 2013 Nomination LA-UR-14-21909.

Munsky, B., S. Sellars, et.al. Automated label free classification of algal lipid accumulation. Presented at 4th International Conference on Algal Biomass, Biofuels and Bioproducts . (Santa Fe, NM, 15-18, June 2014).

A New Hypothesis to Explain the Variability of the Outer Radiation Belt: Can we Predict Post-storm Fluxes of Energetic Electrons Based only on Pre-storm Fluxes of the Lower-energy Population?

Gregory S. Cunningham
20130297ER

Abstract

Earth is surrounded by two radiation belts containing MeV 'killer' electrons that are trapped in earth's geomagnetic field. MeV electrons can deposit dose in sensitive satellite instruments, rendering those instruments or even entire satellites inoperable. Fluxes of MeV electrons in the outer radiation belt can vary by orders of magnitude during geomagnetic events driven by the sun, and the scientific community has a poor ability to predict the changes that are observed. An ability to reliably predict fluxes in the outer radiation belt driven by changes in the sun's output would be of great utility to satellite operators, who could anticipate and accurately attribute anomalies to space weather as opposed to a hostile attack by an adversary.

In our LDRD ER project, we tested a hypothesis that explains the variability of outer radiation belt MeV electron fluxes. The hypothesis was that outer-belt fluxes of MeV electrons are determined by the source population of lower-energy electrons that are convected earthward by electric fields, and diffused upward in energy (accelerated) through interaction with electromagnetic waves. Given the source population and intensity of electromagnetic waves, we believed that we could quantitatively predict the acceleration and hence the fluxes of MeV electrons that would result. Underlying assumptions in the hypothesis were that 1) MeV electrons are first wiped out at the start of the event, and 2) the effect of the electromagnetic waves that accelerate the lower-energy source population to higher energies can be predicted using quasilinear theory for specific events using an empirical model. The project was successful in showing that if the low-energy source population and intensity of electromagnetic waves is known, then the acceleration of the source population to MeV energies can be predicted for a specific event. Because the process of acceleration takes hours to days, this enables forecasting of the hazardous MeV population hours to days in advance, an important capability.

Background and Research Objectives

The radiation belt modeling community has a qualitative understanding of phenomena that can affect flux levels of MeV electrons in the outer radiation belt. Solar output ultimately delivers the energy needed to cause variability of MeV electron fluxes in the outer radiation belt, but the details are still being integrated into quantitative models. For many years, it was thought that inward radial diffusion of lower-energy electrons was the dominant energization mechanism that creates MeV electrons, and indeed the equilibrium two-belt structure of inner magnetospheric electrons was well-described by radial diffusion in the 1970's. However, our team at LANL argued in recent years that electrons in the outer belt must be accelerated locally by wave-particle interactions in order to produce the observed peaks in phase-space density (PSD) versus radial distance from earth, since radial diffusion can only produce a monotonically increasing PSD versus radial distance from earth [3]. Other groups had shown prior to our LDRD project that chorus waves were capable of accelerating electrons, and appeared to be the only effective mechanism for the degree of acceleration that is needed to produce the peaks in phase space density; however, it had not yet been proven with quantitative calculations that chorus waves were responsible for recovery of fluxes after dropouts during geomagnetic events. This is the hypothesis that we tested in the project.

Scientific Approach and Accomplishments

We were able to test the hypothesis that chorus waves are responsible for creating the MeV electron population in the outer belt during geomagnetic events using 1) event-specific measurements of the low-energy source population (100 keV electrons) and 2) event-specific measurements of the intensity of the chorus waves, to drive a LANL computational model called DREAM3D, which computes the temporal evolution of the phase space density of electrons in response to interactions of the electrons with ultra low-frequency (ULF) and very

low-frequency (VLF) waves that interact resonantly with the periodic motion of the electrons as they gyrate around field lines and drift around earth. The time-varying source population was measured by the MagEIS instrument on the Van Allen Probes mission (nee Radiation Belt Storm Probes), which was launched in August 2012 just prior to the start of the LDRD project. The measured source population was used as a time-varying low-energy boundary condition in the DREAM3D diffusion code. The event-specific intensity of chorus waves was inferred indirectly from measurements of precipitating low-energy electrons at low altitude provided by the Polar-Orbiting Environmental Satellite (POES), normalized to actual electromagnetic wave measurements at high altitude by the Van Allen Probes [2]. The wave intensities were extrapolated to all latitudes using statistical models binned by geomagnetic activity. Using the event-specific source population and wave intensities, we were able to show that the enhancement of MeV electrons that was observed by the Van Allen Probes during the October 2012 storm was due to acceleration by chorus waves, thus confirming our hypothesis [1]. We also showed that using a purely statistical model for either the source population or the waves does not produce the enhancement, making event-specific models critical to the successful test of the hypothesis.

Impact on National Missions

The work done in the LDRD ER project was an outgrowth of the Dynamic Radiation Environment Assimilation Model (DREAM) project, which began as an LDRD/DR ~10 years ago. DREAM has spun off several projects, including a $6M 18-month study of HANE impact on low-earth orbiting (LEO) assets that supported the development of the 3D diffusion code, DREAM3D, that was used in this LDRD ER project. The fact that, in this LDRD ER project, we were able to show that enhancement of MeV electrons following a geomagnetic storm is due to chorus waves, and that we can quantitatively predict the enhancement given event-specific information on the low-energy source population and chorus wave intensities, means that it may be possible to forecast the buildup of MeV electrons in the outer radiation belt a few hours to days in advance. Given LANL's heritage in space environment instrumentation on geosynchronous, GPS, and scientific satellites, the potential to use the data from these satellites to build a space weather prediction capability with DREAM3D would seem to be at hand, and we are actively pursuing funding to build this capability.

References

1. Tu, W., G. S. Cunningham, Y. Chen, S. K. Morley, G. D. Reeves, J. B. Blake, D. N. Baker, and H. Spence. Event-specific chorus wave and electron seed population models in DREAM3D using the Van Allen Probes. 2014. Geophysical Research Letters. 41 (5): 1359.
2. Chen, Y., G. Reeves, R. Friedel, and G. S. Cunningham. Global time-dependent chorus maps from low-Earth-orbit electron precipitation and Van Allen Probes data. 2014. Geophysical Research Letters. 41 (5): 755.
3. Tu, W., G. S. Cunningham, Y. Chen, M. G. Henderson, E. Camporeale, and G. D. Reeves. Modeling radiation belt electron dynamics during GEM challenge intervals with the DREAM3D diffusion model. 2013. Journal of Geophysical Research-Space Physics. 118 (10): 6197.

Publications

Chen, Y., G. D. Reeves, G. S. Cunningham, M. G. Henderson, and R. J. Redmon. Forecasting and Remote Sensing Outer-belt Relativistic Electrons from Low-Earth-Orbits. Geophysical Research Letters.

Chen, Y., G. Reeves, R. Friedel, and G. S. Cunningham. Global time-dependent chorus maps from low-Earth-orbit electron precipitation and Van Allen Probes data. 2014. Geophysical Research Letters. 41 (5): 755.

Cunningham, G. S.. Radial diffusion of radiation belt particles in non-dipolar magnetic fields. Journal of Geophysical Research-Space Physics.

Ripoll, J. F., J. M. Albert, and G. S. Cunningham. Electron lifetimes from narrowband wave-particle interactions within the plasmasphere. 2014. Journal of Geophysical Research-Space Physics. 119 (11): 8858.

Tu, W., G. S. Cunningham, Y. Chen, M. G. Henderson, E. Camporeale, and G. D. Reeves. Modeling radiation belt electron dynamics during GEM challenge intervals with the DREAM3D diffusion model. 2013. Journal of Geophysical Research-Space Physics. 118 (10): 6197.

Tu, W., G. S. Cunningham, Y. Chen, S. K. Morley, G. D. Reeves, J. B. Blake, D. N. Baker, and H. Spence. Event-specific chorus wave and electron seed population models in DREAM3D using the Van Allen Probes. 2014. Geophysical Research Letters. 41 (5): 1359.

Zheng, L., A. A. Chan, T. P. O'Brien, W. Tu, G. S. Cunningham, J. M. Albert, and S. R. Elkington. Effects of magnetic drift shell splitting on electron diffusion in the radiation belts. Geophysical Research Letters.

Multidisciplinary Studies of Long Non-coding RNAs: Towards a Structural Basis for RNA in Epigenetics

Karissa Y. Sanbonmatsu
20130319ER

Abstract

Epigenetics focuses on changes in gene expression, which are passed on to subsequent generations of cells without changing DNA sequence. The field has revolutionized traditional notions of genetics and inheritance, producing new insight into environmental response, cell differentiation, and hereditary disease. Two major modification events, site- specific DNA methylation and histone modification on chromatin, alter the gene expression profiles. Nevertheless, the specifics of how DNA and histone-modifying enzymes find these unique locations on chromatin remain a mystery. Long non-coding RNAs (LncRNAs or lincRNAs, pronounced 'link RNAs') have emerged in the past 2 years as major players in epigenetics, recruiting many factors to chromatin. These RNAs are interesting in their own right: they are as big as the ribosome, have unknown structure, and are mission critical for a large number of biological processes. The number of lncRNAs rivals the number of proteins, conjuring an image of a nucleus teaming with RNA-based molecular machines. Harvard and MIT have led the recent explosion in cell-biology studies of lncRNAs; however, to date, there are no structural studies. With our decade of experience in structural studies of the ribosome and state-of- the-art expertise in RNA biochemistry, LANL is in a prime position to lead this new, high impact field. We have recently published a large amount of preliminary data on lncRNA experiments taking the first steps in lncRNA structural studies. In this project, we will focus on four high impact systems and address fundamental unanswered questions:

(1) Are lncRNAs structured?, (2) Do they have subdomains?, (3) Where on lncRNAs do epigenetic proteins bind?, and (4) Do the binding domains contain a tertiary core?

An arsenal of innovative experimental and computational techniques (including SHOT-GUN chemical probing, structure-based molecular simulation, and in vivo single-molecule co-localization imaging) will help us lead this field, laying the structural foundation for lncRNA epigenetics.

Background and Research Objectives

RNA (ribonucleic acid),DNA's molecular cousin, is similar to DNA in composition; however, it often performs a function in the cell, unlike DNA, which is considered solely an information carrier. In all living systems, including humans and bacteria, the information for the blue print of the organism resides in DNA. The blue print is implemented by transferring the genetic information from DNA to RNA. Next, the genetic information is converted from the RNA into proteins, which make up the structures of the cells and perform the biochemistry. RNA has long been thought to mainly serve as a transferring medium, moving information from DNA to proteins. However, in the past five years, it has been found that the vast majority of the human genome (more than 90%) is converted into RNA, but never gets converted into proteins. It has been found that much of this RNA is in the form of long non-coding RNA (lncRNA, or 'link' RNA). These gigantic RNAs do not 'code' for protein, but instead are thought to have a function themselves: turning on and off other genes. The RNAs are often associated with epigenetics. Epigenetics has exploded in the past five years and is closely related to stem cell programming. In epigenetics, Larmarkian-like effects occur, where the environment modifies, but does not mutate DNA. These modifications are passed down to future generations of organisms. For example, babies undergoing extreme stress shortly after birth have an altered stress response, which is passed down to the grandchildren. While many long RNAs have been found to be critical for cancer, hereditary disease, brain function and development, the mechanism of long RNA action is not understood. We have successfully performed and published the first ever structural study of long RNAs and laid the foundation for mechanistic studies.

Scientific Approach and Accomplishments

We accomplished our goals. We were able to complete the first secondary structure of an intact long non-coding RNA, resulting in several publications and invited talks. We employed our novel shotgun secondary structure (3S) method, which did garner significant attention in the RNA community (especially at the recent RNA 2013 conference). In this method we perform several rounds of structural chemical probing. In chemical probing, a special reagent is added that only reacts with highly mobile nucleotides, allowing us to map which nucleotides are base paired in double helices and which nucleotides are single stranded. Thus, we perform 1 round of chemical probing on the entire long non-coding RNA. We then perform successive rounds on fragments of the RNA. If we obtain a match between signals for the full RNA and its fragments, this demonstrates that the fragments have a modular fold and comprise modular subdomains. By probing smaller and smaller fragments, we are able to determine the complete fold of the long noncoding RNAs, a hard problem, which has been long sought after. To verify the fold, we performed comparative studies.

We applied our structure technique (shotgun secondary structure) to several more long non-coding RNA systems. The first system is COOLAIR, a canonical epigenetic switch in plants that allows plants to flower only after prolonged exposure to cold. The second system is Braveheart, a long non-coding RNA that plays a key role in heart cell development. The third system is Gas5, which is critical for hormone signaling. To accomplish this, we transcribed the RNA for each system, denatured the RNA, folded the RNA and chemically probed the RNA. In chemical probing, a special reagent is added that only reacts with highly mobile nucleotides, allowing us to map which nucleotides are base paired in double helices and which nucleotides are single stranded. In this way, we determined candidate secondary structures of the long non-coding RNAs.

In the past year, we finalized the secondary structures of COOLAIR, Braveheart, and Gas5, which is critical for hormone signaling. We validated these folds in vivo in collaboration with Laurie Boyer (MIT) and Caroline Dean (John Innes Centre). We completed a study on a new system called HULC that is a long non-coding RNA thought to interact with microRNAs. The three manuscripts for the 3 systems are almost ready for submission.

In conclusion, we have performed the first structural study of long non-coding RNAs (ribonucleic acids). The only example of a large RNA complex whose 3-D structure has been solved is the ribosome, which took 3 decades of work. We took the first step in structural studies of long non-coding RNAs by determining the 2-D structure. For large systems, 2-D structures are impossible to accurately determine computationally due to the large number of permutations and possible structures. We have devised a novel experimental technique called SHOT-GUN structure determination. We used this to obtain the 2-D structure experimentally.

Impact on National Missions

We have produced preliminary data for NIH calls in cancer-related non-coding

RNAs and several calls for NIH's epigenomics program for epigenetic mark discover, including the role of noncoding RNAs in regulation of transcription (Jerome Garcia). The project is directly related to DARPAs CLIO Memory thrust, including "basic research towards use of epigenetic systems to report environmental events" (Cathy Cleland). It is indirectly related to DOE BER Biological Systems Science "Low dose radiobiology effects on epigenetic regulation". The ER project culminated with an invited talk at the Royal Society in England given September 29, 2015. In addition, a TEDxABQ talk was given for the general public in September 2014 which currently has ~500,000 views on YouTube. The talk was directly related to this ER project. These two presentations have helped raise the visibility of LANL in the life sciences.

Publications

Computational & Experimental Studies: Ribosomes, Riboswitches & Long non-coding RNAs. Invited presentation at Fourth Annual Summer Symposium on Cellular Dynamics of Macromolecular Complexes. (Montreal, May 2014).

Structural Studies of Intact LncRNAs in Plants and Mammals. Invited presentation at Long non-coding RNAs: Marching towards Mechanism Keystone meeting. (Santa Fe, March 2014).

Hayes, R. L., J. K. Noel, A. n. a. Mandic, P. C. Whitford, K. Y. Sanbonmatsu, Mohanty, and J. N. Onuchic. Generalized Manning Condensation Model Captures the RNA Ion Atmosphere. 2015. PHYSICAL REVIEW LETTERS. 114 (25).

Hayes, R. L., J. K. Noel, P. C. Whitford, Mohanty, K. Y. Sanbonmatsu, and J. N. Onuchic. Reduced Model Captures Mg2+ -RNA Interaction Free Energy of Riboswitches. 2014. BIOPHYSICAL JOURNAL. 106 (7): 1508.

Hayes, R. L., J. K. Noel, P. C. Whitford, Mohanty, K. Y. Sanbonmatsu, and J. N. Onuchic. Reduced Model Captures Mg2+ -RNA Interaction Free Energy of Riboswitches. 2014. BIOPHYSICAL JOURNAL. 106 (7): 1508.

Hennelly, S. P., I. V. Novikova, and K. Y. Sanbonmatsu. The

expression platform and the aptamer: cooperativity between Mg2+ and ligand in the SAM-I riboswitch. 2013. NUCLEIC ACIDS RESEARCH. 41 (3): 1922.

Novikova, I. V., A. Dharap, S. P. Hennelly, and K. Y. Sanbonmatsu. Shotgun secondary structure determination of long non-coding RNAs. 2013. Methods. 63 (170): 1.

Novikova, I. V., S. P. Hennelly, C. S. Tung, and K. Y. Sanbonmatsu. Rise of the RNA machines: Exploring the structure of long non-coding RNAs. 2013. Journal of Molecular Biology. 425 (19): 3731.

Novikova, I. V., S. P. Hennelly, and K. Y. Sanbonmatsu. Do lncRNAs have secondary and tertiary structure?. 2012. RNA BIOLOGY. 9 (12): 1398.

Novikova, I. V., S. P. Hennelly, and K. Y. Sanbonmatsu. Structural architecture of the human long non-coding RNA, steroid receptor RNA activator. 2012. NUCLEIC ACIDS RESEARCH. 40 (11): 5034.

Novikova, I. V., S. P. Hennelly, and K. Y. Sanbonmatsu. Sizing up long non-coding RNAs: Do lncRNAs have secondary and tertiary structure?. 2012. Bioarchitecture. 2 (6): 189.

Novikova, I. V., S. P. Hennelly, and K. Y. Sanbonmatsu. Experimentally determined secondary structures of cancer-related long non-coding RNAs. Invited presentation at 245th ACS National Meeting & Exposition. (New Orleans, 7-11 April, 2013).

Novikova, I. V., S. P. Hennelly, and K. Y. Sanbonmatsu. Tackling Structures of Long Noncoding RNAs. 2013. INTERNATIONAL JOURNAL OF MOLECULAR SCIENCES. 14 (12): 23672.

Sanbonmatsu, K. Y.. Rise of the RNA Machines: Long Non-Coding RNAs. Invited presentation at 10th Horizons in Molecular Biology Conference International. (Max Planck Institute, Gottingen, Germany, 9-12 Sept. 2013).

Sanbonmatsu, K. Y.. Integrating simulations and experiments of the SAM-I riboswitch. Invited presentation at RNA Dynamics. (Telluride, CO, 22-26, July 2013).

Sanbonmatsu, K. Y.. Large-scale simulations of biomolecular machines. Invited presentation at Biosupercomputing. (Tokyo, Japan, Dec. 2012).

Sanbonmatsu, K. Y.. Understanding the atomistic mechanism of magnesium effects of RNA dynamics. Invited presentation at Mini-symposium on Modeling, Simulation and Function of Biomolecular Assemblies.. (University of Tokyo, Tokyo, Japan, Nov. 2012).

Sanbonmatsu, K. Y.. Dynamics of riboswitches: Molecular simulations. 2014. BIOCHIMICA ET BIOPHYSICA ACTA-GENE REGULATORY MECHANISMS. 1839 (10): 1046.

Sanbonmatsu, K. Y.. Towards structural classification of long non-coding RNAs. To appear in Biochimica et Biophysica Acta (BBA)-Gene Regulatory Mechanisms. 1 (1): 1.

Sanbonmatsu, K. Y.. Structural architecture of long non-coding RNAs in plants and animals. Invited presentation at Long non-coding RNAs: evolution of new epigenetic and post-transcriptional functions. (Royal Society, UK, 28-29 Sept. 2015).

How Trees Die: Multi-scale Studies of Carbon Starvation and Hydraulic Failure during Drought

Sanna A. Sevanto
20130442ER

Abstract

In this project we have developed a portable Nuclear Magnetic Resonance (NMR) system for measuring changes in tree water content in field conditions, and used the system to monitor water dynamics in living trees during drought and a leaf senescence-bud break cycle. The system uses light and inexpensive electromagnets instead of permanent magnets and operates at ultra-low magnetic fields (<μT). These features allow operation in the natural setting and environment of trees, and use of the system with other instrumentation without interference. We have developed a temperature correction protocol for the NMR signal to allow operation without external temperature control, and successfully used the system for measuring plant water uptake simultaneously with neutron radiography visualization of water movement in trees, as well as leaf gas exchange and diurnal stem diameter variation measurement. The visualization experiments confirmed that the majority of our NMR signal results from water moving fast in the conduits of the xylem, the tissue specialized in water transport. These experiments also led to identification of a new parameter, hydraulic conductivity between the xylem and phloem (tissue responsible for carbohydrate transport), that seems to be a key to identifying the most likely tree mortality mechanism during drought. Mortality mechanisms influence the expected lifetime under stress, and therefore identifying them improves predictions of forest mortality. Our drought experiments show that the NMR system can detect gas-filled water conduits in the xylem, but the arid-zone tree species that we used do not allow gas bubble formation in their xylem on a regular basis at an observable scale. Gas bubble formation in the water conduits is a hypothesized mechanism for tree mortality during drought. When excessive it could lead to a catastrophic failure of the water conducting system and consequent mortality of trees. Species at moist environments, however, can also use it as an extra water reserve to boost photosynthesis in a controlled manner during short drought episodes. Our species, adapted to low and unpredictable precipitation, do not use this extra reserve, but conserve water whenever possible.

Background and Research Objectives

Vegetation mortality events are observed and predicted to worsen with future climate [1], but our ability to predict where and when these could occur is rudimentary [2]. At the heart of this incapability is a lack of basic understanding of fundamental physiological processes relating water and carbon use and transport to plant function and mortality [3] due largely to a lack of tools to monitor these processes in intact plants [3, 4]. The key metabolic and hydraulic failure mechanisms leading to plant mortality have been identified theoretically [3, 4], but tests have been impossible due to a lack of non-invasive measurement techniques. Revealing the mechanisms and irreversible processes leading to plant mortality requires a non-invasive method that simultaneously detects changes in water and carbohydrate content of the key tissues, namely the xylem (water transport tissue) and the phloem (sugar transport tissue). These tissues strongly interact in a functional plant, but they operate under opposite pressure gradients and invasive measurements alter their state and operation, affecting the results obtained.

NMR and MRI are ubiquitous tools for non-invasive studies of soft-tissue anatomy and function in medicine and biology [5]. Atomic nuclei possessing an odd number of nucleons (e.g. 1H or 13C) can be magnetized (polarized) in an externally applied field, and will emit and absorb electromagnetic radiation at a frequency specific to the isotope and the strength of the applied magnetic field. By manipulating this magnetization, one can non-invasively detect and analyze the chemical structure of materials. The frequency of the NMR signal depends on magnetic field strength. Thus a magnetic field gradient can be used to spatially encode the NMR signal and produce structural images (MRI) or track the move-

ment of materials. However, because the strength of the NMR signal is proportional to the applied magnetic field, typically NMR is performed in very high (> 1T) magnetic fields requiring specialized permanent or superconducting magnets housed in buildings rendering the technique somewhat restrictive for in vivo applications with plants. In laboratory conditions NMR and MRI have been used to non-invasively study the distribution and transport of water in different plant tissues [6, 7]. There has also been growing interest in specially designed "plant focused" systems that adapt to the plant, maintaining a vertical geometry and not inhibiting the plant's access to light [8, 9] but all these systems still require rather large and exotic high strength permanent magnets (to increase signal) that make it difficult to measure many plants (or locations on a plant) simultaneously for high throughput studies, or studies in the greenhouse or field.

Our goal was 1) to develop the Ultra-Low-Field (ULF) NMR technique so that we can accurately quantify water and carbon dynamics from tissue level to whole-plant scales in the greenhouse and in the field over time scales from minutes to months; and 2) to use this tool together with traditional plant physiological measurements to test hypotheses about water allocation during drought and progress of plant mortality.

Scientific Approach and Accomplishments

To reach our goals we employed a three-stage process. At the first stage we developed the special tree NMR system (Fig 1), calibrated it against known water content changes in stems of different tree species, and developed a temperature correction model for the signal [10].

The temperature of the magnet as well as the sample affects the NMR signal strength. Therefore, NMR measurements are usually done in temperature-controlled environments where the magnet is cooled actively. We aimed at building a portable NMR system for field use, and a cooling system would have been impractical adding to the power demands in the field. Natural temperature cycles thus affected our signal. These cycles correlate with any plant physiological responses, such as stomatal opening and transpiration rate that depend on temperature or incoming radiation making separating the temperature-induced part of the NMR signal from the plant physiological response essential if NMR is to be used for plant physiological studies. To characterize the temperature responses of our system, we attached a second solenoid near the detector and applied a constant AC signal to it. By observing the variation in this test signal over one week, we created a temperature correction function that adds the linear temperature responses of our electronics to the known inverse proportionality of the NMR signal strength to sample temperature in the natural temperature range [11]. Using this temperature correction we are now able to separate the plant physiological signal from the temperature signal and detect stomatal closure in plants under drought (Fig 2) as long as the air temperature is measured simultaneously with NMR.

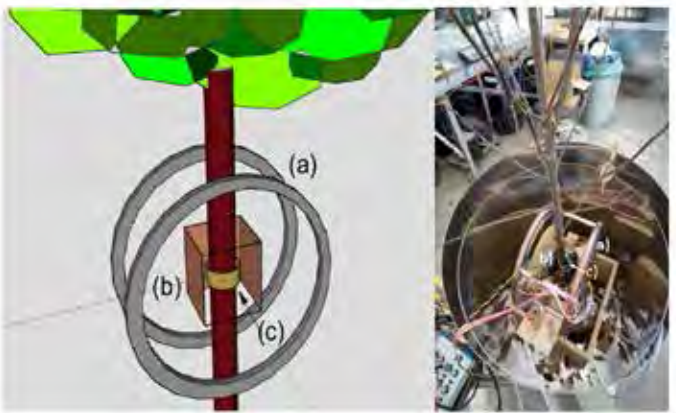

Figure 1. A schematic presentation and a photograph of our low field NMR system for measuring water content changes in trees shows (a) the 41 cm diameter Helmholtz coils which produce the magnetic field; b) copper shielding used to block radio frequency (rf) noise with one panel removed for clarity; c) the solenoid which both excites the 1H nuclei and detects the rf NMR signal their relaxation produces. The solenoid is wrapped around a former on the tree.

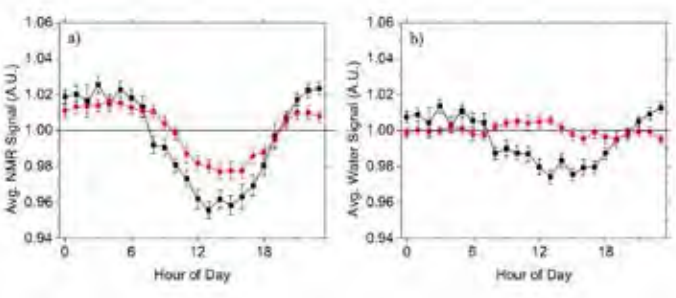

Figure 2. The average diel NMR signal without temperature correction (a) and with temperature correction (b) for a well watered (black line) and water limited (red line) period in our greenhouse experiments. Without temperature correction, the water-limited signal resembles well-watered signal contradicting the information on water transport and use rates measured with other plant physiological method. Once temperature correction is applied, the water-limited period clearly shows no changes in water content supporting the data obtained with other plant physiological measurements.

At the second stage, we focused on improving our system to provide information on the contributions of xylem and phloem tissues, and water bound to the cell walls vs. water moving freely in the conduits. Water, first allocated to phloem tissue and then taken out to support xylem func-

tion as drought progresses, could be an indicator of when the tree becomes dysfunctional, even before visible signs of degradation, such as leaf browning or wilting, appear [12]. Changes in proportions of bound and free water in the xylem could be indicators of bubble formation in the water conduits. Excessive bubble formation during drought is one of the hypothesized mortality mechanisms of plants, but currently there are no methods for detecting this non-destructively in field conditions. During drought, bubble formation in xylem conduits (cavitation) could become excessive if soil water availability does not match transpiration rate. The bubbles could block the water pathway from the soil to the leaves and lead to a hydraulic failure and mortality of the plant [13].

In NMR the relaxation of magnetization after excitation can be described by a two-component exponential decay function with two different time constants. The shorter time constant (T1) is related to the proportion of water bound to the cell walls or living cells, the longer time constant (T2) reflects the amount of freely moving water in the conduits [14]. Changes in these time constants thus contain information on water distribution in the sample. They also could contain signals of bubble formation in the xylem, which would both reduce the signal strength (fewer hydrogen atoms in the sample) and reduce the amount of free water in the sample.

To measure these time constants, we improved our system by increasing the magnetic field strength so that the time constants could be determined separately. We also built a replica of the system for short experiments, while the first system was used for long-term drought experiments in a greenhouse and in the field (see stage 3 below).

In the short-term experiments we measured water movement in branches of pinon pine and one-seed juniper simultaneously with our NMR system, leaf gas exchange measurements and neutron radiography at Paul Scherrer Institute in Switzerland and at LANSCE in Los Alamos. To calibrate our detection limits for bubble formation, we also used a surfactant to promote bubble formation in the conduits [15]. In the neutron radiography measurements we used heavy water (D2O) as a tracer that both NMR and neutron signal intensity react to. Pinon pine and one-seed juniper were selected for these experiments because they are two co-existing species that have a very different stomatal response strategy to drought. Pinon pine closes stomata very early during drought, allowing very little variation in xylem hydration state. One-seed juniper, on the other hand, keeps the stomata open longer during drought and allows its xylem to dry out and theoretically risks more bubble formation in its conduits [13]. These strategies should be reflected in water distribution and tissue anatomy of these plants [16].

Combined with x-ray tomography analysis of sample anatomy, performed at Paul Scherrer Institute, these experiments showed that the majority of our NMR signal comes from water in the xylem (Fig 3). They also indicated that, as predicted by our theoretical work on hydraulic coupling between the xylem and the phloem [16], pinon pine has a higher hydraulic conductivity between the xylem and the phloem than one-seed juniper (Fig 3). This is in line with the stomatal control strategy of transpiration of these species. One-seed juniper that allows xylem dehydration during drought protects the living phloem cells from turgor loss with a low hydraulic conductivity between the xylem and the phloem [16]. These results also show that the hydraulic conductivity between the xylem and the phloem is one of the key parameters to understanding the interaction of carbon and water transport in plants, and the susceptibility of the plant to different mechanisms of mortality during drought [16]. Our approach, which combined NMR and neutron radiography measurements, allows, for the first time, direct, in-vivo measurements of this parameter, which is very difficult to measure with traditional methods [17, 18]. Our tests for detecting bubble formation in the branches were inconclusive. We managed to produce a decline in the NMR signal from a branch using the surfactant once, but that signal was not strong enough to be reflected in the neutron radiography images, and despite several re-trials, we did not manage to reproduce the result in NMR.

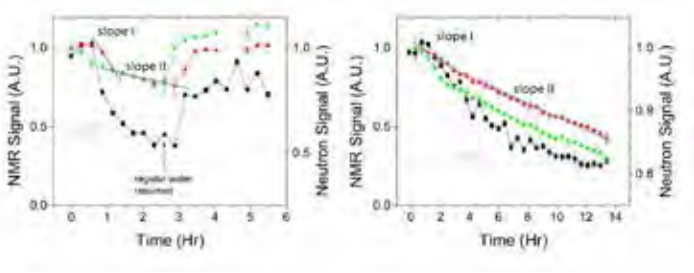

Figure 3. The NMR (black) and neutron (green measured below and red above the NMR detector coil; see Figure 4) signal intensity for juniper (a) and pinon (b) branches. In both cases the signal intensity declined when D2O replaced H2O in the tissues. The NMR signal saturated at the low level (47% of the original in juniper and 27% in pinon) in both species while the neutron signal did not saturate in pinon even after 14 hours of experiment. The neutron signal is directly proportional to sample thickness whereas the NMR signal is focused on the location of maximum magnetic field strength. The difference in saturation of these signals indicates that the majority of the NMR signal originates at the water conductive tissue (xylem), while the neutron signal sees the living tissue (bark and phloem) surrounding the xylem. Two different slopes representing two compartments of water can be identified in the decline of the neutron signal for both spe-

cies. The first one (slope I) represents fast filling compartment in the xylem; the second one slow filling in the living cells. In juniper the first slope is much steeper than in pinon suggesting lower hydraulic conductivity between xylem and phloem tissues.

To further study the capabilities of NMR for detecting bubble formation in the xylem we performed experiments with saturated and unsaturated cellulose sponges with known water content using a powerful commercial NMR system (NMR-MOUSE®, Magritek, San Diego, CA) to allow for higher resolution in time constant determination. These experiments revealed that separating the effects of bubble formation from the effects of elastic shrinkage in the NMR signal amplitude or time constants requires very large scale bubble formation to occur. Tree stems are elastic and shrink and swell diurnally with changing transpiration rate [19]. This serves as elastic water reserve, balancing any mismatch of transpirational demand and water availability from the soil. If this reserve is consumed, and the soil water availability does not match the transpiration rate, trees risk hydraulic failure (cavitation in xylem conduits). On the other hand, some bubble formation, if controlled and repairable, can act as an extra water source for the plant and boost photosynthetic productivity during short periods of drought [20]. The balance between severity of, and benefit from, bubble formation is one of the hot debate topics in plant physiology and vegetation mortality [4]. Unfortunately, our experiments showed that studying the balance with ULF-NMR is not straight forward, and if anything is detected, bubble formation has to be so excessive that the tree is very close to death already.

At the third stage, we conducted long-term experiments in a greenhouse and in the field to test our system and demonstrate the capability for long-term measurements in natural environments. We performed drought-rewatering experiments on aspen trees to investigate indicators of physiological changes in water and carbon allocation in the NMR signal. We also continued tackling the question whether bubble formation could be detected with our system by combining NMR with continuous stem diameter variation measurements. Stem diameter variations are known to follow a diurnal cycle and correlate strongly with transpiration and sapflow rates [21] indicating the magnitude and consumption of the elastic storage capacity [22]. If measured simultaneously on bark and on the xylem, stem diameter variations can be used for calculating the osmotic pressure in the phloem tissue. This pressure fluctuates with carbohydrate availability [23], and loss of it predicts tree mortality relatively accurately [12]. The low magnetic field of our NMR system allowed for uninterrupted measurements with these two systems simultaneously for several months. For field measurements the NMR system was protected from moisture by covering the coils with silicone grease. During these measurements the tree was also tied with guy-wires and ropes to eliminate noise caused by wind shaking the tree. Traditional plant physiological parameters, such as leaf gas exchange, leaf water potential and soil moisture content were measured regularly during these experiments to allow for linking the changes in NMR signal with changes in plant physiology. We also erected a small micrometeorological weather station in the vicinity of these experiments to measure variation in environmental drivers of plant function such as photosynthetically active solar radiation, air temperature relative humidity, and precipitation.

The drought experiment consisted of observing plant responses to several degrees of drought severity from well-watered to a girdled tree to speed up xylem dehydration in the greenhouse. In the field the drought period was maintained until the tree lost all its leaves. After that watering was resumed and NMR and stem diameter signals observed until new leaves were fully grown. Losing leaves and producing new ones induces a major carbon and water reallocation event where resources are transported from storage to the actively growing parts. These experiments thus served both as tests of NMR signal responses to changing water content and reallocated carbon.

Our results from the greenhouse show ceasing of the diurnal use of the elastic storage of water (shrinking and swelling) once watering is stopped, which is consistent with stomatal closure of the plant (Fig 4). Surprisingly, the overall water content of the trees declined very slowly, and only after the bark was removed close to the NMR system. This indicates that aspen trees are very well sealed against water loss when the stomata are closed, and large-scale bubble formation occurs in these trees only when their metabolic processes have already ceased.

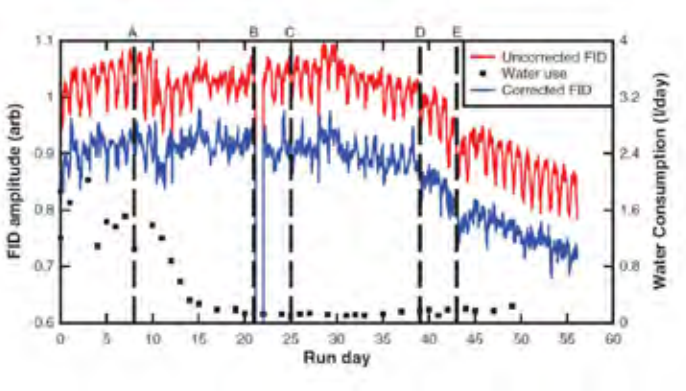

Figure 4. Time series of FID amplitude of the NMR signal and water use of an aspen tree in our greenhouse experiment starting July 11, 2013. Water use was measured by placing the tree on a balance. The temperature corrected FID amplitude (blue) is sifted down by 0.1 to allow for clarity. To encourage water

loss the tree was manipulated in several ways: A) watering was stopped; C) tree crown was cut 1m above the NMR coil; D) tree was cut 10cm above NMR coil, and E) tree was girdled above and below the NMR coil. B marks a gap in data resulting from magnet power supply reset. The reversible diurnal fluctuation in water content ceases in a few days once watering is stopped, but to detect real overall water loss (overall declining trend in the end), the tree had to be cut and girdled.

Interestingly, leaf loss resulted in a clear decline in the NMR signal indicating water loss, but this was not reflected in the xylem diameter variations as shrinkage of the tissue (Fig 5). Xylem tissue shrank earlier during the drought period indicating depletion of the xylem elastic water storage capacity. The sharp decline in NMR signal in the absence of decline in xylem diameter during leaf loss could thus be due to emptying of xylem conduits. The NMR and xylem diameter signals did not resume their original level 20 days after watering resumed, but the whole stem diameter did recover completely. This indicates that the tree refilled its water reserves in the phloem and bark tissues rapidly after watering was resumed, but it did not completely refill the empty xylem conduits. After new leaves flushed, the diurnal variation indicative of elastic storage use resumed both in the NMR and stem diameter signals, but with a lower amplitude indicating changes in water-carbon balance of bark and phloem tissues. The sharp decline in whole stem diameter during leaf loss shows that the water lost from xylem did not end up in the phloem and bark storage tissue. Losing water from the xylem conduits to the benefit of e.g. roots during leaf loss could be beneficial for plant survival during drought to reduce osmoregulation demands or ensure maintenance of soil-root connection. As long as the conduits can be refilled, or new ones built to resume the water transport capacity to support new leaves, no permanent harm would be done. Our observation of potential gas bubble formation in the xylem during leaf loss is the first of its kind and replication of the experiment is needed to confirm the result, and if confirmed, to investigate the abundance of this resource allocation strategy in trees.

Our measurements thus show that in the arid-zone species such as aspen, pinon pine and one-seed juniper, bubble formation rate is so low that we cannot distinguish it from the use of elastic water stores at daily scale, but we can detect it during drought or major reallocation events such as leaf loss. The low diurnal bubble formation rate is contradictory to many studies performed with acoustic emission detection methods that claim regular bubble formation in trees [24]. But it is in line with our own observations about stomatal control of transpiration in these arid-zone species. These species cannot rely on continuous water source to refill gas-filled conduits regularly and close their stomata well before bubble formation becomes detectable [25].

For these species, in this environment, bubble formation is thus rather a threat than a means to boost productivity. The observation of water loss from the xylem during leaf loss was unexpected and emphasizes how little we actually know about how trees cope with environmental stress, and how new measurement methods lead to new discoveries. In this project we developed new methods for in-vivo, non-destructive measurements of water content fluctuations and imaging water movement in woody plants to the level at which these methods can be applied to further studies of plant responses to environmental stress. With these methods we identified one new parameter that should be considered when modeling tree mortality during drought, and observed a new possible strategy of plants to control water stress during environmental changes.

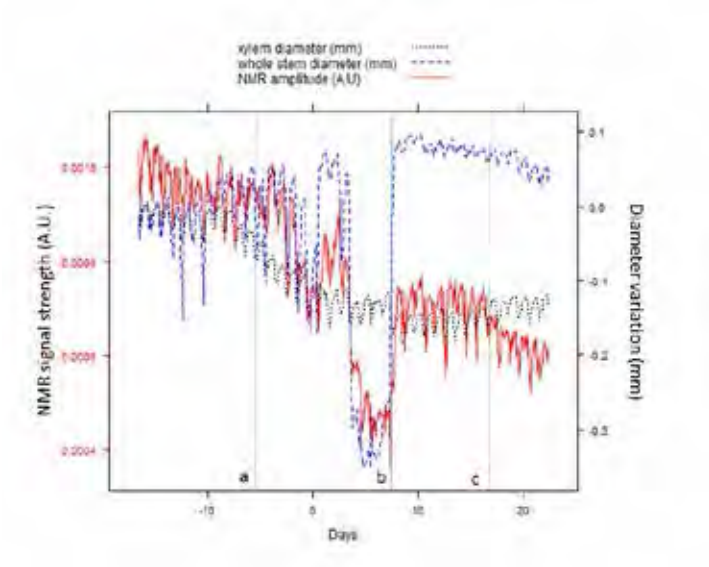

Figure 5. Time series of simultaneous measurements of NMR and tree stem diameter variations in an aspen tree in the field. Time is adjusted to zero when the tree lost all its leaves under imposed drought. The vertical lines mark moments when watering was stopped (a), resumed (b) and new fully grown leaves observed (c). The NMR signal and diameter measured on bark (whole stem) increase slightly and the xylem stops shrinking right after leaf fall as a response to an increase in water availability after a thunderstorm. After that NMR and whole stem signals drop dramatically suggesting water lost from the stem. The xylem diameter does not shrink at this stage indicating that the change in the NMR signal could be due to bubble formation in the xylem (most of NMR signal reflects xylem water). With production of new leaves, the diurnal fluctuations in all signals slowly resume.

Impact on National Missions

Capability to predict vegetation responses to changing climate is needed to support formulating policies and strategies for mitigating the global and national threat of climate change. Vegetation regulates the terrestrial water and

carbon balance, acting as a carbon sink and water redistributor within the soil as well as between the soil and the atmosphere. The presence or absence of vegetation, and forests especially, influences the local climate and weather and has a direct impact on natural resources as well as energy consumption and production. In this project we have developed new methods for measuring plant physiological responses to drought. These methods have allowed us to identify new key parameters that could help in predicting plant responses to drought and their susceptibility to mortality under droughts of different duration more accurately. While more measurements of these parameters are needed to build a global picture of plant susceptibility to drought for global scale vegetation modeling, this project has allowed our method to reach the stage at which it can be used in further studies that assist in developing mechanistic presentations of plant mortality for the models.

References

1. Allen, C. D., A. K. Macalady, Chenchouni, Bachelet, McDowell, Vennetier, Kitzberger, Rigling, D. D. Breshears, E. H. (. Hogg, Gonzalez, R. o. d. Fensham, Zhang, Castro, Demidova, Lim, Allard, S. W. Running, Semerci, and Cobb. A global overview of drought and heat-induced tree mortality reveals emerging climate change risks for forests. 2010. FOREST ECOLOGY AND MANAGEMENT. 259 (4): 660.

2. Xu, , N. G. McDowell, Sevanto, and R. A. Fisher. Our limited ability to predict vegetation dynamics under water stress. 2013. NEW PHYTOLOGIST. 200 (2): 298.

3. McDowell, N. G., and Sevanto. The mechanisms of carbon starvation: how, when, or does it even occur at all?. 2010. NEW PHYTOLOGIST. 186 (2): 264.

4. McDowell, N. G.. Mechanisms Linking Drought, Hydraulics, Carbon Metabolism, and Vegetation Mortality. 2011. PLANT PHYSIOLOGY. 155 (3): 1051.

5. GOLDMAN, M., M. CHAPELLI, V. H. CHAU, and A. ABRAGAM. PRINCIPLES OF NUCLEAR MAGNETIC-ORDERING. 1974. PHYSICAL REVIEW B. 10 (1): 226.

6. Windt, C. W., E. d. o. Gerkema, and Van As. Most Water in the Tomato Truss Is Imported through the Xylem, Not the Phloem: A Nuclear Magnetic Resonance Flow Imaging Study. 2009. PLANT PHYSIOLOGY. 151 (2): 830.

7. Peuke, A. D., M. Rokitta, U. Zimmermann, L. Schreiber, and A. Haase. Simultaneous measurement of water flow velocity and solute transport in xylem and phloem of adult plants of Ricinus communis over a daily time course by nuclear magnetic resonance spectrometry. 2001. PLANT CELL AND ENVIRONMENT. 24 (5): 491.

8. Windt, C. W., Soltner, van Dusschoten, and Bluemler. A portable Halbach magnet that can be opened and closed without force: The NMR-CUFF. 2011. JOURNAL OF MAGNETIC RESONANCE. 208 (1): 27.

9. Jones, , P. S. Aptaker, Cox, B. A. Gardiner, and P. J. McDonald. A transportable magnetic resonance imaging system for in situ measurements of living trees: The Tree Hugger. 2012. JOURNAL OF MAGNETIC RESONANCE. 218: 133.

10. Yoder, , M. W. Malone, M. A. Espy, and Sevanto. Low-field nuclear magnetic resonance for the in vivo study of water content in trees. 2014. REVIEW OF SCIENTIFIC INSTRUMENTS. 85 (9).

11. Malone, M. W., J. Yoder, J. F. Hunter, M. A. Espy, L. T. Dickman, R. O. Nelson, S. C. Vogel, H. Sandin, and S. Sevanto. In vivo observantion of drought response in a tree with low-field NMR and neutron imaging. Frontiers in Plant Science.

12. Sevanto, , N. G. McDowell, L. T. Dickman, Pangle, and W. T. Pockman. How do trees die? A test of the hydraulic failure and carbon starvation hypotheses. 2014. PLANT CELL AND ENVIRONMENT. 37 (1): 153.

13. McDowell, , W. T. Pockman, C. D. Allen, D. D. Breshears, Cobb, Kolb, Plaut, Sperry, West, D. G. Williams, and E. A. Yepez. Mechanisms of plant survival and mortality during drought: why do some plants survive while others succumb to drought?. 2008. NEW PHYTOLOGIST. 178 (4): 719.

14. Casieri, C., L. Senni, M. Romagnoli, U. Santamaria, and F. De Luca. Determination of moisture fraction in wood by mobile NMR device. 2004. JOURNAL OF MAGNETIC RESONANCE. 171 (2): 364.

15. Holtta, , Juurola, Lindfors, and Porcar-Castell. Cavitation induced by a surfactant leads to a transient release of water stress and subsequent ‘run away’ embolism in Scots pine (Pinus sylvestris) seedlings. 2012. JOURNAL OF EXPERIMENTAL BOTANY. 63 (2): 1057.

16. Sevanto, . Phloem transport and drought. 2014. JOURNAL OF EXPERIMENTAL BOTANY. 65 (7): 1751.

17. Sevanto, , Holtta, and N. M. Holbrook. Effects of the hydraulic coupling between xylem and phloem on diurnal phloem diameter variation. 2011. PLANT CELL AND ENVIRONMENT. 34 (4): 690.

18. Savage, J. A., M. J. Clearwater, D. F. Haines, T. Klein, M.

Mencuccini, S. Sevanto, R. Turgeon, and C. Zhang. Allocation, stress tolerance and carbon transport in plants: How does phloem physiology affect plant ecology?. To appear in Plant, Cell and Environment.

19. Peramaki, M., E. Nikinmaa, S. Sevanto, H. Ilvesniemi, E. Siivola, P. Hari, and T. Vesala. Tree stem diameter variations and transpiration in Scots pine: an analysis using a dynamic sap flow model. 2001. TREE PHYSIOLOGY. 21 (12-13): 889.

20. Holtta, , Cochard, Nikinmaa, and Mencuccini. Capacitive effect of cavitation in xylem conduits: results from a dynamic model. 2009. PLANT CELL AND ENVIRONMENT. 32 (1): 10.

21. Sevanto, , Nikinmaa, A. n. u. Riikonen, Daley, J. C. Pettijohn, T. N. Mikkelsen, Phillips, and N. M. Holbrook. Linking xylem diameter variations with sap flow measurements. 2008. PLANT AND SOIL. 305 (1-2): 77.

22. Sevanto, S., T. Holtta, T. Markkanen, M. Peramaki, E. Nikinmaa, and T. Vesala. Relationships between diurnal xylem diameter variation and environmental factors in Scots pine. 2005. BOREAL ENVIRONMENT RESEARCH. 10 (5): 447.

23. Mencuccini, , Holtta, Sevanto, and Nikinmaa. Concurrent measurements of change in the bark and xylem diameters of trees reveal a phloem-generated turgor signal. 2013. NEW PHYTOLOGIST. 198 (4): 1143.

24. Holtta, T., T. Vesala, E. Nikinmaa, M. Peramaki, E. Siivola, and M. Mencuccini. Field measurements of ultrasonic acoustic emissions and stem diameter variations. New insight into the relationship between xylem tensions and embolism. 2005. TREE PHYSIOLOGY. 25 (2): 237.

25. Garcia-Forner, N., H. D. Adams, S. Sevanto, A. D. Collins, L. T. Dickman, P. J. Hudson, M. Zeppel, J. Martinez-Vilalta, and N. G. McDowell. Responses of two semiarid confer tree species to reduced precipitation and warming reveal new perspectives for stomatal regulation. To appear in Plant, Cell and Environment.

Publications

Cruz, N., J. Yoder, and M. Espy. Active Q-switching in NMR applications. Presented at 13th Annual Student Symposium, Los Alamos National Laboratory . (Los Alamos, NM, July 26-27).

Cruz, N., M. W. Malone, D. J. Hart, S. Sevanto, and M. A. Espy. Tracking water flow in trees using NMR. Presented at 14th Annual Student Symposium. (Los Alamos, NM, 5 Aug, 2014).

Hart, D. J., M. W. Malone, S. Sevanto, M. A. Espy, and N. Cruz. Measuring teh water content in trees using NMR. Presented at 14th Annual Student Symposium. (Los Alamos, NM, 5 Aug, 2014).

Malone, M. W., J. Yoder, M. A. Espy, and S. Sevanto. Disentangling biology and physics to measure water in trees. Presented at Plant Biology. (Portland, OR, 12-16 Jul. 2014).

Malone, M. W., J. Yoder, M. A. Espy, and S. Sevanto. Disentangling biology and physics to measure wayer in trees. Presented at NMR^2. (Albuquerque, NM, 3 May, 2014).

Malone, M. W., J. Yoder, M. A. Espy, and S. Sevanto. Disentangling biology and physics to measure water in trees. Presented at LANL Postdoc Research Day. (Los Alamos, NM, 11 Jun, 2014).

Sevanto, S.. Phloem transport and drought. 2013. In 3rd International Conference on Plant Vascular Biology. (Helsinki, Finland, 26-30 Aug, 2013). , p. 56. Helsinki: Helsinki University Press.

Sevanto, S.. Phloem transport and drought. 2014. Journal of Experimental Botany. : doi: 10.1093/jxb/ert467.

Yoder, J.. Measuring absolute water content of trees in vivo with low field NMR. Invited presentation at Physics Division Summer Seminar PostDoc Series. (Los Alamos, NM, June 26, 2013).

Yoder, J., M. A. Espy, M. W. Malone, and S. Sevanto. In vivo observation of drought response in a tree with low-field NMR. 2014. Review of Scientific Instruments. 85: 095110.

Yoder, J., M. Espy, N. McDowell, J. Resnick, and S. Sevanto. Measuring absolute water content of trees in vivo by low field NMR in an uncontrolled environment. Presented at 54th Experimental Nuclear Magentic Resonance Conference. (Pacific Grove, CA, 14-19 April, 2013).

Pyrocumulus Collapse: Unpredicted Wildfire Dangers

Young-Joon Kim
20130487ER

Abstract

This project aims at understanding the physical mechanisms behind the Las Conchas Fire, which occurred in Santa Fe National Forest near Los Alamos, New Mexico, on June 26, 2011. The Fire surprised everyone when it unexpectedly burned approximately 35,000 acres in less than 7 hours during its first night even though it was burning downhill in sparse vegetation and under milder wind conditions than had been present on that afternoon.

We considered two potential mechanisms for this baffling fire behavior, especially its unexpected nighttime blowup; (1) downdrafts associated with the soot-laden pyro-cumulus column (pyro-cu) that towered above the fire, causing a sustained density current carrying fire at high speed, and (2) downslope windstorms due to the breaking of large-amplitude mountain waves developed over Jemez Mountains near Los Alamos. We discussed some insights on these mechanisms and explored their possible effects on wildfire behavior dynamics.

We first performed simulations using the LANL-developed large-eddy simulation model (HIGRAD; HIGh-GRADient model) that includes a multi-component continuum model to scope the potential dynamics that could result when a soot and water vapor laden column, such as a pyro-cu, looses its support from underneath. The simulations illustrated that a rapid descent of heavier-than-air gas mixture due to its own weight could occur under certain atmospheric and wildfire conditions although the mechanisms to sustain the process were unclear.

We then performed simulations using a mesoscale atmospheric model (WRF; Weather Research and Forecasting model) and found suggestive results that account for the coupled topography-atmosphere interaction and resulting influences on fire, which may be required to fully understand and prepare for atypical wildfire behavior in regions with complex topography. We also performed high-resolution simulations over bell-shaped barrier similar to the topography of the fire area under various atmospheric conditions using HIGRAD and found that a localized wildfire-like heat source is largely affected by topographically generated gusty winds. Our investigation sheds light on the interaction of mountain waves with wildfire to modelers and managers of wildfire.

Observed nominal atmospheric conditions from the first night of the fire are likely to occur in a vast set of fire-susceptible communities bordering mountains across the country. This research addresses important implications for the management as well as research of wildfire in that, in order to prepare for potential wildfire, such environmental conditions should be taken into account.

Background and Research Objectives

Between 8 pm local time (MDT) on June 26 and 3 am on June 27, the Las Conchas Fire (hereafter referred to as the LC Fire) grew from 8,000 to 43,000 acres, spreading downhill in sparse fuels and lighter winds than were present during the first several hours of the fire. Fire behavior experts and fire management officers expected the fire to reach 9,000 to 12,000 acres by sunrise due to the anticipated burning conditions, but it surprisingly increased 440% in size before 3 am, causing significant threat to life and property and eventually forcing the evacuation of nearby towns.

It is important that the fire community deciphers the conditions that increase probability of such events and the phenomenology that controls their intensity. An initial hypothesis for the peculiar behavior in the LC Fire is that a particulate-laden portion of the fire-induced "pyro-cumulus (pyro-cu)" column lost buoyancy and produced strong downdrafts, and unleashed a symbiotic density current that increased fire spread rate and intensity. Another hypothesis is that the interactions between the stable nocturnal atmosphere and the local

topography influenced the fire behavior or pyro-cu column stability. We investigated the viability of such hypotheses with numerical simulations.

Some wildfire anomalies have occurred in the early to late evening period. During typical wildfire seasons (mid-Spring to early Fall), the atmospheric stability profile transitions from an unstable convective boundary layer profile during the mid and late afternoon times to a stably stratified profile in the evening. Most often the intensity of a wildfire will decrease with the onset of evening as surface winds in general decrease and relative humidity increases. Wildfire management activities are often designed in anticipation of this type of behavior and when the fire unexpectedly changes to the contrary and increases its activity, practitioners can be surprised. There is a need to understand what combination of aspects of the evening atmospheric conditions and transitioning fire behavior set the state for such surprises. We focused on phenomenology that might exacerbate surface winds and thereby lead to the blowup of a wildfire such as the LC Fire.

In the early years of wildfire behavior research, several commonalities in meteorology, such as the vertical profiles of wind speed and direction, were noted during several blowup fires. It was hypothesized that each of the anomaly fires was influenced by a vertical wind profile in which substantially higher wind speeds were found near the surface than aloft. One way to achieve such conditions locally pertains to the events occurring when a portion of a pyro-cu column does not have sufficient buoyancy to stay aloft. The potential energy of a particle-laden plume that is heavier than the surrounding air can be converted into kinetic energy as the large air mass begins to descend, just as in the vicinity of some thunderstorms. The intersection of the descending winds and the surface can lead to a strong torrent of horizontal surface winds, a.k.a. a "density current", accelerating and intensifying fires in its path. Collapsing pyro-cu's have been implicated in several devastating historical fire events, including the Dude Fire, the Chisholm Fire, the Canberra Fires, and the Brasstown Fire; nevertheless, the phenomenology and warning signs for such an event are not known.

Another set of phenomena resulting in localized gusty winds or "downslope windstorms" are topographically generated gravity waves, i.e., mountain waves (hereafter referred to as MWs). Stable stratification of the atmosphere can lead to generation of MWs. In fact, strong (especially, nocturnal) winds are often found near steep topography when wildfires grow unexpectedly (e.g., 22 mph for the 2013 Yarnell Hill Fire in Arizona). When these waves are of sufficient magnitude, they can overturn and produce an enhancement of near surface wind speeds on the lee-side of topographic feature on the landscape, i.e., create a downslope windstorm. We investigated the potential that MWs could act as a catalyst for rapid intensification or 'blowup" of a wildfire, i.e., a pronounced increase in the energy output of a wildfire event over a relatively short period of time (say, on the order of an hour).

Our research was inspired by the desire to explore basic physical mechanisms relevant to the first night of the LC Fire and identify what combined fire/atmosphere dynamics could have led to the unexpected observed fire behavior. Our primary research objective is to investigate and understand the interaction between the meteorology, dynamic fire intensity, plume dynamics and topography that would lead to significant downslope acceleration of the LC Fire during the night when the ambient wind slowed down and fuels became less continuous. Our future investigation will ultimately involve detailed explorations of the interactions of winds with a heat source, identification of potential causes of strong downdrafts and subsequent downslope density currents as well as developing a better understanding of the interactions between a density current and a fire front.

Scientific Approach and Accomplishments

Our scientific approach is to investigate available observations as well as perform and validate numerical simulations. We first investigated the likelihood of MWs in the LC Fire area by analyzing available observation and analysis/forecast data, e.g., using selected LANL meteorological tower data. We then performed scoping numerical simulations using the Weather Research and Forecast model (WRF) and main simulations using our large-eddy-resolving model, HIGRAD, in order to identify the conceivable magnitude of the wind changes due to rapid decent of a portion of the pyro-cu column under the topographic setting of the LC Fire. Through numerical simulations, we investigated the interaction of an isolated heat source with an atmosphere conducive to the presence of MWs. We report on our qualitative characterization of the manner in which MWs interact with a heat source plume.

First, HIGRAD was modified to include the multi-phase property of fire-contaminated air. With a multi-component continuum model included, simulations were performed to scope the potential dynamics that could result when a soot and water vapor laden column, such as a pyro-cu, looses its support from underneath. The loss of such support could for instance occur due to shifting wind direction at various altitudes diminishing fire intensity. An idealized column of a gaseous mixture containing heat, dry air, water vapor, and fullerene was initialized over the LC Fire area topography where the fire occurred, where the gas col-

umn represented an idealized fire plume. The simulation illustrated the expected rapid descent heavier-than-air gas mixture due to its own weight under certain atmospheric and wildfire conditions. However, the proposed physical mechanism did not fully explain how the vertical motion is sustained for the duration of the fire blowup.

The area surrounding the LC Fire is highly mountainous and strong surface winds are often observed in the area. In order to validate the likelihood of the topographic influence on the fire, a series of MW simulations using WRF were performed and the presence of MW activity around the LC Fire period was investigated. The simulations were initialized at 0000 UTC 26 June 2011 (or 1800 MDT 25 June 2011) before the fire started (at 1300 MDT 26 June 2011) using the local atmospheric conditions before and during the fire together with the area topography. When fully developed (at 09 UTC or 06 MDT 27 June 2011), MWs were found very nonlinear in the entire area of the cross section and a large portion of the low-level flow over mountains reached a "hydraulic jump" state. The low-level flow was separated from the flow above and became well mixed due to the turbulence created by wave breaking with flow reversal (associated with "rotors") in the downstream.

HIGRAD was further modified to represent the buoyancy source-sink term in the prognostic subgrid-scale turbulent kinetic energy equation, which is critical to the formation of MWs. Monin-Obukhov formulations for both surface heat flux and momentum flux were added, respectively, to characterize a stably stratified flow environment and to provide a mechanism for momentum sink at the surface. Also implemented are grid-dependent and dynamic stability-aware prescription of an appropriate subgrid-scale turbulence length, and stability-dependent turbulent Prandtl number. We successfully simulated both linear and nonlinear MWs over idealized bell-shaped ridge-type topography, designed to mimic the Las Conchas Fire area. In nonlinear case (Fr-1=1.2), downstream turbulence and gusty winds due to MW breaking were clearly simulated. The simulations were continued with a heat source added in order to study the interaction of nonlinear MWs with heat source crudely representing wildfire. The turbulent wakes and gusty winds generated by breaking of nonlinear MWs sweep the fire represented by heat source downstream. The fire has spread downstream along the downslope faster and more widely than without MW influence. Further downstream with turbulent wakes/rotors, the winds were weaker and reversed, which could potentially cause unexpected fire behavior.

The rotors of turbulent air along the downstream of the mountain can complicate the behavior of wildfire because the wind directions under the rotors are reversed near the region of strong surface winds. This phenomenon could reverse the flow in the vicinity of wildfire or change it erratically, putting firefighters at unpredicted risk, i.e., fire can unexpectedly strike them from behind. These types of erratic wildfire behavior due to mountains should be investigated systematically and applied to saving precious lives of firefighters.

In this work, we demonstrated that the high-resolution MW dynamics may be crucial to explain the Las Conchas Fire surrounded by complex terrain. This finding has important implications for fire management community and can provide knowledge to better prepare for future wildfires. The physical interpretation of Las Conchas Fire in the context of MW simulation in eddy-resolving scale is not found in the literature. The results out of this project are original and of high quality as was confirmed during the 2014 Fall AGU Meeting where the work was first presented. This work also drew some public attention through a media interview and a subsequent magazine article [The Earth Magazine, May 2015].

Impact on National Missions

LANL's capacity to perform its primary missions was threatened by the Las Conchas Fire, an unexpectedly grown wildfire near high complex topography. According to our investigation, this wildfire developed into much large scale with much greater magnitude possibly due to the generation of strong density currents associated with a collapse of pyro-cumulus and/or wind accelerations by the breaking of MWs, which was channeled by street canyons, thereby focusing the kinetic and thermal energy and potentially increasing damage by an order of magnitude. It is essential that this kind of potential threat be understood in order to save lives and safeguard critical facilities of LANL and other national laboratories under similar environments. Discerning this type of erratic wildfire behavior is crucial for elucidating the fire-related effects from an urban nuclear event (on US soil or elsewhere).

LANL is involved in activities supporting DHS (Department of Homeland Security), STRATCOM (Strategic Command), and DTRA (Defense Threat Reduction Agency) to understand potential damage and lives at risk from an urban conflagration that could likely result from this type of disasters. It will enhance LANL's unique capacity to study coupled fire/atmosphere phenomena in realistically complex environments and therefore will help secure LANL's role supporting the USDA (US Department of Agriculture) Forest Service wildfire research and management missions, and position LANL to serve a larger research role and to assume direct relevance to the fire management sector of the USDA Forest Service. More generally, this work will

help establish the capability to enable wildfire and CBRN (Chemical, Biological, Radiological, and Nuclear) material dispersion risk assessment across the DOE complex.

References

1. Sauer, J., J. Canfield, R. Linn, E. Koo, J. Winterkamp, and Y. -J. Kim. Assessing fire behavior with fundamental fluid dynamics theory. 2014. In International Association for Wildland Fire, Large Wildland Fires Conference. (Missoula, 19-23 May 2014). , p. 00. Missoula, MT: International Association of Wildland Fire.

2. Kim, Y. -J., R. Linn, J. Sauer, J. Canfield, K. Costigan, and D. Munoz-Esparza. Enhanced Risk of Wildfire Resulting from the Interactions between Pyro-Cumulus and Mountain Waves: Implications for Fire Research and Management. 2014. In American Geophysical Union Fall Meeting. (San Francisco, CA, 15-19 December 2014). , p. 00. Washington, DC: American Geophysical Union.

3. The Las Conchas Fire, the largest wildfire in New Mexico history, threatened the town of Los Alamos and Los Alamos National Laboratory in June and July 2011. 2015. The Earth Magazine http://www.earthmagazine.org/article/fire-driven-clouds-and-swirling-winds-whipped-record-setting-new-mexico-blaze.

4. Sauer, J., D. Munoz-Esparza, J. Canfield, K. Costigan, R. Linn, and Y. -J. Kim. New Insights into Boundary Layer Influence on Stratified Atmospheric Flows over Terrain through Large-Eddy Simulations. Journal of the Atmospheric Sciences.

5. Kim, Y. -J., J. Sauer, R. Linn, J. Canfield, K. Costigan, and D. Munoz-Esparza. Identification of Potential Mechanistic Drivers in Anomalous Behavior of Large Wildland Fire: The 2011 Las Conchas Fire Blowup. International Journal of Wildland Fire (To be submitted by 10/16/2015).

Publications

The Las Conchas Fire, the largest wildfire in New Mexico history, threatened the town of Los Alamos and Los Alamos National Laboratory in June and July 2011. 2015. The Earth Magazine http://www.earthmagazine.org/article/fire-driven-clouds-and-swirling-winds-whipped-record-setting-new-mexico-blaze.

The Role of Mesoscale Parameterized Turbulence in Development of Trapped-Lee and Breaking Waves over Complex Terrain. Journal of the Atmospheric Sciences (To be submitted by 10/31/15).

Canfield, J.. Wildfire dynamics: Understanding some behavior trends. 2014. PhD Dissertation, Florida State University / LANL LA-UR-14-22933. 28 Apr. 2014.

Canfield, J., R. Linn, J. Sauer, M. Finney, and J. Forthofer. A numerical investigation of the interplay between fireline length, geometry, and rate of spread. 2014. Agricultural and Forest Meteorology. 189 (190): 48.

Kim, Y. -J., J. Sauer, R. Linn, J. Canfield, K. Costigan, D. Munoz-Esparza, and S. Goodrick. Identification of Potential Mechanistic Drivers in Anomalous Behavior of Large Wildland Fire: The 2011 Las Conchas Fire Blowup. International Journal of Wildland Fire (To be submitted by 10/16/15).

Kim, Y. -J., R. Linn, J. Sauer, J. Canfield, and K. Costigan. Enhanced Risk of Wildfire Resulting from the Interactions between Pyro-Cumulus and Mountain Waves: Implications for Fire Research and Management. 2014. In American Geophysical Union Fall Meeting. (San Francisco, 15-19 Dec. 2014). , p. 00. San Francisco: American Geophysical Union.

Linn, R., J. Winterkamp, J. Canfield, J. Sauer, J. L. Dupuy, M. Finney, C. Hoffman, R. Parsons, P. Fancois, C. sieg, and J. Forthofer. An Emerging Role for Numerical Modelling in Wildfire Behavior Research: Explorations, Explanations, and Hypothesis Development. 2014. In American Geophysical Union Fall Meeting. (San Francisco, 15-19 Dec. 2014). , p. 00. San Francisco: American Geophysical Union.

Sauer, J.. Towards improved capability and confidence in coupled atmospheric and wildland fire modeling. 2013. PhD Dissertation, Florida State University, 12 Nov. 2013.

Sauer, J., D. Munoz-Esparza, J. Canfield, K. Costigan, R. Linn, and Y. -J. Kim. New Insights into Boundary Layer Influence on Stratified Atmospheric Flows over Terrain through Large-Eddy Simulations. Journal of the Atmospheric Sciences.

others, D. Munoz-Esparza and. Winds, Mountains, and Wildland Fire: Improved Understanding of Coupled Atmosphere-Topography-Fire Interactions Through Large-Eddy Simulation. To appear in American Geophysical Union Fall Meeting. (San Francisco, CA, 14-18 Dec. 2015).

Biocatalysts for Remediation of Uranium Wastes

Francisca Rein Rocha
20130590ER

Abstract

One of the strategic priorities of the U. S. Department of Energy has been the cleanup of numerous sites across the Nation that contain subsurface contamination with radionuclides from legacy nuclear waste. Given the daunting volume scales of soil and groundwater contamination with uranium and toxic heavy metals at low concentrations, in-situ bioremediation has been regarded as a promising approach to cost-effective environmental decontamination. A biological approach is based on the fact that some bacteria contain specific multiheme cytochromes that can catalyze the reduction of uranium from its soluble uranyl form (UO2 2+) to the less mobile state as uraninite (UO2). However, catalysis by microorganisms faces drawbacks owing to slow reactions leading to incomplete reductions and release of contaminants as well as the need for continuous supply of sacrificial chemical reductants, which is impractical and promotes deactivation due to competing re-oxidations by the reversible activity of reductants. Moreover, the difficult molecular manipulation for improvement of key structural properties and functional components in such living systems is a bottleneck for further advances in the derivation of bioremediation technologies. To address this grand challenge, the goal of this ER project has been the development of an abiotic approach to the effective reduction of hexavalent uranium. In this proof-of-concept, the electrocatalytically active reductase found in uranium-reducing microorganisms was produced as artificial biocatalyst films onto electrode surfaces for successful demonstration of the UO2 2+ → UO2 immobilization under small electrochemical potentials. The achieved results represent an important step toward viable strategies for practical remediation of nuclear waste, in addition to creating capabilities of relevance to Laboratory missions in this direction.

Background and Research Objectives

Within the U. S. Department of Energy (DOE) complex alone, thousands of discrete sites are contaminated with toxic and radioactive materials (mostly subsurface) accumulated over 50 years of nuclear activities during the Cold War. Contamination by uranium is especially problematic. Given the large volumes of soil and groundwater contamination with uranium and other heavy toxic metals at low concentrations, bioremediation has been regarded as more cost-effective than other methods involving immobilization or preconcentration of contaminants for ex-situ treatment. Despite significant advances in this area, the development and practical realization of viable technologies for remediation at such daunting scales still rely on research at the fundamental (bio) molecular level.

Unlike organic contaminants, radionuclides and toxic heavy metals cannot be biologically “degraded” but can undergo redox transformations that change their mobility. In natural environments, the transport of uranium is mostly determined by its ability to dissolve and dissipate in water flows; this ability, in turn, is ultimately determined by its redox states. The dramatic decrease in solubility accompanying the reduction of U(VI) ions to produce the insoluble mineral UO2 has been viewed as a path of great potential to the sequestration and trapping of this environmental contaminant in the soil underground, thereby preventing migration of contaminated plumes into aquifers and natural groundwater resources. Although the hexavalent state is the most stable for uranium in aqueous medium (where the dominant species is the uranyl ion, UO22+, free or in some form of complexation), the redox behavior of uranium is remarkably rich and often very complicated due to a range of accessible oxidation states and sensitivity of their thermodynamic potentials to medium effects and coordination environments around the metal [1].

Sulfate-reducing bacteria of the genus Desulfovibrio are anaerobes that derive energy from the dissimilatory reduction of sulfate coupled with oxidation of dihydrogen or organic substrates [2]. Some of these bacteria are also

capable of reducing toxic metals, which is a metabolism relevant to bioremediation applications. The overall reduction is a process involving two electrons, but the mechanism by which toxic metals are reduced in D. desulfuricans has not yet been established, despite its great potential for utilization in bioremediation of hexavalent uranium and chromium [3,4]. Studies have confirmed that the tetraheme cytochrome c3 present in such bacteria is specifically involved in the reductive reaction with U(VI) [5]. Of particular interest here is the metal reductase activity of cytochrome c3 from strain G20 (hereafter, denoted Cyt c3). This Cyt c3 produced by D. desulfuricans G20 contains four unequal c-type hemes that are each attached to a peptide by two thioether bridges with bis-histidinyl axial ligation [6] (Fig. 1). Cyt c3 is negatively charged at neutral pH (with a low isoelectric point of 5.8) and, as a result, it has a negative redox potential. Its molecular weight is only 14.4 kDa, which is similar to some monoheme cytochromes. The four hemes in Cyt c3 are situated relatively close to each other and feature intramolecular heme-heme interactions [7], which are crucial to cooperative electron-transfer mechanisms for multi-electron catalysis. Most importantly, in-vitro tests with purified Cyt c3 showing that the fully reduced species is oxidized upon reduction of metals have provided encouraging evidence toward our goal to develop cell-free systems for applications in both in situ and ex situ reduction of hexavalent uranium.

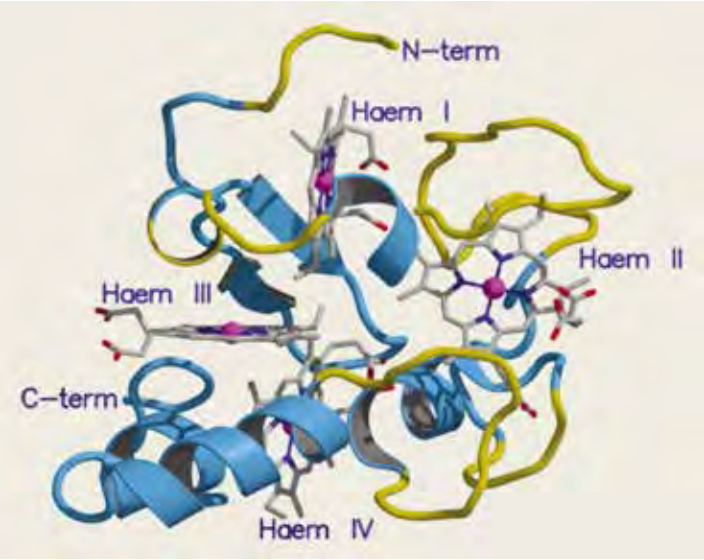

Figure 1. The reductase tetraheme cytochrome c3 (Cyt c3).

Scientific Approach and Accomplishments

Our approach has combined interfacial bioelectrochemistry, in-situ optical spectroscopies, and site-directed mutagenesis into the multi-electron redox catalysis of uranium reduction by D. desulfuricans G20 cytochrome c3 (Cyt c3). The investigations of Cyt c3 alone and its mutants allowed for mapping out physical and chemical factors dictating the proton-coupled redox behavior [8]. Following optimization of conditions and electronic/structural characterizations, we have tackled the interfacial molecular engineering of Cyt c3 electrodes for the electrocatalytic reduction and immobilization of uranium [9,10].

An important milestone in the first phase of the project was the successful implementation of the new preparative methods and bio-analytical techniques needed for the expression, isolation, purification, and structural characterization of our uranium-reducing biocatalyst. Producing the tetraheme reductase Cyt c3 at the target qualitative and quantitative levels was a particularly significant accomplishment because multi-heme cytochromes are generally more difficult to express correctly, since co-factors are needed to enable the proteins to obtain their native fold. In Cyt c3, four hemes must be attached via thioether linkages to the polypeptide chain at the CXX(XX)CH binding sites, and the correct distal axial ligands must be connected to the metal center (trivalent iron) in the nascent protein. In our approaches involving E. coli recombinant expression, specific assembly proteins were required for these critical interactions to form properly. Among the achieved improvements in the expression of Cyt c3, the pC3 plasmid carrying the Cyt c3 gene was co-expressed with the pEC86 plasmid carrying genes of helper maturation proteins. Other systematic changes have also led to further optimizations towards high yields, especially strategies involving auto-induction and temperature effects. We have found that auto-induction processes allow for control over amounts of media and supplements for bacteria growth to high densities prior to protein expression. Another key finding was that decreasing the typical growth temperatures, which causes bacteria to grow slower, has allowed the protein more time to properly fold into its native form. Following expression, the protocols for extraction, purification, and analysis of Cyt c3 have also been implemented and applied, from which the products were purified/analyzed by ion-exchange chromatographic column (Sepharose), gel electrophoresis (SDS-PAGE), Coomassie/heme staining, absorption spectroscopy (UV-Vis and IR), and electrochemistry (cyclic and pulse voltammetries).

As our target application requires surface immobilization of the biocatalyst, we have next produced Cyt c3 tagged with histidines (His-tag Cyt c3) for tethering onto the functionalized electrodes. To this end, a twelve-histidine residue was placed at the C-terminal of the protein, with a cleavage site (TEV protease) introduced between protein and His-tag to provide the flexibility of cleaving the tags and obtain the wild-type Cyt c3 from this same derivative. Following purification via Ni-NTA column, we have structur-

ally and functionally characterized this new His-tag Cyt c3 construct. Measurements by far-UV circular dichroism (CD) showed that this construct is well-folded and has retained its helical structure. Importantly, our spectroscopic and electrochemical characterizations in aqueous solutions as well as immobilized as electrode films (covalently attached monolayers or membrane-embedded multilayers) clearly indicated that His-tagging had no negative impact on either the structural stability or redox potentials of the heme sites, consequently retaining the reductase activity of Cyt c3 [9].

The kinetic and thermodynamic properties of the Cyt c3 catalyzed electron-transfer reaction between uranium(VI) and electrode (gold or glassy carbon) were studied by cyclic voltammetry, both for homogeneous solutions and electrode-attached films. By using in-situ spectroscopy to follow UV-Vis spectral changes associated with heme-based absorption bands, we observed that the heme-Fe(II) sites of the electrochemically reduced biocatalyst are oxidized to their heme-Fe(III) states concurrently with the reduction of U(VI) in solution into U(IV) in the form of uraninite precipitate. In the presence of a complexing agent, such as citrate, the uranyl ions alone (i.e. without the catalyst) can only undergo a one-electron reduction at relatively very negative potentials (below -0.7 V vs Ag/AgCl). Consequently, an aqueous UO22+ solution containing citrate is electrochemically inactive in the range of potentials examined. In contrast, similar measurements for the catalyst in the same medium show a reversible electrochemical response at accessible potentials (above -0.5 V vs Ag/AgCl) for the redox processes associated with the four heme sites of Cyt c3 (Fig. 2). In the presence of uranyl(VI) ions added to the solution, the shape of the voltammograms changes due to a cathodic current that develops upon reduction of Cyt c3. Interestingly, the growth of this cathodic current follows the increase in the concentration of U(VI). This behavior is therefore consistent with the regeneration of oxidized Cyt c3 by the electrocatalytic cycle accompanying the U(VI) → U(IV) reduction (Fig. 2). The immobilization of Cyt c3 into a membrane or ion-exchanger film has not significantly impacted the overall electrocatalytic activity [10].

With our methodologies established and successfully demonstrated for both wild-type and His-tagged Cyt c3, we then turned our studies to improved biocatalyst derivatives by site-directed mutagenesis. The mobile uranyl dication (UO2 2+) is a linear dioxo species that prefers to coordinate up to six donor ligands in the equatorial plan. Uranyl-protein motifs show that binding typically occurs through carboxyl groups such as in aspartate and glutamate. In addition, hydrogen bonds between uranyl and backbone amide groups are predicted to enhance the metal-protein interaction. Therefore, we substituted the binding pocket of Cyt c3 (in the regions of lysine 14 and 56) with glutamate/aspartate residues to enhance specific binding and identify structural features that are essential to uranium reduction. Because glutamate and aspartate have been shown to be good binding partners to uranyl(VI) owing to the negative charges of their side chains, the following mutations have been made to Cyt c3: Asn12 to Asp, Thr13 to Glu, and Phe54 to Glu. Systematic structure-function relationships for these mutants (in comparison to the parent species above) are currently being finalized to provide a better understanding of both the nature of biocatalyst-uranium binding and the mechanism for multi-electron reductase activity.

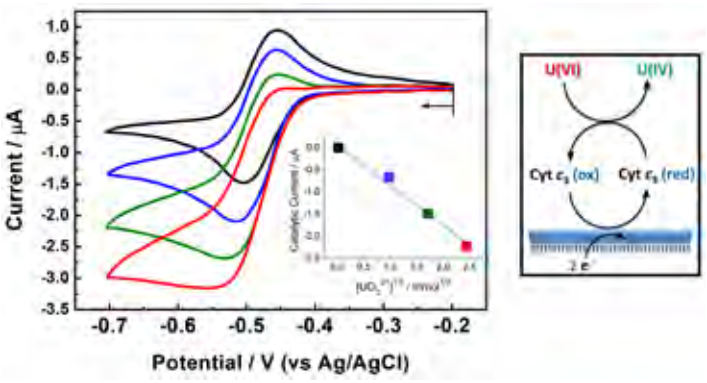

Figure 2. Electrocatalytic activity of uranium-reducing Cyt c3 electrodes.

Impact on National Missions

This research supports our Laboratory missions by providing advancements toward the permanent environmental decontamination of radionuclides and toxic metals in complex subsurface environments. The project ties directly into the LANL/LDRD Grand Challenge “Complex Biological Systems” (specifically “to resolve national challenges in energy, health and environment” as well as “biological interactions and metabolic patterns that control ecosystem functions”). In addition to DOE, this research has high relevance to NNSA, DoD, and DHHS (NIH) programs. With underlying themes related to sensing/detection of radionuclides or toxic substances, nuclear forensics, molecular bioelectronics, and bioenergy, this effort is conducive to programs within DHS, Intelligence Agencies, DoD (DARPA, DTRA, ONR), and DOE (BES, ARPA-E) among some of the identified agencies/sponsors.

References

1. Morris, D. E.. Redox energetics and kinetics of uranyl coordination complexes in aqueous solution. 2002. Inorganic Chemistry. 41: 3542.

2. Louro, R. O.. Proton thrusters: overview of the structural and functional features of soluble tetrahaem cytochromes c3. 2007. Journal of Biological Inorganic Chemistry. 12: 1.

3. LLoyd, J. R.. Microbial reduction of metals and radionuclides. 2003. Microbiology Reviews. 27: 411.

4. Renshaw, J. C., L. J. C. Butchins, F. R. Livens, I. May, J. M. Charnok, and J. R. LLoyd. Bioreduction of uranium: environmental implications of a pentavalent intermediate. 2005. Environmental Science & Technology. 39: 5657.

5. Payne, R. B., L. Casalot, T. Rivere, J. H. Terry, and J. D. Wall. Interaction between uranium and the cytochrome c3 of Desulfovibrio desulfuricans strain G20. 2004. Archives of Microbiology. 181: 398.

6. Pattarkine, M. V., J. J. Tanner, C. A. Bottoms, Y. H. Lee, and J. D. Wall. Desulfovibrio desulfuricans G20 tetraheme cytochrome structure at 1.5 Å and cytochrome interaction with metal complexes. 2006. Journal of Molecular Biology. 358: 1314.

7. Akutsu, H., and Y. Takayama. Functional roles of the heme architecture and its environment in tetraheme cytochrome c. 2007. Accounts of Chemical Research. 40: 171.

8. Rein, F. N., D. M. Vu, and R. C. Rocha. Elucidation of multiple proton-coupled redox microstates in a tetraheme reductase (in preparation). Bioelectrochemistry.

9. Rein, F. N., D. M. Vu, and R. C. Rocha. Direct electron transfer of tetraheme cytochromes at functionalized electrode interfaces (in preparation). Biosensors and Bioelectronics.

10. Rein, F. N., D. M. Vu, and R. C. Rocha. Multi-electron bioelectrocatalysis of uranium reduction by a cytochrome c3 (in preparation). Environmental Science & Technology.

Publications

Rein, F. N., D. M. Vu, and R. C. Rocha. Elucidation of multiple proton-coupled redox microstates in a tetraheme reductase (in preparation). Bioelectrochemistry.

Rein, F. N., D. M. Vu, and R. C. Rocha. Direct electron transfer of tetraheme cytochromes at functionalized electrode interfaces (in preparation). Biosensors and Bioelectronics.

Rein, F. N., D. M. Vu, and R. C. Rocha. Multi-electron bioelectrocatalysis of uranium reduction by a cytochrome c3 (in preparation). Environmental Science & Technology.

Structure Determination of Large and Membrane-Bound Proteins by Nuclear Magnetic Resonance (NMR) Spectroscopy

Ryszard Michalczyk
20130620ER

Abstract

Knowledge of the structures and mechanisms of both large proteins and their complexes and membrane-bound proteins is critical to our understanding of, and intervention in, processes as varied as antibiotic resistance and biosynthesis, biofuels production, and disease development. Application of crystallography to these systems suffers from (1) an inability to crystallize large flexible structures; (2) the effects of crystal packing; and (3) the necessity to include lipid membranes in a full analysis of structure and function. In contrast, Nuclear Magnetic Resonance (NMR) is a versatile technique that can provide structural, dynamic, and kinetic data on biological systems and their interactions in solution.

Presently the size of biomolecules suitable for NMR spectroscopy is limited to <50 kiloDaltons (kDa) for high resolution structures. We propose to address this critical shortcoming by introducing specific, site-selective isotope labeling of amino acids in proteins and optimization of NMR methods for this specific labeling scheme.

We will develop new 3D and 4D NMR experiments for resonance assignments and unambiguous determination of constraints for structure calculation. The methods will use optimized magnetization transfer pathways to minimize signal losses by utilizing new selectively stable isotope labeled amino acids. We will devise new labeling schemes for all twenty natural amino acids to enable these studies. The approach will be validated by applying it initially to structure determination of a large enzyme (34kDa) and finally to structural studies of a protein complex involved in the biosynthesis of enterobactin (132kDa).

The success of this project will open the structural biology field to the detailed mechanistic studies of other large protein complexes and membrane-bound proteins involved in many biological processes placing LANL at the forefront of the field. Leveraging the results obtained here with LANL's synthetic stable isotope capabilities, will open funding possibilities from NIH, DTRA and DOE.

Background and Research Objectives

Crystallography has been successful in structure determination of several large proteins and protein complexes. However, its application to flexible systems, such as described here, suffers from an inability to crystallize large flexible structures as well as the effects of crystal packing on flexible structures. Similarly, application of crystallography to membrane proteins is also limited due to crystallization issues caused by hydrophobicity and the necessity to include lipid membranes in a full analysis of structure and function of these proteins. In contrast, solution NMR is a versatile technique that can provide structural, dynamic, and kinetic data on biological systems and their interactions with each other or with ligands. However, interpretation of complex NMR data of protein complexes or enzymes critically relies on the ability to uniquely assign spectral resonances to distinct nuclei in the molecule. In large biomolecules and molecules with crowded and overlapping resonances, unambiguous assignments or measurements of distance constraints and subsequent structure determination is very challenging and existing methods are frequently inadequate [1].

Characterization of protein structures by NMR requires unambiguous assignment of backbone and side chain resonances and determination of unequivocal distance constraints from nuclear Overhauser effects (nOe) measured in NOESY experiments (Figure 1). These constraints are used for structure calculations. With increasing protein size, the number of resonances increases dramatically leading to crowded or overlapping NMR spectra. Current established strategies rely on proteins uniformly enriched with 13C and 15N and/or with selective enrichment of the methyl groups of Leu, Val and Ile with 13C and full protonation (e.g. 13C1H3). The latter selectively enriched amino acids are introduced into

perdeuterated proteins [2]. The biomolecule is typically uniformly enriched in 15N so that nOes involving those residual protons (amide and methyl groups) can be measured and identified. This sparse labeling approach generates strong methyl-group nOes and allows their assignments but obviously reduces the total number of resulting distance constraints dramatically, leading to less well defined structures. Further, faster relaxation in larger proteins leads to signal losses and decreased peak intensities. Hence, unambiguous data are not easily accessible and structure determination is compromised. To allow for high-resolution NMR studies of large proteins and complexes, a specific combination of amino acid labeling patterns is required to optimize magnetization transfer pathways in NMR experiments (Figure 2).

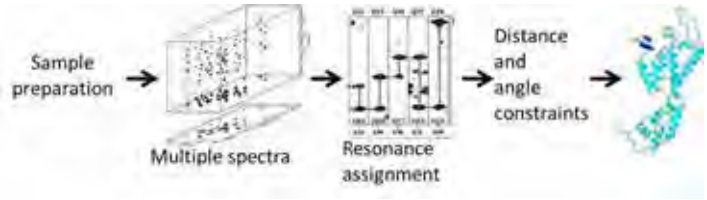

Figure 1. Flow chart of solution structure determination from NMR data.

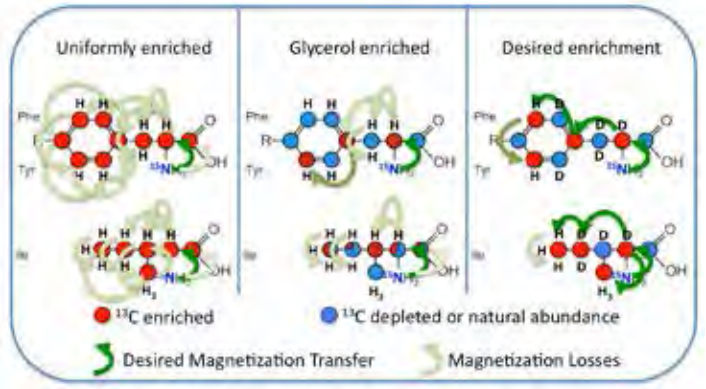

Figure 2. Magnetization transfer pathways in uniformly labeled, glycerol enriched and our 'designer' amino acids.

In this project, we have set out the following goals:

- Develop NMR methods optimized for selectively labeled large proteins and complexes. We aimed to develop new 3D and 4D NMR experiments for resonance assignments and unambiguous determination of distance and orientational constraints with superior sensitivity for large proteins and complexes. The methods are designed to take advantage of optimized magnetization transfer pathways to minimize signal losses by utilizing new amino acids selectively labeled with stable isotopes. We also aimed to optimize non-uniform sampling schemes and data reconstruction algorithms that require only a fraction of all potential data points to be recorded without loss of resolution and sensitivity, shortening data acquisition time, and dramatically improving sensitivity.

- Develop new, selective stable isotope labeling patterns for amino acids and incorporate them into target proteins and complexes. We devised new stable isotope labeling schemes for selected amino acids to simplify NMR studies of large and membrane inserted biomolecules. The isotopic labels were to be incorporated at specific positions to optimize NMR signal and limit relaxation losses during experiments. Co-optimization of sample labeling and NMR methods development will improve the spectral resolution and signal quality allowing very large and membrane-inserted proteins to become accessible by NMR spectroscopy for the first time. We attempted to prepare the selectively labeled amino acids will by direct chemical synthesis and/or by using labeled metabolic precursors (glycerol, pyruvate, glycine, succinate) for in vivo protein production to allow very specific and selective isotopic enrichment.

- Validate the new NMR methods and labeling patterns by applying them to structure determination of a large protein complex. Little is known about the large enzymatic assembly lines responsible for the biosynthesis of bioactive compounds (antibiotics, anti-cancer drugs, virulence factors, toxins, etc.). We employed the stable isotope labeling schemes and the NMR methods developed above to solution NMR studies of a 34kDa enzyme and a large, 132kDa, protein complex involved in the biosynthesis of enterobactin. The complex will be the largest structure determined by solution NMR.

Scientific Approach and Accomplishments

Amino acid labeling for NMR structural studies of large systems. While synthetic schemes for many isotopically labeled amino acids have been fully developed, they have not been used to produce amino acids with the site specific isotopic labels required to support our studies of large biological systems using our new NMR methods. The critical point is that the spin systems (13C-1H, 15N-1H, 15N-13Cα) must be isolated to minimize relaxation losses while still allowing for necessary magnetization transfer to make resonance assignments (Figures 2 and 3). For optimal NMR performance, all amino acids have amino nitrogens labeled with N-15 and α-carbons labeled with C-13 and duterated. The carbonyl carbons are unlabeled and the side chains have C-13 labeled and protonated carbons alternating with unlabeled deuterated carbons. A common precursors to all amino acids is [2-13C, 15N, 2H]-glycine attached to a chiral auxiliary synthon (2,10-camphorsultam, Figure 3). We have synthesized [2-13C, 15N]-glycine

from 2-13C-bromoacetic acid and 15N-potasium succinimide. The reaction can be performed on 1 mole scale and proceeds with good yield. The purified glycine was subsequently protected by esterification with methanol on the carboxyl group and with thiomethyl groups on the amino functionality. Deuteration of amino- and carboxyl-protected glycine proceeded at 25-40oC with catalytic amounts of sodium metal in methanol-d and resulted in 98%+ deuteration and pure product with minimal workup (extraction). The deuterated protected glycine was attached to the sultam and served as the initial building block for all amino acids (Figure 3).

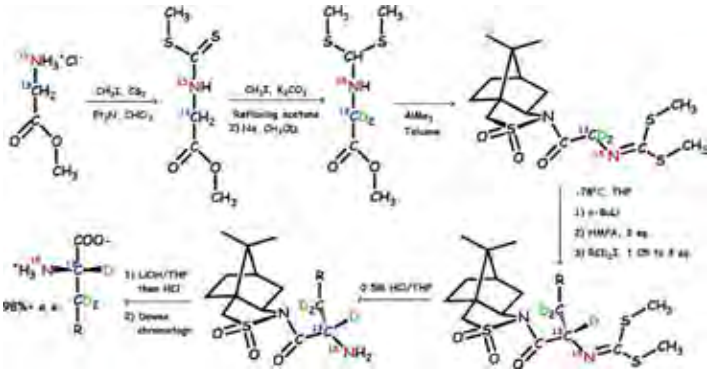

Figure 3. General synthetic scheme for preparation of labeled L-amino acids. The common precursor, glycinate sultam, is inside the blue rectangle.

Synthetic pathways for the production of isotopically enriched amino acids have been worked out over the last decades, with major contributions from the Stable Isotope Resource (SIR) at LANL and Kainosho's group at RIKEN, Japan [3]. While we have the expertise and technology to synthesize all natural amino acids with any site specific isotope labels to allow for the proposed high-resolution NMR studies, the specific combinations of labeling patterns required to optimize magnetization transfer pathways for studies on very large systems have not yet been done. The needed labeling pattern necessary poses its own unique problems, particularly with respect to deuterium incorporation. While 13C and 15N labels cannot undergo exchange to 12C and 14N, depending on the chemical structure, some deuterium positions may be exchangeable with solvent leading to isotopic dilution. For preparation of good NMR samples, amino acids need to be >98% 13C, >98% 15N and >95% D at selected positions. Early on we noticed that several standard synthetic steps lead to isotopic dilution at deuterated positions. One example is silica gel purification during which acidity of the silica gel was sufficient to pull of the deuterium atom and exchange it with the hydrogen from the solvent system. We have also observed isotopic dilution when oxalyl chloride was used in esterification reactions. We mitigated these problems by resorting to alternate purification methods (crystallization, extraction) and/or by substituting reaction solvents with their deuterated versions. While increasing the cost of synthesis, this led to highly deuterated products.

All amino acid side chains were synthesized individually and attached to the glycinate sultam, cleaved and deprotected to yield 18 natural amino acids. Two amino acids, cysteine and tryptophan, were obtained using enzymatic reaction of tryptophan synthase, with labeled serine and benzenethiol (cysteine) or indole (tryptophan) as substrates. Overall, we successfully synthesized all 20 natural amino acids. Our labeling pattern and synthesis, as well as observations of isotopic dilution during deuteration are currently being written up for publication.

In vivo selective protein labeling. For metabolic labeling of proteins, we have cloned the gene for the small protein, ubiquitin (76 amino acids) into E. coli hosts. Expression of this protein under various labeling conditions allowed us to monitor incorporation of isotopes at specific positions in amino acids, since NMR spectra for ubiquitin are well resolved and characterized. We have performed growth in the presence of labeled glycine (which we synthesized), pyruvate or succinate. Analysis of produced ubiquitin showed significant scrambling of all isotopes leading us to conclude that metabolic labeling using these precursors will not be acceptable for NMR of large proteins. Analysis of isotope incorporation in the protein shows that for this approach to be successful we would need to judiciously incorporate inhibitors of amino acid synthesis into growth media to accomplish desired labeling. Since the chemical synthesis can provide large quantities of amino acids with exact labeling patterns, the in vivo approach was abandoned.

NMR methods development. For successful NMR studies of large and complex systems it is critical to limit possible relaxation pathways, reduce the length of pulse sequences to minimize signal losses, and reduce experimental time, which is usually very long (days to weeks). For NMR methods development part of the project, we have modified and tested recently developed 3D TROSY-hNCAnH and 3D TROSY-hN(CO)CAnH NMR experiments [4] by converting them to double-TROSY versions for further increased sensitivity in large proteins. The experiments were tested on a large, 34kDa protein diisopropyl fluorophosphatase (DFPase) from Loligo vulgari, an enzyme that hydrolyses organophosphates. It is an excellent test system – large, very stable and with well-defined structure.

For data acquisition and handling we have implemented and tested on DFPase Non-Uniform Sampling (NUS) schemes based on Iterative Soft Threshold (IST) reconstruction algorithms [5] to determine minimum number of data points in multidimensional experiments that allow

for faithful reconstruction. Since the method allows for collection of significantly reduced number of data points in the experiment, it allows us to reduce experimental time 5-10-fold for 3-dimensional NMR experiments and 15-20-fold for 4-dimensional experiments.

NMR structure determination of large proteins. We have performed all experiments necessary for assignments and structure calculations, including our new and improved NMR experiments, on a sample of DFPase. We have obtained all assignments and distance constraints and are in the final stages of structure validation for publication and release. For the large enterobactin complex, isotopic dilution issues during synthesis have delayed protein synthesis. The protein complex is currently being prepared for NMR analysis. Structure calculation of this large complex will follow and will be the largest de novo single structure obtained by high-resolution NMR.

Summary. During the course of the project, we have synthesized all twenty natural amino acids with well defined, specific stable isotope labeling patterns. The expertise we gained in this area puts us at the forefront of protein labeling methodologies. We explored in vivo protein labeling and decided that it was not selective enough for our needs. We have improved sensitivity of the necessary 3D NMR experiments and applied them to study of an important enzyme, DFPase. We have also implemented non-uniform sampling methods for significantly faster NMR data acquisition. We are in the final stages of DFPase structure validation and began work on the large protein complex, enterobactin synthase, which will be the largest structure solved and will place us at the forefront of modern structural biology.

Impact on National Missions

Knowledge of the structures and mechanisms of both large proteins and their complexes and membrane-bound proteins is critical to our understanding of and intervention in processes as varied as antibiotic resistance and biosynthesis, biofuels production, and disease development (Parkinson's, Alzheimer's, diabetes, etc.). This project is directly related to LANL's missions in Global Security, Biothreat Reduction, and Energy Security and will open the structural biology field to the detailed mechanistic studies of large protein complexes and membrane-bound proteins involved in the above as well as many other processes placing LANL at the forefront of the field. Leveraging the results obtained here with LANL's synthetic stable isotope capabilities, will open funding areas from NIH, DTRA and DOE. We will work closely with program managers in Global Security (Kirsten McCabe) and DOE (BES/BER) so that future funding for these efforts can be developed.

The project resulted in conversion of Alex Koglin from Oppenheimer Postdoctoral Fellow to Scientist 2. Alex brought to LANL new capabilities in fast discovery of natural therapeutics using genome mining and analysis of gene clustering, work that he is continuing as an independent scientist.

References

1. Hyberts, S. G., D. P. Frueh, Arthanari, and Wagner. FM reconstruction of non-uniformly sampled protein NMR data at higher dimensions and optimization by distillation. 2009. JOURNAL OF BIOMOLECULAR NMR. 45 (3): 283.

2. Tugarinov, V., and L. E. Kay. Ile, Leu, and Val methyl assignments of the 723-residue malate synthase G using a new labeling strategy and novel NMR methods. 2003. JOURNAL OF THE AMERICAN CHEMICAL SOCIETY. 125 (45): 13868.

3. Ohki, , and Kainosho. Stable isotope labeling methods for protein NMR spectroscopy. 2008. PROGRESS IN NUCLEAR MAGNETIC RESONANCE SPECTROSCOPY. 53 (4): 208.

4. Frueh, D. P., Arthanari, Koglin, C. T. Walsh, and Wagner. A Double TROSY hNCAnH Experiment for Efficient Assignment of Large and Challenging Proteins. 2009. JOURNAL OF THE AMERICAN CHEMICAL SOCIETY. 131 (36): 12880.

5. Hyberts, S. G., A. G. Milbradt, A. B. Wagner, Arthanari, and Wagner. Application of iterative soft thresholding for fast reconstruction of NMR data non-uniformly sampled with multidimensional Poisson Gap scheduling. 2012. JOURNAL OF BIOMOLECULAR NMR. 52 (4): 315.

Redox active Catalysts for C-C Coupling Reactions Relevant to Renewable Energy

John C. Gordon
20130672ER

Abstract

The majority of glycerol is currently sourced from animal fats and vegetable oils, with a small amount made synthetically for ultrapure applications. Production is rapidly increasing due to biofuel directives being implemented. Projections suggest that by 2020 the production of glycerol will be six times that of the demand, as usage is limited to food additives, the pharmaceutical industries and some chemical applications, including conversion to acrolein, acetol, ethanol and epichlorohydrin. Novel approaches to sustainable fuel sources have been focused on generation of bio-diesel from various feedstocks. As a major by-product of biodiesel production, glycerol has found some use as a food additive, in coolant applications, and currently there is a great deal of interest in conversion of glycerol into other chemicals including propanediol, acrolein, and polyethers along with many other useful chemicals. Thus far there has been little discussion of creating larger carbon chains derived from glycerol or its derivatives, aside from Fisher-Tropsch chemisties. This proposal aims to generate a method based on iron catalysts to convert renewable glycerol derived C3 fragments into C6 species that can then be used in subsequent fuels and feedstocks chemistry.

Background and Research Objectives

The research in this project has targeted the development of inexpensive catalysts, comprised of earth abundant metals, which are capable of supporting multiple electron reductions pertinent to biomass derived molecule upgrading. This chemistry was aimed towards the promotion of carbon-carbon bond forming reactions of ketonic and aldehydic moieties, with the ultimate goal being the conversion of readily available three-carbon fragments derived from glycerol (e.g. acrolein, acetol (hydroxyacetone), etc.) into six (or higher) carbon containing fragments that are then potentially viable as fuel precursors or can be further converted into higher value added feedstock chemical feedstocks. A recent DOE report highlights a list of targeted Top Value-Added Chemicals from Biomass. To the best of our knowledge there are currently no useful methods available to take advantage of these kinds of glycerol derived synthons in this regard. This is in spite of the low cost of glycerol due to its abundance as a by-product of biodiesel production. As mentioned above, glycerol is readily converted into species such as acetol and acrolein, which contain carbonyl (C=O) functionalities potentially amenable to participation in Pinacol type self- and cross-coupling reactions with other C3-C6 biomass derived molecules. Current approaches for glycerol conversion are essentially limited to use in the energy inefficient Fischer-Tropsch process. The Pinacol coupling reaction is a 2-electron process that can aid in forming C-C bonds, however this presents significant challenge for Fe as this metal more readily facilitates 1-electron chemistry. Nonetheless, the goal of using an Fe-based catalyst for this reaction type is attractive due to the pairing of an inexpensive metal with potentially very large scale biomass-derived substrates

Scientific Approach and Accomplishments

This work has attempted to use redox active ligands capable of conferring up to two-electron redox behavior. This is a possible way to promote bond-making reactions and carbon chain extension reactions involving carbonyl containing substrates. We began with the interrogation of diimine ligands to try to facilitate the desired chemistry. A series of (diimine)Fe complexes were made and their efficacy towards carbonyl (C=O) containing substrate coupling reactions was investigated. This provided mixed results. In retrospect, we believe that this particular class of ligands was insufficently oxidizing with respect to the iron centers to which they were bound. When we used model substrate compounds such as benzophenone, acetophenone, etc. to interrogate reactivity, instead of the desired coupling reactions, we primarily observed substrate binding via an arene group, rather than through binding of the carbonyl group by the metal center. This led us to the conclusion that the Fe centers

were less oxidized by these ligand systems (therefore lower valent and less oxophilic) than we had hoped for in order to facilitate the targeted Pinacol chemistry. These arene complexes are interesting in their own right and a publication should result on their chemistries.

From our initial results, the more a prospective complex can present itself as containing Fe(II), the better it should be able to facilitate the desired chemistry. This poses the question of how can the redox activity of the ligand be chosen such that we can exercise more granular control over the electronic state and hence the reactivity of the metal center? Two possible approaches to this question are the incorporation of an oxidant into the ligand and the creation of an internal barrier to ligand oxidation. Quinone and various derivatives thereof are well-known 2-electron organic oxidants, and as several 1,2-diimino quinones have been synthesized and, in one case, used as a ligand for Cu. We have considered this kind of ligand motif as one that can faciiltate the desired redox chemistry. We have most recently used computations to probe the redox behavior of potentially dianionic quinone supported catalysts and have set about synthetically accessing these.

Impact on National Missions

This work advances our understanding of the chemistry and chemical methods that directly bear upon energy security. Success in this area would seed the development of future approaches to more efficient chemistries, potentially providing a bridge from basic science to global scale energy solutions. This is a high profile area of renewable energy. Work in this area is relevant DOE Office of Basic Energy Sciences (Catalysis Science) and DOE Office of Energy Efficiency and Renewable Energy (BETO).

Novel Chemical Architectures for Supercapacitor Electrolytes: Comparing In Situ Scattering Measurements to Theory and Simulation

Cynthia F. Welch
20130681ER

Abstract

Many renewable energy sources produce only intermittent electricity generation. Supercapacitors promise to be one leading scheme for storing that energy for stable use. If their energy densities can be improved, they may find application in a range of devices since they can deliver an order of magnitude more power than chemical batteries. Recent studies suggest that matching electrolyte size to electrode pore geometry yields dramatic increases in capacitance. Most efforts to improve supercapacitor performance focus on optimizing the electrode. In this study, we took the novel approach of optimizing the electrolyte by controlling its constituent size and shape distributions. In addition to our integrated experimental and modeling tools, we developed a new theoretical method to describe these complex systems; this method enabled linking specific chemistries to our multi-scale simulation models. The primary product of this study is a predictive framework that ties electrolyte chemistry to ultimate device performance for standard electrode configurations, as well as new fundamental insight into the molecular-level behavior of these complex systems.

Background and Research Objectives

Many processes involved in manufacturing and transporting goods suffer from inefficiencies due to wasted energy. Similarly, many renewable energy sources (such as wind and solar) yield only intermittent electricity generation. We therefore require advanced devices that quickly capture and release stored energy. If their energy densities can be improved, given that supercapacitors may deliver an order of magnitude more power than chemical batteries, they may dramatically improve the performance of dynamic energy capture and reuse systems. This may be achieved by improvements to either the electrode designs or to the electrolyte. Nanoporous carbon in various forms often serves as the electrode material. Key properties for a successful electrolyte material include high ionic conductivity for fast charge/discharge rates, strong chemical durability for long device lifetimes, good thermal stability to provide function over a very broad range of temperatures, and low volatility and flammability for enhanced safety [1]. Recently, Gogotsi [2] and coworkers demonstrated that carefully matching the pore size in the electrode to the electrolyte moieties enhances capacitance dramatically. They accomplished this via a clever fabrication route to control the electrode pore structure. Little attention has been paid to electrolyte size and shape.

We propose that tailoring the size and shape of the electrolyte in supercapacitors to match the electrode surface geometry will lead to enhanced energy densities, forming our central hypothesis. This hypothesis leads us to consider dendrimer electrolytes as candidates for use in supercapacitors, as well as to study their behavior near and in the electrode pores. The novelty of our proposal lies in optimizing the electrolyte rather than the electrode; this approach may prove more potent and robust than modifying the electrode. Certain dendritic chemistries possess all of the key properties needed in a good electrolyte, and several specific aspects of the physical chemistry recommend them for application in supercapacitors. These characteristics include precisely controlled size and shape, broad range of available sizes, high charge densities, low viscosities at relevant concentrations, and the ability to capture impurities. Many key questions about the behavior of the electrolytes near electrodes must be answered for progress to be made. By combining experiment, theory, and simulation in this project, we provide insight into many of these questions.

Scientific Approach and Accomplishments

Theoretical description of conditions needed for dendrimer electrolyte adsorption to flat electrode surface

Our envisioned application of dendrimers as supercapacitor electrolytes revolves around placing these molecules at and removing them from charged surfaces. Thus, we need a prescription for the conditions needed to re-

lease a charged dendrimer from an oppositely charged flat substrate. We developed this prescription by (a) identifying an effective segment step length that reflects the intramolecular repulsions due to excluded volume and electrostatics, as well as the dendrimer's branching, and (b) using that effective step length to derive an analytical equation that describes the boundary between captured and free dendrimers. We validated this theoretical prediction by performing Monte Carlo computer simulations of coarse-grained model dendrimers escaping from charged surfaces. The simulations considered generations 2 through 6 with a range of lengths between the branch points, as well as a range of solution ionic strengths and surface charge densities. Full details can be found in our publication on this subject: J. Chem. Phys. 2013, 139, 164906.

Scaling theory and simulations to describe interactions between concentrated dendrimer electrolyte solution and flat electrode surface

A single dendrimer electrolyte molecule can contain a large number of charged groups that are available to interact with an oppositely charged electrode surface. We need to understand how to maximize these interactions, thereby maximizing capacitance. To aid in this effort, we used the results of (1) above to develop a scaling theory that describes the thickness of an adsorbed dendrimer layer at an electrode surface, as well as the fraction of segments within the dendrimer that touch the surface, and the total number of dendrimers adsorbed as a function of generation of growth (i.e., dendrimer size), surface charge density, and dendrimer concentration. We demonstrate that these predictions agree well with extensive molecular dynamics simulations, which span a range of concentrations, electrode surface charges, and dendrimer electrolyte size. Combined, the simulations and scaling argument indicate that simultaneous adsorption and compression at the interface take place. Full details can be found in our publication on this subject: ACS Macro Lett. 2014, 3, 180.

In situ experiments to probe structure of dendrimer electrolyte-electrode interface

Building on (2) above, we conducted a series of experiments on poly(amido amine) (PAMAM) dendrimer electrolytes in combination with flat oppositely charged electrodes to better understand electrolyte-electrode interactions. For the experiments, we performed in situ neutron reflectivity (NR) experiments using an electrochemical cell [3] at the SPEAR beam line at the Los Alamos Neutron Science Center (LANSCE). This cell features a quartz substrate coated with palladium as the working electrode and a counter electrode of stainless steel coated with gold. With this cell, we varied the voltage applied across the electrodes and then measured changes in the in-plane averaged scattering length density (SLD) profile of the dendrimers normal to the electrode. This gives information on the thickness of the dendrimer layer adsorbed to the electrode surface, as well as on how that thickness changes with applied voltage. Though our initial results suggested a confirmation of the theory and simulation results described in (2) above, we were unable to follow up with further experiments at SPEAR or any other neutron reflectivity beam line, due to budget cuts in both the BES-supported Lujan Center at LANSCE and in the LDRD program.

Simulations to explore behavior of PAMAM dendrimer electrolyte at an oppositely charged flat electrode surface

Molecular dynamics simulations were performed to observe structural features at the electrode-electrolyte interface in order to aid in the interpretation of the NR data described in (3) above. These simulations were aimed at specifically modeling PAMAM dendrimer chemistry in the presence of an oppositely charged carbon flat electrode. To do so, we used two different united atom models: an extended version of the TraPPE-UA force field [4] (Transferable Potentials for Phase Equilibria – United Atom; parameterized for PAMAM as part of this project) and the coarse-grained MARTINI force field (parameterized for PAMAM by Lee and Larson [5]). Various simulations were performed to test the effectiveness of these models in simulating PAMAM dendrimers.

Both models give reasonable results for the size of PAMAM dendrimers at different generations of growth and charge densities. Both were also used to simulate the mobility of PAMAM dendrimers in the presence of electric fields and to model dendrimer-dendrimer interactions in concentrated solutions. Overall, the TraPPE model was able to explore a larger range of electric field strengths and produce more realistic PAMAM dendrimer electrolyte / carbon electrode interactions in the presence of aqueous solvent molecules. The fully charged PAMAM dendrimer does not adsorb to the carbon electrode surface at zero field (as expected).

On the other hand, a high electric field causes the dendrimer to adsorb and flatten on the surface, while the counterions move to the opposite surface. When the field is removed, both the dendrimer and counterions desorb. This behavior is consistent with the results obtained in (2) above for the molecular dynamics simulations that did not account for specific chemical interactions. Further details on the chemistry-specific simulations will be described in manuscripts in preparation for submission to peer-reviewed journals. In summary, the results suggest that PAMAM dendrimers will behave as good electrolytes in a supercapacitor with carbon electrodes.

Simulations to evaluate stability of PAMAM dendrimers against chemical degradation due to exposure to electric fields

We carried out first-principles molecular dynamics simulations using the finite element density functional theory code FEMTECK, which was developed in Japan by E. Tsuchida [6]. FEMTECK is an efficient simulation code with the ability to apply an electric field. To gain access to this unique capability, we developed a collaboration with Drs. Tsuchida and Choe at Japan's National Institute of Advanced Industrial Science & Technology (AIST), and we sent one of our postdoctoral researchers to AIST in Japan to learn how to use the code and port it to LANL's Institutional Computing resources. We then carried out simulations of solvated G0 PAMAM at high, neutral, and low pH (corresponding to uncharged, partially charged, and fully charged PAMAM, respectively), with and without an applied electric field. We see more proton transfers between the dendrimer and the water for charged dendrimers with the electric field applied, but we do not see any evidence of carbon-carbon or carbon-nitrogen bonds breaking, suggesting that PAMAM dendrimers are stable against electrolytic degradation.

Scaling theory and device-level simulations to describe capacitance of dendrimers

Based on geometrical considerations of dendrimer electrolytes, we developed a scaling theory to predict their capacitance at a flat electrode surface. This theory shows that for electrode surfaces that are saturated with dendrimer electrolytes, capacitance should decrease with increasing dendrimer generation of growth (or size). We have also examined the partitioning of dendrimer electrolytes into pores that mimic those of porous electrodes. These simulations show optimal behavior for capacitance when dendrimer size matches that of the pore. More specifically, dendrimers whose size is smaller than the pore can easily enter and exit the pore, while those that are too large tend to get stuck at the pore entry, thereby blocking the pore. Dendrimers whose size matches the pore enter readily and then remain inside the pore for extended periods of time. These results are described in more detail in 1 – 2 manuscripts being prepared for submission to peer-reviewed journals.

Simulations and experiments aimed at testing the central hypothesis of this study, that the use of dendritic electrolytes will lead to higher charge storage in supercapacitors

We propose that dendrimer polyelectrolytes may provide enhanced supercapacitor performance relative to small molecule electrolytes when paired with porous electrodes with confining geometries commensurate with the size of the electrolyte molecules. To test this hypothesis, we built on the work described in (2) and (6) above to perform a series of coarse-grained Brownian dynamics simulations on a set of model dendrimers, linear oligomers, and small electrolyte ions in the presence of a model porous electrode stack. Motivated by the computational results and guided by all previous results obtained in (1) – (6) above, we subsequently tested the performance of generation 3 and generation 5 PAMAM dendrimer electrolytes in supercapacitors composed of both flat carbon and porous activated carbon electrodes. Those results are compared against the performance of a typical supercapacitor electrolyte, sulfuric acid. We find that: a) there exists a minimum charge density required for electrolyte molecules of different molecular sizes to enter the pores; b) the amount of cationic electrolyte charge partitioned into the cathode pores grows linearly with electrode charge density once this minimum electrode charge has been met; c) the total net charge on the electrodes depends on the molecular architecture; and d) dendrimers outperform a typical small molecule electrolyte at the same molarity of charge in experimental measurements of charge accumulation at porous activated carbon cathodes, as predicted by the simulations and supporting our proposition. We are in the process of submitting this work for publication in a peer-reviewed journal.

Impact on National Missions

We expect agencies such as DOE EERE and ARPA-E, as well as the renewable energy industrial sector, to find the results of this study a solid foundation for future funded programs. Therefore, we are preparing proposals aimed at these DOE agencies, and we are discussing our results with LANL's Feynman Center for Innovation to establish a path forward for potential patents and collaborations with industry. The collaboration with AIST (see (5) above) brought a new theory and modeling capability (FEMTECK) to LANL. This project also produced two peer-reviewed publications (with 4 – 5 more expected submissions), as well as multiple presentations at local, national, and international venues. Furthermore, it supported the hiring of two postdoctoral researchers, both of whom have brought new expertise and capabilities to LANL. One of these postdocs has recently been awarded a Seaborg Institute Postdoctoral Fellowship. In addition, this project provided partial support for 3 graduate student interns at LANL, 2 of whom were converted to LANL Technologists.

References

1. Basic Research Needs for Electrical Energy Storage. 2007. Office of Basic Energy Sciences, U.S. Department of Energy.

2. Chmiola, , Yushin, Gogotsi, Portet, Simon, and P. L.

Taberna. Anomalous increase in carbon capacitance at pore sizes less than 1 nanometer. 2006. SCIENCE. 313 (5794): 1760.

3. Zamlynny, V., I. Burgess, G. Szymanski, J. Lipkowski, J. Majewski, G. Smith, S. Satija, and R. Ivkov. Electrochemical and neutron reflectivity studies of spontaneously formed amphiphilic surfactant bilayers at the gold-solution interface. 2000. LANGMUIR. 16 (25): 9861.

4. Wick, C. D., J. M. Stubbs, N. Rai, and J. I. Siepmann. Transferable potentials for phase equilibria. 7. Primary, secondary, and tertiary amines, nitroalkanes and nitrobenzene, nitriles, amides, pyridine, and pyrimidine. 2005. JOURNAL OF PHYSICAL CHEMISTRY B. 109 (40): 18974.

5. Lee, , and R. G. Larson. Effects of PEGylation on the Size and Internal Structure of Dendrimers: Self-Penetration of Long PEG Chains into the Dendrimer Core. 2011. MACROMOLECULES. 44 (7): 2291.

6. Tsuchida, E., and M. Tsukada. Adaptive finite-element method for electronic-structure calculations. 1996. PHYSICAL REVIEW B. 54 (11): 7602.

Publications

Maerzke, K. A., N. J. Henson, P. M. Welch, and C. F. Welch. Deformation of poly(amido amine) dendrimers at surfaces. Presented at 249th American Chemical Society National Meeting. (Denver, CO, 22-26 Mar. 2015).

Maerzke, K. A., N. J. Henson, P. M. Welch, and C. F. Welch. Deformation of poly(amido amine) dendrimers at charged surfaces. Invited presentation at National Institute of Advanced Industrial Science and Technology (AIST). (Tsukuba, Japan, Oct. 2014).

Welch, C., P. Welch, N. Henson, V. Hartung, T. Lin, S. Edwards, and J. Stull. Novel chemical architectures for supercapacitor electrolytes: Comparing in situ scattering measurements to theory and simulation . Invited presentation at Los Alamos National Laboratory Materials for the Future Capability Review. (Los Alamos, NM, 4-7 May 2014).

Welch, P. M.. The escape of a charged dendrimer from an oppositely charged planar surface. 2013. Journal of Chemical Physics. 139: 164906.

Welch, P. M., C. F. Welch, and N. J. Henson. The flattening of dendrimers from solutions onto charged surfaces. 2014. ACS Macro Letters. 3: 180.

One-step Supercritical Fluid Extraction (SFE) and Separation of Rare Earths (RE)

Stephen L. Yarbro
20140186ER

Abstract

We have demonstrated a prototype system (Figure 1) that exploits the solvent power of supercritical carbon dioxide (SCCO2) with co-solvents for lanthanide (rare earth) separation from oxides and potentially ore. Also, we have demonstrated that the different lanthanide-organic species can be separated in a curved diverging nozzle while still in the supercritical gas phase. The key results are:

- Essentially 100% extraction in 100 minutes
- Nd Predicted separation factor – 1.3 Measured separation factor – 1.2 to 1.8
- Separation factor is the ratio of concentration ratios: ([Nd]/[Yb])Output1¬ / ([Nd]/[Yb])Output2

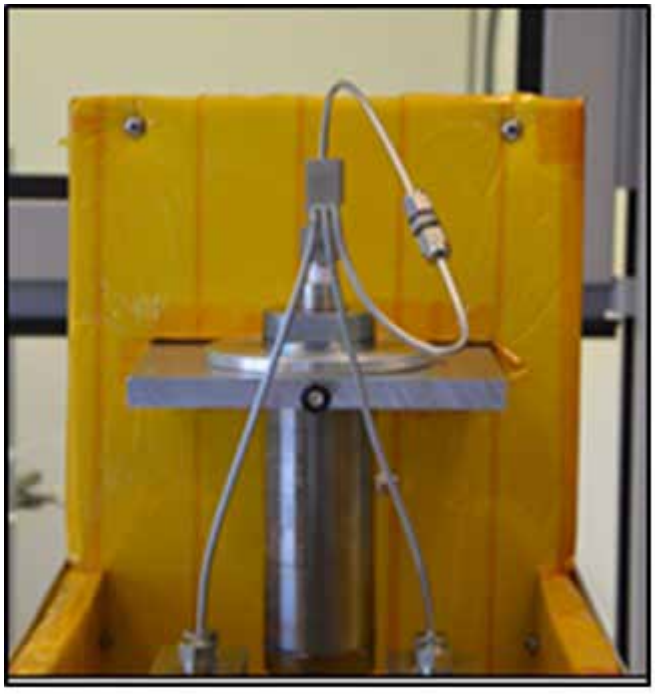

Figure 1. Prototype SCCO Lanthanide Extraction and Separation System.

In this case, the separation factor is calculated on the basis of the heavier organic molecule and a separation factor greater than one indicates the nozzle is separating the two components. Therefore, this approach has the potential to simplify lanthanide processing and separation. Essentially, in one-step, rare earth elements are extracted directly from oxide with the SCCO2/co-solvent mixture (typically tri-butyl phosphate (TBP)) and separated with an aerodynamic method. The aerodynamic method separates the heavier elements from the lighter elements while dis-solved in the supercritical fluid using the centrifugal force. Current production methods require complex equipment and many steps such as dissolution, flotation, and filtration, and washing, separation requiring hun¬dreds of separation stages, precipitation, and calcination. Supercritical fluids are powerful sol¬vents. Coupled with the right co-solvents, the supercritical fluid can selectively remove the lan¬thanide from the ore, and then use an aerodynamic technique developed for isotope separation to separate the lanthanides while still in the homogeneous supercritical fluid. After separation, reducing the pressure recovers the lanthanide solids thereby eliminating the majority of the current production steps along with the associated complexity, cost, and waste.

Background and Research Objectives

Rare earth elements (REEs) are a group of 15 chemical elements in the periodic table, specifically the lanthanides. Although relatively abundant in the earth's crust, REEs rarely occur in concentrated forms, making them economically challenging to obtain. These elements constitute critical components of many important technologies and products, such as hybrid vehicles, wind turbines, and cell phones. Given this global demand for green and sustainable products in energy, military, and manufacturing industries, REE demand in the United States and throughout the world is projected to increase. In recent years, China has been providing 95 to 97 percent of REEs worldwide. Because China has

Chamber Temperature (°C)	Chamber Pressure (psi)	Extractant Acidity (H+, M)	Extraction Conditions	Co-solvent inlet flow rate (mL/min)	CO_2 inlet flow rate (mL/min)	Nd:Yb Separation Factor
85	2180	2.52	Dynamic (120 min)	0.5	14-16	1.22
60	2180	4.54	Dynamic (120 min)	0.5	14.5-16	1.87

Table 1. Key results from extraction and separation tests

demonstrated its ability to control and limit REE exports, it is crucial that the United States expand its ability to obtain REE resources. Mining in the natural environment is the primary means of REE acquisition; however, it results in a large quantity (greater than 90 percent) of excess and unused materials and other environmental impacts. If the United States is to ensure a continuous supply of REEs, responsible mining and extraction practices will need to be developed and enhanced. Additionally, effective recycling, recovery, and reuse of spent consumer and industrial products may reduce the need to develop new mineral resource areas.

The increasing importance of REEs for the manufacture of modern devices, upon which society has become reliant, along with uncertain supplies, is encouraging exploration and development of new mining sites. While REEs are an important resource needed to sustain our modern technologies, the waste footprint and environmental impact from conventional REE mining and extraction operations is significant. The requirements, regulations, and financial obligations and assurances for a new mine and associated processing are usually complex and take years of planning. Therefore, enhanced technology that reduces the complexity and waste generation with a high recovery and separation efficiency would have a large economic benefit and reduce the current environmental impact.

We have measured the solubility and separation efficiency of selected strategic lanthanides (Nd, Yb) from oxide samples using SCCO2 and a co-solvent TBP. Our plan was: (1) based on the literature, choose successful co-solvent (TBP) and measure solubility at different conditions, and (2) develop a simple aerodynamic system based on the Becker nozzle for demonstration and measure separation efficiencies at different conditions. We have demonstrated the technical feasibility and ability for reducing the com¬plexity and cost of production of strategic lanthanide metals.

Long-term goal of this work: Ultimately, we intend for this work to provide the engineering basis for developing a program for using supercritical fluids to process a variety of different stra-tegic materials, including uranium ores and potentially spent fuel. Our long-term goal is for Los Alamos to be a world leader in using novel methods, such as supercritical fluids for producing strategic metals that are critical to US defense and security needs.

Scientific Approach and Accomplishments

Experimental Accomplishments

We used a commer¬cially available "off-the-shelf" (COTS) SuperCritical Fluid Technologies SFT-110 unit (Figure 2). We collaborated with the LANL Center for Inte¬grated Nanotechnologies (CINT) and their mico-fabrication capa¬bility to build simple nozzles for testing. Essentially, there were two phases to the R&D plan: (1) Measure lanthanide solubility's from a well-characterized oxide substrate to develop the procedures and analytical support, then (2) Use the solubility data to design and fabricate a simple nozzle device and with select SCCO2 streams, measure separation factors and validate the CFD model. The nozzle was designed based on the maximum pressure and flowrate through the SFT-110 unit. After the nozzle design was completed, monolithic stainless steel nozzle construction was achieved via 3-D laser printing, and stainless tubing was brazed for installation (Figure 3). Once the unit was installed a series of solubility tests at varying flowrates and acid concentrations was completed to measure the average extraction efficiency and extraction rate. With this data, a series of tests was completed to measure separation factors.

Figure 2. SFT-110 COTS SCCOExtraction System without Separator

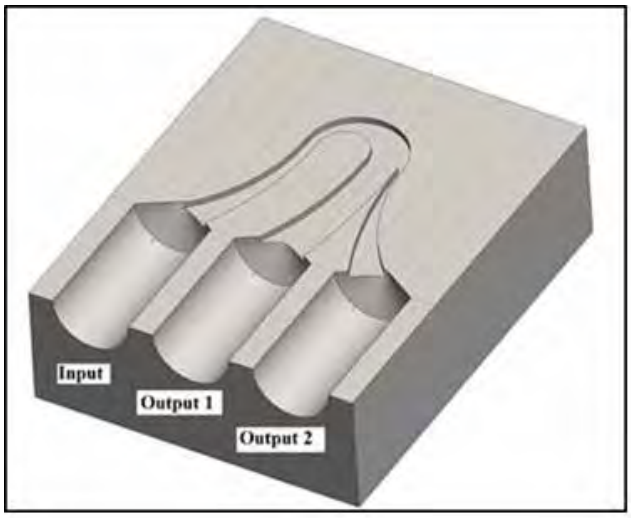

Figure 3. Cutaway View of Separator Nozzle with Output Streams Identified

Modeling

In the Becker process for uranium enrichment [1], a gas jet of ~96% hydrogen and 4% UF6 expands through a narrow slit. The gas moves at high speeds (comparable to those in a modern centrifuge) parallel to a semicircular wall of very small radius of curvature (Figure 3). At gas velocities approaching 400 m/s, with a radius of curvature of 0.1 mm, the centrifugal acceleration achieved is 1.6 x l09 m/s2 or 160 million times gravity. This acceleration exceeds those achieved in centrifuges by a factor of a thousand or more, in an apparatus with no moving parts. The centrifugal force causes the heavier components to move closer to the curved wall than the lighter components as it flows around the semicircle. At the other side, where the gas has changed direction by 180°, a knife-edge separates the flow into a light fraction and a heavy fraction. We have demonstrated that lanthanides dissolved in the supercritical fluid phase can be separated by a similar technique. As a part of the investigation of the solubility of lanthanides in supercritical carbon dioxide with co-solvents, we have developed a 2-D model of curved flow in a Becker nozzle to provide the basis for a preliminary design for testing. The model is based on the non-dimensionalized Navier-Stokes equations for incompressible flow in Cartesian coordinates. In order to calculate the pressure field, the fluid is assumed to be slightly compressible and a penalty method is used along with the divergence of the velocity field. This model has been combined with a second model that calculates the separative performance of a single stage assuming that sonic velocity and equilibrium distribution of the species has been achieved. The results are summarized below.

The key result is that the predicted separation factor and the measured separation factor are close with the measured results bracketing the predicted number. This indicates that additional chemistry is changing the weight ratio and therefore the separation factor.

Impact on National Missions

In 2012, Congress commissioned a study on the defense implications of China's control of the rare earth supply and the impact on US security [2]. Con¬gress is encouraging DOD to develop a long-term strategy to identify material weaknesses and vulnerabilities associ¬ated with RE's and to protect long-term U.S. national se¬curity interests. In addition, The Department of Energy (DOE) Energy Efficiency and Renewable Energy (EERE) Advanced Manufacturing Office is providing $120M to fund a Critical Materials Strategy focusing on critical materi¬als supply issues (Figure 4) [3]. A portion of their mission is to enable new sources of critical materials not now commercially viable, improve the economics of processing existing sources, and identify new uses for co-products and by-products that do not currently contribute to the economics of materials production. This mission integrates well with LANL's Materials for the Future Science Pillar's vision, "Pursuing the discovery sci¬ence and engineering required to establish design principles, synthesis pathways, and manufac¬turing processes ...". We envision demonstrating the process on lanthanides to build a relation¬ship with EERE and then extend the work to actinides to build programs related to nuclear material processing issues.

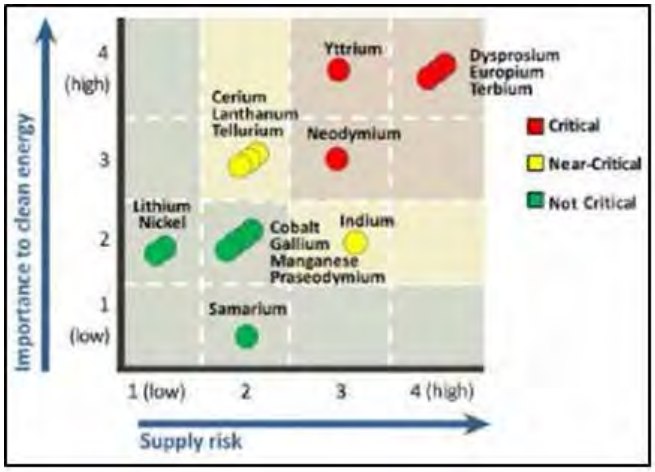

Figure 4. Relation of Supply Risk to Mission Critical Elements

References

1. Becker, E. W., K. Bier, W. Bier, R. Schütte, and D. Seidel. Separation of the isotopes of uranium by the separation nozzle process. 1967. Angewandte Chemie International Edition in English. 6 (6): 507.

2. Rare earth elements in national defense: Background, oversight issues, and options for Congress. 2012. Congressional Research Service.

3. U.S. Department of Energy Critical Materials Strategy. 2011. U.S. Department of Energy.

Publications

Yarbro, S. L., R. M. Chamberlin, P. Martinez, L. Meyers, and Q. McCulloch. Two-dimensional model of curved flow with supercritical carbon dioxide in a diverging nozzle. 2014. Los Alamos National Laboratory unclassified release.

Low-Grade Thermal Energy Recovery

Robert P. Currier
20150303ER

Abstract

Energy-intensive industrial processes, such as electric power production, refineries, chemical plants, and smelters, routinely discard enormous quantities of low-grade thermal energy, known as waste heat, to the environment. This lowers the net energy efficiency. Waste heat rejection usually involves evaporating water in cooling towers, which in turn results in high water demand. For example, US electric power plants use approximately 196 billion gallons per day (8587 cubic meters/sec). This leaves electricity security dependent on the water supply. Cost-effective techniques that can utilize even a portion of this waste heat will improve efficiency, reduce water consumption, and thus improve energy security. Methods proposed to date have low efficiency, are expensive, and/or do not scale-up favorably. This project evaluated an alternative thermal energy recovery concept that uses only conventional, affordable, and scalable processing equipment such as pumps, heat exchangers, and turbines. The following steps, executed in a circulating flow system, are the essence of the concept: water and gas are used to form an incompressible mixture that entraps a gas; the mixture is then pumped to high pressure; waste heat is used to release the entrapped gas at elevated pressure; the liberated gas is further warmed by waste heat; then the warmed gas is expanded to recover usable energy (electricity or shaft work). Some of the recovered energy is used to power the pump. Established engineering principles were used to elucidate key design parameters, evaluate the best working fluids using performance calculations, and identify efficiency improvement and cost-saving opportunities. Assessments of three methods based on this concept were conducted. Crystalline clathrates, reversible chemical reactions, and non-volatile solvents that can absorb large amounts of gas were evaluated. The solvent approach using tailored ionic liquids appears to be the most promising. It may foster the elimination of some process equipment, resulting in reduced capital costs.

Background and Research Objectives

A common cooling task in many industrial processes is to transfer residual energy (in the form of sensible waste heat) to the environment. Water is typically the cooling medium of choice because of its availability, high specific heat capacity, and large heat of vaporization. Most industrial operations use variations of two different wet cooling technologies - once through and closed-loop (cooling tower) cooling systems. A small portion of industry does use dry cooling (convective heat transfer to air rather than evaporation). However, once-through wet cooling is involved in delivering almost 25% of the U.S. electricity. Closed-loop wet systems consumed about 88% of water used in electricity generation in 2011. It is now recognized that U.S. thermoelectric power generation is vulnerable to disruptions in the water supply. Recovery of waste heat (even partially) would clearly be of benefit to U.S. industry. The fundamental challenge in effective waste heat recovery is associated with the fact that the low temperatures involved leave little thermodynamic driving force for conversion to more useful forms of energy.

One low water consumption waste heat recovery option involves solid-state thermoelectric generators (TEGs). However, a major scale difference remains between the Rankine-gas turbine cycles used in thermoelectric power plants (producing hundreds of megawatts of electricity) and TEGs that individually generate only a few watts. Retrofitting a large coal-fired power plant with a thermoelectric recovery system will undoubtedly require significant capital investment [1]. Thus no operational TEG systems have been constructed at scale. Other waste heat conversion options use conventional process equipment (compressors, heat exchangers, expanders). For example, closed-loop Brayton cycles based on supercritical CO2 have been examined at the pilot scale [2]. However commercial-scale implementation remains a challenge. Specifically, materials that can withstand the pressures and temperatures over economically mean-

ingfully product lifetimes are needed. Turbo-expanders unique to supercritical CO2 power cycles still face significant design challenges, e.g., high fluid density near the critical point leads to high wheel loading while material compatibility and operating temperatures impose a significant limitation on seal and bearing design. Also, the heat exchanger requirements may dictate high-cost designs and manufacturing. In addition, robust process control under supercritical conditions will require deeper knowledge of physical parameters near the critical point, and their fluctuations. Kalina absorption cycles, which involve a binary working fluid, are also being pursued [3,4]. The Kalina cycle involves a mixture of two working fluids instead of a single fluid as traditionally employed in conventional Rankine cycles. A mixture of two fluids with different boiling points results in a solution that boils over a range of temperatures as its liquid composition changes. By appropriate choice of the ratio between the components of the solution, the boiling point of the working solution can be adjusted to suit the heat input temperature. Water and ammonia is the most widely used combination, but other combinations are feasible. The change in boiling temperature can be exploited so that a larger average temperature difference is achieved between the heat source and the working fluid being vaporized. This results in more heat being extracted from the source than with a single component working fluid. Present-day Kalina cycles have relatively low efficiency and involve numerous thermal recuperators and heat exchangers [5]. The objective of this project was to evaluate some conceptually simple and scalable alternatives that could offer improved conversion efficiency and/or reduced process costs.

In pursuit of viable alternatives, our focus was on the use of the low-grade heat to generate gas suitable for driving a turbine. The work extractable from a turbine is, thermodynamically speaking, just the difference between the inlet gas enthalpy and the gas enthalpy at the exit (enthalpy is the internal energy of the gas, which is temperature dependent, plus the pressure times the volume). Thus to maximize power generation, one would like to have a high enthalpy gas fed into the turbine. This generally corresponds to achieving the highest possible gas temperature and pressure. At the same time, parasitic energy losses associated with generating such gas must be minimized in order to achieve high net efficiencies. For example, simply compressing low-pressure recycled gas to the inlet pressure will require a compressor that will consume most of the turbine output, resulting in a low efficiency. However, if working fluids could be identified that can bind (or trap) gas in an incompressible form such parasitic losses might be greatly reduced. This is because far less work is required to pressurize a dense, incompressible fluid than is needed to compress gas to the same pressure. It is important to recognize that any alternative cycles and working fluids based on trapping gas in an incompressible form must satisfy certain operational constraints. For example, the thermo-physical and phase behavior of the fluids must match the temperature range of intended operation. Other constraints also exist, which may be either thermodynamic or kinetic. To provide some perspective on these, consider first the heat associated with formation/dissociation of the trapped gas (conservation of energy dictates that the heat of formation equals exactly the heat of dissociation). Some insight into the role this heat plays in overall conversion efficiency can be obtained by comparing a power generating cycle involving trapped gas with a conventional refrigeration cycle.

For the refrigeration cycle, a fluid with a high heat of vaporization is desirable. A large heat of vaporization minimizes the amount of fluid that must be pumped, or circulated through the cycle (that pumping involves energy consumption). The power generation situation is somewhat different. Here the overall efficiency is directly related to the fraction of total heat supplied (QT + QM) that is successfully converted to electricity by the turbine/generator assembly. Since QT is ultimately dumped to the low temperature sink (i.e. to the environment), it is advantageous in a power generating cycle to minimize its magnitude. The ideal working fluid (capable of trapping gas) must also possess physical properties that minimize parasitic losses and enable affordable operation. These properties include not only the heat associated with trapping a gas molecule, but also the viscosity and density, both of which affect the pumping costs. The heat capacity and thermal conductivity must also be considered as these affect the heat transfer coefficients and thus the required heat exchange area. Rate parameters, including diffusion coefficients, mass transfer coefficients, and possibly even chemical reaction rate parameters, must also be considered in selecting and designing a system.

Scientific Approach and Accomplishments

Crystalline clathrates, chemical reactions involving a sizable shift the number of moles of gas, and solvents that display ultra-high gas solubility were all evaluated as possible options.

Clathrates are structured inclusion compounds, in which one component forms a crystalline structure (the “host”) that facilitates the inclusion another component (the “guest”). Interaction between the guest and the host framework is through van der Waals forces, as opposed to chemical bonds. Gas hydrates are sub-set of the clathrates consisting of a water-based host framework. The guests are smaller gas molecules that are captured within

polyhedral cages of hydrogen bonded water molecule. Calculations were performed using CH2F2 as the candidate hydrate-forming gas. It was discovered that the relatively large heat of formation for gas hydrate slurries (50-70 kJ/mole of gas) lead to net conversion efficiencies below those reported for the Kalina cycle. This is due to the need to pass the heat of formation to the ambient sink. Since relatively high heat of formation is seen in all the water-based hydrates, focus shifted to other non-water based inclusion compounds. This included urea, thiourea, cyclodextrins, calixarene, Dianin compounds, crown ethers, phenols, quinols, and hydroquinols as hosts. The list of candidates was narrowed by first considering their stability range (temperature and pressure), heat of formation, the number of gas molecules included per mole of host, gas solubility in the host liquid, viscosity of the host liquid, and the anticipated kinetics. Phenol-based clathrates proved the most attractive as they form clathrates within the temperature range of interest and the heat of formation (20-30 kJ/mole) and most other physical properties were reasonable. However, the gas molecule loading (on the kilogram gas per kilogram phenol basis) proved problematic. The viscosity together with gas molecule loading in the slurry translated into high pumping costs (high in-process parasitic energy losses) and low net efficiency.

Reversible chemical reactions also provide an opportunity to accomplish low-grade heat recovery. For an exothermic reaction, lowering the temperature drives the reaction in the forward direction thereby increasing the moles of products at equilibrium. Likewise, raising the temperature drives the equilibrium back towards the reactants, increasing their quantity. A properly chosen chemical reaction would lower the number of moles of compressible gas at the cool portion of the cycle and release gas upon heating. A thermo-chemical analysis was conducted to identify attributes of the ideal reaction - gas molecules react with one liquid (the reactants) to form another incompressible liquid (the product). Following compression and warming, the reaction equilibrium ideally shifts back towards reactants, liberating high-pressure gas. A large change in the number of moles is sought, along with a small heat of reaction. A heat of reaction too large will again lower the net conversion efficiency since that heat is ultimately dumped to the ambient sink in the cool part of the cycle. Once the ideal system was identified, synthesis of the necessary ingredients could follow. However, the analysis showed the small heat of reaction adversely affected the ability to liberate gas upon modest warming. A small heat of reaction corresponds to only a small change in the equilibrium constant. Attempts to liberate gas by warming increases the concentration of reactants, which pushes the reaction equilibrium back towards the liquid product at high pressures. Also, in the high-pressure part of the process, gas solubility in the liquid mixture increases with pressure, also limiting the amount of pressurized gas available. The basic difficulty is thermodynamic - the need for a small heat of reaction limits attainable changes in the equilibrium constant with only a modest swing in temperature. In a gas-liquid reaction whose stoichiometry involves a large number of gas molecules, the reaction will be pushed strongly towards the liquid (product) phase at the high-pressure portion of the cycle, contrary to the objective. Finding purely vapor phase reactions with a large change in number of moles and just the optimal thermo-chemistry was deemed to be improbable.

Another property that can be exploited is ultra-high gas solubility in a non-volatile liquid solvent that is for all practical purposes incompressible. The gas solubility must be very high, must vary significantly with temperature, and the heat of absorption must not be too large. Ionic liquids (ILs) were examined for this purpose as they offer numerous potential advantages: (1) they match the temperature ranges of interest; (2) they can absorb large quantities gas; (3) the enthalpy of absorption is favorable (typically 10–20 kJ/mole); (4) most have negligible vapor pressure; and (5) the physical properties (e.g. viscosity, thermal conductivity) can be modified by tuning the molecular structures. Heat and material balances were performed for a power cycle involving absorption of ammonia in an IL (1-hexyl-3-methylimidazolium chloride) as a test case. Despite the relatively high viscosity, which increases the energy required for pumping, the conversion efficiencies were comparable to a Kalina cycle. However due to the low vapor pressure of the ILs, other advantages were evident. Specifically, very low pressures can be set on the downstream side of the turbines. In comparison, downstream pressures must be limited in a Kalina cycle to avoid condensation of the water that is mixed with the ammonia gas. The heat remaining in the water-ammonia mixture is partially recovered using a costly rectifier and/or recuperator units in a Kalina cycle. It was shown that use of an ammonia-ionic liquid mixture as a power cycle working fluid has a conversion efficiency equivalent to a Kalina cycle. However, the ammonia-ionic liquid mixture offers practical and capital cost saving advantages: 1) the cycle does not require a complicated rectifying column to purify the ammonia, 2) turbine outlet temperatures can be significantly lower in the ammonia-ionic liquid cycle compared to the Kalina cycle, and 3) the ammonia liquid system does not require a large recuperator heat exchanger. Use of non-volatile ILs removes the need for these pieces of equipment for heat recovery thus reducing the capital investment. Since IL-based absorption proved the most attractive option examined, a plan for further development and testing was developed. The next

step in process development should be design, construction, and operation of an engineering test module demonstrating a fully integrated power production cycle.

Impact on National Missions

This work directly supports Energy Security by increasing the net efficiency of conventional electric power production. Also, reducing water consumption in such processes translates into more secure U.S. energy (less vulnerability to diminishing fresh water supplies). While electric power plants are the initial focus, similar waste heat streams exist in energy-intensive industries such as cement, metals smelting, refining, chemicals, and steel production.

References

1. Yazawa, K.. Optimization of thermoelectric topping combined steam turbine cycles for energy economy. Applied Energy . 109: 1.

2. Turchi, C.. 10 MW supercritical CO2 turbine. 2013. US Department of Energy.

3. Lolos, P., and E. Rogdakis. A Kalina power cycle driven by renewable energy sources. 2009. Energy. 34: 457.

4. Ibrahim, M. B., and R. M. Kovach. A Kalina cycle application for power generation. 1993. Energy. 18: 961.

5. Nasruddin, A., R. Usvika, M. Rifaldi, and A. Noor. Energy and exergy analysis of kalina cycle system (KCS) 34 with mass fraction ammonia-water mixture variation. 2009. Journal of Mechanical Science and Technology. 23: 1871.

Building a Foundation for Understanding How Pathogens Subvert the Host Immune System

Thomas C. Terwilliger
20150715ER

Abstract

This research brings together a team from three LANL Divisions to integrate LANL capabilities to understand how pathogens subvert host immune defenses. Our short-term goal was to bring together key LANL teams and develop a foundation for our long-term plan. Our demonstration system will be influenza virus escaping autophagy. In this LDRD-Directors' Reserve project we developed a foundation for detailed modeling of how influenza interferes with autophagy and for making experimental measurements to evaluate those models. Further we generated antibodies to influenza proteins that we will be able to use to perturb the system and to monitor the interactions between influenza proteins and host proteins.

Background and Research Objectives

One of the key strategies used by the human immune system to eliminate pathogens is to engulf and destroy the pathogen, a process termed "autophagy". In response, many pathogens have developed counter-strategies in which they turn off the destruction step in autophagy, and some even co-opt the autophagy system to provide themselves with a safe haven to reproduce. The normal autophagy process occurs in several steps. The first is initiation of an intracellular vesicle that engulfs the pathogen. This is followed by expansion, closure, and maturation of the vesicle, and finally by digestion of the pathogen inside the vesicle. Many of the host proteins involved in autophagy are known, and some pathogen proteins responsible for inhibiting autophagy have been identified. However, neither the exact gene/protein networks that are induced during the various stages of autophagy nor the specific mechanism of interference by intracellular pathogen proteins is known.

Our long-term goal to develop a quantitative understanding of how an intracellular pathogen escapes and takes advantage of host autophagy. Success in achieving this goal will position us to identify critical host-pathogen interactions responsible for pathogen evasion and to target these interactions for developing new drugs. We will form a multi-disciplinary team to identify and model different stages of autophagy and how they are inhibited by intracellular pathogens. This will be supported by experimental measurements of transcriptome and proteome levels in infected hosts corresponding to different stages of autophagy, and by structural analysis of specific host-pathogen protein-protein complexes critical to pathogen evasion.

Our short-term goal is to bring together key LANL teams and develop a foundation for our longterm plan. Our demonstration system will be influenza virus escaping autophagy. We will develop a foundation for detailed modeling of how influenza interferes with autophagy and for making experimental measurements to evaluate those models. Further we will generate antibodies to influenza proteins that we will be able to use to perturb the system and to monitor the interactions between influenza proteins and host proteins.

Scientific Approach and Accomplishments

Development of models describing influenza interference with autophagy

As proposed, we have extended our models of gene/protein networks in autophagy to include the effects of influenza proteins. These models will now allow us to make predictions about the effects of interfering with specific steps in the autophagy process or in the interference of autophagy by influenza proteins. The extended models include interactions that have been identified in the literature such as influenza proteins M2, H1, and NS1 and their interactions with host proteins LC3-II, Atg5, Atg12, Atg16L, Beclin-1, Vps4, and p150. As described below, this theoretical framework is already a powerful tool for integrating our experimental results with our understanding of the system.

Development of experimental approaches for testing our

models of autophagy and interference by influenza

We carried out exploratory genome-wide transcriptome and proteome analyses on influenza-infected and uninfected epithelial cells. These showed that we could identify many human genes and their expression levels over time after infection, an important prerequisite for further work on this project. We additionally carried out experiments to visualize autophagosomes inside uninfected and infected cells using stable epithelial cell lines expressing green fluorescent protein fused to host protein LC3. An exciting outcome of this part of the work is that our theoretical work (prior to this project) had suggested there may be situations where the levels of autophagy proteins might oscillate between low and high levels. Our experimental work has indicated the presence of such oscillations, suggesting that the theory may indeed be on the right track.

Impact on National Missions

The scientific impact of our current and future work on this project will be a quantitative understanding of how an intracellular pathogen evades autophagy. The project will provide crucial clues for identification of new therapeutic targets and discovery of new drugs. Our comprehensive approach to the problem will enhance our understanding of human proteomics (using antibody technology) and protein-protein interactions (using split-green fluorescent protein technology). Our approach will yield both new approaches for network modeling and new network models, and it will identify the structural biology of key protein-protein interactions.

Ultrafast Vacuum Ultraviolet Spectroscopy of Complex Materials

Dmitry A. Yarotski
20130814PRD4

Introduction

Exotic properties of strongly correlated electron materials, such as high-temperature superconductivity and multiferroicity, have inspired an extensive research effort to harness these properties for technological applications. However, the labyrinthine pattern of competing interactions between charge, spin and lattice has prevented the development of predictive theoretical frameworks and establishment of basic material design principles. In general, it is a rather elaborate task for regular time-averaging probes to decipher the nature of the quasiparticles and the interactions involved in collective material behavior because they give little information on the specific degrees of freedom and underlying microscopic physics. In contrast, ultrafast optical spectroscopy offers unsurpassed ability to discriminate the coupling between charge, spin, and lattice in the time domain because their dynamics differ by several orders of magnitude (e.g., tens of picoseconds for phonons vs hundreds of ps for spins).

In this research, we will apply novel ultrafast vacuum ultraviolet photon sources to perform time-resolved X-Ray magnetic linear (and circular) absorption dichroism spectroscopy of a number of strongly correlated electron materials and heterostructures where spin interactions with other degrees of freedom determine material functionality. These techniques will provide new insight into the spin dynamics in these materials with unprecedented time resolution, element specificity, and sensitivity to antiferromagnetic ordering and dynamics near buried interfaces. The results of our advanced characterization effort will directly feedback to the theoretical effort of our colleagues from Theoretical Division. We strongly believe that such a combined ultrafast theory and characterization approach aimed at resolving spin, charge and lattice interactions, as well as the associated quasiparticle dynamics, will ultimately result in a predictive framework for understanding emergent phenomena in strongly correlated electron materials. As such, this work is poised to make a broad impact on condensed matter physics and will open new directions in complex materials research.

Benefit to National Security Missions

Our work directly addresses the Grand Scientific Challenges identified in the Basic Energy Sciences Advisory Committee report, which are central to DOE's missions in energy, science, and security in general, and to the LANL Nuclear Security and National Defense mission and the Materials Pillar in particular. Our thrust to couple modeling, complex materials synthesis, and ultrafast optical/X-Ray science aligns well with MaRIE vision of "material co-design" and further develops new capabilities for MaRIE science. During this project, we anticipate to access large BES X-Ray facilities at LCLS and APS in accord with institutional priority in supporting national user facilities. The proposed experiments are critical to achieving design and synthesis of new materials with controlled functionalities. Materials with tunable and novel functionality are an enabling component in the development of next-generation devices for sensing, information storage, and spintronics applications. We believe that our integrated capabilities in complex material design, synthesis and characterization will be of great interest to multiple sponsors, including DOE-BES, DOD, IC, and industry.

Progress

The goal of this project is to probe ultrafast spin dynamics in strongly correlated materials using time-resolved X-ray magnetic linear absorption dichroism (XMLD) spectroscopy. The XMLD technique probes p->d transitions of magnetic ions and is valuable tool for understanding how the spin order is coupled to other degrees of freedom (charge, orbital, lattice), because electrons on d-orbitals of transition metal ions are usually responsible for magnetism in complex materials. In particular, our recently developed ultrafast table top soft x-ray source is capable of spanning the 3p-3d transitions (M-edges) of

many transition metal components in strongly correlated electron compounds. The dynamics of spin degrees of freedom is studied by photo-exciting (pumping) a sample with a femtosecond near-infrared laser pulse which takes the material out of equilibrium and perturbs the spin alignment through transient modulation of charge density or lattice distortions affecting exchange interactions. Subsequently, a soft x-ray pulse probes the dynamics by monitoring absorption dichroism (polarization dependence) of the magnetic ion of interest.

In FY15, we focused on investigations of the mechanisms of complex spin-charge interplay in chromium (Cr). Cr is a peculiar material which undergoes several phase transitions involving antiferromagnetic (AFM) spin alignment in spin density waves and formation of charge density waves. Prior to obtaining a novel insight into the Cr non-equilibrium properties, we had to overcome several technical challenges related to unusually high surface sensitivity of M-edge XMLD measurements. First, we discovered that even under high vacuum and the cryogenic temperatures, the thin water layer can contaminate the sample surface and absorb large portion of extreme ultraviolet (XUV) probe pulse. This problem has been mitigated by introducing a liquid nitrogen cooled shield around the sample that freezes out any water remaining in the vacuum chamber before the sample is cooled. A second obstacle was a high sensitivity of XMLD signal to the sample roughness. By closely monitoring and controlling the position of the beam on the sample surface we could consistently measure the same region of the sample thus reducing signal variations cause by inhomogeneous surface profile. The new experimental system configuration now allows continuous measurements of magnetic dynamics in a broad temperature range (5-450 K) in samples that move due to temperature dependent cryostat arm expansion/contraction.

Subsequent measurements of temperature-dependent XMLD dynamics in Cr crystals showed an increase in XMLD signal at ~310K consistent with the onset of AFM spin ordering in this material. Interestingly, another transition at ~120K was also observed, which corresponds to the spin flip from transverse to longitudinal spin density wave order. Both of these observations clearly demonstrate high sensitivity of our table-top XMLD method to AFM spin order variations which were only observed before at large synchrotron facilities. Moreover, our ability to resolve sub-50 fs transients in photoinduced XUV absorption allowed us to follow the dynamics of spin and charge degrees of freedom across the AFM phase transition. Below the transition temperature, XMLD signals show a very fast (~1 ps) amplitude change that relaxes on time scales of >10 ps following photoexcitation. As the temperature is increased through the AFM transition, the amplitude of the ultrafast transient decreases and oscillations (~100 GHz) develop which correspond to coherent excitations in the material. The oscillation strength increases with increasing temperature. This behavior clearly indicates that magnetic order suppresses coherent excitation of charge density waves in Cr which implies strong coupling between these two orders. We are working with theorists in both T-4 and Uppsala University to understand the origins of such multiple-order coupling and its implications on the material functionality. The results of these experiments were presented at the 2015 APS March Meeting, and we are currently working on the manuscript that will summarize our findings and describe physical mechanisms responsible for the observed effects.

Future Work

Exotic properties of complex materials emerge from the strong interactions among spin, charge, and lattice degrees of freedom (DOF). Existing theories cannot predict the emergent behavior, largely because available time-averaging experimental probes cannot decipher the interactions between particular DOFs. In this regard, ultrafast optical spectroscopy (UOS) offers an unmatched ability to separate various DOF and coupling among them in time domain. Our goal is to apply advanced UOS techniques to study time-dependent and element-specific processes that are important for understanding the DOF interplay in complex materials.

In FY15, we applied our optimized table-top ultrafast X-Ray linear absorption dichroism probe to directly reveal the dynamics of spin and charge orders in chromium. In FY16 we will complete the experimental data analysis and develop theoretical understanding of the strong charge-spin coupling and its signatures in ultrafast X-Ray dynamics. These results will be summarized in the manuscript and submitted for publication in peer-reviewed journal. We strongly believe that these results will provide novel insight into element-specific magnetic dynamics in complex materials. In the FY16, we will also continue the ultrafast XMLD experiments on multiferroic materials where magnetic and ferroelectric polarizations are strongly coupled and allow manipulation of electric polarization with magnetic field and magnetization with electric field. Our focus will be single-phase material BiFeO3 where optical pulses will be used to disturb the magnetic ordering and X-Ray pulses will be applied to probe the ensuing modulations in strain, charge or orbital orders. These experiments will shed a new light on the coupling between charge/lattice and spin systems responsible for emergence of magnetoelectric coupling in multiferroics. In addition, we will start extending our ultrafast measurements to ferromagnetic systems

using the transverse magneto-optical Kerr effect or X-Ray magnetic circular absorption dichroism techniques.

Conclusion

We expect that experimental and theoretical insights developed here will lead to a leap in our comprehension of the competing interactions in complex materials. Our novel ultrafast coherent photon probes will allow direct visualization of the real-time formation of competing orders, and will ultimately enable manipulation and coherent control of materials functionality. Our approach will fill the urgent need in integrated modeling, synthesis, and ultrafast nanoscale characterization capabilities essential to address several challenges in materials science. The understanding of complex materials properties developed here will have a significant impact on wide ranging technologies from information storage to energy applications.

Publications

Ahmed, T., B. McFarland, A. Chen, Q. X. Jia, D. A. Yarotski, and J. X. Zhu. Site dislocation between Fe and Mn sites in double perovskite Bi2FeMnO6: A theoretical explanation for XMCD anomaly. Physical Review Letters.

McFarland, B. K., J. X. Zhu , R. P. Prasankumar, G. Rodriguez, R. L. Sandberg, A. J. Taylor, S. A. Trugman, and D. A. Yarotski. Ultrafast X-Ray Probe of Dynamics in Chromium. Presented at 2015 CINT User Meeting. (Santa Fe, September 21-22, 2015).

McFarland, B. K., J. X. Zhu, R. P. Prasankumar, G. Rodriguez, R. L. Sanberg, A. J. Taylor, S. A. Trugman, and D. A. Yarotski. Soft X-Ray Probe of Ultrafast Dynamics in Spin Ordered Chromium. Physical Review Letters.

McFarland, B., J. X. Zhu, R. Prasankumar, G. Rodriguez, R. Sandberg, A. J. Taylor, and D. A. Yarotski. Ultrafast Dynamics near the M-edge in Chromium. Presented at American Physical Society March Meeting. (San Antonio, Texas, March 2–6, 2015).

Bayesian Information Gap Decision Analysis

Velimir V. Vesselinov
20140000PRD4

Introduction

Bayes theorem is a mathematical technique that provides a way to determine the likelihood of different models given some observed data. Bayes theorem is mathematically rigorous, but its application is not always rigorous for two reasons: (1) We can enumerate the possible outcomes of dice-rolling, but not the possible outcomes of groundwater remediation. (2) We can determine conditional probabilities for coin-tossing, but substantial uncertainty surrounds the conditional probabilities in groundwater remediation. We circumvent these issues with a three-layered-onion approach. The middle layer employs Bayes theorem. The inner and outer layers employ a non-probabilistic uncertainty quantification (UQ) methodology called Information-Gap to overcome (1) and (2), respectively. This Bayesian-Information-Gap (BIG) UQ approach provides robust decision support for selecting a remediation approach after the site characterization been performed.

This project will extend this methodology to provide decision support throughout the site characterization process. A probabilistic model will be used to generate hypothetical data that might be obtained from a site characterization effort. The BIG UQ framework will be used to arrive at a decision before and after hypothetical site characterization. Characterization efforts that have a high chance of altering the decision are more worthwhile than those that have a low chance of altering the decision. This also informs the transition from uncertainty reduction to remedy selection. If all site characterization options are unlikely to alter the remedy selection, it is time to suspend site characterization and begin remediation. Techniques for estimating the progress and execution time of the analyses will also be developed.

The combination of flexible computational demands that arises from model independence and open source software means that this framework can also be used out at tens of thousands of contaminated groundwater sites across the USA. Applications to other fields are easily achieved due to the model independence.

Benefit to National Security Missions

This research aligns with the LANL mission and the strategic EES research goals as it aims to provide optimal decisions for national problems related to energy and environmental security; these national problems require development of strategic scientific capabilities to improve decisions in energy and water production, carbon capture and sequestration, waste disposition and storage, and restoration of contaminated sites. In all these areas, real-world applications require robust and accurate methods for capturing the existing uncertainties in the model analyses and decision process. The methods and tools developed in this work will satisfy these needs and strengthen existing research at LANL. This work will provide opportunity for future basic science and programmatic research growth working with new sponsors (e.g., DoD, SERDP, NSF, industry) and new research areas that require decision analyses for complex national security problems.

Progress

The fundamentals of the Bayesian-Information-Gap decision theory (BIG-DT) described in a published paper: O'Malley, D., Vesselinov, V.V., A combined probabilistic/non-probabilistic decision analysis for contaminant remediation, Journal on Uncertainty Quantification, SIAM/ASA, doi: 10.1137/140965132, 2014. The paper summarizes the theory and applies the methodology to solve a synthetic contaminant remediation problem.

Bayesian-Information-Gap decision theory applied to solve CO2 sequestration problem. A paper submitted: O'Malley, D., Vesselinov, V.V., Bayesian-Information-Gap decision theory with an application to CO2 sequestration, Water Resources Research, submitted, 2015.

An initial version of a code in Julia for Bayesian-Information-Gap analysis developed. The code has been tested on 64 processor computational clusters. It needs to be extended to be executable on the LANL HPC distributed clusters.

An initial version of a code in Julia for Bayesian-Information-Gap Optimal Experimental Design (BIG-OED) developed. The code has been tested on 64 processor computational clusters. It needs to be extended to be executable on the LANL HPC distributed clusters. The code has applied to solve a synthetic test problem. The initial results are encouraging.

Future Work

- Develop a probabilistic model that describes the possible outcomes of site characterization efforts. Site characterization efforts that should be considered include pumping tests and groundwater sampling campaigns.
- Develop a methodology that incorporates the site characterization model into the Bayesian-Information-Gap (BIG) uncertainty quantification (UQ) framework.
- Demonstrate the methodology on a synthetic test problem.
- Develop an approach for estimating progress and execution time of these analyses.
- Write a paper describing the methodology.
- Demonstrate the methodology on a real-world problem. Most probably the real-world problem will be related to the LANL Chromium contamination site.

Conclusion

This project will provide a framework for making decisions related to complex problems with a focus on groundwater remediation. Groundwater contamination is an important national problem with over $100 billion dollars in liabilities including around $20 billion within the DOE complex. A substantial challenge in groundwater remediation scenarios is to select between a variety of site characterization efforts and remediation options. This framework will provide insight into the value of different characterization efforts, inform the transition from studying the problem to solving the problem, and help select the best solution to the problem.

Publications

O'Malley, , V. V. Vesselinov, and J. H. Cushman. Diffusive mixing and Tsallis entropy. 2015. PHYSICAL REVIEW E. 91 (4).

O'Malley, , V. V. Vesselinov, and J. H. Cushman. A Method for Identifying Diffusive Trajectories with Stochastic Models. 2014. JOURNAL OF STATISTICAL PHYSICS. 156 (5): 896.

O'Malley, , and V. V. Vesselinov. Groundwater remediation using the information gap decision theory. 2014. WATER RESOURCES RESEARCH. 50 (1): 246.

O'Malley, , and V. V. Vesselinov. Analytical solutions for anomalous dispersion transport. 2014. ADVANCES IN WATER RESOURCES. 68: 13.

Tracking Microbial Activity to Predict the Impacts of Climate Change on Ecosystem Function

Cheryl R. Kuske
20140662PRD1

Introduction

Ecosystem processes such as nutrient cycling sustain life on earth, and are controlled in large part by communities of fungi and bacteria (collectively termed microbes) that reside in the soil. Global changes, such as nitrogen deposition, warming, elevated CO2, and altered precipitation, alter the abundance and biodiversity of microbial communities and significantly alter ecosystem functions. Soil microbial communities largely determine whether terrestrial ecosystems act as carbon sources or sinks under elevated CO2. However, biochemical processes mediated by complex microbial interactions in the soil remain a black box in terrestrial ecosystem models. A major hurdle in linking complex soil communities to major ecosystem processes is the ability to distinguish among the active and dormant members of the community. Understanding how dormancy structures microbial communities is of particular concern because it is a strategy for survival under unfavorable environmental conditions, and could be a pathway for resiliency of microbial communities to climate changes. I will use a combination of high-throughput DNA and RNA sequencing with surveys of functional genes in two different field-collected soils in the laboratory to determine the relative contributions of the active populations, and to elucidate the biological and ecological constraints on the ability of microbial populations to enter and exit from dormancy. Collectively, these studies will help us understand how the microbial community regulates climate change responses and feedbacks in the soil. We have completed two soil microcosm experiments: one that compares microbial community responses to increased moisture, increased nitrogen, and warming temperatures, and another that examines microbial response to environmental stress, including temperature, desiccation and starvation.

Benefit to National Security Missions

First, this project will help fill a significant information gap in our knowledge of and ability to predict the outcomes of processes that are mediated by complex microbial communities in soils. Soils are an enormous reservoir of carbon (C) on Earth, and the concerted activities of soil microbes regulate the storage or release of this C. Second, the project directly contributes to DOE missions in biological systems science and climate change responses. It also advances metagenomics technologies and basic environmental surveys that enable more accurate, specific detection of target microorganisms in environmental samples, thus contributing to a technology base supporting biothreat detection. Third, this project advances our understanding of fungal and bacterial biomass and metabolic capabilities; these are organisms from which we have historically derived most of our antibiotics, as well as other pharmaceuticals and industrial enzymes. Fourth, many of the fungi we will be studying also have potential in processing C for biofuels applications.

Progress

A soil microcosm experiment that compares microbial community responses to increased moisture, increased nitrogen, and warming temperatures is complete. Measures of soil respiration have been collected over the time-course experiment. Extraction of total soil RNA and DNA have been completed, and sequencing of fungal and bacterial communities from both RNA and DNA has been initiated. In addition, using funds received through the LDRD program, we generated 24 metatranscriptomes from a subset of the treatments, and analysis of community shifts based on mRNA is currently underway.

In addition to manipulating soils with the above additions, we used three different stresses in order to determine which community members are able to survive harsh environmental conditions, including heating to 65C, freezing at -80C and long-term desiccation. Measurements of soil respiration and community composi-

tion are planned for the next two months. In addition, we are in the process of constructing contrived communities of known composition to link known functional genes to ribosomal genes to gain a greater understanding of using rRNA as an indicator of activity. Co-extraction of RNA and DNA are complete, and sequencing of fungal and bacterial communities is ongoing.

We expect to finish the community analysis of fungal and bacterial communities generated by high throughput amplicon sequencing within the next two months. The timeline to complete the statistical analysis of communities from the two experiments is estimated at an additional four months.

In terms of publications, we expect to generate two from the initial experiments, one linking soil respiration with community composition of fungal and bacterial communities, and another examining the dynamic rank abundance curves of active and dormant fungal and bacterial communities, which will also incorporate the findings from the metatranscriptome survey. We expect to generate an additional manuscript contrasting stress responses in fungi and bacteria within the two different soil types to further explore the relative effects of anthropogenic perturbations on community shifts and ecosystem functions.

Future Work

Objective: To investigate how dormancy determines community response to global change and the implications of dormancy on soil processes

Rationale: The major goal of the SFA is to understand how global change, primarily nitrogen deposition, will affect microbial communities, and in turn, important ecosystem functions, such as carbon cycling. Understanding how dormancy structures microbial communities is important for understanding both the long and short-term impacts of global change on microbial biodiversity because it is a strategy for survival under unfavorable environmental conditions, and is a potential pathway for resiliency of microbial communities to global change.

Approach: We are analyzing controlled laboratory approaches to study the response of natural microbial communities in two contrasting soils to a multiple environmental manipulations, including increased water availability, increased temperature and increased nitrogen availability. The responses to these perturbations were tracked over time by quantifying soil respiration using gas chromatography. The active and total communities are currently being measured using molecular analysis of rRNA and rDNA in order to both link the composition of the active community to measures of soil respiration, as well as to quantify shifts in the active community over time. These measures will allow us to determine the short-term community responses to predicted global changes, and to link those shifts with ecosystem function.

Conclusion

The goals of this project are to understand the relative contributions of active soil bacterial and fungal populations, and constraints on their ability to enter and exit from dormancy, to enable accurate predictions of C or N fluxes from the soil. By quantifying microbial activity and dormancy under dynamic environmental conditions, my proposed studies will determine how the microbial community regulates climate change responses and feedbacks in the soil, which are critical for development of soil process models and to define appropriate input variables in regional climate models.

Publications

Dunbar, , L. V. Gallegos-Graves, Steven, Mueller, Hesse, D. R. Zak, and C. R. Kuske. Surface soil fungal and bacterial communities in aspen stands are resilient to eleven years of elevated CO2 and O-3. 2014. SOIL BIOLOGY & BIOCHEMISTRY. 76: 227.

Kuske, C. R., C. N. Hesse, J. F. Challacombe, Cullen, J. R. Herr, R. C. Mueller, Tsang, and Vilgalys. Prospects and challenges for fungal metatranscriptomics of complex communities. 2015. FUNGAL ECOLOGY. 14: 133.

Mueller, R. C., Belnap, and C. R. Kuske. Soil bacterial and fungal community responses to nitrogen addition across soil depth and microhabitat in an arid shrubland. 2015. FRONTIERS IN MICROBIOLOGY. 6.

Mueller, R. C., L. Gallegos-Graves, D. R. Zak, and C. R. Kuske. Assembly of active bacterial and fungal communities along a natural environmental gradient. 2015. Microbial Ecology. : 1.

Mueller, R. C., M. M. Balasch, and C. R. Kuske. Contrasting soil fungal community responses to experimental nitrogen addition using the large subunit rRNA taxonomic marker and cellobiohydrolase I functional marker. 2014. MOLECULAR ECOLOGY. 23 (17): 4406.

Complexes Containing Redox-Active Ligands for the Synthesis of Fuels from Readily-Available Carbon Sources

John C. Gordon
20140664PRD2

Introduction

The proposed work will investigate the development of catalytic systems that convert readily available, highly oxidized precursors such as carbon dioxide, acetic acid, and glycerol into higher-order compounds containing more carbon atoms that can readily be converted into alkanes, which are the main components of transportation fuels. This work addresses both the synthesis of the higher order fuel precursors and their defunctionalization to produce hydrocarbons that would be suitable as fuels. This has the potential to convert biorenewable and abundant molecules into molecules with potential use as fuels.

Benefit to National Security Missions

The goal of the project is the synthesis of molecules that can serve as fuels from readily available and sustainable molecules such as CO2, acetic acid, and glycerol. These goals are directly in line with DOE BES's interests in fundamental chemistry and catalysis science and DOE EERE's interests in sustainable and biorenewable chemistry. This work also directly impacts the area of climate and energy impact vis-a-vis the conversion of biorenewable and abundant small molecules into higher order carbon containing species with potential use as hydrocarbon fuels for transportation applications.

Progress

The synthesis of a significant number of metal complexes supported by redox active ligands, including those containing iron and nickel have been achieved. In FY15 these were screened towards a number of reactions, including carbon-carbon bond coupling reactions, hydroboration, etc. In particular, we prepared a nickel based system that appears to exhibit interesting and unexpected redox behavior upon binding a ketonic (C=O bond containing) substrate that may have implication for how redox active metal complexes behave. We are currently working on a manuscript that describes this work.

Future Work

In FY16 we will work on the synthesis and characterization of quinone based systems that can support two electron redox chemistries. The spectral and structural characteristics of these molecules will be used in conjunction with electronic structure calculations to evaluate their potential in promoting chemistries of interest. We will also use electrochemistry to guide subsequent synthetic efforts towards catalytic redox chemistries and this will also be useful in identifying stoichiometric reaction conditions that facilitate carbon-carbon bond coupling reactions and the reduction of highly oxygenated substrates.

Conclusion

The goal of the project is the synthesis of molecules suitable as fuels from readily available and sustainable molecules such as carbon dioxide (CO2), acetic acid, and glycerol. This has the potential to convert biorenewable and abundant molecules into molecules with potential use as hydrocarbon fuels.

Bottom-up Chemical Synthesis of Large, Well-Defined, and Organo-Processable Nanographene-based Triarylamine for Optoelectronic Applications

Hung-Ju Yen
20140666PRD2

Introduction

The main focus of this project is to develop synthetic strategies for making triarylamine-based nano-graphene (TAA-NG), a small piece of graphene with well-defined molecular structure. NG with flexible alkyl chains attached to the periphery of NG renders solubility in organic solvents and allows self-assembly of NGs with phase separation into nanoscaled morphology in composite materials. More importantly, the incorporation of heteroatoms such as triarylamine (TAA) into the graphene frameworks leads to a triangular shape and charge transfer characteristics, which, to the best of our knowledge, have never been attempted. The challenge of this project lies in the fact that the organic synthetic scheme for TAA-NG requires more than 20 steps. This is a costly and time-consuming process. Although synthesis of simple NGs have been demonstrated, synthesis of TAA-NG remains a challenge and the final yield of this compound may be low, which could impede us from developing applications using this materials. Therefore, our challenges are not only in the synthesis of TAA-NG, but also in finding ways to increase the yield of the final product.

We expect the as-prepared TAA-NG will reveal fine-tuned optoelectronic properties tailored for the applications in electrochromic, memory device, LED, photovoltaic cell, fuel cell, lithium battery, and super-capacitor. Success in demonstrating derivatized NGs in the above devices could have intellectual property value and warrants publications in high impact journals.

Benefit to National Security Missions

This project aims to develop nanographenes (NGs) with tunable electronic structures and optical properties. The integration of functional NGs into clean energy technologies could bridge the gap between basic research and commercialization of graphene-based energy devices. Further development of NG-based materials will strengthen our leadership role in NG research, which has strong ties to Laboratory mission in the areas of exotic materials and energy security.

Progress

The main accomplishments for FY15 were the synthesis of heteroatom (N, or B) doped nano-graphenes (NGs) through a newly designed synthetic route. Such synthesis includes Curtis rearrangement, Sonogashira coupling, Suzuki coupling, Diels-Alder cycloaddition, and Ullmann reactions. Nanographenes containing various functional gropus such as hydroxy, methoxy, tert-butyl, fluorine, and bromine. These molecules have been thoroughly characterized using a series of organic spectroscopy probes such as proton and C13 NMR, Infrared, matrix assisted laser desorption ionization spectroscopy. All of the spectroscopy results show perfect agreement with the proposed molecular structure.

In addition, we have found these molecules form hierarchical structure through self-assembly. Such self-assemblies have a d-spacing between nanographene that is functional group dependent. The average d-spacing of the NGs in the domains is around 3.95-4.36 Å, which is much larger than that of pristine graphite (3.34-3.37 Å). NGs with hydrogen, methoxyl, tert-butyl, hydroxy, bromo, and fluoro functional groups attached to the NG flakes have corresponding d-spacing of 3.95, 4.08, 4.36, 4.04, 4.30, and 4.0 Å respectively. It is notable that the d-spacing between flakes is consistent with the size of the functional groups (OMe-tBu > Br > OMe > OH > F > H. XRD of the NGs and is consistent with the TEM measured d-spacing, although they all reveal overall amorphous structure, lacking of a sharp diffraction peak. We use the center of the amorphous peak as a rough estimate of the representative d-spacing, the t-BuOMe HBC appears to has two peaks center at ~ degree, the low angle peak is corresponding to 4.29 A, consistent with the estimated 4.3 A. In addition, these is a trend of XRD peak shifting

to a higher angles from t-BuOMe-, OMe-, H-, Br- F- and OH-, consistent with the our hypothesis of using functional groups to control d-spacing and electron density which allow us to ascertain and optimize Li incorporation and diffusion.

Future Work

In FY16, we will focus on the synthesis of heteroatom (N, or B) doped nano-graphenes through a newly designed synthetic route. Such synthesis includes Curtis rearrangement, Sonogashira coupling, Suzuki coupling, Diels-Alder cycloaddition, and Ullmann reactions. The molecular structures and crystallinity of these nitrogen/boron doped nanographenes will be characterized by X-ray diffraction, scanning electron microscopy, scanning tunneling microscopy, atomic force microscopy, MALDI-TOF Mass spectroscopy, infrared spectroscopy and nuclear magnetic resonance spectroscopy. Electronic and optical properties of these nitrogen doped nanographene will be determined by UV-Vis spectrometer and fluorescence spectrometer. We will measure the redox potentials of these nanographenes by cyclic voltametry, coupled with the absorbance spectra to construct the band diagram of nanographenes. The incorporation of nitrogen/boron in the nanographene is expected to increase the incorporation of metal atoms and rate of diffusion. Therefore, we will incorporate these nitrogen-doped nanographenes as part of anode material in lithium ion battery (LIB) and evaluate the performance characteristics in terms of capacity, stability through hundreds of charging-recharging cycles. We will also evaluate the use of these novel nanographenes as new electrochromic material, and demonstrate the use of these materials for memory devices.

Conclusion

We expect to achieve synthesis of processable nanographene (NG). Our proposed synthesis promises ways to control NGs with size-dependent band gap, optical absorptivity, and charge transfer functionality. If successful, this project will likely generate a new class of materials with emergent functionality previously not accessible through fabrication methods. The integration of functional NGs into clean energy technologies could bridge the gap between basic research and commercialization of graphene-based energy devices. Further developing NG-based materials will strengthen our leadership role in NG research, which has strong ties to Laboratory mission in the areas of exotic materials and energy security.

Publications

Cheruku, P., J. H. Huang, H. J. Yen, R. S. Iyer, K. D. Rector, J. S. Martinez, and H. L. Wang. Tyrosine-Derived Stimuli Responsive, Fluorescent Amino Acids. 2015. CHEMICAL SCIENCE. 6: 1150.

Kuo, C. Y., W. Nie, H. Tsai, H. J. Yen, A. D. Mohite, G. Gupta, A. M. Dattelbaum, D. J. William, K. C. Cha, Y. Yang, L. Wang, and H. L. Wang. Structural Design of Benzo[1,2-b:4,5-b ']dithiophene-Based 2D Conjugated Polymers with Bithienyl and Terthienyl Substituents toward Photovoltaic Applications. 2014. MACROMOLECULES. 47 (3): 1008.

Park, Y. I., O. Postupna, A. Zhugayevych, S. W. Kyu, , Y. S. Park, B. Kim, H. J. Yen, P. Cheruku, J. S. Martinez, J. Park, S. Tretiak, and H. L. Wang. A new pH sensitive fluorescent and white emissive material through controlled inter-molecular charge transfer. 2015. CHEMICAL SCIENCE. 6: 789.

Yen, H. J., H. Tsai, C. Y. Kuo, W. Nie, A. D. Mohite, G. Gupta, J. Wang, J. H. Wu, G. S. Liou, and H. L. Wang. Flexible memory devices with tunable electrical bistability via controlled energetics in donor-donor and donor-acceptor conjugated polymers. 2014. JOURNAL OF MATERIALS CHEMISTRY C. 2 (22): 4374.

Yen, H. J., H. Tsai, M. Zhou, A. Chen, E. F. Holby, S. Choudhury, X. Wang, L. Zhu, H. Lin, L. Dai, G. Wu, and H. L. Wang. Bottom-up Chemical Synthesis of Three-Dimensional Nanographene Assemblies with Controlled d-Spacing and Enhanced Electron Density for Efficient Li Storage. Journal.

Yen, H. J., P. W. Liang, C. C. Chueh, Z. Yang, H. L. Wang, and A. K.-Y. Jen. Single Crystal Perovskite Powders for Large Grained Perovskite Solar Cells. J. Mater. Chem. A.

Petabyte-Scale Computational Analyses of Genomic Data to Elucidate Aging Mechanisms

William S. Hlavacek
20140670PRD2

Introduction

The project has two objectives: 1) analyses of data from different species and 2) analyses of data from thousands of individuals and multiple human tissue types.To achieve the first objective, we will use the reference genome data available from NCBI to perform comparative genomics analysis across 25 species. A preference will be given to non-human primates and rodents because the species in each of these groups have similar genomes but diverse lifespans. For example, the naked mole rat lives up to 30 years, whereas its relative the house mouse lives only about four years. Additionally, in-depth analysis will be performed for different breeds of dogs due to the large amounts of available molecular data. Although all dogs share essentially the same genetic material, different breeds exhibit up to 2-fold differences in life expectancy.

The main outcome of this part of the project will be the identification of homologous genes responsible for lifespan differences across species and the genes affected by nucleotide changes in different breeds of dogs. The second objective is focused on humans. We will use predominately the data generated by initiatives such as the International Cancer Genome Consortium (ICGC). The primary goal of the ICGC is the identification of critical genes involved in oncogenesis, but a byproduct of this large-scale worldwide initiative is an exhaustive genetic and epigenetic characterization of the normal tissues (usually blood) and cancers of 25,000 individual patients. In a study recently reported in a Nature article, it has been demonstrated that these abundant molecular data can be used to identity signatures of molecular processes causing somatic mutations. Moreover, these signatures can be mapped to molecular mechanisms.

This study sheds new light on the origins of cancer but it just scratches the surface of what is possible. To achieve the second project objective, we will use the molecular data available for up to 25,000 individuals to identify molecular differences associated with age. We expect to be able to characterize the rates of several distinct mutational processes occurring in 50 different tissue types.

Benefit to National Security Missions

The project will entail petabyte-scale data science. The methods used and lessons learned are likely to be relevant to many DOE mission areas such as biothreats and DOE Office of Science. The specific problem that will be addressed is highly relevant to the public health mission of NIH. By analyzing large amounts of genomic data, we hope to elucidate molecular signatures and causes of aging. Aging has been identified by the World Health Organization as one of the main healthcare and economic challenges of the 21st century. Remarkably, our current understanding of the mechanisms of aging is extremely limited and as a 2012 review in Cell concluded, “The underlying cause of aging remains one of the central mysteries of biology.” Two (not necessarily exclusive) hypotheses have been put forward to explain aging. The first postulates that aging is due to the accumulation of damage, which can come both from the external environment and from within our bodies and cells. The second theory suggests that aging follows a predetermined biological timetable in which certain genes get switched on and/or off to control lifespan.

Progress

In the past year, we were able to build a capability to download large quantities of data from external sources. Currently, we have a working pipeline that allows downloading ~30TB per day of external data. Note that the download capability of the pipeline is throttled to adhere to LANL’s internal requirements and practically the capacity of the pipeline could be further increased.

In total, we have downloaded ~300TB of data to a staging area and are currently working on the most effective strategy for transferring data from this staging area to

the HPC resources, where the data will be processed and analyzed. We envision having this workflow completed in the next few months and to able to process at least 2 PB of data by the end of this calendar year. Overall, we plan to download the majority of available genomics/biomedical data from around the world by the end of this project.

In the past year, we were also able to perform big data analysis outside of the hitherto mentioned pipelines. The analysis was performed in regards to cancer and human aging, and more specifically to elucidate the activity of mutational processes in neoplastic and aging cells. This work resulted in significant scientific output in regards to high impact peer-reviewed publications as well as a patent application. Additionally, there are another seven manuscripts that are currently under preparation and we expect them to be submitted (and some of them accepted) by the end of this calendar year.

Future Work

We plan to complete and fully automate our pipelines for downloading and processing large-scale genomics data. This will provide LANL with an automated workflow for processing Big Data from any external sources.

From a scientific perspective, we plan to processes ~5 PB of data in the next fiscal year accounting for about ~20,000 individual pairs of cancer-normal genomes. These data will allow us to have the final roadmap on both mutational processes in human cancer as well as mutational processes that are part of normal ageing processes. We will attempt to associate the activity of these processes to gene expression patterns, epigenetics profiles, and clinical outcome. We envision that this work will results in between 10 and 20 high impact scientific publications.

Conclusion

The expected outcome is an in-depth characterization of the genetic changes that occur with age and the mutational processes responsible for these changes, which will have far-reaching implications for human health. In overcoming the technical challenges of the proposed work, we will establish a Big Data Science capability in Los Alamos that could be applied to diverse problems. The planned analyses will encompass roughly 25 petabytes of data and involve the use of advanced methods of multivariate statistics, novel method development, and new approaches to the use of computational resources to solve a Big Data problem.

Publications

Hong, M. K., G. Macintyre, D. C. Wedge, P. Van Loo, K. Patel, S. Lunke, L. B. Alexandrov, and e. t. al. Tracking the origins and drivers of subclonal metastatic expansion in prostate cancer. 2015. Nature Communications. 6: 6605.

Schulze, K., S. Imbeaud, E. Letouze, L. B. Alexandrov, J. Calderaro, and e. t. al. Exome sequencing of hepatocellular carcinomas identifies new mutational signatures and potential therapeutic targets. 2015. Nature Genetics. 47 (5): 505.

Wegener, R., L. B. Alexandrov, M. Montesinos-Rongen, M. Schlesner, A. Haake, H. G. Drexler, J. Richter, G. R. Bignell, U. McDermott, and R. Siebert. Analysis of mutational signatures in exomes from B-cell lymphoma cell lines suggest APOBEC3 family members to be involved in the pathogenesis of primary effusion lymphoma. 2015. Leukemia. 29 (7): 1612.

Yates, L. R., M. Gerstung, S. Knappskog, C. Desmedt, G. Gundem, P. Van Loo, T. Aas, L. B. Alexandrov, and e. t. al. Subclonal diversification of primary breast cancer revealed by multiregion sequencing. 2015. Nature Medicine. 21: 751.

Access to Industrially Important Optically Active beta-X-alcohols via Direct Enantioselective Ester Hydrogenation

Pavel Dub
20140672PRD2

Introduction

Contrary to ketones, limited progress in the hydrogenation of less-electrophilic esters has been made during the last few decades. Industrial homogeneous reduction of esters still relies mostly on the use of metal hydride reagents such as LiAlH4 or NaBH4. Using these reagents, hydrogenation selectivities cannot be controlled and such spent (waste) reductants require energetically intensive regeneration input or disposal. Also the use of heterogeneous catalysis dictates the use of high temperatures and pressures and again selectivities cannot be controlled.

No reports describe detailed enantioselective ester hydrogenation despite the tremendous potential for synthetic organic chemistry. Current "state-of-the-art" catalysis in this area of chemistry has required complicated multi-step ligand synthesis as well and these ligands once synthesized often exhibit air-sensitivity. This work will thus focus on developing new well-defined chiral bifunctional molecular catalysts incorporating air-stable ligands for the enantioselective hydrogenations of esters via dynamic kinetic resolution.

Benefit to National Security Missions

Success in this chemistry could have significant positive impact for LANL, vis-à-vis the application of new approaches to polymers and materials synthesis, in energy applications, and in health related (e.g. pharmaceutical) R&D. This work if successful will potentially lead to high profile publications (Angew. Chemie., JACS, etc.) for the Laboratory and will place LANL at the forefront of this developing area of chemistry.

Progress

In FY15, we have made very good progress during the last year, making a large variety of catalysts based on ligands that are supported by NNS (nitrogen, nitrogen and sulfur) donors. These have demonstrated efficacy in the hydrogenation of a variety of C=O bonds that are relevant to catalytically relevant industrial processes. One paper has been accepted and we have several others being worked on for publication including an invited review article. We have also gone to quite some effort to protect the intellectual property surrounding this technology. This includes the filing of four provisional US patents and a recent non-provisional PCT application.

Future Work

In FY16 we will further develop our ligand chemistries to support new and effective catalysts for the hydrogenation of ketonic substrates. These new complexes will potentially be used in other important catalytic transformations as well, (e.g hydrosilylations, hydroborations, transfer hydrogenations, allylic substitutions, Michael additions, Henry reactions, etc.), so if time permits we will examine some of these reactions.

Conclusion

In addition to the environmentally benign processes outlined above, our goals will go further: currently, the ruthenium (Ru) catalyzed asymmetric hydrogenation of ketones (R. Noyori, Nobel Prize 2001) is the main route to produce optically active secondary alcohols. The utilization of expensive Ru catalysts however is unattractive in terms of cost. It is envisioned that if the enantioselective hydrogenation of ketones could be catalyzed by less-expensive base metal complexes. We will incorporate newly developed and synthesized air-stable chiral ligands onto cheap metals such as copper in order to perform catalytic asymmetric ketone hydrogenation.

Publications

Dub, P. A., B. L. Scott, and J. C. Gordon. "Air-Stable NNS (ENENES) Ligands and their Well Defined Ru and Ir Complexes for Outer-Sphere Molecular Catalysis". 2015. Organometallics. 44: 4464.

Synthesis and X-ray Spectroscopy of Actinide Thiocyanates

Stosh A. Kozimor
20140677PRD3

Introduction

As the need to develop a closed nuclear fuel cycle grows, there are a number of technological challenges that need to be overcome. One of the most difficult challenges is the separation of the minor actinides (Am3+ and Cm3+) from the trivalent lanthanide fission products as they share many physical properties. A number of studies have shown that this separation is possible by employing soft ligands (such as those containing S or N donors), which preferentially bind the actinides (An) over the lanthanides (Ln). One particularly promising extractant is the SCN1- anion that provides enhanced separation of An over Ln. Although little is understood about why the SCN1- extractant is successful, it seems likely to be associated with the propensity of NCS1- to form more covalent An–NCS vs Ln–NCS bonds. We propose to characterize the M–NCS interactions by synthesizing An(NCS)xy- (An = Pu, Am, Cm) complexes and subsequently analyzing the An(NCS)xy- compounds using ligand K-edge X-ray absorption spectroscopy (XAS) and DFT calculations.

Benefit to National Security Missions

This investigation will develop a fundamental understanding of bonding for plutonium and the other actinide elements. The results will be applied to DOE's efforts to design practical and efficient separations of the lanthanides and minor actinides. Moreover, the research will provide discrete probes for quantifying covalency that will be used in future efforts to analyze strategically important actinide materials and aid the DOE in its mission to support the national nuclear agenda that includes expanding nuclear power for energy security, preventing the spread of nuclear weapons, securing nuclear materials against theft, reducing the size of nuclear arsenals, and cleaning up the legacy of the Cold War.

Progress

Over FY15 Cross has made considerable advances in preparing M(NCS)x(y-) compounds. This includes the structural characterization of over 40 compounds by single crystal X-ray diffractometry. Additional, preliminary measurements have been carried out at SSRL and the ALS synchrotrons.

Future Work

Work in FY16 will focus on developing a synthetic route to trivalent f-block SCN1- complexes, and (b) establishing the bonding character of these complexes through multiple spectroscopic and theoretical techniques, primarily S, N, and C K-edge XAS and TDDFT.

Conclusion

Completion of this work will mark the first synthesis of trivalent An3+(NCS)xy- compounds and the first transplutonium S, N, and C K-edge XAS experiments. Developing an understanding of the bonding in these complexes will shed light on both the differences in Ln/An–NCS interactions and highlight how An–NCS bonding varies as the 5f series is traversed from Pu to Cm.

Publications

Macor, J. A., J. L. Brown, J. N. Cross, S. R. Daly, A. J. Gaunt, G. S. Girolami, M. T. Janicke, S. A. Kozimor, M. P. Neu, A. C. Olson, S. D. Reilly, and B. L. Scott. Coordination Chemistry of 2,2'-Biphenylenedithiophosphinate and Diphenyldithiophosphinate with U, Np, and Pu. 2015. DALTON TRANSACTIONS. ASAP (ASAP): NA.

Anaerobic, Solvothermal Synthesis of Lanthanide and Actinide Kagomé Antiferromagnets

Stosh A. Kozimor
20140681PRD4

Introduction

We propose to synthesize these 2D kagomÁ 4f and 5f materials for the first time. The lanthanide/actinide analogs of the jarosite minerals (A1+)(Fe3+)3(OH)6(SO42–)2 will be sought. The choice of monovalent cations (A1+; Ag, Rb, Cs, etc) and the oxo dianions (MO42–; M = S, Se, Te, Mo, W, etc) will template the kagomÁ network and expand the lattice to incorporate the f elements. Initially, we will focus on Ce3+ (4f1) and Yb3+ (4f13) materials and apply the developed methods across the lanthanide series. The 4f studies will provide a basis for expanding to plutonium and the early actinides. Finally, the structural, magnetic, and electronic properties of the new materials will be characterized in collaboration with Bauer, Batista, and Marten.

Benefit to National Security Missions

This research complements LANL's efforts associated with DOE's Office of Basic Energy Science heavy element chemistry program. The work focuses on understanding fundamental concepts associated with plutonium bonding and electronic structure. Overall, these efforts will provide a strong scientific foundation for the DOE and its laboratories to directly support the national nuclear agenda and the Integrated Plutonium Strategy.

Progress

In FY15, La Pierre has developed a new capabilities in solid state synthesis and in hydrothermal synthesis. A number of new teranary oxides were also synthesized. Additionally, La Peirre prepared for the first time (NMe4) NpCl6, which was fully characterized and is being written up for publication. These compounds have been characterized by X-ray powder diffraction. Additionally samples have been prepared for analysis at the SSRL synchrotron.

Future Work

In FY16 we will continue our synthetic efforts to generate methods for preparing a series of lanthanide/actinide analogs of the jarosite minerals (A1+)(Fe3+)3(OH)6(SO42–)2. These materials have never before been prepared. In the first year we will focused heavily on setting up the capability for the hydrothermal synthetic method. Now with this in place, we are working hard on developing methods to crystalize compounds that contain Ce3+ (4f1) and Yb3+ (4f13) metals. The compounds will be characterized by UV-Vis, XAFS, magetometry, and XRD. The synthetic method will serve as a basis for syntheses for other lanthanide elements and eventually be used to expand to plutonium and the early actinides.

Conclusion

A new two-year effort to synthesis 2D frameworks containing magnetically frustrated f elements is proposed. The synthetic component of this project will establish new design principles for unconventional actinide/lanthanide materials that might provide access to new types of actinide superconductors. Spectroscopic results will be used in advancing f element theory. Overall, These efforts will provide a strong scientific foundation for the DOE and its laboratories to directly support the national nuclear agenda and the integrated Plutonium Strategy.

A Physics-Based Numerical Model for Next-Generation Laminar Flow Batteries

Qinjun Kang
20150700PRD1

Introduction

Flow batteries have emerged as an efficient and economical device for the storage of large quantities of energy. They have also received much attention for their promising applications as power sources for vehicles and portable electronics, due to its quick recharge characteristics compared to lithium-ion batteries. Membranes are the most costly and unreliable component of the flow batteries. The membrane-less laminar flow battery can eliminate the need for an ion-exchange membrane by relying on laminar flow and slow diffusion to separate the reactants in anode and cathode. However, power densities as high as membrane-based counterparts have not been achieved. A recently developed membrane-less hydrogen bromine laminar flow battery (HBLFB) can achieve a high power density of 0.795 Wcm-2 at room temperature and atmospheric pressure. In this battery, the characteristics of the microporous anode (composition, structure, wettability, porosity) and the cathode (flow field design, surface structure) have not been optimized. Previous work has shown that these parameters can have an impact on the power density by nearly an order of magnitude.

In this project, we will develop a physics-based multiscale numerical model to understand the coupled physicochemical processes in membrane-less flow batteries, with the ultimate goal to optimize cell parameters to achieve higher power density. We plan to approach this problem in two stages by: 1) developing a microscale model accounting for the complex structures of the microporous anode and all the relevant physico-electrochemical and transport processes; and 2) developing a macroscopic model considering the entire cell, using the upscaled microscale model results as input.

Processes including two-phase distributions within the porous anode, electrolyte flow between the anode and cathode, as well as the electrochemical reactions at both electrodes, will be considered, and the electrode structure, wettability, porosity, as well as the overall cell geometry and dimension will be optimized.

Benefit to National Security Missions

The successful accomplishment of the proposed research will (1) result in a comprehensive multiscale numerical model for coupled transport and electrochemical processes in flow batteries; (2) provide optimal electrode characteristics, overall cell geometry, and operational conditions (e.g. flow rate) for improved cell performance. These results may lead to next-generation membrane-less high power density flow batteries and facilitate their applications in energy storage and power supply. The capabilities to be developed in this project also have direct application to other earth and energy programs, including geological storage of nuclear waste and carbon dioxide, development of petroleum and geothermal reservoirs, fuel cells, and micro reactors. This project will support the LANL Grand Challenge to develop transformative new energy technologies and to significantly enhance and extend the use of current technologies in a manner that is sustainable and that mitigates negative environmental, social, and national security impacts. It will also support DOE goals in promoting energy security.

Progress

Since this project started in January 2015, Dr. Li Chen, has made significant progress towards developing a microscale model accounting for the complex structures of the microporous electrodes and all the relevant physico-electro-chemical and transport processes. Particularly, he has developed a numerical model for coupled diffusion, conduction, and electrochemical reaction. The governing equations for proton transfer in electrolyte and reactant transport in porous electrodes are solved using the lattice Boltzmann method (LBM), with the electrochemical reactions occurring at the electrolyte/electrode interface treated in the source term.

Dr. Chen is currently working on adding fluid flow and convection of reactants in this newly developed model, and solving the coupled governing equations for fluid flow (Navier-Stokes equation), ion transport (Nernst-Plank equation), and electronic potential (Poisson equation) within the LBM framework in an iterated fashion. The resulting model will be the first physics-based, comprehensive pore-scale model for coupled transport and electrochemical processes in the electrodes of flow batteries, taking into account electrolyte flow, advection, diffusion, electrochemical migration and reaction. The transport model will be utilized to fully understand various physiochemical phenomena involved in flow batteries to help minimize transport losses and facilitate optimized material design and architectures, leading to increased flow battery performance and reduced cost.

Future Work

The overarching goal of this project is to develop a novel, physics-based numerical model to simulate coupled physico-electro-chemical and transport processes in flow batteries, to optimize cell parameters for achieving high power densities. We planned to approach this problem in two stages by: 1) developing a microscale model accounting for the complex structures of the microporous anode and all the relevant physico-electro-chemical and transport processes; and 2) developing a macroscopic model considering the entire cell, using the upscaled microscale model results as input.

In the past five months, we have made significant progress in stage 1 by developing a microscopic numerical model for coupled diffusion, conduction, and electrochemical reaction. In FY16, we will first finish developing the microscale model (stage 1) by incorporating fluid flow and convection of reactants in the newly developed model. We will then start developing the macroscopic model considering the entire cell, using the upscaled microscale model results as input. Finally, we will consider all involved processes in the flow battery, including two-phase distributions within the porous anode, electrolyte flow between the anode and cathode, as well as the electrochemical reactions at both electrodes. We will optimize the electrode structure, wettability, porosity, as well as the overall cell geometry and dimension for better flow battery performance.

Conclusion

This project will (1) result in a comprehensive multiscale numerical model for coupled transport and electrochemical processes in flow batteries; and, (2) provide optimal electrode characteristics, overall cell geometry, and operational conditions (e.g. flow rate) for improved cell performance. These results may lead to next-generation membrane-less high power density flow batteries and facilitate their applications in energy storage and power supply.

Publications

Chen, L., G. Wu, E. F. Holby, P. Zelenay, W. Tao, and Q. Kang. Lattice Boltzmann Pore-Scale Investigation of Coupled Physical-electrochemical Processes in C/Pt and Non-Precious Metal Cathode Catalyst Layers in Proton Exchange Membrane Fuel Cells. 2015. Electrochimica ActaElectrochimica Acta. 158: 175.

Resolving Kinetic Scales in 3D Global Magnetosphere Simulations

William S. Daughton
20150703PRD1

Introduction

The magnetic field of the Earth protects our planet against the stream of energetic particles that are continually emitted from the sun. This interaction leads to the formation of the magnetosphere, a bubble of hot ionized gas (plasma) surrounding our planet. During large solar storms, eruptions from the sun compress the magnetosphere and give rise to the injection of energetic particles that can damage satellites. It is a major challenge to understand and properly model how these energetic particles are able to penetrate into the magnetosphere. This project will develop a new simulation approach to accurately describe the dynamics of this complex system, and offer detailed predictions that can be compared with spacecraft observations. This new simulation approach will be far more accurate than current models of the magnetosphere, since it will solve the most basic underlying equations for the ions in the plasma using some of the largest supercomputers in the country. In addition, the electrons will be modeled with a new theoretical approach that has demonstrated improved accuracy in small test problems, but has not yet been applied to large-scale modeling. With these innovations, we anticipate this new kinetic model will leapfrog beyond the present models and provide a wealth of new scientific results and predictions. To test these new predictions, comparisons will be made with satellite observations that measure the energetic particles in the Earth's magnetosphere.

Benefit to National Security Missions

This research will exploit the newest generation of petascale supercomputers using a kinetic simulation code specially optimized for these machines. Some of these calculations will be performed locally at Los Alamos using NNSA computers, while other calculations will be performed on flagship DOE supercomputers such as Titan at Oak Ridge. These efforts are at the very forefront of high performance computing, both in terms of scaling the calculations to large numbers of cores (~100,000) and in remote visualization and analysis of the results. The scientific results from this research may benefit current and upcoming NASA missions focused on understanding the near-Earth space environment. In particular, the upcoming Magnetospheric Multi-Scale (MMS) mission will focus on the kinetic physics of magnetic reconnection with the Earth's magnetosphere. The simulations performed in this project will be among first to study the complex coupling between these kinetic scales and the global dynamics, supporting LANL scientific discovery and innovation in space science and nuclear, particle, cosmology, and astrophysics.

Progress

Excellent progress has been made towards the goals of this PRD project, which started only four months ago (February, 2015). First, we have ported the plasma simulation code H3D to computer clusters at LANL in order to perform global modeling of the Earth's magnetosphere. The H3D code has a rigorous description of the ions in the plasma, but only an approximate fluid description of the electrons. One of the primary goals of this project is to implement an improved fluid model for the electrons into the H3D code. During the past few months, we have already implemented a new equation-of-state that accounts for the effects of electron pressure anisotropy, which in previous work has been shown to be a critical feature. Next, we have tested this new closure relationship for the electrons using a simple two-dimensional test problem involving magnetic reconnection in a current sheet. Magnetic reconnection is a basic progress that converts magnetic energy into plasma kinetic energy, while giving rise to changes in connectivity of the magnetic field. This process is critical to model accurately, since it gives rise to the entry of solar wind plasma into the Earth's magnetosphere. Our preliminary hybrid simulation results agree quite well with first-principles kinetic simulations performed with

VPIC, the standard tool for these problems at LANL. These results show the development of intense current sheets in the reconnection outflow, which are expected to be key observational signatures in spacecraft data. We are currently investigating the influence of grid resolution and dissipation on these results within the H3D code. Meanwhile, we have begun performance testing the 3D version of H3D on LANL HPC machines using a new allocation of resources that were awarded to this project under the Institutional Computing Program. Small 3D reconnection simulations have been performed including the new equations of state. Working towards our goal of 3D global simulations of the Earth's magnetosphere, our initial 3D test problem is to simulation the magnetosphere of Ganymede, one of Jupiter's moons. This problem is computationally much easier than the Earth's magnetosphere, which will allow us to more carefully test the H3D code. Preliminary simulations for Ganymede look very promising and a full-scale production run on a 512-cubed grid is currently being computed on the Mustang computer at LANL.

Future Work

The dynamical coupling between the solar wind and the Earth's magnetosphere is crucially dependent on a number of key regions where kinetic effects are important. This includes the bow shock that develops upstream of the Earth, the shocked solar wind plasma (called the magnetosheath) and a very thin boundary layer along the periphery of the magnetosphere called the magnetopause. Depending upon the orientation of the interplanetary magnetic field (IMF), there are several key processes that can lead to the entry of solar wind plasma into the magnetosphere. This includes magnetic reconnection, which occurs due to changes in the connectivity of field lines across the magnetopause, and the Kelvin-Helmholtz instability, which leads to vortex formation and turbulent transport along the magnetopause boundary. The goal of this project is to describe the entire system with a kinetic description, in order to better understand the entry of solar wind plasma across the magnetopause and into the magnetosphere. In FY 15, we ported this hybrid code to LANL computer clusters, and implemented a new closure model for the electrons that will more accurately describe this physics.

In FY16, we will carefully test this new electron model for a series of test problems, and publish this comparison in a paper. In addition, during FY16 we will continue the small scale 3D simulations of Ganymede (one of Jupiter's moons) that we recently started, and compare the results with recently published papers from fluid models. Finally, during FY16 we will begin performing global simulations of the magnetosphere, starting with the limit of southward IMF where the dominant entry process is due to magnetic reconnection at the dayside magnetopause. Depending on how far we get, we will also look for opportunities to compare our initial results with spacecraft observations.

Conclusion

The fluid models currently used to model the magnetosphere are not fully justified, particularly in critical regions such as shock waves and thin boundary layers. While more accurate simulations have been performed in these local regions, the feedback on the global dynamics remains poorly understood. In this project, we will demonstrate the feasibility of simulations that more accurately describe the entire system. We anticipate this project may dramatically improve our ability to model the space weather environment surrounding the Earth, in regions where communication satellites play a crucial role in modern society.

Chemically Modifying the Uranyl Ion

Jaqueline L. Kiplinger
20120750PRD2

Abstract

This is the final report of a three-year Frederick Reines Distinguished Postdoctoral Fellowship project (March 2012 to June 2015) at Los Alamos National Laboratory. During this project, several different areas of actinide research were explored and they are summarized below.

Background and Research Objectives

Since the Manhattan Project, which sought to identify volatile compounds for the separation of fissionable isotopes for nuclear applications, there has been significant interest in actinide chemistry. Understanding the fundamental chemistry and speciation of actinides is critical to properly handling and processing nuclear materials and disposing of radioactive waste. For many years, the majority of studies on thorium and uranium involved aqueous systems of direct relevance to nuclear fuel processes. However, under these conditions, systems are operating at, or close to, thermodynamic sinks (e.g., uranyl) and important chemistry of the actinides can be masked. Under non-aqueous conditions, chemistry is performed in anhydrous organic solvents, giving opportunities to prepare actinide complexes that would not normally exist and thus gain glimpses of the "hidden" and "true" character of thorium and uranium. This permits the study of novel thorium–ligand and uranium–ligand bonds and their reactivity, which enables us to address fundamental questions regarding the extent and nature (5f vs. 6d) of covalency in actinide chemical bonding and how it impacts reactivity and physicochemical properties. This knowledge could impact on waste remediation where a key approach to minimize the volume of radioactive waste, and recycle useful components, involves separation technologies; these aim to deploy ligands that exploit the different levels of covalency in the chemical bonding of the myriad of elements that are present in radioactive waste.

Scientific Approach and Accomplishments

Thorium Starting Materials: (CpR)2ThCl2. In 2010, LANL reported the development of a convenient and safe solution route to the thorium starting material ThCl4(DME)2 (DME = dimethoxyethane), using inexpensive commercially available reagents, and avoiding the use of thorium metal. During research studies on metallocene thorium azides (see Metallocene Thorium Diazides, below), it was discovered that adding dimethoxyethane (DME) to the reaction mixture when ThCl4(DME)2 is the starting material had a significant effect on reaction times, conditions, and yields. This finding was then acutely demonstrated using the syntheses of known metallocene dichlorides (C5Me5)2ThCl2, (1,2,4-tBu3-C5H2)2ThCl2, and (C5Me4Et)2ThCl2 (Figure 1).

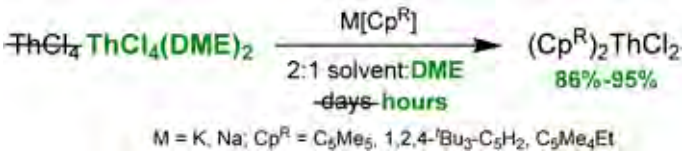

Figure 1. General scheme depicting the synthesis of metallocene thorium dichlorides from ThCl(DME); shows that the addition of DME to a reaction mixture improves synthetic efficacy of ThCl(DME).

The original syntheses of these dichlorides had all involved harsh conditions with long reaction times from the now-outdated starting material ThCl4. These results were communicated in the peer-reviewed journal Inorganic Chemistry Communications in 2014. Importantly, also in 2014, the new starting materials NpCl4(DME)2 and PuCl4(DME)2, which are the transuranic analogs of ThCl4(DME)2 and developed in collaboration with LANL colleague Andrew Gaunt, were reported in the journal Dalton Transactions. This is significant because it shows that findings in thorium chemistry can be applied to the transuranics, meaning it is likely that the results from this project can be translated to the Np and Pu starting materials as well.

Thorium Starting Materials: ThI4(DME)2

Since the synthesis, solubility, structure, and reactivity of actinide halide starting materials are strongly influenced by the nature of the halide, and also because there had been limited progress in the field of thorium tetraiodide chemistry, we were motivated to target the synthesis of the thorium tetraiodide complex, ThI4(DME)2. A synthetic route to ThI4(DME)2 from ThCl4(DME)2 was developed and optimized. It was discovered that ThI4(DME)2 exhibits excellent thermal stability compared to ThI4(THF)4, which undergoes rapid ring-opening of THF at ambient temperature. In a test reaction, it was found that salt metathesis between ThI4(DME)2 and K(LMe) (LMe = (2,6-iPr2C6H3) NC(Me)CHC(Me)N(2,6-iPr2C6H3)) cleanly gives (LMe) ThI2[O(CH2)4I](THF), which is a rare example of a thorium β-diketiminate complex. A demonstration of the synthetic utility of ThI4(DME)2 was completed by the preparation of thorium(IV) alkoxide, amide, and organometallic compounds. This work was published in 2012 in Dalton Transactions and was selected for the cover of the issue (Figure 2).

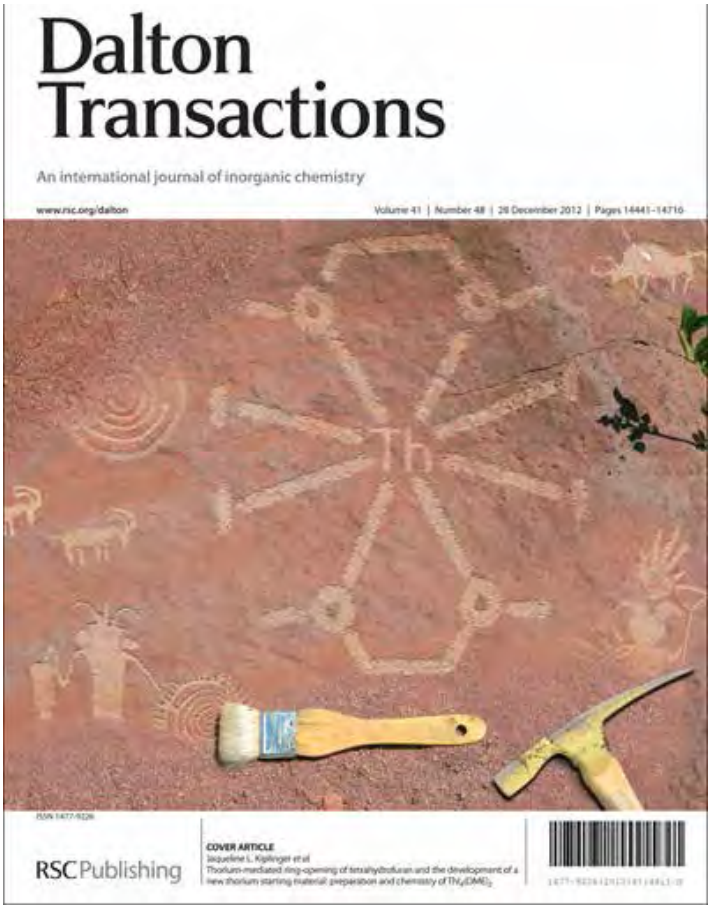

Figure 2. Cover of the issue of Dalton Transactions containing the ThI(DME) report.

Metallocene Uranium Bipyridyl Halides

A series of metallocene uranium bipyridyl halides was synthesized from the U(III) complex (C5Me5)2U(bipy) and halide salts (Figure 3). This family of new uranium-centered complexes is interesting due to being ligated by the redox-active chelating ligand 2,2'-bipyridine (bipy), making the complexes electronically flexible and calling into question the oxidation states of the uranium center and the bipy ligand. This will be a high-impact contribution to the field of actinide chemistry with a full study of the electronic properties across the series of compounds using absorption spectroscopy and electrochemistry. Of special note is the fluoride example, due to (1) the rarity of uranium fluorides relative to the other halides, and (2) the fact that the fluoride ligand is poised to react with silicon reagents, a relatively unexplored type of reactivity with the potential to yield highly sought-after synthetic targets.

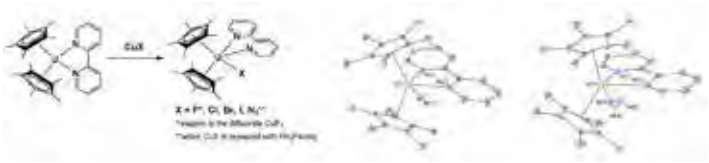

Figure 3. General scheme for the synthesis of (CMe)UX(bipy). X-ray crystal structures of (CMe)UBr(bipy) (structures for X = F and Cl are analogous) and (CMe)U(N)(bipy).

Futhermore, it was found that a different type of metallocene uranium bipyridyl halide is formed when the same U(III) starting material, (C5Me5)2U(bipy), was treated with benzyl (bz) halides. Here, the halide oxidatively adds to the uranium while the bz group migrates to the 5-position on the bipy ligand, forming a new carbon-carbon bond and a new "bipy-bz" ligand (Figure 4). The next step is to use benzyl fluoride; cleaving the very strong C-F bond will be significant, and based on our results with the other halides it is expected this reaction will proceed in a facile manner.

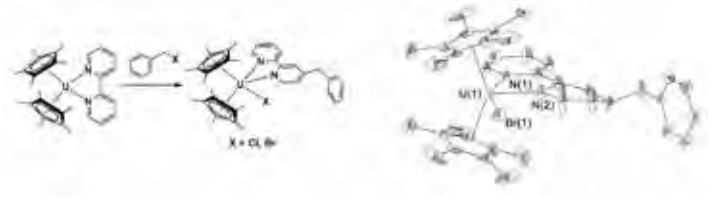

Figure 4. General reaction scheme for the synthesis of (CMe) U(bipy-bz). Representative X-ray crystal structure of (CMe) UBr(bipy-bz) (structure for X = Cl is analogous).

Metallocene Thorium Diazides. The first molecular uranium nitride was reported by LANL in 2010; it was generated by photolysis of a uranium azide complex. In general, actinide nitride ceramics are of interest as alternative nuclear fuels, but very little is known about their chemical properties or reaction behavior due to the challenges surrounding the study of extended materials. An alternative approach is to generate well-defined molecular analogs, which are

simpler to study. Since the 2010 LANL report, there have been only two other molecular uranium nitrides reported, and no molecular nitrides of any other actinides have been reported.

With the generation of molecular thorium nitrides as a long-term target, this project's goal was to generate a series of molecular thorium azides, since azides are a classic entry into nitride chemistry via photolysis, thermolysis, or chemical reduction. There are only two molecular thorium azides in the literature, and neither of them are ideal candidates for conversion to nitrides due to the steric and electronic profiles of their ancillary ligands.

This work has resulted in a series of new metallocene thorium diazide complexes synthesized using salt metathesis between (CpR)2ThCl2 and NaN3 (Figure 5, left), all of which have been fully characterized. It was discovered that their diverse solid-state structures were governed by the size of the ancillary ligands (Figure 5, right). All new compounds were characterized using elemental analysis, X-ray crystallography, multinuclear nuclear magnetic resonance (NMR) spectroscopy, infrared (IR) spectroscopy (solution and solid), and for the first time for any structurally characterized actinide azide, Raman spectroscopy. These results will be submitted to the high-impact peer-reviewed journal Angewandte Chemie International Edition. Work is currently underway to convert these azide complexes to nitrides; initial photolysis experiments have yielded exciting preliminary results, which inspired new actinide chemistry proposals.

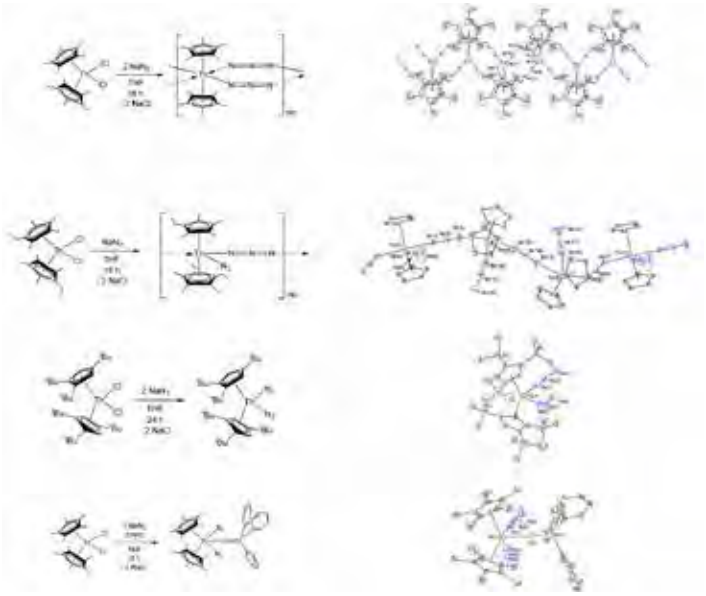

Figure 5. Syntheses of metallocene thorium diazides with corresponding X-ray crystal structures on the right. Trend: smaller ancillary ligands multinuclear complexes (), while larger ancillary ligands mononuclear complexes ().

Impact on National Missions

The DOE complex and LANL clearly benefit from exploratory research into the chemistry of the actinide elements, because of their criticality to DOE nuclear weapons mission areas. The synthesis of new actinide compounds not only provides important information about metal-ligand bonding but also improves our ability to reliably predict their chemical behavior in a variety of applications from performance validation of waste repositories, to the design of selective chemical separation methodologies, to mitigation of corrosion processes in aging weapons components. The recent focus on energy security and the tacit acknowledgment that nuclear energy must be part of the mix to achieve energy independence and reduce greenhouse gas emissions has served to heighten this interest even further.

Publications

Monreal, M. J.. Metallocene Thorium Azide Complexes: Diverse Solid-State Structures Governed by Ancillary Ligand Steric Effects. Invited presentation at 249th National Meeting of the American Chemical Society . (Denver, CO, 22-26 March 2015).

Monreal, M. J.. Establishing a Surrogate Pyrochemical Capability at LANL (Round Table Discussion Leader). Invited presentation at Joint Working Group (JOWOG) 22/2 Technical Exchange @ Lawrence Livermore National Laboratory. (Livermore, CA, September 2015).

Monreal, M. J., B. L. Scott, and J. L. Kiplinger. Organometallic thorium azide complexes: using steric pressure to control structure . Invited presentation at LANL Postdoctoral Women's Group Colloquium. (Los Alamos, February 26, 2014).

Monreal, M. J., B. L. Scott, and J. L. Kiplinger. Organometallic thorium azide complexes: using steric pressure to control structure. Invited presentation at LANL Women's History Month Panel and Poster Session. (Los Alamos, NM, March 31, 2014).

Monreal, M. J., B. L. Scott, and J. L. Kiplinger. Organometallic thorium azides: metallocene sterics govern structure . Invited presentation at Laboratory Directed Research and Development Program Review. (Los Alamos, NM, ay 14, 2014).

Monreal, M. J., B. L. Scott, and J. L. Kiplinger. Organometallic thorium azide complexes: steric pressure controls structure . Presented at LANL Postdoc Research Day. (Los Alamos, NM, June 11, 2014).

Monreal, M. J., B. L. Scott, and J. L. Kiplinger. Organometallic thorium azide complexes . Invited presentation at 27th Rare Earth Research Conference. (Squaw Valley, CA, 22-26 June 2014).

Monreal, M. J., R. J. Wright, J. T. Golden, D. E. Morris, B. L. Scott, P. P. Power, and J. L. Kiplinger . Thorium(IV) and uranium(IV) halide complexes supported by bulky β-diketiminato ligands. 2013. Organometallics (Invited Article – Special Issue: Recent Advances in Organo-f-Element Chemistry). 32: 1423.

Monreal, M. J., R. K. Thomson, B. L. Scott, and J. L. Kiplinger. Enhancing the synthetic efficacy of thorium tetrachloride bis(1,2-dimethoxyethane) with added 1,2-dimethoxyethane: Preparation of metallocene thorium dichlorides. 2014. INORGANIC CHEMISTRY COMMUNICATIONS. 46: 51.

Travia, N. E., M. J. Monreal, B. L. Scott , and J. L. Kiplinger. Thorium-mediated ring-opening of tetrahydrofuran and the development of a new thorium starting material: Preparation and chemistry of ThI4(DME)2. 2012. Dalton Transactions. 41: 14441.

Travia, N. E., M. J. Monreal, B. L. Scott, D. E. Morris , and J. L. Kiplinger. Developing the next generation thorium iodide starting materials. Invited presentation at 243rd American Chemical Society National Meeting. (San Diego, California, 25-29 March 2012).

Travia, N. E., M. J. Monreal, B. L. Scott, and J. L. Kiplinger. A new starting material for thorium chemistry: ThI4(DME)2. Presented at Gordon Research Conference on Inorganic Chemistry. (University of New England, Biddeford, Maine, 17-22 June 2012).

Catalytic Mechanism and Inhibition of Metallo-beta-lactamases (MBL), the Ultimate Threat Against Antibiotics

Ryszard Michalczyk
20120776PRD4

Abstract

A number of bacterial pathogens produce enzymes able to inactivate β-lactam antibiotics, which comprise more than 80% of the world's market of antimicrobials. These enzymes, known as β-lactamases, rank among the most proficient enzymes known. At present, there are no clinically useful MBL (metallo-β-lactamases) inhibitors available. Our research efforts aimed to discover MBL inhibitors or novel antibiotics resistant to inactivation.

Joint Neutron and X-ray crystallography is the only methodology providing details about H atom positions in these enzymes and potential inhibitors, details that will be fundamental for future drug design efforts. Three broad lines of research were explored for NDM-1 and BcII metallo-β-lactamases: (1) Water activation, (2) Substrate binding, and (3) Inhibition.

This research has direct implications for understanding of these enzymes' reaction mechanism and enabling the design of clinically useful MBL inhibitors that will allow re-introduction of many powerful antibiotics currently withdrawn because of their sensitivity to β-lactamases. This has direct impact on the public health security, the well-being of millions of people and the world pharmaceutical industry.

Background and Research Objectives

A number of bacterial pathogens produce enzymes able to inactivate β-lactam antibiotics, which comprise more than 80% of the world's market of antimicrobials. These enzymes, known as β-lactamases, rank among the most proficient enzymes known. Due to their readiness for horizontal transfer and evolution, MBLs entail a serious public health issue. A special group of Zn(II)-dependent β-lactamases, termed metallo-β-lactamases (MBLs), display a worrisome substrate promiscuity, hydrolyzing penicillins, cefalosporins, and carbapenems, the latest generation of β-lactams (Figure 1). Although monobactams are the only known poor MBL substrates, the ever-changing nature of MBLs ensure that this is not a long-term solution.

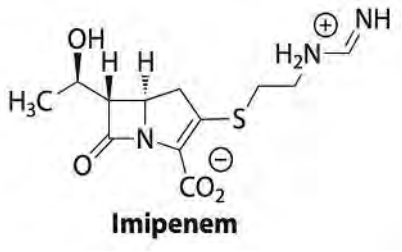

Figure 1. Carbapenems like imipenem (above) are readily inactivated by MBLs.

At present, there are no clinically useful MBL inhibitors available. Research efforts aim to discover MBL inhibitors or novel antibiotics resistant to inactivation. However, our limited knowledge of the MBL's structure-function thwarted such efforts thus far. The MBL's reaction mechanism has been shown not to involve covalently bound intermediates, making unfeasible the classic "suicide substrate" inhibition approach.

Joint Neutron and X-ray crystallography is the only methodology providing details about H atom positions (i.e. water, H-bonds, protonation state of amino acids), fundamental for future drug design efforts. During my time at LANL I characterized the enzyme NDM-1, an MBL of major concern. Three broad lines of research were explored: (1) Water activation, (2) Substrate binding, and (3) Inhibition. This work required all the Protein Crystallography Station resources: the deuteration and protein expression laboratory, protein purification and crystallization laboratory as well as the neutron beamline and X-ray diffraction suite.

Scientific Approach and Accomplishments

As outlined in the Research Proposal, the project comprises three main objectives centered on the structure-function relationships of metallo-β-lactamases (MBLs): (1) Mechanism of water activation, (2) Mechanism of

substrate binding, and (3) Inhibition. The progress on each of these points is detailed below.

Mechanism of water activation

Two MBLs are currently being studied: NDM-1 from K. pneumoniae and BcII from B. cereus. Both wild-type enzymes are being expressed under BSL-2 conditions under IBC-127-2013. This objective will be achieved through solving neutron structures, for which mm-size crystals are needed, which requires large amounts of pure protein. The wild-type NDM-1 enzyme proved to be difficult to express in E. coli BL21(DE3) in a native form due to proteolysis. After several unsuccessful attempts to determine conditions in which NDM-1 would express in a native form (adjusting induction growth temperature and length, use of IPTG or autoinducing media, use of protease inhibitor cocktails) we decided to focus first on the other MBL, BcII (which expresses very well), in order to pursue the neutron structure.

It was determined that BcII does not grow mm-size crystals using the vapor-diffusion method in 9-well plates and 0.5–1 ml drops. Instead, large BcII crystals grow using dialysis method, using commercially available dialysis buttons with 3,000-Da cutoff membrane. BcII crystals are prone to degradation through oxidation of residue Cys221 upon long incubation times (weeks to months). Since neutron beamtime is scarce, BcII crystals will need to be freshly grown close to the data collection time. I plan to grow mm-size BcII crystals for the upcoming neutron beam cycle starting in October 2014, for which the corresponding beamtime request application has been submitted and is pending approval.

Mechanism of substrate binding

For reasons outlined above, this research is also focused on BcII. Two double mutants were designed, cloned, purified, crystallized, and their structures were solved through x-ray crystallography, namely, BcII-DDE (Cys221Asp, His263Glu) and BcII-DDQ (Cys221Asp, His263Gln). As expected, both display an empty second-zinc site and no β-lactamase activity. The next step is to co-crystallize these mutants with different metals and intact β-lactam antibiotics. Crystals have already been grown in the presence of ampicillin and different concentrations of Zn2+ (as a negative control), Ca2+, Mg2+, Sr2+, Ba2+, Fe3+, Co2+, Mn2+, Ni2+, Cu2+, Al3+, and Sm3+, in order to screen conditions in which these metals would enable substrate binding but no catalysis. These crystals will be flash-frozen and shipped to the Stanford Synchrotron Radiation Lightsource (SSRL) for x-ray data collection, for which I have been awarded beamtime on July 8-9th, proposal SSRL 4B25A.

Protein/Ligand	Apo-BcII	BcII-CS319 (CS3)*	BcII-GM256 (GM2)*	BcII-VC26 (VC2)*	BcII-DDQ	BcII-DDE
Data collection						
Spacegroup	$C2_1$	$C2_1$	$C2_1$	$C2_1$	$C2_1$	$C2_1$
Cell constants (Å,°)	a = 53.12 b = 60.81 c = 69.25 β = 93.00 (α=γ= 90°)	a = 53.17 b = 60.83 c = 69.41 β = 93.01 (α=γ= 90°)	a = 53.08 b = 61.28 c = 69.51 β = 93.04 (α=γ= 90°)	a = 53.60 b = 60.42 c = 69.51 β = 93.28 (α=γ= 90°)	a = 53.18 b = 60.00 c = 69.51 β = 93.17 (α=γ= 90°)	a = 53.14 b = 61.39 c = 69.64 β = 93.30 (α=γ= 90°)
Resolution (Å)	1.67	2.29	1.80	2.25	1.39	1.15
Unique reflections	22468	9757	20292	9274	38871	40837
Completeness (%)	87.6	96.9	97.8	87.5	92.5	95.2
Wilson B factor (Å^2)	29.9	49.0	32.6	44.6	22.0	16.1
<I/σI>	3.6	5.5	7.4	4.9	2.7	1.1
Refinement						
PDB accession	4NQ4	4NQ5	4NQ6	4NQ7	–	–
Resolution range (Å)	34.6–1.67 (1.71–1.67)	35.3–2.29 (2.35–2.29)	40.12–1.80 (1.85–1.80)	35.4–2.25 (2.30–2.25)	30.5–1.47 (1.47–1.39)	26.9–1.18 (1.18–1.15)
R_{cryst} (overall) (%)	24.6 (28.8)	19.9 (26.6)	19.3 (37.6)	20.1 (25.5)	16.1	15.5 (34.5)
R_{free} (5 % reflections) (%)	30.0 (38.7)	25.6 (32.2)	24.8 (44.5)	25.3 (37.6)	20.7	18.5 (34.1)
Unit cell contents (chains)	1	1	1	1	1	1
Atoms	1853	1718	1871	1711	1825	1883
Protein	1385	1636	1444	1636	1650	1663
Water	465	66	411	57	174	219
Ligands & ions	3	16	16	18	1	1
Mean B factor (Å^2)	22.6	40.7	28.7	34.8	23.7	17.5
Deviations from ideality						
RMSD bonds (Å)	0.018	0.014	0.019	0.016	0.024	0.023
RMSD angles (°)	1.925	1.798	2.065	1.931	0.019	0.019

Figure 2. X-ray data collection and refinement statistics.

Inhibition of MBLs

This part of the project is focused on two families of potential inhibitors: sulfonamides and bisthiazolidines. The sulfonamides 3-[(2-oxo-1,3-oxazolidin-3-yl)carbonyl]-2-pyridinesulfonamide (OCPS), 6-methoxy-3-nitro-2-pyridinesulfonamide (MNPS) and 3-(4-methyl-5-oxo-4,5-dihydro-1,3,4-oxadiazol-2-yl)-2-pyridinesulfonamide (DOPS) are commercially available, and were selected based on their central 2-pyridine sulfonamide moiety. These compounds have the potential to bind to the second-zinc of MBLs thereby inhibiting the enzyme competitively (through preventing substrate binding) or uncompetitively (through removing the second-site zinc). As a proof-of-concept, the structure of BcII complexed with 2-pyridine sulfonamide was solved at pH 6, showing the expected binding mode, i.e. bidentate binding to the second-zinc site through nitrogen atoms present in the probably deprotonated sulfonamide –NH2 and the pyrimidine. Crystallization trials are in progress for BcII complexed with compounds OCPS, MNPS and DOPS. These crystals will also be shipped and data collected in the upcoming trip to SSRL.

The second group of compounds, bisthiazolidines (BTZs), is bicyclic heterocyclic compounds with two fused thiazolidine rings, thereby emulating penicillins. These compounds were obtained through a collaborative work with researchers from Uruguay and Argentina, who synthesized and isolated them. I have solved the x-ray structures of BcII complexed with three of them (CS319, GM256 and VC26), and measured their inhibition constants in vitro, which resulted to be in the micromolar range. These structures have shed light on possible modifications leading to improved inhibiting properties in these compounds, particu-

larly VC26, which are being introduced by our collaborators in Uruguay.

Impact on National Missions

The proposed work utilized an innovative research strategy that is LANL-unique for novel antibiotics. MBLs comprise a massive global human health issue causing many deaths and substantial economic losses around world, due to the innumerable complications associated with untreatable infections caused by some of the most dangerous bacteria present in clinical settings and intensive care units. This work, which can only be performed at LANL's world-class facilities, will provide the first neutron structures for antibiotic resistance enzymes found in multidrug resistant pathogens, with direct implications for understanding of these enzymes' reaction mechanism and enabling the design of clinically useful MBL inhibitors that will allow re-introduction of many powerful antibiotics currently withdrawn because of their sensitivity to β-lactamases. This has direct impact on the public health security, the well-being of millions of people and the world pharmaceutical industry.

Publications

Gonzalez, J. M., M. M. Gonzalez, M. Kosmopoulou, C. Saiz, V. Castillo, G. Mahler, R. Bonomo, J. Spencer, and A. J. Vila. Inhibition of Metallo-β-Lactamases by Bisthiazolidines. . Presented at 2014 American Crystallographic Association Annual Meeting. (Albuquerque, 24-28 May 2014).

John, F. J. St, D. Dietrich, C. Crooks, E. Pozharski, J. M . Gonzalez, E. Bales, K. Smith, and J. C. Hurlbert. A Novel Member of Glycoside Hydrolase Family 30 Subfamily 8 with Altered Substrate Specificity. To appear in Acta Crystallographica Section D.

Marti-Arbona, R., J. M. Gonzalez, and C. J. Unkefer. Crystal Structure of Phosphoenolpyruvate Carboxylase from Methylobacterium extorquens. Presented at 2014 American Crystallographic Association Annual Meeting. (Albuquerque, 24-28 May 2014).

Turra, G., C. Faugel, J. M. Gonzalez, D. Presello, C. Andreo, and V. Campos-Bermudez. La glioxalasa I de maíz regula niveles de metilglioxal, una molécula señal de estrés en Fusarium verticilloides?. Presented at XXX Argentine Meeting of Plant Physiology. (Mar del Plata, Argentina, 21-24 September 2014).

Unkefer, C. J., J. Chen, S. Z. Fisher, J. M. Gonzalez, J. P. Bacik, and M. J. Waltman. Time-of-flight Laue Neutron Crystallography at the Protein Crystallography Station (PCS) at LANSCE. . Presented at 2014 American Crystallographic Association Annual Meeting. (Albuquerque, 24-28 May 2014).

Stimuli Responsive, Functional Biopolymers: Quinic Acid-Based Polymers and Their Assemblies

Hsing-Lin Wang
20130778PRD1

Abstract

This project aimed to develop functional biomolecules with emergent (mechanical, optical, and electronic) properties that are not accessible through conventional synthetic methods. The approach uses molecules that are known to form polymers compatible with biological systems with side chains that are active to which functional groups can be attached. Depending on the distribution and density of these functional groups on the side chains, a wide spectrum of mechanical and optical properties, and electronic structures can be accessed. Our goal is to exploit the emergent properties, and through the analysis of structure-property relationships, obtain valuable insight regarding the

design of functional biomolecules with enhanced functionality that can be used toward sensing, bioimaging, drug delivery, optical, electronic and energy applications. Such an approach has not yet been studied in a systematic manner mainly because multidisciplinary knowledge ranging from organic synthesis, self-assembly, to materials chemistry and biochemistry is needed. The challenge is to develop synthetic chemistry routes that are facile and effective. Further, we will demonstrate control of functional groups on in order to render desired structures and properties.

Background and Research Objectives

Stimuli-responsive polymers are polymers that respond with dramatic property changes to small changes in their environment such as chemicals, temperature, pH etc. Development of the materials based on stimuli responsive molecules represents an emerging and interdisciplinary topic at the border of life sciences,[1] material sciences[2] and nanotechnology[2] as these polymers are ideal candidates for many applications in the sensor systems, drug delivery, multivalent drug scaffolds, and tissue engineering.

In this context, we would like to investigate the development of functional biomolecules in which the existing functionalities can be coupled with conjugated oligomer[3][4], dye or other complex biomacromolecule for sensing and electronic applications. The functional groups can interact or self-assemble in ways that dominate the formation of hierarchical structure and their corresponding properties. Understanding the source of these interactions between specific components will allow us to achieve functional materials with emergent properties.

Specifically, we proposed to investigate the development of functional biopolymers in which the existing functionalities can be coupled with oligomer, dye or other complex biomacromolecules for sensing and electronic applications. We also proposed to develop biomolecules with build-in functionality resulting from its natural occurrence, such as chirality, which allows us to further incorporate functional groups with control in spatial resolution. We planned to develop unnatural amino acid biomolecules and their self-assemblies and explore their properties against various stimuli such as temperature, pH etc., striving to synthesize a series of biomolecules belong to the category of unnatural amino acid and demonstrate their use for bioimaging and organic electronic devices. These biomolecules can act as spectroscopic reporters on the state of the polymer conformation and on the state of protonation levels. Conformational changes within the polymer trigger the arrangement/proximity of the fluorophores to put them in different environments and thus lead to a modulation of fluorescence. Biomolecules with conjugated structure and amine end group leads to a pH-dependent optical properties as they can turn on/off the intermolecular charge transfer process by varying the pH value of the solution.

Scientific Approach and Accomplishments

Synthesis and characterization of non-natural fluorescent amino acid and their applications to bioimaging

We have synthesized a series of fluorescent unnatural amino acids (UAAs) bearing stilbene and meta-phenylenevinylene (m-PPV) backbone and their optical properties were studied using a suite of spectroscopy probes. These novel amino acids were derived from protected diiodo-L-tyrosine using palladium-catalyzed heck couplings with a series of styrene analogs. Unlike the other fluorescent UAAs, whose emissions are restricted to a narrow range of wavelengths, these new amino acids display emission peaks at a broad range of wavelengths (from 400 to 800 nm); including NIR with a quantum yield of 4% in HEEPS buffer. The incorporation of both pyridine and phenol functional groups lead to distinct red, green, and blue (RGB) emission, in its basic, acidic and neutral states, see Fig. 1. More importantly, these amino acids showed reversible pH and redox response showing their promise as stimuli responsive fluorescent probes.

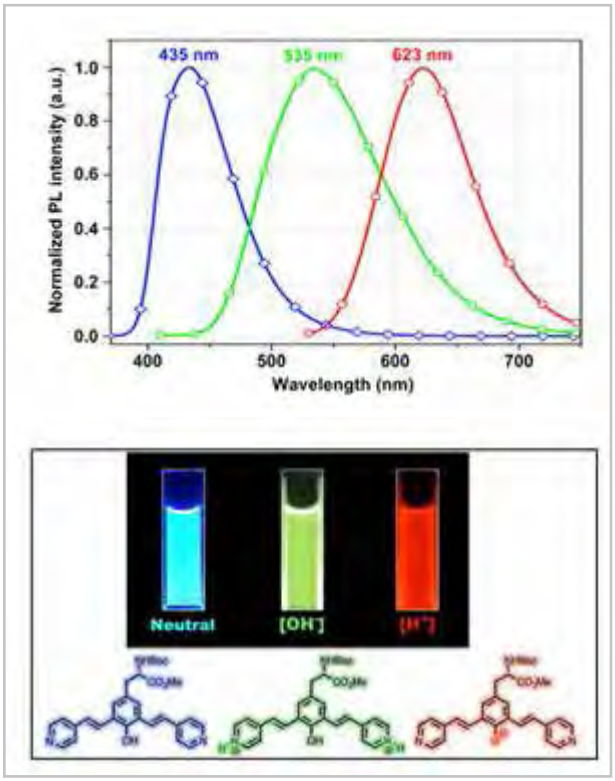

Figure 1. Emission spectra of unnatural amino acid in neutral (blue), acidic (green) and basic (red) environment showing the RGB emission.

To further demonstrate the utility of these UAAs in peptide synthesis, one of the amino acids in this series was incorporated into a cell penetrating peptide (CPP) sequence through standard solid phase peptide synthesis. The general use of these UAAs for cell imaging has been demonstrated by applying CPP to two different cell lines using confocal fluorescence microscopy.

Water-soluble biopolymers for bioimaging

Water-soluble cationic conjugated polymers (WSCPs) [5] show a strong affinity toward the negatively charged cell membranes, staining cell surface using WSCPs is a relatively unexplored area due to the endocytosis problem. However, the ability to functionalize these polymers with specific recognition ligands enables selective detection among the various cell lines and different organelles. To date, only one report has appeared in the literature disclosing the ability of WSCPs to be stable cell staining agents. Water-soluble polythiophene conjugated with lapatinib, an anticancer tyrosine kinase inhibitor, can be used to induce the polymer interaction with transmembrane proteins and thus achieve stable cell membrane staining.

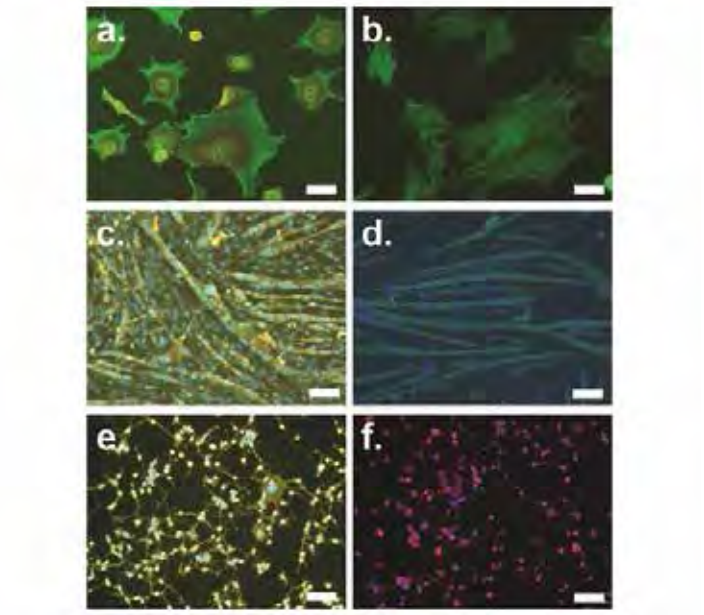

Figure 2. WS-PPV staining of various cell types. (a) Fixed and stained mouse fibroblast cell line 3T3 cells were stained with WS-PPV and imaged using two different filter channels (red, 670 nm/ green, 519 nm). (b) Fixed 3T3 cells were stained with actin staining reagent. (c) Fixed mouse myoblast cell line C2C12 cells were stained with WS-PPV (yellow) and DAPI (blue). The serial muscle cells composed differentiated myotubes were clearly observed via WS-PPV staining. (d) C2C12 cells were fixed and stained with anti-myosin heavy chain antibody (green) and nucleus staining (blue). (e) Fixed and stained mouse motor neuron cell line (NSC-34). The extension of neurite network can be observed through the staining of WS-PPV polymer (yellow). Cell nucleuses were localized using DAPI staining (blue). (f) Mouse motor neuron cells (NSC-34) were fixed and stained with anti-beta III tubulin antibody (magenta) and nucleus staining (blue). All cells were stained with WS-PPV (1 μM) for 10 min. Scale bar = 100 μm.

To further evaluate the robustness of WS-PPV in cell imaging, we extended our studies to a series of different cell lines. Mouse fibroblast (3T3) cells, mouse myoblast

(C2C12) cells, mouse motor neuron cells (NSC-34) and human alveolar basal epithelial cells (A549) were stained independently using 0.5 µM WS-PPV for 10 min. As shown in Fig. 4, different cells could be easily visualized after WS-PPV staining.

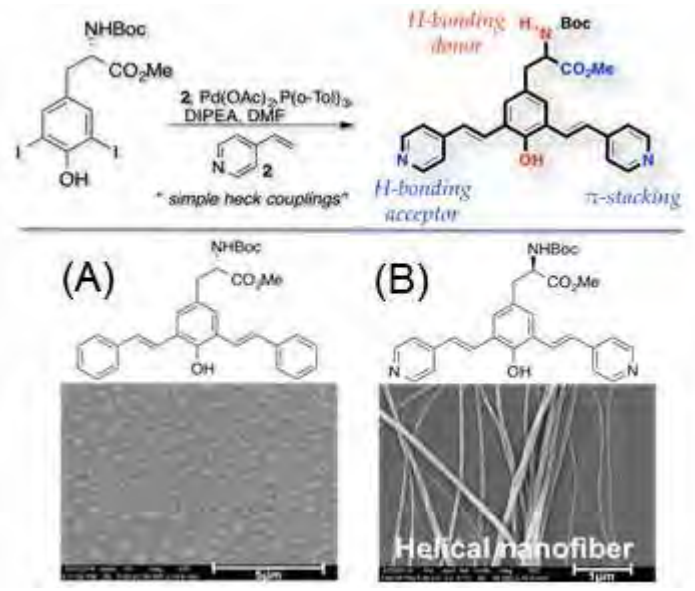

Figure 3. (top) Synthetic scheme of unnatural amino acids, and (bottom) molecular structure of two conjugated oligomers and the SEM images of the hierarchical self-assembled structures.

Actin based filaments (i.e. filopodia) have been shown to play a critical role in controlling the cell migration, exploring their environments and wound healing. However, to observe the formation of filament network, the staining method is usually restricted to immunostaining and fluorescently labeled phallotoxins. These methods have limitations in terms of their cost-effectiveness and long staining time, usually greater than 48 hours. Therefore, the discovery and evaluation of alternate staining agents is a valuable addition to this field and to the best of our knowledge, polymeric imaging agents for filaments staining are barely explored.

While imaging fixed 3T3 cells, we found that WS-PPV polymer effectively stained the cytoskeleton and the obtained images are almost comparable to that of standard staining images. Interestingly, actin fiber and nucleus can be stained at the same time in a single stain by WS-PPV and can be observed simply by using different microscope filters (Fig. 2a), where as, in case of commercial actin staining agents (Fig. 2b), a separate secondary staining is required to visualize the nucleus. This is particularly advantageous as staining with WS-PPV serves as a dual staining agent and lowers the cist and time required for the imaging.

The C2C12 myoblast cell line is a widely used model to study myogenesis in vitro. Immunostaining of the myotubes is commonly used methods to quantify in vitro myogenic differentiation. Despite the selectivity and specificity of immunostaining, this widely used approach suffers from time-consuming staining protocols and cost-effectiveness. Myotube staining by using other than fluorescent antibodies is hardly explored so far. Thus, we wanted to validate the ability of WS-PPV in myotube staining. It is particularly noteworthy that when C2C12 mouse muscle cells were incubated with WS-PPV, myotubes were stained within 10 min (Fig. 2c) as compared to immunostaining that takes 2 days to be visualized (Fig. 2d).

In case of NSC-34 cells, neurites (cell body of a neuron) were stained (Fig. 2e) with WS-PPV in the same staining condition while standard immunocytochemistry staining of neuron cells (Fig. 2f) has longer staining time. Furthermore, the visualization of cells cultured on 3-D substrates sometimes can be a big challenge. For example, the absorption of fluorescent molecules in the substrate (e.g. hydrogel, porous scaffold) can easily increase the high fluorescent background when 3-D substrate is observed through microscopy analysis. Here, we demonstrated the other capability of WS-PPV to stain the cells inside 3-D substrate. The key technique is staining the cells in advance using suspension staining. After staining, the WS-PPV stained cells were spun down and then seeded in the lumen of cellulose based hollow fiber. After 3 days of culturing, A549 cells were still spotted inside hollow fiber. This advantage allows us to monitor a long-term cell culture in 3-D substrate without using any additional post staining which will significantly reduce the fluorescent background.

Cell membrane staining using WSCPs without any targeting ligands for bio recognition is not known. We have shown very exciting results using cationic poly(p- phenylene

vinylene) (PPV), a WSCP for cell imaging. P2 as bioimaging polymer exhibits stability allowing long-term cell tracking, distinguishing live and dead cells, and multi- functional cell staining. Overall, our results show that using WSCP is far superior than state-of-the art staining commercial dyes as WSCP has a much faster staining time at a much lower cost (100 times cheaper than existing commercial dye), while providing more details and imaging resolution as opposed to the commercial dyes. Such unprecedented properties suggest that certain WSCPs may serve as next generation imaging dyes for biomedical research.

Programmed self-assembly of unnatural amino acid

Initially we have studied the self-assembly of three newly synthesized m-PPV analogs (structures A, B in Fig. 3) to test our hypothesis. The only difference between A and B is that a pyridine ring in molecule B replaces the phenyl ring in A. The pyridine moiety in compound B brings

in additional H-bonding source along with π-stacking. As anticipated, structure B self-assembles to form nanostructures due to the nicely positioned two pairs of H-bonding acceptors (Fig. 3_blue) and donors (Fig. 3_red). Electron microcopy studies revealed that the compound B showed the nanofiber formation. Further morphological characterization with SEM, TEM and AFM revealed that the tiniest nanofiber (fibril) has a diameter of 20 nm and several nanofibers can come together to give 60 -100 nm nanofiber (bundles). This is particularly interesting as the morphology of these fibers is in close agreement with the amyloid fibers.19-22 As shown in Fig. 3, it is evident that the build in chiral center leads to helical nanofiber as compare to dotted morphology for molecule without the H-bonding acceptor, Fig, 3A. Our results reveal a novel programmed self-assembly of chiral conjugated oligomer, an amino acid precursor, with enhanced optical properties. To the best of our knowledge, nanofibers comprised of conjugated oligomers with enhanced optical properties have never been reported.

Impact on National Missions

These new classes of biomolecules and their self-assemblies may exhibit high temperature thermal transitions and strong mechanical properties due to the high degree of hydrogen bonding and rigid carbocyclic backbone. The correlation between nanoassembly structures and their associated properties yield insights on the interplay between structure, dynamics and functions of the materials. We also expect this research to feed into novel strategies for the design and synthesis of nanoassemblies with adaptive control to enable the materials with technological relevance in areas of optics, electronics, photovoltaic, and biomedical devices that impact our missions in energy security and threat reduction.

References

Shim, M. S., and Y. J. Kwon. Stimuli-responsive polymers and nanomaterials for gene delivery and imaging applications. 2012. Advanced Drug Delivery Reviews. 64: 1046.

Stuart , M. A. C., W. T. S. Huck, , J. Genzer, M. Müller, C. Ober, M. Stamm, et.al. Minko. Emerging applications of stimuli-responsive polymer materials. 2010. NATURE MATERIALS. 9: 01.

Cheruku, P., J. H. Huang , H. J. Yen, R. S. Iyer,, Kirk D. Rector, J. S. Martinez, and H. L. Wang. Tyrosine-derived stimuli responsive, fluorescent amino acids . 2015. CHEMICAL SCIENCE. 6: 1150.

Park, Y. I., O. Postupna, A. Zhugayevych, H. Shin, Y. -S. Park, B. Kim, H. -J. Yen, P. Cheruku, J. S. Martinez, J. W. Park, S. Tretiak , and H. -L. Wang. A new pH sensitive fluorescent and white light emissive material through controlled intermolecular charge transfer. 2014. CHEMICAL SCIENCE. : DOI: 10.1039/C4SC01911C.

Gao, Y., C. C. Wang , L. Wang , and H. L. Wang. Conjugated polyelectrolytes with pH-sependent conformations and optical properties. 2007. LANGMUIR. 23: 776.

Publications

Cheruku, P., J. H. Huang , H. J. Yen, R. S. Iyer,, Kirk D. Rector, J. S. Martinez, and H. L. Wang. Tyrosine-derived stimuli responsive, fluorescent amino acids . 2015. CHEMICAL SCIENCE. 6: 1150.

Park, Y. I., O. Postupna, A. Zhugayevych, H. Shin, Y. -S. Park, B. Kim, H. -J. Yen, P. Cheruku, J. S. Martinez, J. W. Park, S. Tretiak , and H. -L. Wang. A new pH sensitive fluorescent and white light emissive material through controlled intermolecular charge transfer. 2014. CHEMICAL SCIENCE. : DOI: 10.1039/C4SC01911C.

Single-Cell Genomics for Better Control of Plant Pathogens

Shunsheng Han
20130779PRD1

Abstract

Many bacteria establish long-term populations on their hosts or within specific environments. One strategy for bacterial persistence is the formation of biofilms, bacterial aggregates embedded in a self-produced matrix. Compared to free-living cells, the cells living in the biofilm microenvironment may be exposed to smaller amounts of free iron, oxygen, and nutrients. In this study, we examined the transcriptional and genomic alterations associated with the phenotype changes in the beneficial root-colonizer P. chlororaphis 30-84. This work comprises a genome-wide evolutionary analysis of a phenotypic switching event in P. chlororaphis. Genes identified by genomic or transcriptomic approaches will provide novel insights to better understand genetic adaptations during biofilm formation.

Background and Research Objectives

Microbes survive under unfavorable conditions by undergoing a number of morphological and genetic changes. Consequently, natural populations often contain variants with beneficial mutations that contribute to the public good. However, due to technical limitation, the identity and mechanism of environment-induced mutations remains poorly understood. Genome sequencing allows us to sequence bacterial genomes and thus provide valuable information on genomic variation in response to environmental changes. The proposed research used the rhizosphere-colonizing bacterium Pseudomonas chlororaphis strain 30-84. The strain was first identified due to its ability to inhibit fungal pathogens and has become a model for a beneficial commensal bacterium. Strain 30-84 demonstrates phenotypic variations resulting from spontaneous mutations during rhizosphere colonization. These phenotypic variants (such as small colonies or pigment deficient mutants) are beneficial to the wild type population by increasing cell attachment, biofilm formation and thus biological control activity. The goal of this research was to identify signature genomic and transcriptomic changes in response to environmental signals and investigate how these changes benefit the wild type population.

Scientific Approach and Accomplishments

To identify mutational events during P.chlororaphis colonization, bacterial cells was grown in biofilm conditions. Small colony variants were identified by visual inspection of bacterial colonies on plates. 2. SCV genome was sequenced using next sequencing technology in Dr. Cliff Han's group. To identify beneficial mutations, resulted genome sequences were compared with published genome sequence in collaboration with Dr. Patrick Chain and Chien-chi Lo. A number of mutations were identified and experimentally verified to be responsible for phenotypical changes. The results provide us with a complete set of mutations that are involved in host association. 3. To study the role of these genomics changes in bacterial persistence, beneficial populations was compared with the wild type strain in their ability to produce fungal-inhibiting metabolites and form biofilms. The SCVs exhibited high resistance to antimicrobials and adherence ability. 4. Genomic mutations often lead to changes in gene expression. To understand the beneficial mutation at transcritpome level, RNA sequencing has been conducted to identify differentially expressed genes between wild type and beneficial mutant strains. We found that genes involved in iron uptake and stress responses were highly expressed. Together, these data give us a comprehensive understanding of cell differentiations in response to environmental signals. 5. The above analysis has identified candidate genes involved in successful disease control. This data has been published in the journal Applied Environmental Microbiology, which is the #1 cited journal in Microbiology.

Impact on National Missions

Our results have demonstrated that bacteria can adapt to adverse environmental conditions by altering their genome composition and global gene expression pattern. This project is a model on future analysis of micro-

bial evolution. This is particularly important for the study of clinical antibiotic-resistant bacteria e.g. how they alter their genomes and transcriptomes to overcome antibiotic killing. Deciphering the molecular diversity in vivo is a significant breakthrough in Microbiology and results in a comprehensive understanding of molecular process involved in bacterial adaptation. Knowing how bacteria couple environmental inputs with genomic changes is important in the development of disease management strategies.

Publications

Tao, Y., F. Wang, D. Jia, J. Li, Y. Zhang, C. Jia, D. Wang, and H. Pan. Cloning and functional analysis of the promoter of a stress-inducible gene (ZmRXO1) in maize. 2014. Plant Molecular Biology Reporter. : 1.

Wang, D., C. Han, A. Dichosa, C. D. Gleasner, S. Johnsons, H. E. Daligault, J. M. Yu, E. A. Pierson, and L. S. III Pierson. Draft genome sequence of Pseudomonas putida strain S610, a seedborne bacterium of wheat. 2013. Genome Announcement. 1 (6): e01048.

Wang, D., C. Han, A. Dichosa, C. D. Gleasner, S. Johnsons, H. E. Daligault, J. M. Yu, E. A. Pieson, and L. S. III Pieson. Draft genome sequence of Enterobacter cloacae strain S611 . 2014. Genome Announcement. 2 (6): 00710.

Wang, D., R. J. Dorosky, C. Han, C. H. Lo, A. Dichosa, P. Chain, J. M. Yu, L. S. III Pierson, and E. A. Pierson. Genomic adaptations of a small colony variant in the biofilm of Pseudomonas chlororaphis 30-84. 2015. Applied Environmental Microbiology. 81 (3): 890.

Exploring Doubly Parasitic Radioisotope Production Via Secondary Neutron Fluence From the 100 MeV IPF Irradiations

Eva R. Birnbaum
20130782PRD2

Abstract

The spallation neutron flux produced from the standard proton irradiation of rubidium chloride and gallium targets at the Los Alamos National Laboratory (LANL) Isotope Production Facility (IPF) was investigated as a tool for an innovative route for isotope production and materials science studies. Routine irradiations have been found to produce neutron fluxes as high as 1012 n cm-2 s-1, with approximately 50% of the total flux having energy in excess of 1 MeV. Experimental measurements of radionuclide production using this flux were compared with the predicted radionuclide yield using nuclear excitation functions from MCNPX event generators, evaluated nuclear data, and the TALYS nuclear code via a collaboration with computational nuclear data experts in XCP-3. Practical application of the secondary neutron flux in the realm of radioisotope production is considered, and has been explored experimentally for multiple productions undertaken by the Isotope Program in the past two years. Several small-scale production experiments have been successfully completed to produce tracer amounts of radionuclides from this unique neutron flux. Findings have further been used in support of a DOE Early Career Award proposal application aimed at the characterization of unstudied nuclear reactions using quasimonoenergetic neutron fluxes at multiple international facilities.

Background and Research Objectives

The 100 MeV Isotope Production Facility (IPF) at Los Alamos National Laboratory operates in conjunction with the Los Alamos Neutron Science Center (LANSCE), producing 82Sr, 68Ge, and other isotopes under the purview of the Isotope Production Program. A typical target stack for the large-scale production of 82Sr and 68Ge includes two targets of Inconel-encapsulated rubidium chloride powder and a third target of liquid gallium metal. The IPF's high proton beam current and lengthy irradiations produce a secondary neutron flux with a utilitarian scale that is beyond the reach of the many medical energy cyclotrons around the nation, and energetically distinct from reactor neutron fluences. The potential of this unique capability for research in novel methods of isotope production and materials science is unexploited. Several radioisotopes named in the Isotopes Subcommittee's recent report to the Nuclear Science Advisory Committee (NSAC) are potentially suitable for such neutron-based production. These radioisotopes are necessary to a variety of scientific and medical fields, and in many cases their future, uninterrupted supply is uncertain. This research project intended to establish new production routes for these important isotopes.

Scientific Approach and Accomplishments

Custom target assemblies were fabricated to isolate neutron activation samples from cooling water at the rear of the standard RbCl-RbCl-Ga IPF target stack. In this way, exposure of the foils to the neutron flux created from a typical production run at IPF was assured, changes to the proton targets' configuration (and hence on routine production deliverables) were avoided completely, and a geometry was established which could be utilized again for future irradiations and potentially for isotope production. Activation studies of multiple sample types were performed over a period of two years, with extensive comparison of experimental yields (quantified by gamma spectroscopy and radiochemisty) and theoretical predictions in collaboration with XCP-3 (Figure 1). The results of this work have been summarized in conference proceedings [1] and in Nuclear Instrumentation and Methods in Physics Research [2], and have also resulted in student presentations at a national meeting [3].

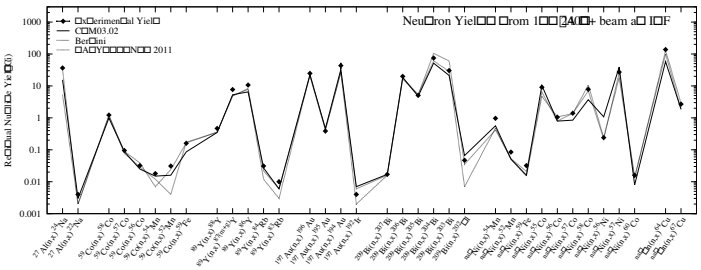

Figure 1. Experimental yields for isotopes generated in the IPF secondary neutron flux as compared to yields predicted by three different modeling programs.

Impact on National Missions

Characterization of the secondary neutron flux by a combination of experiment and theoretical prediction has already enabled the flux to be put to use producing small quantities of radionuclides needed for neutrino mass measurement efforts, developmental radiochemistries, and to collect preliminary data for multiple additional funding proposals. As a result of this work, the Isotope Program has at its disposal an accessible, cost-efficient, and parasitic means of radionuclide production. Accurate flux characterization has resulted in multiple expressions of interest from materials science and fusion energy communities, and before the end of the 2014 calendar year, first shipments of tracer radiolanthanides produced in the secondary neutron flux will be shipped from the Isotope Program at LANL to university collaborators. As a preliminary means to study the potential of spallation energy neutrons for radioisotope production, the secondary neutron flux at IPF has been responsible for the inception of multiple novel isotope production schemes for which funding support has been requested from DOE sponsors.

References

1. Engle, J. W., C. T. Kelsey, H. Bach, B. D. Ballard, M. E. Fassbender, K. D. John, E. R. Birnbaum, and F. M. Nortier. Preliminary investigation of parasitic radioisotope production using the LANL IPF secondary neutron flux. 2012. In 14th International Workshop on Targetry and Target Chemistry. (Cancun, Mexico, 26-29 Aug. 2012). Vol. 1, 1 Edition, p. 1. New York: American Institute of Physics.

2. Engle, J. W., M. R. James, S. G. Mashnik, C. T. Kelsey, L. E. Wolfsberg, D. A. Reass, M. A. Connors, H. T. Bach, M. E. Fassbender, K. D. John, E. R. Birnbaum, and F. M. Nortier. MCNPX characterization of the secondary neutron flux at the Los Alamos Isotope Production Facility. 2014. NUCLEAR INSTRUMENTS & METHODS IN PHYSICS RESEARCH SECTION A-ACCELERATORS SPECTROMETERS DETECTORS AND ASSOCIATED EQUIPMENT. 754: 71.

3. Delorme, K. A., J. W. Engle, F. M. Nortier, and B. R. Kowash. Production potential of Sc-47 using spallation neutrons at the Los Alamos Isotope Production Facility. Presented at Society of Nuclear Medicine and Molecular Imaging. (St. Louis, MO, 7-11 Aug. 2014).

Publications

Delorme, K. A., J. W. Engle, F. M. Nortier, E. R. Birnbaum, and B. R. Kowash. Production potential of Sc-47 using spallation neutrons at the Los Alamos Isotope Production Facility. Presented at Society of Nuclear Medicine and Molecular Imaging. (St. Louis, MO, 7-11 Aug. 2014).

Engle, J. W., C. T. Kelsey, Bach, B. D. Ballard, M. E. Fassbender, K. D. John, E. R. Birnbaum, and F. M. Nortier. Preliminary Investigation of Parasitic Radioisotope Production Using the LANL IPF Secondary Neutron Flux. 2012. 14TH INTERNATIONAL WORKSHOP ON TARGETRY AND TARGET CHEMISTRY. 1509: 171.

Engle, J. W., C. T. Kelsey, H. Bach, B. D. Ballard, M. E. Fassbender, K. D. John, E. R. Birnbaum, and F. M. Nortier. Preliminary investigation of parasitic radioisotope production using the LANL IPF secondary neutron flux. 2012. In 14th International Workshop on Targetry and Target Chemistry. (Cancun, Mexico, 26-29 Aug. 2012). Vol. 1, 1 Edition, p. 1. New York: American Institute of Physics.

Engle, J. W., E. R. Birnbaum, F. M. Nortier, J. A. Rau, K. D. John, and H. R. Trellue. Purification of (PU)-P-242 by irradiation with thermal neutrons. 2013. NUCLEAR INSTRUMENTS & METHODS IN PHYSICS RESEARCH SECTION B-BEAM INTERACTIONS WITH MATERIALS AND ATOMS. 298: 70.

Engle, J. W., E. R. Birnbaum, F. M. Nortier, J. A. Rau, K. D. John, and H. R. Trellue. Purification of (PU)-P-242 by irradiation with thermal neutrons. 2013. NUCLEAR INSTRUMENTS & METHODS IN PHYSICS RESEARCH SECTION B-BEAM INTERACTIONS WITH MATERIALS AND ATOMS. 298: 70.

Engle, J. W., E. R. Birnbaum, H. R. Trellue, K. D. John, M. W. Rabin, and F. M. Nortier. Evaluation of Ho-163 production options for neutrino mass measurements with microcalorimeter detectors. 2013. NUCLEAR INSTRUMENTS & METHODS IN PHYSICS RESEARCH SECTION B-BEAM INTERACTIONS WITH MATERIALS AND ATOMS. 311: 131.

Engle, J. W., E. R. Birnbaum, H. R. Trellue, K. D. John, M. W. Rabin, and F. M. Nortier. Evaluation of Ho-163 production options for neutrino mass measurements with microcalorimeter detectors. 2013. NUCLEAR INSTRUMENTS & METHODS IN PHYSICS RESEARCH SECTION B-BEAM INTERACTIONS WITH MATERIALS AND ATOMS.

311: 131.

Engle, J. W., J. W. Weidner, B. D. Ballard, M. E. Fassbender, L. A. Hudston, K. R. Jackman, D. E. Dry, L. E. Wolfsberg, L. J. Bitteker, J. L. Ullmann, M. S. Gulley, Pillai, Goff, E. R. Birnbaum, K. D. John, S. G. Mashnik, and F. M. Nortier. Ac, La, and Ce radioimpurities in Ac-225 produced in 40-200 MeV proton irradiations of thorium. 2014. RADIOCHIMICA ACTA. 102 (7): 569.

Engle, J. W., M. R. James, S. G. Mashnik, C. T. Kelsey, L. E. Wolfsberg, D. A. Reass, M. A. Connors, H. T. Bach, M. E. Fassbender, K. D. John, E. R. Birnbaum, and F. M. Nortier. MCNPX characterization of the secondary neutron flux at the Los Alamos Isotope Production Facility. 2014. NUCLEAR INSTRUMENTS & METHODS IN PHYSICS RESEARCH SECTION A-ACCELERATORS SPECTROMETERS DETECTORS AND ASSOCIATED EQUIPMENT. 754: 71.

Engle, J. W., S. G. Mashnik, Bach, Couture, Jackman, Gritzo, B. D. Ballard, Fassbender, D. M. Smith, L. J. Bitteker, J. L. Ullmann, M. S. Gulley, Pillai, K. D. John, E. R. Birnbaum, and F. M. Nortier. Cross sections from 800 MeV proton irradiation of terbium. 2012. NUCLEAR PHYSICS A. 893: 87.

Engle, J. W., S. G. Mashnik, J. W. Weidner, L. E. Wolfsberg, M. E. Fassbender, Jackman, Couture, L. J. Bitteker, J. L. Ullmann, M. S. Gulley, Pillai, K. D. John, E. R. Birnbaum, and F. M. Nortier. Cross sections from proton irradiation of thorium at 800 MeV. 2013. PHYSICAL REVIEW C. 88 (1).

Engle, J. W., S. G. Mashnik, J. W. Weidner, L. E. Wolfsberg, M. E. Fassbender, K. Jackman, A. Couture, L. J. Bitteker, J. L. Ullmann, M. S. Gulley, C. Pillai, K. D. John, E. R. Birnbaum, and F. M. Nortier. Cross sections from proton irradiation of thorium at 800 MeV. 2013. PHYSICAL REVIEW C. 88 (1): -.

Fassbender, M. E., Ballard, E. R. Birnbaum, J. W. Engle, K. D. John, J. R. Maassen, F. M. Nortier, J. W. Lenz, C. S. Cutler, A. R. Ketring, S. S. Jurisson, and D. S. Wilbur. Proton irradiation parameters and chemical separation procedure for the bulk production of high-specific-activity Re-186g using WO3 targets. 2013. RADIOCHIMICA ACTA. 101 (5): 339.

Gott, M. D., B. D. Ballard, L. N. Redman, J. R. Maassen, W. A. Taylor, J. W. Engle, F. M. Nortier, E. R. Birnbaum, K. D. John, D. S. Wilbur, C. S. Cutler, A. R. Ketring, S. S. Jurisson, and M. E. Fassbender. Radiochemical Study of Re/W Adsorption Behavior on a Strongly Basic Anion Exchange Resin. 2014. RADIOCHIMICA ACTA. 102 (4): 325.

Jackman, K. R., J. W. Engle, F. M. Nortier, K. D. John, E. R. Birnbaum, and D. E. Norman. Synthetic spectra for radioactive strontium production QA/QC. 2014. JOURNAL OF RADIOANALYTICAL AND NUCLEAR CHEMISTRY. 302 (1): 347.

Medvedev, D. G., J. W. Engle, F. M. Nortier, S. V. Smith, and L. F. Mausner. Theoretical approach to the production of Ti-44 (T-1/2=59.1 years) using high energy protons: Expanding Sc-44 availability. 2013. ABSTRACTS OF PAPERS OF THE AMERICAN CHEMICAL SOCIETY. 245.

Hybrid Nanostructures for Photoreduction of CO_2 to Hydrocarbons

Hongwu Xu
20130787PRD2

Abstract

High-quality ZnTe/CdS core/shell nanorods and ZnTe/CdS-Pt hybrid nanostructures have been successfully synthesized and characterized. The growth of CdS shell on ZnTe core forms a type-II alignment in terms of the relative conduction/valence band edge of the core/shell. This also significantly enhances the stability of ZnTe nanorod cores, while maintaining their long charge carrier lifetimes, ultrafast charge separation dynamics, and extended absorption spectra. Our results support the potentiality of utilizing ZnTe-based hybrid nanomaterials for photocatalysis and solar energy conversion applications including CO2 photoreduction.

Background and Research Objectives

Photocatalytic conversion of CO2 into fuels or useful chemicals is a promising approach to both reducing atmospheric CO2 level and fulfilling the increasing energy demands for hydrocarbon-based fuels. Although extensive efforts have been made on development of semiconductor-based nanomaterials for solar-to-fuel conversion, the efficiencies achieved so far are too low for practical applications [1]. Previous studies suggest that single-electron reduction of CO2 is thermodynamically unfavorable. While the proton-coupled, multiple-electron reduction is more favorable, it is a multi-step process requiring transfer of multiple electrons, which is kinetically hindered. For example, conversion of CO2 to CH4 needs four steps involving transfer of eight electrons, which leads to high-overpotential reduction of CO2 to hydrocarbons and alcohols. There are also other factors that limit photocatalytic efficiencies, including inefficient absorption of solar energy, fast recombination of photo-excited electron-hole pairs, and backward redox reactions. A major challenge lies in the fact that the performance of energy materials/systems depends on their multiple properties, such as redox activity, light absorption, mechanical property and stability. However, it is difficult to find simple, single-phase materials that satisfy all the criteria [2].

To develop efficient photocatalytic systems for conversion of CO2 into fuels, three major challenges need to be addressed: 1) absorption of the visible part of the solar spectrum, 2) design of structures that facilitate transfer processes of multiple electrons and hydrogen atom with sufficient energy for reduction of CO2 and oxidation of H2O, and 3) design of structures that promote adsorption of CO2 and water close to the source where the photo-generated electrons and holes are formed. The objectives of this project are to design, synthesize and characterize multi-component, composite nanostructures, particularly core/shell structures, with controlled nanoparticle size, shape and composition, allowing exploration of their potential photocatalytic applications including CO2 reduction.

Scientific Approach and Accomplishments

As a critical step towards photoreduction of CO2 to hydrocarbons, we design/synthesize hybrid nanostructures of photoactive materials that have both effectively separated charges and catalytic sites for chemical conversion. Semiconductor core/shell nanostructures are used for initial photo-induced charge separation, while the metallic components provide catalytic sites for subsequent chemical conversion. Compared to many other semiconductors, ZnTe has a more negative conduction band (-1.9 V) while still having a suitable band gap for visible light absorption. Thus ZnTe has a larger driving force for electron transfer, which may facilitate photoreduction of CO2 [3]. However, ZnTe nanoparticles, while stable under reducing conditions, often undergo light-induced anodic oxidation in aqueous solutions. Hence, coating their surfaces with shells of a more stable phase, e.g. CdS, is a plausible approach to protecting ZnTe nanoparticles from dissolution during the charge separation process. Moreover, these core/shell nanostructures can facilitate charge separation by forming a barrier to control back electron transfer. Adding a co-catalyst, such Pt to the ZnTe/CdS core/shell, can further help accumulate the photo-induced electrons and facilitate CO2 conversion.

ZnTe nanorods were synthesized using an organic-solution method [4]. In a typical synthesis, first, 0.13 g of zinc acetate was mixed with 10 mL of octadecene and 2 mL of oleic acid in a 50 mL three-neck flask. The mixture was heated to 200 °C under a N2 gas flow through a Schlenk-line, forming a clear Zn-containing solution. The temperature was then decreased to 160 °C by cooling the flask. Second, a Te precursor was prepared by mixing Te-trioctylphosphine (1M for Te) solution (0.5 mL), 0.7 M superhydride solution (0.7 mL) and 2 mL of oleylamine in a vial in a glovebox. Third, this precursor was transferred into a 10 mL plastic syringe and was directly injected into the Zn solution. Then the temperature was increased to 300 °C with a rate of about 10 °C/min. The resulting product was separated by adding 10-20 mL of ethanol followed by centrifugation. The isolated nanorods were re-dispersed in 10 mL of hexane, producing ZnTe colloidal suspensions. Figure 1A is a representative transmission electron microscope (TEM) image of the sample, showing uniform nanorod morphology.

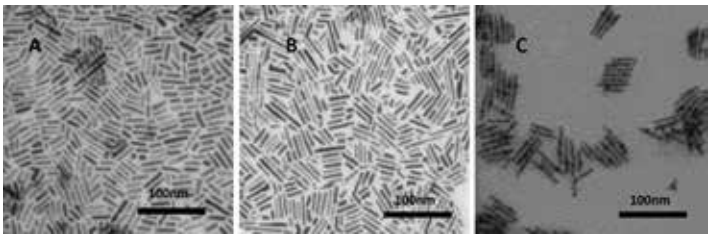

Figure 1. TEM images of (A) ZnTe nanorods, (B) ZnTe/CdS core/shell nanorods and (C) ZnTe/CdS-Pt hybrid nanostructures.

ZnTe/CdS core/shell nanorods were synthesized via successive growth of CdS on ZnTe nanorods. In a typical synthesis, 5 mL of ZnTe nanorod colloidal solution, 10 mL of octadecene, 0.5 mL of sulfur-oleylamine (1M) and 0.2 mL of trioctylphosphine were mixed in a flask attached to the Schlenk-line and slowly heated to 170 °C under an Ar gas flow. 1 mL of Cd precursor solution (0.1 M) was added dropwise into the flask during a period of 10 min. The reaction system was kept at 170 °C for an additional 10 min allowing for CdS shell growth. The product was separated by using the same procedure as for bare ZnTe nanorods and was re-dissolved in 10 mL hexane or chloroform. TEM imaging of ZnTe/CdS core/shell nanorods reveals that after CdS coating, ZnTe cores maintain their original rod-like morphology (Fig. 1B). Because of the small lattice mismatch between ZnTe and CdS (about 4.4%), the growth of CdS overlayer on ZnTe is considered to be epitaxial; high-resolution TEM image (Fig. 2A) of ZnTe/CdS core/shell [see powder X-ray diffraction (XRD) pattern in Fig. 2B] does not reveal noticeable interfaces between ZnTe and CdS. With the addition of CdS shells, the stability of ZnTe was found to be dramatically enhanced relative to that of bare ZnTe nanorods, with a shelf life of at least several months. The ultraviolet-visible (UV-vis) absorption spectra of ZnTe/CdSe nanorods and the corresponding ZnTe seeds are shown in Figure 3. The bare ZnTe nanorods exhibit the first exciton absorption peak at 500 nm. By contrast, ZnTe/CdSe core/shell rods have the corresponding absorption peak at 600 nm. This red shift is consistent with the occurrence of CdS shell on ZnTe core, which form a type-II nanostructure.

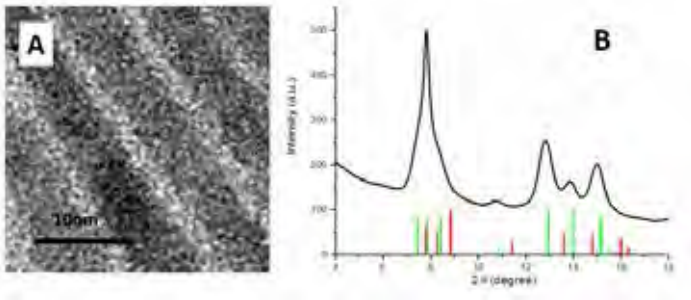

Figure 2. (A) HRTEM and (B) powder XRD pattern of ZnTe/CdS core/shell nanorods. Green and red lines denote the reflections of wurzite ZnTe and CdS, respectively.

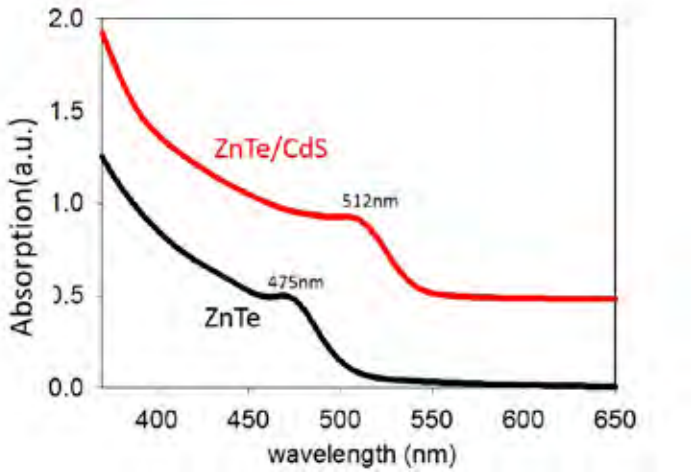

Figure 3. UV-vis absorption spectra of ZnTe nanorods and ZnTe/CdS core/shell nanorods.

Transient absorption (TA) spectra of ZnTe/CdSe quantum dots (QDs) at different delay times after excitation at 400 nm are shown in Figure 4A, and their energy level diagram is shown in Figure 4B. There are three possible electronic transitions: T1, T2 and T3 (Fig. 4B), which are responsible for absorption bands 1, 2 and 3 (Fig. 4A), respectively. T1 is the transition from the lowest energy valence-band (VB) 1sh level in ZnTe to a delocalized conduction-band (CB) electron level in ZnTe. T2 is the spatially indirect transition from the VB 1sh level in ZnTe to the lowest energy CB 1se level in CdS. T3 is the transition from the lowest energy delocalized VB hole level to the CB 1se level in CdS. The correlation among the kinetics at T1, T2 and T3 transitions indicates the presence of an internal charge separation process from the ZnTe core to the CdSe shell. The TA

results indicate attractive properties of ZnTe/CdS core/shell nanorods. First, the ZnTe/CdS nanorods maintain the advantageous properties of the type-II nanostructures. They have a longer charge carrier lifetime compared with that of bare ZnTe nanorods, ultrafast charge separation dynamics, and red-extended absorption spectra. Second, the ZnTe/CdS nanorods have a higher reductive potential compared to other type II heterostructures, making a promising photocatalytic system for reduction of CO2 under photo-illumination.

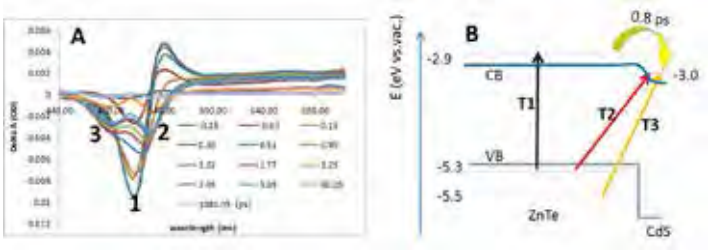

Figure 4. (A) TA spectra of ZnTe/CdS core/shell nanorods at different delay times after 400 nm excitation. B) The energy level diagram of ZnTe/CdS core/shell nanorods. The arrows indicate three possible electronic transitions (T1, T2 and T3). CB - conduction band; VB - valence band.

Previous studies have demonstrated that adding a metal tip to semiconductor nanocrystals will enhance charge separation and transfer properties at metal-semiconductor interfaces. In addition, the metal tip may also serve as a catalytic site for photoreactions. To enhance the photo-induced charge separation and transfer properties of ZnTe/CdS nanorods, we synthesized Pt decorated ZnTe/CdS nanorods following a previously developed method [5]. A typical reaction is as follows: 0.015 g of Pt acetylacetonate was added to 5 mL of dichlorobenzene along with 0.5 mL of oleylamine, 0.5 mL of oleic acid and 20 mg of 1,2-hexadecanediol. The mixture was heated at 70 °C for 10 min under an Ar flow, forming a Pt precursor solution. The freshly prepared Pt precursor was introduced into ZnTe/CdS nanorods colloidal solution in diphenyl ether (10 mL) that was pre-heated to 200 °C. After several minutes, the reaction was stopped by removal of the heat. The product was separated by adding excessive ethanol followed by centrifugation. TEM image shows that almost all ZnTe/CdS nanorods have been decorated with Pt nanoparticles (Fig. 1C).

In addition to the ZnTe/CdS core/shell nanoparticles, we investigated the stability of CdSe/ZnSe core/shell QDs at high pressures up to 10.7 GPa using in-situ synchrotron XRD coupled with diamond-anvil-cell (DAC) technique. Core/thick-shell giant quantum dots (gQDs) possessing type II electronic structures exhibit suppressed blinking and diminished nonradiative Auger recombination. Our results demonstrate that the CdSe core and ZnSe shell behave independently under high pressure, despite that stresses may exist at the interface due to the CdSe/ZnSe lattice mismatch. Namely, consistent with precious studies [6], the wurtzite CdSe core transforms to the rock salt structure above about 5.6 GPa and then to the zincblende structure upon decompression to ambient condition (Fig. 5). As expected for ZnSe, which has a phase transition at about 13 GPa [7], the shell is unaffected by our experiment (10.7 GPa). This post-synthesis integrity of core/shell CdSe/ZnSe further supports our hypothesis that surface-related processes during shelling are key to effecting shell vs. alloy formation [8].

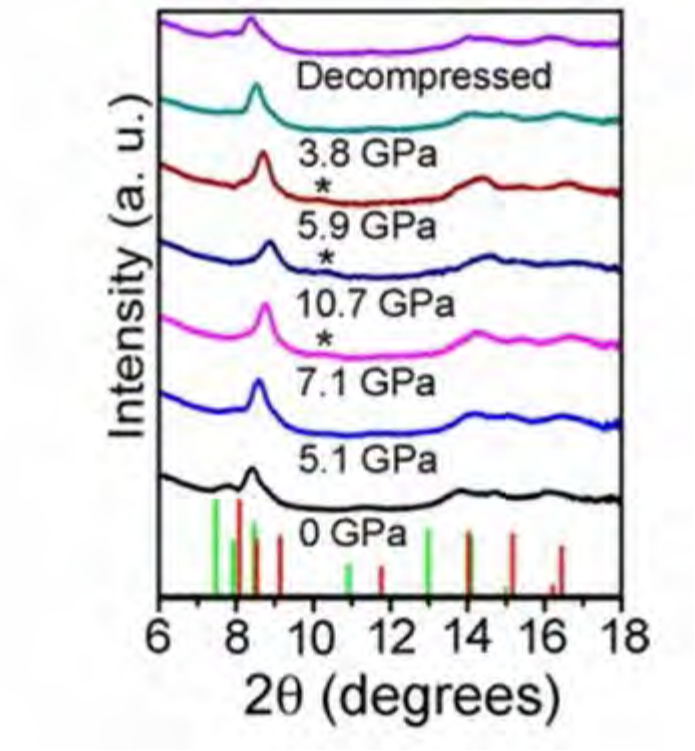

Figure 5. XRD patterns of CdSe/ZnSe core/shell quantum dots under different pressures. Rock salt (200) reflection indicated by asterisk. CdSe and ZnSe wurtzite reference patterns are green and red, respectively.

Impact on National Missions

Through controllable synthesis and systematic characterization of core/shell nanomaterials, we have shown potential utilization of these materials for practical applications including efficient photocatalytic conversion of CO2 plus H2O into hydrocarbon fuels and chemicals. The results will lay the foundation for the ultimate development of solar-to-fuel conversion devices and have broad implications for rational design of functional nanomaterials.

References

1. Roy, S. C., O. K. Varghese, Paulose, and C. A. Grimes. Toward Solar Fuels: Photocatalytic Conversion of Carbon Dioxide to Hydrocarbons. 2010. ACS NANO. 4 (3): 1259.

2. Amirav, , and A. P. Alivisatos. Photocatalytic Hydrogen Production with Tunable Nanorod Heterostructures. 2010. JOURNAL OF PHYSICAL CHEMISTRY LETTERS. 1 (7): 1051.

3. Jin, , J. u. n. Zhang, R. D. Schaller, Rajh, and G. P. Wiederrecht. Ultrafast Charge Separation from Highly Reductive ZnTe/CdSe Type II Quantum Dots. 2012. JOURNAL OF PHYSICAL CHEMISTRY LETTERS. 3 (15): 2052.

4. Zhang, J., S. Jin, H. C. Fry, S. Peng, E. Shevchenko, G. P. Wiederrecht, and T. Rajh. Synthesis and Characterization of Wurtzite ZnTe Nanorods with Controllable Aspect Ratios. 2011. JOURNAL OF THE AMERICAN CHEMICAL SOCIETY. 133 (39): 15324.

5. Habas, S. E., Yang, and Mokari. Selective growth of metal and binary metal tips on CdS nanorods. 2008. JOURNAL OF THE AMERICAN CHEMICAL SOCIETY. 130 (11): 3294.

6. Alivisatos, A. P.. Perspectives on the physical chemistry of semiconductor nanocrystals. 1996. JOURNAL OF PHYSICAL CHEMISTRY. 100 (31): 13226.

7. KOFFERLEIN, M., H. KARZEL, W. POTZEL, W. SCHIESSL, M. STEINER, G. M. KALVIUS, D. W. MITCHELL, and T. P. DAS. HIGH-PRESSURE PHASE-TRANSITION IN ZNSE. 1994. HYPERFINE INTERACTIONS. 93 (1-4): 1505.

8. Acharya, K. P., H. M. Nguyen , M. Paulite , A. Piryatinski, J. Zhang, J. L. Casson , H. Xu, H. Htoon, and J. A. Hollingsworth. Elucidation of two giants: challenges to thick-shell synthesis in CdSe/ZnSe and ZnSe/CdS core/shell quantum dots . 2015. Journal of the American Chemical Society. : DOI: 10.1021/jacs.5b00313.

Publications

Acharya, K. P., H. M. Nguyen , M. Paulite , A. Piryatinski, J. Zhang, J. L. Casson , H. Xu, H. Htoon, and J. A. Hollingsworth. Elucidation of two giants: challenges to thick-shell synthesis in CdSe/ZnSe and ZnSe/CdS core/shell quantum dots . 2015. Journal of the American Chemical Society. : DOI: 10.1021/jacs.5b00313.

Joint Inversions of Seismic and Gravity Data in Volcanic Areas to Advance Hazards Assessment: A Focus on the Alaskan Subduction Zone and Kilauea, Hawaii

Monica Maceira
20130807PRD3

Abstract

Alaska and Hawaii present significant seismic and volcanic hazards to the U.S. By studying the causes of these hazards and the environments in which they occur, we can work toward better characterizing the hazards they present. Three-dimensional passive-source seismic velocity tomography is a powerful imaging technique that utilizes seismic waves produced by earthquakes to image complex subsurface structures, such as subducting slabs or magma distributions beneath volcanoes. The resolutions of these studies are generally limited by the natural distribution of earthquakes. Gravity data, however, provide alternate sources of information regarding subsurface structures, and are available at a variety of scales. Due to the inherent relationship between density and seismic velocity, gravity and seismic data can be jointly inverted, leading to the characterization of Earth structures that is not limited by the distributions of seismicity. Joint inversion also places stronger constraints on the temperature, compositional, fluid, and magmatic distributions.

Background and Research Objectives

The Alaskan subduction zone provides an ideal location to explore the geophysical expressions of volcanism, including regions of elevated temperature, fluid content, and melting in the earth's mantle and crust. The current distribution of seismic stations is focused near the relatively two-dimensional volcanic arc located above the subducting oceanic plate, limiting the ability to resolve these anomalies. The inclusion of gravity data in a joint inversion will markedly increase the ability to resolve these features in three dimensions. In this study we addressed questions regarding the sources of volcanism such as 1) How are anomalies associated with magma genesis spatially related to volcanic centers? 2) Can the cause(s) of these anomalies be independently constrained?

Kilauea Volcano, Hawaii, presents a unique opportunity to study one of Earth's most active volcanoes, in a location that has produced historical M>7 tsunamigenic earthquakes. While previous seismic studies have focused on studying the near-surface beneath the summit caldera, portions of Kilauea's rift zones, or the seismically active tsunamigenic decollement fault beneath the volcanic material and the underlying oceanic crust, the extents of these studies are limited by the natural seismic distributions. By combining gravity and seismic data, we can address questions such as 1) What volume of magma is stored beneath the summit and rift zones, and has the potential to erupt? 2) Can the aseismic and seismic portions of the decollement be imaged, constraining the maximum magnitude of earthquake this fault can produce? 3) How does neighboring Mauna Loa Volcano contribute to the structure of Kilauea?

Scientific Approach and Accomplishments

During her Director's Postdoctoral Fellowship, Ellen focused on studying Akutan and Makushin volcanoes in Alaska, the Colombian subduction zone (as a new dataset became available), and Kilauea Volcano. Her work focused in two areas: 1) algorithm and methodology improvement and 2) better understanding of the tectonics of these regions.

Algorithm improvements include the extension of the inversion method to Cartesian (as opposed to geographic) coordinates; the addition of multiple optional types of regularization and smoothing; altering how gravity partial derivatives are treated; reducing the computational time; and the inclusion of topography and its effects on gravity predictions. Outside of the algorithm itself, Ellen developed an objective method of determining the optimal combination of regularization parameters and relative weights for different datasets. Several of these improvements are particularly important for applications to more local-scale problems, which is a relatively new direction for this joint-inversion algorithm.

In her work with Akutan and Makushin Volcanoes, Ellen used body and surface waves to develop a 3D P-wave and S-wave velocity model for the two volcanoes and improve earthquake locations. The body wave measurements and continuous seismic data are from the Alaska Volcano Observatory, and she developed the surface wave dataset from ambient noise analysis of the continuous seismic data. The combined analysis of the velocity structure at each volcano and the distributions of seismicity have provided insight to near-surface faulting, magma pathways to the surface, and regions of the long-term storage of magma. In comparison to other nearby volcanoes, this work demonstrates the breadth of magmatic structures at different volcanoes, even those that share many similarities. This work was published in March 2015 in the Journal of Geophysical Research, and it has been presented at several meetings.

Her work on Colombia demonstrates for the first time the benefits of including gravity data in a joint inversion with body waves and surface waves. Using data from the national Colombian seismic network, Ellen refined the body wave dataset and measured surface waves from local earthquakes. Gravity data are from a global satellite-based model and constrain velocities (via densities) in the shallow subsurface. The structure of the Colombian subduction zone has been a longstanding topic of debate, with several proposed models. The results of her study provide evidence for a tear in the subducting tectonic plate in central Colombia, with a boundary between two neighboring plates at the Bucaramanga nest, a small region of some of the most intense seismicity globally. Ellen is currently finishing up a manuscript of this work for submission to the journal Geochemistry Geophysics Geosystems in the next month or so. She has also presented this work at several national and international meetings.

Ellen's work at Kilauea Volcano builds upon her previous research in the area. Here, the joint inversion of body wave, surface wave, and gravity data is complicated by the significant topography in the area and its effects on gravity at the local scale. She worked to better understand the magma plumbing system of the volcano, particularly how deeper magma reservoirs are connected to eruptions at the surface at the summit caldera and Southwest and East Rift Zones. This volcano poses both eruptive and tsunami hazards to the area.

Starting this last 2015 summer, Ellen also began applying the joint inversion technique to Iran, in order to begin her transition from a Director's Postdoc to a programmatic postdoc. This region is of interest both tectonically and for global security, and working on a velocity model for the region will allow her to validate the predictions of the technique through comparison with independent constraints on earthquake locations, as well as to collaborate more closely with several members of the ground-based nuclear explosion monitoring team in EES-17.

Ellen has also been working with a fellow postdoc (now staff member) at the Lab in his work to further improve computational and regularization aspects of joint inversions, specifically to improve the recovery of sharp structural boundaries, which tend to be smoothed out in most inversions. This work has been published in Geophysical Journal International. She has also worked with two summer students, one with using body-wave seismic data from Bhutan (summer 2014) and one with using surface-wave seismic data from Antarctica (summer 2015).

Outside of her own research, Ellen has participated in several activities at the Lab and in the geosciences community. In October 2015, she will give an invited talk at the GeoPRISMS Theoretical and Experimental Institute for the Subduction Cycles & Deformation Meeting on her work at Akutan and Makushin Volcanoes. In September 2014, she had an invited webinar for the Incorporated Research Institutions for Seismology on seismic and geodynamic constraints on subduction zone structure and volcanism. In April 2014, she gave a similar invited colloquium talk at the University of Minnesota. Ellen convened a session with two external collaborators at the American Geophysical Union 2013 Fall Meeting, entitled 'Geophysical Observations and Models of Subduction', and she chaired a session at the 2014 Fall Meeting. Ellen has reviewed proposals for the National Science Foundation, as well as manuscripts for Nature Geoscience, Geology, Journal of Geophysical Research, and Geochemistry Geophysics Geosystems. In March 2014, she participated in a discussion panel at the Lab as a part of Women's History Month, and she has been the postdoc representative to the EES Worker Safety and Security Team since summer 2014.

Impact on National Missions

The research discussed under this project will enhance the capability of the Laboratory through unique expertise in imaging Earth structure. This expertise has applications to Nonproliferation R&D under Nuclear Nonproliferation, where accurate Earth models are needed to locate, identify and determine yield for seismic events of interest such as underground nuclear explosions. The relationship to assessing hazards in volcanic zones could be of interest to DHS/FEMA as they are responsible for domestic preparedness and response regarding, among other things, natural disasters, and perhaps to the Department of the Interior's USGS. High-resolution Earth models are also required for characterization and monitoring within several other

areas of LANL mission space including geothermal energy development (Applied Energy Programs Office) carbon sequestration (Fossil Energy, within the Office of Science Programs), and used fuel disposition and salt repository science (both within the office of Civilian Nuclear Programs), as well as the new DOE initiative SubTER in which LANL – and in particular EES-17 – is participating.

Publications

Holt, R. A., M. K. Savage , J. Townend , E. M. Syracuse , and C. H. Thurber . Crustal stress and fault strength in the Canterbury Plains, New Zealand. Presented at American Geophysical Union Fall Meeting. (San Francisco , 9-13 Dec. 2013).

Holt, R. A., M. K. Savage, Townend, E. M. Syracuse, and C. H. Thurber. Crustal stress and fault strength in the Canterbury Plains, New Zealand. 2013. EARTH AND PLANETARY SCIENCE LETTERS. 383: 173.

Lemon, S., C. H. Thurber, M. M. Haney, E. Syracuse, H. Zhang , X. Zeng , and S. G. Prejean. Ambient noise tomography of the Katmai Volcanic Complex, Alaska. Presented at Seismological Society of America Annual Meeting . (Anchorage, 30 April - 2 May, 2014).

Lin, Y., E. Syracuse, M. Maceira, C. Larmat, and H. Zhang. Joint inversion for Kilauea volcano with an edge-preserving constraint. 2014. In Seismological Society of America Annual Meeting. (Anchorage, 29 April - 2 May, 2014). Vol. 85, p. 502. El Cerrito: BSSA.

Lin, Y., E. Syracuse, M. Maceira, H. Zhang, and C. Larmat. Double-difference travel-time tomography with edge-preserving regularization and a priori interfaces. 2015. Geophysical Journal International. 201: 574.

Segall, , A. L. Llenos, S. -. Yun, A. M. Bradley, and E. M. Syracuse. Time-dependent dike propagation from joint inversion of seismicity and deformation data. 2013. JOURNAL OF GEOPHYSICAL RESEARCH-SOLID EARTH. 118 (11): 5785.

Syracuse, E. M., J. D. Pesicek, H. Zhang , and C. H. Thurber . Exploring the connection between intermediate-depth seismicity, slab hydration, and dehydration. Presented at American Geophysical Union Fall Meeting. (San Francisco, 9-13 Dec., 2013).

Syracuse, E. M., M. Maceira , H. Zhang , C. Larmat, C. Ammon, and C. Chai. Advanced Multivariate Inversion Techniques. Invited presentation at Review of Monitoring Research. (Albuquerque, 17-19 June, 2014).

Syracuse, E. M., M. Maceira , G. A. Prieto , H. Zhang , and C. J. Ammon . Joint inversion of seismic and gravity data for velocity structure and hypocentral locations of the Colombian subduction zone. Presented at American Geophysical Union Fall Meeting. (San Francisco, 15-19 Dec., 2014).

Syracuse, E. M., M. Maceira , G. A. Prieto , H. Zhang, and C. J. Ammon . Joint inversion of seismic and gravity data for velocity structure and hypocentral locations of the Colombian subduction zone. Presented at Seismological Society of America Annual Meeting. (Pasadena, 21-23 April, 2015).

Syracuse, E. M., M. Maceira , E. Bergman , W. S. Phillips, M. Begnaud , and H. Zhang. Velocity structure of the Iran region using seismic and gravity observations. Invited presentation at Comprehensive Test Ban Treaty: Science and Technology 2015 Conference. (Vienna, Austria, 22-26 June, 2015).

Syracuse, E. M., M. Maceira, G. A. Prieto , H. Zhang, and C. J. Ammon . Joint inversion of seismic and gravity data for velocity structure and hypocentral locations of the Colombian subduction zone. Presented at International Union of Geodesy and Geophysics General Assembly. (Prague, Czech Republic, 22 June - 2 July, 2015).

Syracuse, E. M., M. Maceira, G. A. Prieto, H. Zhang, and C. J. Ammon. Multiple plates subducting beneath Colombia: Results of the joint inversion of seismic and gravity data. Geochemistry Geophysics Geosystems.

Syracuse, E., M. Maceira, H. Zhang, and C. Thurber. Seismicity and structure of Akutan and Makushin Volcanoes, Alaska, using joint body- and surface-wave tomography. 2015. Journal of Geophysical Research. 120 (2): 1036.

Syracuse, E., M. Maceira, and H. Zhang. Joint inversion of seismic and gravity data for velocity structure and hypocentral locations at Akutan and Makushin volcanoes. 2014. In Seismological Society of America Annual Meeting. (Anchorage, 30 April - 2 May, 2014). Vol. 85, p. 500. El Cerrito, California: BSSA.

Discovery of Novel Bioactive Natural Products

Alexander Koglin
20130815PRD4

Abstract

Natural evolution designed highly efficient enzymatic systems with an incredible and often enough not reproducible chemical diversity. Secondary metabolites, natural products with bioactive properties, represent the class of compounds with the highest diversity in their chemical structures, functional groups and properties. This class contains often heavily alternated non-ribosomal peptides; ketides or acyl-derived small molecules and combinations thereof. The diverse biological functions include the vast majority of antibacterial, antifungal, antiviral, anti-cancer, immunosuppressant, analgesic, signal transducing, energy-storage compounds and toxins. A variety of tailoring enzymes associated with the biosynthetic assembly lines define the chemical structure of all products and can tremendously modify these step-by-step synthesized molecules.

As DNA sequences encode ribosomal peptides and resulting protein functions, the order and assembly of enzymes in biosynthetic clusters responsible for secondary metabolite synthesis define the chemical structure of secondary metabolites. We investigate the genetic encoding and organization of enzymatic functions in newly discovered assembly lines to predict the chemical composition of those natural products. We will isolate those compounds and characterize their bioactivity for the development of drug candidates that are urgently needed to counter emerging threats to public health caused by bacteria, viruses, fungi and human cell altering events.

This project is focused on the prediction, identification and characterization of a series of novel secondary metabolites. Cultures of strains listed below have been established in the laboratory to isolate some of these predicted natural products. These strains include: Streptosporangium roseum, Myxococcus xanthus, Chlamidomonas acidophila, Herpetosiphon aurantiacus, Clostridium thermocellum and Desulvovibrio aerotolerans.

All enzymes that are predicted to be in involved in the biosynthesis of these novel natural products have been cloned into E. coli expression systems. Among those novel compounds are two completely new siderophores. Siderophores are metal, in this case primarily iron, ion chelators produced for bacterial iron homeostasis and it has been also demonstrated that siderophores are virulence markers of pathogenic strains and can contribute to the path and severity of infections.

Background and Research Objectives

In this project, available genomic DNA data of soil and marine bacteria will be exploited in a multidisciplinary approach to allow fast natural product discovery and characterization. The research employs five key steps.

Genome Analysis

Bioinformatics analysis of genomes of selected bacteria (e.g. Myxococcus xanthus and Streptosporangium roseum) will identify natural product biosynthetic machineries and predict product building blocks (e.g. amino acids, sugars).

Isolation of Predicted Natural Products

The bacterial strains will be cultivated, isotopically enriched (e.g. 13C, 15N, 1H or 3H, 14C) by feeding labeled substrates, and the natural products extracted from the culture. Incorporated isotopes will readily identify proposed compounds by NMR and high-res mass spec (MS) for stable isotopes, or by β- or γ-detection for radioactive isotopes, after chromatographic separation. The availability of high-field NMR and excellent MS resources will uniquely enable the project at LANL.

Structure Elucidation

Once separation from the culture is achieved, large scale culturing without labels will follow. NMR, elemental analysis, high-res MS, and x-ray SAS will be applied to elucidate structures of newly identified compounds.

Validation of the Biosynthetic Machinery
Isolated genes of putative clusters will be transformed into E. coli strains, expressed and biochemically characterized in vitro to validate the underlying biosynthesis of newly isolated compounds. Also, the entire biosynthetic cluster can be cloned into an overproduction bacterial strain, where high expression of the biosynthetic machinery will make the natural product a major component of the cells. In case the transgenic natural products are toxic for E. coli, a cell-free translation/transcription system is available and will be employed.

Bioactivity Studies
The bioactivity of newly isolated natural products and their potency will then be evaluated in vitro by incubation with either bacterial, fungal, human cell lines or viral systems. This will give insights into the natural product's properties and potency.

Meeting the great demand for novel bioactive agents requires improved discovery processes of bioactive compounds. It is clear that microbes continue as a major source of new drug leads. With short evolutionary cycles and natural pressure to protect their biological niches, soil and marine microbes are prime targets for identification of novel compounds. This project couples advances in DNA sequencing and bioinformatics with biochemical and labeling techniques, structure elucidation methods and advanced knowledge in natural product biosynthesis. High level expertise in these areas, combined with Stable Isotope Resource, give LANL potential to be an outstanding contributor to this field. This strategy will give further insights into nature's way to produce bioactive compounds, significantly shorten the time span for natural product discovery, and consequently speed up and reduce costs for drug development. It will guide future developments of accurate prediction of natural product structures exclusively based on genomic DNA information. This supports the mission of Bioscience Division in biosecurity and LANL's mission in threat reduction and global security.

Scientific Approach and Accomplishments
For the bioinformatic part of the project, it was proposed to identify at least 10 new gene clusters encoding for biosynthetic machineries for natural product production. Instead, we used a more sophisticated approach by systematically analyzing all available microbial genomes deposited in the NCBI database. The analysis was carried out using Perl-scripts developed by Alex Koglin and was compared to an adapted and heavily modified stand-alone version of the publically available bioinformatic tool, AntiSMASH1. Within the analyzed 2,773 genomes of bacterial strains, more than 19,000 of these gene clusters were found. From this vast amount of available strains, five were chosen (Myxococcus xanthus DK 1622, Corallococcus coralloides DSM 2259, Streptosporangium roseum DSM 43021, Catenulispora acidiphila DSM 44928, Herpetosiphon aurantiacus DSM 785) in which the biosynthetic clusters are unusual, i.e. not following the classical linear, multimodular organization2. This approach significantly reduces the probability of isolating compounds similar to known or identified natural products. Within these five strains a total of 124 gene clusters have been identified. Bioinformatics analysis revealed that 25 of these clusters showed unusual organization and hence are likely to yield poteniallt novel bioactive natural products. Subsequently, these clusters were analyzed in-depth using additional bioinformatic tools, such as pfam3, nrpspredictor24 and 2metdb5 to facilitate structure and building block prediction of the natural products.

The practical goals were to establish growth of five different bacterial strains and the isolation as well as structural characterization of three novel natural products produced by these strains, facilitated by feeding isotopically enriched, predicted building blocks. To meet these goals, the five above mentioned strains were successfully cultured under laboratory conditions. In addition to the bioinformatics prediction of the amino acid building blocks, it is important to biochemically correlate the identified gene clusters to the 25 predicted natural products by cloning and expression of the amino acid building block activation enzymes. This gives valuable insights into natural product assembly mechanisms and allows estimation of how the predictions match the actual substrate building blocks. In total 197 genes and gene fragments within the 25 clusters were annotated to be involved in building block (amino acid) activation. The 92 essential of these genes have been successfully cloned and the generated expression plasmids were used to transform E. coli BL21 (DE3*) cells to yield expression strains for the building block activating enzymes. In initial test expression studies using 23 of these heterologous strains protein production was observed. In the subsequent large scale expressions, soluble protein was obtained in sufficient amount for biochemical characterization. By carrying out photometric assays6 with the 20 natural amino acids for each individual building block activating enzyme, it was possible to confirm the activation of the predicted building blocks in 90% of the cases.

The feeding experiments for fast natural products isolation are currently limited to stable isotope labels (13C), a radiological permit for the faster 14C-feeding experiments was not provided in time. Practically, this means the compounds within the cell/supernatant extracts are separated by liquid chromatography (HPLC), the individual fractions

are freeze-dried, the yielded solids are analyzed by NMR (Nuclear Magnetic Resonance) spectroscopy for 13C-carbon enrichment and hence the proposed natural product. For one bacterial strain this whole process can take up to four months for one novel natural product. Isotopic enriched (13C)-cysteine was fed to Streptosporangium roseum in order to facilitate isolation of a natural product that was predicted to be composed of three cyclized cysteines. From analysis of individual fractions by the procedure stated above, isolation conditions for that predicted natural product were established, large scale isolation without label was carried out and the structure was elucidated by NMR. The isolated natural product showed three cyclized cysteines and an additional aromatic amino acid. We predicted structural similarity to pyochelin, a thiazole-siderphore that is produced by several pathogenic strains including Pseudomonas syringae, Pseudomonas aeruginosa, and several B. pseudomallei strains and yersiniabactin the siderophore and virulence factor produced by Yersinia pestis. We demonstrated that the determined structure of this secondary metabolite is as predicted. We further identified and characterized all enzymes that are involved in the biosynthesis of this novel siderophore in vitro. Due to the delay in obtaining the radiological permit, only two of the targeted three natural products has been structurally characterized. These entirely novel siderophores, or iron chelators, demonstrate the strength to predict chemical structures of natural products for a directed search for novel bioactive compounds that assemble the pool for our drugs, known toxins and virulence factors. Both new structures and their biochemical characterization have been submitted for publication.

Impact on National Missions

This project supports the LANL public health mission (Homeland Security Act 2002, DOE Strategic Plan 2011, Public Health Security and Bioterrorism Preparedness and

Response Act 2002) as well as its mission in global threat reduction. It also has direct appeal to our WFO sponsors and the base knowledge acquired can be applied to increasing efficiency of novel product synthesis to make it more cost effective. It will both leverage and strengthen our capabilities in bioinformatics computing, genomic/meta-genomic analysis and isotopic enrichment in a multidisciplinary project utilizing Matthias's skills to bridge the disciplines in support of the laboratory's missions in renewable energy, biosurveillance and biosecurity and development of countermeasures for bacterial infections under the Advanced Therapeutics Program.

References

1. Blin, K. a. i., M. H. Medema, Kazempour, M. A. Fischbach, Breitling, Takano, and Weber. antiSMASH 2.0-a versatile platform for genome mining of secondary metabolite producers. 2013. NUCLEIC ACIDS RESEARCH. 41 (W1): W204.

2. Strieker, , Tanovic, and M. A. Marahiel. Nonribosomal peptide synthetases: structures and dynamics. 2010. CURRENT OPINION IN STRUCTURAL BIOLOGY. 20 (2): 234.

3. Finn, R. D., Bateman, Clements, Coggill, R. Y. Eberhardt, S. R. Eddy, Heger, Hetherington, Holm, Mistry, E. L. L. Sonnhammer, Tate, and Punta. Pfam: the protein families database. 2014. NUCLEIC ACIDS RESEARCH. 42 (D1): D222.

4. Roettig, , M. H. Medema, K. a. i. Blin, Weber, Rausch, and Kohlbacher. NRPSpredictor2-a web server for predicting NRPS adenylation domain specificity. 2011. NUCLEIC ACIDS RESEARCH. 39: W362.

5. Bachmann, B. O., and Ravel. METHODS FOR IN SILICO PREDICTION OF MICROBIAL POLYKETIDE AND NONRIBOSOMAL PEPTIDE BIOSYNTHETIC PATHWAYS FROM DNA SEQUENCE DATA. 2009. COMPLEX ENZYMES IN MICROBIAL NATURAL PRODUCT BIOSYNTHESIS, PART A: OVERVIEW ARTICLES AND PEPTIDES. 458: 181.

6. Wilson, D. J., and C. C. Aldrich. A continuous kinetic assay for adenylation enzyme activity and inhibition. 2010. ANALYTICAL BIOCHEMISTRY. 404 (1): 56.

Publications

Inglis, S. R., Strieker, A. M. Rydzik, Dessen, and C. J. Schofield. A boronic-acid-based probe for fluorescence polarization assays with penicillin binding proteins and beta-lactamases. 2012. ANALYTICAL BIOCHEMISTRY. 420 (1): 41.

Koglin, A., and M. Strieker. Biosynthesis of two novel antibacterial compounds. Nature Chemical Biology.

Strieker, M., J. Schmidt, and A. Koglin. Identification and characterization of an unusual siderophore in S. roseum. Natural Product Reports.

From Food to Fuel: Making Ammonia Synthesis Viable for Energy Storage Applications

James M. Boncella
20130817PRD4

Abstract

The use of ionic liquids as media for the homogeneous, catalytic reduction of nitrogen to ammonia was investigated. Novel and reproducible methods for the synthesis of extremely pure ionic liquids were discovered. The reduction of nitrogen to ammonia in organic solvents was reproduced as reported in the literature, but transferring this methodology to various ionic liquids gave much poorer catalytic activity. It is likely that the differing solubility of the reagents in ionic liquids as compared to conventional organic solvents was responsible for the diminished reactivity of these catalytic systems. The partial synthesis of a tridentate phosphine ligand that can be covalently bound to an electrode surface was completed.

Background and Research Objectives

Room temperature ionic liquids (ILs) are salts characterized by a melting point below 100 °C. Whereas many inorganic salts can require temperatures many hundreds of degrees Celsius to acquire a molten state, the salt pairs in ILs are prevented from interacting strongly with one another through a variety of approaches, including the incorporation of sterically demanding functional groups with little polarizability, the distribution of charge over a large area, and asymmeterization of functional groups about a charged ion. All of these strategies work to prevent ready incorporation of the ions into a crystal lattice, which result in a salt with a very low temperature melting point. The use of these various approaches has led researchers in this field to develop a large library of ILs, which have been incorporated into a growing body of research that takes advantage of the unique physical properties afforded by ILs when compared to traditional organic solvents.

Our work in this area was driven by an interest in performing the electrocatalytic reduction of N2 to NH3. It was envisioned that ILs would provide a superior medium in which to perform this reduction due to the low vapor pressures of ionic liquids, their high charge mobilities and wide electrochemical window. Needed, then, were electrochemically pure ionic liquids, free of the nearly ubiquitous trace contaminants that accompany commercially available ILs. Even in research labs, it was thought until recently that the pale yellow color of many ILs – now known to result from impurities – was an inherent property of the materials. This work expanded on previous LANL research and resulted in the development of protocols for generating large quantities of electrochemically pure ionic liquids.

Scientific Approach and Accomplishments

In order to facilitate N¬2 reduction, Pyrrolidinium and imidazolium cations were chosen for their relative inertness under reducing conditions, and the fluorinated bis(trifluoromethylsulfonyl)amide (Tf2N–) and trifluoromethanesulfonate (TfO–) anions (Figure 1) were used due to their chemical stabilities and the noted propensity of the former for forming ionic liquids that are immiscible with water. The details of the synthetic procedures that resulted from our research will be outlined in a forthcoming publication. The course of our research identified the following factors as being crucial to the synthesis of electrochemically pure, as illustrated in Figure 2.

- Repeated distillations of the starting materials
- Maintenance of the amine alkylation reaction temperature at or below room temperature
- Thermal and vacuum activation/purification of the charcoal used for decolorization of the ILs
- Filtration through a 0.8 µm nylon filter
- Repeated washings of the product with distilled water
- Removal of residual water from the product with either ultra-low pressures (turbopump) or activated molecular sieves

The use of the methods described above led to ionic liquids that were suitably pure to be used in the study of the gas absorption, conductivity, and electrochemical properties of these materials under various temperature and pressure regimes. The details of this work will be communicated in a manuscript currently under preparation by our collaborators. A surprising discovery that resulted from this work was that several ionic liquids under consideration aggressively retained acetone within the material, obviating extraction methods that used acetone. The physical origin of this effect is not obvious given the lack of coordination sites in the ionic liquid and the vast difference in boiling points between the two materials.

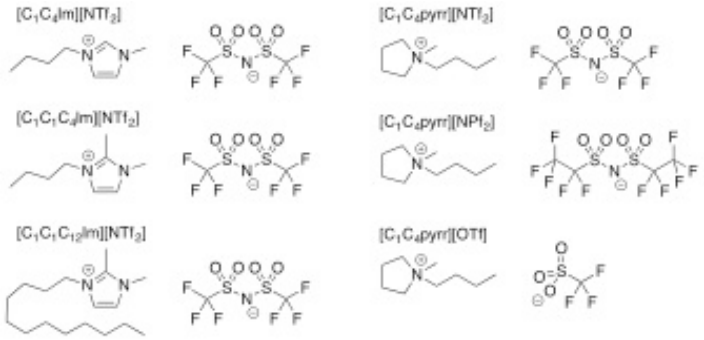

Figure 1. Ionic liquids synthesized and purified for gas absorption and N reduction studies.

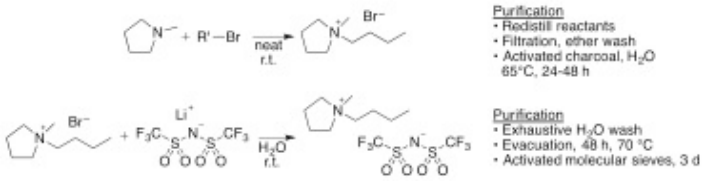

Figure 2. General reaction scheme used for synthesizing electrochemically pure ionic liquids.

Synthesis of Nishibayashi complex and N2 reduction to NH3

The low-valent dimolybdenum complex [(PNP)Mo(N2)2]2(μ-κ1,κ1-N2) (Mo, PNP = 2,6-bis(di-tert-butylphosphinomethyl)pyridine) has been reported by Nishibayashi and co-workers to perform the catalytic reduction of dinitrogen to ammonia under 1 atm of N2 and at 298 K, using lutidinium triflate ([LutH][OTf]) and cobaltocene [(C5H5)¬2Co] to deliver hydrogen equivalents to the coordinated dinitrogen ligands (Figure 3). Our interest lay in determining whether or not the unique physical properties of ionic liquids could be used to enhance the catalytic output of this reaction.

Commercial sources of the PNP ligand were found to contain significant quantities of an unidentified impurity (ca. 15%). Clean PNP ligand needed to synthesized, we first alkylated 2.0 equiv of tBu2PH with 1.0 equiv of 2,6-bis(chloromethyl)pyridine, by stirring in MeOH at 45 °C for 48 h. After cooling to room temperature, the addition of excess Et3N caused a white solid to precipitate. The solution was evacuated to dryness then the mixture was extracted with Et2O to afford the product in high yields and purities. This ligand was next metallated by heating a mixture of the ligand with MoCl3(thf)3 in THF at 50 °C for 16 h. Crystallization of the product from DCM/hexane yields orange-brown blocks of (PNP)MoCl3.

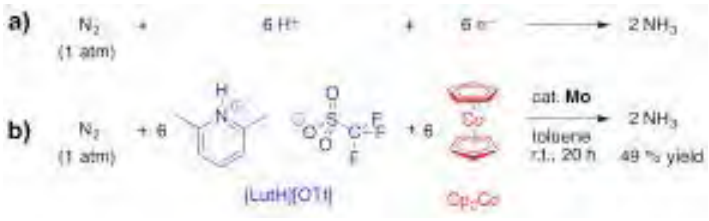

Figure 3. (a) General reaction for the reduction of dinitrogen to ammonia. (b) Synthetic protocol used by Nishibayashi and co-workers to perform the homogeneous chemical reduction of dinitrogen under ambient conditions.

Nishibayashi and co-workers described the reduction of (PNP)MoCl3 to Mo as being effected by 6 equiv of 0.5 wt % Na/Hg amalgam. We found that the reduction could be performed with sodium metal, with or without a catalytic amount of naphthalene. In the absence of naphthalene, the reaction proceeds slowly, requiring up to four days for the reduction to complete. The addition of 10 mol % naphthalene allows the reaction to finish in ca. 24 h (Figure 4); lower naphthalene loadings negatively impacted the reaction time and higher loadings led to diminished product purities.

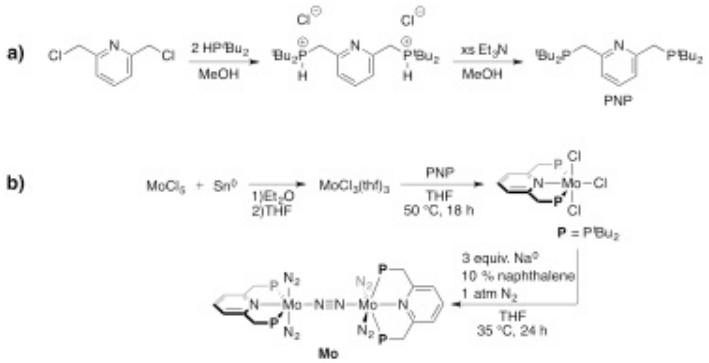

Figure 4. (a) Synthesis of the neutral tridentate ligand PNP. (b) Synthetic scheme describing the modified synthesis.

Despite our ability to generate the desired Mo complex from this method, we encountered significant differences from the synthetic protocol reported by Nishibayashi and co-workers. Our best rational of these differences was

consistent with reversible N2 binding to the complex, including solvatochromism and pressure- and atmosphere-dependent color changes. Dinitrogen ligands are poor σ-donors and moderate π-acceptors. In Mo complex, the terminal N2 ligands have both cis- and trans-π-accepting ligands. Such a coordination environment should limit back-bonding into the N2 π* orbitals, leading to a weak interaction between the terminal N2 ligands and the metal center. In the original report on this complex, Nishibayashi and co-workers report that satisfactory elemental analyses could only be obtained by drying a solution of Mo under a stream of nitrogen, consistent with the idea that N2 coordination is weak for this species. Under the lower atmospheric pressure of Los Alamos compared to Tokyo, it is conceivable that the chemistry of a complex with a weakly bound gaseous ligand could be altered from that at sea level.

Despite the differences in the solution chemistry, we successfully accomplished N2 reduction in a manner similar to that reported previously. In toluene, the solvent used in the original report, we obtained 14 equivalents of NH3, a marginal increase over the 12 equivalents reported under analogous conditions. The use of ionic liquids as a reaction medium was hypothesized to stabilize charged intermediates, facilitating the catalytic process. A variety of reaction conditions, including the rate and order of addition of hydrogen atom equivalents, the nature of the ionic liquid, and the reaction stoichiometry were screened, but only trace quantities of ammonia were detected. When performing the reaction in toluene, the acid (lutidinium triflate) is largely insoluble. It may be that this insolubility is instrumental in controlling the acidity of the solution and the stability of the metal complex. Paradoxically, it appears that the insolubility of lutidinium triflate is responsible for the success of the reaction in toluene.

Attempted synthesis of modified PNP ligand

Only limited mechanistic information has been presented in the literature to elucidate the manner in which Mo reduces dinitrogen to ammonia. We were thus interested in synthesizing a ligand that retained the coordination properties of PNP while offering a means of attaching the ligand to a surface through which the reaction details could be probed by in situ IR and/or UV-vis monitoring. Our approach to this problem involved attempting to append a linker group in the 4 position of the pyridine ring. The linker would then be used to attach the molybdenum complex to indium tin oxide, boron-doped diamond, or a similarly transparent, conductive surface. Such a surface bound complex could be studied using spectro-electrochemistry.

The synthetic scheme in Figure 5 outlines our approach to synthesizing a ligand that would meet the demands described above. Starting with chelidamic acid, a para-bromo functionality was installed prior to reduction of the 2,6-substituents to hydroxymethyl groups. Conversion of the alcohols into halides was accomplished with either phosphorus tribromide (PBr3) or trichlorotriazene (TCT). Subsequent attempts to alkylate tBu2PH with these species were unsuccessful, leading to complex mixtures of products with no clear evidence for formation of the desired product. Changes to the reaction conditions (solvent, temperature, reaction time, base) similarly failed to yield the desired product. Considering the high yield of PNP when using the parent 2,6-bis(chloromethyl)pyridine, we are left to conclude that the para-bromo substituent is deleterious to this reaction.

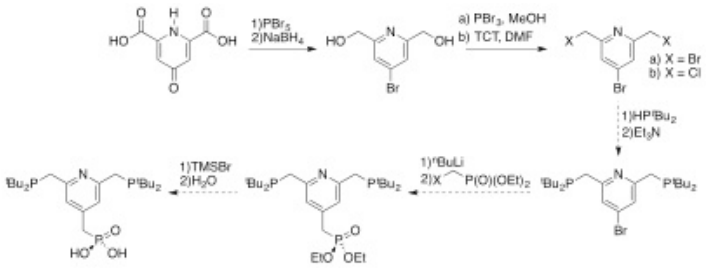

Figure 5. Synthetic scheme used for the attempted synthesis of modified PNP ligands.

Impact on National Missions

This work has demonstrated that the use of homogeneous catalysts for the reduction of nitrogen in ionic liquids is viable, though not nearly as efficient as in organic solvents. The discovery of novel methods for the purification of ionic liquids demonstrates that it is possible to take advantage of the novel properties of ionic liquids for electrochemistry, and by extension, electrochemical devices. This will have a positive impact on research that relates to energy security. This work has spawned an ongoing outside collaboration with Michigan State University on the electrochemical synthesis of ammonia.

Genetically Encoded Tools for Light-controlled Molecular Assembly

Geoffrey S. Waldo
20140660PRD1

Abstract

Tools to study protein interactions with high spatio-temporal resolution would advance our understanding of biology. Attaching proteins whose assembly could be controlled by light is one way to achieve this goal. Photo-switchable phototropin 1 and light-oxygen-voltage sensor proteins (LOV) domains are large and perturb the proteins they are attached to. GFP is a highly fluorescent barrel-shaped molecule with 11 beta strands. To overcome the issue of bulky tags, our group has developed two-part split GFPs. Strand 11, the 'tag', (15 amino acids) is attached to other proteins. The rest of the GFP, the 'detector', (strands 1-10) is added or expressed in the cell separately, spontaneously binding the strand 11 to form fluorescent GFP. We developed a three-part split GFP whose reassembly is not spontaneous. Strand 10 and strand 11 are attached to two different proteins. Only if the proteins interact with each other, are the small GFP strands near enough to be detected by GFP strands 1 to 9. This three-part split GFP is thus a protein-protein interaction detector. Recently Boxer showed that violet light reversibly displaces strand 10 from the rest of our two-part GFP. In this project we proposed developing a light-activated three-part split GFP system so that the small target strands could be removed by light. This technique could then be applied to study spatio-temporal details of protein-protein interactions in influenza infections of human cells using light control. We have shown the light exchange property is slow in our three-part GFP, likely because the affinity of strand 10 is higher for the rest of the GFP, compared to the two-part split GFP. From this we have learned what is needed to make robust light-activated three-part split GFP system. We expressed and purified human and influenza proteins that interact for use with the new split GFP technology.

Background and Research Objectives

Optical control of proteins could allow unparalleled control of protein-protein interactions. Many important biological events rely on the protein interaction, modification, or alternant conformation in response to a second protein. This concept has been illustrated with a Rac-protein light switch phototropin 1 (LOV2 domain) fusion protein that was able to control cell mobility when activated by light [1]. Several photo switchable versions of fluorescent proteins have also been investigated for their use in live-cell fluorescence microscopy because multiple proteins could be labeled with one of the labels being switched on or off after exposure to blue light [2]. The disadvantage of these photo switchable proteins is that the entire protein needs to be affixed onto a target protein, and they are simply passive reporters, not assembling or disassembling with light. The goal of this project was to develop a three-part split green fluorescent protein (GFP) technology that is light activated, i.e. the GFP fragments could be driven apart with light and reassemble in the dark. The split GFP technique would have an advantage over other photo switchable proteins since the GFP tags are only 15 amino acids long. Waldo et al. previously developed a version of GFP that can be split at either strand 10 or strand 11 leading to a tag that can be placed on a target protein [3]. Once GFP strands 1-9 is added to the solution with the labeled target protein, the complete GFP is formed leading to a fluorescent system. This system can then be applied to many different applications, including in vivo labeling of proteins, a tool to determine protein solubility, and most recently, a means to improve protein crystallography.

The purpose of this Director's Fellowship was to modify this existing system to incorporate a light activated component. Currently, the binding of GFP strands 1-9 + S10-target-S11, GFP strands 1-9 + target-S10-S11, or GFP strands 1-9 + targetA-S10 + targetB-S11 (when targetA and target interact) is nearly irreversible (Figure 1). Research by the Boxer lab indicated that the dissociation of our GFP 11-1-9 + S10 could be sped up by the addition of 405 nm light [4]. Then, by incorporating a mutation in S10 that changes the color from green to yellow, two different versions of S10 could be used to monitor when

photo-dissociation and reassembly occurred. I proposed using this new light activated system to look at proteins involved in the human-influenza interaction. A number of influenza proteins are known to interact transiently with human proteins, which aids in influenza's ability to evade the human immune system.

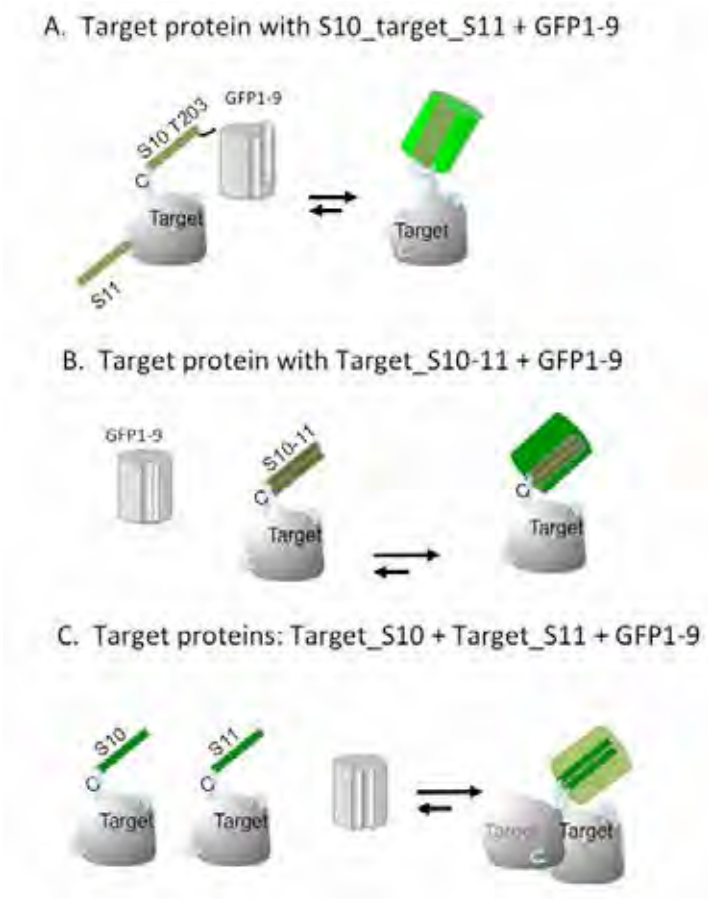

Figure 1. An overview of current GFP split technology developed in Geoff Waldo's lab. A. A target protein is labeled with strand 10 of GFP on the N-terminus and strand 11 on C-terminus, when GFP1-9 is added to a solution containing the target protein GFP is able to form a complete barrel and fluoresces green. B. A second split protein configuration involves a target labeled with strands 10 and 11 on the C-terminus. When GFP1-9 is added to solution the missing strands 10-11 can combine with GFP1-9 and fluoresce green. C. The third split system labels one target protein with strand 10 from GFP and a second target protein with strand 11 from GFP. After addition of GFP1-9, if the two target proteins interact green fluorescence will result.

Scientific Approach and Accomplishments

The first step in this project was to develop a split GFP light activated system that could then be modified through genetic engineering to be used in in vivo cell studies of human-influenza protein interactions. I started with the existing three-part split GFP system that had previously been developed by the Waldo lab [3]. Since the binding rate of 10-test protein-11 + GFP strands 1-9 is much slower than test protein-10-11 + GFP strands 1-9, we used this to look for photo-exchange (Figure 2A). The 10-test protein-S11 with the addition of GFP 1-9 is green. A second target protein with the higher affinity tag of GFP strand 10-11 with the mutation T203Y (mutation that confers a yellow fluorescent spectral shift) is added to the solution at a higher concentration. After exposing to 405 nm laser pointer, the green strands would be displaced and the higher affinity yellow strand 10-11 would bind. In concept this experiment is straightforward. Exchange was much slower than in the GFP 11-1-9 + S10 system, consistent with a higher affinity of S10 for the rest of the GFP in the three-part split GFP.

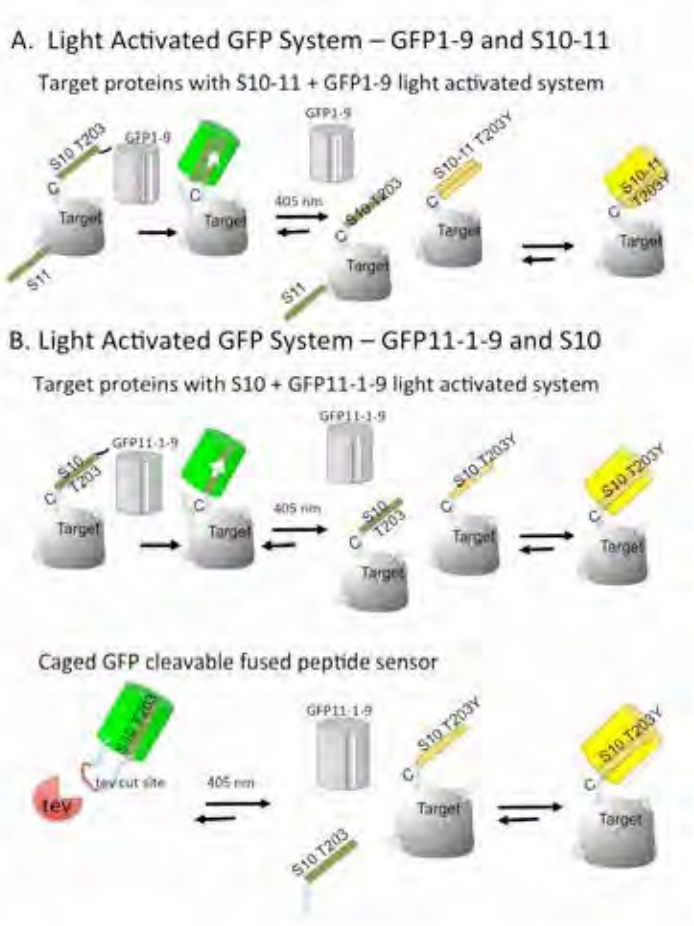

Figure 2. Proposed light-activated GFP systems. A. A target protein is labeled with S10 T203Y on one terminus and S11 on the other terminus and when combined with GFP1-9 fluoresces green. Exposure to 405 nm light causes S10 and S11 to dissociate. Excess target protein labeled by GFP10-11 T203Y is present in solution and binds with a higher affinity than the S10_target_S11 version. This is reflected by exchange to yellow (T203Y) fluorescence. B. Either a target protein is labeled with S10 or alternatively, S10 is connected to GFP11-1-9 with a designed protease cut site. The protease cut site can be utilized to separate S10 from GFP11-1-9. After 405 nm light exposure, excess target protein with S10 T203Y (yellow) is added. S10 T203Y, which has higher affinity, binds preferentially over S10 T203.

After this we moved to a different light activated system, utilizing only S10 as a leaving group (Figure 2A). A sample of target protein-S10 + GFP strands 11-1-9 was incubated, resulting in green fluorescence. The sample was then illuminated with 405 nm with excess target protein-S10 T203Y (yellow) added. Exchange would result in a yellow solution. Slow exchange was observed, under room light for 48 hours (Figure 3). A different experiment was designed utilizing a caged GFP cleavable fused peptide of GFP strand 10 (Figure 2A). To test the effect of the mutations in the three-part split GFP vs. the two-part split GFP, a light activated experiment was designed with both our GFP strands 11-1-9 version from the optimized GFP strands 1-9 complementation system (Figure 1) and a version based on our two-part split GFP (Figure 4) [4]. In this experiment, both versions of GFP 11-1-9-(protease site)-10 were expressed and purified. The protease sites allowed the strand 10 to be cut using tabacco etch virus protease, but the GFP would remain assembled in the dark. This cut protein was incubated with excess of sulfate reductase-S10 T203Y. Exposure to 405nm laser pointer for 15 minutes resulted in significant exchange (520 nm excitation, 550 nm emission) for the GFP based on the two-part split construct but none for the version based on the GFP1-9 optimized system (Figure 5).

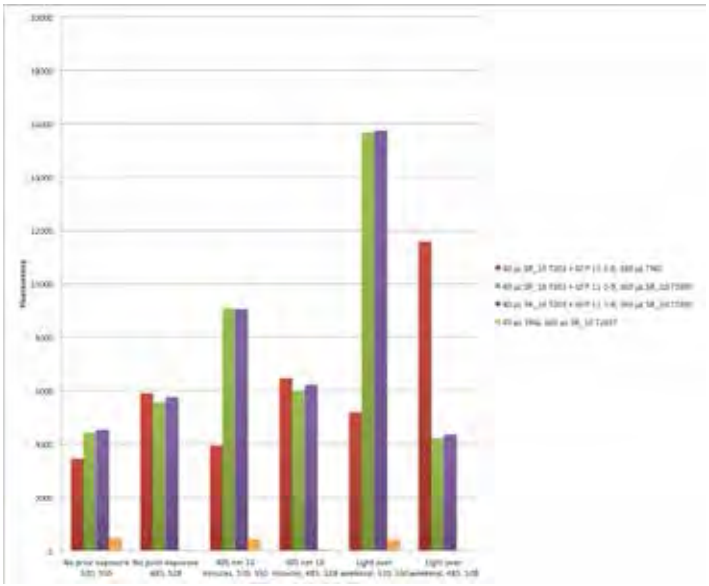

Figure 3. Light exchange experiment with sulfate reductase with C-terminal GFP strand 10. An increase in yellow fluorescence (520 nm excitation, 550 nm emission) is seen in light exposed samples with excess SR_10 T203Y as expected. There is a further increase after exposure to room light over 48 hours. A higher rate of exchange was expected.

This experiment finally established some rationale for why all the previous trials failed with GFP 1-9 system. As figure 4 illustrates, the version based on the two-part GFP construct and the GFP 1-9 optimized version are 94% identical. The residue at position 65 cannot be the only residue responsible for the different response to 405 nm light, as this residue was already investigated. Since strand 10 was extensively engineered to increase its affinity for the three-part split GFP, it is most likely that the difference in off rate is due to the three residues that differ in strand 10 from the three-part GFP versus the two-part GFP. There are two possible follow up experiments to identify the difference. Ideally, we would want a system that has the benefits of the GFP 1-9 optimized system (strong fluorescence, good solubility, protein interaction dependence on assembly) but maintains the light exchange properties of the two-part GFP system. It is clear that a possible route is to start with the two-part system and mix mutations in from the GFP 1-9 three-part system, and throughout the entire selection process, select for variants that maintain or improve the ability to exchange with 405 nm light but have improved fluorescence and solubility. This new split system could then be used for photoswitching experiments. A second experiment could be designed to specifically look at the different affinities of strand 10. This would essentially just require altering the protease constructs to have the strand 10 of the corresponding two-part or three-part split GFP. It could be that the residues present in strand 11 could significantly alter the affinity of strand 10.

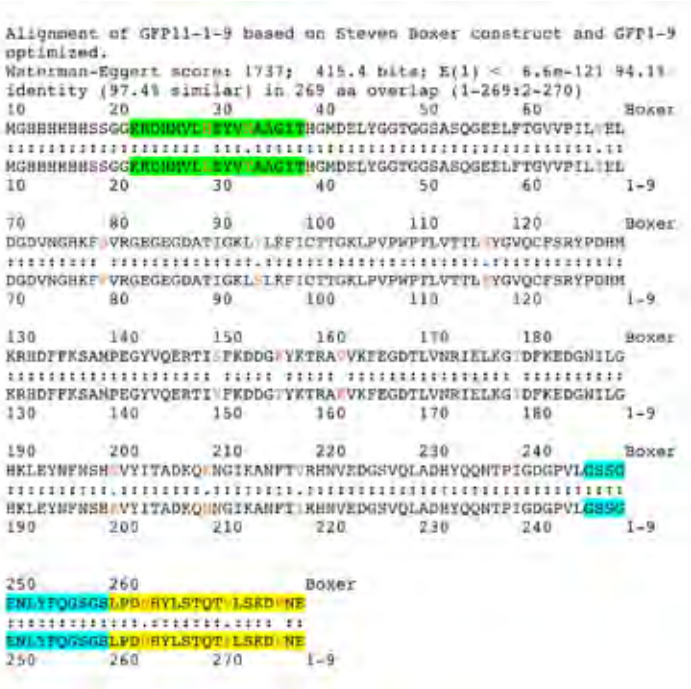

Figure 4. Protein sequence alignment of GFP11-1-9 based on the optimized GFP1-9 system developed in the Waldo lab and the version of GFP11-1-9 used by the Boxer lab for caged GFP cleavable fused peptide sensor. The Blue highlighted regions is the tev cut sites, red text is residues that differ, green highlighted sections are strand 11, and yellow highlighted section are strand 10.

In addition, I expressed, purified, and began crystallization trials of human protein p85 and influenza protein NS1 that are known to interact with each other. These proteins would be ideal targets to use with the new light activated split GFP system. The expression, co-purification, and some crystallization conditions were identified for these two proteins. Once the light activated system with GFP is optimized these two proteins could make an ideal test system. P85 could be labeled with S10, NS1 with S11, and when GFP1-9 is added to solution the light activated studies could be conducted.

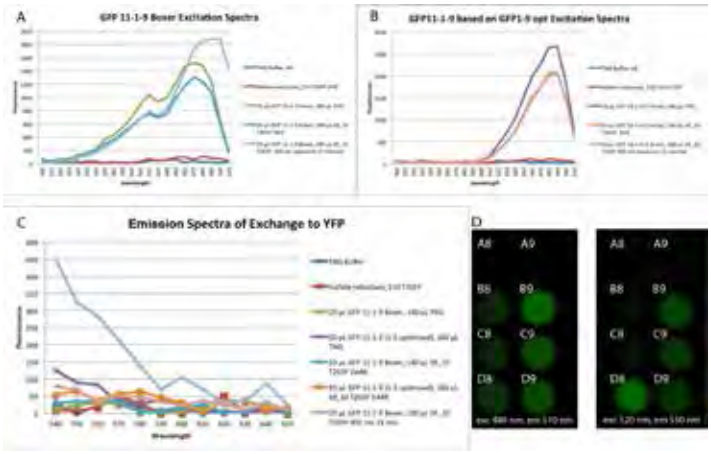

Figure 5. Light exchange experiment with caged GFP 11-1-9-tev-10 constructs. A. Excitation spectra of GFP11-1-9-tev-10 Boxer version with controls and sample with excess sulfate reductase_10 T203Y (SR_10) added to solution. There is a marked shift toward 510 nm as excitation max in 405 nm exposed sample (purple trace). B. Excitation spectra of GFP11-1-9-tev-10 based on GFP1-9 optimized with controls and samples with excess SR_10 T203Y. No shift in excitation sample was noted as compared to sample in dark or control GFP11-1-9-tev-10. C. Emission spectra in light exchange experiment. Only the GFP11-1-9-tev-10 boxer construct exposed to 405nm light after excess SR_10 T203Y was added had an increase in emission over the other samples. D. Plate photographed after excitation at 488 nm, emission at 510 nm (exposure time 1/15 sec). Second image is the same plate photographed after excitation at 520 nm, emission at 550 nm (exposure time 4 sec). Wells correspond to: A8 200 µL TNG buffer: A9 20 µL TNG, 180 µL SR_10 T203Y: B8 20 µL Boxer, 180 µL TNG: B9 20 µL 11-1-9-rev-10 1-9 opt, 180 µL TNG: C8 20 µL Boxer, 180 µL SR_10 T203Y kept in dark: C9 20 µL 11-1-9-rev-10 1-9 opt, 180 µL SR_10 T203Y kept in dark: D8 20 µL Boxer, 180 µL SR_10 T203Y after 15 minutes 405 nm exposure: D9 20 µL 11-1-9-rev-10 1-9 opt, 180 µL SR_10 T203Y after 15 minutes 405 nm exposure. D8 has a marked increase in yellow fluorescence.

Conclusions. Six major conclusions can be drawn. (1) The results show that the two-part split GFP can be photodissociated, and that the fragments spontaneously reassemble in the dark. (2) Since the assembled GFP can transit through cell membranes, this offers an immediate tool for the delivery of caged peptides via GFP. (3) Once at the desired location, the caged GFP would be photo dissociated, releasing the caged peptide for activating desired biological responses. (4) Further, this allows the selective detection of proteins tagged with S10 T203Y, by observing the appearance of yellow fluorescence that can be specifically excited using 520 nm light (this wavelength does not excite GFP based on S10 T203). (5) Thus for the first time, it will be possible to monitor proteins in specific sites in living cells, sites which have been off-limits to conventional live-cell labeling experiments. (6) In future research directions, the two-part split GFP and three-part split GFP can be tweaked by evolution to increase photo exchange rate and solubility.

Impact on National Missions

This work firmly establishes precedence for using green fluorescent proteins for light-activated assembly and disassembly. Since the split GFP fragments are small and non-perturbing, this technology is disruptive since tagged proteins can be studied with less perturbation compared to existing tags.

Biosecurity

Many pathogen/host interactions have been hampered by the bulky size of tags in the past. Up to now, GFPs have been passive tags, simply fluorescing in response to light. For the first time, this new light-activated split GFP provides a tool for controlling protein localization, aggregation, and interactions with light. This tool has strong positive impact on our mission to study, understand, and ultimately control host-pathogen biology.

Energy independence

The ability to control gene networks using light, using the very stable and robust GFP scaffold, means we can more easily engineer organisms for synthetic biology. This impacts the production of biofuels and bio-derived natural products.

References

1. Cabantous, S., T. C. Terwilliger, and G. S. Waldo. Protein tagging and detection with engineered self-assembling fragments of green fluorescent protein. 2004. Nature Biotechnology. 23: 102.

2. Cabantous, S., H. B. Nguyen, J. D. Pedelacq, F. Koraichi, A. Chaudhary, K. Ganguly, M. A. Lockard, G. Favre, T. C. Terwilliger, and G. S. Waldo. A new protein-protein interaction sensor based on tripartite split-GFP association. 2013. Scientific Reports. 3: 1.

3. Do, K., and S. G. Boxer. GFP variants with alternative beta strands and their application as light-driven pro-

tease sensors. 2013. Journal of the American Chemical Society. 135: 10226.

4. Wu, Y.. A genetically encoded photoactivatable RAC controls the motility of living cells. 2009. Nature. 461: 104.

5. Zhou, X. X., and M. Z. Lin. Photoswitchable fluorescent proteins: ten years of colorful chemistry and exciting applications. 2013. Current Opinion Chemical Biology. 17: 682.

Publications

Leibly, D. J., M. A. Arbing, I. Pashkov, N. DeVore, G. S. Waldo, T. C. Terwilliger, and T. O. Yeates. A suite of engineered GFP molecules for oligomeric scaffolding. 2015. Structure. 23 (9): 1754.

Mesoscopic Lattice Boltzmann Modeling and Investigation of Boiling Multiphase Flows

Qinjun Kang
20140669PRD2

Abstract

Boiling multiphase flow is pervasive in nature and industrial applications. However it is not well understood despite many years of research effort. Novel methods are badly needed for a better understanding of boiling multiphase flows. The main objectives of this research were to develop a novel, physics-based thermal lattice Boltzmann (LB) model for modeling boiling multiphase flows and to obtain new insights into the mechanisms of boiling heat transfer. Scientific accomplishments of this project include the development of a novel, physics-based thermal LB model for modeling multiphase flow with phase change, as well as numerical investigation of boiling multiphase flow and self-propelled Leidenfrost droplets on ratchet surfaces. This project supports physics-based prediction models of departure from nucleate boiling, one of the grand challenge problems of the DOE Consortium for Advanced Simulation of Light Water Reactors. The approach will also have significant implications in other research areas including spray cooling, nucleate boiling heat transfer of nanofluids, and cooling of micro-electronic devices. This project has resulted in four publications in barely one year.

Background and Research Objectives

Boiling multiphase flows are ubiquitous in nature as well as in many industrial applications. Nucleate boiling, a well-known boiling phenomenon, has been recognized as one of the most effective heat transfer modes and used in a wide field of high-tech devices and systems such as nuclear reactors, heavy-vehicle engines, computer chips, and micro-electronic devices. However, despite years of tremendous research effort, many aspects of boiling are still not well understood, e.g., the physical mechanism causing the critical heat flux is not revealed. This is due to (1) the correlations developed by experiments rely heavily on empirical parameters which are only valid for a narrow parameter range and (2) numerical simulations based on traditional numerical methods usually involve many assumptions and empirical correlations. Novel methods are highly demanded for a better understanding of boiling multiphase flows. In the past years, the mesoscopic LB method has been developed into an alternative approach for simulating multiphase flows, in which the interfaces can arise, deform, and migrate naturally as a result of particle interactions, without needing a cluster of marker points to track the interfaces or capturing the interfaces via the evolution of an order parameter. Moreover, this method has been recently demonstrated to be capable of modeling phase change without any assumptions, though the model is limited to low density ratios.

The main objectives of this research were to develop a novel, physics-based thermal LB model for modeling boiling multiphase flows, and to obtain improved understanding of boiling phenomena, e.g., new insights into the physics of critical heat flux at different scales through mesoscopic modeling.

Scientific Approach and Accomplishments

Novel, physics-based thermal LB model for modeling boiling multiphase flows

We developed a hybrid thermal LB model for simulating thermal multiphase flows, which employs an improved pseudopotential LB model and a finite-difference scheme to simulate the fluid flow and the temperature field, respectively. The pseudopotential LB model and the finite-difference solver of temperature are coupled via the equation of state. Numerical simulations of boiling heat transfer have been conducted using the model. The complete three boiling stages, nucleate boiling, transition boiling, and film boiling, as well as the boiling curve were successfully reproduced in our simulations with the bubble nucleation, growth, departure, and coalescence being well captured. Some basic features of boiling heat transfer were clearly observed in the numerical results, such as the severe fluctuation of transient heat flux in the transition boiling regime, the critical heat flux in the boiling curve, and the feature that

the maximum heat transfer coefficient lies at a lower wall superheat than that of the maximum (critical) heat flux. Furthermore, the influences of the heating surface wettability on boiling heat transfer have also been studied. The numerical results show that the critical heat flux decreases when the contact angle increases, which also causes the boiling process to enter the film boiling regime at a lower wall superheat. Besides, increasing the contact angle will reduce the required wall superheat for the onset of boiling (Figure 1). All of these findings are consistent with the experimental studies in the literature, demonstrating that the proposed model is capable of reproducing the basic features and the fundamental characteristics of boiling heat transfer.

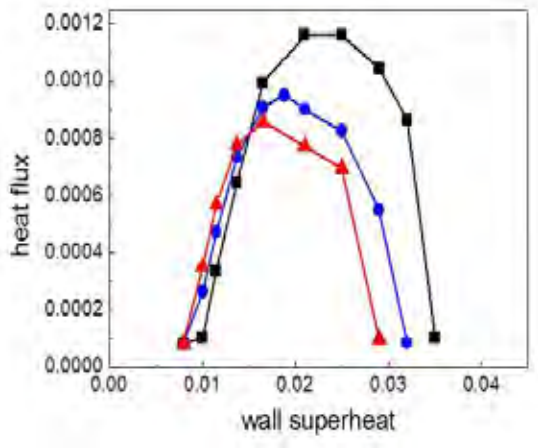

Figure 1. Boiling curves at different contact angles. The squares, circles, and triangles represent the results of static (liquid) contact angles around 44.5, 50, and 55.5 degrees.

Numerical investigation of self-propelled Leidenfrost droplets on ratchet surfaces

Using the developed model, we have also investigated the self-propelled motion of Leidenfrost droplets on ratchet surfaces, a phenomenon that liquid droplets perform self-propelled motion when placed in contact with hot surfaces with asymmetric textures. This phenomenon has important applications in cooling systems with no moving parts, such as microprocessor cooling.

We have investigated the dynamic behavior of Leidenfrost droplets on horizontal ratchet surfaces. Numerical results show that the self-propelled motion of Leidenfrost droplets originates from the asymmetry of the ratchets and the vapor flows below the droplets (see streamlines in Figure 2). It is found that the Leidenfrost droplets move in the direction toward the slowly inclined side from the ratchet peaks, which agrees with the experimental observation. The effects of the initial droplet radius and the influences of the ratchet aspect ratio have been studied. We have found that there exists a critical value of the aspect ratio. Moreover, we have also studied the performances of Leidenfrost droplets on inclined ratchet surfaces. Different inclination angles have been investigated. It is found that the droplet moves downhill in the early stage due to the downhill acceleration caused by the gravitational force. Later, the droplet turns around at a certain time with the help of the uphill acceleration, which is generated by the vapor flow beneath the droplet. The maximum inclination angle at which a Leidenfrost droplet can still climb uphill successfully is found to be related to the initial radius of the droplet.

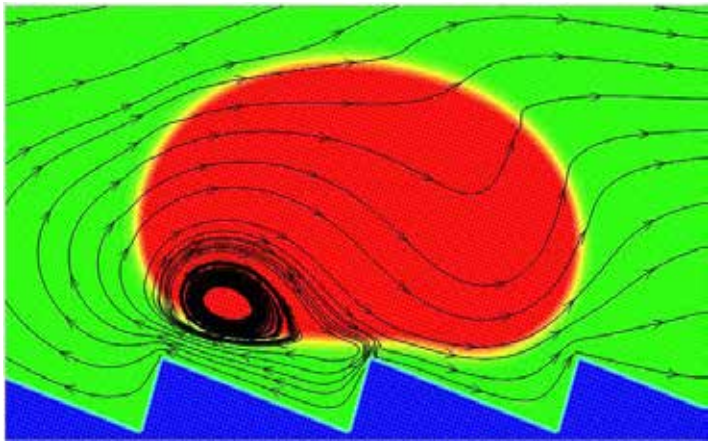

Figure 2. The streamlines for the case of initial droplet radius 45 at dimensionless time 1.45.

Impact on National Missions

This project supports the DOE/NNSA missions in Energy Security, Environmental Quality, and the missions of the Office of Science by enhancing our understanding of boiling multiphase flow and heat transfer. The project supports physics-based prediction models of departure from nucleate boiling, one of the grand challenge problems of the DOE Consortium for Advanced Simulation of Light Water Reactors. The approach will also have significant implications in other research areas including spray cooling, nucleate boiling heat transfer of nanofluids, and cooling of micro-electronic devices.

Publications

Li, Q., K. Luo, Q. Kang, Y. He, Q. Chen, and Q. Liu. Lattice Boltzmann methods for multiphase flow and phase-change heat transfer. 2015. arXiv preprint arXiv:1508.00940arXiv preprint arXiv:1508.00940.

Li, Q., K. Luo, Q. Kang, and Q. Chen. Contact angles in the pseudopotential lattice Boltzmann modeling of wetting. 2014. Physical Review EPhysical Review E. 90 (5): 053301.

Li, Q., Q. Kang, M. Francois, Y. He, and K. Luo. Lattice Boltzmann modeling of boiling heat transfer: The boil-

ing curve and the effects of wettability. 2015. International Journal of Heat and Mass TransferInternational Journal of Heat and Mass Transfer. 85: 787.

Li, Q., Q. Kang, M. Francois, and A. Hu. Lattice Boltzmann modeling of self-propelled Leidenfrost droplets on ratchet surfaces. 2015. arXiv preprint arXiv:1506.00700arXiv preprint arXiv:1506.00700.

Information Science & Technology

Information-Driven Materials Discovery and Design

Turab Lookman
20140013DR

Introduction

The goal of this project is accelerated materials discovery by advancing the state-of-the-art statistical inference and optimization tools to find materials with desired or targeted properties. This data-centric approach narrows the possible search space for improved prediction by teasing out hidden information that is present in the data for known materials. Until very recently, new materials have almost exclusively been discovered by intuition and costly trial and error. However, literally overnight the use of simple statistical inference tools is just starting to define the new field of materials informatics. Our key innovation is an integrated design loop - an excellent example of the paradigm of codesign. It is a departure in how to think about the problem of Materials Discovery by using sophisticated information theoretic tools developed in various contexts including pattern recognition, operations research, bioinformatics, but applying them in a unique way to materials science issues. As an example, we will focus on the class of functional materials known as piezoelectrics. These are materials which produce a large strain if an electric field is applied, or a large polarization if stress is applied. The need is to find materials with a large response and high working temperatures. Such materials have numerous applications, from energy harvesting devices to sensors, and N. America has been gradually and continuously losing market share in these markets. These predominantly lead-based compounds are now banned in many parts of Europe. Our objective will be to search for new lead-free piezoelectrics. However, the paradigm we will develop will also be applicable to other materials classes with their own targeted properties, and where possible, we will examine within this project other related materials classes.

Benefit to National Security Missions

Accelerated materials discovery is of strategic importance and relevance to DOE/SC initiatives. Moreover, the development of information science predictive tools to enable accelerated materials discovery is also a fundamental aspect of innovation in the above agencies. These tools are based on machine learning methods and are widely applicable to fields such as pattern recognition, statistical analysis and operation research, areas that are also of interest to these agencies. Our focus in this proposal is to demonstrate the new capability on the class of materials known as piezoelectrics and other functional materials. These are of interest to DOE/SC as they find applications as sensors and energy harvesting devices. More broadly, we will pioneer a new approach to materials discovery using information science predictive tools that will impact all missions that depend on materials, including the weapons program. The design loop we propose is also an example of the paradigm of codesign (which is gaining greater traction within DOE, for example,) - where learning a “model” is performed iteratively guided by experiments and computer calculations, which in turn are guided by statistical analysis.

Progress

- Prediction, synthesis and characterization of NiTi-based ultra low thermal dissipation alloys. Several new alloys have been discovered by implementing our design framework. The alloys belong to the class: NiTiCuFePd. One of these compounds has the smallest thermal dissipation of any known compound. Our adaptive design framework is general and can be applied to any materials class.
- Prediction, synthesis and characterization of new BaTiO3 based Pb-free alloys that are easier to synthesize. Further characterization work is underway to determine the piezoelectric coefficients.
- Discovery of a new feature (Excess Born charge) that classifies AB solids with fewer misclassifications than any other scheme (work to appear in Phys. Rev. B). This has been a classic problem studied over the last 50 years and may be considered to be the earliest

example using materials design ideas.

- An approach to classification learning which uses orbital radii to design new ductile intermettalic compounds. Our predictive models indicate that the compounds SoCo, ScIr and YCd should be ductile, whereas each was previously predicted to be brittle (to appear in Nature Scientific Reports, 2015).
- Discovery of new polymer based dielectrics with large wide band gaps and dielectric constants using high through put electronic structure calculations.
- Discovery of new water-splitting catalysis compounds using high through put electronic structure calculations.
- An understanding of how the adaptive design algorithms are forgiving of issues and drawbacks of the inference training model.
- In the design of Light emitting diodes (LEDs), industry standard simulation codes (e.g. APSYS) are used to predict the internal quantum efficiency before fabrication. We have demonstrated how adaptive design (using a Gaussian model coupled to efficient global optimization) can be used to guide APSYS to optimally design LEDs with better performance than what has been done so far.

Future Work

A key component of the project has been the adaptive design strategy to suggest the next experiments for finding materials with single targeted properties. This will be studied in greater detail in its own right and applied to a number of other materials data sets to test robustness. It includes a number of machine learning tasks (e.g. batch mode or multiple experiments other than Kriging believer algorithm, Bayesian approach), coupled with tight coupling to synthesis, characterization and DFT (electronic calculations) efforts. Specific materials classes include Heusler alloys and Bi based piezoelectrics.

Our materials design has so far involved a single property or objective. Our goal will be to formulate a multi-objective optimization strategy so that we can optimize two or more properties. This will be performed with data sets (Max phases and Apatites) that will facilitate benchmarking, as well as the data set for NiTi based compounds for which we have successfully searched for new low thermal dissipation alloys. We will now also optimize for large transition temperatures and large strains.

A number of our materials problems (e.g. Heuslers) require addressing the classification problem in an adaptive, iterative manner (e.g. finding new phase transforming Heuslers). We will therefore study a feedback loop for classification to guide experiments.

Conclusion

If successful, we will establish a new paradigm for addressing complex optimization problems that include multiple sources and choices to incorporate domain knowledge. Further, we will have developed tools and algorithms to deal with error estimation, with experimental design and employing materials domain knowledge in machine learning. Our success will be measured by our discovery of new materials with desired properties and greater insight into the dominant mechanisms (structure-property relationships) underlying materials phenomena. A main deliverable will be an Information Science & Technology based materials discovery capability for accelerated materials discovery.

Publications

Information Science for Materials Discovery and Design. 2015.

Balachandran, P. V., D. Xue, J. Theiler, J. E. Hogden, and T. Lookman. Adaptive design strategies for materials design. Scientific Reports (2015).

Balachandran, P. V., Theiler, J. M. Rondinelli, and Lookman. Materials Prediction via Classification Learning. 2015. SCIENTIFIC REPORTS. 5.

Gubernatis, J.. Data Visualization and Structure Identication. 2014. LA-UR-14-22628.

Gubernatis, J.. Data Visualization and Structure Identication. 2015. In Information Science for Materials Discovery and Design. Edited by Lookman, T., F. J. Alexander, and K. Rajan. Vol. 225, First Edition, p. 1. Berlin: Springer Verlag.

Lookman, T.. Heterogeneities, The Mesoscale and Multifunctional Materials Codesign: Insights and Challenges. 2014. In Mesoscopic Phenomena in Multifunctional Materials. Edited by Saxena, A., and A. Planes. Vol. 198, First Edition, p. 57. Berlin: Springer.

Lookman, T., P. V. Balachandran, D. Xue, G. Pilania, T. Shearman, J. Theiler, J. Hogden, J. E. Gubernatis, K. Barros, E. Ben-Naim, and F. J. Alexander. A perspective on materials informatics: state-of-the-art and challenges. 2015. In Information Science for Materials Discovery and Design. Edited by Lookman, T., F. J. Alexander, and K. Rajan. Vol. 225, First Edition, p. 3. Berlin: Springer-Verlag.

Mannodi-Kanakkithodi, A., G. Pilania, T. Doan Huan, T. Lookman, and R. Ramprasad. Informatics-Driven Strategy for the Accelerated Design of Polymer Dielectrics. Scientific Reports (2015).

Pilania, G., J. E. Gubernatis, and T. Lookman. Classification of octet AB-type binary compounds using dynamical

charges: A materials informatics perspective. To appear in Scientific Reports (2015).

Pilania, G., P. V. Balachandran, J. E. Gubernatis, and T. Lookman. Classification of ABO3 perovskite solids: a machine learning study. 2015. Acta Crystallographica, Section B: Structural Science, Crystal Engineering and Materials. 71 (5): 507.

Pilania, G., T. Lookman, and J. Gubernatis. Structure classification and melting temperature prediction in AB solids via machine learning. 2015. Physical Review B, Vol 91, Issue 21, 214302 (2015).

Pilania, G., and T. Lookman. Electronic structure and biaxial strain in RbHgF 3 perovskite and hybrid improper ferroelectricity in (Na,Rb)Hg 2F 6 and (K,Rb)Hg 2F 6 superlattices. 2014. Physical Review B (Condensed Matter and Materials Physics) . 90 (11): 115121.

Xue, D., P. V. Balachandran, J. E. Hogden, J. Theiler, and T. Lookman. Accelerated search for materials with targeted properties by adaptive design. Nature Communications.

Next Generation Quantum Molecular Dynamics

Anders M. Niklasson
20140074DR

Introduction

Quantum mechanical Born-Oppenheimer molecular dynamics (QMD) provides a highly powerful, but computationally expensive, multidisciplinary tool to predict, understand and design materials and processes directly from the fundamental principles of quantum physics. Merging QMD with future extreme-scale computing therefore holds the promise of a major paradigm shift in materials science, chemistry, and biology. Unfortunately, this potentially revolutionary opportunity will never be realized without a radical re-design of current approaches to QMD, overcoming a number of interconnected fundamental shortcomings. Based on several LANL-unique innovations, including a conceptually new graph-based approach to quantum mechanics, we propose a major coordinated interdisciplinary effort to develop a truly transformative computational framework for a new generation QMD that is specifically tailored for extreme-scale computing on heterogeneous architectures and allows simulations for time and length scales that are multiple orders of magnitude beyond current capacity. A key element of the proposed work is the development of a radical alternative to the traditional computational algorithms that are unsuited to large-scale simulations. Our new graph-based approach for solving the electronic structure problem will enable us to combine, for the first time, high on-node computational efficiency with massive parallelism for QMD simulations, including on-the-fly interrogation of the electronic degrees of freedom for visualization or quantum response properties. We will develop and demonstrate this capability on two test-bed applications (involving aspects of nuclear fuels, and protein structures and dynamics) where classical MD methods are inadequate or fail, and where QMD simulations have thus far been too expensive. This unique computational capability will strengthen LANL's leadership in numerous mainstream priority areas in materials science, chemistry and biology, and it will have a lasting multidisciplinary impact on diverse applications that advance our missions.

Benefit to National Security Missions

This project will provide a new capability that will (a) benefit our mainstream Laboratory missions in weapons science and energy security by enabling the predictive modeling of fundamentally quantum mechanical processes occurring in energetic materials, nuclear fuels, actinide chemistry, and fuel cells; and (b) provide a competitive advantage to LANL as we target new opportunities in emerging areas such as the Materials Genome Initiative, biofuels, and partnerships with industry. To give one example, equations-of-state and opacities in highly nonequilibrium conditions important to the weapons mission rely increasingly on quantum mechanical molecular dynamics simulations, but are constrained by the small length and short time scales presently accessible. A number of recent DOE workshops have highlighted "the need to advance theoretical models of physical and chemical objects and processes, and to develop algorithms that effectively enable those models to be simulated on modern computing systems", in particular: 1) advancing the speed and accuracy for quantum chemistry modeling on extreme-scale platforms, and 2) bridging length and time scales to enable seamless multiscale chemical reactivity modeling.

Progress

We have made significant progress on all deliverables and milestones over the last 12 months. Notable highlights include our project review, where all aspects of our work and project were ranked highly, and we hired an outstanding postdoctoral fellow who is making good progress. We are heavily involved in the 2015 IS&T summer school where 6 graduate students are exploring graph partitioning approaches to electronic structure theory, their implementation on modern computational architectures, and application to problems in chemistry and materials science. The project has already generated several peer-reviewed publications, invited talks at international conferences, as well as strong representa-

tion from team members at the CECAM workshop 'Next Generation Quantum Molecular Dynamics: Challenges and Perspectives' in Bremen, Germany. Various technical highlights and progress toward our deliverables are listed below:

A shared memory ELLPACK-R implementation of our workhorse SP2 algorithm was shown to scale linearly on 1 to 16 threads for poly(ethylene) and liquid water systems. A poly(ethylene) molecule and solvated protein were shown to scale linearly on a single Intel MIC node and a Haswell node. The ELLPACK-R SP2 algorithm was developed and shown to outperform existing sparse matrix libraries, such as MKL (CPU and MIC) and CuSparse (GPU). Additionally the distributed multi-node/multi-core graph partitioning SP2 approach was shown to exhibit good performance for a large systems using structure-based partitioning. The beginnings of a single node/multi-core/GPU graph partitioning of the SP2 algorithm has shown improved single node performance over a CPU-only version.

We designed a novel merge-based sparse-matrix multiplication algorithm for use in the SP2 algorithm which guarantees stride 1 access to the working data and thus minimizes memory divergence. This is especially important for accelerated architectures with limited cache, and disordered (large-bandwidth) matrices.

Accelerated versions of the merge-based SP2 algorithm were developed in OpenCL and CUDA. The CUDA version was co-developed with Nvidia and results presented at the 2015 GPU Technology Conference. Notably, the merge-based algorithm was shown to be more than 5x faster than Nvidia's in-house cuSparse library routines for disordered matrices, and Nvidia is interested in incorporating the method into their packages.

We are designing and implementing a basic matrix library (bml) with several internal matrix representations (dense, sparse, and graph-based). Through a common API, the application code can seamlessly utilize and switch between any of the supported internal formats. We are also addressing O(>N)bottlenecks in the LATTE code that will enables its use in simulations containing >100000 atoms.

We have investigated the use of the extended Lagrangian Born-Oppenheimer molecular dynamics formalism constant temperature dynamics. Three different approaches were considered: the NosÁ and Andersen thermostats, and Langevin dynamics. We find that the simulations based on the extended Lagrangian Born-Oppenheimer framework provides accurate canonical distributions even under approximate SCF convergence, often requiring only a single diagonalization per time step, whereas regular Born-Oppenheimer formulations exhibit unphysical fluctuations unless a sufficiently high degree of convergence is reached at each time step. The thermostated extended Lagrangian framework thus offers an accurate approach to sample processes in the canonical ensemble at a fraction of the computational cost of regular Born-Oppenheimer molecular dynamics. The algorithm, as implemented in the LATTE code, has been coupled to the accelerated molecular dynamics framework, AMDF, providing a powerful tool to the study of rare event processes with quantum accuracy.

Large-scale calculations at zero electronic temperature were demonstrated using the DFTB+ code, and we are pursuing QMD simulations using the nonorthogonal method in LATTE using the 3ob parameter set from dftb.org, which includes a parameterization for sulfur. Finally, we have demonstrated crystallographic refinement of the charge density of urea computed using DFT (VASP) and DFTB (DFTB+, LATTE) against high-resolution experimental data (0.35 Angstrom). The refinements yield a figure of merit comparable to traditional methods (SHELX), but with substantially different hydrogen displacement parameters. These results have important implications for interpretation of hydrogen displacement parameters in small-molecule crystal structure models.

An automated algorithm and code for the parameterization and optimization of tight binding models was developed for both the Hamiltonian matrix elements and the interatomic pair potentials. This code has enabled us to rapidly derive new parameterizations or improve existing models parameterization. We have also explored a novel use of the extended Lagrangian Born-Oppenheimer MD formalism in simulations of metals.

Future Work

- We shall complete the development of our graph-based, parallel density matrix build in the stand-alone PROGRESS library and link it with the LATTE quantum molecular dynamics code. Rapid, positive progress was made in the last 12 months, supported in part by the 2015 IS&T summer school.
- Application of accelerated MD to organic systems (liquids and biological) based on both adaptive self-consistent field calculations and parallelism. Publications in these areas are currently in preparation.
- Investigation of the utility of TB+U in obtaining good electronic densities of states for actinide-based materials. The continued development of automated, machine-based algorithms for parameterizing TB models (both bond integrals and the corresponding repulsive terms).

- Continued exploration of sparse matrix methods on traditional architectures as well as graphics processing units (via the cuSPARSE libraries), and more exotic devices such as MICs.
- Further work on the computation of charge densities from density functional tight binding for the simulation of protein structures and associated X-ray diffraction patterns.
- Elimination of all parts of the LATTE quantum MD code that have worse than linear scaling in terms of performance and memory use. These steps will enable > 100000 atoms to be simulated using our existing code base. Our development of the new, general 'BML' library and interface will facilitate this work.
- Publication and continued testing of our new, linear scaling algorithm for obtaining the inverse factorization of the overlap matrix in electronic structure theory.

Conclusion

Our chief result will be a general, interdisciplinary, computational capability that will enable us to analyze, understand, predict and design materials and processes directly from quantum theory, at time and length scales that are multiple orders of magnitude beyond current capacity. This will be delivered in the form of the portable and openly available program package that can be used with a broad class of electronic structure codes. The development will be guided through two testbed application systems of LANL mainstream mission relevance: 1) protein structures and 2) nuclear fuels.

Publications

Cawkwell, M. J.. Fast quantum molecular dynamics simulations of shock-induced chemistry in organic liquids. Invited presentation at American Physical Society March Meeting 2014. (Denver, 3-7 March 2014).

Cawkwell, M. J., A. M. N. Niklasson, and D. M. Dattelbaum. Extended Lagrangian Born-Oppenheimer molecular dynamics simulations of the shock-induced chemistry of phenylacetylene. 2015. JOURNAL OF CHEMICAL PHYSICS. 142 (6).

Cawkwell, M. J., J. D. Coe, S. K. Yadav, X. -. Liu, and A. M. N. Niklasson. Extended Lagrangian Formulation of Charge-Constrained Tight-Binding Molecular Dynamics. 2015. JOURNAL OF CHEMICAL THEORY AND COMPUTATION. 11 (6): 2697.

Cawkwell, M. J., M. A. Wood, A. M. N. Niklasson, and S. M. Mniszewski. Computation of the Density Matrix in Electronic Structure Theory in Parallel on Multiple Graphics Processing Units. 2014. JOURNAL OF CHEMICAL THEORY AND COMPUTATION. 10 (12): 5391.

Martinez, E., M. J. Cawkwell, A. F. Voter, and A. M. N. Niklasson. Thermostating extended Lagrangian Born-Oppenheimer molecular dynamics. 2015. JOURNAL OF CHEMICAL PHYSICS. 142 (15): 154120.

Mniszewski, S. M., M. J. Cawkwell, J. Mohd-Yussof, N. Bock, T. C. Germann, and A. M. N. Niklasson. Efficient parallel linear scaling calculation of the density matrix for Born-Oppenheimer Molecular Dynamics. 2015. Journal of Chemical Theory and Computation.

Niklasson, A. M. N., M. J. Cawkwell, E. H. Rubensson, and E. Rudberg. Canonical density matrix perturbation theory. 2014. Submitted to Phys. Rev. E, under review.

Niklasson, A. M. N., S. Mniszewski, C. F. A. Negre, M. J. Cawkwell, P. Swart, J. MohdYusof, T. C. Germann, M. Wall, N. Bock, E. H. Rubensson, and H. Djidjev. Fermi operator expansion using graph partitioning. 2015. To be submitted to Phys. Rev. Lett..

Niklasson, A. M. N., and M. J. Cawkwell. Generalized extended Lagrangian Born-Oppenheimer molecular dynamics. 2014. Journal of Chemical Physics. 141 (16): 164123.

Optimization and Control of Dynamic Networks

Angel E. Garcia
20140565DR

Introduction

Network science research has been primarily focused on the simplification of dynamic graphs to static graphs and their topological characteristics. But processes on networks such as the spread of a virus on a social network, traversal through a cyber network, and cascading failures in a power grid are critically dependent on the dynamic nature of the underlying network.

These dynamic graphs are at the heart of technological and scientific problems in electrical power grids. Deployment of new technologies, such as renewable generation and electric vehicles, is rapidly transforming electrical power networks by coupling previously distinct spatiotemporal scales and challenging traditional approaches for designing, analyzing, and operating power grids. The interactions of spatiotemporal scales in power systems are pushing the limits power engineering best practices and we need to develop general complex system models at the appropriate level of network detail necessary to isolate and analyze the relevant static, dynamic, and stochastic phenomena.

Computer networks are also inherently dynamic and non-stationary. Capturing the dynamics of user activity through coarse-level and high-fidelity modeling is critical to understanding normal activity and detection of anomalous activity. Only recently has a network-wide (graph theory) viewpoint been taken.

The CNLS brings a unique perspective in the integration of interdisciplinary approaches and ideas to the subject of network science. The CNLS has been a leader and innovator in Information Science and Technology. In particular the CNLS has helped provide new approaches in theory and modeling of networks for more than 10 years. The CNLS has helped nucleate efforts at LANL for applications of networks in neurocomputation, smart grid, and cybersecurity.

Benefit to National Security Missions

Information Science and Technology is a Laboratory strategic pillar that touches a broad spectrum of science at LANL from discovery science to pivotal program needs. This proposal directly addresses Complex Networks capabilities through the modeling of dynamic networks and with applications to cybersecurity and power systems (``smart grids'').

This proposal develops core information science and technology capabilities needed to address the open questions of the Office of Electricity that intersect with the scientific goals of DOE's Office of Advanced Scientific Computing Research (ASCR) Applied Mathematics Program such as uncertainty quantification in complex engineered networks.

This project will innovate with basic research supporting LANL's internal cybersecurity programs and Global Security programs. Effective cyber defense of the weapons complex is essential to its security and effectiveness.

Progress

We developed methods for reconstruction of spreading couplings from partial observations with a dynamic message-passing algorithm. The problem of network reconstruction and parameters estimation from diffusion data is important in many applications including understanding the structure of the epidemic spread of disease. A number of recent papers introduced efficient algorithms, based on the maximization of the likelihood of observed cascades, assuming that the full information for all the nodes in the network is available.

In this work, we focus on a more realistic and restricted scenario, in which only a partial information on the cascades is available, and show that a robust reconstruction of spreading parameters can be achieved with an algorithm based on recently introduced dynamic message-

passing equations for the spreading processes. This work is being prepared for publication.

Distributed stability and control algorithms were designed for large-scale dynamical networks. Using recent tools from semi-definite programming and sum-of-squares methods, we have been been designing computationally efficient and parallel algorithms to certify stability of interconnected systems. We have proposed two such algorithms --- 1) a decentralized "stability-ring algorithm" to certify asymptotic stability, and 2) a comparison systems based algorithm to certify exponential stability of large-scale systems. With these algorithms we designed distributed and local control policies. We are also looking at applying these stability and control algorithms to real-world systems, such as the power systems network including design of a distributed optimal reactive power dispatch algorithm for an electrical distribution feeder, with application to photovoltaic inverters.

This work is under review in the papers 1) S. Kundu and M. Anghel, "An iterative expanding-contracting ring algorithm for decentralized stability analysis", 54th IEEE Conference on Decision and Control, 2015; and 2) S. Kundu and M. Anghel, "Computation of linear comparison equations for stability analysis of interconnected systems", 54th IEEE Conference on Decision and Control, 2015

Models and control algorithms were developed for flow in natural gas pipeline systems. This area of research is becoming urgent because the recent advances in hydro-fracking for gas production have significantly increased the utilization of gas pipeline systems and made the operation and control of these systems much more challenging. We constructed models for distributed network flow systems where flows on edges are driven by node potentials. These structure of these models is very interesting and can be exploited to find optimal solutions. We showed that the network flow equations are unique and can be equivalently recast as the solution of a strictly convex optimization problem. We also analyzed the maximum throughput problem to maximize the amount of flow that can be delivered to the loads while satisfying bounds on the node potentials. We illustrated application of these general results to balanced, i.e. steady, natural gas networks and validated the theoretical results with simulations on a test case.

This work generated three papers currently under review.

We created new dynamic network models as "temporal random graphs" by generalizing two well known static random graph models. These models are relevant for studying questions about the dynamic structure of centralized computer authentication systems such as those found at most large corporate environments. he connectivity of the authentication systems creates risk that malicious users can traverse the network to gain unauthorized access computers and databases. Using these models we can study the temporal structure to answer reachability questions such as how long it would take, starting at a single computer node, to connect to most of the other computers in the network. We proved asymptotic theorems that give lower and upper bound for these times. The work has been submitted as the chapter, "Temporal Reachability in dynamic networks."

Future Work

For FY16 we will focus on the following tasks.

- Complete results on reconstruction of spreading networks and further development of dynamic message passing techniques for this application.
- Construct ODE/PDE models for power and gas systems that incorporate the different devices and controls that are making inroads into electrical distribution networks, e.g., PV systems, electric vehicle charging, and frequency responsive loads. The ODE/PDEs approach will address the interaction of emergent phenomena arising from the interaction of new smart-grid components.
- Develop reduced models for natural gas pipe network flow along with strategies for optimization and control. Seek theorems about the structure and optimization of these networks and develop algorithms that exploit the theoretical results.
- Sponsor two workshops: "Physics informed machine learning," which will build a new community of researchers aiming to exploit physics to create higher performance algorithms for learning and classification; and "Conference on Data Analysis (CODA). The 3rd conference on big data and statistics will focus of research across the DOE complex.

Conclusion

We expect to develop research results with three interlocking themes:
Dynamic Networks: develop models and algorithms for temporal random graphs; seek theorems for connectivity and reachability in the models; and explore the range of possible temporal correlation patterns.
Power Systems: create comprehensive ODE/PDE models for power systems; develop reduced-order stochastic models of network power-outage cascades; develop mathematical tools to capture system energy and thermal states.
Cybersecurity: model as dynamic networks; develop tech-

niques including hierarchical models to capture statistics of bursty network communication patterns; create inference methods and fit cyber authentication network data to the temporal random graph models.

Publications

Bienstock, , Chertkov, and Harnett. Chance-Constrained Optimal Power Flow: Risk-Aware Network Control under Uncertainty. 2014. SIAM REVIEW. 56 (3): 461.

Catanach, T., and M. Garcia. Power System Dynamic State Estimation using a Layered Local-Global Method. IEEE Transactions on Power Systems.

Chernyak, V. Y., Chertkov, Bierkens, and H. J. Kappen. Stochastic optimal control as non-equilibrium statistical mechanics: calculus of variations over density and current. 2014. JOURNAL OF PHYSICS A-MATHEMATICAL AND THEORETICAL. 47 (2).

Doerfler, , M. R. Jovanovic, Chertkov, and Bullo. Sparsity-Promoting Optimal Wide-Area Control of Power Networks. 2014. IEEE TRANSACTIONS ON POWER SYSTEMS. 29 (5): 2281.

Farrell, M., T. Goodrich, N. Lemons, F. Reidle, F. Villaamil, and B. Sullivan. Hyperbolicity, degeneracy, and expansion of random intersection graphs. 2014. arXiv.

Frolov, , Backhaus, and Chertkov. Efficient algorithm for locating and sizing series compensation devices in large power transmission grids: I. Model implementation. 2014. NEW JOURNAL OF PHYSICS. 16.

Frolov, , Backhaus, and Chertkov. Efficient algorithm for locating and sizing series compensation devices in large power transmission grids: II. Solutions and applications. 2014. NEW JOURNAL OF PHYSICS. 16.

Garcia, M., S. Backhaus, and R. Bent. Power Flow-Based Adaptive Generator Controls. Invited presentation at 52nd Annual Allerton Conference on Communication, Control, and Computing. (Allerton, Illinois, 1-3 Oct. 2014).

Garcia, M., T. Catanach, S. V. Wiel, and R. Bent. Line Outage Localization using Phasor Measurement Data in Transient State. IEEE Transactions on Power Systems.

Generous, N., G. Fairchild, A. Deshpande, S. Y. Del Valle, and R. Priedhorsky. Global disease monitoring and forecasting with Wikipedia. . 2014. arXiv.

Goddard, , Klose, and Backhaus. Model Development and Identification for Fast Demand Response in Commercial HVAC Systems. 2014. IEEE TRANSACTIONS ON SMART GRID. 5 (4): 2084.

Hagberg, , and Lemons. Fast Generation of Sparse Random Kernel Graphs. 2015. PLOS ONE. 10 (9).

Jaworsky, , Turitsyn, and Backhaus. THE EFFECT OF FORECASTING ACCURACY ON THE SIZING OF ENERGY STORAGE. 2014. In 7TH ANNUAL DYNAMIC SYSTEMS AND CONTROL CONFERENCE, 2014, VOL 2.

Kundu, S., and I. A. Hiskens. Overvoltages due to Synchronous Tripping of Plug-in Electric-Vehicle Chargers Following Voltage Dips. 2014. IEEE Transactions on Power Delivery. 29 (3): 1147.

Kundu, S., and I. Hiskens. Nonlinear dynamics of hysteresis-based load controls. 2014. In The 19th World Congress of the International Federation of Automatic Control. (Cape Town, South Africa, 24-29 Aug. 2014). , p. 5419. Cape Town: IFAC.

Lubin, M., and Y. Dvorkin. A Robust Approach to Chance Constrained Optimal Power Flow with Renewable Generation. IEEE Transactions on Power Systems.

Mak, T., P. Van Hentenryck, A. Zlotnik, H. Hijazi, and R. Bent. Efficient Dynamic Compressor Optimization in Natural Gas Transmission Systems. Invited presentation at American Control Conference 2016. (Boston, 6-8 Jul. 2016).

Mehta, , N. A. Sinitsyn, Backhaus, and B. C. Lesieutre. Safe control of thermostatically controlled loads with installed timers for demand side management. 2014. ENERGY CONVERSION AND MANAGEMENT. 86: 784.

Misra, S., M. W. Fisher, S. Backhaus, R. Bent, M. Chertkov, and F. Pan. Optimal compression in natural gas networks: A geometric programming approach. 2015. IEEE Transactions on Control of Network Systems. 2 (1): 47.

Nagarajan, H., E. Yamangil, R. Bent, S. Backhaus, and P. Van Hentenryck. Optimal Resilient Transmission Grid Design. Invited presentation at Power Systems Computation Conference 2016. (Genoa, Italy, 20-24 Jun. 2016).

Nagarajan, H., and S. Rathinam. On maximizing algebraic connectivity of networks for various engineering applications. Invited presentation at European Control Conference (ECC). (Linz, Austria, 15-17 Jul. 2015).

Stolbova, , Backhaus, and Chertkov. Fault-induced delayed voltage recovery in a long inhomogeneous power-distribution feeder. 2015. PHYSICAL REVIEW E. 91 (2).

Sulc, , Backhaus, and Chertkov. Optimal Distributed Control of Reactive Power Via the Alternating Direction Method of Multipliers. 2014. IEEE TRANSACTIONS ON ENERGY CONVERSION. 29 (4): 968.

Sundar, K., H. Nagarajan, M. Lubin, L. Roald, S. Misra, R. Bent, and D. Bienstock. Unit Commitment with N-1 Secuity and Wind Uncertainty. Invited presentation at

Power Systems Computation Conference 2016. (Genoa, Italy, 20-24 Jun. 2016).

Tapia, A., N. LaLone, E. MacDonald, R. Priedhorsky, and M. Hall. Crowdsourcing rare events: Using curiosity to draw participants into science and early warning systems. . 2014. In International Conference on Information Systems for Crisis Response and Management (ISCRAM), 2014. (University Park, Pennsylvania, 18-21 May, 2014). , p. 135. Pennsylvania: ISCRAM.

Turcotte, M.. Detecting localised anomalous behaviour in a computer network . 2014. In Advances in Intelligent Data Analysis XIII, LNCS 8819 . (Leuven, Belgium, 30 Oct - 1 Nov, 2014). , p. 321. Belgium: Springer.

Yamangil, E., R. Bent, and S. Backhaus. Designing Resilient Electrical Distribution Grids. 2014. arXiv:1409.

Yamangil, E., R. Bent, and S. Backhaus. Designing Resilient Electrical Distribution Grids. Invited presentation at Proceedings of the 29th Conference on Artificial Intelligence. (Allerton, Illinois, 1-3 Oct. 2014).

Scalable Codesign Performance Prediction for Computational Physics

Stephan J. Eidenbenz
20150098DR

Introduction

We will develop a performance-prediction capability that relies on modeling architectural and algorithmic details of a computational-physics code running on a specified high-performance computing (HPC) architecture. This capability will fundamentally benefit a large number of HPC code projects by providing techniques for rapid evaluation of novel algorithmic ideas; rapid evaluation of middleware "mapping" concepts; optimizing method & architecture parameters for performance; and perhaps most intriguing semi-automated code generation for crucial subroutines. After the project ends, the performance prediction capability will be useable with minimal additional effort for other computational physics domains and architectures of the generations after next, and for decision support in HPC platform procurement to test vendor proposals against request specifications.

Building the performance prediction capability is our first goal, which will have a focus on models for state-of-the-art and conjectured architectures. Our second goal is to use the capability to assess novel solutions to the key exa-scale challenges of the data motion/movement, high-parallelism, and fault tolerance applied to radiation transport and hydrodynamics methods.

Our initial algorithmic ideas that we will develop, model and assess for the applications include: Determining optimal ways to hide communication and/or memory latencies on specific devices for discrete ordinates mesh sweeps and analyzing tradeoffs of non-sweep-based algorithms that increase independent work units and data movement for deterministic radiation transport. Models of the random access of memory and stochastic work generation of a Monte Carlo fixed source calculation and various approaches to task-based parallelism for stochastic radiation transport. Rapid analysis of tree-code algorithms on different architectures for hydrodynamics.

An initial set of middleware technologies that we will develop includes: Polyhedral optimization methods to minimize data motion, load-balancing schemes vs. data movement requirements, static graph-based automated parallelization approach for innermost loop computations of physics domain codes, Just-In-Time Parallelization schemes and alternatives to checkpoint-restart paradigm for failure tolerance.

Benefit to National Security Missions

Our future computational physics code base for hydrodynamics and radiation transport are of fundamental importance to DOE and LANL. Maintaining LANL's leadership role in national security will depend on our ability to consistently provide performance improvement in our codes for emerging architectures. Additionally, these techniques will be applicable to other application domains, in particular climate simulations and large-scale infrastructure simulations. Previous work related to AMD resulted in a successful transition of that project to the DOE Office of Science BES, which will now support the implementation and physics discovery work. Similarly in this project: If we are successful at identifying algorithmic variations with substantial predicted performance gains, programmatic sources, e.g., ASC, may be willing to support follow-on code development made possible by a successful LDRD project.

Progress

The performance prediction project has structured its work along three focus areas: i) Develop and validate hardware models, ii) develop and validate software models, and iii) design and implement the required scalable discrete event simulation framework. The main results are as follows.

Detailed models were developed for the Cielo supercomputer architecture and are in the process of validating these models on benchmark applications. We have developed a model for the upcoming Trinity super-

computer as far as its specification is known and will run predictive runs of benchmark software and also radiation transport models as next steps. (iii) We have also built and already partially validated a few desktop machine architectures.

A model of the radiation transport mini-app SNAP that we call SNAPSim was build and validated. We have designed a similar model for the SPH oct tree code. We will validate this in a next step. We have also built models for the POlyBench benchmark suite. In addition, a large molecular dynamics project called SpecTADSim has been built in our Simian framework that is ready for publication

We developed a Lua or Python-based parallel discrete event simulation system called Simian that we have open sourced. Three publications are under review for it.

Future Work

For FY16 (year two of the DR), we plan to continue to improve upon the work performed in FY15. We have created a Python-based discrete event simulation system called Simian that will serve as our primary simulation tool going forward. We consider our work going forward as categorized into three broader tasks:

1. Continue to add more features to the hardware models that describe the function of relevant architectures, including internode data movement (interconnect modeling), intranode data movement (memory hierarchy and cache structure modeling), failure resilience, and power consumption. Each new addition to the hardware modeling framework will be generalized and parameterized for simple extension to different architectures.
2. Expand our catalog of physics application domains to include stochastic radiative transport. Consider the inclusion of different computational kernels associated with radiative transport and hydrodynamics applications to ensure we are capturing all the relevant computational challenges associated with these types of numerical simulations. Begin exploring parallel solution algorithmic alternatives and their suitability for our existing suite of hardware models.
3. Hardware and software model validation will be an important part of our second year activities. Ensuring that we have sound models will allow us to explore variations with confidence that alternatives are analyzed fairly and warrant further examination.

Validation in the sense of Task 3 refers to the comparison of relevant numerical simulation with an actual code on an actual cluster compared to the simulated result. It is an important step in our ability to demonstrate the value in rapid performance prediction using discrete event simulation software. Task 2 may also include the development of a semi-formal process for evaluating the computational intensity of existing production codes for easier implementation within the discrete event simulator framework.

Conclusion

Based on results for different application domains and on preliminary analysis for transport and hydrodynamics, we anticipate to achieve at least one order of magnitude performance improvement for stochastic radiation transport codes as these codes have undergone few optimization efforts for current node designs of many cores and more complicated memory hierarchies. Deterministic radiation transport codes and smoothed particle hydrodynamics codes have seen some optimization and we expect our models to predict another 2-3X improvement in performance.

Publications

Chapuis, G., S. Eidenbenz, N. Santhi, and E. J. Park. Simian integrated framework for parallel discrete event simulation on GPUs. To appear in WinterSim 2015. (Huntington Beach, California, 6-9 Dec. 2015).

Chapuis, G., S. Eidenbenz, and N. Santhi. GPU Performance Prediction Through Parallel Discrete Event Simulation and Common Sense. To appear in Valuetools 2015. (Berlin, Germany, 14-16 Dec. 2015).

Park, E. J., S. Eidenbenz, N. Santhi, G. Chapuis, and B. Settlemyer. Parameterized benchmarking of parallel discrete event simulation systems: communication, computation, and memory. To appear in The Winter Simulation Conference. (Huntington Beach, CA, 6-9 Dec. 2015).

Santhi, N., S. Eidenbenz, and J. Liu. The Simian Concept: Parallel Discrete Event Simulation with Interpreted Languages. To appear in 2015 Winter Simulation Conference. (Huntington Beach, CA, 6-9 Dec. 2015).

Zamora, R. J., A. F. Voter, D. Perez, N. Santhi, S. M. Mniszewski, S. Thulasidasan, and S. Eidenbenz. Discrete Event Performance Prediction of Speculatively Parallel TAD. SIAM Journal on Scientific Computing.

Cyberphysical Systems and Security

Scott N. Backhaus
20150215DR

Introduction

Many critical infrastructures, e.g., electric power grids and natural gas pipelines, are cyberphysical systems—physical networks whose flows are governed by the law of physics but are regulated by a control system coupled to cyber networks that transmit the information required to optimize and control the physical networks for reliability and efficiency. Crucial to the defense of cyberphysical systems is the concept of intrusion detection and localization, however, this is not sufficient. If a system is under attack, it cannot simply be brought down to purge the attacker. Doing so would grant the attacker his objectives, i.e. wide spread denial of the services from the cyberphysical network. A proportional response is required.

The overarching objective of this work is to develop advanced approaches to cyberphysical defense, which can be broken down into the following goals:

- Detect and localize an attacker within the cyberphysical network without reference to a predefined attack vector. Attackers are creative and detection methodologies cannot be based on scripted attack scenarios.
- Develop algorithms for proportional response and designing resilient cyberphysical networks—Proportional responses to attacks should weigh the estimated network degradation from the attack and the degradation caused by the response. Resilient cyberphysical designs will greatly improve this balance in favor of the cyberphysical operators.
- Deploy, demonstrate and validate—The efficacy of cyberphysical intrusion detection and response methodologies will improve at much faster rates when their development and refinement is closely coupled with real-world experimentation that validates strengths and reveals weaknesses.

Benefit to National Security Missions

Cyberphysical systems are crucial to the reliable delivery of energy, water, and other resources, creating strong connections to LANL's National Security and Energy Security missions including those US Government agencies that monitor, analyze, or develop technology for critical infrastructure, e.g. DOE Office of Electricity, DOE Energy Efficiency and Renewable Energy, DOE Fossil Energy, and Department of Homeland Security.

These systems are composed of interdependent complex networks described by disparate mathematical models creating scientific challenges that go well beyond the modeling and analysis of the individual networks. Integration of approaches from complex systems, statistical physics, machine learning, and optimization will create a holistic and uniquely LANL approach that is able to localize attacks and develop appropriately scaled proportional responses. Both DOE and DHS are creating and running new programs in cyberphysical systems a creating significant programmatic pull. Many efforts in these programs are based on best practices or standard engineering analyses. Our approach based on the science of complex networks and probabilistic methods will advanced detection and defense capabilities to the US Government agencies identified above. Components of the NNSA Complex, including our own Laboratory, are cyberphysical systems with complex security issues, and this work will build capabilities for protecting the Complex.

Progress

- Established automated process for collecting large data sets and building a data base for collection of physical data from the NSSB
- In process and near completion: Established a communications monitoring capability to detect communication events on the control/serial network in the NSSB. The combination of this data and the

data in #1 forms a unique data set for our research and the rest of the community investigating cyberphysical systems.
- Exploring two signal processing/statistical methods for removing background signals and tends to extract fluctuations in the physical data time series.
- Exploring two methods for reconstructing graphical models of the NSSB cyberphysical system from correlations in the physical data streams.

Future Work

Planned milestones by FY16 year end:

- Begin intrusion detection experiments on NSSB
- Develop machine learning algorithms for graphical models of continuous variables and apply to data from NSSB test bed. Extend methods for continuous variables to discrete variables
- Build an interdependent network model of the NSSB suitable for network optimization and optimal network defense task in BY2.

Conclusion

Information theory: We will develop algorithms for online learning of graphical models using operational time-series data collected from sparse measurements on cyberphysical systems.

Network optimization: We will develop new algorithms for decomposing and efficiently solving difficult multi-level optimization problems that involve discrete and continuous variables.

Experimental validation: We will develop a unique cyberphysical test bed where we will deploy and test the tools and methods developed in the information theoretic and optimization thrusts.

Disruptive Innovation in Numerical Hydrodynamics

Jacob I. Waltz
20130005DR

Abstract

We describe the accomplishments and impact of the LDRD Directed Research Project "Disruptive Innovation in Numerical Hydrodynamics," executed over the time frame FY2012-FY2015. The goal of this project was to develop a new class of numerical methods applicable to shock hydrodynamics phenomena and designed for advanced computer architectures. The research led to several key breakthroughs and conclusions, which are expected to influence a variety of LANL programs.

Background and Research Objectives

This project was fundamentally motivated by two observations: first, a decreased rate of progress in the development of modeling and simulation tools by the Advanced Simulation and Computing (ASC) program; and second, the imminent (at the time of the proposal) large-scale transition in High Performance Computing (HPC) from conventional to so-called advanced or emerging architectures. The high-level goal of this project, therefore, was to develop a novel simulation methodology that combined algorithmic advances with effective utilization of new hardware systems. Taken together, the combined capability was expected to enable a dramatic leap forward in predictive capability.

The particular focus of this project was numerical methods for the simulation of shock hydrodynamics problems, which we define as the study of material response to shock waves and associated physical phenomena. This field of physics is central to a broad portion of the LANL mission space (e.g. Inertial Confinement Fusion, Stockpile Stewardship, and dynamic experiments) as well as numerous fundamental science and engineering areas (e.g. astrophysics and materials science). Mathematically, this physics is described by a set of coupled, nonlinear partial differential equations. These equations are supplemented by constitutive models, such as an equation of state, that describe material-specific characteristics. Computer codes that simulate shock hydrodynamics problems – often referred to as "hydro codes" –solve these equations numerically given some specific problem description that includes geometry information, material densities, initial pressures and temperatures, etc. In this manner the governing equations are transformed from a continuous form with no closed-form analytic solution, to a discrete system that can be solved numerically on a computer. The approach used to carry out this transformation is the numerical method.

Historically, these equations have been solved using a discrete representation of the problem based on quadrilateral (in 2D) or hexahedral (in 3D) cells: the spatial domain of the problem is subdivided into a collection of non-overlapping cells (referred to in toto as the computational "mesh" or "grid"), and the governing equations are solved numerically for each cell or alternatively the cell vertices. An additional choice is the reference frame in which the governing equations are solved. In the so-called Eulerian description, the governing equations are written for and solved in a reference frame that is at rest relative to the material, i.e. the "Laboratory" frame. In the so-called Lagrangian description, the governing equations are written for and solved in a reference frame that moves with the material, i.e. the "co-moving" frame. A third description, referred to as the Arbitrary Lagrangian-Eulerian (ALE) approach, also is possible. In the ALE description the equations are written for and solved in a reference frame that moves arbitrarily relative to the laboratory frame and the material; the ALE description therefore contains both the Eulerian and Lagrangian descriptions as limiting cases, and can be viewed as the most general.

ALE methods based on triangular (in 2D) or tetrahedral (in 3D) cells have been explored for LANL applications, but had not been successfully developed for a number of reasons; detailed technical explanations can be found in both the original proposal and in two of the journal articles produced by the project: N Morgan et al, J Com-

put Phys 281:614-652 (2015); and J Waltz et al Int J Numer Meth Fluids 76:129-146 (2014). However, numerical methods based on triangular and tetrahedral meshes have some key advantages over quadrilateral and hexahedral approaches, the most important of which for this project are rapid problem definition using commodity tools; simpler and more easily optimized data structures; and potentially higher accuracy. For these and other reasons, tetrahedral-based approaches have gained widespread acceptance in the Computational Fluid Dynamics (e.g. aircraft aerodynamics) and Computational Electromagnetics communities, but were not yet demonstrated to be suitable for shock hydrodynamics applications.

The primary technical goal, therefore, was to develop a tetrahedral-based numerical method for shock hydrodynamic simulations that overcame the historical difficulties associated with such methods. However, the imminent transition to advanced computer architectures created an additional constraint, namely, that any new method should also be designed a priori for these new platforms. Without taking this constraint into account, any new method might become a dead-end path on future HPC technology. Likewise, deployment of existing algorithms on emerging architectures would not fundamentally change the predictive capability of those algorithms. With this perspective in mind, a secondary technical goal was that the new method be designed a priori for advanced computer architectures.

Based on these goals and the intended future application of the research results, the original project proposal defined the following three milestones (one per fiscal year):

FY2013: Demonstrate a tetrahedral-based numerical method for single-material shock hydrodynamic problems in the ALE reference frame

FY2014: Demonstrate effective use of advanced computer architectures

FY2015: Extend the single-material tetrahedral-based ALE method to multiple materials with strength

The order of these milestones was based on the level of perceived risk associated with each task. In what follows we describe the R&D approach and the accomplishments for each of the above.

Scientific Approach and Accomplishments

The task with the most perceived risk in this proposal involved the development of a tetrahedral-based numerical method for single-material shock hydrodynamic problems in the ALE reference frame. Two parallel R&D approaches with different risks were therefore pursued. The first approach involved the extension of a proven Eulerian method to the more general ALE description, and subsequently into a Lagrangian-like regime. The major uncertainty with this approach was whether or not the method would be susceptible to large errors when applied to shock hydrodynamics problems. The second approach involved the extension of a modern Lagrangian method for quadrilateral cells to the more general case of tetrahedral cells, and subsequently into the more general ALE description. The major uncertainty with this approach was whether or not the method could be successfully adapted to tetrahedral cells.

Ultimately, both approaches proved to be successful, and together were described in a total of six journal articles. Three of these articles have been ranked among the top downloaded articles for their respective journals. More importantly, the tetrahedral-based methods developed in this project were demonstrated to be 1000-10000 times faster than the methods used in production ASC codes, when measuring time to solution for a given level of accuracy.

The primary focus in FY14 was effective utilization of advanced architectures. The original target architecture described in the proposal was the Graphics Processing Unit (GPU). However, the target architecture was changed to the Intel Many-Integrated-Core (MIC) architecture based on the anticipated results (which were later confirmed) of the Trinity supercomputer procurement. The basic approach for this work was to take proven techniques for conventional computer architectures, and attempt to apply them to the MIC-type systems. An initial performance comparison of different data structures used by the most compute intensive portions of the numerical methods was first performed (L. D. Risinger et al, LA-UR-13-28518, 2013). This was followed by a more detailed study of overall application performance, which was eventually published in J. Waltz et al, Int J Numer Meth Fluids 77:319-333 (2015). These studies led to two important conclusions: first, although the vector performance of the Intel MIC is often cited as a key advantage over conventional architectures, these studies demonstrated that effective use of threads was key to maximizing performance on the Intel MIC; second, data structures and optimization techniques originally developed for conventional architectures could make effective use of the Intel MIC with little to no modification.

Due to a budget cut of approximately $200k in FY14, detailed performance optimization studies originally planned for FY15 were deferred so that hierarchical parallelism could be explored. Parallelism in shock hydrodynamic codes is typically based on the concept of domain decomposition: the spatial extent of the problem is decomposed

into sub-domains, and the governing equations are solved in parallel on each sub-domain by separate compute units. Domain decomposition has been the standard approach for ASC codes since the advent of the ASCI era. An alternative parallelization strategy is the shared memory approach. In this method, a single memory image of the problem (or a subset of the problem) is shared by multiple compute units. Each unit then operates on a portion of this memory image using e.g. threads. Both approaches have their relative advantages and disadvantages, and are appropriate for different computing regimes. The relevant consideration for this work however was that advanced computer architectures were expected to require a hybrid approach that employed domain decomposition across major compute units, and shared memory within the major compute units. For example, the Intel MIC architecture consists of 60-70 individual compute cores, each of which can further support up to four individual processes (threads). On a large system composed of Intel MIC chips (i.e. a Trinity-like system), one could envision using domain decomposition to parallelize across the different MIC chips, and using threads to parallelize within each MIC chip. Domain decomposition was therefore implemented into the computer software in use for this research, and a detailed performance study was undertaken to assess the performance characteristics of the hybrid approach. While the results of this analysis have not been published (again due to resource limitations), they were described in various presentations (e.g. LA-UR-15-21734). The important conclusion from these studies is that on the Intel MIC, hybrid parallelization strategies were faster than a pure domain decomposition approach.

The final milestone, extension of the tetrahedral-based method to multiple materials with strength, was considered from the beginning of the project to be lower risk than the previous two milestones. The approach used for this milestone was to extend techniques demonstrated for Eulerian methods to the ALE reference frame. This extension was successfully demonstrated without strength for some very basic initial test problems, but the work was somewhat impacted by staff availability and a $200k budget reduction in FY15. Progress on demonstrating the methodology with material strength also was impacted by staff availability.

On the other hand, some unexpected research breakthroughs were accomplished in FY15 in the area of level set methods. Level set methods are a class of numerical techniques used to compute the motion of surfaces and interfaces. Examples relevant to this work include both material interfaces and high explosive burn fronts. This project was able to demonstrate, for the first time, a fast, accurate level set method for tetrahedral grids. Unfortunately, although the technical work was completed in FY15, documentation of the work in journal articles was not yet complete by the time of this writing; however, the ASC program has a high level of interest in this work.

Impact on National Missions

The impact of this work on National Missions has yet to be fully determined. The ASC Program Office declined to fund a proposal to develop a new production simulation tool based directly on the results of this research project, but has agreed to support a low-level of follow on research to address certain remaining questions – in particular, how to simulate contact mechanics within the tetrahedral-based formulation. The outcome of these studies could potentially lead to a more direct adoption of this project's research results. The results of this project also are expected to impact technical choices made within existing ASC projects. For example, the new level set methods are a strong candidate for implementation into existing simulation tools, and the performance studies on the Intel MIC architecture are expected to influence how existing tools are ported to the Trinity Phase 2platform.

The results of this project also have generated strong interest in communities beyond ASC. These include the nuclear detection and seismo-acoustic coupling community; the nuclear blast effects modeling community; the high-explosives experimental community; and the DOE/DOD Joint Munitions Program. Discussions with all of these programs are ongoing and are expected to result in future mission contributions.

Publications

Canfield, T. R., M. R. J. Charest, N. R. Morgan, L. D. Risinger, J. Waltz, and J. G. Wohlbier. Simulation of multi-material flows using a finite element Riemann solver and adaptive unstructured grids. Presented at Conference on Numerical Methods for Multi-Material Flows. (San Francisco, CA, 2-6 Sep. 2013).

Canfield, T. R., N. R. Morgan, L. D. Risinger, J. Waltz, and J. G. Wohlbier. Manufactured solutions for the three-dimensional Euler equations with relevance to inertial confinement fusion. Presented at American Society of Mechanical Engineers Verification and Validation Symposium. (Las Vegas, NV, 22-24 May 2013).

Long, A. R., R. G. McClarren, J. Waltz, and J. G. Wohlbier. Implicit Monte Carlo adaptions for tetrahedral meshes with node-based unknowns. Presented at American Nuclear Society Joint International Conference on Mathematics and Computation. (LaGrange Park, IL, April 2015).

Long, A. R., T. R. Canfield, M. R. J. Charest, N. R. Morgan, J. Waltz, and J. G. Wohlbier. Implicit Monte Carlo discretizations for tetrahedral meshes with node-based unknowns. Presented at Nuclear Explosives Code Developers Conference. (Los Alamos, NM, 20-24 Oct. 2014).

Morgan, N. R., J. Waltz, D. E. Burton, M. R. J. Charest, T. R. Canfield, J. G. Wohlbier, J. Bakosi, and A. R. Long. A 3D Arbitrary Lagrangian Eulerian (ALE) hydrodynamic approach for tetrahedral meshes. Presented at Conference on Numerical Methods for Multi-Material Fluid Flow. (Wurzburg, Germany, 7-11 Sep 2015).

Morgan, N. R., J. Waltz, D. E. Burton, M. R. J. Charest, T. R. Canfield, and J. G. Wohlbier. A Godunov-like point-centered essentially Lagrangian hydrodynamic approach. 2015. Journal of Computational Physics. 281: 614.

Morgan, N. R., J. Waltz, D. E. Burton, M. R. J. Charest, T. R. Canfield, and J. G. Wohlbier. A point-centered arbitrary Lagrangian Eulerian hydrodynamic approach for tetrahedral meshes. 2015. Journal of Computational Physics. 290: 239.

Morgan, N. R., J. Waltz, D. E. Burton, T. R. Canfield, L. D. Risinger, J. G. Wohlbier, and M. R. J. Charest. A Godunov-like point-centered ALE finite element hydrodynamic approach. Presented at Conference on Numerical Methods for Multi-Material Fluid Flow. (San Francisco, CA, 2-6 Sep. 2013).

Morgan, N. R., J. Waltz, D. E. Burton, T. R. Canfield, M. R. J. Charest, and J. G. Wohlbier. Application of a multidimensional approximate Riemann solution to point centered hydrodynamics on tetrahedral meshes. Presented at Nuclear Explosives Code Developers Conference. (Los Alamos, NM, 20-24 Oct. 2014).

Risinger, L. D., J. Waltz, T. R. Canfield, M. R. J. Charest, N. R. Morgan, and J. G. Wohlbier. Threading of indirect gather-scatter algorithms for 3D unstructured flow solvers. 2013. Internal LANL report LA-UR-13-28518.

Waltz, J.. GPU and multicore acceleration of a 3D unstructured mesh Eulerian-AMR hydrocode. Presented at Nuclear Explosives Code Developers Conference. (Livermore, CA, 22-26 Oct. 2012).

Waltz, J.. Multimaterial hydrodynamics simulation for advanced architectures. 2015. Presentation given to DOE/DOD Joint Munitions Program 10th Annual Users' Forum, Arlington, VA (2015); LA-UR-15-21374.

Waltz, J., J. G. Wohlbier, L. D. Risinger, T. R. Canfield, M. R. J. Charest, A. R. Long, and N. R. Morgan. Performance analysis of a 3D unstructured mesh hydrocode on multi- and many-core architectures. 2015. International Journal for Numerical Methods in Fluids. 77: 319.

Waltz, J., N. R. Morgan, T. R. Canfield, M. R. J. Charest, L. D. Risinger, and J. G. Wohlbier. A 3D finite element arbitrary Lagrangian-Eulerian method for shock hydrodynamics on unstructured grids. 2014. Computers & Fluids. 92: 172.

Waltz, J., N. R. Morgan, T. R. Canfield, M. R. J. Charest, and J. G. Wohlbier. A nodal Godunov method for Lagrangian shock hydrodynamics on unstructured tetrahedral grids. 2014. International Journal for Numerical Methods in Fluids. 76: 129.

Waltz, J., N. R. Morgan, T. R. Canfield, M. R. J. Charest, and J. G. Wohlbier. A Godunov ALE method for 3D unstructured grids. Presented at Nuclear Explosives Code Developers Conference. (Los Alamos, NM, 20-24 Oct. 2014).

Waltz, J., T. R. Canfield, M. R. J. Charest, N. R. Morgan, L. D. Risinger, and J. G. Wohlbier. Operator splitting and time accuracy in Lagrange plus remap methods. Presented at Conference on Numerical Methods for Multi-Material Fluid Flow. (San Francisco, CA, 2-6 Sep. 2013).

Waltz, J., T. R. Canfield, N. R. Morgan, L. D. Risinger, and J. G. Wohlbier. Verification of a three-dimensional unstructured finite element method using analytic and manufactured solutions. 2013. COMPUTERS & FLUIDS. 81: 57.

Waltz, J., T. R. Canfield, N. R. Morgan, L. D. Risinger, and J. G. Wohlbier. Manufactured solutions for the three-dimensional Euler equations with relevance to Inertial Confinement Fusion. 2014. Journal of Computational Physics. 267: 196.

Wohlbier, J. G., L. D. Risinger, T. R. Canfield, M. R. J. Charest, N. R. Morgan, and J. Waltz. Programming for modern architectures in the CHICOMA hydrocode. Presented at Conference on Numerical Methods for Multi-Material Fluid Flow. (San Francisco, CA, 2-6 Sep. 2013).

Empowering the Expert: Machine Learning with User Intelligence

Reid B. Porter
20130013DR

Abstract

Experts are very good at understanding and exploiting domain-specific data, but in nearly all science and defense applications, there is too much data for experts to look at it all. Machine Learning provides tools that can clean up, filter, and identify the most relevant subsets of data. However, because these tools lack domain-specific input, they are not as accurate as they could be and experts do not fully trust them. Machine Learning with User Intelligence advances the field of Interactive Machine Learning (IML) to provide a middle ground that combines the complementary strengths of experts and machines in data analysis.

This project has made a wide range of contributions to Interactive Machine Learning that span theory, algorithms and applications. These contributions have been recognized in the broader research community with multiple best paper and invited speaker awards, and acceptance to the highest impact machine learning conferences. The project's contributions have also been recognized in programmatic activities, and a number of new projects are underway to transition the theoretical and algorithmic advances made by the project into practical software and operational tools.

In science and defense, we have critical applications where experts must understand and validate tool outputs before making a decision. Fortunately, experts are also highly motivated and willing to interact with the tools in a much more sophisticated way than current systems allow. This project has shown that Los Alamos, where experts in machine learning can work side-by-side with experts in science and defense, is well positioned to exploit the more motivated and informed user base and address the fundamental challenges holding back machine learning in specialized domains.

Background and Research Objectives

Scientists and intelligence analysts are very good at understanding and exploiting the specialized datasets with which they work; the problem is that there is too much of this data for them to look at. Data processing tools help to clean up, filter and identify the most relevant subsets of data, but recent developments in machine learning indicate that there is an opportunity to enhance the efficiency and accuracy of this process, by involving the user in a more interactive dialog.

Traditional machine learning employs a fixed set of labels, supplied up-front by the user, to optimize data processing tools before they are applied to a larger dataset or data archive. This approach has proven successful both in theory (rigorous proofs) and in practice (commercial applications). Machine Learning with User Intelligence pushes the state of the art in two main directions:

From up-front learning to interactive learning: Traditional machine learning tools stop when the human steps in. This means the expert is still the bottleneck in data exploitation: spending too much time in tedious and repetitive post-processing tasks and not enough time on validation and research. Interactive machine learning starts when the human steps in, and tools are a force multiplier, where the user's intelligence is the force to be multiplied, not an expense to be minimized.

From label learning to relational learning: Machine learning with user intelligence formalizes the interactive dialog with relational objects, stated in terms of motifs, clusters, alignments, matches and other generalizations of standard labels. By providing additional interface "bandwidth" between the domain expert and the data processing tool (and thus creating a better expression of the dialog in terms of Graphical Models), higher quality associations are produced, and more effective tools can be built.

The project has three main objectives:

- Identify and formalize new classes of user-interac-

tion that would benefit experts

- Develop learning algorithms that translate these interactions into tools
- Apply these tools to analysis bottlenecks in the expert's application

Scientific Approach and Accomplishments

Over the course of this project Interactive Machine Learning has gained momentum within the broader research community, and due to the timing of this project, we have been privileged to have played a role in this emerging field. One of our first accomplishments was to publish a comprehensive review article in the IEEE, Computers in Science and Engineering [1]. We were invited to present this material at one of the first workshops on Interactive Machine Learning, which was held in the spring of 2013. In the spring of 2014, we hosted our own workshop on Interactive Machine Learning at Los Alamos. This event attracted leading researchers from academia (Caltech, Cornell, CMU, Indiana and UCSC), industry (Microsoft, Google) and government (JPL) and we continue to benefit from students and collaborations from this event. Interactive Machine Learning now appears to be a regular workshop in mainstream machine learning conferences, and our team presented at the most recent workshop on Interactive Data Exploration and Analysis at the Knowledge Discovery and Data Mining (KDD) conference.

Our review article provided a unified view of Interactive Machine Learning research and also a road-map for our project (and the research community). The roadmap articulates two main technical thrusts, which we call the 'Training Dialog' (moving from up-front learning to interactive learning) and the 'Training Vocabulary' (moving from label learning to relational learning). Common to both of these thrusts is the need to balance theory and practice, and our project contained a diverse range of staff (from statistical physicists to application specialists) in order to advance both the underlying mathematics, and the specific tools used by end-users in particular applications. We now describe the projects main contributions in more detail under these two broad categories of work.

Training Vocabulary

Graphical Models provide a general purpose framework for learning and representing dependencies among variables in multivariate data. Graphical Models are key to expanding the training vocabulary because they provide a balance of rigor and flexibility on the theory front and domain adaptability on the interactivity front.

Theory: A significant theoretical accomplishment was to advance the theory of Belief Propagation. Belief Propagation is one of the most important algorithms for Graphical Models because it provides distributed, scalable prediction based on message passing. As science and defense applications grow in size, the need for message passing algorithms increases, and our work currently defines the largest provable correct class of problem that can be predicted with Belief Propagation. Two papers on this topic were accepted at the high impact Neural Information Processing Systems (NIPS) conference [2][3].

Prediction is a fundamental component of learning and therefore advances in prediction feed directly into advances in learning. In addition, our team was inspired by the specific theoretical approach used to advance Belief Propagation, and this led to a number completely novel research directions for learning that we hope to continue in future work [4][5].

Supervised Semantics: Scientists and data analysts are very good at recognizing patterns and identifying important relationships in the data they are analyzing, but generally lack mechanisms to annotate relationships in a way that machine learning can understand. Our accomplishments move IML far beyond labels, and include:

- Semantic interactions (such as merging and splitting) were formalized as prediction in a Graphical Model and learning algorithms developed to enable a new type of interactive image analysis tool [6]. These tools have been applied to applications in nuclear material forensics, geo-spatial analysis and bio-medical image analysis (see Figure 1 and 5), and provide significant benefit to a number of expert users. This is discussed in more detail under impact.
- New connections were made between Graphical Models and a number of widely used hierarchical image segmentation methods including the Watershed algorithm [7]. These connections enable these popular methods to be more easily adapted and evaluated for particular applications and a software library implementing these ideas was developed.
- New mechanisms to inject an expert's 'relational advice' into Graphical Models were developed that help control what parts of the model are learnt from data, and what parts are based on prior knowledge. To demonstrate the generality of the approach we evaluated it on a wide range of applications from image analysis, to autonomous driving. This work was accepted for presentation at the high impact AAAI (Advances in Artificial Intelligence) conference [8].

- A statistical framework for estimating the uncertainty associated with the Graphical Models was developed for materials image analysis. This framework contextualizes the variability in feature patterns of materials and the imaging process, provides greater insight into the performance of different algorithms, and is used to identify where user feedback can improve accuracy [9].

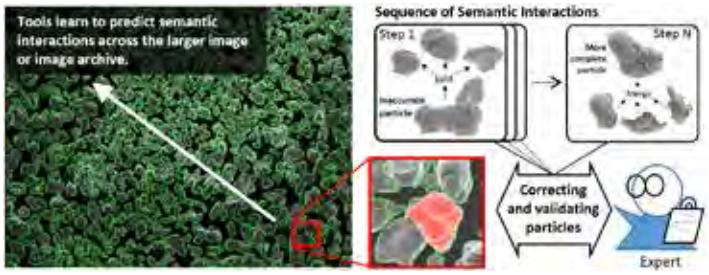

Figure 1. Supervised Semantic tools learn more from experts than standard machine learning tools because they understand semantic interactions like splitting and merging. These interactions are encoded into the Graphical Model and then propagated across the larger data set or data archive.

Model Discovery

In supervised semantic tools, the approximate structure of the Graphical Model is known, and the expert interaction is encoded into parameters. However, in other applications the potential dependencies within data are unknown, and the expert's goal is to identify these dependencies with the help of data. In this type of application prediction accuracy is often less important than the Graphical Model structure, since the structure can identify dependencies that the scientist may not have thought of. Our accomplishments with respect to these types of tools included:

- A new computationally efficient mechanism to incorporate expert knowledge into Graphical Model structure learning was developed. It enables experts to encode known dependencies, and known dependency directions, and it won a best poster award at the Los Alamos Postdoc Research Day [10].

- We worked with experts from the ChemCam science team to identify and analyze chemical depth trends in laser-induced breakdown spectroscopy (LIBS) data. There have been over 300,000 observations to date, and each observation has over 600 channels, making manual evaluation of depth trends almost impossible. Our model discovery tools were used to summarize and make this data more interpretable to the expert which helped elucidate rock surface weathering (see Figure 2) [11].

- Experts are often more interested in the changes in dependencies that occur as experimental parameters are varied than they are in the dependencies found in a single experiment. We developed new methods for this use-case and demonstrated its utility with experimental data that included co-collected time series and video data (see Figure 3) [12].

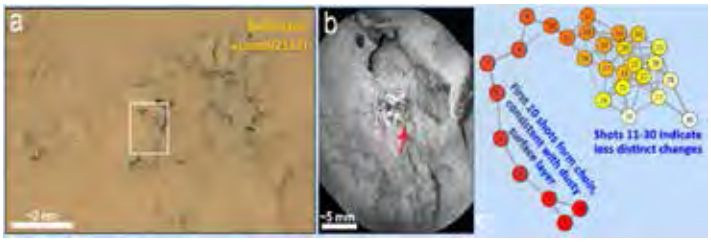

Figure 2. (a) Mars Rover mast camera image of rock with ChemCam sampling region in white. (b) Image from ChemCam microimager with sampling location indicated by the red arrow. (c) Graphical Model of shot-to-shot depth profile (30 shots) is consistent with a dusty surface layer and increased mixing with depth.

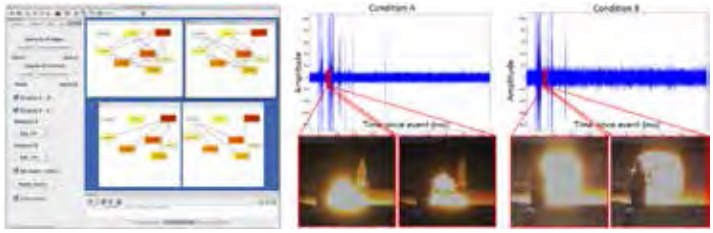

Figure 3. Left) Interface to enable users to explore and search for differences in dependencies in experimental datasets. Right) Radio Frequency (RF) signal data and video associated with two settings of an experiment parameter.

Training Dialog

One of the most common interactions between humans and machine learning is data triage: machine learning tools are applied to large datasets to identify subsets of data, which are then passed to the expert to discard or follow up.

Theory

Another significant theoretical accomplishment formalized anomaly detectors and provided quantitative methods for evaluating their performance. Broadly speaking, anomalies are rare and 'interesting', and this idea can be placed on firmer footing by defining anomaly detection in terms of characterizing the background. This approach illuminates how different anomaly detection methods relate, and provides tools to characterize the quality of anomaly detection in the absence of ground truth [13]. We were invited to present this material as a plenary talk at two high impact Hyperspectral Imaging conferences.

Hemi-Supervised Learning: Anomaly detection provides the framework for a wide range of data triage applications, but does not provide a mechanism for incorporating user feedback (or triage results). Since 'interesting' is rare, this feedback corresponds (primarily) to experts labeling data as 'not-interesting' (note, when interesting data is found, experts typically move into more focused analysis where 'Supervised Semantics' and 'Model Discovery' tools can be more helpful). We developed a new algorithm for incorporating one-sided negative feedback into anomaly detection, called Hemi-Supervised Expectation Maximization [14]. We also created and released a large open dataset to better compare interactive anomaly detection methods, and found our method was one of the few to consistently beat random sampling over large numbers of problem instances (previous comparisons typically involved a small number of hand selected problems, and statistical significance was hard to evaluate).

User Sampling Bias

Another significant accomplishment was motivated by image analysis tools where we observed experts interacting with machine learning in a different way. Instead of the tool going first, the expert would go first. They would label a small amount of 'interesting data' and then iterate with the machine learning system to find more. We called this unexplored form of Interactive Machine Learning 'User Driven Sampling Bias' and we showed how expert bias, interacting with small amounts of data, can consistently outperform automated methods with all of the data (see Figure 4). This work received a Best Paper award at the SPIE/IS&T Visualization and Data Analysis Conference (VDA-2014) [15]. In related work, our team used Amazon Turk to investigate human cognitive bias in the expression of numerical uncertainty. This led to an algorithm for finding new linguistic hedges in unstructured text [16] and also to recommendations and methods for quantifying uncertainty in reporting qualitative analysis results for forensic evidence.

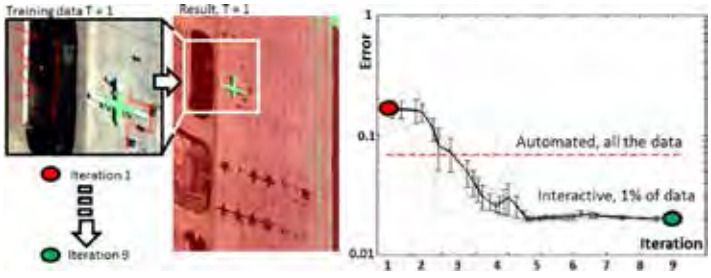

Figure 4. Left) The expert selects pixels to label (red or green) in iteration 1 producing a prediction result with error 0.108 (red dot in plot). Right) Over 9 iterations the experts adds more training data (totaling 1% of the data) and the machine learning system outperforms the machine learning system trained with all of the data (red dashed line).

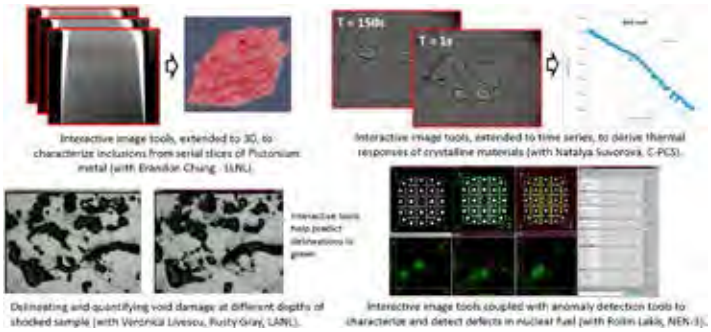

Figure 5. This project has produced a set of general purpose, yet easily tailored tools, that can help experts automate time-consuming analysis in a number of advanced material applications.

Impact on National Missions

Our accomplishments empower experts to exploit specialized data in less time, and with greater accuracy, both by automating tedious and repetitive tasks and by enabling them to focus on validation and higher-level objectives. Specific applications successfully transitioned to programmatic funding during the course of the project include:

Nuclear Material Forensics

The 'supervised semantic' tools developed in this project are now in operational use within a number of nuclear forensics laboratories throughout DOE, FBI and NIST. The Domestic Nuclear Detection Office (DNDO) within the Department of Homeland Security (DHS) has been funding software maturation since the summer of 2014, and beta versions of the tools were recently delivered to DNDO for external Independent Validation and Verification. LANL now has an ongoing program with DNDO to support the image analysis needs of approximately 40 scientists in research activities and forensic exercises.

Human Guided Sense Making

The Defense Threat Reduction Agency (DTRA) has recognized semantic interactions as a key technology for multimodal data enrichment. In the summer of 2015, they funded LANL to develop a prototype for the geospatial image analysis domain, as part of their Advanced Analytics Program to strengthen national capabilities in countering weapons of mass destruction (CWMD).

Interactive Image Search and Triage

Interaction was also recognized by intelligence community sponsors as a low-risk way to incorporate image search tools into operational databases. We were funded to provide a baseline capability for image search and our tools became operational in the summer of 2014. We are now responding to requests for enhancements and extensions to meet the specific needs of particular datasets and end users.

The project also explored a number of other mission relevant applications that we believe are high value targets for follow on work.

Advanced Materials: Building on our success with interactive image analysis tools for nuclear material forensics we worked with experts who are acquiring increasing volumes of image data for stockpile stewardship and the weapons enterprise (Figure 5). Experts need these images to derive quantitative measurements, and define uncertainty, but there is also increasingly need for prediction, and anomaly detection, as part of process monitoring and certified material production. The tools developed under this project provide a much needed middle ground between commercial tools, which experts find are not quite right for their particular problem, and custom analysis tools, which must be developed at significant cost in time and resources.

Cybersecurity: Improving anomaly detection accuracy and maximizing the limited expert feedback has the potential of making a significant impact in cybersecurity applications and we hope to identify opportunities for future work in this area.

References

1. Porter, R., J. Theiler, and D. Hush. Interactive Machine Learning in Data Exploitation. 2013. IEEE Computing in Science and Engineering. 15 (5): 12.
2. Ahn, S., S. Park , M. Chertkov, and J. Shin. Minimum weight perfect matching via blossom belief propagation. (Montreal Canada, 7-12 Dec).
3. Shin, J., A. E. Gelfand, and M. Chertkov. A Graphical Transformation for Belief Propagation: Maximum Weight Matchings and Odd-Sized Cycles . 2013. (Lake Tahoe, 5-10 Dec). p. 2022. : .
4. Porter, R., and B. Zimmer. Links between binary classification and the assignment problem in ordered hypothesis machines . 2015. (San Francisco, 2015). p. doi:10.1117/12.2083994. San Francisco: SPIE/IS&T.
5. Johnson, J., D. Oyen, P. Netrapalli, and M. Chertkov. Learning planar ising models . Machine Learning Research .
6. Porter, R., S. Lundquist, and C. Ruggiero. Learning to Merge: A New Tool for Interactive Mapping. 2013. (Baltimore, Maryland, 18 May, 2013). p. 87431F. Baltimore, Maryland: SPIE.
7. Porter, R., D. Oyen, and B. Zimmer. Learning watershed cut energy functions . 2015. (Rejijeck, Iceland, May). p. 497. Rejijeck, Iceland: Springer.
8. Odom, P., T. Khot, R. Porter, and S. Natarajan. Knowledge Based Probabilistic Logic Learning. 2015. (Austin, Texas, 25-30 Jan. 2015). p. 83. Austin, Texas: AAAI.
9. Director, H., J. Gattiker, and R. Porter. A multi-scale noise model for estimating uncertainty in computer vision algorithms. Technometrics.
10. Oyen, D., K. Sentz, B. Anderson, and C. Anderson-Cook. Bayesian discovery of bayesian networks with order priors . (Phoenix, AZ, Feb).
11. Oyen, D., R. Porter, and N. Lanza. Discovering Compositional Trends in Mars Rock Targets from ChemCam Spectroscopy and Remote Imaging. (Washington DC, 13-15 Oct).
12. Oyen, D., R. Porter, and K. Sentz. Interactive comparative analysis for multi-modal data exploitation and fusion. (Washington DC, 13-15 Oct).
13. Zimmer, B., and R. Porter. Hemisupervised Expectation maximization for rare category detection . ACM Transactions on Knowledge Discovery From Data.
14. Harvey, N., and R. Porter. User-Driven Sampling Strategies in Image Exploitation. 2014. (San Francisco, 23 Dec). p. 90170B. San Francisco: SPIE.
15. Sentz, K., and S. Ferson. Natural language of uncertainty: numeric hedge words . 2015. International Journal of Approximate Reasoning. 57 (Feb.): 19.

Publications

Ahn, S., S. Park , M. Chertkov, and J. Shin. Minimum weight perfect matching via blossom belief propagation. To appear in Proceedings of Neural Information Processing Systems (NIPS) 2015. (Montreal Canada, 7-12 Dec).

Burr, T., and A. Skurikhin. Conditional Random Fields for inverse problems in structured data. 2015. Algorithms. 8: 466.

Chertkov, M., A. E. Gelfand, and J. Shin. Loop Calculus and Bootstrap-Belief Propagation for Perfect Matchings on Arbitrary Graphs. 2013. In International Meeting on 'Inference, Computation, and Spin Glasses'. (Sapporo, Japan, July). , p. . Sapporo, Japan: .

Director, H., J. Gattiker, and R. Porter. A multi-scale noise model for estimating uncertainty in computer vision algorithms. Technometrics.

Gelfand, A. E., J. Shin, and M. Chertkov. Belief Propagation for Linear Programming. 2013. In IEEE International Symposium on Information Theory (ISIT). (Istanbul, Turkey, July). , p. 2249. Istanbul, Turkey: IEEE.

Grosklos, G., and J. Theiler. Ellipsoids for anomaly detection in remote sensing imagery . 2015. In Proc. SPIE 9472. (Baltimore, March). , p. 94720P. Baltimore: SPIE.

Harvey, N., and R. Porter. User-Driven Sampling Strategies in Image Exploitation. 2014. In IS&T / SPIE Visualization and Data Analysis VDA'2014. (San Francisco, 23 Dec). , p. 90170B. San Francisco: SPIE.

Harvey, N., and R. Porter. User-Driven Sampling Strategies in Image Exploitation. 2014. Information Visualization. (Nov): 1.

Johnson, J., D. Oyen, P. Netrapalli, and M. Chertkov. Learning planar ising models . Machine Learning Research .

Matteoli, S., M. Diani, and J. Theiler. An overview of background modeling for detection of targets and anomalies in hyperspectral remotely sensed imagery. 2014. Selected Topics in Applied Earth Observations and Remote Sensing (JSTARS)Selected Topics in Applied Earth Observations and Remote Sensing (JSTARS). 7: 2317.

Odom, P., T. Khot, R. Porter, and S. Natarajan. Knowledge Based Probabilistic Logic Learning. 2015. In AAAI'15. (Austin, Texas, 25-30 Jan. 2015). , p. 83. Austin, Texas: AAAI.

Oyen, D., K. Sentz, B. Anderson, and C. Anderson-Cook. Bayesian discovery of bayesian networks with order priors . To appear in Advances in Artificial Intelligence, AAAI'16.. (Phoenix, AZ, Feb).

Oyen, D., R. Porter, and K. Sentz. Interactive comparative analysis for multi-modal data exploitation and fusion. To appear in 2015 IEEE Applied Imagery Pattern Recognition workshop (AIPR2015). (Washington DC, 13-15 Oct).

Oyen, D., R. Porter, and N. Lanza. Discovering Compositional Trends in Mars Rock Targets from ChemCam Spectroscopy and Remote Imaging. To appear in 2015 IEEE Applied Imagery Pattern Recognition workshop (AIPR2015). . (Washington DC, 13-15 Oct).

Oyen, D., and T. Lane. Bayesian structure discovery of multitask Bayesian networks. 2015. Knowledge and Information Systems. 43 (1): 1.

Oyen, D., and T. Lane. Bayesian discovery of multiple Bayesian networks via transfer learning. 2013. In IEEE International Conference on Data Mining. (Dallas, Texas, 7-10 Dec). , p. 577. Dallas, Texas: IEEE.

Oyen, D., and T. Lane. Interactive Exploration of Comparative Dependency Network Learning . 2014. In Workshop on Interactive Data Exploration and Analysis at KDD, August 2014.. (New York, 24-27 August). , p. 88. New York: ACM.

Porter, R., D. Oyen, and B. Zimmer. Learning watershed cut energy functions . 2015. In International Symposium on Mathematical Morphology. (Rejijeck, Iceland, May). , p. 497. Rejijeck, Iceland: Springer.

Porter, R., D. Oyen, and J. Theiler. Data adaptive affinity functions in unsupervised segmentation . To appear in Computational Imaging, IS&T Electronic Imaging. 2016.. (San Francisco, Jan).

Porter, R., J. Theiler, and D. Hush. Interactive Machine Learning in Data Exploitation. 2013. IEEE Computing in Science and Engineering. 15 (5): 12.

Porter, R., N. Harvey, and C. Ruggiero. Investigation of Segmentation Based Pooling for Image Quantification. 2014. In IS&T / SPIE Image Processing: Machine Vision Applications VII. (San Francisco,). , p. 90240F. San Francisco: SPIE.

Porter, R., S. Lundquist, and C. Ruggiero. Learning to Merge: A New Tool for Interactive Mapping. 2013. In Algorithms and Technologies for Multispectral, Hyperspectral, and Ultraspectral Imagery XIX. (Baltimore, Maryland, 18 May, 2013). , p. 87431F. Baltimore, Maryland: SPIE.

Porter, R., and B. Zimmer. Links between binary classification and the assignment problem in ordered hypothesis machines . 2015. In Proceedings of IS&T/SPIE Electronic Imaging, Image Processing: Algorithms and Systems XIII . (San Francisco, 2015). , p. doi:10.1117/12.2083994. San Francisco: SPIE/IS&T.

Porter, R., and C. Ruggiero. Data Integration and Entity Resolution: Challenges and Opportunities for Nonproliferation and Arms Control. 2014. In Information Analysis Technologies, Techniques and Methods for Safeguards, Nonproliferation and Arms Control Verification. (Portland, Oregon, May). , p. . Portland, Oregon: INMM.

Ruggiero, C., A. Ross, and R. Porter. Segmentation and learning in the quantitative analysis of microscopy images. 2015. In Proceedings of IS&T/SPIE Electronic Imaging, Image Processing: Machine Vision Applications VIII. (San Francisco , Jan.). , p. 94050L. San Francisco: SPIE/IS&T.

Sentz, K., and F. Hemez. The Future of Intelligent Systems for Safeguards, Nonproliferation, and Arms Control Verification. 2014. In INMM Information Analysis Technologies, Techniques and Methods for Safeguards, Nonproliferation and Arms Control Verification. (Portland, OR , May). , p. . Portland, OR : INMM.

Sentz, K., and S. Ferson. Natural language of uncertainty: numeric hedge words . 2015. International Journal of Approximate Reasoning. 57 (Feb.): 19.

Shin, J., A. E. Gelfand, and M. Chertkov. A Graphical Transformation for Belief Propagation: Maximum Weight Matchings and Odd-Sized Cycles . 2013. In Advances in Neural Information Processing Systems 26 (NIPS-2013). (Lake Tahoe, 5-10 Dec). , p. 2022. : .

Shin, J., A. Gelfand, and M. Chertkov. A graphical transformation for belief propagation. IEEE Transactions on Information Theory .

Skurikhin, A. N.. Learning tree-structured approximations for Conditional Random Fields. 2014. In IEEE Applied Imagery Pattern Recognition Workshop. (Virginia, 14-16 Oct. 2014). , p. 1. Virginia: IEEE.

Theiler, J.. Transductive and Matched-Pair Machine Learning for Difficult Target Detection Problems. 2014. In Proc. SPIE 9088, Algorithms and Technologies for Multispectral, Hyperspectral, and Ultraspectral Imagery XX. (Baltimore, Maryland, 13 June, 2014). , p. 90880E . Baltimore, Maryland: SPIE.

Theiler, J.. Spatio-spectral anomalous change detection in hyperspectral imagery. 2013. In Global Conference on Signal and Information Processing. (Austin,Texas, 3-5 Dec, 2013). , p. 953. Austin, Texas: IEEE.

Theiler, J.. Matched-pair machine learning . 2013. Technometrics. 55 (4): 536.

Theiler, J.. By definition undefined: adventures in anomaly (and anomalous change) detection. To appear in Proc. 6th IEEE Workshop on Hyperspectral Image and Signal Processing: Evolution in Remote Sensing (WHISPERS 2014). (,).

Theiler, J.. Anomalousness: how to measure what you can't define. 2015. In Fourier Transform Spectroscopy and Hyperspectral Imaging and Sounding of the Environment. : JT1A.2.

Theiler, J., and G. Grosklos. Problematic projection to the in-sample subspace in a kernelized anomaly detector. Geosciences and Remote Sensing Letters.

Wolpert, D., and D. Rajnarayan. Using Machine Learning to Improve Stochastic Optimization. 2013. In Late Breaking Papers in the Twenty-Seventh Conference on Artificial Intelligence (AAAI). (Bellevue, Washington, 14-18 July). , p. . Bellevue, Washington: AAAI.

Zimmer, B., and R. Porter. Hemisupervised Expectation maximization for rare category detection . ACM Transactions on Knowledge Discovery From Data.

Reducing Data Dimensionality in Seismic Inversion

Gowri Srinivasan
20150691ECR

Introduction

Seismic inversion (SI) refers to the problem of using seismic observations to estimate the geophysical properties of the earth through a wave equation. Inversion techniques are an integral part of DOE-critical mission areas such as energy production (natural gas extraction) and national security (aspects of Comprehensive Test Ban Treaty verification) that rely on accurate estimations of geophysical properties. Errors in inversion are costly; the result is inefficient extraction of natural gas since fractures cannot be located, or inability to ascertain if an explosion was nuclear due to incorrect yield determination.

Matching 1000s of terabytes of seismogram data to estimate a large number of nonlinearly related parameters in the wave equation is challenging and often computationally prohibitive. Hence simplifying but inaccurate assumptions of elasticity and isotropy are currently made to make the problem tractable. However, applying methods that reduce the dimensionality of the problem without simplifying the physics will also make the problem tractable and also greatly increase the accuracy of predictions. Currently used Dimension Reduction Techniques (DRTs) assume linear correlations between parameters which is often not justifiable. The goal of this proposal is to develop DRTs that capture nonlinear correlations between parameters allowing for accurate and efficient inversion. We will investigate two separate approaches to accelerate the convergence of large scale viscoelastic SI problems. We propose a kernel-based method to account for nonlinear correlations between parameters known as Kernel Principal Component Analysis. We will also consider joint dimension reduction and emulation, by learning quantitative relationships between parameters that replace computationally expensive simulators. We will validate our methods using field-scale datasets, a challenging but necessary step since methods that work well on synthetic datasets often do not scale well. Doing so will be transformational for large scale data analytics in a wide range of inversion problems.

Benefit to National Security Missions

This project will advance LANL's Integrating Information, Science, and Technology for Prediction pillar by closely integrating new analytical and computational aspects to advance predictive capabilities for large scale problems. Aspects of the inversion problem include characterizing the nature and source of seismic activity, which is a topic very relevant to LANL's Science of Signatures (SoS) pillar. Results of the proposed project will directly provide new computational tools that will support existing programs in extraction of subsurface resources (e.g., natural gas recovery) and CTBT verification. Aspects of the modeling framework developed here are relevant for any high-dimensional nonlinear complex system, and will be of great interest to several DOE programs, positioning LANL to compete for new program space. Methods developed here will be attractive to the new DOE SubTer initiative, where the state of stress in the ground is a key quantity of interest.

Progress

The project started on June 15, 2015, which is a week into it at the time of this progress report. However, leading up to now, we have demonstrated both linear and kernel PCA on simple data sets including the Swiss roll dataset. We are in the process of setting up quadratically constrained quadratic programming (QCQP) algorithms to investigate whether there is significant speedup of the KPCA method using the three standard kernels.

Future Work

In FY16 we will use quadratically constrained quadratic programming methods (QCQP) and other computationally efficient methods investigated in FY15 to learn the kernel for a seismic inversion problem. We will start with the assumption of elastic, slightly homogeneous me-

dium and gradually progress to visco-elastic medium with anisotropy.

We will also attempt joint dynamic dimension reduction of basis and emulation using both linear PCA and kernel PCA methods. We will try this first on the elastic slightly homogeneous medium modeled in FY15 using the kernel identified from our work leading up to this point.

Conclusion

We expect that applying Kernel Principal Component Analysis (KPCA) methods will lead to accurate and accelerated convergence of Seismic Inversion problems. We will verify our results against the high dimensional model to ensure that critical features are captured with far fewer parameters. Multivariate emulation is also unmanageable when the number of parameters exceeds 10. We expect that our joint emulation and dimension reduction technique will yield results that are more efficient that using either only emulators or lower dimensional models. The key is in combining the advantages of the two methods.

Publications

Hickmann, K., J. Hyman, and G. Srinivasan. Robust classification through dimension reduction using kernel principal component analysis. Siam Journal on Scientific Computing.

Quantum Methods for Fast Signal Processing and Metrology

Rolando D. Somma
20130741ECR

Abstract

The development of novel quantum methods or transformations for fast signal processing is paramount in science and technology. A generalization of the well-known Fourier transform (FT) to design transformations that could be implemented on a quantum processor with dramatic speedups is highly desirable. Such a quantum transformation could be applied to problems in signal analysis and quantum metrology. In particular, fractional Fourier transforms (frFTs) play an important role in signal analysis. frFTs are more powerful than the FT because they can eliminate noise and improve the signal to noise ratio in more general scenarios. Quantum versions of frFTs suitable for exponentially fast implementation could then revolutionize signal processing.

This project aims at developing quantum fractional Fourier transforms for fast signal processing. In particular, for a sample of size N, a quantum frFT that could be implemented using subpolynomial in N operations on a quantum information processor would be ideal. (The same transformation requires significantly more operations on a conventional computer.) A quantum frFT will be used to build methods for radar analysis and image processing that are exponentially faster than conventional ones. The potential of such transformation for quantum metrology (high-precision sensing) and related quantum algorithms is also of interest.

Background and Research Objectives

The Fourier transform (FT) is ubiquitous in signal processing. Interestingly, it also occupies a hallowed place in quantum information: a quantum variant can be implemented very rapidly on a quantum processor. Such quantum FT yields a number of exceptional applications such as in the famous Shor's algorithm for factoring. There are also useful non-quantum generalizations of the Fourier transform, including the fractional Fourier transform (frFT), which represent other powerful tools for conventional signal processing. Previous to this project, quantum frFTs have never been proposed, constructed or applied. Such transformations have the potential to revolutionize signal processing and provide a fundamentally new tool for fast quantum information tasks.

The research objective is to fill this gap by constructing and applying quantum variants of the frFT that, like the quantum FT, can be implemented efficiently on a quantum processor. The same transformation requires significantly more operations when implemented on a conventional computer. We seek advanced quantum methods for solving signal processing and algorithmic problems faster than currently possible.

Scientific Approach and Accomplishments

We followed several approaches and developed a quantum transformation that is an excellent approximation to the desired quantum fractional Fourier transform. The basic idea is to relate the fractional Fourier transform to the evolution operator of the quantum harmonic oscillator. A discrete quantum harmonic oscillator was then proposed suitable for quantum computer implementations, and Trotter-Suzuki approximations were used to implement such a transformation. The approximation error decreases very fast (exponentially fast) with the dimension of the space of the problem, making it an excellent candidate for applications. The most remarkable property is that the implementation cost of our approximate quantum fractional Fourier is subpolynomial in the dimension, that is, significantly smaller (almost exponentially smaller) than the implementation cost of the corresponding conventional fractional Fourier transform. Thus, the main objective of this research project was achieved.

We applied our approximate quantum fractional Fourier transform to different problems. In particular, for the simulation of quantum systems and signal processing problems, attaining substantial speedups with respect

to the corresponding classical algorithms in both cases. All our results have been published [1] and presented in conferences, and the goals of this ECR project were successfully accomplished.

Impact on National Missions

This project constitutes a novel approach in quantum science with interdisciplinary impact that has already generated new interdisciplinary collaborations. This research is a direct response to the FY13/FY14 IS&T Grand Challenge on quantum information science. The project also enhances other capabilities at LANL, Sensing, Metrology, and Quantum Cryptography, and brings integration between the pillars of the LDRD "Quantum Initiative". Previous LANL research on quantum information led the PI to start new collaborations with Sandia National Labs on building a small-scale quantum computer, to obtain an NSF grant bringing summer students to LANL, and to obtain an AFOSR grant in collaboration with the University of Pittsburgh. The current project has enhanced LANL's capabilities in the quantum arena for a sustainable future. It also allowed the ECR investigator to start a new program in quantum methods to solve other important science problems of mission relevance – a recently funded project by NRO in collaboration with JHU/APL and the Joint Quantum Institute in Maryland.

References

1. Somma, R. D.. Quantum simulations of one dimensional quantum systems. 2015. arXiv: 1503.06319.

Publications

Somma, R. D.. Quantum simulations of one dimensional quantum systems. 2015. arXiv:1503.06319.

Stochastic Modeling of Phase Transitions in Strongly Interacting Quantum Systems

Christopher Ticknor
20130749ECR

Abstract
We studied the collective behavior of quantum systems and developed methods to understand quantum gases near a phase transition. Specifically, we studied a trapped two-component Bose Einstein Condensate and thoroughly explored and characterized the excitations. We used this knowledge to explore magnetic fluctuations that diverge near a phase transition. We found that experiments should be able to observe scaling behavior.

Background and Research Objectives
Quantum systems of reduced dimensions exhibit enhanced quantum fluctuations compared to 3D systems. In a homogeneous 2D system, a Bose Einstein Condensate (BEC) will never form as quantum fluctuations prevent this. But there is a Berezinskii-Kosterlitz-Thouless (BKT) transition, a topological phase transition in 2D systems, wherein the coherence of the gas changes decay behavior from exponential to algebraic as the temperature is lowered. (Phase coherence can be thought of as: if we know the phase here at x, then we know something about the phase there at x'). The BKT transition is physically motivated by vortex pairs unbinding due to thermal energy. Once vortex pairs are unbound, they destroy phase coherence as they move through the gas. The BKT transition occurs in a variety of 2 dimensional systems.

Theoretical modeling of temperature dependent dipolar gases has largely been neglected due to the numerical challenges. The first theory looking at temperature dependence was several years ago, but neglected the thermal correlation function. Additionally, this work was restricted to Cr, the weakest dipolar gas. I completed the first full treatment of non-zero temperature trapped dipolar gases. This resulted in a theory that has been used to study correlations in a single component dipolar gases. More recently other groups have followed suit. Now experiments with Dy and Er are producing strongly interacting dipolar BECs, but these BECs are not very degenerate ($T/T_c>0.25$). There is a pressing need to develop methods capable of studying strongly interacting, "warm" dipolar BECs.

Scientific Approach and Accomplishments
We analyzed the excitation spectrum for a two-component quasi-two-dimensional Bose-Einstein condensate. We studied how excitations change character across the miscible to immiscible phase transition.

We furthered the understanding of the two component BEC by studying the dispersion relation and comparing the character of the excitations of a single- and two-component BEC. We studied the single-component dispersion for a finite BEC system and look at examples of quasiparticles to understand and characterize the dispersion relation. Next we presented the dispersion relation for a two-component BEC in both the miscible and immiscible parameter regimes. Then we presented examples of the quasiparticles for both regimes.

Finally, we studied fluctuations in these trapped systems. We demonstrated that measurements of number fluctuations within finite cells provide a direct means to study susceptibility scaling in a trapped two-component Bose-Einstein condensate. This system supports a second-order phase transition between miscible (co-spatial) and immiscible (symmetry-broken) states that is driven by a diverging susceptibility to magnetic fluctuations.

This body of work provides a path forward to understand the quantum excitations in a multi-component BEC.

Impact on National Missions
Understanding finite quantum systems is essential to engineering quantum materials. The study of phase transitions in the presence of non-local interactions has wide reaching impacts. Additionally, computational methods developed here could be transferred to the study

of warm dense matter via quantum molecular dynamics (QMD using a hybrid Kohn-Sham and Thomas-Fermi (orbital free) density function theory of the electronic structure. The numerical implementation is similar to that of the PGP method. This development is of great interest to the Laboratory because it presents a means to produce thermal conductivities at much higher temperatures than are currently possible.

Publications

Baillie, , R. N. Bisset, Ticknor, and P. B. Blakie. Number Fluctuations of a Dipolar Condensate: Anisotropy and Slow Approach to the Thermodynamic Regime. 2014. PHYSICAL REVIEW LETTERS. 113 (26).

Bisset, R. N., R. M. Wilson, and Ticknor. Scaling of fluctuations in a trapped binary condensate. 2015. PHYSICAL REVIEW A. 91 (5).

Bisset, R. N., Ticknor, and P. B. Blakie. Finite-resolution fluctuation measurements of a trapped Bose-Einstein condensate. 2013. PHYSICAL REVIEW A. 88 (6).

Ticknor, C.. Excitations of a trapped two-component Bose-Einstein condensate. 2013. PHYSICAL REVIEW A. 88 (1): 013623.

Ticknor, C.. Dispersion relation and excitation character of a two-component Bose-Einstein condensate. 2014. PHYSICAL REVIEW A. 89: 053601.

Ticknor, C., and R. Bisset. Finite-resolution fluctuation measurements of a trapped Bose-Einstein condensate. 2013. PHYSICAL REVIEW A. 88: 063624.

From the Finite Element Method to the Virtual Element Method

Gianmarco Manzini
20140270ER

Introduction

This project aims at the development of a new family of numerical methods on polygonal and polyhedral unstructured meshes for diffusion, reaction-diffusion and convection-diffusion problems, the Stokes equations and compressible and incompressible elasticity equations.

These methods are a generalization of the Finite Element Method (FEM) to polygonal and polyhedral meshes and are based on the very new paradigm of Virtual Element Methods (VEMs). In the virtual framework, only the part of the finite element space that refers to polynomials is constructed, while the behavior of the method on the rest of the space is approximated following a stability criterion. This fact has a dramatic impact on the computational complexity that is greatly simplified as the implementation of virtual elements does not require the explicit construction of the shape functions anymore.

Benefit to National Security Missions

The success of this research will provide unique capabilities in the DOE complex that combine world-class algorithms, their theoretical foundation and high-end HPC technologies. This new class of numerical algorithms is outstanding for mathematical models used in Environment (Climate and Energy Impact), and Scientific Discovery and Innovation (Nuclear, Particle, Cosmology, Astrophysics, Basic Understanding and Modeling of Materials, Information Science and Technology).

Progress

The research activity of the first year of this project mainly concerned mentoring a summer study, and the development of:

1. virtual element methods for diffusion problems with convection and reaction terms;
2. a non-conforming formulation suitable to 2D and 3D diffusion problems; and
3. a general stabilization technique for elliptic equation to fix the hourglass instability.

The summer student worked mainly on the topics of item (1). The results of his work are in a LANL technical report and will be the content for a future research paper.

In (1) Virtual Element Methods were developed for any order of accuracy in the diffusive regime and stabilization techniques will be developed and investigated in the convection dominated regime. Results from this work was presented in a international congress and are submitted for publication to an international research journal.

In (2) we developed the non-conforming formulation for the VEM, carry on the convergence analysis and established the connection with the non-conforming MFD method. This work was presented in an international workshop and a paper is submitted for publication to an international research journal.

In (3) we investigated how the classical stabilization "a la Belytschko" for the hourglass instability can be restated in the virtual framework and a new family of stabilization techniques (including the one mentioned above) can be derived. The results of the work will be published by International Journal for Numerical Methods in Engineering.

Future Work

The research team will extend the development and implementation of the virtual element method (VEM) formulation for reaction-diffusion problems and convection-diffusion problems. This is a highly non-trivial process.

We will develop and implement the VEM formulation for

the steady Stokes problem. The numerical approximations will have the following features suitable for 2D applications, and order of accuracy higher than one.

Conclusion

The expected results are the developments of new classes of methods and their characterization with respect to accuracy, efficiency, and effectiveness for important applications where the VEM can outperform the existing computational technologies by providing high-order continuity and accuracy for the numerical approximation and improved properties of the scheme (e.g. dispersion reduction for wave propagation). The virtual element algorithms may impact a wide range of modeling multi-physics applications, including climate and environmental modeling (e.g., climate, ocean and sea-ice modeling, ASCEM Project, Arctic Terrestrial Simulator), plasma physics (e.g., Fokker-Planck equation in inertial confinement fusion simulations) and other CFD-based applications.

Publications

Cangiani, , Manzini, Russo, and Sukumar. Hourglass stabilization and the virtual element method. 2015. INTERNATIONAL JOURNAL FOR NUMERICAL METHODS IN ENGINEERING. 102 (3-4): 404.

Cangiani, A., G. Manzini, and O. Sutton. Numerical results using the conforming VEM for the convection-diffusion-reaction equation with variable coefficients. 2014. Los Alamos National Laboratory LA-UR-14-27709.

Dios, B. Ayuso de, K. Lipnikov, and G. Manzini. The nonconforming virtual element method. SIAM Journal of Numerical Analysis.

Gyrya, V., G. Manzini, and D. McGregor. A non-comforming virtual element discretization for singularly perturbed advection di usion reaction equations. 2014. Los Alamos National Laboratory LA-UR-14-27995.

Manzini, Gianmarco. The nonconforming virtual element method for the convection-reaction-diffusion equation. 2015.

Manzini, Gianmarco. The Virtual Element Method. 2015.

Manzini, Gianmarco. The virtual element method for flow and transport in porous media. 2015.

Manzini, Gianmarco, Andrea Cangiani, and Oliver J. Sutton. Conforming and nonconforming virtual element methods for elliptic problems. 2015. Mathematics of Computation.

Manzini, Gianmarco, Andrea Cangiani, and Vitaliy Gyrya. The non-conforming Virtual Element Method for the Stokes equations. 2015. SIAM Journal on Numerical Analysis.

Veiga, L. Beirao da, and G. Manzini. RESIDUAL A POSTERIORI ERROR ESTIMATION FOR THE VIRTUAL ELEMENT METHOD FOR ELLIPTIC PROBLEMS. 2015. ESAIM-MATHEMATICAL MODELLING AND NUMERICAL ANALYSIS-MODELISATION MATHEMATIQUE ET ANALYSE NUMERIQUE. 49 (2): 577.

Large Fluctuations in Stochastic Dynamical Systems

Timothy C. Wallstrom
20140302ER

Introduction

The goal of this project is to understand dynamical systems in the presence of large random fluctuations. Such systems are common in economics, physics, and several areas of biology. The usual analyses of random systems make certain technical assumptions on the size of the fluctuations, which are invalid when the fluctuations are too large. For these types of random systems, the usual analyses are invalid, and new methods are required.

We focus on the dynamical systems that govern evolution, and specifically on the area of population genetics, which is the mathematical framework for the study of evolution. On the one hand, these systems are sufficiently rich to exhibit a broad range of phenomena. On the other hand, striking recent mathematical results have led to a complete characterization of the solution classes, under large fluctuations, of the equations of population genetics, in certain simple cases. Thus, these systems should be tractable, but rich enough to provide general insights.

Our objective is to illuminate the dynamics of specific realistic dynamical systems by connecting such systems to the general theory. In short, we want to connect the data to the theory. The value of such an analysis has been amply demonstrated in the case of small fluctuations, and we expect similar dividends in the case of large fluctuations.

We will test our formalism by applying it to the understanding of HIV evolution in the infected individual. HIV is the Human Immunodeficiency Virus, which is the causative agent in AIDS. Existing models of HIV evolution have led to a number of stubborn mysteries, which we trace to an inadequate modeling framework, which does not account for large fluctuations. There is empirical evidence of large fluctuations in HIV, and modern sequencing technology will permit detailed comparison of our models with experimental data.

Benefit to National Security Missions

Our work will contribute to the understanding of dynamical systems in the presence of large fluctuations, which is an area of mathematics of importance to both the Office of Science (DOE/SC) and the NSF (Other Federal Agencies). The particular application on which we will focus on is evolutionary dynamics, which is of broad interest, and is a central concern of Fundamental Bioscience. We believe our models will describe evolutionary dynamics in a large number of areas of biology. We will be focusing specifically, however, on the evolution of HIV in the infected patient. Such research is of direct interest to the National Institutes of Health (NIH). The tools we develop will be valuable for future advances in our understanding of HIV and other pathogens, such as influenza, which will have importance for Basic Health Research.

Progress

Over the past year, we have made progress in three main areas. First, we have obtained extensive high-quality pathogen sequence data, and analyzed this data using models of large fluctuations. Second, we have established new mathematical results for models with large fluctuations. Third, we have written computer simulation programs for simulating models with large fluctuations. We discuss these advances in more detail.

Sequence data: One of the key goals of our project is to connect the abstract mathematical theory of large fluctuations in population genetics with actual genomic data from pathogen populations. To this end, we have been successful in obtaining extensive, high-quality sequence data for studying the evolution of pathogens within an infected patient. We have obtained data for both the Human Immunodeficiency Virus (HIV), and for the Hepatitis C virus (HCV), so that we can compare the similarities and differences between how these pathogens evolve within the patient. Both of these pathogens

are expected to exhibit large fluctuations. The sequences are several thousand bases long, which helps with statistical significance, and were obtained using the technique of single genome amplification (SGA), an expensive technique that ensures that the sequences are highly accurate. Our datasets contain dozens of sequences taken at several times, spanning the period from acute to chronic infection in multiple patients.

We have used this data to demonstrate that the usual genealogical model, which assumes small fluctuations, does not fit either HIV or HCV. We are in the process of fitting the data to models with large fluctuations and writing up our results. The paper should be completed in a few months.

New mathematical results: Most of the existing results for models of large fluctuations assume, as a mathematical idealization, that the population size is infinite. This limit leads to useful simplifications, since the probability of certain types of genealogical events becomes so small that these events can be ignored. Although this is a good starting approximation, actual populations are finite, and for this reason the actual probability of these events, though small, is not zero. We would like to know how likely they are. We have used mathematical analysis to calculate these probabilities in the case of a large but finite population. This is an important step in making these models more realistic, and connecting them to the actual biological data. A paper describing these results is in preparation.

New simulation codes: We have written computer code to simulate our models of large fluctuations. Much of the behavior of our models cannot be obtained through mathematical analysis, because the full models are too complex. Thus, we are dependent on computer simulations to determine many of the properties of these models. To gain the best understanding of our models, the simulation results are used in conjunction with mathematical analysis. We have used these simulation codes to explore the range of different genealogies that arise from our models, and to evaluate how well we can determine model parameters from a sample of sequences. The simulation codes complement our mathematical results, as described in the previous paragraph, in that they help us to understand the behavior of these models for finite populations.

Future Work

In the upcoming year, the third and last of this project, we will complete work in several areas.

First, we will complete the analysis of the Human Immunodeficiency Virus (HIV) and Hepatitis C Virus (HCV) datasets obtained over the past year, and publish this analysis. We will also complete and publish the mathematical analysis of models with large fluctuations and finite population sizes.

A second goal will be to use our methods to try to obtain clinically significant insights into the biology of pathogen infection. The genealogies of both HIV and HCV appear to undergo a qualitative change a few years into infection, a change which may correspond to disease progression. However, this apparent change has not yet been understood quantitatively. We hypothesize that this change may correspond to a change in the size of the fluctuations in the evolutionary process, and may be detectable as a change in the parameter quantifying these fluctuations.

A third goal will be to develop our methods to accommodate common complications that arise in the analysis of real datasets: sequencing errors, and recombination. In our analysis so far, we have had the benefit of very high quality sequence data. In many cases, we will want to apply a similar analysis to poorer quality data, which is more readily available because it is less expensive to obtain. We will study the robustness of our inference techniques in the presence of the types of sequencing errors that occur commonly in the usual sequencing technologies. A second complication is recombination. In recombination, a virus contains genetic material from two parent viruses. Recombination is much more prevalent in HIV than in HCV. Through a combination of computer simulation and comparative studies between HIV and HCV, we will assess the impact of recombination on our inference methods.

Conclusion

This project will lead to methods for connecting realistic stochastic dynamical systems to their solution classes, to an understanding of how progressive adaptation takes place in a predator-prey environment, and to clarification of the appropriate framework for modeling HIV evolution within the host.

Publications

Bhattacharya, T., E. Giorgi, T. Wallstrom, P. Hraber, G. Learn, T. Kreider, Y. Li, F. Gao, B. Korber, B. Hahn, and G. Shaw. Detecting Selective Sweeps in HIV. 2014. Presentation to Scientific Leadership Group of Center for HIV/AIDS Vaccine Immunology (CHAVI), July 30, 2014. Chosen for presentation to full CHAVI collaboration meeting, and presented there on September 29, 2014..

Accelerating Time Integration for Multi-scale Simulations

Shengtai Li
20140323ER

Introduction

One of the most difficult challenges in multiscale simulations is to bridge the gap between different time scales. The time step for the fast timescale variables tends to be so small that the slow-scale variables have to wait a long time until the micro-step simulation finishes a macro-step. To overcome this limitation in time scales is becoming the key for the practical use of the multiscale simulations.The primary goal of this proposal is to develop an innovative numerical framework to accelerate the time integration for the multi-time-scale problems. To achieve this goal, we identify two major objectives. First, we will construct low dimensional, coarse-grained, effective reduced order models (ROM) via analytical and numerical approximations. The ROM serves two purpose in our simulations: either the cost of each time step of simulation is sharply reduced, or a large time step is allowed by removing the dynamics of fast components, or both.

Second, we will accelerate the time integration via parallel-in-time (PIT) strategy. By construction, the ROMs only capture the original full microscopic dynamics approximately. In many cases, the microscopic simulations with small time step is needed over the entire time domain to capture long time dynamics correctly, or at least in some small regions. The PIT strategy proposes to break the global problem of time evolution into a series of independent evolution problems on smaller intervals. Initial states for these problems are supplied by a less accurate but fast sequential time integrator, for example by using ROM. The smaller independent evolution problems can then be solved in parallel using more expensive and more accurate integrators. An iterative procedure is used to ensure that the algorithm converges to the solution one would have obtained using a purely sequential fine propagator over the entire time-domain.

Benefit to National Security Missions

The need for multiscale simulation capability is pervasive in many areas of science and engineering, including environmental and geosciences, climate, materials, combustion, high energy density physics, fusion, bioscience, chemistry, power grids and information networks. In the past 20 years, numerical techniques, such as domain decomposition and adaptive mesh refinement (AMR), have been developed to bridge different length scales. However, the total elapsed time of the simulation is limited by the fastest timescale in the system, because it is often necessary to use the same small time step for the whole system to avoid instability and unphysical artifact.

We are developing a reduced order model (ROM) and parallel in time method to accelerate the time integration in multiscale simulations, and to resolve the parallel saturation issue for future exa-scale computing. Our numerical techniques can be applied to many multiscale problems, including but not limited to defect (e.g., crack) formation and propagation in solid material, magnetic reconnection layer in plasma physics, interface or front propagation in combustion, interface formation and propagation during phase transition in multi-phase flow simulations, and the dust and gas coupling in disk-planet simulations.

Progress

The research team developed a new reduced model for the coupled dynamics of dust and gas. Our previous reduced order model (ROM) uses a bi-fluid model and treats the dust as a pressureless fluid. This has a drawback that the stiff source term (drag force between dust and gas) appears in both the gas and dust equations. The partial equilibrium state must be reached in both equations, which increases the complexity to solve the equilibrium state. That is why in the old model, we do not implement the dust feedback to the gas. In the new ROM, we combine the gas and dust as one fluid. Only one equation in the one-fluid model contains the stiff source term, which is the velocity difference between

dust and gas. Therefore the equilibrium state is easy to solve. The dust feedback to the gas is easier to implement than the old model.

We also developed a new Riemann solver for the new ROM and a new second-order method to solve the one-fluid model. The method has been verified and tested.

A parallel-in-time algorithm was implemented by embedding our algorithm and code into a general framework XBRAID to achieve the parallel in time capability. The framework XBRAID greatly reduced our code development time and effort.

Our simulation package was enhanced with additional capabilities. We extended our method to multiple planets, which is necessary for simulating the newly-observed HL Tau proto-planetary disks and its surrounding multiple gaps. We also allow the initial disk to be exponential decaying at the outer-disk so as to avoid the gravitational instability issues. We have developed a non-uniform log-grid method so that we can simulate a much larger disk with relatively small number of grid points. We have coupled the coagulation code from Til Bernstil of Harvard University with our disk simulations code.

The research team also adapted a radiative transfer code RADMC-3D for our use and generated observations images from our numerical simulation results.

The newly (Dec 2014) observed HL Tau disk was stimulated using our coupled dust and gas dynamics with our super-fast disk self-gravity solver. The observation images from our simulated data match quite well with those from the ALMA telescope. Our results have been presented on the international conference and have gained world-wide recognition.

Through simulations, we find it is essential to simulate the dust and gas together to obtain accurate dust distribute in a disk. It is also important to include the disk self-gravity in the simulations to obtain a clear picture of the gap formation by the planet in the HL Tau disk. We also obtain upper and lower limit on the total disk mass for the future observations.

Future Work

The following tasks are planned for the next fiscal year:

- Develop an adaptive algorithm to achieve better accuracy and efficiency for the coupled dust and gas dynamics. We have found for many problems the time scales vary continuously over a wide range and there is no clear scale separation. The conventional multi-scale technique does not work well for these type of problems. We will develop an adaptive algorithm to identity when and where the reduced order model can be safely used, when and where the parallel-in-time method must be done to improve the accuracy, and when and where the conventional model can be used. We will develop techniques to bridge the gap between different regions and methods.
- Develop a new algorithm to improve the accuracy of our operator-splitting approach. For multi-physics and multi-scale problems, we will combine the spectral deferred correction (SDC) algorithm with our second-order operator-splitting approach to improve the accuracy. We will also implement this algorithm to the XBRAID parallel-in-time framework.
- Apply the new algorithm to the dusty disk simulations to simulate more observed proto-planetary disks, and compare the simulation results with the observations.

Conclusion

The primary goal of this project is to develop an innovative numerical framework to accelerate the time integration for the multiscale problems. By using reduced order model and parallel in time strategy, we expect to speed up our current simulation of planet formation in dusty disks by at least two order of magnitude. Our proposed space-time parallelism can also solve spatial parallelization saturation issue: using more processors above a critical number will slow down the simulation due to the communication overhead. Our proposed algorithm can be easily applied to other multiscale problems to accelerate the simulation by orders of magnitude.

Publications

Deng, W., H. Li, B. Zhang, and S. Li. Relativistic MHD Simulations of Collision-induced Magnetic Dissipation in Poynting-flux-dominated Jets/outflows. 2015. The Astrophysical Journal. 805 (2): 1.

Fu, W., H. Li, S. Li, and S. Lubow. Effects of dust feedback on vortices in protoplanetary disks . 2014. Astrophysical Journal Letter. 795 (2): L39.

Fu, W., H. Li, S. Lubow, and S. Li. LONG-TERM EVOLUTION OF PLANET-INDUCED VORTICES IN PROTOPLANETARY DISKS . 2014. The Astrophysical Journal Letters. 788 (2): L41.

Guan, X., H. Li, and S. Li. Relativistic MHD Simulations of Poynting Flux-Driven Jets . 2013. The Astrophysical Journal 12/2013; 781(1). . 781 (1): 1.

Li, S.. Modified FARGO Algorithm and its Combination with Adaptive Mesh Refinement. Journal of Computational

and Applied Mathematics.

Li, S., and H. Li. Numerical treatment of dust diffusion in dusty proto-planetary disks. 2014. In NUMERICAL MODELING OF SPACE PLASMA FLOWS: ASTRONUM-2013. (Biarritz, France, 1-5 Jul 2013). Vol. 488, 1 Edition, p. 96. San Francisco: Astronomical Society of Pacific Conference Series.

Li, S., and H. Li. Long-Time Sustainability of Rossby Wave Instability in Protoplanetary Disks with Dead Zone. 2015. In Numerical Modeling of Space Plasma Flows: ASTRONUM-2014. (Long Beach, CA, 23-27 Jun. 2014). Vol. 498, 1 Edition, p. 92. San Francisco: Astronomical Society of Pacific Conference Series.

Su, H., and S. Li. Structure-Preserving Numerical Methods for Infinite-Dimensional Birkhoffian Systems. 2015. Journal of Scientific Computing. 46 (1): 196.

Su, H., and S. Li. Energy/Dissipation-Preserving Birkhoffian Symplectic Methods for Maxwell's Equations with Dissipation Terms. Journal of Computational Physics.

Zhai, X., H. Li, P. Bellen, and S. Li. Three-Dimensional MHD Simulation of Caltech Plasma Jet Experiment: First Results . 2014. The Astrophysical Journal . 791 (1): 1.

Zhang, X., H. Li, S. Li, and D. Lin. RESONANCES OF MULTIPLE EXOPLANETS AND IMPLICATIONS FOR THEIR FORMATION . 2014. The Astrophysical Journal Letters . 789 (1): L23.

Automated Identification and Reverse Engineering of Malware

Christine M. Anderson-Cook
20140355ER

Introduction

Malware (i.e., malicious program) analysis is a multi-Billion dollar industry. Beyond that, malware analysis is critical to our national security both to protect national secrets and to prevent corporate espionage. Almost all large government facilities and corporations employ trained cyber professionals to reverse engineer (RE) suspected malware so that they can respond appropriately. A highly trained professional can spend days to weeks uncovering the purpose of the malware, in an effort to discover who sent it, and the extent of the attack. An organization cannot adequately respond to a malware infection until they understand what it does.

The main goal of this project is to develop an automated framework for the reverse engineering of malware. We propose to develop a procedure that will take a program trace (static or dynamic), and classify the subroutines as a particular functionality (e.g., disk I/O, network, GUI, registry, exploit, etc). The results will be a list of likely classifications of a subroutine's functionality, with corresponding probabilities. This is precisely what a reverse engineer would do in a more qualitative manner when they are unraveling the purpose of a program. However, classifying subroutines manually is an incredibly time consuming task. Thus, this work will substantially speed up RE times, providing a swifter response and thus reducing the expense and possibly the severity of a malware infection.

A second important consequence of this work is that the task classification results can be used to automatically assess the high-level functionality of a program as a whole with far more accuracy than in previous work (i.e., trojan, adware, IRC, advanced persistent threat, etc.). There has been no attempt until now to automatically arrange and classify the various tasks of a program, hence, the potential for a large impact due to this work.

Benefit to National Security Missions

Malware analysis is a multi-Billion dollar industry. Beyond that malware analysis is critical to our national security both to protect national secrets and to prevent corporate espionage. Almost all large government facilities and corporations employ trained cyber professionals to reverse engineer suspected malware. This work will allow them to not only investigate more of the large amount of suspected malware discovered on their systems, but also allow a swifter response to these threats. The preliminary classification work is already mature enough to be implemented on any enterprise network just as it already has been at LANL in Code Vision. We intend to ultimately implement the new reverse engineering methodology developed in this work in a tool suitable for use by cyber professionals. This will allow the methodology to be transitioned into practice at other government agencies and corporations. As the NNSA complex is a prime target for cyberattack, cybersecurity is an enabling technology for the nuclear weapons mission.

Progress

New methodology for identification and classification of malware was developed. The current focus is on Advanced Persistent Threat (APT) malware. One new approach uses the static trace of the program. A static instruction trace can be viewed as a graph with nodes representing subroutines and directed edges representing calls between subroutines. Thus, techniques which involve comparing graphs by checking for node and structure similarity may be useful. We expect static traces from related programs to have similar static traces, so they should have several common subroutines and much of the graphs should be isomorphic. The research looks at malware at the program level and classifies programs based on their similarity with known malware subroutines. Malware and benign programs can share a substantial amount of code, implying that classifica-

tion should be based on malicious subroutines that occur infrequently, or not at all in benign programs. Various approaches to accomplishing this task are investigated, and a particularly simple approach appears the most effective. This approach simply computes the fraction of subroutines of a program that are similar to malware subroutines whose likes have not been found in a larger benign set.

The second area of research considers the problem of identifying the function of different subroutines. Our goal is to automate the task of identifying the general function of the subroutines in the function call graph of the program to aid the reverse engineers in timely triage of where to focus their efforts. Two approaches to model the subroutine labels are investigated, a multiclass Gaussian process and a multiclass support vector machine. The output of these methods is the probability that the subroutine belongs to a certain class of functionality (e.g., file I/O, exploit, etc.). Promising initial results illustrate the efficacy of this method based on evaluation based on a sample of 201 subroutines taken from two malicious families.

Another area of research is to examine methods for identifying the family of malware from which newly identified programs are associated. Again an early diagnosis of malware phylogeny can help with efficiently determining if new programs represent new families of APT, or if the commonalities between existing programs for which reverse engineering has been performed can be leveraged.

Future Work

The research team will continue to explore the local subroutine approach to classification of APT malware that has shown promise. We will take advantage of the fact that only a handful of subroutines tend to make a program look malicious, to produce a subroutine importance measure. This could be displayed graphically to provide a useful reversing tool. We also intend to leverage the graphical nature of "malicious" subroutines to provide a more informative indicator of maliciousness if certain subroutines are connected than if the subroutines were not calling each other. We will finish the papers in development and start writing up the new results described above for scholarly journals. We will also continue to present this work at professional meetings.

Conclusion

This work is expected to result in a transformational approach to the reverse engineering of malware. We expect to understand the limits of the methodology in terms of how well it can provide likely purposes of each subroutine and program. We will validate the classification out-of-sample to ensure good performance. We further expect the subroutine classification results to provide extremely informative features for an overall program classification (benign, trojan, adware, IRC, advance persistent threat) routine. This overall classification routine will also be thoroughly validated on a large dataset.

Publications

Anderson, B., C. Storlie, M. Yates, and A. McPhall. Automating Reverse Engineering with Machine Learning Techniques. 2014. In The 7th ACM Workshop on Security and Artificial Intelligence. (Scottsdale, 7 Nov. 2014). , p. 103. Scottsdale: ACM Digital Library.

Anderson, B., T. Lane, and C. Hash. Malware Phylogenetics Based on the Multiview Graphical Lasso. 2014. In The Thirteenth International Symposium on Intelligent Data Analysis. (Leuven, Belgium, 29-31 Oct. 2014). , p. 1. Leuven, Belgium: Springer.

Bolton, A.. Malware static trace analysis through bigrams and graph edit distance. 2015. LANL Report.

Kao, Y., B. Reich, C. Storlie, and B. Anderson. Malware detection using nonparametrcis Bayesian clustering and classification techniques. To appear in Technometrics.

Neil, J., C. Hash, A. Brugh, M. Fisk, and C. Storlie. Scan statistics for the online detection of locally anomalous subgraphs. 2013. Technometrics. 55 (4): 403.

Oyen, D., C. Anderson-Cook, K. Sentz, and B. Anderson. Bayesian discovery of Bayesian networks with order priors: A new approach to combining knowledge and statistical data. To appear in The Thirteenth AAAI Conference . (Phoenix, 12-17 February 2016).

Oyen, D., K. Sentz, B. Anderson, and C. Anderson-Cook. Application of Bayesian discovery with order priors to combining knowledge and statistical data. 2015. LANL Report.

Sexton, J.. Anomaly detection of multistage network intrusions. 2015. LANL report.

Sexton, J., C. Storlie, and B. Anderson. Subroutine based detection of APT malware. To appear in Journal of Computer Virology and Hacking Techniques.

Sexton, J., C. Storlie, and J. Neil. Attack chain detection. To appear in Statistical Analysis and Data Mining .

Sexton, J., and C. Storlie. Internal stepping stone detection. To appear in Technometrics.

Storlie, C., B. Anderson, S. Vander Wiel, D. Quist, C. Hash, and N. Brown. Stochastic Identification of Malware with Dynamic Traces. 2014. Annals of Applied Statistics. 8 (1): 1.

Temporal Graphs

Aric A. Hagberg
20140389ER

Introduction

Graphs are increasingly being used to model complex techno-social networks such as the power grid, the internet, as well as computer and social networks. Understanding how these networks function and behave under changing circumstances is vital to several areas of national security.

This project will focus on developing temporal graph models for certain classes of complex networks such as computer and social networks. The scientific research will elucidate the interplay between the structural evolution of the network, temporal properties of the network, and dynamic processes, such as the spread of a virus or information, occurring on the network. The research will examine how sensitive networks are to perturbation, how to slow the speed of a virus and how to increase cybersecurity in the face of persistent attacks. We will develop efficient algorithms to generate random instances of these models as well as algorithms to fit data to the models. This project develops methods and techniques for network science. Network science is one of three cross-cutting themes in the Integrating Information, Science, and Technology for Prediction pillar at Los Alamos.

Benefit to National Security Missions

Network science is one of three cross-cutting themes in the Integrating Information, Science, and Technology for Prediction pillar at Los Alamos. Our work develops new models, techniques and theorems for dynamically changing graphs which are the underpinnings for many applications of network science. For example temporal graphs are a major research interest in cybersecurity and fill a missing gap in random graph models. Progress in modeling temporal graphs will provide capability relevant to DOD missions in cybersecurity anomaly detection.

The DOE ASC program sponsors research in the area of complex networks related to big data challenges. Our research develops new algorithms to efficiently generate large instances of random graphs for modeling and testing of high-performance computing applications.

Progress

We continued to refine our approach to the modeling and analysis of the graph structure of computer authentication events. These models are helping understand the risk of using centralized authentication systems such as those found in most large organizations such as Los Alamos National Laboratory. Our article “Connected components and credential hopping in authentication graphs,” published as part of the International Conference on Signal-Image Technology & Internet-Based Systems (SITIS) in November 2014 described our first results. We extended that research with a longer paper “The structure of authentication networks”, currently in review, that describes in detail the changes in degree (connectivity) of authentication networks over time and experiments in restricting the length of time credentials are valid. Along with these papers we released a companion public data set on which we based our modeling and analysis results.

The research team investigated metrics for connectivity in temporal graphs that are relevant for real systems such as the authentication event data. For static graphs the connectivity of a node has a single simple definition of the set of other nodes that you can reach by crossing links. We developed a new definition of “reachability” that captures the dynamics of unauthorized credential usage in a computer network with centralized authentication. This definition provides a measure of how long it takes, starting at a given computer, to traverse the credential network and crossing as many edges as are available at the current time.

Two new random temporal graph models were constructed based on the well-known static models, the Erdos-Renyi and Chung-Lu random graphs. The models allow an adjustable rate of change for dynamic edges with preservation of the original static random graph structure. For these two models we proved theorems for the reachability time and the mixing time (the time it takes to thoroughly randomize any initial graph correlations). These theorems will appear in the chapter "Temporal reachability in dynamic networks" of the book "Dynamics of Networks and Cybersecurity", Imperial College Press in 2015.

We submitted for publication our fast algorithm for generating large-scale random kernel graphs with specified small subgraph properties. This new algorithm dramatically speeds up the time it takes to generate kernel graphs from quadratic scaling to linear scaling in the number of graph nodes. In addition to the manuscript we released a Python software implementation of the algorithm to show the practical performance and simplicity. We have new preliminary further results on this class of kernel models that appear to make it practical to generate networks with specified distributions of triangle, square, and higher order subgraphs.

Future Work

For FY16 we will continue with our three-part approach of data, algorithms, and theorems for the dynamics of cybersecurity network systems. We will continue to seek definitions and theorems for random temporal graphs. We will apply our definition and knowledge of reachability to analyze authentication networks. We will seek to develop and publish new cybersecurity graph data sets for modeling and analysis, and we will develop models and inference methods to fit cyber authentication network data. Our results will be published in leading journals and top conferences in mathematics, statistics and cybersecurity. The algorithms for generating models will be tested and published in the NetworkX Python software package.

Conclusion

We target a fundamental challenge in network science, namely modeling the time-dependent changes in complex networks. Networks targeted in this work are cyber and social networks. We anticipate that this project will have a broad impact in the network science communities: we will contribute new insights and basic methodologies for understanding network evolution affects both the network topology, and those dynamical processes occurring on the network.

Publications

Farrell, M., T. Goodrich, N. Lemons, F. Reidl, F. S. Villaamil, and B. D. Sullivan. Hyperbolicity, degeneracy, and expansion of random intersection graphs. 2015. In to appear in the 12th Workshop on algorithms and models for the web graph.

Hagberg, A., N. Lemons, A. Kent, and J. Neil. Connected Components and Credential Hopping in Authentication Graphs. 2014. In Signal-Image Technology and Internet-Based Systems (SITIS), 2014 Tenth International Conference on. , p. 416.

Hagberg, A., N. Lemons, and S. Misra. Temporal reachability in dynamic networks. In Dynamics of Networks and Cybersecurity. Imperial College Press.

Hagberg, A., and N. Lemons. Fast generation of sparse random kernel graphs. 2015. PloS one. 10 (9): e0135177.

Keszegh, B., N. Lemons, and D. P'alvolgyi. Online and Quasi-online Colorings of Wedges and Intervals. Order. : 1.

Efficient Method for Large Scale Simulations of Fermionic Gases Interacting with Classical Fields

Kipton M. Barros
20140458ER

Introduction

We will develop a tool to simulate a broad range of quantum mechanical phenomena that arise from strongly correlated electrons in actinide, lanthanide, and transition metal based compounds. These compounds are of special interest due to the formation of mesoscale super-structures that produce novel macroscopic functionality. Interacting quantum mechanical systems are notoriously difficult to simulate; existing numerical methods cannot span the gap between atomic and mesoscale. Our new algorithm improves state of the art efficiency by orders of magnitude and makes the mesoscale accessible.

It applies to condensed matter systems of electrons interacting with a classical field that might represent local magnetic moments, charge density or a superconducting order parameter. We focus on the Kondo lattice model (KLM), where itinerant electrons interact with localized classical magnetic moments. Over the past decade, the KLM has been widely used to study giant and colossal magneto-resistance. In recent years, KLM studies have focused on a variety of new phases that have special transport properties. These new phases arise due to the complicated, effective many-body interactions of the classical field, obtained by "integrating out" the conduction electrons. Because electrons are quantum mechanical in nature, tracking the effective interactions for an evolving classical field requires repeated diagonalization of an NxN matrix, where N is the number of atoms in a finite lattice. A direct approach fails for lattices beyond N=400 lattice atoms. In our algorithm, the computational cost scales linearly with system size and preliminary studies of a triangular lattice of N=40,000 atoms lead to a variety of phenomena consistent with experiments: chiral vortices and domains, skyrmions, bound hedgehog dipoles, and interacting vortices. We will extend our method to study a broad variety of 2D and 3D models relevant to real materials and implement a version optimized for parallel execution.

Benefit to National Security Missions

We will develop a tool that will create fundamentally new capabilities for bridging two LANL grand challenges: "Information, Science and Technology" (IS&T) and "Materials: Discovery Science to Strategic Applications"(MDSSA). This research is a direct response to FY13 IS&T Grand Challenge priorities: development of methods for inference and prediction of large-scale complex systems and design of algorithms to efficiently extract information from massive amounts of data. Our project also responds specifically to the LDRD "Materials for the Future" focused area and addresses the priorities of realizing design principles towards controlled functionality and developing multifunctional materials to transform structural and functional performance and integration, and tunable and emergent properties. In the BES report on Basic Research Needs, multifunctional materials are emphasized as solutions to a range of energy problems. The main bottleneck for understanding the complex behavior of interacting quantum systems is the lack of efficient algorithms for simulating the corresponding models. Developing this capability is crucial for addressing future Laboratory mission challenges such as inference and prediction of large-scale complex systems, and prediction and control of emergent phenomena in complex materials. The innovative codes that will be developed under this project will be applied to the simulation of real compounds that are being investigated in our experimental groups. These codes will support new program developments for modeling and simulating complex materials. This challenging task will have a major worldwide impact on the fundamental understanding of unconventional states of matter. Such states have great application potential due to their unusual physical responses.

Progress

The research team refactored and generalized our KPM code to facilitate new application areas. For example,

adding support for a new Kondo Lattice Model now typically involves writing a couple new functions to specify the matrix hopping elements.

Various aspects of the code were optimized to improve builds times of the Hamiltonian matrix. In particular, we now calculate Hamiltonian matrix elements in a multi-threaded way using Intel's Thread Building Blocks (TBB) library. We also use TBB's parallel-sort capability to speed up construction of the Compressed Sparse Row (CSR) matrix format. Finally, using Cuda 6.5, our optimized code can now use Block-compressed Sparse Row (BSR) format, which takes advantage of the block matrix structure typically seen in multi-orbital Hamiltonians. The BSR format eliminates storage of most sparse matrix indices, thereby reducing GPU bandwidth loads, and enabling an effective speed-up of a factor of 2 for typical Hamiltonians. We are still working on the multi-GPU, MPI version of our code.

We also discovered a surprising and beautiful mathematical identity that enables much better scaling with the number of random vectors. As discussed in our report last year, we now benefit from the decay of the density matrix by using "correlated" random vectors. This year, we analyzed the "energy matrix", which can be thought of as the anti-derivative of density matrix (i.e. the anti-derivative of the Fermi function, applied to the Hamiltonian). It turns out that the energy matrix has better decay properties than the density matrix. By using automatic differentiation, we can stochastically estimate the density matrix while still benefiting from the superior decay properties of the energy matrix. In the naive KPM method (our original ER proposal) the stochastic error scales like 's^{-1/2}', in the number of random vectors s. With our improvements, the error decreases exponentially with 's' for insulators. For metals, the error now scales like s^{-1} and s^{-5/6} for 2d and 3d systems respectively. Our code is likely the only one capable of simulating the dynamics of metals in a linear scaling way.

Last summer, our student Julien Roussel successfully implemented a Monte Carlo approach for the graph color problem necessary to effectively choose correlations among KPM random vectors.

The research team's experience with Molecular Dynamics simulations has helped us to improve our methodology also for dynamical simulations of magnetic spin systems. In particular, we have implemented a predictor-corrector scheme for time integration of "stochastic Landau-Lifshitz" (SLL) dynamics. This has had three benefits: (1) integration error now scales O(dt^2), making finite-temperature simulations much more accurate, (2) this richer dynamics now includes effective dynamical waves, which appear to decrease decorrelations times for equilibrium measurements, and (3) SLL dynamics is realistic, enabling us to perform non-equilibrium and dynamical magnet studies.

Interaction with local quantum chemistry experts has suggested fruitful new research directions. For example, after discussions with Anders Niklasson (T-1), we have learned that the Extended Lagrangian formalism could be very useful for solving dynamical self-consistency constraints that appear in condensed matter physics, such as strong magnets. These discussions have spun off a new ER proposal currently under consideration by the CNM committee.

We applied the above-described algorithms to study new physical problems, including:

Using our recent numerical developments to include correlations in quantum molecular dynamics via the so-called Gutzwiller approximation. We have produced the first prototype for modeling single-orbital systems (like Hydrogen). By using this approach, we have computed the self-diffusion coefficient as a function of the strength of the intra-orbital Coulomb interaction. Interestingly enough, we found that the self-diffusion coefficient exhibits a rather sharp maximum near the Mott transition. We are currently finishing a manuscript on this topic.

We have found that crystals of merons and antimerons are solutions of Kondo Lattice Models on high-symmetry lattices. This important result shows that the Ruderman-Kittel-Kasuya-Yosida interaction is not enough to characterize the magnetic ordering of frustrated itinerant magnets. By combining our novel numerical approach with analytical treatments, only valid in the weak-coupling regime, we have discovered that exotic crystals of topological defects can also be stabilized in itinerant magnets. We are currently starting to write a manuscript on this topic.

Future Work

The research team will develop a truly high-performance C++/MPI version of our code, which will be scaled to hundreds of GPUs in order to reach tens or hundreds of thousands of atoms.

We will also use the code developed in 1. to simulate the propagation of topological defects in atomic crystals.

Finally, the team will start simulations of Kondo Lattice Models (KLM) with small Fermi surface pockets. This is a precondition for stabilizing the desired emergent mesoscale structures.

Conclusion

The algorithm and codes to be developed in this project will allow us to study phases that were previously inaccessible. We will study the emergence of complex mesoscale magnetic patterns that we know should occur in low-density electron gases interacting with magnetic ions. Our codes will include a tool for incorporating the band structure parameters of the itinerant electrons which are computed via a tight-binding parameterization of the conduction bands obtained from first principle calculations [Local Density Approximation (LDA)]). We will deliver a high-performance implementation of our algorithm, and many associated analysis tools, to the LANL community.

Publications

Barros, , Sinkovits, and Luijten. Efficient and accurate simulation of dynamic dielectric objects. 2014. JOURNAL OF CHEMICAL PHYSICS. 140 (6).

Barros, K., F. Venderbos, G. Chern, and C. D. Batista. Novel magnetic orderings in the kagome Kondo-lattice model. 2014. Physical Review B. 90: 245199.

Barros, K., and E. Luijten. Dielectric Effects in the Self-Assembly of Binary Colloidal Aggregates. 2014. Physical Review Letters. 113: 017801.

Gan, , Wu, Barros, Xu, and Luijten. Comparison of efficient techniques for the simulation of dielectric objects in electrolytes. 2015. JOURNAL OF COMPUTATIONAL PHYSICS. 291: 317.

Lin, , C. D. Batista, Reichhardt, and Saxena. ac Current Generation in Chiral Magnetic Insulators and Skyrmion Motion induced by the Spin Seebeck Effect. 2014. PHYSICAL REVIEW LETTERS. 112 (18).

Lin, , C. D. Batista, and Saxena. Internal modes of a skyrmion in the ferromagnetic state of chiral magnets. 2014. PHYSICAL REVIEW B. 89 (2).

Lin, S., C. Reichhardt, C. D. Batista, and A. Saxena. Dynamics of skyrmions in chiral magnets: dynamic phase transitions and equation of motion. 2014. Journal of Applied Physics. 115: 17D109.

Lin, S., X. Wang, Y. Kamiya, G. Chern, F. Fan, D. Fan, B. Casas, Y. Liu, V. Kiryukhin , W. Zurek, C. D. Batista, and S. Cheong. Topological defects as relics of emergent continuous symmetry and Higgs condensation of disorder in ferroelectrics. 2014. Nature Physics. 10: 970–977.

Coupled ALE-AMR for 3D Unstructured Grids

Jacob I. Waltz
20150414ER

Introduction

This project researches and develops novel methods for the numerical modeling of high-speed material flows that are applicable to a wide range of scientific and national security problems. The basic concepts under exploration involve the combination of historically proven but heretofore independent techniques. The primary scientific challenge for the project lies in the development of a mathematical approach that couples the different techniques in a consistent manner. Such approaches have not been previously developed either at Los Alamos National Laboratory or within the broader computational science community. The new methods are designed to enhance fidelity and computational efficiency relative to existing methods.

Benefit to National Security Missions

We expect our research to lead to significant improvements in fidelity and computational efficiency for work related to NNSA Defense Programs, Nonproliferation, and Science Campaigns. The impacts of these improvements will include faster responses to programmatic questions; increased population sizes for Uncertainty Quantification and other sensitivity studies; greater detail in discovery-scale simulations; and an enhanced ability to model realistic 3D features.

Future Mission: The jump in simulation capability that results from our research will enable the solution of entirely new classes of problems and therefore has the potential to significantly expand the scope of the Laboratory's simulation tools. New application areas might include design of blast mitigation structures for urban environments, energetic disablement calculations of Improvised Explosive Devices, anti-personnel and anti-structural analysis, high-resolution studies of mix and ignition in Inertial Confinement Fusion targets, and astrophysics.

Progress

The primary goal of the project for FY15 was to develop the theory for and implement mathematical techniques to compute physics-based motion of the moving reference frame. Both the theoretical development and the initial implementation have been successfully completed. Initial verification of the technique also has been completed, and its application to more complex problems is in progress. A presentation on this topic and the overall project will be given at a leading domestic conference in July 2015; a journal article is expected in late FY15 or early FY16.

Future Work

The research team will extend the FY15 work on moving reference frame techniques to include mesh adaption. Specific tasks include:

- implement mathematical techniques to couple mesh adaption to a moving reference frame.
- test the techniques on standard problems involving high-speed material flows
- document the research results in journal articles and/or conference presentations

Conclusion

The goal of this project is to develop a novel method for the numerical modeling of high-speed material flows. The impacts of this work will include significant enhancements in detail and accuracy; reduced uncertainty in simulation-based responses to programmatic issues; and advances in scientific understanding in the broader numerical modeling community. Given the unique nature of the work, it also will establish Los Alamos National Laboratory as an international leader in this area.

Publications

Waltz, J., J. Bakosi, and N. R. Morgan. A coupled ALE-AMR approach for shock hydrodynamics on tetra-

hedral grids. Presented at United States National Congress on Computational Mechanics. (San Diego, CA, 27-31 Jul 2015).

Globally Optimal Sparse Representations

Brendt E. Wohlberg
20150467ER

Introduction

One of the major computational challenges in the modern world is the processing and analysis of the growing deluge of data from such diverse sources as automated telescopes collecting astronomy data, physics data from particle accelerators, and intelligence data from remote sensing satellites, to name but a few. Many of these processing and analysis tasks require an effective model for the data at hand. Such a model is provided by sparse representations, which have found an extremely wide range of applications, often with state-of-the-art results. These representations are mathematically simple to define, but usually involve relatively expensive optimization algorithms to compute them. For practical reasons, this type of model is usually applied independently to small blocks of signal or image data. An alternative form of this representation that jointly models an entire signal or image exists, and has numerous advantages, but is not very widely applied, primarily due to the great computational cost.

Motivated by the recent development of significantly for efficient algorithms for these globally optimal sparse representations, this project will explore and develop the mathematical theory, algorithms, and applications of this approach. While there are numerous clear advantages of this form of sparse representation, there are a number of technical challenges in fully exploiting them. Potential applications include processing of and feature detection in hyperspectral remote sensing imagery, change detection in wide-field automated sky surveys, structural health monitoring for critical machinery and buildings, and detection and classification of features in radio frequency signals for non-proliferation monitoring. This work also has the potential for significant impact in the fields of signal and image processing, where sparse representations have become a major subject of research.

Benefit to National Security Missions

The project will develop a general data modeling technique, primarily with relevance to data in the form of sampled signals, images, or video. Given the generality of the method, it has potential relevance to any of the areas above that require processing or analysis of these types of data. As such, the primary mission relevance is to Information Science and Technology. Nevertheless, specific potential application areas that have already been identified include analysis of radio frequency data for non-proliferation monitoring (relevant to agency DOE/NNSA and mission Remote Sensing for Nuclear Nonproliferation), analysis of remote sensing data for non-proliferation and intelligence acquisition (relevant to DOE/NNSA and Intelligence Agencies, and mission Remote Sensing for Nuclear Nonproliferation), modeling of material properties and analysis of multiple modalities of materials science data (relevant to Basic Understanding of Materials mission), structural health monitoring for machinery, including vehicles (relevant to agency DOT and Commerce and Transportation mission), and analysis of astronomical and sky-survey data (relevant to agency NASA and mission Nuclear, Particle, Cosmology, and Astrophysics).

Progress

Substantial progress has been made in the seven months since the start of the project. To summarize:

A new method has been developed to improve algorithm convergence, reducing the time required to compute the data representation. This method has potential benefits for a general class of optimization algorithms, of which the problem at the core of this project is just one example. A journal paper has been submitted to IEEE Transactions on Signal Processing, and is currently under review.

The main algorithm has been refined and improved in a

number of ways, and a careful comparison has been made with competing approaches, showing that it provides substantial computational advantages in most problem regimes. A journal paper describing this work has been submitted to IEEE Transactions on Image Processing, and is currently under review.

The general method has been extended to additional image processing applications, and work is ongoing in improving application performance. A journal paper describing this work is in preparation.

In line with the commitment to open source expressed in the project proposal, an initial version of an open source software library has been completed and publicly released.

Two difference collaborations have been established with external groups (at University of Rochester and at Academia Sinicia in Taiwan) working on audio signal processing problems. Thus far, these collaborations have led to a conference paper presented at ICASSP 2014, and another conference paper recently submitted to MLSP 2015.

Ongoing collaboration on applications of sparse representation and convolutional sparse representation methods to anomaly detection problems, with collaborators at Politecnico di Milano and Tampere University of Technology, have led to two conference papers that have already been presented, and an additional one accepted for presentation.

Joint work with a collaborator at Pontifical Catholic University of Peru (with a joint UNM appointment) has led to a conference paper accepted for presentation and a joint UNM/LANL patent on a novel video background modeling method that exploits ideas from convolutional sparse representations.

Invited research seminars have been presented at the UCLA Math department and at Microsft Research at Redmond.

Future Work

The second fiscal year of the project will focus on the following main aspects of the project:

Signal representation

Initial experiments, and some initial reports in the literature, indicate that convolutional sparse representations are most effective when applied to signals and images that have been pre-processed to remove smoothly varying components. The most effective choice of this preprocessing, which can have a major performance impact, is far from clear, and substantial theoretical and experimental work is required to resolve this question. Progress was made on this aspect during the first fiscal year of the project, but a proper understanding of the optimal approach is still to be developed.

Dictionary learning

Even in the case of standard sparse representations, the problem of learning a "dictionary" (the set of basic components from which the linear representation is assembled) is still rapidly developing, and is far from being a solved problem. Learning effective dictionaries in the convolutional setting presents an additional set of challenges related to the vastly increased redundancy of the representation. The possibility of constructing multiscale dictionaries is one of the major advantages of this form, but also provides a further set of technical challenges. Some progress was made on this aspect during the first year, but significant work remains to be done.

Algorithm development

Efficient algorithms have recently been developed, but further increases in efficiency would both aid the computational experiments required for other aspects of the project, and expand the range of potential applications. Considerable progress has been made in this area, but there are some possible improvements remaining to be explored.

Conclusion

The major technical goals are the development of theory, algorithms, and applications of the globally optimal sparse representations. This work will primarily involve the development of signal processing theory and methods, together with associated algorithms. If successful, these developments have the potential to change the standard practice in the application of sparse representation methods to a wide variety of problems, together with improved performance and new capabilities of these methods. An open-source library will be released to make these techniques widely available to researchers in the field, as well as to practitioners in application areas.

Publications

Boracchi, Giacomo, Diego Carrera, and Brendt Wohlberg. Novelty Detection in Images by Sparse Representations. 2014. In Proceedings of the IEEE Symposium Series on Computational Intelligence (IEEE SSCI). , p. 47.

Carrera, Diego, Giacomo Boracchi, Alessandro Foi, and Brendt Wohlberg. Detecting Anomalous Structures by Convolutional Sparse Models. 2015. In The International Joint Conference on Neural Networks (IJCNN).

Cogliati, Andrea, Zhiyao Duan, and Brendt Wohlberg. Piano

Music Transcription With Fast Convolutional Sparse Coding. 2015. In IEEE International Workshop on Machine Learning for Signal Processing.

Jao, Ping-Keng, Yi-Hsuan Yang, and Brendt Wohlberg. Informed Monaural Source Separation of Music based on Convolutional Sparse Coding. 2015. In Proceedings of IEEE International Conference on Acoustics, Speech, and Signal Processing (ICASSP). , p. 236.

Rodriguez, P., and Brendt Wohlberg. Incremental Principal Component Pursuit for Video Background Modeling. To appear in Journal of Mathematical Imaging and Vision.

Rodriguez, Paul, and Brendt Wohlberg. Translational and Rotational Jitter Invariant Incremental Principal Component Pursuit for Video Background Modeling. 2015. In Proceedings of IEEE International Conference on Image Processing (ICIP).

Wohlberg, Brendt. Endogenous Convolutional Sparse Representations for Translation Invariant Image Subspace Models. 2014. In Proceedings of IEEE International Conference on Image Processing (ICIP). , p. 2859.

Wohlberg, Brendt. Efficient Algorithms for Convolutional Sparse Representations. To appear in IEEE Transactions on Image Processing.

Enabling Automatic Parallelism and Transparent Fault Tolerance

Marion K. Davis
20150485ER

Introduction

One of the three major challenges in harnessing the potential of an extreme-scale computing system, as identified by the 2010 Summary Report of the DOE Office of Science Advanced Scientific Computing Advisory Committee (ASCAC), is exploiting massive parallelism. In particular, they state that software implementations will need new programming paradigms to make effective use of unprecedented levels of concurrency. Yet more recent is the 2011 DOE Advanced Scientific Computing Research (ASCR) Exascale Programming Challenges Report, specifically calling out the need to revisit functional-language concepts. DOE and DARPA have also recognized the potential of domain-specific languages (DSLs) for raising the level of abstraction of programming. In the broader scientific computing community it is becoming more widely understood that the only programming paradigm that can so scale will be data-dependence-based asynchronous scheduling of purely functional compute tasks. In turn, this paradigm enables a fault-tolerance mechanism much more light-weight than checkpoint/restart because compute tasks, being pure (side-effect free), can be safely restarted if their failure is detected. This project will develop and evaluate a robust and performant implementation of this paradigm in its purest form wherein compute tasks are both internally and externally (observationally) pure. While such systems have been proposed, and their theoretical properties are well-understood, no non-trivial implementation exists with an evaluation mechanism that is strict by default, i.e., exhibiting the behavior most commonly expected by programmers and required for high performance. By its nature such a system will be able to automatically extract maximal parallelism from a program, and in the presence of uncommitted compute resources allow speculative evaluation of results that may or may not be needed in the future. Further, it enables transparent (to the programmer) fault tolerance mechanism as previously described, and a type system that supports efficient deep embedding of DSLs.

Benefit to National Security Missions

High performance computing is fundamental to the advancement of many areas of science. While innovations in hardware technologies continue to allow us to build ever more powerful and complex computing systems, our modes of programming them have advanced conservatively. Both DOE and DARPA have recognized the need to re-examine the entire software stack that ranges from operating systems, runtime systems, programming systems, and applications. At the level of programming systems, the need to re-explore functional language concepts has been explicitly identified. This project directly addresses this need, as well as its corresponding runtime system. Breakthroughs in this area will benefit high performance scientific computing at large, and all scientific disciplines that use it.

Progress

The research team determined that the appropriate break-out point from GHC (Glasgow Haskell Compiler) is at the STG (spineless tagless G-machine) intermediate representation. Our system then will compile STG, with our non-standard semantics, to executable code. The greater part of the overall effort is the runtime system, initially supporting serial execution and garbage collection, later parallel execution, and then some degree of parallel garbage collection.

We have established that we can modify and build a recent version of GHC from source, thus allowing the possibility of not needing to parse GHC's STG dump. However, given that STG is itself a complete higher-order, polymorphic, pure functional programming language in its own right, we regard the bridging of the gap between the GHC specifics and STG as reported in the literature to be of lesser immediate priority than realizing the missing parts of the toolchain--the compilation of STG to machine code and the creation of the supporting runtime system, which are the core functionality needed for the

overall goals of the project.

Our initial proof of concept was the modification of an existing STG interpreter to provide variable-strictness semantics: from the provided "lazy" (call-by-need, or non-strict with sharing) to, e.g., strictness in function arguments, constructors, or "let" expressions, while preserving the sharing. This provides our reference semantics for a compiler-based implementation.

We defined an abstract machine that is implemented by the code generator. Analogously to the simulator, it is a modification of the STG machine as reported in the literature, using variants of the "eval/apply" evaluation strategy appropriate for the specified degree of strictness, and later parallelization.

This latter is rather more general than originally envisioned: as proposed only fully strict semantics would be supported. We determined, however, that to be "currying friendly," that is, to efficiently support closures and partial function application with proper scoping and lifetimes, required machinery that readily generalizes to the STG model and so implemented it in its full generality.

Critical to such an implementation is the ability to realize efficient tail calls (interprocedural "jumps"). Our original proposal was to directly generate LLVM (Low Level Virtual Machine) code. However, given the unusual nature of the control structure it was more expedient to implement a subset of the portable machine language C-- that is compilable with a C compiler, including GCC and and Clang/LLVM. Serendipitously we now have two independent mechanisms for tail calls: via C--, and directly from the C compilers given mild constraints on the C-- implementation, and still benefit from the LLVM (or GCC back-end) optimization.

We set up a distributed revision control system (Git), an automated building/testing system (Jenkins), project wiki, etc., to manage our project documents and code, and as a template for the eventual open-sourcing of the software.

The research team also implemented a parser, a constraint-based Hindley-Milner-Damas type inferencer, a compiler (serial code only at this point) from STG to our implementation of C--, a supporting runtime system, and a small test suite. The runtime system includes a 2-space copying garbage collector. In other words, we have an operational, demonstrable compiler toolchain. As such we are right on target with the Gannt progress chart in the original proposal.

Future Work

Our goals for FY16 are as follows:

- Largely complete serial implementation
- Begin implementation of runtime support for parallel evaluation

The corresponding tasks are as follows:

Serial implementation

1. Implement variably-sized heap and stack objects
2. Generalize support for unboxed types
3. Re-implement garbage collector for (1) and (2)
4. Investigate performance implications of using native tail calls
5. Generally improve code generation
6. Add explicit compiler flags for specifying strictness properties

Parallel evaluation

1. Design and implementation of thread pool
2. Design and implementation of multiple-heap mechanism
3. Add par language construct for explicit task parallelism

Conclusion

First is the strict pure functional language implementation itself, as open source--the first of its kind, even disregarding the automatic parallelization, explicit speculative evaluation, and resilience mechanism that this system will implement. Second, the practical validity of arguments for and against the strict but pure functional paradigm, in the context of scientific computing, while maintaining purity, will be testable. Third is the demonstration of utility of an environment in which embedded DSLs may be developed and their space/time performance meaningfully evaluated.

Inserting Nonlinear N-Material Coupling PDF Information into Turbulent Mixing Models

Jozsef Bakosi
20150498ER

Introduction

The project develops new mathematical models for turbulent mixing. We target applications in which the detailed simulation of turbulence is intractable and the purpose of "turbulence models" is to predict the statistics of turbulent mixing which is far more tractable. We address the mixing problem of multiple materials with very different densities. In such problems the velocity affects the material fields and more importantly, the material fields affect the velocity field. This results in strong two-way coupling between the fields that is not accounted for in current statistical computations.

The work introduces a new principle: Any model for the statistics must be derived from a relevant underlying probability density function (PDF), a higher order mathematical object that is consistent with the physics of coupled hydrodynamics and material mixing and contains information on all statistics. This ensures physical correctness at the mathematical and theoretical levels and has never been done.

We synthesize two evolution equations governing mass transport in two realms describing turbulent mixing: the mass fractions transport in physical space, and the Master Equation describing the transport of statistical information in probability state space. We also apply two averaging methods: Reynolds averaging in physical space and sample space averaging. This allows instantaneous constraints to be inserted into statistically averaged equations. This synthesis has never been done.

Also, we bridge the multi-fluid and single-fluid descriptions of turbulent mixing. The Master Equation allows accounting for widely different underlying PDFs of the state space, representing very different non-equilibrium stages of the mixing process. This two-pronged strategy allows representing both sharp and diffusive material interfaces within the same method and allows a continuous bridging between multi and single fluid models, which has never been done.

The project entails mathematics, theory, computation, and validation, resulting in implementation of new models in a LANL production code.

Benefit to National Security Missions

Multi-component variable-density turbulent material mixing is a central element in many LANL programs. Material fields are required for a predictive science of turbulent mixing, reaction, and opacity. This work will directly and immediately impact modeling efforts and advance the predictive science in ASC (XCP) and several campaigns. The work will result in engineering models, directly relevant to LANL's large physics codes, in which the resolution of all scales are intractable and statistical methods are the only practical approach.

The results of the work will be translated in the 3rd year into programmatic engineering efforts by implementation of the developed equations into LANL's RAGE production code. To this end we are in contact with Robert Gore (XTD-IDA), project lead of two campaigns.

Progress

Part of the first FY was spent exploring different probability density functions (PDFs) to see which provide signature behavior of high-order statistical information seen in high-density-difference turbulent material mixing. The developed necessary theoretical principles we have (so far) focused on binary mixing, which then will be extended to the mathematics of multiple materials mixing models now and next FY. Based on data of high-fidelity direct numerical simulations (DNS) of variable-density turbulent mixing between fluids of very different densities, we selected a beta-distributed stochastic process to describe the time-evolution of the binary materials PDF due to its favorable characteristics.

We have compared to data how the stochastic beta process mixes the density,the mass fractions, and the volume fractions, in order to choose the correct variable for a mixing process. We have studied the three mixing processes to see which Master Equation (ME) mixing process best represents material mixing physics, specifically, which produces a unique non-monotonic behavior of skewness only seen variable-density mixing. We derived multiple hierarchies of moment equations for statistics describing variable-density mixing to study which has the proper mathematical structure. A stochastic beta process for the mass fractions (not density or volume fractions) is the only process capable of correctly emulating observations in variable-density turbulent mixing.

The ME for the stochastic beta process for variable-density mixing has three unknown parameters (b, kappa, S) that depend on the statistics of the mixing process. We derived mathematical forms of b, kappa, and S, that ensure the correct asymptotic behavior of the mass fractions PDF and its statistics. These results constitute an important step toward the mathematical model not only for the ME but also for the moment equations derived from the ME. This will lead to engineering models that are applicable and can be inserted into moment closures for binary mixing. These theoretical results for the binary process provide a crucial step towards treating the multi-material problem and also has some important and direct practical applications for binary mix models of programmatic interest (see below).

We have also developed a Monte Carlo simulation code to explore the mathematical behavior of the stochastic processes described by Master Equations. This is an unexpected development of a novel methodology that was not part of the original proposal and which produces several unanticipated and important results. For example: one is faced with developing closure approximations for terms in the moment equations derived from the ME and from Navier-Stokes. Using this methodology, we are now in the position to test the validity of the modeled mixing closures using Monte Carlo simulations of a realizable mixing process. The importance of this technique becomes clear when one considers the established practice in turbulence modeling of mixing processes. In established practice a closure for an unknown unclosed term is first proposed then tested against data of a quantity in the physical equation with the unknown term. Using a Monte Carlo simulation we can directly test the closure approximation for the unknown term independent of other physical effects and their approximations.

We have also started work on performing simulations for model validation purposes. We will use an existing verified and validated large eddy simulation (LES) code for a number of simulation cases that will be used to produce data currently non-existent in the literature. Specifically, we compute two different types of variable-density turbulent binary mixing flow for validation: a spatially homogeneous but non-stationary and a spatially inhomogeneous but statistically stationary flow -- both with various initial configurations not computed previously. The LES results together with the existing DNS data will be used to validate and guide our final specification of the binary material mix model as well as the work in the next FYs on the multi-component model.

Besides the new and unexpected Monte Carlo simulations and the LES simulations for validation, we are also planning to validate our moment equation binary mix model in an XTD division research code solving for our validation cases. This step will help evaluate (1) the principles in our binary moment equation mix model before proceeding to the theory of the multi-material problem, and (2) how our work fits into the existing moment method (BHR) currently used in XTD.

Future Work

Going forward, the research temam will connect the first year's work on binary mixing to the existing moment method (BHR) currently used in XTD division. In particular, we investigate how some of the statistics computed by BHR can be specified based on our model. This identifies differences between the models and sheds light on how BHR can be improved.

Theoretical work on multi-component (ternary) variable-density mixing will begin. We derive moment equation hierarchies from the Master Equation (ME) and Navier-Stokes. We work on specifying approximations of the unknown terms in our model. This will yield a testable and directly useful engineering method for multi-component mixing.

Our Monte Carlo simulation code will continute to be used to validate closure approximation hypotheses but now for the multi-component case with ternary mixing. The goals here are similar to that of the binary case: using a physically realizable mixing process we test the validity of the modeled mixing closures as well as the correct asymptotic behaviors.

We continue the large eddy simulations to produce validation data with various initial conditions. Specifically, we compute two different types of variable-density turbulent binary mixing flow for validation: a spatially homogeneous but non-stationary and a spatially inhomogeneous but sta-

tistically stationary flow -- both with various initial configurations not computed previously. We will also extend the capability of the LES code to compute ternary mixing.

Also, the research team will run various test cases with an XTD division research code that solves our simpler validation cases using ordinary differential equations governing spatially homogeneous mixing. This is a crucial intermediate step in model validation as well as comparing our model to BHR and is used for testing only parts of the modeled process independent of spatial transport.

Conclusion

The new turbulent material mix model will correctly account for the nonlinear coupling and constrained statistics in the mixing of multiple materials that do not exist in current approaches and will avoid the conventional passive-scalar approximations that are inadequate for LANL problems. The new model will be implemented in a production code for immediate impact on programmatic efforts. We expect sizable improvements over the currently used passive-scalar approximations for multi-material mixing problems and highly visible breakthrough-level results in the area of material mixing to be published in the open literature.

Long-time Dynamics using Trajectory Splicing

Arthur F. Voter
20150557ER

Introduction

Molecular dynamics (MD), the simulation of the evolution of individual atoms in a material, is an essential tool to further our understanding of materials at the nanoscale. Due to its inherently serial nature, however, MD is strongly limited in the timescales it can reach, a problem that becomes even more crippling on large-scale parallel computers. There is thus a pressing mission need for massively-parallel long-time MD simulation techniques. Building on our many years of experience addressing this issue, we are introducing a new paradigm in long-timescale simulation: parallel trajectory splicing (ParSplice). In this ParSplice approach, a long trajectory of arbitrary accuracy is assembled from many short, independent segments generated efficiently in parallel. Through the use of simulation simulators, i.e., simple models of the simulation framework, we will systematically explore the large design space of ParSplice methods to identify the best performing methods on existing and expected next-generation (or exascale) computer architectures, taking into account massive core counts, shorter mean times between failures, and energy costs dominated by data-motion. We will demonstrate the efficiency of the approach in production conditions by investigating problems important to the mission of the lab such as void and bubble evolution, annealing of defects at grain boundaries, and ionic transport in complex oxides. For systems where the trajectory is trapped in small regions of configuration space, we expect efficiency gains of several orders of magnitude at extreme computational scales compared to current approaches. ParSplice will revolutionize the way large-scale long-time MD simulations are performed.

Benefit to National Security Missions

The project directly addresses fundamental challenges of direct relevance to the lab and to DOE/SC/BES and DOE/SC/ASCR. Our project supports the Scientific Discovery and Innovation mission of the lab through two pillars: the basic understanding of materials, and IS&T. Indeed, our goal is to develop a novel capability that would enable the direct simulation of materials at the atomic scale over extremely long timescales. Such a capability is invaluable to investigate the microstructural evolution of materials and understand their performance in operation conditions. Applications to materials in extreme condition are directly relevant to the lab's mission, for example in support of the MaRIE effort. Application to nuclear materials are also directly relevant to BES and OFES. A second crucial aspect of the project is to develop a novel simulation paradigm that exploits state-of-the-art concepts in computer science. We are especially interested in the scalability of simulations up to the peta and exa-scales. Doing so requires the development of architecture-aware algorithms and codes that are scalable and fault-tolerant. Our project contains an important performance prediction component that will be used to predict and optimize the performance of the code on various architecture. These activities directly address challenges identified by ASCR.

Progress

During the first FY of the project, we have analyzed the "certification rules" (which enforce that the result is free from bias) and determined that they could be safely relaxed from what we had proposed in the initial proposal. This flexibility improves the performance of ParSplice and simplifies the implementation. We have also explored "placement rules", i.e., the assignation of work on the different replicas. We have compared two strategies: one based on the current end point of the trajectory, and one on its projected end point once the work unit that is about to be scheduled is completed. The latter strategy proved to be extremely efficient, but it can be computationally expensive compared to the former. The simple strategy however was surprisingly efficient as compared to the previous state of the art, and could be leveraged at larger computational scales, when minimiz-

ing the scheduling effort will be paramount.

We have developed and implemented a first production version of ParSplice within LANL's AMDF code. We have validated it using a simple defect, a trimer on a silver surface. We have assessed its scalability up to hundreds of cores and compared its performance to previous approaches. The initial results are extremely encouraging and show that improvements of up to an order of magnitude are possible with the current code. We are currently applying the code to more complex systems and initial results are very positive. We are now working on a manuscript that reports on our new method.

Future Work

During the next fiscal year, we will concentrate on improving the scalability of ParSplice in order to be able to exploit peta-scale computational resources, and beyond. This will require designing tailored certification and placement rules that require minimal computational work, little or no synchronization, and built-in fault tolerance. It will also require the development of scalable software components (such as segment and state databases) that are able to handle large throughputs. This will likely require the development of a hierarchical management structure, in contrast to the current master/slave implementation. We will develop such scaling strategies and demonstrate them on IC resources or on application simulators for extrapolation to extremely large scales.

Concomitantly, we will apply our current code at intermediate scales (~1000 cores) in order to further demonstrate its practical uses in research settings. We will identify systems for which current methods are inadequate and demonstrate how ParSplice can overcome current limitations. Possible application areas include complex defects in metals and nanoscale clusters.

Conclusion

The research team will develop the ParSplice method and deliver an implementation that is nominally exascale ready. This state of readiness will be validated through extensive simulations using our performance prediction approach. The design and parameter spaces will be thoroughly explored so as to be ready to adjust the implementation novel architectures emerge. We will also deliver a thorough formal understanding of the method. Based on this analysis, the class of systems that would optimally benefit from ParSplice will be identified. The power of the approach will be demonstrated on leadership-class computers on physical problems of interest to the lab.

Spatial and Extreme Value Processes for Bridging Micro- and Macro-Scales in Materials

Scott A. Vander Wiel
20150594ER

Introduction

Advances in computing power have made it possible to simulate very small physical systems in remarkable detail, often making use of "first principles," or at least very reliable mathematical models for system evolution. However, bridging information from simulations at very small scales to the macro-scale required for modeling large-scale systems (e.g. the global ocean, a nuclear reactor, an implosion) remains a challenging and open problem. In materials science, advances in bridging scales are needed to develop more predictive models of material behavior given its micro-scale composition, enabling more reliable predictions of material properties in new, extreme environments, and enabling the design of new materials.

This project focuses on a basic problem in material science: How do heterogeneous, micro-scale descriptions of a polycrystal affect macro-scale mechanical response properties? Here the seemingly random spatial distribution of micro-scale material properties often results in spatially coherent stress fields (under loading), leading to damage or failure in the material. This project will focus on developing statistical theory, models, and tools to advance our ability to estimate macro-scale mechanical response properties from heterogeneous, random, microscale material descriptions.

Benefit to National Security Missions

There is a demonstrated need for advancement in computational prediction of damage and failure in polycrystalline metallic materials, particularly for our weapons calculations. This is largely a result of inadequate physics and material statistics representation. Although the computation mechanics and mechanics of materials communities continue to make advances in this arena, much of the work is lacking proper rigor in how extreme value physical processes are represented mathematically. This project is designed to address this shortcoming in how we represent such processes. The programs here at LANL with interest and need in these technological areas are ASC PEM Materials Modeling, and several campaigns. With increased interest in advanced and additive manufacturing processes, a rigorous statistical linkage to the material microstructure as we are proposing to do here will be important. In addition, the Office of Science is interested in funding work which offers the potential to promote energy efficiency. By improving our ability to predict damage and failure events in metallic materials, transportation sector industries can make more efficient use of materials and reduce the weight of vehicles and reduce manufacturing energy intensity.

Progress

Flyer plate experiments on tantalum samples in combination with macro-scale damage model calculations of these experiments have provided quantitative information on stress conditions at the estimated point when material voids begin to grow. These boundary conditions are used as inputs to meso-scale polycrystalline models to interrogate the behavior of interacting tantalum grains.

Finite element models of tantalum microstructure have been created with a 3D voxel structure that matches distributions of grain size, shape and crystal orientations. We can provide an endless supply of statistically equivalent microstructure realizations for further modeling efforts.

We apply external stresses with time, representative of those in flyer plate experiments to the polycrystalline finite element meshes to produce stress fields throughout a representative volume of tantalum grains. These calculations show that stress tends to elevate at interfaces between two grains and more-so where three grains meet.

We have developed a statistical model to represent the stress field in a multi-grain volume. The model incorporates several features observed in meso-scale computations: (i) each grain has its own nominal stress level, (ii) stresses tend to elevate at some, but not all, grain boundaries, (iii) boundary locations with elevated stress are correlated across grains. Fitting of the statistical model is challenging because meshes are on the order of half a million elements and this translates into vary large covariance matrices that represent spatial dependence in stress fields.

Implementation of the statistical model is nearly complete. We represent stress fields as integrals of Gaussian Markov random fields. The structure of this model allows large-scale correlated fields to be computed blockwise in a Monte Carlo Markov chain (MCMC) calculation. The result is a posterior distribution of parameters that control correlation length scales and distances that elevated boundary stresses penetrate into grain bodies.

This is a totally new approach to characterizing stress fields in polycrystalline materials with the potential to statistically bridge the gap between meso-scale and macro-scale models describing and predicting how materials fail. Writing the initial implementation of the statistical model has been challenging, but we are just now getting results and enhancements to the model form will be much easier to implement than creation of the initial code from whole cloth.

Sparse matrix derivations of likelihood calculations required for MCMC implementation have been written up and will form the core technical portion of a paper to be submitted to a statistics journal.

Curt Bronkhorst presented some of this work in invited presentations at three conferences in 2015: (i) Mach Conference for Multiscale Materials; (ii) TMS Annual Meeting; (iii) International Symposium on Plasticity.

Future Work

This effort will be conducted in two main phases. In the first phase, statistical theory and methodology will be developed in concert with a simulation campaign focused on simulated materials. Once methodology has been sufficiently refined, and kinks and problems have been worked out in the synthetic setting, we expect to move focus to actual materials.

Over the next fiscal year, we will:

- Design and carry out dynamic loading simulations of polycrystalline structures, under different initial conditions for the polycrystal, as well as under different dynamic loads.
- Develop statistical models of the spatial dependence and strength anisotropies describing the polycrystal.
- Develop statistical models of the resulting stress field, characterizing the extremes of the field, as well as their spatial dependence.
- Search out and catalog physical data on polycrystal configurations that are relevant to this effort.

Conclusion

This effort will demonstrate a viable approach for statistically characterizing micro-scale properties of a polycrystal, and using these properties to predict the material's strength and damage properties at a macro-scale, under some rather simple loading scenarios. We also expect this effort will illuminate promising new directions for analysis approaches that can bridge the micro- and macro-scales. In particular, we will seek new statistically rigorous representations of damage nucleation in polycrystalline materials. As new experimental facilities come online, this work will serve to get some of the necessary analytical tools in place for gaining understanding from such experiments.

Publications

Bronkhorst, C. A., N. Bourne, G. T. Gray III, V. Livescu, C. B. Storlie, S. A. Vander Wiel, E. K. Cerreta, D. J. Luscher, M. Ardeljan, and M. Knezevic. Deformation Induced Porosity Nucleation Mechanisms in Polycrystalline Metallic Materials (keynote lecture). Invited presentation at International Symposium on Plasticity 2015. (Montego Bay, Jamaica, 4-8 January, 2015).

Bronkhorst, C. A., N. Bourne, G. T. Gray III, V. Livescu, C. B. Storlie, S. A. Vander Wiel, E. K. Cerreta, D. J. Luscher, M. Ardeljan, and M. Knezevic. Deformation Induced Porosity Nucleation Mechanisms in Polycrystalline Metallic Materials. Presented at Mach Conference 2015. (Montego Bay, Jamaica, 8-10 April, 2015).

Bronkhorst, C. A., N. Bourne, G. T. Gray III, V. Livescu, C. B. Storlie, S. A. Vander Wiel, F. L. Addessio, D. J. Luscher, M. Ardeljan, E. K. Cerreta, and M. Knezevic. Porosity Based Damage and Failure in Polycrystalline Tantalum – Structural Linkages (invited). Invited presentation at TMS 2015. (Orlando, Florida, 15-19 March, 2015).

A Computationally Efficient Model for Warm Dense Mixtures

Didier Saumon
20130244ER

Abstract

Warm dense matter (WDM) encompasses ionized fluids at the confluence of condensed matter physics, plasma physics, and dense fluids and cannot be described adequately by the theories of these well-established fields. It is a frontier of high energy density physics (HEDP) that presents considerable challenges to theory and experiments.

We developed theoretical and computational tools to model mixtures in the WDM regime. This is evolving into a new, state-of-the-art capability to model extreme states of matter at LANL that will support future experiments at HEDP facilities and numerous programmatic applications involving the hydrodynamics of dense plasma mixtures.

Our approach is based on a suite of approximate models that account for the most important physics of warm, dense plasmas while remaining computationally economical. It is ideally suited to produce large tables of constitutive physical properties of materials such as the equation of state (EOS) and transport coefficients for a wide range of applications. Most notably, we have developed tools of remarkable computational efficiency and very good accuracy to generate tables of diffusion coefficient for WDM mixtures. We have demonstrated the validity of our models by extensive comparisons with results obtained with state-of-the-art ab initio simulations methods. We present applications to dense plasma mixtures encountered in white dwarf stars.

Background and Research Objectives

Warm dense matter conditions typically occur at temperatures of 1eV to several 100eV and densities from 0.1 to 100 times normal solid densities [1]. WDM is too hot to be treated by the standard methods of condensed-matter and liquid-state physics, but too cool to be modeled as a weakly coupled plasma. It lies in an intermediate region where simplifying approximations are elusive. It is a frontier of HEDP of great practical importance.

WDM mixtures lie at the heart of problems in planetary science and stellar astrophysics. Examples include the phase diagram of hydrogen and helium in Jupiter and Saturn and the gravitational stratification of elements in white dwarf stars. WDM mixtures also occur during the implosion phase of inertial confinement fusion (ICF) capsules.

WDM can be modeled successfully with large scale ab initio simulations, primarily with quantum molecular dynamics (QMD) [1]. However, this method becomes prohibitively expensive at temperatures above 10eV for most systems. At higher temperatures, a simpler version that uses the Thomas-Fermi model of the electron - rather than the physically more accurate Schrödinger equation - can be applied. Nonetheless, this orbital-free molecular dynamics (OFMD) method remains computationally expensive [2].

Our main goal is to develop a new approach to model WDM that is computationally much more efficient than QMD and OFMD with a more approximate yet realistic description of the physics of dense plasmas. It would then become practical to generate large tables of WDM properties for many different applications. In this project, we extended our single-component model to mixtures and computed EOS and diffusion coefficients. We have made several important advances and we have been very successful in reaching our goal.

Scientific Approach and Accomplishments

This LDRD project is an extension to mixtures of our research on dense, single-component plasmas which is funded separately. Thus the following exposition necessarily involves some discussion of our single-component work.

Formalism for mixtures

We formulated a multiple-component mixture theory by expanding that of our single-component microscopic model of dense plasmas called Quantum Hyper-Netted Chain (QHNC) [3]. We arrived at a much simpler form than we originally anticipated. This set of equations is not only valid for binary mixtures but is readily extended to mixtures of an arbitrary number of ion species and quantum mechanical electrons [4].

Pseudo-atom model

The microscopic model for the bound states of the plasma ions, the electronic screening, and the fluid structure of the plasma is no longer the QHNC model, but evolved into an original variation that has proved far superior for modeling WDM. This new model, called PYRRHO, assumes that the plasma is made of identical pseudo-atoms. The pseudo-atom is composed of a nucleus and its surrounding spherically symmetric electron cloud of bound and screening electrons [5]. The structure of the pseudo-atom is obtained with an average atom model in which the electrons can be described either with a full quantum mechanical (Kohn-Sham, or KS) model or in the orbital-free (OF) approximation. The pseudo-atom is combined with the integral equations of fluid theory for a complete, self-consistent model of the plasma. The solution of the set of equations gives a detailed microscopic description of the plasma without free parameters. The PYRRHO model is far more stable numerically than the original QHNC. The KS mode of PYRRHO runs well up to several 100eV, retaining a full quantum mechanical description of the plasma over the full regime of WDM, which is generally not possible with QMD. The PYRRHO model was generalized to mixtures within the formalism described above.

The PYRRHO model has been extensively tested against single-component warm dense plasmas and turns out to be very successful [4-7]. We have demonstrated the ability to solve the system of equations for up to seven-component mixtures of dissimilar elements and mixtures where one component is a trace species, as well as ions with very different charges and/or masses. Such plasmas are difficult to model with ab initio methods.

The ion pair distribution function is the quantity predicted by PYRRHO that is most readily compared with other calculations. We have made such comparisons in the WDM regime with pair distribution functions from QMD and OFMD simulations of elements as varied as hydrogen, carbon, beryllium, aluminum, iron and tungsten for temperatures of a few to hundreds of eV, all with excellent agreement [5, 6].

We have validated the underlying PYRRHO model of mixtures against published QMD simulations of a plasma of carbon and hydrogen relevant to ICF capsules [4]. The pair distribution functions of ions in the C-H plasma are in excellent agreement at high temperatures and high densities. Deviations arise and grow steadily at lower temperatures and densities because of the formation of C-C chemical bonds in the plasma, something that PYRRHO cannot describe. This pointed out a fundamental limitation of our pseudo-atom model for those material that are not fully dissociated in the WDM regime. Nonetheless, we were able to validate PAMD for mixtures against OFMD simulations of the C-H mixture for the same conditions since chemical bonds cannot form in the OF approximation.

We have compared our ionic pair distribution functions with published OFMD simulations for a mixture of copper-deuterium and for a carbon-oxygen mixture computed with our own OFMD code, all with excellent agreement. We also found excellent agreement with the OFMD EOS of a Fe-He mixture (Figure 1) [15].

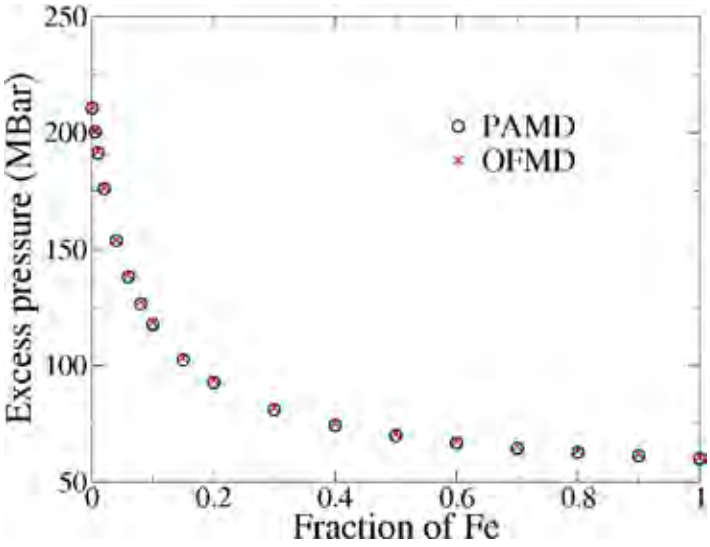

Figure 1. Excess pressure (contributions other than non-interacting gas) of mixtures of iron (Fe) and helium (He) at a temperature of 50eV and density of 10g/cm3. Our OF-PAMD calculations are shown by open circles which are compared to state-of-the-art OFMD simulations [15]. The agreement is better than 1.5% for all Fe:He mixing ratios, which validates the OF-PAMD moled for a highly asymmetric plasma mixture in the WDM regime. From [7].

Pseudo-atom molecular dynamics

The PYRRHO model is described by a set of algebraic equations and is static by construction. However, it generates ion-ion potentials for all components pairs in the mixture. Those potentials can be used in a classical molecular dynamics simulation from which we can extract quantities that are intrinsically dynamic in character, i.e. those that

involve particle collisions. The combination of PYRRHO and classical molecular dynamics, which we call Pseudo-Atom Molecular Dynamics (PAMD) is a significant advance and has become the central tool of our program to model WDM [7].

PAMD is similar to QMD and OFMD: it combines a quantum mechanical (or orbital free) description of the electrons with the classical motion of the ions. With PAMD we can calculate the same plasma quantities as ab initio simulations but 10-100 times faster with MD simulations that typically contain 10-100 times more particles and run for 10 times more time steps. These larger and longer simulations reduce the statistical noise due to random fluctuations in the system. QMD and OFMD simulations, being limited to small numbers of particles, typically give noisy or inaccurate results for transport coefficients. Furthermore, PAMD allows the modeling of mixtures where one species is a trace component (1:100 or smaller mixing ratio) which is currently not possible with ab initio methods. Its relative speed makes it possible to calculate large tables of physical properties, something that still requires a rather heroic effort with ab initio methods.

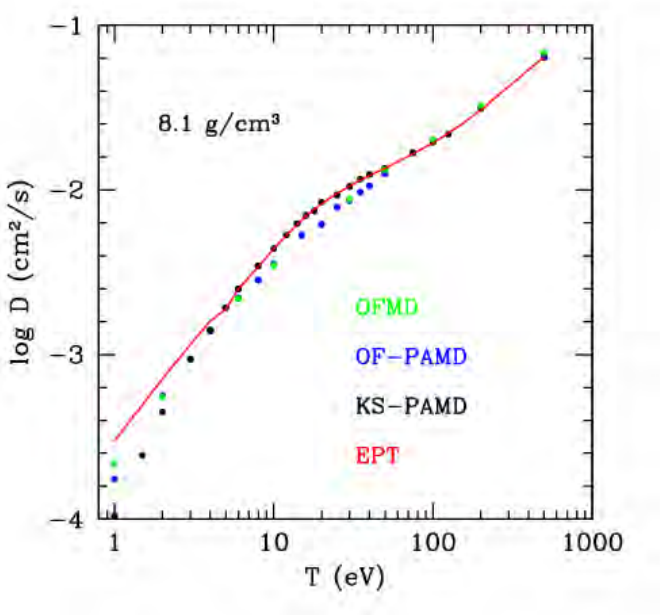

Figure 2. Coefficient of self-diffusion of aluminum at 8.1g/cm3 and temperatures from 1 to 500eV calculated with several models. The excellent agreement between the reference calculation of OFMD (green dots) with our OF-PAMD (blue dots) validates latter. The full quantum mechanical calculation KS-PAMD (black dots) diverges from the two OF calculations because it is a physically more realistic description of the electrons. This is clearly important at temperatures below 100eV. KS-PAMD merges smoothly with OF-PAMD at higher temperatures, as expected. The red curve shows the results of the effective potential theory (EPT) using the same ion-ion effective potential as in KS-PAMD. The agreement with KS-PAMD is essentially perfect (within the uncertainty in the KS-PAMD result) as long as the interactions are not too strong (T>5eV at this density). We obtain very similar results at densities of 2.7 and 27 g/cm3. Adapted from [7].

A main goal of our project is to compute ion diffusion coefficients, which are a much more sensitive test of the model's ion-ion effective potential than pair distribution functions. The OF-PAMD diffusion coefficients for deuterium, boron, iron and copper, over a wide range physical regimes all fall within the uncertainty of the published OFMD values [8, 9]. Figure 2 shows the diffusion coefficient of aluminum computed with OF-PAMD compared to our OFMD. Except for the lowest temperatures of 1-2eV, they agree within 10%, which is on par with the state-of-the-art. Figure 2 also shows the quantum mechanical KS-PAMD results which differ from the OFMD result for T<100eV because of their more accurate treatment of the electrons. KS-PAMD and OF-PAMD agree very well at higher temperatures, as expected on physical grounds. This demonstrates that the PAMD model works very well over a wide range of conditions for a quantity as sensitive as the self-diffusion coefficient, it can also be run in the full quantum mechanical mode to very high temperatures, thus providing a continuous description of the physics with a single model over a wide range of conditions, unlike QMD/OFMD.

Effective potential theory

In collaboration with Scott Baalrud (U. of Iowa), we developed a new approach to compute ionic diffusion coefficients in dense plasmas. In dilute plasmas, diffusion can be treated by considering only binary collisions between ions through the Chapman-Enskog formalism. This approach is known to fail dramatically as the interactions in the plasma grow and multiple collisions dominate. Introducing an effective ion-ion potential that accounts for ion correlations, the "effective potential theory" (EPT) extends the domain of applicability of the Chapman-Enskog formalism to moderately coupled plasmas [10, 11]. This is extremely fast computationally. Since the PYRRHO model generates the effective potential that is the input to the EPT model, we had an exciting opportunity to apply the EPT model to WDM and extend it to mixtures.

The power of the EPT model is demonstrated in Figure 2 where it agrees with the KS-PAMD values to better than 2% over nearly the full range of conditions shown. At the lowest temperatures, deviations rise rapidly as the plasma interactions become very strong and the EPT model fails. Figure 2 summarizes our accomplishments in our ability to calculate diffusion coefficients in WDM: 1) OF-PAMD gives very nearly the same values as the reference OFMD calculation, 2) the more physically accurate KS-PAMD can be run over the full range of density and temperature and recovers the OF-PAMD results at high temperatures, and 3)

the EPT model agrees perfectly with KS-PAMD over most of the WDM regime.

This is a remarkable result. We have demonstrated that we can compute the diffusion coefficient by combining the PYRRHO calculation of the effective ion pair potential with the EPT model over much of the range of WDM conditions. There is no need to resort to noisy and lengthy MD simulations, except in the strong coupling cases where EPT fails. This results in enormous savings in computing time. It is a transformative development for the computation of transport properties.

Diffusion in white dwarf stars

The calculation of ionic inter-diffusion coefficients in white dwarf demonstrates the new capability that we have developed for mixtures.

The very large surface gravity of white dwarf stars causes heavier elements to sink below the surface. This results in a layered structure with a very thin surface layer often composed of pure hydrogen, with an underlying layer of pure helium, on top of a core of carbon. The hydrogen layer is missing in about 25% of white dwarfs. Many white dwarf stars show traces of heavier elements (Mg, Ca, Si, Fe, etc.) at the surface that are thought to be of planetary origin, such as a dust disk or an asteroid belt. Those elements diffuse downward in the star below the observable surface. The exciting astrophysical implication is that by measuring the amount of these accreted elements at the surface, and with a theoretical knowledge of how fast they diffuse downward, we can infer the composition of the orbiting planetary material which is otherwise invisible.

In collaboration with Gilles Fontaine (U. de Montréal) we have calculated the coefficient of diffusion of traces of Ca and Si for a range of white dwarf models with both H and He surface layers. The results for the diffusion of Si in He are shown in Figure 3. The agreement between KS-PAMD and EPT is quite good but not perfect. The reason is that Si is at a trace concentration (1:200), which is challenging for any MD simulation (and impossible to do with ab initio simulations) giving noisy KS-PAMD values. The smoothness of the EPT result illustrates that our novel approach can handle the diffusion of traces without difficulty. We find that the diffusion coefficients that are universally used in white dwarf models [12] are usually within 50% of our more accurate calculation, but are up to a factor of two lower at the highest density.

Another class of white dwarfs shows traces of carbon at the surface [13]. The carbon comes from the core and is brought up to the surface by a convective/diffusive process [14] whose modeling requires the coefficient of C-He inter-diffusion over a wide range of densities, temperature and mixing ratios. We estimate that a table of about 1000 points is necessary. No one would consider doing such a calculation with ab initio methods but it is manageable with our new tools. We have computed the PYRRHO potentials for 700 points in the parameter space of interest. The completed table will be made available for inclusion in white dwarf evolution codes.

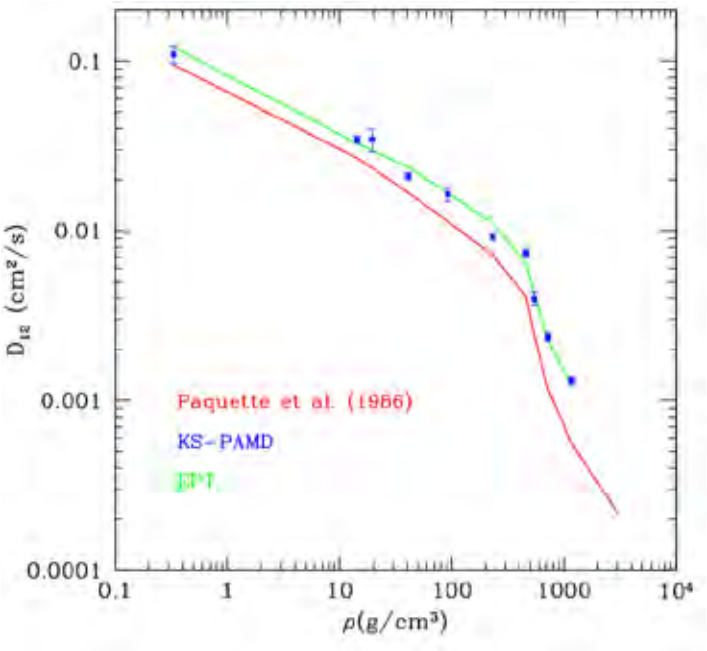

Figure 3. Coefficient of diffusion of a trace of Si in a dense He plasma. The values of temperature and density follow those along the bottom of the convection zone in a sequence of cooling models of white dwarf stars, with hotter/younger white dwarfs on the left and cooler/older white dwarfs on the right. Temperature varies along the density axis. Three calculations of the coefficient of inter-diffusion of Si-He are shown. Paquette et al. (1986) [12] is the theory of diffusion used in all white dwarf models that we seek to update. KS-PAMD is our model for dense plasmas coupled with molecular dynamics. The error bars and the scatter of those points reflect the statistical uncertainty in the calculation of the diffusion coefficient in a mixture containing a trace element (Si:He = 1:200 here). The green curve show the EPT result, which is not only very smooth but is also computationally much faster. Our more sophisticated model for dense plasmas lead to diffusion coefficients that are consistently 25-100% larger than those of Paquette et al. [12].

Impact on National Missions

NASA and NSF: The primary applications thrust of our research is astrophysical – with an initial focus on understanding heavy-element diffusion in white dwarf stars. In a broader sense, this research created a robust capability for scientists to develop accurate equations of state and transport coefficients for wide varieties of astrophysical phenomena.

DOE/Understanding of Materials: Warm dense matter is a frontier of materials physics. Because it describes a region of temperature and density space devoid of simplifying approximations, all of the physics matters. It is also a region difficult to probe experimentally. The capability to model mixtures in this regime advances our basic knowledge of materials behavior in extremes and our ability to design and analyze HEDP experiments.

NNSA/DP & Nuclear Weapons: During a nuclear explosion, and in inertial confinement fusion, mixtures of warm dense matter can be created. This research potentially enhances our capability of modeling materials as they pass though this regime.

NNSA/Non-proliferation: The ability to make accurate equations of state for a wide variety of warm, dense, mixed materials lends itself to better anticipating and ameliorating the effects of rogue WMDs. A calculation for a mixture of programmatic interest was initiated in FY15.

References

1. Desjarlais, M. P., J. D. Kress, and L. A. Collins. Electrical conductivity for warm, dense aluminum plasmas and liquids. 2002. PHYSICAL REVIEW E. 66 (2).

2. Lambert, F., J. Clerouin, and G. Zerah. Very-high-temperature molecular dynamics. 2006. PHYSICAL REVIEW E. 73 (1).

3. CHIHARA, J.. UNIFIED DESCRIPTION OF METALLIC AND NEUTRAL LIQUIDS AND PLASMAS. 1991. JOURNAL OF PHYSICS-CONDENSED MATTER. 3 (44): 8715.

4. Starrett, C. E., Saumon, Daligault, and Hamel. Integral equation model for warm and hot dense mixtures. 2014. PHYSICAL REVIEW E. 90 (3).

5. Starrett, C. E., and Saumon. A simple method for determining the ionic structure of warm dense matter. 2014. HIGH ENERGY DENSITY PHYSICS. 10: 35.

6. Starrett, C. E., and Saumon. Electronic and ionic structures of warm and hot dense matter. 2013. PHYSICAL REVIEW E. 87 (1).

7. Starrett, C. E., Daligault, and Saumon. Pseudoatom molecular dynamics. 2015. PHYSICAL REVIEW E. 91 (1).

8. Lambert, , Clerouin, and Mazevet. Structural and dynamical properties of hot dense matter by a Thomas-Fermi-Dirac molecular dynamics. 2006. EUROPHYSICS LETTERS. 75 (5): 681.

9. Danel, J. -. F., Kazandjian, and Zerah. Numerical convergence of the self-diffusion coefficient and viscosity obtained with Thomas-Fermi-Dirac molecular dynamics. 2012. PHYSICAL REVIEW E. 85 (6).

10. Baalrud, S. D., and Daligault. Effective Potential Theory for Transport Coefficients across Coupling Regimes. 2013. PHYSICAL REVIEW LETTERS. 110 (23).

11. Baalrud, S. D., and Daligault. Modified Enskog kinetic theory for strongly coupled plasmas. 2015. PHYSICAL REVIEW E. 91 (6).

12. PAQUETTE, C., C. PELLETIER, G. FONTAINE, and G. MICHAUD. DIFFUSION-COEFFICIENTS FOR STELLAR PLASMAS. 1986. ASTROPHYSICAL JOURNAL SUPPLEMENT SERIES. 61 (1): 177.

13. Dufour, P., P. Bergeron, and G. Fontaine. Detailed spectroscopic and photometric analysis of DQ white dwarfs. 2005. ASTROPHYSICAL JOURNAL. 627 (1): 404.

14. PELLETIER, C., G. FONTAINE, F. WESEMAEL, G. MICHAUD, and G. WEGNER. CARBON POLLUTION IN HELIUM-RICH WHITE-DWARF-ATMOSPHERES - TIME-DEPENDENT CALCULATIONS OF THE DREDGE-UP PROCESS. 1986. ASTROPHYSICAL JOURNAL. 307 (1): 242.

15. Danel, , Kazandjian, and Zerah. Orbital-free molecular dynamics simulations of a warm dense mixture: Examination of the excess-pressure matching rule. 2009. PHYSICAL REVIEW E. 79 (6).

Publications

Saumon, D., C. E. Starrett, and J. Daligault. Diffusion coefficients in white dwarfs. 2015. In 19th European White Dwarfs Workshop. (Montreal, Canada, 11-15 Aug. 2014). Vol. 493, p. 419. San Francisco: Astronomical Society of the Pacific.

Starrett, C. E., J. Daligault, and D. Saumon. Pseudoatom molecular dynamics. 2015. PHYSICAL REVIEW E. 91: 013104 (5).

Starrett, C. E., Saumon, Daligault, and Hamel. Integral equation model for warm and hot dense mixtures. 2014. PHYSICAL REVIEW E. 90 (3): 033110 (8).

Software/Hardware Mapping for Data Locality Optimization

Hristo N. Djidjev
20130252ER

Abstract

This project addresses the problem of software-hardware codesign for next-generation computing systems as an optimization problem. Compute-intensive portions of an application software and a hardware architecture are parameterized by a set tunable of software and hardware parameters and the problem is to find a combination of these parameters that optimizes the software-hardware pair with respect to performance characteristics. A key step of such an approach is to be able to model the energy consumption and the running time, key components of any cost function, as analytical functions of the software and hardware parameters, only having the abstract hardware model available (and not the real hardware).

In order to develop an energy model, we assume that the code portion of interest is a stencil kernel and that it has already been optimized in a way that is beneficial for any modern architecture, namely, into a form that minimizes the number of data transfer operations. For this purpose, we have used existing tools based on the polyhedral method that divide the set of all operations into blocks of code called tiles that can be executed independently of each other. Then our energy model evaluates the energy needed to execute each tile, and represents the total energy as a sum of the energies for the individual tiles. A similar approach is used to model the time.

Having analytical formulas for the time and energy as functions of the tunable parameters makes it possible to run very efficient optimizations in order to find the best choice of parameters for minimizing the time, the energy, or a combination of both. Our validation analysis on a Graphics Processing Unit (GPU) architecture shows that both models are very accurate and that the associated optimization problem can determine optimal tile sizes with respect to the energy consumption with average error less than one percent.

Background and Research Objectives

A new approach to addressing the challenges of solving computational problems at the exascale is to apply a software-hardware codesign approach, in which the software and the corresponding hardware for solving a class of application problems are jointly co-developed and co-optimized. In contrast, the current approach to high performance computing (HPC) consists of two separate and independent phases, first, hardware is designed and delivered to users; second, software for the application of interest is developed or adapted to run on that new hardware. However, in the overwhelming majority of cases, it is realized that, because of mismatch between the data communication patterns and the hardware architecture, the available computing resources cannot be efficiently exploited, and the originally promised performance is hard or impossible to achieve.

In order to develop a methodology for the codesign of software and hardware, we first look at properties that are desirable for most software applications, regardless of the specifics of the hardware architecture. One of the most desired properties of a good mapping is the locality of the data access. Modern computer processors such as Graphics Processor Unit (GPU) and Cell have limited amount of local memory and the time of data transfer between that memory and the global memory is huge compared to the cost of computation or the cost of local access. Hence, it is important to develop a method that maps the operations of a software code onto the hardware in a way that maximizes locality and data reuse, i.e., such that as large as possible amount of computations are performed on the data in the local memory before that data is replaced with new data. In addition, one wants to preserve the semantics of the original code and hence guarantee that the mapping will not affect the code correctness. The corresponding mapping optimization problem is very difficult to solve efficiently as it is in the NP-hard class and because it needs to be run multiple times, since it is a step of the software/

hardware space exploration loop that is invoked iteratively. Hence, we will look at a subclass of all software codes, namely nested-loops, and at a subclass of all transformations, namely affine transformations. Previous research has shown that those subclasses capture the most relevant types of codes and transformations from a practical point of view (as loops are usually responsible for most of the total computation time) and, on the other hand, result in optimization problems of manageable computational complexity. Our goal is to address the algorithmic challenges and to design mapping algorithms that are both accurate and scalable and to test their performance on a prototype mapping tool.

We focus in our analysis on a subclass of the tiled nested loop codes called dense stencils, which occur frequently in the numerical solution of PDEs and in many other contexts such as high-end graphics, signal and image processing, numerical simulation, scientific computing, and bioinformatics. We chose stencils for our case studies since that would allow us to model an entire class of algorithms in a hierarchical way with a single generic model representing the whole class, while model parameters that are stencil-dependent have to be separately specified for each stencil of interest to complete its model. (However, the approach is applicable to any other class of nested-loop codes that allows tiling.) We completely develop and validate the detailed models (including the stencil-dependent parameters) of three specific stencils. Models for other stencils can be developed in a similar way.

In order to increase the amount of parallelism and improve the locality of memory accesses, it is often useful to divide the set of all computations of a code into groups called tiles [3]. Tiles are considered atomic, i.e., all the data needed to perform the computations in a tile can be made available before the computation begins and there are no cyclic data dependencies between tiles (tiling is legal). We also note that in order to obtain the best performance, tiling is often applied hierarchically at multiple levels.

Unfortunately, in most cases tiling is only possible after the code is transformed into equivalent, but easier to tile code. There are many transformations that can result in tillable codes, and they can be further distinguished by the amount of data communication and the amount of parallelism they offer. One can find an optimal transformation using the polyhedral method and some of the publicly available tools based on it such as PLUTO [1].

Finally, in order to choose an optimal software/hardware combination, one needs an objective (cost) function that can be used to rank the candidate solutions. Typical components of such cost functions are the running time and the consumed energy of a software implementation. While energy and, especially, time are easy to measure, our task is much more difficult, as we need to estimate these parameters on abstract representations of the hardware and software.

Scientific Approach and Accomplishments

Approach overview

One of the most challenging issues of the proposed optimization framework is searching the space of all possible software-hardware pairs and finding the one that is optimal with respect to the chosen cost function. The difficulty of this problem is that the space is huge and it will not be possible to exhaustively look at and evaluate all of its members. On the other hand, it is not clear how can one explore the structure of this space. One of the important observations made in this project is that the computational complexity of the optimization procedure can be significantly reduced, compared with the procedure originally described in the proposal, by eliminating the need to search the space of all hardware parameters for an optimal solution. Previously, for each set of hardware parameters (each point in the search space), one had to run a problem for optimally mapping the software representation onto the corresponding hardware. The new approach directly finds the sets of the optimal hardware parameters by including them as variables in the mapping optimization problem. For this to work, we need to be able to model as an analytical function the energy and the running time of a software implementation of a parameterized algorithm on a parameterized hardware, in particular, a parameterized model of a Graphics Processing Unit (GPU). We next describe the development of such models.

Energy and time modeling

The input to our model is a tiled nested-loop code that is optimized for execution time. Therefore, we assume the code is free of shared memory bank conflicts and the global memory accesses are coalesced. Then, we model energy of the code as an analytical function of software parameters and GPU hardware parameters. For example: tile sizes, program input parameters, the number of operations in the loop body are software parameters and the energy consumed by an operation (i.e., addition, multiplication, etc.) is a hardware parameter. The list of all parameter used is given in Figure 1.

We chose to model energy since energy efficiency has been recognized as one of the biggest challenges in the roadmap to higher performance (exascale) systems for a number of reasons including cost of usage, reliability, energy conservation, and environmental impact [7]. The most powerful computers today consume megawatts of power,

enough to power small towns, and at cost of millions per year.

Name	Type	Description
$\mathtt{S_i}$	EP	i-th space dimension
$\mathtt{T}$	EP	time dimension
$\mathtt{op_j}$	EP	# of operations of type $\mathtt{j}$ in loop body
t_{S_i}	ES	tile size along the i-th space dimension
t_T	ES	tile size along time dimension
s_{S_i}	ES	subtile size along the i-th space dimension
P_{stat}	EH	static power of device
e_{gr}	EH	Energy per word of global↔register transfer
e_{sr}	EH	Energy per word of shared↔register transfer
e_{gs}	EH	Energy per word of global↔shared transfer
e_{sync}	EH	energy for a single synchronization
e_{j}	EH	energy per operation of type j
E_{iter}	CD	energy for a single iteration computation
E_{gs}	CD	Energy per tile for global↔shared transfers
E_{sr}	CD	Energy per tile for shared↔register transfers
E_{ar}	CD	Energy per tile for arithmetic
E_{sync}	CD	Energy per tile for synchronizations
M_{io}	CSD	I/O volume per tile (global↔shared)
V_{tile}	CSI	volume of a tile (# of iteration points)
N_{tiles}	CSI	total number of tiles
T_{alg}	CI	total execution time of stencil
E_{obs}	CI	total observed/experimental energy consumption
E_{stat}	CI	total static energy
E_{dyn}	CI	total dynamic energy
E_{alg}	CI	total energy

Figure 1. List of the parameters. S/H/P stand for software/ hardware/problem type, D/I stand for problem dependent/independent, and E/C--for elementary/composite; MA stands for multiply-add operation. is measured in 4-byte words.

We compute the hardware parameters using microbenchmarks as well as regression. Then we apply the analytical model to compute total energy consumption of a program for a given set of software parameters without having to really run the program. We report the error of our model by comparing the modeled energy against the actual (measured) energy consumed by the GPU. Finally, we use our energy model to select the optimal tile size for energy efficiency and report the number of non-optimal tile size selections and hence the error in energy due to the selection of non-optimal tile sizes.

We model the time using a similar approach and using parameters that correspond to the ones of the energy model. For instance one energy parameter characterixing the hardware is the energy consumed for one multiply-add operation; for the time model the corresponding parameter is the time needed for one such operation. In general, modeling time is more difficult than modeling the energy. The reason is that, while for the energy the total amount for running an algorithm is the sum of the energies spent performing individual operations, for the time this is not always the case as the execution of some operations can overlap in time due to parallelism. Another important feature is that the value of the predicted time is used as a parameter in the energy model. The reason is that energy has two main components: static energy, which is the energy consumed when the processor is idle, and the dynamic energy, which is the energy needed to do the computation. Time is needed to evaluate the static energy portion, which is a product of the run time and the static power.

One of the advantages of our modeling approach is that our models predict energy and time parameters of a software implementation on a given hardware by analyzing source code only, unlike other approaches [4], [5] that rely on parameters computed by running benchmarks for each individual code. We do use micro-benchmarks, but they are needed to characterize hardware, rather than codes.

Validation: We validated our energy model on three stencil codes, Smith Waterman, Jacobi 1D and Jacobi 2D. Given two molecular sequences (like genomes), the Smith-Waterman algorithm (SW) solves the problem of finding an optimal alignment of the sequences that maximizes the overlap or other similarity measure. Using the dynamic programming methodology, SW iteratively constructs a table that identifies the optimum alignment. This algorithm for the iterative construction of the table has the structure of a stencil code. The second algorithm, Jacobi 1D (1-dimensional 3-point stencil), is defined by a recurrence where the value at each point at a given time instance is evaluated by taking the average of its neighboring elements along with itself from the previous time step. Jacobi 2D is the two-dimensional 5-point analog of Jacobi 1D.

These stencils were implemented on a GPU. A GPU has an array of Streaming Multiprocessors (SMs) each one with a set of SIMD (Single-Instruction Multiple Data) Vector Processors. The number of such processors can vary from 8 to 192 depending on the GPU. All SMs share an off-chip global memory and have a private memory and a register file. The programming model consists of a grid of thread blocks. The threads of a thread block execute concurrently on one SM and multiple thread blocks may execute concurrently on one SM (depending on available shared memory and register resources). As thread blocks terminate, new thread blocks are launched [8]. The computations in a thread block are expected to be independent of those in other thread blocks. Hence, the execution order of the thread blocks in a grid can be arbitrary. Within a thread block, all the threads can access shared memory collaboratively and explicitly synchronize to have a uniform view of shared memory data among threads.

We used NVIDIA K20c GPU [9] to experimentally validate

our models. Since NVIDIA has not disclosed energy or power data for memory and compute operations for K20c, we needed to obtain these parameters experimentally. We used two methods: benchmarking and regression. Micro-benchmarks are short pieces of code, each of which stresses an operation of interest. We used the NVIDIA NVML library to measure instantaneous power at any time of the execution of a micro-benchmark. The total consumed energy is then the product of the average measured power and the execution time of the micro-benchmark.

We designed micro-benchmarks for each parameter of interest to determine the value of that parameter experimentally. The micro-benchmarks were implemented in such a way that the execution time and total energy consumption is dominated by the operation of interest.

The second method we used to determine the value of the hardware energy parameters is based on nonlinear regression, as described next. We create a set of combinations of software parameters and, for each such combination, experimentally measure the energy consumed by the corresponding code. We then plug in the values of the known parameters into the formula for the energy derived in the previous section and obtain, for each experiment, an equation with the values of the elementary hardware parameters as unknowns. The left-hand side of the resulting system of equations contains the energy values predicted by the model and the right-hand side contains the corresponding measured values. We then use an optimization method to find values of the unknown parameters that minimize the error defined as a norm of the difference between the left and right-hand sides of the equations.

The values of the parameters and the corresponding modeling errors are given in Figure 2 [6]. The errors are quite low, less than 18% for the micro-benchmark method and less than 9% for the regression method.

Using the models for energy optimization: Having the analytical models, we can use them for optimization, for instance, for finding a combination of software parameters that minimizes]energy consumption. We did such an optimization in order to find a combination of tile sizes that minimize the energy consumption. We solve an optimization problem, where the objective function is that analytical function we found during the energy modeling and the free variables are the tile sizes. This is a nonlinear optimization problem, but of relatively small size, and we were able to solve it using the nonlinear solver Knitro [2] in a matter of seconds. We validated the results of the optimization by comparing the energy consumption by codes using optimal sets of parameters found through measurements with ones found through solving the optimization problem. The results are shown on Figure 3. The errors in all cases are less than 1%, with average error 0.2%.

Parameter Name [unit]	Micro-benchmarks	Regression
P_{stat} [W]	48	53
e_{gs} [J]	2.2×10^{-9}	3.17×10^{-09}
e_{sr} [J]	2.23×10^{-10}	1.84×10^{-10}
e_{fadd} [J]	5.3×10^{-11}	5.02×10^{-11}
$e_{\text{fmultiply}}$ [J]	3.7×10^{-11}	3.51×10^{-11}
e_{iadd} [J]	7.2×10^{-11}	0
e_{imax} [J]	4.8×10^{-11}	0
error SW [RMSE]	12.77%	2.59%
error J1D [RMSE]	17.14%	2.35%
error J2D [RMSE]	8.30%	3.95%

Figure 2. Table of the energy parameter values from the micro-benchmark approach and the regression approach.

Stencil	# Experim.	# Wrong	RMSE	Max error
SW	298	2	0.05%	0.75%
J1D	265	1	0.02%	0.4%
J2D	125	0	0.00%	0.0%

Figure 3. Energy optimization error. SW, J1D, and J2D stand for Smith-Waterman, Jacobi 1D, and Jacobi 2D, respectively.

Impact on National Missions

Co-design has been recognized as one of the high-priority areas of research for Information Science and Technology at LANL. This project focuses on a key step of the software/hardware co-design process – mapping the software representation onto the hardware model in order to maximize data reuse and locality and increase the amount of parallelism. The optimization framework and the energy and time models developed in this project make it possible to find optimal sets of software and hardware parameters with respect to cost function of the energy consumption and execution time. The project helped establish collaborations with Colorado State University (Prof. Sanjay Rajopadhye and his group) and the University of Rennes at France (Prof. Rumen Andonov) and led to the hiring of Guillaume Chapuis (University of Rennes) as a postdoc at LANL.

References

1. Bondhugula, U., A. Hartono, J. Ramanujam, and P. Sadayappan. PLuTo: A Practical and Fully Automatic Polyhedral Program Optimization System. 2008. In ACM Conference on Programming Language Design and Implementation. (Tuscon, AZ, 2008). , p. 101. Tuscon, AZ: ACM.

2. Byrd, R. H., J. Nocedal, and R. A. Waltz. Knitro : An Integrated Package for Nonlinear Optimization. 2006. Energy. 83: 1.

3. Grosser, T., A. Cohen, Holewinski, Justin and Sadayappan, , and S. Verdoolaege. Hybrid Hexagonal/ Classical Tiling for GPUs. 2014. In CGO. , p. 66.

4. Leng, J., T. Hetherington, A. ElTantawy, S. Gilani, N. S. Kim, T. M. Aamodt, and V. J. Reddi. GPUWattch: Enabling Energy Optimizations in GPGPUs. 2013. In Proceedings of the 40th Annual International Symposium on Computer Architecture. , p. 487. ACM.

5. Nagasaka, H., N. Maruyama, A. Nukada, T. Endo, and S. Matsuoka. Statistical power modeling of GPU kernels using performance counters. 2010. In Green Computing Conference, 2010 International. , p. 115.

6. Ranasinghe, W., S. Rajopadhye, H. Djidjev, R. Andonov, V. Krishna Tandrapati, and N. Prajapati. Energy Modeling and Optimization for Tiled Nested-Loop Codes. 2015. In 11th Workshop on High-Performance, Power-Aware Computing. IEEE Computer Society.

7. Rodero, I., and M. Parashar. Energy Efficiency in HPC Systems . 2012. In Energy-Efficient Distributed Computing Systems . By Zomaya, A. Y., and Y. C. Lee. , p. 81–108. Hoboken, NJ, USA: John Wiley & Sons.

8. CUDA C Programming Guide v6.0. 2014. NVIDIA.

9. NVIDIA Next Generation CUDA Compute Architecture: Kepler GK110. 2012.

Publications

Aleksandrov, L., H. Djidjev, A. Maheshwari, and J. R. Sack. An Approximation Algorithm for Computing Shortest Paths in Weighted 3-d Domains. 2013. DISCRETE & COMPUTATIONAL GEOMETRY. 50 (1): 124.

Chapuis, , Le Boudic-Jamin, Andonov, Djidjev, and Lavenier. Parallel Seed-Based Approach to Protein Structure Similarity Detection. 2014. PARALLEL PROCESSING AND APPLIED MATHEMATICS (PPAM 2013), PT II. 8385: 278.

Chapuis, , Le Boudic-Jamin, Andonov, Djidjev, and Lavenier. Parallel Seed-Based Approach to Multiple Protein Structure Similarities Detection. 2015. SCIENTIFIC PROGRAMMING.

Chapuis, G., and H. Djidjev. Shortest-Path Queries in Planar Graphs on GPU-Accelerated Architectures. 2015. In Large-Scale Scientific Computing (LSSC). Vol. 9374, p. 51. Springer-Verlag.

Djidjev, , Thulasidasan, Chapuis, Andonov, and Lavenier. Efficient Multi-GPU Computation of All-Pairs Shortest Paths. 2014. 2014 IEEE 28TH INTERNATIONAL PARALLEL AND DISTRIBUTED PROCESSING SYMPOSIUM.

Djidjev, H., S. Thulasidasan, G. Chapuis, R. Andonov, and D. Lavenier. Efficient multi-GPU computation of all-pairs shortest paths. 2014. In IEEE International Parallel & Distributed Processing Symposium (IPDPS) . (Phoenix, May 19-23, 2014). , p. 360. Phoenix: IEEE.

Djidjev, H., S. Thulasidasan, G. Chapuis, R. Antonov, and D. Lavenier. Accelerating graph algorithms using graphics processors: shortest paths for planar graphs. 2014. ADTSC Science Highlights.

Djidjev, H., and M. Onus. Using graph partitioning for efficient network modularity optimization. 2013. GRAPH PARTITIONING AND GRAPH CLUSTERING. 588: 103.

Djidjev, Hristo N.. Parallel seed-based approach to protein structure similarity detection. 2013. Los Alamos National Laboratory, LA-UR-13-27448.

Djidjev, Hristo N.. Efficient Shortest Path Computations on Multi-GPU Platforms. 2013. Los Alamos National Laboratory, LA-UR-13-26585.

Djidjev, Hristo N., Guillaume Chapuis, Sunil Thulasidasan, and Rumen Andonov. On Solving the Shortest Path Problem for Planar Graphs using Graphics Processors. 2012. Los Alamos National Laboratory, LA-UR-12-25700.

Djidjev, Hristo N., Rumen Andonov, Sanjay Rajopadhye, and Vamsi Tandrapati. Co-Design Optimization of Jacobi Kernel for GPU Architectures. 2013. Los Alamos National Laboratory, LA-UR-13-28110.

Djidjev, Hristo N., Sunil Thulasidasan, Rumen Andonov, Guillaume Chapuis, and Dominique Lavenier. Efficient Multi-GPU Computation of All-Pairs Shortest Paths. 2013. Los Alamos National Laboratory, LA-UR-13-28111.

Djidjev, Hristo, Guillaume Chapuis, Rumen Andonov, Sunil Thulasidasan, and Dominique Lavenier. All-Pairs Shortest Path algorithms for planar graph for GPU-accelerated clusters. 2015. Journal of Parallel and Distributed Computing. : -.

Ranasinghe, W., S. Rajopadhye, H. Djidjev, R. Andonov, V. Krishna Tandrapati, and N. Prajapati. Energy Modeling and Optimization for Tiled Nested-Loop Codes. 2015. In 11th Workshop on High-Performance, Power-Aware Computing. IEEE Computer Society.

Wohlers, , Le Boudic-Jamin, Djidjev, G. W. Klau, and Andonov. Exact Protein Structure Classification Using the Maximum Contact Map Overlap Metric. 2014. ALGORITHMS FOR COMPUTATIONAL BIOLOGY. 8542: 262.

Wohlers, I., M. Le Boudic-Jamin, H. Djidjev, G. Klau, and R. Antonov. Exact Protein Structure Classification Using the Maximum Contact Map Overlap Metric, , 2014. Presented at International Conference on Algorithms for Computational Biology (AlCoB). (Tarragona, Spain, July 1-3, 2014).

Contextual Learning and Recognition

Alexei N. Skurikhin
20130265ER

Abstract

The potential of big data holds a unique opportunity for global transparency, geographic profiling of activities of interest and many other problem domains. At the same time, in spite of growing quantities of data, object recognition and data interpretation often remains ill-posed. This problem of object disambiguation is extremely common in a broad spectrum of applications, including computer vision, image analysis, social network analysis, bioinformatics and text analytics. The object interpretation ambiguity can be addressed by exploiting the fact that objects rarely occur in isolation; they tend to co-occur and co-vary, and this correlation structure, known as context, provides important information for the disambiguation of the object. However, context-aware machine learning typically leads to a significant increase in the computational complexity of the data interpretation, known as inference process. Modeling contextual information and scaling context aware machine learning methods to large problems are among the most challenging issues in developing the next generation of information extraction approaches.

We developed a computationally tractable machine learning approach based on conditional random fields (CRFs) for context aware object recognition in imagery data. Learning and inference in the developed approach is computationally efficient. This efficiency is achieved due to the approximation of the original intractable CRF probabilistic graph model with an ensemble of computationally tractable spanning tree-structured graph models. The developed approximation based technique demonstrated competitive performance on publicly available datasets used in computer vision and machine learning areas. The approach can be used as a foundation for learning more accurate approximations based on graphs that are more structurally complex than spanning trees.

Background and Research Objectives

Many real-world machine learning problems require recognizing objects whose interpretation depends on the context that is represented in the form of interdependencies among potential data interpretations. The problem is known as context aware structured machine learning. This stands in contrast to the conventional approaches of machine learning, which map input observed instances to output variables, such as classification labels, independently of each other, and thus often cannot address the problem of object disambiguation (Figure 1).

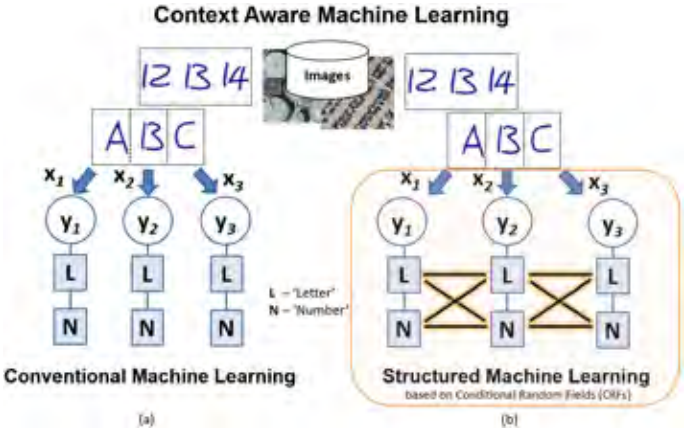

Figure 1. Illustration of context aware machine learning. (a) Conventional machine learning approaches classify input observed entities described with feature vectors x(i) independently of each other. (b) Our project focused on context aware structured machine learning approach based on conditional random fields (CRFs). CRF-based approach classifies input observed entities jointly (collectively) by exploiting dependencies y(i)-y(j) in the output domain, i.e. labeling of objects impacts each other interpretation. Context aware recognition of the central object y(2) is primed by how the adjacent objects y(1) and y(3) are recognized. y(2) is most likely to be "B" when its neighbors are recognized as "letters". y(2) is most likely to be "13" when its neighbors are "numbers."

CRFs offer a mathematically consistent approach for reasoning under uncertainty and modeling contextual dependencies. CRFs are probabilistic graphical models that model conditional probabilistic distributions and support probabilistic inference to answer queries about the output variables y(i) (Figure 1). A graph consists of a set of nodes corresponding to random variables y(i) and a set of undirected edges encoding independence relations among the random variables (Figure 1). Given the evidence, i.e. the observed values of x(i) in Figure 1, probabilistic inference aims to find labeling y_i corresponding to the observed evidence. In the CRF framework, classification labeling of objects acts as context for interlinked objects by constraining potential interpretation (labeling) of each other. The challenge arises due to the computational intractability of probabilistic inference (of classification labeling) over general graphs; this is known to be NP-hard.

There are several classes of CRF graphs, and probabilistic graphical models in general, where inference is tractable. They include tree structured graphs [1], graphs with low treewidth [2], and binary pairwise Markov Random Fields (MRFs) with submodular energy constraints [3]. For a model satisfying the sub-modularity constraints the MAP labeling can be found in polynomial time using graph cuts approach [3]. Graph cuts, however, do not scale up well to large problems and do not provide the probabilities of individual variables assignment associated with a solution.

Due to the intractability of the exact inference in most graphical models, there has been a growing research effort to develop tractable approaches to approximate inference. Most known and often used approaches to approximate inference for general graphs are loopy belief propagation (LBP) [1] and generalized belief propagation (GBP) [4]. However, while belief propagation inference on trees is exact and computationally efficient, for general graphs LBP is not guaranteed to converge and when it converges the result is not guaranteed to be a unique fixed point (a global optimum). For GBP there is neither guarantee of convergence nor guarantees on the accuracy of the estimated probabilities when inference does converge.

Our objective was to develop methods for developing computationally efficient algorithms for context aware learning and inference in CRF-based probabilistic graphical models. This broadly entailed development of (1) the approximation of an arbitrary graph by computationally tractable subgraphs, and (2) learning with approximate subgraphs.

Scientific Approach and Accomplishments

To characterize contextual cues used in CRF models, we developed algorithms to estimate similarities of image elements (such as image pixel patches) by considering longer range interactions between the elements across multiple spatial scales, using descriptors based on edge orientation histograms, phase congruency, differential invariants, and scale invariant interest points [5, 6]. These descriptors are used to characterize pixel patches and their relationships (e.g., similarities), while patches themselves constitute complex objects which are modeled as flexible constellations of parts augmented with interpart contextual relations. This representation provides a context modeling framework with statistical summary of the whole image, spatial layout properties within local image regions surrounding pixel patches. This also reduces the graph size, as nodes of the graph correspond to the partitions of the image, which are larger than individual pixels. If, prior to graph modeling, image is partitioned into pixel patches, this drastically reduces the number nodes in the graph. As a result, computational complexity of the inference in the graph that that is based on pixel patches (instead of individual pixels) is reduced.

Initially we investigated approximate inference based on pseudo-likelihood (PL) approach done over original graph model. Instead of calculating the probability of individual variables at sites in MRF/CRF given all other variables at different sites, the PL approach approximates the joint probability of the variables at nodes in MRF/CRF as a product of individual conditional probabilities over each variable, where the conditioning is on the neighbors of the variable. This property makes it a very efficient parameter learning method with some loss of accuracy, for it avoids exactly calculating the likelihood partition function. The PL-based approximation has been shown to produce consistent estimates in the large lattice limit and demonstrated reduced performance level otherwise [6, 7]. Finally, when the data and/or parameter dimension is extremely large, particularly whenever the likelihood involves summing probabilities over many unobserved states such as genealogies in biology, and, for example, in applications in astronomy and cosmology, and corresponding models do not have an analytical likelihood function, we developed and investigated an approach to choose summary statistics for approximate Bayesian computation to enable inference without explicit likelihood [8, 9]. While, particularly, the PL approach can be considered as an approximation of the original graph using ‘simple’ composite blocks covering nearest neighbors of each graph node, the quality of such an approximation often needs to be more accurate for real-world applications.

We posed the problem of intractable inference over general CRF graph as computationally efficient inference over tractable approximations of the original graph model. A key challenge to this approximation is a choice

of subgraphs in the original graph such that the quality of approximation of the original model can be adjusted, while inference over subgraphs should be tractable.

To build approximations to the original graph model, we have chosen a set of spanning trees. Spanning trees are graph ultra-sparsifiers of treewidth=1. Inference in tree-structured graphs can be implemented efficiently using belief propagation that is an iterative message passing algorithm for computing approximate marginal distributions of each variable in a graphical model [1]. The algorithm is based on the idea of message passing along the edges of the graph, where the message indicates how much each node should update its belief based on the neighboring node's current information. In tree-structured graphs the message passing schedule can be considered as a two-pass schedule, with forward message propagation followed by backward propagation. The algorithm begins by defining one of the variables (nodes) as the root. In the forward sweep the algorithm sends messages from leaves towards the root. In the backward sweep the messages are propagated in the opposite direction, from the root through tree edges to all leaves. After the completion of the backward sweep, the full set of messages over every edge in both directions is estimated. This allows one to compute all the node and edge (joint) marginals. In general loopy graphs, neither convergence nor correctness of this procedure is guaranteed as the message of one node can pass back to itself through the loops. In tree-structured graphs, both convergence and exactness of the inference process is guaranteed.

The important question is how to choose trees to approximate the original graphical model. The number of spanning trees of the graph is exponential in the size of the graph. The exact number of spanning trees can be estimated using the matrix-tree theorem by evaluating the determinant of the combinatorial Laplacian of the graph. We took an approach that assumes a lack of prior information on how subgraph should be structured. We also assume that objects which have to be recognized can be present in any location inside the image. Therefore, we randomly sample spanning trees corresponding to the original graph model. Each of sampled trees captures some aspect of the original model. The use of randomly sampled trees allows us to compensate to some extent for weakness of each of the individual spanning trees. Spanning trees are generated uniformly at random from among all spanning trees of the original graph using the algorithm, introduced in [10], that simulates a loop-erased random walk. The complexity of this generation is the mean hitting time of a graph, which can be much smaller than the cover time of a graph.

We developed two approaches to the CRF general graph approximation based on generated spanning trees. First, we developed ensemble based spanning tree CRF approximations [11]. Spanning trees are randomly generated and are then trained independently on the whole training dataset. Classification is done by majority voting over the ensemble of these trained trees. Second, we developed a deep architecture structured (hierarchical) approximation consisting of multiple layers [12]. Each layer of this architecture contains one randomly generated spanning tree whose structure varies across the layers. Learning of this approximate model begins with one layer architecture containing one generated spanning tree that serves as the initial approximation of the original graphical model. Adding new spanning tree layers continues until the classification error reduction becomes acceptably small. Classification is produced by the spanning tree on the top layer. In both approaches, generated trees are computationally tractable acyclic sub-graphs which allow efficient and exact inference. Our approaches, results of their evaluations and opportunities for further development of our approaches are summarized in [11, 12, 13, 14, 15]. Results of evaluations of our CRF-based ensemble approach is shown in Figure 2.

Figure 2. Results of evaluations of CRF-based ensemble approach.

Impact on National Missions

This project contributes to the development of mathematics and computer science required to extract knowledge from massive quantities of data. Current approaches to object recognition are overwhelmed by the sheer volume of data (e.g., the increasing Earth observation image data volume is going beyond zettabytes, 10^21 bytes), and the diversity of features associated with objects of interest. Additionally, in a variety of applied domains, e.g., broad area search, increasing efforts at concealment and deception make finding and correctly characterizing activities of interest very challenging. The developed CRF based approach can facilitate object interpretation disambiguation and provide an ability to focus human analysts on "hot spots" in the data. The approach can also be expanded to

the analysis and interpretation of multi-source data, e.g., data from optical, hyperspectral, SAR and LiDAR sensors.

References

1. Pearl, J.. Probabilistic reasoning in intelligent systems: networks of plausible inference. 1998.

2. Bach, F. R., and M. I. Jordan. Thin junction trees. 2002. ADVANCES IN NEURAL INFORMATION PROCESSING SYSTEMS 14, VOLS 1 AND 2. 14: 569.

3. Kolmogorov, V., and R. Zabih. What energy functions can be minimized via graph cuts?. 2004. IEEE TRANSACTIONS ON PATTERN ANALYSIS AND MACHINE INTELLIGENCE. 26 (2): 147.

4. Yedidia, J. S., W. T. Freeman, and Y. Weiss. Generalized belief propagation. 2000. In Advances in Neural Information Processing Systems. (Denver, CO, USA, 28–30 November 2000). , p. 7 pp.. Denver, CO, USA: NIPS.

5. Skurikhin, A. N., S. R. Garrity, N. G. McDowell, and D. M. Cai. Automated tree crown detection and size estimation using multi-scale analysis of high resolution satellite imagery. 2013. Remote Sensing Letters. 4 (5): 465.

6. Burr, T., and A. N. Skurikhin. Approximate inference options in data models for image analysis. 2013. presented at the Statistical Image Analysis Workshop, Santa Fe, NM, LAUR 13-21603.

7. Burr, T., and A. Skurikhin. Pseudo-likelihood inference for Gaussian Markov random fields. 2013. Statistics Research Letters. 2 (3): 63.

8. Burr, T., and A. Skurikhin. Selecting summary statistics in approximate Bayesian computation for calibrating stochastic models. 2013. BioMed Research International. 2013: 10 pages.

9. Burr, T., and A. N. Skurikhin. Algorithms for approximate Bayesian computation. 2015. In Encyclopedia of information science and technology. Edited by Khosrow-Pour, M.. Third Editionp. 1559. Hershey, PA, USA: IGI Global .

10. Wilson, D. B.. Generating random spanning trees more quickly than the cover time. 1996. In Annual ACM Symposium on Theory of Computing (STOC). (Philadelphia, Pennsylvania, USA, 22-24 May, 1996). , p. 296. New York, NY, USA: ACM.

11. Skurikhin, A. N.. Learning tree-structured approximations for conditional random fields. 2014. (Washington, DC, USA, 14-16 Oct. 2014). p. 8 pp.. Piscataway, NJ, USA: IEEE.

12. Skurikhin, A. N.. Hierarchical spanning tree-structured approximation for conditional random fields: an empirical study. 2014. (Las Vegas, NV, 8-10 Dec. 2014). Vol. 8888p. 85. BERLIN, GERMANY: SPRINGER-VERLAG.

13. Skurikhin, A. N.. Hidden conditional random fields for land-use classification. 2015. (Milan, Italy, 26-31 July, 2015). p. 4 pp.. Piscataway, NJ, USA: IEEE.

14. Burr, T., and A. N. Skurikhin. Conditional random fields for pattern recognition applied to structured data. 2015. Algorithms. 8: 466.

15. Burr, T., and A. N. Skurikhin. Conditional random fields for modeling structured data. 2015. In Encyclopedia of information science and technology. Edited by Khosrow-Pour, M.. Third Editionp. 6167. Hershey, PA, USA: IGI Global.

Publications

Burr, T., and A. N. Skurikhin. Approximate inference options in data models for image analysis. 2013. presented at the Statistical Image Analysis Workshop, Santa Fe, NM, LAUR 13-21603.

Burr, T., and A. N. Skurikhin. Conditional random fields for modeling structured data. 2015. In Encyclopedia of information science and technology. Edited by Khosrow-Pour, M.. , Third Edition, p. 6167. Hershey, PA, USA: IGI Global.

Burr, T., and A. N. Skurikhin. Algorithms for approximate Bayesian computation. 2015. In Encyclopedia of information science and technology. Edited by Khosrow-Pour, M.. , Third Edition, p. 1559. Hershey, PA, USA: IGI Global .

Burr, T., and A. N. Skurikhin. Conditional random fields for pattern recognition applied to structured data. 2015. Algorithms. 8: 466.

Burr, T., and A. Skurikhin. Pseudo-likelihood inference for Gaussian Markov random fields. 2013. Statistics Research Letters. 2 (3): 63.

Burr, T., and A. Skurikhin. Selecting summary statistics in approximate Bayesian computation for calibrating stochastic models. 2013. BioMed Research International. 2013: 10 pages.

Skurikhin, A. N.. Learning tree-structured approximations for conditional random fields. 2014. In 2014 IEEE Applied Imagery Pattern Recognition Workshop (AIPR). (Washington, DC, USA, 14-16 Oct. 2014). , p. 8 pp.. Piscataway, NJ, USA: IEEE.

Skurikhin, A. N.. Hierarchical spanning tree-structured approximation for conditional random fields: an empirical study. 2014. In Advances in Visual Computing (ISVC 2014), Lecture Notes in Computer Science. (Las Vegas, NV, 8-10 Dec. 2014). Vol. 8888, p. 85. BERLIN, GERMANY: SPRINGER-VERLAG.

Skurikhin, A. N.. Hidden conditional random fields for land-use classification. 2015. In the International Geoscience and Remote Sensing Symposium (IGARSS 2015). (Milan, Italy, 26-31 July, 2015). , p. 4 pp.. Piscataway, NJ, USA: IEEE.

Skurikhin, A. N., S. R. Garrity, N. G. McDowell, and D. M. Cai. Automated tree crown detection and size estimation using multi-scale analysis of high resolution satellite imagery. 2013. Remote Sensing Letters. 4 (5): 465.

A New Approach to Multiscale Plasma Physics Simulations

Gian L. Delzanno
20130334ER

Abstract

Collision-less magnetized plasmas offer a formidable challenge to the numerical modeler because of the high-dimensionality of the model (the plasma distribution function lives in a six dimensional space), the high level of non-linearity and anisotropy that governs the dynamics of the plasma, and the wide variety of spatial and temporal scales that have to be bridged between the characteristic plasma scales and the system size.

The most widely used numerical approach to collision-less magnetized plasmas is the Particle-In-Cell (PIC) technique, where the plasma distribution function is discretized by macro-particles that move in a computational mesh under the action of the self-consistent electromagnetic field. PIC is relatively simple, extremely robust and fairly easily parallelized, but suffers from the inherent statistical noise associated with the macro-particles. This implies that PIC becomes extremely resource-intensive for problems that require a high signal-to-noise ratio.

In this project we have developed a new spectral capability for the numerical modeling of collision-less magnetized plasmas. We have combined spectral discretizations in velocity space (based on Hermite functions and Legendre polynomials) and in physical space (either global Fourier basis or local discontinuous-Garlekin discretization). We have successfully formulated, implemented, and tested these methods, and studied their numerical stability and conservation properties. A comparison against PIC shows that the spectral method can be several orders of magnitude faster or more accurate than PIC, at least for the standard benchmark problems considered.

Background and Research Objectives

Magnetized plasmas are at the cornerstone of many interesting phenomena in astro, space and laboratory physics [1]. Important examples are the Earth's magnetosphere or laboratory experiments aimed at achieving sustained nuclear fusion energy. In many applications the collision frequency is much smaller than the typical scales of interest, implying that a collision-less kinetic description of the plasma is necessary (as opposed to a fluid/macroscopic description characterized by macroscopic fluid moments like density, momentum and energy). In addition, the characteristic spatial scales of the plasma (such as the Debye length, namely the characteristic length on which electric fields are shielded by the plasma, or the plasma gyro-radii) can be several orders of magnitude smaller than the characteristic system size. Similar considerations apply to the temporal scales, implying that plasmas are very multi-scale. Indeed, the highly non-linear, strongly anisotropic behavior of magnetized plasmas and their multi-scale nature, combined with the high dimensionality of the kinetic description (the plasma distribution function, namely the plasma density in phase space, lives in a six dimensional space consisting of three spatial coordinates and three velocity coordinates), make the numerical modeling of collision-less magnetized plasmas a formidable challenge.

The most widely used approach to the numerical solution of the collision-less magnetized plasma model, i.e. the Vlasov-Maxwell equations, is the Particle-In-Cell (PIC) method [2]. In PIC, the plasma distribution function is discretized with macro-particles that move in a computational mesh due to the electromagnetic field generated self-consistently. PIC owes its popularity to its simplicity, robustness and the relative ease for parallelization that allows one to tap into the impressive recent advances in computing power. The major shortcoming of PIC, however, is due to the statistical noise associated with the macro-particles, which has a rather unfavorable scaling proportional to the inverse of the square root of the number of particles per cell [2]. This implies that problems requiring a large signal-to-noise ratio also require a lot of computational resources. As a figure of merit of the resource-intensive nature of PIC, a single

run using the global gyrokinetic PIC code developed within the SciDAC Gyrokinetic Particle Simulation Center for investigating the long-time evolution of turbulent transport in nuclear fusion devices was estimated, in 2008, to take approximately 25 million CPU hours, on 100,000+ cores [3]. Interestingly, the monetary cost of such simulation can be estimated at about $1,000,000 [4].

A second class of numerical methods for the Vlasov-Maxwell equations is called Eulerian-Vlasov and discretizes phase space by introducing a six dimensional computational mesh [5]. As such, Eulerian-Vlasov methods do not suffer from statistical noise from particles (there are no particles) but require significant amount of memory. For instance, storing a field in double precision on a mesh with one trillion cells requires ~8 Tb of memory. Memory is probably the main reason for the somewhat limited diffusion of Eulerian-Vlasov methods (at least relative to PIC), although other issues such as lack of discrete conservation laws or lack of positivity of the plasma distribution function are also important.

This project deals with the development of spectral methods for the numerical solution of the Vlasov-Maxwell equations that are alternative to PIC and Eulerian-Vlasov methods. In particular, the velocity part of the plasma distribution function is expanded into basis functions, resulting in a system of moment equations for the coefficients (moments) of the expansion. A spectral method is clearly immune to particle noise, but the most important aspect of this approach is that with a suitable basis the low-order moments of the expansion correspond to the typical moments of a fluid. This allows a smooth transition from a fluid to a kinetic description of the plasma by simply increasing the number of moments retained. This feature of the spectral method is critical in approaching multi-scale problems and assessing the importance of kinetic effects, and is not available in PIC or Eulerian-Vlasov methods that are instead forced to treat the full distribution function.

Scientific Approach and Accomplishments

Capability development. We have developed a new capability for the solution of the Vlasov-Maxwell equations for a collision-less magnetized plasma. The velocity part of the plasma distribution function is expanded in Hermite basis functions [we have tried both the symmetrically- (SW) and asymmetrically-weighted (AW) basis] or Legendre polynomials. The resulting set of partial differential equations is discretized in the spatial coordinate by a spectral discretization using a (global) Fourier decomposition or a (local) discontinuous-Galerkin (DG) discretization. The final set of ordinary differential equations is discretized in time with a second-order accurate, fully implicit Crank-Nicholson scheme. The discretized set of non-linear equations is solved with a Jacobian-Free Newton-Krylov (JFNK) technique using the GMRES solver for the inner linear iterations and with the possibility of applying a preconditioner to speed-up the convergence cycle. These techniques have been implemented in a Fortran code, which has been successfully tested against a number of benchmark problems. The code is interfaced to the PETSc library in order to take advantage of PETSc routines for efficient parallelization both on shared- and distributed-memory architectures. The code is open source (LA-CC-14-021). Below we highlight the main accomplishments of our study.

Successful comparison against PIC techniques. We have performed several standard tests (Langmuir waves, Landau damping, two-stream instability, ion acoustic waves) where we have compared our Fourier-Hermite (FH) capability against PIC in terms of accuracy, computational time of the simulation and efficacy. Efficacy combines both numerical error and computational time into a single measure of the cost-effectiveness of an algorithm. Naturally algorithms with higher efficacy are better. These tests have been conducted on the Vlasov-Poisson equations, i.e. the electrostatic limit of the Vlasov-Maxwell equations, in one dimension. The comparisons have been performed both for an explicit time discretization of the FH algorithm (mainly because the overwhelming majority of PIC techniques are explicit) and for the implicit Crank-Nicholson time discretization. In all cases FH has outperformed PIC by producing results that are either orders of magnitude more accurate in the same computational time or orders of magnitude faster for the same accuracy. Consistently, the efficacy is orders of magnitude higher for FH than for PIC, as exemplified in Figure 1 where results of our efficacy study for the two-stream instability problem are shown. In addition, we have performed the comparison for the echo problem. In this case a wave is excited at the beginning of the simulation and decays. A second wave is excited at a later time and also decays. The non-linear interaction between the two waves creates a third wave (the echo) at a later time. This test requires high resolution and has been inaccessible to PIC because of the statistical noise mentioned above, despite using an astonishing 2,000,000 particles per cell in our implementation (PIC simulations normally use a few hundred particles per cell as a rule of thumb). FH, on the other hand, could easily handle the echo problem and reproduce the known theoretical results. This is shown in Figure 2, where the first three Fourier modes of the electric field are shown (the echo is in E1, while E2 and E3 correspond to the excited waves). These results are in Refs. [6,7]. An example of another test problem, the interaction between a plasma and a beam, is shown in Figure 3, where the nonlinear modifications of the beam are captured very

well by the spectral method.

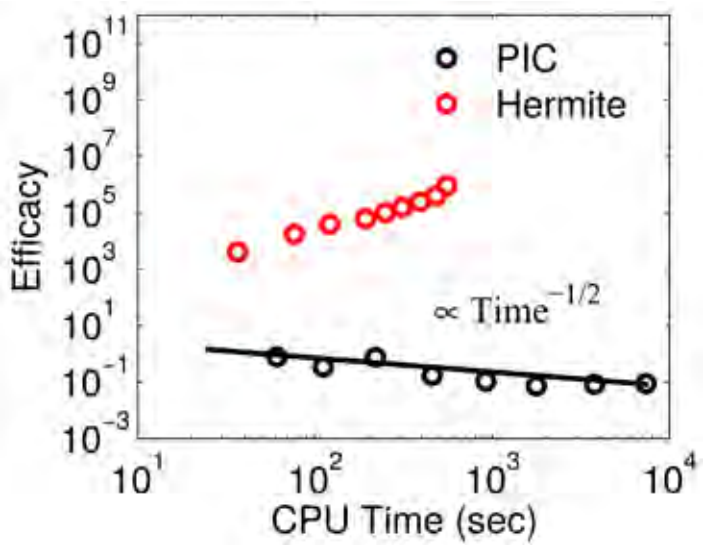

Figure 1. A comparison between the implicit Fourier-Hermite (FH) spectral method and the implicit Particle-In-Cell (PIC) technique on a two-stream instability problem, showing the computational time to complete the simulation versus the efficacy (defined as the inverse of the numerical error times the computational time). On this example FH has orders of magnitude higher efficacy than PIC, namely it is a much more cost-effective algorithm.

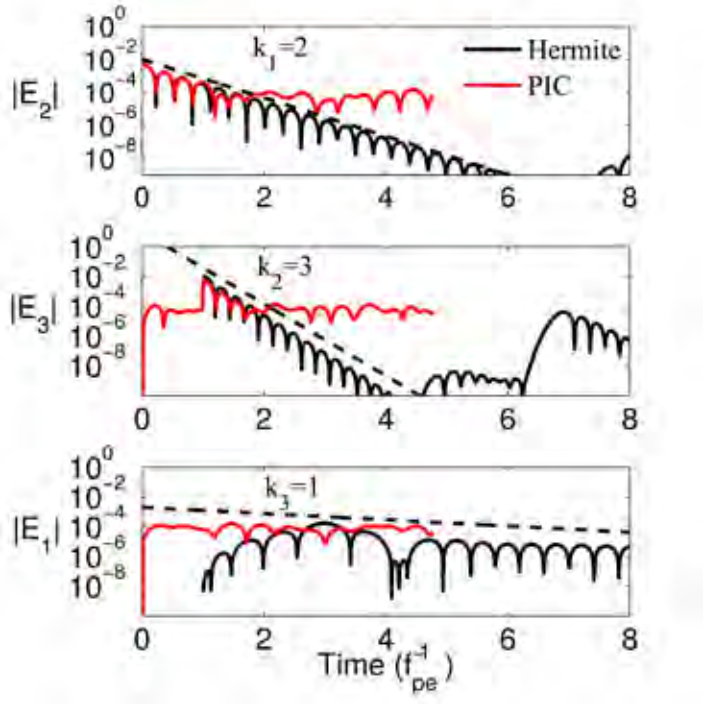

Figure 2. Comparison between the spectral Fourier-Hermite (FH) method and the Particle-In-Cell (PIC) method on the echo problem. The picture shows the first three Fourier modes of the electric field versus time. At time t=0 a wave is initialized (E2) in the system and decays. At time t=1 a second wave is initialized (E3) and decays. The two waves interact non-linearly to produce a third wave (the echo, E1) at time t=3. The FH methods clearly shows the echo and reproduces its known theoretical aspects. PIC, on the other hand, cannot reproduce the echo because of the statistical noise due to the particles (despite 2,000,000 particles per cell were used in this simulation, while typical PIC runs normally use few hundreds particles per cell).

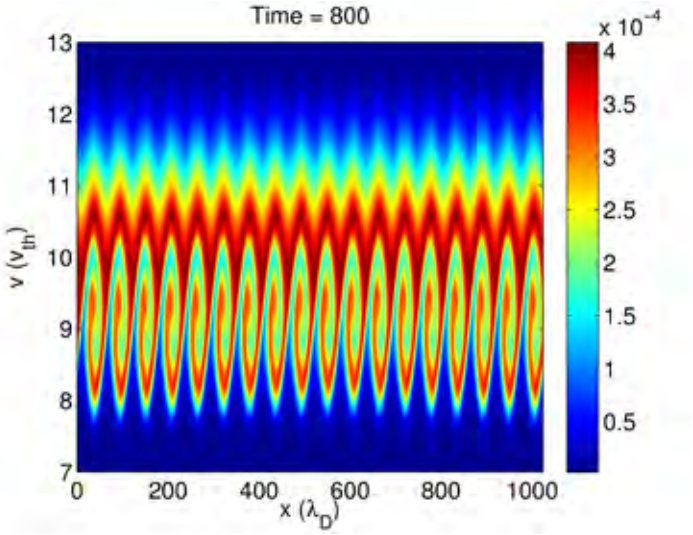

Figure 3. The interaction of a weak beam with a background plasma studied with the FH method. The picture shows part of the phase space during the saturation phase. The spectral method captures accurately the nonlinear distortion of the beam after the development of a beam-plasma instability.

Formulation of spectral algorithms with stability properties and exact conservation laws in discrete form. A lot of effort has been devoted to devise numerical algorithms with certain important properties. For the Hermite expansion, it is possible to prove the numerical stability of the SW algorithm in a finite time step. This is not guaranteed for AW Hermite and one has to resort to an artificial collisional operator to stabilize the method. On the other hand, it is possible to prove that AW Hermite features exact conservation laws in discrete form for total mass, momentum and energy, while these are valid for SW Hermite only in certain limits. The Legendre expansion, on the other hand, can be numerically stable and can feature exact conservation laws in discrete form. For comparison, this is something that has never been achieved in PIC, where either total mass or momentum or total mass and energy can be conserved simultaneously. All these considerations have been proven theoretically and confirmed by numerical experiments. Most of the work has been performed on the Vlasov-Poisson equations in one dimension, with a Fourier or DG spatial discretization. Exact conservations laws in discrete form have been established for AW Hermite in multi-dimensions and for the full Vlasov-Maxwell equations (i.e. the electromagnetic case). These results can be found in

Refs. [7,8,9,10].

Optimization of the spectral basis. As we have argued above, the main advantage of spectral methods is their potential to bridge between a fluid/macroscopic and a kinetic/microscopic description of the plasma by retaining more moments. This is true for both AW Hermite and Legendre discretizations. We have exploited this feature for the FH method, for which we have developed a technique where the number of moments is changed dynamically during the simulation. This is achieved by a double-threshold strategy: if the last moment of the simulation is below a certain threshold, it is removed from the simulation; if it is above a (higher) threshold, we add a moment and its equation to the code. We have successfully tested this technique on Landau damping and two-stream instability problems showing that a sizeable gain of performance can be achieved in this way. These results are published in Ref. [11]. For the Hermite discretization, another form optimization can be obtained acting on the basis itself. This is because the Hermite basis contains two free parameters (the velocity shift and scaling) that, if adjusted properly, can significantly increase the rate of convergence of the series. We have formulated some physics-based criteria for dynamically changing the free parameters during the simulation. The preliminary results are encouraging and show a significant improvement in the simulation.

Formulation, implementation and testing of a spectral method based on a Legendre expansion in velocity space. A spectral method based on a Hermite discretization is very suitable when the plasma distribution function is nearly Maxwellian (this is because the basis functions contain a Maxwellian weight function). In cases of strong non-Maxwellian behavior, the effectiveness of the Hermite expansion is tightly coupled to a robust optimization of the velocity shift and scaling of the basis. An alternative approach, which bypasses the optimization problem completely, consists of using a Legendre-polynomial expansion where free parameters are not necessary. We have been able to formulate this method by using the Simultaneous Approximation Term technique and deliver an algorithm that is numerically stable and features exact conservation laws in discrete form. This had never been done before in the context of the Vlasov-Poisson equations and its formulation, properties and successful testing can be found in Ref. [9].

Formulation, implementation and testing of a spectral method based on a local (DG) basis in physical space. A crucial aspect of the spectral expansion in velocity space is the ability to optimize the expansion basis, namely to retain only the moments that are necessary for an accurate description (fluid or kinetic) of the dynamics. This feature has already been exploited in the FH method where we have changed the number of moments dynamically in the simulation. The Fourier basis, however, limits the applicability of this approach because one is forced to add or eliminate a moment everywhere in the physical domain. In many problems of interest, however, the plasma could behave as a fluid in part of the domain while a kinetic description is required elsewhere. A necessary step to address this type of problem was to develop a spectral discretization based on a local expansion in physical space. We have accomplished this task by using the DG discretization. We have successfully formulated, implemented and tested a DG spatial discretization combined with both Hermite and Legendre expansions in velocity space. The stability of the resulting method and the conservation laws have been studied theoretically and with numerical experiments. The results of our study are presented in Ref. [10].

Impact on National Missions

Magnetized plasmas lie at the heart of many problems in global and energy security that are critical to the nation. Examples includes geomagnetic storms that develop near Earth and can damage infrastructure on the ground and in space (the potential economic damage from a strong geomagnetic storm has been estimated to $1-2T) or the quest of (magnetic fusion) laboratory experiments to provide a sustainable and virtually infinite source of energy to free the nation from its dependence on oil. We have developed a new capability for the numerical modeling of magnetized plasmas that can be much more computationally efficient/performing than traditional techniques. Although the project has focused on the formulation, implementation and testing of this new capability mostly on toy-problems, it positions us uniquely towards future opportunities in the areas mentioned above. This obviously also includes the exascale initiative signed by President Obama. We are constantly in contact with Dr. Pieter Swart (T-5, LANL point of contact for OASCR programs) and Dr. Luis Chacon (T-5, LANL point of contact for exascale computing) to capitalize on potential opportunities. We are also establishing new collaborations with the international community (in particular, Prof. Jack Scudder of U. Iowa, Dr. Vadim Roytershteyn of the Space Science Institute, Prof. Stefano Markidis of the KTH Royal Institute of Technology of Stockholm), where collaborators are interested in applying our new capability to problems that could not be previously solved. This is also expected to lead to new funding opportunities.

References

1. Goldston, R. J., and P. H. Rutherford. Introduction to Plasma Physics. 1995.

2. Birdsall, C. K., and A. B. Langdon. Plasma Physics via

Computer Simulation. 1991.

3. Tang, W. M.. Scientific and computational challenges of the fusion simulation project (FSP). 2008. Journal of Physics: Conference Series. 125: 012047.

4. Walker, E.. The real cost of a CPU hour. 2009. Computer. 42 (4): 35.

5. Cheng, C. Z., and G. Knorr. The integration of the Vlasov equation in configuration space. 1976. Journal of Computational Physics. 22: 330.

6. Camporeale, E., G. L. Delzanno, B. Bergen, and J. D. Moulton. On the velocity space discretization for the Vlasov-Poisson system: comparison between Hermite spectral and Particle-in-Cell methods. Part 1: semi-implicit scheme. 2013. arXiv:1311.2098.

7. Camporeale, E., G. L. Delzanno, B. Bergen, and J. D. Moulton. On the velocity space discretization for the Vlasov-Poisson system: comparison between implicit Hermite spectral and Particle-in-Cell methods. To appear in Computer Physics Communications.

8. Delzanno, G. L.. Multi-dimensional, fully-implicit, spectral method for the Vlasov-Maxwell equations with exact conservation laws in discrete form. 2015. Journal of Computational Physics. 301: 338.

9. Manzini, G., G. L. Delzanno, J. Vencels, and S. Markidis. A Legendre-Fourier spectral method with exact conservation laws for the Vlasov-Poisson system. LA-UR-15-27359.

10. Manzini, G., J. Vencels, G. L. Delzanno, and S. Markidis. Spectral based-discontinuous Galerkin discretizations of the Vlasov-Poisson system. LA-UR-15-27420.

11. Vencels, J., G. L. Delzanno, A. Johnson, I. Bo Peng, E. Laure, and S. Markidis. Spectral Solver for Multi-scale Plasma Physics Simulations with Dynamically Adaptive Number of Moments. 2015. Procedia Computer Science. 51: 1148.

Publications

Camporeale, E., G. L. Delzanno, B. Bergen, and J. D. Moulton. Fourier-Hermite spectral method for the Vlasov equation. Presented at 55th Annual Meeting of the APS Division of Plasma Physics. (Denver, 11-15 Nov 2013).

Camporeale, E., G. L. Delzanno, B. Bergen, and J. D. Moulton. On the velocity space discretization for the Vlasov-Poisson system: comparison between implicit Hermite spectral and Particle-in-Cell methods. To appear in Computer Physics Communications.

Camporeale, E., G. L. Delzanno, B. Bergen, and J. D. Moulton. On the velocity space discretization for the Vlasov-Poisson system: comparison between Hermite spectral and Particle-in-Cell methods. Part 1: semi-implicit scheme. 2013. arXiv:1311.2098.

Delzanno, G. L.. Multi-dimensional, fully-implicit, spectral method for the Vlasov-Maxwell equations with exact conservation laws in discrete form. 2015. Journal of Computational Physics. 301: 338.

Delzanno, G. L., B. Bergen, J. D. Moulton, B. Srinivasan, and E. Camporeale. Spectral method for the solution of the Vlasov equation based on Hermite polynomials. Presented at American Physical Society Division of Plasma Physics Meeting. (New Orleans, 27-31 Oct 2014).

Delzanno, G. L., E. Camporeale, B. Bergen, J. D. Moulton, B. Srinivasan, and G. Manzini. Fully implicit spectral method for the solution of the Vlasov equation based on Hermite polynomials. Invited presentation at 2014 US-Japan JIFT Workshop on Progress in kinetic plasma simulations. (New Orleans, 31 Oct-1 Nov 2014).

Delzanno, G. L., E. Camporeale, B. Bergen, and J. D. Moulton. Fully-implicit Fourier-Hermite spectral method for the Vlasov equation. Presented at Vlasovia 2013. (Nancy, France, 25-28 Nov 2013).

Delzanno, G. L., J. Vencels, G. Manzini, S. Markidis, and E. Camporeale. Spectral method for the solution of the Vlasov-Maxwell equations. Invited presentation at Workshop on Magnetic Reconnection in Plasmas. (Stockholm, Sweden, 10-14 Aug. 2015).

Manzini, G., G. L. Delzanno, J. Vencels, and S. Markidis. A Legendre-Fourier spectral method with exact conservation laws for the Vlasov-Poisson system. LA-UR-15-27359.

Manzini, G., G. L. Delzanno, and J. D. Moulton. Spectral/ Discontinuous Galerkin discretization of the Vlasov-Poisson system. Invited presentation at European Conference on Numerical Mathematics and Advanced Applications. (Ankara, Turkey, 14-18 Sept. 2015).

Manzini, G., J. Vencels, G. L. Delzanno, and S. Markidis. Spectral based-discontinuous Galerkin discretizations of the Vlasov-Poisson system. LA-UR-15-27420.

Vencels, J., G. L. Delzanno, A. Johnson, I. Bo Peng, E. Laure, and S. Markidis. Spectral Solver for Multi-scale Plasma Physics Simulations with Dynamically Adaptive Number of Moments. 2015. Procedia Computer Science. 51: 1148.

Vencels, J., G. L. Delzanno, A. Johnson, I. Bo Peng, E. Laure, and S. Markidis. Spectral Solver for Multi-scale Plasma

Physics Simulations with Dynamically Adaptive Number of Moments. Invited presentation at ICCS 2015 International Conference on Computational Science. (Reykjavík, Iceland, 1-3 June 2015).

Vencels, J., G. L. Delzanno, G. Manzini, V. Roytershteyn, and S. Markidis. Weak turbulence simulations with the Hermite-Fourier spectral method. Presented at 57th Annual Meeting of the APS Division of Plasma Physics. (Savannah, Georgia, 16-20 Nov. 2015).

Vencels, J., G. L. Delzanno, G. Manzini, and S. Markidis. Spectral methods for the solution of the Vlasov-Maxwell equations. Invited presentation at ICNSP 2015 International Conference on Numerical Simulation of Plasmas. (Golden, Colorado, 12-14 Aug. 2015).

Sparse, Distributed, and Robust Network Control

Marian Anghel
20130558ER

Abstract

We developed new methods for the algorithmic construction of Lyapunov functions for the transient stability analysis of dynamic networks including, in particular, power system networks. The proposed methodology uses recent advances in the theory of positive polynomials, semidefinite programming, and sum of squares decomposition, which have provided powerful nonlinear tools for the analysis of systems with polynomial vector fields. In order to apply these techniques to power system networks described by trigonometric nonlinearities we used an algebraic reformulation technique to recast the system's dynamics into a set of polynomial differential algebraic equations. We demonstrated the application of these techniques to the transient stability analysis of power systems by estimating the region of attraction of the stable operating point.

However, such methods scale very poorly with the size of the system. For this reason we developed a decentralized approach to stability analysis of interconnected systems which does not require computing a Lyapunov function for the full system. In this project we have developed a number of scalable and parallel iterative algorithms that decompose a system into a network of interacting subsystems and certify the asymptotic stability of the interconnected systems by using only the subsystems' Lyapunov functions. When this stability cannot be certified we design local and minimal control laws that guarantee asymptotic stability. We have applied these algorithms to a number of dynamic networks including a network of interacting Van der Pol oscillators and a network preserving power system model that includes dynamic loads in addition to the usual swing dynamics of generators. The analysis and control design methods developed in this project can be extended to more general, possibly more complex, networks including, in the case of power systems, voltage dynamics and more complicated generator and load models.

Background and Research Objectives

The analysis and control of complex interconnected systems is a great engineering and operational challenge. Although emerging network control applications include large mechanical structures, distributed sensing, military reconnaissance, and interacting mobile robot agents, the focus of this project is the design of distributed controllers for large-scale power grid systems.

Paradoxically, for a system which is arguably the most influential machine of the 20th century, the modern power systems have not yet fully embraced the technical opportunities of the 21st century (distributed sensors, computers, and advanced communication networks). At the same time, the power systems face the simultaneous convergence of several independent difficulties (intermittent renewable energy sources, frequent transmission congestions, relentless market pressure) which the existing centralized control infrastructure will not be able to solve. A paradigm shift based on modern distributed measurements, control, and management concepts is necessary to modernize the grid.

In response to these challenges, this project seeks to construct an algorithmic synthesis of nonlinear and distributed control techniques for large networked power systems. More specifically, this project developed a decentralized approach that exploits separability and decomposition of the corresponding control problem into nonlinear sub-problems that can be solved locally and efficiently.

Scientific Approach and Accomplishments

A traditional approach to transient stability analysis involves the numerical integration of the nonlinear differential equations describing the system's dynamics. This method provides an accurate description of transient phenomena but has a number of serious disadvantages. First, its computational cost prevents time-domain simulations from providing real-time transient stability

assessments and significantly constraints the number of cases that can be analyzed. Second, numerical simulations alone cannot quantitatively estimate the degree of system stability or produce actionable information to guide preventive control measures.

For these reasons alternative approaches to transient stability analysis have been intensively explored. Among the methods proposed, the Lyapunov function (LF) method can be used to prove the stability of an equilibrium point and avoids the expensive time-domain integration of the system dynamics. The Lyapunov function is a generalization of the energy function for dissipative mechanical systems. As described in Figure 1, a Lyapunov function is positive in a bounded domain around the equilibrium point, except at the equilibrium point where it is zero, and decreases along every trajectory of the dynamical system. As a result the Lyapunov function decreases in time to zero, thus proving that the system's trajectory converges to the equilibrium point (the only point where the Lyapunov function is zero). The largest level set of the Lyapunov function inside the bounded domain is an invariant of the system dynamics (every trajectory starting inside this level set remains inside the level set) and provides an approximation of the region of attraction of the equilibrium point. Unfortunately, there is no general approach for constructing Lyapunov functions for a given dynamical system. Nevertheless, for polynomial dynamical systems, if we restrict the search for Lyapunov function in the space of sum-of-squares (SOS) polynomials (polynomial that can be written as the sum of squared polynomials and that are, therefore, positive) algorithmic approaches for constructing Lyapunov functions have been introduced more than a decade ago. Indeed, testing that a SOS polynomial is positive reduces to solving a linear matrix inequality for which efficient semidefinite programming methods are available.

One of the first contributions of this project was to use SOS techniques in order to develop an algorithm for the construction of Lyapunov functions for classical power system models. We demonstrated the application of these techniques to the transient stability analysis of power systems by estimating the region of attraction of the stable operating point [1]. The application of SOS methods to power system models was innovative for two reasons. First, power system networks are not polynomial dynamical systems because their dynamics is described by trigonometric nonlinearities. Nevertheless, using an algebraic reformulation technique we were able to recast the system's dynamics into a set of polynomial differential algebraic equations. Second, we have also shown that systems with transfer conductances can be analyzed as well without any conceptual difficulties. This is a significant result because analytical energy functions (an alternative to Lyapunov functions that is used in power system transient stability analysis) do not exist for these systems and the proposed SOS analysis provides for the first time a constructive approach for computing analytical Lyapunov functions for realistic power system models with transfer conductances (dissipative power lines). As shown in Figure 2 the proposed SOS method provides better estimates of the ROA when compared to various estimates based on the energy function method that are either very conservative or provide only local estimates of the ROA.

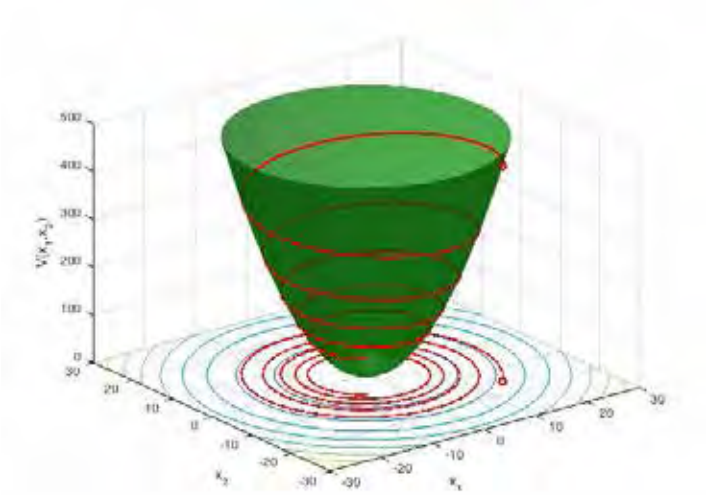

Figure 1. An example of stability analysis using a Lyapunov function. A simple two-dimensional system has a global equilibrium point at the origin. A quadratic Lyapunov function (LF) that is positive everywhere in the phase space of the system is shown in green. The Lyapunov function is zero only at the equilibrium point. After a disturbance the trajectory of the system is shown in red in the two dimensional phase plane. The evolution of the LF itself along the dynamics of the system is also shown in red along the LF surface. The LF decreases along the trajectory and converges to zero. Since the LF is only zero at the equilibrium point, the decrease of the LF to zero certifies the stability of the equilibrium point. Since this system is globally stable the whole phase space belong to the region of attraction. For this reason a LF whose time derivative along the system's dynamics is negative everywhere in phase space can be easily found. Nonlinear systems are generally not globally stable and the search for LFs has to be performed in a local domain around the equilibrium point. The analysis in this case is very difficult but sum-of-squares methods can provide efficient algorithm to searching for LFs.

For large-scale dynamical systems the SOS method becomes inapplicable due to the fast growing computational complexity of the semidefinite programs that need to be solved. For this reason, this project further developed a decentralized approach to stability analysis of interconnected systems that does not require computing a Lyapunov function for the full system. In particular we have

developed a number of scalable and parallel iterative algorithms that decompose a system into a network of interacting subsystems and certify the asymptotic stability of the interconnected systems by using only the subsystems' Lyapunov functions.

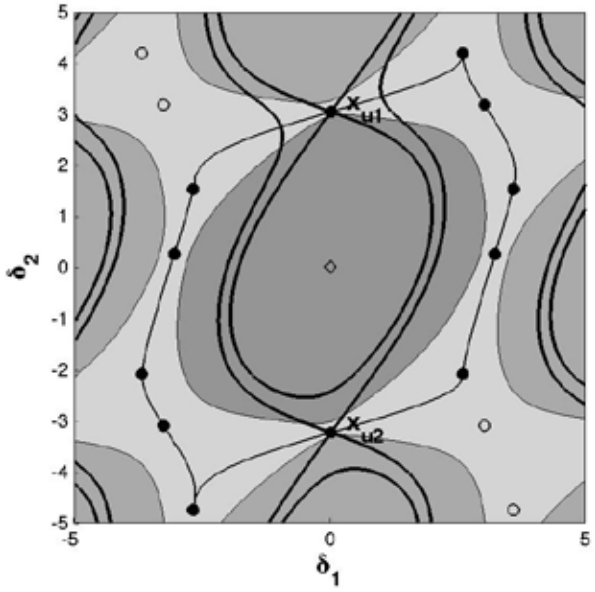

Figure 2. The region of attraction for the equilibrium point located at the origin, projected in the angle space of a simple power system model, is shown in thin black line connecting the unstable equilibria on the boundary of the region of attraction (ROA). The thick black lines show two different approximations to the ROA constructed using energy function methods. The dark gray area shows the best estimate of the ROA according to the proposed sum-of-squares (SOS) algorithm. Unlike the energy function approach, the SOS approach provides a globally optimal estimate.

One algorithm uses the subsystems' Lyapunov functions as state variables and invokes a comparison principle to bind their dynamics by the evolution of a new linear dynamical system. If this linear system is stable and converges to the zero, then each component of the vector LF converges to zero. As a result, each subsystem converges to its zero state (equilibrium state) thus guaranteeing the global convergence of the full, interconnected system. However computing these comparison equations, for a given interconnected system, still remains a challenge. We have shown that SOS methods can be used to study the stability of an interconnected system by computing the vector Lyapunov functions as well as the comparison equation [5, 6]. In Figure 3 we show a network of nine Van der Pol oscillators along with the regions of attraction (ROA) of the isolated subsystem in red lines. For this system we assume an extreme decomposition of the network in which each oscillator (node) describes a subsystem, but this restriction can be relaxed. In [5] and [6] we show that our proposed methodology for computing the comparison system performs better than the traditional approaches found in the literature. In the same papers we show how the comparison equation approach can be used to design decentralized control laws when the comparison approach cannot certify global system stability. This is an application of the comparison equation approach that has not been discussed before in the control literature. The approach presented is parallel and scalable. The method can also be applied to complex real world systems, such as power systems, as we show in a paper that is currently in preparation. Moreover, we have generalized this approach and introduced a new algorithm that uses multiple comparison equations to further improve the performance of the comparison equation approach [7].

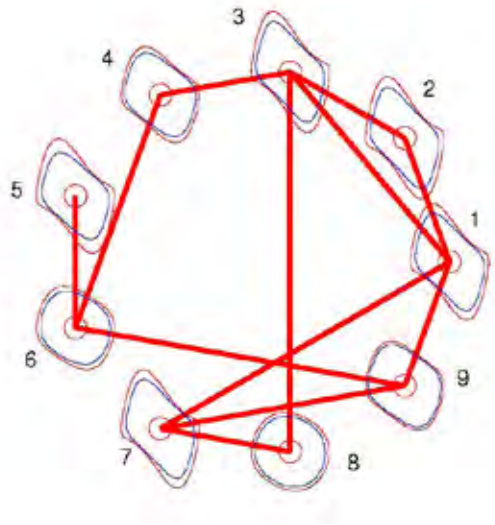

Figure 3. A network of nine Van der Pol oscillators along with the regions of attraction (ROA) of the isolated subsystem in red lines. We assume an extreme decomposition of the network in which each oscillator (node) describes a subsystem. This restriction can be relaxed. Estimates of the ROA of the isolated subsystem are in blue lines. The thick red lines defines the neighbors of each subsystem.

Another suite of algorithms that we have developed has no counterpart in the literature [2,3,4]. They use SOS methods and input to state stability analysis to make local stability estimate for each subsystem under disturbances introduced by the interaction with its neighbors. This approach provides stability estimates that guarantee a suite of contractions of the subsystem's dynamics to a decreasing sequence of local level sets defined by the LF of each subsystem as presented in Figure 4. This approach is iterative and each subsystem updates its stability estimates based on new information received from its neighbors. If for each subsystem this sequence decreases to zero, the algorithm proves the global stability of the fully interconnected system. When the algorithms fail to provide stability guar-

antees, they provide locally computable control laws that restore the asymptotic stability of the full system under a given disturbance. The controls are distributive, adaptive, and minimal, because they are applied to a small number of subsystems and for a limited duration.

This algorithm is applied in [3] to a network of Van der Pol oscillators and in [4] to a power system model of three generators and six load nodes as shown in Figure 5. For the power system model we perform an overlapping decomposition in which the dynamics of the reference node (generator node 3) is shared with all the subsystems. The same iterative convergence analysis described above is applied to this system. The use of overlapping decompositions, in which some subsystems share some degrees of freedom, is very significant. Indeed, if a decomposition fails to have stable isolated subsystems, then the definition of the unstable subsystems can be enlarged to include states from their neighbors until each subsystem become stable.

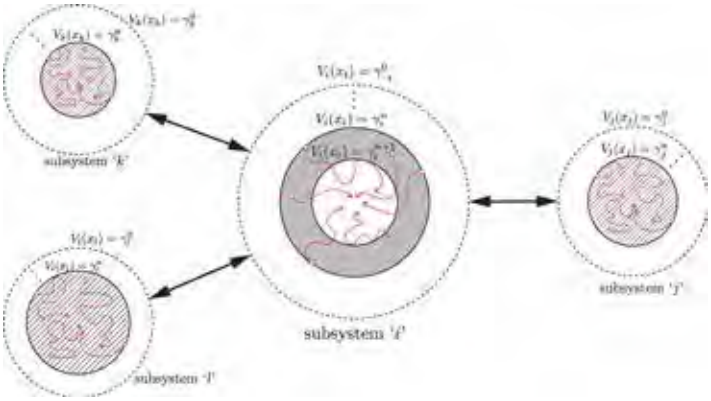

Figure 4. Distributed coordinated sequential stability certification. The central subsystem interacts with three other subsystems. At the end of a disturbance the state of each subsystem moves away from the equilibrium point at zero. The neighbors communicate to the central subsystem their position in phase space by providing the value of their Lyapunov function at their current state. Based on this information the central subsystems determines if its Lyapunov function will decrease in time under the action of the local dynamics AND the influence received from the neighbors. These disturbances are defined by the hashed domains in the figure. This problem is solved locally by each subsystem using sum-of-squares (SOS) methods. If the answer is "yes" then all trajectories of the subsystem (red lines) starting from a ring (gray area) whose outer bound is the current level set will converge to a domain defined by a smaller level set. The central subsystem then communicates this new level set estimate to its neighbors. The same analysis is performed in parallel by all subsystems. As the dynamics evolves each subsystem computes a decreasing sequence of level sets that bound the the global dynamics. If all sequences converge to zero, then the full system is asymptotically stable. If for some subsystems this stability cannot be guaranteed - the answer to the above stability question is "no" - a controller is designed using again SOS methods in order to guarantees the convergence of the subsystem trajectory to a lower level set. The control is local and it adapts to the subsystem state and the disturbance information received from its neighbors.

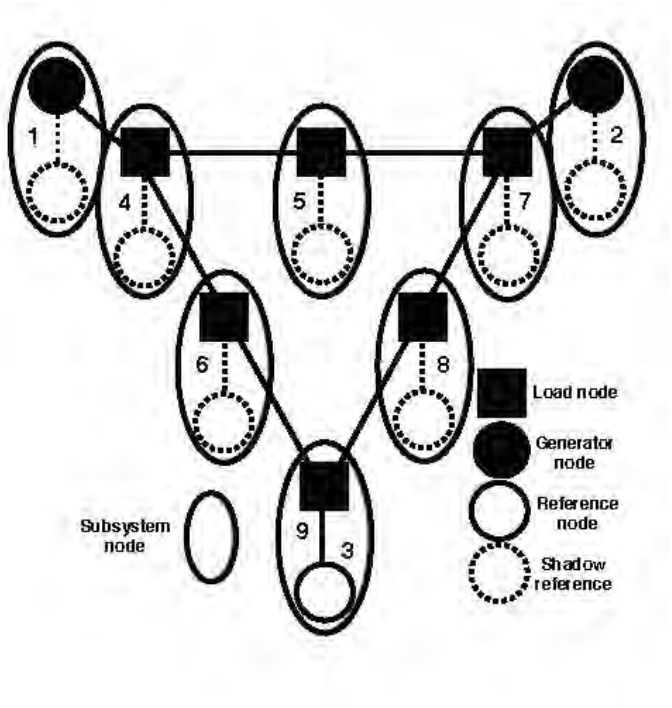

Figure 5. Network of three generators and six load nodes. We perform an overlapping decomposition in which the dynamics of the reference node (generator node 3) is shared with all the subsystems. This results in the following overlapping subsystems: S1 ={1, 3}, S2 = {4, 3}, S3 = {5, 3}, S4 = {7, 3}, S5 = {2, 3}, S6 = {6, 3}, S7 = {8, 3}, S8 = {9, 3}. The same iterative convergence analysis described in Figure 4 is applied to this system. The use of overlapping decompositions, in which some subsystems share some degrees of freedom, is very significant. Indeed, if a decomposition fails to have stable isolated subsystems, then the definition of the unstable subsystems can be enlarged to include states from their neighbors until each subsystem become stable.

All the algorithms developed are parallel and scalable and use limited communications between each subsystem and its neighbors. The analysis and control design methods developed in this project can be extended to more general, possibly more complex, networks including, in the case of power systems, voltage dynamics and more complicated generator and load models.

Impact on National Missions

This project is well aligned with LANL's efforts in energy security. This project addresses some of the challenges of grid modernization efforts, and also addresses the computational needs for the next generation electric grid as expressed in recent workshops organized by the Department of Energy (DOE) in partnership with Office of Electricity Delivery and Energy Reliability (OE).

More specifically, the report on "Advanced Control Methods" conducted by the National Energy Technology Laboratory for the DOE in 2007 has identified the need for the development of distributed intelligent agents that respond rapidly at the local level to unburden centralized control systems. This project directly addresses this problem by developing a distributed control methodology that is robust with respect to system disturbances.

Furthermore, the Smart Grid Research and Development Program of the DOE/OE, identifies in its multi-year program plan the development of advanced control methods. As the smart grid evolves, this program recognizes that more complex automated control systems will be necessary to maintain the grid's optimum operation. Control algorithms investigated in this project directly address the fundamental conceptual challenges posed by such automated control systems.

Finally, the April 2011 DOE workshop, "Computational Needs for the Next Generation Electric Grid Proceedings," highlights a class of mathematical and computational problems relevant for potential power systems research. It identifies, in particular, the difficulties currently encountered by direct transient stability analysis methods. Again, this project directly addresses this problem and our preliminary results have already offered significant breakthrough results based on novel algebraic control techniques.

References

1. Anghel, M., F. Milano, and A. Papachristodoulou. Algorithmic construction of Lyapunov functions for power system stability analysis. 2013. IEEE Transactions on Circuits and Systems I: Regular Papers.. 60 (9): 2533.

2. Anghel, M., J. Anderson, and A. Papachristodoulou. Stability analysis of power systems using network decomposition and local gain analysis. 2013. In Bulk Power System Dynamics and Control Symposium. (Crete, Greece, 25-30 Aug. 2013). , p. 1. Explore Digital Library: IEEE .

3. Kundu, S., and M. Anghel. A sum-of-squares approach to the stability and control of interconnected systems using vector Lyapunov functions. 2015. In The 2015 American Control Conference. (Chicago`, 1-3 July, 2015). , p. 5022. Explore Digital Library: IEEE.

4. Kundu, S., and M. Anghel. A sum-of-squares approach to the stability and control of power systems via vector Lyapunov functions. To appear in The 2015 European Control Conference. (Linz, Austria, 15-17 July, 2015).

5. Kundu, S., and M. Anghel. Distributed coordinated control of large-scale nonlinear networks. To appear in 5th IFAC Workshop on Distributed Estimation and Control in Networked Systems. (Philadelphia, 10-11 Sep. 2015).

6. Kundu, S., and M. Anghel. Computation of linear comparison equations for stability analysis of interconnected systems. To appear in The 54th IEEE Conference on Decision and Control . (Osaka, Japan, 15-18 Dec. 2015).

7. Kundu, S., and M. Anghel. A multiple-comparison-systems method for distributed stability analysis of large-scale systems. Automatica.

Publications

Anghel, M., F. Milano, and A. Papachristodoulou. Algorithmic Construction of Lyapunov Functions for Power System Stability Analysis. 2013. IEEE Transactions on Circuits and Systems I: Regular Papers. 60 (9): 2533.

Anghel, M., J. Anderson, and A. Papachristodoulou. Stability Analysis of Power Systems using Network Decomposition and Local Gain Analysis. 2013. In Bulk Power System Dynamics and Control Symposium.. (Crete, Greece, 25-30 Aug. 2013). , p. 1. NA: IEEE Explore.

Kundu, S., and M. Anghel. Sum-of-Squares Approach to the Stability Analysis of Inter-connected Systems. Presented at SCONES 2014, IEEE Symposium on the COntrol of NEtwork Systems.. (Boston, 27-28 Oct. 2014).

Kundu, S., and M. Anghel. A sum-of-squares approach to the stability and control of interconnected systems using vector Lyapunov functions. 2015. In The 2015 American Control Conference. (Chicago, 1-3 July). , p. 5022. Explore Digital Library: IEEE .

Kundu, S., and M. Anghel. A sum-of-squares approach to the stability and control of power systems via vector Lyapunov function. To appear in European Control Conference. (Linz, Austria, 15-17 July 2015).

Kundu, S., and M. Anghel. Computation of linear comparison equations for stability analysis of interconnected systems. To appear in 54th IEEE Conference on Decision and Control. (Osaka, Japan, 15-18 December, 2015).

Kundu, S., and M. Anghel. Distributed coordinated control of large-scale nonlinear networks. To appear in 5th IFAC Workshop on Distributed Estimation and Control in Networked Systems. (Philadelphia, 10-11 September, 2015).

Motter, A. E., S. A. Myers, M. Anghel, and T. Nishikawa. Spontaneous synchrony in power-grid networks. 2013. NATURE PHYSICS. 9 (3): 191.

Integrated Photonics Pathfinder (IPP)

Kevin P. Mccabe
20140507ER

Abstract

Single-photon, quantum communications (QC) offers "future proof", lightweight cyber security solutions for networks. The rapidly evolving network environment (cloud computing, handheld devices, SmartGrid and other critical infrastructure) presents cyber challenges such as low latency one time signatures that are difficult or impossible to meet with conventional cryptography. In addition to the myriad technical challenges, there is a huge cost to continuously upgrade network infrastructure based on the larger and larger key sizes needed for the temporary security offered by our current public key infrastructure. The value proposition of quantum communications drives the QC client (transmitter) to be manufacturable and lightweight in terms of computation, size and power. By leveraging U.S. investment in emerging integrated photonics processes it is possible to replace the current state of the art large and expensive, hand-built, optical and electrical transmitters with a monolithic integrated device and thus make quantum secured networks commercially viable. This research extends monolithically integrated photonics into an 11 orders-of-magnitude smaller optical power (quantum) regime to address key risks.

Background and Research Objectives

Communications networks have revolutionized the way we work, live, operate computer systems and run our national infrastructure. But hardly a day goes by without a report highlighting the pressing need for improved cyber security technologies to protect our economic and National security. The widespread deployment of cryptography provides confidentiality, authentication, identification and other security functions for the protection of private data in motion as well as ensuring that control, access and network management can only be performed by authorized parties. Critical to these functions is the secure distribution of the secret random number sequences known as cryptographic keys to authorized users [6]: secret keys are used as parameters within cryptographic algorithms.

Single-photon quantum communications (QC) has the potential to finally give defenders dominance over attackers in cyber space. QC has "future-proof" security rooted in laws of physics: today's quantum-secured communications cannot be compromised by unanticipated future technological advances. But QC today only exists in point-to-point instantiations that have limited ability to address the cyber security challenges of our increasingly networked world.

The IPP project, by use of emerging Si integrated electro-photonics has the overarching goal to reduce the QC transmitter size and cost by 100x each, and improve controllable attenuation by 4 orders of magnitude. By design, fab and testing of photonic die we seek to validate performance models of optical components necessary for the coexistence of quantum communications (QC) with conventional optical network communications. While LANL has demonstrated QC using modular integrated photonics, QC has never before been performed with monolithically integrated photonics. Our research leverages the US investment in the underlying technology of optical telecommunications infrastructure and applies it to the quantum regime.

Scientific Approach and Accomplishments

Previous experience with integrated optics for QC has shown that there are several areas of risk that will have to be managed in order for Si photonic systems to be applicable to QC. The first is the modulation scheme. We have found that photon polarization qubits are superior to phase-based qubits even for optical fiber systems that require polarization correction. However, polarization based transmitters and receivers must support multiple polarization states. This means that integrated photonics waveguides must work with both orthogonal polarizations within a polarization basis. In prior research our Gen1 modular QC transmitter uses a GaAs phase

modulator whose waveguide supports propagation of both transverse electric (TE) and transverse magnetic(TM) modes and modulates only the TE mode. That way we can produce the minimum desired number of polarization states, four, with a single modulator. However in Si photonics, the waveguides do not support both TE and TM polarizations simultaneously and the modulation methods, injection of charge carriers into the waveguide, do not selectively delay one polarization over the other. Therefore we must split the single, TE-mode polarization into two waveguides, modulate one and recombine the two waveguides with one of them rotated by 90° relative to the other one. We need to experimentally test combining the two polarizations in a Si oxide waveguide on the same substrate. The other area of risk is in the isolation needed to protect our quantum channel and detectors from the conventional communication channel that must operate over the same optical communication fiber but be split and isolated in the photonics. In general the highest available controllable extinction ratio in directional couplers is 60 dB, but we require 110 dB. We believe that Si photonic couplers, unlike other directional couplers, can achieve higher isolation ratios by cascading several components on the same substrate because there is little scattering or mode mixing to reduce the extinction ratio as is the case with discretely coupled components.

In year 1 of our 2 year research plan we collaborated with the University of Delaware that had a program called OpSIS for Optoelectronic Systems Integrated in Silicon. OpSIS separates design from fabrication and combines many designs on a single wafer to provide low cost access to cutting edge foundries. Through training and dialog with OpSIS we drafted specifications for the optical components of a monolithic quantum communications module. A photonic conceptual level design showing feasibility was completed. As we were preparing for a fabrication run of our first test chips, OpSIS lost its primary funding source and fabrication services ceased. LANL continued the research by collaborating with a senior researcher at Acacia Communications Inc., a recognized leader in optical transceivers used for the internet backbone. Physical designs are process dependent so the LANL developed physical designs for OpSIS had to be adapted by OpSIS for their process. This had some advantages because the Acacia process is more optimal for our application than the OpSIS was. Two fabrication runs were planned. The first run was with simple test structures: a tunable splitter and phase shifters. This fabrication run had a yield failure unrelated to our research. The second run combines some of the structures from the first run with cascaded splitters used as an attenuator and added an amplitude modulator. The second run did yield and characterization of the test structures on those die will be a subject of future research. In working with researchers at OpSIS and Acacia no fundamental problems were identified so we have gained insight and confidence in our research approach.

Impact on National Missions

Cyber-security is a top national security threat. QC can address long-duration/high-value security needs within many network environments, such as: highly secure DoD and DOE complexes; between government agencies in the Washington, DC area; financial networks; supervisory, control and data acquisition (SCADA) systems for critical infrastructure (power, water and SmartGrid) networks; or within a US Embassy compound. Further applications will extend security to constrained network environments. Examples include: warhead verification and IAEA treaty monitoring. Miniaturized QC systems will enable a handheld quantum secured devices to be used for identification, authentication, access control and secure telephone calls. An aircraft or satellite acting as a trusted node could establish ad hoc secure networks of ground, sea and air-based users on a continental or even a global scale.

Quantum secured communications technology at the Laboratory has been licensed to Whitewood Encryption Systems, Inc. a wholly owned subsidiary of Allied Minds.

Mixing and Diffusion in Granular Flows

Ivan Christov
20130792PRD2

Introduction

This project aims to understand the complexity of force-carrying contacts in a granular medium, which can often lead to its destabilization (due to external forcing) along unexpected fault lines, as commonly observed in geophysical situations including earthquakes, mudslides, and avalanches. The approach will be twofold. First, a model of how granular materials flows will be developed for the types of conditions encountered in geophysical processes. This is a high-potential scientific problem because, in over three decades of research, this most basic question regarding granular materials remains unsettled. Second, the force-chain network structure of granular materials will be obtained from model experiments, being conducted at Los Alamos, of a granular medium between sheared plates responding to the stimulus of their relative motion. The mathematical techniques of network analysis will be used to better understand the dynamic behavior of the medium under such loads. This is a cutting-edge endeavor because few such laboratory scale experiments and analysis have been carried out previously. Additionally, new algorithms for simulating universal emergent behaviors (clustering, ordering, topology) arising from the interplay between discontinuous granular mixing dynamics and microscopic physics will be developed as part of this project. This is a high-risk undertaking because scaling dynamics of granular materials in geophysical situations to laboratory scale experiments has yet to be demonstrated. Success in the project would imply the ability to extend the scaling concepts that have been so successful in fluid dynamics and aerodynamics to a new area: solid mechanics.

Benefit to National Security Missions

Granular materials are ubiquitous and are found in a host of applied programs. Hence, understanding mixing and flow of granular materials has impacts on many applied programs. This project aims to develop a modeling and simulation capability for describing mixing and flow of granular materials. The ability to improve model mixing of granular matter will impact energy applications including storage and transportation of energy-related materials (e.g., coal and biofuels). Granular materials tend to segregate according to size, a property that can be an obstacle in manufacturing and transportation processes. This project addresses precise mixing characteristics of granular materials and could lead to the design of optimized container design for improved mixing and more efficient transportation. The capabilities developed in this project will also be relevant for other DOE programs and needs including waste storage, waste handling and transportation, high explosives, and handling of materials produced in powder form.

Progress

The scientific accomplishments of the project in FY15 include the construction of a flow regimes diagram for injection of a buoyant liquid into a confined porous medium. Although the dynamics of granular media under various forcing and excitations are of interest on their own, a common geophysical problem involves the penetration of a liquid into the pore space between static grains. Specifically, such fluid injection into a porous medium occurs in a large variety of geophysical and industrial processes such as seawater intrusion into coastal aquifers, geological sequestration of carbon dioxide, waste fluid disposal, and oil and gas recovery. When the injected and displaced fluids are immiscible, a free boundary problem can be formulated to describe the time evolution of the fluid-fluid interface. It is of interest to know how this interface evolves over time in order to understand the sweep efficiency of the injection process. Work performed under this project in FY15 focused on the case of two-dimensional (Cartesian) vertically confined porous media. Assuming the injected fluid is denser than the displaced fluid, then the injected fluid only attaches to the bottom boundary at early times for point source injection. As time

progresses, the injected fluid contacts the top boundary, and the fluid flow becomes confined. Results obtained in this project establish that during the propagation process, because of the change of the horizontal and vertical length scales, the interface exhibits a transition from an early time unconfined behavior to a late time confined behavior, and we derived a nonlinear advection-diffusion equation to describe the time evolution of the fluid- fluid interface. We analyzed this partial differential equation in two distinguished asymptotic limits (early and late time) and found exact solutions in each case, resolving the structure of the moving front. Through detailed numerical simulations, we were then able to construct a phase diagram depending on two dimensionless quantities: the viscosity ratio of the displaced fluid to the injected fluid, and a dimensionless time. In doing so, the transition processes between the early and late time asymptotic limits were elucidated and the relevance of the early time and late time exact solutions were demonstrated for the first time in the literature.

Another scientific accomplishment of this project in FY15 is the Hamiltonian formulation of the equations for wave propagation in continua with microstructure such as a granular material. Although a granular materials' microstructure is quite complex in practice, the collective (continuum) behavior has been observed and well documented. The simplest way to study wave propagation in such a context is to derive a generic (universal) model, based on extended thermodynamics, for a continuum with one inherent length scale (e.g., the grain size). Then, by standard techniques, one can obtain weakly nonlinear dispersive evolution equations for wave propagation through this continuum. What had not been appreciated in previous discussion of such equations in the literature is that they possess Hamiltonian structure, endowing them with a number of desirable physical properties. We constructed the Hamiltonian formulation of such nonlinearly dispersive wave equations for the first time, showing there is in fact a hierarchy of such nonlinearly dispersive evolution equations. Additionally, as another novel feature of our work, we derived exact solitary wave solutions of these equations with curious properties: namely, waves that are compact and peaked.

In FY15, this project has yielded over a dozen invited presentations and two contributed presentations (international and regional conferences such as the American Physical Society's Division of Fluid Mechanics Annual Meeting). In addition, two journal publications have appeared in top disciplinary and multidisciplinary journals (Journal of Fluid Mechanics, Physical Review E), three more have been submitted for review, and a number are in preparation.

Future Work

In FY16, we will perform theoretical modeling of the experiments being conducted at Los Alamos on sheared granular media confined between two moving plates. In FY16, we will further expand our stated focus on geophysics, connecting to ongoing work at LANL on subsurface transport of particulate materials with applications to hydraulic fracturing. The latter systems consist of granular materials undergoing (potentially large) deformation and shear. A new aspect of this problem, then, is the possibility of comminution (or grinding, breakage, etc). Furthering the ongoing theoretical modeling we are performing, we will incorporate comminution into the models. The models will be analyzed to produce predictions that will be compared against observational data and benchmarked numerical simulations being performed at Los Alamos. Additionally, in FY16, the theory will be extended to account for non-uniformities of the flow conduits due to fracturing, comminution and other physical effects present in such high-pressure situations. We will also study the effects of grain fragmentation on granular flow, a problem with relevance to geophysical granular flows and earthquake physics.

Conclusion

The outcome of the first part of this work will be improved prediction of rare and destructive seismic events, which have significant implications for society at large. The outcome of the second part of this work will be improved understanding of how localized processes affect structure formation, which can lead to better prediction of dynamics as diverse as percolation in porous medium and spread of infections on networks.

Publications

Christov, I. C.. On a hierarchy of nonlinearly dispersive generalized KdV equations. 2015. PROCEEDINGS OF THE ESTONIAN ACADEMY OF SCIENCES. 64 (3): 2012.

Christov, I. C.. Comment on "The velocity field due to an oscillating plate in an Oldroyd-B fluid" by C.C. Hopkins and J.R. de Bruyn [Can. J. Phys. 92, 533 (2014)]. 2015. CANADIAN JOURNAL OF PHYSICS. 93 (12): 1651.

Christov, I. C., R. M. Lueptow, J. M. Ottino, and R. Sturman. A Study in Three-Dimensional Chaotic Dynamics: Granular Flow and Transport in a Bi-Axial Spherical Tumbler. 2014. SIAM JOURNAL ON APPLIED DYNAMICAL SYSTEMS. 13 (2): 901.

Christov, I. C., R. M. Lueptow, J. M. Ottino, and R. Sturman. A Parametric Study of Mixing in a Granular Flow a Bi-Axial Spherical Tumbler. Dynamical Systems - Modelling. Edited by Awrejcewicz, J..

Christov, I. C., and H. A. Stone. Shear dispersion in dense

granular flows. 2014. GRANULAR MATTER. 16 (4): 509.

Christov, I. C., and P. M. Jordan. On an instability exhibited by the ballistic-diffusive heat conduction model of Xu and Hu. 2014. ROCEEDINGS OF THE ROYAL SOCIETY A-MATHEMATICAL PHYSICAL AND ENGINEERING SCIENCES. 470 (2161): 20130557.

Christov, I. C., and P. M. Jordan. Corrections to Morse and Ingard's variational-based treatment of weakly-nonlinear acoustics in lossless gases. 2015. JOURNAL OF THE ACOUSTICAL SOCIETY OF AMERICA. 138 (1): 361.

Christov, I. C., and P. M. Jordan. Maxwell's "other" equations. 2015. The Royal Society Publishing Blog.

Khare, A., I. C. Christov, and A. Saxena. Successive phase transitions and kink solutions in phi(8), phi(10), and phi(12) field theories. 2014. PHYSICAL REVIEW E. 90 (2): 023208.

Zheng, Z., B. Guo, I. C. Christov, M. A. Celia, and H. A. Stone. Flow regimes for fluid injection into a confined porous medium. 2015. JOURNAL OF FLUID MECHANICS. 767: 881.

Zheng, Z., I. C. Christov, and H. A. Stone. Influence of heterogeneity on second-kind self-similar solutions for viscous gravity currents. 2014. JOURNAL OF FLUID MECHANICS. 747: 218.

Thermodynamics and Information Processing at the Nanoscale

Wojciech H. Zurek
20140667PRD2

Introduction

Sebastian Deffner is an emerging leader in the field of nonequilibrium statistical mechanics (as recognized by the community, and current leaders in the field). As a postdoctoral fellow, he will bring his cutting-edge expertise in nonequilbrium processes to LANL with direct relevance across disciplines. His research program is directly aligned with one of the Los Alamos mission to foster energy security.

Nanodevices running thermodynamic cycles---Deffner's principal area of research---provides optimal ways of converting different types of energy (e.g. thermal into mechanical) and is important for a variety of applications.

The engineering of highly efficient quantum engines and thermodynamic cycles is a low risk, cutting edge area of research with the potential to advance efficient energy conversion techniques and to directly impact ongoing experimental progress around the world.

There is already significant related interest at LANL. In addition to ongoing research in nanotechnology, current efforts at P-21 (Boshiers's lab), are devoted to the implementation of a superadiabatic quantum piston [A. del Campo, M. G. Boshier, Sci. Rep. 2, 648 (2012)], one of the key components to realize the engineered energy systems proposed by Deffner for optimizing energy conversion and use.

Benefit to National Security Missions

Deffner will explore laws of thermodynamics as they apply on a nanoscale. At that level thermal and quantum fluctuations become important, and modify optimal strategies for extraction of useful work. Efficient acquisition of energy is one of the missions of DOE, and of keen interest to LANL. Moreover, at the level at which Sebatian will explore thermodynamics, information gained in course of the engine cycle can be comparable to thermodynamic entropy, and its efficient processing using available hardware (which includes quantum information processing) is important. Information processing, including its quantum aspects, is of interest to LANL and DOE.

Progress

In the last fiscal year we have significantly advanced our understanding of quantum thermodynamic devices and of optimal quantum processes. Our progress is reflected in five publications and two preprints.

Together with our collaborator Haitao Quan (Peking University, formerly LANL director funded postdoc) we computed the work distribution for quantum pistons operating with non-interacting bosons and fermions. This work has been published in Phys. Rev. E 90, 062121 (2014).

Similar results have also been obtained for quantum processes in diatomic molecules. Chem. Phys. 446, 18 (2015) reports the analytical treatment of the quantum work statistics in driven Morse oscillators.

In Phys. Rev. Lett. 114, 150601 (2015) we generalized the quantum Jarzynski equality to non-linear quantum systems. In particular, we showed how quantum thermodynamic relations generalize to PT-symmetric quantum mechanics, i.e., a non-hermitian quantum theory. These results will also be present in an upcoming CNLS workshop on PT-symmetry and a CNLS workshop on related topics for Feb 2016 is in preparation.

Our insight in the foundations of statistical mechanics attracted the attentions of Nature Physics. In an invited News and Views article Deffner summarized the state-of-art and future perspectives of the role played by quantum entanglement in the foundations of statistical

mechanics. Nature Physics 11, 383 (2015)

In particular, we were able to show that the foundations of statistical physics can be built from purely quantum symmetries -- entanglement assisted envariance: arXiv:1504.02797

We also furthered our understanding of optimal quantum processes. A recent PRL reports the experimental study of environment assisted speed-ups in cavity QED. This experiment has been performed in the group of Luis Orozco at the University of Maryland: arXiv:1503.02591

Finally, in arXiv:1503.03455 Gardas and Deffner showed that no quantum heat engine can be more efficient than a Carnot engine. This result settled a discussion brewing in the literature for over ten years. The main novel insight is how to properly define heat and work for quantum systems with non-negligible coupling to the environment.

Future Work

The main objective of this project research is the development of a coherent framework for the understanding, the design, and the theoretical foundations of nanothermodynamic devices, whose modes of operation allow the implementation of information processing, and which generically operate far from thermal equilibrium. In collaboration with the experimental group of Ferdinand Schmidt-Kaler, we developed only recently the smallest possible quantum heat engine, whose working medium consists of a single trapped ion.

The experimental principle can be extended in two directions: (i) To date, we only studied a single ion trapped in a one-dimensional harmonic oscillator. Optical lattices are, to very good approximation, a network of harmonic oscillators. Thus, the working principles of the one-ion heat engine can be readily generalized to multiple particles evolving in an optical lattice. Such a device would enable the experimental study of the thermodynamic properties of fully controllable multi-particle quantum systems. (ii) In previous research, we also have been interested in the interplay of (quantum) information and thermodynamics. However, how to describe a quantum information reservoir, i.e. a fully quantum mechanical hard disk, and its thermodynamic properties is to date still an open question. To this end, we will be aiming at simple generalizations of the on-ion heat engine towards a minimal quantum Maxwell demon - a perfect device to study quantum thermodynamics and information theory. We are also planning to investigate fluctuation relations generalizing the statements of the second law of thermodynamics and their consequences on the dynamics of nanodevices.

In a new collaboration with the experimental group of Luis Orozco we have built expertise in optimizing quantum processes in cavity QED. In a next step we will be aiming at the development of an 'optimal' quantum heat engine based on this novel technology.

Conclusion

We expect our results to have impact on the design of quantum systems in the development of quantum computers, and in the fundamental understanding of nanotechnology experiencing quantum effects. Our research will open new avenues in the fundamental understanding of time-dependent quantum systems operating arbitrarily far from thermal equilibrium, and thereby process information. Highly efficient quantum cycles will be designed.

Publications

Acconcia, T. V., M. V. S. Bonança, and S. Deffner. Shortcuts to adiabaticity from linear response theory. To appear in PHYSICAL REVIEW E.

Cimmarusti, A. D., Z. Yan, B. D. Patterson, L. P. Corcos, L. A. Orozco, and S. Deffner. Environment assisted speed-up of the field evolution in cavity quantum electrodynamics. 2015. PHYSICAL REVIEW LETTERS. 114: 233602.

Deffner, . TEN YEARS OF NATURE PHYSICS From spooky foundations. 2015. NATURE PHYSICS. 11 (5): 383.

Deffner, , and Saxena. Jarzynski Equality in PT -Symmetric Quantum Mechanics. 2015. PHYSICAL REVIEW LETTERS. 114 (15).

Deffner, S., and A. Saxena. Quantum work statistics of charged Dirac particles in time-dependent fields. 2015. PHYSICAL REVIEW E. 92: 032137.

Gardas, B., and S. Deffner. Thermodynamic universality of quantum Carnot engines. 2015. PHYSICAL REVIEW E. 92: 042126.

Gong, , Deffner, and H. T. Quan. Interference of identical particles and the quantum work distribution. 2014. PHYSICAL REVIEW E. 90 (6).

Leonard, , and Deffner. Quantum work distribution for a driven diatomic molecule. 2015. CHEMICAL PHYSICS. 446: 18.

A Quadrature Approach for Non-Gaussian Uncertainty Representation and Propagation

David Palmer
20130784PRD2

Abstract

If the position and velocity of an object is known, and with forces affecting its motion, good predictions as to where it will be in the future can be made. However, in the real world, the quantities are only approximately known, and only estimates of the region where the object might be found in the future can be made. This project looked at predicting satellite positions, but the techniques being developed are more general and can be applied to a number of practical problems.

Current standard prediction techniques simplify the uncertainty to regions that are described by spheroids that may be stretched like a football, but not bent like a banana, coiled like a spring, or split into multiple regions. These more complicated uncertainty regions can be explored by simulations.

In more technical terms; this work sought to improve on the traditional sigma point approaches to nonlinear filtering by considering a more general formulation, and applying the new sigma point filtering method to highly relevant problems. Our study was focused on space situational awareness, which is a key topic in the Grand Challenge for Sensing and Measurement Science for Global Security. However, more generally, it covers many fields of simulation.

Background and Research Objectives

Recent events in space, including the collision of Russia's Cosmos 2251 satellite with Iridium 33 and China's Feng Yun 1C anti-satellite demonstration, have stressed the capabilities of Space Surveillance Network (SSN) and its ability to provide accurate and actionable impact probability estimates. The SSN network has the unique challenge of tracking more than 18,000 resident space objects (RSOs) and providing critical collision avoidance warnings to military, NASA, and commercial systems. However, due to the large number of RSOs and the limited number of sensors available to track them, it is impossible to maintain persistent surveillance resulting in large observation gaps. This inherent latency in the catalog information results in sparse observations and large propagation intervals between measurements and close approaches. The large propagation intervals coupled with nonlinear RSO dynamics results in highly non-Gaussian probability distribution functions (pdfs). In particular, low-Earth orbiting (LEO) satellites are heavily influenced by atmospheric drag, which is very difficult to model. Uncertainties in atmospheric influences must be folded into estimation models to accurately represent the position uncertainties in calculating impact probabilities. This process then separates naturally into a prediction and correction cycle, where estimates are used to predict the orbital position at a future time and observations are used to improve or correct these predictions while decreasing uncertainty. The difficulty in this process lies in representing the non-Gaussian uncertainty and accurately propagating the uncertainty through the orbital dynamics model. Accurate assessment of confidence in position knowledge will be a significant improvement, particularly for the space situational awareness (SSA) community and the warfighter.

Scientific Approach and Accomplishments

This postdoctoral fellowship work focused on the development of the next generation of sigma point filters; improving on the traditional approaches by considering a more general formulation, and applying the new method to the highly relevant problem of SSA. The new approach to uncertainty propagation was developed by using the theory of Gauss-Hermite Quadrature (GHQ) integration and extending GHQ using Generalized Gaussian Cubature (GGC). The approach was applied to a number of problems to study the convergence properties, robustness, and accuracy of the proposed method.

Our new approach, named GGC filter, is a novel method for nonlinear filtering based on a generalized Gaussian cubature approach. Specifically, it is a new point-based

nonlinear filter that is not based on one-dimensional quadrature rules, but rather uses multi-dimensional cubature rules for Gaussian distributions. The new generalized Gaussian cubature filter is not in general limited to odd-order degrees of accuracy, and provides a wider range of order of accuracy. The method requires the solution of a set of nonlinear equations for finding optimal cubature points, but these equations need only be solved once for each state dimension and order of accuracy. This rule can also be extended to anisotropic cases where the order of accuracy is not isotropic in dimension. This method allows for tuning of the cubature rules to develop problem specific rules that are optimal for the given problem. The generalized Gaussian cubature filter is applied to benchmark problems in astrodynamics, and it is compared against existing nonlinear filtering methods.

To test the performance of the new GGC rules for propagation of uncertainty through a dynamic system, a simple nonlinear two-dimensional example is used. This example models a nonlinear spring-mass system with a nonlinear friction term. The system dynamics for this simple example used a cubed term for the spring force. The simulation time considered is 200 seconds with a sampling interval 0.1 seconds. Monte Carlo simulations were conducted to test the GGC approaches for different orders. The Monte Carlo samples are taken from the initial distribution, and 1,000 samples are used in the comparisons.

The errors in the means of the system's state is computed for the different order of the GGC method and compared to the means calculated from the Monte Carlo samples at each time step. These errors are shown in Figure 1 for the system state mean calculated with GGC. From this figure it can seen that as the order increases, the mean is more accurately estimated. During the initial portion of the simulation the errors are large for all the models since the nonlinear spring is fluxing greatly but the higher-order GGC still has better performance. As the energy dissipates the system fluctuation is lower but the higher-order models still show better performance.

A second example is considered, a nonlinear spring-mass model state estimation example with nonlinear measurements. The nonlinear spring-mass model is the same as the one used in the first example to test the uncertainty propagation performance of the GGC approach. Measurements are simulated assuming a measurement model that consists of the exponential of the first state and additive random noise. Measurements are sampled at 0.1 second intervals for a total of 200 second simulation time.

The state estimates for UKF, GGC order 3, and GGC 5 are shown in Figure 2. From Figure 2 it can be seen that the UKF has the worst performance while the GGC method does a better job at tracking the truth. All filters diverge initially, but the UKF has the largest divergence. Also the UKF takes the longest amount of time to converge to the true state.

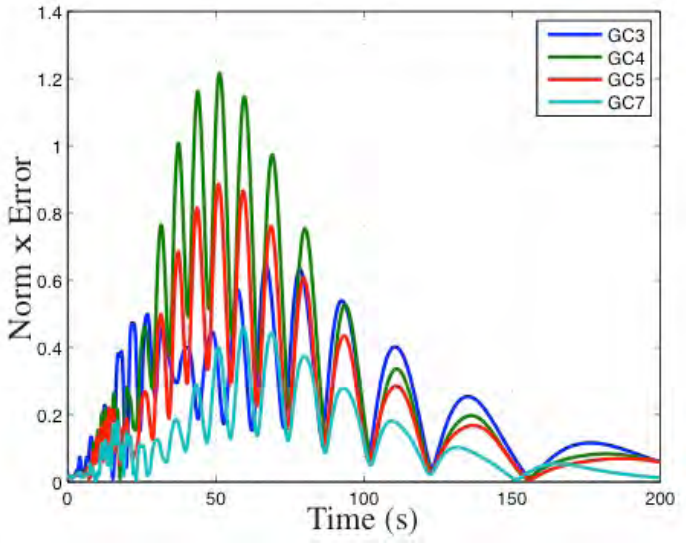

Figure 1. Errors in a model estimator at different Gaussian Cubature orders. The modeled system is a mass on a non-linear spring (force proportional to the cube of the displacement) with non-linear friction. The fit improves rapidly as the order increases.

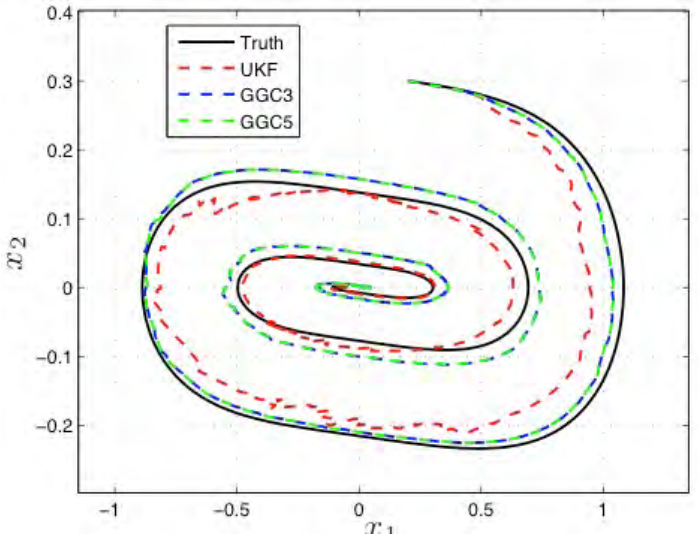

Figure 2. The state space (position and velocity) trajectory of the model system as in Figure 1, and some estimator outputs. In this case, the estimator input was the exponential of the position, plus noise. Because the Unscented Kalman Filter (UKF, red) was developed for simple conditions, it has trouble with the non-linear measurements (which lead to non-Gaussian noise in the derived position) showing much more erratic variation than the Gaussian Cubature models.

The final example considered is an attitude estimation example satellite orientation estimation. The performance

of the GGC filter, UKF, and the EKF are compared. The GGC uses the approach for representing the pdf as sigma points discussed earlier. Large initial errors are considered. It is important to note that with large initial errors the attitude distribution becomes highly nonlinear. Attitude errors of -50, 50, and 160 degrees for each axis, respectively, are added into the initial-condition attitude estimate. The initial attitude standard deviation is set to (50 degrees) for each attitude component. Gyro biases are also estimated. The initial bias standard deviation is set to (20 deg/hr) for each axis. A plot of the norm of the attitude errors for this simulation case is shown in Figure 3. The EKF does not converge for this case since the first-order approximation cannot adequately capture the large initial condition errors. The UKF does have better convergence properties than the EKF for this case, however the GGC provides the best convergence performance. Both the EKF and the UKF are more sensitive to the initial conditions than the GGC. The performance of the GGC is checked by running the filter 100 times. It always converges and the statistics of the estimation results in the 100 runs are almost identical.

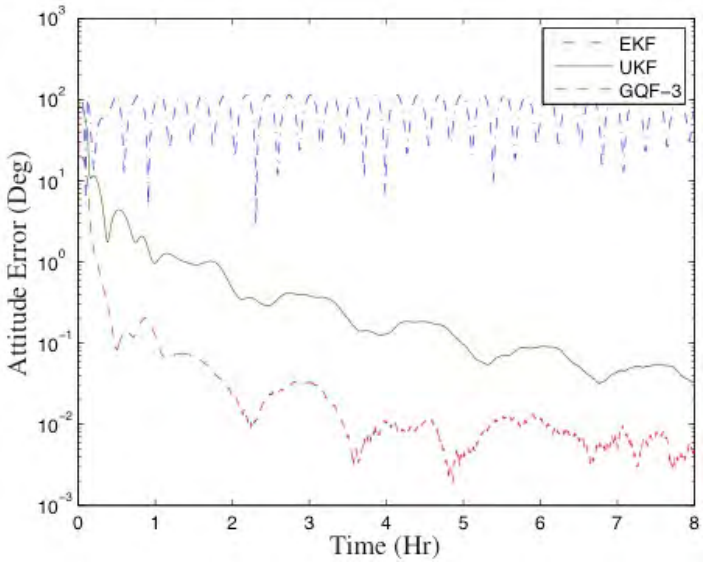

Figure 3. Attitude estimation of a satellite. Given an initially large uncertainty in the attitude, the Extended Kalman Filter (EKF) never develops a good approximation to the satellite attitude. An Unscented Kalman Filter (UKF) does discover the attitude and gradually improve its estimate, while the new algorithm gives a large improvement in both speed and accuracy.

For a general nonlinear problem, the Gaussian cubature method requires less function evaluations as compared to existing approaches to achieve equivalent accuracy. Figure 4 shows a comparison of the number of terms (function evaluations) as a function of order required by the GGC method vs the number required by current existing approaches. From this figure it is clear that the number of function evaluations required grows slower with GGC method than it does with competing approaches.

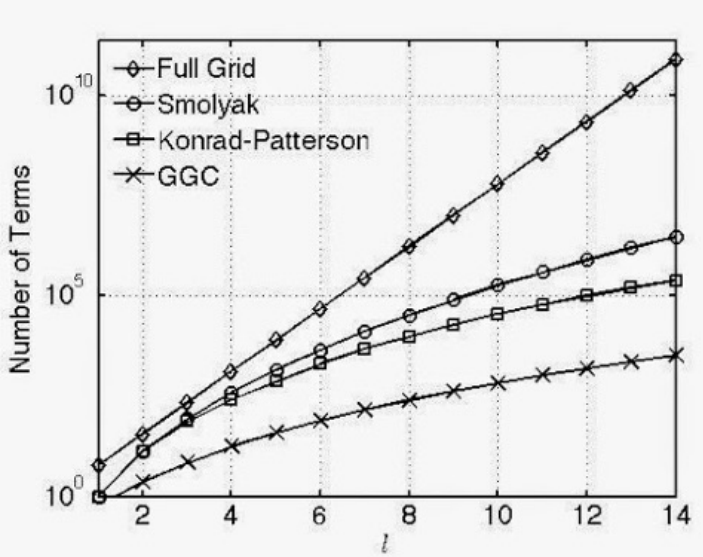

Figure 4. Comparison of growth of computational requirements vs order for different analysis schemes. Note the extreme logarithmic scale, indicating that for 14th order accuracy, a full-grid approach would need millions of times more calculations than the Cubature approach. Even the more sophisticated previous approaches require 100-1000x the calculations.

Impact on National Missions

This research represents a novel and ground-breaking approach to uncertainty quantification that has application across a number of areas in LANL's portfolio. In particular, the development of accurate and consistent methods of characterizing uncertainty is highly relevant for the space situational awareness, which is key to insuring the security of national space systems critical to nonproliferation and other security challenges. This research offered an exciting opportunity to further solidify the theoretical underpinning of powerful and well-known methods in nonlinear/non-Gaussian estimation while developing a new and computational efficient technique.

This work investigated a technique called Generalized Gaussian Cubature, where the rules are constructed to integrate a set of functions exactly. Hermite and Sparse Tensor products approaches for multi-dimensional integrals were discussed. The generalized cubature approach was used to solve multi-dimensional integrals of Gaussian distributions. The solution was simplified greatly by using the generalized cubature technique along with properties of Gaussian distributions. Additionally, the solution of nodes and weights for the generalized cubature of a Gaussian distribution was also greatly simplified by using the multi-dimensional Hermite polynomials. Cubatures were derived for a number of orders and dimensions and used for both uncertainty propagation and sequential state estimation.

Good results were shown with the new methods with three example problems. The authors are very optimistic about the approach and believe that it can greatly improve the uncertainty quantification results for a large number of practical problems.

References

1. Linares, R., and I. Impact-Team. A Framework for Integrated Modeling of Perturbations in Atmospheres for Conjunction Tracking (IMPACT). 2014. (Pasadena, CA, 2014). p. 0. Pasadena, CA: AIAA.

2. Linares, R., W. Andrew, M. A. Shoemaker, and J. L. Crassidis. Characterization of Inactive Rocket Bodies Via Non-Resolved Photometric Data. 2014. (Maui, Hawaii, 2014). p. 0. Maui, Hawaii: AMOS.

3. Klimenko, A., A. Brennan, H. Godinez, D. Higdon, J. Koller, E. Lawrence, R. Linares, D. M. Palmer, M. Shoemaker, D. Thompson, A. Walker, B. Wohlberg, M. K. Jah, E. Suton, T. Kelecy, A. Ridley, and C. McLaughlin. A Framework for Integrated Modeling of Perturbations in Atmospheres for Conjunction Tracking (IMPACT). 2015. In AIAA Book on Space Operations, 2015. By AIAA, . p. 0. Reston, VA, USA: AIAA.

4. Mehta, P. M., A. Walker, E. Lawrence, R. Linares, D. Higdon, and J. Koller. Modeling Satellite Drag Coefficients with Response Surfaces. 2014. Advances in Space Research. (Oct): 00.

Publications

Klimenko, A., A. Brennan, H. Godinez, D. Higdon, J. Koller, E. Lawrence, R. Linares, D. M. Palmer, M. Shoemaker, D. Thompson, A. Walker, B. Wohlberg, M. K. Jah, E. Suton, T. Kelecy, A. Ridley, and C. McLaughlin. A Framework for Integrated Modeling of Perturbations in Atmospheres for Conjunction Tracking (IMPACT). 2015. In AIAA Book on Space Operations, 2015. By AIAA, . , p. 0. Reston, VA, USA: AIAA.

Linares, R., W. Andrew, M. A. Shoemaker, and J. L. Crassidis. Characterization of Inactive Rocket Bodies Via Non-Resolved Photometric Data. 2014. In Advanced Maui Optical and Space Surveillance Technologies (AMOS) Conference. (Maui, Hawaii, 2014). , p. 0. Maui, Hawaii: AMOS.

Linares, R., and I. Impact-Team. A Framework for Integrated Modeling of Perturbations in Atmospheres for Conjunction Tracking (IMPACT). 2014. In AIAA - Space Operations Conference. (Pasadena, CA, 2014). , p. 0. Pasadena, CA: AIAA.

Mehta, P. M., A. Walker, E. Lawrence, R. Linares, D. Higdon, and J. Koller. Modeling Satellite Drag Coefficients with Response Surfaces. 2014. Advances in Space Research. (Oct): 00.

Materials for the Future

Photoactive Energetic Materials for Quantum Optical Initiation

Robert J. Scharff
20140005DR

Introduction

This project provides an innovative approach to establish design principles and a scientific methodology for generating photoactive energetic materials with controllable optical functionality. The project aims to increase the controllability of chemical dynamics in novel photoactive materials through a concerted experimental and theoretical effort that characterizes the dynamics of energy localization, chemical bond activation, and chemical reactions. This approach will provide critical insight on how to manipulate electronic structure through synthesis in order to generate the desired material response to overcome mechanisms that limit controllability.

The authors propose a three-part solution for the successful design of photoactive energetic materials for quantum optical initiation. The first part involves the development of new explosives derivatized with an optical chromophore. The optimization of optical response properties (e.g. 1-photon and 2-photon absorption cross-sections and resonant wavelengths) of the photon absorbing chromophore will enable efficient coupling of the laser field to the explosive and facilitate control of excited state dynamics. The second part addresses the need for the elucidation of electron-vibrational dynamics following photoexcitation. Our feasibility studies support our main idea that exothermic NO2 formation could be achieved photochemically: following absorption, photochemistry can be accomplished through non-adiabatic conversion of the excess electronic energy into specific vibrational degrees of freedom on the explosive and controlling the onset of exothermic chemical reactions in the surrounding material. The third part of the proposal uses fs laser pulse shaping quantum control to optimize photodissociation quantum yields and photoinitiation exothermic chemistry.

The achievement of optically driven control over the chemical reaction dynamics of energetic materials will not only have an immediate and profound impact on the Weapons Program, but will also provide significant advancements towards utilizing laser pulses as powerful sources for manipulating and controlling atomic and molecular processes on unprecedented time and length scales.

Benefit to National Security Missions

The overarching goal of this project – to achieve quantum control of explosive initiation – utilizes the theory-guided, materials-by-design approach outlined in the Materials Pillar Extreme Environments theme of "predicting and controlling functionality of materials in these extremes". Critical to the Materials Pillar mission is the establishment of design principles and scientific protocols for manufacturing advanced materials to control functionality for predefined performance criteria central to LANL mission needs. DOE programmatic drivers exist for the development of photoactive energetic materials that can address future milestones for enhanced safety, security, and use-control of the nuclear stockpile. Moreover, there are DoD directives for the development of new energetic materials that are insensitive to unplanned stimuli (e.g., spark, impact, and friction). The development of photoactive energetic materials that optically initiate through quantum controlled photochemistry would yield a "quantum lock-and-key" capability valuable not only in applications for improved detonator optical isolation, but also for enhancement of use-control protections, explosive optical logic, and other dual-use technologies to support initiatives concerning DoD insensitive munitions or planned Life Extension Programs.

Progress

In our first 17 months, we have established a very interdisciplinary research program aimed at understanding the photochemical reaction dynamics of several tetrazine-derivatized energetic molecules. Tetrazine is a promising high nitrogen energetic chromophore that has a large heat of formation and versatile chemistry

for attachment to a number of ligands. Petrin tetrazine chloride was the initial focus of detailed study, since petrin is the trinitrate analog of PETN, the current DOE detonator explosive. Replacing PETN with a PETN derivatized with an energetic chromophore was a logical first step. Tetrazine was also derivatized with 2 PETN molecules, with dinitroazetidine (DNAZ), 2 DNAZ molecules, and nitroglycerin. More complex molecules with 2 DNAZ and tetrazines linked through an azo group were tested as a means to achieve extended conjugation and increase the two photon absorption. High nitrogen tetrazine metal complexes were produced to enhance absorption through charge transfer. Several triazine-based energetics were also formed, which are accessible to irradiation in the near ultraviolet.

A number of new experimental capabilities were developed to enhance the level of detail and the speed of characterization of the photoactive energetic materials. One of the initial objectives was the capability to screen the numerous materials the synthesis team had produced to determine which were worth scaling up to larger quantities. We determined that photochemical bleaching through laser irradiation in an FTIR would allow the use of 10-20 mg of material to answer many of the relevant questions: How photoactive are the HEs? What is the chemistry produced? What type of laser irradiation will they be accessible to? Do the properties determined match those expected by the synthesis team or predicted by the theory team?

Initial studies of FTIR photobleaching used CW lasers at nonhazardous levels within the energetic material synthesis area at TA-9. While we were able to obtain photobleaching data, sometimes days of irradiation were necessary. Since this was not a laser laboratory, the use of pulsed or high intensity lasers was not allowed. The simplest solution was to purchase a small FTIR and integrate it into the laser laboratory at TA-40. This allowed us to port high power CW, pulsed nanosecond, and pulsed femtosecond lasers of various wavelengths into the FTIR. We wrote software to quantitatively analyze the hundreds of photobleaching spectra that could now be acquired in a day. We now have the capability to determine the photochemical quantum yield and basic photochemistry through FTIR of novel photoactive explosives excited at a broad range of wavelength and intensity conditions.

The next stage of experiments focused on nanosecond frequency-doubled Nd:YAG excitation at 532 nm that would be relatively straightforward to transition to engineering applications, while also taking advantage of the large absorption of the tetrazine complexes at 532 nm. We quickly determined that the quantum yield was very low, but could be increased dramatically with intensities easily achieved with common nanosecond lasers. We were not seeing signs of NO2 elimination predicted by the NA-ESMD predictions, but could have been missing small changes in the FTIR. Since many of the products of energetic material dissociation are expected to be small gas phase molecules, we designed an experiment to measure these products as well.

We built a photochemical mass spectrometry experiment to measure relative yields of gas phase products. This experiment is essentially a windowed vacuum cell coupled to a rough pump and turbopump with a commercial quadrupole mass spectrometer attachment. We adapted an existing vacuum cell to hold 4 KBr pellets that could be irradiated individually in vacuum while pumping and monitoring the mass spectrum. The new capability to measure gas phase photoproducts proved decisive in determining when the chemistry was localized on the chromophore and when energy transfer led to chemistry on the conventional energetic moiety.

Future Work

Synthesis: Synthesis efforts will focus on pi extended conjugated systems in an effort to increase cross sectional areas of the molecule. Efforts will also focus on polycyclic materials in an effort to increase polarizability. We will also begin to scale-up molecules we have created in FY14.

Theory: Currently we are benchmarking the non-adiabatic dynamics with solvent using well studied model systems. In the next year this means we will be able to perform non-adiabatic dynamics simulations of our target molecules using solvent environment.

Characterization: We will perform CW laser photo degradation, fluorescence quantum yield and spectral measurements, and measure the optical absorption of the remaining newly synthesized photoactive energetic materials to identify the one photon active excited states and use FTIR to measure the photo decomposition chemistry. We will begin time resolved photochemical measurements (FSRS) on the novel photoactive HE. We will begin to measure two photon absorption spectra of photoactive HE in solution for comparison and validation to theory.

Conclusion

As the primary goal is the design and development new energetic materials with controllable photochemical reactions, the expected outcome is a transformational and universal paradigm for the development of advanced future materials with structure-function relationships leading to applications based on quantum control of chemistry. The development of photoactive energetic materials that initiate through the quantum control of photochemis-

try addresses future surety themes outlined in the FY12 Stockpile Stewardship and Management Plan and provides an enabling technology for future Directed Stockpile Work. The project will pave the way for new explosives that perform like RDX yet are insensitive to unplanned stimuli.

Publications

Bjorgaard, J. A., K. A. Velizhanin, and Tretiak. Solvent effects in time-dependent self-consistent field methods. II. Variational formulations and analytical gradients. 2015. JOURNAL OF CHEMICAL PHYSICS. 143 (5).

Bjorgaard, J. A., Kuzmenko, K. A. Velizhanin, and Tretiak. Solvent effects in time-dependent self-consistent field methods. I. Optical response calculations. 2015. JOURNAL OF CHEMICAL PHYSICS. 142 (4).

Bjorgaard, J. A., Nelson, Kalinin, Kuzmenko, K. A. Velizhanin, and Tretiak. Simulations of fluorescence solvatochromism in substituted PPV oligomers from excited state molecular dynamics with implicit solvent. 2015. CHEMICAL PHYSICS LETTERS. 631: 66.

Greenfield, M. T., S. D. McGrane, C. A. Bolme, J. A. Bjorgaard, T. R. Nelson, Tretiak, and R. J. Scharff. Photoactive High Explosives: Linear and Nonlinear Photochemistry of Petrin Tetrazine Chloride. 2015. JOURNAL OF PHYSICAL CHEMISTRY A. 119 (20): 4846.

Hernandez, Alfonso, Nelson, Tretiak, and Fernandez-Alberti. Photoexcited Energy Transfer in a Weakly Coupled Dimer. 2015. JOURNAL OF PHYSICAL CHEMISTRY B. 119 (24): 7242.

Kilina, , Kilin, and Tretiak. Light-Driven and Phonon-Assisted Dynamics in Organic and Semiconductor Nanostructures. 2015. CHEMICAL REVIEWS. 115 (12): 5929.

White, A. J., V. N. Gorshkov, Tretiak, and Mozyrsky. Non-adiabatic molecular dynamics by accelerated semiclassical Monte Carlo. 2015. JOURNAL OF CHEMICAL PHYSICS. 143 (1).

White, A. J., V. N. Gorshkov, Wang, Tretiak, and Mozyrsky. Semiclassical Monte Carlo: A first principles approach to non-adiabatic molecular dynamics. 2014. JOURNAL OF CHEMICAL PHYSICS. 141 (18).

Multiferroic Response Engineering in Mesoscale Oxide Structures

Dmitry A. Yarotski
20140025DR

Introduction

Multiferroic (MF) materials exhibit strongly coupled magnetic and ferroelectric (FE) orders and promise transformative technologies in energy, security, and information processing. However, the inability to synthesize epitaxial materials with the desired three-dimension (3D) structure and to probe the emergent properties resulting from the atomic-to-mesoscale evolution poses significant challenges to modern condensed matter theory in providing a predictive description of the strong coupling among spin, charge, orbital, and lattice degrees of freedom. As a result, new materials discovery has often relied on serendipitous findings rather than on scientific principles underpinning the magnetoelectric (ME) functionality. We target to use a systematic co-design approach to the discovery of MFs based on a closed synthesis-characterization-modeling loop. We emphasize the rapid feedback from the experimental validation to theoretical prediction and vice versa. Our approach is enabled by a combination of recent LANL breakthroughs in first-principles modeling of complex electron correlation phenomena, controllable synthesis of 3D mesoscale films, and novel coherent photon probes of intrinsic dynamics of competing orders in MF composites.

Built on our team's unique expertise in theoretical simulation of multifunctional metal-oxide materials, the effort starts with ab-initio identification of prominent composite structures having high ME response. Experimental results is then used to refine model Hamiltonians and to provide a better estimate for the geometry and constituent materials, quite possibly beyond the initial compounds and structures, for the next optimization iteration. For a particular choice of materials (BiFeO3:CoFe2O4 or La0.7Sr0.3MnO3:BiFeO3), we synthesize these epitaxial 3D composite films and systematically characterize their structural and physical properties.

Benefit to National Security Missions

This project aims to develop basic principles to control macroscale multiferroic (MF) functionality in mesoscale composites through tuning the interactions on the nanoscale. This research directly supports all three central themes of the Materials for the Future pillar in harnessing defects, interfaces and electromagnetic field extremes to control collective behavior in MF materials. Our approach also addresses LANL's priorities in 'meso'-science development and practical realization of design principles towards both tunable and controlled functionality of complex materials. The proposed effort aligns well with the MaRIE vision of 'material co-design' and develops new integrated capabilities in synthesis, theory, and ultrafast x-ray characterization for MaRIE. This project further leverages the user programs at LCLS, APS, CINT, NHMFL, and the Lujan Center in accord with the LANL institutional priority in supporting national user facilities. Materials with tunable functionality are enabling components in energy, sensing, and information technologies. Therefore, we expect this work to have a direct and significant impact on near- and long-term LANL programs in Advanced Materials, Global Security, Information Science and Technology, and Clean Energy.

Progress

In the second year of the project we have continued a synergistic theoretical and experimental effort to understand and control the magneto-electric (ME) coupling in single-phase and heterostructured multiferroic systems. In particular, we used first-principles density functional theory (DFT) to reveal the mechanisms of magnetic coupling across the interface between multiferroic (ferroelectric (FE) and antiferromagnetic (AFM)) BiFeO3 (BFO) and ferromagnetic (FM) La1-xSrxMnO3 (LSMO). In order to understand the implications of BFO pillar structure in LSMO matrix on the ME coupling, we calculated the net magnetization induced in BFO and LSMO in the proximity of interface. Using initially AFM ordered BFO and FM ordered LSMO, we electronically relaxed both system

and found that collinear alignment of magnetization axis in both LSMO and BFO is more favorable than their perpendicular mutual orientation. These results explained the dependence of induced magnetization in BFO on the LSMO termination plane at the interface that was observed in our neutron scattering experiments. Moreover, this effect should also lead to reduced magnetization in LSMO near the interface due to spin disorder induced by the exchange bias, which was initially confirmed in our ultrafast optical spectroscopy measurements on BFO/LSMO superlattices and, recently in our X-Ray magnetic circular dichroism (XMCD) experiments on BFO/LSMO nanopillars samples. Dependence of this effect on the pillar density and structure will provide essential insight for engineering ME coupling through manipulation of interfacial exchange bias in multiferroic composites.

We have also studied the problem of strain and electronic localization/delocalization in disordered ferromagnetic systems. We constructed a numerical algorithm to calculate the conductance within the transfer matrix method. By targeting the structural disorder relevant to BFO or MgO pillar in LSMO matrix structure, we have found that with a given strength of an impurity barrier, there is a critical thickness, below which the low-energy electronic wave functions become localized. This work gives a correspond explanation to the experiment which measure the transport property for the LSMO system with a critical thickness. To test this prediction, we created a series of LSMO films of varying thickness and nanopillar samples where effective "thickness" of LSMO was continuously varied by changing LSMO fraction in LSMO/MgO composite from nanoscale pillar to mesoscale matrix. Magnetization and XMCD (using synchrotron facilities) measurements have clearly shown continuous degradation of conductivity and FM response with increased strain in LSMO. These results should aid in optimization of multiferroic functionality of the nanocomposites by controlling strain field distribution across the interfaces. Time-resolved second harmonic spectroscopy has also demonstrated charge accumulation at the interfaces of BFO/LSMO nanopillars which leads to enhancement of FE response in BFO. This effect is thought to be relevant to the predicted electron localization and will be more thoroughly investigated in the following experimental/modeling effort.

In parallel to optimizing composite multiferroic architectures, we are continuously searching for new single-phase materials with enhanced magnetization, polarization, and ME coupling that can be used in nanostructure fabrication. For example, double perovskite Bi2FeMnO6 (BFMO) is a potential candidate for the highly sought room-temperature multiferroic system. We have studied the magnetic, electronic and optical properties and their interplay in double perovskite Bi2FeMnO6 (BFMO) by using both the first-principles computation and experiment. Our ab initio calculations captured the complex exchange interactions between Fe and Mn sites which cause ferromagnetic (anti-parallel) spin alignment on these ions. The predicted magnetic moment qualitatively agrees well with Goodenough-Kanamori theory but our calculations reveal the importance of onsite (on both Mn and Co) correlations that should be accounted for using Hubbard model. These correlations open up insulating band gap providing the possibility for simultaneous existence of ferrimagnetic and FE ordering in BFMO. Initial modeling results disagreed with our XMCD spectra and measurements of magnetic moments of Fe and Mn ions which provided immediate feedback for improving our first-principle computation routines. Better match to experimental data could be achieved by accounting for complex interplay between the distortions and the disorder of the cation (Fe, Mn) sites as well as the magnetic structure. Improved accuracy of the calculations will enable better understanding and design of interfaced systems: recently, we used it to demonstrate dependence of net magnetization on strain in BFMO nanostructures which can be tested by varying substrate materials in XMCD and magnetization measurements.

Future Work

Theory: We will continue to use density functional theory (DFT) to advance our microscopic understanding of magneto-electric coupling mechanisms in multiferroic materials. In particular, we will use DFT to calculate the XMCD response as a function of strain and validate them by comparison with experiments. With our first-principles approach, we will perform ionic relaxation in BFMO and calculate ferroelectric moment using state-of-the-art Berry's phase approach. We will continue investigating the mechanisms and optimal conditions for coupling FE/AFM/FM orders across the interfaces. Depending on the mismatch of the lattice parameters across the interface, we will employ either a coherent DFT framework or incoherent molecular dynamical simulations to study the interface structure-function relationship. Finally, we will study the multiferroic functionality in composites within our effective model aimed at finding design principles for raising the figure of merit.

Synthesis: We will use laser molecular beam epitaxy to synthesize both 3D multiferroic architectures with desired structural properties. Vertically aligned epitaxial BiFeO3:CoFe2O4, BaTiO3:CoFe2O4 and BiFeO3/La(1-x)Sr(x)MnO3 films with appropriate volume ratios as determined by the theoretical modeling will be extensively investigated. To establish the baseline, we will also grow

and study the layered structures and single layer films, e.g. BFMO. To systematically manipulate the strain state in the nanocompistes, we will further vary the film thickness and substrate materials.

Characterization: The films synthesized will be systematically studied not only by the conventional characterization techniques but also by advanced probing tools such as neutron diffraction and magnetoelectric measurements at high magnetic fields. We will apply time-integrated and time-resolved optical tools, covering the terahertz (THz) through the x-ray frequencies, to investigate the mechanisms underlying magnetoelectric functionality in these materials. We will also perform static x-ray magnetic circular/linear dichroism (XMCD/XMLD) experiments in order to directly probe spin alignment on particular magnetic ions as a function of composition.

Conclusion

We expect to identify an optimal geometry of 3D composites and develop initial concepts underpinning their functionality. Continuous iterations through co-design loop will result in better understanding of the ME functionality in 3D structures. We anticipate to delivering a complete theoretical suite for reliable prediction of MF functionality in any possible 3D geometry and materials combination. When combined with refined 3D synthetic and characterization tools, we expect to develop a complete set of capabilities for accelerated materials discovery that will be applicable to a broad class of correlated electron materials, well beyond the MF heterostructures.

Publications

Ahmed, , La-o-Vorakiat, Salim, Y. M. Lam, E. E. M. Chia, and Zhu. Optical properties of organometallic perovskite: An ab initio study using relativistic GW correction and Bethe-Salpeter equation. 2014. EPL. 108 (6).

Ahmed, T., A. Chen, D. A . Yarotski, S. A. Trugman, Q. Jia, and J. X, Zhu. Magnetic, Electronic and Optical Properties of Double Perovskite Bi2FeMnO6. To appear in Scientific Reports.

Ahmed, T., A. Chen, Q. X. Jia, D. A . Yarotski, and J. X . Zhu. Site dislocation between Fe and Mn sites in double perovskite Bi2FeMnO6: A theoretical explanation for XMCD anomaly. Physical Review Letters.

Ahmed, T., Q. X. Jia, M. R. Fitzsimmons, Z. Bi, S. Rudin, and J. X. Zhu. First-principles Study of Magnetic Coupling at the BiFeO3-La(1-x)SrxMnO3 Hetero-structured Interface. Physical Review B.

Atkins, R., M. Dolgos, A. Fiedler, C. Grosse, S. Fischer, S. P. Rudin, and D. C. Johnson. Synthesis and Systematic Trends in Structure and Electrical Properties of [(SnSe)1.15]m(VSe2)1, m = 1, 2, 3, and 4. 2014. Chemistry of Materials. 26: 2862.

Chen, , Weigand, Bi, Zhang, Lu, Dowden, J. L. MacManus-Driscoll, Wang, and Jia. Evolution of microstructure, strain and physical properties in oxide nanocomposite films. 2014. SCIENTIFIC REPORTS. 4.

Chen, A.. Role of vertical strain and microstructure on magnetoresistance in vertically aligned nanocomposites. Invited presentation at Materials Science &Technology 2014. (Pittsburgh, PA, October 12-16, 2014).

Chen, A. P., W. Zhang, J. L. MacManus-Driscoll, H. Wang, M. R. Fitzsimmons, and Q. X. Jia. Role of interfaces on competing interactions of ferroic films. Invited presentation at 2015 MRS Fall meeting. (Boston, Massachusetts, 29 Nov - 4 Dec, 2015).

Chikara, S., J. Singleton, N. Lee, H. Y. Choi, Y. J. Choi, and V. S. Zapf. Electric polarization observed in single crystals of multiferroic Lu2CoMnO6. Applied Physics Letters.

Choi, E. M., T. Fix, A. Kursumovic, C. J. Kinane, D. Arene, S. L. Sahonta, Z. Bi, J. Xiong, L. Yan, J. S. Lee, H. Wang, S. Lamgridge, Y. M. Kim, A. Y. Borisevich, I. MacLaren, Q. M. Ramasse, M. G. Blamire, Q. X. Jia, and J. L. MacManus-Driscoll. Room temperature ferrimagnetism and ferroelectricity in strained, thin films of BiFe0.5Mn0.5O3. 2014. Advanced Functional Materials. 24 (47): 7478.

Dowden, P. C., Z. Bi, and Q. X. Jia. Method for controlling energy density for reliable pulsed laser deposition of thin films. 2014. Rev. Sci. Instrum.. 85: 025111.

Fang, , Tai, Deng, Wu, Ding, J. u. n. Sun, and E. K. H. Salje. Fe-vacancy ordering in superconducting K1-xFe2-ySe2: first-principles calculations and Monte Carlo simulations. 2015. SUPERCONDUCTOR SCIENCE & TECHNOLOGY. 28 (9).

Haeusler, , Atkins, Falmbigl, S. P. Rudin, Neumann, and D. C. Johnson. Insights from STEM and NBED studies into the local structure and growth mechanism of misfit layered compounds prepared using modulated reactants. 2015. ZEITSCHRIFT FUR KRISTALLOGRAPHIE. 230 (1): 45.

Haeusler, , Atkins, Falmbigl, S. P. Rudin, Neumann, and D. C. Johnson. Insights from STEM and NBED studies into the local structure and growth mechanism of misfit layered compounds prepared using modulated reactants. 2015. ZEITSCHRIFT FUR KRISTALLOGRAPHIE. 230 (1): 45.

Jain, , Wang, Roldan, Glavic, Lauter, Urban, Bi, Ahmed, Zhu, Varela, Q. X. Jia, and M. R. Fitzsimmons. Synthetic

magnetoelectric coupling in a nanocomposite multiferroic. 2015. SCIENTIFIC REPORTS. 5.

Jia, Q. X.. Effect of Interfaces on Ferroic Properties of Composite Films. Invited presentation at International Symp. on Emerging Multifunctional & Bio-Directed Mater.. (San Antonio, TX, 10 - 111, Oct.).

Kogoj, J., L. Vidmar, M. Mierzejewski, S. A. Trugman, and J. Bonca. Thermalization after photoexcitation from the perspective of optical spectroscopy. Physical Review Letters.

Lee, , S. A. Trugman, C. L. Zhang, Talbayev, X. S. Xu, S. -. Cheong, D. A. Yarotski, A. J. Taylor, and R. P. Prasankumar. The influence of charge and magnetic order on polaron and acoustic phonon dynamics in LuFe2O4. 2015. APPLIED PHYSICS LETTERS. 107 (4).

Lee, , Sangle, Lu, Chen, Zhang, J. S. Lee, Wang, Jia, and J. L. MacManus-Driscoll. Novel Electroforming-Free Nanoscaffold Memristor with Very High Uniformity, Tunability, and Density. 2014. ADVANCED MATERIALS. 26 (36): 6284.

Li, , R. u. n. Zhao, Tang, Chen, Zhang, X. i. n. Lu, Wang, and H. a. o. Yang. Vertical-Interface-Manipulated Conduction Behavior in Nanocomposite Oxide Thin Films. 2014. ACS APPLIED MATERIALS & INTERFACES. 6 (8): 5356.

Li, , W. e. i. Zhang, L. e. Wang, Gu, Chen, R. u. n. Zhao, Y. a. n. Liang, Guo, Tang, Wang, Jin, Wang, and H. a. o. Yang. Vertical Interface Induced Dielectric Relaxation in Nanocomposite (BaTiO3)(1-x):(Sm2O3)(x) Thin Films. 2015. SCIENTIFIC REPORTS. 5.

Li, B. o., Pan, Tai, M. J. Graf, Zhu, K. E. Bassler, and C. S. Ting. Unified description of superconducting pairing symmetry in electron-doped Fe-based-122 compounds. 2015. PHYSICAL REVIEW B. 91 (22).

Mun, E. D., Chern, Pardo, Rivadulla, Sinclair, H. D. Zhou, V. S. Zapf, and C. D. Batista. Magnetic Field Induced Transition in Vanadium Spinels. 2014. PHYSICAL REVIEW LETTERS. 112 (1).

Mun, E., D. F. Weickert, J. Kim, B. L. Scott, C. Miclea, R. Movshovich, J. Wilcox, J. Manson, and V. S. Zapf. Partially disordered antiferromagnetism and multiferroic behavior in a frustrated Ising system, CoCl2-2SC(NH2)2. To appear in Physical Review B.

Pan, , Li, Tai, M. J. Graf, Zhu, and C. S. Ting. Evolution of quasiparticle states with and without a Zn impurity in doped 122 iron pnictides. 2014. PHYSICAL REVIEW B. 90 (13).

Rudin, S.. Magnetic Structure, Cation Disorder, Octahedral Rotations, and Antiferroelectric Distortions in Bi2FeMnO6. Invited presentation at Electronic Structure Approaches and Applications to Quantum Matter. (Santa Fe, 20 May, 2015).

Rudin, S. P., and D. C. Johnson. Density functional theory calculations of the turbostratically disordered compound [(SnSe)(1+y)](m)(VSe2)(n). 2015. PHYSICAL REVIEW B. 91 (14): 144203.

Sandberg, R., B. Mafarland, R. Prasankumar, G. Rodriguez, A. Chen, Q. X. Jia, A. Taylor, D. Yarotski, A. Ried, and H. Ohldag. Probing multiferroic materials with soft X-ray spectroscopy and imaging. Invited presentation at SLAC User Workshop. (Menlo Park, CA, Oct. 10, 2014).

Sheu, Y. M., S. A. Trugman, L. Yan, J. Qi, Q. X. Jia, and A. J. Taylor. Polaronic transport induced by competing interfacial magnetic order in a La0.7Ca0.3MnO3/BiFeO3 heterostructure. 2014. Phys. Rev. X. 4: 021001.

Sheu, Y. M., S. A. Trugman, L. Yan, Q. X. Jia, A. J. Taylor, and R. P. Prasankumar. Ultrafast optical manipulation of magnetoelectric coupling at a multiferroic interface. 2014. Nature Communications. 5: 5832.

Sing, S., J. H. Haraldsen, J. Xiong, E. M. Choi, P. Lu, D. Yi, X. D. Wen, J. Liu, H. Wang, Z. Bi, P. Yu, M. R. Fitzsimmons, J. L. MacManus-Driscoll, R. Ramesh, A. V. Balatsky, J. X. Zhu, and Q. X. Jia. Induced magnetization in La0.7Sr0.3MnO3/BiFeO3 superlattices. 2014. Phys. Rev. Lett.. 113: 047204.

Tai, , C. -. J. Wang, M. J. Graf, Zhu, and C. S. Ting. Emergent topological mirror insulator in t(2g)-orbital systems. 2015. PHYSICAL REVIEW B. 91 (4): 041111.

Tai, Y. Y., H. Choi, T. Ahmed, C. S. Ting, and J. X. Zhu. Edge states and local electronic structure around an adsorbed impurity in a topological superconductor. Nature Physics.

Talbayev, , Lee, S. A. Trugman, C. L. Zhang, S. -. Cheong, R. D. Averitt, A. J. Taylor, and R. P. Prasankumar. Spin-dependent polaron formation dynamics in Eu0.75Y0.25MnO3 probed by femtosecond pump-probe spectroscopy. 2015. PHYSICAL REVIEW B. 91 (6).

Talbayev, , Lee, S. A. Trugman, C. L. Zhang, S. -. Cheong, R. D. Averitt, A. J. Taylor, and R. P. Prasankumar. Spin-dependent polaron formation dynamics in Eu0.75Y0.25MnO3 probed by femtosecond pump-probe spectroscopy. 2015. PHYSICAL REVIEW B. 91 (6).

Trugman, S. A .. High temperature transport in the Holstein model. Invited presentation at Conference on Dynamics of Quantum Many Body Systems far from Equilibrium. (Krvavec, Slovenija, 15 December, 2014).

Xiong, J., V. Matias, B. W. Tao, Y. R. Li, and Q. X. Jia. Ferroelectric and ferromagnetic properties if epitaxial

BiFeO3-BiMnO3 films on ion-beam-assisted deposited TiN buffered flexible Hastelloy. 2014. J. Appl. Phys.. 115: 17D913.

Zapf, V.. Multiferroic behavior investigated at high magnetic fields: CdV2O4. Invited presentation at Telluride Workshop on oxide materials. (Telluride, CO, June, 2015).

Zhang, , Chen, J. i. e. Jian, Zhu, L. i. Chen, Lu, Jia, J. L. MacManus-Driscoll, Zhang, and Wang. Strong perpendicular exchange bias in epitaxial La0.7Sr0.3MnO3:BiFeO3 nanocomposite films through vertical interfacial coupling. 2015. NANOSCALE. 7 (33): 13808.

Zhang, , Li, Lu, Fan, Su, Khatkhatay, Chen, Jia, Zhang, J. L. MacManus-Driscoll, and Wang. Perpendicular Exchange-Biased Magnetotransport at the Vertical Heterointerfaces in La0.7Sr0.3MnO3:NiO Nanocomposites. 2015. ACS APPLIED MATERIALS & INTERFACES. 7 (39): 21646.

Zhang, W., A. Chen, Z. Bi, Q. X. Jia, J. L. MacManus-Driscoll, and H. Wang. Interfacial coupling in heteroepitaxial vertically aligned nanocomposite thin films: from lateral to vertical control. 2014. Curr. Opin. Solid State Mater. Sci. . 18: 6.

Zhang, W., J. Jian, A. Chen, L. Jiao, F. Khatkhatay, L. Li, F. Chu, Q. X. Jia, J. L. MacManus-Driscoll, and H. Wang. Strain relaxation and enhanced perpendicular magnetic anisotropy in BiFeO3:CoFe2O4 vertically aligned nanocomposite thin films. 2014. Appl. Phys. Lett.. 104: 062402.

Zhao, , Tai, and C. S. Ting. Phase diagram of the isovalent phosphorous-substituted 122-type iron pnictides. 2015. PHYSICAL REVIEW B. 91 (20): 205110.

Exploring Mechanisms of Catalysis on Plutonium Surfaces (U)

Marianne P. Wilkerson
20140051DR

Introduction

Characterization of the molecular rearrangements that occur on metal surfaces can provide insight into important catalytic processes. Uncovering the role a metal surface plays in catalyzing molecular transformations is critical to obtaining a thorough understanding of its performance in a given environment. High-resolution imaging (Atomic Force Microscopy/Scanning Tunneling Microscopy), Secondary Ionization Mass Spectrometry, and Fourier Transform Infrared Absorption Spectroscopy are being applied to characterize molecular and materials states on Pu surfaces, providing unprecedented information about their roles in materials/environment interactions. We are using electronic structure and atomistic methods to model reaction mechanisms and thermodynamic stability of various materials. Furthermore, a comprehensive organometallic chemistry study is being conducted to provide complementary information about metal-molecule binding and factors controlling reactivity.

Benefit to National Security Missions

The response of Pu materials to molecular environments is a key component of laboratory missions related to Stockpile Stewardship. Furthermore, the development of the materials science and chemistry of the actinides, particularly Pu, will advance and strengthen our position as the national Plutonium Center of Excellence.

Progress

The fiscal year was marked by several major project accomplishments. A series of 7 at.% Ga delta-stabilized plutonium samples, specifically designed to accommodate each analytical system, have been cut and prepared in PF-4. All experimental systems are advancing towards plutonium readiness, while others are awaiting receipt of the first Pu samples. The modeling efforts have made substantial gains as well, with the advancement of DFT calculations that explore the role of defects in the oxide layer and the interaction of those defects with bound intermediates.

Experiments on surrogate materials with the FTIR reflectance accessory revealed that Polarization Modulation Infrared Refection Adsorption Spectroscopy (PM-IRRAS) is preferred to properly investigate the surface chemistry of actinide surfaces. The system is now fully configured to run in this mode. A plutonium readiness review with the Radiation Protection group was completed in June, and the instrument is undergoing final testing with surrogates prior to accepting the first plutonium sample, scheduled for the month of July.

Various aspects of the ultra-high vacuum scanning tunneling microscopy (UHV-STM) have been tested, modified, repaired, or replaced as needed. A service technician is scheduled to visit LANL the week of June 22nd to address a lingering noise problem. Once the final issues have been addressed, initial experiments on surrogates will begin in the 3rd quarter of FY15 and will move quickly on to thin film Pu oxides and, ultimately, plutonium metal.

Final facility tie-in of the glovebox that supports the Atomic Force Microscopy (AFM) is scheduled for completion in June. The glovebox is now leak tight, and boasts an oxygen and water concentration measured at the ppm level. During the final preparation phase, extensive analysis of surrogate films have aided in the selection of the best AFM tip for plutonium. The first ever AFM images of Pu metal surfaces will be analyzed in FY15 and published the following year.

Experiments with the Time-of-Flight Secondary Ion Mass Spectrometer have identified several interesting surface species following gas exposures on plutonium metal samples. As this work marks the first known application of ToF-SIMS to a plutonium metal surface, time has been spent developing peak identification protocols. Isotopically labeled gas exposures will commence this year to

compliment the infrared work.

The goal of the synthetic chemistry work is to develop molecular complexes that exhibit the relevant structural characteristics, react them with small molecules, and determine the molecular transformations that occur using molecular and spectroscopic techniques. To this end, the synthetic chemistry work has successfully prepared organometallic cerium complexes and exposed them to gases of interest. Solid state crystal structures of these molecules have been obtained to confirm atom connectivity and infrared (IR) spectra have been recorded. These IR spectra show good agreement to the theoretical spectra provided by T-1. Current experiments are focused on translating both the experimental and theoretical IR spectroscopy to well defined metallic surfaces and translating the molecular synthesis to plutonium to determine the effect on the IR stretching frequency for further spectroscopic comparison.

The theory and modeling team has made progress in understanding the structure of the Pu oxide surface as well as its interactions with molecules of interest. In particular, we have identified that high concentrations of oxygen monovacancies are thermodynamically stable under UHV experimental condition on the <110> surface, and must be considered as possible actives sites for catalysis. Vibrational calculations of various moieties are complete, and will be compared with IR spectroscopy measurements. We are working to explore other possible reaction sites/surfaces including Pu6Fe, <111> PuO2 surfaces with and without defects, Pu2O3 surfaces, and Fe/C defected PuO2 <110> surfaces. Identification of these sites is a key step for making further progress in understanding surface reactions. Finally, great progress has been made in using Density Functional Theory (DFT) modeling to interface synthesized molecular structures with bound intermediates to their spectroscopic signatures for understanding relevant reactions on molecular sites. Synthetic cerium compounds and their IR spectra have been identified and anticipated shifts when moving to Pu are in the process of being determined. Such findings and their agreements with experimental spectra will aid in the interpretation of future data and give confidence in DFT predictions for molecular site/adsorbate interactions.

Future Work

The Scanning Tunneling Microscope (STM) system will commissioned for plutonium during FY15. The first ever STM images of Pu metal surfaces will be acquired. An additional gas manifold system will be constructed and integrated into the system for gas exposure experiments.

Building on Atomic Force Microscope (AFM) measurements of UO2 and U3O8 PAD films, images of PuO2 PAD films will be completed, and additional Pu coupons will be imaged, both before and subsequent to various exposures.

Surface measurements on Pu6Fe material will be conducted using the Secondary Ion Mass Spectrometry (SIMS). Experiments will include exposures to isotopically labelled gases to identify dynamic reaction products.

Polarization Modulation Infrared Reflection Absorption Spectroscopy Synthesis work will be accelerated and reactions to prove the ability of cerium to facilitate the reverse water-gas shift reaction will be carried out to help determine the mechanism of this reaction. New complexes and intermediates will be synthesized and reaction with appropriate gases will be performed.

Modeling work will focus on further validation of modeling methods via the use of all-electron based codes that include relativistic effects and hybrid exchange-correlation functionals. Vibrational spectra will be calculated which will allow our findings to be directly compared with experimental data, aiding in model validation and experimental interpretation of data. Other surface defect structures (step edges, kinks, etc.) will also be considered.

Conclusion

We will gain a deeper understanding of the fundamental connections that exist between the composition, valence state and structural properties of a given defect center and its propensity for catalysis through the following areas:

- Reaction mechanisms of Pu-catalyzed molecular transformations.
- Thermodynamic models
- High-resolution imaging of Pu surfaces.
- Surrogate Pu coordination complexes with hitherto unexplored properties.

Publications

Beaux, M. F., T. Durakiewicz, K. S. Graham, J. N. Mitchell, S. Richmond, E. D. Bauer, D. P. Moore, F. J. Freibert, P. H. Tobash, and J. A. Kennison. Electronic structure of polycrystalline d-Pu metal: a review of photoemission spectra interpretations. 2014. In Pu Futures - The 'Science' 2014. (Las Vegas, NV, 7-12 Sept. 2014). , p. CMP.9. Las Vegas NV: American Nuclear Society.

Hernandez, S. C., D. S. Schwartz, C. D. Taylor, and A. K. Ray. Ab initio study of Ga-Stabilitzed d-Pu bulk and surfaces. 2014. In Pu Futures - The 'Science' 2014. (Las Vegas, NV, 7-12 Sept. 2014). , p. M&MS.15. Las Vegas NV: American Nuclear Society.

Hernandez, S. C., D. S. Schwartz, C. D. Taylor, and A. K. Ray. Ab initio study of gallium stabilized d-plutonium alloys and hydrogen-vacancy complexes. 2014. Journal of Physics: Condensed Matter. 26 (3): 235501/1.

Hernandez, S. C., M. P. Wilkerson, and M. N. Huda. Understanding oxygen adsorption on 9.375 at.% Ga-stabilized delta-Pu(111) surface: A DFT study. 2015. Journal of Alloys and Compounds. 653: 411.

Hernandez, S. C., T. J. Venhaus, and M. N. Huda. Atomic oxygen adsorption on 3.125 at.% Ga stabilized delta-Pu(111) surface. 2015. Journal of Alloys and Compounds. 643: 253.

Hernandez, S. C., and C. D. Taylor. Density functional theory studies on atomic adsorptions on Ga stabilized d-Pu (111) surfaces. 2014. In Materials Research Society 2014 Spring Meeting and Exhibit. (San Franscisco, CA, 21-25 April 2014). , p. S6.05. San Franscisco CA: Materials Research Society.

Holby, E. F.. Oxygen vacancies in PuO2 (110) surfaces via density functional theory. 2014. In Pu Futures - The 'Science' 2014. (Las Vegas, NV, 7-12 Sept. 2014). , p. III. Las Vegas NV: American Nuclear Society.

Pugmire, A. L., C. H. Booth, T. J. Venhaus, and D. L. Pugmire. Structural insights into the oxide formed during the room temperature corrosion of Plutonium. 2014. In Pu Futures - The 'Science' 2014. (Las Vegas, NV, 7-12 Sept. 2014). , p. SS&C.7. Las Vegas NV: American Nuclear Society.

Richmond, S., P. H. Tobash, and D. Schwartz. The synthesis of Pu6Fe from plutonium deuteride and iron powders. 2014. In Pu Futures - The 'Science' 2014. (Las Vegas, NV, 7-12 Sept. 2014). , p. M&MS.13. Las Vegas NV: American Nuclear Society.

Schwartz, D. S., S. Richmond, C. D. Taylor, A. I. Smith, and A. L. Pugmire. Hydrogen effects in Pu-Ga alloys: defects and thermodynamics. 2014. In Pu Futures - The 'Science' 2014. (Las Vegas, NV, 7-12 Sept. 2014). , p. II. Las Vegas NV: American Nuclear Society.

Smith, A. I., K. L. Page, S. Richmond, J. Siewenie, T. A. Saleh, M. Ramos, and D. S. Schwartz. Local structural investigation of the Pu-7at%Ga using neutron total scattering. 2014. In Pu Futures - The 'Science' 2014. (Las Vegas, NV, 7-12 Sept. 2014). , p. M&MS.7. Las Vegas NV: American Nuclear Society.

Sutton, A. D., and M. P. Wilkerson. Catalysis with cerium organometallic complexes. 2014. In Pu Futures - The 'Science' 2014. (Las Vegas, NV, 7-12 September 2014). , p. CCCC.11. Las Vegas NV: American Nuclear Society.

Venhaus, T. J., and D. P. Moore. Analysis of Pu surfaces with time-of-flight SIMS. 2014. In Pu Futures - The 'Science' 2014. (Las Vegas, NV, 7-12 Sept. 2014). , p. SS&C.8. Las Vegas NV: American Nuclear Society.

Wagner, G. L., M. T. Paffett, K. D. Rector, B. L. Scott, and M. P. Wilkerson. Characterization of products from hydrolysis of UF6. 2014. In Pu Futures - The 'Science' 2014. (Las Vegas, NV, 7-12 Sept. 2014). , p. CCCC.4. Las Vegas NV: American Nuclear Society.

Mesoscale Materials Science of Ductile Damage in 4 Dimensions: Towards the Computational Design of Damage-Tolerant Materials

Ricardo A. Lebensohn
20140114DR

Introduction

The failure of structural materials has a significant impact on vast sectors of the economy, including energy, transportation and defense. The costs arise both from rare catastrophic events to the more mundane expenses of over-engineering or preventive part replacement. Consequently, there has been enormous effort in the past to gain fundamental understanding of failure mechanisms and thus enable the development of more reliable components.

Most structural materials are polycrystalline aggregates, in which the constituent crystals are irregular in shape, have anisotropic mechanical properties, and contain a variety of defects. The deformation of these heterogeneous materials results in very dynamic and complicated responses. While centuries of metallurgical experience and post-failure analysis have given us insight into general aspects relating material processing and performance, our failure models remain empirically calibrated because we have yet to achieve a thorough understanding of the controlling processes at the scale of the materials' heterogeneity, i.e. the mesoscale.

This project addresses one of the most difficult outstanding problems in Materials Science: the development of a predictive, microstructure-sensitive ductile failure model. This will be achieved by integrating time-resolved three-dimensional (3-D) microstructural characterization of polycrystalline materials with state-of-the-art modeling and advanced data analysis tools, to ensure maximal and optimal data extraction. Increasingly complex model materials will be used to develop this integrated capability, which will be then tested and applied to the predictive design of damage-tolerant microstructures.

We intend to draw upon existing High Energy Diffraction Microscopy (HEDM) techniques, integrating and combining them with appropriate modeling and data analysis formulations, to discover relationships between microstructure and ductile damage in selectively prepared polycrystalline aggregates. We will follow the volumetric deformation through time, i.e. in four dimensions. The proposed integration will allow us to achieve the full inversion of this 4-D data, and extract the controlling aspects of ductile damage.

Benefit to National Security Missions

DOE's Office of Basic Energy Sciences (OBES) has recently highlighted the area of mesoscale science as the next grand-challenge in Materials Science. The two top capability gaps for this were defined as the seamless integration of theory, modeling and simulation with synthesis and characterization, and the dynamic characterization of mesoscale phenomena. This project directly addresses both topics. Success of this paradigm will establish LANL's leadership in this growing initiative, expected to be central to future DOE programs.

The development of improved predictive damage models that incorporate mesostructural sensitivity will be of interest to several Defense Programs (DP) stakeholders. Extension to dynamic regimes will especially extend its application to DP programs. The MaRIE campaigns will be a beneficiary of experience in the development of in-situ diffraction and associated data processing. Application of the integrated approach to material development should attract interest from advanced manufacturing initiatives.

Progress

Experimental

- Using powder metallurgy, we have manufactured Cu-W and Cu-Nb plates with fully dense structure [1].
- We are executing a General User Proposal (GUP) in Advanced Photon Source (APS) and requested six days for the fall 2015 cycle.

- We have submitted and executed a beam-time proposal in Cornell High Energy Synchrotron Source (CHESS) to collect tomographic, nf- and ff-HEDM data in Cu-W (December 2014). We are scheduled to perform similar measurements on Cu-Nb samples in July 2015.

Data Analysis

- We demonstrated the feasibility and accomplished the registration of orientation field and tomography in a post-shocked Cu sample [9].

- Compressive sensing techniques were used to solve efficiently the inverse lattice orientation problem in far-field high-energy diffraction microscopy. We are extending this approach to solve both orientation and spatial grain information [7].

- C++/MPI framework is in development to estimate model parameters directly from measurements. Strategies to compute reduced order models are being implemented, yielding encouraging results in terms of small approximation error and computation time [8].

- 100TB data storage was acquired, and we created the "meso4d" Unix group in CCS's cluster Darwin to store experimental raw data, install and run data reduction and simulation codes. All data reduction codes IceNine (nf-HEDM), HEXRD (ff-HEDM), FABLE (box-beam HEDM) and Recon (tomo) have being successfully installed in Darwin.

Modelling

- The feasibility of using the viscoplastic FFT model (VPFFT) with direct input from HEDM data [2] was demonstrated.

- The dilatational viscoplastic FFT model (DVPFFT) was extended to consider void growth in polycrystalline materials and applied to the interpretation of microstructural effects on porosity evolution of shocked Cu.

- A moment-based method for calculating interface normals in voxelized 3D images was developed. The normal determination is required to investigate microstructural effects on void nucleation [3]. Simulations of existing HEDM experiments in post-shocked Cu are in progress [9].

- The FFT-based formulation was extended to consider microstructural effects on stress concentration promoting crack propagation [4, 5], and we have implemented a non-local EVPFFT formulation [6].

Future Work

HEDM measurements on Cu-W samples performed during FY15 are being analyzed and modeled and new experiments on pure Cu and Cu-Nb will be conducted in APS and CHESS, respectively, to measure damage evolution in polycrystalline aggregates synthesized to maximize the extraction of relevant microstructural information. The measured microstructures are being used as input for our improved spectral model, whose predictions and underlying physics will be tested against the measured damage evolution.

The major bottleneck of the proposed work, which lies on the difficulty in inverting the low-quality diffraction data arising from heavily deformed and damaged materials, will continue to be addressed. All four proposed strategies we be continued: 1) collecting the synchrotron data simultaneously in tomography, orientation and stress mapping modes; 2) using correlations between multiple snapshots during the deformation process; 3) employing direct simulations; and 4) using compressive sensing and hierarchical sparse representations.

We will capture microstructural and micromechanical information correlated with ductile damage, obtaining HEDM snapshots during quasi-static tensile tests performed on notched bars. The measurements will be performed on a volume of ~0.5 mm3 in the notch region of the samples. In the third year, we will study polycrystalline Cu-Nb composites (in CHESS), and we will repeat HEDM measurements in pure Cu (in APS).

3-D tomographic reconstructions will allow us to detect void formation at early stages of deformation. The grain orientation data will inform us of plastic deformation at the grain scale, in particular near voids, while the local stress mapping will provide information on stress concentrations, which presumably drive void nucleation, and stress relaxations once voids have formed.

Conclusion

Our overarching goal is to be able to formulate a quantitative, microstructure-sensitive, experimentally-validated mesoscale model of ductile damage, paving the way towards a truly predictive failure model. This will also result in the advancement of novel experimental and analytical techniques that can then be extended and applied to other problems of strategic interest for the Laboratory and the Nation.

Publications

Anglin, B. S., R. A. Lebensohn, and A. D. Rollett. Validation of a numerical method based on Fast Fourier Transforms for heterogeneous thermoelastic materials by comparison with analytical solutions. 2014.

Computational Materials Science. 87: 209.

Bingert, J. F., R. M. Suter, J. Lind, S. F. Li, R. Pokharel, and C. P. Trujillo. High-Energy diffraction microscopy characterization of spall damage. 2014. In Dynamic Behavior of Materials, Volume 1. , p. 397. : Springer International Publishing.

Chen, C. F., D. Dombrowski, R. A. Lebensohn, B. Clausen, R. Forsyth, and R. Pokharel. Processing and consolidation of copper for mesoscale materials science of ductile damage in four dimensions. 2014. In 2014 World Congress on Powder Metallurgy & Particulate Materials (PM 2014) . (Orlando, FL, 18-22 May 2014). , p. 0946. Orlando, FL: APMI International.

Landecker, W., R. Chartrand, and S. DeDeo. Robust sparse coding and compressed sensing with the difference Map. 2014. In European Conference on Computer Vision. (Zurich, 6-12 September, 2014). Vol. 8691, p. 315. Zurich: Springer International Publishing Switzerland.

Lebensohn, R. A., J. P. Escobedo, E. K. Cerreta, Dennis-Koller, C. A. Bronkhorst, and J. F. Bingert. Modeling void growth in polycrystalline materials. 2013. Acta Materialia. 61 (18): 6918.

Lebensohn, R. A., and A. Needleman. Numerical implementation of non-local polycrystal plasticity using Fast Fourier Transforms. Journal of the Mechanics and Physics of Solids.

Lebensohn, R. A., and R. Pokharel. Interpretation of microstructural effects on porosity evolution using a combined dilatational/crystal plasticity computational approach. 2014. Journal of the Minerals, Metals and Materials Society (JOM). 66 (3): 437.

Lieberman, E., A. D. Rollett, R. A. Lebensohn, and E. M. Kober. Calculation of grain boundary normals directly from 3-D microstructural images. 2015. Modelling and Simulation in Materials Science and Engineering. 23: 035005.

Ozturk, T., C. Stein, R. Pokharel, C. Hefferan, H. Tucker, S. Jha, R. John, R. A. Lebensohn, P. Kenesei, R. M. Suter, and A. D. Rollett. Simulation domain size requirements for elastic response of 3-D polycrystalline materials. To appear in Modelling and Simulation in Materials Science and Engineering.

Pokharel, R., J. Lind, A. K. Kanjarla, R. A. Lebensohn, S. F. Li, Kenesei, R. M. Suter, and A. D. Rollett. Polycrystal Plasticity: Comparison Between Grain-Scale Observations of Deformation and Simulations. 2014. Annual Review of Condensed Matter Physics. 5: 317.

Pokharel, R., J. Lind, S. F. Li, P. Kenesei, R. A. Lebensohn, R. M. Suter, and A. D. Rollett. In-situ observation of bulk 3-D microstructure evolution of polycrystalline copper using synchrotron radiation. 2015. International Journal of Plasticity. 67: 217.

Rovinelli, A., R. A. Lebensohn, and M. D. Sangid. Influence of microstructure variability on short crack growth behavior. 2015. Engineering Fracture Mechanics. 138: 265.

Sidky, E. Y., R. Chartrand, J. M. Boone , and X. Pan. Constrained TpV minimization for enhanced exploitation of gradient sparsity: application to CT image reconstruction. 2014. IEEE Journal of Translational Engineering in Health and Medicine. 2: 1.

Stein, C. A., A. Cerrone, T. Ozturk, S. Lee, P. Kenesei, H. Tucker, R. Pokharel, J. Lind, C. Hefferan, R. M. Suter, A. R. Ingraffea, and A. D. Rollett. Fatigue crack initiation, slip localization and twin boundaries in a nickel-based superalloy. 2014. Current Opinion in Solid State and Materials Science. 18 (4): 244.

Subedi, S., R. Pokharel, and A. D. Rollett. Orientation gradients in relation to grain boundaries at varying strain level and spatial resolution. 2015. Materials Science and Engineering A. 638: 348.

Aging in Delta Plutonium Alloys: A Fundamental Approach

Franz J. Freibert
20150057DR

Introduction

The mission of LANLs' Stockpile Stewardship program is to assess aging of our nation's stockpile materials. Both α-decay and thermodynamics are powerful physical processes in δ-Pu, with potential to couple strongly to phase changes in δ-Pu. Understanding the relative contributions of these processes is necessary to identify important aging mechanisms and accurately extrapolate induced effects on δ-Pu properties and performance over decades. This project, founded in Defects and Interfaces theme of the Materials for the Future Focus Area, is focused on the development of a mechanistic multi-scale understanding and control of defects and He bubbles, intrinsic and enhanced, across significant length, time and temperature scales of δ-Pu aging.

The goal is to quantify and understand the radiogenic changes in δ-Pu induced by the drivers of He ingrowth, defect accumulation and δ-Pu phase instability as determined by consensus of state-of-the-art experimental, computational and modeling tools. We will work to understand radiogenic defect accumulation as the mechanism of ambient temperature lattice swelling over a 1-2yr. transient ingrowth period; to control numbers and configurations of various defects separately from He bubbles and determine the influence radiogenic defects have on electronic and structural properties from nanometer to bulk spatial scale correlated with δ-Pu phase instability; and to understand defect accumulation interaction with He ingrowth as functions of experimental variables sufficient to induce and control void swelling.

This work will lay the fundamental groundwork for a Pu aging strategy by revealing the importance, rate, and scale of radiogenic changes in δ-Pu with exceptionally sensitive measurements, capable of showing aging effects in real time over a wide temperature range, with computational approaches describing defect structures and their relative stability. This approach supports unprecedented advances in understanding the physics of radiogenic damage process in δ-Pu exploring materials of controlled thermal histories, Ga compositions and alpha-decay dose.

Benefit to National Security Missions

The single most important mission of LANLs' Stockpile Stewardship program is to assess aging of our nation's stockpile; nonetheless, there are certain fundamental science questions that are not addressed in the program. Direct reuse of δ-Pu components expected to be in service for many decades requires that physics and engineering assessments have a firm scientific basis. Both a-decay and thermodynamics are powerful physical processes in δ-Pu, with potential to couple strongly to phase changes in δ-Pu. Understanding the relative contributions of these processes and their coupling are necessary to identify the important aging mechanisms and to accurately extrapolate induced effects on δ-Pu properties and performance margins over decadal time scales. Current physics-based lifetime estimates for US pits are approximately 100yr. These estimates were developed within a Quantifying Margins and Uncertainties (QMU) formalism for primary physics performance. However, the physics models for the QMU determinations do not contain fundamental physics and therefore are not predictive. The scientific work of understanding the effects of Pu aging must continue; otherwise today's solution to a Life Extension Program (LEP) problem might induce two or more unforeseen problems in the future.

Progress

The project team now includes a joint LANL/LBNL postdoctoral researcher in support of collaborations at the Stanford Linear Accelerator.

Local Structure and Nascent State Defect Evolution

The project team has made progress towards the goal of using extended X-ray absorption fine structure (EXAFS) spectroscopy, as a probe of the local structure around defect sites. A proposal has been written for synchrotron

time to conduct extended aging and annealing experiments, and was favorably received by the peer review committee. Anticipate receiving time to conduct these experiments on the next available scheduling period. To further leverage the unique capabilities of the synchrotron experiments, are redesigning sample holders to make resistivity measurements simultaneously with X-ray measurements. Design, prototyping, testing, and safety approval processes are moving forward on schedule. Anticipate being able to make a full-scale test of the system in advance of next synchrotron experiment. Progress has been made in the data analysis and modeling of EXAFS data. A new manuscript is in preparation, using previously unpublished data, detailing a method to quantify the amount of radiation damage present in a material relative to it's undamaged state. Expect this to be submitted to a peer-reviewed journal for publication by the end of the summer, and to use the developments therein to analyze the results of future experiments.

Thermally Activated Defect Evolution and Kinetic Behavior

Physical property measurements and characterization measurements have been made on delta Pu alloys. These include low temperature heat capacity and electrical resistivity to determine cryogenic aging behavior of the materials. This currently involves allowing the samples to accumulate damage at 4 K for a short time and then heating the samples in-situ in the cryostat at various rates in order to investigate the annealing out of damage. Preparing for the upcoming beamline experiments, new equipment is being assembled in order to perform isochronal annealing experiments. A high resolution resistance bridge and preamp will be used in conjunction with the physical property measurement system. System will be sent to Stanford for the fall beamline experiments in order to measure electrical resistivity while performing EXAFS. Furthermore, characterization of the samples before and after various treatments, using X-ray diffraction technique (phase identification, any changes in peak position, shape and intensity, identification of any additional phases and/or impurities).

Time Dependent/Defect Induced Thermodynamic Properties Changes

Using high-resolution, high temperature resonant ultrasound spectroscopy (RUS), measuring in real time at the 10^-7 level changes in the elastic moduli of unalloyed Pu and delta Pu alloys to understand the relative contributions of radiogenic daughter product ingrowth, phase stability, and radiation damage. With the ability to observe changes in elastic moduli to 100 parts per billion, observing changes in the elastic moduli of Pu and Pu-Ga alloys in real time. Changes due to ingrowth of radioactive decay products, the thermodynamic stability of Pu-Ga phases, and the introduction of radiation damage. By changing temperature (4K-700K), Ga concentration, sorting out the relative importance of the three effects, and the temperatures at which they are most active. Expect that at temperature ranges greater than 450K the face centered cubic of lattice Pu-Ga alloys can no longer support lattice damage and defect accumulation. This assertion is based upon thermal expansion measurements, which exhibit the final stages of radiogenic defect annihilation with temperature. Expect to validate this assertion within the next month of continuous elastic modulus monitoring at increasingly high temperatures.

Modeling and Theory

Development of new molecular dynamics models that account for known aging behavior of plutonium alloys. Revised an existing meso-scale (100-10,000 nm) model to account for radiation-damage-suppression terms from a reaction-rate model. Estimation of interstitial defect transport rates as a function of gallium concentration in plutonium alloys. Developed a global damage-to-defect-to-effects pathway mapping as a means to semi-quantify the balance between damage accumulation and damage annihilation, thus implement a means to discriminate the strength of the various radiogenic/phase stability mechanisms including daughter product ingrowth, irradiation damage and phase stability. Also, of concern is sustaining a LANL molecular dynamics modeling capability given limited resources, so training early career staff in radiation damage molecular dynamics modeling.

Future Work

The goal of this project is to quantify and understand the radiogenic changes in δ-Pu induced by the drivers of He ingrowth, defect accumulation and δ-Pu phase instability as determined by consensus of state-of-the-art experimental, computational and modeling tools. This project, founded in the Defects and Interfaces theme of the Materials for the Future Focus Area for LDRD Strategic Investment, is focused on the development of a mechanistic multi-scale understanding and control of inhomogeneities (i.e., defects and He bubbles), intrinsic and enhanced, across significant length, time and temperature scales that govern δ-Pu aging.

We propose implementing the following objectives by testing the associated hypotheses.

Objective #1: Understand radiogenic defect accumulation as the mechanism of ambient temperature lattice swelling over a 1-2yr. transient ingrowth period.

Hypothesis #1: The transport mechanisms observed dur-

ing ambient temperature initial swelling transient are the same mechanisms that eventually will lead to void swelling. Evolution and accumulation of ambient temperature defects are controlled by thermal vacancy migration and recovery processes occur as annealing of a defected state against defect stabilizing factors.

Objective #2: Understand defect accumulation interaction with He ingrowth as functions of experimental variables sufficient to induce and control void swelling.

Hypothesis #2: Point defect (i.e., interstitials, vacancies, clusters, etc.) structures anneal and thermally activate distinctly and separately from those associated with He (i.e., bubbles and voids). However, with experimentally provided vacancies to be absorbed by bubbles, void swelling can be induced in δ-Pu.

Conclusion

This project will form the basis for pit lifetime estimates that are physically sound and advance the understanding of fundamental radiogenic processes in δ-Pu. Because the focus of Defense Science Campaigns is the development of science impacting stockpile performance, an understanding of radiogenic effects in δ-Pu will impact experiment implementation. Because the focus of Directed Stockpile Work is the function of stockpile technology, aging indicators of performance impact could influence programmatic decisions on Pit Reuse and Lifetime Extension Programs and bound thermo-mechanical processing and supporting technological development for better definition of performance margins and uncertainties

Publications

Conradson, S. D., Bock, J. M. Castro, D. R. Conradson, L. E. Cox, Dmowski, D. E. Dooley, Egami, F. J. Espinosa-Faller, F. J. Freibert, A. J. Garcia-Adeva, N. J. Hess, E. K. Holmstroem, R. C. Howell, Katz, J. C. Lashley, R. J. Martinez, D. P. Moore, L. A. Morales, J. D. Olivas, R. A. Pereyra, Ramos, S. P. Rudin, and P. M. Villella. Nanoscale heterogeneity, premartensitic nucleation, and a new plutonium structure in metastable delta fcc Pu-Ga alloys. 2014. PHYSICAL REVIEW B. 89 (22).

Conradson, S. D., Bock, J. M. Castro, D. R. Conradson, L. E. Cox, Dmowski, D. E. Dooley, Egami, F. J. Espinosa-Faller, F. J. Freibert, A. J. Garcia-Adeva, N. J. Hess, Holmstroem, R. C. Howell, B. A. Katz, J. C. Lashley, R. J. Martinez, D. P. Moore, L. A. Morales, J. D. Olivas, R. A. Pereyra, Ramos, J. H. Terry, and P. M. Villella. Intrinsic Nanoscience of delta Pu-Ga Alloys: Local Structure and Speciation, Collective Behavior, Nanoscale Heterogeneity, and Aging Mechanisms. 2014. JOURNAL OF PHYSICAL CHEMISTRY C. 118 (16): 8541.

Freibert, F. J.. Current research into the self-irradiation effects of δ-phase Pu-Ga alloys . 2015. In NUCAR 2015 . (Mumbai, India, 9-13 February 2015). , p. 42. Mumbai: Bhabha Atomic Research Centre.

Freibert, F. J., J. N. Mitchell, D. S. Schwartz, and A. Migliori. Radiogenic-thermally coupled lifetimes for defects of aged δ-phase Pu-Ga alloys. 2015. In Plutonium Futures 2014, The Science. (Las Vegas, NV, 7-12 September 2014). , p. 220. La Grange Park, IL: American Nuclear Society.

Maiarov, B. A., J. B. Betts, F. J. Freibert, and A. Migliori. Real-time aging studies and some high temperature measurements of Ga-stabilized δ-phase 239Pu . 2015. FY15 Annual Report.

Mitchell, J. N., F. J. Freibert, T. E. Mitchell, and D. S. Schwartz. Aging and the δ → α′ transformation in Pu-Ga alloys . To appear in PTM: International Conference on Solid-Solid Phase Transformations in Inorganic Materials. (Whistler, Canada, 28 June-3 July 2015).

A New Approach to Mesoscale Functionality: Emergent Tunable Superlattices

Marc Janoschek
20150082DR

Introduction

The future availability of multifunctional materials is essential for the country to remain globally competitive and to ensure our energy and defense security. We must move beyond the current age of 'informed serendipity' towards a new era of 'materials by design' enabling controlled functionality that would allow rapid creation of novel applications required for an ever-changing world. Important technological functionalities are a consequence of mesoscale objects that respond to an external stimulus; e.g. magnetic memories and sensors are built upon the ability to switch mesoscale domains with magnetic fields. Here the mesoscale describes objects that have typical size in between the atomic-scale (i.e. sub-nanometer) and the macroscale (~1 mm). The critical step for mastering the designed functionality will be to achieve control of materials directly on this mesoscale. This is the potential promised by the recent discovery of a mesoscale object, a magnetic vortex called a "skyrmion" that emerges in magnetic materials . The stability of these topological objects makes them behave as particles when driven by external stimuli. Put differently, skyrmions are the new atoms of the mesoscale world. Similarly, just as different combination of atoms produce materials with different properties, different arrangements of skyrmions lead to distinct functionalities through coupling to electrical currents, magnetic and electrical fields, and temperature gradients. The resulting mesoscale architecture build from skyrmions is moreover clean, tunable, and movable, qualities that are vital for achieving enhanced macroscale functionality. This project will exploit the promising properties of those mesoscale magnetic whirls to find design principles for new functional materials, such as ultra-low-power high-density memory materials.

Benefit to National Security Missions

Our project responds specifically to the over-arching grand challenge of LANL's materials strategy. It addresses the priorities of realizing design principles towards controlled functionality and developing multi-functional materials to transform structural and functional performance, as well as tunable and emergent properties. In particular, the mesoscale magnetic whirls (so called "skyrmions") that will be investigated in this proposal hold great potential for multi-functional remote sensing, memory storage applications, and new computing technologies. In each case future devices using this technology will have ultra-low power consumption. Those new sensing, storage and computing devices are directly relevant for a new generation defense and prevention technologies, as well as improving information science and technology. The development of new mesoscale computational capabilities within this project that will be used to design these materials will additionally enable molecular dynamics calculations on the mesoscale, which is of broad relevance to the lab's material's strategy, and stockpile stewardship , weapon's research, and the study of matter at extremes in general. The mesoscale imaging and synthesis methods developed in this program will be crucial to study further functional materials directly on the mesoscale as required for stockpile stewardship, weapons research, and new materials for example required for the automotive, renewable energy, and defense industries.

Progress

Obtaining an improved understanding of the functionality that derives from magnetic mesoscale architecture based on skyrmion building blocks represents a multi-scale material science problem. Notably the competition of two or more atomic-scale magnetic interactions leads to the emergence of skyrmions, and controls their size and arrangement on the mesoscale. Those mesoscale parameters, in turn dictate the functionality of this assembly of skyrmions on the macroscale. In order to tackle this problem our team has tailored and improved our computing, synthesis and imaging capabilities to investigate these materials on each of those three length scales in the first year of this project. These capabilities

have been used to initiate a tightly integrated modeling-making-measuring loop that will be used through the entire project to create design principles for mesoscale magnetic mesoscale architecture based on skyrmions.

To make progress on the understanding of the atomic-scale interactions that control the emergence of magnetic mesoscale architecture based on skyrmions, we have carried out first-principle electronic structure calculations for prototypical skyrmion materials from which the strength of these interactions may be determined theoretically. Simultaneously, we have used neutron spectroscopy on the prototypical skyrmion material manganese silicide to measure the strength of these interactions in order to verify our calculations (manuscript submitted and under review at Phys. Rev. Lett.). This effort is currently applied to more materials.

We have also used and expanded a new algorithm developed at Los Alamos to predict the emergence of various arrangements of skyrmion architectures directly on the mesoscale based on atomic-scale interactions in a given material. This effort has already led to novel and exciting theoretical results that suggests a new mechanism for the emergence of skyrmion architecture based on a type of atomic-scale magnetic interactions that typically exist in rare earth and actinide materials, which are of interest to Los Alamos. In addition, this type of new magnetic calculation has shown that magnetic anisotropy that can be tuned either via crystal chemistry or external parameters such as strain, controls the symmetry of the arrangement of skyrmions in materials (manuscript published: S.-Z. Lin et al., Phys. Rev. B 91, 224407 (2015)). To test this experimentally, we have built a prototype of a strain cell that can be used in combination with small angle neutron scattering (SANS). SANS is able to probe the symmetry of a skyrmion assembly directly on the mesoscale. First tests with the strain cell prototype have shown how to improve it for experiments with skyrmion materials and a full-blown strain cell is currently being assembled for measurements in the second year of this project.

To address the challenge of functionality on the macroscale, we are currently testing real time imaging of skyrmion movement and rotation using transmission electron microscopy. The expected velocity of skyrmions under the application of external stimuli such as electrical current or temperature and magnetic field gradients is also simulated using so-called micro-magnetic calculations that have the skyrmion size as input parameters.

Finally, the first year has also been used to ramp up our efforts in synthesizing known skyrmion materials as well as candidate materials identified through theory. Currently, this efforts yields 1-2 materials every week, and has recently lead to the discovery of skyrmions in a so far unreported cobalt-zinc-manganese alloy at a temperature of 260 K (30 K below room temperature), making this an ideal material for applications (manuscript in preparation). Moreover, promising preliminary data on a related material with a different cobalt-zinc-manganese concentration suggests that skyrmions may even exist above room temperature. This new family of cobalt-zinc-manganese compounds thus represents a prototypical test bed for establishing design principles and functionality for skyrmion materials for the second year of our project.

In summary, our project is making outstanding progress in all efforts (modeling-making-measuring) on all the relevant length scales that define the properties of skyrmion architecture. Our team is therefore well setup for the second year of the project that will verify basic design principles on the choice of magnetic ions, local environments and overall crystallographic symmetry that yield skyrmion lattices for distinct functionalities.

Future Work

Understanding the functionality of skyrmions represents a multi-scale material science problem that stretches from the atomic- over the meso- to the macroscale. During the first year, our team has tailored and improved our computing, synthesis and imaging capabilities to investigate these skyrmion materials on each of those three length scales. Using these tools we have already identified a new class of skyrmion cobalt-zinc-manganese alloys that show skyrmions near room temperature and thus represents an optimal test-bed for establishing design principles and functionality for skyrmion materials for the second year of our project. In the second year, we will use these new materials to establish and test basic principles on choice of magnetic ions, local environments and overall crystallographic symmetry that yield skyrmion lattices with different sizes and symmetries that can be used for distinct functionalities. From our modeling efforts, we know that in particular magnetic anisotropy is a useful parameter to tune skrymions. Magnetic anisotropy can be tuned via strain. Using a strain cell for small angle neutron scattering that we have developed in the first year, we will test the design rules postulated by theory. Our new magnetic mesoscale algorithm developed at LANL has further suggests a new mechanism for the emergence of skyrmion architecture based on a type of atomic-scale magnetic interactions that typically exist in rare earth and actinide materials, which are of interest to Los Alamos. Our synthesis effort will therefore make materials to test these design rules for rare earth and actinide based skyrmions. Finally, we will use real time imaging of skyrmion movement and rotation

as function of external stimuli such as electrical current or temperature and magnetic field gradients using transmission electron microscopy. The results will be compared with micro-magnetic calculations that have the skyrmion size as input parameters.

Conclusion

In pursuing our objective, we will not only pioneer a new direction for material science at LANL, as well as for the international community, and respond directly to national, Laboratory and DOE priorities, but have the real potential of transforming the research on functional materials. Using our fully-integrated modelling-making-measuring loop we will find “design principles” for various mesoscale skyrmion architectures, which will immediately yield designed functionality via their unique properties. In particular, we expect to identify magnetic mesoscale architecture optimized for new memory or sensing applications.

Publications

Choi, H., S. Z. Lin, and J. X. Zhu. Density functional theory study of skyrmion pinning by atomic defects in MnSi. Physical Review B.

Kugler, M., G. Brandl, J. Waizner, M. Janoschek, R. Georgii, A. Bauer, K. Seemann, A. Rosch, C. Pfleiderer, P. Böni, and M. Garst. Band structure of helimagnons in MnSi resolved by inelastic neutron scattering. 2015. Physical Review Letters. 115 (9): 097203.

Lin, S. Z.. Generation of skyrmions by chopping magnetic chiral stripe domains with an electric current. Physical Review Letters.

Lin, S. Z., A. Saxena, and C. D. Batista. Skyrmion fractionalization and merons in chiral magnets with easy-plane anisotropy. 2015. Physical Review B. 91: 224407.

Lin, S. Z., and A. Saxena. Non-circular skyrmion and its anisotropic response in thin films of chiral magnets under tilted magnetic field. 2015. Physical Review B. 92: 180401.

Lin, S. Z., and A. Saxena. Dynamics of Dirac strings and monopole-like excitations in chiral magnets under a current drive. Physical Review Letters.

Lin, S. Z., and J. Zang. Skyrmion dynamics in chiral magnets. Skyrmion: the topological structures, magnetic and transport properties, and potential applications.

Lin, S. Z., and S. Hayami. Ginzburg-Landau theory for skyrmions in inversion-symmetric magnets with competing interaction. Physical Review B.

Ozawa, R., S. Hayami, K. Barros, G. W. Chern, Y. Motome, and C. D. Batista. Vortex crystals with chiral stripes in itinerant magnets. Physical Review Letters.

Saxena, A., and S. Z. Lin. Skyrmions in Functional Materials. To appear in Integrated Ferroelectrics.

Meso-Photonic Materials for Tailored Light-Matter Interactions

Houtong Chen
20150109DR

Introduction

Building on our internationally recognized expertise in metamaterials, we propose to tackle key science issues underpinning some "grand challenge" scale problems in photonics by developing transformational meso-photonic materials based on two core innovations: a meta-molecule concept and the integration of functional materials into meso-photonic structures. Meta-molecules are a collection of meta-atoms (sub-wavelength metal/dielectric resonators) with tailored internal interactions, enabling designer light coupling and propagation. Integration of functional materials (semiconductors, complex oxides, graphene, and transition metal dichalcogenides) results in tunable and reconfigurable photonic functionalities, enables novel optoelectronic architectures, and provides a means to exploit the greatly enhanced light-matter interactions to study a wealth of basic physics phenomena.

In our joint experiment-theory effort, we will demonstrate the unusual power of this meso-photonic platform in two connected focus areas: (a) Photonic phenomena and functionalities enabled by meta-molecule structures. We will demonstrate a host of photonic functionalities, including complete polarization control and arbitrary wavefront shaping based on the meta-molecule concept, and develop an efficient proof-of-concept solar thermophotovoltaics device for energy harvesting; (b) Enhanced meso-photonic functionalities through integration of functional materials into meta-molecule structures. We will realize real-time control of photonic functionalities, develop meso-photonic cavities for greatly improved optoelectronics, and explore the fundamental physics of strong light-matter interactions in low dimensional quantum materials.

Benefit to National Security Missions

Our proposed work supports the Emergent Phenomena central theme in the Materials for the Future science pillar. This project addresses some grand challenge questions regarding key technological gaps in photonics. The development of compact, lightweight, flexible, and integrated optical elements and optoelectronic devices will impact Threat Reduction and Global Security applications, such as flat lens antennas and focal plane array detectors for communications, imaging, and sensing, such as effluent detection, particularly for space and satellite sensing of nuclear nonproliferation. Indeed, in a recent presentation DoD has listed metamaterials and plasmonics as one of its six high priority S&T areas. The proof-of-concept meso-photonic solar thermophotovoltaics will create a pathway that greatly impacts renewable solar energy harvesting for our national energy security, a core mission of LANL and DOE. The exquisite control of photonic and electronic density of states in meso-photonic cavities will be of great interest to BES for fundamental studies of light-matter interactions enabling emergent meso-scale material properties and functionalities. The proposed research aligns with New Mexico's Technology21 Roadmap for Science and Technology, and contributes to the potential New Mexico Advanced Photonics Hub. It will also prepare us for the Mesoscale Science, Advanced Manufacturing, and National Photonics Initiatives.

Progress

- A broadband omnidirectional absorber was demonstrated based on a metallic metasurface architecture, which accomplished greater than 90% absorptance in the visible and near-infrared range of the solar spectrum, and exhibited low emissivity to prevent thermal radiation losses at mid- and far-infrared wavelengths. A manuscript has been submitted to Nano Letters.

- New metasurfaces were designed, fabricated, and characterized for optical antireflection coatings operating at terahertz and mid-infrared frequencies. A paper has been published in Applied Physics Letters.

- We finished the design and numerical simulations of metasurface structures for a flat lens operating at THz frequencies.
- A plasmonic metasurface structure was demonstrated; it accomplished the simultaneous manipulation of polarization and phase of the transmitted light, which was further used to demonstrate a broadband near-perfect anomalous refraction and the generation of a radially polarized beam. A paper has been published in Advanced Functional Materials.
- An ultra-broadband free-space terahertz modulator based on a semiconductor-integrated metasurface was demonstrated. Experimental validations confirm a bandwidth of at least 100%, spanning 0.5-1.5 THz with -10 dB modulation depth. A paper has been published in Applied Physics Letters.
- Through numerical simulations, we demonstrated that the integration of graphene into metasurface structures enabled independent tuning of two absorption bands of metasurface structure by application of voltage biases to tune the graphene Fermi level. A manuscript has been submitted to Scientific Reports.
- We computed the radiative heat transfer between two sheets of 2D Dirac materials, within the framework of the local approximation for the optical response of these materials. A paper has been published in Journal of Physics: Condensed Matter.
- The spontaneous emission rate of a two-level quantum emitter near a graphene-coated substrate under the influence of an external magnetic field was investigated. We demonstrated that the application of the magnetic field can substantially increase or decrease the decay rate. Our findings strongly suggest that a magnetic field could act as an efficient agent for on-demand, active control of light-matter interactions in graphene at the quantum level. A paper has been submitted to Physical Review Letters and deposited to arXiv: 1506:02176.
- We are processing the requirement of a solar simulator, a vacuum chamber, and a temperature control system for the characterization of the metasurface intermediate structure for solar thermophotovoltaics.

Future Work

- Fabricate new metasurface structures for broadband meso-photonic absorbers and narrowband emitters, and explore the use of refractory plasmonic materials to construct the key component (intermediate structure) of solar thermophovoltaics that can operate at elevated temperatures.
- Build the characterization capability for metasurface intermediate structures to be used in solar thermo-photovoltaics.
- Explore new metasurface structures that enable multi-band or broadband antireflection performance.
- Fabricate and characterize the performance of a metasurface flat lens to focus broadband terahertz radiation.
- Integrate semiconductors 2D Dirac materials to enable polarization switching/modulation.
- Fabricate and characterize graphene-enabled independent tuning of a dual-band metasurface absorber.
- Model heat transfer and structural disorder of the metasurface absorber/emitter within the intermediate structure.
- Integrate 2D materials for enhanced photodetection.
- Model light-matter interactions of 2D Dirac materials within metasurface cavities.

Conclusion

The anticipated deliverables are: a) Novel photonic functionalities from meso-photonic structures; b) Proof-of-concept highly efficient meso-photonic intermediate structure for solar thermophotovoltaic energy harvesting; c) Development of modeling and simulation capabilities for designing and understanding light-matter interactions in meso-photonic materials; d) Enhanced photonic functionalities enabled by functional materials integration; and e) Fundamental studies of strong light-matter interaction between meta-molecules and two dimensional electronic quantum materials. Our proposed work supports the Emergent Phenomena central theme in the Materials for the Future science pillar, and will have great impact on renewable energy, communications, imaging and sensing.

Publications

Azad, A. K., W. J. M. Kort-Kamp, M. Sykora, N. R. Weisse-Bernstein, T. S. Luk, A. J. Taylor, D. A. R. Dalvit, and H. T. Chen. Broadband metasurface absorber – Toward solar thermophotovoltaics. Scientific Reports.

Bartolo, N., F. Intravaia, D. A. R. Dalvit, and R. Messina. Non-Equilibrium Casimir-Polder plasmonic interactions. Physical Review A.

Chen, H. T.. Semiconductor activated terahertz

metamaterials. 2015. Frontiers of Optoelectronics. 8 (1): 27.

Heyes, J. E., W. Withayachumnankul, N. K. Grady, D. R. Chowdhury, A. K. Azad, and H. T. Chen. Hybrid metasurface for ultra-broadband terahertz modulation. 2014. Applied Physics Letters. 105 (18): 181108.

Intravaia, F., V. E. Mkrtchian, S. Y. Buhmann, S. Scheel, D. A. R. Dalvit, and C. Henkel. Friction forces on atoms after acceleration. 2015. Journal of Physics-Condensed Matter. 27 (21): 214020.

Kort-Kamp, W. J. M., B. Amorim, G. Bastos, F. A. Pinheiro, F. S. S. Rosa, N. M. R. Peres, and C. Farina. Active magneto-optical control of spontaneous emission in graphene. 2015. Physical Review B. 92: 205415 .

Kort-Kamp, W. J. M., N. A. Sinitsyn, and D. A. R. Dalvit. Quantized beam shifts in graphene. Physical Review B, Rapid Communications.

Li, J. X., S. Q. Chen, H. F. Yang, J. J. Li, P. Yu, H. Cheng, C. Z. Gu, H. T. Chen, and J. G. Tian. Simultaneous control of light polarization and phase distributions using plasmonic metasurfaces. 2015. Advanced Functional Materials. 25 (5): 704.

Liang, L., M. Qi, J. Yang, X. Shen, J. Zhai, W. Xu, B. Jin, W. Liu, Y. Feng, C. Zhang, H. Lu, H. T. Chen, L. Kang, W. Xu, J. Chen, T. J. Cui, P. Wu, and S. Liu. Anomalous terahertz reflection and scattering by flexible and conformal coding metamaterials. To appear in Advanced Optical Materials.

Rodriguez-Lopez, P., W. K. Tse, and D. A. R. Dalvit. Radiative heat transfer in 2D Dirac materials. 2015. J. Phys.: Condens. Matter. 27: 214019.

Sinitsyn, N. A.. Exact results for models of multichannel quantum nonadiabatic transitions. 2014. Physical Review A. 90: 062509 .

Sun, C., and N. A. Sinitsyn. Exact transition probabilities for a linear sweep through a Kramers-Kronig resonance. 2015. J. Phys. A: Math. Theor.. 48: 505202.

Woods, L. M., D. A. R. Dalvit, A. Tkatchenko, P. Rodriguez-Lopez, A. W. Rodriguez, and P. Podgornik. A materials perspective on Casimir and van der Waals interactions. To appear in Review of Modern Physics.

Wu, L., W. K. Tse, M. Brahlek, C. M. Morris, R. V. Aguilar, N. Koirala, S. Oh, and N. P. Armitage. High-Resolution Faraday Rotation and Electron-Phonon Coupling in Surface States of the Bulk-Insulating Topological Insulator Cu0.02Bi2Se3. 2015. Physical Review Letters. 115: 217602.

Yang, L., N. A. Sinitsyn, W. Chen, J. Yuan, J. Zhang, J. Lou, and S. A. Crooker. Long-lived nanosecond spin relaxation and spin coherence of electrons in monolayer MoS2 and WS2. 2015. Nature Physics. 11: 830–834.

Zhang, B., J. Hendrickson, N. Nader, H. T. Chen, and J. Guo. Metasurface optical antireflection coating. 2014. Applied Physics Letters. 105 (24): 241113.

Zhang, Y., T. Li, B. Zeng, H. Zhang, H. Lv, X. Huang, W. Zhang, and A. K. Azad. A graphene based tunable terahertz sensor with double Fano resonances. 2015. Nanoscale. 7: 12682.

Zhang, Y., T. Li, Q. Chen, H. Zhang, J. F. O'Hara, E. Abele, A. J. Taylor, H. T. Chen, and A. K. Azad. Independently tunable dual-band perfect absorber based on graphene at mid-infrared frequencies. Scientific Reports.

Fighting Carbon with Carbon: All-Carbon Nanomaterial Photovoltaics

Stephen K. Doorn
20130026DR

Abstract

This DR effort focused on studies related to development of carbon nanomaterials (CNM) as active light harvesting components in solar photovoltaics (PV). Goals were to demonstrate the benefits these materials can bring to enhancing performance of solar cells and understanding system behaviors to enhance future performance. Our areas of focus included development of two complementary PV device architectures, supporting materials development (synthesis, purification, processing), fundamental studies of materials photophysics and electrochemistry as a basis for tailoring energy and charge flow in our complex systems, and establishing and applying theory to understand and guide the design of our underlying processes. A few highlights of notable results include demonstration of best-in-class PV performance in our devices. We also provide clear direction for future efficiency enhancements and new roles our materials can play in other hybrid PV systems. Our development of ultra-efficient, one-step purification processes will enhance many new applications of CNM. At a fundamental level, we have provided a first determination of critical energetics that drive photogeneration and collection of electrons. We also established a first understanding of dopant-induced emitting states behind unprecedented new photoluminescence behaviors in carbon nanotubes. Surprising discoveries are leading to unforeseen development of electrochromic devices and novel photonic materials for quantum information processing. The project has thus resulted in major leaps in scientific understanding of CNM, produced unexpected discoveries, and new opportunities for follow-on work. The effort has been extremely productive, being on target for generating ~50 publications, responsible for over 50 invited talks, and resulting in 4 patent disclosures. Towards future opportunities, our work will have significant impact in areas including energy harvesting, storage, and efficiency; development of new photonic and optoelectronic materials and devices; and for growing interest in photon-based quantum information processing.

Background and Research Objectives

Pioneering developments on nanographenes and compositionally-defined carbon nanotubes (CNTs) indicate these materials possess many properties of ideal light harvesters for thin-film photovoltaic (PV) applications. These benefits include more efficient light absorption, tunability of optical and electrochemical properties to match the solar emission spectrum and allow optimization of interfacial charge flow between other device materials, and extremely efficient photogeneration of long-lived free charges available for collection as electrical power [1]. A compelling opportunity thus exists to create new PV device types based on these materials as active light-harvesting components for overcoming performance bottlenecks imposed by current light-harvesting chromophores. By project-end we aimed to harness these properties within functioning PV-devices based on two platforms suitable for follow-on development. In establishing these prototype platforms, our primary goals were:

- Demonstrate the benefits of carbon nanomaterials (CNM) as active light harvesting components and roles they may play in enhancing performance of solar cells.
- Probe and understand system characteristics from the individual materials level to integrated devices to establish new design principles for future performance improvements.

Towards these goals we: Probed the fundamental photophysical and electrochemical behaviors of CNM chromophores and the means to control and tune the associated energy and charge flows. Established CNM materials integration into functioning photovoltaic devices. Pursued these objectives within two promising device architectures for realizing all-CNM photovoltaics: a layered thin-film platform and as dye-sensitized solar cells, with CNM as active dye.

Our end results demonstrated best-in-class devices enabled by improved materials processing. We revealed key behaviors not previously established and used the new understanding to establish design principles for further device improvements. Finally, we produced surprising discoveries and new capability that establish significant opportunity for future advances in energy harvesting, storage, and efficiency; thin film optoelectronics; and quantum information processing.

Scientific Approach and Accomplishments

Materials Development

Graphene oxide was studied as an initial chromophoric material, but dropped in favor of our other candidates. However, with it we established for the first time how charge transport and dynamics in this material change with surface composition thru the first electrostatic force microscopy [2] and correlated photocurrent imaging on it. Direct photoluminescence microscopy also demonstrated dependence of its optical properties on surface composition.

Isolating highly enriched semiconducting CNTs was critical to our PV device development. We developed a single-step aqueous two-phase (ATP) separation for isolating (6,5) or (7,5) nanotubes (Figure 1) that gave dramatic improvements in speed, efficiency, reproducibility, and purity [3]. We also demonstrated the approach as a rapid method for benchtop removal of unwanted nanotube bundles (eliminating the need for expensive ultracentrufugation steps). The approach is also capable of producing long (microns) tubes essential for improving transport of energy and charge in our devices. Most importantly the ATP processing was shown to be compatible with our PV film development. We also established a breakthrough understanding of the ATP separations mechanism. Using chemical modifications and innovative direct photoluminescence imaging of separated tubes, we showed the mechanism works on diameter-dependent changes in surface composition, rather than through direct interactions between the nanotube surface and separation medium (as previously thought).

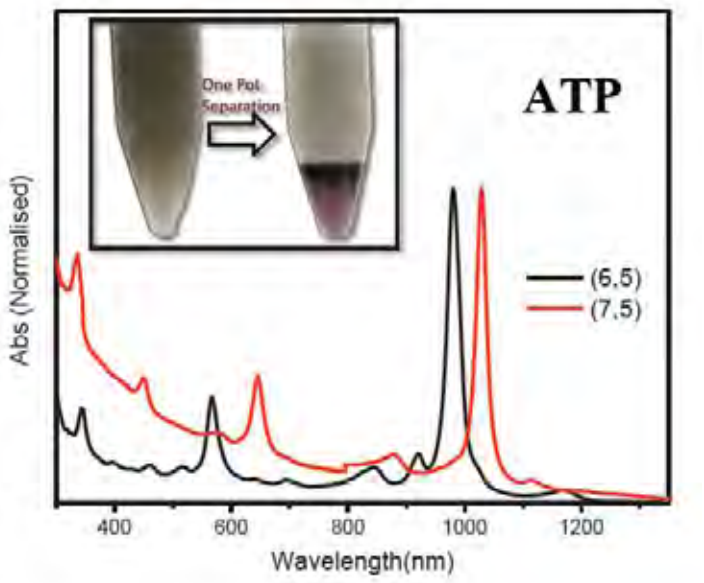

Figure 1. Illustration of effectiveness of one and two-step separations. Inset shows one-step isolation of (6,5) CNTs (bottom phase, purple color) from starting material. Absorption spectra of (6,5) and (7,5) CNTs isolated in two steps. High spectral purity demonstrated.Color variation is shown as applied voltage is varied.

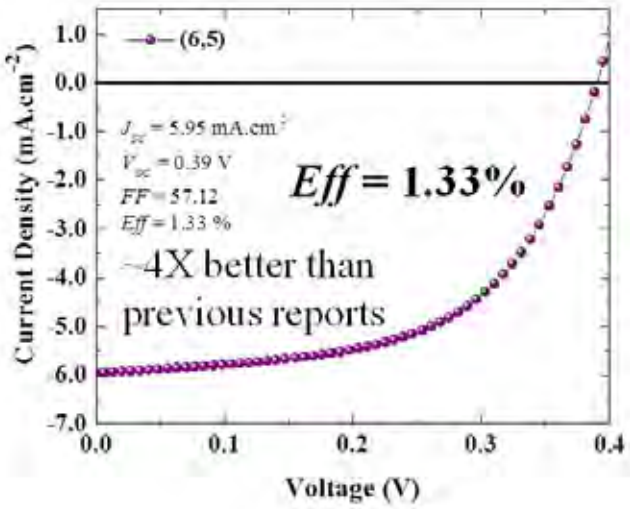

Figure 2. Current-voltage curve showing 4X improvement in (6,5) device performance.

Thin Film Advances

Thin film device advances required both chromophore development and integration with other device materials. Through improved processing, film deposition, optimizing interlayer interactions, and tailoring of film component thicknesses, we produced CNT-based PV devices yielding best in class performance for monochiral structures designed from (6,5) or (7,5) nanotubes (Figure 2). The (7,5) devices showed a 4-fold improvement in performance, while the (6,5) devices yielded 4-fold improvements in power conversion efficiency over past reports. That efficiencies are still in the 1% range, however, shows they are limited by the narrow CNT wavelength response. We next demonstrated this limitation could be overcome by generating the first multi-chiral devices in which performance was shown to be the sum of response from each chiral component, while extending wavelength coverage.

By making hybrid devices with other chromophores, we also showed CNTs can act in tandem to create charge

and energy cascades. This important result shows CNTs have potential for enhancing performance of other PV device architectures in hybrid assemblies. This finding will form the basis for expanding the CNT role to harvest light wavelengths at which only limited response occurs in other materials.

We have made significant advances in understanding of CNT films towards improving design principles in the areas of effectively expanding to multiple CNT structures, film morphology, and the function of other component materials. In particular, rather than acting merely as a suspension agent, we have discovered that the polymer PFO plays an active role in photogeneration of charges; a surprising finding that opens new routes to enhancing performance. In contrast, PFO-bpy can play a limiting role. We have shown via photoluminescence imaging of CNT surface structures that these contrasting behaviors originate in part from formation of very different surface structures. PFO forms an open structure that enhances charge transport and intertube interaction, while a more closed structure for PFO-bpy blocks such behavior. This important finding will drive new design in film morphology and has motivated our pursuit of other active polymers that can harness the full range of nanotube structures we can now access via ATP separations.

Fundamental Photophysics and Lifetime Engineering

This effort has yielded significant opportunity for probing new exciton physics in CNTs and for developing novel techniques as probes of newly revealed behaviors. Some brief examples include Raman probing of intertube interactions in defined-composition CNT bundles. Our discovery of ultranarrow Raman responses superimposed on normal excitation profile behavior in these bundles reveals delocalized exciton states, useful for directing energy flow and opening a new area of study in defined structural interactions. Single-tube optical measurements were developed for probing exciton transport in such bundles. Results have shown intriguing coupling between exciton-exciton annihilation processes and photon emission statistics [4].

Our most significant fundamental breakthroughs have come from studies of covalently doped tubes as routes to improving efficiencies via extending excitation lifetimes by using a localization strategy. Exciton localization at dopant sites is an emerging area of CNT studies with great promise for improved quantum yields and new functionality, yet little is known about the new optical states that arise. Our studies have revealed for the first time the electronic structure and chemical functionality of novel dopant sites [5], definitively show exciton localization at these sites, and show one consequence of localization to be an unprecedented 10-fold increase in excited-state lifetimes (Figure 3). These could be used to enhance charge generation in doped PV devices. As a result of our efforts, we now understand for the first time the structural and dopant dependences of the lifetimes and environmental dependences of dopant-state emission, which will guide dopant development for applications [6]. Most significantly, we discovered that the dopant states can be utilized as single photon emitters at telecom wavelengths at room temperature [7] (Figure 3). Overcoming this long-standing challenge in quantum optics places CNTs for the first time as compelling sources for photonic-based quantum information processing.

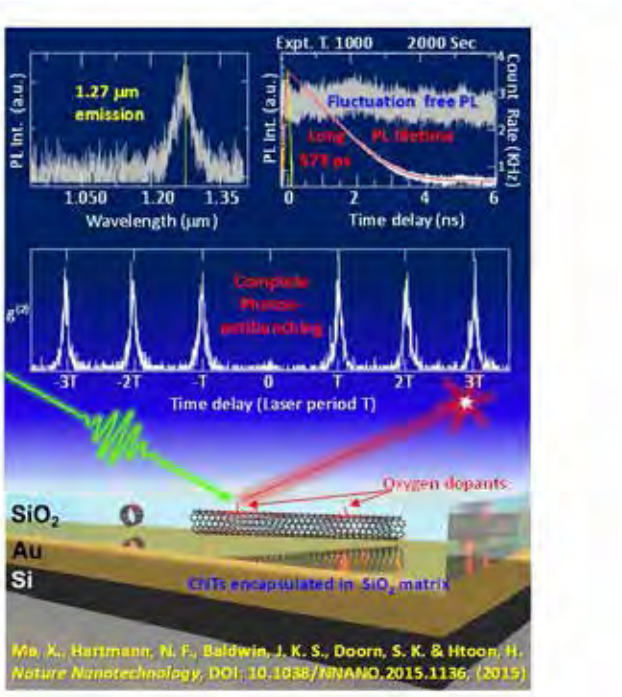

Figure 3. Illustration of single photon emission behavior arising from carbon nanotubes doped in a solid-state process developed in the project. Exciton localization at dopant trap sites yields extended emission lifetimes and complete antibunching at room-temperature as signature of single photon emitter.

Theory

Theory has been an integral part of all the above studies. In addition to developing tight-binding approaches to understanding intertube interactions, efforts at quantum chemical modeling of our various systems have ranged from enhancing LANL-developed codes for modeling excited-state dynamics and testing on model conjugated ring systems (Figure 4), to understanding the dynamics of localized charging events. These results are essential for understanding energy and charge flow in CNM devices. Capability for such studies was also greatly strengthened through efforts at quantum-chemical modeling of the doped nanotubes described above [5]. Density Functional Theory elucidated dopant structure, provided the basis to understand the interplay of excitonic states and spa-

tially localized dopant states, how these define extended lifetimes, and provided a basis for understanding thermal stability of these exciton traps. Deep insights into photo-excited dynamics of chemically functionalized CNM thus resulted. Theory continues to provide a guide to ongoing nanographene synthesis and dopant design efforts.

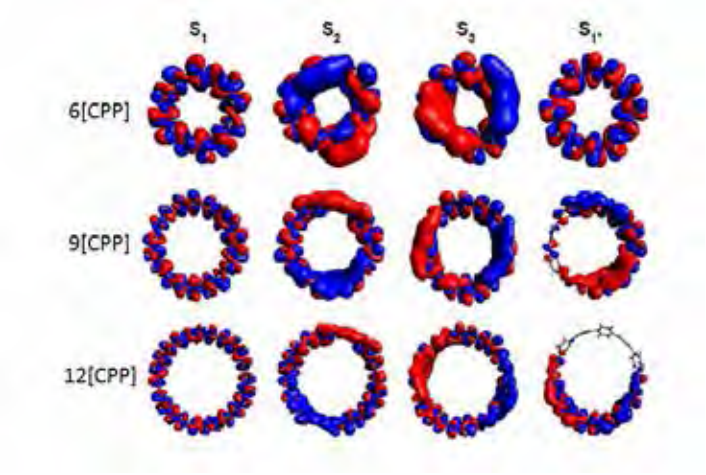

Figure 4. Quantum chemical calculations of ground (S1), and excited state (S2, S3, and S1) exciton wavefunctions for various model cycloparaphenylene [CPP] ring structures as CNT surrogates. Localization in S1* yields high quantum yields for photoluminescence.*

DSSC Cells

Nanographene molecules were studied as light harvesting chromophores in dye-sensitized solar cells (DSSCs). Our success in this area followed directly from the enabling breakthrough development of an in-situ synthesis approach that overcame severe barriers to integration of these chromophores into the parent TiO2 charge-accepting structures [8]. The key innovation was to only perform the final synthesis step after adsorption of precursors to the TiO2 support. This strategy completely overcame previous loading limits to give a 10-fold improvement in PV response for these systems. More importantly, this breakthrough also led to our ability to probe key behaviors of nanographenes towards developing strategies for further improvements.

In situ synthesis was extended to nanographene deposition on transparent electrode surfaces. This allowed us to determine for the first time the critical values of their oxidation and reduction potentials [9]. These values are essential for engineering appropriate driving forces for charge transport in PV cells and in developing potential battery applications as well. These results were produced from an innovative spectroelectrochemical technique developed within the project that overcame lack of energy resolution plaguing previously existing techniques. Size control over the nanographene synthesis allowed us to directly determine quantum confinement effects in optical and electrochemical properties, providing critical information for tuning materials properties. These results also allowed the first determination of exciton binding energies in nanographenes. Finally, access to these unique hybrid materials allowed us to make the first ever excited-state dynamics measurements of charge and energy flow in these systems, which are leading directly to new DSSC design principles. In particular, inefficient charge injection into TiO2, in competition with fast optical relaxation, was revealed as the primary performance bottleneck in these systems. The results point towards development of improved adsorption chemistry, introduction of fixed dipole moments and reducing exciton binding energies as key synthesis targets for improvements.

As a surprise development, our spectroelectrochemical studies resulted in the discovery of electrochromism in these materials [9] (Figure 5): the ability to change color under applied voltage. Electrochromic materials are of significant interest for color display technology and as a basis for smart windows for enabling advances in energy efficiency. Nanographene size tunability provides a full color palette to the effect. Our first generation device performance in areas such as coloration efficiency, contrast, switching time and cost are as good or better than for existing devices based on inorganic materials.

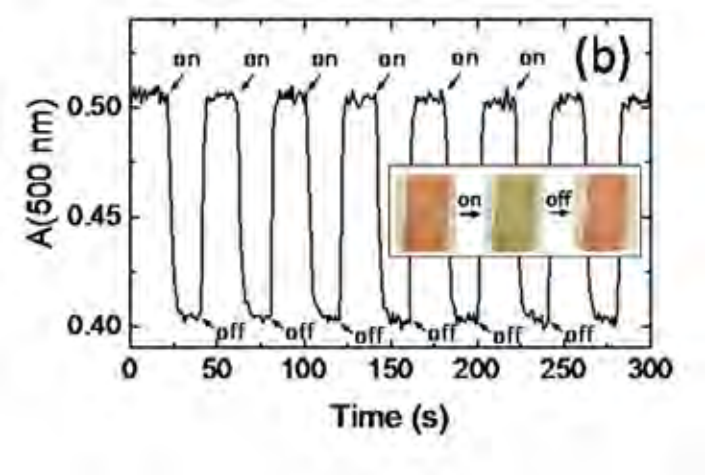

Figure 5. Absorbance vs. time-plot demonstrating breakthrough discovery of electro-chromism in nanographenes. Color variation is shown as applied voltage is varied.

In support of DSSC efforts, effective solid-state electrolytes were generated via incorporation of ionic liquids into sol-gels via a microwave driven process. Anticipate replacement of liquid cells will enhance DSSC lifetimes. Exciting side-development showed solid-state electrolyte can form basis for graphene supercapacitors, showing highest energy storage densities to date.

Summary

In summary, this project was highly successful in producing breakthrough discoveries and new understanding across areas spanning CNM materials development, unveiling of new photophysical behaviors, and exciting new applications unforeseen at project start. The primary efforts on PV device development produced best-in-class performance and clear strategies for future improvements and integration. Our efforts also generated state-of-the-art capabilities for thin film processing, optoelectronic device development, optical probes, and CNM chemistry as just a few examples. Our outstanding productivity resulted in 25 currently published papers, three submitted, and 20 additional papers in preparation. The work is also responsible for over 50 invited talks as well as three invention disclosures.

Impact on National Missions

The results of this effort enhance LANL's portfolio in renewable energy research, which must continue to grow and strengthen to meet the critical challenges facing the nation in areas of climate disruption and energy security. While our CNM device efficiencies remain at the 1-2% level, the understanding developed in this project point towards compelling roles CNM can play as components for enhancing performance of hybrid PV systems. The capabilities and expertise developed in this project are also translating directly into rapid LANL development of perovskite materials that are pushing PV efficiency limits into commercially interesting terrain. Our nanographenes as promising electrochromic materials and novel solid-state electrolytes for high-energy density supercapacitors will play future roles in energy efficiency and storage.

Beyond energy-related applications, advances from our effort will also impact threat reduction needs through detector and sensors development and photonics applications, all of which rely on similar photophysical processes as were studied here. Hybrid nanotube/graphene photodetectors demonstrated in the project have the potential for enhancing spatial resolution of near-IR imaging arrays. Newly established capabilities for optoelectronic device development are also enhancing LANL studies of 2D materials including technologically important transition metal dichalcogenides. The discovery of doped CNTs as room-T single photon sources at telecom wavelengths forms a strong basis for their pursuit as photonic materials for quantum information (QI) needs. This is a growing area of interest for global security applications and there is significant opportunity to grow the role of photonic based QI through these materials. Strengthened capabilities for optical probes and theory developments are also enhancing the user program at the Center for Integrated Nanotechnologies (CINT, part of the DOE nanoscience user facility program). In particular, our efforts in doped nanotubes are drawing in large numbers of new users.

References

1. Arnold, M. S., J. L. Blackburn, J. J. Crochet, S. K. Doorn, J. G. Duque, Mohite, and Telg. Recent developments in the photophysics of single-walled carbon nanotubes for their use as active and passive material elements in thin film photovoltaics. 2013. PHYSICAL CHEMISTRY CHEMICAL PHYSICS. 15 (36): 14896.
2. Yalcin, S. E., Galande, Kappera, Yamaguchi, Martinez, K. A. Velizhanin, S. K. Doorn, A. M. Dattelbaum, Chhowalla, P. M. Ajayan, Gupta, and A. D. Mohite. Direct Imaging of Charge Transport in Progressively Reduced Graphene Oxide Using Electrostatic Force Microscopy. 2015. ACS NANO. 9 (3): 2981.
3. Subbaiyan, N. K., Cambre, A. N. G. Parra-Vasquez, E. H. Haroz, S. K. Doorn, and J. G. Duque. Role of Surfactants and Salt in Aqueous Two-Phase Separation of Carbon Nanotubes toward Simple Chirality Isolation. 2014. ACS NANO. 8 (2): 1619.
4. Ma, , Roslyak, J. G. Duque, Pang, S. K. Doorn, Piryatinski, D. H. Dunlap, and H. a. n. Htoon. Influences of Exciton Diffusion and Exciton-Exciton Annihilation on Photon Emission Statistics of Carbon Nanotubes. 2015. PHYSICAL REVIEW LETTERS. 115 (1).
5. Ma, , Adamska, Yamaguchi, S. E. Yalcin, Tretiak, S. K. Doorn, and H. a. n. Htoon. Electronic Structure and Chemical Nature of Oxygen Dopant States in Carbon Nanotubes. 2014. ACS NANO. 8 (10): 10782.
6. Hartmann, N. F., S. E. Yalcin, L. Adamska, E. H. Haroz, X. Ma, S. Tretiak, H. Htoon, and S. K. Doorn. Photoluminescence imaging of solitary dopant sites in covalently doped single wall carbon nanotubes. Nanoscale.
7. Ma, , N. F. Hartmann, J. K. S. Baldwin, S. K. Doorn, and H. a. n. Htoon. Room-temperature single-photon generation from solitary dopants of carbon nanotubes. 2015. NATURE NANOTECHNOLOGY. 10 (8): 671.
8. Ji, , Wu, Adamska, K. A. Velizhanin, S. K. Doorn, and Sykora. In Situ Synthesis of Graphene Molecules on TiO2: Application in Sensitized Solar Cells. 2014. ACS APPLIED MATERIALS & INTERFACES. 6 (22): 20473.
9. Ji, , S. K. Doorn, and Sykora. Electrochromic Graphene Molecules. 2015. ACS NANO. 9 (4): 4043.

Publications

Adamska, L., G. V. Nazin, S. K. Doorn, and S. Tretiak. Self-trapping of charge carriers in semiconducting carbon nanotubes: Structural analysis. 2015. Journal of Physical Chemistry letters. 6: 3873.

Adamska, L., I. Nayyar, H. Chen, A. K. Swan, N. Oldani, S. Fernandez-Alberti, S. K. Doorn, and S. Tretiak. Self-trapping of excitons, violation of the Condon approximation and efficient fluorescence in conjugated cycloparaphenylenes. 2014. Nano Letters. 14: 6539.

Arnold, M. S., J. L. Blackburn, J. J. Crochet, S. K. Doorn, J. G. Duque, A. Mohite, and H. Telg. Recent developments in the photophysics of single-walled carbon nanotubes for their use as active and passive material elements in thin film photovoltaics. 2013. Physical Chemistry Chemical Physics. 15: 14896.

Crochet, J. J., J. G. Duque, J. H. Werner, B. Lounis, L. Cognet, and S. K. Doorn. Disorder limited exciton transport in colloidal single-wall carbon nanotubes. 2012. Nano Letters. 12: 5091.

Duque, J. G., L. Oudjedi, J. J. Crochet, S. Tretiak, B. Lounis, S. K. Doorn, and L. Cognet. Mechanism of electrolyte-induced brightening in single-wall carbon nanotubes. 2013. Journal of the American Chemical Society. 135: 3379.

Fagan, J. A., E. H. Haroz, Ihly, H. u. i. Gui, J. L. Blackburn, J. R. Simpson, Lam, A. R. H. Walker, S. K. Doorn, and Zheng. Isolation of > 1 nm Diameter Single-Wall Carbon Nanotube Species Using Aqueous Two-Phase Extraction. 2015. ACS NANO. 9 (5): 5377.

Galande, , W. e. i. Gao, Mathkar, A. M. Dattelbaum, T. N. Narayanan, A. D. Mohite, and P. M. Ajayan. Science and Engineering of Graphene Oxide. 2014. PARTICLE & PARTICLE SYSTEMS CHARACTERIZATION. 31 (6): 619.

Hartmann, N. F., S. E. Yalcin, L. Adamska, E. H. Haroz, X. Ma, S. Tretiak, H. Htoon, and S. K. Doorn. Photoluminescence imaging of solitary dopant sites in covalently doped single-wall carbon nanotubes. Nanoscale.

Ji, , S. K. Doorn, and Sykora. Electrochromic Graphene Molecules. 2015. ACS NANO. 9 (4): 4043.

Ji, Z., R. Wu, L. Adamska, K. Velizhanin, S. K. Doorn, and M. Sykora. In-situ synthesis of graphene quantum dots on TiO2: Applications in sensitized solar cells. 2014. ACS Applied Materials and Interfaces. 6: 20473.

Kilina, , Kilin, and Tretiak. Light-Driven and Phonon-Assisted Dynamics in Organic and Semiconductor Nanostructures. 2015. CHEMICAL REVIEWS. 115 (12): 5929.

Lawrence, D., C. Tran, A. T. Mallajosyula, S. K. Doorn, A. Mohite, G. Gupta, and V. Kalra. High-energy density nanofiber-based solid state supercapacitors. To appear in Journal of Materials Chemistry A.

Liu, J. i. n., Adamska, S. K. Doorn, and Tretiak. Singlet and triplet excitons and charge polarons in cycloparaphenylenes: a density functional theory study. 2015. PHYSICAL CHEMISTRY CHEMICAL PHYSICS. 17 (22): 14613.

Ma, , N. F. Hartmann, J. K. S. Baldwin, S. K. Doorn, and H. a. n. Htoon. Room-temperature single-photon generation from solitary dopants of carbon nanotubes. 2015. NATURE NANOTECHNOLOGY. 10 (8): 671.

Ma, , and H. a. n. Htoon. Tailoring the photophysical properties of carbon nanotubes by photonic nanostructures. 2015. MODERN PHYSICS LETTERS B. 29 (17).

Ma, X., J. K. S. Baldwin, N. F. Hartmann, S. K. Doorn, and H. Htoon. Solid-state approach for fabrication of photostable oxygen-doped carbon nanotubes. To appear in Advanced Functional Materials.

Ma, X., L. Adamska, H. Yamaguchi, S. E. Yalcin, S. Tretiak, S. K. Doorn, and H. Htoon. Electronic structure and chemical nature of oxygen dopant states in carbon nanotubes. 2014. ACS Nano. 8: 10782.

Ma, X., O. Roslyak, J. G. Duque, S. K. Doorn, A. Piryatinski, D. H. Dunlap, and H. Htoon. Influences of exciton diffusion and exciton-exciton annihilation on photon emission statistics of carbon nanotubes. 2015. Physical Review Letters. 115: 017401.

Ma, X., S. Cambre, S. K. Doorn, and H. Htoon. Temperature-dependent photoluminescence of water-filled carbon nanotubes: Thermal expansion of a single chain of water molecules. Nano Letters.

Martin, E. J. J., Berube, Provencher, Cote, Silva, S. K. Doorn, and J. K. Grey. Resonance Raman spectroscopy and imaging of push-pull conjugated polymer-fullerene blends. 2015. JOURNAL OF MATERIALS CHEMISTRY C. 3 (23): 6058.

Sau, J. D., J. J. Crochet, S. K. Doorn, and M. L. Cohen. Multiparticle exciton ionization in shallow doped carbon nanotubes. 2013. Physical Chemistry Letters. 4: 982.

Solenov, D., C. Junkermeier, R. L. Reinecke, and K. A. Velizhanin. Tunable adsorbate-adsorbate interactions on graphene. 2013. Physical Review Letters. 111: 115502.

Subbaiyan, N. K., Cambre, A. N. G. Parra-Vasquez, E. H. Haroz, S. K. Doorn, and J. G. Duque. Role of Surfactants and Salt in Aqueous Two-Phase Separation of Carbon Nanotubes toward Simple Chirality Isolation. 2014. ACS NANO. 8 (2): 1619.

Subbaiyan, N. K., and S. K. Doorn. Nanotube micellar surface chemistry: Surfactant surface structure, modification, and application. 2015. In Handbook of carbon nanomaterials. Edited by D'Souza, F., and K. M. Kadish. Vol. 8, p. 1. New Jersey: World Scientific.

Subbaiyan, N., A. N. G. Parra-Vasquez, S. Cambre, M. A. Santiago Cordoba, S. E. Yalcin, C. E. Hamilton, N.

H. Mack, J. Blackburn, S. K. Doorn, and J. G. Duque. Benchtop extraction of isolated individual single-walled carbon nanotubes. 2015. Nanoscale. 9: 5377.

Velizhanin, K. A., Dandu, and Solenov. Electromigration of bivalent functional groups on graphene. 2014. PHYSICAL REVIEW B. 89 (15).

Yalcin, S. E., Galande, Kappera, Yamaguchi, Martinez, K. A. Velizhanin, S. K. Doorn, A. M. Dattelbaum, Chhowalla, P. M. Ajayan, Gupta, and A. D. Mohite. Direct Imaging of Charge Transport in Progressively Reduced Graphene Oxide Using Electrostatic Force Microscopy. 2015. ACS NANO. 9 (3): 2981.

Yamaguchi, H., S. Ogawa, L. Adamska, A. M. Dattelbaum, G. Gupta, S. K. Doorn, H. Htoon, M. Chhowalla, K. A. Velizhanin, A. Mohite, and Y. Takakuwa. Valence band electronic structure evolution of graphene oxide upon thermal annealing fo optoelectronics. Journal of Physical Chemistry Letters.

Design Principles for Materials with Magnetic Functionality

Joe D. Thompson
20130052DR

Abstract

A significant challenge to materials physics and chemistry is the designed control of materials functionalities, a challenge that must be met to satisfy ever increasing demands for advanced materials that underpin the Nation's energy security and competitiveness. Strongly magnetic materials, whose functionality results from a delicate balance of complex interactions among electrons, are key to numerous energy-efficient technologies, but their useful function presently relies on rare and expensive elements, almost always imported. The goal of this project has been to discover scientific principles that, for the first time, allow designed control of materials that are paradoxically both strongly magnetic and free of expensive rare elements. Substantial progress in meeting our goal has allowed first-principles calculation of desirable magnetic properties in a strong magnet devoid of rare elements and the identification of essential design principles for discovering new magnetic materials with technologically useful functionality.

Background and Research Objectives

Advanced materials have been and will continue to be essential for the country to remain globally competitive and to ensure our energy and defense security. Indeed, recent national Materials Genome and Computational Materials Science and Chemistry Initiatives are motivated by the need to develop design principles that accelerate the discovery and application of advanced materials with useful function — a radical departure from traditional discovery of materials and functionality by 'informed serendipity'. Initial success in these initiatives is promising. For example, first-principles calculations and computational algorithms have reached the point where it is possible to predict useful properties of compounds relevant for photovoltaic, battery and thermoelectric applications. These materials properties and their applications are dominantly independent-electron functionalities, which are relatively straightforward to calculate. Like these independent-electron functionalities, magnetism also underpins many energy-efficient technologies, notably wind turbines and 'green' automobiles, but magnetism is an intrinsically highly complex and delicate collective-electron function that is a far more challenging problem.

All magnets in wind turbines and other green technologies presently rely on a material with a 3d-element, like Fe or Co, and a rare-earth element Nd or Sm. The 3d-element provides a large saturated magnetic moment and the 4f-element is the source of atomically derived magnetic anisotropy that hinders magnetic moments from reversing their orientation as a magnetic field changes sign and is essential for 'strong' magnetic properties. The Department of Energy has recognized the high demand and high supply risk of critical rare-earths in its 2011 'Critical Materials Strategy' that calls specifically for the long-term need for research aimed at creating rare-earth-free strong magnets. Despite decades of making-and-measuring to find such ferromagnets that are free of 4f-electron elements, this approach has not been successful. Progress requires a strategy based on scientific principles that ultimately will allow the design of a suitable magnet with magnetic anisotropy even in the absence of a 4f-element. Though some magnetic anisotropy can be derived from d-electron elements, in virtually all cases the coupling between electron spin and orbital moments (spin-orbit coupling) that gives rise to magnetic anisotropy is quenched by the metallic crystal-chemical environment in which the d-element resides. A successful strategy must understand conditions from atomic to macro scales that enable retention of d-electron magnetic anisotropy, and this is the strategy that this project has taken.

Scientific Approach and Accomplishments

Our computationally motivated, experimentally validated approach to this problem used two closely coupled loops – a relatively quick turn-around loop of computations, make and measure fed lessons learned into a sec-

ond slower loop of in-depth theoretical and experimental understanding. Iteratively closing these loops has produced a set of experimentally validated design principles for strong magnets without rare-earth elements. From work discussed below, these design principles are: (1) the crystal structure should be lower than cubic, ideally tetragonal or hexagonal, and contain a high density of magnetic 3d elements; (2) strong electron-electron (Coulomb) interactions are essential and become prominent when the electronic bandwidth of d-elements is comparable to the Coulomb interaction energy, which tends to be realized in ternary compounds that include Si, Ge, or P; (3) including a heavy 4d- or 5d element in the material can be useful for promoting magnetic anisotropy on the 3d element.

Our initial hypothesis was that a family of rare-earth-free materials, with compositions T23-xT'xZ6 (where T is a 3d-element Cr, Mn, Fe, Co and Ni, T' is a heavier 4d- or 5d-element and Z=B, C, or Al) was a promising starting point for exploring design principles. Density functional electronic structure and ordered magnetic moment were calculated for 35 new variants of this family, and based on those calculations, the most promising materials were made and their magnetic properties were measured. Trends in magnetic properties predicted from calculations were supported qualitatively, and often quantitatively, by experiments. Though many of these materials had large saturated magnetic moments and high ferromagnetic ordering temperatures, which are desirable characteristics, none of these materials had substantial magnetic anisotropy. As learned by closing the two loops, the relatively strong hybridization between electrons of the T and T' elements and the absence of strong crystalline electric fields in the cubic structure of these materials caused the spin-orbit coupling, and hence magnetic anisotropy, to be negligible. This family was not pursued further but did establish the design principle that structural anisotropy, for example in tetragonal or hexagonal structure types, was important.

In parallel, substantial effort, particularly in the second loop, was devoted to understanding why the rare-earth free magnet YCo5 had a magnetic anisotropy and associated magnetic anisotropy energy (MAE) that is comparable to that of the most widely used strong ferromagnet Nd2Fe14B. Though hexagonal YCo5 has been known for decades to have a large MAE, there was no microscopic understanding, in spite of numerous theoretical attempts, of precisely why this was the case. To address this problem, we developed a theoretical framework (Local Density Approximation + Dynamical Mean Field Theory – LDA+DMFT) that included realistic electron-electron (Coulomb), crystal-field and spin-orbit interactions on all five d-orbitals of Co in its two inequivalent crystal structure sites. Such a calculation was the first of its kind. These calculations showed that the MAE density is double-valued as a function of the Coulomb energy U, but our photoemission and specific heat measurements constrained the value of U to be about 3.5 eV, which from our calculations gave the measured MAE density. This large U predicted theoretically implies that electronic correlations are important, a fact that we also have demonstrated by comparing the measured electronic specific heat with calculations that ignore these correlations. This is a significant new design principle that had not been appreciated previously by anyone. It is important to note that the energy of the critical property, MAE, is more than three orders of magnitude smaller than U and much smaller than any other energy scale in the problem, highlighting the difficulty of accurately predicting the MAE from first principles as we have done so successfully. These calculations further predicted that the MAE of YCo5 might increase by a factor of six if we could tune the value of U to half its intrinsic value and also predicted with remarkable accuracy (and with no adjustable parameters) the orbital moment on Co atoms that we confirmed by x-ray magnetic circular dichroism measurements.

These LDA+DMFT calculations are extremely demanding and time consuming, prohibiting their use for exploratory searches. For this, we turned to computational expertise in the first loop. Using full-potential linearized augmented plane-wave (FP-LAPW) density functional (LDA) calculations of electronic structure, we correctly predicted trends in the MAEs of XCo5, X={Th, Y, La, Ce} and the XCo4B, X={Y, La} series of compounds, many of which we made and measured. (As an experimental aside, we note that single crystals are needed to determine the MAE, but finding experimental conditions under which these materials might be prepared as single crystals also was prohibitively time consuming. We found, however, a simple solution to this obstacle. Because these materials are magnetically anisotropic, we prepared them in polycrystal form, ground the polycrystals into a powder, and aligned the powder embedded in pre-hardened epoxy and subject to a magnetic field while the epoxy hardened. From several tests, we showed that the aligned powders accurately reproduced the MAE measured in single crystals. This 'make' process took about a day instead of weeks to months to grow single crystals of a given material.) Despite predicting correct trends, the quantitative accuracy of computed MAEs compared to experimental values was poor, as shown in the left panel of Figure 1; however, the accuracy of the magnetic moments was generally superior, which is useful because the anisotropy of the orbital moment μL is related to the MAE of a material. From a large number of computational variations, we verified that anisotropy of μL mimics that of the MAEs (right panel of Figure 1). Because

these calculations converge very quickly, we may have identified a proxy for MAEs that is less computationally demanding, an important step in implementing our design principles in practice.

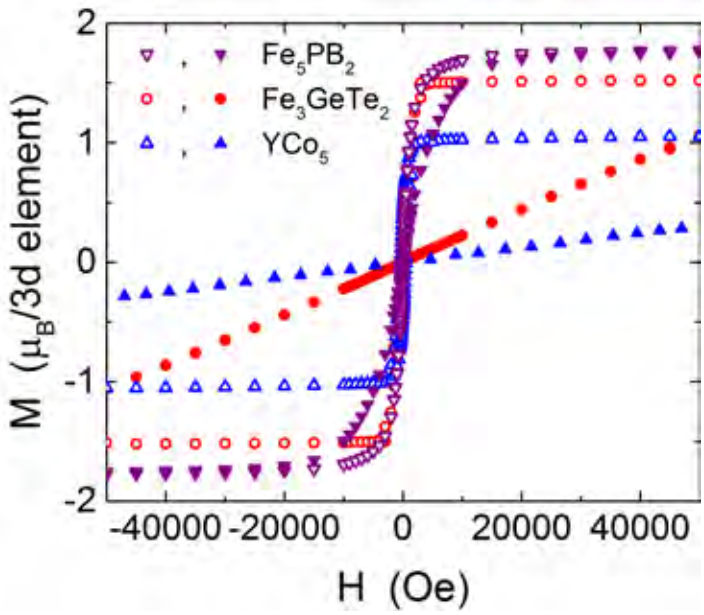

Figure 1. Magnetization in units of Bohr magnetons per 3d element versus applied magnetic field. Open symbols correspond to field applied along the easy magnetic axis, where the magnetization saturates rapidly, and closed symbols are for field perpendicular to the easy axis. Fe5PB2 has the largest saturated magnetization, but it is only weakly anisotropic and consequently has a modest MAE, which is related to the area bounded by the easy and hard axis magnetization curves for this compound. Of the three ferromagnets, YCo5 has the smallest saturated magnetization but is highly anisotropic and has the largest MAE. Fe3GeTe2 has an intermediate MAE that is very large for an Fe-based ferromagnet.

Guided by initial design principles, the first loop performed a total of nearly 1000 density functional calculations on potentially magnetically anisotropic compounds, and about 90 of the more promising materials were made, many as aligned powders, and measured for comparison to predictions. From those calculations and measurements, we identified two particularly promising materials Fe5PB2 and Fe3GeTe2 whose magnetic anisotropy is compared to YCo5 in Figure 2. These ternary compounds contain elements P and Ge, which, like Si, do not 'dissolve' Fe, and this is a condition that favors retention of Fe's orbital moment. We found that the MAE of Fe5PB2 was relatively high, about 8% of that of YCo5, and at low temperatures exceeded that of SrFe12O19 and BaFe12O19, which have applications in microwave and small motor technologies but are not useful for green technologies. Consequently, except for a few substitution studies, Fe5PB2 was not pursued in-depth because we showed that Coulomb interactions still were not sufficiently optimized to produce significant magnetic anisotropy. In contrast, we found that Coulomb interactions were very strong in Fe3GeTe2, giving an MAE about 35% of that in YCo5 and that is among the highest of any rare-earth free ferromagnet, and single crystals of it were studied in detail as were variations on its chemical composition. We note that the heavy 4d-element Te, like other 4d-and 5d-elements at the end of their row in the periodic table, has relatively large atomically derived spin-orbit coupling, which can be transferred to Fe and thus enhance Fe's orbital moment. From x-ray circular dichroism, we determined the orbital and spin moments on Fe atoms, from photoemission found that the electronic bandwidth was quite narrow, consistent with strong electron-electron interactions, and imaged magnetic domains using magnetic force microscopy. Besides initial calculations that identified this material as promising, we applied LDA+DMFT methods to calculate the photoemission spectra and spin and orbital moments. These calculations compared favorably with experiments but still could not account quantitatively for all measured atomic properties. We do not understand the origin of these quantitative differences but note that Fe3GeTe2 is an important validation of our design principles.

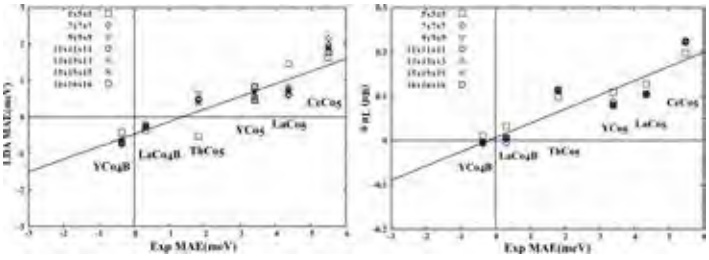

Figure 2. Comparison of calculated and measured magnetic properties of the series XCo5, where X is Th, Y, La and Ce, and of related compounds XCo4B. Symbols correspond to calculations using different numbers of k (momentum) points in a three dimensional grid used to calculated the LDA electronic structure. The number of k-points is given in the legends, and the larger this number, the longer calculations take to converge but they become more accurate. The left panel compares magnetic anisotropy energies (MAEs) and the right panel shows the relation between calculated orbital moment anisotropy and measured MAE.

As mentioned earlier LDA+DMFT calculations, though quantitatively accurate, are extremely time consuming, and, therefore, we wanted to develop a much faster alternative that also captured strong electron-electron correlations, which LDA does not. To this end, substantial effort went into developing a general code that incorporates correlations within the Gutzwiller approximation for treating multi-orbital correlated electron systems, like the 3d-based materials of interest for our project. This code includes the

automatic generation of variational parameters based on the crystal symmetry of the compound. In particular, we applied our code to YCo5 based on a tight-binding parametrization, which we computed for this purpose. The tight-binding parametrization turned out to be challenging because of the hybridization of 3d-orbitals with s-character electrons. We also faced convergence problems when applying the Gutzwiller approximation to YCo5 because of the very large set of variational parameters (about 7000) imposed by the rather low crystal symmetry of this compound. It is important to emphasize, however, that our Gutzwiller+tight-binding code represents the first attempt to use this approach for computing the MAE of correlated electron materials. In spite of these challenges, we have demonstrated that this is a promising approach towards a reliable, accurate computation of MAE in correlated electron materials. Preliminary Gutzwiller-based calculations based on a simpler band structure of YCo5 reproduced the experimental value of the MAE, and importantly these calculations are over an order of magnitude faster than LDA+DMFT.

A spin-off of our Guzwiller+tigh-binding code was the implementation of the first quantum molecular dynamics algorithm, which includes correlations in the Gutzwiller approximation (QMD+GW). We wrote a code for a single-orbital model and as a first test studied the change of the transport properties of a liquid metal as a function of increasing Coulomb interaction. In particular, we calculated the electronic conductivity and the ionic self-diffusion constant when the liquid metal undergoes a Mott-Anderson transition.

Besides demonstrating success in meeting our scientific goal, this project also pursued programmatic funding opportunities and reached out to the broader scientific community. In response to the DOE call for a Critical Materials Hub proposal, we participated actively in the Laboratory's response to that call. Though the proposal was among the three finalists, it was not selected. Additionally, project members were chosen to submit proposals or contribute to proposals in response to DOE calls for Computational Materials Science and Chemistry and an Energy Frontier Research Center, with emphasis in each case on our approach and successes in developing design principles. Again, these proposals were highly ranked, but unfortunately not funded. In coordination with Laboratory ARPA-E program managers, the concept of this project was discussed with two APRA-E program offices, the Rare-Earth Alternatives in Critical Technologies and the Vehicle Technology office. Both considered our concept attractive, but both also judged that it was premature to invest in it at this time. Out-reach activities included one team member co-organizing an international workshop on Electronic Structure Approaches and Applications to Quantum Matter, which included advances in the theory of strong magnets, and another team member serving as a guest editor of the special issue of the Journal of Physics: Condensed Matter that was devoted to rare-earth replacement magnets.

Impact on National Missions

By implementing Materials Genome initiative concepts, this project of computationally motived, experimentally validated science has developed a set of principles for the design of new materials with a specific functionality. Besides realizing a priority of the Laboratory's strategy of Materials for the Future, success in this project has been a first step in realizing the Department of Energy's Critical Materials Strategy of designing rare-earth-free strong magnets. Methodologies developed in this project are broadly applicable to Laboratory materials-by-design problems in which electron-electron interactions are a fundamental component of materials' functionalities, ranging from new types of sensing and near lossless transmission of energy to the response of Pu to environmental changes. In the course of this project, a project-supported postdoc was converted to staff in T-1.

Publications

Brito, N. L., E. D. Bauer, F. Ronning, J. D. Thompson, and R. Movshovich. Study of magnetic microstructure of Fe3GeTe2 using magnetic force microscopy. Applied Physics Letters.

Brito, N. L., E. D. Bauer, F. Ronning, J. D. Thompson, and R. Movshovich. Surface magnetometry of Fe3GeTe2 via magnetic force microscopy. Journal of Physics: Condensed Matter.

Chern, G. W., K. Barros, C. D. Batista, J. D. Kress, and G. Kotliar. Mott transition in a metallic liquid - Gutzwiller molecular dynamic simulations. Physical Review Letters.

Janoscheck, M., J. C. Cesar, F. Ronning, E. D. Bauer, and J. D. Thompson. Physical properties of the ferromagnet Fe3GeTe2. Journal of Physics:Condensed Matter.

Leiding, J., J. K. Ellis, and R. L. Martin. FP-LAPW/LDA calculations of magnetic properties of XCo5, X={Th, Y, La, Ce}, and XCo4B, X={Y. La} magnets. Physical Review B.

Ronning, F., and J. L. Sarrao. Material's prediction scores a hit. 2013. Physics . 6: 109.

Ronning, F., and S. Bader. Rare earth replacement magnets. 2014. Journal of Physics: Condensed Matter . 26: 060301.

Sarrao, J. L., F. Ronning, E. D. Bauer, C. D. Batista, J. X. Zhu, and J. D. Thompson. Building blocks for correlated su-

perconductors and magnets. 2015. APL Materials. 3: 041512.

Zhu, J. X., M. Janoschek, R. Rosenberg, F. Ronning, J. D. Thompson, M. A. Torrez, E. D. Bauer, and C. D. Batista. LDA+DMFT approach to magnetocrystalline anisotropy of strong magnets. 2014. Physical Review X. 4: 021027.

Zhu, J. X., T. Durakiewicz, F. Ronning, M. Janoschek, E. D. Bauer, and J. D. Thompson. Electronic correlations and magnetism in the Hund ferromagnetic material Fe3GeTe2. Physical Review B.

Non-Precious Metal Electrocatalysts for Clean Energy

Piotr Zelenay
20130065DR

Abstract

In order to fully realize the clean energy conversion and storage technologies (fuel cells, batteries, and water electrolyzers), development of highly-active, durable, and inexpensive electrocatalysts for the oxygen reduction and evolution reactions (ORR/OER) is necessary. This project has responded to that grand challenge by combining experimental and multi-scale modeling approaches for the purpose of (1) elucidating the nature of ORR and OER activity, (2) probing the interaction between meso- and nanoscale controls on electrocatalyst performance, and (3) designing and synthesizing non-precious metal catalysts (NPMCs) via a rational design.

Active site characterization from density functional theory (DFT) and model system experiments have provided insights into the nature of the active site and critical role of water for the NPMC development graphitic NPMCs. Mesoscale/multiphysics studies using lattice Boltzmann method (LBM) has developed the first physics-based model to account for coupled fluid flow, ion transport, and electrochemical reactions for applications in energy conversion/storage technologies. Catalyst synthesis of next-generation NPMC has produced the highest reported activity from two-dimensional graphene oxide (GO) ORR electrocatalysts in acid electrolytes obtained from highly ordered “dry” GO precursors. Further, a bifunctional ORR/OER NPMC with low ORR-OER potential gap (0.6 V, ca. 0.1 V less than the lowest value reported to date) has been developed from earth-abundant La-Sr-Co-Fe-C catalyst.

Through advancing the fundamentals of oxygen electrocatalysis and developing novel materials and concepts for energy applications this project has directly tackled two top research priorities in the LDRD Energy & Earth Systems Challenge, including the need to utilize earth-abundant elements in place of precious metals. This work also positions LANL to target major new initiatives in clean-energy catalysts in the future.

Background and Research Objectives

The oxygen reduction (ORR) and evolution (OER) reactions are crucial to a variety of electrochemical energy storage and conversion technologies. The lack of understanding and control of ORR and OER electrocatalysis is a critical barrier to low-temperature fuel cells, metal-air batteries, and water electrolyzers for hydrogen generation. High ORR and OER overpotentials are the main obstacle to making these technologies viable. Pt- and Ir-based catalysts are state-of-the-art in terms of activity and durability for the ORR and OER, respectively. However, the prohibitive cost and scarcity of these precious metals have limited their widespread implementation in clean energy applications. To fully realize these technologies, highly active, durable, and inexpensive catalysts, based solely on earth-abundant elements, are desperately needed for oxygen electrodes.

Research objectives of this project have been:

(1) Molecular Level Insights into the Nature of Non-Precious Metal Active ORR and OER Sites. Two-dimensional carbon systems, such as graphene and graphene oxide (GO), can be readily modified and described theoretically, making them ideal for elucidating electrocatalytic active sites. Model electrocatalyst systems based on nitrogen-doped graphene and GO functionalized with nonprecious metals have been synthesized and characterized using spectroscopic and imaging tools to identify most active reaction sites. These graphene systems have been modeled using density functional theory (DFT) calculations to assign experimental spectra and interrogate active-site geometry and electronic structure. Hence, the scientific framework critical for optimization of non-precious metal ORR, OER, and bi-functional ORR/OER electrocatalysts for clean energy production/storage have been developed in this project.

(2) Theory and Optimization of the Mesoscale Catalyst Structure. The electrochemical activity of NPMCs is

highly coupled to the mesoscale structure of the catalyst: unlike precious metal catalysts there is no distinction between catalyst and support in NPMCs. Catalytic activity is multiscale and requires theory to bridge the nano- and mesoscales. Fundamental kinetic quantities for active sites, based on DFT, have been reconciled with mass-transport phenomena via the LBM method. The resulting models have provided an understanding of the linkage between three-dimensional mesoscale catalyst structure, mass-transport effects, and active-site kinetics.

(3) Rational Design and Synthesis of Next-Generation NPMCs. Based on the rational design derived from studies of model graphene electrocatalysts, novel non-precious metal electrocatalysts have been synthesized. Carbon and a few oxide templates have been investigated for the stabilization and promotion of active sites. Such synthesis-based approach for new catalysis optimization, as well as a focus on the OER represents a major extension of NPMC research to date, both at LANL and elsewhere. While practical NPMCs are more complex than the model systems, theoretical calculations have helped elucidate the catalytic processes observed spectroscopically, as in the case of the model graphene electrocatalytic system.

This work creates a foundation for next-generation NPMC systems as a basis of a large electrochemical energy conversion and storage program at LANL.

Scientific Approach and Accomplishments

Model Systems

In this project, simpler carbons were utilized to better understand the process required for the formation of active NPMCs. Typically, NPMCs are formed when nitrogen heteroatoms and non-precious metals that, once incorporated into the carbon lattice, can form a metal-nitrogen-carbon complex. State-of-the-art NPMCs are commonly synthesized from complex carbon precursors; by reducing the complexity of such systems utilizing two-dimensional carbons such as graphene, graphene oxide (GO), and graphite we were able to identify the critical role of water in the formation of active NPMCs.

In the GO studies, we developed a simple solvent-drying technique based on Hansen's solubility parameters (dispersion, δd, hydrogen bonding, δH, and polarity, δp) to obtain NPMC precursors that resulted in electrocatalysts with high degree of ORR catalytic activity (the highest reported to date for GO NPMC in acid electrolytes). The process involves monitoring of intercalated water, which exists abundantly within GO sheets, using several characterization techniques: X-ray diffraction (XRD), X-ray photoelectron spectroscopy (XPS), and infrared spectroscopy (FTIR). Exfoliation and functionalization of graphite to GO increases the interlayer graphene spacing from 3.3 Å to 10.8 Å due to the formation of oxygen-containing functional groups on the graphene basal plane and simultaneous intercalation of water. Effective removal of intercalated water was obtained by rinsing GO sheets with solvents of similar δd-, but lesser δp- and δH-character than water (e.g. ethanol and diethyl ether), leading to partially reduced GO materials (Figure 1a). The effect of solvent rinsing on the removal of intercalated water revealed a decrease in d-spacing from 10.8 Å to 7.5 Å, along with an increase in graphitic carbon content causing a confinement of water as observed from the sharpening of the O-H stretch vibrational modes from FTIR (Figure 1c).

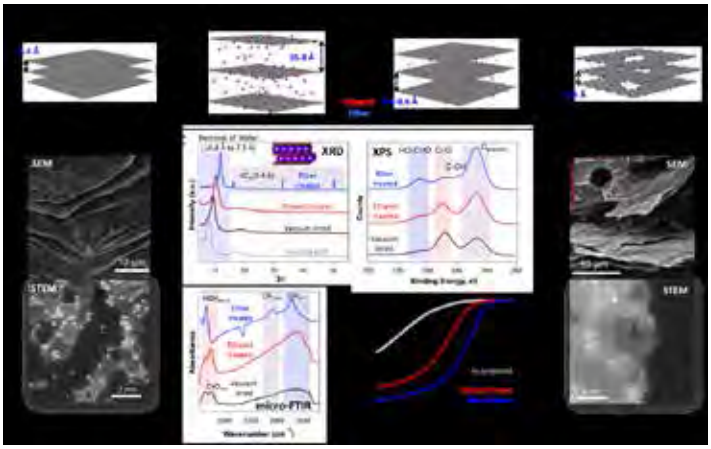

Figure 1. (a) Design principle of GO catalysts. (b) Electron micrographs of initial 2-D carbon GO. (c) Various characterization techniques employed for the monitoring of intercalated water. (d) Resulting GO NPMCs.

Molecular dynamics models were used to find relaxed GO structures with intercalated water and various solvents in order to aid the understanding of solvent effects on multi-layer GO materials. Calculated averaged d-spacing between GO sheets showed values in good agreement with the decreasing d-spacing trend observed from experimental XRD data, supporting the hypothesis that solvents can substantially alter the structure of water-intercalated GO. Thus, certain solvents can pull GO layers together close enough that they would react with residual alkali and transition metal ad-atoms leftover from the GO synthesis process. Upon nitrogen incorporation via high temperature treatment in ammonia, these domains impede the egress of intercalated water molecules, leading to the formation of active GO catalysts with increased ORR activity. Overall, the two-dimensional sheet-like structure of GO is preserved, but large (5-20 μm) holes are formed in the graphitic sheets after nitrogen incorporation (Figure 1d). Such holey sheets address a significant challenge in using 2-D materials for catalysis, i.e., inaccessibility of active sites deep within the layered material. These findings are cur-

rently under review in the sister journal of Science magazine, Science Advances.

Model catalyst systems were also developed from graphene, the simplest carbon structure. In this work, a novel systematic bottom-up approach for the investigation of the role of each component in NPMCs was developed via nitrogen the incorporation on graphene structures using energetic neutral atom beam (ENABLE), a unique novel technique exclusive to LANL. ENABLE offers the ability to utilize high kinetic energy reactive neutral atoms to overcome thermal barriers, allowing for direct scission and formation of chemical bonds without disrupting graphene's pristine lattice structure. The correlation of chemical-structure to ORR activity of these model nitrogen-doped systems was investigated using ultrathin film electrodes. These findings revealed significant control towards the incorporation of different N species into the graphene structure based on substrate temperature or sequential atom doping (Figure 2).

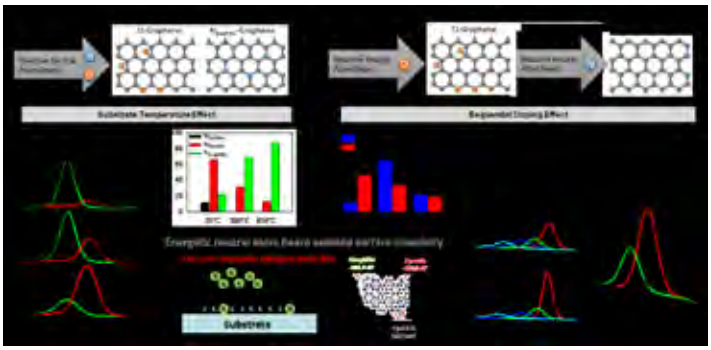

Figure 2. Nitrogen doping of graphene structures via ENABLE-assisted surface chemistry. Effect of substrate temperature and sequential doping on nitrogen speciation as observed from XPS characterization.

Theory

The quantum-chemical modeling component of this project was successful in understanding the atomic-scale behavior of probable ORR active site structures. The goal of linking atomic scale non-precious metal active site structures to ORR activity was achieved and, for the first time, coupled with structural stability considerations. Unlike previous studies, structural stability motifs were established and used to identify target sites for activity studies. Four structural motifs were discovered: (1) Fe is most stable in graphene with N nearest neighbors between the Fe and C atoms, (2) resulting Fe-N structures are more stable embedded at graphene edges as compared to the bulk, (3) edge Fe-N structures are thermodynamically driven to form small edge clusters (multi-metal atom sites), and (4) in-situ conditions (with applied potential in an aqueous environment) can lead to spontaneous *OH formation from water, significantly modifying the active site structure and ORR activity. The fourth motif, spontaneous *OH ligand modification of sites, has been shown to apply to FeN4 structures (both bi-vacancy and porphyrin). This understanding from modeling helps guide interpretation of experiments, as in-situ and ex-situ observations of same initial structures are likely to be different (changed bond lengths, planarity, etc.) due to this ligand modification.

These stability studies point to a novel active-site structure [FeCoN5(*OH) on a graphene zig-zag edge, Figure 3]. Interestingly, this site was determined based on maximizing stability but was found to also have the highest calculated thermodynamic limiting potential (Ul) reported to date for NPMC active sites. (Ul serves as a computationally accessible measure of ORR activity.) Thus, increasing the density of these active sites is predicted to significantly improve ORR catalyst activity. The capabilities and structures developed are already aiding in follow-on projects for relating structure to experimental signatures via computation as well as guiding further improvement in activity via structural fine tuning.

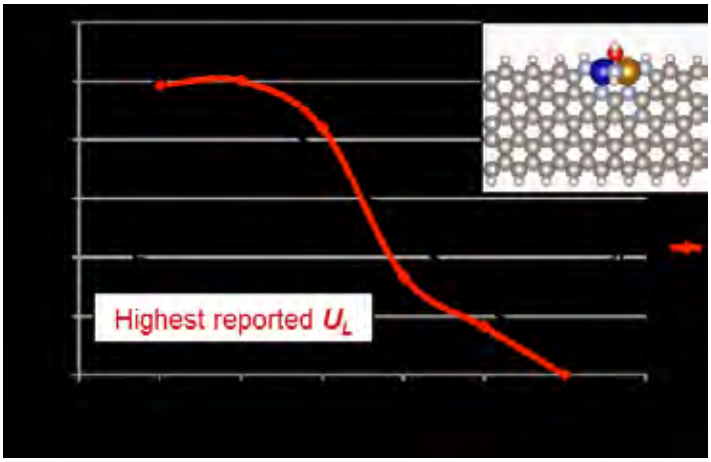

*Figure 3. Free energy ORR (associative) pathway as a function of reaction coordinate on the FeCoN(*OH) structure.*

A pore-scale model based on the lattice Boltzmann method (LBM) was developed for the coupled physico-electrochemical processes in both carbon/platinum (C/Pt) and NPMC cathode catalyst layers (CLs) for proton exchange membrane fuel cells (PEMFCs). The model was applied to CLs to evaluate effects of nanoscale structural characteristics on the macroscopic transport properties, improving fundamental understanding of reactive transport processes in nanostructured CLs. Application of the model to reactive transport processes is the first such study on NPMC CL systems.

High-resolution CL porous structures for PEMFCs were reconstructed using the quartet structure generation set,

which follows the experimental fabrication process including carbon seed generation, carbon phase growth, Pt deposition and ionomer coverage. Detailed distributions of Pt, carbon, ionomer and void space were obtained from the reconstruction process (Figure 4, left). It was found that the detailed layer structures significantly affect the effective diffusivities. The tortuosity predicted is much higher than that commonly used in the Bruggeman equation. Additionally, Knudsen diffusion plays a significant role in oxygen diffusion and significantly reduces oxygen's effective diffusivity. The effective proton conductivity predicted is close to the simulation results reported in literature and much lower than experimental results, indicating other proton transport mechanisms such as proton transport in liquid water.

Figure 4. Reconstructed 3D nanoscale structure of a cathode CL (left). Oxygen concentration in the NPMC CL obtained from the LBM simulations (right).

Reactive transport processes in NPMC CLs and Pt CLs were numerically investigated at the nanoscale using the LBM (Figure 4, right). The simulation results show that although the total reaction surface area of NPMC CL considered in this study is larger than that of the Pt CL, the reaction rate within the NPMC CL is lower than that in Pt CL, due to a much smaller reaction rate coefficient. To further improve the performance of the NPMC CL, the reaction surface area needs to be increased to overcome the slow reaction rate coefficient. In addition, the effects of micro- and mesopores on mass transport were studied. Our results show that micropores (a few nm) contribute little to mass transport. Mesopores (few tens of nm) or macropores (larger than 50 nm) are required to increase the mass transport rate. Our study suggested that pore-scale modeling can be used to optimize the CL microstructures for more desirable reaction surface area. This part of the work has resulted in six peer reviewed journal articles. Additionally, significant progress was made in incorporating fluid flow and ion transport into our model. The resulting model will be the first physics-based to account for coupled fluid flow, ion transport, and electrochemical reactions and will have applications in many other energy conversion/storage systems.

Catalyst Synthesis

Bifunctional OER/ORR catalysts were developed from lanthanum-strontium-cobalt perovskites, (La0.85Sr0.15) CoO3-δ (LSC). LSC demonstrates high OER activity compared to state-of-the-art precious metal catalyst, IrO2, however, its ORR activity is negligible (Figure 5a). Significant improvement in ORR activity was obtained by modifying LSC using a nitrogen precursor, cyanamide (CM), and iron. Elemental energy-dispersive X-ray spectroscopy (EDS) mapping (Figure 5b) and XRD analysis (not shown) revealed a phase separation of LSC into lanthanum oxides and a perovskite with more equal La:Sr ratio. Interestingly, strontium was found atomically dispersed atop of graphene sheets throughout the catalyst as observed from high-resolution transmission electron microscopy. Thus, catalytically active bifunctional OER/ORR catalysts were obtained when the initial perovskite structure (La0.85Sr0.15) CoO3-δ was converted into A-site defective perovskite. This A-site vacancy induces changes in the molecular orbital structure of the catalyst, favorably affecting OER activity. The catalyst activity observed from modified-LSC catalysts with nitrogen and iron demonstrate the lowest ORR-OER potential gap (0.6 V, ca. 0.1 V less than the lowest reported value) to date.

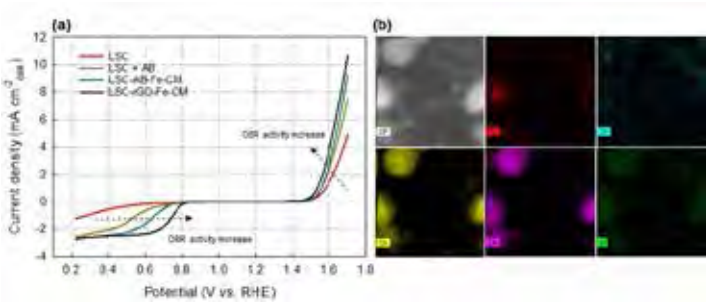

Figure 5. (a) ORR/OER activities of LSC and modified-LSC catalysts: LSC+AB, LSC-AB-Fe-CM, and LSC-rGO-Fe-CM. (b) Elemental EDS mapping from LSC-rGO-Fe-CM bi-functional catalyst.

Lastly, based on our understanding gained of the critical role of water for the synthesis of graphitic NPMCs, a novel approach was developed to incorporate non-precious metals and nitrogen precursors into graphite using a water-free process. Successful intercalation of dry metal and/or nitrogen precursors into graphite was obtained via high temperature and pressure in an oxygen-free environment obtaining a new catalyst precursor, graphite intercalated compound (N-GIC). Manuscripts for this process as well as the study furthering the effect of solvent treatments in alkaline environments are in preparation. These findings have been reported in a number of peer-reviewed journal articles, as well as conference presentations, many of which were invited contributions.

Impact on National Missions

This research supported the Los Alamos LDRD Energy & Earth Systems Grand Challenge "concepts and materials for clean energy". In particular, it tackled top research priorities of "new materials, for energy applications, containing earth-abundant elements that mimic properties of rare and expensive materials" and "energy generation and efficiency". This research will enable sustainable and low-cost energy devices with enhanced energy efficiency/capacities, targeting new initiatives in mesoscale catalysis, which are scheduled to be announced by DOE-BES in the near future. Particularly, this research is relevant to the DOE-EERE mission of developing alternative energy sources, especially for transportation and stationary applications (fuel cells, hydrogen generation). By being directly relevant to renewable energy, this research earns the highest mark in the energy security category. Finally, this effort has focused on the fundamental understanding of materials for possibly the two most challenging reactions in electrochemistry, oxygen reduction and evolution, using a combination of modeling, experimentation with model systems, and catalyst development making this project relevant to essential understanding of materials and fundamental chemistry.

Publications

Chen, L., G. Wu, E. F. Holby, P. Zelenay, W. Tao, and Q. Kang. Lattice Boltzmann Pore-Scale Investigation of Coupled Physical-electrochemical Processes in C/Pt and Non-Precious Metal Cathode Catalyst Layers in Proton Exchange Membrane Fuel Cells. 2015. 158: 175.

Chen, L., Q. Kang, Q. Tang, B. A. Robinson, Y. He, and W. Tao. Pore-scale simulation of multicomponent multiphase reactive transport with dissolution and precipitation. 2015. International Journal of Heat and Mass Transfer. 85: 935.

Chen, L., Q. Kang, Y. L. He, and W. Tao. A critical review of the pseudopotential multiphase lattice Boltzmann model: methods and applications. 2014. International Journal of Heat and Mass Transfer. 76: 210.

Chen, L., Y. L. He, Q. Kang, and W. Tao. Coupled numerical approach combining finite volume and lattice Boltzmann methods for multi-scale multi-physicochemical processes. 2013. Journal of Computational Physics. 255: 83.

Chung, H. T., G. Wu, Q. Li, and P. Zelenay. Role of two carbon phases in oxygen reduction reaction on the Co-PPy-C catalyst. 2014. International Journal of Hydrogen Energy. 39: 15887.

Chung, H. T., J. H. Won, and P. Zelenay. Active and stable carbon nanotube/nanoparticle composite electrocatalyst for oxygen reduction. 2013. Nature Communications. 4: -.

Elbaz, L., G. Wu, and P. Zelenay. Heat-treated non-precious-metal-based catalysts for oxygen reduction. 2013. In Electrocatalysis in fuel cells: A non- and low-platinum approach. Edited by Shao, M.. , p. 231. London: Springer-Verlag.

Gao, W., G. Wu, M. T. Janicke, D. A. Cullen, R. Mukundan, J. K. Baldwin, E. L. Brosha, C. Galande, P. M. Ajayan, K. L. More, A. M. Dattelbaum, and P. Zelenay. Ozonated graphene oxide film as a proton exchange membrane. 2014. Angewandte Chemie International Edition. 53: 3588.

Higgins, D., G. Wu, H. T. Chung, U. Martinez, S. Ma, Z. Chen, and P. Zelenay. Manganese-based non-precious metal catalysts for oxygen reduction in acidic media. 2014. ECS Transactions. 61 (31): 35.

Holby, E. F., G. Wu, P. Zelenay, and C. D. Taylor. Modeling non-precious metal matalyst mtructures and mheir relationship to ORR activity. 2013. ECS Transactions. 58 (1): 1859.

Holby, E. F., and C. D. Taylor. Activity of N-coordinated multi-metal-atom active site structures for Pt-free oxygen reduction reaction catalysis: Role of *OH ligands. 2015. Scientific Reports. 5: 9286.

Holby, E. T., G. Wu, P. Zelenay, and C. D. Taylor. Structure of Fe-Nx-C defects in oxygen reduction reaction catalysts from first principles modeling. 2014. Journal of Physical Chemistry C. 118: 14388.

Hussey, D. S., D. L. Jacobson, D. Liu, B. Khaykovich, M. V. Gubarev, D. Spernjak, G. Wu, J. Fairweather, R. Mukundan, R. Lujan, P. Zelenay, and R. L. Borup. Neutron imaging of water transport in polymer-electrolyte membranes and membrane-electrode assemblies. 2013. ECS Transactions. 58 (1): 293.

Li, Q., K. Luo, Q. Kang, Y. He, Q. Chen, and Q. Liu. Lattice Boltzmann methods for multiphase flow and phase-change heat transfer. To appear in Progress in Energy and Combustion Science.

Liu, H., Q. Kang, C. R. Leonardi, B. D. Jones, S. Schmieschek, A. Narvaez, J. R. Williams, A. J. Valocchi, and J. Harting. Multiphase lattice Boltzmann simulations for porous media applications - a review. 2014. Computational Geosciences. eprint: 1404.7523.

Martinez, U., G. M. Purdy, E. F. Holby, K. Artyushkova, J. H. Dumont, A. Singh, N. H. Mack, P. Atanassov, D. A. Cullen, K. More, M. Chhowalla, P. Zelenay, A. M. Dattelbaum, A. Mohite, and G. Gupta. Critical Role of Intercalated Water for Electrocatalytically Active Nitrogen-

Doped Graphitic Systems. Science Advances.

Martinez, U., T. L. Williamson, K. Artyushkova, N. H. Mack, G. M. Purdy, J. H. Dumont, D. Kelly, W. Gao, A. M. Dattelbaum, A. Mohite, G. Gupta, and P. Zelenay. Thin-film non-precious metal model catalysts for oxygen reduction reaction. 2014. ECS Transactions. 64 (3): 293.

Wu, G., and P. Zelenay. Nanostructured Nonprecious Metal Catalysts for Oxygen Reduction Reaction. 2013. Accounts of Chemical Research. 46 (8): 1878.

Yalcin, S. E., C. Galande, R. Kappera, H. Yamaguchi, U. Martinez, K. A. Velizhanin, S. K. Doorn, A. M. Dattelbaum, M. Chhowalla, P. M. Ajayan, G. Gupta, and A. D. Mohite. Direct imaging of charge transport in progressively reduced graphene oxide using electrostatic force microscopy. 2015. ACS Nano. 9 (3): 2981–2988.

Yamaguchi, H., J. Granstrom, W. Nie, H. Sojoudi, T. Fujita, D. Voiry, M. Chen, G. Gupta, A. D. Mohite, S. Graham, and M. Chhowalla. Reduced graphene oxide thin films as ultrabarriers for organic electronics. 2013. Advanced Energy Materials. : DOI: 10.1002/aenm.201300986.

Phase Stability of Multi-Component Nanocomposites Under Irradiation

Blas P. Uberuaga
20130118DR

Abstract

The design of materials that are essentially "immune to radiation," as called for by DOE, is one of the grand challenges in the materials science discipline. This is because energetic radiation damages a material by a variety of very different mechanisms, such as void swelling, embrittlement, irradiation creep, and phase instabilities from radiation induced solute redistribution (RISR). Typically, the solution for one problem either has no effect on or exacerbates the other damage mechanisms. For example, using interfaces as sinks for vacancies and interstitials can reduce void swelling but the same interfaces that mitigate void swelling can increase RISR.

RISR causes phase instabilities that lead to catastrophic failure through embrittlement, fracture and corrosion. We examine an innovative solution to the chronic problem of radiation-induced phase instability: nanocomposite materials design via interfaces that minimize defect fluxes, which is the origin of RISR. We hypothesize several factors can be used to control defect fluxes and suppress RISR. Using a materials co-design R&D approach where experiments and multi-scale modeling are closely integrated to test our hypotheses, we have gained fundamental new insights of RISR to interfaces, and developed initial design principles for next-generation materials for nuclear energy applications that maintain chemical composition profiles that are critical for many materials properties in extreme environments.

Background and Research Objectives

Recent DOE workshops [1] have called for the development of materials that are "self-healing" or immune to radiation to enable future advanced nuclear energy systems. "Developing a first-principles description of mechanical properties and phase stability in multi-component, multiphase systems under extreme conditions" has been specifically called out as a grand challenge that involves many scientific issues, including [BES-ANES report, ref. 1].

While these reports call for "radiation tolerant materials," it is crucial to recognize that radiation damage is not a single problem; it is a generic umbrella that refers to a host of very different problems. Broadly, one can categorize these into two fundamentally different effects, see Figure 1 [2-7]. On the left, void swelling, caused by clustering of radiation-induced point defects (vacancies and interstitials), leads to void formation in materials resulting in swelling and embrittlement. Grain boundaries and interfaces are sinks for defects and can annihilate defects before they cluster, mitigating void swelling. On the right is a qualitatively different problem observed only in multi-component alloys, the current focus: radiation-induced solute redistribution (RISR). RISR leads to changes in the local chemical composition of the material, with enrichment of some and depletion of other solutes near interfaces. As the composition profile becomes heterogeneous near interfaces, new phases might form or enough segregation can occur to adversely affect properties, leading to brittle intergranular fracture, increase in the ductile-to-brittle transition temperature (DBTT), and accelerated stress corrosion cracking. Interfaces are the source of RISR. The end result of either void swelling or RISR is failure of the material, but the reasons are completely different.

Why does Cr deplete and Ni enrich at interfaces, as in Figure 1d? The literature provides the following insight [5,8,9]: at high temperatures, radiation-induced vacancies and interstitials migrate to interface sinks. Depending on how solutes couple to these defects, they will either be enriched or depleted at those interfaces. Different solutes couple differently with interstitial and vacancy fluxes. Many years of experimental effort have generated a substantial knowledge database and phenomenological models of RISR [10,11]. However, these models have little predictive power. Recent observations have shown that Cr enriches at GBs in ferritic-martensitic steels [12,13], the opposite behavior observed in fcc steels (Figure 1d). Cr is a vacancy diffuser. The under-

standing of interstitial solutes is poorer still, yet interstitial segregation can have a profound impact on interface brittleness. A key challenge is to understand how solutes segregate to sinks to develop predictive models of their behavior.

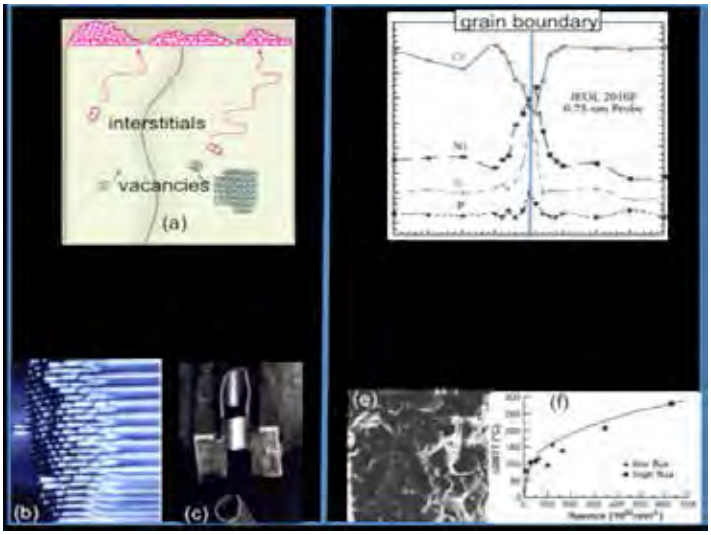

Figure 1. Two different aspects of radiation damage. : (a) schematic of radiation-induced defect agglomeration [2]; (b) swelling of fuel rods in a reactor [3]; (c) void-induced embrittlement of fuel cladding [4]. : (d) solute redistribution [5] at GBs in fcc steel due to radiation leading to (e) brittle intergranular fracture (irradiation-assisted stress corrosion cracking) [6] and (f) increase in DBTT [7].

The state-of-the-art of research in radiation damage is summarized in the BES-ANES report:

[I]t is often possible to empirically discover… materials that exhibit good resistance to a specific radiation damage process, but it is extremely challenging to develop a material that simultaneously exhibits high resistance to all the radiation damage mechanisms. [14]

As pointed out in Ref. [15], this is in large part due to RISR.

Guided by three hypotheses, we have examined how interfaces influence RISR in an effort to develop design principles that can guide future materials development. Our hypotheses are:

Hypothesis #1: RISR will depend on the atomic structure, chemistry and energetics of interfaces.

Hypothesis #2: RISR can be influenced by using intentionally added 'sacrificial' elements.

Hypothesis #3: For a given system and irradiation condition, solute redistribution will depend on spacing between interfaces.

In what follows, we describe our efforts in examining these hypotheses and the insight gained. We focus on Hypotheses #1 and #3. For several reasons, we were not able to pursue Hypothesis #2. However, during the course of the project, we developed a fourth hypothesis related to phase-stability under irradiation:

Hypothesis #4: The phase stability of chemically complex precipitates under irradiation is dictated by, and can be controlled by, the minor alloying element chemistry.

Scientific Approach and Accomplishments

Hypothesis #1

Hypothesis #1 states that the atomic structure and chemistry of interfaces will dictate RISR in a given materials system. To systematically study the role of interfaces on RISR, we developed a series of model metal/oxide two-dimensional bi-layer composite systems. We focused on metal/oxide composite systems as these most closely mimic the nanostructured ferritic alloys (NFAs) [16] that are of interest for advanced nuclear energy systems. Using magnetron sputtering, we deposited a series of oxide films on Fe-Cr alloys [17, 18]. These samples were then irradiated with ion beams. Once irradiated, they were then characterized using advanced microscopy techniques (transmission electron microscopy (TEM), electron dispersion spectroscopy (EDS), and electron energy-loss spectroscopy (EELS)). These techniques provide information about the structure and chemical evolution induced by the irradiation. Three systems were synthesized and analyzed: Fe+Cr/MgO, Fe+Cr/TiO2, and Fe+Cr/Y2O3. In each case, the system was annealed as well as irradiated, to separate out the role of temperature and radiation damage.

Figure 2 summarizes the results of these experiments. Each of the systems examined exhibits unique and surprising behavior. In the case of MgO, there is strong evidence of irradiation-assisted segregation of Cr to the interface, but no interdiffusion of Cr into the oxide. However, for both TiO2 and Y2O3, in addition to segregation from the Fe layer to the oxide, we see significant interdiffusion of Cr into the oxide itself. In the case of TiO2, this occurs to a limited degree during annealing, but is strongly enhanced by the irradiation such that the Cr completely interpenetrates the oxide. In the case of Y2O3, only minimal interdiffusion occurs during annealing. However, after irradiation, significant concentrations of Cr have diffused into the oxide.

Thus, important conclusions from these experiments are that (a) all of the metal/oxide interfaces attract Cr, (b) this attraction is strongly enhanced by the irradiation, and (c) in many cases there is significant interpenetration of Cr into the oxide. This interpenetration is often accompanied by phase changes. In the TiO2 and Y2O3 films, incorpo-

ration of Cr leads to amorphization of the oxide. This is particularly dramatic in the Y2O3 film, as bulk Y2O3 would not normally be susceptible to amorphization. Cr significantly enhances the rate of failure of these oxides. In the case of MgO, even more complicated phase changes have occurred, in which the Cr substitutes the Mg to form a crystalline spinel-like phase (MgCr2O4).

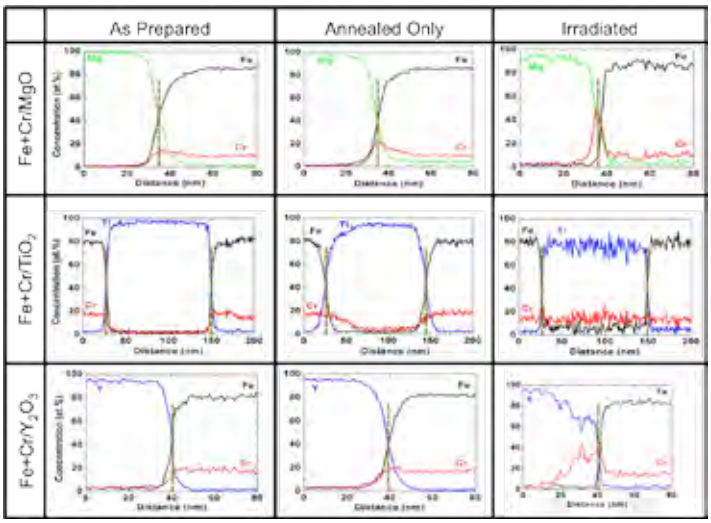

Figure 2. Chemical profiles at metal/oxide interfaces after both annealing and irradiation. Of particular interest is the distribution of Cr in the three sets of samples. The location of the interfaces are indicated by the dashed lines. The behavior of Cr both after annealing and after irradiation depends significantly on the nature of the interface.

Assisted by density functional theory (DFT) calculations, we have found that it is much easier for Cr to interdiffuse into these oxides than Fe. Thus, once the defects are created during the irradiation, Cr can diffuse into the oxide structures while Fe, even if it is forced into the oxide by the damage processes, will not mix with the oxide.

Together, the experiments and theory indicate that certain types of metal/oxide interfaces are much more stable against RISR than others. In particular, radiation-enhanced diffusion of Cr destabilizes many otherwise stabile interfaces. These results confirm hypothesis #1, that RISR, and the consequences of RISR, are very sensitive to the nature of the interfaces involved.

Hypothesis #3

Hypothesis #3 states that RISR can be controlled via the density of interfaces. This hypothesis is motivated by the fact that simple models found that, if the density of interfaces is increased, the flux of radiation-induced defects is reduced. Given that RISR depends on defect fluxes, we hypothesized that the flux of alloying elements is also influenced by interfacial density.

To test this hypothesis, we performed extensive kinetic Monte Carlo (KMC) simulations on the segregation of Cr to ideal sinks during irradiation. We specifically focused on a low damage flux regime, as this means that defects will not accumulate quickly and thus the concentration of defects will always be low, ideal conditions for the KMC simulations.

The KMC model simulations the motion of vacancies and interstitials in a Fe matrix, near an ideal sink. Cr atoms interact with the vacancies and interstitials and are thus pushed and pulled accordingly. Once defects reach the sink, they are “perfectly annihilated” meaning that the sink eliminates them from the system. Defects are generated at a given rate to mimic irradiation conditions in real experiments. Finally, the concentration of Cr and temperature are varied to determine how the observed behavior depend on these variables. The results provided in Figure 3 are for a particular condition.

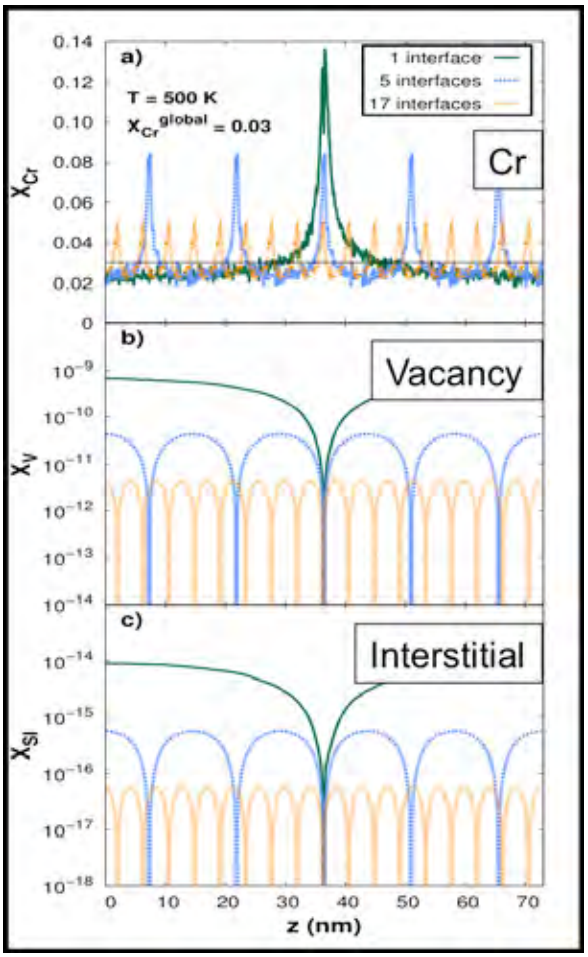

Figure 3. Results of kinetic Monte Carlo (KMC) simulations examining the behavior of Cr near ideal sinks as a function of sink spacing, or sink density. As the sink density is increased, the concentrations and fluxes of defects in the material decreases. This leads to lesser amounts of Cr segregation as the sink density is increased, mitigating RISR.

As hypothesized, and as shown in Figure 3, increasing the density of interfaces does indeed decrease the amount of Cr that segregates to those interfaces. As the interfacial density increases, the concentrations and, more importantly, the flux of interstitials and vacancies correspondingly decrease. This decreases the overall flux and build-up of Cr to the interfaces.

Hypothesis #4

The last hypothesis developed during the course of the project and focused on the stability of pre-existing chemical precipitates within the material under irradiation, states that this stability is a consequence of the minor chemical species in the precipitate. This hypothesis grew out of our experiments on engineering alloys showing that, under irradiation, the major elements within the material remained essentially where they were, but it was the minor elements that redistributed significantly and led to the instability of the material. This is illustrated in Figure 4, in which the engineering material Rene N4 was irradiated to various doses up to 75 dpa (displacements per atom) at room temperature [19]. Rene N4 is a Ni-based superalloy with many minor elements. In particular, the weight percent of those elements highlighted in Figure 4 are: 9.8% Al, 3.5% Ti, 7.5% Co, 9.8% Cr, and 1.5% Mo. Of these elements, Mo exhibits the greatest amount of redistribution under irradiation. By 0.75 dpa, the chemical structure of the other elements is strongly intact, but the distribution of Mo has become much more diffuse, originally residing at the interphase boundaries between the cuboids forming the structure and quickly becoming dispersed throughout the matrix. At the same time, structural ordering within the material is quickly lost during irradiation, with a concurrent drop in the mechanical hardness of the material. Given that the structural ordering is associated with the minor elemental species, this indicates that the mechanical properties of the material are very sensitive to the redistribution of these species under irradiation. Future work will work towards quantifying this effect and designing new alloying chemistries that mitigate radiation-induced disordering and dissolution of the material.

Phase Field Development

An important target of our research plan was the development of a phase field model, informed by atomistics, that could computationally probe the hypotheses to a level not possible with other computational approaches. In particular, because of the relative efficiency of the phase field approach, larger systems with more heterogeneities in terms of microstructure and chemistry could be considered. Unfortunately, development of the phase field model progressed more slowly than anticipated, for a number of reasons. Development accelerated with the addition of more personnel and we are close to a final model that will be able to examine more complex materials than our KMC capability currently can. Figure 5 shows results from the phase field simulations when ideal sinks are modeled. These are sinks that perfectly annihilate any defect that reaches them. The phase field model shows that there is a dependence on both the temperature and the Cr content for whether such sinks lead to Cr enhancement or depletion at the sinks. This is in qualitative agreement with recent results from CEA [20]. As the model is continued to be developed, more realistic sink behavior will be incorporated.

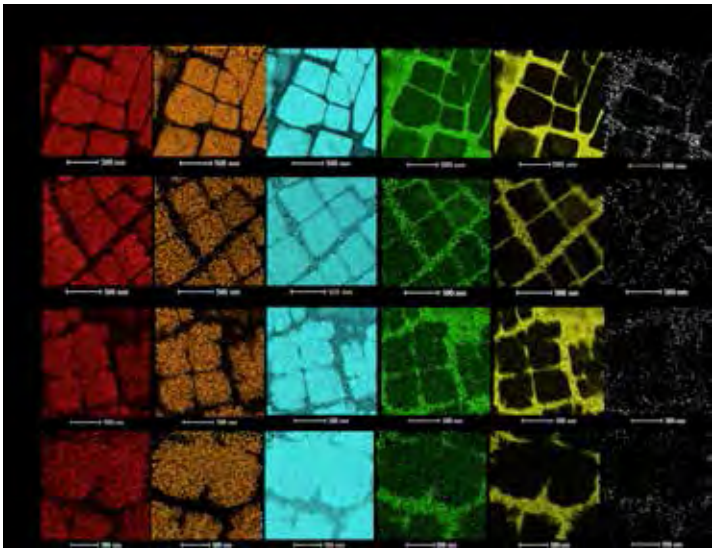

Figure 4. Chemical distributions within Rene N4 after irradiation to various doses. The distributions of the major elements remains mostly intact, even to the high doses, but the distribution of minor elements such as Mo becomes quickly dispersed, even at the lowest level of damage considered.

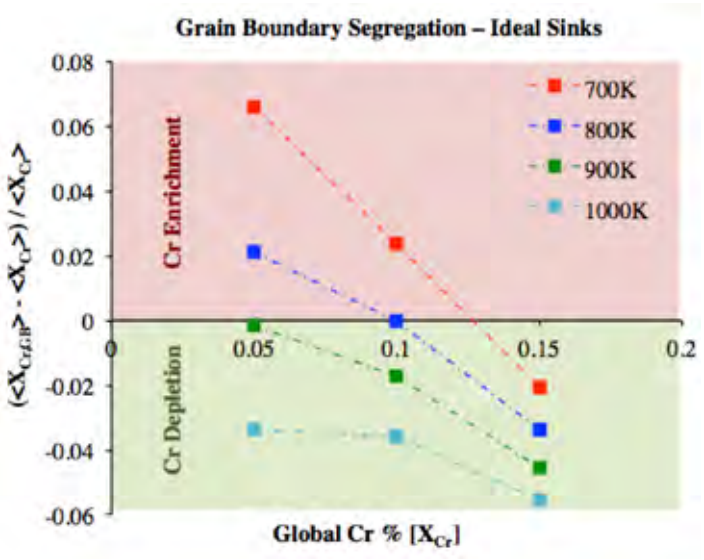

Figure 5. Phase field simulations showing the behavior of Cr near ideal sinks as a function of temperature and Cr concentra-

tion, revealing that whether Cr is enriched or depleted at the sinks depends on the irradiation conditions and the alloy content. The next step in developing this phase field model is to include more realistic properties for the sinks.

Summary

To summarize, we have proposed and tested several hypotheses that provide new insight into the design of advanced materials for nuclear energy applications that can mitigate radiation-induced segregation. In particular, we have demonstrated that, indeed, RISR is sensitive to the nature of the interfaces in the material, the density of interfaces in the material, and the minor alloying chemistry in the material

These insights provide new design principles for exploring new materials systems. In particular, nanostructured materials, already pursued to mitigate void swelling, may be just as effective at mitigating RISR. However, care must be made in choosing the appropriate composite materials. Some oxides, for example, will not only act as sinks for alloying elements, but will undergo potentially detrimental phase changes as a consequence of gettering those species.

This project has laid the foundation for future efforts in developing advanced materials in which more realistic chemistries are considered. It has provided new fundamental insights into the role of interfaces in influencing RISR that, in turn, provide new directions for developing materials that mitigate RISR. Finally, the capabilities developed during the course of this project should find utility in other scientific efforts ongoing within the laboratory. We are currently pursuing such opportunities.

Finally, as with all such projects, a number of other results were also generated. Due to a lack of space, we cannot highlight those here. However, they appear in our Reference list [21-31].

Impact on National Missions

As of now, while the work performed during the course of this project has motivated and inspired several proposals to outside funding agencies, particularly the Office of Nuclear Energy, no such proposals have won funding. We continue to be cognizant of funding opportunities that would leverage our work and capabilities. We expect that, once the phase field model has been completed, it will be of interest to internal programs. Further, the work in this project was highlighted during a recent workshop on developing research directions for the Office of Environmental Management. We thus expect that, once the results of that workshop have been evolved into a Funding Opportunity, we will be very competitive because of the fruits of this project.

Finally, a number of postdocs were converted to staff as a consequence of this project. In particular, Nan Li (MPA-CINT), Osman Anderoglu (MST-8), Enrique Martinez (MST-8), and Samrat Choudhury (MST-8) were postdocs who were converted to staff positions at least in part as a consequence of their involvement in this project.

References

1. DOE-BES Workshop Reports: Advanced Nuclear Energy Systems, Materials Under Extreme Environments; Scientific Grand Challenges in National Security: The Role of Computing at the Extreme Scale, DOE Workshop Report. 2007. DOE-BES Workshop Reports.
2. Ackland, G.. Controlling radiation damage. 2010. Science. 327: 1587.
3. Porollo, S. I., S. V. Shulepin, Y. V. Konobeev, and F. A. Garner. Influence of silicon on swelling and microstructure in Russian austenitic stainless steel EI-847 irradiated to high neutron doses. 2008. Journal of Nuclear Materials. 378: 17.
4. Garner, F. A., and D. L. Porter. Irradiation creep and swelling of AISI 316 to exposures of 130 dpa at 385–400 C. 1988. Journal of Nuclear Materials. 155: 1006.
5. Was, G. S.. Fundamentals of radiation materials science. 2007.
6. Busby, J. T., G. S. Was, and E. A. Kenik. Isolating the effect of radiation-induced segregation in irradiation-assisted stress corrosion cracking of austenitic stainless steels. 2002. Journal of Nuclear Materials. 302: 20.
7. Lu, Z., R. G. Faulkner, and P. E. J. Flewitt. The role of irradiation-induced phosphorus segregation in the ductile-to-brittle transition temperature in ferritic steels. 2006. Materials Science and Engineering: A. 437: 306.
8. Ardell, A. J.. Materials issues for generation IV systems. 2008. NATO Science for Peace and Security Series B - Physics and Biophysics.
9. Wiedersich, H., P. R. Okamoto, and N. Q. Lam. A theory of radiation-induced segregation in concentrated alloys. 1979. Journal of Nuclear Materials. 83: 98.
10. Was, G., and J. T. Busby. Role of irradiated microstructure and microchemistry in irradiation-assisted stress corrosion cracking. 2005. Philosophical Magazine. 85: 443.
11. Allen, T. R., and G. S. Was. Modeling radiation-induced segregation in austenitic Fe–Cr–Ni alloys. 1998. Acta Materialia. 46: 3679.
12. Gupta, G., Z. Jiao, A. N. Ham, J. T. Busby, and G. S. Was. Microstructural evolution of proton irradiated T91.

2006. Journal of Nuclear Materials. 351: 162.

13. Lu, Z., R. G. Faulkner, G. S. Was, and B. D. Wirth. Irradiation-induced grain boundary chromium microchemistry in high alloy ferritic steels. 2008. Scripta Materialia. 58: 878.

14. Klueh, R. L.. Elevated temperature ferritic and martensitic steels and their application to future nuclear reactors. 2005. International Materials Review. 50: 287.

15. Zinkle, S. J.. Fusion materials science: Overview of challenges and recent progress. 2005. Physics of Plasmas. 12: 058101.

16. Odette, G. R.. Recent progress in developing and qualifying nanostructured ferritic alloys for advanced fission and fusion applications. 2014. JOM. 66: 2427.

17. Xu, Y., S. K. Yadav, J. A. Aguiar, O. Anderoglu, J. K. Baldwin, Y. Q. Wang, J. A. Valdez, A. Misra, H. M. Luo, B. P. Uberuaga, and N. Li. Solute redistribution and phase stability at FeCr/TiO2-x interfaces under ion irradiation. 2015. Acta Materialia. 89: 364.

18. Xu, Y., S. K. Yadav, J. A. Aguiar, O. Anderoglu, J. K. Baldwin, Y. Q. Wang, A. Misra, H. M. Luo, B. P. Uberuaga, and N. Li. Irradiation-induced formation of a spinel phase at the FeCr/MgO interface. 2015. Acta Materialia. 93: 87.

19. Sun, C., M. Kirk, M. Li, K. Hattar, Y. Wang, O. Anderoglu, J. Valdez, B. P. Uberuaga, R. Dickerson, and S. A. Maloy. Microstructure, chemistry and mechanical properties of Ni-based superalloy Rene N4 under irradiation at room temperature. 2015. Acta Materialia. 95: 357.

20. Soisson, F.. Private communication. 2015. Private communication.

21. Choudhury, S., J. A. Aguiar, M. J. Fluss, L. L. Hsiung, A. Misra, and B. P. Uberuaga. Non-uniform solute segregation at semi-coherent metal/oxide interfaces. 2015. Scientific Reports. 5: 13086.

22. Lee, T., A. Caro, and M. J. Demkowicz. Atomistic modeling of radiation-induced disordering and dissolution at a Ni/Ni3Al interface. 2015. Journal of Materials Research. 30: 1456.

23. Martinez, E., and B. P. Uberuaga. Mobility and coalescence of small stacking fault tetrahedra in Cu. 2015. Scientific Reports. 5: 9084.

24. Sun, C., E. Martinez, J. A. Aguiar, A. Caro, J. A. Valdez, K. Baldwin, Y. Xu, B. P. Uberuaga, O. Anderoglu, and S. A. Maloy. Thermally induced interdiffusion and precipitation in a Ni/Ni3Al system. 2015. Materials Research Letters. 3: 169.

25. Watkins, E. B., Kashinath, Wang, J. K. Baldwin, Majewski, and M. J. Demkowicz. Characterization of a Fe/Y2O3 metal/oxide interface using neutron and x-ray scattering. 2014. APPLIED PHYSICS LETTERS. 105 (4).

26. Martinez, , B. P. Uberuaga, and A. F. Voter. Sublattice parallel replica dynamics. 2014. PHYSICAL REVIEW E. 89 (6).

27. Aguiar, J. A., O. Anderoglu, S. Choudhury, J. K. Baldwin, Y. Q. Wang, A. Misra, and B. P. Uberuaga. Nanoscale morphologies at alloyed and irradiated metal/oxide bilayers. 2015. Journal of Materials Science. 50: 2726.

28. Bach, H. T., O. Anderoglu, T. A. Saleh, T. J. Romero, C. T. Kelsey, E. R. Olivas, B. H. Sencer, P. O. Dickerson, M. A. Connors, K. D. John, and S. A. Maloy. Proton irradiation damage of an annealed Alloy 718 beam window. 2015. Journal of Nuclear Materials. 459: 103.

29. Senninger, , Martinez, Soisson, Nastar, and Brechet. Atomistic simulations of the decomposition kinetics in Fe-Cr alloys: Influence of magnetism. 2014. ACTA MATERIALIA. 73: 97.

30. Sun, C., S. Zheng, C. C. Wei, Y. Wu, L. Shao, Y. Yang, K. T. Hartwig, S. A. Maloy, S. J. Zinkle, T. R. Allen, H. Wang, and X. Zhang. Superion radiation-resistant nanoengineered austenitic 304L stainless steel for applications in extreme radiation environments. 2015. Scientific Reports. 5: 7801.

31. Yuryev, D. V., and M. J. Demkowicz. Computational design of solid-state interfaces using O-lattice theory. 2014. Applied Physics Letters. 105: 221601.

Publications

Aguiar, J. A., O. Anderoglu, S. Choudhury, J. K. Baldwin, Y. Q. Wang, A. Misra, and B. P. Uberuaga. Nanoscale morphologies at alloyed and irradiated metal/oxide bilayers. 2015. Journal of Materials Science. 50: 2726.

Bach, H. T., O. Anderoglu, T. A. Saleh, T. J. Romero, C. T. Kelsey, E. R. Olivas, B. H. Sencer, P. O. Dickerson, M. A. Connors, K. D. John, and S. A. Maloy. Proton irradiation damage of an annealed Alloy 718 beam window. 2015. Journal of Nuclear Materials. 459: 103.

Choudhury, S., J. A. Aguiar, M. J. Fluss, L. L. Hsiung, A. Misra, and B. P. Uberuaga. Non-uniform solute segregation at semi-coherent metal/oxide interfaces. 2015. Scientific Reports. 5: 13086.

Klaver, T. P. C., E. del Rio, G. Bonny, and A. Caro . Inconsistencies in modelling interstitials in FeCr with empirical potentials. Modelling and Simulation in Materials Science and Engineering.

Lee, T., A. Caro, and M. J. Demkowicz. Atomistic modeling of radiation-induced disordering and dissolution at a Ni/Ni3Al interface. 2015. Journal of Materials Research. 30: 1456.

Martinez, , B. P. Uberuaga, and A. F. Voter. Sublattice parallel replica dynamics. 2014. PHYSICAL REVIEW E. 89 (6).

Martinez, E., and B. P. Uberuaga. Mobility and coalescence of small stacking fault tetrahedra in Cu. 2015. Scientific Reports. 5: 9084.

Senninger, , Martinez, Soisson, Nastar, and Brechet. Atomistic simulations of the decomposition kinetics in Fe-Cr alloys: Influence of magnetism. 2014. ACTA MATERIALIA. 73: 97.

Senninger, O., F. Soisson, E. Martinez, M. Nastar, C. C. Fu, and Y. Brechet. Modeling radiation induced segregation in iron-chhromium alloys. Acta Materialia.

Sun, C., E. Martinez, J. A. Aguiar, A. Caro, J. A. Valdez, K. Baldwin, Y. Xu, B. P. Uberuaga, O. Anderoglu, and S. A. Maloy. Thermally induced interdiffusion and precipitation in a Ni/Ni3Al system. 2015. Materials Research Letters. 3: 169.

Sun, C., M. Kirk, M. Li, K. Hattar, Y. Wang, O. Anderoglu, J. Valdez, B. P. Uberuaga, R. Dickerson, and S. A. Maloy. Microstructure, chemistry and mechanical properties of Ni-based superalloy Rene N4 under irradiation at room temperature. 2015. Acta Materialia. 95: 357.

Sun, C., S. Zheng, C. C. Wei, Y. Wu, L. Shao, Y. Yang, K. T. Hartwig, S. A. Maloy, S. J. Zinkle, T. R. Allen, H. Wang, and X. Zhang. Superion radiation-resistant nanoengineered austenitic 304L stainless steel for applications in extreme radiation environments. 2015. Scientific Reports. 5: 7801.

Watkins, E. B., Kashinath, Wang, J. K. Baldwin, Majewski, and M. J. Demkowicz. Characterization of a Fe/Y2O3 metal/oxide interface using neutron and x-ray scattering. 2014. APPLIED PHYSICS LETTERS. 105 (4).

Xu, W., L. Li, J. A. Valdez, M. Saber, C. C. Koch, R. O. Scattergood, and Y. Zhu. Effect of nano-oxide particle size on radiation resistance of iron-chromium alloys. Journal of Nuclear Materials.

Xu, Y., S. K. Yadav, J. A. Aguiar, O. Anderoglu, J. K. Baldwin, Y. Q. Wang, A. Misra, H. M. Luo, B. P. Uberuaga, and N. Li. Irradiation-induced formation of a spinel phase at the FeCr/MgO interface. 2015. Acta Materialia. 93: 87.

Xu, Y., S. K. Yadav, J. A. Aguiar, O. Anderoglu, J. K. Baldwin, Y. Q. Wang, J. A. Valdez, A. Misra, H. M. Luo, B. P. Uberuaga, and N. Li. Solute redistribution and phase stability at FeCr/TiO2-x interfaces under ion irradiation. 2015. Acta Materialia. 89: 364.

Yuryev, D. V., and M. J. Demkowicz. Computational design of solid-state interfaces using O-lattice theory. 2014. Applied Physics Letters. 105: 221601.

Quantum Chemistry, Information, Materials and Metrology

Angel E. Garcia
20130727DR

Abstract

From quantum information to condensed matter materials, the tools of quantum mechanics underpin the science and enable the exploration of new ideas and opportunities for applications. We proposed an integrated and interdisciplinary set of problems including the quantum chemistry of nanoscale materials, quantum communication, information and computing, quantum frustration in materials, quantum magnets, cold atom physics, Casimir AMO physics, quantum phase transitions, and quantum metrology. Our approach integrates these topics by looking for unexpected synergies. For example, quantum information research provides new tools that can be applied to condensed matter problems. Similarly, new materials such as topological insulators may provide an effective medium for implementing quantum memory. We also explore fundamental topics such as quantum friction and novel materials with soft-matter-like phases and investigate practical applications such as sensing device with ultra-high sensitivity. Examples of the latter include scanned probes, cold atom magnetometry, and nano-scale opto-mechanical devices. The integration of these topics will build capability in quantum science and enable new exciting applications.

Background and Research Objectives

Quantum mechanics is at the center of the properties of matter at the microscopic level. These properties determine the macroscopic properties of materials. The goals of this project are to develop scientific progress at the interfaces of quantum chemistry and materials, quantum information, and quantum optics. Of particular interest are the relations between spectroscopic and chemical properties of organic nanomaterials. The tools of quantum chemistry are used to understand how chemical variations of nanomaterials change their properties. Spectroscopic properties of materials require the understanding of quantum excited-states. For this purpose, our interdisciplinary team developed and employed new theoretical methods, including time-dependent density functional and semi empirical methods, algorithms, and new computer codes. We also explored the intersection of quantum information, communications and computing with new materials such as chiral superconductors and topological insulators and also with novel detection technologies such as ultra sensitive scanned approaches. We studied how strong electronic correlations give rise to new topological materials. These materials have possible applications in photovoltaics, quantum computing, and in the development of advanced functional materials. Another areas of interest are the physics of ultracold atoms, Bose-Einstein condensates, and the possible use of these systems for quantum computing.

Scientific Approach and Accomplishments

Our scientific approach is based on the use of quantum theory and statistical mechanics, applied mathematics, and computational methods to study complex materials and systems under extreme conditions (e.g., ultra cold atoms). These approaches are combined with experimental data to validate our models. The methods developed are applied to specific problems of interest, and, through collaborations with experimental collaborators we help develop new nanomaterials. Our work on this project resulted in 73 publications in refereed journals. Here we present highlights of our accomplishments on this project.

The understanding of the electronic properties of materials is crucial for the design of new functional photoactive materials. When activated by light, organic materials show dynamics that is often characterized by large non-adiabatic couplings between multiple excited states. As part of this project, we developed a non-adiabatic excited state molecular dynamics (NA-ESMD) framework that describes photoinduced phenomena in (conjugated) organic materials [1]. These methods have been used to describe the planarization of polyfluorenes, and the energy transfer of poly phenylene vinulene (PPV), among other applications [2-8]. The NA-ESMD framework pro-

vides a computationally efficient and accurate description of photoinduced dynamics that cannot be accomplished by sophisticated ab initio methods.

In condensed matter theory we have studied the properties of magnetic systems. Magnets are natural realizations of gases of interacting bosons whose relevant parameters, such as dimensionality, lattice geometry, amount of disorder, nature of the interactions, and particle concentration can vary widely between different compounds [9]. The particle concentration can be easily tuned by applying an external magnetic field, which plays the role of a chemical potential. This rich spectrum of realizations offers a unique possibility for studying the different physical behaviors that emerge in interacting Bose gases from the interplay between their relevant parameters.

In this project we demonstrated that exotic magnetic vortex crystals can emerge near the magnetic field induced quantum critical point of frustrated magnets [10-11]. It is important to note that this was the first proposal for the observation of magnetic vortex lattices in Mott insulators. In addition, we demonstrated that frustration can change the nature of this quantum critical point in one-dimensional systems [12].

Also, by combining numerical and field theory techniques, we demonstrated that an antiferromagnetic Ising model on stacked triangular layers exhibits a very exotic phase diagram with a number of Berezinskii-Kosterlitz-Thouless transitions (0, 2 or 4) that depends on the number of layers [13]. In a similar context, we demonstrated the proliferation of Z6 vortices at the structural transition of a family of multi-ferroic materials [14].

An important part of this project is the organization of workshops in the areas of quantum physics and its application to nanomaterials and materials. In May 2013 we organized a workshop “Organic Solar Cells: Theory and Experiment, From Description to Prediction”. This workshop brought together the leading researchers in the field of organic semiconductors with the primary focus on photovoltaic applications. The emphasis was on deep understanding of fundamental processes occurring in organic solar cells, as well as on improving practical tools for modeling/characterization of existing and prediction/design of new photovoltaic materials and devices.

In February 2014 we organized the workshop “Information Science for Materials Discovery and Design”. The aim of this conference was to bring together the materials and information science communities to evaluate the opportunities and challenges in the emerging field of materials informatics. Researchers presented contrasting but complementary approaches, such as those based on high throughput calculations or data driven discovery, together with the merits of machine-learning methods to accommodate searches with multiple objectives or higher dimensional databases.

Impact on National Missions

The understanding of the electronic properties of materials is relevant to the properties of actinides and other f-electron systems. These materials are crucial for the laboratory and DOE mission on nuclear materials. The work on spectroscopic properties of organic nanomaterials is relevant to the development of efficient photovoltaics, which in turn are important for developing renewable energy devices. The work on ultracold atoms is relevant for quantum computing. We strongly impact DOE Office of Science mission in the fundamental understanding of electronic and magnetic materials with applications to energy, electronics, and computing. The algorithms and codes generated to study excited states contribute to our national competitiveness in high performance computing.

References

1. Nelson, , Fernandez-Alberti, A. E. Roitberg, and Tretiak. Nonadiabatic Excited-State Molecular Dynamics: Modeling Photophysics in Organic Conjugated Materials. 2014. ACCOUNTS OF CHEMICAL RESEARCH. 47 (4): 1155.

2. Fernandez-Alberti, , V. D. Kleiman, Tretiak, and A. E. Roitberg. Nonadiabatic Molecular Dynamics Simulations of the Energy Transfer between Building Blocks in a Phenylene Ethynylene Dendrimer. 2009. JOURNAL OF PHYSICAL CHEMISTRY A. 113 (26): 7535.

3. Nelson, , Fernandez-Alberti, A. E. Roitberg, and Tretiak. Artifacts due to trivial unavoided crossings in the modeling of photoinduced energy transfer dynamics in extended conjugated molecules. 2013. CHEMICAL PHYSICS LETTERS. 590: 208.

4. Nelson, , Fernandez-Alberti, A. E. Roitberg, and Tretiak. Nonadiabatic excited-state molecular dynamics: Treatment of electronic decoherence. 2013. JOURNAL OF CHEMICAL PHYSICS. 138 (22).

5. Nelson, , Fernandez-Alberti, A. E. Roitberg, and Tretiak. Conformational disorder in energy transfer: beyond Forster theory. 2013. PHYSICAL CHEMISTRY CHEMICAL PHYSICS. 15 (23): 9245.

6. Adamska, , Nayyar, Chen, A. K. Swan, Oldani, Fernandez-Alberti, M. R. Golder, Jasti, S. K. Doorn, and Tretiak. Self-Trapping of Excitons, Violation of Condon Ap-

proximation, and Efficient Fluorescence in Conjugated Cycloparaphenylenes. 2014. NANO LETTERS. 14 (11): 6539.

7. Ma, , Adamska, Yamaguchi, S. E. Yalcin, Tretiak, S. K. Doorn, and H. a. n. Htoon. Electronic Structure and Chemical Nature of Oxygen Dopant States in Carbon Nanotubes. 2014. ACS NANO. 8 (10): 10782.

8. Liu, J. i. n., Adamska, S. K. Doorn, and Tretiak. Singlet and triplet excitons and charge polarons in cycloparaphenylenes: a density functional theory study. 2015. PHYSICAL CHEMISTRY CHEMICAL PHYSICS. 17 (22): 14613.

9. Zapf, , Jaime, and C. D. Batista. Bose-Einstein condensation in quantum magnets (vol 86, 2014). 2014. REVIEWS OF MODERN PHYSICS. 86 (4).

10. Kamiya, , and C. D. Batista. Magnetic Vortex Crystals in Frustrated Mott Insulator. 2014. PHYSICAL REVIEW X. 4 (1).

11. Wang, , Kamiya, A. H. Nevidomskyy, and C. D. Batista. Three-Dimensional Crystallization of Vortex Strings in Frustrated Quantum Magnets. 2015. PHYSICAL REVIEW LETTERS. 115 (10).

12. Rahmani, , A. E. Feiguin, and C. D. Batista. Anyonic Liquids in Nearly Saturated Spin Chains. 2014. PHYSICAL REVIEW LETTERS. 113 (26).

13. Lin, , Kamiya, Chern, and C. D. Batista. Stiffness from Disorder in Triangular-Lattice Ising Thin Films. 2014. PHYSICAL REVIEW LETTERS. 112 (15).

14. Lin, , Wang, Kamiya, Chern, F. e. i. Fan, Fan, Casas, Y. u. e. Liu, Kiryukhin, W. H. Zurek, C. D. Batista, and Cheong. Topological defects as relics of emergent continuous symmetry and Higgs condensation of disorder in ferroelectrics. 2014. NATURE PHYSICS. 10 (12): 970.

Publications

Adamska, L., I. Nayyar, H. Chen, A. K. Swan, N. Oldani, S. Fernandez-Alberti, M. R. Golder, R. Jasti, S. K. Doorn, and S. Tretiak. Self-trapping of excitons, violation of Condon approximation and efficient fluorescence in conjugated cycloparaphenylenes. 2014. Nanotechnology Letters. 14 (11): 6539.

Baratz, A., A. White, and M. Galperin. Effects of electromagnetic coupling on conductance switching of a gated tunnel junction. 2014. Journal of Physical Chemistry Letters. 20: 3545.

Barros, K., and Y. Kato. Efficient langevin simulation of coupled classical fields and fermions. 2013. Physical Review B. 88: 235101.

Bechtold, A., D. Rauch, F. Li, T. Simmet, P. Ardelt, A. Regler, K. Müller, N. A. Sinitsyn, and J. J. Finley. Three-stage decoherence dynamics of an electron spin qubit in an optically active quantum dot. 2015. Nature Physics. : 1.

Behunin, R. O., D. A. R. Dalvit, R. Decca, and C. C. Speake. Limits on the accuracy of isoelectronic gravity measurements at short separation due to patch effects. 2014. Physical Review D. 89: 051301.

Bel, G., and F. L. Brown. Theory of single molecule emission spectroscopy. 2015. The Journal of Chemical Physics. 142 (17): 174104.

Bisset, R. N., C. Ticknor, and P. B. Blakie. Finite-resolution fluctuation measurements of a trapped Bose-Einstein condensate. 2013. Physical Review A. 88 (6): 063624.

Bisset, R. N., R. M. Wilson, and C. Ticknor. Scaling of fluctuations in a trapped binary condensate. 2015. Physical Review A. 91 (5): 053613.

Bjorgaard, J. A., K. A. Velizhanin, and S. Tretiak. Solvent effects in time-dependent self-consistent field methods. II. Variational formulations and analytical gradients. 2015. The Journal of Chemical Physics. 143 (5): 054305.

Bjorgaard, J. A., T. Nelson, K. Kalinin, V. Kuzmenko, K. A. Velizhanin, and S. Tretiak. Simulations of fluorescence solvatochromism in substituted PPV oligomers from excited state molecular dynamics with implicit solvent. 2015. Chemical Physics Letters. 631–632: 66.

Bjorgaard, J. A., and M. E. Kose. Simulations of Singlet Exciton Diffusion in Organic Semiconductors: A Review. 2015. RSC Advances. 5: 8432.

Campo, A. Del, and W. H. Zurek. Universality of phase transition dynamics: Topological defects from symmetry breaking. 2014. International Journal of Modern Physics A. 29 (08): 1430018.

Campo, A. del. Shortcuts to Adiabaticity by Counterdiabatic Driving. 2013. Physical Review Letters. 111 (10): 100502.

Campo, A. del, I. L. Egusquiza, M. B. Plenio, and S. F. Huelga. Quantum Speed Limits in Open System Dynamics. 2013. Physical Review Letters. 110 (5): 050403.

Campo, A. del, J. Goold, and M. Pasternostro. More bang for your buck: Towards super-adiabatic quantum engines. 2013. Scientific Reports. 4: 6208.

Campo, A. del., T. W. Kibble, and W. H. Zurek. Causality and non-equilibrium second-order phase transitions

in inhomogeneous systems. 2013. Journal of Physics: Condensed Matter. 25 (40): 325701.

Candia, R. D., J. S. Pedernales, A. d. Campo, E. Solano, and J. Casanova. Quantum Simulation of Dissipative Processes without Reservoir Engineering. 2015. Scientific Reports. 5.

Chen, H., Y. Y. Tai, C. S. Ting, M. J. Graf, J. Dai, and J. X. Zhu. Disorder effects in multiorbital s±-wave superconductors: Implications for Zn-doped BaFe2As2 compounds. 2013. Physical Review B. 88 (18): 184509.

Chern, G. W., C. C. Chien, and M. Di Ventra. Dynamically generated flat-band phases in optical kagome lattices. 2014. Physical Review A. 90 (1): 013609.

Chern, G., A. Rahmani, I. Martin, and C. Batista. Quantum Hall Ice. 2012. PHYSICAL REVIEW B.

Cimmarusti, A. ., Z. Yan, B. . Patterson, L. . Corcos, L. . Orozco, and S. Deffner. Environment-Assisted Speed-up of the Field Evolution in Cavity Quantum Electrodynamics. 2015. Physical Review Letters. 114 (23): 233602.

D'Alessio, L., and A. Rahmani. Thermally isolated Luttinger liquids with noisy Hamiltonians. 2013. Physical Review B. 87 (17): 174301.

Deffner, S.. Ten years of Nature Physics: From spooky foundations. 2015. Nature Physics. 11 (5): 383.

Deffner, S., and A. Saxena. Jarzynski Equality in PT-Symmetric Quantum Mechanics. 2015. Physical Review Letters. 114 (15): 150601.

Delgado, F., C. D. Batista, and J. Fernando-Rosa. Local probe of fractional edge states of S=1 Heisenberg spin chains. 2013. Physical Review Letters. 111 (16): 167201.

Gan, Z., H. Wu, K. Barros, Z. Xu, and E. Luijten. Comparison of efficient techniques for the simulation of dielectric objects in electrolytes. 2015. Journal of Computational Physics. 291: 317.

Glasenapp, P., N. A. Sinitsyn, L. Yang, D. G. Rickel, D. Roy, A. Grelich, M. Bayer, and S. A. Crooker. Spin noise spectroscopy beyond thermal equilibrium and linear response. 2014. Physical Review Letters. 113 (15): 156601.

Impens, F., R. Behunin, C. C. Ttira, and P. Maia. Neto. Nonlocal double-path Casimir phase in atom interferometers. 2013. EPL (Europhysics Letters). 101 (6): 60006.

Intravaia, F., R. O. Behunin, and D. A. Dalvit. Quantum friction and fluctuation theorems. 2014. Physical Review A. 89: 050101.

Kamiya, Y., and C. Batista. Magnetic vortex crystals in frustrated Mott insulator. 2014. Physical Review X. 4: 011023.

Karzig, T., A. Rahmani, F. von Oppen, and G. Refael. Optimal control of Majorana zero modes. 2015. Physical Review B. 91 (20): 201404.

Kato, Y.. Multidiscontinuity algorithm for world-line Monte Carlo simulations. 2013. Physical Review E. 87 (1): 013310.

Kilina, S., D. Kilin, and S. Tretiak. Light-Driven and Phonon-Assisted Dynamics in Organic and Semiconductor Nanostructures. 2015. Chemical Reviews. 115 (12): 5929.

Kim, J. W., Y. Kamiya, E. D. Mun, M. Jaime, N. Harrison, H. Yi, Y. S. Oh, S. W. Cheong, C. D. Batista, and V. S. Zapf. Coexistence of Ising and Heisenberg moments in multiferroic Ca3Co2-xMnxO6. 2014. Physical Review B. 89: 060404.

Kim, J. W., Y. Kamiya, E. D. Mun, M. Jaime, N. Harrison, J. D. Thompson, H. T. Yi, Y. S. Oh, S. W. Cheong, C. D. Batista, and V. S. Zapf. Multiferroicity with coexisting isotropic and anisotropic spins in Ca3Co2−xMnxO6. 2014. Physical Review B. 89: 060404.

Knolle, J., G. W. Chern, D. I. Kovrizhin, R. Moessner, and N. B. Perkins. Raman Scattering Signatures of Kitaev Spin Liquids in A2IrO3 Iridates with A=Na or Li. . 2014. Physical Review Letters. 113: 187201.

Koutroulakis, G., T. Zhou, C. D. Batista, Y. Kamiya, J. D. Thompson, S. E. Brown, and H. D. Zhou. Magnetic Phases of the Spin-1/2 Triangular-Lattice Antiferromagnet Ba3CoSb2O9. 2015. Physical Review B. 91: 024410.

Li, F., A. Saxena, D. Smith, and N. Sinitsyn. Higher-order spin noise statistics. 2013. New Journal of Physics. 15 (11): 113038.

Li, H., M. Catanzaro, S. Tretiak, and V. Chernyak. Excited-State Structure Modifications Due to Molecular Substituents and Exciton Scattering in Conjugated Molecules. 2014. Journal of Physical Chemistry Letters. 5 (4): 641.

Li, H., S. Malinin, S. Tretiak, and V. Chernyak. Effective tight-binding models for excitons in branched conjugated molecules. 2013. The Journal of Chemical Physics. 139 (6): 064109.

Lin, S. Z., X. Wang, Y. Kamiya, and G. W. Chern. Topological defects as relics of emergent continuous symmetry and Higgs condensation of disorder in ferroelectrics. 2014. Nature Physics. 10: 970.

Lin, S., Y. Kamiya, G. W. Chern, and C. D. Batista. Stiffness

from disorder in triangular-lattice ising thin films. 2014. Physical Review Letters. 112 (15): 155702.

Lin, S., and D. Roy. Role of kinetic inductance in transport properties of shunted superconducting nanowires. 2013. Journal of Physics: Condensed Matter. 25 (32): 325701.

Liu, J., L. Adamska, S. K. Doorn, and S. Tretiak. Singlet and triplet excitons and charge polarons in cycloparaphenylenes: a density functional theory study. 2015. Physical Chemistry Chemical Physics. 17 (22): 14613.

Mun, E. D., G. W. Chern, V. Pardo, F. Rivadulla, R. Sinclair, V. S. Zapf, and C. D. Batista. Magnetic field induced transition in vanadium spinels. 2014. Physical Review Letters. 112 (1): 017207.

Muniz, R., Y. Kato, and C. D. Batista. Generalized spin-wave theory: application to the bilinear-biquadratic model. 2014. PTEP. : 083I01.

Nei, W., H. Tsai, R. Asadpour, J. C. Blancon, A. J. Neukirch, G. Gupta, J. Crochet, M. Chhowalla, S. Tretiak, M. Alam, H. L. Wang, and A. Mohite. High efficiency solution-processed Perovskite solar cells with millimeter-scale grains. 2015. Science. 347 (6221): 522.

Nelson, T., S. Fernandez-Alberti, A. E. Roitberg, and S. Tretiak. Artifacts due to trivial unavoided crossings in the modeling of photoinduced energy transfer dynamics in extended conjugated molecules. 2013. Chemical Physics Letters. 590: 208.

Pershin, Y., V. Slipko, D. Roy, and N. Sinitsyn. Two-beam spin noise spectroscopy. 2013. Applied Physics Letters. 102 (20): 202405.

Pyka, K., J. Keller, H. L. Partner, R. Nigmatullin, T. Burgermeister, D. M. Meier, K. Kuhlmann, A. Retzker, M. B. Plenio, W. H. Zurek, A. del Campo, and T. E. Mehlstäubler. Topological defect formation and spontaneous symmetry breaking in ion Coulomb crystals. 2013. Nature Communications. 4: 3291.

Rahmani, A.. Quantum dynamics with an ensemble of hamiltonians. 2013. Modern Physical Letters B. 27 (26): 1330019.

Rahmani, A., R. Muniz, and I. Martin. Anyons in Integer Quantum Hall Magnets. 2013. Physical Review X. 3 (3): 031008.

Rahmani, A., T. Kitagawa, E. Demler, and C. Chamon. Cooling through optimal control of quantum evolution. 2013. Physical Review A. 87 (4): 043607.

Rahmani, A., and G. Chern. Universal Rényi mutual information in classical systems: The case of kagome ice. 2013. Physical Review B. 88 (5): 054426.

Roy, D.. Cascaded two-photon nonlinearity in a one-dimensional waveguide with multiple two-level emitters. 2013. Scientific Reports. 3: 02337.

Roy, D.. Two-photon scattering of a tightly focused weak light beam from a small atomic ensemble: An optical probe to detect atomic level structures. 2013. Physical Review A. 87 (6): 063819.

Roy, D., L. Yang, S. Crooker, and N. Sinitsyn. Cross-correlation spin noise spectroscopy of heterogeneous interacting spin systems. 2014. Nature.

Roy, D., L. Yang, S. Crooker, and N. Sinitsyn. Cross-correlation spin noise spectroscopy of heterogeneous interacting spin systems. 2015. Nature Scientific Reports. 5: 9573.

Roy, D., N. Bondyopadhaya, and S. Tewari. Topologically trivial zero-bias conductance peak in semiconductor Majorana wires from boundary effects. 2013. Physical Review B. 88 (2): 020502.

Roy, D., Y. Li, A. Greilich, Y. Pershin, A. Saxena, and N. Sinitsyn. Spin noise spectroscopy of quantum dot molecules. 2013. Physical Review B. 88 (4): 045320.

Roy, D., and N. Bondyopadhaya. Statistics of scattered photons from a driven three-level emitter in a one-dimensional open space. 2014. Physical Review A. 89 (4): 043806.

Savukov, I., T. Karaulanov, and M. G. Boshier. Ultra-sensitive high-density Rb-87 radio-frequency magnetometer. 2014. Applied Physics Letters. 104 (2): 023504.

Savukov, I., and T. Karaulanov. Magnetic-resonance imaging of the human brain with an atomic magnetometer. 2013. Applied Physics Letters. 103 (4): 043703.

Savukov, I., and T. Karaulanov. Anatomical MRI with an atomic magnetometer. 2013. Journal of Magnetic Resonance. 231: 39.

Savukov, I., and T. Karaulanov. Multi-flux-transformer MRI detection with an atomic magnetometer. 2014. Journal of Magnetic Resonance. 249: 49.

Shimada, H., J. L. Jacobsen, and Y. Kamiya. Phase diagram and the strong-coupling fixed point in the disordered O(n) loop model. 2013. Journal of Physics A. 47: 122001.

Sonner, J., A. del Campo, and W. H. Zurek. Universal far-from-equilibrium dynamics of a holographic superconductor. 2015. Nature Communications. 6: 7406.

Torrontegui, E., S. Ibáñez, S. Martínez-Garaot, M. Modugno, A. del Campo, D. Guéry-Odelin, A. Ruschhaupt, X. Chen, and J. G. Muga. Chapter 2 - Shortcuts to Adia-

baticity. 2013. In Advances in Atomic, Molecular, and Optical Physics. Edited by Arimondo, E., P. R. Berman, and C. C. Lin. Vol. Volume 62, p. 117. -: Elsevier.

Wang, Z., Y. Kamiya, A. H. Nevidomskyy, and C. D. Batista. Three-Dimensional Crystallization of Vortex Strings in Frustrated Quantum Magnets. 2015. Physical Review Letters. 115 (10): 107201.

White, A. J., V. N. Gorshkov, S. Tretiak, and D. Mozyrsky. Non-adiabatic molecular dynamics by accelerated semiclassical Monte Carlo. 2015. The Journal of Chemical Physics. 143 (1): 014115.

White, A., S. Tretiak, and M. Galperin. Raman scattering in molecular junctions: a pseudoparticle formulation. 2014. Nano Letters. 14 (2): 699.

White, C. E., N. J. Henson, L. L. Daemen, M. Hartl, and K. Page. Uncovering the True Atomic Structure of Disordered Materials: The Structure of a Hydrated Amorphous Magnesium Carbonate (MgCO3·3D2O). 2014. Chemistry of Materials. 26 (8): 2693.

Zhang, Z., K. Wierschem, I. Yap, Y. Kato, C. Batista, and P. Sengupta. Phase diagram and magnetic excitations of anisotropic spin-one magnets. 2013. Physical Review B. 87 (17): 174405.

Non-Equilibrium Phenomena in Materials, Fluids, and Climate

Angel E. Garcia
20130728DR

Abstract

Materials and fluids are, on macroscopic scales, governed by continuous classical fields, often exhibiting highly nonlinear phenomena under non-equilibrium conditions. On the microscopic scale, however, the granularity of the system can become important and interesting new behavior emerges from the particle discreteness. A variety of non-equilibrium processes that involve both regimes were investigated in this project. We used simulations of atomic interactions on intermediate length scales to characterize the properties of geopolymer concretes and compared with data from neutron scattering studies, investigated a coupled granular continuum model of earthquake dynamics, described complex interactions arising in colloidal particle suspensions, developed new algorithms and mathematical approaches to fluid flow in porous media to help assess carbon sequestration scenarios and enhanced hydraulic fracture methods, and probed the fundamental flow properties of rotating and/or stratified fluids. We also explored exciting areas of plasma physics including wave-particle interactions in the Earth's magnetosphere using kinetic simulations and magnetic reconnection in coupled fluid and magnetic field models of real plasmas. In all these areas, we focused on both science and application to solve national challenges in energy, climate, and environment. The approach was primarily theory and modeling with application to related experimental efforts involving neutron scattering, earthquake laboratory studies, and physical realizations of rotating and/or stratified fluid systems. Our interdisciplinary approach helped bridge these problems and suggest multi-scale methods to couple discreteness to continuum field models. Our work was well aligned with LANL materials strategy, had strong components of information science and technology to deal with data management and analysis, and broadly supported capability in physics, applied math, materials science, and climate science.

Background and Research Objectives

Systems driven far from equilibrium constitute many of the most difficult scientific challenges of the modern era. Some prominent examples are materials strength, where plastic (irreversible) motion involves the interactions of many dislocations as a material is strained past its elastic limit, fluid turbulence – a venerable problem involved in transport of heat in oceans and atmospheres as well as in the sun and Earth's interior, plasma instability associated with the interaction of the Earth's magnetosphere with the solar wind and with the generation of that wind through coronal mass ejection, the intrinsic behavior of materials with unique properties arising from geometric frustration, and the behavior of fluid flow in porous media which is important in carbon sequestration scenarios, oil extraction methodologies, and improved hydraulic fracture technologies. Our research objectives including developing novel algorithms to more effectively study these difficult problems, providing unique quantitative understanding of mechanisms that form the basis for practical applications, and discover new scientific principals underlying the physics of complex systems.

Scientific Approach and Accomplishments

This project has developed collaborative scientific progress in materials, soft matter, fluid dynamics and plasma physics, all of which manifest important and challenging aspects of systems driven out of equilibrium. Our scientific approach melds theory, modeling, and numerical simulation using tools of nonlinear science, statistical physics, applied mathematics, and advanced scientific algorithms. In some cases, we also collaborate with or directly perform experimental investigations that complement the theory/modeling/simulation approach. Our work resulted in over 50 publications in refereed journals so we present here some of the highlights of our research efforts.

In this project, we focused on the structure and dynamics of a variety of materials of importance in funda-

mental science and in applications. The manufacture and preparation of conventional concrete releases significant amounts of carbon dioxide, a greenhouse gas. Geopolymer concrete is a material that can substitute for conventional concrete but its properties are still being explored and discovered. Using a combination of molecular dynamics modeling and scattering experiments (neutrons and x-rays), we have advanced the structural characterization of these promising materials [1]. Another novel new material, that takes advantage of geometric frustration to create novel structural properties, is artificial spin ice for which much of the theory has been developed by CNLS postdocs. In this project, we proposed a new material structure by considering geometric frustration on an irregular lattice structure [2], providing a window into possible applications in which topological effects produce advanced functional materials. We also developed a new approach to creating novel structures using nanotechnology [3]. Our work on elastic-plastic deformation encompassed the coupling of granular material with a continuum elastic material to replicate stick-slip motion in earthquakes, the characterization of interfacial defects [4], a possible explanation for the anomalous behavior of solid helium, and the onset of irreversibility in amorphous solids under periodic shear. Using similar computational tools, we explored the classical response to driving of topological arrangements of spins called "skyrmions" [5].

Solitons are a classical nonlinear solution to wave equations that arise in many systems including Bose-Einstein condensates and optical fibers. In our work, we showed how these soliton systems could become unstable through nonlinear interactions despite being seemingly quite stable from a linear (small amplitude) perspective [6]. We described many other interesting properties of these nonlinear states. We also applied our methodology to traveling waves in granular systems [7].

Our research on fluid flows in porous media and fractured rock sought to yield insights into the complicated nature of sedimentary formations under the Earth's surface. In one approach, we investigated the flow regimes for fluid injection into a confined porous medium [8]. In another, we developed an algorithm for explicitly generating pore structures (see Figure 1) similar to those created by hydraulic fracture [9]. We held a conference entitled "Grand Challenges in Geological Fluid Dynamics" in September 2015 under the auspices of this project that brought together many world experts from academic, governmental and industrial institutions to explore novel theoretical, empirical, numerical and experimental approaches to subsurface fluid processes.

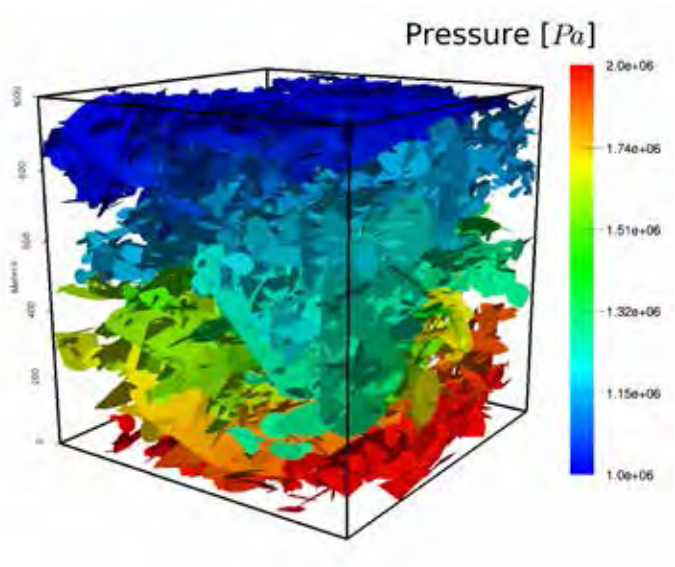

Figure 1. Geophysical rock domain with complex structure of rock fracture filled with fluid computed using a novel algorithm. Pore pressure is shown as color coded with pressure difference vertical from bottom to top.

Fluid dynamics underpins both the short and long term evolution of the Earth's oceans and atmospheres, i.e., weather and climate, and controls, through stratification and rotation, the eruption of coronal mass ejections on the sun, the transport of heat in the core of the earth, and the mixing necessary for understanding supernova explosions. In this area, we studied how turbulent shear flows induce fluid mixing using a combination of experimental measurements and novel data analysis [10]. Such flows develop in key portions of the oceanic large-scale circulation that controls the global distribution of heat. Parameterizing the mixing properties of such flows is critical for modeling climate evolutions. Another accomplishment was extending the domain of measurements of heat transport in thermal convection under rotation [11], a system highly relevant to stellar convection and to Earth's outer core transport. We also used equations for general rotating and stratified flows to develop a novel new algorithm to speed up computations in systems where there is a combination of slow fluid modes and fast wave modes such as exist in the atmosphere and ocean [12]. We applied this in several contexts including a rotating and stratified atmosphere [13]. Rotation and stratification both drive fluid systems to be more planar, i.e., they create flows that are anisotropic and in certain limits they approach a quasi two-dimensional fluids. We conducted experiments and analysis on a laboratory based two-dimensional fluid as an analog of the more complex geophysical system [14]. Our conference entitled "Ocean Turbulence" in 2013 brought together world experts in all aspects of turbulence in ocean flows, building on our continuing work in fluid dynamics and our interactions with climate modeling efforts at Los Alamos.

When fluids are conducting, they can become unstable to a combination of hydrodynamic and magnetic instabilities. Such fluids are known as "magnetohydrodyamic" and can support the spontaneous generation of a magnetic field through a dynamo effect and the reordering (or reconnection) of magnetic field lines as those lines are acted upon by hydrodynamic forces. Indeed, magnetic reconnection is one of the most important and poorly understood phenomena in astrophysics. In Figure 2, we illustrate a "tearing mode" instability from a 3D calculation of a two-fluid model of magnetic reconnection. We also suggested that conventional explanations of magnetic reconnection may be incorrect in not properly including the properties of the turbulence [15]. Finally, we performed an analysis of the role of the magnetic field geometry in determining the dynamic properties for a 2013 magnetic storm, where the Van Allen Probes observed very rapid electron accelerations. Our work [16] shows that conventional dipolar descriptions work well for higher energy electrons but that details of the magnetic field determine the motions of lower energy electrons.

Figure 2. Three dimensional realization of magnetic reconnection illustrating tearing mode mechanism computed using a two-fluid plasma model in a triply-periodic domain. Lines denote magnetic field lines and color map shows charge density.

Impact on National Missions

The materials research that we performed is in the mesoscopic regime, an important area for the MaRIE program and is applicable to recent DOE/BES priorities in fundamental materials research. Our work on the fundamentals of earthquakes may find application in the detection and triggering of earthquakes. The theoretical work on subsurface flows is relevant to energy recovery and carbon sequestration efforts in Applied Energy Programs. We continue to work on geophysically motivated problems relevant to climate evolution and developed a novel parallel-in-time algorithm that may find application in those efforts. The space plasma applications are relevant to global security efforts. We sponsor postdoctoral fellows working in areas relevant to the Laboratory mission. These postdoctoral fellows are candidates for future staff positions at the Laboratory.

References

1. Provis, J., A. Hajimohammadi, C. White, S. Bernal, R. Myers, R. Winarski, V. Rose, T. Proffen, A. Llobet, and J. J. van Deventer. Nanostructural characterization of geopolymers by advanced beamline techniques. 2013. Cement and Concrete Composites. 36: 56.

2. Gilbert, I., G. W. Chern, S. Zhang, L. OBrien, B. Fore, C. Nisoli, and P. Schiffer. Emergent ice rule and magnetic charge screening from vertex frustration in artificial spin ice. 2014. Nature Physics. 10 (9): 670.

3. Chern, G. W., C. Reichhardt, and C. Nisoli. Realizing three-dimensional artificial spin ice by stacking planar nano-arrays. 2014. Applied Physics Letters. 104 (1): 013101.

4. Wang, J., R. Zhang, C. Zhou, I. Beyerlein, and A. Misra. Characterizing interface dislocations by atomically informed Frank-Bilby theory. 2013. Journal of Materials Research. 28 (13): 1646.

5. Reichhardt, C., D. Ray, and C. J. Reichhardt. Collective Transport Properties of Driven Skyrmions with Random Disorder. 2015. Phys. Rev. Lett.. 114: 217202.

6. Kevrekidis, P. ., D. . Pelinovsky, and A. Saxena. When Linear Stability Does Not Exclude Nonlinear Instability. 2015. Physical Review Letters. 114 (21): 214101.

7. Xu, H., P. G. Kevrekidis, and A. Stefanov. Traveling waves and their tails in locally resonant granular systems. 2015. Journal of Physics A: Mathematical and Theoretical. 48 (19): 195204.

8. Zheng, Z., B. Guo, I. Christov, M. Celia, and H. Stone. Flow regimes for fluid injection into a confined porous medium. 2015. Journal of Fluid Mechanics. 767: 881.

9. Hyman, J. D., and C. L. Winter. Stochastic generation of explicit pore structures by thresholding Gaussian random fields. 2014. Journal of Computational Physics. 277: 16.

10. Odier, P., J. Chen, and R. Ecke. Entrainment and mixing in a laboratory model of oceanic overflow. 2014. Journal of Fluid Mechanics. 746: 498.

11. Ecke, R., and J. Niemela. Heat transport in the geostrophic regime of rotating Rayleigh-Bernard convec-

tion. 2014. Physics Review Letters. 113: 114301.

12. Haut, T., and B. Wingate. An asymptotic parallel-in-time method for highly oscillatory PDEs. 2014. SIAM Journal of Scientific Computing. 36 (2): A693.

13. Whitehead, J. P., T. Haut, and B. Wingate. The effect of two distinct fast time scales in the rotating stratified Boussinesq equations. 2015. IMA Journal of Numerical Analysis. : 1.

14. Rivera, M., H. Aluie, and R. Ecke. The direct enstrophy cascade of two-dimensional soap film flows. 2014. Physics of Fluids. 26 (5): 055105.

15. Eyink, G., E. Vishniac, C. Lalescu, H. Aluie, K. Kanov, K. Bürger, R. Burns, C. Meneveau, and A. Szalay. Flux-freezing breakdown in high-conductivity magneto-hydrodynamic turbulence. 2013. Nature. 497 (7450): 466.

16. Zhao, L., Y. Yu, G. L. Delzanno, and V. K. Jordanova. Bounce averaged diffusion coefficients in a physics based magnetic field geometry from RAM-SCB. 2015. Journal of Geophysical Research: Space Physics. 120 (4): 2616.

Publications

Aluie, H.. Scale decomposition in compressible turbulence. 2013. Physica D: Nonlinear Phenomena. 247 (1): 54.

Barros, K., and W. Klein. Liquid to solid nucleation via onion structure droplets. 2013. Journal of Chemical Physics. 139 (17): 174505.

Beylkin, G., and T. S. Haut. Nonlinear approximations for electronic structure calculations. 2013. Proceedings of the Royal Society A. 469 (2158): 20130231.

Chern, C. W., M. Morrison, and C. Nisoli. Degeneracy and criticality from emergent frustration in artificial spin ice. 2013. Physical Review Letters. 111 (17): 177201.

Chern, G. W., C. Reichhardt, and C. J. Olson Reichhardt. Avalanches and disorder-induced criticality in artificial spin ices. 2014. New Journal of Physics. 16 (6): 063051.

Chern, G. W., C. Reichhardt, and C. Nisoli. Realizing three-dimensional artificial spin ice by stacking planar nano-arrays. 2014. Applied Physics Letters. 104 (1): 013101.

Christov, I. C., and P. M. Jordan. Corrections to Morse and Ingard's variational-based treatment of weakly-nonlinear acoustics in lossless gases. 2015. The Journal of the Acoustical Society of America. 138 (1): 361.

Christov, I., R. Lueptow, J. Ottino, and R. Sturman. A study in three-dimensional chaotic dynamics: granular flow and transport in a bi-axial spherical tumbler. 2014. SIAM Journal on Applied Dynamical Systems. 13 (2): 901.

Christov, I., and H. A. Stone. Shear dispersion in dense granular flows. 2014. Granular Matter. 16 (4): 509.

Christov, I., and P. M. Jordan. On an instability exhibited by the ballistic-diffusive heat conduction model of Xu and Hu. 2014. Proceedings of the Royal Society A. 470 (2161): 20130557.

Chu, H., C. Zhou, J. Wang, and I. J. Beyerlein. An Analytical Model for the Critical Shell Thickness in Core/Shell Nanowires Based on Crystallographic Slip. 2013. J. 61 (11): 2147.

Ecke, R. E.. Scaling of heat transport near onset in rapidly rotating convection. 2015. Physics Letters A. 379 (37): 2221.

Ecke, R., and J. Niemela. Heat transport in the geostrophic regime of rotating Rayleigh-Bernard convection. 2014. Physics Review Letters. 113: 114301.

Eyink, G., E. Vishniac, C. Lalescu, H. Aluie, K. Kanov, K. Bürger, R. Burns, C. Meneveau, and A. Szalay. Flux-freezing breakdown in high-conductivity magnetohydrodynamic turbulence. 2013. Nature. 497 (7450): 466.

Gertjerenken, B., and P. G. Kevrekidis. Effects of interactions on the generalized Hong–Ou–Mandel effect. 2015. Physics Letters A. 379 (30–31): 1737.

Gilbert, I., G. W. Chern, S. Zhang, L. OBrien, B. Fore, C. Nisoli, and P. Schiffer. Emergent ice rule and magnetic charge screening from vertex frustration in artificial spin ice. 2014. Nature Physics. 10 (9): 670.

Haim, L., A. Hagberg, and E. Meron. Non-monotonic resonance in a spatially forced Lengyel-Epstein model. 2015. Chaos: An Interdisciplinary Journal of Nonlinear Science. 25 (6): 064307.

Haut, T. S., T. Babb, P. G. Martinsson, and B. A. Wingate. A high-order scheme for solving wave propagation problems via the direct construction of an approximate time-evolution operator. 2014. arXiv.

Haut, T. S., T. Babb, P. G. Martinsson, and B. A. Wingate. A high-order time-parallel scheme for solving wave propagation problems via the direct construction of an approximate time-evolution operator. 2015. IMA Journal of Numerical Analysis.

Haut, T., and B. Wingate. An asymptotic parallel-in-time method for highly oscillatory PDEs. 2014. SIAM Journal of Scientific Computing. 36 (2): A693.

Hyman, J. D., and C. L. Winter. Stochastic generation of ex-

plicit pore structures by thresholding Gaussian random fields. 2014. Journal of Computational Physics. 277: 16.

Karamatskos, E. T., J. Stockhofe, P. G. Kevrekidis, and P. Schmelcher. Stability and tunneling dynamics of a dark-bright soliton pair in a harmonic trap. 2015. Physical Review A. 91 (4): 043637.

Kevrekidis, P. G., B. A. Malomed, A. Saxena, A. R. Bishop, and D. J. Frantzeskakis. Solitons and vortices in two-dimensional discrete nonlinear Schrodinger systems with spatially modulated nonlinearity. 2015. Physical Review E. 91 (4): 043201.

Kevrekidis, P. G., R. L. Horne, N. Whitaker, Q. E. Hoq, and D. Kip. Bright discrete solitons in spatially modulated DNLS systems. 2015. Journal of Physics A: Mathematical and Theoretical. 48 (34): 345201.

Kevrekidis, P. ., D. . Pelinovsky, and A. Saxena. When Linear Stability Does Not Exclude Nonlinear Instability. 2015. Physical Review Letters. 114 (21): 214101.

Khare, A., I. Christov, and A. Saxena. Successive phase transitions and kink solutions in φ8, φ10, and φ12 field theories. 2014. Physical Review E. 90 (2): 023208.

Middleton, R. S., J. W. Carey, R. P. Currier, J. D. Hyman, Q. Kang, S. Karra, J. Jiménez-Martínez, M. L. Porter, and H. S. Viswanathan. Shale gas and non-aqueous fracturing fluids: Opportunities and challenges for supercritical CO2. 2015. Applied Energy. 147: 500.

Nisoli, C., D. Abraham, T. Lookman, and A. Saxena. Quasi-one-dimensional thermal breakage. 2013. Physical Review E. 88 (4): 042409.

Nisoli, C., and A. R. Bishop. Attractive inverse square potential, U(1) gauge, and winding transitions. 2014. Physical Review Letters. 122 (7): 070401.

Odier, P., J. Chen, and R. Ecke. Entrainment and mixing in a laboratory model of oceanic overflow. 2014. Journal of Fluid Mechanics. 746: 498.

Provis, J., A. Hajimohammadi, C. White, S. Bernal, R. Myers, R. Winarski, V. Rose, T. Proffen, A. Llobet, and J. J. van Deventer. Nanostructural characterization of geopolymers by advanced beamline techniques. 2013. Cement and Concrete Composites. 36: 56.

Regev, I., T. Lookman, and C. Reichhardt. Onset of irreversibility and chaos in amorphous solids under periodic shear. 2013. Physical Review E. 88 (6): 062401.

Regev, I., and C. Reichhardt. Rheology and shear band suppression in particle and chain mixtures. 2013. Physical Review E. 87 (2): 201.

Reichhardt, C. J., G. Chern, A. Libál, and C. Reichhardt. Disordered artificial spin ices: Avalanches and criticality (invited). 2015. Journal of Applied Physics. 117 (17): 172612.

Reichhardt, C., D. Ray, and C. J. Reichhardt. Magnus-induced ratchet effects for skyrmions interacting with asymmetric substrates. 2015. New Journal of Physics. 17 (7): 073034.

Reichhardt, C., D. Ray, and C. J. Reichhardt. Reversible ratchet effects for vortices in conformal pinning arrays. 2015. Physical Review B. 91 (18): 184502.

Reichhardt, C., D. Ray, and C. J. Reichhardt. Collective Transport Properties of Driven Skyrmions with Random Disorder. 2015. Phys. Rev. Lett.. 114: 217202.

Reichhardt, C., J. Drocco, C. J. Reichhardt, and A. R. Bishop. Statics and Dynamics of Vortex Matter with Competing Repulsive and Attractive Interactions. 2013. Journal of Superconductivity and Novel Magnetism. : 1.

Rivera, M., H. Aluie, and R. Ecke. The direct enstrophy cascade of two-dimensional soap film flows. 2014. Physics of Fluids. 26 (5): 055105.

Wang, J., R. Zhang, C. Zhou, I. Beyerlein, and A. Misra. Characterizing interface dislocations by atomically informed Frank-Bilby theory. 2013. Journal of Materials Research. 28 (13): 1646.

Wang, X., and J. Whitehead. A bound on the vertical transport of heat in the 'ultimate' state of slippery convection at large Prandtl numbers. 2013. Journal of Fluid Mechanics. 729: 103.

White, C., G. Kearley, J. Provis, and D. Riley. Structure of kaolinite and influence of stacking faults: Reconciling theory and experiment using inelastic neutron scattering analysis. 2013. The Journal of Chemical Physics. 138 (19): 4501.

White, C., J. Provis, B. Bloomer, N. Henson, and K. Page. In situ X-ray pair distribution function analysis of geopolymer gel nanostructure formation kinetics. 2013. Physical Chemistry Chemical Physics. 15 (22): 8573.

White, C., K. Page, N. Henson, and J. Provis. In situ synchrotron X-ray pair distribution function analysis of the early stages of gel formation in metakaolin-based geopolymers. 2013. Applied Clay Science. 73: 17.

Whitehead, J. P., T. Haut, and B. Wingate. The effect of two distinct fast time scales in the rotating stratified Boussinesq equations. 2015. IMA Journal of Numerical Analysis. : 1.

Xu, H., P. G. Kevrekidis, and A. Stefanov. Traveling waves and their tails in locally resonant granular systems. 2015. Journal of Physics A: Mathematical and Theoreti-

cal. 48 (19): 195204.

Zhao, L., Y. Yu, G. L. Delzanno, and V. K. Jordanova. Bounce averaged diffusion coefficients in a physics based magnetic field geometry from RAM-SCB. 2015. Journal of Geophysical Research: Space Physics. 120 (4): 2616.

Zheng, Z., B. Guo, I. Christov, M. Celia, and H. Stone. Flow regimes for fluid injection into a confined porous medium. 2015. Journal of Fluid Mechanics. 767: 881.

Zheng, Z., I. Christov, and H. Stone. Influence of heterogeneity on second-kind self-similar solutions for viscous gravity currents. 2014. Journal of Fluid Mechanics. 747: 218.

Zhou, C., J. Su, M. Graf, C. Reichhardt, A. Balatsky, and I. Beyerlein. Plastic response of dislocation glide in solid helium under dc strain-rate loading. 2013. Physical Review B. 88 (2): 4513.

Attosecond Dynamics of Correlated Electrons in f-Electron Materials

Steve M. Gilbertson
20140622ECR

Introduction

The purpose of this project is to develop an experimental setup capable of tracking electron dynamics in correlated electron systems. The time scales involved will be on the order of attosecond (10^-18 s). This will be the first system of its type and what we are attempting to measure will be the first observations of such dynamics. The goal of the project is to gain insight into quantum coherent electron behavior in solid state materials. The majority of attosecond experiments thus far conducted have concentrated on single atom dynamics in gases and molecules, while applications to condensed matter, especially coherent dynamics, are few. The project will focus on the measurement and first observations of quantum multi-path interference in 5f Mott insulators and 4f heavy fermion materials. The materials will be optically pumped with an infrared laser pulse and probed with a soft x-ray, attosecond laser pulse. This will enable the transient recording of the excited state dynamics. The experiments will require development of an attosecond transient reflectivity apparatus - a unique setup currently not in exsitence in the U.S.

The system itself will be constructed using the most cutting-edge techniques in interferometer stabilization, nonlinear optics, and state-of-the-art attosecond pulse generation methods. Such techniques have only been demonstrated a few times worldwide. Once the experimental attosecond source setup is demonstrated, materials of interest to the Department of Energy, namely f-electron systems and systems with correlated electrons, will be tested. The expected observed phenomena will be the first ever of such measurements. The data analysis will be conducted with the expertise of Los Alamos material scientists.

Benefit to National Security Missions

The specific contributions that our work makes are almost entirely in the areas of the basic understanding of materials as well as overall scientific advancement. The work will be of particular interest to DOE/SC and the scientific discovery and innovation missions. We will be looking at the fundamental time evolution of electron dynamics within solid materials using newly developed attosecond spectroscopy techniques. The questions we can address involving correlated electrons in Mott insulators and 4-f heavy fermion materials should greatly expand the laboratory's knowledge base and will be compared to theoretical models that have been developed at LANL. The materials chosen for this work were also specifically selected to address issues pertaining to nuclear nonproliferation, and nuclear fuel research. The initial experiments will be performed on Indium-rich CeCoIn5 which shares similar properties to nuclear fuel compounds while secondary experiments will address issues in UO2, a known nuclear fuel product, directly. Finally, the work will address issues related to the MaRIE project. Our work will enable an important in situ characterization capability for materials that can be studied with the MaRIE facility in the future. Even more basically, the attosecond source and spectrometer that will be developed can easily be applied for studying simpler atoms, molecules and possibly even biological samples. This will provide another tool for time resolved studies in the areas of fundamental chemistry and biology.

Progress

Over the past year we have met our goals. The attosecond transient reflectivity setup was completed and tested yielding a very bright high harmonic extreme ultraviolet light source. Additional chirped mirrors were purchased to give more control over the few-cycle femtosecond laser pulses produced from the hollow core fiber and a variety of laser pulses have been measured. We have now characterized pulses from 30 femtoseconds all the way down to 9.5 femtoseconds with >1.5 mJ per pulse making our laser the shortest amplified system at LANL. We next implemented the double optical gating technique after acquiring the necessary optics. This was a major milestone for the project because we

were able to measure the first attosecond laser pulses at LANL. The attosecond pulses were spectrally characterized under a variety of conditions and with different types of generating gases giving estimates on total photon flux and bandwidths. The interferometer was rearranged to allow for more flexibility in adding optics and both spatial and temporal overlap were found again within a few femtoseconds. More recently, the uranium dioxide sample was added to the setup and we are currently trying to get static reflectivity data from the sample. Once this is accomplished, we will optically pump the sample to try and see transient reflectivity.

Along with these accomplishments, we also received supplemental funding which we are planning to use to implement an attosecond time step piezo electric transducer (pzt) stage used for making fine temporal steps as well as locking the setup. When the funding was first awarded for this project, there were sufficient cuts that meant we had to reduce the total scope of our work. We decided at the time to use the attosecond pulses as a delta function probe after optical excitation allowing us the see dynamics that occur on a few femtosecond timescale. This meant we could save resources by not purchasing the closed loop pzt as well as reducing the strict requirements on interferometer stabilization. However, with the supplemental funding, the pzt stage has been purchased along with several passive stabilization methods. We are hoping to get this implemented in the near term which may allow us to measure dynamics with attosecond precision before the experiment is over. In any event, the passive stabilization methods will help reduce temporal jitter and give us more temporal resolution in the data.

Future Work

In the upcoming fiscal year, we plan to begin the source development during the first couple of months followed by data acquisition. The plan of the previous year was modified so that all equipment was purchased at once and up front so as to maximize the amount of time spent taking data in the second year. Since the hollow-core fiber assembly is complete as well as the upgrades for the laser system, the next step will be vacuum chamber construction and alignment of the XUV optics. This will be followed by characterization of the attosecond laser pulses via reflectivity measurements off of gold mirrors. Upon satisfactory completion of the attosecond pulse characterization, spatial and temporal overlap will be found at the location of the sample position. Once this is complete, samples that are already available will be installed for preliminary data acquisition.

Conclusion

The ultimate goal of the project is to gain unprecedented insight into quantum coherent electron behavior in solid state materials. We propose to exploit unique phenomena in 5f Mott insulators and 4f heavy-fermion materials to demonstrate quantum multi-path interference effects in the attosecond response of these materials to an infrared laser pulse. This will require development of an attosecond transient reflectivity apparatus. We will show that the application of attosecond pulses to solid state materials can provide essential information about the dynamics and coherence of electrons.

Controlling the Electronic Structure of Emerging Atomically Thin Materials Through Heterostructuring

Jinkyoung Yoo
20150659ECR

Introduction

The overarching goal of the research is controlling the physical properties of emerging two-dimensional atomically thin materials (2D-ATMs, e.g. graphene, monolayer transition metal dichalcogenides) through heterostructure formation with conventional semiconductor (silicon, germanium, gallium arsenide) growth on 2D-ATMs.

Though the emerging 2D-ATMs have attracted great attention in the last decade due to their exotic physical properties, there has not been methodology to control the physical characteristics of 2D-ATMs since chemical doping and alloying of 2D-ATMs are not permanently stable. Applying bias to 2D-ATMs through semiconductor on 2D-ATM enables us to control the electronic properties of 2D-ATMs in precise and on-demand manner. The preliminary results of the team show that high-quality semiconductor layers and nanowires can be grown on the 2D-ATMs through unconventional crystal growth mechanism. The project can make the breakthrough for 2D-ATM research field hindered by the absence of reliable method of controlling physcial properties of 2D-ATMs and for conventional semiconductor research field which has been suffered from the limit of inherent characteristics of conventional semiconductors.

The synergistic output through a combination of low dimensionality of 2D-ATMs and established science of semiconductors has broad impact in materials science and device manufacturing.

The research has four key goals:

1. Provide a reliable and robust way of tuning properties of 2D-ATMs in precise manner since the main approach of semiconductor growth on 2D-ATMs employs established semiconductor science and technology.
2. Control carrier transport characteristics of 2D-ATMs through semiconductors grown on 2D-ATMs.
3. Open novel opportunities of observation of emergent phenomena in the novel heterostructures.
4. Utilize the exotic physical phenomena (e.g. band gap opening in atomically thin materials, tunneling-mediated p-n junction properties) for semiconductor devices such as ultra-efficient photodetectors and artificial photosynthesis.

Benefit to National Security Missions

The goals of the LDRD project are closely related to semiconductor heterostructure formation and control of physical properties of emerging materials. Integrated studies, from materials preparation to device demonstration, offer benefits to basic science and applied research.

For basic science the project is directly relevant to the grand challenges set by DOE SC, ‘control at the level of electrons’ and ‘energy and information on the nanoscale’. The project provides materials systems composed of ultimately (atomically) thin material and semiconductors of which properties are precisely controlled to tackle the grand challenges.

The project provides a reliable way to utilize the exotic properties such as abnormally large optical absorptance of two-dimensional atomically thin materials (2D-ATMs) which are useful to develop ultrafast and highly efficient detectors (especially for MaRIE) due to extremely small capacitance and ultimately thin heterojunction expediting excited carrier separation and energy harvesting devices such as photovoltaic cells and water splitting for hydrogen production (Energy security, Renewable energy). Furthermore, the ultimate thinness of the semiconductor/ 2D-ATMs makes it possible to transfer high-quality heterostructures onto various substrates such as plastics and glasses without loss of physical characteristics. The transferrable heterostructures are the key building blocks of embedded and flexible devices.

Thus, the concepts explored in the project can also find diverse applications in electronic/photonic devices based on charged carrier management. Project success will pave the way for future research funded by Department of Homeland Security, Department of Defense, Department of Commerce, and pursuing initiatives in national nanotechnology and manufacturing.

Progress

Since the beginning of CY2015 (the project's start date), 2 milestones have been achieved: 1) Growth of Ge(Si) thin films and nanowires on monolayer MoS2 and graphene, 2) Cross-sectional transmission electron microscopy (TEM) imaging of the interface between Ge and MoS2. Moreover, three-terminal electronic device fabrication and theoretical calculation are in progress. The research results were presented in 2015 Materials Research Society Spring Meeting in San Francisco in April.

In detail, a single crystalline Ge thin film was successfully grown on monolayer and multi-layer MoS2 via chemical vapor deposition. Single crystallinity of Ge thin film was confirmed by the cross-sectional TEM image. The same approach was employed to grow Ge and Si thin films on graphene. Growth of Ge and Si nanowires was also achieved by catalyst-assisted vapor-liquid-solid growth method in a chemical vapor deposition chamber. The nanowires are also single crystalline and vertically aligned. Additionally, the positions of Ge(Si) nanowires on graphene and MoS2 were controlled by positioning catalysts.

The electrical properties of Ge(Si)/MoS2(graphene) heterostructures are under investigation. For the research, multi-terminal field effect transistor-type devices have been fabricated with the heterostructures. The multi-electrodes on Ge(Si) thin film and on MoS2(graphene) layer enable us to monitor electrical properties of semiconductor thin film grown on atomically thin materials (MoS2, graphene) and of atomically thin materials independently. Moreover, we are comparing the electrical properties of atomically thin materials before and after Ge(Si) thin film growth. According to our recent observations, the electrical conductivity type of MoS2 is converted from n-type to p-type by growth of undoped Ge thin film. This behavior has been observed in more than 10 samples. The origin of the conductivity type conversion is under investigation through theoretical calculation (Density functional theory). Currently, charge transfer between Ge and MoS2 generates the phenomenon. Since doping in atomically thin materials to control conductivity type is a quite difficult issue, our observation provides a novel way and insight to control physical properties of atomically thin materials.

Future Work

In the next year, three milestones are set as the followings:

- Growth of semiconductors (silicon (Si), germanium (Ge)) thin films or nanowires on two-dimensional atomically thin materials (2D-ATMs, graphene and monolayer molybednum disulfide (MoS2)) with controlled conductivity type of silicon and germanium. Chemical vapor deposition in ultra-high/high vacuum chamber will be employed for the growth. The target of this goal is making both single crystalline semiconductor thin film with grain size of >10 micrometer and single crystalline semiconductor nanowires with diameter and length of <100 nm and >1 micrometer on graphene and MoS2, respectively. N-type, intrinsic, P-type semiconductors will be grown on 2D-ATMs via introducing dopant precursors during the growth.

- Cross-sectional scanning transmission electron microscopy studies of semiconductor/2D-ATMs to characterize the structural properties of the heterointerfaces. The atom arrangements of grown semiconductor and 2D-ATM at the heterointerface will be investigated. The detailed information obtained from the structural characterizations is employed to set the boundary condition of electronic band structure calculation.

- Theoretical calculation of electronic band structures (mainly band gaps) of the heterostructures. Density-Functional-Theory will be used for the calculation.

Conclusion

The achievements are closely related to fundamental materials science from the perspectives of materials preparation and control of properties, which can be directly expanded to various device applications.

The ideal outcome of the research is the control of the physical properties of 2D-ATMs through semiconductor/2D-ATM heterointerfaces and the observation of emergent phenomena in the heterostructures such as tunneling-mediated transport, band gap opening, reversible strong localization of carriers, and other unexpected behaviors.

Additionally, the unconventional crystal growth mechanism, which is not based on chemical bonding between substrate and grown material, provides novel insights of preparing high-quality heterostructures composed incompatible materials.

Publications

Lin, Y. -C., J. Yoo, I. Bilgin, A. Mohite, S. Kar, and D. Pete. Growth and characterizations of germanium/monolayer MoS2 heterostructures. 2015. 2015 Materials Research Society Spring Meeting.

A Novel Crystal Plasticity Model that Explicitly Accounts for Energy Storage and Dissipation at Material Interfaces

Jason R. Mayeur
20150696ECR

Introduction

This project is focused on developing a novel mesoscale theory and computational framework that can be used to enhance our understanding of the role that interfaces play in dictating microstructural evolution in nanoscale material systems. Recent work at LANL on fabricating bulk two-phase lamellar bimetallic nanocomposites has shown that these material systems possess superior strength and radiation damage resistance as compared the constituent metals and/or composites with more conventional layer thicknesses, e.g. larger than one micron. Experiments show that these nanocomposites have highly oriented microstructures and that there is a predominant interface relationship between grains along the bi-phase interfaces, which gives rise to their exceptional properties. The resulting microstructure in these nanoscale composites was unexpected based on conventional understanding of the fabrication process and active material deformation mechanisms. Earlier conventional mesoscale and atomistic simulations suggest that this unique microstructure arises due to a competition between the energy stored at the bi-phase interfaces and the stability of certain crystallographic orientations under the imposed deformation. In order to test this hypothesis, a mesoscale theory and computational framework that accounts for interface energy, the relevant plastic deformation mechanisms, and the associated lattice reorientation is needed. Such a modeling framework does not currently exist, and the goal of this project is to develop a tool to bridge this gap in understanding. The proposed path of model development would build upon an existing state-of-the-art nonlocal single crystal plasticity theory developed by the principal investigator to include the interface energy effects. The model would truly be one-of-kind and would uniquely position LANL to answer fundamental questions related to the role of interfaces in nanoscale polycrystalline material systems.

Benefit to National Security Missions

This project will deliver a simulation tool that addresses relevant physics of mesocale deformation mechanisms in polycrystalline metals with an emphasis on the role played by material interfaces. This enhanced understanding will enable the design of materials with properties tailored for specific applications, which is directly aligned with the Laboratory's Materials for the Future Science Pillar. The proposed modeling framework is also suited for bridging the mesoscale gap between atomistic and macroscale continuum methods, and would complement the modeling component of the Making, Measuring, and Modeling Materials (M4) facility as a part of the MarIE vision.

Progress

Since the funding for this project was appropriated in Feb of 2015, the efforts of the PI and collaborators, in accordance with the project plan, have been directed towards: the simulation of size-dependent mechanical response of fcc nanocrystalline metals, the development and implementation of a new constitutive model for bcc nanocrystalline metals into the existing computational framework, and a continuing literature review and initial efforts at theory development for the interface constitutive model that is to be completed/implemented in FY16. Some of the teams efforts have also been directed at developing additional computational methods and capabilities to generate more realistic synthetic microstructures that are higher fidelity representations of the actual nanocomposite microstructures of interest to this project. The PI was recently invited to and participated in a workshop in Poitiers, France on "Interface-Mediated Plasticity in Nanostructured and Architectured Materials". At the workshop, the PI presented research results highlighting our efforts made towards understanding the novel mechanical properties of these materials systems as well as our path forward for incorporating these essential interface physics that are currently missing from existing modeling frameworks. Our presentation was

well-received and a potential collaboration with the group in France that is fabricating a complementary set of nanocomposite materials remains a possibility. This collaboration could directly benefit from the computational model development being undertaken as part of this project.

Future Work

- Develop a single crystal constitutive law applicable for body-centered cubic (bcc) materials.
- Implement the bcc single crystal constitutive law within the nonlocal finite element framework.
- Develop the constitutive theory for the interface energy terms.
- Implement the interface energy constitutive theory within the nonlocal finite element framework.
- Perform nonlocal finite element simulations of face-centered cubic (fcc) nanocrystalline materials systems without interface energy effects.
- Perform nonlocal finite element simulations of bcc nanocrystalline materials systems without interface energy effects.
- Perform nonlocal finite element simulations of nanocrystalline fcc/bcc multilayer materials systems without interface energy effects.

Conclusion

The primary goal of this research is to develop a nonlocal crystal plasticity model to study the competition between bulk-dominated and interface-dominated polycrystalline plasticity at the mesoscale. The model will be used to study mechanical response of nanocrystalline face-centered cubic (fcc), body-centered cubic (bcc), and fcc/bcc lamellar composites. It is anticipated that the improved understanding of these nanoscale material systems obtained via simulation will facilitate next generation materials design by identifying relationships between process parameters and the resulting microstructure.

Room Temperature Oxidation and Corrosion of Plutonium

Alison L. Pugmire
20130738ECR

Abstract

Previous work on plutonium oxidation and corrosion has primarily focused on ultra-high vacuum or accelerated aging (e.g. high temperature) conditions. As a result, a significant gap exists in our understanding of the oxide layer formed at room temperature. This research has focused on performing a systematic study of plutonium oxidation and corrosion in carefully controlled environments at various times throughout the corrosion process. Samples of delta-phase plutonium alloyed with 1.9 at. % gallium were corroded for 1 month in dry air, humid air, and humid argon environments. After one month, both plutonium and gallium oxides were observed. After storage in a dry/inert atmosphere for six and 16 months, further corrosion (and most likely radiogenic aging) occurs to form non-crystalline plutonium oxides and gallium oxides. Based on the results of this work and previous preliminary studies in our group, the plutonium oxide formed in the initial stages of oxidation appears to be disordered and non-crystalline (with no long-range order), contrary to the historical depiction of this oxide. The detection of gallium oxide has only rarely been observed, particularly for delta-phase plutonium. Its formation here has been attributed to the presence of an additional surface phase (alpha'-phase plutonium) that was formed during sample preparation. Although unexpected, this result shows that gallium can be oxidized and may play a role in the oxidation. Overall, this work has improved our understanding of the structural and chemical composition of the oxide layer formed under ambient conditions and has changed our model for the oxide layer developed in conditions relevant to the safe storage and potential reuse of the material.

Background and Research Objectives

The unpredictable behavior and reactivity of plutonium has led to a very poor understanding of its metallurgy and corrosion process. This not only poses a basic scientific challenge, but directly affects the safe, long term storage of this material. In an effort to understand the surface chemistry and corrosion of plutonium, knowledge of the surface oxide composition is paramount. The currently accepted description of the oxide layer is shown in Figure 1. At ambient temperatures, the corrosion products have been described as a thick PuO_2 surface layer over a thin Pu_2O_3 layer at the metal interface (Figure 1, left). Under inert/non-oxidizing conditions, e.g. ultra high vacuum (UHV), the PuO_2 layer auto-reduces to form a thick Pu_2O_3 layer (Figure 1, right) [1].

This generalized view of the oxide layer is based on years of experiments encompassing a wide array of experimental conditions [2, 3]. While this description appears to be straightforward, several aspects regarding the corrosion mechanism and products are still debated. First, in an attempt to explain the increased corrosion rate in the presence of H_2O, a hyperstoichiometric oxide (PuO_{2+x}) has been proposed. However, this species has only been observed by a few groups in extreme conditions (i.e. high temperatures, low pressures) [1,4] while others debate its existence [5]. Second, the presence of the Pu_2O_3 layer at room temperature is questionable because it has not been experimentally observed but is only assumed based on its formation in very specific atmospheres (non-oxidizing/inert atmospheres) [1]. Third, the initial weight gain studies in the 1950s demonstrating the effects of alloying have yet to be explained. In wet air, unalloyed, α-Pu corrodes 1.7 times faster than alloyed, δ-Pu (3.3 at. % Ga), while in wet inert atmospheres, δ-Pu (3.3 at. % Ga) corrodes 6.5 times faster than unalloyed, α-Pu [1,6]. Fourth, the surface oxide layer has been characterized as crystalline based on x-ray diffraction (XRD) results. However, XRD is only sensitive to the crystalline form, and preliminary work from our group using EXAFS, spectroscopic ellipsometry (SE), Augur electron (AES) and x-ray photoelectron spectroscopies (XPS) indicate this layer is not as simplistic as once thought, but may have amorphous Pu-O components [7,8]. Finally, because the plutonium oxidation process is very slow at room temperature in O_2 (~ 0.02 nm/hr)

and is accelerated with elevated temperatures (> 25 °C) or a moist environment [5, 8], the vast majority of previous work has utilized accelerated growth conditions to produce oxide layers quickly for easier studies. This has resulted in a significant gap in previous corrosion studies and leaves the room temperature growth of the oxide layer not well understood. This regime is perhaps the most relevant regime as it directly applies to the storage and potential reuse of this material in the nuclear stockpile.

Thus, many questions regarding the oxide layer remain, and the goal of this research has been to address several key questions. What is the chemical composition of the corrosion products (PuO_2, Pu_2O_3, PuO_{2+x}, $PuO_x(OH)_y$)? Is the surface layer oxide crystalline PuO_2, an amorphous oxide, or a non-crystalline oxide? Is Pu_2O_3 present at the dioxide-metal interface? Why is a different rate observed for unalloyed, alpha plutonium versus alloyed delta plutonium? The goal of this work was to answer these fundamental questions using a combination of surface sensitive (SE, AES, XPS) and bulk techniques (XRD, EXAFS) on a variety of sample types (i.e. unalloyed versus alloyed plutonium). However, in June 2013, the LANL director issued a pause of the facility where much of the work was to be performed (TA-55, PF-4). As a result, the work was refocused such that the goals of the project could still be addressed using available materials and techniques. An additional corrosion regime was added to the original work scope (investigating the corrosion/radiogenic aging of materials as they were stored). The bulk and surface was characterized using EXAFS at an off-site location (the Stanford Synchrotron Radiation Lightsource, SSRL) and the surface was interrogated using XPS at another LANL facility (TA-35, Bldg 0213, TFF, the Target Fabrication Facility). Most importantly, perhaps, a new plutonium capability (SE) was developed and installed at TFF to complement the techniques used here. While XPS is sensitive to only the top 5 nm and EXAFS probes the bulk material up to 2. 5 microns, SE probes the bulk with extreme sensitivity to the surface oxide layer. In this way a suite of techniques were used and developed to probe the oxide layer formed in ambient conditions.

Scientific Approach and Accomplishments

The overall approach of this work was to study the ambient oxidation/corrosion of plutonium as a function of humidity, oxygen content, and exposure and study the structural and chemical components of the oxide layer using multiple techniques (EXAFS, SE). This work investigated the initial formation of the oxide layer on delta-phase plutonium alloyed with 1.9 at. % gallium exposed for 1 month to: 1) dry air (O_2); 2) wet air (O_2 + H_2O); and 3) wet argon (Ar + H_2O). Experimental repeatability was tested using a duplicate sample placed in one of the exposure conditions (wet air). The bulk chemical and structural components of the oxide layer were investigated using EXAFS, and the surface components were studied using XPS (when available) and surface EXAFS (a synchrotron experiment new to the PI).

After one month of exposure, the samples exposed to dry air, wet air, and wet argon were photographed (Figure 2). These photographs are the first recorded images of the color changes that occur after plutonium has oxidized/corroded at room temperature after one month. As seen in Figure 2, distinct color changes and oxide growth are observed [Manuscript in preparation]. Using previous work correlating the calculated spectral reflectivity (using SE) and the color of the surface, the oxide layer thickness was estimated [10, 11]. For dry air (A), the gold color is indicative of a ~40 nm oxide layer. For wet air (B) and wet argon (B), the overall blue surface indicates the oxide layer is ~ 80 - 100 nm, and the olive-green powder is characteristic of PuO_2 [12]. This visual inspection has allowed for an initial assessment regarding the extent of corrosion. The dry environment is the least corrosive; the humid environments are more corrosive, and the wet argon is most corrosive, producing the thickest oxide layer with the largest areas of green PuO_2 powder.

EXAFS was used to investigate the bulk material from both the gallium edge (providing structural information surrounding the gallium atoms) and the plutonium edge (which provides structural information surrounding the plutonium atoms). After 1 month, the gallium EXAFS showed two metallic components corresponding to alpha'- and delta-phase plutonium. The alpha'-phase commonly occurs after hand-polishing plutonium metal, but can be removed with electropolishing. The electropolishing performed in this sample preparation clearly did not remove all of the stress-induced alpha'. Perhaps the most striking result from the gallium EXAFS data was the presence of a gallium oxide. This has only rarely been observed in the oxide layer, and it's presence indicates that even though the plutonium alloy only contains 1.9 atomic percent gallium (2 gallium atoms for every 50 plutonium atoms), the gallium is being oxidized. In the plutonium EXAFS data, two metallic phases were also observed (alpha'- and delta-phase plutonium). However, unlike the gallium data, the plutonium EXAFS data only showed indications of an oxide layer (i.e. peaks with low amplitude that could not be modeled). Given the oxophilic nature of plutonium compared to gallium and its visible presence (Figure 2), it likely follows that if a gallium oxide is formed, a plutonium oxide would be formed. Thus, the inability of EXAFS to detect the oxide after 1 month indicates there is not a sufficient amount of

plutonium oxide present, or it is very disordered and does not correspond to a crystalline plutonium oxide.

After 6 months of storage in a dry or argon (for the wet argon sample only) environment, EXAFS and XPS data were acquired. Both the gallium and plutonium EXAFS data showed a large increase in the amount of gallium and plutonium oxide, in addition to small amounts of the original metallic surface. Both the gallium and plutonium oxides were disordered in the EXAFS data and did not correspond to crystalline oxides, as has been the historical interpretation (Figure 1). The XPS data also corroborates these results and shows gallium and plutonium oxides. After 16 months, no observable metal fractions are observed in either the gallium or plutonium EXAFS, and only disordered oxides are observed. As in the 6 month data, only peaks associated with non-crystalline gallium and plutonium oxides were observed. Clearly, some local order is retained (up to 5 angstroms away from the plutonium/gallium atom). If the oxide was completely amorphous (no order), it would not be detectable by EXAFS. Finally, surface EXAFS (an experiment new to the PI) was performed at all time points (1 , 6, and 16 months). The preliminary results corroborated those detailed above, but highlighted the need for improved sample holder design and more calibrated experiments.

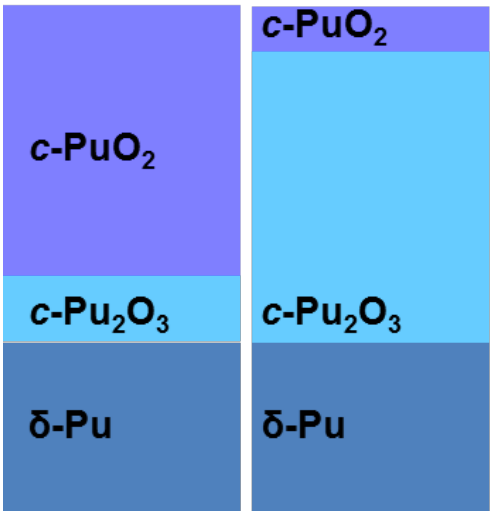

Figure 1. Historical depiction of oxide products formed on delta-plutonium under ambient (left) and UHV (right) conditions ("" refers to the crystalline form).

In order to compliment these studies, the last year of the project was focused on adding a new Pu capability (SE). The necessary equipment was acquired and assembled, including all the necessary radiological safety components to allow for plutonium studies. Non-radiological testing was performed on standards, and the first plutonium sample (a PuO2 sample prepared by the Polymer Assisted Deposition method (PAD) is scheduled for January 2015. This first sample is not only readily available, but is the most common room temperature form of a crystallographic plutonium oxide, providing a benchmark, or "standard" for PuO2 using SE. A key feature that was included during assembly is the inclusion of gas sample bottles that will allow for introduction of air or water, allowing for in-situ measurements of the oxidation and corrosion process. This capability has generated much interest in the weapons and dynamic testing community, and will hopefully result in future funding for these studies.

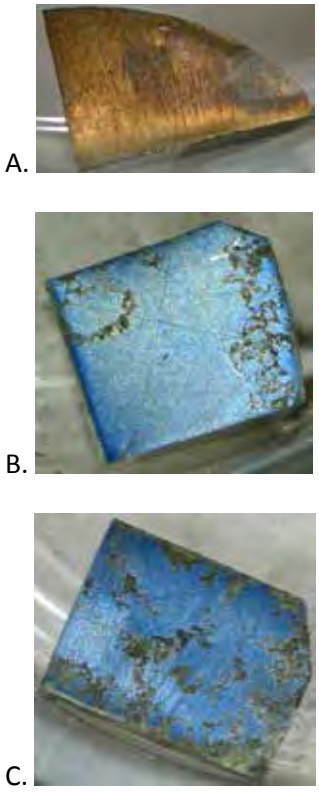

Figure 2. Pu with 1.9 at. % Ga after one month of exposure to dry air (A); wet air (B), and wet argon (C).

Overall, the results from this research indicate a non-crystalline oxide layer (not c-Pu2O3, c-PuO2) is formed in the initial stages of corrosion. If removed from the corroding elements and left to corrode (and radiogenically age) for up to 16 months, this oxide will further corrode, but not to a crystalline form of any known plutonium oxide (i.e. PuO2). This result is contrary to our historical view of the corrosion products, and has led to the modern depiction of the oxide products shown in Figure 3. Another interesting result was the formation of a gallium oxide that has rarely been observed. These results, in addition to discussions with experts in the field, have led to the postulation that the surface alpha' layer is promoting gallium oxidation. Gallium metal is not known to readily oxidize, and the alpha'-phase is known to be a meta-stable phase in which

gallium is trapped or 'frozen' in an alpha-phase plutonium lattice. If this is the surface that is readily available for oxidation, and gallium is intrinsically unstable in the alpha'-phase, the gallium will be thermodynamically favored to oxidize. It is the PIs hope that programs will support future studies in this area so that the room temperature oxidation and corrosion products and mechanism can be fully understood. Two manuscripts are in preparation and will be submitted in the upcoming months.

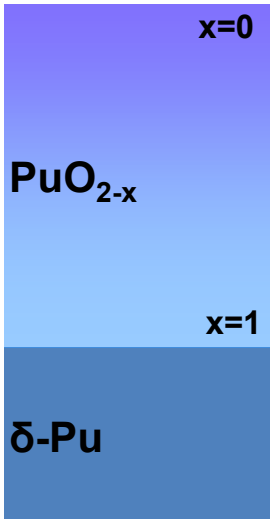

Figure 3. Modern depiction of the oxide layer formed on delta-plutonium based on this research and recent work by our group [7,8].

Impact on National Missions

Pu corrosion has been identified as a key issue in pit aging and reuse, and this research has directly impacted our understanding of the oxide layer that is formed in three ambient environments relevant to the storage and reuse of this material. The corrosion process is more complicated than originally thought. The oxide layer contains many non-crystalline components, particularly at the surface. This research has also allowed a new plutonium capability to be developed that will be of interest to both the dynamic testing community and the weapons community in general. This research has fostered and strengthened LANL's scientific collaboration with another facility in the DOE complex, SSRL at the SLAC National Accelerator Laboratory in Menlo Park, CA, as well as with other experts in the EXAFS field at Lawrence Berkeley National Laboratory.

References

1. Haschke, J. M., T. H. Allen, and L. A. Morales. Surface and corrosion chemistry of plutonium. 2000. Los Alamos Science. 26: 252.

2. Butterfield, M. T., T. Durakiewicz, J. J. Joyce, A. J. Arko, K. S. Graham, D. P. Moore, and L. A. Morales. Photoemission of surface oxides and hydrides of delta plutonium. 2004. Surface Science. 571 (1-3): 74.

3. Waber, J. T.. The corrosion and oxidation of metals. 1948. U.S. Atomic Energy Commision Report, LA-1381.

4. Conradon, S. D., B. D. Begg, D. L. Clark, C. Den Auwer, F. J. Espinosa-Faller, P. L. Gordon, N. J. Hess, R. Hess, D. W. Keogh, L. A. Morales, M. P. Neu, W. Runde, C. D. Tait, D. K. Veirs, and P. M. Villella. Speciation and unusual reactivity in PuO2+x. 2003. Inorganic Chemistry. 42 (12): 3715.

5. Martin, P., S. Grandjean, M. Ripert, M. Freyss, P. Blanc, and T. Petit. Oxidation of plutonium dioxide: an x-ray absorption spectroscopy study. 2003. Journal of Nuclear Materials. 320 (1-2): 138.

6. Raynor, J. B., and J. F. Sackman. Some observations on the oxidation of unalloyed and d-stabilized plutonium metal. 1965. In Plutonium 1965: Proceedings of the 3rd International Congress on Plutonium. (,). , p. 575. : Institute of Metals.

7. Costello, A. L., F. J. Espinosa-Faller, and S. D. Conradson. Corrosion in Ga-stabilized plutonium. Presented at Plutonium Futures – The Science 2012. (Cambridge, UK, 15-20 July 2012).

8. Pugmire, D. L., and H, G. G. Flores. The optical properties of the Pu/Pu oxide thin film system. Presented at Plutonium Futures – The Science 2012. (Cambridge, UK, 15-20 July 2012).

9. Raynor, J. B., and J. F. Sackman. Oxidation of plutonium in moist air and argon. 1963. Nature. 197 (4867): 587.

10. Larson, D. T., and D. L. Cash. Plutonium oxide thickness - color correlation. 1968. The Dow Chemical Company.

11. Pugmire, D. L., F. J. Freibert, and J. P. Baiardo. The optical properties of the plutonium/plutonium oxide thin film system. 2013. Actinide Research Quarterly 2013. August : 47.

12. Clark, D. L., S. S. Hecker, G. D. Jarvinen, and M. P. Neu. Plutonium. 2011. In The chemistry of the actinide and transactinide elements. Edited by Morss, L. R., N. M. Edelstein, and J. Fuger. , p. 1. Dordrecht: Springer Science+Business Media B.V..

Publications

Booth, C. H., Y. Jiang, S. A. Medling, D. L. Wang, A. L. Costello, D. S. Schwartz, J. N. Mitchell, P. H. Tobash, E. D. Bauer, S. K. McCall, M. A. Wall, and P. G. Allen. Self-irradiation damage to the local structure of plutonium

and plutonium intermetallics. 2013. JOURNAL OF APPLIED PHYSICS. 113 (9): -.

Pugmire, A. L.. Spectroscopic Analysis of Actinyl Systems. 2013. Actinide Research Quarterly. (3): 18.

Pugmire, A. L., C. H. Booth, T. J. Venhaus, and D. L. Pugmire. Structural insights into the oxide formed during the room temperature corrosion of plutonium . Presented at Pu Futures - The Science 2014. (Las Vegas, NV, 7-12 Sept 2014).

Pugmire, A. L., C. H. Booth, T. J. Venhaus, and D. L. Pugmire. Understanding the oxidation and corrosion of plutonium with EXAFS. Invited presentation at SSRL/LCLS Users' Meeting and Workshop. (Menlo Park, CA, 7 - 10 Oct. 2014).

Pugmire, D. L., H. G. Garcia Flores, and A. L. Costello. The room temperature oxidation/corrosion of delta plutonium. Presented at XIII International Workshop: Fundamental Properties of Plutonium. (Sarov, Russia, 8-13 Sept. 2013).

Pugmire, D. L., H. Garcia Flores, A. L. Pugmire, and D. P. Moore. The room temperature oxidation/corrosion of delta-Pu: historical perspective vs. modern understanding . Invited presentation at Pu Futures - The Science 2014. (Las Vegas, NV, 7-12 Sept 2014).

Novel Mesoscale Modeling Approach for Investigating Energetically Driven Nanoscale Defect/Interface Interactions

Abigail Hunter
20130745ECR

Abstract

The primary goal of this project is to investigate nanoscale defect/interface interactions, such as nucleation and growth of deformation twins, and dislocation dynamics as controlled by interfaces through development of an innovative three-dimensional (3D) phase field dislocation dynamics (PFDD) mesoscale model that links atomic-scale and nanoscale physics. Development of this computational tool enables the study of deformation mechanisms at interfaces not possible with current mesoscale methods.

This project proposed three key goals that all include investigation of a physical problem and novel extensions to the PFDD model. These goals focus on (1) investigating the formation of deformation twins and dependencies with respect to temperature and grain size variations, (2) slip transmission of dislocations through bimetallic interfaces, and (3) extending to deformation behavior in body-centered cubic (bcc) crystal structures. All goals were met successfully during the project; however, temperature dependence was not successfully included in the PFDD framework. This project produced 8 journal publications with 3 more in preparation that detail results including discovery of an unprecedented grain size effect and previously unreported twin formation mechanism. This project has also fostered several collaborations between laboratory scientists and universities including Purdue and Iowa State Universities. Three students were also funded at different times during the duration of this project.

Background and Research Objectives

Plasticity in metals is mediated by the nucleation, motion, and interaction of line defects in the crystalline lattice structure known as dislocations. In nanomaterials (grain sizes less than 100nm), experimental studies and atomistic simulations show that when the characteristic length scale (ex: layer thickness, grain size) decreases many deformation mechanisms arise that are not active in bulk and coarse-grained material counterparts, such as deformation twinning [1-12]. As grain sizes reach ~30-50nm in face-centered cubic (fcc) materials, plasticity becomes primarily driven by the motion and interaction of partial (or extended) dislocations, which unlike perfect dislocations leave behind stacking faults (SFs) in the crystal lattice [9, 13]. The increased number of individual partial dislocations and wide SFs are thought to be responsible for the alternative deformation mechanisms seen at the nanoscale [14-18]. These alternative deformation mechanisms, along with grain boundaries and bimetallic interfaces, can result in unique material behavior including high strength and improved ductility [12, 19-23]. As applications for nano-devices increases, there is not only a growing need to ensure reliability, but also the opportunity to engineer materials for specific applications, yet a predictive model to address all of these issues still does not exist.

Increased research efforts have been invested into developing models that can accurately describe partial dislocation behavior. Many of the above observations are from atomistic methods; however, these microscopic models are computationally intensive and limited in both time and length scales. Consequently, atomistic attempts to address the issues of deformation twinning and dislocation behavior at interfaces have only led to controversy due to inappropriate time and length scales. Conversely, classical continuum models focus on a macroscopic level accounting for dislocation densities rather than individual dislocations. While this is effective for modeling deformation processes in bulk material, on the micron and sub-micron scales it is difficult to study dislocation interactions and many nanoscale deformation behaviors fail to be predicted. The gap in this intermediate or mesoscale regime that lies between atomistic and continuum scales has been recognized by Basic Energy Sciences (BES), particularly in regards to the evolution and understanding of defect microstructure [24].

Formulation of dislocation models, including discrete dislocation dynamics (DDD) and phase field models, aim to fill this gap at the mesoscale. DDD models are a more developed approach for modeling deformation behavior at the mesoscale; however, they were originally developed for bulk crystals and have difficulty accounting for deformation processes at interfaces and grain boundaries, and deformation twinning [25]. DDD is also based on empirical rules, generally motivated by atomistic simulation. This basic framework impedes transformational changes, such as accounting for temperature dependence and the effects of surfaces and interfaces. On the other hand, phase field models have been only recently applied to investigate dislocation behavior and interactions at the mesoscale [26, 27]. Phase field models are directly dependent on minimization of the total system energy, which is especially advantageous when accounting for partial dislocations, deformation twinning, and interface interactions. Unlike DDD models, the phase field framework does not rely on rules or directly incorporate self-consistent atomic-scale information to influence dislocation behavior.

The goals of this project include innovative extensions of the 3D PFDD model that are not only of great interest to the scientific community, but also answer many questions about dislocation behavior on the nanoscale, particularly at interfaces. This project focuses on the following three goals that each address (a) an interesting physical problem, and (b) a novel extension of the PFDD model:

- Investigate the effects of grain size variation and temperature dependence on deformation twinning in fcc materials, such as copper, nickel, and silver. (b) Include temperature dependence in the PFDD model.
- Study dislocation behavior in fcc/fcc multilayers. (b) Implement a complex description of bimaterial interfaces that includes both local interface effects (lattice mismatch, residual Burgers vectors) and bulk effects (elastic moduli mismatch) in the PFDD model.
- Account for dislocation behavior in bcc materials, such as tantalum and niobium. (b) Reformulate the PFDD model to account for the appropriate bcc slip systems, Burgers vector geometry, and dislocation mobility.

Overall, all of these goals were met with one exception. Temperature dependence has still not been included in the PFDD framework. Preliminary simulations in which the elastic moduli were changed to reflect temperature changes did not impact results as expected. We concluded that in order to accurately account for temperature the fundamental formulation of the phase field framework needed to be developed in a way that includes temperature from the very beginning. In order to meet the other project objectives, this was not completed.

Despite not including temperature dependence, this project still investigated important issues surrounding the formation of deformation twins in fcc metals. Specific focus was given to the impact of material properties and grain size variations on the formation of extended stacking faults (SFs) and two-layer deformation twins. While the primary focus of this goal changed slightly, valuable studies were completed resulting in several journal publications. The remaining two goals focusing on fcc/fcc multilayers and bcc metals were fully met.

Scientific Approach and Accomplishments

The 3D PFDD model is unique to Los Alamos National Laboratory (LANL), and has great potential to answer many questions about the effects of SFs, deformation twinning, and the impact of grain boundaries and heterophase interfaces on dislocation and material strength behavior. By tracking the motion of individual dislocations via a scalar-valued phase field variable defined on each active slip plane, phase field models can account for a number of dislocation behaviors, such as nucleation, annihilation, and dislocation interaction with obstacles and externally applied stresses [27-30]; however, at the beginning of the project the PFDD framework was designed to study dislocation characteristics of only fcc materials in bulk crystals with a very limited description of some types of interfaces. The PFDD model does have a detailed energetic description of the SF region between partial dislocations, which is in contrast to most other predictive dislocation models that rely on only one parameter [31-35]. This energetic description for the SF region is directly informed by atomistics [36, 37].

Deformation Twinning

As discussed above, temperature effects were not studied as initially outlined by this project, but rather the effects of grain size variations and material dependence. Experimental results and numerical simulations demonstrate that partial dislocations are the basic defect responsible for deformation twins, which occur when SFs form on adjacent planes [1, 3, 19, 38-40]. Hence, to fully understand deformation twin formation we also investigated extended SFs.

Figure 1 shows a PFDD simulation of a leading partial dislocation emerging from a grain boundary defect, propagating into the grain until the trailing dislocation in emitted in a 31.87nm grain in nickel. The green region represents the SF. Energetically, the SF will reach a maximum (or critical) width at which it becomes more energetically favorable to emit the trailing partial rather than continue to expand the SF.

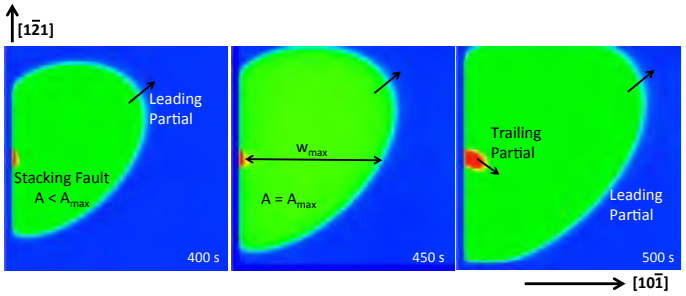

Figure 1. PFDD simulation of partial dislocation motion in a 31.87nm nickel grain. The leading partial emits from a grain boundary defect and extends into the grain until it becomes more energetically favorable to nucleate a trailing partial than to continue to expand the SF (green region). The SF width at this point is the critical or maximum SF width. The trailing partial emits from the same grain boundary defect.

We ran several simulations similar to Figure 1 for grain sizes varying from 10-120nm for several fcc metals including nickel, aluminum, and copper [41]. Interestingly we discovered a previously unreported grain size effect in which the critical SF width increases with increasing grain size [41, 42]. At first, this finding appeared to contradict prior results from experiments [15] and atomistic simulations [17, 43], which generally report that SF widths are wider in smaller grains. Our study shows that as the grain size increases, the critical SF width also increases, but the fraction of the grain cross-sectional area taken up by the critical SF region decreases. These grain size effects are intriguing and cannot be explained by any model to date.

Additionally, we found that monolayer SF formation (when the SF covers the entire grain cross-section without trail emission) is a necessary but insufficient condition for twin formation [44]. This led to the discovery of another likely elementary mechanism for twin formation called the alternate emission (AE) mechanism [44]. Many twinning processes have been proposed most of which assume that the partial dislocations emit from the same grain boundary [3, 45, 46]. Conversely, the AE mechanism considers participation of two grain boundaries on opposite sides of a nanoscale grain. Figure 2 shows the formation of a two-layer deformation twin in a 65.8nm grain of copper via the AE mechanism [44]. This mechanism may be energetically favorable over other proposed mechanisms because it accommodates deformation without generating detrimental backstresses.

This physical picture translates into two conditions that can help determine whether or not a two-layer twin will form via AE. First, the material system should be sufficient to accommodate a monolayer SF. Second, the energy required to nucleate a trailing partial must also be sufficiently high. If both conditions are fulfilled, leading partials on adjacent planes can propagate stable SFs across the entire grain cross-section without exceeding the energy penalty to provoke emission of a trailing partial. Achieving both criteria translates to a high propensity for twinning, which we see most strongly in silver and copper. Overall, this study resulted in 8 journal publications in collaboration with Dr. Irene Beyerlein (LANL).

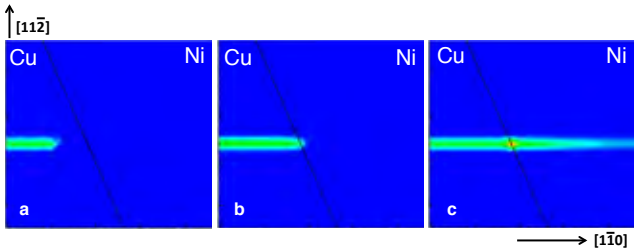

Figure 2. PFDD simulation of two-layer twin formation via the AE mechanism in a 65.8nm copper grain [44]. Frames (a) and (b) show the topmost glide plane, and frames (c) and (d) present cross-sectional views of the grain. The SFs are shown in green, and hashed regions represent grain boundaries. Grain boundary defects are on opposing grain boundaries and adjacent glide planes.

Fcc/fcc Multilayers

Thickness-dependent strengthening phenomena have been observed in bimetallic multilayers, and the interfaces between the metals drastically impact the strengthening mechanisms [21]. Furthermore, the strengthening mechanisms, such as dislocation pile-ups, elastic moduli mismatch, and misfit dislocations, themselves are not fully understood and have been a recent topic of study and debate [21]. Modeling dislocation behavior across nanolayer interfaces had never been attempted with a phase field model prior to this project.

The problem of heterophase interfaces is very complex. In an effort to simplify the initial simulations only perfect dislocations (no partial dislocations) were considered in a cube-on-cube orientation (no misorientation/rotation between the fcc metals). Model extensions focused on accounting for bulk effects, such as elastic moduli mismatch. Furthermore, energetic expressions for local interface properties, such as lattice parameter mismatch and residual Burgers vectors, were included in the PFDD model.

The PFDD model can now model slip transmission of perfect dislocations through fcc/fcc bimaterial interfaces for a variety of systems with cube-on-cube orientation. Figure 3 shows an example simulation for a perfect dislocation moving from copper to nickel. The green line represents the dislocation that approaches, meets, and then passes through the interface (thin black line). The red point at the

interface of Figure 3c represents the residual Burgers vector in the interface.

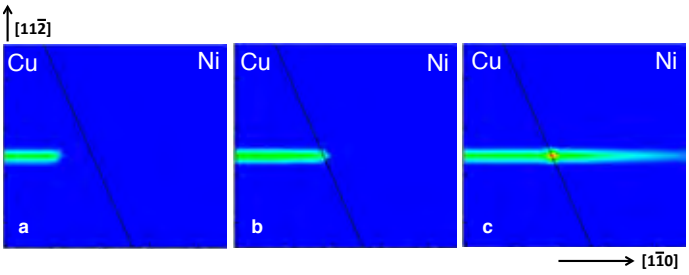

Figure 3. PFDD simulation of a perfect dislocation approaching, meeting, and transmitting through a copper-nickel interface. The dislocation line is green and the red point at the interface in frame (c) represents the residual Burgers vector.

Similar simulations have been completed for various fcc/fcc bimaterial systems. This work has led to the formulation of an analytical solution for the minimum stress required for slip transmission to occur (i.e. the threshold stress). Notably, we can analytically investigate the dependence of the threshold stress on key material properties. This can also be used for predictive modeling. This work was completed in collaboration with Prof. Marisol Koslowski and Yifei Zeng (Purdue University) and publications are in preparation. Future research includes extending to partial dislocations, systems with misorientation, and subsequent slip transmission studies.

Bcc Materials

Dislocation behavior in bcc materials had never been studied using a phase field model prior to this project and was a major step for the PFDD framework. Accounting for bcc materials required reformulation of much of the PFDD algorithm. Most notable modifications include redefining dislocation and system geometry (Burgers vectors and slip systems), and describing the dislocation core in bcc materials. In bcc materials, edge and screw oriented dislocations have very different core structures [47]. Edge dislocations have planer core structures, similar to fcc materials, and move very quickly through the crystal lattice [47]. Conversely, screw dislocations have non-planar core structures, meaning that the core region can be spread across non-parallel crystallographic planes [47]. This causes screw-type defects to be less mobile and produce larger amounts of inelastic strain making them key to the dominant deformation mechanisms in bcc materials [47, 48]. Clearly, there are fundamental differences between line defects in fcc and bcc materials that cannot be ignored when modeling plasticity in bcc materials.

Initially, we approached a simplified problem that considered only perfect dislocations moving in a single active slip system. We considered an infinite medium with a single dislocation loop in niobium (Figure 4). The dislocation loop includes edge, screw, and mixed-type orientations. Since different parts of the loop have different mobilities the loop will not expand evenly across the silp plane, as the PFDD simulations show in Figure 4. The edge oriented dislocation lines move much faster creating an oval shape. For comparison, Figure 4 also shows results for the same configuration in copper, a fcc metal. In this case, the loop expands evenly because there is no notable different between edge and screw mobilities.

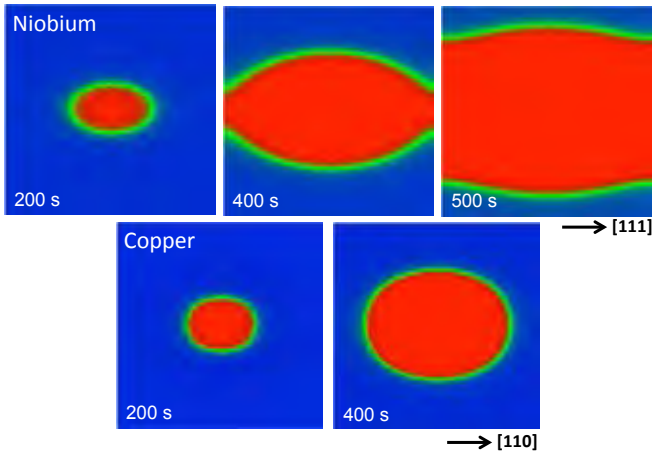

Figure 4. PFDD simulations of an expanding perfect dislocation loop in niobium and copper. Green lines represent the dislocation line, red indicates slipped regions, and blue regions are unslipped areas. In niobium the dislocation loop does not expand evenly due to the difference in mobilities between edge and screw oriented dislocation lines. There is no such difference in the edge and screw mobilities in fcc metals, hence the loop in copper expands evenly.

This extension of the PFDD model to bcc metals creates opportunities for many studies that are of interest to the scientific community including investigation of kink and cross-slip mechanisms and fcc/bcc interfaces. This work was completed in collaboration with Rebecca Runnels (New Mexico Tech) and Dr. Irene Beyerlein (LANL) and publications are in preparation.

Impact on National Missions

A primary mission of the Advanced Simulations and Computing (ASC) Program is to provide simulation capabilities required to maintain a safe, secure and reliable stockpile. While LANL has advanced atomistic and continuum simulation tools, it is not clear how to connect information on these two very different length scales; hence, there remains a computational gap at the mesoscale that translates into a gap in our understanding of material deformation. The PFDD model aims to fill this gap, and produce predictive multiscale simulations crucial for stockpile stew-

ardship. Furthermore, understanding the effects of defects on material behavior as materials age becomes increasingly important for determining the performance, reliability, and safety of weapon systems. The PI is intimately involved with developing and implementing material models for Integrated Codes and Physics and Engineering Models. This work is also in line with anticipated DOE/BES proposal calls on mesoscale modeling [24].

References

1. Chen, M. W., E. Ma, K. J. Hemker, H. W. Sheng, Y. M. Wang, and X. M. Cheng. Deformation twinning in nanocrystalline aluminum. 2003. Science. 300 (5623): 1275.

2. Farkas, D., S. Van Petegem, P. M. Derlet, and H. Van Swygenhoven. Dislocation activity and nano-void formation near crack tips in nanocrystalline Ni. 2005. Acta Materialia. 53 (11): 3115.

3. Liao, X. Z., F. Zhou, E. J. Lavernia, S. G. Srinivasan, M. I. Baskes, D. W. He, and Y. T. Zhu. Deformation mechanism in nanocrystalline Al: Partial dislocation slip. 2003. Applied Physics Letters. 83 (4): 632.

4. Schiotz, J., and K. W. Jacobsen. A maximum in the strength of nanocrystalline copper. 2003. Science. 301 (5638): 1357.

5. Shan, Z. W., E. A. Stach, J. M. Wiezorek, J. A. Knapp, D. M. Follstaedt, and S. X. Mao. Grain boundary-mediated plasticity in nanocrystalline nickel. 2004. Science. 305 (5684): 654.

6. Swygenhoven, H. Van, P. M. Derlet, A. G. Froseth, S. Van Petegem, Z. Budrovic, and A. Hasnaoui. Nanocrystalline fcc metals: bridging experiments with simulations. 2004. Nanoscale Materials and Modeling-Relations among Processing, Microstructure and Mechanical Properties. 821: 285.

7. Swygenhoven, H. Van, M. Spaczer, and A. Caro. Microscopic description of plasticity in computer generated metallic nanophase samples: A comparison between Cu and Ni. 1999. Acta Materialia. 47 (10): 3117.

8. Swygenhoven, H. Van, M. Spaczer, A. Caro, and D. Farkas. Competing plastic deformation mechanisms in nanophase metals. 1999. Physical Review B. 60 (1): 22.

9. Vo, N. Q., R. S. Averback, P. Bellon, S. Odunuga, and A. Caro. Quantitative description of plastic deformation in nanocrystalline Cu: Dislocation glide versus grain boundary sliding. 2008. Physical Review B. 77 (13): 134108.

10. Yamakov, V., D. Wolf, S. R. Phillpot, A. K. Mukherjee, and H. Gleiter. Deformation-mechanism map for nanocrystalline metals by molecular-dynamics simulation. 2004. Nature Materials. 3 (1): 43.

11. Zhu, Y. T., X. Z. Liao, S. G. Srinivasan, Y. H. Zhao, M. I. Baskes, F. Zhou, and E. J. Lavernia. Nucleation and growth of deformation twins in nanocrystalline aluminum. 2004. Applied Physics Letters. 85 (21): 5049.

12. Zhao, Y. H., Y. T. Zhu, X. Z. Liao, Z. Horita, and T. G. Langdon. Tailoring stacking fault energy for high ductility and high strength in ultrafine grained Cu and its alloy. 2006. Applied Physics Letters. 89 (12): 121906.

13. Hirth, J. P., and J. Lothe. Theory of dislocations. 1982.

14. Cockayne, D. J., M. L. Jenkins, and I. L. Ray. Measurement of Stacking-Fault Energies of Pure Face-Centred Cubic Metals. 1971. Philosophical Magazine. 24 (192): 1383.

15. Liao, X. Z., S. G. Srinivasan, Y. H. Zhao, M. I. Baskes, Y. T. Zhu, F. Zhou, E. J. Lavernia, and H. F. Xu. Formation mechanism of wide stacking faults in nanocrystalline Al. 2004. Applied Physics Letters. 84 (18): 3564.

16. Schoeck, G.. The cross-slip energy unresolved. 2009. Philosophical Magazine Letters. 89 (8): 505.

17. Yamakov, V., D. Wolf, M. Salazar, S. R. Phillpot, and H. Gleiter. Length-scale effects in the nucleation of extended dislocations in nanocrystalline Al by molecular-dynamics simulation. 2001. Acta Materialia. 49 (14): 2713.

18. Zhao, Y. H., X. Z. Liao, Y. T. Zhu, Z. Horita, and T. G. Langdon. Influence of stacking fault energy on nanostructure formation under high pressure torsion. 2005. Materials Science and Engineering A-Structural Materials Properties Microstructure and Processing. 410: 188.

19. Yamakov, V., D. Wolf, S. R. Phillpot, A. K. Mukherjee, and H. Gleiter. Dislocation processes in the deformation of nanocrystalline aluminium by molecular-dynamics simulation. 2002. Nature Materials. 1 (1): 45.

20. Liao, X. Z., F. Zhou, E. J. Lavernia, D. W. He, and Y. T. Zhu. Deformation twins in nanocrystalline Al. 2003. Applied Physics Letters. 83 (24): 5062.

21. Liu, Y., D. Bufford, H. Wang, C. Sun, and X. Zhang. Mechanical properties of highly textured Cu/Ni multilayers. 2011. Acta Materialia. 59 (5): 1924.

22. Zhang, J. Y., G. Liu, X. Zhang, G. J. Zhang, J. Sun, and E.

Ma. A maximum in ductility and fracture toughness in nanostructured Cu/Cr multilayer films. 2010. Scripta Materialia. 62 (6): 333.

23. Zhang, J. Y., X. Zhang, G. Liu, G. J. Zhang, and J. Sun. Scaling of the ductility with yield strength in nanostructured Cu/Cr multilayer films. 2010. Scripta Materialia. 63 (1): 101.

24. From Quanta to the Continuum: Opportunities for Mesoscale Science. 2012. Basic Energy Science Advisory Committee Mesoscale Science Subcommittee .

25. El-Awady, J. A., S. B. Biner, and N. M. Ghoniem. A self-consistent boundary element, parametric dislocation dynamics formulation of plastic flow in finite volumes. 2008. Journal of the Mechanics and Physics of Solids. 56 (5): 2019.

26. Wang, Y. U., Y. M. Jin, A. M. Cuitino, and A. G. Khachaturyan. Nanoscale phase field microelasticity theory of dislocations: Model and 3D simulations. 2001. Acta Materialia. 49 (10): 1847.

27. Koslowski, M., A. M. Cuitino, and M. Ortiz. A phase-field theory of dislocation dynamics, strain hardening and hysteresis in ductile single crystals. 2002. Journal of the Mechanics and Physics of Solids. 50 (12): 2597.

28. Hunter, A., and M. Koslowski. Direct calculations of material parameters for gradient plasticity. 2008. Journal of the Mechanics and Physics of Solids. 56 (11): 3181.

29. Koslowski, M.. Scaling laws in plastic deformation. 2007. Philosophical Magazine. 87 (8-9): 1175.

30. Koslowski, M.. Effect of grain size distribution on plastic strain recovery. 2010. Physical Review B. 82 (5): 054110.

31. Asaro, R. J., P. Krysl, and B. Kad. Deformation mechanism transitions in nanoscale fcc metals. 2003. Philosophical Magazine Letters. 83 (12): 733.

32. Douin, J., F. Pettinari-Sturmel, and A. Coujou. Dissociated dislocations in confined plasticity. 2007. Acta Materialia. 55 (19): 6453.

33. Gu, P., B. K. Kad, and M. Dao. A modified model for deformation via partial dislocations and stacking faults at the nanoscale. 2010. Scripta Materialia. 62 (6): 361.

34. Martinez, E., J. Marian, A. Arsenlis, M. Victoria, and J. M. Perlado. Atomistically informed dislocation dynamics in fcc crystals. 2008. Journal of the Mechanics and Physics of Solids. 56 (3): 869.

35. Wang, Z. Q., and I. J. Beyerlein. Stress orientation and relativistic effects on the separation of moving screw dislocations. 2008. Physical Review B. 77 (18): 184112.

36. Hunter, A., I. J. Beyerlein, T. C. Germann, and M. Koslowski. Influence of the stacking fault energy surface on partial dislocations in fcc metals with a three-dimensional phase field dislocations dynamics model. 2011. Physical Review B. 84 (14): 144108.

37. Shen, C., and Y. Wang. Incorporation of gamma-surface to phase field model of dislocations: simulating dislocation dissociation in fcc crystals. 2004. Acta Materialia. 52 (3): 683.

38. Ogata, S., J. Li, and S. Yip. Energy landscape of deformation twinning in bcc and fcc metals. 2005. Physical Review B. 71 (22): 244102.

39. Venables, J. A.. Electron Microscopy of Deformation Twinning. 1964. Journal of Physics and Chemistry of Solids. 25 (7): 685.

40. Christian, J. W., and S. Mahajan. Deformation Twinning. 1995. Progress in Materials Science. 39 (1-2): 1.

41. Hunter, A., and I. J. Beyerlein. Stacking fault emission from grain boundaries: Material dependencies and grain size effects. 2014. Materials Science and Engineering A. 600: 200.

42. Hunter, A., and I. J. Beyerlein. Unprecedented grain size effect on stacking fault width. 2013. Applied Physics Letters Materials. 1: 032109.

43. Swygenhoven, H. Van, P. M. Derlet, and A. Hasnaoui. Atomic mechanism for dislocation emission from nanosized grain boundaries. 2002. Physical Review B. 66 (2): 024101.

44. Hunter, A., and I. J. Beyerlein. Predictions of an alternative pathway for grain-boundary driven twinning. 2014. Applied Physics Letters. 104 (23): 233112.

45. Wu, X. L., X. Z. Liao, S. G. Srinivasan, F. Zhou, E. J. Lavernia, R. Z. Valiev, and Y. T. Zhu. New deformation twinning mechanism generates zero macroscopic strain in nanocrystalline metals. 2008. Physical Review Letters. 100 (9): 095701.

46. Yamakov, V., D. Wolf, S. R. Phillpot, and H. Gleiter. Deformation twinning in nanocrystalline Al by molecular dynamics simulation. 2002. Acta Materialia. 50 (20): 5005.

47. Wang, Z. Q., and I. J. Beyerlein. An atomistically-

informed dislocation dynamics model for the plastic anisotropy and tension-compression asymmetry of BCC metals. 2011. International Journal of Plasticity. 27 (10): 1471.

48. Zhang, R. F., J. Wang, I. J. Beyerlein, and T. C. Germann. Twinning in bcc metals under shock loading: a challenge to empirical potentials. 2011. Philosophical Magazine Letters. 91 (12): 731.

Publications

Beyerlein, I. J., J. S. Carpenter, A. Hunter, L. S. Toth, and W. Skrotzki. Nano-enabled orientation alignment via extreme shear strains. To appear in Scripta Materialia.

Cao, L., A. Hunter, I. J. Beyerlein, and M. Koslowski. The role of partial mediated slip during quasi-static deformation of 3D nano crystalline metals. To appear in Journal of the Mechanics and Physics of Solids.

Hunter, A., R. F. Zhang, I. J. Beyerlein, T. C. Germann, and M. Koslowski. Dependence of equilibrium stacking fault width in fcc metals on the gamma-surface. 2013. MODELLING AND SIMULATION IN MATERIALS SCIENCE AND ENGINEERING. 21 (2): -.

Hunter, A., R. F. Zhang, and I. J. Beyerlein. The core structure of dislocations and their relationship to the material g-surface. 2014. Journal of Applied Physics. 115: 134314:1.

Hunter, A., and I. J. Beyerlein. Unprecedented grain size effect on stacking fault width. 2013. Applied Physics Letters Materials. 1: 032109.

Hunter, A., and I. J. Beyerlein. Stacking fault emission from grain boundaries: Material dependencies and grain size effects. 2014. Materials Science & Engineering A. 600: 200.

Hunter, A., and I. J. Beyerlein. Predictions of an alternative pathway for grain-boundary driven twinning. 2014. Applied Physics Letters. 104: 233112:1.

Hunter, A., and I. J. Beyerlein. Relationship between monolayer stacking fault and twins in nano crystals. To appear in Acta Materialia.

Magnetic Field Effects on Convection-Modified Solid-Liquid Interfaces

Amy J. Clarke
20130755ECR

Abstract

In-situ characterization techniques are now affording direct interrogations of materials during synthesis and processing, in part because of first experiments performed by this team to monitor metal alloy melting and solidification with x-rays and protons. X-rays permit microstructural examinations of small fields-of-view in thin metal sections, whereas protons allow for imaging of larger fields-of-view in thin and thick metal sections. In this project, the influence of static magnetic field on tin-bismuth alloys during solidification was explored, demonstrating a new approach to further control microstructural evolution and fluid flow. Dendritic pattern development at the solid-liquid interface and macro-scale fluid flow during solidification in a static magnetic field were examined with real-time x-ray imaging at Argonne National Laboratory's Advanced Photon Source (APS) and 800 MeV proton radiography (pRad) at Los Alamos National Laboratory, respectively. Proton imaging revealed the macroscopic influences of magnetic field on casting mold filling, whereas x-ray imaging captured early-stage microscopic dendritic growth. From this initial exploration of the effect of static magnetic field on metal alloy solidification, it was determined that primary dendritic spacing decreased with a static magnetic field. Qualitative differences in casting mold filling and alloy melt flow behaviors were also observed with a static magnetic field, compared to the results obtained without one. This work highlights the potential use of static magnetic field as an effective way to modify metal alloy solidification at the micro- and macroscopic length scales.

Background and Research Objectives

Metal alloy melt flows interact with solid interfaces at a variety of length scales, from the microscopic scale dendritic tips that develop at the solid-liquid interface to the macroscopic interactions with the casting mold during filling. The flows that arise in the alloy melt during casting and solidification will influence the distribution of solute, potentially leading to enhanced macro- and microsegregation (i.e., chemical inhomogeneity), reduced casting quality, and microstructural variations.

Specific types of micro- and macroscopic fluid flows may be achieved during casting and solidification by controlling the geometry and heat flux. In addition to these variables, the application of a magnetic field may constitute a way to further influence alloy melt fluid flows and solidification structural development. For example, Imhoff et al. have applied a 35 Tesla magnetic field to metal alloys during solidification, which resulted in microstructures with enhanced crystallographic anisotropy and different phase morphologies compared to those solidified without a magnetic field [1]. Weak magnetic field has also been used to create zirconia- and alumina-magnetite aligned solidification structures and aligned titania-magnetite scaffolds that exhibit substantially higher strengths than similar (unaligned) structures produced without a magnetic field [2]. In early work, Li et al. reported increasing primary dendritic spacing with increasing magnetic field intensity from 0 to 14 Tesla and larger dendritic spacing for a lower solid-liquid interface velocity and a given magnetic field intensity for an aluminum-4.5 wt.% copper alloy [3]. However, in more recent work Li et al. reported decreasing primary dendritic spacing with increasing magnetic field intensity from 0 to 1 Tesla and larger primary dendritic spacing for a higher solid-liquid interface velocity and a given magnetic field intensity [4].

The effect of a weak (0.08 Tesla) transverse magnetic field on convection and microstructural evolution in aluminum-4 wt.% copper and aluminum-10 wt.% copper alloys was examined by Li et al. with in-situ x-ray imaging. The observed microscopic flows were reportedly linked to the microstructural evolution and the final microstructure [4]. Apart from post-mortem microstructural examinations and the qualitative in-situ x-ray imaging examinations described above, quantitative and in-situ

characterizations of the effect of weak magnetic field on microstructural evolution are lacking.

At the macroscopic scale, electromagnetic breaking (EMBr) is used to control alloy melt fluid flow during continuous casting, as flow control is critical for avoiding the entrapment of inclusions and achieving the desired heat transfer and solidification behavior. Visualizing the complex flows produced by EMBr is challenging, but large-scale eddy current simulations have been used to model these flows for continuous casting scenarios with EMBr and insulating or conducting walls [5]. Experimental observations of macroscopic fluid flow during metal casting are challenging and are typically only simulated with water modeling. Liu et al. recently visualized macroscopic fluid flows during continuous casting without and with air gas injection by water modeling [6]. Although computational and experimental simulations of macroscopic flows during metal casting have been performed, direct observations of metal casting, especially those that include variables like magnetic field, are nonexistent at scales relevant for industry.

Turbulent flow and convection in the liquid may be altered by changing the effective liquid viscosity by the application of magnetic field [7], perhaps changing the local flow conditions at the solid-liquid interface to impact microstructural evolution or the large-scale flows encountered during casting mold filling and subsequent solidification. We use x-ray and proton imaging to make movies during solidification to explore the potential of static magnetic field for the modification of alloy melt fluid flow and the formation and growth of solid-liquid interface patterns (e.g., the formation and growth of dendrites). Understanding how static magnetic field may be used to control fluid flow and microstructural development in metal alloys will enable improved casting design and quality and the creation of intended microstructures.

Scientific Approach and Accomplishments

The role of magnetic field on macro-scale alloy melt fluid flow and micro-scale solid-liquid interface pattern development has been examined using real-time x-ray and proton imaging at Argonne and Los Alamos National Laboratories, respectively. X-rays permit microstructural examinations of a small field-of-view in thin metal sections, whereas protons allow for imaging of larger fields-of-view in thin and thick metal sections. Proton imaging was used to measure the macro-scale influences of a magnetic field on casting mold filling and x-ray imaging was used to observe initial microstructural development in the presence of a magnetic field. These complementary experiments enable the relative effectiveness of the imposed magnetic field to modify fluid flow and structural evolution to be directly assessed.

For both the x-ray and proton imaging experiments, permanent neodymium-iron-boride magnets were used to provide a uniform static magnetic field. During casting and solidification, one magnet was placed on either side of the metal alloy sample, as shown schematically Figure 1a. Ideally, the field strength between two the two large parallel magnets would be constant, however the required spacing needed to achieve this would impede the ability to conduct the experiments. Therefore, the field strength between the two magnets varied with position, and the magnet strength and positioning were chosen after systematic calculations that directly aided in the experimental design to provide the proper field strength profile. The result of these calculations for the casting experiments is also shown in Figure 1a. A diminishing strength is observed toward the center of the experimental set-up, and must be accounted for when selecting the experimental parameters.

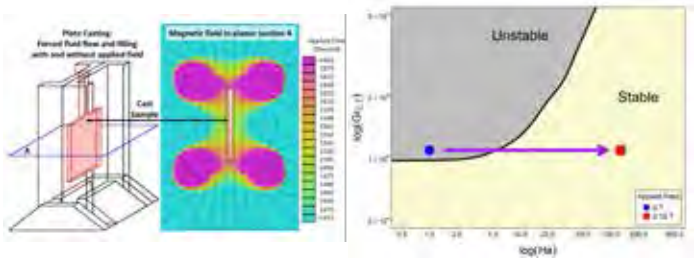

Figure 1. (a) The geometry used for the proton imaging experiments of casting mold filling with and without the application of a static magnetic field and the magnetic field in the indicated cross-section and (b) Grashof (Gr) and Hartmann (Ha) numbers indicating the regimes of unstable and stable flow with the application of a static magnetic field.

For the experiments, the potential effect of field interactions on flow must be considered. For magneto-hydrodynamic flow, there are two dimensionless numbers we used to predict the magnetic damping of thermal convection in field, namely the Hartmann and Grashof numbers. The Hartmann number represents the amount of magnetic damping and is the ratio of the induced magnetic force to the viscous force. In contrast the Grashof number is a predictor of the strength of the convection forces and is calculated by taking the ratio of the thermosolutal buoyant force and the liquid's viscous force. At high Hartmann numbers, the thermosolutal convection is sufficiently damped to have little direct influence on local structural development; while at high Grashof numbers, there is sufficient buoyant driving force to transition to significant convection cell development. When both thermosolutal and magnetic forces are at play, the destabilization of the liquid

(i.e. development of convection cells) can be predicted by balancing both effects. The calculated regions of stability and instability are plotted in Figure 1b. By imposing a sufficiently large magnetic field on a sample, the Hartman number may be increased to eliminate undesired convection in a system. For the present experiments, the size, strength and location of the magnets with respect to the area of interest for imaging were selected to sufficiently modify the flow behavior during metal alloy casting and solidification. For the relevant geometries, this required an effective magnetic field minimum of ~1200 gauss. The experiments were designed so that the saddle point in the field strength was no lower than this limit. The experiments presented here were performed using a tin-27 at.% bismuth alloy to take advantage of the high x-ray absorption contrast between the tin-rich initial solid and the bismuth enriched liquid during solidification.

Synchrotron x-ray imaging was performed at the Sector 32 Insertion Device beamline at Argonne National Laboratory's Advanced Photon Source. For imaging, a monochromatic 28 keV x-ray beam was used. X-rays pass through a metal foil sample and impinged upon scintillator where they were converted to visible light. The movie camera captured 1024 x 1280 pixel images at an approximate frame rate of 0.85 Hz, with a pixel size of 1.3 microns. The imaging field of view (FOV) was ~1.4 x 1.7 mm. Each metal alloy sample was placed between two boron nitride crucible halves with a ~0.1 mm thick window and then inserted into a slotted steel rod with a 5 mm through hole perpendicular to the flat plane of the crucible to accommodate the beam path. The images were post processed to remove the background and normalize the gray-scale to a constant reference; all image analysis was performed using ImageJ software. Primary dendrite tip velocities were measured using manual tracking in ImageJ, beginning with the frame in which the tip of the first dendrite entered the FOV, and ending when the dendrite exited the FOV.

Direct imaging of solidification with x-rays enabled the measurement of branched dendritic structures that formed as the first solid in the metal alloy. Figure 2 shows representative images from the solidification sequence without an imposed magnetic field (Figure 2a) and in a 0.12 T static magnetic field orthogonal to the vertical axis of the image (Figure 2b). Individual dendrite velocities were measured multiple times and the average tip velocity was determined. The primary and secondary dendrite arm spacing for the alloys was also determined. The center-to-center distance between adjacent dendrite arms was measured, and these values were averaged over multiple measurements to determine the overall spacing. The dendrite spacing measurements were performed on an image where a dendrite had traversed half the FOV. Secondary dendrite spacings were measured near the tip of the primary dendrite arms.

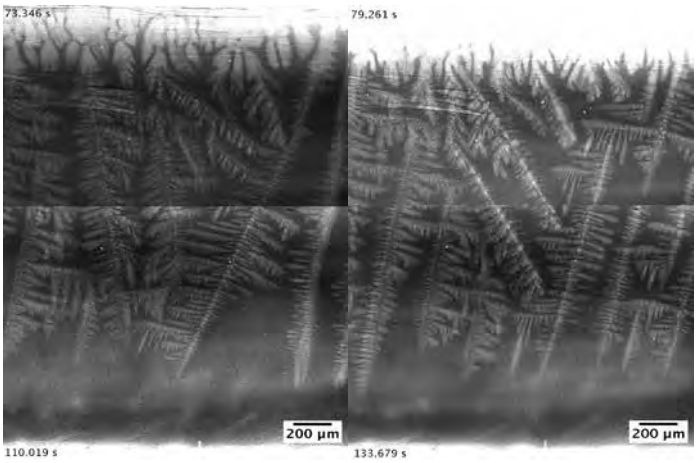

Figure 2. X-ray images from directional solidification of a tin-27 at.% bismuth alloy parallel to gravity with (a) no externally applied magnetic field and (b) an 0.12 T static magnetic field orthogonal to the nominal dendritic growth direction.

For the directional solidification experiments without and with the static magnetic field, a thermal gradient (G) of 27 K/cm and a solid-liquid interface velocity (V) of 20 microns/s and a G of 27 K/cm and a V of 15 microns/s were determined, respectively. In the presence of the static magnetic field, overall refinement of the dendritic structure was observed (i.e., a decrease in primary dendritic spacing from 288 to 200 microns). Reduced dendritic spacing is essential for improving the properties and performance of as-cast parts. The appearance of dendritic side branches also changed with application of the static magnetic field. The branches became more frequent, but less prone to further growth, implying that the fluid flow and mixing adjacent to the dendrite arms was effectively suppressed. However, it must be recalled that this system is not over damped. In continuous casting where EMBr is employed, the forced convection velocities are high so the effect of convection on the microstructure may be in the form of remelting solidified regions as the liquid jets impinge upon a cooler region. The effect here is less dramatic, but has a strong effect on the local environments. Reduction in liquid velocity requires that both solute and thermal boundary layers near the growth front of the dendrites will be more spread out than without magnetic damping. Most importantly, this means that the solute is enriched near the dendrite tips, thereby changing the side branching environment and consequently the primary spacing. These findings fit into a larger overall picture of convection effects on morphology development during solidification, supporting the trend reported by Li et al. of

decreasing primary dendritic spacing with increasing magnetic field intensity and larger primary dendritic spacing for a higher solid-liquid interface velocity and a given magnetic field intensity [4].

For the pRad imaging experiments, a plate geometry was selected for the casting mold filling experiments to limit projection artifacts from overlapping features. Graphite was used for the mold material; no coating was applied to the inside surfaces of the mold cavity. The casting mold was directly filled from the downsprue, without a gating system. A funnel shaped crucible was placed on top of the graphite mold, and a pure bismuth plug was pre-melted in to the bottom of the crucible. A 40 g charge of a tin 27at.% bismuth alloy was loaded into the crucible. During heating, the alloy charge melted first. When the bismuth plug finally melted, the alloy melt was released into the mold cavity. This enabled relatively repeatable pouring conditions, without mechanical control within the radiation enclosure of the proton beamline. A thinned window area was machined into the sides of the mold walls to facilitate the proton imaging. The mold stack was clamped in a water-cooled aluminum stand to develop a large gradient in the vertical axis of the mold and promote directional solidification. Each mold was instrumented with sheathed 0.5 mm diameter thermocouples to provide temperature monitoring and feedback control. The thermocouples were placed approximately 1.5 mm away from the plate cavity directly below the downsprue, near each corner of the plate. The crucible and top of the mold were heated using independently controlled induction heaters. Additional thermocouples were placed in the crucible above the mold cavity and adjacent to the downsprue to monitor the crucible heating.

For the proton imaging of the casting mold filling, the identity lens configuration was used. This permits an imaging FOV with nominal dimensions of 120 × 120 mm and approximately 100 micron spatial resolution. Imaging rates were 10 and 20 Hz for the castings, with and without the imposed magnetic field, respectively. The entire mold cavity was visible within the FOV during the filling, while the base of the funnel was just visible in the images, as shown in Figure 3. The transmission radiographs were post processed to maximize local contrast and to normalize the gray-scale to a consistent reference. To remove artifacts in the proton images resulting from local variations in brightness due to deviations in beam intensity, the images were divided by representative images of the beam.

The proton imaging suggests that introduction of a static magnetic field across the casting mold cavity subtly, but significantly, modified the behavior of the liquid metal alloy during filling. These images enabled the first measurements of the fluid stream and initial splashing during the filling of the mold cavity to be made. Increased width of the metal alloy stream was observed with the static magnetic field, suggesting that the velocity of the falling liquid was effectively decreased. In addition, less splashing and droplet separation were observed during the introduction of the metal alloy into the cavity, resulting in improved filling behavior, as shown in Figure 4, and a decrease in the susceptibility of the casting to surface defects that could influence the casting quality. Subtle changes in the liquid surface shape during filling were also observed with application of the static magnetic field.

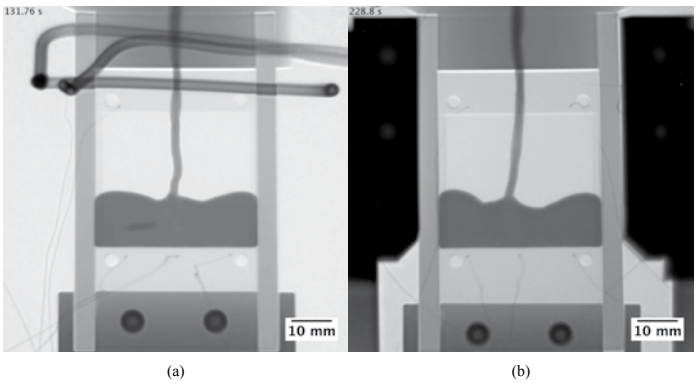

Figure 3. Proton images of a casting mold filling of a tin-27 at.% bismuth alloy with (a) no externally applied magnetic field (20 Hz imaging rate) and (b) a 0.12 T static magnetic field aligned orthogonal to gravity (10 Hz imaging rate).

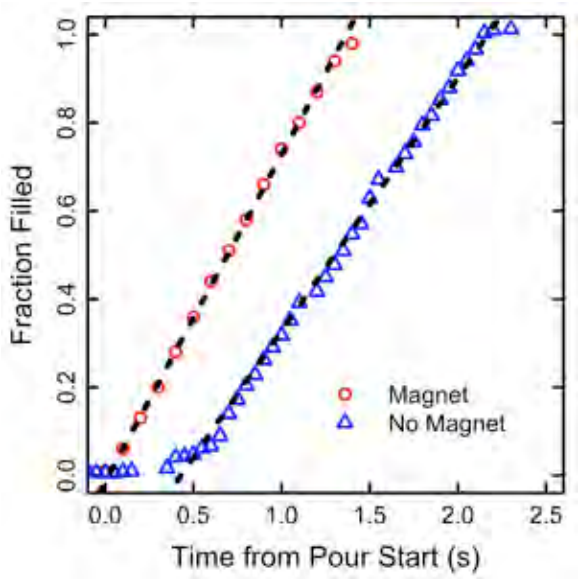

Figure 4. Normalized fraction filled measured from the proton images of casting mold fillings of a tin-27 at.% bismuth alloy with and without a 0.12 T static magnetic field.

Impact on National Missions

Convection of an alloy melt during casting mold filling plays a critical role in the solute segregation that develops at

the macro-scale, whereas localized convection cells that develop during solidification drastically influence micro-scale solute segregation and morphological and micro-structure evolution. Application of a static magnetic field during solidification provides an opportunity to control alloy melt fluid flow characteristics and the interface shape and dynamic equilibrium at that interface. Materials for the future, including the creation of materials with application-tailored properties to achieve controlled functionality by directed synthesis and processing, is one of three science pillars at Los Alamos National Laboratory. Controlling materials synthesis and processing and the design of materials functionality through the exploitation of defects and interfaces, understanding the dynamic evolution of materials, defect structures, and interfaces, and the use of novel characterization techniques, especially at extremes, are priorities listed in Los Alamos National Laboratory's Directed Research and Development Defects and Interfaces in Materials (DIM) Exploratory Research Category. These priorities are also reflected in the laboratory's Matter-Radiation Interactions in Extremes (MaRIE) Signature Facility vision, and are deeply rooted in nationally recognized needs identified by the U.S. DOE Basic Energy Sciences, The National Academies, and the White House Office of Science and Technology Policy's Materials Genome Initiative (MGI).

References

1. Imhoff, S. D., T. J. Ott, T. J. Tucker, M. R. Katz, and J. C. Cooley. Primary phase alignment in the Mg-Sb system with a 35-T DC magnetic field. 2013. Emerging Materials Research. 2 (EMR2): 5.

2. Porter, M. M., J. Mckittrick, and M. A. Meyers. Biomimetic materials by freeze casting. 2013. JOM. 65 (6): 720.

3. Li, X., Y. Fautrelle, and Z. Ren. Influence of an axial high magnetic field on the liquid – solid transformation in Al – Cu hypoeutectic alloys and on the microstructure of the solid. 2007. Acta Materialia. 55: 1377.

4. Li, X., Y. Fautrelle, A. Gagnoud, D. Du, J. Wang, Z. Ren, H. Nguyen-Thi, and N. Mangelinck-Noel. Effect of a weak transverse magnetic field on solidification structure during directional solidification. 2013. Acta Materialia. 64: 367.

5. Singh, R., B. G. Thomas, and S. P. Vanka. Effects of a magnetic field on turbulent flow in the mold region of a steel caster. 2013. Metallurgical and Materials Transactions B. 44: 1201.

6. Liu, Z., B. Li, and M. Jiang. Transient asymmetric flow and bubble transport inside a slab continuous-casting mold. 2014. Metallurgical and Materials Transactions B. 45: 675.

7. Easter, S., V. Bojarevics, and K. Pericleous. Numerical modelling of liquid droplet dynamics in microgravity. 2011. Journal of Physics: Conference Series. 327: 012027.

Effects of Joining Processes on Bimetal Interface Content and Radiation Damage Resistance

John S. Carpenter
20130764ECR

Abstract

This document is a final report on the LDRD-ECR awarded in January 2013 entitled 'Effects of Joining Processes on Bimetal Interface Content and Radiation Damage Resistance'. The proposed work stemmed from the desire to provide an industrially practical joining method for bimetallic nanolayered composite materials that exhibit highly desirable traits such as high strength, radiation damage resistance, and thermal stability. The key to maintaining these properties is control of the joining process such that interface density (or layer thickness for a multilayered composite) and the atomic structure of the interfaces is maintained. The model system of Cu-Nb was selected and the solid state joining process of friction stir welding (FSW) was chosen as the focus of the proposed work. Successful friction stir welds were accomplished for the first time in a nanolayered bimetallic composite material over the course of this study. In addition, through careful design of the FSW tooling and process parameter combinations, near full-strength butt welds were achieved. These same high-strength butt welds also exhibited large scale stability of both interfacial density and interfacial structure. Although further refinement is needed in FSW process parameters and tool design, this study shows that the FSW methodology can be applied to join nanostructured metal composites successfully. With industrially scalable processing techniques available for the bulk nanostructured metals, an industrially practical joining technique was the remaining obstacle to utilizing these synthetic materials in a multitude of applications including those in the fields of defense, transportation, and energy.

Background and Research Objectives

During the late 90's LANL scientists showed that as the length scale of bimetal composites began to decrease, novel increases in strength [1-3], radiation damage resistance [4,5] and thermal stability [6,7] were noted that far exceeded what was measured in bulk metals. The enhancements in properties, through a combination of experimental and modeling studies, were found to emanate primarily from the high density of interfaces and the specific atomic-level interfacial structures in the composites [5,8-11]. Various applications within the defense, transportation, and energy arenas were envisioned for material exhibiting this collection of desirable characteristics [4,12]. However, the physical vapor deposition (PVD) process used to manufacture these nanoscale bimetal composites was too slow for scale up due to its dependence on building up the structure atom-by-atom. Within the past five years, work at LANL through an LDRD-DR grant has provided an industrially scalable methodology for manufacturing bulk sheets of nanostructured bimetal composites through a top-down methodology [13,14]. These bulk sheets were manufactured using accumulative roll bonding (ARB) and they exhibited microstructures, properties, and performance in extreme conditions similar to the PVD material [15-18]. An example microstructure for the ARB material can be seen in Figure 1. In order to realize the potential for this class of materials in engineering applications, industrially feasible joining techniques are required. The planned objective for this work was to find a suitable industrially feasible joining technique that maintained the nanostructure (both density and structure of interfaces).

A prior LDRD-DR at LANL focused on the fabrication of bulk bimetal layered composites using the ARB technique. Success was achieved for the Cu-Nb system and characterized material for this study was provided via this route. An initial attempt at joining was made utilizing electron beam welding but, as expected, the melting of the material lead to a loss of both the density and structure of the interfaces. Through this seed study, it was concluded that any joining methodology that relied on fully melting the parent material for joining purposes would destroy the desirable properties that make the Cu-Nb material unique. The focus of this research then became solid-state joining methods, or methods that did not require full melting of the material. The most

promising of the solid-state joining methods was friction stir welding.

Friction stir welding (FSW) is a solid-state welding process that makes use of friction and deformational heating to plastically deform and coalesce materials to create a joined structure [19,20]. This technique was initially developed for aluminum because the microstructural instabilities encountered during fusion welding required additional post-weld heat treatments [19-21]. Figure 2 shows a schematic of the FSW process in the inset [22]. In FSW, a rotating tool is inserted through the material thickness and travels down the joint line between two separate pieces of material [20,23]. A predetermined load maintains the shoulder contact as the rotating tool travels down the joint line and physically mixes the materials.

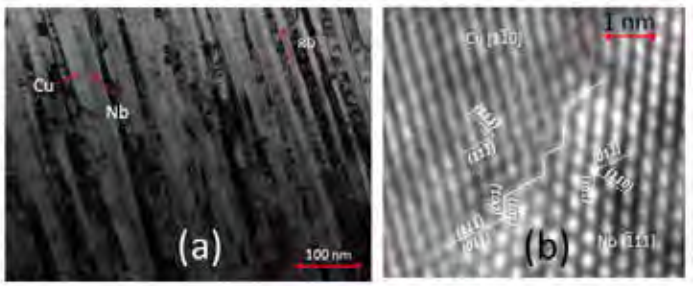

Figure 1. (a) Micrograph of ARB Cu-Nb with defined lamellar structure at h = 10 [15]. (b) High resolution TEM micrograph of an interface at h = 18 nm. Interfacial structure consists of joined {112} planes with epitaxial orientation relationship [15].

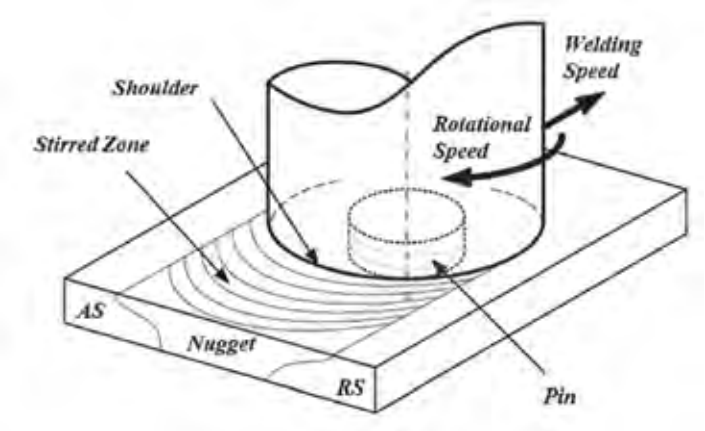

Figure 2. Diagram describing general FSW process with advancing (AS) and retreating (RS) sides labeled [22].

FSW, to this point, has been largely utilized on materials comprising only a single metal or phase since the process brings the material close to melting temperature. Cu and Nb have substantially different melting temperatures that add a complicating factor to any attempts at FSWing. FSW is also commonly applied to soft metals with low melt temperatures to minimize tool wear. The competing melting temperatures coupled with the high strength of this material made for a difficult challenge without even taking into account the desire to maintain the material's initial nanostructure. Despite these challenges, an aggressive set of research objectives was outlined for this study:

Year One: Perform initial studies of FSW on ARB nanoscale material to give fully dense, high quality welds. Deliverable: Publish results on FSW and fusion weld parameters and the interfacial effects on weld quality, hardness, and post-processing interfaces in a peer-reviewed journal.

Year Two: Continue to refine FSW joining technique parameters to tailor strength and interfacial structure. Integrate radiation damage resistance studies on all samples, if warranted. Deliverables: (A) Provide a butt-welded plate with minimal reductions in strength and radiation damage resistance. (B) A set of optimized parameters for joining ARB Cu-Nb plates that maintains the desirable properties. (C) Publish results on effects of weld parameters on microstructure, individual interface content and radiation damage resistance in peer-reviewed journal.

Success would have a three-fold impact:

- LANL would maintain its leadership status in cutting-edge research in the field of bimetallic nanolayered composite materials.
- The number and type of materials to which the FSW method could be applied would be expanded.
- A pathway for joining industrial-sized quantities of bimetal nanolayered composites would be realized allowing for a transition from a model material to a real engineering material.

Scientific Approach and Accomplishments

In this section, the scientific approach and accomplishments will be conveyed in the context of the two year set of research objectives seen in the previous section.

In year 1, bead-on-plate FSWs were performed on nanoscale Cu-Nb layered composites using a tungsten alloy for tooling. Several sets of processing parameters were utilized in order to obtain a fully consolidated (i.e. defect-free) weld zone. The tool geometry was simplistic, consisting of an unadorned cylindrical pin and a flat shoulder region. The best result obtained using this initial pin can be seen in Figure 3. A large defect on the advancing side is seen indicating that the pin failed to draw the material in during the stir processing. In addition, it can be seen that the microstructure within the weld nugget is nanocrystalline and equiaxedl in grain shape with grain diameters of ~7 nm. The measured strength, utilizing nanoindenta-

tion methods, exhibited a near 250% increase in the weld nugget when compared with the parent material. The increase in strength observed in this region when compared with the parent material is a product of having 3D nanograins as opposed to only a single nanoscale dimension within the composite sheet structure. Although the strength was improved, the fine (~ 7 nm) grain diameters made it impossible to investigate interfacial structures. No characterization method currently available would be able to provide orientation information from these small volumes. These results have been communicated via a peer-reviewed journal publication [24].

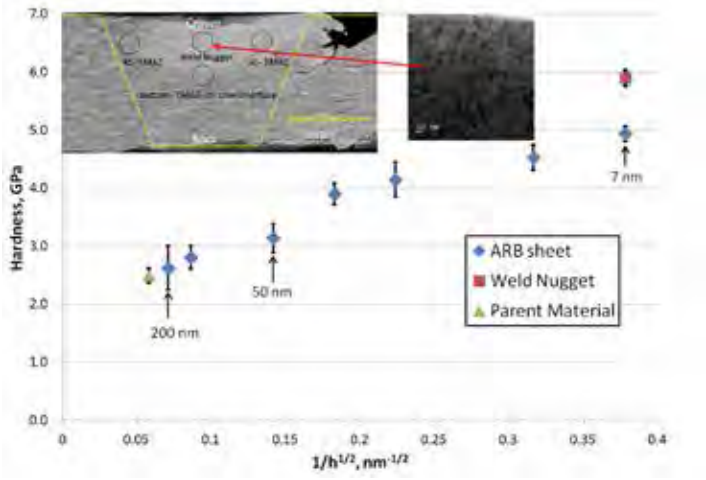

Figure 3. Hardness versus interfacial spacing plot showing the large increase in hardness between the weld nugget and the parent material. Blue diamonds represent data points for refined ARB material without FSW. The inset electron microscopy images show the best case bead-on-plate weld and the equiaxed nanocrystalline structure within the weld nugget [24].

Previous work using high pressure torsion (HPT) [25] suggested that an ideal strain was present during rotational straining of the ARB Cu-Nb material. Similar to FSW, HPT involves a shoulder in contact with a material with the tooling having both a load and a rotational speed. Unlike FSW, HPT does not involve a translational movement of the shoulder contact nor include a pin. The HPT work showed that at high strains a nanocrystalline, equiaxed microstructure of Cu and Nb grains was created while at more moderate strains, the lamellar structure was maintained. This indicated a need to reduce the level of strain during FSW via process parameters such as rotational speed, downward load on the tool, and translational speed. In addition, the large defect seen in Figure 3 revealed a need for a pin geometry redesign to pull more material in during the stirring process.

At the beginning of year 2, initial focus was placed on redesigning the pin geometry. Pin size and geometry is restricted by the overall thickness of the Cu-Nb sheets. Efforts were, therefore, made in the beginning of the year to manufacture thicker Cu-Nb sheets and the outcome was an increase from a 500 um overall thickness to a 3 mm overall thickness. With this increase in sheet size, further design space was opened up in FSW tooling design. A single scroll, or channel, was carved into the shoulder in a helical pattern in order to promote better welding. In addition, flats were placed on the sides of the pin to create a more triangular shape which has been shown to promote enhanced welding. Technical obstacles that needed to be overcome during this part of the work included the small scale machining of the tungsten alloy used in the tooling as well as modifying the ARB process to accommodate a thicker final sheet.

Butt welding, or the joining of two separate plates, was performed while investigating the proper process parameters to achieve a fully consolidated weld. Success in this endeavor was achieved through careful manipulation of process parameters in conjunction with the new tool design. Two fully consolidated welds were achieved for two sets of process parameters with the material either undergoing one pass or two passes to achieve effective joining. Images of the single pass weld can be seen in Figure 4. Through optical and electron microscopy it was noted that in the single pass weld, a layered microstructure was still visible throughout the weld nugget. In the two-pass weld, on the other hand, a nanocrystalline and equiaxed microstructure was observed.

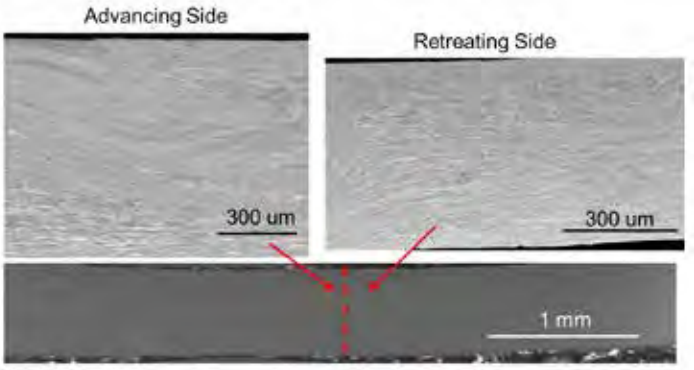

Figure 4. Micrographs showing the fully consolidated one pass butt weld (bottom) where red dashed line indicates where the material was joined. No defects on either the advancing or retreating side were noted. Detailed micrographs show that a layered structure is maintained during joining.

Tensile testing was conducted on the one and two pass welds, with the one-pass weld exhibiting a higher strength than the two-pass weld. In addition, the one-pass weld compared favorably with tensile test results for the parent material with no weld as seen in Figure 5. Failure of both the one and two-pass welds was a normal chisel-edge type

fracture surface (not shown in this report) that is indicative of a ductile failure. This is an important result because it indicates that if this weld had been put into service, noticeable deformation would have occurred prior to failure.

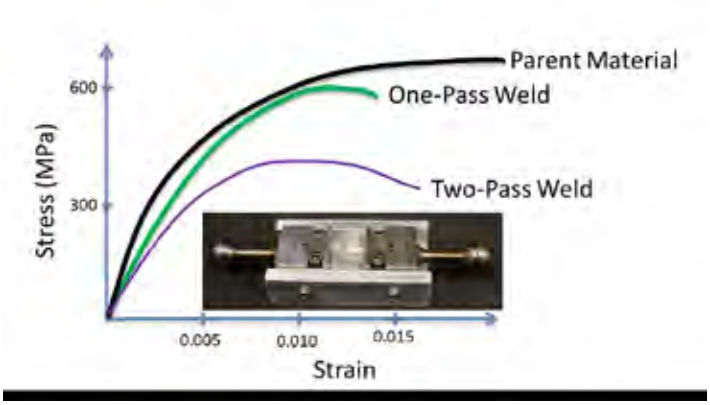

Figure 5. Plot summarizing mechanical testing data for the one-pass and two-pass welds. The welds are compared with the mechanical behavior of the parent material [26]. The one-pass weld shows that it reaches more than 90% of the strength of the parent material with limited decrease in ductility. The inset shows the experimental setup which included dog-boned shaped tensile specimens.

Utilizing electron backscatter diffraction (EBSD) methods, the atomic structure of the interface was inferred as well as the density of interfaces. Strain levels within a weld nugget or stir zone vary. The maximum value occurs near the leading edge of the shoulder's interaction with the material during tool rotation, also known as the advancing side. The minimum strain level is found on the opposite side of the weld nugget from the advancing side. In Figure 4, the advancing or high strain side is on the left of the image while the retreating or low strain side of the weld nugget is seen on the right. The EBSD results (not shown in this report) indicated that the interface density and atomic structure of the interface were both maintained in the single pass weld on the retreating side. On the advancing side, the layered composite microstructure was more tortured making an assessment of the interfaces more difficult. This result suggests that with further refinement of process parameters and a more complicated tool design, butt welds could be made that provide little to no change in the microstructural features responsible for the enhanced mechanical properties.

Radiation damage tolerance testing is currently underway in order to see if the resistance to radiation damage is maintained following the FSW process.

This work has directly led to three invited conference talks, one invited seminar, one publication in print, and two publications in preparation.

Impact on National Missions

The technical results outlined above have lead to new collaborations with outside academic institutions, new capabilities within the laboratory, and the introduction of new students and postdocs to the laboratory. The reaction of the Cu-Nb nanolamellar composite to FSW caught the attention of wear researchers from Clemson University. A collaboration with Professor Molly Kennedy and her research team has begun by studying the wear properties of the parent material with the eventual goal of exploring the wear properties of the equiaxed nanocrystalline material as described in Cobb et al. [24]. A second academic collaboration has also begun with the University of New Hampshire and is centered on understanding the mechanisms that lead to the plastic deformation seen during FSW in these composites. Initial characterization indicates that the lamellar composite geometry leads to distinct differences in plastic flow. Professor Marko Knezevic is excited to apply his plasticity model and incorporate a second phase in order to understand the physics of flow in the confined layer geometry presented by the nanolamellar composites.

This work has enabled new capabilities within the lab. Through the fabrication of tooling for the FSWing, machinists here at the lab have become familiar with the response of W-La2O3 to milling and machining. This ultra-hard metal can be used to manufacture FSW tools in the future and for other applications that require strength coupled with high temperature stability. Another capability developed at the laboratory through this work has been the introduction of a nanoindentation technique that can extract elastic moduli for indents of limited (<50 nm) depth. Finally, this work has lead to the new capability of performing FSW on bimetallic nanolamellar composite materials.

Shraddha Vacchani, a former graduate student from Georgia Tech, assisted on this project during the summer of 2013 by using the FSWed material in order to develop the aforementioned nanoindentation methodology. She has since started a post-doctoral researcher position here at the laboratory due, in part, to the excellent experience she had as a summer student. Josef Cobb of Mississippi State University (MSU) was also involved in this project and performed work in this area during academic years at MSU and during summers at LANL. This research will form the core of his PhD thesis and the PI will serve on the dissertation committee.

References

1. Misra, A., M. Verdier, Y. C. Lu, H. Kung, T. E. Mitchell, M. Nastasi, and J. D. Embury. Structure and mechanical properties of Cu-X (X = Nb,Cr,Ni) nanolayered compos-

ites. 1998. Scripta Materialia. 39: 555.

2. Clemens, B. M., H. Kung, and S. A. Barnett. Structure and strength of multilayers. 1999. MRS Bulletin. 24: 20.

3. Mara, N. A., D. Bhattacharyya, P. Dickerson, R. G. Hoagland, and A. Misra. Deformability of ultrahigh strength 5 nm Cu/Nb nanolayered composites. 2009. Applied Physics Letters. 92: 231901.

4. Zhang, X., N. Li, O. Anderoglu, H. Wang, J. G. Swadener, T. Hochbauer, A. Misra, and R. G. Hoagland. Nanostructured Cu/Nb multilayers subjected to helium ion-irradiation. 2007. Nuclear Instruments & Methods In Physics Research Section B-Beam Interactions With Materials And Atoms. 261: 1129.

5. Misra, A., M. J. Demkowicz, X. Zhang, and R. G. Hoagland. The radiation damage tolerance of ultra-high strength nanolayered composites. 2007. JOM. 59: 62.

6. Misra, A., R. G. Hoagland, and H. Kung. Thermal stability of self-supported nanolayered Cu/Nb films. 2004. Philosophical Magazine. 84: 1021.

7. Misra, A., and R. G. Hoagland. Effects of elevated temperature annealing on the structure and hardness of copper/niobium nanolayered films. 20. Journal of Materials Research. 2005: 2046.

8. Demkowicz, M. J., Y. Q. Wang, R. G. Hoagland, and O. Anderoglu. Mechanisms of He escape during implantation in CuNb multilayer composites. 2007. Nuclear Instruments & Methods In Physics Research Section B-Beam Interactions With Materials And Atoms. 261: 524.

9. Demkowicz, M. J., R. G. Hoagland, and J. P. Hirth. Interface structure and radiation damage resistance in Cu-Nb multilayer nanocomposites. 2008. Physical Review Letters. 100: 136102.

10. Demkowicz, M. J., D. Bhattacharyya, I. Usov, Y. Q. Wang, M. Nastasi, and A. Misra. The effect of excess atomic volume on He bubble formation at fcc-bcc interfaces. 2010. Applied Physics Letters. 97: 161903.

11. Mara, N. A., D. Bhattacharyya, J. P. Hirth, P. Dickerson, and A. Misra. Mechanism for shear banding in nanolayered composites. 2010. Applied Physics Letters. 97: 021909.

12. Han, W. Z., A. Misra, N. A. Mara, T. C. Germann, J. K. Baldwin, and T. Shimada. Role of interfaces in shock-induced plasticity in Cu/Nb nanolaminates . 2011. Philosophical Magazine. 91 (32): 4172.

13. Carpenter, J. S., S. C. Vogel, J. E. LeDonne, D. L. Hammon, I. J. Beyerlein, and N. A. Mara. Bulk texture evolution of Cu-Nb nanolamellar composites during accumulative roll bonding. 2012. Acta Materialia. 60 (4): 1576.

14. Carpenter, J. S., R. J. McCabe, S. J. Zheng, T. A. Wynn, N. A. Mara, and I. J. Beyerlein. Processing Parameter Influence on Texture and Microstructural Evolution in Cu-Nb Multilayer Composites Fabricated via Accumulative Roll Bonding. 2014. Metallurgical and Materials Transactions A. 45A (4): 2192.

15. Han, W. Z., J. S. Carpenter, J. Wang, I. J. Beyerlein, and N. A. Mara. Atomic-level study of twin nucleation from face-centered-cubic/body-centered-cubic interfaces in nanolamellar composites. 2012. Applied Physics Letters. 100 (1): 011911.

16. Carpenter, J. S., S. J. Zheng, R. F. Zhang, S. C. Vogel, I. J. Beyerlein, and N. A. Mara. Thermal stability of Cu-Nb nanolamellar composites fabricated via accumulative roll bonding. 2013. Philosophical Magazine. 93 (7): 718.

17. Han, W. Z., M. J. Demkowicz, N. A. Mara, E. G. Fu, S. Sinha, A. D. Rollett, Y. Q. Wang, J. S. Carpenter, I. J. Beyerlein, and A. Misra. Design of Radiation Tolerant Materials Via Interface Engineering. 2013. Advanced Materials. 25 (48): 6975.

18. Han, W. Z., E. K. Cerreta, N. A. Mara, I. J. Beyerlein, J. S. Carpenter, S. J. Zheng, C. P. Trujillo, P. O. Dickerson, and A. Misra. Deformation and failure of shocked bulk Cu-Nb nanolaminates. 2014. Acta Materialia. 63: 150.

19. Dawes, C. J., and W. M. Thomas. Friction stir process welds aluminum alloys. 1996. Welding Journal. 75 (3): 41.

20. Rhodes, C. G., M. W. Maloney, W. H. Bingel, R. A. Spurling, and C. C. Bampton. Effects of friction stir welding on microstructure of 7075 aluminum. 1997. Scripta Materialia. 36 (1): 69.

21. Johnsen, M. R.. Friction stir welding shows great promise for joining of difficult-to-weld materials. 1997. Welding Journal. 76 (6): 20.

22. Galvao, I., C. Leitao, A. Loureiro, and D. Rodrigues. Friction stir welding of very thin plates. 2012. In Soldagem & Inspecao. (Sao Paulo, Brazil, March 2012). , p. 2. Sao Paulo: Soldagem & Inspecao.

23. Jata, K. V., and S. L. Semiatin. Continuous dynamic

recrystallization during friction stir welding of high strength aluminum alloys. 2000. Scripta Materialia. 43 (8): 743.

24. Cobb, J., S. Vachhani, R. M. Dickerson, P. O. Dickerson, W. Z. Han, N. A. Mara, J. S. Carpenter, and J. A. Schneider. Layer stability and material properties of friction stir welded Cu-Nb nanolamellar composite plates. 2014. Materials Research Letters. 2: 227.

25. Ekiz, E. H., T. G. Lach, R. S. Averback, N. A. Mara, I. J. Beyerlein, M. Pouryazdan, H. Hahn, and P. Bellon. Microstructural evolution of nanolayered Cu-Nb composites subjected to high-pressure torsion. 2014. Acta Materialia. 72: 178.

26. Beyerlein, I. J., N. A. Mara, J. S. Carpenter, T. Nizolek, W. M. Mook, T. A. Wynn, R. J. McCabe, J. R. Mayeur, K. W. Kang, S. J. Zheng, J. Wang, and T. M. Pollock. Interface-driven microstructure development and ultra high strength of bulk nanostructured Cu-Nb multilayers fabricated by severe plastic deformation . 2013. Journal of Materials Research. 28 (13): 1799.

Publications

Cobb, J., S. Vachhani, R. Dickerson, P. Dickerson, W. Han, N. Mara, J. Carpenter, and J. Schneider. Layer stability and material properties of friction stir welded Cu-Nb nanolamellar composite plates. 2014. Materials Research Letters. 2 (4): 227.

Probing Interface Reactions of Calcite Nanocrystals at Elevated Temperatures and Pressures

Rex P. Hjelm Jr
20130772ECR

Abstract

Calcite (the most stable form of calcium carbonate, CaCO3) is an important mineral phase in both environmental systems and energy applications. Calcium carbonate is considered the long-term sink for atmospheric carbon dioxide (CO2), and thus the process by which CO2 is trapped and transformed to stable carbonate minerals is of great fundamental and practical interest. The main goal of this project was to isolate and characterize the atomic interface structures that facilitate precipitation and dissolution of carbonate species under conditions found in underground reservoirs for CO2 sequestration. Our efforts produced three sets of results: (1) the design, building, and commissioning of a high pressure and temperature sample environment compatible with neutron local structure studies; (2) novel experimental observation of the atomic structure of the first few layers of growth and dissolution in carbonate mineral growth in an aqueous environment; and (3) methodology advancements for finite material structure refinement.

Background and Research Objectives

There are many challenges to probing the relevant interface reactions experimentally: first, the solid/fluid interface represents a very small proportion of the total system, resulting in low signal strength for many experimental measurements. Second, standard diffraction (the usual means of determining atomic structure) is intrinsically complex due to the amorphous nature of the fluid phase and the non-periodic/highly disordered interface within the solid phase. Third, the sequestering of CO2 in underground reservoirs occurs under hot, pressurized conditions. Sample environments used to achieve these conditions (e.g., pressure cell) further reduce signal from the interface structure during experiments. As a further complication, CO2 trapping mechanisms are governed by emergent processes from pore (micro) down to molecular (atomic) scales, and experimental approaches typically focus on one length scale or another. All these factors have hindered progress in experimentally probing the atomic interface structures controlling precipitation and dissolution of carbonates at conditions encountered in the Earth's crust.

This ECR project was designed to reduce the complexity of calcium carbonate mineral growth behaviors (which depend on substrate and solution chemistries, as well as macroscopic variables such as temperature, transport and thermodynamic stability) into elementary processes. Specifically, we pursued advanced total scattering techniques based on neutron and X-ray total scattering measurements to target the atomic structure at the interface between substrate minerals and water/CO2 fluids at elevated temperatures and pressures. The approach involved the use of porous substrates with tunable surface chemistry, a size dependent (and therefore surface area dependent) set of carefully characterized nanocrystalline carbonate samples, high pressure and temperature sample environment development for local structure measurements, and differential total scattering measurements with fluid-solid mixtures. A complementary effort targeting the integration of multi-length scale scattering measurements was also supporting this work.

Scientific Approach and Accomplishments

The original project scope had four tasks associated with it: (1) careful synthesis and characterization of size dependent nanocrystalline materials; (2) development of high pressure and temperature cells compatible with local structure measurements on the Neutron Powder Diffractiometer (NPDF) instrument; (3) neutron total scattering measurements of calcite-fluid solutions at elevated pressure and temperature; and (4) a data simulation and data modeling effort to interpret experimental results. The progress in each of these areas is described below.

Task 1: We have identified that very small and monodisperse calcite nanocrystal samples are quite difficult

to synthesize. Nonetheless, a large (100 gram) calcite nanoparticulate sample with an average particle diameter of 40 nm has been prepared at the Lujan Center by a senior advisor for this project, Dr. Luke Daemon. This sample has been characterized by laboratory X-ray diffraction, thermogravimetric analysis, transmission electron microscopy (for morphology), and surface area measurements. Plans for both mechanical milling and digestive ripening of this sample have been made in hopes to produce smaller and larger average particle size samples, respectively. Additionally, neutron and X-ray total scattering measurements and atomic pair distribution function (PDF) analyses of calcium carbonate crystalline polymorphs, including calcite (micron-sized bulk grains and 40 nm particles), aragonite and monohydrocalcite have been completed during the 2014 run cycle at the Lujan Center, LANL and the Advanced Photon Source (APS), ANL. Characterization of these carbonate polymorphs provides reference structural information and model-independent local structure comparisons for the early stages of carbonate mineral growth. Figure 1 shows the comparison of NPDF data measured for both bulk and 40 nm calcite samples.

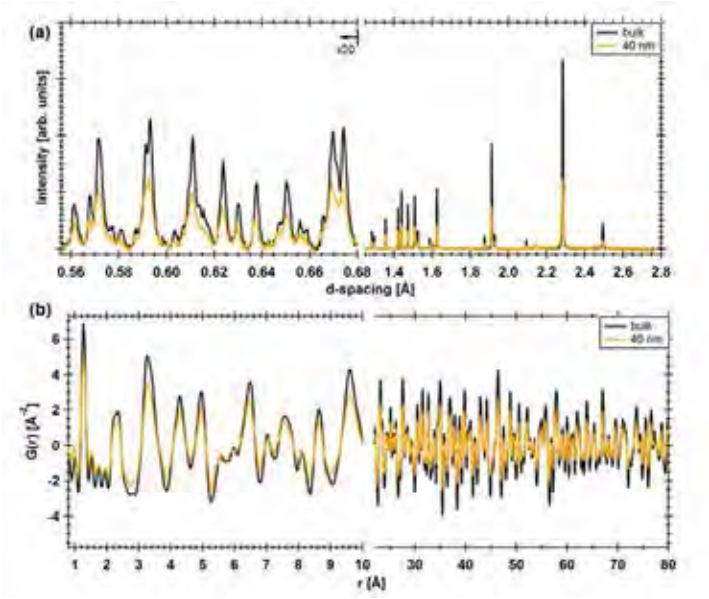

Figure 1. (a) Time-of-flight neutron powder diffraction pattern at a detector angle of 148° (bank 4) for both bulk and 40 nm calcite samples. Only one of four banks of neutron data is shown. (b) Corresponding PDF G(r) obtained through Fourier transformation of neutron total scattering data (after merging all four banks). For 40 nm sample, note the presence of broad Bragg reflections in plot (a) and the finite size effects resulting in reduced correlation intensity in plot (b).

Task 2: Our team, in collaboration with the Lujan Center's sample environment, high pressure, and mechanical design teams, completed the engineering design of a series of high pressure and temperature cells compatible with neutron total scattering measurements (which require a very low and stable background scattering signal). The suite of gas pressure cells includes both the vanadium and titanium-zirconium materials, and two different cell thicknesses. Finite element analysis was applied to the final designs to validate safety factors for experimental measurements. The commissioning of the new NPDF fluid cell apparatus for pressure and temperature ranges up to 100 MPa and 350 K was completed in the 2014 Lujan Center run cycle. High quality PDF data were collected in the apparatus for calibration samples (Si powder) at room temperature, and additionally for supercritical and subcritical CO2 fluids at elevated temperatures and pressures. This result and high pressure/temperature fluid cell applications were advertised at the 2014 ACS spring meeting (March 16-20) and 2014 American Crystallography Association Annual Meeting (May 17-21) and American Conference on Neutron Scattering (June 1-6). This work was published in the Review of Scientific Instruments, describing the new sample environment capability at the Lujan Center.

Task 3: Investigation of the first series of nanoparticulate calcite samples with the commissioned high temperature and high pressure cells on the NPDF instruments was originally scheduled in the 2014 Lujan Center run cycle for four days of neutron scattering beamtime. This part of the investigation was postponed to a later run cycle due to the difficulty in producing a size dependent set of calcite nanoparticles. As an alternative, the idea of following calcite and carbonate mineral growth within controlled pore glass (CPG) substrates was nucleated. Two days of synchrotron X-ray total scattering beamtime were awarded through the APS competitive proposal review process to investigate the interfacial reactions and growth of calcium carbonate minerals in CPG. The approach involved the use of well characterized CPG powders (with tunable pore wall chemistry) and a fixed chemistry of carbonate growth solution as a reasonable proxy for studying the carbonate mineral precipitation in reservoir rock for sequestration. The results from this initial experiment prove the signal sensitivity of total scattering difference methods for monitoring CaCO3-H2O-CO2 fluid/solid interfaces and growth processes. While the analysis is still preliminary (and on-going), the results provide a completely novel experimental observation that the initial stages of interface growth follow monohydrocalcite-like building blocks. Detailed modeling of the difference experiments will allow us to track the rate and size of particulate growth. Follow-on experiments are planned with different growth solutions and at different temperatures.

Task 4: Neutron and x-ray pair distribution function data modeling efforts have been incorporated in Tasks 1-3,

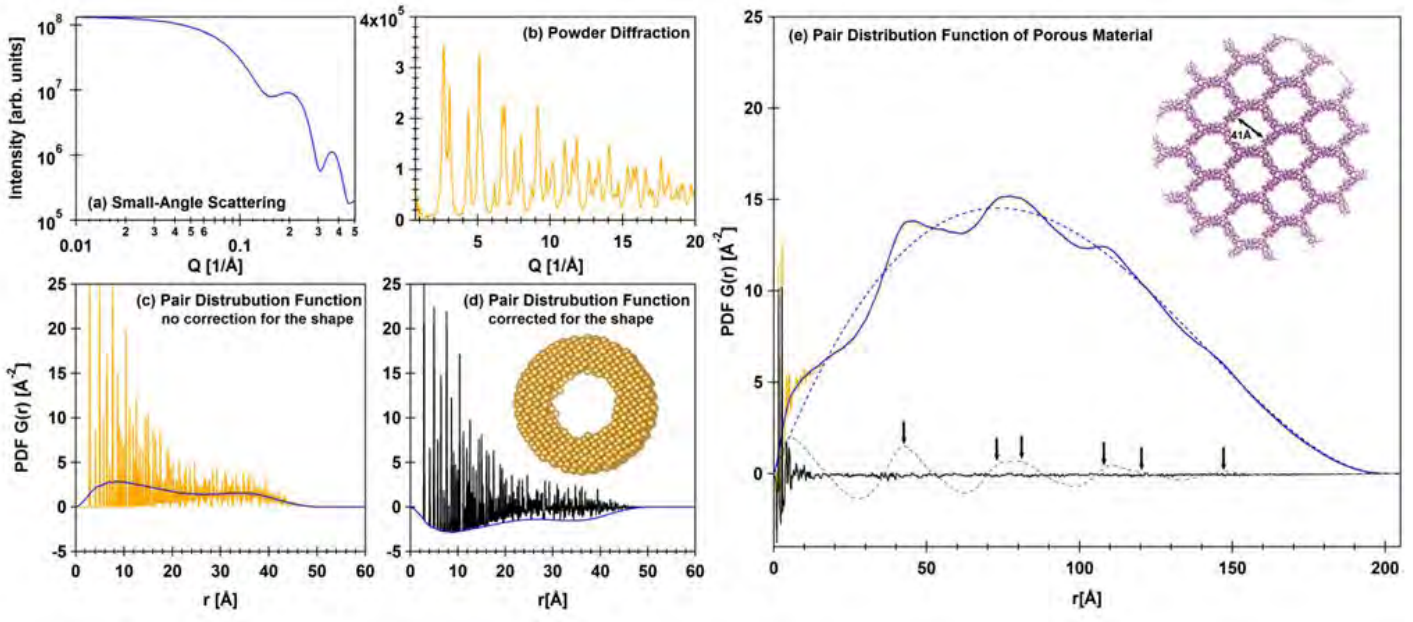

Figure 2. Example of current approach.

discussed above. Current approaches are focused on simulating nanocrystalline materials as well as porous substrates from the atomic scale through the nanoscale. Two examples are given in Figure 2. The first example (Figures 2a-d) features a single donut-shaped nanoparticle. At low-Q (Figure 2a), the scattering arises from the whole particle, allowing one to deduce information related to particle shape. At high-Q (Figure 2b), the Bragg diffraction peaks give information about the internal atomic structure of the particle. The simulated PDF G(r) (Figure 2c; orange curve) of such a configuration cannot be directly compared with the experimental PDF data. This is due to the fact that the simulation is completed in vacuum while the experimental PDF data contains the structural features of an "assembly" of many uncorrelated nanoparticles (all constituting an infinite but structure-less "background" of average non-zero density). To take the environment of a real system into account during modeling, a correction function (Figure 2c; blue curve) must be applied to the model of a finite nanoparticle to compare it to real data. With a correction, the computed model PDF oscillates around zero (Figure 2d; black curve) and can be directly compared with the experimental PDF data. The correction function (Figures 2c and d; blue curve) is actually the characteristic form factor of a finite-shaped particle. In the second example, the uncorrected model PDF of ordered mesoporous silica MCM-41 (Figure 2e; orange curve) contains both the sharp peaks at low-r (i.e., bonding pairs of the amorphous silica) and the broad structure bump/oscillation at high-r. By analogy with the first example, the broad structure feature at high-r in Figure 2e (solid blue curve) come from the nature of the channel packing (hexagonal close packing array; dashed gray curve) and the overall particle shape (spherical form factor; dashed blue curve). The black curve in Figure 2e is what one would observe for the experimental PDF of MCM-41 material (real experimental data is not shown here). PDF analysis based on diffraction only reflects the amorphous nature of the silica framework and would not show significant high-r oscillations beyond ~10 Å. Multiple length scales are important for accessing features such as pore network connectivity and degree of pore filling. While PDF measurements inform on length scales of large Q-range of ~0.8-50 Å-1 (corresponding to ~1-100 Å length scale), the low-Q diffractometer measurements can probe on the Q-range of ~0.03-0.5 Å-1 (corresponding to ~5-200 nm length scale). It will be important to experimentally merge these length scales to approach applied scientific problems in CO2 sequestration. Our developed methods for combining simulated information from multiple length scales into a single atomic structure refinement have been published in the Journal of Applied Crystallography.

In summary, our efforts produced three sets of results: (1) the design, building, and commissioning of a high pressure and temperature sample environment compatible with neutron local structure studies; (2) novel experimental observation of the atomic structure of the first few layers of growth and dissolution in carbonate mineral growth in an aqueous environment; and (3) methodology advancements for finite material structure refinement. Two publications have appeared and another is in progress. Three publications resulted from this work and another manuscript is in draft form.

Impact on National Missions

Understanding the behavior of mineral interfaces in

geothermal fluids is important for expanding many of the earth's energy options, including geothermal production, hydrocarbon extraction, remediation of contaminants, and geologic carbon sequestration. Successful study of the interface reactions in the CaCO3-H2O/D2O-CO2 system directly supports the missions of reducing climate and energy impacts, and enabling environmental remediation and restoration.

Sample environment capabilities and modeling methodology developed as part of this work will also provide new or improved research tools for probing complex materials, relevant to the MARIE and NNSA missions of LANL and the DOE Office of Science, as well as DOE Fossil Energy, and Nuclear Energy Programs. For instance, the temperature and pressure regimes and length scales of interest in this study are directly applicable to optimizing hydrocarbon extraction from oil and gas reservoirs and understanding corrosion and scaling in nuclear reactors.

The developed sample environment remains at LANL's Lujan Center, to be applied to NNSA and Geosciences related scientific studies on the NPDF beamline. A range of energy applications are possible, such as catalysis, clathrate inhibition, carbon capture, ion exchange, and gas storage. The developments can also extend to combined methods. Isotherm sorption and neutron diffraction measurements, for instance, can be joined for elucidating the adsorption mechanism and the structure of molecules confined in porous solids. Another example is the derivation on equation-of-state for a system of interest from neutron diffraction data collected with a range of macroscopic thermodynamic parameters.

The work on methods to combine data over multiple length scales will provide scientists with tools to understand the atomistic to mesoscale structure of materials. This work will support LANL's effort in emergent phenomena and defects and interfaces to be responsive to Office Science initiatives in mesoscale science. This work will also benefit NNSA and potentially DOD funded projects in explosives and propellants.

Spin-state Transitions as a Route to Multifunctionality

Vivien Zapf
20140177ER

Introduction

The ability to sense and manipulate magnetic spins with tuning parameters such as electrical current, light, or voltage, underlies a great number of technologies. Of the three, current and light are well-established or on their way to technological use. However, coupling magnetic spins to voltage, e.g. the ferroelectric or dielectric properties of a material, remains a fundamental scientific challenge. Yet, coupling between magnetic spins and voltage has significant potential to reduce energy consumption and dissipation in the process of sensing and manipulating spins, and the need for this is specified in a number of recent funding calls especially by military agencies and metrology researchers seeking room-temperature low-powered magnetic sensors, in addition to civilian applications in sensing, computation circuits and memory, liquid crystal displays, and electronics. We take a novel approach by investigating the coupling between spin-state transitions and ferroelectricity. Specifically, we focus on metal-organic materials where these spin-state transitions are common under ambient conditions.

When the spin-states in neighboring spins communicate via magnetic exchange or structural distortions, the resulting orderings and phase transitions can become complex and fascinating, and their understanding requires a careful collaboration between analytic, computational, and experimental understanding. Spin-state transitions in metal-organics have been found in the last decade to be sensitive to chemical absorption, light and small pressures, and to be inherently coupled to the lattice and in some cases drive structural phase transitions. We explore using spin-state transitions to drive structural changes in materials that modify their ferroelectricity and/or dielectric constant. We build on our recent and intriguing results in a metal-organic. The potential for multifunctional cross-coupling between the magnetic-electric properties as well as the incident light, pressure, and chemical sensitivity opens the door to other potent multifunctional devices.

Benefit to National Security Missions

Our work primarily seeks to understand the chemistry and physics of metal-organic materials where magnetism such as spin-state transitions couples to the ferroelectric properties. Secondary to that, the coupling to light, pressure, and chemical absorbents can be studied. The ultimate applications of these materials are new magnetic and electric sensors, tunable high-frequency devices, and computer memory have eventual applications to energy security and remote sensing. This work closely relates to the DOE/SC. If we demonstrate this new approach to magneto-electric coupling, follow-on funding for applications of this work can be envisioned. Applied work on the very similar topic of multiferroics, which targets the same applications, is currently funded by DARPA, the ORNL, the Army, the Navy, and by the electronics industry.

Progress

The research team is exploiting the flexible design and unique magnetic characteristics of organic materials instead of the more traditionally-studied inorganic materials to create and understand the coupling between magnetism and electric dipoles in insulating materials. The advantages of organic-based materials is their flexibility for design, the softness of the lattice that can easily deform to create electric dipoles, and the ability to encapsulate different types of polar molecules within pores of the structure. By ‘organic’ materials we refer to several classes of materials. The first class consists of organic m, where the magnetism resides within a carbon-based molecule. The second consists of metal-organic coordination compounds. Here the magnetism is created by a transition-metal ion like Fe or Co, that is coordinated by organic ligands into a crystal structure. These coordination compounds can form porous frameworks (“metal-organic frameworks”, or MOFs) where pores within the structure can host additional atoms or molecules. Finally, molecular magnets are compounds where again a transition-metal ion is the source of the

magnetism, but this magnetic ion resides in an organic molecular structure. These molecules pack together into a crystalline structure. In all cases we are exploring single crystals of these materials.

Our search for new magnetoelectric coupling mechanisms in organic-based materials is three-pronged, exploring three different mechanisms for magnetoelectric coupling.

In the first prong of this project, we search for trimerized magnetic structures in organic magnets. This is an example of theory driving experiment. Here we predicted the existence of magnetoelectric coupling due to competing interactions within trimer compounds and subsequent distortion of the electronic wave function or trimer structure. We have identified this phenomenology at work in the organic magnet TNN#CH3CN and computed the phase diagram and electric polarization. Our theoretical results agree well with the set of experiments by performed Yasu Takano (these experiments are described in the previous progress report). We are currently writing a manuscript on this topic.

The second prong of this project is to investigate metal-organic framework compounds where magnetism in the porous framework can couple to ferroelectricity of a molecule trapped within the pore. On this topic we have discovered two perovskite metal-organic framework compounds with magnetoelectric coupling and investigated the mechanisms. We actually find a magnetic order directly creating ferroelectricity at the magnetic transition in one of these materials, which is rare within metal-organics. We use the uniquely sensitive measurement techniques at LANL in pulsed magnetic fields to measure the magnetoelectric coupling. Our results are in fact surprising because magnetoelectric coupling appears to be not the simplistic idea of a magnetic framework with electric dipoles encapsulated, but rather a more complex scenario of ferroelectricity originating both within the framework and within pores, influenced by the coupling between them. Two papers are in final draft form, and third paper is published.

Finally the third prong of this project is to investigate spin-state transitions as a route to multiferroic behavior. Spin-state transitions occur in certain transition-metal ions with partially-filled d shells. When a local distortion of the lattice changes the crystal electric field environment of the magnetic ion, the electrons in the partially-filled d-orbitals can occupy a different pattern of orbitals that creates a different total magnetic moment for the ion. This is a mechanism for strong coupling between magnetism and crystal structures, that we in turn exploit to create coupling between magnetism and electric dipoles.Here we discovered the first example of a spin-state transition, rather than long-range magnetic order, creating ferroelectricity. We synthesized the compound and performed magnetic and electric experiments to very high magnetic fields at LANL and at the DC facility of the National High Magnetic Field Facility in Florida. We are in the process of completing this work, extending the experiments to more voltages, measuring the electron spin resonance. We have modeled this compound and are refining the modeling parameters in a tight iterative loop with experiments. Building on this work we have identified further spin-state transition compounds that are promising for observing this phenomenology even at high temperatures up to room temperature. Synthesis of these materials is in progress.

Future Work

- Complete the phase diagram of TNNCH3CN and compute the electric polarization in order to compare our results with the future experiments by Yasu Takano that are described in the progress report.
- Propose a model and compute the corresponding phase diagram for the new trimer compound that was recently synthesized by the experimentalists in our team.
- Provide theoretical input for the new metal-organic multiferroic that Nathan Smythe is producing in his new lab.
- Continue exploration of new materials including the La1-xSrxCoO3 family of spin-state transition materials, andmagnetic variants of the ferroelectric tris-sarcosine calcium chloride
- Flesh out our understanding of the most promising materials discovered in the first year; this includes the frustrated trimer materials where magnetoelectric coupling will be explored.
- Magnetoelectric coupling in tris[2-(pyrrol-2-ylmethyleneamino)ethyl]amine-Manganese(II) will be measured, and we will grow family members with different magnetic ions and ligands.
- Variants of triethylmethylammonium tetrabromoferrate (III) with different ligand lengths will be explored to tune the magnetoelectric coupling above room temperature.

Conclusion

Our deliverable will be an enhanced understanding of spin-state transitions and their coupling to the crystalline lattice and it's electrically polar properties, as well as new metal-organic materials and materials approaches to magneto-electric coupling. The applications of magneto-electric coupling are devices such as computer memory, filters, sensors, and antennas. Our approach achieves magneto-electric coupling with less power dissipation than

existing spintronics devices due to the insulating nature of our materials.

Publications

Gomez-Aguirre, L. C., B. Pato-Doldan, J. Mira, S. Castro-Garcia, M. A. Senaris-Rodriguez, M. Sanchez-Andujar, J. Singleton, and V. S. Zapf. Magnetic field-induced multiferroic behavior in [CH3NH3][Co(HCOO)3] Metal-Organic Framework. To appear in Journal of the American Chemical Society.

Kamiya, , and C. D. Batista. Magnetic Vortex Crystals in Frustrated Mott Insulator. 2014. PHYSICAL REVIEW X. 4 (1).

Koutroulakis, , Zhou, Kamiya, J. D. Thompson, H. D. Zhou, C. D. Batista, and S. E. Brown. Quantum phase diagram of the S=1/2 triangular-lattice antiferromagnet Ba3CoSb2O9. 2015. PHYSICAL REVIEW B. 91 (2).

Lin, , Barros, Mun, Kim, Frontzek, Barilo, S. V. Shiryaev, V. S. Zapf, and C. D. Batista. Magnetic-field-induced phases in anisotropic triangular antiferromagnets: Application to CuCrO2. 2014. PHYSICAL REVIEW B. 89 (22).

Ma, J., Y. Kamiya, T. Hong, H. B. Cao, G. Ehlers, W. Tian, C. D. Batista, Z. L. Dun, H. D. Zhou, and M. Matsuda. Static and Dynamical Properties of the Spin-1/2 Equilateral Triangular-Lattice Antiferromagnet Ba3CoSb2O9. Physical Review Letters.

Mun, E. D., Chern, Pardo, Rivadulla, Sinclair, H. D. Zhou, V. S. Zapf, and C. D. Batista. Magnetic Field Induced Transition in Vanadium Spinels. 2014. PHYSICAL REVIEW LETTERS. 112 (1).

Mun, E. D., J. Wilcox, J. L. Manson, B. Scott, P. Tobash, and V. S Zapf. The Origin and Coupling Mechanism of the Magnetoelectric Effect in TMCl2-4SC(NH2)2 (TM = Ni and Co). 2014. Advances in Condensed Matter Physics. 2014: 512621.

Zapf, , Jaime, and C. D. Batista. Bose-Einstein condensation in quantum magnets. 2014. REVIEWS OF MODERN PHYSICS. 86 (2): 563.

Zhu, S., Y. Q. Li, and C. D. Batista. Spin-orbit coupling and electronic charge effects in Mott insulators . 2014. Physical Review B. 90: 195107.

Beyond the Chemical Reaction Zone: Detonation Product Gases in the Warm Dense Regime

Dana M. Dattelbaum
20140261ER

Introduction

The chemical reaction zone behind a detonation front comprises a dense fluid mixture of components such as N2, CO2, CO, CH4, and NH3, at densities ranging from 0.09 to 1.5 g/cm3. There is considerable overlap between the constituents of detonation product mixtures and those of planetary ices and atmospheres. Conditions relevant to planetary physics are often those of the warm dense matter (WDM) regime: too dense for weakly-coupled plasma models but too hot for standard condensed matter techniques. While these states are hotter and denser than those of the chemical reaction zone, multiple shocks may readily carry the product mixture through the WDM and into the dense plasma region: standard SESAME tables extend to T~10 keV and ρ/ρ0~10^6. Despite their vital importance in these contexts, however, molecular dissociation and ionization at elevated pressure and temperature are poorly characterized and constitute a significant source of potential error in our equations of state. To address these gaps, we will establish a synergistic experiment-theory-simulation effort focused on quantifying the P-V-T surfaces, and associated dissociation and ionization processes for the principal detonation product species: N2, CO2, CH4 and NH3.

Benefit to National Security Missions

The successful execution of this experimental-theoretical project provides critical and foundational data and models for improved confidence in weapons simulations. This project will enable rapid development of the experimental and theoretical tools to demonstrate transformational improvements in the treatment of detonation product gases. The results of this project are relevant to the National Boost initiative, Predictive Capability Framework, and objectives of some DOE/NNSA Campaigns, and Advanced Certification. In addition, the fundamental data obtained is relevant to planetary physics, and definitions of the conditions of the large gas giant planets.

Progress

Measured the Hugoniot of low-density ammonia based on gas gun experiments. Determined temperature of first- and second-shocked states based on pyrometry up to 7000-8000 K. These were compared to values calculated in hydrodynamic simulation using a legacy SESAME table and the PAGOSA software package. Calculated temperatures were systematically low relative to measurement. From the data we also determined that ammonia does not ionize on first shock. This work is being reported at the Shock Compression Conference in June, and a journal manuscript is in preparation.

Safety and procedures were completed to start firing methane at various initial densities this quarter. We performed the first gas shock experiments on the LANL 2-stage high performance gun. We also designed an asymmetric cell to reach shock conditions three times greater in pressure for the same impact condition; this innovation is being published in HVIS Proceedings 2015.

We developed an interferometric fiber Bragg strain sensor to provide early triggers for spectroscopic diagnostics. Again, there is a manuscript in preparation.

The research team also completed theoretical investigations of ammonia in a warm dense matter regime, using newly developed simulation methodology. This enabled us to more accurately assess the extent of molecular decomposition. These results are being prepared for publication in the Journal of Chemical Physics.

Future Work

The objectives of the experimental effort are: 1) to quantitatively resolve the shocked states in N2, CO2, CH4 and NH3 on the principal Hugoniot, and along a quasi-isentropic path to very high compression ratios and temperatures, and 2) to determine at what conditions dissociation and ionization (and possibly metallization) occur, and attempt to measure spectroscopic evidence

of dissociation products. On- and off-Hugoniot states in molecular gases will be achieved via gas gun-driven plate impact using a suite of high performance gas guns with impact velocities up to 8 km/s. The experimental program will consist of two directions. The first, and lower risk, are shock experiments on fluid (liquefied) species, with a focus on reaching higher compression-rate, off-Hugoniot states, and applying in situ spectroscopies for the first time. The second, parallel direction will be to apply our newly developed experimental approach on elevated density gases. To determine the temperatures along the compression path, and to measure dissociation and ionization in the gases, we have a variety of time-resolved optical spectroscopic tools at our disposal.

Ab initio molecular dynamics (AIMD) simulation will be performed at fixed (ρ,T) states matched to those of experiment. Average degrees of coordination (bonding) will be used to calibrate atomic fluid models that more effectively capture dissociation transitions. Ionization states, however, are very difficult to infer directly from AIMD, because the imposed periodic boundary conditions prevent electron density from actually leaving the simulation cell. Our initial approach to this problem will be to calculate electrical conductivity (ac) and interpret the degree of charge transport using the Drude model for a free electron gas.

Simulations of the plate impact experiments will be performed using PAGOSA, a three-dimensional Eulerian hydrocode used to simulate compressive flow and high strain-rate deformation.

Conclusion

The expected result of this program is a significantly improved modeling capability for simple molecular gases that are relevant to detonation products and weapons simulations for the Laboratory. New EOS methodologies will provide a physics-basis to bridge the gap between compressed fluid and Thomas-Fermi-Dirac regimes. Furthermore, we will lead the field by applying a comprehensive suite of advanced spectroscopic diagnostics under shock conditions. Lastly, new models, based on experimental results, will be evaluated in the Eulerian code PAGOSA.

Publications

Gibson, L. L., B. D. Bartram, D. M. Dattelbaum, J. M. Lang, and J. S. Morris. A gas-loading system for LANL two-stage gas guns. To appear in Shock Compression of Condensed Mater - 2015. (Tampa, FL, 14-19 June 2015).

Goodwin, P. M., B. R. Marshall, R. L. Gustavsen, J. M. Lang, A. H. Pacheco, E. N. Loomis, and D. M. Dattelbaum. Fiber-interferometric detection of gun-launched projectiles. To appear in Shock Compression of Condensed Matter - 2015. (Tampa, FL, 14-19 June 2015).

Topological Kondo Insulators

Joe D. Thompson
20140271ER

Introduction

Metals are materials in which there is a band of electronic states that is only partially filled, allowing electrons to flow easily in response to a weak electric field. In a pristine insulator, however, possible electronic states are fully occupied, and there is a large energy gap between filled and unfilled electronic states. As a result, no electrons are available to move in response to an electric field and, hence, the electrical resistivity is infinite. An entirely new state of electrons has been proposed that combines both electrically conducting and electrically insulating electrons in a single material. The concept underlying this state of electrons is highly non-trivial and relies on the mathematical notion of topology that 'protects' conducting electrons from acquiring the insulating behavior of the vast majority of other electrons. As long as time-reversal symmetry is preserved (that is, an electron with spin 'up' moving with momentum +k is identical to an electron with spin 'down' moving with momentum –k), and there is strong coupling between the electron spin and the electron angular momentum, this very unusual state of electrons should appear. The goal of this project is to establish experimentally the validity of this idea of topologically protected conducting electrons in materials that are electrically insulating because of strong electron-electron correlations. Just as the theory is non-trivial, so is its experimental validation because of the inevitable complication of material's imperfections which produce responses that mimic those of topologically protected conducting electrons.

Benefit to National Security Missions

The theoretical proposal that certain materials should have electrically insulating interiors but electrically conducting surfaces has profound implications for our basic understanding of how electrons can organize themselves as a consequence of rules of quantum mechanics. Experimentally validating this theoretical proposal in materials where strong electron-electron interactions also are present would open opportunities for manipulating electrons for energy applications, such as thermoelectric cooling, as well as for discovering an exotic state in which elementary charge carriers act as their own antiparticles, so-called Majorana fermions. This project is primarily one of discovery science, focused on understanding the fundamental consequences of theoretical predictions that also have implications for new interpretations of electronic behaviors in plutonium-based materials. But, research will be pursued as well with potential technological applications in mind, including the use of those discoveries in the development of new spin-based logic devices that have broad relevance to DOE energy and defense missions.

Progress

A metallic topological surface state is theoretically predicted to be robust to perturbations that do not break time-reversal symmetry. To test the robustness of the surface state of the theoretically proposed topological Kondo insulator SmB6, we have continued experiments in which we measure the response of SmB6 to surface damage created by systematically irradiating the surface with heavy ions (krypton and argon) to controlled depths ranging from 10Å to over 400Å. In work published in Physical Review B we showed that, upon significant damage of the surface by these non-magnetic ions, the surface state is not destroyed. Instead, the surface state reconstructs beneath the heavily damaged region that becomes a poor conductor. This is consistent with expectations for a topological surface state and an important confirmation of the theoretical prediction that SmB6 is a topological Kondo insulator. In further work we have shown that this reconstruction only occurs once the concentration of defects in the damaged layer is sufficiently high, on the order of 1 displacement per atom. At small levels of damage, the electrical conductivity of the surface state appears to be moderately reduced, possibly indicating the presence of a 'Kondo hole' (the absence of a Sm atom from its expected position in the lattice) that scatters the metallic surface electrons

and reduces the surface conductivity. A further theoretical prediction is that the topologically protected metallic surface should be sensitive to the introduction of magnetic impurities that break time-reversal symmetry. We have tested this prediction by irradiating the surface of SmB6 with magnetic iron-ions. Surprisingly, we found that the surface state is not destroyed by this damage but reconstructs below the damaged surface, as with non-magnetic irradiation. This observation is not understood fully but may be a consequence of the orientation of the magnetic moments of implanted iron ions. Nevertheless, this result has important implications for both the study of SmB6 with magnetic field and also for the application of topological surface states, for example in magnetic heterostructures form with SmB6.

The design of an experimental setup to measure the thermal conductivity of single crystals of SmB6 under applied pressure has made good progress. Initial tests of several experimental setups have led to the selection of a dynamic method, the so-called '3-Omega' technique. In this method the thermal conductivity of a sample is measured by measuring the 3rd harmonic of the voltage that is induced across a crystal in the presence of a small oscillating thermal gradient generated by an oscillating current through a metallic strip on the crystal's surface. Isolation of the small 3rd harmonic signal from the background is a challenge using conventional electronics but has been achieved through a special experimental arrangement. The application of a narrow metallic strip to the sample is also challenging, but good progress has been made in that regard as well. The next step will be to show we get accurate and reproducible data for samples in a high pressure environment.

Future Work

To achieve our goal of experimentally validating the theoretical prediction of topologically protected electronic states in strongly correlated electron materials, we will use heavy-ion irradiation to damage the surface systematically to controlled depths ranging from approximately ten to several hundred nanometers depth and measure and model the effect of this damage on the temperature-dependent electrical resistivity of proposed topological Kondo insulators. If this damage does not break time-reversal symmetry, theoretically the metallic surface should survive damage, but if this symmetry is broken by irradiation damage, it is possible that the metallic surface state would be destroyed. This possibility has not been settled by theory but will be by proposed experiments. In parallel, we will pursue the use of pressure-dependent measurements of the thermal and electrical resistivities of SmB6 to probe the evolution of the metallic surface as the insulating gap in the bulk is systematically suppressed by applied pressure. With this range of techniques, we expect to prove or disprove several theoretical predictions. If theory is proven to be correct, this work will lay the foundation for an entirely new field of research on strongly correlated electron materials and the substantial technological consequences of topologically protected quantum states of matter.

Conclusion

This project will establish a new field of research on electronic states that emerge in materials as a consequence of strong electronic correlations and that hold promise for enabling new technologies ranging from thermoelectric cooling and spintronic devices to quantum computing.

Publications

Wakeham, N., Y. Wang, Z. Fisk, F. Ronning, and J. D. Thompson. Surface state reconstruction in ion-damaged SmB6. 2015. Physical Review B. 91: 0851007.

Semiclassical Modeling of Non-adiabatic Processes in Molecular Materials

Dima V. Mozyrsky
20140293ER

Introduction

Present day computational quantum chemistry and material science attempt to evaluate not only equilibrium properties of molecular materials, but also their dynamics under different physical conditions. For example, by absorbing a quantum of laser radiation a molecule goes to an excited electronic state, which may lead to various possibilities in its subsequent evolution: It may dissociate into to new molecules or atoms or, emitting a phonon, it may go to a long-living excited vibronic state without splitting into new molecules. Understanding and control over these processes (photoinduced pathways) lies at the heart of all our efforts to design functional photoactive materials for many technological applications. Such molecular dynamics is inevitably accompanied by the transitions between neighboring electronic states in a molecule that are not easy to describe within the existing approximation schemes. The majority of the existing schemes are either too computationally expensive or based on ad-hoc approximations that lead to inconsistencies between quantum and classical mechanics. Therefore there is a clear need for a novel computational paradigm that, on one hand, would be sufficiently precise and based on well controlled physical approximations rather than ad hoc assumptions, and, on the other hand, would be computationally feasible to allow for efficient numerical simulations of molecular dynamics in realistic multi-atomic molecules. In this project we aim to accomplish this goal.

Benefit to National Security Missions

First and foremost our project upon completion will provide novel computational capabilities critical for understanding light-induced dynamics in many technologically relevant nanostructures. In fact, for the first time, experimental ultrafast spectroscopy will have its theoretical counterpart able to treat the material on the same footing. Consequently, we envision extremely broad applications of developed tools, relevant to the current and future LANL/DOE missions. Our project primarily addresses Energy and Earth Systems LANL Grand challenge by providing computational means for molecular materials suitable for clean energy (solar energy capture and energy storage). Secondly, it strongly relates to Materials: Discovery Science to Strategic Applications challenge by discovering emergent phenomena in complex systems. In particular we expect that the project will attract the attention of the world-wide community of spectroscopists and computational material scientists and will establish new collaborations with LANL and attract new CINT users.

Progress

The research team tested the relative error on the Semi-Classical Monte-Carlo algorithm (SCMC) and found that it scales as a square root of the number of trajectories. We have also shown that the error is approximately independent on the number of nuclear degrees of freedom. The details can be found in Ref. (1).

In order to apply the semiclassical Monte-Carlo approach to the realistic models we needed to significantly improve the convergence of the algorithm, i.e., by factor ~ 50. This is because the electronic structure calculations for realistic molecules are typically very computationally expensive and constitute a major bottleneck for the use of the semiclassical methods since these methods typically require a large number of trajectories. For example, our initial approach (SCMC method) had required several thousands of trajectories to evaluate the transition probabilities for a system at a single level crossing, while the contemporary computational resources at LANL would not allow for “such luxury”: Typical non-adiabatic surface hopping simulations of realistic molecular systems would involve several hundred trajectories, at most a thousand of trajectories. The problem of convergence was resolved by developing two new methods, the accelerated-SCMC and the accelerated-SCMC with re-Gaussianization, which reduce the cost of the SCMC algorithm up to two orders of magnitude for certain systems. In the first

approach the cost efficiency is achieved by avoiding the repetitive trajectories, which increases the efficiency by several times. Furthermore, the accelerated-SCMC method is "hybrid", - it only uses Monte-Carlo method for evaluating the integrals only higher order terms in the expansion, while the first order integral is evaluated by finite differences. This leads to a significant decrease in the number of trajectories because Monte-Carlo method is efficient only for the integration of higher-dimensional functions. The re-Gaussianization procedure (i.e., the second method) turned out to be a very efficient approach in problems involving several level crossings. It allows us to reconstruct the wavefunction after the system passes through a level crossing, which leads to significant computational savings for two reasons: (1) It reduces the number of interfering wavepackets at the next crossing, which leads to a very strong reduction in the number of needed trajectories; (2) It removes the necessity to run multiple trajectories between level crossings, - instead one runs a single, re-Gaussianized wavepacket between the non-adiabatic regions, which also significantly reduces the number of needed trajectories to maintain a desired accuracy. In most cases the new procedures are nearly as efficient as the commonly used surface hopping schemes, with little to no loss of accuracy. This implies that these modified SCMC algorithms will be practical numerical solutions for simulating non-adiabatic dynamics in realistic molecular systems. The details for the two approaches can be found in Ref. (3).

We have studied analytically a model involving non-adiabatic dynamics in a system with a few slow degrees of freedom. It was shown in such problems that one can introduce an order parameter that properly describes the collective dynamics of slow degrees of freedom. Such study is relevant for better general understanding of non-adiabatic dynamics. The details can be found in Ref. (2).

Future Work

- Generalize the existing algorithm to multi-dimensional situations, i.e., for multi-atomic molecules. Apply the algorithm for several molecular systems of interest
- Include description of noise and dissipation effects. In the majority of experimental situations the forces produced by molecule's surrounding medium (typically a solution) are sufficiently strong and may significantly modify the system's dynamics. Accounting for such forces is, therefore, imperative for the reliable numerical simulation of realistic molecules in realistic physical conditions.
- Test a deterministic approach developed in the course of the project. If successful, this approach may significantly improve the numerical cost of the non-adiabatic modeling algorithm. This direction represents a slight deviation from the work plan stated in the original proposal. However, it may provide a more efficient solution to the problem of non-adiabatic dynamics (which is the main goal of this project).

Conclusion

The major technical goal of this project is to provide a computational algorithm to evaluate molecular dynamics in situations involving transitions between different electronic states in a molecule. The algorithm will allow for a reliable and efficient evaluation of reaction pathways and product ratios in a variety of problems of photoinduced molecular dynamics and will complement, and, in some cases, replace the existing approaches. We also intend to apply our method to study non-adiabatic dynamics in several molecular systems involving interaction of molecules with light relevant for photovoltaic applications.

Publications

White, A. J., V. N. Gorshkov, S. Tretiak, and D. Mozyrsky. Non-adiabatic molecular dynamics by accelerated semiclassical Monte Carlo. 2015. The Journal of Chemical Physics . 143: 014115.

White, A., V. N. Gorshkov, R. Wang, S. Tretiak, and D. Mozyrsky . Semiclassical Monte-Carlo: A First Principles Approach to Non-adiabatic Molecular Dynamics . 2014. The Journal of Chemical Physics . 141: 184101.

Zhou, N., L. Chen, Y. Zhao, D. Mozyrsky, V. Chernyak, and Y. Zhao. Ground state properties of sub-Ohmic spin-boson model with simultaneous diagonal and off-diagonal coupling . 2014. Physical Review B. 90: 155135.

Making nano-Mg a reality

Irene J. Beyerlein
20140348ER

Introduction

With the need to reduce gas consumption, Mg alloys have risen to the top of the list as the next lightweight structural materials to replace steel. However, even if all the steel in your car (e.g., 30 mpg) were replaced with today's Mg, the weight reduction would boost fuel efficiency by only 54.6% (to 46 mpg), well below the Corporate Average Fuel Economy standards for 2020 (61 mpg). But if the strength of bulk Mg were to increase ten-fold, the gas mileage would boost from 30 mpg to 76 mpg, leading to a transformational impact on the automotive industry. For other structural metals (e.g., Al, Cu, Ni, steel), up to ten-fold increases have been realized by severe plastic deformation (SPD) techniques, which transform coarse-grained metals to nano-grained metals. Unfortunately, all attempts to make "nano- Mg" in bulk sizes have failed. Bulk nano-Mg cannot be made because SPD causes deformation twinning in Mg. For this ER, we propose a breakthrough in microstructural processing by design, where the key is to create a composite of Mg and a smaller amount of second metal phase, metal X, such as Nb, Fe, or V, and tune the Mg-X interfaces to suppress twinning, permitting Mg refinement to the nanoscale. This innovative approach gives rise to new scientific issues of Mg-X interface/defect processes. To tackle them, we pose two original hypotheses and use them to direct an integrated experimental and modeling s trategy. By the end of the ER, we will deliver nano-Mg-X in bulk sheet form, wherein the Mg crystals are <100 nm in size. Being sought after for a decade, our bulk nano-Mg-X, as well as the science that enabled it and synthesis pathways that made it, will be in high demand by countless reputable research groups and industry (automotive, bio, and aerospace).

Benefit to National Security Missions

Being sought after for a decade, our bulk nano-Mg-X, as well as the science that enabled it and synthesis pathways that made it, will be in high demand by countless reputable research groups and industry (automotive, bio, and aerospace). Nano-Mg-X will no doubt exhibit many other interesting properties apart from ultra high strength, such as corrosion resistance (aging), magnetism, conductivity, thermal stability, biodegradation resistance, and fracture toughness. Our project will fundamentally transform Mg research and manufacturing and make LANL the leader of this rapidly growing market. This ER notably fulfills all three pillars of LANL's Materials Strategy. 1) Defects and Interfaces: our innovation tunes interfaces to suppress emission of twinning dislocations. 2) Emergent Phenomena: all matter is controlled by their atomic structure and nearly 30% of nano-Mg-X will be Mg-X interface with a differing atomic structure than Mg or X. Hence new effects can be expected. 3) Extreme Environments: we exploit one extreme (severe strains) to produce nano-Mg-X, a material that will be tolerant in extremes of high stress, high strains (formable), and we expect, high temperatures.

Progress

This past year, we made progress towards our goal of developing a ground-breaking method for synthesizing a nano layered composite metal that combines two phases, one metal with a hexagonal close packed (hcp) crystal structure and another metal with a body centered cubic crystal (bcc) structure. Our main innovation behind this plan is the recognition that deformation twinning is the chief obstacle that has prevented so many scientists before us from achieving this goal. Specifically last year, we achieved many milestones. First, we determined how to make nanolayered composite Zr/Nb, where Zr is an hcp metal and Nb is a bcc metal. We determined that in order to refine from coarse-layered sizes to nano-layered sizes, it is necessary to eliminate shear banding, an instability that happens during the initial stages of SPD processing. Once shear banding begins, the layers no longer co-deformed and layer refinement via mechanical processing stops. Second, we characterized the microstructure and we determined the interface crystallography. The texture of the Zr phase and Nb phase corre-

sponded to the texture that would develop in each phase when rolled alone. However, when the layer thickness reduced below 100 nm, the texture strongly deviated from the conventional rolling texture. Instead it became sharp and correspondingly, a few predominant interfaces are suspected to emerge. From our analysis, the textures suggest that the two predominant interfaces are (a) {110}Nb||{1 -1 0 0}Zr and {111}Nb||{1 -2 1 10}Zr and (b) {110}Nb||{1 -1 0 0}Zr and {100}Nb||{1 -2 1 10}Zr. Third, we then developed a multi-scale model to determine the microstructural evolution during the processing of Zr/Nb, namely its dislocation defect structure, its bimetal interface structure, and texture. Through this work, we also determined that it did not twin, why it did not twin, and why the predominant interfaces emerged. We also determine the microstructural features that caused shear banding. The fact that annealing reduced the dislocation density postponed shear banding. Thus, the changes annealing caused in grain size and texture were not the main reasons it postponed shear banding.

Fourth, we made progress towards our ultimate goal of making Mg/Nb composites. To this end, we made Mg-Nb nano layered composites via physical vapor deposition. With this fabrication method, we were able to modify the interface structures in a controlled manner and to determine the deformation behavior via micro pillar testing. We found that when the layers are thin, 5 nm, the Mg takes on a body center cubic (bcc) crystal structure. However, when they are 50 nm, while still being nano in size scale, the Mg keeps its hcp crystal structure. As a result, we found that the two pillars had very different constitutive behaviors. The 5 nm Mg/Nb composite achieved both outstanding ductility and strength. At the same time we also carried out atomic scale simulations to determine which interface structures are energetically favorable and which crystal structure is preferred as a function of layer thickness. The simulations predicted that due to the coherency strains in the interface, the Mg transforms from hcp to bcc. The coherency strains for bcc Mg are less than that for hcp Mg.

Using this knowledge, we performed crystal plasticity finite element (CPFE) simulations to understand microstructure evolution during bulk deformation processing. In order to extend these methods to Mg, we had to characterize the hardening law for Mg, which is non-trivial since Mg deforms by several distinct slip and twinning modes and develop a way to treat the formation of twin lamellae. The latter turned out to be the first modeling technique to treat deformation twinning in a microstructural materials model. We also had to extend these models to Nb. For this, we had to develop for the first time a CPFE model for bcc materials that accounted for non-Schmid effects. The above three accomplishments in CPFE led to three papers, either being reviewed or accepted for publication. For the upcoming year, we are now ready to carry out fabrication process simulations for Mg/Nb using our novel CPFE model.

Future Work

The overarching goal of this project by the end of the three years is to develop a ground-breaking method for synthesizing nano layered composite metal that combines two phases, one metal with a hexagonal close packed (hcp) crystal structure and another metal with a body centered cubic crystal (bcc) structure. In this past year, we made a novel nanocomposite material in bulk form using severe plastic deformation (SPD). In these composites, the hcp material was Zr and the bcc material was Nb. We were able to model these Zr/Nb nano layered composites using crystal plasticity finite element techniques. In the next year, we plan to work our way towards making Mg/Nb composites. We plan to first apply our SPD technique to single phase Mg. Two types of Mg materials will be used. One will be pure Mg, which is known to twin at room temperature. The second material will be an Mg alloy, called Mg-4Li. In planning for these tests, we have developed constitutive crystal plasticity based models to study the effect of starting microstructure (grain size, texture) on twinning in both Mg materials. We find that we can postpone twinning in Mg at elevated temperatures and we also found that twinning is postponed in Mg due to the lower activation barrier for pyramidal <c+a> slip. We will at the same time carry out crystal plasticity finite element (CPFE) simulations of Mg and Mg/Nb for understanding microstructure evolution during bulk deformation processing. We have already started developing the CPFE models for Mg and for modeling twin formation in Mg. In the next year, we will complete these efforts and begin extending it to consider Mg/Nb. This model will help guide the processing steps for achieving target interface configurations and character.

Conclusion

By the end of the ER, we will deliver 1) nano-Mg-X in bulk sheet form, 2) characterization of its nanostructure and mechanical properties, and 3) processing path designs for making nano-Mg-X in the form of bulk sheets and tubes. In addition, we will offer new understanding in the nascent field of hcp-X interfaces, the associated hcp-X interface models, and patentable SPD techniques.

Publications

Ardeljan, , I. J. Beyerlein, and Knezevic. A dislocation density based crystal plasticity finite element model: Application to a two-phase polycrystalline HCP/BCC

composites. 2014. JOURNAL OF THE MECHANICS AND PHYSICS OF SOLIDS. 66: 16.

Ardeljan, M., I. J. Beyerlein, and M. Knezevic. A dislocation density based crystal plasticity finite element model: application to a two-phase polycrystalline HCP/BCC composites. 2014. Journal of the Mechanics and Physics of Solids. 66: 16.

Ardeljan, M., M. Knezevic, T. Nizolek, I. J. Beyerlein, S. J. Zheng, J. S. Carpenter, R. J. McCabe, N. A. Mara, and T. M. Pollock. A multi-scale model for texture development in Zr/Nb nanolayered composites processed by accumulative roll bonding. 2014. Journal of Materials Science and Engineering. 63: 012170.

Beyerlein, I. J., J. S. Carpenter, Hunter, L. S. Toth, and Skrotzki. Nano-enabled orientation alignment via extreme shear strains. 2015. SCRIPTA MATERIALIA. 98: 52.

Cao, L. e. i., Hunter, I. J. Beyerlein, and Koslowski. The role of partial mediated slip during quasi-static deformation of 3D nanocrystalline metals. 2015. JOURNAL OF THE MECHANICS AND PHYSICS OF SOLIDS. 78: 415.

Carpenter, J. S., Nizolek, R. J. McCabe, Knezevic, S. J. Zheng, B. P. Eftink, J. E. Scott, S. C. Vogel, T. M. Pollock, N. A. Mara, and I. J. Beyerlein. Bulk texture evolution of nanolamellar Zr-Nb composites processed via accumulative roll bonding. 2015. ACTA MATERIALIA. 92: 97.

Carpenter, J. S., R. J. McCabe, J. R. Mayeur, N. A. Mara, and I. J. Beyerlein. Interface-Driven Plasticity: The Presence of an Interface Affected Zone in Metallic Lamellar Composites. 2015. ADVANCED ENGINEERING MATERIALS. 17 (1): 109.

Hunter, , R. F. Zhang, and I. J. Beyerlein. The core structure of dislocations and their relationship to the material gamma-surface. 2014. JOURNAL OF APPLIED PHYSICS. 115 (13).

Hunter, , and I. J. Beyerlein. Relationship between monolayer stacking faults and twins in nanocrystals. 2015. ACTA MATERIALIA. 88: 207.

Hunter, , and I. J. Beyerlein. Unprecedented grain size effect on stacking fault width. 2013. APL MATERIALS. 1 (3).

Hunter, , and I. J. Beyerlein. Predictions of an alternative pathway for grain-boundary driven twinning. 2014. APPLIED PHYSICS LETTERS. 104 (23).

Hunter, , and I. J. Beyerlein. Stacking fault emission from grain boundaries: Material dependencies and grain size effects. 2014. MATERIALS SCIENCE AND ENGINEERING A-STRUCTURAL MATERIALS PROPERTIES MICROSTRUCTURE AND PROCESSING. 600: 200.

Jahedi, , Ardeljan, I. J. Beyerlein, M. H. Paydar, and Knezevic. Enhancement of orientation gradients during simple shear deformation by application of simple compression. 2015. JOURNAL OF APPLIED PHYSICS. 117 (21).

Jahedi, , M. H. Paydar, Zheng, I. J. Beyerlein, and Knezevic. Texture evolution and enhanced grain refinement under high-pressure-double-torsion. 2014. MATERIALS SCIENCE AND ENGINEERING A-STRUCTURAL MATERIALS PROPERTIES MICROSTRUCTURE AND PROCESSING. 611: 29.

Knezevic, , Drach, Ardeljan, and I. J. Beyerlein. Three dimensional predictions of grain scale plasticity and grain boundaries using crystal plasticity finite element models. 2014. COMPUTER METHODS IN APPLIED MECHANICS AND ENGINEERING. 277: 239.

Knezevic, , I. J. Beyerlein, M. L. Lovato, C. N. Tome, A. W. Richards, and R. J. McCabe. A strain-rate and temperature dependent constitutive model for BCC metals incorporating non-Schmid effects: Application to tantalum-tungsten alloys. 2014. INTERNATIONAL JOURNAL OF PLASTICITY. 62: 93.

Knezevic, , Jahedi, Y. P. Korkolis, and I. J. Beyerlein. Material-based design of the extrusion of bimetallic tubes. 2014. COMPUTATIONAL MATERIALS SCIENCE. 95: 63.

Knezevic, , Nizolek, Ardeljan, I. J. Beyerlein, N. A. Mara, and T. M. Pollock. Texture evolution in two-phase Zr/Nb lamellar composites during accumulative roll bonding. 2014. INTERNATIONAL JOURNAL OF PLASTICITY. 57: 16.

Knezevic, , Zecevic, I. J. Beyerlein, J. F. Bingert, and R. J. McCabe. Strain rate and temperature effects on the selection of primary and secondary slip and twinning systems in HCP Zr. 2015. ACTA MATERIALIA. 88: 55.

Knezevic, M., T. Nizolek, M. Ardeljan, I. J. Beyerlein, N. A. Mara, and T. M. Pollock. Texture evolution in two-phase Zr/Nb lamellar composites during accumulative roll bonding. 2014. International Journal of Plasticity. 57: 16.

Kumar, A., I. J. Beyerlein, and J. Wang. First-principles study of the structure of Mg/Nb multilayers. 2014. Applied Physics Letters. 105: 071602.

Lentz, , Klaus, I. J. Beyerlein, Zecevic, Reimers, and Knezevic. In situ X-ray diffraction and crystal plasticity modeling of the deformation behavior of extruded Mg-Li-(Al) alloys: An uncommon tension-compression asymmetry. 2015. ACTA MATERIALIA. 86: 254.

Lentz, , Klaus, Wagner, Fahrenson, I. J. Beyerlein,

Zecevic, Reimers, and Knezevic. Effect of age hardening on the deformation behavior of an Mg-Y-Nd alloy: In-situ X-ray diffraction and crystal plasticity modeling. 2015. MATERIALS SCIENCE AND ENGINEERING A-STRUCTURAL MATERIALS PROPERTIES MICROSTRUCTURE AND PROCESSING. 628: 396.

Xu, X. F., Y. Jie, and I. J. Beyerlein. A note on statistical strength of carbon nanotubes. 2013. Computers, Materials & Continua. 38: 17.

Xu, X. F., Y. Jie, and I. J. Beyerlein. A probability model for the strength of carbon nanotubes. 2014. American Institute of Physics Advances. 4: 077116.

Yuan, R. u. i., I. J. Beyerlein, and Zhou. Emergence of grain-size effects in nanocrystalline metals from statistical activation of discrete dislocation sources. 2015. ACTA MATERIALIA. 90: 169.

Zhou, , C. J. O. Reichhardt, Reichhardt, and Beyerlein. Random organization in periodically driven gliding dislocations. 2014. PHYSICS LETTERS A. 378 (22-23): 1675.

Zhou, , Reichhardt, C. J. O. Reichhardt, and I. J. Beyerlein. Dynamic Phases, Pinning, and Pattern Formation for Driven Dislocation Assemblies. 2015. SCIENTIFIC REPORTS. 5.

Toward Tunable Functionalties Using Epitaxial Nanoscaffolding Films

Quanxi Jia
20140371ER

Introduction

Lattice-strained epitaxial nanoscaffolding films (epi-NSFs), in which a parallel array of nanoscaled material A interfaces with another material B and forms a regular lateral arrangement of A:B on a substrate, provide a new design paradigm to tune/manipulate functionalities that cannot be obtained in individual constituents (A or B). Tuning/controlling functionality of a broad range of materials is emerging as an exciting direction in materials research community. Built on our expertise, integrated capabilities (from CINT, NHMFL, and T-4), and preliminary experimental results, this project aims to develop new capabilities toward tunable functionalities using epi-NSFs where the vertical interface can act as an "active device". Specifically, we will, for the first time in the field, investigate the tunable optical and resistive switching properties based on La0.7Sr0.3MnO3:ZnO (LSMO:ZnO) and SrTiO3:Sm2O3 (STO:SmO) epi-NSFs, respectively. The impact of this project reaches far beyond these materials systems.

Leveraging CINT's well controlled laser-MBE for the growth of complex metal-oxide films, we target to synthesize both LSMO:ZnO and STO:SmO epi-NSFs with controlled microstructures. In parallel with modeling effort, we also use computational results to optimize the processing parameters (which can affect the surface morphology of the film) and to tune the optical properties of ZnO and resistive switching property (or so called "memristive" behavior) of STO. Combining our unique characterization tools (such as transport measurement and photoluminescence (PL) spectroscopy at a wide range of magnetic fields and temperatures) with advanced TEM and high-resolution x-ray diffraction capability, our objective is to establish the processing-structure-functionality relationship of epi-NSFs.

Benefit to National Security Missions

This work supports and strengthens the Laboratory's core scientific capabilities essential to discovering, understanding, and exploiting emergent phenomena in materials. In particular, this research develops/expands our key capabilities outlined in the EPM ER category, e.g. i) functional design and optimization, ii) novel control and metrology techniques exploiting emergent phenomena, iii) understanding mechanisms for control of material properties, and iv) synthesis and processing techniques that lead to control of emergent phenomena. Furthermore, this project enables the development of new experimental (advanced synthetic and diagnostic techniques) and theoretical capabilities to probe the state of complex nanoscale materials. This effort can ensure LANL's continued and expanded leadership in nanostructured materials, innovative probing methods, and theoretical predication and design of new/improved functional materials.

The success of this project enables LANL to respond effectively to future BES calls since our proposed work directly addresses the Grand Scientific Challenge identified in the BESAC report: how do remarkable properties of matter emerge from the complex correlations of atomic or electronic constituents and how can we control these properties? Beyond BES, this work will have enormous ramifications in technological sectors such as memory and electro-optical devices. Finally, this work enables an important capability for MaRIE, since the ability to design, synthesize, measure, and model functionality at different length scales in complex materials is the central competence underpinning MaRIE's M4 facility. Additionally, this work exploits and expands the capabilities at two LANL National User Facilities: CINT and NHMFL.

Progress

In the past year, we made tremendous progress for this project. This can be testified by our many refereed journal articles published in 2014 and patent application related to this project. In the following, we summarize the key technical accomplishments.

We, using LSMO:ZnO epitaxial nanoscaffolding films (epi-NSFs) as a model system, have studied the effect of film thickness on the physical properties of nanocomposites. We show that strain, microstructure, as well as magnetoresistance strongly rely on film thickness. These results confirm the critical role of film thickness on the microstructures, the strain, and functionalities. It further shows that one can use film thickness as a key design parameter to design nanocomposite with optimum functionalities.

Optimizing the processing parameters for high quality LSMO:ZnO epi-NSFs

LSMO:ZnO films with different thicknesses (10 nm to 200 nm) were grown on r-plane sapphire, c-plane sapphire, and LAO (001) by using pulsed laser deposition (PLD) with a KrF excimer laser (Lambda Physik LPX 300, λ = 248 nm, 2Hz). The rectangle laser beam with an area of 5.55 mm2 was focused onto the composite target with an energy density of 2.0 J/cm2. A substrate temperature of 750 °C and an oxygen pressure of 100 mTorr were found to be optimal for high quality epi-NSF LSMO:ZnO.

Structural characterization using x-ray diffraction

The structures of epi-NSFs with different film thicknesses on various substrates have been analyzed by X-ray diffraction (XRD). It is noted that both LSMO and ZnO phases are preferentially oriented out-of-plane. The Φ-scans of LSMO {202} and LAO {202} show a fourfold symmetry, suggesting that the LSMO phase on the LAO substrate is epitaxially grown (cube-on-cube). Different from the films on sapphire substrates, the out-of-plane lattice constant of films on LAO (001) strongly depends on film thickness. The LSMO (002) peak monotonically shifts to the larger angles with increasing film thickness, indicating that the strain varies with the thickness. We believe that when the nanocomposite films are thin enough, the strain in the LSMO phase is controlled by the LAO substrate. However, the strain of LSMO phase is dominated by the secondary ZnO phase when the films become thicker (200 nm).

Microstructural characterization using transmission electron microscopy

To investigate the thickness dependent microstructures of the ei-NSFs, transmission electron microscopy (TEM) and scanning TEM (STEM) in high-angle annular dark-field (HAADF) mode were conducted. We have found that the ZnO nanopillars tend to embed in the LSMO matrix. The LSMO phase is connected into much larger domains. It is interesting to note that both LSMO and ZnO nanodomains are vertically and alternatively aligned on LAO substrate with uniform feature size through the film thickness. The plan-view STEM image further reveals that the ZnO rectangular nanopillars are embedded in the LSMO matrix. These perpendicular ZnO domains are consistent with the x-ray Φ-scan results. Detailed analysis also shows that the microstructure of epi-NSF LSMO:ZnO on LAO is independent of the film thickness.

Magnetic properties of epi-NSF LSMO:ZnO

To reveal the property-structure correlation in these epi-NSFs, the magnetotransport and magnetoresistance (MR) of these films have been investigated at different temperatures and magnetic fields. We have found that the microstructure evaluation with the film thickness should be the dominating factor in determining the transport properties of the films on sapphire substrates. In the case of LSMO:ZnO films on LAO substrates, TEM results show that the microstructure does not change with the film thickness. Thus, the metal-insulator transition temperature and resistivity variation with the film thickness could be correlated with the strain effect.

Parallel connection channel model

In order to fit the magnetotransport results in the whole temperature range, including the abnormal high resistance at low temperatures, a modified parallel connection channel model was used to analyze the experimental results. We have found that our results are consistent with the microstructure variations of the nanostructures on sapphire substrates. The phenomenological model is not suitable for the thin nanocomposite films on LAO substrates since the large strain effect can significantly alter the ferromagnetic behavior of the LSMO phase.

Future Work

- Probe both the transport and the structural properties of La0.7Sr0.3MnO3:ZnO (LSMO:ZnO) and SrTiO3:Sm2O3 epitaxial nanoscaffolding films.
- Tune the optical properties of LSMO:ZnO using external magnetic field.
- Understand the structure-property relationship of these materials.

Conclusion

Our integrated capabilities to design, synthesize, and characterize different epi-NSFs with a range of controllable and tunable properties make it possible to explore new physics. This project has also great technological impact on areas of functional materials for application in memories, photonic devices, and sensing components. The following outlines the expected scientific and technical results:

- Development of a set of principles to design epi-NSFs with targeted functionalities.
- Demonstration of magnetic field tunable optical prop-

erties of ZnO in LSMO:ZnO epi-NSFs.

- Illustration of much enhanced tunable memristive switching in STO:SmO epi-NSFs.

Publications

Chen, A., M. Weigand, Z. Bi, W. Zhang, X. Lv, P. Dowden, H. Wang, J. L. MacManus-Driscoll, and Q. X. Jia. Role of microstructure and strain on the magnetoresistance of nanocomposite films. 2014. Scientific Reports. 4: 5426.

Jia, Q. X.. Self-assembled epitaxial nanocomposite films: their strain control and functionalities. Invited presentation at New Mexico Tech. (Socorro, NM, 7 March, 2014).

Jia, Q. X.. Effect of interfaces on competing interactions of functional complex metal-oxides. Invited presentation at Univ. of Connecticut. (Storrs, CT, 17 OCt. 2014).

Lee, S. B., A. Sangle, P. Lu, A. Chen, W. Zhang, J. S. Lee, H. Wang, Q. X. Jia, and J. L. MacManus-Driscoll. Novel electroforming-free nanoscaffold memristor with very high uniformity, tunability and density. 2014. Adv. Mater.. 26: 6284.

Lee, S. B., W. Zhang, F. Khatkhatay, H. Wang, Q. X. Jia, and J. L. MacManus-Driscoll. Ionic conductivity increased by two orders of magnitude in micrometer-thick vertical yttria-stabilized ZrO2 nanocomposite films. To appear in Nano Lett..

Lee, S. B., W. Zhang, Q. X. Jia, H. Wang, and J. L. MacManus-Dris. Strain tuning and strong enhancement of ionic conductivity in SrZrO3-RE2O3 (RE = Sm, Eu, Gd, Dy, and Er) nanocomposite films. 2015. Adv. Functional Mater.. 25: 4328.

Lu, P., E. Roemro, S. B. Lee, J. L. MacManus-Driscoll, and Q. X. Jia. Chemical quantification of atomic-scale EDS maps under thin specimen conditions. 2014. Microscopy & Microanalysis . 20: 1782.

MacManus-Driscoll, J. L., A. Suwardi, A. Kursumovic, Z. Bi, C. F. Tsai, H. Wang, Q. X. Jia, and Q. J. Lee. New strain states and radical property tuning of metal oxides using a nanocomposite thin film approach. 2015. APL Mater.. 3: 062507.

Yang, S. M., S. B. Lee, J. Jian, W. Zhang, Q. X. Jia, H. Wang, T. W. Noh, S. V. Kalinin, and J. L. MacManus-Driscoll. Strongly enhanced oxygen ion transport through samarium-doped CeO2 nanopillars in nanocomposite films. To appear in Nat. Commun..

Zhao, R., W. Li, J. H. Lee, E. M. Choi, Y. Liang, W. Zhang, R. Tang, H. Wang, Q. X. Jia, and J. L. MacManus-Driscoll. Precise tuning of (YBa2Cu3O7)1-x:(BaZrO3)x thin film nanocomposite structures. 2014. Adv. Funct. Mater.. 24: 5240.

Direct-gap Group-IV Nanocrystals:Cheap, Versatile Materials for Solar Cells

Sergei A. Ivanov
20140446ER

Introduction

Cheap, non-toxic and abundantly produced, Group IV semiconductors (silicon (Si), germanium (Ge), tin (Sn)) are versatile materials for a broad range of devices. However, Si and Ge are indirect semiconductors, which make their interactions with light (absorption or emission) much less efficient than those of direct-gap semiconductors. This places severe limitations on how these materials can be used in solar cells, driving prices up and holding utilization down. If one could, instead, convert these materials into a more versatile form that could be handled and processed cheaply, and that offered better absorption properties, the effect on solar cell development and deployment would be transformative. Even simply rendering these materials amenable to, e.g., screen printing, spray deposition and other fabrication techniques suitable for roll-to-roll processing or the coating of surfaces of complex morphology, would enable a host of new civilian and military applications that are incompatible with rigid, brittle crystalline-Si. We propose to use the unique power and flexibility of colloidal synthesis to accomplish exactly that. The use of colloidal nanocrystal (NC) synthesis places the ability to create size-/composition-/shape-controlled NCs in device-relevant quantities into the hands of nearly any researcher. Importantly, colloidal NCs are amenable to low-cost solution-based processing techniques, making them extremely versatile. We seek to exploit the power of colloidal synthesis to create a new class of Group IV alloy NCs with direct band-gap behavior at solar-relevant energies (1.0-1.5 eV) for use in a wide-range of emerging solar technologies.

Benefit to National Security Missions

This work combines a number of marquee capabilities of the Laboratory, including world-recognized nanoscience efforts towards a goal of tremendous potential impact, especially with direct relevance to applications in solar energy capture and energy-efficient solid-state lighting. In this way, our work is directly tied to the LANL Science Mission in the Basic Understanding of Materials, and in the process will involve exploration of Fundamental Chemistry. These studies directly seek to understand and exploit the power of Defects and Interfaces in a material system of unique potential importance to applications in Energy Security, particularly in the area of Renewable Energy, and as such lie at the core of the LANL “Materials for the Future” Pillar. The development of direct band gap Group IV NCs by low-cost methods is also extremely relevant to ongoing and future DOE Office of Science programs. Development of low-cost silicon-based photovoltaic materials will result in long-term benefits to LANL efforts and eventually to federal stakeholders in these areas.

Progress

In the second year of our project, we continued the development of the versatile procedure for the synthesis of SnGe alloy nanoparticles together with the investigation of the mechanism leading to their formation. As we achieved deeper understanding of the factors beneficial for the increased load of tin in germanium lattice, we were able to synthesize SnGe alloy nanoparticles with 95% of tin load. As such, we have achieved full compositional variation of SnGe alloy, where we can change its composition from pure Ge to Sn0.95Ge0.05 nanocrystals!

Synthesized nanocrystals were also studied with absorption spectrometry in the attempt to elucidate the nature of changes in the electronic structure of those products as a function of the amount of tin. The results obtained to date indicate that previous theoretical models might have underestimated the amount of tin needed to convert germanium into the direct-gap material.

In parallel with the synthesis of single-source Ge-Sn and Si-Sn precursors, where the same molecule contains both needed elements, we are working on the modification of our original approach to the synthesis of SnGe

nanocrystals so that we could introduce the third element – silicon – into the composition of the alloy. Preliminary results have already revealed that this approach appears to be more productive than the originally proposed synthesis of SnSi followed by the introduction of germanium. Introduction of silicon during the SnGe nanoparticle synthesis allowed us to obtain the first batch of ternary composition SiGeSn nanoparticles! Direct incorporation of Sn into Si is yet an elusive goal, but the discovered modification of this approach with the initial synthesis of the ternary alloy followed by the minimization of germanium content is a viable alternative that might lead to the SnSi alloy formation, the ultimate goal of our project.

Future Work

As the project is continues to be short funded, the theoretical investigation of the systems of interest will again have to be de-emphasized (but not fully abandoned). In the year to date, the following tasks will be performed.

We will model the alloy NCs with different compositions and type of protecting molecules on the NC surface seeking to understand the best formulations for stable GexSn(1-x) and SixSn(1-x) alloy NCs. Together with theoretical assessment of NC stability, we will continue the development of a synthetic procedure for heavily alloyed germanium-tin NCs (with tin more than 90%).

The research team will fully switch to the silicon-germanium-tin formulations utilizing the same synthetic approach to map the composition boundaries of alloyed nanocrystals.

Additionally, we will develop the approach to prepare uniform films of synthesized nanocrystals to assess their application in photovoltaics as well as a cathode in lithium batteries.

All synthesized nanocrystals will be continued to be spectroscopically characterized in order to establish the understanding of their electronic structure on the way from poor to efficient light absorber.

Conclusion

Utilizing two different synthetic approaches combined with two methods of reaction activation, the goal is to synthesize nanocrystals with formulations SixSn1-x and GexSn1-x. The synthetic efforts will benefit greatly from the theoretical component, predicting compositions of greatest stability and Sn-distribution effects. Technologically, the alloy NCs with enhanced absorption will have an immediate, direction-changing impact on research within solar-cell community in general. Fundamental studies of these formulations will provide an insight into the fascinating and underexplored interplay of bulk and small size effects in semiconductors, advancing the understanding of electronic structure and behavior in essentially all nanomaterial and atomically disordered systems.

Publications

Ramasamy, , P. G. Kotula, A. F. Fidler, M. T. Brumbach, J. M. Pietryga, and S. A. Ivanov. SnxGe1-x Alloy Nanocrystals: A First Step toward Solution-Processed Group IV Photovoltaics. 2015. CHEMISTRY OF MATERIALS. 27 (13): 4640.

Metal and Semiconductor Nanocrystal Superlattices Under Pressure: Multiscale Tuning of Structure and Function

Jennifer A. Hollingsworth
20140456ER

Introduction

The overarching goal of this project is to explore and exploit high pressure as a novel means to precisely tune colloidal nanocrystal superlattices (NCSLs) from the atomic to the nano- and mesoscales to realize: (1) new understanding of forces and interactions affecting supercrystal stability, (2) novel NCSLs structures by controlled compression of self-assembled NCSLs, and (3) collective behavior as a function of interparticle distance.

On their own, nanoparticle colloids of carefully controlled size/shape and surface properties will self-assemble into a surprisingly wide array of ordered two-dimensional (2D) and three-dimensional (3D) NCSLs that mimic atomic lattices. These can comprise single or multiple components, e.g., binary and ternary superlattices (SLs), where the latter afford a richer variety of accessible structures and opportunities for developing collective functional properties compared to their single-component counterparts. Significant progress has been made over the last decade in "nanoparticle-colloid self-assembly," with ~20 binary NCSLs now known. These have been constructed from two metals, two semiconductors, two magnetic nanoparticles, or combinations thereof.

Surprisingly, however, efforts to exploit new functionality resulting from ordered arrays of dissimilar but interacting nanoparticles has been limited to ~six examples, including interactions in magnetic-nanoparticle pairs, enhanced electronic conductivity in semiconductor mixtures, and fluorescence quenching of a metal/semiconductor pair. In addition, there are interesting, but limited, examples of enhanced stability imparted to nanoparticle components as a result of superstructuring, in particular, stability against effects of elevated temperature. Beyond this, however, understanding of the comparative stability of different nanocolloidal-crystal lattices and their tendency to transform into other structures remains lacking.

Therefore, we aim to apply a novel approach—high-pressure methods as an analytical and synthesis tool—to establish new understanding of NCSL formation and stability toward design of new structures and controlled functionality.

Benefit to National Security Missions

The effort directly addresses Basic Science focus areas, including Materials for the Future Pillar Focus Area 2: Advancing the understanding of materials functionality through co-design using extreme conditions, in situ measurements and User Facilities, as we make use of capabilities located at LANL CINT and LANSCE, as well as Cornell's High-energy synchrotron source for x-ray scattering analysis (the CHESS facility). The work is also clearly responsive to envisioned MaRIE mission areas, especially "high-pressure nanoscience." We also support Focus Area 3: Developing multi-functional materials architectures to transform structure/function integration, performance and emergent properties. A successful program will lay the groundwork for a predictive "closed-loop" capability for designing/implementing novel/functional nanocrystal superlattice structures that take advantage of collective, "emergent" behavior to realize important optical performance, especially "superradiance." Superradiance can significantly enhance the efficiency of nanoscale light sources without the need for an external cavity, with the potential to transform solid-state lighting and telecommunication technologies. Also, the ability to couple otherwise discrete quantum emitters over distance is likely to play an important role in the realization of quantum computation. Beyond superradiance, the effort will enable other "collective functionality," such as the ability to manipulate fundamental statistical properties of light emission through, with implications for the development of single-photon and entangled-photon-pair sources that are critically needed for quantum-communication applications. Beyond "light": the targeted ability to precisely organize interacting-nanocrystal superstructures comprising

components of selected composition/functionality is key for energy harvesting (solar, thermoelectrics), catalysis, energy storage, and sensing, where coupled interfacial (e.g., charge-separation/transfer) and extended-transport issues dominate.

Progress

The research team completed high-pressure diamond-anvil-cell (DAC) synchrotron X-ray diffraction (XRD) studies of two series of core/shell QDs. Here, core/shell systems were compared with different tendencies for alloy formation. Namely, one system was anticipated to be highly susceptible to alloy formation via cation-cation migration and alloying, while the other was presumed less likely to alloy as the mechanism of alloy formation would have to be mediated by anion-anion exchange. Results from this analysis were published.

In addition, we completed an analysis of observed variations of phase transformation pressures with shell thickness and core/shell composition. These results afford key insight into fundamental stability parameters (bulk moduli/compressibility) of the core/shell quantum dots, and are currently being written up for a late-summer submission.

Beyond these fundamental studies of the effects of pressure on nanocrystal stability (as input into our superstructure analyses), we have made significant progress this FY in other key aspects of the program. Namely, a DAC with optical windows for conducting in situ observations of NCSL photoluminescence under pressure (Research Goal 3) was purchased and installed in the CINT "single-nanostructure" spectroscopy laboratory. This instrument has a built-in capability for exciting/recording photoluminescence as part of a ruby luminescence method for pressure calculation. Our initial aim was to "piggy-back" on this capability and attempt to simultaneously pull our emission spectra from our NCSLs. However, although not explicitly stated in the company's technical specs, the wavelength window that can be accessed is very limited due to the optics integrated in the system. That said, we have designed a "work-around" (physical modification to the setup) that will allow us to couple the DAC to our spectroscopy setup and, thereby, to still obtain direct/correlated assessment of NCSL emission performance with a precise pressure measurement.

We have also made significant progress in our efforts to prepare phase-pure/discrete NCSLs in micronfluidic droplet "microreactors." We have identified this approach (only a single report in the literature on this novel application of microfluids to crystal growth) as the only route to obtaining large NCSLs phase separated from amorphous NC aggregates and even other NCSLs. We have demonstrated that for NCSLs of reasonable size (~1 micron or more) we can physically manipulate them into the DAC. We have characterized NCSLs by optical spectroscopy and obtained parameters for realizing NCSL formation for both electrostatic assembly and hard-sphere self assembly (latter in hydrophobic media), e.g., concentration of "screening" ions (as small charged NCs or salt additives), NC concentration, time, non-solvent concentration. We now have a good understanding so that in year 3 we will be able to shift our emphasis from NCSL nucleation/growth to in situ pressure studies. That said, thus far we have prepared NCSLs from "well-behaved" NCs of uniform size/shape. In year 3, we will transition to larger and less uniform thick-shell quantum dots (giant QDs) and the hybrid gQD-Au systems toward realizing truly "collective" optical properties from the mixed excitonic-plasmonic systems.

Future Work

Overall, we aim to apply a novel approach—high-pressure methods as an analytical and synthesis tool—to establish new understanding of colloidal nanocrystal superlattice (NCSL) formation and stability toward design of new structures and controlled functionality. To this end, we are pursuing three Research Goals, with specific Year 3 Goals delineated as follows:

NCSL stability studies

High-pressure diamond-anvil-cell (DAC) synchrotron x-ray diffraction (XRD) has now been completed of two series of core/shell QDs. In year 3, we will follow-up with some iterations of one of these systems -- variations of the core/thick-shell CdSe/CdS system to assess unexplored effects of crystal structure (cubic vs. hexagonal) and particle shape (hexagonal/faceted, pyrimidal, elongated/asymmetric) as key parameters potentially influencing optical properties (quantum yield and stability). That said, our focus in year 3 will transition to Goals 2 and 3.

New NCSL structures through pressure

NCSLs (QD-QD; QD-Au) prepared in microfluidic-droplet reactors will be transferred to our PL-integrated DAC for in situ measurements of PL as a function of pressure. The resulting novel fused structures will be further characterized structurally/optically outside the DAC. Furthermore, we have also established a capability for fabricating 2-D NCSLs using Langmuir-Blodgett techniques. Thus, we now have access to both types of superstructure, representing two extremes of NC-NC interactions. We will perform molecular dynamics simulations using the LAMMPS software to study the differing self-assembly dynamical processes that are active in the formation our 2-D/3-D nanoparticle arrays.

New binary NCSL functionality through pressure: In the

second half of year 3, a few of the “most interesting” binary systems explored in (2) will be investigated for collective optical properties, where we target “superradiant” modes that spread over the entire supercrystal domain. Realization of optimized, extended superradiance is anticipated for Year 3 of the effort.

Conclusion

Until now, the development of new nanocrystal superlattices (NCSLs) has depended upon empirical observations of effects of size-ratio, surface-ligand/charge, solvent dielectric constant and electrophoretic mobilities. By combining our expertise in synthesis and computational chemistry with in situ high-pressure x-ray scattering and optical spectroscopy, we will establish correlated structure-stability relationships and principles for predictive development of new superstructures, aided by “pressure sintering.” We will also demonstrate unprecedented collective behavior (e.g., superradiance) by precise tuning of inter-nanocrystal distances toward designed “colloidal metamaterials” for applications from light-emission to catalysis, photovoltaics & thermoelectrics; whereas, current examples are limited to small-cluster behavior or uncontrolled/disordered assemblies.

Publications

Acharya, K. P., H. M. Nguyen, Paulite, Piryatinski, J. u. n. Zhang, J. L. Casson, Xu, H. a. n. Htoon, and J. A. Hollingsworth. Elucidation of Two Giants: Challenges to Thick-Shell Synthesis in CdSe/ZnSe and ZnSe/CdS Core/Shell Quantum Dots. 2015. JOURNAL OF THE AMERICAN CHEMICAL SOCIETY. 137 (11): 3755.

Li, , Bian, Wang, Xu, J. A. Hollingsworth, Hanrath, Fang, and Wang. An Obtuse Rhombohedral Superlattice Assembled by Pt Nanocubes. 2015. NANO LETTERS. 15 (9): 6254.

Quan, Z., D. Wu, J. Zhu, W. H. Evers, J. M. Boncella, L. D. A. Siebbelese, Z. Wang, A. Navrotsky, and H. Xu. Energy landscape of self-assembled superlattices of PbSe nanocrystals. 2014. Proceedings of the National Academy of Sciences . : 9054–9057.

Interactions of Electrons with Quantum-Confined Systems Probed by Scanning Tunneling Spectroscopy

Victor I. Klimov
20140495ER

Introduction

The beneficial aspects of quantum confinement as a means for controlling light-matter interactions are well documented. On the other hand, the influence of confinement on interactions of solids with charged particles (electrons and holes) still remains largely unexplored. The case of charge injection is particularly important as most practical devices make use of this type of excitation. One expected effect of confinement is a diminished role of momentum conservation, which might lead to an intriguing situation where interactions of electrons with matter are constrained only by energy conservation. This would have major implications for several detection/sensing technologies, where the use of nanostructures could greatly increase sensitivity, potentially up to the fundamental limit defined only by energy conservation. Here, we address this problem via comprehensive studies of interactions of single electrons/holes with individual semiconductor nanocrystals (NCs). The specific focus is on impact ionization (ImI), that is, the collision of an injected charge with a valence-band electron, which is subsequently promoted to the conduction band. Electrons at well-defined energies will be injected into the NCs from the tip of a scanning tunneling microscope and the ImI efficiency will be inferred from measurements of the resulting luminescence. In addition to single-NC sensitivity in detecting ImI events, this study will provide comprehensive information on how the ImI efficiency relates to NC morphology and the structure of electronic states. Based on these measurements, we will answer an important fundamental question: can the ImI efficiency in NCs approach the energy-conservation-defined limit? We also aim to unequivocally demonstrate that ImI performance in nanostructures is superior to that of bulk solids.

Benefit to National Security Missions

The proposed work directly addresses the Science Pillar "Science of Signatures" especially the second theme "Revolutionize Measurements". This project pushes the boundaries in advanced instrumentation for studies of interactions of charged particles with individual nanostructrues by combing scan-probe and optical techniques. Further, this project exploits quantum confinement effects (e.g., relaxation of momentum conservation) for enhancing the detection sensitivity. Since interactions of energetic radiation with matter are mediated by "hot" electrons, the effects under investigation are directly relevant to radiation detection. Further, due to their potential use in IR avalanche photodiodes, these studies also enhance capabilities in remote sensing and quantum communication making these studies relevant to the "Energy Signatures" strategy. Further, impact ionization can be exploited to enhance solar photovoltaics. Additionally, our studies support the "Materials" Pillar under the theme emergent phenomena. Specifically, an underlying theme of this project is materials by design, which is the central vision of the controlled functionality strategy. The fundamental aspects of our work are of interest to the DOE Office of Science.

Progress

Experimental results

Light-modulated scanning tunneling microscopy/spectroscopy of PbS quantum dots (QDs)

One of the goals of this project is to investigate light-matter interactions within an individual quantum-confined semiconductor nanocrystal using methods of scanning tunneling microscopy (STM). Toward this goal, we have measured a tunneling current through the individual PbS QD as a function of voltage applied to the STM tip with and without illumination. Using the laser beam directed towards the QD sample through an optical port of the STM, we were able to modulate the tunneling current using excitation rates of 0.01 – 0.1 photons absorbed per QD per ms. Furthermore, the high spatial resolution of the STM combined with the light-modulation capability enabled spatial mapping of both the photocurrent and the dark current in QD monolayer

and multilayer films, providing information on correlations between the film morphology and photoconductivity.

While our initial room-temperature measurements yielded current-voltage characteristics with sufficient signal-to-noise ratio for determining a QD band gap, further noise suppression via cryogenic cooling is required for resolving individual quantized transitions within the QDs. To achieve this goal, we have modified the STM design to allow for cooling of the sample holder with liquid nitrogen. First test measurements of this cryogenic capability are underway.

Sample preparation
Sample preparation is perhaps the most critical step in ensuring the success of STM measurements. To this end, we have explored a large parameter space for preparing "STM-grade" QD samples including various ligand treatments, different regimes of annealing, different film thicknesses, and several different substrate materials. We found that depending on the amount of short ligands such as 1,2-ethanedithiol (EDT), the films can exhibit either metallic or semiconducting behavior. As these samples are highly air-sensitive with surfaces prone to oxidation, we are developing an ultra-high vacuum heater/dock bundle that allows for in situ annealing of the sample in the main STM chamber for convenient transfer to the STM head. Using the high-resolution spatial imaging capability of the STM, we ensure that annealing and ligand treatment do not change the morphology of the close-packed QD films (avoiding, for example, fusion of the QDs).

STM upgrades
Integration with optics: We have integrated a laser system into the STM setup. This system is equipped with a modulator for high-sensitivity, low-noise lock-in measurements of excited photocurrents. For all QD sizes used in the measurements excitation intensities are sufficient to maintain average QD occupancies close to or exceeding unity. This ensures a large modulation of the tunneling photocurrent excited by the incident laser beam.

Low-temperature capability: We have acquired a special custom-designed liquid nitrogen Dewar that enables safe transfer of liquid nitrogen through a flexible transfer line with a special "Z" shape. Our initial tests have demonstrated successful cooling of the STM head to about 165 Kelvin.

Heating capability We have designed an ultra-high vacuum heater/dock allowing for in situ sample annealing. It consists of a one-inch diameter heater unit surrounded by a heat shield with a sample dock on the top of the shield. The sample dock is designed to allow for transfer of our annealed samples from the heater dock to the STM sample stage using the wobble stick. The design has been completed and sent for manufacturing.

System for tunneling gap monitoring: Precise control and evaluation of tip/sample spatial separation is crucial for STM measurements. Therefore, we have developed a tip/sample spatial gap monitoring system using a telescope and a CCD camera. This system allows for the sample/tip spatial gap inside the ultra-high vacuum chamber to be monitored on the computer screen.

Future Work
During the next year, we will focus on the following two tasks:

The research team will continue studies of PbS and PbSe nanoplatelets using scanning tunneling spectroscopy (STS) measurements in order to determine the structure of electronic states in these novel nanostructures. Specifically, we plan to investigate the difference (if any) between the edge and the interior states. We will also probe the effect of nanoplatelet stacking on the structure/energies of STS features and attempt to derive the strength of interplatelet coupling. The results of the STS measurements will be analyzed using model calculations conducted within a multi-band effective mass approximation.

We will continue our instrument development work. The next stage is the incorporation of the optical system into the STM to allow for efficient pick-up of light emitted by a nanostructure in the course of excitation with a tunneling current. The mechanical parts of the pick-up system have been already machined. The fiber optical elements have been acquired. After optical and mechanical pick-up parts are assembled and installed in the STM chamber, we will test the complete system by analyzing scanning tunneling emission from bulk substrates (e.g., CdSe and CdS). Eventually these measurements will be extended to CdSe-based nanocrystals.

Conclusion
- Development of a novel STL technique for quantitative characterization of ImI with single-NC sensitivity and complete morphological information.
- Development of a quantitative theoretical model for treating ImI in semiconductor NCs of various compositions, shapes and internal structures.
- Detailed experimental information on ImI yields in NCs as a function of composition, size, shape (dots vs. rods) and internal structure (e.g., core-only vs. core/shell).
- Development of nanostructures with ImI yields approaching those for the energy-conservation-defined limit.

Unraveling Interfacial Charge and Energy Transfer Processes in Single Layer 2D Transition Metal Dichalcogenides

Aditya Mohite
20140540ER

Introduction

Graphene research has initiated rejuvenated interest and served as a catalyst for the birth of a new field, beyond graphene, in the form of novel two-dimensional (2D) layered materials also referred to as Transition metal dichalcogenides (TMDs). TMDs exhibit remarkable electronic and optical properties arising from the reduced dimensionality of a single unit cell perpendicular to the crystal plane that hold the promise for transformational research and development for next generation thin film optoelectronic applications. Unlike the semi-metal graphene (zero electronic band-gap), TMDs such as MoS2, MoSe2, WS2, WSe2, GaS, GaSe, InAs etc. are intrinsic semiconductors with band gaps spanning the entire solar spectrum. This provides a unique opportunity to create layered homo and heterostructures by combining two or more layers of these 2D materials and tailoring their interfacial properties to pave the path for current applications in phototransistors, photovoltaics, photodetectors, photocatalysis (H2 evolution/water splitting) and light emitting devices (LEDs) and transformational technologies in spin and valleyoptoelectronics. However in order to take advantage of the rich optoelectronic properties, it is critical to understand the charge generation, recombination and separation processes at the homo (create by two layers with semiconducting phase (2H) and/or metallic phase (1T) or and hetero interfaces (created by dissimilar TMDs with semiconducting or metallic phase). In this project, we will combine single atomic layers of MoS2 and MoSe2 to form the first of its kind, layered TMD heterostructures that will enable us to establish the interfacial design rules, vital for the understanding, control and manipulation of the flow of charge and energy across the TMD heterostructure interfaces.

Benefit to National Security Missions

The novel physical phenomena we aim to explore in this project will pave the way to make transition metal dichalcogenides (TMDs) viable assets in LANL's science pillar of Materials for the Future. The formation of inter-face states between TMDs with an understanding of their fate and transport will allow us to go beyond intrinsic optical and electronic properties. This project, therefore, directly addresses the materials strategy of controlled functionality by tailoring materials to perform beyond their basic properties. The successful completion of this ER will have tremendous implications for agencies like DoD, Space Research, NASA etc for the use of thin film optoelectronic devices for remote applications and as power sources for on field personnel.

Progress

In the past year we have made significant progress in the synthesis and optoelectronic characterization of heterostructures with similar and different layered transition metal di-chalcogenides (TMD) and achieved most goals established at the beginning of the year.

The main highlight was our work on creating highly efficiency metal-semicondcutor contacts using a novel phase engineering approach, which can reversibly convert a TMD from a semiconductor to a metal. We developed this approach to make clean and perfect metal -semiconductor interfaces with TMDs and demonstrated that excellent, loss free charge transfer can be achieved. Specifically, we showed that by we can reduced the contact resistance in an optoelectronic device and achieve highly efficiency photoresponse as compared to the pristine semiconductor device. This work was published in several high impact papers (Nature Materials, ACS Nano and APL) and most recently in a review article in Chem. Soc Reviews, which is a high impact journal (impact factor of 33). The phase transformation strategy also allowed us to test the catalytic performance of the TMDs and by comparing the performance of 2-dimensional TMDs to 1-dimensional nanowires, we were able to show that the mechanism of catalytic activity in 1D and 2D TMDs is different. We also demonstrated that the origin of catalytically activity in 2D sheets is from the

edges and not from the basal plane. This work is expected to resolve a long standing controversy in the use of layered 2D sheets as catalysts.

In addition to this work, we also demonstrated a unique CVD growth of TMDs using a modified precursor, which leads to the growth of high quality single-crystalline TMDs. The optical and electrical characterization of the grown TMDs demonstrated properties that are consistent with high optical grade semiconductors. For e.g. we were able to observe new features in the photocurrent and Raman spectrum that have not been observed before. We worked with theorists and collaborators at Northeatern university and OIST (Japan) to validate our experimental observations using theory and structural characterization using diffraction techniques such as LEEM and PEEM. This work is now accepted in ACS Nano and is expected to be a significant step in achieving high quality TMD samples for research groups across the world. Furthermore, extended our growth strategy to growth heterostructures of TMDs such as MoS2/MoSe2 or MoS2/WS2 etc. Preliminary characterization of these heterostructures has shown that the interface between the two TMDs is atomically sharp that should allow for extremely efficient charge and energy transfer process between these layers. This also gives us a handle on understanding the interface states that are known to be associated with loss mechanisms in optoelectronic devices.

In the coming fiscal year, we will continue our efforts on the characterization of heteorstructures created using our novel growth technique and demonstrate a highly efficient TMD device with performance close to that predicted through theoretical calculations. We are on track to achieve our goal and the work is expected to lead to several high impact publications. Currently, we have published, 9 peer reviewed papers and the work has led to 5 invited talks at international conferences and 3 invited seminars at Universities in the US.

Future Work

The goals for FY16 are:

- CVD growth of vertical and lateral TMD hererostructures made from MoS2/MoSe2
- Correlated photo current and photoluminescence to understand charge and energy transfer processes at the interface of these hererostructures.
- Based on the measurements above, understand design principles for stacking 3 or more hererostructures with cascading energy levels to obtain high performance optoelectronic devices.

Conclusion

We will combine single atomic layers of MoS2 and MoSe2 to form the first of its kind, layered TMDC heterostructures that will enable us to establish the interfacial design rules, vital for the understanding, control and manipulation of the flow of charge and energy across the TMDC heterostructure interfaces.

The success of this proposed work promises to redefine the field of thin film optoelectronic devices that have tremendous advantages in their overall performance, form factor, flexibility and cost over existing thin film technologies based on Silicon.

Publications

Bilgin, , Liu, Vargas, Winchester, M. K. L. Man, Upmanyu, K. M. Dani, Gupta, Talapatra, A. D. Mohite, and Kar. Chemical Vapor Deposition Synthesized Atomically Thin Molybdenum Disulfide with Optoelectronic-Grade Crystalline Quality. 2015. ACS NANO. 9 (9): 8822.

Cummins, D. R., Martinez, Kappera, Voiry, Martinez-Garcia, Jasinski, D. a. n. Kelly, Chhowalla, A. D. Mohite, M. K. Sunkara, and Gupta. Catalytic Activity in Lithium-Treated Core-Shell MoOx/MoS2 Nanowires. 2015. JOURNAL OF PHYSICAL CHEMISTRY C. 119 (40): 22908.

Kappera, , Voiry, S. E. Yalcin, Branch, Gupta, A. D. Mohite, and Chhowalla. Phase-engineered low-resistance contacts for ultrathin MoS2 transistors (vol 13, pg 1128, 2014). 2014. NATURE MATERIALS. 13 (12).

Kappera, , Voiry, S. E. Yalcin, Jen, Acerce, S. o. l. Torrel, Branch, Lei, Chen, Najmaei, J. u. n. Lou, P. M. Ajayan, Gupta, A. D. Mohite, and Chhowalla. Metallic 1T phase source/drain electrodes for field effect transistors from chemical vapor deposited MoS2. 2014. APL MATERIALS. 2 (9).

Lei, , A. l. i. Sobhani, Wen, George, Wang, Huang, P. e. i. Dong, B. o. Li, Najmaei, Bellah, Gupta, A. D. Mohite, Ge, J. u. n. Lou, N. J. Halas, Vajtai, and Ajayan. Ternary CuIn7Se11 : Towards Ultra-Thin Layered Photodetectors and Photovoltaic Devices. 2014. ADVANCED MATERIALS. 26 (45): 7666.

Lei, S., L. Ge, S. Najamaei, A. George, R. Kappera, J. Lou, M. Chhowalla, H. Yamaguchi, G. Gupta, R. Vajtai, P. Ajayan, and A. Mohite. Evolution of the Electronic Band Structure and Efficient Photo-Detection in Atomic Layers of InSe. 2014. ACS NANO. 8 (2): 1263.

Voiry, , Mohite, and Chhowalla. Phase engineering of transition metal dichalcogenides. 2015. CHEMICAL SOCIETY REVIEWS. 44 (9): 2702.

Microstructure Based Continuum Process Modeling of Weapons Metals

Rodney J. Mccabe
20140630ER

Introduction

We will develop an engineering scale modeling capability that describes the evolution of microstructure, properties, and performance that accompany production processes of uranium weapons components. We will accomplish this by experimentally measuring and modeling the change in microstructure and properties that accompany thermal processes such as annealing and heat treating. This newly developed thermal processing evolution law will be coupled with our well established deformation based evolution law for uranium that describes the evolution of microstructure and properties accompanying mechanical processes such as rolling and forming. A novel aspect of this approach is that the microstructure and property evolution accompanying a mechanical deformation process will propagate into the model of a subsequent thermal process and vice versa. Thus, microstructure and property evolution will be tracked from the initial process through the final part. We will also develop a novel, computationally efficient representation of our evolution laws in order to overcome the computational challenges of implementing microstructure based evolution laws within engineering scale simulations. In addition, this new modeling capability will be validated using MaRIE-like experiments. Our deliverables will enable LANL to 1) gauge the properties of existing stockpile components, 2) analyze the sensitivity of manufacturing process variables, 3) examine alternative manufacturing processes resulting in similar microstructures and properties, and 4) directly assess the engineering performance of metal weapons parts in service.

Benefit to National Security Missions

Our deliverables fill a large gap in the processing/microstructure/property knowledge of weapons metals, an achievement that will have widespread impact on several National Security missions. Manufacturing of uranium and other metal weapons components traditionally relies on process control to ensure that parts have reproducible, desired performance. However, despite its importance, process control decisions do not involve the effect of the evolving microstructures and properties of these complex metals. Lacking this effect prevents the weapons complex from moving forward into process-aware manufacturing and product-based qualification.

For posterity, we will have an experimentally validated, computationally efficient microstructure based modeling capability. This capability is a long sought after tool for processing-aware manufacturing and engineering performance analysis. Within the project we intend to focus on the physics of the microstructure evolution of uranium during both deformation and thermal drives. The methods can be adapted to other weapons and non-weapons metals.

The innovative processing modeling framework developed will not be limited to only the cases and approaches we employ here. The continuum modeling platform will be adaptable to other regimes provided the microstructure based constitutive law can be developed. Validation of the developed models will ultimately be accomplished using MaRIE like experiments. This type of experiment is important in the science it will uncover, but also because it will drive the needs for improved in situ capabilities; temporal, spatial, and angular resolution; analysis and handling of large data sets; and forward modeling needs that will be desired with MaRIE.

Progress

Our objective is to develop a computationally efficient engineering scale modeling capability that describes the evolution of microstructure, properties, and performance that accompany production processes of weapons components. To accomplish this, the project consists of manufacturing operations, experimental characterization, and model and computational development. In the past 12 months, the research time has accomplished the following tasks:

- Specimens have been machined from uranium plates having undergone seven different rolling schedules (rolled in FY14).
- Recrystallization experiments have been performed on specimens from all seven different rolling schedules.
- The microstructures of specimens from all seven have been electron backscatter diffraction (EBSD) characterized in the as-rolled and recyrstallized conditions as well as characterization of the starting materials.
- Correlations between the as-deformed microstructure and recrystallized microstructure, particularly the texture evolution, have been experimentally determined for clock-rolled uranium and the results have been published (McCabe et. al., J. Nucl. Mat., 265 (2105) 189-195) and presented at the TMS 2014 annual conference.
- Uranium shapes have been formed from cross-rolled uranium (from FY14) with experimental measures of local strain for model validation.
- Modeling of uranium cross-rolling (from FY14) is finished and results will soon be submitted for publication (Zecevic et al., "Origin of texture formation in orthorhombic alpha-uranium under simple compression and rolling to high strains", J. Nucl. Mat. in preparation.
- Computationally efficient, spectral crystal plasticity for a surrogate material was successfully coupled with the implicit version of the commercial finite element package Abaqus. These results have been published (Zecevic et al., "A new implementation of the spectral crystal plasticity framework in implicit finite elements", Mech. of Mat., 84 (2015) 114-126)
- An efficient computational framework to model the mechanical processing operations has been implemented for surrogate materials using previously published data. Benchmarking of this framework is nearly complete; preliminary results were presented at the 2015 Mach Conference in Annapolis, MD, and finished results will soon be submitted for publication (Richards et al., "Acceleration of macroscale plasticity simulations using GPUs", in preparation). Integration of additional material models into the framework is underway.
- A toy model to visualize the effects of different recrystallization laws has been implemented, and is being used to identify the necessary parameters to develop physically realistic models of recrystallization.
- Based on experiments and the toy model, the foundation for using the output from our deformation model as the input for the recrystallization model has been established. The tasks necessary to modify the deformation model to account for the microstructure characteristics important for the recrystallization model have been laid out and modifications to the deformation model have begun.

Future Work

Our objective is to develop a computationally efficient engineering scale modeling capability that describes the evolution of microstructure, properties, and performance that accompany production processes of weapons components. To accomplish this, the project consists of manufacturing operations, experimental characterization, and model and computational development. Whereas, most of these efforts during the first 15 months of the project have been to develop the physically based models and computational tools, most of the efforts in the next 12 months concern model validation and improvement.

Tasks for the next 12 months will include:

- Machine, test, and characterize specimens for in situ neutron and X-ray diffraction studies at LANSCE and APS. These tests will simulate a complete thermo-mechanical processing mapping the microstructure evolution throughout a deformation and recrystallization step on individual samples.
- Form parts with experimental strain mapping from straight and clock rolled uranium that have been experimentally characterized and modeled through an entire mechanical and thermal processing. Characterize the microstructures of the formed parts.
- Finish analyzing the straight rolled electron backscatter data to quantitatively define the relationship between initial grain size and rolling reduction to final recrystallized grain size.
- Finish integration of additional material models into our computationally efficient framework. Develop spectral plasticity representation for uranium and test its validity against the visco-plastic self-consistent model we have been using to successfully model uranium.
- Finish making modifications to our deformation model to allow us to account for the microstructure characteristics important for the recrystallization model.
- Run modeling simulations equivalent to our three processing step validation experiments (rolling, forming, recrystallizing) and compare with experimental results

Conclusion

The overall technical goal is to develop a computationally efficient, deformation and thermal processing physics based modeling capability allowing for accurate prediction of microstructure, property, and performance evolution at the engineering level. This work will provide scientific understanding of the evolution of the defects that are the mechanisms of deformation and the driving force for thermally driven microstructure changes. The developed mod-

eling capability will allow for reliable modeling of metals processing and engineering performance in uranium and other complex metals. The computational tools developed will allow better physics to be added to larger simulations of components and engineering systems.

Publications

Ardeljan, , R. J. McCabe, I. J. Beyerlein, and Knezevic. Explicit incorporation of deformation twins into crystal plasticity finite element models. 2015. COMPUTER METHODS IN APPLIED MECHANICS AND ENGINEERING. 295: 396.

Knezevic, M., J. Crapps, I. J. Beyerlein, D. R. Coughlin, K. D. Clark, and R. J. McCabe. Anisotropic modeling of structural components using embedded crystal plasticity constructive laws within finite elements. To appear in International Journal of Mechanical Sciences.

Lebensohn, R. A., M. Zecevic, M. Knezevic, and R. J. McCabe. Average intragranular misorientation trends in polycrystalline materials predicted by a viscoplastic self-consistent approach. Acta Materialia.

McCabe, R. J., A. W. Richards, D. R. Coughlin, K. D. Clarke, I. J. Beyerlein, and M. Knezevic. Microstructure effects on the recrystallization of low-symmetry alpha-uranium. 2015. Journal of Nuclear Materials. 465: 189.

Zecevic, M., M. Knezevic, I. J. Beyerlein, and R. J. McCabe. Origin of texture formation in orthorhombic alpha-uranium under simple compression and rolling to high strains. Journal of Nuclear Materials.

Zecevic, M., R. J. McCabe, and M. Knezevic. A new implementation of the spectral crystal plasticity framework in implicit finite elements. 2015. Mechanics of Materials. 84: 114.

Solute and Microstructure Prediction during Processing (U)

Amy J. Clarke
20140639ER

Introduction

All metallic alloys experience solidification, which occurs over multiple length and time scales. Thus, achieving intended solidification structures in metallic alloys is key to achieving properties and performance. To predict solidification structural development, we must understand how solidification structure develops from the micro- to the macroscale. This can only be achieved through a coupled experimental and modeling campaign. Our goal is to make Los Alamos National Laboratory's macroscopic (or continuum engineering) scale casting simulation code, Truchas, microstructure-aware. Our work will combine direct observations of solidification in high-density metallic alloys at the micro- and macroscale using synchrotron x-ray and high-energy proton imaging, along with computational microstructural modeling, to permit the identification, development, and incorporation of important analytical expressions for structural development into Truchas. Our coupled experimental and modeling campaign will make unprecedented processing and microstructural linkages for high-density metallic alloys; it will also create the necessary infrastructure for future application to actinides.

Benefit to National Security Missions

We currently do not have experimentally informed casting or solidification microstructural development models at Los Alamos National Laboratory. While detailed microscale structure predictions over engineering length scales (i.e., centimeters) are still a distant goal, from this work first order approximations of structure at the continuum level will be attainable with current computational tools. Casting simulations have been performed at Los Alamos National Laboratory for over 20 years with casting codes based on continuum architecture that consists of coupled differential equations solved in a meshed environment. They perform well for fluid flow and macroscopic heat flow and are able to predict what temperature exists at any given cell. Nonetheless, continuum codes currently do not include the physics needed to capture non-continuum events that dictate the microstructure, such as pattern formation at the solidification front or the geometric form of a dendrite. Our coupling of in-situ characterization during processing with our materials and modeling expertise will enable unprecedented processing and microstructural linkages for high-density metallic alloys; it will also create the necessary infrastructure for future application to actinides. The integration of multiscale physics into a continuum, engineering-scale code for structural development is the critical link needed to perform process-aware manufacturing. Our proposed work will also highlight the need for advanced experimental and computational tools to extend our predictive capabilities to emerging manufacturing technologies, such as additive or in-situ fabrication.

Progress

We have performed in-situ casting mold filling and solidification experiments at pRad (the 800 MeV proton radiography facility at Los Alamos National Laboratory, LANL) to improve our understanding of alloy melt fluid flow and the role of thermal conditions on microstructural development during the casting process. We also performed initial in-situ x-ray imaging at Argonne National Laboratory's Advanced Photon Source (APS) to monitor dendritic microstructural development in an aluminum-silver alloy and subsequent chemical redistribution (homogenization) during iso-thermal holding at an elevated temperature. The casting experiments are particularly valuable for assessing larger length-scale solute segregation information and generating a range of microstructural characteristics for comparison with Truchas modeling. We have performed ex-situ microstructural (electron microscopy) and chemical (EDS, energy dispersive spectroscopy and MXRF (Macro X-Ray Fluorescence) examinations of the castings we produced at pRad. The measurements are ongoing for tin-bismuth and gold-zinc-aluminum alloy castings, and we are beginning to explore mechanical properties for selected

samples. We have also evaluated the deformation of aluminum-copper alloy samples made previously at APS to start linking microstructural development to mechanical performance, both experimentally and computationally. We also evaluated phase selection in gold-zinc-aluminum and bismuth-antimony alloys during solidification with HIPPO (High-Pressure-Preferred Orientation) at the Los Alamos Neutron Science Center (LANSCE) at LANL to help provide modeling inputs.

A flexible mathematical framework has been developed within Truchas, which can accept analytical models for solidification that produce predictions of final microstructural features. The next step, which is underway, is to incorporate solute information into the final predictions. Our modeling focus this year has been to treat the flow conditions that assume rapid solute mixing in the liquid and minimal diffusion in the solid. Our methodology of incorporating analytical expression into Truchas permits the rapid assessment of model applicability and systematic improvements.

Exploration of various micro-scale modeling schemes (i.e., phase-field, front tracking, and dynamic needle network (DNN)) has led us to two important conclusions. Phase-field simulations, in conjunction with experimental microstructure development, have helped to identify trouble areas for both analytical models and other types of modeling schemes. The combination of computational speed and good experimental matching of DNN for features such as primary dendrite spacing has made it the primary candidate for conducting simulations based upon Truchas outputs. Due to enhanced applicability to typical casting conditions, the micro-modeling focus has naturally shifted back to diffusion-limited, rather than kinetically-limited, growth conditions.

Future Work

The scope of work has changed due to continued uncertainty and reduction in budget allocation. While the end goal to make Truchas microstructure-aware has not changed, we have strengthened our focus on predicting dendritic microstructural evolution, especially in larger volumes relevant to casting, with comparisons to experimental microstructures and mechanical properties. We will focus less on homogenization, and more on dendritic microstructures produced by solidification. Essentially, we will perform dendritic microstructural predictions with Truchas and micro-scale models, evaluate solidification microstructures produced by in-situ and ex-situ micro- and macro-scale experiments for comparisons with modeling, and will explore the link to mechanical properties. Our end milestones will be the development of a process (casting) model that can predict microstructure, tested against local predictions made with microstructural modeling and experiments, and the demonstration of MaRIE-like experiments that follow solidification microstructural development to mechanical properties (i.e., certification-type experiments). We will not develop a micro-scale homogenization model or link homogenized microstructures to properties, but we will have performed preliminary in-situ homogenization experiments, identified suitable alloy(s) for follow-on studies, and have the modeling framework within Truchas.

For FY16, our primary goal will be to inform and validate solute and structure predictions from Truchas. We will also explore the link of solidification microstructural evolution to mechanical properties. To exploit opportunities for strengthening the structure models, we will also use thermal parameters from Truchas as boundary conditions for local micro/meso-scale modeling of microstructural development with other techniques for comparisons.

Conclusion

We will create a flexible computational framework for the multiscale prediction of high-density metallic alloys during solidification from the micro- to the macroscale by extending a continuum casting model (Truchas) to include fast, analytical models for microstructure. We will use proton imaging to experimentally measure macroscale phenomena and x-ray imaging to watch the evolution of key microstructural features, similar to those in actinides, in high-density alloys. Our experiments will allow us to identify the critical parameters needed for the prediction of microstructure in a casting with Truchas at a length scale never before accomplished.

In situ X-ray Imaging and Diffraction to Understand the Mechanics of Initiation Mechanisms in Explosive Single Crystals

Kyle J. Ramos
20140643ER

Introduction

The project is a joint experimental/theoretical investigation of the deformation mechanisms in the energetic molecular crystal (cyclotrimethylene trinitramine) RDX. The localization of mechanical deformation in explosives under shock compression has been linked to the on-set of chemical reactions and the initiation of detonation. New capabilities for real-time, in situ X-ray diffraction and imaging using the IMPULSE capability at the Advanced Photon Source will be employed to measure the evolution of the average lattice strain and spatially localized material failure in RDX single crystals during dynamic compression. These data will be interpreted and eventually predicted through the development of a single crystal plasticity model. The development of a validated, predictive thermomechanical model for RDX will enable us to model the response of more complex microstructures and defects at the completion of the project. The single crystal plasticity models will take as input existing data from the literature, in situ data from IMPULSE and the results of first principles electronic structure calculations of the orientation-dependent thermophysical properties of RDX. The use of first principles calculations are critical when we will model the high-pressure phase of RDX that cannot be recovered for characterization in the laboratory. The single crystal plasticity model will be validated via its implementation into a finite element simulation code from which we will compute diagnostics, including interface velocimetry and X-ray diffraction patterns that can be compared directly with in situ experiments.

The ability to measure the structure response of complex materials in the nanosecond time scales before they are destroyed during shock compression is a major innovation that this project will advance. Nevertheless, the integration of these measurements with theory and simulation that can rationalize and predict responses based on the activity of the underlying deformation mechanisms breaks new ground in shock physics.

Benefit to National Security Missions

Success in this project will motivate and guide technological development and further experimental work at the NNSA's Dynamic Compression Sector at the Advanced Photon Source and proposed facilities such as LANL's MaRIE.

The development of a mechanistic understanding of the response of energetic constituents to impact will provide the first framework for predicting the material conditions for initiation. This capability will significantly affect high explosive science at LANL and beyond and is critical to our national security mission. NNSA Advanced Simulation and Computing (ASC) and the Department of Defense (DoD) strongly support in situ measurements and emphasize the need for predictive materials models. In addition, new thermomechanical models and the ability to predict initiation are indispensable to the development of reduced sensitivity explosives for DoD and Department of Energy (DOE) insensitive munitions via particle and crystal engineering.

Progress

The research team made outstanding progress on all aspects of the project over the last 12 months. Significant advances in theory and simulation have been achieved and in situ X-ray diffraction experiments at the Advanced Photon Source (APS) have moved ahead. Details on specific technical advances are as follows.

Major contributions were made to a recently published review article on the elasticity of energetic molecular crystals [D. E. Hooks, K. J. Ramos, C. A. Bolme, and M. J. Cawkwell, Propellants Explosives Pyrotechnics, 40, 333 (2015)]. This review article allowed us to dissect the experimental protocols for measuring the elastic constants of brittle, low symmetry molecular crystals and how elastic tensors may be predicted by first principles or molecular dynamics simulations. Since accurate tensors of elastic constants are of critical importance to

modeling the mechanical response of explosives, this work satisfied major deliverables of the project and made a significant contribution to the scientific literature.

A new equation of state for alpha RDX was developed based on extremely accurate density functional theory calculations and quality literature data. We are currently making good progress on the development of an equation of state for the high pressure gamma polymorph of RDX that will allow us to model phase transformations in the material, and the tetragonal explosive PETN. A novel anisotropic constitutive model has been proposed, parameterized to available literature and calculated data, and implemented in the ABAQUS finite element simulation package. Continuum-scale simulations of impact problems in RDX single crystals, using known systems for plastic flow, are currently underway.

A state-of-the-art single crystal plasticity model was developed and implemented in a 1-D hydrocode. Small-scale simulations using these methods highlighted deficiencies in our understanding of dislocation-mediated plasticity in RDX. These gaps in our knowledge will be addressed with new, carefully designed plate impact experiments.

Code was developed for simulating X-ray diffraction patterns with the beam parameters used at the APS. We have tested the code using datasets obtained from earlier large-scale molecular dynamics simulations.

We performed large-scale atomistic and molecular dynamics simulations of the core structure of a dislocation in alpha RDX. We hope these simulations will allow us to better understand the slip in molecular crystals at a fundamental level.

Our 'anomalous hardening' model for the unusual shock response of specific orientations of RDX single crystals to shock was reevaluated. By reanalyzing data from large-scale molecular dynamics simulations we discovered a previously unknown monoclinic phase of RDX that can only be accessed by dynamic compression. Based on unit cell parameters obtained from density functional theory calculations and simulated X-ray diffraction patterns, we will perform a series of in situ X-ray diffraction experiments at the APS during the next run cycle to confirm the presence of the hypothetical new phase.

The first in situ diffraction patterns from explosives were recorded during impact at the APS. The hardware for the X-ray diffraction was designed and successfully implemented on the IMPact System for Ultrafast Synchrotron Experiments (IMPULSE). Single crystal RDX samples were prepared for impact on {210} and {021}-orientations to test our 'anomalous hardening' model and subsequent discovering of a monoclinic phase as described in item six above. Four frames of data were captured per experiment with very high signal-to-noise and detailed the deformation process.

Next steps include analyzing the X-ray diffraction patterns and comparing them to results from recently developed finite element model and X-ray diffraction simulations of the crystalline deformation during shock loading. The analysis will enable the extraction of previously unattainable equation-of-state information and the development and validation of an anisotropic plasticity model crucial for predicting thermomechanical localization of deformation and associated heating. Further experiments have already been designed and built and will be completed in July.

Future Work

Our goals for the third year of the project include:

- Continued application of shear stress to dislocations in alpha-RDX in atomistic simulations to evaluate barriers to dislocation motion. These data will inform the generation of single crystal plasticity models.
- Continued development of an anisotropic equation of state, based on our new formalism, for gamma-RDX and/or other potential phases that are discovered in atomisitic simulations and XRD (X-ray diffraction) experiments.
- Perform plate impact experiments for phase transformation investigation using XRD diagnostic.
- Compare XRD experimental results with computed diagnostic from simulations.
- Apply the new models in the simulation of more complex microstructures

Conclusion

We will deliver a validated, anistropic thermomechanical model for the response of single crystals of the explosive RDX to shock compression. We shall construct anisotropic, temperature-dependent equation of state for RDX based on experiment and theory. The equation of state will be employed in a single crystal plasticity model that incorporates deformation mechanisms and phase transformations that have been observed experimentally. Rates for the deformation mechanisms will be parameterized to experimental data. The ability to model deformation processes in explosives pertains directly to explosive initiation and safety, both of which are of considerable importance to ongoing NNSA and DoD missions.

Publications

Hooks, D. E., K. J. Ramos, C. A. Bolme, and M. J. Cawkwell. Elasticity of Crystalline Molecular Explosives. 2015. PROPELLANTS EXPLOSIVES PYROTECHNICS. 40 (3): 333.

Enabling Mesoscale Science: Nonlocal Dislocation-Flux Crystal Plasticity Under Shock Loading Conditions

Darby J. Luscher
20140645ER

Introduction

Our team will develop and implement a novel physics-based model for dislocation-mediated single crystal plasticity, applicable under shock loading regimes characterized by large deformation, deformation rate, and high pressure and temperature. This endeavor is motivated by challenging mesoscale problems such as damage nucleation at material interfaces. The novelty of the proposed formulation stems mainly from its explicit representation of dislocation flow through the crystal lattice, coupled with a detailed accounting for elastic interactions between dislocations. These features establish a new paradigm for crystal plasticity, which is fundamentally different from existing models in that arena.

Specifically, our single crystal plasticity model will include (1) a proper treatment of the evolution of dislocation fields, built upon balance laws governing their transport through the lattice, (2) a physically consistent representation of long-range nonlocal interactions of dislocations, and their role in resisting (or enhancing) slip, (3) kinetics models for (a) dislocation nucleation, multiplication, and annihilation, consistent with large deformation rates and for (b) dislocation velocity, accounting for phonon-drag and inertial effects acting on dislocations, and (4) boundary conditions that have a direct physical interpretation. Our work will deliver (1) a coupled-physics, mixed-field implementation of the theory, amenable to numerical simulations of polycrystal response, and (2) novel simulations of dislocation pile-up leading to damage nucleation in copper polycrystals under shock loading.

High-risk aspects are numerical issues related to the computational implementation of mixed-field physics calculations, development of models for computing stress fields in the vicinity of dislocations, and the aggressive schedule of code implementations.

Benefit to National Security Missions

The length and time scales relevant in simulations of weapon performance motivate the development of macroscale models that capture the essence of dominant physical processes at finer scales. Examples include plastic slip, void nucleation, growth, and coalescence, phase transformation, and twinning. These physical processes depend critically upon microstructural details, such as grain morphology, orientation distributions, grain boundary characteristics, and defects. The development of macroscale models reflecting these processes demands an understanding of the underlying physics, which is often gained through experiment. Currently available diagnostic measurements for shock-regime experiments are often ambiguous in identifying specific mechanisms of these processes. For example, measurements of free surface velocity (VISAR) require speculative inference to draw conclusions about damage nucleation kinetics.

Development of new in-situ diagnostic technologies, for example, through MaRIE, promises to provide detailed data associated with these im-portant physical processes. In many cases, such newly available data would not be amenable to direct comparison with results obtained using existing models. The connection between microstructural processes and simulations of weapon performance demands insight from mesoscale modeling, to provide more detailed interpretation of currently available measurements and to be predictive on a commensurate level of resolution with anticipated diagnostics.

Our research will deliver a mesoscale simulation capability implemented into an ASC LAP code. These simulation tools are expected to deliver on the promise of nonlocal modeling strategies, namely the ability to predict scale-dependent material response as part of the solution of a multi-physics problem, without requiring any length-scale parameters to be specified as inputs.

Progress

In FY15, we continued to develop the prototype code and apply this code to solving relevant boundary value problems. The extensions of the prototype code include a translation from the relatively slow running python source code into fortran code that typically runs two orders of magnitude faster. In several cases, numerical testing revealed deficiencies in the implementation scheme that were subsequently resolved. At this point, the 1D prototype code is relatively mature and the overall implementation strategy has stabilized.

Theoretical development continued in FY15, focusing on constitutive relations; specifically, we have compared the competing influence of various dislocation evolution terms. This work has led to an increased understanding of the role of dislocation nucleation, multiplication, annihilation, and motion within the context of shock loading.

We modeled the response of single-crystal plate impact problems with various combinations of simulation parameters in order to help identify where the computational algorithms should be improved. We have demonstrated application of the theory to a notional interface problem where dislocations are unable to slip across an explicit interface within the problem. We have also developed a test problem that explores the notion of mixed-domain strategy where the DMB problem is solved everywhere throughout the problem domain, but the CDT and DDC problem is only solved near interfaces that would resist dislocation motion.

The overall theoretical framework and application to three plate impact scenarios has been included in a manuscript accepted for publication in the International Journal of Plasticity. The reviews for this publication were favorable reinforcing the timeliness of this coordinated multi-physics approach to dislocation mediated plasticity for shock loading environments. The numerical implementation and an associated parameter sensitivity study were included in a manuscript submitted for publication. Two invited lectures have been given based on this work in FY15.

We initiated the multi-dimensional implementation of each sub-problem into an Advanced Simulation and Computing (ASC) Lagrangian Applications Project (LAP) code. The DMB problem comprises a solution scheme to satisfy conservation of momentum and a constitutive integration scheme to update crystal plasticity calculations. Our DMB problem will leverage the existing solver within FLAG. Implementation of the crystal plasticity update has been initiated via the creation of a “node” within the database hierarchy of FLAG. The subroutines to evaluate the constitutive model are being ported to this FLAG node. The CDT problem will be solved within FLAG by leveraging the advection schemes within FLAG to remap solution variables for arbitrary Lagrange/Eulerian (ALE) calculations. Identifying the solution strategy for the DDC problem within FLAG continues. We anticipate that these tasks will be preliminarily completed by the end of FY15 and will leave us in good position to successfully achieve FY16 stage gate.

Future Work

In FY16 we will continue to apply the prototype 1D code to simulations of various plate impact scenarios. These simulations are intended to challenge the numerical implementation and reveal where improvements to the reliability of the coupling and integration schemes can be made. Also, we will develop an improved kinematic theory for solving the DDC problem. The original FY15 goal of multi-dimensional implementation of each sub-problem into an Advanced Simulation and Computing (ASC) Lagrangian Applications Project (LAP) code will be completed during FY16. Full coupling of these sub-problems will begin toward the latter part of FY16.

Stage Gate 3: Tested implementation of each sub-problem into ASC code. A demonstration of the full coupling of these sub-problems to a 3D shock loading problem.

Conclusion

We will deliver simulation tools built around the mesoscale physics-based nonlocal models of plasticity developed by our research that will deliver on the promise of nonlocal modeling strategies, namely the ability to predict scale-dependent material response as part of the solution of a multiphysics problem, without requiring any length-scale parameters to be specified as inputs. Our research will have significant impact to LANL, the DOE’s Office of Science, and the U.S., by virtue of its critical role in enabling mesoscale science needed for modeling nucleation and evolution of defects at material interfaces.

Publications

Luscher, D., J. Mayeur, H. Mourad, A. Hunter, and M. Kenamond. Coupling continuum dislocation transport with crystal plasticity for application to shock loading conditions. 2016. International Journal of Plasticity. 76: 111.

Embedded Fiber Sensor Approach for Dynamic Pressure and Temperature Measurements in Explosives

George Rodriguez
20140650ER

Introduction

From the standpoint of high explosive (HE) engineering and science, there is a critical need across the Departments of Energy and Defense for in-situ probes that can continuously measure thermodynamic state variables (pressure, temperature, and detonation velocity) under conditions of extremes. To date, very few approaches exist that are capable of accurately measuring state variables independently without referring to a model or inferring from other parameters such as velocity or density. This project will use an embedded fiber optic approach that places sensors at the point where the measurements need to be made, and makes it possible to measure gradients from violent HE chemical reactions if the sensors can be distributed in the HE. Furthermore, the sensors need to be impervious to harsh environments where HE reaction chemistry can produce extreme temperature and pressure in conditions from slow burn cookoff to detonation. Under this project, we will establish a new Laboratory diagnostic capability in high pressure science and thermometry. The diagnostic is transformative, because it will provide the Laboratory the ability to measure conditions of HE burn, deflagration, and detonation propagation. The diagnostic is intimately tied to Laboratory models for fundamental material inputs that initialize HE equation-of-state models (EOS), reaction rates, and by-product EOS for predictive HE science. The probe is indifferent to material type, and the diagnostic should be applicable to inert materials (metals, plastics, liquids, etc.) where internal conditions are often impossible do diagnose with surface limited techniques. In this project, we focus on violent HE reactive conditions because of its complex thermodynamic behavior that challenges science models linking thermal explosion and detonation. The data resulting from from this project will bound critical HE initiation models relevant to Laboratory mission and put into place a baseline diagnostic for pressure and temperature of materials in extremes.

Benefit to National Security Missions

The project relevance is intimately tied to new diagnostic capability for the Laboratory's core mission activities that include high explosive (HE) campaign science, weapons surety and engineering, explosives chemistry and equation-of-state, initiation systems, and others that will immediately benefit Department of Energy and Department of Defense programs in HE science, materials dynamics, and surety. The diagnostic probe developed under this project will yield dynamic measurements of pressure and temperature conditions in controlled thermal explosions with secondary explosives. The experimental information will advance the Laboratory's understanding of explosives by providing validation data needed for reactive explosive models. The in-situ pressure and temperature probe being developed is clearly aligned with Laboratory Mission relevance including Matter in Extremes call Topical Area 3: Diagnostics to Measure Temperature, Pressure (Stress), Strain, Velocity, and their Gradients. Mission relevance to Nuclear Weapons Programs in performance validation for Directed Stockpile Work, Surety, and Campaign Science is identified because the project develops a desirable sensor diagnostic capability currently not available. It is expected that other agencies involved in high explosive burn reactive flows (i.e., NASA) would be interested in the technology as well.

Progress

In FY15 we successfully completed our pressure-only based measurements in thermal explosion cook-off experiments comparing response between PBX9501 and PBX9502. We related reaction violence to pressure response in these secondary explosives. Reaction violence of a thermal explosion is determined by the energy release rate of the explosive and the coupling of that energy to the case and surroundings. For the HMX (PBX9501) and TATB (PBX9502) based secondary high explosives studied, we have observed that temperature controls the time to explosion and pres-

sure controls the final energy release rate subsequent to ignition. Pressure measurements in the thermal explosion regime have been notoriously difficult to make due to the extreme rise in temperature which is also occurring during a thermal explosion. We utilized several different pressure measurement techniques for several different secondary high explosives. These techniques include commercially available piezoelectric and piezoresistive sensors which we have utilized in the low pressure (sub 30 MPa) range of PBX9502 thermal explosions, and fiber Bragg grating sensors for the higher pressure range (up to GPa) for PBX9501 and PBX9502 experiments. Simultaneous x-ray radiography measurements of burn velocity were also made, and correlations between pressure, burn velocity, and reaction violence studied.

Design modifications to our pressure-only fiber Bragg instrumentation were completed to accommodate the extraction of pressure and temperature independently with a single fiber Bragg grating sensor. The modifications included the switch over of the instrument from a design that was optically insensitive to fiber light polarization to one that is polarization dependent. This required all optical components in the system to be exchanged for polarization based encoded illumination and detection, including the fiber Bragg grating sensor. By using polarization encoded pulses to interrogate the sensor, the temperature-pressure extraction method relies on the polarization mode dispersion properties of fiber (i.e, both polarizations propagate thru the fiber system but because of the difference in the speed of light between each mode, a difference in response of the fiber Bragg grating sensor yields a difference in time-delay between modes). We use polarization mode dispersion to simultaneously detect the pressure and temperature while monitoring the polarization mode dispersion time-delay to yield a set of two measurements that can only be satisfied by a unique combination of pressure and temperature. Our first experimental tests of these temperature-pressure based HE thermal explosion measurements are to be made in late summer of 2015.

Results from our fiber Bragg grating based sensor development and instrumentation for high-speed pressure diagnostics were published in the the peer-reviewed journal Optics Express ("Coherent Pulse Interrogation System for Fiber Bragg Grating Sensing of Strain and pressure in Dynamic Extremes of Materials, Opt. Express Vol. 23, 014219 (2015)), and a invited SPIE conference proceedings paper was also published ("Insight into Fiber Bragg Sensor response at 100 MHZ Interrogation Rates Under Various Dynamic Loading Conditions," SPIE Vol. 9480, 948004 (2015)). The results showing details of the pressure response differences between PBX9501 and PBX9502 were also presented this summer at the 2015 American Physical Society's topical conference on Shock Compression of Condensed Matter ("Relationship Between Pressure and Reaction Violence in Thermal Explosions," Paper # K3.00001). We are following up the presentation of this work with a peer reviewed journal publication.

Future Work

In FY16, we will complete the our studies of simultaneous temperature and pressure extraction in the thermal response of the HMX based PBX9501 explosive and of the TATB based insensitive high explosive PBX9502. After these studies, the plan is to switch to elongated rate sticks of high explosives (PBX9501 and PBX 9502) where initial burn is followed by the sub-sonic burn regime of deflagration before crossover to full detonation. Recording of deflagration pressure and temperature histories will be attempted with pressures expected to eventually exceed the maximum range available with fused silica based fiber optic Bragg sensors when reaching full detonation pressures. Nonetheless, the build-up of pressure and temperature in the deflagration regime is of valuable interest in understanding the crossover from low velocity convective burn to pressures at high sub-sonic speeds.

Conclusion

The project will yield a field tested rack-mounted portable diagnostic detection system for simultaneous dynamic pressure and temperature sensing for explosive burn, blast waves, and detonation physics. This system will be a first-of-a-kind embedded probe for measuring dynamic pressure and temperature for a variety of extreme environments including shocked samples, deflagration-to-detonation transition and high explosive cookoff, and other experiments. We expect a diagnostic that will be capable of measuring dynamic events (nanosecond time scale) of pressure up to 100 kilobar and temperature up to 1000 degrees Celsius.

Publications

Rodriguez, G., M. Jaime, C. H. Mielke, F. F. Balakirev, A. Azad, R. L. Sandberg, B. Marshall, B. M. La Lone, B. F. Henson, L. Smilowitz, M. Marr-Lyon, and T. Sandoval. Insight into fiber Bragg sensor response at 100 MHz interrogation rates under various dynamic loading conditions. 2015. In 2015 SPIE International Society for Optics and Photonics Defense, Security, and Sensing Conference: Fiber Optic Sensor and Application XII. (Baltimore, 20-24 Apr. 2015). Vol. 9480, p. 948004. Bellingham: SPIE.

Rodriguez, G., M. Jaime, F. F. Balakirev, C. H. Mielke, A. Azad, B. Marshall, B. M. Lalone, B. H. Henson, and L. Smilowitz. Coherent pulse interrogation system for

fiber Bragg grating sensing of strain and pressure in dynamic extremes of materials. 2015. Optics Express. 23 (11): 14219.

Smilowitz, L., B. F. Henson, G. Rodriguez, D. Remelius, E. Baca, D. Oschwald, and N. Suvorova. Relationship between pressure and reaction violence in thermal explosions. To appear in Journal of Physics Conference Series.

Smilowitz, L., B. Henson, G. Rodriguez, R. Sandberg, M. Holmes, A. Novak, E. Baca, and D. Oschwald. Following reaction progress from thermal decomposition to ignition and internal burning. To appear in Proceedings of the 15th International Detonation Symposium. (San Francisco, 13-18 Jul. 2014).

Thin-Film Heat Switch for Active Thermal Management of CubeSat Payloads

Alexander H. Mueller
20150375ER

Introduction

Satellites are exposed to a complex thermal environment: external heat loads change rapidly between solar exposure and eclipse (Fig. 1a), and internal heat loads are dictated by the operation of electronic payloads1. While heat is most efficiently dissipated from the satellite during eclipsed ("cold") periods, payload operation may follow different patterns as dictated by the mission. The resulting thermal management problems are magnified in small form factor CubeSats that have limited space to move, store, and release thermal energy.

The goal of this project is to fabricate the next generation heat switch and demonstrate its performance in a satellite environment. Starting from our existing device and modeling capabilities, we will scale up the heat switch area and improve the thermal conduction ratio between the "on" and "off" states. The new heat switch will then be integrated with a CubeSat thermal management system to maintain a nbatteryu pack at optimal operating temperature using the batteries own waste heat. If successful, the heat switch will be tested to General Environmental Verification Standards (GEVS) in anticipation of a possible CubeSat launch scheduled for late 2016.

Development of this active and compact thermal management system will allow for a denser packing of payloads on cubesats, and after proven performance, full size satellites. After development and production, this technology can be applied to terrestrial applications such as industrial waste heat management and concentration, thermal regulation of buildings, and electronic component cooling in consumer electronics.

Benefit to National Security Missions

Success in this project will advance the utility of cubesats and have future applications in the thermal management of full size satellites. These platforms are important in our nation's remote sensing, information collecting, and communication missions in support of nuclear non-proliferation, and intelligence missions. Future application in waste heat capture and thermal regulation of buildings extends the relevance of this research to energy security and environmental stewardship missions.

Progress

This LDRD project is developing an active thermal transfer technology to maintain optimal temperatures of cubesat electronic components. The initial component for demonstration of the integrated device was to be a power amplifier, however the research team decided that maintaining a Li-ion battery pack at optimal charging and discharging temperatures would be a more general, less mission-specific application whose demonstration would have higher impact in the community. This required an increase in the active area of the device to 7.5 sq.in., and a more complex geometry involving a phase change material (PCM) for thermal storage that would be sandwiched between two heat switches capable of controlling the flow of heat into and out of the PCM.

The team successfully demonstrated the scale up (by 50x from previous devices) of the heat switch device and the fabrication of the PCM layer in time for the first mid-year review of the project. The large area heat switch was fabricated from photolithographically pattered Ti/Au electrode on sapphire wafer a planar copper electrode and 3M Novec 7500 dielectric fluid in between. The thermal transport properties of the heat switch were demonstrated and shown to be capable of a rapidly changing its thermal conduction coefficient in a tunable manner for differing heat loads. The thermal storage layer between the two heat switches was assembled by melt casting a commercial PCM into a mold formed by the planar copper electrodes. Several thermistors were embedded into the PCM for measuring and controlling the heat flows during operation. The PCM was shown to be able to store 2 kJ of heat in a 35 ml volume while

maintaining an overall temperature near 25°C. The material accomplishes this by undergoing a solid-solid phase transition that absorbs thermal energy upon heating above 25 oC and will subsequently release this heat upon cooling below 12 oC due to the reverse phase transition. The device will use the stored heat in anticipation of charging the batteries as soon as the satellite moves out of the eclipse part of its orbit. To do so, the heat switch is activated to moving heat from the PCM to the battery pack so that the battery temperature is optimal for rapidly accepting charge from the solar panels as soon as they are illuminated. This new mode of operation makes better use of the existing power and enables advanced payload capabilities.

Currently a test frame for the integrated PCM / heat switch device with the battery pack is being fabricated. This first prototype will be tested in an environmental chamber that is capable of simulating the thermal environment that the assembly will be exposed to in space. The team is awaiting delivery of the battery charger in order to simulate the entire coordinated cycle of charging and discharging the batteries during orbit. The cycle consists of capturing the heat generated during discharge of the batteries in the illuminated (hot) part of the orbit in the PCM using the heat switch to mediate the heat transfer. This heat will be stored in the PCM during the eclipse (cold) cycle. Once the satellite moves towards the end its the eclipsed position, the stored heat will be used to increase the batteries temperature in anticipation of charging immediately upon leaving eclipse as the solar panels are illuminated. We anticipate testing the first prototype in the environmental chamber at end FY15 or early FY16.

Future Work

Project goals for FY 16 are to integrate the heat switch, phase change material (thermal storage) and battery pack into one monolithic device. This device will be tested in an environmental chamber and subjected to GEVS testing. Upon completion of testing, a revised device will be assembled into a cubesat housing.

Project goals for FY15 will be to fabricate a large area (25 cm2) electrohydrodynamic (EHD) heat switch and evaluate its performance. Once the operational parameters and performance are determined we will refine the design in order to reach the 150 W/ 100cm2 heat transfer rate necessary for integration with a cubesat battery pack. This will involve iterative micro-fabrication of electrode geometries and investigation of stacked serial and parallel configurations.

Conclusion

We expect to develop an active, compact thermal management system capable of moving 150W / 100cm^2 of waste heat into a thermal storage medium. If successful, the system will undergo NASA standard reliability testing and be deployed on a cubesat scheduled for future launch. Development of such a system will allow for increased cubesat payload densities and higher operational duty cycles, and thus increase the utility of the cubesat's sensing and communication hardware.

Sub-Grid Meso-Scale Model for Twinning and Slip Processes

Curt A. Bronkhorst
20150431ER

Introduction

Plastic deformation in metallic materials occurs by two physical processes - dislocation motion (slip) and mechanical twinning. Representing plasticity by slip processes is computationally more straightforward since dislocations are very small (comparable to atomic length scales) relative to most computational cells used in problems requiring models for plastic deformation. This is true even when modeling single crystals explicitly. Mechanical twinning is a mechanism which physically spans an entire single crystal and forms a plate-like morphology. The formation of these plate-like structures during deformation transforms the nature of the material microstructure. These plate like structures have been impossible to represent numerically within single crystal models within traditional finite element codes since they are many times larger than a single computational cell. Their representation has been limited to homogenized theories which do not model microstructures or highly resolved phase-field theory which are extremely expensive computationally. This project offers a new technique to explicitly represent the morphological transformation due to mechanical twinning within polycrystal plasticity models. This will be a transforming development which will allow us to directly study both slip and twinning processes computationally under general 3D loading conditions. If successful, this work will allow us to directly study all deformation involving both plastic mechanisms and more accurately quantify structural evolution of materials under dynamic loading conditions. Under these conditions, mechanical twinning is generally more prominent and is believe to contribute substantially to shock hardening in strategic materials.

Benefit to National Security Missions

Much of our present weapon assessment and certification strategy relies upon numerical simulation of the shock and dynamic deformation behavior of metallic materials. At present, this deformation behavior is represented by highly phenomenological equations with only notional representation of complex physical processes leading to tenuous quantitative accuracy. In addition, this highly phenomenological material modeling strategy leads to numerical difficulties under certain loading conditions. At present, these models completely ignore the physical process of twinning on the shock hardening of metallic materials and also the impact that twinning has upon the structural evolution of materials and its impact upon their damage and failure response. This project will capitalize on LANL's expertise in plasticity modeling and begin to develop the meso-scale modeling tools to allow us to begin to quantitatively compute both dislocation slip and twinning processes in a way which is structurally accurate and allow us to quantify the influence of both of these processes on the way in which it changes under dynamic loading conditions. These developments can be used directly in weapons calculations in the future (selected regions of interest) or used to motivate the proper high length scale models to enable representation of slip and twinning together in a physically accurate way across the entire weapons system.

Progress

The new numerical finite element which includes an embedded region of additional deformation within a planar region of finite thickness has been completed. Implementation of this new numerical tool has been performed in two-dimensions within a user-element subroutine within ABAQUS. This numerical tool is specifically being used in this project to represent the explicit deformation mechanism of mechanical twinning which exhibits planar, laminar topology within individual single crystals of metallic and organic crystalline material. This numerical technique offers the opportunity to finally represent this deformation mechanism explicitly. The element has been successfully tested using an elasto-viscoplastic material model under dynamic loading conditions using a macroscale continuum model. These are the same loading conditions of interest to this project. The new technique has demonstrated adequate

numerical robustness under these conditions.

Integration of a finite deformation model for the viscoplastic deformation of single crystal titanium will begin in the fourth quarter of this year. Currently there is a difference in the strain measures used within the single crystal model and the embedded region finite element under finite strain conditions. Changes in the measure of strain and the variables used to represent the kinematics will be changed within the embedded region finite element to be consistent with that used within the single crystal model to be based upon the deformation gradient experienced locally within the element. This will facilitate the merging of the two currently separate subroutines into a single user element subroutine containing the model of the single crystal.

Implementation of a model for twin nucleation and growth within the single crystal model code is underway. When completed, the single crystal model will be capable of representing thermally activated based dislocation slip process as well as the nucleation and growth of mechanical twinning based upon the power law representation of the rate of twin growth. The twin nucleation model is based upon the mechanism of partial dislocation accumulation at a grain boundary providing the driving force. Our first mechanical problem to exercise the above-mentioned tools will be a simple two-dimensional periodic bi-crystal system allowing for twin nucleation and growth within a single row of computational cells. Differing orientation relationship between the two crystals will allow for probing of the driving force for twin propagation. Simple shear loading conditions will be applied to this simple boundary value problem to properly exercise the new numerical tool for robustness. In addition, we will also probe the physics of nucleation and growth of a single twin within this simple system. Bi-crystal combinations of interest as defined by the experiments will also be easily examined.

High purity polycrystalline titanium has been acquired for this project and a procedure for combined cold-rolling and heat-treatment to achieve a target equiaxed grain size of 50 microns has been developed. This is a grain size which is larger than traditionally achieved with high purity titanium to facilitate detailed examination of individual twin regions. A matrix of mechanical experiments has been defined for the 50 micron grain size titanium. The variables in the experimental component of this project include strain rate (0.1/s, 1.0/s, 100/s, and 2000/s), strain (total strains of 0.01, 0.02, and 0.05), and the three principal plate directions. All experiments will be conducted at an initial temperature of 20 C. Execution of these experiments is underway. Once completed, in addition to the mechanical behavior data which will be used by the single crystal model, metallographic EBSD characterization will be performed on the deformed samples to characterize the statistics of twin formation in this material. These experimentally results will define specific grain boundaries of interest which can be explore computationally with the above-mentioned model and embedded element.

Future Work

The anticipated tasks and accomplishment goals for this project in fiscal year 2016 are as follows:

- Develop the sub-grid twinning model within the framework of the existing single crystal model for slip based plastic processes. Consistency of strain and kinematic quantities between the sub-grid and crystal model will be developed. This step will be completed by mid-second year with implementation to follow.

- Develop and implement the analytical nucleation criteria for the initiation of twin lamellae within the ABAQUS code. We anticipate the development of the nucleation model to be completed in the first year and its implementation in the second year together with twin growth.

- Develop the twin growth model for expansion of the laminate twin(s) with deformation. This model will be completed early in year two and will be coupled with the nucleation model and sub-grid code. Bi-crystal calculations will begin in year two to test numerical stability and begin to test the nucleation and growth criteria for growth of twins under simple shear conditions.

- Demonstrate the feasibility of the newly developed model by performing polycrystal simulations of dynamic experiments conducted on high purity Ti and comparing results to the new experiments and quantitative metallographic information. A test plan has been developed and will be executed throughout the duration of this project. We will draw upon these experimental results in the simulations we choose to focus upon.

Conclusion

This project will develop the numerical element to represent the morphological deformation of mechanical twinning in single crystal metallic materials. The kinetic and kinematic theory to represent the mechanism of twinning will be developed and taken from existing work. The theory will be coupled with the developments of the new numerical element. This development will be coupled with existing theory for dislocation slip processes. This work will be coupled with experimental data for HCP materials. This is exciting work and is anticipated to produce several publications. This will also allow us to institutionally

broaden our computational material science capability.

Publications

Mourad, H. M., and C. A. Bronkhorst. Finite Element Simulations of Dynamic Shear Localization in Elasto-Viscroplastic Solids under Adiabatic Conditions. Presented at U. S. National Congress of Computational Mechanics. (San Diego, 26-30 July, 2015).

Higher Order Spin Noise Spectroscopy: From Foundation of Quantum Mechanics to Applications

Nikolai Sinitsyn
20150504ER

Introduction

Complete information about an interacting system is contained in the full set of correlators of its variables. However, one of the central results in statistical physics, called the fluctuation-dissipation theorem tells us that information provided by standard experimental measurement tools (e.g. conductivity, susceptibilities, or pump-probe experiments) is intrinsically limited: Accessible linear response characteristics are equivalent to measurements of only 2nd order correlators taken at thermodynamic equilibrium. Our main idea is that Spin Noise Spectroscopy, an optical technique pioneered at LANL, opens a unique opportunity to escape from the constraints of the fluctuation-dissipation theorem and measure higher-order correlators, which we will use to:

- characterize decoherence mechanisms in solid state qubits made of InGaAs quantum dots,
- reveal interactions and disorder characteristics of conducting electrons in semiconductors,
- explore spins entanglement in atomic gases and test quantum mechanics at new scales.

Studies of higher-order spin correlations will constitute a significant advance in the field of quantum measurement science. We will achieve the most precise understanding of the physics of a nuclear spin bath, determine whether macroscopic systems of ~109 interacting spins can still exhibit quantum properties that cannot be found in classical physics, and obtain qualitatively new information about many-body quantum electron interactions.

Benefit to National Security Missions

This project will build capabilities in the novel measurement methods that enable new scientific discovery at LANL. It is based on recent technological advancements that use the large data storage and manipulation capabilities. Until very recently this technology simply did not exist. The proposal will advance new Laboratory capabilities that underpin a wide variety of Laboratory missions including Nanotechnology and Quantum Information Science. Demonstration of new effects by measurements of higher order correlators in spin systems will generate worldwide attention and will form a robust platform for a mesoscopic spintronics program at LANL. The present project will lay the groundwork for future proposals for external funding to address national problems, including energy efficient applications (DOE). The team will work with A.Taylor to develop a BES Materials Science funded project.

Progress

Project is going well and on track. The team has already published one combined experimental-theoretical paper in Scientific Reports about the invention of the “Cross-Correlation Spectroscopy” - the technique that allows measurements of new types of spin correlators in condensed matter systems.

Several work are currently either submitted or at the final stage of preparation. This includes:

- PI (Nikolai Sinitsyn) with a CNLS postdoc - Dr. Fuxiang Li have collaborated with the group of experimentalists in Germany, lead by Prof. Jonathan Finley at Technische Universitat, Munchen. We already prepared a LA-UR internal LANL publication that reported the discovery of three-stage decoherence mechanisms of a solid state qubits. Article is currently submitted to Nature Physics.
- All members of the project have performed research (both measurements and theory) on the 4th order spin correlations for hot atomic vapors in external noisy magnetic fields. We are at the stage of working on the final experiment that would generate figures of good quality for publication.
- PI and Fuxiang Li have been working on a very complex fundamental theory of higher order spin corre-

lators of conducting electrons and constraints imposed by higher order fluctuation relations on such correlations. We already obtain main results and are working currently on the final version of the article.

- Dr. Scott Crooker (CI) has performed test measurements of the 4th order correlator of spins in hole doped quantum dots in GaAs. Despite observing a complex signal, our analysis revealed that it is strongly affected by nonlinearities in the detector, so that alternative approaches are needed. PI and Fuxiang Li have proposed a different type of correlator that is expected to be free of the problems observed by experimentalists. However, this requires the change in the setup, which will take time (about 1/2 year) to make but it is totally within our capabilities.

Future Work

Experimental studies will focus on measuring third-order correlator of the solid state spin qubit realized in InGaAs quantum dots. These spins are entangled with a dense bath of ~105 nuclear spins. Measurements of 3rd order correlators should provide considerable new insight in physics of this interaction. They will allow us to use our the central spin qubit as a nanoscale probe of local nuclear spin dynamics. Recently, we discovered that these correlators can be used to probe fundamental questions of quantum mechanics. Our team already obtained preliminary experimental results in this direction.

Theoretically, we will focus on higher order correlators of conduction electrons. We will explore the universality of their behavior due to thermodynamic constraints described by the higher order fluctuation dissipation relations. We will identify a small number of independent parameters that control the shape of higher order correlators and make predictions for their behavior in specific systems.

Conclusion

The goal of this project is to demonstrate the new material characterization method and use it to explore essentially new physical phenomena, previously unreachable by conventional means including some of the most fundamental problems in science such as the emergence of the macroscopic classical realism from microscopic quantum mechanics.

We will show that considerable stream of information provided by the spin noise signal is sufficient to precisely and non-invasively determine higher-than-2nd order correlators of variables even in mesoscopic quantum systems at thermodynamic equilibrium.

Publications

Bechtold, A., D. Rauch, F. Li, T. Simmet, P. Ardelt, A. Regler, K. Müller, N. A. Sinitsyn, and J. Finley. Three-stage decoherence dynamics of an electron spin qubit in an optically active quantum dot. 2015. Nature Physics. : x.

Li, F., and N. A. Sinitsyn . Universality in higher order spin noise spectroscopy. Physical Review Letters.

Rice, W., T. Baker, W. Liu, N. A. Sinitsyn, V. A. Klimov, and S. A. Crooker . Revealing Giant Internal Magnetic Fields due to Spin Fluctuations in Magnetically-Doped Colloidal Nanocrystals. To appear in Nature Nanotechnology.

Roy, D., L. Yang, S. A. Crooker , and N. A. Sinitsyn. Cross-correlation spin noise spectroscopy of heterogeneous interacting spin systems. 2015. Scientific Reports. 5: 9573.

Sinitsyn, N. A.. Exact transition probabilities in a 6-state Landau-Zener system with path interference. 2015. Journal of Physics A: Mathematical and Theoretical. 48: 195305.

Sinitsyn, N. A.. Solvable four-state Landau-Zener model of two interacting qubits with path interference. 2015. Physical Review B. 92: 205431.

Three-Dimensional Porous Nanographene for Highly Efficient Energy Storage

Hsing-Lin Wang
20150532ER

Introduction

Graphene, due to its unique chemical and physical properties, has emerged as a new energy storage material for lithium ion battery anodes. However, over 50% of the graphene charge capacity is lost during charge-discharge cycles due mainly to restacking of graphene sheets into graphite-like structures. A lack of ideal model graphene systems that can be easily incorporated into Li battery anodes has hindered scientific investigation of Li reaction mechanisms and prevented development of robust graphene-based anode materials.

Using a novel synthetic method developing at C-PCS/MPA-11, we are able to synthesize a series of nitrogen-doped nanographene structures that allow for finely-tuned nitrogen doping and molecular structures and sizes. In this proposal, using these ideal nanographene model systems, we aim to elucidate Li ion adsorption/desorption/diffusion kinetics as functions of nitrogen dopant, molecular size, and structures of the synthesized nanographene. Based on the acquired knowledge, the 3D porous nanographene anodes with desired chemical and structural properties will be further prepared via a crosslinking synthetic strategy in order to maximize the specific Li storage capacity, diffusivity, and long-term charge/discharge stability.

In order to achieve these goals, we propose an innovative R&D approach by integrating theoretical predictions from density functional theory calculations and nanoscale dynamic simulations with experimental characterization using well-defined nanographene model systems. In turn, nanographene with optimally designed electronic and geometric structures will be realized though molecularly controlled synthetic methods. By combining the multidisciplinary expertise, we expect to understand fundamental reaction mechanisms of lithium on the doped nanographene structures and ultimately, to propose a path forward to designing structurally stable and high-capacity graphene anodes for energy storage applications.

Benefit to National Security Missions

The proposed research enables a better understanding of fundamental mechanisms for Li behavior in porous graphene structures and provides a viable approach for fabricating functional nanomaterials for advanced battery technologies with high-power and high-rate performance. The project addresses fundamental challenges in materials, energy, and nanotechnology. Success will have wide-spread impact on the fabrication of high-performance rechargeable batteries for efficient energy storage. This research will strengthen our capability in addressing key LANL missions of materials functionality and energy security, positioning LANL in a new frontier of energy storage research. With this proposed LDRD-ER effort, understanding the mechanisms that underpin battery reactions and developing high-performance electrode materials for energy storage will support new fundamental and applied follow-on projects in the Basic Energy Science (BES) and Energy Efficiency and Renewable Energy (EERE) offices, respectively.

Progress

One of our main goals is to develop Such synthesis is regarded as highly challenging as there is no guarantee success of such molecules. In the fiscal year 2015, we have made significant progress in several fronts. First, we have demonstrated synthesis of two dimensional (2D) and three dimensional (3D) nanographene molecules through multi-step organic synthesis. Complete characterization of such molecules through a suite of organic spectroscopy probes and the results are in perfect agreement with the hypothesized structure.

Second, the electronic, optical and redox properties of these molecules have been fully characterized. These molecules reveal structure and redox potentials that are functional group-dependent. Although such results are somewhat expected, once fabricated into lithium ion

battery, varying functional group have a huge impact in the performance in terms of the specific capacitance and stability.

Third, Lithium battery from these nanographene anode have been prepared and the highest capacity is ~950-1000 mAh/g, the highest number ever reported for carbon based anode. We collaborate with Professor gang Wu 9A former scientist at MPA-11) at University Buffalo and Liming Dai at Case Western Reserve who is the world expert in energy conversion and storage devices. Some of the results have been reproduced by more than one group. These results have been written and submitted for publications. One of the manuscripts was sent to "Science" and currently evaluated by the Advisory board.

Future Work

In FY16, we will (1) realize atomic level control over the chemical synthesis of the nanographenes which include two dimensional (2D) and three dimensional (3D) nanographene structures. We strive to show chemical synthesis of nanographenes and demonstrate how these nanographenes self-assemble to form hierarchical structures, which is critical to the performance of lithium ion batteries with respect to their charge capacity and stability, and (2) optimize the electronic and geometric properties of nanographene for efficient Li ion adsorption and diffusion determined by electrochemical measurement. Batteries tests will provide the correlation between functional group, geometry and redox properties. Such correlation has never been realized and the demonstration of such correlation will represent a major advancement in rational design of anode materials for energy storage devices.

Conclusion

We expect to: (1) Develop new synthetic protocols to prepare a series of nanographenes with various functional groups (linker) and nitrogen doping to finely tune their physical and electronic properties. (2) Gain fundamental understanding of lithium adsorption/desorption and diffusion kinetics on doped graphene by using well-defined (e.g., molecular size, structure, and doping content and location) nanographene model systems. (3) Based on insight provided from experimental results and DFT predictions, design and synthesize novel 3D porous nanographene anodes with optimal chemical and structural properties to maximize Li capacity, diffusion rate, and cyclic stability for energy storage applications.

Controlled Helium Release from Composite Plasma Facing Materials through Interface Design

Yongqiang Wang
20150567ER

Introduction

The overall project goal is to demonstrate a tungsten (W) based plasma-facing material that continually outgasses helium (He) as it is being implanted, thereby preventing He assisted cavity growth and yielding a morphologically stable plasma-facing surface. This demonstration will be accomplished by designing and testing a tungsten-metal (W-M) nano-composite containing interfaces that provide stable pathways for controlled and continuous He outgassing. The interfaces will be designed such that the pathways self-organize under He implantation.

This project is built on recent research by our team into the interaction of He with solid-state interfaces in bcc-fcc multilayer composites, in which we discovered that that certain metal-metal interfaces are capable of stably storing up to several atomic % of He without forming He bubbles: far in excess of the bulk He solubility limit. The reason for this surprising lack bubbles as compared to the bulk counterparts is that implanted He aggregates into platelets that wet high-energy parts of the interfaces of interest and do not grow into voids even in the presence of radiation-induced vacancy supersaturations.

We plan to use this insight to design W-M interfaces with high-energy regions patterned into continuous pathways (nanochannels) that will first trap (or store) He and then allow it to outgas while maintaining morphological flatness, mechanical cohesion and thermal conductivity across the interface. Successful demonstration of this novel interface design concept will enable breakthrough improvements in the performance of W based plasma-facing materials under fusion-relevant conditions, and the insights gained will become a broader "toolkit" of materials science and engineering methods that may later be used in other fusion and non-fusion related applications where precipitation of impurities play an important role.

Benefit to National Security Missions

This research is important to LANL's core materials capabilities: discovering, understanding,and exploiting defects and interface in materials. To achieve the vision of prediction and control of materials functionality set by MaRIE vision, it is noted that "a key grand challenge is the ability to predictively manipulate microstructures to achieve desired macroscopic performance. Central to this challenge is the potency of defects, either to be exploited intentionally for enhanced performance or to suffer their deleterious effects." Our proposed research directly addresses this vision and will strengthen LANL's competency in the design of functional materials through exploiting defects and interfaces.

A recent report by the DOE Office of Fusion Energy Sciences' Advisory Committee emphasized that "the majority of [plasma facing component] materials research should be oriented towards tungsten" (p. xvi) with the specific goal of identifying and characterizing W-based materials suitable for fusion-relevant environments. The proposed project directly addresses the needs in this report.

We plan to design W-M interfaces with high-energy regions patterned into continuous pathways (nanochannels) that will first trap (or store) He and then allow it to outgas while maintaining morphological flatness, mechanical cohesion and thermal conductivity across the interface. Successful demonstration of this novel interface design concept will enable breakthrough improvements in the performance of W based plasma-facing materials under fusion-relevant conditions, and the insights gained will become a broader "toolkit" of materials science and engineering methods that may later be used in other fusion and non-fusion related applications where precipitation of impurities play an important role.

Progress

Experimental efforts: the key accomplishment is to synthesize nanostructured thin films with high quality Cu-V interfaces and to capture the interface dislocation network by transmission electron microscope. To capture dislocation network at Cu-V interfaces is one of the grand challenges in this project. Here we hypothesize that the diffusivity of helium along dislocation line will be much faster than that in bulk and the dislocation network at interfaces has been treated as the channel to effectively diffuse out the extra helium in materials. To form effective channels for helium diffusion, the interface structure needs to be atomic sharp between Cu and V and also needs large grain size in both Cu and V layers. In order to synthesize high quality thin films, we have performed many batches of depositions with different sputtering rate, temperature, film thickness, and substrate. The grain size has been improved from 20 nm at very beginning of the project to 200 nm, an increase of one order of magnitude. The large grain size provides us the possibility to see the structure of dislocation network under transmission electron microscope (TEM). We think we have found the recipe to synthesize high quality Cu/V bilayer, tri-layer and multi-layer thin films. Helium implantation has been arranged in this month along with the following up TEM characterization to observe the nanochannel structure. We believe within the first 12 months of this project, we will figure out how helium atoms diffuse out of the Cu/V thin films with presence of the dislocation network at Cu/V interface.

Modeling effort: During the first year, the team has constructed a phase field model of He precipitate growth at patterned interfaces. This approach uses the Cahn-Hilliard equation to evolve an order parameter field that describes the He precipitates as well as the metal into which the He precipitates grow (Cu, in the case of Cu-V precipitates). The interface is described as a surface with a location dependent energy, which gives rise to wetting at specified contact angles. The non-wettable part of the interface is modeled by a Dirichlet boundary condition that fixes the order parameter at the value corresponding to the metal. A custom, quasistatic helium loading algorithm was developed whereby the net helium content is increased by changing the order parameter in the helium precipitates. After each helium loading step, the precipitate morphology is relaxed by solving the time-dependent Cahn-Hilliard equation until a static state is reached. The process is then repeated as often as needed to simulate the desired extent of precipitate growth. We use the MOOSE phase field code developed at Idaho National Laboratory to run these simulations. We are currently conducting a parametric study that investigates the critical helium content needed to cause precipitates to de-wet from the interface as a function of wetting angle and spacing of misfit dislocation intersections.

We have presented our modeling work at the 2014 MRS Fall Meeting (contributed talk) and at the 15th International Conference on Plasma Facing Materials and Components held at Aix en Provence, France in May 2015 (poster). The experimental results have been accepted to present at the 17th International Conference on Fusion Reactor Materials to be held at Eurogress Aachen, Germany in October 2015 (poster). By invitation, we gave a presentation and submitted a white paper on this subject at a recent Plasma-Materials Interactions Workshop organized by Princeton Plasma Physics Laboratory for Office of Fusion Energy Sciences in May, 2015.

Future Work

The goal of the second year is to demonstrate through modeling, simulation and experiment that W-Cu nanocomposites possess nanochannel structures for desired helium storage and controlled helium release. Experimentally, we will first synthesize theory-predicted W-Cu interfaces (bi-layer, tri-layer, and multi-layer) using physical vapor deposition methods; then perform He ion implantation in these structures using various beam energies, ion fluences, beam fluxes, and temperatures; and finally perform detailed characterizations of the as-deposited and ion implanted samples for nanochannel distribution, He-bubble formation, He retention and release, and surface morphology etc. On the modeling side, we will investigate the large-scale morphology evolution during continuous vacancy loading both at isolated interfaces and in multilayers. These simulations will be performed both for Cu-V and Cu-W interface structures. Preparation of two publications is anticipated: one that describes the phase field method developed during the first year and another that explores the He large-scale precipitate morphology evolution. Graduate student D. Y. Yuryev will spend the fall semester of 2015 at Los Alamos National Laboratory working with Project PI, Y. Q. Wang, on integration of her simulations with experiments being performed at LANL. Her stay will be supported by a DOE Office of Sciences Graduate Fellowship. We plan to present our work at the 2015 fall MRS meeting in Boston.

Conclusion

The overall technical goals are to demonstrate a tungsten (W) based plasma-facing material that continually outgasses helium (He) as it is being implanted, thereby preventing He assisted cavity growth and yielding a stable plasma-facing surface. This demonstration will be accomplished by designing and testing a tungsten-metal (W-M) nano-composite containing interfaces that provide stable

pathways for controlled and continuous He outgassing. Successful demonstration of this novel concept will enable breakthrough improvements in the performance of W based plasma-facing materials under fusion-relevant conditions as well as enhancing other applications where precipitation of impurities play an important role.

Publications

Li, N., M. Demkowicz, N. Mara, Y. Q. Wang, and A. Misra. Hardening due to interfacial He bubbles in nanolayered composites . To appear in MATERIALS RESEARCH LETTERS.

Zhang, H. X., F. Ren, Y. Q. Wang, M. Q. Hong, X. H. Xiao, W. J. Qin, and C. Z. Jiang. In situ TEM observation of helium bubble evolution in V/Ag multilayer during annealing. To appear in Journal of Nuclear Materials.

Precision 'Bottom-Up' Fabrication of Non-classical Photon Sources

Jennifer A. Hollingsworth
20150604ER

Introduction

"Quantum" light sources deliver photons in a strictly regulated fashion that defies the statistical distribution of photons that result from classical light sources, such as lasers, light-emitting diodes and thermal sources. A true single-photon source yields one photon when optically or electrically prompted, while non-quantum sources are always subject to a Poisson distribution in their photon statistics. Single-photon sources are needed as 'building blocks' toward next-generation quantum-information technologies – secure quantum communication (optical quantum bits/'qubits'), quantum networking (optical 'messengers'), quantum cryptography, quantum computation, and quantum sensing (including aiding development/qualification of sensors for quantum-information experiments and performance testing of low-light imaging systems).

Nanowire (NW) elements are nearly ideal structures for assembling photonic circuits due to their extreme shape asymmetry, which can afford optical confinement in two dimensions and opportunities for extensive transport in the long, third dimension, followed by photon out-coupling at the distal end. Integrating individual, otherwise isolated single quantum emitters within a NW cavity affords clear benefits for both systems – the wire is functionally "activated" by the emitter, while the emitter becomes accessible for a range of excitation routes, as well as to photon-information transport and collection. Although significant progress has been made in the past decade in emitter-in-wire single-photon sources by epitaxial-growth methods (top-down etching of planar structures containing self-assembled QDs, QDs self-assembled in a NW, and bottom-up nanodisc-in-wire structures), outstanding challenges remain.

The overarching goal is to address these challenges by combining novel fabrication principles with unique emitters to create quantum-emitter/NW-waveguide hybrid structures exhibiting: (1) on-demand single photons, (2) room-temperature photon purity, and (3) fast emission. Specifically, we will embed our so-called 'giant' QDs (g-QDs) within zinc oxide NWs, where the g-QDs will be structured to afford both room-temperature spectral purity and single-dot level optical stability (photons-on-demand), while the NWs will provide efficient subwavelength waveguiding.

Benefit to National Security Missions

With respect to our Science Mission, especially in regard to Materials Chemistry, Materials-by-Design, and Materials Properties, we will establish new methods for fabricating functional hybrid nanoscale structures that will exhibit designed emergent properties. We will establish new knowledge/new understanding regarding how to enhance/tune fundamental semiconductor radiative rates by field effects (proposed novel quantum-dot/dielectric metamaterial couple) and/or charge enhancement (quantum-dot/diode couple). More practically, we will demonstrate the first waveguided optically and electrically pumped single-photon sources based on solution-synthesized quantum emitters, characterized by an unprecedented combination of: ultra-pure photon statistics, high room-temperature efficiencies, and "on-demand" response that is not possible using conventional approaches. We also anticipate proving a path-forward to very low-threshold lasing resulting from our coupling of a novel emitter with a nanowire cavity (for strong cavity-emitter coupling). Thus, our Discovery Science aims will enable understanding/controlling collective properties of excitonic/dielectric hybrids using advanced spectroscopies, in-situ measurements & CINT (user facility). Toward applications relevant to nuclear nonproliferation, DoD, NIST, and IC, the work aims to establish new single-photon source capabilities for next-generation quantum information technologies – secure quantum communication, networking, cryptography, computation and sensing, with low-threshold lasers also useful for next-gen solid-state lighting and conventional

communications. More specifically -- Photon-on-demand are needed for DoD, DARPA secure communication, as well as non-proliferation programs (e.g., next-gen NCAM) - performance testing of low-light imaging systems, development & qualification of sensors for quantum information (QI) experiments, while entangled photon source will serve broad needs in QI science & secure communication (QKD & beyond).

Progress

In the first nine months of this project, we made significant progress toward research Objective 1, which is the foundational science on which Objectives 2 and 3 will build. Specifically, a key aspect of the proposed program was to establish a method for coupling quantum emitters with optical waveguide structures. The proposed method was to use the 'direct-write' capability afforded by dip-pen nanolithography (DPN) to literally place from few to a single giant quantum dot (g-QD) onto the tops of ZnO nanowire (NW) waveguides, where the ZnO NWs are sub-micron in diameter and grown in organized arrays across a solid substrate. Such post-synthesis "nanoscale manipulation" would be unprecedented for a mask-less technique in creating coupling between two nanoscale materials systems over many such systems (as opposed to "one-off" approaches). We successfully used DPN to precisely position g-QDs exclusively on top of dielectric nanowires. However, for this initial work, we employed silicon nanodisk antennas as opposed to ZnO nanowires. The former were obtained from an external collaborator, while the ZnO structures had to be synthesized by our team. Several months of development were required to realize the desired ZnO diameters, aspect ratios and pitch (rod-to-rod spacing). We recently achieved this level of control and are ready to move forward with the initially targeted ZnO nanowires in year 2, as the DPN approaches developed in year 1 using Si nanodisks are directly applicable to the ZnO structures.

Importantly, we established a new DPN strategy to obtain accurate nanoscale integration of the nanocrystals with their nano-sized substrates. Namely, we developed a novel three-step 'reading-inking-writing' approach, where atomic force microscopy (AFM) images of the pre-patterned substrate topography are used as 'maps' to accurately place nanocrystal ink. We also explored two methods for the 'inking' step -- dip-coating and scan-coating of the AFM 'writing' tip. Only the latter was found to afford controlled nanocrystal deposition (number of particles deposited per pillar) and repeatable deposition across the array of nanodisks. For the first time, we demonstrated that DPN is indeed a viable technique to fabricate multicomponent (hybrid) nanostructures that would be challenging or impossible to create using traditional lithographic techniques. We have also established a quantitative 'guide' for correlating pen-substrate contact time with the number of nanoparticles deposited per writing step. Prior to our work, this type of "predictive" capability was believed to be limited to simpler, molecular (rather than nanoparticle) inks. Finally, we demonstrated this level of control for a range of nanocrystal compositions (red-emitting CdSe/CdS and IR-emitting InP/CdSe QDs), sizes (~10-50 nm) and surface chemistries (bare g-QDs and silica-coated g-QDs), thereby addressing another project goal – to have the flexibility in the fabrication approach to use emitters 'as-needed' for proper emitter-waveguide coupling and to modify the emitter structure/chemistry to ensure properties stability throughout the processing/integration steps. We have recently submitted this work for publication:

The rapid progress in integration aspects of the project will be complemented in Year 2 by equally rapid progress in photo-physical characterization of the hybrid QD-ZnO structures and in the synthesis of doped ZnO NWs.

Future Work

In the second year of the project we will transition our success in nanoscale precision integration of 'Giant' quantum dot (g-QD) quantum emitters with silica dielectric nanodisks by dip-pen nanolithography (DPN) to coupling gQDs with in-house synthesized ZnO nanowires (NWs). This will allow us to establish functional coupling via the proposed "post-synthesis nanomanipulation" strategy. We will characterize color and NW-diameter/length-dependent waveguiding and assess single-photon emission performance. Tasks to be accomplished include an initial assessment of ZnO NW waveguide properties, which will entail further g-QD synthesis and ZnO NW synthesis (400-600 nm diameter – sizes initially guided using finite-domain time-difference (FDTD) calculations); preparation of simple gQD/ZnO NW couples for study of basic wave-guiding behavior of ZnO NWs for red (CdSe/CdS gQD: ~650 nm) and near-infrared (InP/CdS gQD: 1 μm) emission, and confocal microscopy studies to determine the efficiency of ZnO NW waveguiding as a function of NW diameter/length and gQD color. Based on this baseline assessment, we will attempt to fabricate a waveguided single-photon source comprising a gQD embedded in a ZnO-NW, which will entail: synthesis of an array of partially grown ZnO NWs; direct-writing of g-QD emitters using DPN onto the tops of the ZnO NWs, and completion of NW growth. Emission characteristics (stability, linewidth, emission rate, polarization, waveguiding) of the new hybrid gQD/ZnO NW structures will be determined by performing single-nanostructure time-tagged, time-resolved photoluminescence spectroscopy, including Hanbury Brown and Twiss and Hong-Ou-Mandel experi-

ments to assess the purity and indistinguishability of the single-photon emission events (employing a new superconducting NW single-photon detector for experiments in the near-infrared). Toward Objectives 2 (Electrically driven single-photon emission) and 3 ('Speeding up' colloidally synthesized emitters), we will begin efforts to fabricate and test stable ZnO p-n junctions. Also, Objective 1 will lay the groundwork for Objectives 2 and 3.

Conclusion

We will demonstrate the first waveguided optically (Objective 1) and electrically (Objective 2) pumped single-photon sources based on solution-synthesized quantum emitters, where our gQD emitters possess the unique advantages of ultra-pure photon statistics (complete antibunching) and high room-temperature efficiencies compared to epitaxially grown emitters, combined with "on-demand" (non-blinking) response that is not possible using conventional colloidal QDs. We will also provide new understanding toward enhancing radiative rates by field effects (gQD/dielectric couple) and/or charge enhancement (gQD/diode couple) (Objective 3). Each new property will "emerge" as a direct result of the proposed design for a novel hybrid-material constructs.

Publications

Dawood, F., P. A. Schulze, C. J. Sheehan, M. R. Buck, A. M. Dennis, N. Karan, I. Staude, J. Dominguez, G. S. Subramania, A. R. James, I. Brener, N. A. Amro, and J. A. Hollingsworth. Precision Placement of Nanocrystals Onto Sub-Micron Three-Dimensional Dielectric Antenna by Dip-Pen Nanolithography. ACS Nano.

Perovskite Solar Cells: The Next Frontier in Energy Harvesting

Aditya Mohite
20150612ER

Introduction

Recent discovery of incorporating organic–inorganic hybrid perovskites such as CH3NH3PbX3 (X = Cl, Br, I) as donor materials in a simple planar bilayer photovoltaic devices has revealed very high power conversion efficiency exceeding 15%1-4 without the need for nanostructuring or creating complex device architectures. In less than eight months, this work published in Nature1, 3 and Science4 has been cited more than 200 times. In spite of the celebrity status for this amazing new material, there is extremely limited scientific understanding on what intrinsic properties are responsible for endowing it with near ideal optical and electrical properties. Building on our extensive expertise in the organic photovoltaic (PV) devices 5, through a combined experimental and modeling effort, here we will formulate critical design strategies for high-performing devices based on hybrid perovskites by achieving synthetic control over light absorption properties, conversion of optical-to-electric energy, manipulation over charge separation and recombination.

Benefit to National Security Missions

This proposal focuses on developing perovskites and to gain unprecedented power conversion efficiency in photovoltaic (solar cell) devices. Perovskites with controlled crystallite domain size, defects, and morphology, coupled with an interfacial layer could redefine photovoltaic research as next generation solar cells with unprecedented high efficiency. The proposed work will strengthen our capability in addressing laboratory missions, particularly in the areas of materials development and energy security, and support new program development in Office of Science.

Progress

Work by our team at LANL that was recently published in Science has demonstrated a simple solution-based approach to grow films of CH3NH3PbIxCl3-x perovskite films consisting of large crystal grains. Our unique solution growth process led to reproducible and efficient hysteresis-free solar cells with peak efficiency approaching ~18%. We are now among only 3 teams in the world able to fabricate hysteresis-free devices with this efficiency; the others include H. Snaith's vapor deposition approach (Cambridge, UK) and M. Graetzel's mesoporous architectures (Switzerland). There are several distinct advantages to our process over the other systems. Notably, our subsequent preliminary studies suggest that these high crystalline quality perovskite films are potentially behaving as classical direct band-gap crystalline semiconductors like GaAs. Specifically, we observe that like GaAs optically excited electrons and holes occurs via broadband absorption and predominately recombine radiatively (so called bimolecular recombination. The PL quantum yield is near unity, and the PV device ideality factor is close to 1 indicating defect-free behavior. Our theoretical DFT calculations [Science] explained these observation by predicting the presence of blue-shifted electronic states at the interfaces due to excess chlorine (Cl) at the grain-boundaries, providing a natural passivation layer that minimizes internal charge carrier losses thus contributing to the high efficiencies.

Further, our initial measurements of perovskite photostability under constant solar illumination reveal a major breakthrough in obtaining stable perovskite solar cells with high efficiency. The observed degradation depends on the experimental conditions. Theoretical modeling attributes photo degradation to the formation of macroscopic charged domains, which is confirmed by experiments. Such a joint theory-experimental effort can clarify the observed physical phenomena and suggests synthetic strategies to control photo degradation (elaborated below). These examples also highlight ongoing integrated efforts between theory, synthesis and characterization. These results place our LANL team at a distinct advantage over other research groups across the world and as we stand today, we are perceived as among

the top 3 research groups in the area of perovskite solar cells.

Future Work

In the coming fiscal year, we will focus on two aspects:

- Ferroelectric effect in perovskite grains: We will understand through experiments and theoretical efforts tif the large grain perovskites demonstrated exhibit ferroelectric effect. We will perform charge polarization measurements in the dark and also study light induced polarization. We will use this information to understand the role of ferroelectricity in photovoltaic devices. We will answer questions like what is the origin of the high open circuit voltage and high current.
- We will perform detailed structure function relationship between the large grains and its optical properties. We will perform temperature dependent XRD and optical measurements to understand how the structural phases play a role in perovskites and how do they influence the overall macroscopic behavior.

Conclusion

We expect to achieve an understanding of the intrinsic source of high photocurrent and voltage (open circuit voltage; Voc) in perovskite-based solar cell devices, as well as how the emergent ferroelectric properties of these unique materials can be tuned to surpass current device efficiencies and develop high efficiency low cost PV devices.

Publications

Nie, , Tsai, Asadpour, Blancon, A. J. Neukirch, Gupta, J. J. Crochet, Chhowalla, Tretiak, M. A. Alam, Wang, and A. D. Mohite. High-efficiency solution-processed perovskite solar cells with millimeter-scale grains. 2015. SCIENCE. 347 (6221): 522.

Tsai, , Nie, Cheruku, N. H. Mack, Xu, Gupta, A. D. Mohite, and Wang. Optimizing Composition and Morphology for Large-Grain Perovskite Solar Cells via Chemical Control. 2015. CHEMISTRY OF MATERIALS. 27 (16): 5570.

Defect-Induced Emergent Magnetism in (Nonmagnetic) Complex Oxides and their Interfaces

Scott A. Crooker
20150613ER

Introduction

Interest in oxide-based electronics has exploded in recent years, fueled by the ability to grow atomically-precise interfaces and heterostructures of various complex oxides. Strontium titanate (SrTiO3) -- a nonmagnetic wide-bandgap insulator -- is a foundational material in this field. Owing to its widespread use in materials science, its dielectric and lattice properties are well known. However, tantalizing evidence in recent years indicates that there may yet be much more to SrTiO3 than previously realized: Several groups around the world have recently reported unexpected emergent phenomena at these oxide interfaces, most strikingly magnetism and superconductivity. This is particularly remarkable because the constituent oxides (e.g., SrTiO3 and LaAlO3) are nominally nonmagnetic and insulating. Crucially, the formation and distribution of oxygen vacancies defects (VO) – which form readily in SrTiO3 and are mobile – are widely suspected to play an essential but as-yet-poorly understood role in these emergent interfacial phenomena.

Our team recently applied powerful magneto-optical techniques to bulk SrTiO3 crystals for the first time and discovered that, surprisingly, VO defects can generate an optically-induced and persistent magnetism in this nominally nonmagnetic material. However, the underlying physical mechanisms remain unknown. Nor is it known how deeply these findings inform on the interfacial magnetism discussed above. Therefore, motivated by these results and coupled with our state-of-the-art capabilities for pulsed-laser deposition (PLD) oxide growth at LANL, we propose to reveal the origin of (and ultimately engineer) the defect-related emergent magnetic properties in these bulk and interfacial complex oxides, focusing on the archetype SrTiO3. We will apply a powerful suite of magneto-optical techniques to SrTiO3 epilayers and SrTiO3/LaAlO3 interfaces grown by PLD and MBE techniques, including Optically-Coupled SQUID Magnetometry and also ultrafast magnetization dynamics via Time-Resolved Faraday Rotation. Controlled introduction and removal of VO defects via annealing protocols is a key component of this program.

Benefit to National Security Missions

This research is vital to LANL's core materials capabilities: Discovering, understanding, and exploiting defects and interfaces in materials. It not only strengthens LANL's existing competency, but also significantly expands capabilities for our future nanostructured materials via "external" control of interfaces and defects. Furthermore, the MaRIE Workshops report indicates that "interfaces and defects" must be addressed to solve the decadal challenges for accelerating materials discovery. To achieve the vision of prediction and control of materials functionality, it states "a key grand challenge is the ability to predictively manipulate microstructures to achieve desired macroscopic performance. Central to this challenge is the potency of defects, either to be exploited intentionally for enhanced performance or to suffer their deleterious effects. The role of defects is a microcosm of the broader impact of rare events and fluctuations that are a key stumbling block in achieving prediction and control." Our project directly addresses this vision. The ability to control defects will yield new and unique results since the materials we are going to explore will provide us the opportunity to obtain new and/or improved functionalities not obtainable through bulk materials or by simply changing material chemistry. Moreover, this research represents an opportunity for LANL to take the global lead in the fundamental understanding of oxide materials. LDRD's investment in such an effort will ensure continued leadership in nanotechnology and functional materials, which will enable LANL to respond effectively to future calls by BES and other funding agencies.

Progress

Over the past year, postdocs Bill Rice and Luyi Yang have made substantial progress on various aspects of this

project. Bill has established a fully-functional capability for Time Resolved Faraday Rotation, which is an ultrafast optical technique for measuring the picosecond-resolved dynamics of spin and magnetization in semiconductor (and metallic) materials. This new LANL capability employs an ultrafast Ti:sapphire laser coupled to an optical parametric oscillator, which can deliver 100fs optical pulses at wavelengths spanning the optical spectrum. This new capability has been tested and benchmarked in two semiconductor systems: 1) magnetically-doped semiconductor nanocrystals, and 2) new atomically-thin MoS2 semiconductors. Both material systems have yielded new and exciting experimental results. In the first case, we have a nearly-completed draft of a paper written up, entitled "Revealing Giant Internal Magnetic Fields due to Spin Fluctuations in Magnetically-doped Colloidal Nanocrystals", that we intend to submit to Nature Nanotechnology. In the second case, we have written up a paper, "Long-lived Nanosecond Spin Relaxation and Spin Coherence of Electrons in Monolayer MoS2 and WS2", that is currently under review at Nature Physics (in fact, we just recently received very favorable reviews in the first round of refereeing). In parallel with the above, we obtained new SrTiO3 crystals that we have characterized and are intending to measure in the SQUID magnetometer within the next month.

Future Work

Growth and preparation of SrTiO3 epilayers and SrTiO3 / LaAlO3 interfaces will be performed at CINT-Los Alamos using our state-of-the-art PLD techniques. Direct comparison with similar samples grown by MBE forms a key piece of this proposal; these will come from established connections with Chris Leighton & Bharat Jalan (Minnesota) and Suzanne Stemmer (UCSB). Reduced concentrations of elemental impurities in MBE samples will allow us to ascertain whether, e.g., VO-Fe complexes play any role in the observed magnetic phenomena. In parallel, we will also continue to measure commercial "pure" SrTiO3 crystals as well as crystals that are intentionally and very lightly doped (0.01%) with Fe and Nb.

Magneto-optical studies will primarily rely on our "workhorse" setup for magnetic circular dichroism (MCD;), which has proven extremely effective at revealing magnetism in SrTiO3. Our Oxford Spectramag split-coil magnet at the NHMFL has direct optical access and is ideally suited for this purpose (T=1.5-300 Kelvin, B= 0-8 Tesla). Tunable light sources include a spectrally filtered Xe lamp and tunable dye / Ti:sapphire /OPO lasers. Planned modifications include more efficient frequency-doubling crystals to access deeper UV wavelengths (~350 nm), necessary for above-bandgap studies of SrTiO3 interfaces and thin epilayers. Controlled introduction and removal of VO via annealing in UHV and oxygen environments. This essential capability currently exists in U. Minnesota but we will emulate and improve it here at CINT to ensure quick turnaround of samples and rapid convergence on ideal annealing recipes.

Conclusion

The overall technical goal of this project is to study and ultimately reveal the origin of the recently-discovered magnetism and magnetic effects that emerge in many (nominally nonmagnetic) oxide semiconductors. We will focus on strontium titanate, which is the archetypical and foundational material in this new burgeoning field of 'complex oxide electronics'. Our plan is to directly compare magnetism and magneto-optical phenomena in SrTiO3 grown by bulk (commercial) methods, by pulsed laser deposition (PLD), and by molecular beam epitaxy (MBE). A key component is the rapid iteration of samples following controlled introduction and removal of oxygen vacancies.

Publications

Yang, L., N. A. Sinitsyn, W. Chen, J. Yuan, J. Lou, and S. A. Crooker. Long-lived nanosecond spin relaxation and spin coherence of electrons in monolayer MoS2 and WS2. 2015. Nature Physics. 11: 830.

Energetic Materials Cocrystal Engineering: Toward Superior Munitions

Philip Leonard
20150623ER

Introduction

This research is developing energetic materials with new and hopefully superior performance and safety properties via cocrystallization. Cocrystallization will allow us to exploit synergistic properties in existing energetic materials (EM) by alloying on a molecular level. Property modification via creation of stoichiometric cocrystals has been demonstrated with great success in pharmaceuticals and is beginning to bear fruit for explosives as well. For example, two EM that are powerful performers in terms of detonation velocity and shock pressure may separately be highly sensitive to impact, by cocrystallizing those molecules one might be able to achieve a layered structure where planar dislocations dissipate energy non-violently resulting in an acceptable safety margin. In the same vane, two insensitive materials which are non-performers due to inadequate density could cocrystalize into a form with a higher than average density as a result of superior packing. Given challenges in scaling and adopting new materials, creating better EM through cocrystallization has great advantages. Cocrystallization of HE is also critical as an alternative to formulation where the properties of molecules are always averaged - often with trade-offs in sensitivity and performance.

One great challenge in this effort is coupling modeling and experiment. We are applying the latest in density functional theory (DFT) functionals to predict packing structures as well as modeling of single crystal X-ray data to determine structures. This active discourse will accelerate experimental achievement while also providing insight into the failings of our modeling assumptions.

Benefit to National Security Missions

Cocrystals have great potential for technological innovation. This project will perform fundamental research into the nature of intermolecular interactions in condensed matter that will enlighten cocrytallization in defense-related applications as well as life-science applications.

An increased understanding of intermolecular bonding will be crucial to the development of explosives with superior properties in terms of energy density, handling safety, and specialized properties such as high melting and decomposition temperatures. Because explosives are widely used in the harvesting of fossil fuels, this research will improve our ability to extract energy resources from deeper or more difficult terrain. Improved explosive safety has direct application to DOD safety and DOE safety and surety missions. We envision that the capability to modify detonation velocity and pressure as a function of density will have important implications for the design of precision explosive applications such as linear and conical shaped charges and explosive lenses, applications which may be of interest to DARPA or NASA for controlled demolition such as rocket stage separation.

Progress

This project comprises three main pursuits, development of computational ability, synthesis of cocrystalline material, and characterization by X-ray and other methods. X-ray characterization has been delayed due to instrument problems which have now been resolved, the other two focus areas are proceeding well.

A systematic screening for cocrystal formation between sixteen target molecules was initiated and is ongoing. Cocrystallization from solvent and during solvent grinding has been used for screening. The effects of the two different crystallization methods on cocrystalization formation and phase purity are being assessed. Characterization by x-ray diffraction and vibrational spectroscopy is ongoing. Reitveld refinement of powder x-ray diffraction data is being developed to provide unit cell parameters and quantitative measures of phase purity. Assessing and attaining phase purity is crucial before transitioning to explosive property testing because of deleterious effects of remaining pure parent phases used to form the cocrystal.

A new approach and code for the prediction of the atomic structure of co-crystals has been implemented in our 'APES' code (Automated Prediction of Explosive Structures). APES employs efficient algorithms to scan and rank potential crystal structures as a function of unit cell parameters (lattice parameters and angles), the position and orientation the molecules, and stoichiometry. All of these degrees of freedom are searched using a stochastic, simulated annealing algorithm and the code is heavily parallelized (MPI) such that extremely high throughputs can be achieved. The code makes no assumption of the space group, leaving that step instead to the post-processing of promising crystal structure with ab initio electronic structure codes.

While APES can quickly scan and rank millions of potential structures, the accuracy of its predictions are controlled by the molecular geometries and descriptions of intermolecular interactions that we input. We found that the set of Buckingham potentials developed for C, H, N, O-containing molecules developed by D. E. Williams provides an adequate and transferable description of non-bonded interactions in organic molecular crystals. The set of partial charges assigned to every atom are extremely sensitive to the method used in their calculation. Hence, we discovered that only relatively high-level approaches such at CHELPG give reliable sets of partials charges whereas sets of simple Mulliken partial charges do not give the correct ranking of crystal structures in APES simulations. We will soon use spectroscopic data from the experiments mentioned above to estimate the number of unique molecule in each unit cell in order to narrow the search space for APES in terms of stoichiometry.

We are continuing to improve the purity of our most promising candidate, TNX. We have discovered that solvent choice is critical for producing material with acceptable phase purity. TNX possesses special challenges for scale up because it is a co-crystal of melamine and trinitrophloroglucinol which have very different solubilities. Nevertheless, by transitioning from DMSO to ethylene glycol followed by washing with methanol, we have been able to produce high-purity material in excellent yield (~70- 75%). Combustion studies on pure parent HE (TNPG) and TNX have been performed. TNPG was found to behave anomalously: it burned at low pressures (< 800 psi), but would not sustain combustion at high pressures. Due to smoke obscuring the burn front at low pressures (≤ 1000 psi), TNX could only have data fit between 1200 and 1800 psi. Scale up to 100 g scale of TNX for 1" rate stick will proceed next quarter.

Future Work

Initial screening

Cocrystal formation will be performed using solvent grinding and wet chemistry techniques. Solvent grinding has been used as an efficient method for pharmaceuticals but not in explosives because of the inherent hazards which we have overcome. The LANL HE Crystal Lab has constant temperature and continuous circulation growth vessels, specifically designed for growth of cocrystals. Our goal is to create multiple highly crystalline materials for X-ray analysis.

X-ray analysis

In order to understand intermolecular interactions in the synthesized co-crystals we must determine their full atomic structure. We will apply atomistic simulation techniques to aid solution. Powder XRD on the cocrystals will enable us to identify their Bravais lattice and unit cell parameters. We will also measure vibrational spectroscopy in order to determine the number of unique molecules per unit cell. Our goal is to generate data sets for each new material for modeling.

Modelling

Armed with the Bravais lattice, unit cell parameters, possible synthon structures, and the number of unique molecules per unit cell, we will perform a series of Monte Carlo simulations with a generic force field to determine an optimal set of coordinates for the molecules of that lattice. The stability and heats of formation of those structures will be computed by condensed phase DFT calculations in order to identify which is energetically most favorable. Our goal is to be able to solve single crystal X-ray data and predict the correct packing structure (although possibly not exclusively).

Sensitivity and performance characterization

Sensitivity of new cocrystals will be assessed by the WX-7 analytical team using standard drop-hammer, BAM friction, and electrostatic discharge (ESD) testing. Performance testing is not envisioned as occurring in the first year. Our goal is to make safe energetic materials.

Conclusion

Our technical goals are to (1) develop and utilize rational crystal engineering strategies to discover cocrystals and (2) demonstrate superior explosive safety and performance and improved material properties. The first goal has broad relevance to chemistry in general as modification of physical properties are significant to everything from pharmeceuticals to non-linear optical (NLO) materials. Achieving a rational design process for cocrystallization based on more than intuition is critical to the future of the field. Developing new explosives is no less critical to national security as

existing mainstays are being threatened due to environmental concerns.

Publications

Bowden, P. R., P. W. Leonard, J. P. Lichtardht, B. C. Tappan, B. L. Scott, and K. J. Ramos. Energetic salt of trinitrophloroglucinol and melamine. To appear in APS Shock Compression of Condensed Matter. (Tampa, 14-19 Jun. 2015).

Majorana Fermions for Quantum Information

Filip Ronning
20150628ER

Introduction

Quantum information processing offers great potential in terms of National Security, fundamental science, and commercial applications. However, quantum information is notoriously sensitive to small amounts of noise. A solution to this problem lies in using so-called fault tolerant topologically protected states to store quantum information. Majorana fermions, which were predicted over 70 years ago, but not yet definitely observed in nature, are examples of a topologically protected state that could be used for quantum information technology. Recent progress has suggested that appropriately engineered structures in solid state systems could realize Majorana fermions. Several promising first experiments have been performed, but disorder has limited further progress on existing materials. Instead, strongly correlated f-electron materials, such as SmB6 (samarium hexaboride), can also host Majorana fermions in appropriately engineered structures, and are much cleaner.

Benefit to National Security Missions

This work will address DOE Office of Science and national security mission needs. We propose to provide evidence for an exotic particle known as a Majorana fermion. A Majorana fermion has potentially a huge impact on national security as it can provide the platform for quantum information processing, which enables computations not possible on a classical computing architecture. The advantage of Majorana fermions is that they are much less sensitive to noise effects which can destroy other quantum information architectures. We will work on a material known as Samarium hexaboride. This material is interesting by itself as it may possess a unique surface state. Thus our studies will also shed light on a new type of matter found in Samarium hexaboride.

Progress

The objective of this proposal is to find evidence for a Majorana fermion in a condensed matter system with the prospect of using them for quantum information technology. The most promising route to accomplish this employs superconductivity in a topologically non-trivial material. Here topology refers to the “curvature” of the electronic structure in analogy to the curvature of a sphere versus a donut in geometry. The work we performed in the first year took three approaches. First, we aimed to identify that the semimetal, niobium arsenide (NbAs) is topologically non-trivial, and whether superconductivity could be found in this material. Second, we attempted to create clean interfaces of superconducting aluminum (Al) on the surface of samarium hexaboride (SmB6), a proposed “topological insulator.” Third, we are exploring the robustness of using Majorana fermions for quantum memories in the presence of thermal decoherence effects.

NbAs was recently predicted to be a so-called Weyl-semimetal. This metallic state has many unique properties due to the electronic structure being topologically non-trivial. We were able to synthesize single crystals of NbAs, and found that they have an amazing mobility at low temperatures (2 K), which is even larger than that found in graphene. Furthermore, by studying the electronic structure using ultra high magnetic fields we could determine that the electronic structure is indeed topologically non-trivial as predicted by theory. Unfortunately, our attempts to discover superconductivity in this material have been unsuccessful down to 0.050 K.

As originally proposed, we are exploring devices made out of the topologically non-trivial material SmB6, and superconducting aluminum. We have been able to deposit superconducting pads of Al on SmB6 that are 100 nm thick. Importantly, these pads have been shown to be consistently and robustly adhered to the sample surface, and fully superconducting from resistance measurements. Initial problems with the Al not becoming superconducting were resolved through changing the metal source to reduce any contaminants. In early work

the resistance of the patterned samples showed irreproducibility because of intermittent contact between the SmB6 and the Al. These issues were overcome by improving the process by which the sample surface is prepared. The samples are now aggressively cleaned and undergo a thorough oxide removal step. In addition, a 3nm titanium layer is deposited in between the SmB6 and Al layer to improve adhesion.

Progress has also been made on the patterning of the narrow junction between two Al strips. Small samples are difficult to process due to surface non-uniformities and the small dimensions required during the lithographic process. A procedure has been developed that has resulted in 70 nm gaps between contacts, but progress still needs to be made to reduce the linewidth variation in the gap and to improve the adhesion of the e-beam resist to the sample.

In order for us to show evidence for Majorana fermions in the junctions it is necessary to perform low power measurements of the current-voltage characteristics of the junctions. The experimental setup to perform these measurements is now operational. Initial measurements show qualitatively that the contact between the Al and SmB6 is good. The next step will be to get quantitative information on the contact quality, and once patterned junctions are produced we can further optimize the electronic setup for their characterization.

A self-correcting quantum memory is a quantum many-body system that can protect its quantum state against errors for a period of time that grows rapidly with the system size. Most proposals for quantum memories in 2 dimensions, such as those using Majorana fermions, have issues that make them unstable with respect to small local static perturbations. We recently introduced a new approach to quantum memories where the interactions of the system are random, according to particular distribution. Small-scale numerical simulations show that this approach may also work at larger sizes. Our line of research for the next few months is to investigate the role of thermal fluctuations in these systems and whether practical methods for "storing" and "reading" a quantum state are possible.

One paper was published in JPCM, and another submitted to PRX on the above work. Also, the PI gave an invited talk at an international conference on SmB6.

Future Work

Samarium hexaboride (SmB6) may or may not possess an exotic electronic state on the surface of the material. If it exists, and can be made superconducting one has the chance of creating the particle called a Majorana fermion, which could be used in quantum information processing. We will explore the properties of devices which induce superconductivity on the surface state of SmB6. This will be done by depositing aluminum (itself a superconducting material) on top of the SmB6 crystal. If the interface between the SmB6 crystal and the aluminum is clean enough, then we will have the possibility of creating non-linear transport in such a device from which we could identify if the SmB6 does indeed possess the exotic electronic state. In fact, the signatures in the transport measurement if successful may also reveal the first evidence of a Majorana state. We will also investigate how thermal decoherence can affect the utility of Majorana fermions for quantum memories.

Conclusion

We propose to provide evidence for the existence of the elusive Majorana fermions in hybrid structures using SmB6, and to further demonstrate that the position of the Majorana fermion can be moved. The physical exchange of Majorana states leads to exotic properties, which in the future can form the basis for quantum computation.

Publications

Ghimire, N. J., Y. Luo, M. Neupane, D. J. Williams, E. D. Bauer, and F. Ronning. Magnetotransport of single crystalline NbAs. 2015. JOURNAL OF PHYSICS-CONDENSED MATTER. 27 (15): 152201.

3-Dimensional Characterization of Nuclear Fuels: Microstructural Evolution under Representative Temperature and Thermal Gradients

Donald W. Brown
20130232ER

Abstract

X-rays and neutrons have been used as probe particles to monitor the microstructure of nuclear fuel under conditions simulating those perceived by the fuel in reactor. Ceramic (UO2) has been the focus of the experimental work, but other metallic and composite fuels have been studied when strategic. High energy x=ray diffraction microscopy (HEDM) has been used to monitor grain morphology under extreme temperature (~2000°C), x-ray micro-tomography (μT) has been used to monitor pore and crack structure under temperature and irradiation (separately) conditions, and small angle scattering (SAS) has been used to monitor void and pore evolution under high temperature. In many cases, the analysis of the scattering data is still on-going, but clear effects are available.

Diffusion of xenon gas (a fission product) from within the microstructure to the volume external to the fuel and within cladding (the plenum) is critical to the useful lifetime of ceramic nuclear fuel. The xenon atoms initiate as interstitial impurities and diffuse to form clusters, voids, and finally pores on their way to the plenum. The HEDM data shows clearly that increases in the oxygen stoichiometry (UO2+x, where x~0.1) increases the grain size following sintering under the same conditions. This is important because grain boundaries act as short circuits for the fission produced xenon to reach the plenum. Thus, large grains slow the transfer of fission gases (e.g. Xe and Kr) from the microstructure to the plenum). Small angle x-ray scattering (SAXS) has been utilized to provide statistical information related to the development of xenon bubbles at temperature. X-ray μT shows clearly the development of small pores at the interface of a metallic fuel and its bonded cladding during irradiation. This is possibly related to the formation of bubbles on the surface of the metallic fuel which block coolant flow channels resulting in dangerous hot spots in research reactors.

Background and Research Objectives

Recently, interest in nuclear energy in the Unites States (and worldwide) has surged, with increased efforts to extend the lifetime of the current fleet of reactors and to develop advanced reactors that operate at higher temperatures and use fuel to higher burn-up. The accident at Fukushima has not changed the fact that nuclear energy will remain part of the US energy mix for the foreseeable future, but has shifted research priorities to accident tolerant designs.

Nuclear fuel functions in possibly the most extreme environment. The extreme thermal gradient drives radial grain growth and void migration in ceramic (UO2) fuel which degrades thermal conductivity and facilitates transport of fission products which is important in the case of cladding failure. Current models attempt to predict useful lifetimes of fuel assemblies. Safety margins and predictions of the engineering performance of nuclear reactor fuel rely on modeling codes used to predict dimensional change, stress state and fission gas release as a function of burn-up and temperature history. Thermal conductivity is the single most important material parameter in these codes and is heavily dependent on microstructure (e.g. grain morphology, porosity, etc.), oxygen stoichiometry, chemical segregation, etc. To date, empirical and phenomenological descriptions of the evolution of the microstructure of fuel materials are used to calculate the thermal conductivity, but this leaves huge uncertainties and necessarily results in large safety margins and inherently inefficient use of resources as well as increased production of waste.

Microstructural evolution occurs in nuclear fuels due to the high temperature, extreme thermal gradient and radiation damage. In ceramic fuels, grains grow in the direction of extreme thermal gradient, that is, radially, while voids elongate along the gradient. Cracks develop during the first thermal cycle due to the stresses associated with the strong thermal gradient. Oxygen stoichi-

ometry in pure UO2 and actinide content in mixed oxide fuels (MOX), evolve under these conditions. All of these changes in the microstructure affect both the thermal conductivity and transport of fission products in ways which we can neither predict accurately nor fully understand, but these are the lifetime limiting behavior of ceramic nuclear fuels.

The objective of the research was to characterize the microstructural evolution of the fuel under conditions simulating those perceived during operation, that is, at high temperature and high thermal gradient. High energy x-ray diffraction and imaging can probe the microstructure of bulk nuclear fuel at relevant length (μm) and time (seconds) scales while in this demanding environment. The understanding gleaned from the experimental work has been used to develop microstructural models associated with the MARMOT code being developed at Idaho National Lab.

Scientific Approach and Accomplishments

We have used x-ray scattering experiments on nuclear fuels to monitor the grain morphology, orientation, void structure, and chemical segregation in their respective microstructures as a function of external perturbation, such as time at temperature. The primary subject has been ceramic UO2 in an extreme thermal gradient. However, strategic studies of other fuel types were completed as well to 1.) develop techniques for probable use in MaRIE and 2.) develop strategic partnerships in the arena of nuclear fuel with other institutions such as INL and UC Berkeley.

High energy diffraction microscopy (HEDM) was used to probe the grain morphology before and after time at elevated temperature to inform microstructural models (e.g. MARMOT) of the growth of grains in specific neighborhoods under operation conditions. X-ray micro-tomography (μT) has been used to characterize the evolution of pores (a key component of the microstructure) both under high temperature and after irradiation. Finally, Small Angle Scattering (SAS) has been used to characterize heterogeneities on nm length scales during manufacture of the fuel and as bubbles develop in fuel that was implanted with Xe atoms as interstitials.

High-Energy Diffraction Microscopy The HEDM technique was developed in parallel by the Suter group at Carnegie Mellon University and by the Poulson group in Denmark to study grain and sub-grain level crystal orientation, strain and defect density. The technique uses a near field area detector to record diffraction spots and directly image grains in a polycrystal based on orientation. To date, the technique has been used on annealed metals with relatively low z-number, e.g. copper, and recently in-situ measurements during deformation (Cu) and annealing (Al and Ni) have been completed.

We have evolved the technique as necessary to study high-Z materials. In particular, we have completed studies of ceramic UO2 as a function of processing and after time at temperature simulating operation conditions. Figures 1a-c show grain maps and grain size distributions in UO2, UO2.11 and UO2.16 material sintered at 1450°C for 4 hours. Note the difference in scale of figure 1a. Clearly, the higher oxygen content leads to larger grain sizes in the as sintered material.

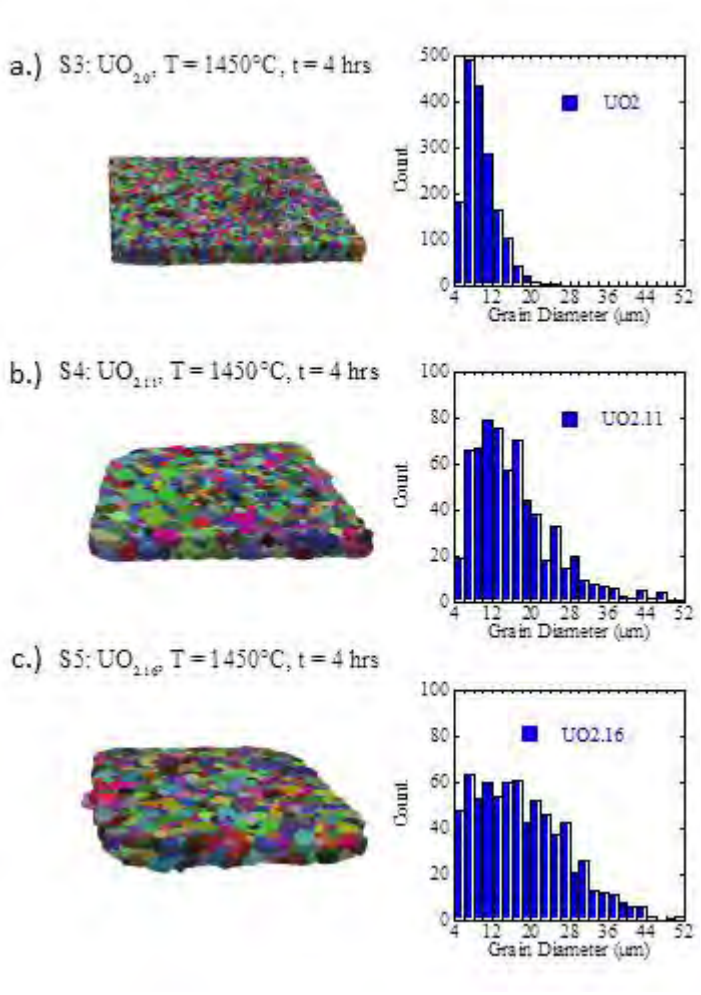

Figure 1. Grain map and grain size distribution for a.) UO2, b.) UO2.11, and c.) UO2.16.

The HEDM technique allows us to pick out specific grains that are, for instance, far in the tails of the grain size distribution to search for the cause of such anomalous grains and evaluate if they have an inordinate control on the properties of the overall sample. Figure 2 shows an inverse pole figure with all of the 20018 identified grains located. The colors are indicative of the size of the individual grains. There is no obvious correlation between grain size and orientation. Six grains have been extracted from the micro-

structure which have sizes of greater that 3x the average grain size. Again, these six grains span the range of orientations, indicating that grain orientation does not play a role in the anomalous growth of these specific grains. A deeper search into the effect of the grain neighborhood effect on the grain growth is ongoing.

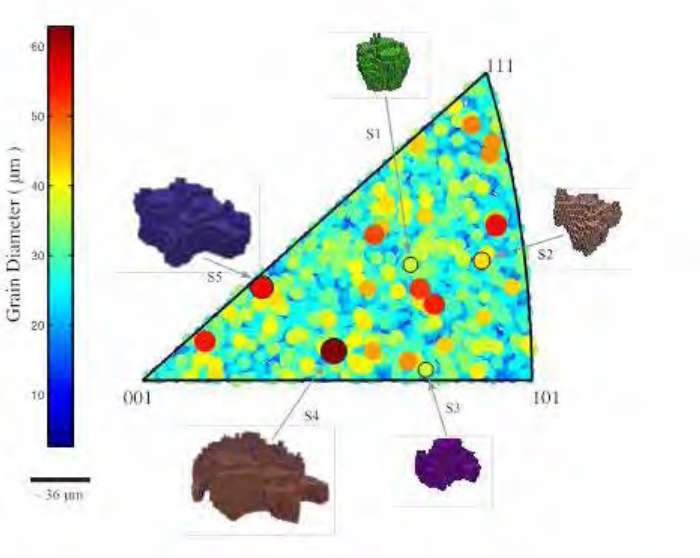

Figure 2. Mapping of the orientations of identified grains on the stereographic projection. The color of each spot (grain) is indicative of the grain size, as per the color bar. Six grains with anomalously large size have been identified and located on the stereograph.

Figure 3 shows grain maps and grain size distribution of UO2 in the as-sintered state and after 3 hours at 1950°C. Grain growth during time at temperature is readily apparent. As above, we are currently searching the local grain morphologies in an attempt to understand the driver for selection of preferred grains for growth. This information will prove critical for the development of models that can predict grain growth, which controls the diffusion of fission gases from the microstructure to the space surrounding the fuel.

Micro-Tomography The pore and crack morphology has been imaged with x-ray µT. Several groups have pushed the limits of µT to sub-micron resolution in some highly optimized cases, but in general, the current resolution limit is ~1-2µm. To study the growth and migration of pores and cracks in UO2, we have pushed this resolution to ~0.7 µm as well as adapt the technique to higher energy incident x-rays. Limitations in scintillator technology prevent further reduction of the resolution at high x-ray energy. Figures 4a and b show (a.) a relatively low resolution (6µm) tomographic slice through an engineering scale (5mm diameter) ceramic nuclear fuel pin as well as (b.) a micrograph of the same area. The x-ray tomograph was collected with 250keV X-rays at the 10BM beamline at the Advanced Photon Source. This clearly demonstrates the ability to non-destructively visualize the interior of a full fuel pellet using high energy x-rays.

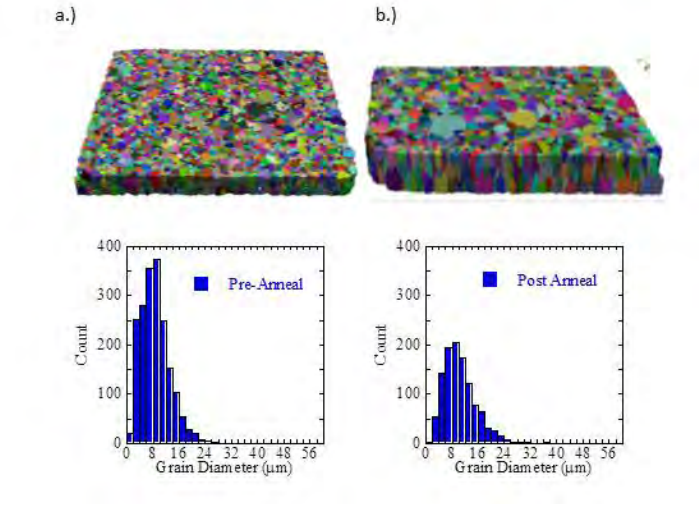

Figure 3. Grain map and grain size distribution for UO2 a.) as-sintered and b.) after 3 hours at 1950C.

Figure 4c shows a very high resolution tomographic slice of a section from a metallic uranium fuel foil after irradiation, demonstrating the ability to characterize very active material. The sample is a monolithic uranium-molybdenum alloy clad aluminum, with a 15 µm thick zirconium interaction barrier separating fuel from the cladding. Each pixel is 0.7µm. The three layers of the sample are clearly evident as are pores that have formed during the irradiation. The failure mechanism of these monolithic fuel plates is debonding of the fuel from the cladding, resulting in bubbles forming on the surface of the fuel and block coolant flow channels. The mT not only probes the possible failure mechanism of the research reactor fuel, it also demonstrates the capability to non-destructively probe highly activated spent fuels.

Small Angle Scattering SAS techniques are well established but application to UO2 at high temperature is novel. Thin film samples (1µm) of UO2 were grown using Ion Bombardment Assisted Deposition (IBAD). A pure UO2 sample was grown as well as samples with 2 and 4 weight percent xenon. The xenon atoms are trapped in the lattice as interstitials in a similar fashion to the xenon produced as a fission product during use. Small Angle Xray Scattering (SAXS) was completed during heating of the samples to monitor the motion of the xenon from individual interstitials to form clusters, voids, bubbles, etc.

Figure 5 shows SAXS data from a.) pure UO2 and b.) UO2 with 4wt% xenon with time at 225°C. The pure UO2

sample shows absolutely no evolution in the scattering over a 4 hour period. In contrast, the 4wt% xenon sample shows an increase of scattering at ~0.02 1/Å in 10's of minutes, which indicates the development of a heterogeneity (presumably bubbles) with a length scale of ~30nm. Transmission electron microscopy (TEM) analysis has just begun. Figure 5c shows elemental maps on a line across the sample. The xenon content fluctuates with a length scale on the order of 10's of nm, consistent with the heterogeneity indicated by the SAXS data. Complete analysis of this data will inform models of the motion of xenon in the microstructure as the release of the xenon from the microstructure is a primary driver in the overall burn-up of the fuel.

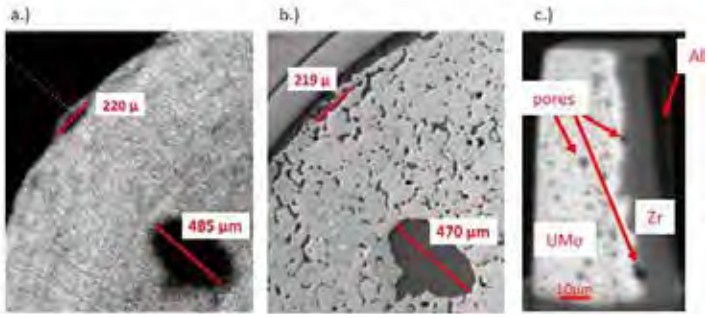

Figure 4. a.) Slice from a tomographic reconstruction of a 5mm diameter UO2 fuel pin. b.) Optical micrograph of same. c.) Tomographic reconstruction of a section of an irradiated metallic (uranium molybdenum) fuel.

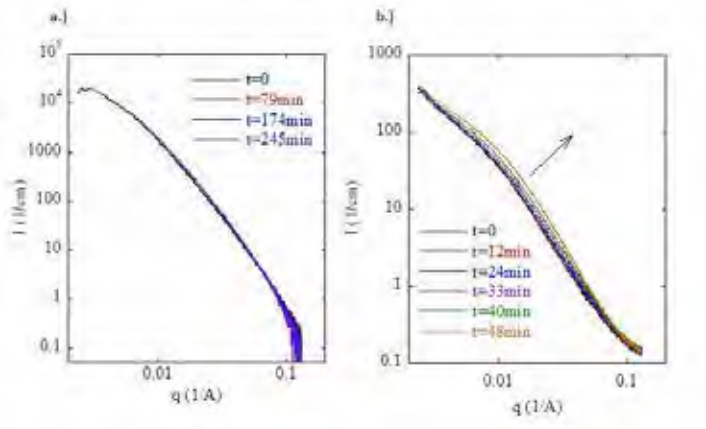

Figure 5. SAXS data collected on (a.) pure UO2 and (b.) Xe implanted UO2 during time at 225°C .

In-Situ Experiments Above is an example of a very successful in-situ x-ray experiment completed as part of this project, i.e. monitoring the microstructure while at temperatures approaching 700°C. While not shown here because of space limitations, in-situ SANS experiments during sintering of UO2 powder to 1200°C were also successfully completed. However, a goal of this project was to complete in-situ HEDM to ~2000°C. At Diamond Light Source, in-situ experiments designed to reach 2000°C were halted at 1500°C when oxide was detected in the diffraction pattern, suggesting (correctly) that the tantalum sample containment had oxidized. The experiments were stopped with no breach of containment. Further development of a boron-nitride container for in-situ experiments occurred. BN was chosen because it is both more stable than refractory metals, and is transparent to high energy x-rays. However, we were unable to demonstrate the robustness of the BN containment to the satisfaction of either the experimental team or the APS radiation safety committee in time for the final experimental run of this project. Because the ramifications of a containment breach on a radioactive sample at a synchrotron light source are considerable, a very conservative approach was taken.

Future Much of what is shown in this report is "preliminary" results which have not been analyzed to the fullest extent. Following the completion of this project, Reeju Pokharel (postdoc) will continue with roughly 0.3FTE of support from the civilian nuclear energy project to finish processing this data as well as continue work on UN/U3Si5 composite fuels. The team is part of multiple proposals to the DOE Office of Nuclear Energy. In 2014, Brown headed an effort from which a full proposal was requested. The proposal was not funded, but has been re-submitted in 2015 with more results and suggested revisions requesting $1M over 3 years. Proposals from Idaho National Lab (metallic uranium fuels) and Advanced Photon Source (cladding) including significant participation from the LANL team have also been submitted.

Impact on National Missions

The work described here-in has provided previously unobtainable microstructural data useful for the CASL, NEAMS and Fuel Cycle R&D programs residing at LANL, as well as the MARMOT code developers at INL (and now Penn State University). Mike Tonks at PSU and Brad Fromm at INL are currently using the 3D microstructures generated with HEDM in the as-sintered state as starting points for predictive calculations. The models will evolve the microstructure under the same conditions achieved in our experiments, to be compared directly to the final microstructures we observed. This provides unprecedented validation opportunities for the code developers.

Publications

Brown, D. W., Balogh, Byler, C. M. Hefferan, J. F. Hunter, Kenesei, S. F. Li, Lind, S. R. Niezgoda, and R. M. Suter. Demonstration of Near Field High Energy X-Ray Diffraction Microscopy on High-Z Ceramic Nuclear Fuel Material. 2014. MECHANICAL STRESS EVALUATION BY NEUTRONS AND SYNCHROTRON RADIATION VII. 777: 112.

Very Low Temperature Scanning Point Contact Spectroscopy Investigation of Inhomogeneous States on the Nano-scale

Roman Movshovich
20130285ER

Abstract

This project aims to push the latest advances in scanned probes techniques to a new state-of-the-art level to address a number of outstanding problems from the "top shelf" issues in condensed matter physics. It combines our expertise in several Scanning Probe Microscopy (SPM) and Spectroscopy (SPS) techniques and a dilution refrigerator, instrumented with a 14 Tesla magnet, to develop a novel Very Low Temperature Scanning Point Contact Spectroscopy (VLTSPCS) apparatus. The VLTSPCS can be used to investigate several outstanding high profile problems in correlated electron physics, where our group at LANL has both demonstrated expertise and world leadership. Point Contact Spectroscopy (PCS) has been used extensively for investigating homogeneous superconducting (SC) states mostly in zero magnetic field. At the interface between the normal tip and superconducting sample, Andreev Reflection (AR) of quasiparticles creates a bound state, which reveals itself as a zero-voltage resonance peak in the dI/dV spectra inside the SC energy gap. Our unique VLTSPCS apparatus will go well beyond state-of-the-art PCS capabilities: sub-nanometer resolution of the PCS combined with the scanning capability and in-situ control of the force between the PCS tip and the sample, high magnetic fields, and very low temperatures will allow us to explore the spatially inhomogeneous states in an unprecedented part of the phase space. Within this proposal we will address some of the hottest topics in correlated electron physics: (1) spatial variation of the energy gap in the postulated Fulde-Ferrell-Larkin-Ovchinnikov [1,2] superconducting state in CeCoIn5 at high fields [3]; (2) direct visualization of the exotic high-field vortex structures, up till now studied only by Small Angle Neutron Scattering (SANS) techniques, e.g., in CeCoIn5 [5,6] and UPt3 [7]; (3) high-field capability will give access to field-tuned Quantum Critical Points (QCP), where some theories predict the breakdown of the quasiparticle concept [8]. We will be able to test this directly, as PCS spectra are sensitive to the sample's local electronic density of states. The unique apparatus developed within this proposal will open new avenues of the correlated electron research, notably within unconventional superconductivity and quantum critical phenomena, an area of LANL's traditional excellence and world leadership

Background and Research Objectives

Our proposal involves a broad spectrum of outstanding topics of research. It is the result of the confluence of new capabilities afforded by the proposed novel VLTSPCS apparatus and our interests, demonstrated by research conducted both at present and in recent past at LANL.

The High-Field Superconducting (HFSC) state of CeCoIn5 [3] is one of the confluences, and will be one of the focal points of this proposal. This state was proposed [3] as realization of a spatially inhomogeneous superconducting state, predicted by Fulde and Ferrell and Larkin and Ovchinnikov (FFLO) [1,2] in the early 1960's.

The FFLO state is a straightforward consequence of the very successful BCS (Bardeen-Cooper-Schrieffer) theory of superconductivity, and a direct outcome of the pair-breaking effect of the magnetic field acting on the spins of the superconducting electrons. In spite of the apparent theoretical simplicity (Fig. 1), an FFLO state was not observed so far, likely due to several stringent requirements on materials and physics aspects needed to support an FFLO state.

Experimental results stimulated great theoretical activity in this field, with diverse scenarios based on attraction or competition between superconductivity and magnetism. A number of theories even suggest that the FFLO state underlies the physics of the HFSC state of CeCoIn5 [14-16]. In particular, enhancement of the normal quasiparticle density of states at the nodes of the FFLO state, where the superconducting energy gap goes to zero, was shown to lead to the formation of the MLRO [15]. On the other hand, there are also theories that do not require

FFLO for formation of the HFSC phase of CeCoIn5. Some of these theories show that MLRO can be a result of coupling of the superconducting and magnetic order, usually with a third fast-spatially-varying (on the order of a unit cell) superconducting order parameter [5,17,18]. Furthermore, pair-breaking along the nodes of the d-wave superconductor by a magnetic field due to the Zeeman effect was also shown to lead to MLRO [19].

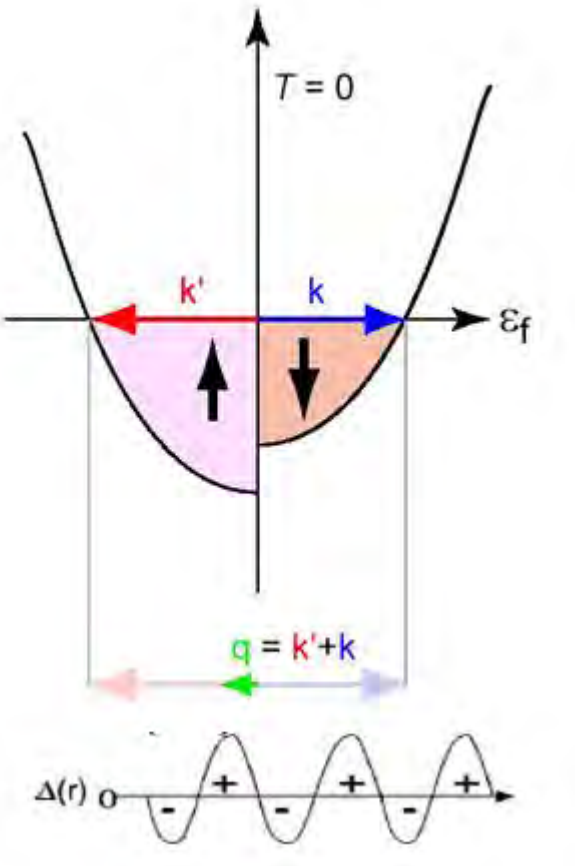

Figure 1. Zeeman splitting of the spin up and spin down bands leads to a finite momentum of superconducting Cooper pairs of electrons with opposite spins, resulting in the spatially varying energy gap D() with nodal (D() =0) planes perpendicular.

Whether or not the FFLO physics plays an important role in the formation of the HFSC state, the MLRO state is unique in its own right: magnetism is confined to the superconducting state, and disappears when CeCoIn5 is driven into the normal state with increasing magnetic field or temperature. These properties are contrary to the canonical paradigm of competition between superconductivity and magnetism. Therefore, the HFSC state in CeCoIn5 is a new exotic state of matter and understanding it is of paramount importance.

Bulk measurements, whether thermodynamic, transport, or spectroscopic (NMR and neutron scattering), so far have failed to provide a definitive “smoking gun” result either for or against an FFLO state. We will resolve this controversy by directly visualizing the spatial variation of the superconducting energy gap on the sub-nanometer scale, using the VLTSPCS apparatus to be developed within this proposal (details below).

The VLTSPCS apparatus will enable the visualization of vortex lattices in high magnetic fields, a table-top capability complimentary to the Small Angle Neutron Scattering (SANS). The VLTSPCS will fill several niche applications, for example, in cases where no large samples are available (required for SANS), or for studies of thin films. The PCS couples directly to the quasiparticles in the SC state and thus to the superconducting order parameter. Therefore, the contrast at high fields will be much greater than in SANS experiments that couples to variations of the magnetic field only.

The significance of such apparatus itself cannot be overestimated. The combination of a dilution refrigerator with a new 14 T superconducting magnet, a scanning platform for a variety of surface probes options, including conventional Magnetic Force Microscopy (MFM), Atomic Force Microscopy (AFM), and Kelvin Force Microscopy (KFM), and the technical focus of this proposal - an innovative Scanning Point Contact Spectroscopy (SPCS) probe, capable of probing the magnitude of the superconducting energy gap on the sub-nanometer scale – is unique. It will open a vast experimental phase space and a new capability to interrogate correlated electrons at very low temperatures and high fields, and help assure the continued preeminent position of LANL in this research field.

Scientific Approach and Accomplishments

The phase space occupied by the HFSC phase of CeCoIn5 presents formidable challenges of very low temperatures (below 300 mK) and high magnetic fields (up to 12 T). Probing the spatial dependence of the SC energy gap in CeCoIn5, visualizing the vortex lattice, or the SC energy gap around an impurity, requires a scanned probe capability. The STM is a powerful tool that has been used to investigate a number of unconventional superconductors, such as BSCCO, a high-temperature copper-oxide superconductor. However, no STM system exists that satisfies the extreme requirements listed above (the field range; the tunneling current in existing STMs is always parallel to the direction of the magnetic field, contrary to some of our measurement requirements, see below). The STM is extremely sensitive to the sample surface quality and cleanliness. In addition, atomic resolution of STM imposes stringent requirements on the control of the distance between the STM tip and the substrate, since the tunneling current is exponentially sensitive to the probe-sample separation.

Therefore the STM is very sensitive to the mechanical vibrations and electrical noise in the system. The superior atomic resolution of the STM is not required, however, to achieve our goals, since the characteristic length scales of the FFLO state, vortex separation, and impurity-induced suppression of the SC energy gap are all on the order of the superconducting coherence length ξ ≈ 2-10 nm. The sub-nanometer spatial resolution of the PCS is therefore fully sufficient to achieve our experimental goal. The SPCS will employ the Contact-mode Atomic Force Microscopy (CAFM) technique. It presents us with a perfect compromise: the spatial resolution will increase to sub-nm range (still satisfying the experimental requirements), with a benefit of drastically reduced sensitivity to surface cleanliness and preparation and to mechanical and electrical noise. The "lower tech" SPCS presents us with the best tool to address the science objectives within this proposal.

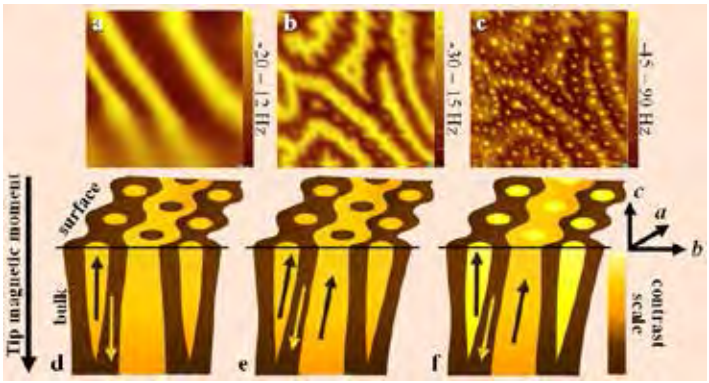

Figure 2. Magnetic domain structure of FeGeTe observed with MFM for the (a) (101) surface (lift height = 300 nm). (b) (001) surface for a lift height 1,500 nm. (c) (001) surface for a lift height of 600 nm. All MFM images, a - c, were taken at the same scanning size (28 × 28 μm) and experimental conditions (zero field cooled; T = 4.0 K; P the schematic) (d) schematic of the domain structure near the surface of uniaxial ferromagnets, where the c-axis is the magnetic easy axis, showing how the branching of bulk stripe domains of alternating magnetization near the sample edge results in a surface magnetic structure consisting of wavy stripes with rows of dagger domains with the opposite magnetization; (e) the unperturbed FeGeTe microstructure where the easy axis is tilted away from the c-axis and only two MFM contrast states (indicating only two domain magnetization directions) are observed, and (f) the microstructure observed with MFM for lift heights ≤ 600 nm due to influence of the field H of cantilever on the sample, creating a third magnetization direction and an MFM contrast.

Within experimental part of the proposal the focus was on developing MFM expertise of Dr. Neliza Leon Brito – a postdoc who started to work on this project in December 2013. Neliza needed to become an expert in operation of MFM, crucial for development of the SPCS technique. She ran MFM in several modes, successfully performing Meissner force technique penetration depth measurements, and imaging of the ferromagnetic domains. This resulted in three recent articles on the details of formation and evolution of the ferromagnetic domains in electron correlated materials (two submitted), see the publication section of the report.

Dr. Neliza Leon Brito was hired to take over from Dr. Jeehoon Kim, who left the project to take a professor position in Postech, South Korea. Neliza came with experience in designing and building a Scanning Hall Microscopy, for Alex de Lozanne group in University of Texas, Austin, the same group where Dr. Jeehoon Kim obtained his Ph.D.

First, to get up to speed with MFM technique, Dr. Leon Brito used Meissner technique of measuring magnetic penetration depth in several pnictide superconductors of interest (and Nb, our standard for these measurements). These experiments require fine field control, and ability to take cantilever response at a single point over the sample.

Next step was to extend the operation of the MFM apparatus into scanning mode and for Neliza to acquire this expertise, a necessary part of the SPCS technique. Subsequent MFM investigations focused on several ferromagnetic (FM) compounds, and in particular, an easy-axis ferromagnet Fe3GeTe2. For the easy-axis FM compound the expected domain structure observed on the surface perpendicular to the easy axis display a very characteristic domain branching structure (see Figure 2(d)), where the large domains in the bulk of the material break up into smaller and smaller domains as they approach the surface, thereby reducing the leakage (or stray) field outside of the sample and lowering the total magnetic energy of the system. One expects just two dominant magnetizations of the domains: up and down. The resulting color image of the surface would correspondingly be expected to have two dominant colors (contrasts), consistent with the image shown in Figure 2(b). Instead, we observed that the smallest "dagger" domains (seen as dots within the stripe domains) became bright color, indicating repulsion of the cantilever from the sample, as shown in Figure 2(c). This effect appeared only when the lift height of the cantilever (distance above the surface) was reduced below a critical value. Two possible scenarios need to be considered: (1) MFM magnetic tip flips the smallest domains of the sample, illustrated in Figures 2(e,f) or (2) the stray field from the sample is large enough to flip the magnetization of the tip of the MFM cantilever (so called soft cantilever regime). We initiated a collaboration on the modeling of the MFM signal (in this case the resonant frequency of the magnetic cantilever, which is proportional to the second gradient of magnetic field) in a complicated geometry of the surface branching domains, with Dr. Denis Pelekhov of the Ohio State University. One simulation for a cantilever lift height

of 600nm is shown in Figure 3. Such simulations point towards the second scenario (cantilever direction is influenced by the sample's stray field) as the most likely one, but not completely, as the cantilever's behavior is somewhere between the soft and hard regimes. These results are being written up two papers, one focusing of physical properties of Fe3GeTe2, and another on general subtleties of the MFM investigation of magnetic compounds, and a great care that needs to be taken while interpreting MFM data. This paper will be of significant value to the scanning probes community.

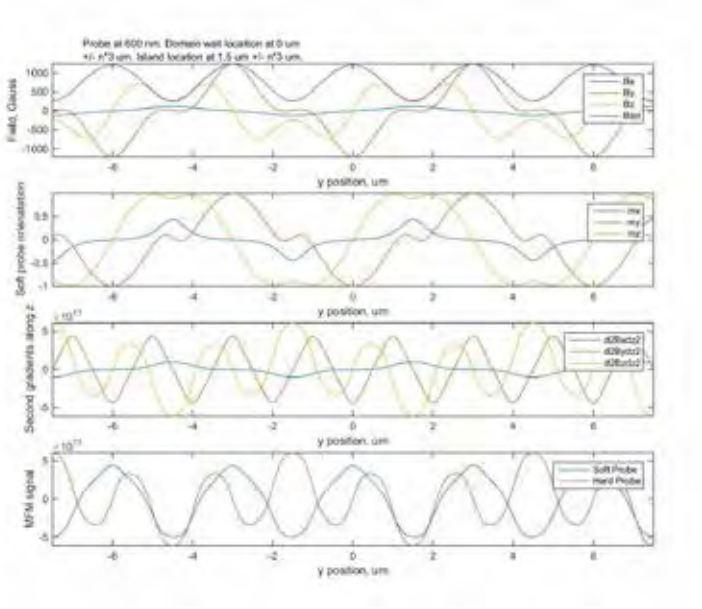

Figure 3. Micro-magnetic LLG simulations of a model sample system, with stripes of alternating up-down magnetization perpendicular to the sample's surface, with small cylindrical islands in the middle of the all stripes and regularly spaced along them. The top graph gives the total stray field of the sample, next is the orientation of the soft cantilever that follows the direction of the resulting combined magnetic field. Second graph from the bottom gives a second gradient of field components along the z-direction, which determines the forces on the MFM tip. The bottom graph shows the expected MFM signal (proportional to the second derivative of field along z) for soft (magnetization follows the direction of the external field) and hard (magnetization is constant, parallel to z-axis).

On the theory side, the objective was to explore the question of how the FFLO state will be revealed by SPCS. Our combined expertise in both FFLO physics [18] and PCS of heavy-fermion superconductors [19] enables the modeling of the SPCS spectra and extraction of the superconducting energy gap in scanned mode of operation, when the point contact parameters may vary during the surface scan. The model calculations include the effects of high magnetic fields and strong Pauli limiting of CeCoIn5 on the SPCS spectra.

We continue a strong collaboration with Pr. Jeehoon Kim from Postech, Korea, who is continuing the work of developing low temperature SPCS that he started as a postdoc here at LANL. We have hosted several of his students, and exchanged samples and components. In particular, he supplied us with several home-made platinum point contact cantelevers. This collaboration resulted in several publications, one to be submitted to Nature Physics (see publication section of the progress report).

Theoretically, previous studies of various aspects of unconventional heavy-fermion superconductivity, such as the FFLO state, vortex state and tunneling into the HFSC have thoroughly prepared us for this project. We developed theoretical modeling capabilities to tackle the spatially nonuniform FFLO state [22] as well as vortex state [4] in unconventional superconductors. More recently, we developed a multi-channel tunneling model for point-contact spectroscopy (PCS) in heavy-fermion systems and applied it to CeCoIn5 [23,24]. This unique problem presented several challenges, as the available PCS data on heavy fermion compounds cannot be fitted by the standard BTK (Blonder-Tinkham-Klapwijk) theory of PCS, which was extremely successful for conventional superconductors. It turned out, for example, that one needed to account for the localized states at the surface, as well as for both heavy electron (correlated) and light electron bands. The quantum interference between localized and itinerant electrons sufficed to describe the asymmetric (Fano) line shape of the differential conductance. Detailed modeling was required to extract the Fano and superconducting parameters of interest from measured dI/dV spectra, such as the superconducting energy gap and energy level of the localized f-electron state. That work demonstrated that a full understanding of the SPCS data and extraction of relevant physics (energy gap and other parameters) requires state-of-the-art modeling capabilities of surfaces within a multi-channel model for electrons hopping from the tip to the sample. Based on the previous expertise we have accomplished the following within the theoretical component of this project:

1) We derived an analytic formulation of the tunneling conductance in the normal state based on our multi-channel point-contact tunneling model for heavy-fermion materials. This new formulation provides a great simplification over previous formulations and allows us to better understand qualitatively the normal state properties of electrons tunneling from a metallic tip into a heavy-fermion metal beyond numerical results. We will continue with our efforts of the construction of a tunneling Hamiltonian that incorporates the magnetic field, correlations effects, and other ordered states, such as a spin-density wave.

2) We investigated the evolution of the spectral function,

tunneling density of states of quasiparticles, and the local magnetic penetration depth in doped 122 iron pnictide superconductors. Since our main interest is toward scanned probes, a special emphasis was given to the local effects in the presence of a single Zn impurity and the overall suppression of superconductivity at arbitrary impurity concentrations.

Technical details

We introduced a two-channel tunneling model to generalize the widely used BTK (Blonder-Tinkham-Klapwijk) theory of point-contact conductance between a normal metal contact and superconductor. Tunneling of electrons can occur via localized surface states or directly, resulting in a Fano resonance in the differential conductance G=dI/dV. We presented an analysis of G within the two-channel model when applied to soft point-contacts between normal metallic silver particles and prototypical heavy-fermion superconductors CeCoIn5 and CeRhIn5 at high pressures. In the normal state the Fano line shape of the measured G was well described by a model with two tunneling channels and a large temperature-independent background conductance (see Figure 4). In the superconducting state a strongly suppressed Andreev reflection signal was explained by the presence of the background conductance. We reported Andreev signal in CeCoIn5 (shown in Figure 5) consistent with standard d_(x2-y2)-wave pairing, assuming an equal mixture of tunneling into [100] and [110] crystallographic interfaces. Whereas in CeRhIn5 at 1.8 and 2.0 GPa the signal was described by a d_(x2-y2)-wave gap with reduced nodal region, i.e., increased slope of the gap opening on the Fermi surface. The is a possibility is that the shape of the high-pressure Andreev signal is affected by the proximity of a line of quantum critical points that extends from 1.75 to 2.3 GPa, which is not accounted for in our description of the heavy-fermion superconductor.

Recent experiments on Zn-doped 122-type iron pnictides, Ba(Fe,Co,Zn)2As2, challenged our understanding of electron doping the 122s and the interplay between doping and impurity scattering. To resolve this enigma, we investigated the disorder effects of nonmagnetic Zn impurities in the strong (unitary) scattering limit on various properties of the system in the s+- wave superconducting pairing state. The lattice Bogoliubov–de Gennes equation (BdG) was solved self-consistently based on a minimal two-orbital model with an extended range of impurity concentrations. We found that Zn impurity is best modeled as a defect, where charge is mainly localized, but scattering is extended over a few lattice sites. With increasing Zn concentration, the density of states showed a gradual filling of the gap, revealing the impurity-induced pair-breaking effect. Moreover, both the disorder configuration-averaged superconducting order parameter and the superfluid density were dramatically suppressed toward the dirty limit, indicating the violation of the Anderson theorem for conventional s-wave superconductors and the breakdown of the Abrikosov-Gorkov theory for impurity-averaged Green's functions. Furthermore, we found that the superconducting phase was fully suppressed close to the critical impurity concentration of roughly n_(imp) ≈ 10%, in agreement with recent experiments.

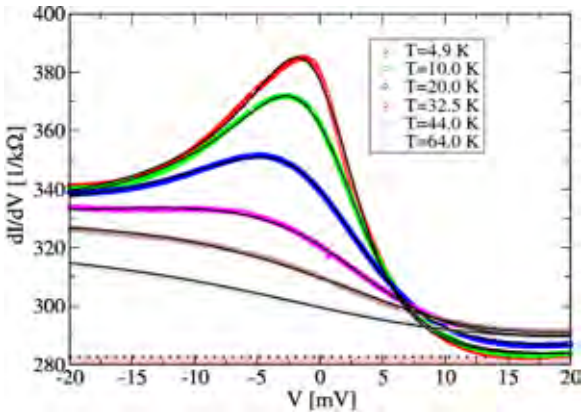

Figure 4. Fitting the Fano line shape of CeCoIn at ambient pressure in the normal state. The transparency D = 0.210 is in the tunneling rather than high transparency limit. The solid (black) lines are fits with constant background conductance G0 = 282.6 (kΩ), which is shown as red-shaded background.

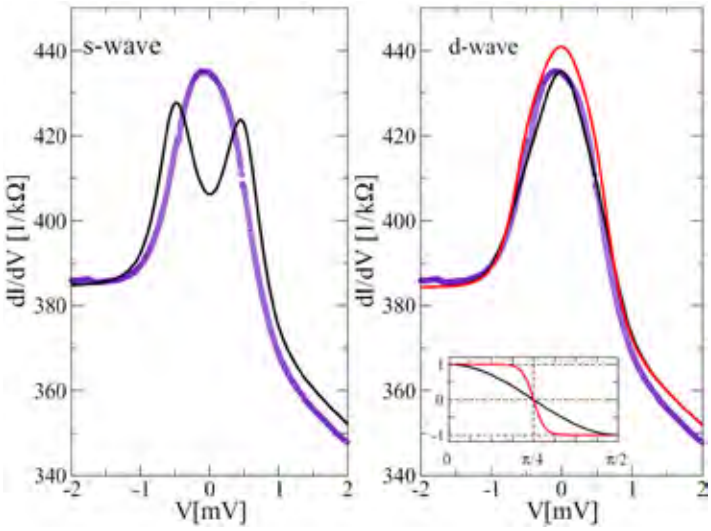

Figure 5. Fitting the Andreev signal of CeCoIn in the superconducting state at ambient pressure and at 1.31 K with = 23K. We assumed isotropic -wave gap (left) and -wave gap (right). The wave is plotted for standard (black) and five times steeper (red) slope of the gap at nodes with equal weight of tunneling into [100] (0°) and [110] (45°) surface orientations. Inset: angle dependence of the gap function.

Impact on National Missions

This project supports several BES programs: Novel Materials (PI Joe D. Thompson) and Vortex Physics (PI- L. Civale).

It will open new areas of research in the areas of the Strongly Correlated Electron Physics, magnetism, and general superconductivity. This project supports both themes of Emergent Phenomena and Defects and Interfaces, two of the three areas of the Materials Strategy at LANL.

References

1. FULDE, P., and R. A. FERRELL. SUPERCONDUCTIVITY IN STRONG SPIN-EXCHANGE FIELD. 1964. PHYSICAL REVIEW. 135 (3A): A550.

2. LARKIN, A. I., and Y. N. OVCHINNI. INHOMOGENEOUS STATE OF SUPERCONDUCTORS. 1965. SOVIET PHYSICS JETP-USSR. 20 (3): 762.

3. Bianchi, A., R. Movshovich, C. Capan, P. G. Pagliuso, and J. L. Sarrao. Possible Fulde-Ferrell-Larkin-Ovchinnikov superconducting state in CeCoIn5. 2003. PHYSICAL REVIEW LETTERS. 91 (18).

4. Young, B. -., R. R. Urbano, N. J. Curro, J. D. Thompson, J. L. Sarrao, A. B. Vorontsov, and M. J. Graf. Microscopic evidence for field-induced magnetism in CeCoIn5. 2007. PHYSICAL REVIEW LETTERS. 98 (3).

5. Kenzelmann, , Straessle, Niedermayer, Sigrist, Padmanabhan, Zolliker, A. D. Bianchi, Movshovich, E. D. Bauer, J. L. Sarrao, and J. D. Thompson. Coupled superconducting and magnetic order in CeCoIn(5). 2008. SCIENCE. 321 (5896): 1652.

6. Kenzelmann, , Gerber, Egetenmeyer, J. L. Gavilano, T. h. Straessle, A. D. Bianchi, Ressouche, Movshovich, E. D. Bauer, J. L. Sarrao, and J. D. Thompson. Evidence for a Magnetically Driven Superconducting Q Phase of CeCoIn5. 2010. PHYSICAL REVIEW LETTERS. 104 (12).

7. Gannon, W. J., W. P. Halperin, Rastovski, M. R. Eskildsen, Dai, and Stunault. Magnetization in the superconducting state of UPt3 from polarized neutron diffraction. 2012. PHYSICAL REVIEW B. 86 (10).

8. Si, Q. M., S. Rabello, K. Ingersent, and J. L. Smith. Locally critical quantum phase transitions in strongly correlated metals. 2001. NATURE. 413 (6858): 804.

9. Koutroulakis, , M. D. Stewart Jr., V. F. Mitrovic, Horvatic, Berthier, Lapertot, and Flouquet. Field Evolution of Coexisting Superconducting and Magnetic Orders in CeCoIn5. 2010. PHYSICAL REVIEW LETTERS. 104 (8).

10. Kakuyanagi, K., M. Saitoh, K. Kumagai, S. Takashima, M. Nohara, H. Takagi, and Y. Matsuda. Texture in the superconducting order parameter of CeCoIn5 revealed by nuclear magnetic resonance. 2005. PHYSICAL REVIEW LETTERS. 94 (4).

11. Kumagai, , Shishido, Shibauchi, and Matsuda. Evolution of Paramagnetic Quasiparticle Excitations Emerged in the High-Field Superconducting Phase of CeCoIn5. 2011. PHYSICAL REVIEW LETTERS. 106 (13).

12. Tokiwa, , Movshovich, Ronning, E. D. Bauer, Papin, A. D. Bianchi, J. F. Rauscher, S. M. Kauzlarich, and Fisk. Anisotropic effect of Cd and Hg doping on the Pauli limited superconductor CeCoIn(5). 2008. PHYSICAL REVIEW LETTERS. 101 (3).

13. Ikeda, . Impurity-induced broadening of the transition to a Fulde-Ferrell-Larkin-Ovchinnikov phase. 2010. PHYSICAL REVIEW B. 81 (6).

14. Miyake, . Theory for Coupled SDW and Superconducting Order in FFLO State of CeCoIn5. 2008. JOURNAL OF THE PHYSICAL SOCIETY OF JAPAN. 77 (12).

15. Yanase, , and Sigrist. Antiferromagnetic order in the FFLO state. 2009. In 25TH INTERNATIONAL CONFERENCE ON LOW TEMPERATURE PHYSICS (LT25), PT 5A. Vol. 1505a Edition.

16. Ikeda, , Hatakeyama, and Aoyama. Antiferromagnetic ordering induced by paramagnetic depairing in unconventional superconductors. 2010. PHYSICAL REVIEW B. 82 (6).

17. Agterberg, D. F., Sigrist, and Tsunetsugu. Order Parameter and Vortices in the Superconducting Q Phase of CeCoIn5. 2009. PHYSICAL REVIEW LETTERS. 102 (20).

18. Aperis, , Varelogiannis, P. B. Littlewood, and B. D. Simons. Magnetic Properties of an Antiferromagnetic d-Wave Singlet and pi-Triplet Superconductor. 2009. JOURNAL OF SUPERCONDUCTIVITY AND NOVEL MAGNETISM. 22 (2): 115.

19. Suzuki, K. M., Ichioka, and Machida. Theory of an inherent spin-density-wave instability due to vortices in superconductors with strong Pauli effects. 2011. PHYSICAL REVIEW B. 83 (14).

20. Bianchi, A. D., Kenzelmann, DeBeer-Schmitt, J. S. White, E. M. Forgan, Mesot, Zolliker, Kohlbrecher, Movshovich, E. D. Bauer, J. L. Sarrao, Fisk, Petrovic, and M. R. Eskildsen. Superconducting vortices in CeCoIn5: Toward the Pauli-limiting field. 2008. SCIENCE. 319 (5860): 177.

21. Das, , J. S. White, A. T. Holmes, Gerber, E. M. Forgan, A. D. Bianchi, Kenzelmann, Zolliker, J. L. Gavilano, E. D.

Bauer, J. L. Sarrao, Petrovic, and M. R. Eskildsen. Vortex Lattice Studies in CeCoIn5 with H perpendicular to c. 2012. PHYSICAL REVIEW LETTERS. 108 (8).

22. Vorontsov, A. B., J. A. Sauls, and M. J. Graf. Phase diagram and spectroscopy of Fulde-Ferrell-Larkin-Ovchinnikov states of two-dimensional d-wave superconductors. 2005. PHYSICAL REVIEW B. 72 (18).

23. Fogelstrom, , W. K. Park, L. H. Greene, Goll, and M. J. Graf. Point-contact spectroscopy in heavy-fermion superconductors. 2010. PHYSICAL REVIEW B. 82 (1).

24. Park, W. K., and L. H. Greene. Andreev reflection and order parameter symmetry in heavy-fermion superconductors: the case of CeCoIn(5). 2009. JOURNAL OF PHYSICS-CONDENSED MATTER. 21 (10).

Publications

Chen, H., Y. Y. Tai, C. S. Ting, M. J. Graf, D. Jianhui, and J. Zhu. Disorder effects in multiorbital s(+/-)-wave superconductors: Implications for Zn-doped BaFe2As2 compounds. 2013. PHYSICAL REVIEW B. 88 (18): 184501.

Fogelstrom, , M. J. Graf, V. A. Sidorov, X. i. n. Lu, E. D. Bauer, and J. D. Thompson. Two-channel point-contact tunneling theory of superconductors. 2014. PHYSICAL REVIEW B. 90 (10).

Jeong, , Yang, Yang, O. E. Ayala-Valenzuela, Wulferding, J. -. Zhou, J. B. Goodenough, de Lozanne, J. F. Mitchell, Leon, Movshovich, Y. H. Jeong, H. W. Yeom, and Kim. Magnetic domain tuning and the emergence of bubble domains in the bilayer manganite La2-2xSr1+2xMn2O7 (x=0.32). 2015. PHYSICAL REVIEW B. 92 (5).

Kim, , Haberkorn, Kim, Civale, P. C. Dowden, and Movshovich. Ferromagnetic bubble clusters in Y0.67Ca0.33MnO3 thin films. 2013. APPLIED PHYSICS LETTERS. 102 (19).

Kim, J., N. Haberkorn, K. Gofryk, M. J. Graf, L. Civale, F. Ronning, A. S. Sefat, and R. Movshovich. Intrinsic superconducting properties and vortex dynamics in heavily overdoped Ba(Fe0.86Co0.14)2As2 single crystal. 2015. Solid State Communications. 201: 20.

Leon-Brito, N., E. D. Bauer, F. Ronning, J. D. Thompson, and R. Movshovich. Study of magnetic microstructure of Fe3GeTe2 using magnetic force microscopy. Apllied Physics Letters.

Leon-Brito, N., E. D. Bauer, F. Ronning, J. D. Thompson, and R. Movshovich. Surface magnetometry of Fe3GeTe2 via magnetic force microscopy. Journal of Physics: Condensed Matter.

Pan, , Li, Tai, M. J. Graf, Zhu, and C. S. Ting. Evolution of the Fermi surface topology in doped 122 iron pnictides. 2013. PHYSICAL REVIEW B. 88 (21).

Yang, J., I. Yang, D. Wulferding, S. Chung, R. Movshovich, H. W. Yeom, K. S. Kim, and J. Kim. Confinement of projective vortices via an extra dimension. Nature Physics.

Excited State Quantum Interactions in Carbon Nanotubes

Stephen K. Doorn
20130309ER

Abstract

This project was motivated by two unexpected discoveries revealed in our work at LANL. The first was the discovery of strong asymmetries in the Raman excitation profiles of carbon nanotubes (CNTs), when previous expectations were that no such asymmetries should exist. The second was the discovery of strong quantum interference effects occurring between closely spaced electronic levels of CNTs. Our project goals were to study these behaviors in depth to develop an understanding of the origins and CNT structural (or (n,m)) dependence of these behaviors. We also wished to explore the consequences these behaviors may have for other photophysical responses of CNTs. As a result of this project, we significantly advance the state-of-the-art in CNT separations for isolation of specific (n,m) species. We established the metallicity, excited-state, and diameter dependences of the REP asymmetry behavior. We developed a robust model for the asymmetries showing they originate in non-Condon behaviors as a result of state-mixing of different exciton levels. We revealed the (n,m) dependence of several new vibrational modes of CNTs. And finally, we probed and accurately modeled the excited state dynamics of model ring compounds that served as molecular mimics of CNTs. The implications of these results are far reaching. They further demonstrate the importance of access to pure (n,m) samples for revealing new CNT behaviors. Our understanding of fundamental optical processes in the nanotubes is greatly strengthened. We have also significantly strengthened LANL capabilities for theory and experimental probing of photonic behaviors at the nanoscale. Together, these results form a robust basis for future efforts targeting emerging applications of nanotube optics.

Background and Research Objectives

Our recent first-time demonstration of quantum interference [1] and violation of the Condon approximation [2] in carbon nanotubes (CNTs) overturns long-held assumptions regarding their optical response and opens the way for new quantum physics to be explored in these systems. In particular, Raman excitation profiles (REPs) of pure, single-nanotube chirality samples, demonstrated for the first time two peaks in the REPs. These corresponded to the long-expected incoming and outgoing resonances. Surprisingly, however, the outgoing resonance was significantly weaker than the incoming (Figure 1), as a consequence of non-Condon effects. While these fundamental behaviors are fascinating by themselves, they have the potential to alter relaxation pathways and dynamics underlying anticipated applications in photonics, optoelectronics and energy harvesting. It is therefore important to understand both the origins and consequences of these phenomena in CNTs. Our goal was to understand how the interplay of electronic and vibrational structure in CNTs gives rise to non-Condon and interference behaviors and determine what consequences they hold for observed photophysical responses.

We focused on three objectives:

1) Non-Condon Behaviors were probed for multiple nanotube structures, vibrational modes, and excited states using Raman and modeled with quantum chemical theory and condensed matter approaches to gain an understanding of their origins.

2) We advanced the state of the art in nanotube purification to access more tube structures and to enable extensive probing of other phonon mode behaviors to contrast to those exhibiting the non-Condon response.

3) Relaxation Pathways and Dynamics were probed in model systems using time-resolved spectroscopies to learn the fate of optical excitations as determined by phonon-mediated electronic state interactions.

Each of these focal areas represents pioneering studies that open significant new areas of CNT physics for further investigation. No other molecular or condensed-

matter system offers the ability to study non-Condon and interference behaviors in such a controlled and systematic way and the information gained impacts our understanding of photophysical behaviors of broad classes of optical materials and serves as a bridge between molecular and condensed matter systems.

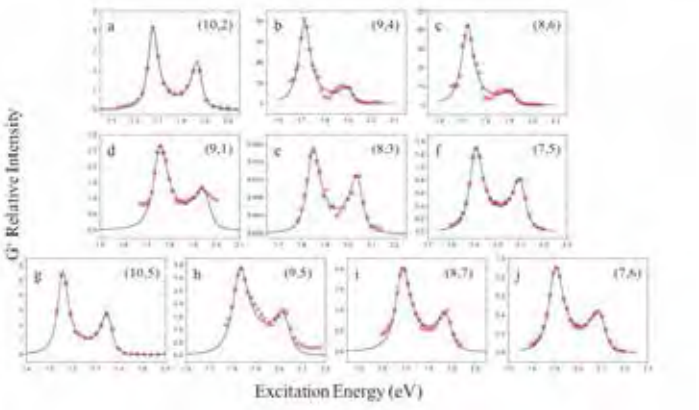

Figure 1. Example Raman excitation profiles of the LO mode for several semiconducing carbon nanotube structures. REPs show two peaks arising from incoming and outgoing resonances. Clear asymmetry is seen, with the outgoing resonance peak always being weaker.

Scientific Approach and Accomplishments

Generation of targeted nanotube structures

To meet our goals, advances in nanotube separations needed to be made. These provided specific new chiralities while efficiently generating large quantities (up to mL scale) of enriched material. We established a new technique based on aqueous two-phase separation concepts that allow rapid separation and efficient scale-up of targeted chiralities [3]. We produced up to 10+ mL scale volumes of new armchair metallic species ((8,8), (7,7), (6,6), and (5,5)), for metallic studies, advances in large-diameter separations (a particularly difficult range intended to give (10,5), (10,2), (12,4) for pump probe and interference studies) [4], novel non-armchair metallics ((10,4), (7,4)) for interference work and (7,5) and (7,6) for our work on isotopically substituted tubes. Isotopically enriched (10,5) tubes produced via a selective polymer suspension technique were also available. Finally, we also pushed the ability to generate new small-d and intermediate diameter chiralities (including (5,4), (10,0), and (11,0) structures) at the extremes of the diameter and chiral angle distributions of our samples.

Such a broad range of structures is an unprecedented range of pure chiralities. These were essential for generating the high quality Raman excitation profiles in our studies. They allowed probing the limits of chirality-dependent quantum behaviors. They also were critical for establishing new unambiguous information on (n,m) dependent frequencies of additional modes not previously accessible.

Origins, Transition Level, and Structural Dependences of Non-Condon Behavior

With our advances in separations we had the opportunity to significantly expand our Raman excitation profile (REP) data beyond the original work on semiconductors [2]. We produced REPs for four so-called "armchair" metallic structures ((8,8), (7,7), (6,6), (5,5); diameter of 0.68 to 1.09 nm) [5]. In all cases significant REP asymmetry was demonstrated (Figure 2), extending our observed trends to metallic tubes and further cementing our finding that the behavior is intrinsic and is a general behavior across all nanotube types (semiconducting and metallic species). The high quality of the new metallic REPs, paired with previous semiconducting results, allowed us to definitively demonstrate the asymmetry weakens as diameter decreases.

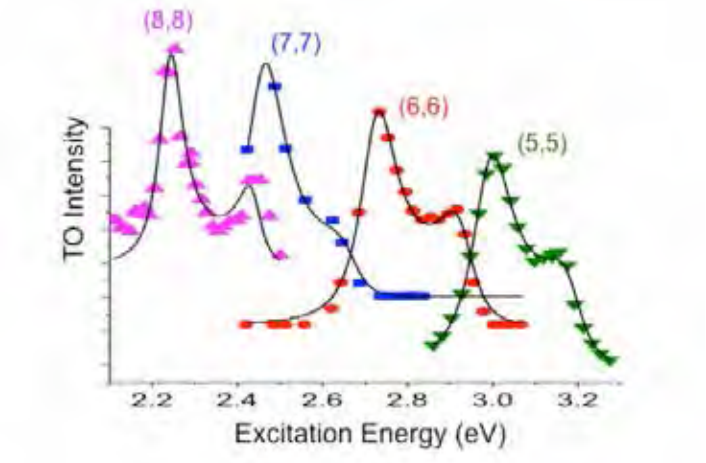

Figure 2. Raman excitation profiles of the TO mode for the (5,5), (6,6), (7,7), and (8,8) armchair metallic nanotube structures. All REPs show an asymmetry similar to that found for semiconducting nanotubes.

Through a collaboration with Eduardo Barros of MIT, we also generated a theoretical description of the REP behaviors that bridged the molecular picture of the result being a non-Condon effect with an approach based on condensed matter theory. We contrasted our results with a competing condensed-matter theory [6] that suggested the asymmetries arise solely as a consequence of features of the nanotube density of states. While we showed this approach can describe our diameter-dependent trends, it is inadequate to describe the magnitude of the asymmetries. As an alternative we have developed a description that combines molecular concepts with condensed matter that shows the asymmetries arise as the result of mixing of transition density between allowed and forbidden exciton states. Such a result is a type of non-Condon effect, thus confirming the originally suggested basis for the observed

asymmetries. The flexible approach is also general to semiconductors (see below). Significantly, the approach is also testable and provides a route to understand the varying effects observed for different transition levels and for different phonon modes.

Transition Energy and Phonon Dependence of REP Asymmetry in Semiconductors

We have established the degree of REP asymmetry in semiconductors for a wide range of chiralities across the first 4 exciton excited states and for the radial breathing mode (RBM), G- (or TO) and G+ (or LO) modes. For transition level dependence, we find that the asymmetry in the lowest transition is weakened for the G modes, and disappears for the RBM (Figure 3). We also always find the TO mode displays a stronger asymmetry than is found for the LO mode [2]. We have recently added data for our smallest diameter nanotube (the (5,4)) to this set and find asymmetry for all modes nearly disappears, which adds significant weight to our assertion that smaller diameter tubes give weaker effects.

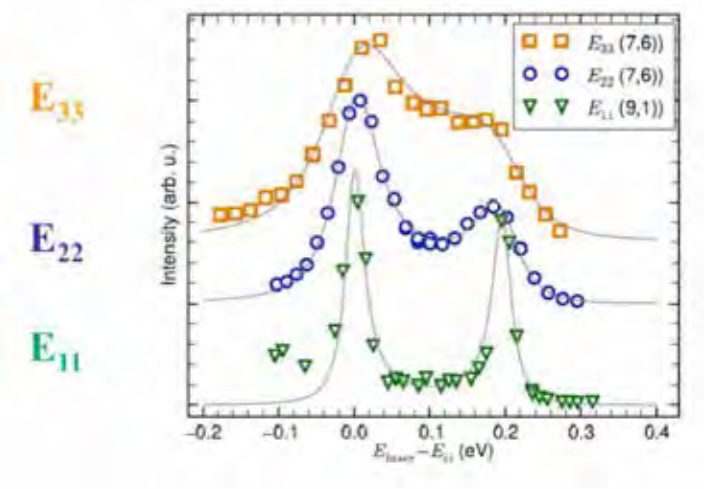

Figure 3. A comparison of how REP asymmetry for the G-mode evolves on going from E11 to E22 to E33. E11 shows the weakest asymmetry.

A theoretical description for understanding these trends had been lacking, but as an extension of the work on armchair structures we have demonstrated the generality of the condensed matter state-mixing approach to non-Condon modeling to include the semiconductor structures. Of significance, we demonstrate the excitonic nature of the optical transitions plays a significant role in the origins of the behavior. State-mixing surprisingly evolves from the strongest allowed excitonic transitions. The modeling results converge on a description that involves mixing of weakly allowed states associated with phonon sidebands. The theory is beginning to have predictive power, suggesting that the closer the phonon mode is in frequency to the energy mismatch between the two mixing exciton states, the stronger the asymmetry will be. This accurately describes the trends we observe for phonon behaviors. The results also suggest that isotopic substitution should modulate the observed asymmetries. This prediction is being tested in the last weeks of this project. We are finishing REP measurements on C13 isotopically substituted nanotubes of the (7,5), (7,6), and (10,5) structures. Preliminary data on the (10,5) is already showing the expected effects, thus supporting the new theoretical framework we have developed.

New Phonon Modes

Access to significant numbers of new pure nanotube chiralities has allowed us to measure unambiguously for the first time the chirality dependence of metallic TO modes and the so-called “M mode” of the semiconductors. These are providing new insights into coupling to the electronic structure of the tubes and also inform back to the non-Condon effects.

The armchair work has allowed us to obtain the first ever detailed frequency values for the TO phonon mode (Figure 4) over 6 different structures ((5,5) through (10,10)). Frequencies show a sharp decrease to smaller diameter tubes and exhibit anomalous behavior of the phonon dispersion. The behavior can be described by introducing a new phonon scattering mechanism in nanotubes. We have confirmed this mechanistic description by implementing electrochemical doping measurements on pure (6,6) structures in our armchair series. Our results now resolve a controversy in the theoretical community over how to describe electron-phonon coupling in metallic nanotubes [7].

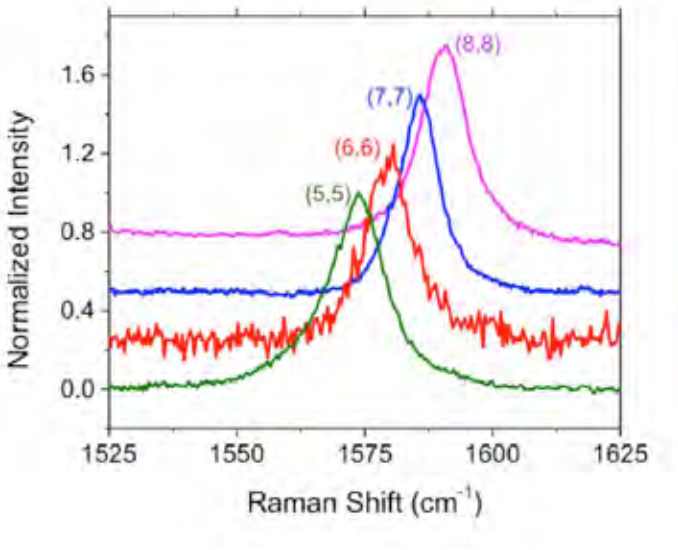

Figure 4. Raman spectra of the TO mode for the labeled armchair metallic nanotube structures. Frequency downshifts significantly as nanotube diameter decreases.

We also obtained M-mode frequencies for 12 separate tube chiralities. Again a strong dependence on diameter is found, but in a unique manner. Within a given (2n+m) family of tubes, the frequencies deviate from an "ideal" armchair behavior in much the same way that nanotube transition energies do! This behavior has no other parallels for other nanotube phonon modes. Additionally, we find strong chirality dependences in the intensities. Most significantly, for tubes like the (11,0), for which we are also able to obtain M-Mode REPs, we find the REP shape is completely unlike the excitonically-determined line shapes found for the RBMs and G-modes (see Figures 1-3 as representative examples). The M-mode REP maxima do not match up with those found for the G and RBM modes. Tied to this behavior is that near resonance, the M-mode peaks themselves show two clear components. This contrasting behavior to the RBM and G modes suggests that the M-mode behavior is completely determined by the nanotube electron and phonon dispersions, as opposed to coupling to exciton levels. This provides an explanation for lack of asymmetry in the M-mode REPs. As determined from our results on the G-mode REPs, such non-Condon effects are driven by coupling to excitons. In the absence of such coupling (as apparently for the M-mode) no asymmetry will be observed!

Excited-State Dynamics in Model Molecular Surrogates
Unfortunately, our separations efforts were not able to provide the levels of (10,5) and (10,2) structures we required to pursue studies of the effects of quantum interference on excited-state dynamics in nanotubes. As an alternative, we pursued studies of dynamics for cycloparaphenylenes, the simplest structural unit of armchair carbon nanotubes, and which we find also display very strong non-Condon effects. In these studies, femtosecond pump probe measurements were paired with quantum chemical theory modeling of exciton behaviors. Our pump probe measurements (see Figure 5 as an example) are the first ever probes of the early time dynamics in these systems. We are able to resolve the growth of optically excited states and initial decay to intermediate states. Most importantly, we are able to spectrally and temporally resolve coupling of the electronic degrees of freedom to phonon-driven localization of excitons.

Our time-dependent density functional theory study provides a simple and conceptually appealing physical picture explaining all experimentally observed trends in optical properties in this family of molecules [8]. We found that the commonly used Condon approximation is invalid in this molecular family and breaks optical selection rules, making these materials superior fluorophores. Using LANL-unique non-adiabatic excited state dynamics modeling we established clear pictures of phonon-mediated exciton behaviors in CPPs. The quantum chemical modeling provides an exact description of the pump probe results. As a complement to the dynamics studies and the armchair nanotube studies, the effort has also pursued Raman studies of the CPPs and has revealed a clear size dependence in many of the vibrational modes, analogous to what is commonly found for many of the nanotube phonon modes.

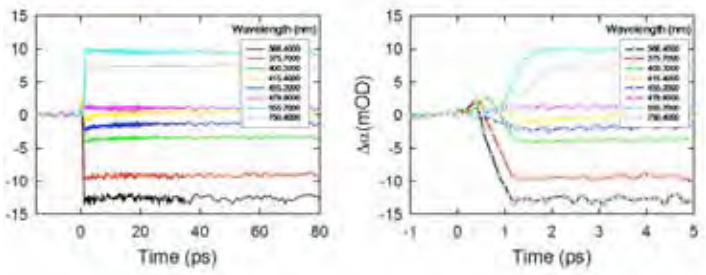

Figure 5. Example pump-probe results for the 12-ring cycloparaphenylene structure 12 [CPP]. Low (left) and high (right) time resolutions of several spectral regions are shown.

In summary, this ER effort has successfully met most of the goals set forth at its beginning. We now understand the excitonic origins of the non-Condon effects observed in their Raman excitation profiles. We have established significant new capability for nanotube processing, probing their behaviors optically, and understanding their photophysics with new theory efforts. Finally, we continue to highlight the importance of pure chirality nanotube samples for revealing new and unexpected nanotube physics. Overall, the effort to date has been highly productive, with nine papers published, one more submitted, and five others in preparation.

Impact on National Missions

Results of this project will have a direct bearing on developing optical and electronic properties of carbon nanotubes for photonic and energy harvesting applications and may also contribute to sensing and spectral tagging applications. As a result, this work will have direct relevance to the mission of the DOE-BES funded Center for Integrated Nanotechnologies and the potential applications will be of interest to agencies including NIH, DOE, DHS, and DOD with potential impact on threat reduction and renewable energy missions. Our efforts have also driven development and understanding of fundamental surface chemistry of low-dimensional

materials. Additionally, the quantum behaviors we studied are found in broad classes of materials, but only carbon nanotubes allow the detailed study that we pursued. As a result, the nanotubes serve as ideal model systems for

obtaining a basic understanding of several novel quantum behaviors. As such, their study supports DOE goals for expanding fundamental understanding of functional nanomaterials.

References

1. Duque, J. G., Chen, A. K. Swan, A. P. Shreve, Kilina, Tretiak, Tu, Zheng, and S. K. Doorn. Violation of the Condon Approximation in Semiconducting Carbon Nanotubes. 2011. ACS NANO. 5 (6): 5233.

2. Duque, J. G., Telg, Chen, A. K. Swan, A. P. Shreve, Tu, Zheng, and S. K. Doorn. Quantum Interference between the Third and Fourth Exciton States in Semiconducting Carbon Nanotubes Using Resonance Raman Spectroscopy. 2012. PHYSICAL REVIEW LETTERS. 108 (11).

3. Fagan, J. A., C. Y. Khripin, C. A. S. Batista, J. R. Simpson, E. H. Haroz, A. R. H. Walker, and Zheng. Isolation of Specific Small-Diameter Single-Wall Carbon Nanotube Species via Aqueous Two-Phase Extraction. 2014. ADVANCED MATERIALS. 26 (18): 2800.

4. Fagan, J. A., E. H. Haroz, Ihly, H. u. i. Gui, J. L. Blackburn, J. R. Simpson, Lam, A. R. H. Walker, S. K. Doorn, and Zheng. Isolation of > 1 nm Diameter Single-Wall Carbon Nanotube Species Using Aqueous Two-Phase Extraction. 2015. ACS NANO. 9 (5): 5377.

5. Haroz, E. H., J. G. Duque, E. B. Barros, Telg, J. R. Simpson, A. R. H. Walker, C. Y. Khripin, J. A. Fagan, Tu, Zheng, Kono, and S. K. Doorn. Asymmetric excitation profiles in the resonance Raman response of armchair carbon nanotubes. 2015. PHYSICAL REVIEW B. 91 (20).

6. Moura, L. G., M. V. O. Moutinho, Venezuela, Fantini, Righi, M. S. Strano, and M. A. Pimenta. Raman excitation profile of the G band in single-chirality carbon nanotubes. 2014. PHYSICAL REVIEW B. 89 (3).

7. Telg, , E. H. Haroz, J. G. Duque, Tu, C. Y. Khripin, J. A. Fagan, Zheng, Kono, and S. K. Doorn. Diameter dependence of TO phonon frequencies and the Kohn anomaly in armchair single-wall carbon nanotubes. 2014. PHYSICAL REVIEW B. 90 (24).

8. Adamska, , Nayyar, Chen, A. K. Swan, Oldani, Fernandez-Alberti, M. R. Golder, Jasti, S. K. Doorn, and Tretiak. Self-Trapping of Excitons, Violation of Condon Approximation, and Efficient Fluorescence in Conjugated Cycloparaphenylenes. 2014. NANO LETTERS. 14 (11): 6539.

Publications

Adamska, , Nayyar, Chen, A. K. Swan, Oldani, Fernandez-Alberti, M. R. , et.al. Self-Trapping of Excitons, Violation of Condon Approximation, and Efficient Fluorescence in Conjugated Cycloparaphenylenes. 2014. NANO LETTERS. 14 (11): 6539.

Berciaud, S., X. Li, H. Htoon, L. E. Brus, S. K. Doorn, and T. F. Heinz. Intrinsic line shape of the Raman 2D mode in freestanding graphene monolayers. 2013. Nano Letters. 13: 3517.

Chen, H., M. R. Golder, F. Wang, S. K. Doorn, R. Jasti, S. Tretiak, and A. K. Swan. Raman-active modes of even-numbered cycloparaphenylenes: comparisons between experiment and DFT calculations with group theory arguments. 2015. Journal of Physical Chemistry C. 119: 2879.

Ciesielski, R., V. Giegold, N. F. Hartmann, E. H. et.al, Electronic and vibrational coherences in single semiconducting carbon nanotubes probed by femtosecond pulse-shaping microscopy at room temperature. Nature Nanotechnology.

Fagan, J. A., C. Y. Khripin, C. A. S. et.al, Isolation of Specific Small-Diameter Single-Wall Carbon Nanotube Species via Aqueous Two-Phase Extraction. 2014. ADVANCED MATERIALS. 26 (18): 2800.

Fagan, J. A., E. H. Haroz, Ihly, H. u. i. Gui, J. L. Blackburn, J. R. Simpson, Lam, A. R. H. Walker, S. K. Doorn, and Zheng. Isolation of > 1 nm Diameter Single-Wall Carbon Nanotube Species Using Aqueous Two-Phase Extraction. 2015. ACS NANO. 9 (5): 5377.

Haroz, E. H., J. G. Duque, J. Simpson, E. Barros, H. Telg, A. Height-Walker, X. Tu, M. Zheng, J. Kono, and S. K. Doorn. Asymmetric excitation profiles in the resonance Raman response of armchair carbon nanotubes. 2015. Physical Review B. 91: 205446.

Haroz, E. H., J. G. Duque, X. Tu, M. Zheng, A. R. Hight Walker, R. H. Hauge, S. K. Doorn, and J. Kono. Fundamental optical processes in armchair carbon nanotubes. 2013. Nanoscale. 5: 1411.

Lim, , A. R. T. Nugraha, Cho, Noh, Yoon, Liu, Kim, Telg, E. H. Haroz, G. D. Sanders, Baik, Kataura, S. K. Doorn, C. J. Stanton, Saito, Kono, and Joo. Ultrafast Generation of Fundamental and Multiple-Order Phonon Excitations in Highly Enriched (6,5) Single-Wall Carbon Nanotubes. 2014. NANO LETTERS. 14 (3): 1426.

Telg, H., E. H. Haroz, J. G. Duque, X. Tu, C. Khripin, J. Fagan, M. Zheng, J. Kono, and S. K. Doorn. Diameter dependence of TO phonon frequencies and the Kohn anomaly in armchair single-wall carbon nanotubes. 2014. Physical Review B. 90: 245422.

Enhancing Thermoelectric Properties of Topological Insulators through Nanostructuring

Nikolai Sinitsyn
20130348ER

Abstract

This project was motivated by the discovery of new materials, called Topological Insulators (TI), which demonstrate a new state of electrons that is topologically distinct from the conventional band insulators or metals. One of the manifestations of the topological properties is the appearance of conducting electron states, on the surface of material, which propagate throughout the sample without elastic scattering. We believe that nanostructuring of TIs can substantially increase the role of these states in charge and thermal transport to the level of obtaining a device structure with record high thermoelectric characteristics. We develop a theory of thermoelectric effects in thin films and nanowires made of TIs. This goal will require an understanding the role of disorder and quantum confinement on the topologically protected surface states. Complimentary experimental efforts were focused on measurements of thermal transport in topological insulator nanowires using state of the art CINT Discovery platform. This provided a selective probe for conflicting processes determining the figure of merit. Theoretical results were benchmarked against experimental data and used to provide a guideline for subsequent experimental studies. Our studies reveal several effects in TI-nanowires that will likely lead to new advances in thermoelectricity.

Background and Research Objectives

The effectiveness of a thermoelectric material is determined by the ratio of electrical (σ) to thermal (κ) conductivity and its thermopower (Seebeck coefficient, S), with a material's figure of merit given by $ZT=\sigma S^2T/\kappa$. For high performance one wants large thermopower, high electrical conductivity and low thermal conductivity, posing an optimization problem involving conflicting materials properties. While there are no fundamental theoretical or thermodynamic limits to increases, ZT~1 has remained the upper limit for materials in use for the last 30 years.

The prediction of TIs in 2005 had quickly evolved to the discovery that some of the most important thermoelectric materials, Bi2Se3 and Bi2Te3, belong to this class. Due to specific topological properties of the electronic band structure, these insulators possess gapless (metallic) modes at the surfaces. Unlike usual 2D electron systems, such surface states have a Dirac spectrum. When geometry is confined to quasi-1D, the Dirac Hamiltonian completely forbids the electron backward scatterings, thus opening up ballistic channels.

By increasing the figure of merit of materials, a wide range of new energy saving technologies is expected to become possible. For example, spinning components of refrigerators will be replaced by energy efficient, compact cheap and silent solid-state devices. Thermoelectric generators and refrigerators are mainly used in applications requiring reliability, including the power generation sources for deep space missions and cooling of computer central processing units. The environmental concerns and demands to explore alternative energy sources (e.g., generation of electric power from waste heat) have been motivating the search for new high-ZT thermoelectric materials. We explored two general strategies for further increasing ZT:

1. Make electrons as ballistic as possible, to increase σS^2.
2. Suppress the phonon heat conductivity, κ.

The above two mechanisms are usually conflicting. However, in TI naonowires, this is not the case for the following reason. Localization of phonons in a confined, quasi-1D, geometry will lead to the reduction of κ, as in other materials, but the product of electronic conductivity and thermopower, σS^2, should actually, substantially increase in Tis due to the protected ballistic character of Dirac electrons in quasi-1D geometry. This distinguishes TI nanowires from other nanostructurs because, in standard quasi-1D materials, transport is suppressed by

elastic scattering both for phonons and electrons.

Scientific Approach and Accomplishments

Our team fabricated the nanowire from a topological insulator SnTe and performed measurements of the transport characteristics, including the thermoelectric figure of merit (Xu et al, Nanoscale, 2015). We achieved particularly interesting progress with relatively thick nanowires (1000-100nm) at which specific topological physics is not expected to play big role. However, experiments revealed unexpected phenomena – the growth of the Seebeck coefficient by a factor 4 (and the increase of figure of merit by an order of magnitude). It is a surprising and very useful effect, meaning that there are additional factors that can improve thermoelectric properties of those materials.

Following studies of SnTe we turned to the nanowires made of lead telluride (PbTe) and its alloy compounds, which are the most promising thermoelectric materials for electric power generation (Xu et al, Nanoscale, submitted). We developed an approach to grow high quality single-crystalline PbTe and PbSnTe nanowires by a vapor transport approach and performed the thermoelectric studies of these individual nanowires. We measured the electrical conductivity, thermopower and thermal conductivity of the same individual nanowires to determine their thermoelectric figure of merit ZTs. In comparison to bulk samples, the PbSnTe nanowires showed both improved thermopower and suppressed thermal conductivity, leading to an enhancement of ZT by a factor of ~ 10. The ZTs of the PbSnTe nanowires were also several times higher than that of PbTe nanowires reported in the literature. Our work clearly demonstrated that nanostructuring, in combination with alloying, is an effective approach to enhancing thermoelectric properties of topological insulators.

Our team has achieved considerable theoretical progress in understanding transport properties in Dirac semiconductors, which class includes topological insulators. The PI has published a series of articles in Phys. Rev. Lett., Phys. Rev. B, J. Phys. A, and contributed to a Nature Physics article with the discovery of unusual behavior of spin relaxation in transition metal dicalcogenides (L. Yang, et al, Nature Physics, 2015).

Impact on National Missions

The project supported the Threat Reduction and Energy Security Mission, and advanced Science and Technology Grand Challenges in Materials: Discovery Science to Strategic Applications (Emerging Phenomena) and Energy & Earth Systems (Concepts & Materials for Clean Energy). It offered a unique opportunity to exploit novel materials - topological insulators - for energy applications, an area that also strongly supports LANL's long-term development of new functional materials capabilities. We built fundamental understanding of topological effects in heat transport.

Publications

Lin, J., and N. A. Sinitsyn. Three level Landau-Zener-Coulomb model: Exact transition probabilities in the three-state Landau-Zener-Coulomb model. 2014. Journal of Physics A: Mathematical Theoretical. 47: 015301.

Lin, J., and N. A. Sinitsyn. The model of a level crossing with a Coulomb band: exact probabilities of nonadiabatic transitions. 2014. Journal of Physics A: Mathematical Theoretical. 47: 175301.

Ren, J., and N. A. Sinitsyn. Braid Group and Topological Phase Transitions in Nonequilibrium Stochastic Dynamics. 2013. Physical Review E. 87: 050101(R) .

Roslyak, O., and A. Piryatisnki. Sonoluminescence of carbon nanotubes. 2013. Unpublished Document.

Sinitsyn, N. A.. Landau-Zener Transitions in Chains. 2013. Physical Review A. 87: 032701.

Sinitsyn, N. A.. Nonadiabatic transitions in exactly solvable quantum mechanical multi-channel model: role of level curvature and counterintuitive behavior. 2013. Physical Review Letters. 110: 150603.

Tse, W., A. Saxena, D. Smith, and N. A. Sinitsyn. Spin and Valley Noise in Two-Dimensional Dirac Materials. 2014. Physical Review Letters. 113: 046602.

Xu, E. Z., Z. Li, J. A. Martinez, N. A. Sinitsyn, N. Li, B. Swartzentruber, and J. A. Hollingsworth. Diameter dependent thermoelectric properties of individual SnTe nanowires. 2015. Nanoscale. 7: 2869.

Xu, E. Z., Z. Li, J. Aviles, N. Li, B. Swartzentruber, N. Sinitsyn, H. Htoon, J. Wang, and S. X. Zhang. Vapor transport growth and enhanced thermoelectric properties of single-crystalline PbSnTe nanowires. Nanoscale.

Yang, L., N. A. Sinitsyn, W. Chen, J. Yuan, J. Zhang, J. Lou, and S. A. Crooker. Long-lived nanosecond spin relaxation and spin coherence of electrons in monolayer MoS2 and WS2. 2015. Nature Physics . : doi:10.1038/nphys3419.

"Upscaling" Nanoscale Thermoelectrics: The Meso-macroscale Design Challenge for Real-World Energy Needs

Jennifer A. Hollingsworth
20130350ER

Abstract

Next-generation thermoelectrics (TEs) have the potential to dramatically impact a wide range of energy harvesting and utilization schemes underpinning a sustainable and secure energy supply for the 21st century. To do so, conventional TE technologies must be transformed to achieve unprecedented performance efficiencies. Nanoscale size effects have been identified as a means to realizing the needed advances, and theoretical and experimental demonstrations of important improvements in TE parameters have been shown at the level of individual nanoscale structures. Critically, however, general strategies are lacking to translate success at the nanoscale into performance requirements at the meso-macroscale. We address this gap with a stepwise approach to the integration of optimized TE nanomaterials into structures of increasing complexity and scale, establishing a path from the single nanostructure to functional bulk composites capable of macroscale manipulation and device-level performance.

Background and Research Objectives

More than half of the energy generated worldwide is lost as heat. Such 'waste heat' can originate from large point sources (e.g., industrial processes) or smaller distributed sources (e.g., automobiles). Even partial recovery of this lost energy would have a dramatic impact on the economic and environmental costs associated with the increasing global appetite for energy. Furthermore, "heat management" problems plague the electronics industry and the emerging solid-state lighting industry. In both cases, performance efficiencies and product lifetime are impacted by high operating temperatures. On-demand/site-specific cooling would eliminate costly, entire system cooling approaches and boost system efficiencies.

TE conversion of heat (temperature gradients) into electricity (the 'Seebeck Effect') or the converse, TE cooling ('Peltier Effect'), is a technology that has the potential to address each of the above problems and, therefore, to have a crosscutting and significant impact on all aspects of Global Energy Security and Climate Change. In addition, TEs can complement other technologies, e.g., solar cell/TE hybrid systems, where the TE component boosts energy output by converting solar-generated heat into "extra" electricity. By improving the economics of other nascent technologies, TEs can hasten their progression to widespread implementation. To date, though, low TE efficiencies—well below the Carnot efficiency limit—have relegated TEs to important but niche applications in remote power generation (e.g., space/deep-sea), remote cooling (e.g., ionizing radiation detector), and specialty applications (e.g., DNA synthesizers), where benefits of reliability, compact size, and no moving parts trump efficiency & cost considerations.

Currently, the TE figure-of-merit, ZT, remains at ~1 for most deployed systems,1 where $ZT = S^2\sigma/\kappa$ and S = Seebeck coefficient, σ = electrical conductivity, κ = thermal conductivity. A ZT of ~2-3 is considered necessary for TEs to significantly penetrate general energy use. Optimizing ZT requires minimizing κ (to prevent short-circuiting the thermal gradient) while simultaneously maximizing σ and S. Referred to as a "combination of opposites," this challenging materials requirement demands separate tuning of bandgap, electronic density-of-states (DOS), and electron/ phonon mean free path, given that in conventional bulk materials these parameters are correlated.

Nanotechnology can address the ZT challenge, and dramatic improvements in specific TE parameters and even in ZT (from ~1.1 to 2.5) have been demonstrated experimentally, with ZTs as high as 10 predicted. Semiconductor NWs are a promising nanomaterial building block for TE applications. Their anisotropic structure provides a path for charge transport, while their width can be manipulated in the nanoscale regime to cause reductions in κ or enhancements in S. In addition, using various in situ

techniques, NW surfaces can be "roughened" or internal composition can be modulated to form axial heterostructures or NW "superlattices." Each synthetic "knob" provides opportunities to tune κ and S, while retaining σ.

In addition to high ZTs, however, TE device efficiency depends on maintaining large temperature differences (ΔTs) across the hot and cold junctions. If device thickness is small (<<1 mm), then extremely large heat fluxes (>100's kW) are required to maintain large ΔTs. The practical limitations on engineering a device for such massive heat input imply that TE devices need to be significantly thicker than the longest dimension of typical nanoscale structures (>>1μm). This requirement constitutes a potential "show stopper" for nano-enabled TEs, and it is this challenge of scale that we address here.

In order to use NWs, for example, as the elementary units of a TE device, they need to be scaled to the above-described device-scale dimensions. It is unlikely that individual NWs will reach the lengths of centimeters with retention of optimized nanoscale features (diameters <10 nm, roughened surfaces, internal superlattice structure, etc.). Therefore, arrays or forests of shorter NWs (microns) will have to be "stacked" or individual NWs interconnected to form 3-D networks. For either scenario, a supporting matrix (array backfill material) or framework is presumably required for bulk-level manipulation and device processing. This aspect of NW-enabled TEs remains little explored in the literature. For these reasons, we aimed to explore the effects on nanoscale TE properties of NW branch and network formation at progressively increasing levels of complexity, as well as assess the impact of matrix integration on these properties.

Thus, the overarching goal of the program was to address the challenge of scale that is uniquely relevant to nano-enabled TEs. In so doing, we discovered an alternative approach to addressing scale issues in TEs, namely, by using non-thermally conductive spacer layers as a means for avoiding "thermal shorting" in TE thin films. We have also addressed an underpinning "knowledge gap" in terms of understanding how the key transport properties—electrical and thermal—change across the extremity of length scales from nano/meso- to macroscale. Though the problem of scale is paramount for TEs, the synthetic strategies and new principles of multi-scale transport can be applied to a wide range of nano-enabled technologies. The three objectives that were pursued are:

1. Assessing and optimizing nanoscale TE functionality by way of baseline studies in single-NW systems of controlled size and surface roughness.
2. Understanding and controlling meso-macroscale TE properties of novel branched/networked NW constructs.
3. Assessing the viability of aerogels as a NW TEs matrix and/or functional spacer layer.

Scientific Approach and Accomplishments

Our original approach is outlined in Figure 1. The strategy of studying differently sized and shaped lead chalcogenide nanowires (NWs) (of increasing network complexity) as building blocks for new thermoelectric (TE) devices was largely followed. However, during the execution of the project, we determined that TE properties could most readily be obtained from thin-film devices and, further, that even thermal conductivity was accessible if we placed an aerogel (non-thermally conducting) spacer in between the NW film and the solid support (Figure 2).

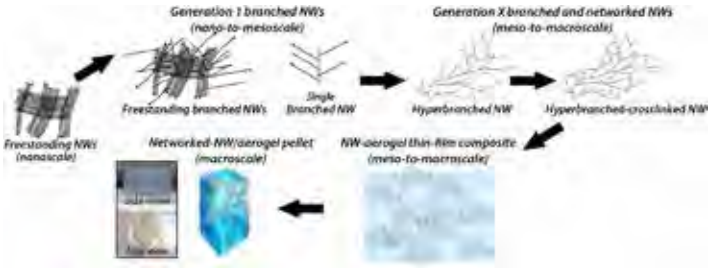

Figure 1. Schematic showing increasing complexity in nanowire structures and integration with aerogel (thermally insulating, structurally supportive) matrix material.

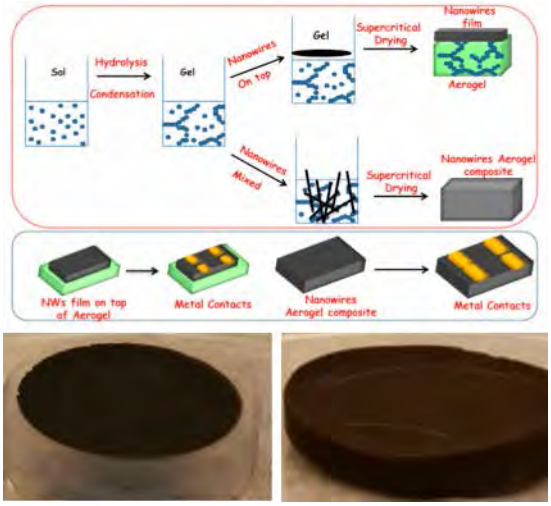

Figure 2. (top) Schematic of the approaches developed in this program to either fabricate a nanowire thin film on top of an aerogel support layer or to fabricate an aerogel-nanowire bulk composite material (with sufficient nanowire density to support electrical conductivity through the construct). (bottom) Photographs of nanowire film grown on top of an aerogel layer (left) and of an aerogel-nanowire bulk composite (right).

Without the aerogel spacer, the thick solid support would cause rapid thermal shorting of the NW thin film, preventing meaningful data from being obtained. In this way, we were able to determine ZT in direct measurements of all ZT components, without having to fabricate macroscale structures comprising aerogel-NW composites. Although these thin-film devices became the focus of our research, we also developed the synthetic strategies to fabricate bulk aerogel-NW composites that can potentially be used as large-scale building blocks for traditional TE device constructs. In addition to this experimental modification, we also expanded our NW materials to include core/shell NWs, rods and tetrapods. Therefore, in addition to the Publications reported within this document, this ER will result in four further publications with project postdoc, Nimai Mishra, as first author: (1) Lead chalcogenide nanowire building blocks for thin-film thermoelectrics: Impact of size, shape and interfaces; (2) Bulk thermoelectrics enabled by hybrid semiconductor-aerogel compositing, (3) Controlled branching in lead chalcogenide nanowires, and (4) Engineering Auger recombination in core/shell rods and tetrapods.

Significant results were obtained in this program in both theory and experiment thrusts. Examples are provided below for each Objective

Objective 1: We completed a systematic study of PbS, PbSSe, and PbSe nanowire (NW) synthesis by catalyzed solution-liquid-solid (SLS) growth, investigating numerous synthetic variables to obtain size, surface, and branching-controlled NW growth. The variables were: bismuth (Bi) nanoparticle catalyst size (5-38 nm diameters); temperature (175-320 oC): purity of coordinating-ligand (e.g., 90% trioctylphosphine versus 97%; 90% trioctylphosphine oxide versus 99%); and precursor (dual-source versus single source). In support of these studies, single-source precursors for PbS and PbSe were synthesized and characterized by NMR (working with Ryszard Michalczyk, B-11, and Koushik Ghosh, MPA-CINT). Overall, we currently favor use of higher purity ligands and single-source precursors, and we discovered that temperature is the key variable for tuning surface morphology from rough to smooth and NW branching from straight to multiply branched, both trending with increasing temperature, where our temperature range spans below and above the melting point of bulk Bi (271 oC). In fact, we obtained uniquely high yields of branched NWs, e.g. 90% for PbSe.

NW building blocks in hand, we fabricated and tested single-NW and thin-film devices, capitalizing on new collaborations within and outside LANL. With external collaborator, Enzhi Xu (Indiana Un.), we fabricated single-NW devices from PbS NWs (dropcast NWs onto substrate with large electrodes; electron-beam lithography and metal deposition to link NWs to electrodes), for which microamp currents were occasionally obtained, confirming reasonable conductivity for these thin wires. Challenges: the consistency of single-NW device performance and lifetime in air would need to be improved to move this aspect of the work forward. More fruitful, we fabricated thin-film devices comprising NW mats, for which we developed a unique procedure for improving electrical conductivity that involved multiple surface-ligand exchanges followed by annealing in forming gas, where anneal temperatures were sufficiently low to avoid particle sintering. With such modified films, we conducted thermoelectric parameter measurements with Marcelo Jaime (MPA-CMMS).

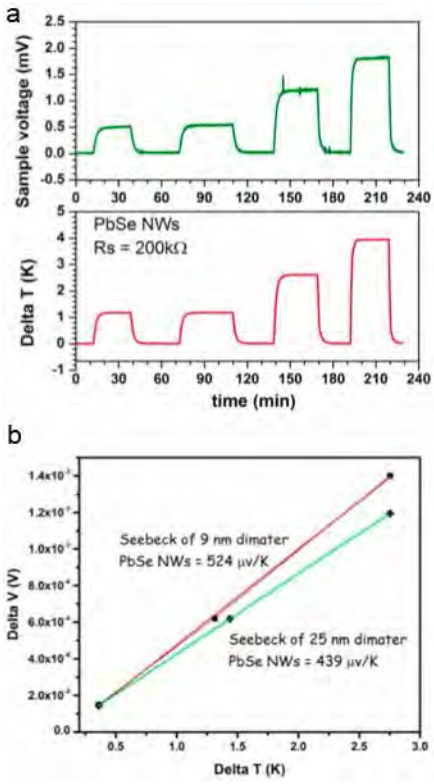

Figure 3. (a) Data demonstrating the thermoelectric effect in thin films comprising PbSe nanowires. Voltage (top) changes as a clear function of changing film delta-temperature (bottom). (b) First Seebeck coefficient values obtained in this program for differently sized PbSe nanowires, demonstrating the expected impact of quantum confinement for the first time in ensembles of ultra-thin nanowires.

Objective 2: Manuscript titled, Enhanced Thermoelectric Properties of Semiconductor Nanowire Networks, was prepared that describes a novel theoretical approach to mapping TE "networks" on two-port networks. Here, Piryatinski argues that in contrast to a conventional single-port (i.e., resistor) network model, our model allows for large-scale calculations and also predicts convergent TE figure-of-merit, ZT, behavior with increasing number of junctions. Using

this model, the numerical simulations of ZT are performed for branched and Cayley-tree NW networks. The simulations show that the phonon impedance of the network junctions plays the dominant role in the enhancement of the network performance. Importantly, depending on the phonon impedance mean value, the ZT enhancement of random networks can vary in the range of 20-150%. To provide connection with experiment, the manuscript further demonstrates how the model parameters can be related to the observables available in TE measurements.

Objective 3: We successfully incorporated PbSe NWs into silica-aerogel monoliths. In addition, we determined optimal NW solution chemistry to realize placement of high quality NW films on top of silica-aerogel supports. Both types of device components have been demonstrated experimentally (conductivity measurement in former case, and full TE characterizations in case of latter construct) to be potentially important approaches to moving nano-enabled TE forward.

Impact on National Missions

The program has impacted multiple national missions. First, with respect to emerging materials technologies underpinned by advanced materials R&D, the program has provided important insights in the areas of nanomaterials synthesis and integration, characterization and theory. These lay the foundation for successful translation of nanoscale thermoelectric phenomena to the macroscale and afford new understanding with respect to how properties scale with changes in length scale and complexity (Mesoscale science impact). This aspect of the work contributes directly to DOE Basic Science initiatives and is relevant to the Scientific Discovery and Innovation Mission in the Basic Understanding of Materials. We have further demonstrated novel functional composites comprising nanowire (NW) networks in aerogels as well as novel multi-layer structures comprising NW thin films on aerogel spacer layers for applications in thermoelectrics. In this way, the work also addresses challenges to the implementation of nano-enabled thermoelectrics in real-world device architectures, where the new “paths forward” provided by the project can have a transformative impact on Energy Security (Renewable Energy) and the Environment (Climate and Energy Impact and even “waste” management), as thermoelectrics tackles both waste heat utilization and heat management issues. Furthermore, we have established new modeling tools for addressing transport processes from simple to branched NWs and their composites over multiple length-scales, bringing new capabilities for theory-guided materials discovery and development and, again, impacting mesoscale science through truly multi-scale theory advances. Lastly, the new composite materials were tested at temperature extremes (cold and hot) and entailed conversion of energy types (e.g., heat to electricity) and energy translation across interfaces, with direct relevance to complex materials design and characterization for MaRIE. In addition, the technology developed can impact longer term development of small-size, rapid-response temperature probes for extreme environments, e.g., explosives.

References

1. Bell, L. E.. Cooling, heating, generating power, and recovering waste heat with thermoelectric systems. 2008. SCIENCE. 321 (5895): 1457.

Publications

Acharya, K. P., T. G. Holesinger, J. A. Crisp, S. A. Ivanov, D. J. Williams, J. L. Casson, M. Sykora, and J. A. Hollingsworth. Layer-by-layer fabrication of nanowire sensitized solar cells: geometry-independent integration. 2014. Advanced Functional Materials. 24: 6843–6852.

Mishra, N., W. Y. Wu, M. S. Bharathi, H. Ramanarayan, J. A. Hollingsworth, Y. W. Zhang, and Y. Chan. Continuous shape-tuning of nanotetrapods and their shape-mediated self-assembly behavior. ACS Nano.

Roslyak, O.. Enhanced thermoelectric effect of branched nano-wire trees. Invited presentation at Fordham University Seminar. (New York, 12 May 2013).

Roslyak, O., and A. Piryatinski. Thermoelectric effects in disordered branched nano-wires. 2013. In American Physical Society Annual Meeting 2013. (Baltimore, MD, 18-22 March 2013). , p. BAPS.2013.MAR.W12.14. College Park, MD: Bulletin of the American Physical Society.

Roslyak, O., and A. Piryatinski. Enhanced thermoelectric properties of semiconductor nanowire networks. 2015. arXiv.org. : arXiv:1501.03229 .

Roslyak, O., and A. Piryatinski. Enhanced thermoelectric properties of semiconductor nanowire networks. To appear in Nano Letters.

Xu, E. Z., Z. Li, J. A. Martinez, N. Sinitsyn, H. Htoon, N. Li, B. Swartzentruber, J. A. Hollingsworth, J. Wang, and S. X. Zhang. Diameter dependent thermoelectric properties of individual SnTe nanowires. 2015. Nanoscale. 7: 2869.

Giving Cold Atoms Weight: Creating Heavy Fermions in Optical Lattices

Cristian D. Batista
20130385ER

Abstract

Lanthanide and actinide based compounds are strongly correlated materials of strategic interest for LANL. The coexistence of localized f-moments with itinerant electrons in broad bands leads to unusual states of matter, such as unconventional superconductivity and heavy fermion behavior, which are far from being understood in spite of more than 30 years of intense research. These novel states typically appear near quantum critical points induced by variations of different external parameters such as pressure, magnetic field or chemical doping. The main bottleneck for characterizing these states is that the experimental characterization is limited by many factors. Consequently, there is a need for finding controllable realizations of this physics that can shed light on the basic and universal properties of the novel states that emerge near quantum critical points. We propose to address this need by modeling a class of atomic gases known as Bose-Fermi resonant systems in an optical lattice, and identifying regimes of parameters for which the atomic system can be mapped into a lattice of local moments (localized f-electrons) that interact via exchange with itinerant electrons. Describing and testing this non-trivial mapping requires a description that bridges the Angstrom-sized atomic physics scale with the micron-sized optical lattice physics. The aim of this interdisciplinary approach is to solve a long-standing problem of strongly correlated materials that are relevant for our LANL's mission.

Background and Research Objectives

The possibility of trapping cold atoms in periodic potentials opens new horizons for the experimental and theoretical study of correlated matter. We are slowly discovering that the physical laws that govern the interactions between these atoms are very similar to the ones that describe the interaction between electrons in actinide based inter- metallic compounds. Besides being the basic materials for nuclear applications, these compounds are among the most complex correlated materials in nature. For this reason, it is very challenging to understand and predict its electronic and structural properties. Cold atoms offer a unique opportunity of isolating the essential ingredients that control the properties of these materials and tuning the most relevant parameters in a way that would not be possible by directly studying these compounds.

We argue that the closed channel amplitude physics of the Feshbach resonance gives access to the "Kondo physics" responsible for heavy fermion behavior in inter-metallic compounds. The first goal of this project is to describe the narrow resonance properties and derive a model for the effective atom-atom interactions from first principles. The second goal is to connect this model with the one that is traditionally used to describe the electronic properties of inter-metallic compounds. By guiding cold atoms towards a first realization of heavy fermion physics, this project will establish the first one-to-one connection between cold atoms and inter-metallic compounds. This research is relevant for understanding the origin of the complex electronic properties of actinide-based materials, which are relevant for the nuclear energy security mission.

Scientific Approach and Accomplishments

In a magnetically controlled cold atom Feshbach resonance, cold alkali atoms are placed in a homogeneous magnetic field of strength B. When interacting, the atoms temporarily rearrange their spins (nuclear spins and valence electron spins) thereby bringing their relative coordinate wave function into a quasi-bound state that we will call "molecule". This process is described by a mixed fermion-boson Hamiltonian, in which the boson represents the amplitude of the quasi-bound state.

We completed the first principles derivation of a model for describing this system of cold alkali atoms. We also mapped the model into a Kondo Lattice Hamiltonian and studied ways of tuning the parameters of the equivalent

Kondo Lattice model (KLM) by controlling the parameters of the original system of alkali atoms. The KLM is relevant for lanthanide and actinide based materials because it describes the interaction between local moments (localized f-electrons) and conduction electrons that form a broad band (itinerant electrons moving in s, p or d-bands).

We used the Density Matrix Renormalization (DMRG) code, developed during the first year of the project, to study the phase diagram of the one-dimensional version of the model derived from first principles. In agreement with our expectations, the phase diagram includes quantum phase transition between a molecular superfluid and a disordered state. The disordered state is the one-dimensional version of the heavy fermion phase that appears in higher dimensions (the Fermi liquid is unstable in one-dimension). In terms of the KLM, the counterpart of the molecular superfluid is a magnetically ordered state in which the local magnetic moments order antiferromagnetically in a plane perpendicular to an effective applied magnetic field. Along this process, we realized that a precondition for obtaining the Kondo Lattice model physics with cold atoms is to have a strong (hard-core) repulsion between the molecules (closed channel). Unfortunately, there is no obvious way of producing this interaction in current implementations of atomic gases. However, this obstacle could be removed in the future by the use of other atomic species or actual molecules.

We have recently submitted a manuscript entitled “The narrow Feshbach Resonance as a long-delay interaction” [1]. The scattering amplitude of cold atom narrow Feshbach resonances exhibits a steep dependence upon scattering energy. We derived the energy dependence of the effective energy-dependent scattering length from the scattering description of two coupled channels and find a universal three-parameter description in the narrow resonance limit. We test the energy dependence for two specific resonances in the 40K-87Rb interaction complex. The energy dependence implies a negative effective range close to resonance with an absolute value that can exceed cold atom inter-particle distances. Rather than attributing the large absolute value of the effective range to an effective interaction-at-a-distance, we point out that the sign and magnitude of the effective range are consequences of a long-lasting interaction. We determined the delay-time and recover the time that the interacting atoms spend in the closed channel during the collision. We pointed out that the long time spent in the vibrationally excited closed channel state can give rise to an effective three-body loss-process that involves the vibrational de-excitation by a third atom.

The scattering amplitude of the cold atom narrow Feshbach resonances depends sensitively on the scattering energy. As demonstrated by the eight-decade old challenge of constructing good effective interactions to describe the nucleon-nucleon interactions in low energy nuclear physics, the effective description of energy-dependent interactions can be daunting. However, we found that in the limit of sufficiently narrow resonances, the two-body resonances fall into two universal categories: potential resonances and quantum tunneling resonances. We show that the narrow Feshbach resonances fall into the latter category and we show that similarity scaling can map results from vastly different cold atom experiments onto each other.

The many-body techniques developed under this project, such as the development of a DMRG code, were applied to solve different many-body problems involving competing interactions and quantum phase transitions [2-5]. The multiple results are described in the manuscripts listed below. In particular, we found new plateux phases induced by pressure in the so-called “Shastry-Sutherland” compound SrCu2(BO3)2 [2] and a novel anyonic liquid at a field-induced quantum critical point [3]. We have also reproduced the inelastic neutron scattering data of the heavy fermion antiferromagnetic compound CeRhIn5 [5]. This work was done in collaboration with experimentalists from MPA Division. We are now applying our many-body (DMRG) techniques to understanding the magnetic field and temperature phase diagram of this compound. Our preliminary results indicate that the competition between Kondo screening and the RKKY interaction leads to non-trivial effects induced by magnetic field, such as a non-monotonic behavior of the ordering temperature as a function of the magnetic field.

Impact on National Missions

Lanthanide and actinide based compounds are strongly correlated materials of strategic interest for LANL and the DOE complex. We have developed methods for studying and emulating the competing phases of these materials under control, i.e., without relying on uncontrolled approximations. As we demonstrated in this project, these unbiased methods can be applied to any correlated electron material and they are promising for achieving predictive power for these classes of complex materials.

References

1. Hazra, J., B. Naduvalath, and E. Timmermans. The narrow Feshbach Resonance as a long-delay interaction. Physical Review B.

2. Haravifard, S., D. Graf, A. Feiguin, C. D. Batista, J. C. Lang, D. M. Silevitch, G. Srajer, B. D. Gaulin, H. A. Dabkowska, and T. F. Rosenbaum. Crystallization of

Spin Superlattices with Pressure and Field in a Layered Magnet. Nature Communications.

3. Rahmani, , A. E. Feiguin, and C. D. Batista. Anyonic Liquids in Nearly Saturated Spin Chains. 2014. PHYSICAL REVIEW LETTERS. 113 (26).

4. Wang, , Kamiya, A. H. Nevidomskyy, and C. D. Batista. Three-Dimensional Crystallization of Vortex Strings in Frustrated Quantum Magnets. 2015. PHYSICAL REVIEW LETTERS. 115 (10).

5. Das, , S. -. Lin, N. J. Ghimire, Huang, Ronning, E. D. Bauer, J. D. Thompson, C. D. Batista, Ehlers, and Janoschek. Magnitude of the Magnetic Exchange Interaction in the Heavy-Fermion Antiferromagnet CeRhIn5. 2014. PHYSICAL REVIEW LETTERS. 113 (24).

Publications

Das, , S. -. Lin, N. J. Ghimire, Huang, Ronning, E. D. Bauer, J. D. Thompson, C. D. Batista, Ehlers, and Janoschek. Magnitude of the Magnetic Exchange Interaction in the Heavy-Fermion Antiferromagnet CeRhIn5. 2014. PHYSICAL REVIEW LETTERS. 113 (24).

Haravifard, S., D. Graf, A. Feiguin, C. D. Batista, J. C. Lang, D. M. Silevitch, G. Srajer, B. D. Gaulin, H. A. Dabkowska, and T. F. Rosenbaum. Crystallization of Spin Superlattices with Pressure and Field in a Layered Magnet. Nature Communications.

Hazra, J., B. Naduvalath, and E. Timmermans. The narrow Feshbach Resonance as a long-delay interaction. Physical Review B.

Rahmani, . QUANTUM DYNAMICS WITH AN ENSEMBLE OF HAMILTONIANS. 2013. MODERN PHYSICS LETTERS B. 27 (26).

Rahmani, , A. E. Feiguin, and C. D. Batista. Anyonic Liquids in Nearly Saturated Spin Chains. 2014. PHYSICAL REVIEW LETTERS. 113 (26).

Rahmani, A., T. Kitagawa, E. Demler, and C. Chamon. Cooling through optimal control of quantum evolution. 2013. PHYSICAL REVIEW A. 87 (4): -.

Wang, , Kamiya, A. H. Nevidomskyy, and C. D. Batista. Three-Dimensional Crystallization of Vortex Strings in Frustrated Quantum Magnets. 2015. PHYSICAL REVIEW LETTERS. 115 (10).

Topology in Superposition: Quantum Decoherence in Many-body Systems

Wojciech H. Zurek
20130409ER

Abstract

Decoherence is responsible for eliminating symptoms of quantumness from the familiar, macroscopic world. Thus, even though our Universe is undeniably quantum, our everyday reality appears to be classical. The origin of decoherence responsible for the emergence of the classical is the immersion of the macroscopic objects in our world in the environments (such as air or photons) that, via incessant interactions, constantly monitor their states. Quantum states – in contrast to classical states – are perturbed by such monitoring. Therefore, only certain states of the systems can survive such "environmental monitoring" intact. They are the candidate classical states. The usual objective of the studies of decoherence was to assess the effect of the environment on the state of the system. This was done using fairly primitive models of the environment that acted as a "quantum garbage dump" for the excess (quantum) information. The aim of this proposal was to shift the focus of attention from the state of the system to the state of the environment. We characterized how many copies of what sort of information about the system becomes deposited in the environment, and assessed its role in the emergence of the classical. We also wanted to study more realistic environments. We have succeeded (to some degree, better than we expected) in meeting the goals of the proposal. Thus, we have arrived at a very satisfying quantitative theory of the amplification that occurs when a photon environment monitors objects (e.g., when sunlight scatters from them). We have also obtained additional insights into excitations arising in many-body environments, and, in particular, into excitations left behind by quantum phase transitions. Understanding quantum decoherence and the quantum-classical border is essential for quantum information processing, and for the quantum aspects materials science, of interest to LANL and DoE because of their impact on national missions.

Background and Research Objectives

Decoherence is by now widely regarded as a "quantum fact of life." It is often cited as the bridge over the quantum - classical divide. Above all, it is investigated as both an obstacle to practical applications of quantum theory (in quantum computing or quantum metrology) and – more recently – as an important resource (e.g., in creating entanglement or in speeding up controlled transitions between quantum states).

Yet, models of the environment used in its study – the central spin model and quantum Brownian motion – were until recently embarrassingly primitive. Both were introduced in the early 80's and suffer from the same oversimplification: An environment consisting of many non-interacting subsystems (spins and harmonic oscillators, respectively) that have only limited relation with realistic environments encountered in condensed matter or everyday life.

We have studied decoherence caused by quantum many – body environments. We have, in particular, investigated the flow of information and its amplification in settings that are more realistic, and that recognize the "facts of life" ignored so far in discussions of the transition form quantum to classical: The information we gain about our quantum Universe is usually obtained indirectly, by measuring fragments of the environment (e.g., photons) that has interacted (e.g., scattered from) the "systems of interest." This is possible because interactions capable of decohering are also imprinting – in many copies the information about the state of such systems in the environment. Thus, in our quantum Universe, at least some of the environments are not just "garbage dumps" for spurious information, but are de facto communication channels that allow observers to gain information indirectly – i.e., without direct interaction – about objects of their interest.

This point of view, championed by our group (and known as "Quantum Darwinism") shifts the focus from the study of the effect of the environment on the "system of interest" to the investigation of the effect of the system of interest on the environment. The basic observation is that the preferred states of the system (so – called "pointer states") that are singled by their stability in spite of decoherence are becoming imprinted, in many copies, on the state of the environment. Observers can than obtain information about such systems by intercepting small fragments of the environment. (For example, you, the reader, are now intercepting fragments of the photon environment to find out the content of this report).

The study of quantum Darwinism requires new tools. These are supplied by the modern developments of quantum information theory. For instance, one of the key questions is the number of copies of the state of the system that are deposited in the environment in the course of decoherence. This is de facto a process of amplification that happens because of decoherence. It can be analyzed using tools such as quantum Chernoff information that allow one to estimate redundancy of the information deposited in the environmnet.

Scientific Approach and Accomplishments

Our study of quantum coherence and decoherence in situations involving many body systems has progressed along several parallel lines, some of them stimulated by recent experimental developments.

Our paper connecting decoherence with amplification (Zwolak, Riedel and Zurek, Amplification, Redundancy, and the Quantum Chernoff Information, Phys. Rev. Lett. 112, 140406 (2014)) has been just published. It provides modern, quantum information–based understanding of the nature and of the role of amplification in the transition from quantum to classical. This is an important step in the development of the "quantum Darwinism" program we have championed.

With Dziarmaga, Zurek has investigated dynamics of phase transitions in the Kosterlitz- Thouless universality class. This is important, as there are several interesting systems that fall into this category, including paradigmatic quantum Bose-Hubbard model in one dimension.

In the Kosterlitz- Thouless universality class the near-critical behavior of quantities such as the relaxation time is not polynomial (as is the norm for most other second order phase transitions) but, rather, exponential. The question is then how to adapt the Kibble-Zurek mechanism (KZM) to this non-polynomial setting. Ongoing experiments on the one–dimensional Bose–Hubbard model (that belongs to the Kosterlitz-Thouless universality class) add urgency to this project.

The unexpected answer is that KZM predictions apply, but not in the naïve form (that depends only on the asymptotic values of critical exponents). Rather, asymptotic scalings are expected only in the limit when the quench is very slow (which also means that the size of the system has to be very large). These advances have been reported in a paper by Dziarmaga and Zurek (Quench in 1D Bose- Hubbard Model: Topological Defects and Excitations from Kosterlitz-Thouless Phase Transition Dynamics).

With Julian Sonner of MIT and del Campo, Zurek has initiated investigation of KZM in the context of holographic duality. Holographic duality is a powerful approach that allows one to treat strongly coupled (i.e., intractable via any "direct" approach) field theoretic and many – body models using a "dual" system – anti de Sitter Universe – that is weakly coupled, and, therefore, more tractable.

Our preprint with these results has just appeared ("Universal far-from-equilibrium Dynamics of a Holographic Superconductor"). It confirms KZM predictions for the winding numbers, but it also opens several interesting questions about KZM and holographic duality we intend to pursue in the future.

Zurek has continued his work on quantum foundations, including an update prepared for the Solvay conference "The Theory of the Quantum World" (edited by D. Gross et al., World Scientific, 2013). These advances have also led to a mini-review in the 2014 Physics Today, and a followup discussion, in May 2015 issue of Physics Today. These papers provide an accessible discussion of the propagation of information through many body environments. The interplay between the process of decoherence and the amplification that is naturally caused by decoherence is especially highlighted and placed in the context of quantum foundations. This (as well as other advances summed up in that article) is a major step forward in the understanding of the transition from quantum to classical. The tools developed in this study (such as quantum Chernoff information) will be also suitable in other contexts (such a detection of weak forces, etc.). They are also essential for the "Quantum Darwinism" program our group has championed.

Impact on National Missions

This research contributed to the condensed matter science at Los Alamos, providing critical insights into quantum technological applications. These are diverse, including superconductors, metrology, etc., and have clear impact on national missions.

Quantum computing may be of the most significant and urgent potential impact. There is the dream of quantum information processing, but even if it turns out to be more distant than some hope, the fundamental elements of computers will reach single atom size this decade (this is based on extrapolation of the famous "Moore's law"). Understanding what happens to superpositions of collective degrees of freedom and of relevant sources of decoherence is then indispensable in these (and similar) applications of interest to LANL, the NSSA and DOE.

Moreover, quantum superpositions in cold atom systems can possibly be used to enhance sensitivity of measuring devices. Capabilities foreseen for MaRIE seem well suited for condensed matter studies related to this project (dynamics of phase transitions).

Publications

Sonner, Julian; del Campo, Adolfo; Zurek, Wojciech H., Universal Far-from-equilibrium

Dynamics of a Holographic Superconductor, NATURE COMMUNICATIONS, Volume: 6 Article Number: 7406 Published: JUN 2015

Partner, Heather L.; Nigmatullin, Ramil; Burgermeister, Tobias; et al. Structural phase transitions and topological defects in ion Coulomb crystals, PHYSICA B-CONDENSED MATTER Volume: 460 Special Issue: SI Pages: 114-118 Published: MAR 1 2015

Zurek, Wojciech H. QUANTUM DARWINISM, CLASSICAL REALITY, and the randomness of quantum jumps PHYSICS TODAY Volume: 67 Issue: 10 Pages: 44-50 Published: OCT 2014

Zwolak, , C. J. Riedel, and W. H. Zurek. Amplification, Redundancy, and Quantum Chernoff Information. 2014. PHYSICAL REVIEW LETTERS. 112 (14) Article Number: 140406.

Campo, del, and W. H. Zurek. Universality of phase transition dynamics: Topological defects from symmetry breaking. 2014. INTERNATIONAL JOURNAL OF MODERN PHYSICS A. 29 (8) Article Number: 1430018.

Dziarmaga, J., and W. H. Zurek. Quench in 1D Bose-Hubbard model: topological defects and excitations from Kosterlitz-Thouless phase transition dynamics. 2014. Scientific Reports. 4: 5950.

Pyka, K., J. Keller, H. L. Partner, R. Nigmatullin, T. Burgermeister, D. M. Meier, K. Kuhlmann, A. Retzker, M. B. Plenio, W. H. Zurek, A. del Campo, and T. E. Mehlstaubler. Topological defect formation and spontaneous symmetry breaking in ion Coulomb crystals. 2013. NATURE COMMUNICATIONS. 4, Article Number: 2291.

Riedel, C. J., W. H. Zurek, and M. Zwolak. The rise and fall of redundancy in decoherence and quantum Darwinism (vol 14, 083010, 2012). 2013. NEW JOURNAL OF PHYSICS. 15: Article Number: 039503.

Streltsov, A., and W. H. Zurek. Quantum Discord Cannot Be Shared. 2013. PHYSICAL REVIEW LETTERS. 111 (4): Article Number: 040401.

Tylutki, M., J. Dziarmaga, and W. H. Zurek. Dynamics of the Mott Insulator to Superfluid quantum phase transition in the truncated Wigner approximation. 2013. 21ST INTERNATIONAL LASER PHYSICS WORKSHOP. 414: Article Number: 012029.

Zurek, W. H.. Wave-packet collapse and the core quantum postulates: Discreteness of quantum jumps from unitarity, repeatability, and actionable information. 2013.

PHYSICAL REVIEW A. 87 (5): Article Number: 052111.

Zwolak, M., and W. H. Zurek. Complementarity of quantum discord and classically accessible information. 2013. SCIENTIFIC REPORTS. 3: Article Number: 1729.

Accurate Interfacial Structures for Atomistic Simulations: Minimizing the Grand-Canonical Free Energy

Danny Perez
20130517ER

Abstract

To carry out effective simulations at the atomic scale, it is crucial to know the details of the atomistic structure of materials. However, obtaining such information experimentally is often impractical due to technical limitations or high costs. It is therefore crucial to be able to directly discover these relevant atomic scale configurations using computer simulations. In this project, we take on this challenge by developing a suite of novel simulation techniques that allow the configuration space of complex systems to be efficiently sampled. We demonstrate their power by investigating the behavior of defects in materials, and more specifically of grain boundaries in metals. Our method provides novel insights into the behavior of these complex systems, insights that were previously out of reach.

Background and Research Objectives

To carry out effective simulations at the atomic scale, it is crucial to know the details of the atomistic structures of materials. Indeed, many of the crucial properties of materials (e.g., strength) are controlled by the details of their atomic structure, for example, the nature of the different defects in the material, the ease at which defects move, and how they interact. In order to be able to make reliable predictions from simulations, one needs to be able to create representative configurations of the atoms in the material, so the properties and evolution of such configurations can be predicted. Even the most accurate methods are useless if such a starting point cannot be obtained. A pressing challenge is that, often, obtaining that information experimentally is impractical due to technical limitations or to the high cost of such a procedure. When lacking better approaches, simple rules of thumb or geometric constructions are often used to fill in the missing details. Sometimes, searches in limited spaces are used to explore the neighborhood of these guesses to assess their thermodynamic stability (i.e., how comparatively stable they are in conditions of interest), which is often a good metric of their practical relevance. However, due to the astronomical size of the accessible configuration space, unconstrained searches are scarcely attempted. While sampling algorithms are available, materials are notoriously difficult to sample thoroughly, because their energy landscape is very rough, so that exploring it in search of stable configurations is extremely time-consuming. This problem is even more severe when the number of atoms in the structures of interest is unknown a priori. This is often the case for defects such as grain boundaries (the interface between regions of the materials with different crystalline orientations). Indeed, these defects are by definition coupled to the bulk material. They can therefore exchange atoms with their environment, which can affect the density, and hence the structure, of the boundaries. In this case, simulations have to tackle the difficulty of accurately accounting for these changes in the number of atoms, which in an ongoing challenge. Overall, this inability to thoroughly search the space of possible configurations severely limits the accuracy of atomistic simulations: again, even the most accurate simulation is only as good as its starting point. Further, being unable to sample the landscape of these materials implies that accurate prediction of their properties in various conditions of interest to applications cannot be expected. In this project, we developed efficient sampling algorithms to systematically and autonomously search for the most relevant structures. Our work is based on a grand-canonical approach where we are able to efficiently stitch together simulations of different number of atoms in order to make predictions on open systems where the number of atoms is able to naturally fluctuate. This framework is coupled to state-of-the-art sampling algorithms that will allow an efficient search of this huge space. Our method is demonstrated on problems related to defects and grain boundary in materials. Our approach could have a profound impact in the field by leveraging modern simulation techniques to turn the “art” of predicting the atomic structure of materials into a systematic search process. This could dramatically improve the accuracy

and predictive power of atomistic simulations.

Scientific Approach and Accomplishments

An important part of the project has been dedicated to the development, implementation, and comparison of different sampling approaches. We first investigated the formal underpinnings of different potential simulation methodologies in order to identify the most promising. In doing so, we uncovered an unexpected equivalence between three simulations methods that are widely used in the field, namely Wang-Landau sampling, statistical temperature molecular dynamics, and metadynamics. The first and last methods are workhorses of computational thermodynamics. While they superficially share some resemblance, their formal relationships were never investigated. This has lead to many "rediscoveries" where very similar enhancement or analysis were proposed for each of the methods, without putting these in the wider context of an "ecosystem" of related techniques. This duplication of effort is costly and slows down the pace of innovation. In our work, we demonstrated that the three methods can be made absolutely identical through a consistent choice of initial conditions and update rules. This unexpected equivalence opens the door to technology transfer between different communities that were previously working mostly independently. We published our findings in the Journal of Chemical Theory and Computation [1]. This work is already well cited, demonstrating the usefulness of this insight. It has also been presented in leading national conferences and was very well received.

Building on this improved understanding of the different methods, we then focused on assessing different techniques that can be applied to the problem of so-called grand-canonical thermodynamics in materials. These methods allow one to simulate systems where the number of atoms is not constant because of a coupling with a reservoir of atoms (usually the extended environment in which a particular configuration is embedded). Upon testing many different approaches, we settled on a combination of "adaptive force biasing" sampling combined with a parallel tempering approach and a thermodynamic integration at different particle number. In simple terms, we first run different simulations with a varying number of atoms. In these simulations, each running on multiple processors, we characterize the thermodynamics on a wide range of temperature. This is done by running simulations at different temperatures side-by-side and allowing them to interact by exchanging configurations between them; this is parallel tempering. This insures the "mixing" of the different simulations and greatly accelerates convergence. We further accumulate crucial information on the density of states of the system during the simulation. A second set of simulations (the thermodynamic integration part) is then carried out at high temperature to "stitch" the different simulations together. This is done by introducing "fractional particles", i.e., particles that can come in and out of the simulation cell in a continuous fashion by scaling their interaction with the rest of the system. This enables us to then predict the probability that the system would contain a given number of particles at a given temperature and to compute any thermodynamic quantity of interest at any temperature. Our approach combines several state-of-the-art approaches into a unique new capability that has not been applied to materials before.

Despite initial encouraging results, we rapidly realized that, in order to be practical, the efficiency of the parallel tempering simulations would have to be improved. This is because the thermodynamic integration part can only be done in a liquid, but we are really interested in the properties of the solid. Therefore, our simulations have to extend across the melting transition in order to make grand-canonical predictions. Crossing phase transitions is a notorious problem in sampling because the configurations on either side of the transitions are extremely different and hard to reach from the other side. Because the simulation cannot easily cross the transition, convergence is extremely slow, which introduces errors in our low-temperature predictions. This is an extremely challenging, and well known, problem that we had to tackle in order to make further progress. Our approach to the problem was two-pronged: first, optimally adjust the set of temperatures during the parallel tempering stage, and second, introduce a novel database resampling strategy that allows replication of important configurations across the different replicas of the system, instead of just shuffling the same configurations around as is usually done in parallel tempering. The first problem is a long-standing one and, since the introduction of parallel tempering, a huge number of solutions have been proposed. These solutions are however very cumbersome to apply in practice. We realized that, because we were using parallel tempering in conjunction with other state-of-the-art methods to compute the density of states, we could directly predict the optimal temperature distribution, instead of slowly pushing the temperatures around in the right direction. This is a major advance, because our method does not require running preliminary simulations: instead we continuously adjust the optimal temperature set based on the latest thermodynamic data gathered during the simulation. This last point is crucial in the case of phase transitions, because the transition point tends to move as it converges. Therefore, a priori identifying the optimal temperature set is just as difficult as solving the original problem. The method is first described in Ref. [2], and will be covered in details in

Ref. [3]. The second improvement is the introduction of a database of configurations that can be used to resample during parallel tempering. The idea is simple but extremely far reaching: by measuring the density of states as we perform parallel tempering, we can automatically discover when some replicas are trapped in "metastable" states, i.e., long-lived states which are nonetheless irrelevant in the conditions of interest. Even better, we can resample a more appropriate state for these replicas from the set of all configurations visited by any other replica at any point in the past [3]. Taken together, these two improvements have delivered dramatic speedups for simulations across the melting transition. These improvements are critical for our needs, but are also extremely widely applicable to other fields, as parallel tempering is a workhorse in atomistic simulations.

We have implemented our approach into our in-house simulations code AMDF and demonstrated its efficiency. We thoroughly validated the codes by comparing the results of different sampling techniques. As a first application, we investigated, in collaboration with an ongoing DOE SciDAC project, the behavior of small helium clusters in bulk tungsten, a system of relevance to fusion energy production. Understanding the behavior of these clusters is critical, as they are known to nucleate helium bubbles, which can lead to dramatic degradation of the performance of the material. We predicted the binding free energies of these clusters over a large range of temperature, which can be used to predict the relative abundance of clusters of different sizes. This result nicely complemented the other techniques used in that project. An article describing our results was published in Physical Review B [5] while the details of the method are discussed in another paper published in Physics Procedia [4].

Using our technique, we have begun exploring the behavior of realistic grain boundaries in copper. Copper is an ideal test material because it can be very well described using empirical potentials. We have selected three boundaries of different character in order to sample from the very wide range of possible boundaries. For each boundary, we have performed a complete grand-canonical scan that enables us to predict their properties at any temperature and chemical potential (the "strength" of the source/sink of atoms the system is coupled with). To our knowledge, this is the first time this was achieved. An example of such a boundary is shown in Figure 1. A typical example of a result of our approach is shown in Figure 2. There, we show the evolution of the probability of observing a given number of atoms in the grain boundary as a function of temperature. The observed behavior is extremely complex. At low temperatures (200K), only one number of atoms is

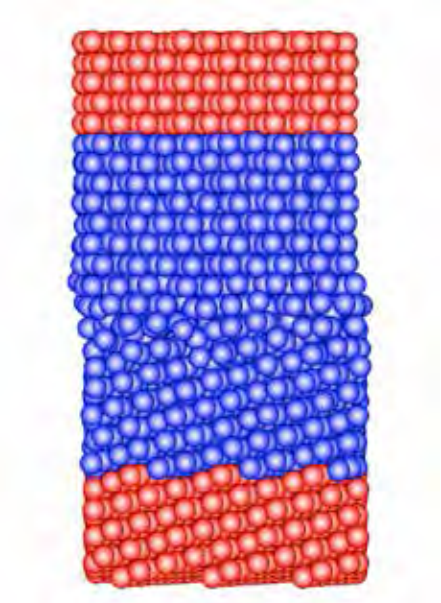

Figure 1. Illustration of a Sigma 45 grain boundary in copper. The atoms in red a constrained to move as rigid blocks in order to impose a specific grain boundary orientation. The configurations of the atoms in blue are fully sampled with our method. This is repeated by changing the number of atoms in the boundary until a whole layer has been added or removed.

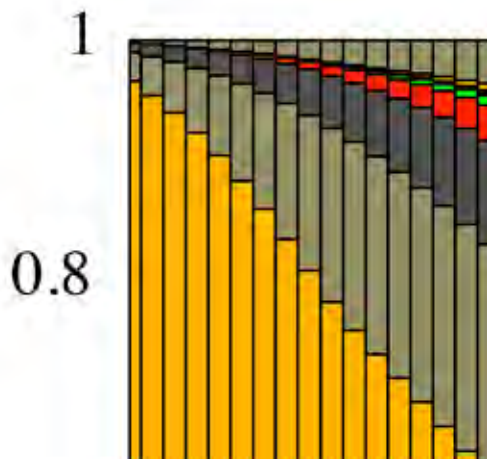

Figure 2. Evolution of the probability of observing a Sigma 45 grain boundary containing a given number of atoms as a function of temperature. The height of each vertical bar is proportional to the probability that the corresponding number of atoms is found in the boundary.

likely. This is expected, as, in the limit as the temperature goes to zero, only the state with the very lowest energy will be observed. However, as the temperature increases, the contribution of that state falls sharply. By the time the temperature reaches 500K, a wide range of different number of atoms, and hence of structures of the boundary can be expected to coexist. Even more interesting, as the temperature keeps increasing, the configurations that dominated at low temperatures become increasingly irrel-

evant. This is a clear demonstration of the need to properly identify structures that are relevant in different conditions: predictions of the properties of the boundary will obviously be adversely affected by the postulate that the relevant structures remain the same at any temperature. Using our approach, we can do away with such assumptions and directly explore the possible configurations of such complex systems in their full complexity, leading to a dramatic improvement in our ability to model, understand, and eventually control, such systems.

Impact on National Missions

Atomistic computer simulations play an increasingly important role in the prediction of properties of materials, or in the interpretation of experimental results. However, to be effective, these simulations need adequate starting points that properly represent the most probable atomic-scale structure of the material. This is crucial for a number of the Laboratory's missions, especially those dealing with materials in extreme conditions. For example, we recently found that adding a small proportion of interstitials to a grain boundary in tungsten (a leading candidate for the first wall of fusion reactors) can dramatically lower the stress at which the boundaries slide, which could lead to creep, but also enhance the ability of the materials to heal radiation-induced defects. To quantify these effects, it is paramount to first identify the structures that are thermodynamically relevant. These same challenges exist everywhere atomistic simulations of materials are used. Our proposed methodology will assist in the sampling of the possible structures and greatly help in the identification of the relevant ones. This has the potentials to significantly increase the power of atomistic simulations across a very wide range of problems of direct relevance to the lab's missions, for example to investigate the properties of cladding materials in nuclear reactors, or to be able to predict the response of polycrystalline materials to shock, to name only a few examples. This capability directly supports mission needs for DOE Office of Science, Nuclear Energy, and MaRIE while enhancing our basic understanding of materials.

References

1. Junghans, , Perez, and Vogel. Molecular Dynamics in the Multicanonical Ensemble: Equivalence of Wang-Landau Sampling, Statistical Temperature Molecular Dynamics, and Metadynamics. 2014. JOURNAL OF CHEMICAL THEORY AND COMPUTATION. 10 (5): 1843.

2. Vogel, T., and D. Perez. Accelerating the convergence of replica exchange simulations using Gibbs sampling and adaptive temperature sets. 2015. Physics Procedia. 68: 125.

3. Vogel, T., and D. Perez. Towards an optimal flow: Density-of-states-informed replica-exchange simulations. Physical Review Letters.

4. Vogel, T., and D. Perez. Sampling in the multicanonical ensemble: small He clusters in W. 2014. Physics Procedia. 57: 104.

5. Perez, , Vogel, and B. P. Uberuaga. Diffusion and transformation kinetics of small helium clusters in bulk tungsten. 2014. PHYSICAL REVIEW B. 90 (1).

Publications

Junghans, , Perez, and Vogel. Molecular Dynamics in the Multicanonical Ensemble: Equivalence of Wang-Landau Sampling, Statistical Temperature Molecular Dynamics, and Metadynamics. 2014. JOURNAL OF CHEMICAL THEORY AND COMPUTATION. 10 (5): 1843.

Perez, , Vogel, and B. P. Uberuaga. Diffusion and transformation kinetics of small helium clusters in bulk tungsten. 2014. PHYSICAL REVIEW B. 90 (1).

Vogel, T., and D. Perez. Sampling in the multicanonical ensemble: small He clusters in W. 2014. Physics Procedia. 57: 104.

Vogel, T., and D. Perez. Accelerating the convergence of replica exchange simulations using Gibbs sampling and adaptive temperature sets. 2015. Physics Procedia. 68: 125.

Vogel, T., and D. Perez. Towards an optimal flow: Density-of-states-informed replica-exchange simulations. Physical Review Letters.

Understanding and Controlling Magneto-Electric Coupling in Multiferroic Materials

Dmitry A. Yarotski
20130525ER

Abstract

The last few decades have seen the discovery of novel classes of correlated electron materials with exotic properties that few would have imagined. Multiferroic materials stand out among them, due to the ability to change their magnetization and/or polarization state with either electric or magnetic fields. This has the potential to revolutionize future energy, sensing and information technologies, as multiferroic circuits will combine the low power consumption and speed of field-effect devices with the permanence of magnetic elements. The remarkable properties of multiferroics emerge from strong coupling between coexisting electric and magnetic orders. Despite recent progress in the synthesis and characterization of single-phase and heterostructured multiferroic materials, the existing understanding of magnetoelectric (ME) coupling mechanisms is still controversial, and the dynamical properties of multiferroics remain practically unexplored. In particular, the role of low-energy excitations (phonons, magnons, etc.) in the emergence of multiferroic functionality has not been clarified.

Our ultimate goal is to leverage the unmatched LANL integration of material synthesis, advanced ultrafast optical techniques and forefront solid-state theory to test the dynamic limits of ME phenomena and reveal the mechanisms governing ME coupling in representative multiferroic materials. In pursuit of this goal, we used sub-picosecond optical and terahertz (THz) pulses to directly excite electronic degrees of freedom and then probe the ensuing energy transfer to the low-energy modes in order to investigate their effect on magnetic and electric orders in each material. Our unique combination of broadband time-resolved probes allowed unambiguous separation of spin, charge and lattice dynamics, and in conjunction with theoretical modeling, revealed the mechanisms of coupling between low-energy modes responsible for the emergence of magneto-electric interactions in multiferroics. The results of this work are poised to make a broad impact on condensed matter physics and will open new directions in complex materials research.

Background and Research Objectives

Multiferroics are technologically important materials with co-existing ferroelectric (FE) and (anti) ferromagnetic (FM/AFM) orders. The allure of these materials lies in the possibility of controlling the electric and magnetic responses with either electric or magnetic fields. This has the potential to revolutionize future technology by combining the low power consumption and speed of field-effect devices with the permanence of magnetic elements. In addition to their technological appeal, multiferroic materials exhibit a variety of novel physical phenomena, e.g. new elementary excitations, like “electromagnons” (magnetic excitations driven by the electric field of light), and offer fertile ground for exploring the fundamental mechanisms governing ME coupling (which differ between various materials). Despite substantial effort over the past decade, single-phase multiferroic materials with strong ME coupling have only been realized at cryogenic temperatures.

Currently, there is a consensus that the major obstacle on the way to implementation of room-temperature multiferroic functionality is the lack of understanding of microscopic mechanisms governing the coupling between magnetization and ferroelectric polarization. In particular, the role of low-energy excitations in emergence of ME coupling and their influence on dynamics of multiferroic response remain practically unexplored. Although great strides have been made in characterization of the static ME response by standard methods consisting of measuring the magnetization as a function of applied electric field or vice versa, they provided little information on the underlying microscopic physics. Arguably, more insight has come from optical spectroscopy, which hinted on an intimate connection between the spectrum of low-energy excitations (phonons, magnons, and electromagnons) and ME coupling. However, there

is still strong disagreement as to whether these low-energy excitations are directly linked to the ME coupling.

In this project, we have leveraged recent developments in nonlinear optical techniques and have taken an innovative approach to resolving this controversy by direct excitation of specific low-energy modes and subsequent observation of their effect on magnetic/electric orders, and, importantly, coupling between them. More specifically, we have targeted systems where either lattice distortions or charge ordering drive ferroelectric response of the materials, and investigated how an introduction of elementary structural (phonons) and magnetic (magnons) excitations affects the spin, lattice and charge behavior and multiferroic properties of the material. Our ultimate objective for this project was to address three longstanding problems in the basic and applied science of ME systems: 1) How fast can the magnetization/polarization be switched, and how can this be improved? 2) What low-energy excitations are responsible for the strong interactions between electric and magnetic orders? 3) How can we manipulate these excitations to enhance the ME coupling and design better multiferroics? The results of our work provide the answers to these questions for several material systems, which are by no means complete but pave the way to better understanding of multiferroic functionality and development of the basic principles of ME material design. The impact of this project is expected to reach well beyond these particular materials as this study has enabled the transition from "passive" observation of quasiparticle and order dynamics to an "active" excitation and control of materials response with coherent photon sources.

Scientific Approach and Accomplishments

Our scientific accomplishments are exceptional considering the scale of the project. This can be testified by our near 11 refereed journal articles published and in preparation. In the following, we highlight most important technical accomplishments.

Strong coupling of charge fluctuations to ferroelectric and magnetic orders in LuFe2O4

Multiferroic LuFe2O4 has attracted much recent attention due to its strong ME coupling near room temperature. Theoretical studies have linked the giant ME coupling in LuFe2O4 bilayers to quantum charge fluctuations, but experimental evidence supporting this hypothesis has been scarce. We used femtosecond optical pump-probe spectroscopy, closely coupled to theory, to examine the effect of photoexciting either intralayer or interlayer Fe2+ -> Fe3+ charge transfer transitions at 1.5 eV and 1.1 eV, respectively, (in effect externally driving polaronic charge fluctuations) on the interlayer charge transfer energy as a function of temperature. Then, by varying the temperature above and below the AFM ordering temperature, TN, while tracking the maximum photoinduced reflectivity change, we revealed the role of these fluctuations in governing the coupling between spin and charge orders. The experimental results were interpreted by developing a model for polaronic hopping between two atomic sites, governed by the double exchange mechanism. Our studies revealed that charge fluctuations are coupled to the electric polarization, and furthermore that magnetic order strongly influences this coupling. This explicitly demonstrates that quantum charge fluctuations may be the mechanism coupling electric polarization and magnetic order in this unique multiferroic material. In addition, our time-resolved data, particularly the temperature dependence of coherent phonon oscillations, indicates that magnetic order influences polaron hopping and also suggests that polarized bilayers in LuFe2O4 are stacked anti-ferroelectrically along the crystal axis, in agreement with recent predictions.

Magnon-assisted relaxation of photo-carriers in multiferroic Eu0.75Y0.25MnO3

One of the most dramatic effects of strong ME interactions is an existence of a new elementary excitations, the electromagnons, that consist of coupled magnons and polar phonons and have resonant frequencies in THz range. However, it is still unclear whether the electromagnons are also coupled to electronic degrees of freedom or not. Here, we address this question by applying optical pump-THz probe spectroscopy to study the effects of photo-induced electronic perturbations on THz electromagnon absorption in a multiferroic Eu0.75Y0.25MnO3. This material belongs to distorted perovskite manganese oxides RMnO3, whose magnetic structure evolves with rare-earth ion R from an A-type antiferromagnet through incommensurate spiral spin order to a collinear E-type antiferromagnet. Onset of the spiral spin order below TN=47 K breaks the spatial inversion symmetry and induces a ferroelectric polarization in the a-c plane at TFE=30 K. In the temperature range of coexisting spin spiral and ferroelectric orders the electromagnon modes at 0.7 and 2.5 THz have been observed, hinting at a strong magneto-electric coupling in this material. We have observed both electromagnon modes in THz absorption spectra of Eu0.75Y0.25MnO3 crystal below TFE. The temporal evolution of THz absorption following an excitation with 1.5 eV pump (above band gap) photons at temperatures below and above magnetic phase transition showed no pronounced changes of electromagnon absorption. This behavior points at relatively weak coupling of electronic degrees of freedom to the electromagnon modes. Alternatively, the changes might be obscured by a strong frequency dependence of photoinduced THz transmission that resembles free carrier response and can

be described by the Drude model with scattering rates of <1 THz for all measured temperatures. Another notable feature of THz transmission dynamics is very slow (>>ns) relaxation at temperatures of 50 K and above, which accelerates significantly (100's fs) at T < 35K. The photo-excited carriers relax by either recombining across the bandgap or depositing the energy to other quasiparticles. Apparently, a new scattering channel opens at lower temperatures and promotes carrier relaxation back to equilibrium. The proximity of crossover temperature to the magnetic transition near TN suggests that this scattering process involves magnons, similar to another multiferroic, TbMnO3, where magnon-assisted hopping is known to contribute to the relaxation dynamics. This behavior clearly reveals strong spin-charge coupling in the dynamic response of this class of multiferroic materials and might have implications for their future application in optoelectronic devices.

We have also applied optical pump-optical probe spectroscopy to the same material to extract more details about electron-magnon coupling. While the THz probe is more sensitive to the collective motion of delocalized photo-excited carriers, optical probes are nearly resonant with d-d transitions of the magnetic ions and provide indirect information about magnetic re-ordering that follows photon absorption. As expected, our results demonstrated that the optical response of Eu0.75Y0.25MnO3 to photons with energies of 1.55 and 3.1 eV is dominated by the d-d and p-d transitions of magnetic Mn ions. The photo-induced charges increase the occupancy of higher d-orbitals and create a localized spin excitation that results in ultrafast switching of super-exchange interactions. The decay of this localized spin state appears as the tremendous increase in the amplitude of photoinduced reflectance due to the strong coupling of optical transitions to the spin-spin correlations. The decay involves emission of spin waves (magnons) and occurs within hundreds of picoseconds of the pump pulse, in agreement with our optical pump-THz probe results. In addition, the relaxation of photoexcited electrons to equilibrium included the formation and trapping of the Jahn-Teller polarons on the Mn sites, which affects the magneto-electric coupling strength in this material.

Complex spin structure in magetoelectric BiFeMnO3

Among single-phase multiferroic materials, BiMnO3 and BiFeO3 have been extensively investigated due to the promise of strong magnetoelectric coupling close to room-temperature. BiMnO3 is a rare multiferroic material which exhibits ferromagnetism. While the ferroelectric transition temperature is relatively high at 400 K, the ferromagnetic transition temperature is far below room temperature (TC = 105 K), and the magnetization is rather small. BiFeO3 has an incommensurate antiferromagnetic structure (TN = 650 K) and ferroelectricity (TC = 1103 K). With the aim of enhancing the magnetic moment in BiMnO3 while maintaining ferroelectricity, various approaches have been followed including attempting to induce a local spin configuration in a B-site ordered structure, or creating a complex chiral or canted spin structure via substitution of different 3d transition metal cations at the B-sites. Using epitaxial scheme, we have achieved co-existence of magnetic and ferroelectric orders in BiFe0.5Mn0.5O3 (BFMO) at room temperature by strain engineering. We have found that the BFMO perovskite phase only forms if there is a close lattice match with the substrate (i.e., (001) SrTiO3), and if the films are very thin and highly strained. Meticulous growth control has achieved clean, highly epitaxial, strained BFMO layers. Using first-principles density-functional theory calculations we predicted anti-parallel alignment of magnetic moments on Fe and Mn ions and revealed the strong dependence of the total magnetic moment on the strain. Subsequent measurements using X-ray magnetic absorption dichroism spectroscopy at Advanced Photon Source confirmed the predicted complex spin structure in this material, while strain effects are yet to be verified by growing Bi2FeMnO6 films on substrates with variable lattice mismatch. These results will provide a solid foundation for modeling and creating more complex heterostructured materials where the interfaces are used to control strain state and order coupling.

Other accomplishments

Experimentally, we have explored several novel materials that hold the promise for magnetoelectric functionality. We used optical pump–THz probe spectroscopy at low temperatures to study the charge dynamics in topological insulator Bi2Se3. Film thickness variation allowed us to separate the bulk from the surface transient response. We demonstrated that for thinner films the photoexcitation changes the transport scattering rate and reduces the THz conductivity, whereas in thicker films the conductivity increases upon photoexcitation and scales with increasing both the film thickness and the optical fluence. These different dynamics are attributed to the surface and bulk electrons, respectively, and demonstrate that long-lived mobile surface photo-carriers can be accessed independently below certain film thicknesses for possible optoelectronic applications. In the large magnetoresistance material WTe2, ultrafast optical pump-probe spectroscopy revealed several characteristic timescales in quasiparticle dynamics. The fast relaxation process occurring on a sub-picosecond time scale was caused by electron-phonon thermalization, allowing us to extract the electron-phonon coupling constant. An additional slower relaxation process, occurring on a time scale of 5-15 picoseconds, could be

attributed to phonon-assisted electron-hole recombination. As the temperature decreased below ambient, the timescale governing this process increased due to the reduction of the phonon population. However, below 50 K, an unusual decrease of the recombination time occurred, most likely due to a change in the electronic structure that has been linked to the large magnetoresistance observed in this material.

Experimental advances were matched by theory development aimed at explaining the data and directing the experiment to discovering the mechanisms underpinning multiferroic response. Beside modeling the static and dynamic signatures of magnetoelectric coupling in optical and THz ranges described above, we have focused on developing the theory of ultrafast time-resolved X-ray magnetic linear and circular dichroism (XMLD/XMCD) spectroscopy of magnetic materials. A model Hamiltonian including the core-levels has been considered. The time evolution for the spin and charge density has been formulated to derive the dielectric function. A numerical algorithm is being developed and will be tested against the data from ultrafast XMLD/XMCD capabilities recently developed at LANL.

Impact on National Missions

Our work directly addresses the Grand Scientific Challenges identified in the Basic Energy Sciences Advisory Committee (BESAC) report, which are central to DOE's missions in energy, science, and security in general, and to the LANL Materials Grand Challenge in particular. The demonstrated integration of material synthesis, novel ultrafast spectroscopic capabilities (intense THz sources and time-resolved X-ray probes) and forefront condensed matter theory represents the LANL Materials Strategy and provides LANL with the capability to investigate emergent properties of complex materials through observation of the dynamical behavior of relevant order parameters and through selective excitation of the low-energy modes responsible for material functionality. Our thrust to interface materials science with ultrafast THz, optical and X-Ray coherent photon probes represents an essential element in the MaRIE strategy that connects the M4 facility to the Multi-Probe Diagnostic Hall. Proposed experiments will provide critical understanding of the mechanisms of magnetoelectric coupling and thus enable the design and synthesis of new multiferroic materials with controlled functionalities. Materials with tunable and novel functionality are an enabling component in the development of next-generation devices for sensing, information storage, and spintronics applications. We believe that our integrated capabilities in complex material design, synthesis and characterization will be of great interest to multiple sponsors, including DOE-BES, DOD, IC, and industry.

Publications

Aguilar, R. V., Qi, Brahlek, Bansal, Azad, Bowlan, Oh, A. J. Taylor, R. P. Prasankumar, and D. A. Yarotski. Time-resolved terahertz dynamics in thin films of the topological insulator Bi2Se3. 2015. APPLIED PHYSICS LETTERS. 106 (1).

Aguilar, R. Valdes, A. Azad, S. W. Cheong, A. J. Taylor, R. P. Prasankumar, and D. A. Yarotski. Slow relaxation of photocarriers and their coupling to magnons in multiferroic Eu0.75Y0.25MnO3. Applied Physics Letters.

Aguilar, R. Valdes, Y. M. Sheu, A. J. Taylor, R. P. Prasankumar, and D. A . Yarotski. Time resolved terahertz and second harmonic investigations in multiferroic RMnO3 and RMn2O5. Presented at 2013 March Meeting of The American Physical Society. (Baltimore, MD, 18-22 March, 2013).

Chen, A. P., H. H. Zhou, Z. X. Bi, Y. Y. Zhu, Z. P. Luo, A. Bayraktaroglu, J. Phillips, E. M. Choi, J. L. MacManus-Driscoll, S. J. Pennycook, J. Narayan, Q. X. Jia, X. H. Zhang, and H. Y. Wang. A New Class of Room-Temperature Multiferroic Thin Films with Bismuth-Based Supercell Structure. 2013. ADVANCED MATERIALS. 25 (7): 1028.

Chen, A. P., W. R. Zhang, F. Khatkatay, Q. Su, C. F. Tsai, L. Chen, Q. X. Jia, J. L. MacManus-Driscoll, and H. Wang. Magnetotransport properties of quasi-one-dimensionally channeled vertically aligned heteroepitaxial nanomazes. 2013. APPLIED PHYSICS LETTERS. 102 (9): -.

Chen, A. P., Z. X. Bi, Q. X. Jia, J. L. MacManus-Driscoll, and H. Y. Wang. Microstructure, vertical strain control and tunable functionalities in self-assembled, vertically aligned nanocomposite thin films. 2013. ACTA MATERIALIA. 61 (8): 2783.

Choi, , Fix, Kursumovic, C. J. Kinane, Arena, Sahonta, Bi, J. i. e. Xiong, L. i. Yan, Lee, Wang, Langridge, Kim, A. Y. Borisevich, I. a. n. MacLaren, Q. M. Ramasse, M. G. Blamire, Jia, and J. L. MacManus-Driscoll. Room Temperature Ferrimagnetism and Ferroelectricity in Strained, Thin Films of BiFe0.5Mn0.5O3. 2014. ADVANCED FUNCTIONAL MATERIALS. 24 (47): 7478.

Dai, Y. M., J. Bowlan, H. Li, H. Miao, Y. G. Shi, S. A. Trugman, J. X. Zhu, H. Ding, A. J. Taylor, D. A. Yarotski, and R. P. Prasankumar. Ultrafast Carrier Dynamics in the Large Magnetoresistance Material WTe2. To appear in Physical Review B Rapid Communications.

Lee, , S. A. Trugman, C. D. Batista, C. L. Zhang, Talbayev, X. S. Xu, S. -. Cheong, D. A. Yarotski, A. J. Taylor, and R. P. Prasankumar. Probing the Interplay between Quantum Charge Fluctuations and Magnetic Ordering in LuFe2O4. 2013. SCIENTIFIC REPORTS. 3.

Lee, , and R. P. Prasankumar. Correlation between quantum charge fluctuations and magnetic ordering in multiferroic LuFe2O4. 2014. EUROPEAN PHYSICAL JOURNAL B. 87 (11).

Lee, J., S. A. Trugman, C. L. Zhang, D. Talbayev, X. S. Xu, S. W. Cheong, D. A. Yarotski, A. J. Taylor, and R. P. Prasankumar. The influence of charge and magnetic order on polaron and acoustic phonon dynamics in LuFe2O4. 2015. Applied Physics Letters. 107 (4): 042906.

Talbayev, , Lee, S. A. Trugman, C. L. Zhang, S. -. Cheong, R. D. Averitt, A. J. Taylor, and R. P. Prasankumar. Spin-dependent polaron formation dynamics in Eu0.75Y0.25MnO3 probed by femtosecond pump-probe spectroscopy. 2015. PHYSICAL REVIEW B. 91 (6).

Xu, B., Y. M. Dai, L. X. Zhao, K. Wang, R. Yang, W. Zhang, J. Y. Liu, H. Xiao, G. F. Chen, A. J. Taylor, D. A. Yarotski, R. P. Prasankumar, and X. G. Qiu. Optical Signatures of Weyl Points in TaAs. Physical Review Letters.

Understanding of Nanoscale Fracture and Its Application in Developing High Fracture Toughness Nanoscale Composites

Nan Li
20140450ER

Abstract

In this project, we for the first time in the world aim at studying fracture toughness of nano/micro-dimensional samples and nanostructured materials. High strength materials generally have low fracture toughness because of reduced plastic deformation at the crack tip. We aim to design materials with high fracture toughness and good damage tolerance as well as high strength. Nanocomposites are promising candidates because of the role of interfaces in plastic deformation, including impeding dislocation motion as a barrier, facilitating the recovery and emission of dislocation at/from boundaries, providing additional plastic deformation pathways, and assisting in accommodation of plastic deformation. These aforementioned roles are strongly determined by the microstructures of nanocomposites and structures and properties of boundaries. Thus, we hypothesize "By virtue of microstructures and structures of nanocomposites, dislocations can be dynamically recovered within interface, preventing the formation of dislocation forest, assisting the further plastic deformation and suppressing the damage nucleation and propagation. The combination of these advantages will enable the development of high strength and high toughness composites." However, the current fracture theory and models are unable to quantitatively and qualitatively test this hypothesis because of the lack of understanding of interface physics. Moreover, the current experimental techniques cannot measure and characterize fracture toughness and fracture behavior of nanocomposites. Therefore, we have (1) for the first time developed a Nanoscale Fracture modeling tool and (2) developed the capability of measuring and characterizing fracture behaviors at nanoscale (including nano-sized specimen and nano-grained composites). Through this ER, we are able to address "what is Nanoscale Fracture?" and measure fracture toughness at nanoscale. With this technique, we are able to design the high strength and high toughness nanoscale materials by virtue of microstructures and boundaries. This significant contribution enables one to address both the science of nanoscale fracture and the engineering issue of designing nanoscale materials with high fracture toughness. The development of both modeling and experimental capability will also benefit other programs at LANL.

Background and Research Objectives

Future energy technologies demand novel materials with high fracture toughness and high strength that far exceed the limits of even the most advanced materials to date. Materials with the high strength can have low fracture toughness provided a crack nucleates. We hypothesize that nanocomposites could hold high strength and high toughness by virtue of their high density of interphase boundaries, largely because irreversible energy is associated with plastic deformation. However, fracture mechanics of nanoscale materials (referred to as Nanoscale Fracture), including the measurement of fracture toughness and characterization of fracture behaviors of nanoscale matertials, is less understood in contrast to fracture mechanics of conventional coarse-grained materials. Understanding "Nanoscale Fracture" involves both (1) defining/evaluating facture toughness and (2) determining the influence of microstructures and boundary structures on fracture behaviors. However, current theoretical and modeling tools are unable to address the two major issues because they do not have the capability of dealing with the influence of boundaries on plastic deformation. Therefore, we propose to develop a first of its kind of Nanoscale Fracture (NF) modeling tool. The most challenging technical part in terms of this theoretical approach is to include the influence of microstructures and boundary structures on the dislocation networks ahead of the crack tip and the sliding of the boundaries. Both determine the plastic work that can be done in the crack propagation process. To do so, we have developed our interface-dislocation dynamics model to deal with interfaces and grain boundaries in polycrystalline composites and integrate it into meso-scale/continuum-scale models to simulate the evolution of dislocation

networks in grains and boundaries and the contribution of boundary sliding to the plastic deformation. These have not been included in any of the existing materials modeling tools because of the lack of systematic fundamental understanding of interface physics at atomic scales.

Scientific Approach and Accomplishments

Atomic-scale: modeling and experimental characterization of cracking zone

By combining in situ high resolution transmission electron microscopic observation and molecular dynamics simulations, we for the first time performed atomistic observation of a crack tip approaching coherent twin boundaries in face centered cubic structures. Coherent twin boundaries (CTBs) in nano-twinned materials could improve crack resistance. However, the role of the CTBs during crack penetration has never been explored at atomic scale. Our in situ observation on nano-twinned Ag under a high resolution transmission electron microscope reveals the dynamic processes of a crack penetration across the CTBs, which involve alternated crack tip blunting, crack deflection, twinning/detwinning and slip transmission across the CTBs. The alternated blunting processes are related to the emission of different types of dislocations at the crack tip and vary with the distance of the crack tip from the CTBs. The results suggest that there is a critical twin thickness corresponding to both high strength and good toughness in nanotwinned materials. This work was published in Nature Group Journals, Scientific Reports 4:4397 (2014).

Meso-scale: modeling and experimental characterization

Combining in situ transmission electron microscopic observation and crystallographic analysis, we characterized twinning-dominated nucleation, propagation and deflection of crack in molybdenum. Corresponding to previous studies, the links between twins and cracks in bcc structures were proposed and demonstrated, including that (1) cracks and twins are independently produced, (2) cracks are induced by twins, and (3) twins are induced by cracks. According to these understandings, a strong correlation between twins and cracks in bcc structure could exist. However, the ex situ experimental setup could not directly demonstrate this correlation. In our work, we demonstrate a strong twin-crack relation in Mo. {112} twinning is characterized to be responsible for the dynamic process of crack zigzag propagation. The activation of the {112} twinning systems at the crack tips is ascribed to the high local stress at crack tips. The deflection is ascribed to the alternative of twinning variants that nucleate at the crack tip and are facilitated by twinning reflection at GBs. Moreover, in situ HRTEM images suggested de-twinning on crack surfaces. These observations demonstrate a twin-crack relation that (a) twins nucleate cracks and dominate a preferred cracking path and (b) a propagating crack also facilitates twinning. This work has published in Philosophical Magazine Letters 94 (4), 225-232 (2014).

Continuum-scale: elastic-plastic deformation in the far-field of crack

To interpret in situ SEM bending testing, we have developed a finite element method to characterize stress intensity factor of crack at a given geometrical dimension. Using this method, we have formulated the dependence of stress intensity factor on sample's dimensions, loading, and materials properties. These results have been used to link with experimental data.

Evaluation of fracture toughness in small sample

Evaluation of fracture toughness of materials is dependent of the geometry and dimensions of the tested samples. For coarse-grained materials, the sample can be made as big as the ASTM standards. Correspondingly, many theoretical models have been developed to evaluate fracture toughness by combining experimental measurements. However, we found such models could not describe fracture toughness for small samples. Figure 1(a) shows the three-point bending sample and loading condition. The sample size is about 30 um in wide and 6~10 um in height. Figure 1(b) shows the simulation model used in finite element modeling. Figure 1(c) shows variation of fracture toughness with the crack length for two different height of samples (6.2 and 9.2 um). The blue dashed lines show the prediction from the existing models. We have developed an empirical model, which can predict fracture toughness for small sample. Currently, we are working on a paper to report our contribution to the field of nanoscale fracture and nanoscale mechanics.

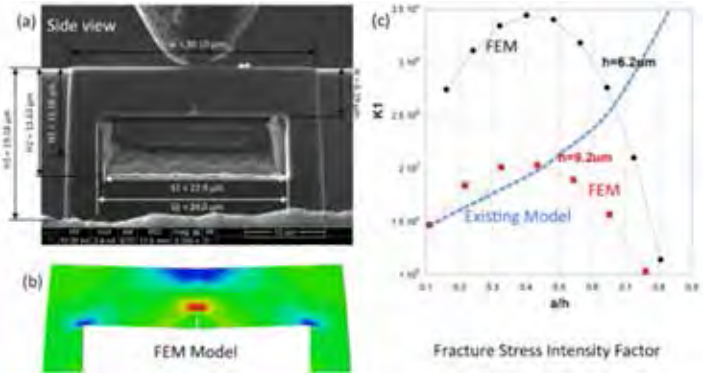

Figure 1. Prediction of fracture toughness for small samples. (a) in situ indentation testing of three-point bending micrometer samples, (b) Finite element simulation model, (c) variation of fracture toughness with crack length.

Phase transformation enhanced fracture toughness

The enhancement of plastic deformability in ceramics will enable the design of novel composites with high hardness and measurable ductility that are used in energy and defense related technologies and aerospace engineering. Metal/ceramic multilayers have come into greater focus due to their promising mechanical, physical and chemical properties, making them practically useful for harsh environments and extreme loading. Compared to metals, ceramics are lacking in room temperature plasticity and fracture toughness, because of a high lattice friction stress on most slip systems at low homologous temperatures. Metal/ceramic layered composites have been fabricated and extensively tested under various types of loading. As the bilayer period is reduced to a few nanometers, plastic co-deformability was inferred in Al-TiN multilayers from compressive stress-strain curves. Besides plastic codeformation, we found that thin ceramics layers can easily undergo phase transformation that releases elastic energy and offer additional plastic deformation. This can enhance fracture toughness in nanolayered metal/ceramics composites. High-resolution TEM (HRTEM) images in Figures 2a and 2b clearly show the initial Al-AlN-TiN trilayers. Cracks initiate in the TiN layer adjacent to the AlN layer. When the crack opens, the AlN layer does not crack, instead a phase transformation occurs in the AlN component from the zinc blende to the wurtzite phase. The crack first initiates in the TiN layer from the AlN-TiN interface (Figure 2b). This is a mode I crack due to the tensile stress resulting from the bending stress state beneath the indenter tip. The second crack initiates in the TiN layer from the top surface (Figure 2c). According to the crystallography of the TiN layer, the second crack surface is close to a {111} plane (Figure 2c). It is also noticed that the AlN and Al layers near the second crack do not fracture associated with the opening of the crack (Figure 2d). We studied the stress state associated with the crack initiation using finite element method and found that both the cracks are initiated by the tensile stress.

To characterize the two phases of AlN and the transition path, we performed in situ TEM indentation tests. Phase transformation processes are revealed with several high-resolution transmission electron microscope (HRTEM) images of the Al-AlN-TiN trilayer during in situ indentation testing. Figures 3b-3e show several TEM images of the AlN layer with respect to the indentation time. Six-atomic layers of w-AlN forms and propagates towards the left direction in Figures 3b-3d. A sharp interface between the z-AlN and w-AlN forms in the AlN layer, as shown in Figure 3d and magnified in Figure 3d'. Finally, the z-AlN layer transforms entirely into the w-AlN layer (Figure 3e). Two microstructural features are worthy of further discussion, i.e., the interface between the z-AlN and w-AlN crystals is sharp and the layer thickness remains unchanged after the phase transformation. These two features can be well addressed based on the collective gliding of three Shockley partials on every two (111) planes. It is worth mentioning that the three Shockley partials have the net zero Burgers vector, attract each other and form the sharp interface between the z-AlN and w-AlN, as demonstrated by our atomistic simulations.

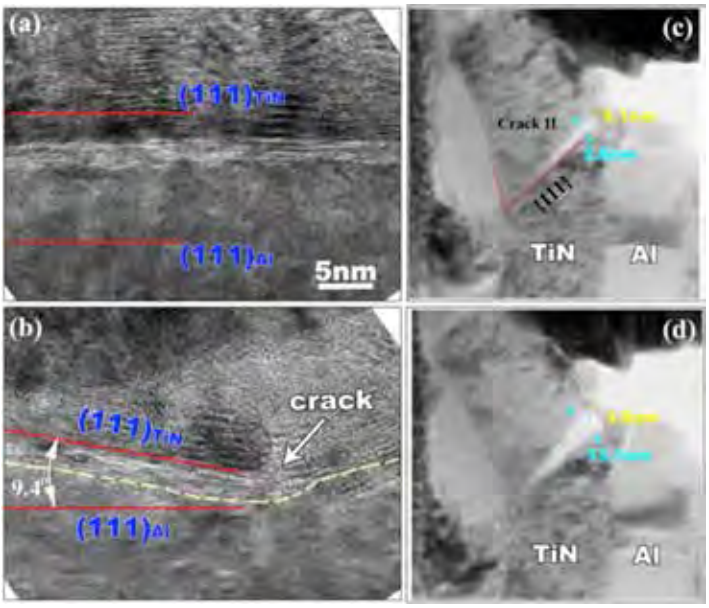

Figure 2. (a) and (b) HRTEM images of the Al-TiN interface before and after indentation. The red lines indicate the (111) plane. (c) and (d) Initiation and propagation of the crack II. The Al layer near the crack II does not fracture and the layer thickness reduces from 6.1 nm to 3.8 nm.

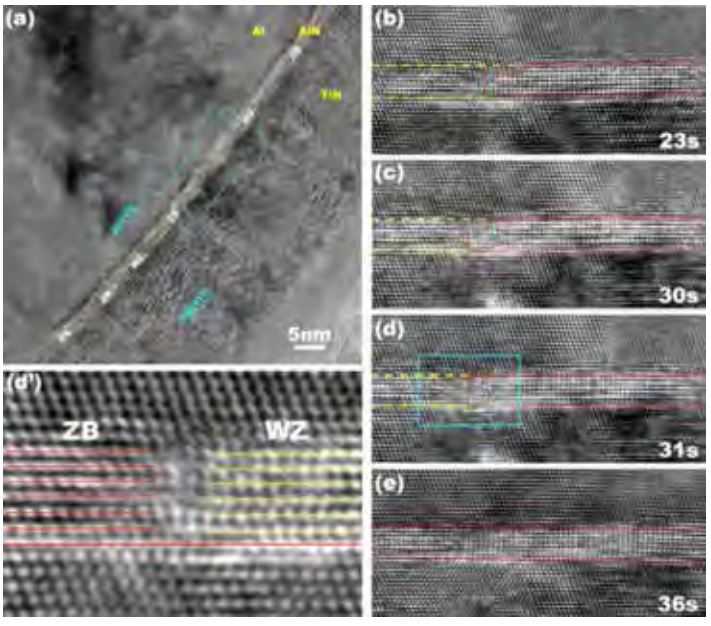

Figure 3. Phase transformation in the AlN layer. (a) one HRTEM image from in situ indentation test. WZ and ZB indicate the

w-AlN and z-AlN phase. Along the layer, phase transformation occurs heterogeneously. (b)-(e) HRTEM images of four snapshots of the region outlined in the blue rectangle in (a), showing the w-AlN nucleated and propagate towards the right direction. A sharp interface between the w-AlN and z-AlN was observed in all images and magnified in (d').

Interface sliding enhanced fracture toughness

Interface sliding for layered composites can be a major plastic deformation mode, especially for weak shear interfaces. We investigated the shape and size of the plastic zone at crack tip in layered composites with respect to interface shear resistance. Figure 4(a) shows the simulation model where interface sliding is described with additional slip system with the shear resistance interface. Crystal plasticity is described with slips that have a shear resistance dislocation. By varying the interface shear resistance, we can study the shape and size of the plastic zone at the crack tip. As shown in Figures 4(b)-4(d), with decreasing interface shear resistance, the plastic zone increases along the interface plane. As a consequence, the loading at same amount displacement decreases as well (Figure 4e). This means more plastic work associated with interface sliding, enhancing fracture toughness.

We recently performed in situ indentation testing for Mg/Nb multilayers in a SEM. We observed formation of a sharp crack from the surface due to the tension stress associated elastic bending (Figure 5a). The crack does not propagate but the crack tip blunts associated with interface sliding (Figure 5b to 5e), as evident from the observation of crack tip and a white strip (marked in a red circle). Finally, the crack propagates and forms a sharp tip again.

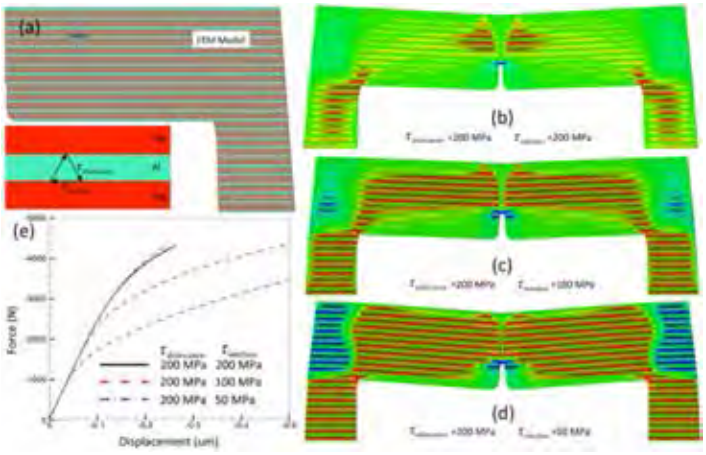

Figure 4. Interface sliding at crack tip. (a) FEM simulation model and method, (b), (c), and (d) Variation of shape and size of plastic zone at crack tip with respect to interface shear resistance, (e) the loading-displacement curves.

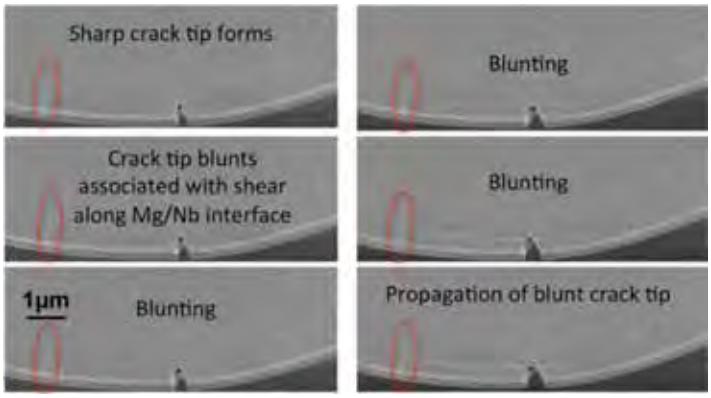

Figure 5. Crack tip blunts associated with interface sliding in Mg/Nb multilayered composites.

Impact on National Missions

The proposed work aligns with the call of "Materials: Discovery Science to Strategic Applications" to address the priority in materials at LANL: "the mechanistic multi-scale understanding and control of inhomogeneities, intrinsic and engineered, across all appropriate length and time scales that govern materials functionality". This ER project addresses two themes of our Materials Grand Challenge: Defects & Interfaces and Extreme environments. This work has developed a new materials modeling tool and provided insights into the roles of interfaces/grain boundaries in fracture resistance, which is of mission relevance to work at LANL.

Publications

Bufford, D.. In situ nanoindentation study on plasticity and work hardening in aluminium with incoherent twin boundaries. 2014. Nature Communications. 5: 4864.

Chen, Y., K. Y. Yu, Y. Liu, S. Shao, H. Wang, M. A. Kirk, J. Wang, and X. Zhang. Damage-tolerant nanotwinned metals with nanovoids under radiation environments. 2015. Nature Communications. 6: 7036.

Huang, , Wang, and Zhou. Effect of plastic incompatibility on the strain hardening behavior of Al-TiN nanolayered composites. 2015. MATERIALS SCIENCE AND ENGINEERING A-STRUCTURAL MATERIALS PROPERTIES MICROSTRUCTURE AND PROCESSING. 636: 430.

Li, , Shao, Li, McCall, Wang, and S. X. Zhang. Single Crystalline Nanostructures of Topological Crystalline Insulator SnTe with Distinct Facets and Morphologies. 2013. NANO LETTERS. 13 (11): 5443.

Li, N., and J. Wang. In-situ TEM Study of Dislocation-Interface Interactions. 2015. In The Transmission Electron Microscope – Theory and Applications. Edited by Maaz, K.. , p. 69. Croatia: InTech.

Liu, L.. Twinning-dominated nucleation, propagation and deflection of crack in molybdenum characterized with

in situ transmission electron microscopy. 2014. Philosophical Magazine Letters. 94 (4): 225.

Liu, L.. Atomistic observation of a crack tip approaching coherent twin boundaries. 2014. Scientific Reports. 4: 4397.

Salehinia, , Shao, Wang, and H. M. Zbib. Interface structure and the inception of plasticity in Nb/NbC nanolayered composites. 2015. ACTA MATERIALIA. 86: 331.

Salehinia, I.. Molecular dynamics simulations of plastic deformation in Nb/NbC multilayers. 2014. International Journal of Plasticity. 59: 119.

Salehinia, I.. Plastic deformation of metal/ceramic nanolayered composites. 2014. The Journal of The Minerals, Metals & Materials Society. 66 (10): 1.

Shao, , Wang, Misra, and R. G. Hoagland. Spiral Patterns of Dislocations at Nodes in (111) Semi-coherent FCC Interfaces. 2013. SCIENTIFIC REPORTS. 3.

Shao, S.. Energy minimization mechanisms of semi-coherent interfaces. 2014. Journal of Applied Physics. 116: 023508.

Shao, S., J. Wang, A. Misra, and R. G. Hoagland. Relaxation of Misfit Dislocations at Nodes. 2014. Materials Science Forum. 783: 515.

Wang, . Atomistic Simulations of Dislocation Pileup: Grain Boundaries Interaction. 2015. JOM. 67 (7): 1515.

Wang, , R. F. Zhang, C. Z. Zhou, I. J. Beyerlein, and Misra. Interface dislocation patterns and dislocation nucleation in face-centered-cubic and body-centered-cubic bicrystal interfaces. 2014. INTERNATIONAL JOURNAL OF PLASTICITY. 53: 40.

Wang, , Zhou, I. J. Beyerlein, and Shao. Modeling Interface-Dominated Mechanical Behavior of Nanolayered Crystalline Composites. 2014. JOM. 66 (1): 102.

Xu, E. Z., Li, J. A. Martinez, Sinitsyn, Htoon, N. a. n. Li, Swartzentruber, J. A. Hollingsworth, Wang, and S. X. Zhang. Diameter dependent thermoelectric properties of individual SnTe nanowires. 2015. NANOSCALE. 7 (7): 2869.

Yu, Q. i. n., Jiang, and Wang. Tension-compression-tension tertiary twins in coarse-grained polycrystalline pure magnesium at room temperature. 2015. PHILOSOPHICAL MAGAZINE LETTERS. 95 (4): 194.

Yu, Q. i. n., Jiang, and Wang. Cyclic deformation and fatigue damage in single-crystal magnesium under fully reversed strain-controlled tension-compression in the [10(1)over-bar0] direction. 2015. SCRIPTA MATERIALIA. 96: 41.

wang, J.. Reactions of lattice dislocations with grain boundaries in Mg: Implications on the micro scale from atomic-scale calculations. 2014. International Journal of Plasticity. 56: 156.

Additive Manufacturing of Mesoscale Energetic Materials: Tailoring Explosive Response through Controlled 3D Microstructure

Alexander H. Mueller
20150753ER

Abstract

Additive Manufacturing (AM) provides control over the mesoscale (micron-to-mm) internal structures of components at a level difficult to achieve through traditional machining techniques. These new structural design parameters have a profound effect on the mechanical properties of the AM parts, and provide a previously unavailable avenue to design damage propagation through the part. Control of the components' microstructure has particularly exciting applications to high explosives (HE) whose sensitivity and performance are dominated by structural features at the mesoscale. Modeling the effects of mesoscale structure on the mechanical properties, and damage and shock propagation within the part will allow for development a predictive capability to fully exploit these new manufacturing capabilities. The methodologies developed within this project will allow for the in-silico building of structures with mesoscale inclusions, three-dimensional mesh generation of these structures, and Finite Element Method (FEM) modeling of the mechanical properties and reaction under shock. This generates a modeling foundation for future handoff to simulations of reactive burn and will allow for the predictive design of the detonation characteristics of additively manufactured mesostructured HE components.

Background and Research Objectives

Additive Manufacturing (AM) provides control over the mesoscale (micron-to-mm) internal structures of components at a level difficult to achieve through traditional machining techniques. Application of AM to high explosives (HE) allows control of the HE microstructure and properties so that the interaction between the structure, reactive chemistry, and detonation properties may be better understood and used.

Modern explosives have stochastic, un-optimized microstructures. AM seeks to change these material limitations by directly assembling hierarchical structures to tailor and control the functionality of high explosives through manipulation of defects, wave interactions leading to the formation of "hot spots," - regions of high temperature and pressure from which chemical reactions initiate, and ultimately control the reactive flow and explosive performance properties.

AM can elucidate the mechanisms that allow control of performance through structure by developing the capabilities and materials to produce reproducible, micro-structured samples for high fidelity dynamic experiments. This includes the foundation for tailored sensitivity, directional performance, vibrational tolerance, and other properties not currently accessible to DoD, DOE and industrial reactive material applications. To achieve this goal, mesoscale HE modeling will play an essential roll.

The first objective of the modeling effort is to be able to determine and predict the mechanical response of a design meso-structured AM-HE. This can be accomplished by using Finite Element Methods (FEM) to perform numerical simulations of AM-HE meso-structures. The meso-structure is usually designed using a CAD (Computer Aid Design) system. For the FEM analysis it is necessary first to mesh the CAD geometry and then to transfer the mesh to the FEM code. This requires an interface between the CAD system and the Mesh Generation program (MG) and an interface between the MG program and the FEM code.

In this report we outline the steps developed to bring meso-structure designs from a CAD modeling to the FEM analysis.

Scientific Approach and Accomplishments

The approach presented in this report for AM-HE meso-structure modeling follows the above mentioned steps: develop CAD geometry, generate the mesh, and perform FEM analysis. In this study CAD design was accomplished using the BRL-CAD program, the TetGen v1.4.3

(tetrahedron generation) program was used for mesh generation, and the FEM analysis was performed using the ABAQUS finite element code.

The meso-structure was designed in BRL-CAD. Then the geometry of the microstructure was extracted as a STL (STereoLithography) file. The STL file represents the triangulated surface of the meso-structure.

In the next step the STL file was used as input for the mesh generation in TetGen and the geometry was discretized in tetrahedrons. Using different options, the size, the aspect ratio of the element, etc. of the mesh can be controlled. TetGen allows for multiple material regions and holes i.e. regions with no material.

In the FEM analysis step the tetrahedron mesh generated with TetGen was used as input for the ABAQUS-FEM analyses. In this step, material models, boundary and initial conditions were added to the problem. For a given mesh, different analyses can be performed: static and dynamic response, frequency and modal analyses, buckling stability, heat transfer, burning models, etc. The analyses can be combined; however, in the present report only the mechanical response was considered. Several examples involving different structures and different analyses are presented.

Geometry and mesh generation

As an example of the aforementioned approach, two types of meso-structures were considered in this report. The first type follows the idea of laminate composites. The meso-structure consists of a stack of layers each layer being composed of a number of cylinders with stacking sequence at 900 and at 450 as shown in Fig 1. One refers to these structures as Ply90 and Ply45. The FEM mesh for these structures is shown in Fig. 2(a,b). For Ply90 the size of the structure was 2 cm in x and y direction and 0.9 cm in z direction. The cylinder diameter was 1 mm. For Ply45 the size of the structure was 1 cm in x and y directions and 0.3 cm in the z direction. The cylinder diameter was 0.35 mm.

The second type of meso-structure follows the idea of particles distributed within a matrix. For this report a distribution of spheres inside of a cube was considered. In this case, an initial sphere was designed in BRL-CAD and then discretized using the extracted STL file from CAD geometry. Then, using this sphere as a pattern, a number of spheres were generated inside of a cube following a given spatial distribution: uniform (refers as Sph01) and a non-uniform gradient-like distribution (refers as Sph02) in x,y, and z direction. Fig. 3 shows the FEM mesh in these cases. In this case the size of the cube was 1 cm in all directions and the spheres size were scaled accordingly.

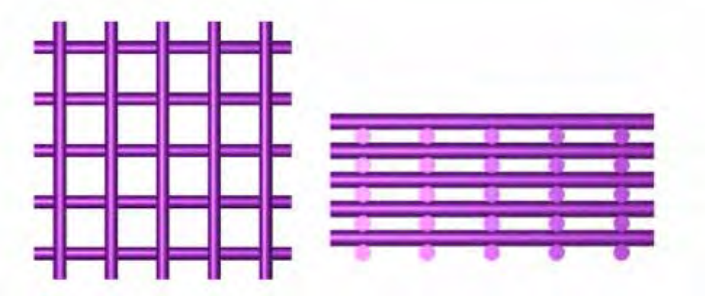

Figure 1. BRL-CAD geometry for Ply90 (a,b) and Ply45 (c,d) meso-structures.

FEM analysis

Once the FEM mesh for the meso-structure is obtained, the different analyses can be performed. In the present study different examples involving dynamic mechanical response are shown. The material in all cases was PBX9501 modeled as a viscoelastic material with damage. The damage in these results models the shear modulus degradation due to microcracking. The analysis was performed using ABAQUS with a user material subroutine implementing the PBX9501 material mechanical model.

Example 1

In this example the meso-structure Ply90 was subjected dynamically to a uniform compression strain rate in z and x direction. Fig. 2(c) shows the damage distribution for loading in z-direction and Fig. 2(d) shows damage distribution for loading in x-direction. The resulting damage is found to be localized at the cylinders intersections between the layers.

Figure 2. TetGen FEM mesh generation for Ply90 (a) and Ply45 (b). (c,d) Damage plot from ABAQUS FEM simulations for Ply90 under differing dynamic loading conditions.

Example 2

In this case natural frequencies were determined for Ply90 and Ply45 meso-structures simple supported in x, y and z direction. Fig 4 shows different vibration modes for Ply90 and Ply45. This analysis used the elastic bulk and shear modulus extracted as instantaneous values forming the viscoelastic PBX9501 material model.

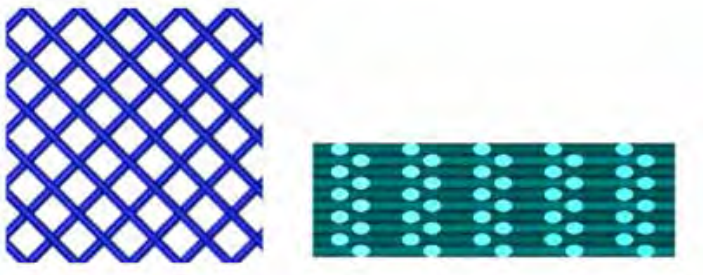

Figure 4. Natural frequency modes of the meso-structures Ply90 (a,b) and Ply45 (c,d).

Example 3

In this example, a meso-structure with non-uniform distribution of spheres Sph02 was subjected to a compressive uniform strain rate in the z-direction. This problem used the mesh shown in Fig. 3(c). The loading was applied on one face of the cube on the z-direction while the opposite face was simply supported in z-direction. Material model was PBX9501 as described above. The analysis was performed for the time duration necessary for the waves to travel along the length of the cube in z-direction.

Figure 3. TetGen FEM mesh generation for uniform (a), (Sph01), and non-uniform (b,c), (Sph02), distribution of spherical defects within a cube matrix.

Figure 5 shows the pressure wave contours at different moments in time as the wave advances in the material. It can be observed that the introduction of particles affects the wave profile compared with the wave profile in a homogeneous material.

It should be noted that for designed AM-HE meso-structures more complex analyses can be performed such as shock problems, modal analyses, heat transfer, burn models, etc. Bulk properties of microstructure can be determined also from global response of the meso-structure. For a meso-structure like Sph01 or Sph02, by adjusting the distribution of spheres or other inclusions in the HE matrix, the wave profile can be modified.

One important aspect of the approach used in this work is that the MG and FEM analysis can be incorporated in more complex code. For example in a shape optimization problem one starts with an initial CAD design. During the optimization the shape changes and the geometry needs to be remeshed and FEM analysis performed on new geometry. In the presented approach the mesh procedure and FEM analysis can be included as internal subroutines in the optimization code. In this case the shape of the object is represented a triangulated surface which can be available from the MG program (TetGen in our case).

In addition, analyses of different array configurations of HE designs can provide a reference database, which can be used later in design and manufacturing of HE.

Figure 5. Dynamic loading of meso-structure Sph02 at uniform compression strain rate in the z-direction, using PBX9501 material model. Isosurfaces of the pressure wave: (a) initial, (b,c,d) intermediate sequences of time, (e,f) wave reaches the end face of the cube.

Impact on National Mission

Achieving control of explosive sensitivity and performance by the hierarchical assembly of energetic materials lies squarely at the intersection of explosives chemistry, materials science, and detonation physics; core and unique competencies of LANL. The materials capabilities developed by this work align with the lab's core mission as detailed by the NNSA Additive Manufacturing Initiative Roadmap, have utility in support of MaRIE, the Materials Strategy in Defects and Interfaces, Extreme Conditions and Emergent Phenomena areas, and the DOE-BES Mesoscale Report; while the modeling and simulation tools developed will position LANL at the lead for HE materials by design.

In the present work an approach for integrating AM-HE design with FEM analysis was presented. Additive manufacturing (AM) of energetic materials has been designated as a priority to the NNSA and their stockpile stewardship mission. The development of this technology with relevant applications in lifetime extension programs (LEPs) and for the development of next generation materials (components of the future) has garnered much support throughout the agency. Furthermore, the development of AM processes

for HE has received considerable interest in DoD programs and Intelligence sponsors to address their particular needs. The 2016 NNSA stockpile stewardship plan specifically acknowledges the importance of AM technologies and their tie-in to MARIE, with the understanding of the interactions of defects in HE during the buildup to detonation being an obvious material interaction in an extreme environment. The understanding that we will gain over the behavior of explosives gives this basic research relevance to the above program areas.

Efficient Carbon Nanotube Growth on Graphene-Metal Surfaces

Enkeleda Dervishi
20130785PRD2

Introduction

The project goal is to optimize the synthesis conditions that promote the catalytic conversion of graphene into high yield few-walled (1-2 layers) carbon nanotubes (CNTs). The approach will overcome typical drawbacks of nanotube synthesis that include use of harsh chemical treatments of growth substrates and include the need for multi-step purification processes. These challenges will be overcome by using graphene sheets as an innovative new substrate for growth that allows one-step synthesis of composite materials. Growth can also be attained at low-temperatures (~200 degrees C vs the typical 800 degrees or higher) which is essential for enabling development of composites based on multiple materials with very different ranges of temperature compatibility. Another innovative aspect is to use dip-pen lithography capability for fine-control over placement and morphologies of metallic nanoparticle growth catalysts. Optimization of our growth processes will require variation and study of the influence of multiple growth parameters. These will include modulation of catalyst particle size, composition, and placement. We will also study the effects of variable temperatures and reactant gas composition and flow rates. The resultant synthesis will directly provide nanotube/graphene composites that will be studied for their energy harvesting and storage potential. Low temperature growth processes are anticipated to also allow the use of gold nanoparticles for growth as well, which will be the key to enabling development of nanotube-nanowire hybrids (not yet attained) of interest for optical and electronics needs. The knowledge gained in these first synthesis directions will also allow us to tailor synthesis conditions to pursue growth of other novel composite materials including carbon nanotube hybrids with complex metal oxides. Such oxide thin films form the basis for superconducting and multi-ferroic materials of technological interest. Interactions with nanoelectronic materials such as nanotubes can introduce emergent electronic behaviors that may enhance the properties of interest.

Benefit to National Security Missions

The work is directly relevant to DOE Office of Science interests in the fundamental science of and development of multifunctional nanoscale materials. The work will also probe the fundamentals of carbon nanomaterial interactions with other materials, also of interest to DOE/SC. The nanotube/graphene materials are of significant interest for energy storage and energy harvesting, giving the work mission relevance for both energy security and the environment (climate and energy impacts). The effort is also directly related to development and basic understanding of nanomaterials with ultimate impact on electronics, sensing, and imaging needs as well.

Progress

Throughout FY15, we made the following progress in the areas of large area and single-domain graphene and grapheme film synthesis, and envelopment of graphene heterostructures with oxides, nano wires, and quantum dots, as well as spectroscopic characterization of graphene molecules.

Large area graphenes for QD heterostructure plasmonics: We studied interaction of semiconducting quantum dots with large area graphenes. Interactions in these heterostructures create new optical responses from the quantum dots. Specifically, optical excitation of the quantum dots creates localized charging of the graphene resulting in optical plasmons that in turn interact with the quantum dots to modify their optical emission properties. The result is an enhanced rate of biexciton emission.

Single domain graphene synthesis: Efforts are proceeding at generating large area, single domain graphenes and evaluating the importance of different growth parameters for optimization. The single domain materials will be incorporated into a number of our heterostructure studies. In particular, we will target generation of twisted bilayer graphenes that produce new optical

resonances. Pairing of these systems with quantum dots should further enhance the plasmonic behaviors discussed in the above paragraph. Towards that end we are experimenting with iron films as growth substrates for preferential large-area bilayer growth and will continue that approach into FY16.

Graphene films: We have generated graphene films from graphene disk syntheses for use by collaborators in biosensing applications and bioviability testing. The bio viability tests are noteworthy in demonstrating that graphene films are capable of killing bacterial populations and may prove to be useful for medical coatings technology.

Nanowire heterostructures: Our goal is to access the potential high performance of Si nanowires for energy storage in batteries, but overcome current limitations of physical degradation of the nanowires on electrochemical cycling by pairing them with a highly conductive overcoat of graphene to provide physical strength. We have pursued Ge nanowires as a test system, but have encountered difficulties in melting of the nanowires during the graphene overcoating process. We have recently discovered that the melting is a function of ambient pressure in the growth chamber and are closing in on functional growth parameters. In parallel we have also developed a number of synthesis strategies for overcoating of Si nanowires by using an etching and catalyst nucleation process. Pursuit of these new strategies will be pursued into FY16.

Oxide heterostructures: Our first target is to integrate large-area graphenes with ZnO for optimal electro-optic behavior. We have worked out the necessary transfer techniques and are currently generating improved ZnO for integration to pursue Raman and electrical transport measurements in these systems. We are pushing to also integrate single domain graphene for performance optimization. We have also begun integrating large area graphene to ferromagnetic oxides with the goal of probing strain transfer to graphene using Raman spectroscopy.

Graphene molecule Raman spectroscopy: In FY15 we have evaluated size dependent trends in the fundamental Raman response of the D, G, and 2D vibrational modesvof synthesized graphene molecules. These systems have well-defined structures produced by direct chemical synthesis, allowing for the first time exact correlation of Raman behaviors to the graphene structure. We observe clear rise and fall of D to G intensity ratios as structures increase in size to the large area graphene sheet limit. These results can be understood as due to explicit structural changes that vary the number of graphene edge/defect states. We also find that the size-dependent vibrational frequency changes can be used to observe the transition of our structures from more molecular-like to large-scale extended behaviors. These results also provide a new characterization tool for molecular graphenes complementary to other approaches but providing more structural information.

Future Work

Large area, single domain graphene synthesis: In FY16 we will continue with optimization of single domain large area growth and push Fe-film catalyzed systems for “twisted” bilayer growth. Large area materials will be fed into our heterostructure studies. The twisted bilayer work in particular will be paired with quantum dot efforts to further probe optical coupling in these systems as follow-on to the FY15 results (see Paste-Year’s Accomplishments).

In FY16, graphene films will continue to be produced to supply collaborators in the areas of biosensing and bioviability.

In FY16 we will also finish up evaluation of the Ge nanowire melting mechanism and proceed with generation of test heterostructures for use in Raman spectroelectrochemical probing of the nanowire expansion process during electrochemical cycling. Si heterostructure growth strategies will be continued.

Oxide heterostructures: We now have all components required for generation of the oxide heterostructures and will proceed through FY16 with their optimized generation and related Raman studies.

Graphen Molecule Raman: In FY16 final spectra will be obtained and analyzed. We are at the intial stages of writing up the work for publication.

Conclusion

Our primary technical goal is now focused on generation of large-area graphene heterostructures. The methods we anticipate using will result in generation of functional hybrid carbon nanomaterials of interest for energy storage, electronic, and multi-ferroic applications. These may include hybrid quantum dot/graphene materials, graphene/nanowire heterojunctions, and graphene composites with complex oxide thin films.

Publications

Gao, Y., O. Roslyak, E. Dervishi, N. S. Karan, Y. Ghosh, C. J. Sheehan, F. Wang, G. Gupta, A. Mohite, A, M. Dattelbaum, S. K. Doorn, J. A. Hollingsworth, A. Piryatinski, and H. Htoon. Hybrid Graphene-Giant Nanocrystal Quantum Dot Assemblies with Highly Efficient Biexciton Emission. . 2015. Advanced Optical Materials Highlighted on the Inside Front Cover. . 3 (1): 39.

Understanding and Controlling Magnetism in Multiferroics with THz Pulses

Rohit P. Prasankumar
20130812PRD3

Introduction

In ferromagnets, the magnetization can be controlled with an external magnetic field, an idea widely used, for example, in magnetic data storage. However, magnetic fields have some drawbacks: there are limitations to how fast they can be switched, they are inconvenient to use, and they consume extra energy. Much effort has thus been devoted to multiferroic materials, in which electric and magnetic polarizations exist simultaneously and can be coupled, enabling control of magnetism with an electric field.

Recently, there have been significant advances in the ability to synthesize these materials, which has led to much effort focused on increasing the magnetoelectric (ME) coupling between magnetic and ferroelectric (FE) order, especially near room temperature. However, the microscopic origin of this coupling can vary across different classes of materials, and is not well understood. Low energy excitations (i.e. soft modes, magnons, etc.) are thought to play a key role in ME coupling, and therefore also offer a promising route to controlling it.

Here, we will use ultrashort optical and terahertz (THz) pulses to shed light on the microscopic origin of magnetoelectric coupling in different multiferroic materials (building on our previous work in this area). In these experiments, we will use these pulses to separately manipulate and probe the magnetic and electric orders in a given material, enabling us to, e.g., modify the magnetic order and probe the resulting changes in ferroelectric order, or vice versa. This will provide much insight into magnetoelectric coupling in multiferroics, which should extend our knowledge of their basic physics and also enable researchers to optimize them for applications.

Benefit to National Security Missions

The proposed experiments will provide LANL, as well as CINT, with the capability to investigate magnetoelectric coupling in multiferroic materials through selectively exciting the low-energy modes responsible for material functionality and probing their effects on this coupling. More generally, our effort to interface materials science with ultrafast terahertz (THz) and optical probes represents an essential element in the MaRIE strategy that connects the M4 facility to the Multi-Probe Diagnostic Hall. This work directly addresses the LDRD Grand Challenge in Materials, which underpins all three Laboratory mission areas. It also addresses several of the Grand Challenges for Basic Energy Sciences identified by the DOE Office of Science. We will work with the Program Director for Basic Energy Sciences to explore future funding opportunities within BES in the growing areas of ultrafast materials science.

Progress

In FY15, one of the main things that we worked on is optical-pump, THz probe (OPTP) measurements in the multiferroic HoMnO3. Unlike typical OPTP measurements, THz probing in HoMnO3 shows changes only at the magnon resonance, allowing us to directly track spin dynamics after optically exciting electrons. We learned from additional measurements at different pumping fluences and temperatures that the excited electrons couple to the spins via phonons, since the optically induced changes in the magnon resonance are consistent with steady state temperature increases. To test this physical picture, we did optical pump, optical probe measurements. A slow rise time is seen in these signals, which is nearly identical to that seen in the THz data. The slow rise time in the optical data can be attributed to spin-phonon relaxation through its temperature dependence. This confirms that the magnon dynamics seen in our THz signals result from a phonon-mediated transfer of energy from electrons to spins, since they correspond to the spin-phonon relaxation time. We have written a manuscript about these results, which should be submitted to Physical Review Letters in in FY15.

The research team gave talks about this work at the Ma-

terials Research Society spring meeting and the Quantum Electronics and Laser Science conference.

We spent some time looking for nonlinear THz pulse driven transport in LCMO and LSMO thin films (which are simultaneously magnetic and conducting). The current conclusion is that our THz fields are not strong enough to drive nonlinear transport, since all measurements seem to reveal a linear response. Considering the measured values for the binding energies of the polarons in these materials, we do expect that 10-100 times larger THz electric fields would be needed to be able to "untrap" or pull electrons out of bound polaronic states. The next step in this project is to work with other colleagues in the LUMOS group to pattern a metamaterial on top of the film, which should enhance the incident THz pulse at the film by a factor of as much as 50.

We recently obtained some TbMnO3 crystals. These are multiferroic, similar to HoMnO3 discussed above, but rather than having a magnetic dipole active magnon mode, it is electric dipole active, or an electromagnon, and also lies within the spectrum of our THz pulse. In initial temperature dependent transmission measurements it was difficult to identify this mode, but we are working to better polish the crystal and solving some other experimental problems so that it should be observable. Then we will optically pump and probe changes in the electromagnon as done in HoMnO3. Since this magnon can be excited with our THz E-field which is significantly stronger than our THz B-field, we will also try to detect changes to the ferroelectricity by probing second harmonic generation after exciting this mode.

Future Work

In FY16, we will initially focus on submitting our optical-pump, THz-probe results on HoMnO3 for publication. We will then optimize our system for performing mid-infrared (IR) pump, THz-probe experiments on HoMnO3, which will shed light on the coupling between lattice and magnetic degrees of freedom. We will then perform similar experiments on the manganite TbMnO3, which is well known for its strong magnetoelectric coupling, albeit at low temperatures. This material possesses an electromagnon resonance that is directly linked to ME coupling, and the proposed experiments should thus shed much light on these phenomena. We should be able to photoexcite the electromagnon resonance while probing ferroelectric order with second harmonic generation, shedding light on the coupling between these degrees of freedom. We will also perform similar experiments on multiferroic heterostructures, consisting of thin FE and magnetic films grown on top of one another to maximize the coupling between them; we have extensively used optical pump-probe spectroscopy to study these heterostructures, and THz pumping should give more insight into ME coupling in these systems.

Finally, we will extend our initial experiments on THz transport in thin manganite films to explore the role of polarons vs. free carriers in transport, particularly under high driving fields. This will likely include the fabrication of a metamaterial structure on top of these films to enhance the field strengths in the manganite layer, since our THz electric fields are not yet strong enough to liberate polarons from their bound states. This is a new regime of transport in these extensively studied systems, which should reveal novel physical phenomena. Overall, the proposed experiments should thus provide much insight into ME coupling in multiferroics and transport in colossal magnetoresistance manganites, with wide ranging impact in physics and materials science.

Conclusion

Multiferroic materials, in which magnetic and ferroelectric order can be closely coupled, offer much promise for a variety of applications in data storage, novel logic elements, and sensing. However, the mechanisms underlying this coupling are not well understood, limiting the potential of these materials. Here, we will use ultrashort optical and terahertz (THz) pulses to shed light on the microscopic origin of magnetoelectric coupling in different multiferroic materials. This will provide much insight into magnetoelectric coupling in multiferroics, which should extend our knowledge of their basic physics and also enable researchers to optimize them for applications.

Publications

Bowlan, P., D. A. Yarotski, N. J. Hur, A. J. Taylor, and R. P. Prasankumar. Direct observation of magnon dynamics in multiferroic HoMnO3. Presented at Quantum Electronics and Laser Science Conference. (San Jose, CA, 10-15 May 2015).

Bowlan, P., S. W. Cheong, D. A. Yarotski, A. J. Taylor, and R. P. Prasankumar. Directly probing antiferromagnetic order in HoMnO3 on an ultrafast time scale using optical-pump, THz-probe spectroscopy. Presented at Materials Research Society Spring Meeting. (San Francisco, CA, 6-10 April 2015).

Design Principles for High Performance Organic Photovoltaics

Aditya Mohite
20140658PRD1

Introduction

In this project we will apply innovative interface modification techniques to alter the charge recombination rates across an organic solar cell interface in a bilayer organic photovoltaic device by incorporating a spacer layer with designed functionality. The photo-generated exciton after migration to the donor-acceptor (D-A) interface dissociates due to a strong built-in field setup by the energy level alignment of the donor and acceptor forming a charge transfer or exciplex state (electron is on the acceptor molecule, C60, and hole on donor P3HT). There is a strong tendency for the exciplex state to recombine, which leads to poor photocurrent and thus low power conversion of sunlight to electricity. A few monolayers of the spacer layers are expected to suppress the electron to recombine with the hole and promote the separated electron away from the hole to generate photocurrent. We will use three different types of spacer layers: (a) Insulator (LiF) (b) Oligomer molecules and (c) Heavy Atom. Each of these spacer layers will result in the suppression of the exciplex recombination using different mechanisms. For example, LiF will act like a tunnel barrier, where an optimum thickness of the barrier is expected to completely suppress back recombination. Similarly, in the case of Oligomers, ordering at the D-A interface will control the recombination rate and for the Heavy Atom case, the exciton lifetime is expected to be long due to enhanced spin-orbit coupling, which will impart some triplet character to the singlet state. These strategies are also expected to bring about a deep scientific understanding of interface photo-physical processes that will be universal for heterostructures interfaces created with nanostructures.

Benefit to National Security Missions

This project aligns with LANL's Energy Security and Environment Mission areas, the DOE-BES Sunshot initiative, and Grand challenges addressed by the BES. Through studying this area of research, we will gain control over the transfer of charge and energy flow across interfaces and specifically provide the following in an attempt to develop high efficiency solar cells:

- Reveal the design principles for the efficient conversion of light to energy
- Develop mesoscale devices starting from model systems
- Apply the fundamental understanding to practical architectures such as bulk heterojunctions (BHJ) for organic solar cells and also for other types of light to energy conversion applications

Progress

There has been significant progress towards the goals described in FY15. We have achieved two key results that are fundamentally transformational.

First, by performing carefully designed experiments on organic solar cell devices, we have understood the role of microscopic ordering at the interface (donor/acceptor), where the exchange of charge and energy takes place. Given the spaghetti like morphology of the polymer systems, this was a challenging problem as different morphologies lead to different optoelectronic response and manifests as a different interface. There was no control over the morphology of the polymers at the interface which led to low efficiency devices. We have demonstrated the role of ordering by using small molecules (Oligothiphenes) with specific functional groups that microscopic ordering can be controlled and this leads to a 500% increase in the overall power conversion efficiency in a bilayer device. These small molecules can be deposited by thermal evaporation or via Langmuir-Blodgett trough process. We determined that when the oligomers are arranged out of plane to the donor (polymer that absorbs the light), extremely efficient charge and energy flow is observed, in contrast to when they are lying in plane or are pi-stacked. The microscopic structure was verified using one and two dimensional XRD at LANL and at the Advanced Photon

Source at Argonne National Lab. Furthermore, using these design principles established on proof of principle bilayer solar cells, we translated them to practical polymer solar cell devices also known as bulk heterojunction solar cells. We observed an increase in the efficiency from 4% to 8% with these strategies in a P3HT/PCBM system. This is the highest efficiency reported for a P3HT/PCBM solar cell to date. This work was in review in Science for 9 months and unfortunately was rejected. It was the editors call. We are writing a manuscript for Nature Materials on the ordering work.

In addition to the ordering work, we have also embarked upon a new research direction of controlling morphology in the recently discovered perovskite solar cells. One of the key challenges in perovskite solar cell is controlling the crystal structure and morphology, which determines its optical and electrical properties. We have developed three new strategies to develop highly crystalline films with large single crystalline grains that have quality similar to that of conventional direct band-gap semiconductors like GaAs and defect purity like crystalline Si. These techniques are (1) Hot casting using an IR heat gun (2) Doctor blading for making large area films and (3) Hot-casting using spin coating.

We get power conversion efficiencies of >18% with thee films and writing several manuscripts for high impact journals like Nature Materials, Nature Photonics and Science. This work is expected to have transformation impact in the field of thin-film solar cells.

Future Work

In FY16, we will focus on the aspect of photostability and reliability in the large grain perovskites that we have developed using several techniques. We will measure the efficiency of the perovskite solar cells as a function of constant solar light using a solar simulator. We will test the device for chemical and structural degradation. We will also explore the effect of UV light on the photostability of perovskite solar cells. In addition, we will also investigate the thermal and mechanical stability in these devices through a collaboration with Prof. Reinhold at Stanford University.

Conclusion

The success of this proposal will result in obtaining universal design rules that will guide the fabrication of high efficiency photovoltaics using nanostructure materials. These design principles will be applicable to several other applications such as organic light-emitting diodes (OLEDs), sensors, photo-catalysis, etc.

Publications

Dun, , Huang, Huang, Xu, Zhou, Y. e. Zheng, Tsai, Nie, D. R. Onken, Li, and D. L. Carrollt. Hydrazine-Free Surface Modification of CZTSe Nanocrystals with All-Inorganic Ligand. 2014. JOURNAL OF PHYSICAL CHEMISTRY C. 118 (51): 30302.

Kuo, , Nie, Tsai, Yen, A. D. Mohite, Gupta, A. M. Dattelbaum, D. J. William, K. C. Cha, Yang, Wang, and Wang. Structural Design of Benzo[1,2-b:4,5-b ']dithiophene-Based 2D Conjugated Polymers with Bithienyl and Terthienyl Substituents toward Photovoltaic Applications. 2014. MACROMOLECULES. 47 (3): 1008.

Liu, , M. R. Kelley, S. A. Crooker, Nie, A. D. Mohite, P. P. Ruden, and D. L. Smith. Magnetoelectroluminescence of organic heterostructures: Analytical theory and spectrally resolved measurements. 2014. PHYSICAL REVIEW B. 90 (23).

Mok, J. W., Lin, K. G. Yager, A. D. Mohite, Nie, S. B. Darling, Lee, Gomez, Gosztola, R. D. Schaller, and Verduzco. Linking Group Influences Charge Separation and Recombination in All-Conjugated Block Copolymer Photovoltaics. 2015. ADVANCED FUNCTIONAL MATERIALS. 25 (35): 5578.

Nie, , Chen, Smith, Xia, Hewitt, and Carroll. Nano graphite platelets enhanced blue emission in alternating current field induced polymer based electroluminescence devices using Poly (9,9-dioctylfluorenyl-2,7-diyl) as the emitter. 2014. ORGANIC ELECTRONICS. 15 (1): 99.

Nie, , Tsai, Asadpour, Blancon, A. J. Neukirch, Gupta, J. J. Crochet, Chhowalla, Tretiak, M. A. Alam, Wang, and A. D. Mohite. High-efficiency solution-processed perovskite solar cells with millimeter-scale grains. 2015. SCIENCE. 347 (6221): 522.

Sun, , Asadpour, Nie, A. D. Mohite, and M. A. Alam. A Physics-Based Analytical Model for Perovskite Solar Cells. 2015. IEEE JOURNAL OF PHOTOVOLTAICS. 5 (5): 1389.

Tsai, , Nie, Cheruku, N. H. Mack, Xu, Gupta, A. D. Mohite, and Wang. Optimizing Composition and Morphology for Large-Grain Perovskite Solar Cells via Chemical Control. 2015. CHEMISTRY OF MATERIALS. 27 (16): 5570.

Xia, , Chen, G. M. Smith, Sun, Yang, Nie, Li, Huang, Ma, and D. L. Carroll. High-performance alternating current field-induced chromatic-stable white polymer electroluminescent devices employing a down-conversion layer. 2015. JOURNAL OF LUMINESCENCE. 161: 82.

Yamaguchi, , Granstrom, Nie, Sojoudi, Fujita, Voiry, Chen, Gupta, A. D. Mohite, Graham, and Chhowalla. Reduced Graphene Oxide Thin Films as Ultrabarriers for Organic Electronics. 2014. ADVANCED ENERGY MATERIALS. 4 (4).

Yen, , Tsai, Kuo, Nie, A. D. Mohite, Gupta, Wang, Wu, Liou, and Wang. Flexible memory devices with tunable electrical bistability via controlled energetics in donor-donor and donor-acceptor conjugated polymers. 2014. JOURNAL OF MATERIALS CHEMISTRY C. 2 (22): 4374.

Yin, S. u. n., Nie, A. D. Mohite, Saxena, D. L. Smith, and P. P. Ruden. Current-voltage characteristics of organic heterostructure devices with insulating spacer layers. 2015. ORGANIC ELECTRONICS. 24: 26.

Synthesis of Novel Energetic Materials

David E. Chavez
20140659PRD1

Introduction

This project will focus on the development of novel energetic materials that are thermally stable but can be initiated through the use of unprecedented mechanisms such as photochemical or electrochemical stimulation to novel excited states. The research will focus on the synthesis of molecules with kinetic barriers large enough to prevent thermally induced detonation and excited states capable of bypassing those barriers in response to non-thermal stimulus (optical or electrochemical stimulation).

Benefit to National Security Missions

Los Alamos National Laboratory is a world leader in the synthesis and development of energetic materials. The design of a new class of explosives with controlled initiation properties has the potential to enhance safety and could have applications in detonator development and weapons programs. The proposed work will contribute to the Laboratory's core missions of new energetic materials development and threat reduction science. The fundamental nature of the work could have an impact in the basic understanding of materials and chemistry.

Progress

In FY15 significant progress was made towards the development of materials explosive for direct optical initiation. The overall goal of the project is the development of new explosive materials, which are stable to external stimuli (impact, friction, heat, and spark) that can be detonated when exposed to laser irradiation. Conventional explosives are unable to undergo this detonation process since they do not strongly absorb laser light. Compounds consisting of explosive tetrazines (tetrazines are nitrogen rich small dye molecules) with metal ions were targeted due to their potential to absorb large amounts of light and their potentially tunable explosive properties. Initial results from previous work had shown that the combination of iron with non-explosive tetrazines led to compounds with exceptional absorption of visible light.

Twelve compounds of non-explosive tetrazines and explosive tetrazines with zinc, copper, nickel, cobalt and iron were synthesized and their optical, explosive and chemical properties characterized in FY15. The iron based compounds had the largest absorption of visible light, the copper based compounds had significant absorption of near-infrared light, while the zinc, nickel and cobalt based compounds did not show any promising absorption of light. In addition it was found that the absorption of light was dependent on the metal used, and independent of whether the compounds were explosive or not. This was significant because it demonstrated that it is possible to control the optical and explosive properties of compounds independently of each other. A manuscript of these efforts has been submitted for publication in Inorganic Chemistry in FY15.

The strong absorption of visible light in iron based compounds prompted further investigation into this class of materials. It was found that chemically altering the tetrazine portion of the compounds could alter the wavelength of light absorbed without significantly affecting the explosive properties of the compounds. This was significant because it allowed for the compounds to be tuned to the wavelengths of light produced by commercially available lasers. This match between the wavelength of light emitted by laser sources and the wavelength of light absorbed by the compounds will lead to move efficient conversion of the laser energy into the initiation of the explosive materials. A collaboration between M division and T division was established to better understand the properties of these new materials. Overall these six new compounds have been synthesized and their optical, explosive, and chemical properties have been characterized. A publication summarizing these efforts is currently (FY15) in preparation.

The absorption of near-infrared light by the copper based compounds was significant since the most common commercially available laser emits near-infrared light. Additional investigation into these materials led to the discovery that the copper based compounds could adopt two different forms. The first form has a higher ratio of tetrazine to copper, while the second form has higher density and more favorable explosive properties. Tetrazines with differing explosive properties were used to synthesize additional copper based compounds of both forms. These resulting compounds have a wide range of explosive properties, but nearly identical optical properties. This is significant because it will allow for the determination of what explosive properties are important for direct optical initiation. A collaboration with W division has been established to test the response of these materials to laser irradiation. A manuscript is being prepared on this work in FY15 with the expectation that publication will occur in FY16.

In FY15 this project allowed additional capabilities to be established. Single crystal X-ray diffraction capability was developed at TA-9 which allows for the determination of the molecular structure of new materials. Although this capability existed off site, the ability to run these experiments at TA-9 avoids the cost and safety concerns of transporting explosive materials off-site. In addition protocols for the elemental analysis of compounds with both organic and metallic components were developed. This type of analysis allows for the determination of the mass composition of new materials.

Overall, a large number of new compounds have been synthesized as candidates for direct optical initiation. In FY16 the existing materials will be further investigated to determine the most promising materials. In addition the results obtained and the collaborations established will be used to guide the design of the next generation of these materials.

Future Work

Thomas was very productive in FY15, developing and characterizing new photoactive energetic molecules. In FY16 he will continue to make new molecules and examine their properties for optical initiation.

Specific FY16 tasks to be accomplished:

- Characterization of tetrazine ligands
- Reactions of tetrazine ligands with metals, characterization of products
- Scale up new selected compounds and collaborate with W division for laser initiation testing.

Conclusion

The technical goals of the project are to produce new optically active energetic materials that respond to non-thermal stimuli. The anticipated impact will be in the area of controlled initiation of energetic materials for applications. Access to such materials will significantly enhance the safety and surety of many systems employing energetic materials.

Publications

Breiner, M. M., D. E. Chavez, T. W. Myers, and R. D. Gilardi. 1,2,4,5-Tetrazinyl-Substituted Amino-1,2,4,5-Tetrazines. 2015. SYNLETT. 26 (4): 557.

Chavez, D. E., T. W. Myers, J. M. Veauthier, M. T. Greenfield, R. J. Scharff, and D. A. Parrish. Pentaerythritol Trinitrate Substituted s-Tetrazine and s-Triazine. 2015. SYNLETT. 26 (14): 2029.

Myers, T. W., D. E. Chavez, S. K. Hanson, R. J. Scharff, B. L. Scott, J. M. Veauthier, and Wu. Independent Control of Optical and Explosive Properties: Pyrazole-Tetrazine Complexes of First Row Transition Metals. 2015. INORGANIC CHEMISTRY. 54 (16): 8077.

Myers, T. W., S. K. Hanson, Jacqueline M. Veauthier, and David E. Chavez. First row transition metal complexes of tetrazine based ligands as a new class of energetic materials . Presented at 249th ACS National Meeting & Exposition. (Denver, CO, 22-26, Mar. 2015).

Investigating Structure-Directing Agents in Nonconventional Nanowire Synthesis Using a Transmission-Electron-Microscope Flow-Cell Holder

Jennifer A. Hollingsworth
20140661PRD1

Introduction

Understanding the growth mechanisms for one-dimensional (1D) semiconductor nanostructures, especially more complex 1D heterostructures including superlattice, core/shell, and dumbbell-like structures, is essential for the controlled synthesis of these novel architectures. Importantly, structural control is anticipated to enable properties control, where the ability to tune transport properties, charge separation efficiencies, and charge or energy transfer processes underpins a range of applications from energy conversion and storage to catalysis and photodetection. To date, however, controlled solution-phase growth of high quality and intentionally designed 1D heterostructures is still in the very early stage. Improved methods for establishing the structure-controlling mechanisms and, thereby, for increasing the pace of materials discovery and development are needed.

The work will take advantage of the postdoc's expertise in glycol-based solution-assisted low-temperature refluxing processes for synthesizing tellurium-based semiconductor nano-heterostructures for thermoelectric applications, along with LANL's new capability in in situ liquid-phase transmission electron microscopy (TEM). The latter will enable an unprecedented systematic assessment of nanowire and nanowire heterostructure formation real-time by direct imaging under the conditions of growth. Nanowires will be synthesized in the TEM flow cell, permitting direct assessment of the impact of reaction parameters on nanowire formation and growth progression. Glycol-based syntheses are scalable and afford a lower temperature alternative compared to higher temperature and more costly solution-phase and vapor-phase approaches. And yet, they are also capable of yielding high-quality, single-crystalline materials. The specific 1D nanostructures studied here will support advances in thermoelectrics and topological insulator applications, with important consequences for waste-heat energy harvesting (more than half of the energy generated worldwide is lost as heat), heat management in the electronics industry, remote power generation, etc. If successful, to our knowledge, this will also be the first real-time in situ imaging of nanowire growth processes in solution.

Benefit to National Security Missions

The work will advance fundamental understanding of nanomaterials growth mechanisms, which will enable new materials-by-design strategies. It will also advance our understanding of chemical processes that take place at nano/meso-interfaces and how these influence structure and ultimately function. Together, these contribute directly to DOE/SC, Basic Understanding of Materials and Fundamental Chemistry missions. It will also advance a new capability in liquid-phase transmission electron microscopy, propelling LANL to the forefront of this emerging and important research area. This capability will enable direct assessments (with enhanced efficiency and accuracy compared to 'post-mortem' assessments) of the impact of growth parameters on morphology, composition and interface evolution. This same technique can also be applied to studying corrosion processes and the impact of chemical or high-energy electron dosing on both growth and degradation of surfaces or three-dimensional structures, with relevance to MaRIE and stockpile stewardship. Finally, the nanowire materials produced will have direct relevance to energy harvesting (energy security, remote power generation) and cooling (e.g., spot cooling in electronics) applications, with fundamental understanding translatable to other nanowire materials systems that have potential applications in chem/bio sensing.

Progress

In FY15, the postdoc focused on flow-enabled synthesis of hetero-structured nanowires (toward addressing a need in the fields of thermoelectrics and topological insulators for ultrathin bismuth or lead chalcogenide nanowires (e.g., Bi2Te3 or PbTe, respectively) and their

heterostructures (e.g., where PbSe/PbTe superlattices were predicted by Dresselhaus (PRB 2003) to afford a game-changing thermoelectric figure-of-merit: ZT >6, if nanowire diameter could be controlled to <5 nm and segment lengths to only 2-3 nm). He has successfully re-established our laboratory's novel flow-solution-liquid-solid method for hetero-nanowire synthesis. He determined that lack of reproducibility in nanowire growth (even whether or not nanowire growth took place, e.g., in competition with quantum dot growth) could largely be attributed to the treatment of the growth substrate prior to deposition of the low-melting metal catalyst (bismuth). So far, only HF treatment ensures that the metal film is sufficiently "active" and able to support/catalyze nanowire growth (without HF treatment, the metal appears not to break apart into the nanoscale catalytic "islands"). More recently, he has successfully synthesized heterostructure nanowires comprising controllably abrupt or alloyed interfaces between segments of defined length. He has controlled interface properties by exploring methods for depleting the catalyst droplets of precursor prior to initiation of growth of a second or third segment (eliminated the "reservoir" effect so common in gas-phase nanowire growth). His nanowires of alternating segments will be explored for thermoelectric properties, while extremely short segments will be analyzed for "quantum dot-in-wire" properties, e.g, enhanced photoemission from an embedded emitter in a wire. Lastly, we have established a capability for templating the growth of catalyst-metal arrays for ordered nanowire growth (polystyrene sphere template for directing metal deposition prepared using Langmuir-Blodgett sphere assembly). This will be the first demonstration of ordered arrays of nanowires grown by a solution-phase method.

Future Work

In FY16, the postdoc will continue to target specific, novel nanowire heterostructures (nano-segmented for thermoelectrics and dot-in-wire for single-photon source application) by solution-phase growth methods. This will entail continuing to pursue significant progress being made in flow-based synthesis as described in the Progress section. He will also pursue a second option: polyol synthesis, where the aim will be to understand the controlling variables in polyol syntheses that determine nanowire diameter and use this understanding to synthesize ultra-thin sub-5 nm wires (currently a key synthetic challenge to access nanowires below 10 nm) and to monitor the impact of molecular "capping agents" or reactive cations on the formation of core/shell or superlattice heterostructures, respectively. Together, these aims address a need in the fields of thermoelectrics and topological insulators for ultrathin bismuth or lead chalcogenide nanowires (e.g., Bi2Te3 or PbTe, respectively) and their heterostructures (e.g., where PbSe/PbTe superlattices were predicted by Dresselhaus (PRB 2003) to afford a game-changing thermoelectric figure-of-merit: ZT >6, if nanowire diameter could be controlled to <5 nm and segment lengths to only 2-3 nm). Notably, the catalyzed flow-based approach may prove even more amenable to addressing this need for ultra-thin / controlled-heterostructure nanowire growth, as we have shown that by simply tuning the flow-rate (addition rate) of the nanowire precursor compounds during growth affords dramatic control over nanowire diameter (faster yields narrower by enhancing supersaturation). We also aim to shift our solution methods to study in situ in LANL liquid-phase TEM holder.

Conclusion

The project will advance the state-of-the-art in liquid-phase transmission electron microscopy (TEM). By pushing boundaries in terms of how the parameters and processes that influence nanomaterial's growth are assessed, the project will also afford new mechanistic understanding that will enable 'materials-by-design' of complex, functional one-dimensional semiconductor nanostructures for applications from energy conversion and storage to catalysis and photodetection.

Publications

Hollingsworth, J. A., G. Zhang, and R. Laocharoensuk. Controlling composition and interfaces in solution-grown semiconductor nanowires. Langmuir (Invited Feature Article).

Quantum Control of Tailor-designed Photoactive Energetic Materials

Tammie R. Nelson
20140668PRD2

Introduction

A critical need for the prediction and control of explosives behavior has been identified as a "grand challenge" in the area of dynamic and energetic materials science. Development of photoactive energetic materials that optically initiate by a laser light, can address future milestones for enhanced safety and security of the nuclear stockpile. Here, photoinitiation requires non-adiabatic (non-radiative) conversion of excess electronic energy into specific vibrational degrees of freedom mediated by the electron-phonon coupling. Excited states have varying electron-phonon couplings, and depending on their localization and energy, lead to different relaxation pathways. This structure provides a "landscape" for optical control (steering the outcome of a chemical reaction with light) based on which excitations are selected. Non-adiabatic excited-state molecular dynamics (NA-ESMD) simulations provide a detailed understanding of key photoinduced phenomena controlling competing interactions and relaxation pathways in complex materials.

Benefit to National Security Missions

The proposed work will increase the controllability of chemical dynamics by predicting and controlling the functionality of materials. The proposed work will further LANL's reputation and prestige in quantum control and molecular design. Control of explosive initiation would be transformational for LANL's core missions of stockpile safety and energetic materials.

Progress

Over the past year, significant changes have been done to the non-adiabatic excited state molecular dynamics (NA-ESMD) codes toward implementation of solvent contributions. A Polarizable Continuum Model (PCM) has been implemented and numerically tested. This allows us to conduct simulations of excited state dynamics in the presence of the simple solvent environment. We have also developed theoretical formalism on how to compute gradients along the excited state potential energy surfaces. Several numerical tests on representative molecules in solvent environment have been conducted and the results have been summarized in an article "Simulations of fluorescence solvatochromisms in substituted PPV oligomers from excited state molecular dynamics with implicit solvent" recently published in Chemical Physics Letters. In terms of applications, using developed theoretical methodology, we have conducted nonadiabatic dynamics simulations that show that the deactivation mechanism of tetrazine photochemistry in PetrinTzCl is due to vibrational excitation of the Petrin moiety during internal conversion. Simulation results along with respective experimental data offer potential for this material to be stable in ambient lighting, yet possible to initiate with short pulsed lasers. An article on this subject "Photoactive high explosives: linear and nonlinear photochemistry of petrin tetrazine chloride" has been recently published in the Journal of Physical Chemistry C.

Future Work

We have already made a prototype code incorporating solvent at the Polarizable Continuum Model (PCM) level. During the second year of the project, our goal is formulate a combined quantum mechanical and molecular mechanical (QM/MM) approach to treat large systems and include solvent and thermal bath effects will be developed. QM/MM is a much more accurate approach in which a system is divided into a quantum mechanical region and a molecular mechanical region allowing realistic modeling of dielectric media. Depending on the molecular system, different force fields will be interfaced with our existing non-adiabatic excited-state molecular dynamics (NA-ESMD) code. In terms of applications, photoactive energetic materials with controllable optical functionality will be studied. Specific vibrational degrees of freedom responsible for bond breakage, rapid decomposition, and the onset of the exothermic chain reactions relevant to explosive initiation processes in the

surrounding material will be identified. In the future, we will use the developed methodology to design and propose controllable materials. Detailed numerical NA-ESMD simulations to investigate photoinduced pathways, timescales, branching effects, and multiple product formation, which can be experimentally validated by ultrafast spectroscopy capabilities, will be performed. Possible photoinduced reaction coordinates and electron-vibrational relaxation pathways to elucidate mechanisms for optical initiation will be assessed. Moreover, first principle electronic structure calculations will be used to quantitatively evaluate the nonlinear optical responses to understand excited-state properties and to provide design strategy for new photoactive energetic materials.

Conclusion

The proposed implementation of the quantum mechanical and molecular mechanical (QM/MM) approach will provide novel computational capabilities critical for understanding light-induced dynamics in many technologically relevant materials. Specifically, this will allow us to simulate large molecular systems where full ab-initio calculations are prohibitively expensive, and to describe systems that interact strongly with solvent environments. Such simulations have been done previously for the ground state but were never attempted for excited states due to computational complexity.

Publications

Bjorgaard, J. A., T. Nelson, K. Kalinin, V. Kuzmenko, K. A. Velizhanin, and S. Tretiak. Simulations of fluorescence solvatochromisms in substituted PPV oligomers from excited state molecular dynamics with implicit solvent. 2015. Chemical Physics Letters. 631: 66.

Greenfield, M. T., S. D. McGrane, C. A. Bolme, J. A. Bjorgaard, T. R. Nelson, S. Tretiak, and R. J. Scharff. Photoactive high explosives: linear and nonlinear photochemistry of petrin tetrazine chloride. 2015. Journal of Physical Chemistry A. 119: 4846.

Nelson, , Fernandez-Alberti, A. E. Roitberg, and Tretiak. Nonadiabatic Excited-State Molecular Dynamics: Modeling Photophysics in Organic Conjugated Materials. 2014. ACCOUNTS OF CHEMICAL RESEARCH. 47 (4): 1155.

Ultrafast Carrier Dynamics in Novel Two-Dimensional Nanomaterials

Victor I. Klimov
20140675PRD3

Introduction

Semiconductor nanomaterials are a versatile materials platform for exploring novel physical phenomena not found in their bulk counterparts. A detailed understanding of the physical factors controlling the electronic properties will allow for the development of materials with tailored electronic properties. Recent advances in synthetic methods have allowed for the synthesis of nearly atomically thin two-dimensional nanoplatelets. These materials have already shown promise for use in next generation transistors as well as other electronic applications. However, the underlying electronic properties of these materials remain largely unexplored. Specifically, it still remains largely unknown how the effect of confinement in only one dimension is different from the effects of the two-dimensional and three-dimensional confinement realized, respectively, in nanorods and quantum dots. To this end, we will conduct a side-by-side study of materials of different dimensionalities with femtosecond spectroscopy. Experiments will elucidate the time scales of carrier relaxation, exciton binding energies, as well as the strength of multicarrier interactions. Due to the quasi-two-dimensional confinement of the electrons in the material, the Coulomb interactions between carriers are expected to be significantly enhanced relative to existing semiconductor nanocrystals. The strong Coulomb interaction can give rise to room temperature excitonic phenomena and enhance multicarrier processes that are typically only observed at extremely low temperatures.

Benefit to National Security Missions

Agency Relevance/DOE/SC. The primary goal of this project is to explore the electronic properties of a new class of two-dimensional semiconductor materials. As such, the results will be valuable to the DOE's Office of Science.

Mission Relevance/MaRIE. Since we are studying charge carrier interactions at extremely high densities in these two-dimensional semiconductors, the insights from this project could potentially benefit MaRIE.

Scientific Discovery and Innovation/Basic Understanding of Materials. Through ultrafast laser spectroscopy of these semiconductor nanosheets, we will establish the role of two-dimensional quantum confinement on intraband carrier cooling, Auger recombination and other multi-carrier interactions, significantly contributing to the basic understanding of these novel nanomaterials.

The materials developed in this project can be used as spectrally tunable light harvesters in photoconversion including both photovoltaics and generation of solar fuels. This makes this project directly relevant to the LANL's Energy Security and Environment missions.

Progress

Our initial target materials in this project were transition metal chalcogenide layered semiconductors that were recently isolated in the form of single-layered plates. We anticipated that following the methodology outlined in the published literature would enable us to prepare colloidal suspensions of single-layered MoS2 and characterize them with femtosecond optical spectroscopy. However, the sample preparation did not produce materials of sufficient quality for spectroscopic studies, with the suspensions containing a mixture of plates of differing thicknesses. Therefore, in FY15, we instead focused on a different class of nanomaterials, namely PbSe. We synthesized two-dimensional platelets of varying thickness of sufficiently high quality for optical studies. Femtosecond transient absorption and time resolved photoluminescence experiments were utilized to characterize the interaction strength between carriers as well as the rate of carrier cooling. Additionally, using a hyperbolic effective mass model we were able to explain the size dependence of the band gap as a function of the thickness of the material. Furthermore, we were able to quantify the magnitude of the carrier-carrier interactions in bulk, two-dimensional plates, one-dimensional nanorods, and

zero-dimensional quantum dots. Interestingly, we found that one-dimensional materials exhibited the strongest interaction between carriers through a combination of dielectric and geometrical effects. These results are currently being prepared for publication.

Future Work

This project focuses on better understanding the role that dimensionality plays in controlling the optical and electronic properties of nanometer-sized objects. In particular, we are interested in how the interactions between electrons are modified when the size of a material was confined to the nanoscale in one (plates), two (rods), and three (dots) dimensions. The extremely thin two-dimensional materials facilitate increased interactions between charge carriers, which should result in novel physical phenomena. To gain insight into the new physics that arise in strongly confined two-dimensional materials we will utilize femtosecond transient absorption spectroscopy in conjunction with time-resolved photoluminescence experiments to probe the carrier dynamics. Through tuning of the power of the excitation beam, the dynamics of multicarrier processes will be measured. Due to the increased interactions between carriers we expect to find a corresponding increase in the multicarrier recombination rate, as well as potentially bound multiexciton states that are typically only observed at temperatures approaching absolute zero. Tuning of the probe wavelength across the spectra will allow for the relaxation process to be directly monitored as well as resolving the energies of higher-lying excited states. Saturation experiments will also reveal the degeneracy of the transitions, providing a detailed understanding of the energy level structures that lead to the unique properties found in ultra thin semiconductor layers.

Conclusion

These studies of two-dimensional nanostructures will help elucidate how the precise shape and size of the nanomaterial control their optical and electronic properties. We expect that the two-dimensional confinement of charge carriers will enable increased interactions between them leading to novel physics. The insights gained from this project will advance our understanding of the fundamental electronic properties of two-dimensional materials and facilitate their applications in real-life technologies.

Publications

Gao, J., A. F. Fidler, and V. I. Klimov. Carrier multiplication detected through transient photocurrent in device-grade films of lead selenide quantum dots. 2015. Nature Comm.. 6: 8185.

New Room Temperature Multiferroic Thin Films Enabled by Strain Engineering

Quanxi Jia
20140676PRD3

Introduction

Multiferroic materials have attracted extensive interests due to their potential technological applications as multifunctional devices. However, the single-phase multiferroic materials are rare because of the distinct nature of magnetism and ferroelectricity. Seeking nanocomposite multiferroic materials, therefore, has become our recent research focus. Strain engineering provides an important approach to yield new functional materials with novel properties. We have demonstrated a new class of multiferroics (BiFe0.5Mn0.5MnO3 or BFMO) based on two partially miscible phases of BiFeO3 and BiMnO3 using epitaxial strain. Fully strained BFMO/LaAlO3 (LAO) superlattices with controlled layer thickness and periodicity could be a very promising way to realize new room temperature multiferroic materials. We will take advantage of the well-equipped capabilities at Los Alamos National Laboratory (such as laser molecular beam epitaxy, high resolution x-ray diffraction, transmission electron microscopy, and transport characterization tools) to systematically study the highly strained BFMO/LAO superlattice structures.

Benefit to National Security Missions

This project focuses on fabrication, properties, and microstructural characterization of advanced nanostructured superlattice with an emphasis on room temperature multiferroic materials. The proposed effort supports and strengthens the Laboratory's core scientific capabilities essential to discovering, understanding, and exploiting emergent phenomena in materials. This project also directly addresses the LANL Energy Security and Environment mission areas as well as the Grand Scientific Challenge identified in the DOE BESAC report: how do remarkable properties of matter emerge from the complex correlations of atomic or electronic constituents and how can we control these properties?

Progress

Owing to the potential applications in the development of high performance solid-state devices, multiferroics materials have recently attracted a great deal of attention. Single-phase multiferroic materials are very scarce due to their exclusive nature origins. Another way to achieve multiferroicity is by combining individual ferroelectric and ferromagnetic materials into composites. This allows to choose components with large ferroelectric properties (d33 and g33) and magnetostriction, so the resulting composites may have superior multiferroic properties and magnetoelectric couplings.

The following highlights our accomplishments from Aug. 2014 to June 2015.

We have fabricated CoFe2O4 films with different thicknesses, grown on MgO substrates. The strain effect on magnetism and magnetic anisotropy were studied. We found that strain plays a critical role in determining the ferromagnetism of CoFe2O4 films. The magnetostriction coefficient of CFO films is estimated to be $\lambda[001] = -188\times10-6$. This study is important for the design and growth of CoFe2O4 based multiferroic superlattices such as BaTiO3:CoFe2O4.

We grew Bi2FeMnO6 (BFMO) thin films with both conventional pseudocubic structure and novel supercell structure on SrTiO3 (001) substrates with different thicknesses of CeO2 buffer layers (ranging from 6.7 to 50.0 nm) using pulsed laser deposition. The correlation between the thickness of the CeO2 buffer layer and the structure of the BFMO films shows that the CeO2 buffer layer, as thin as 6.7 nm, is sufficient in triggering the novel BFMO supercell structure. The buffer layer thickness is found to be critical in controlling the microstructure and magnetism of the BFMO supercell structures. Thin seed layers can produce a smoother interface between the BFMO film and the CeO2 buffer layer, and therefore better ferrimagnetic properties. Our results have

demonstrated that strain and interface could be utilized to generate novel thin film structures and to tune the functionalities of thin films.

We have optimized the growth and characterized the growth rate of perovskite thin films in laser MBE system by the advanced RHEED system.

Future Work

Fully strained superlattices with controlled layer thickness and periodicity provide very promising ways to realize new room temperature multiferroic materials. The well-equipped capabilities at CINT (such as laser molecular beam epitaxy, high resolution x-ray diffraction, transmission electron microscopy, and transport characterization tools) will enable us to carry out the following proposed FY16 tasks with success.

We will grow high quality multiferroic superlattices such as BaTiO3:CoFe2O4 and La0.7Sr0.3MnO3:BaTiO3 by using the Laser MBE system. With the RHEED system, we are able to monitor the layer by layer growth and we can design the interface with atomic sharpness.

We will perform magnetoelectric coupling (ME) measurements of these superlattices using VSM and SANS.

As this project will be complete at the end of July 2016, we will wrap up this project and explore new funding opportunities.

Conclusion

This project focuses on fabrication, properties, and microstructural characterization of advanced nanostructured superlattice with an emphasis on room temperature multiferroic materials. We expect that the structure-functionality relationship of this new class of multifunctional materials can be established at the end of the project.

Publications

Ahmed, T., A. P. Chen, D. A. Yarotski, S. Rudin, S. A. Trugman, Q. X. Jia, and J. X. Zhu. First-principles study of magnetic, electronic and optical properties of double perovskite Bi2FeMnO6. Phys. Rev. B.

Ahmed, T., A. P. Chen, Q. X. Jia, D. A. Yarotski, and J. X. Zhu. Site dislocation between Fe and Mn sites in double perovskite Bi2FeMnO6:A theoretical explanation for XMCD anomaly. To appear in Scientific Reports.

Chen, A. P., W. Zhang, J. L. MacManus-Driscoll, H. Wang, M. R. Fitzsimmons, and Q. X. Jia. Role of interfaces on competing interactions of ferroic films. Invited presentation at 2015 MRS Fall meeting. (Boston, Nov. 29 - Dec. 4).

Choi, E. M., J. E. Kleibeuker, T. Fix, J. Xiong, C. J. Kinane, D. Arena, S. Langridge, A. P. Chen, Z. Bi, J. H. Lee, H. Wang, Q, X. Jia, M. G. Blamire, and J. L. MacManus-Driscoll. Interface coupled BiFeO3/BiMnO3 superlattices with magnetic transition temperature up to 410 K. Adv. Mater..

Zhang, W., A. P. Chen, M. Li, L. Li, Z. Xia, P. Boullay, L. Wu, Y. Zhu, J. L. MacManus-Driscoll, Q. X. Jia, and H. Wang. Two-dimensional layered oxide structures tailored by self-assembled layer stacking via interfacial strain. Adv. Funct. mater..

Search for the Topological States in F-electron Systems

Tomasz Durakiewicz
20140678PRD3

Introduction

The broad category of correlated electron systems, with eminent examples like high-temperature superconductors, also includes a family of f-electron compounds based on lanthanides (4f) or actinides (5f). This area of research is a LANL specialty. This proposal bridges the LANL expertise in basic physical properties of f-electron materials, and the cutting edge novel science of topological surface states so far known only for non-f electrons. An extensive Angle-Resolved Photoelectron Spectroscopy (ARPES) study of several candidate systems will be performed, aimed at identification and characterization of such states. A spin-resolved variant and temperature-dependent studies will provide evidence for spin texture, an important and now still missing indicator of topological protection. Results will be directly applicable to a wider set of problems found in correlated systems and their surface properties.

Benefit to National Security Missions

This project has direct ties to basic research of novel materials, and advancing our ability to provide design principles for future materials. It is linked to e.g. NSF funding efforts in the area of topological insulators. By focusing on f-electrons it is relevant to enhancing and control of the transport properties of lanthanides and actinides, including nuclear fuels.

Progress

During the first six months of his appointment, between Jan 2015 and June 2105, Madhab Neupane was focusing on (1) taking photoemission data at synchrotron facilities, (2) analyzing data and (3) writing manuscripts.

The search for novel topological surface states and novel properties of materials being hosts to such states is ongoing. Madhab measured, for the first time, the electronic structure of a novel system BiPd, continued measurements of SmB6 and CeB6 and performed initial measurements of the topological superconductor, Sr-doped BiSe2. Data reduction and analysis on those systems is ongoing. His work in this period of time resulted in several papers published or at various stages of preparation; see a full list of papers published and in submission for 2015.

Madhab also organized and run several synchrotron based experiments at various beamlines: 4 runs at Advanced Light SOurce in Berkeley (Feb, Mar and twice in Apr) as well as Univ of Tokyo in May and Swiss Light Source in June.

Future Work

During the first year of the project a series of Angle-Resolved Photoelectron Spectroscopy (ARPES) studies will be performed in specialized synchrotron facilities. The goal is twofold: to perform a detailed temperature - dependent study with high energy resolution in order to resolve the band dispersion of the surface states and and to work on the spin-resolved variant in search of signatures of spin texture. These measurement will ultimately provide evidence by identifying (i) the massless (linear) band dispersion and (ii) spin texture characteristic for topological surface states.

During the second year, the results of the first year's work will be prepared for publications. Additional data will be collected if missing information about the electronic structure in specific parts of energy-momentum space is found.

Conclusion

It is expected that this project will lead to (i) proving or disproving the existence of topological surface states in f-electron systems, (ii) measuring the temperature evolution of the hybridization gap and analyzing its influence and role in forming the surface states, (iii) performing an detailed spectral analysis in order to obtain information about the renormalization energy scales and (iv) extending the search for surface states towards a broader class

of f-electron systems.

Publications

Chang, , Das, Chen, Neupane, Xu, M. Z. Hasan, Lin, Jeng, and Bansil. Two distinct topological phases in the mixed-valence compound YbB6 and its differences from SmB6. 2015. PHYSICAL REVIEW B. 91 (15).

Ghimire, N. J., Luo, Neupane, D. J. Williams, E. D. Bauer, and Ronning. Magnetotransport of single crystalline NbAs. 2015. JOURNAL OF PHYSICS-CONDENSED MATTER. 27 (15).

Huang, , Xu, Belopolski, Lee, Chang, Wang, Alidoust, Bian, Neupane, Zhang, Jia, Bansil, Lin, and M. Z. Hasan. A Weyl Fermion semimetal with surface Fermi arcs in the transition metal monopnictide TaAs class. 2015. NATURE COMMUNICATIONS. 6.

Neupane, , Xu, Alidoust, Bian, D. J. Kim, Liu, Belopolski, T. -. Chang, H. -. Jeng, Durakiewicz, Lin, Bansil, Fisk, and M. Z. Hasan. Non-Kondo-like Electronic Structure in the Correlated Rare-Earth Hexaboride YbB6. 2015. PHYSICAL REVIEW LETTERS. 114 (1).

Neupane, , Xu, Alidoust, Sankar, Belopolski, D. S. Sanchez, Bian, Liu, Chang, Jeng, Wang, Chang, Lin, Bansil, Chou, and M. Z. Hasan. Surface versus bulk Dirac state tuning in a three-dimensional topological Dirac semimetal. 2015. PHYSICAL REVIEW B. 91 (24).

Xu, , Liu, S. K. Kushwaha, Sankar, J. W. Krizan, Belopolski, Neupane, Bian, Alidoust, Chang, Jeng, Huang, Tsai, Lin, P. P. Shibayev, Chou, R. J. Cava, and M. Z. Hasan. Observation of Fermi arc surface states in a topological metal. 2015. SCIENCE. 347 (6219): 294.

Xu, , Neupane, Belopolski, Liu, Alidoust, Bian, Jia, Landolt, Slomski, J. H. Dil, P. P. Shibayev, Basak, Chang, Jeng, R. J. Cava, Lin, Bansil, and M. Z. Hasan. Unconventional transformation of spin Dirac phase across a topological quantum phase transition. 2015. NATURE COMMUNICATIONS. 6.

Xu, S. Y., I. Belopolski, N. Alidoust, M. Neupane, G. Bian, C. Zhang, R. Sankar, G. Chang, Z. Yuan, C. C. Lee, S. M. Huang, H. Zheng, J. Ma, D. S. Sanchez, B. K. Wang, A. Bansil, F. Chou, P. P. Shibaye, H. Lin, S. Jia, and M. Z. Hasan. Discovery of a Weyl Fermion semimetal and topological Fermi arcs. 2015. Science. : 1.

Rational Design of Multiferroics and Influence of Cationic Disorder on Multiferroicity in Perovskites

Blas P. Uberuaga
20140679PRD3

Introduction

Ferroelectricity and magnetism in solids have seemingly different origins. While magnetism is related to ordering of spins of electrons in incomplete ionic shells, ferroelectricity results from a delicate balance between long-range coulombic dipole-dipole interactions and short-range repulsive forces. Materials in which ferroelectricity and ferromagnetism exist simultaneously are known as multiferroic materials. Multiferroics can, in principle, enable novel and revolutionary future energy, sensing, and information technologies. However, ferroelectric ferromagnets are exceedingly rare. This research effort seeks to enable rational design of novel thin-film multiferroic materials.

The research team is developing a design strategy to systematically navigate through the chemical space of magnetic perovskite oxides (ABO3 systems) using quantum mechanical computations in combination with thermodynamics based models and materials informatics. State-of-the-art computations are being used to explore and understand coupling between ferroelectricity and magnetism for a range of ABO3 compounds as a function of composition, strain and nominal charge states of A and B site cations. Advanced density functional theory based computations such as those with hybrid functionals (to appropriately account for the self-energy of a many-body system of electrons) are being used for a further careful investigation and validation of the identified promising material candidates with multiferroic behavior.

A key objective of this effort is to assess the effect of crystalline cationic disorder on the magnetism, ferroelectricity and their coupling in perovskites. Crystalline disorder in magnetic perovskites is expected to strongly influence both the local magnetic structure as well as the polar phonon modes. However, the atomic scale mechanisms through which crystalline cationic disorder and multiferroicity couple in magnetic perovskites are not well understood at present and is specifically targeted in this work.

Benefit to National Security Missions

This research is of direct relevance to the missions above as the ability to rationally design multiferroics will enable novel and revolutionary future energy, sensing, and information technologies in which the low power and high speed of field-effect electronics are combined with the permanence and routability of voltage-controlled ferromagnetism. This paradigm has the potential to mitigate the costs, risks and time involved in preparing and testing of multi-functional materials. Further, this research should yield insights into the fundamental factors underlying materials behavior, providing the basic understanding needed to further develop novel materials and material architectures for advanced energy applications. Finally, an atomic-level understanding of the influence of crystalline disorder on multiferroic behavior would directly translate to better device performance.

These goals are of direct relevance to the missions of DOE/BES and LANL, particularly the laboratory's science pillar of Materials for the Future.

Progress

Over the past year, we have built machine learning models to examine various aspects of material discovery. In particular, we have examined important properties of perovskite materials as these hold particular promise for a number of applications involving multiferroic properties and fast ion conduction. We highlight three papers that emphasize this work.

First, in a Journal of Applied Physics paper, we showed how one can combine two perovskite materials (with chemical formula ABX3, where A and B are cations and X is an anion, in this case Cl) to form a double perovskite that emphasized the strengths of each and minimized the weaknesses. In particular, we showed how combin-

ing CsCaCl3 and RbZnCl3 lead to a stable cubic double perovskite that had a strong ferroelectric response to strain. By them selves, CsCaCl3 is a very stable cubic perovskite that shows little sensitivity to strain while RbZnCl3 is unstable and easily distorts. By combining the two, we showed how a perovskite that is stable in the cubic structure but undergoes ferroelectric distortions under small strains leads to a new material with potentially improved functionality.

In a second paper, we used accelerated molecular dynamics methods to examine the kinetic pathways for oxygen vacancies in double perovskites as a function of the cation ordering. Because of the structure of these materials, there are 9 high symmetry orderings of the A and B cations. We examined how oxygen vacancies, the important carrier of ionic conductivity in these materials, move through the material for the different cation orderings. We find that both the absolute mobility as well as the nature (one-dimensional or three-dimensional) depends significantly on the cation ordering. In particular, there are orderings in which the mobility is higher than in either of the component single perovskites (in this case, SrTiO3 and LaAlO3). This work is under review at Chemistry of Materials, where the first round of reviews were very favorable.

These two papers showed the promise of double perovskites for advance functionality, but did not demonstrate their discovery. In a third paper accepted to Phys. Rev. B, we build and critically access state-of-the-art machine machine approaches for materials classification and property predictions by taking a specific example of classical AB crystalline solids. Once validated, these approaches are now being applied to perovskite systems. In a fourth paper submitted to Acta Crystallographica, we have built a machine learning approach that examines those “features” of perovskites that predict their formability. Importantly, predicting which perovskite chemistries lead to stable perovskites with simple heuristics significantly accelerates the discovery process. We found that new features that were not previously considered do a better job of predicting formability than those previously considered. This demonstrates the power of the approach.

Future Work

In the coming fiscal year, we plan to build on our ongoing work by considering double perovskites–ordered perovskites with multiple A and/or B site cations. These materials can be synthesized with a variety of cation orderings, each of which shows a different tendency towards exhibiting ferroelectric polarization and it’s coupling with strain. Furthermore, due to enormous combinatorial possibilities available in the double perovskite chemical space, it lends itself as an ideal test-bed for materials informatics based approaches involving big-data and machine learning methods. We plan to use the data generated in the quantum mechanical computations to develop efficient, robust and validated machine learning models for property predictions for perovskites and double perovskites, which can then be used in a high throughput screening studied to identify potential material candidates with a specific application in mind.

In parallel to these bulk studies, we will also focus on interface structures in complex oxides. Charge transfer effects at hetero-interfaces between two appropriately chosen ferroelectric materials can also lead to an interface magnetization. If the interface magnetization couples strongly with either strain or polarization in either side of the materials, an efficient multiferroic device can be realized. This mechanism has not been explored in detail to date. Furthermore, presence or absence of misfit dislocations or controllable point defects (such as O vacancies) on ferroelectricity, ferromagnetism and their coupling will be studied.

Conclusion

We are systematically screening the chemical space of magnetic perovskites to identify promising multiferroics. This research effort will deliver new insights into the factors that govern coupling between ferroelectricity and ferromagnetism in perovskite materials. By systematically exploring strain-(polar) phonon coupling and spin-phonon coupling in a range of material systems, we will identify and understand mechanisms that control spin-phonon-strain behavior in these materials. An atomic-level understanding of the influence of crystalline disorder on multiferroic behavior would directly translate to a better device performance and an improved control over the functionality.

Publications

Kim, C., G. Pilania, and R. Ramprasad. From organized high-throughput data to phenomenological theory: the example of dielectric breakdown. Chemistry of Materials.

Kumar, A., G. Pilania, T. D. Huan, T. Lookman, and R. Ramprasad. Informatics-driven strategy for the accelerated design of dielectrics. Scientific Reports.

Lookman, T., P. V. Balachandran, D. Xue, G. Pilania, T. Shearman, J. Theiler, J. E. Gubernatis, J. Hogden, K. Barros, E. BenNaim, and F. J. Alexander. A perspective on materials informatics: state-of-the-art and challenges. Information science for materials discovery and design. Edited by Lookman, T..

Pilania, , J. E. Gubernatis, and Lookman. Structure classifi-

cation and melting temperature prediction in octet AB solids via machine learning. 2015. PHYSICAL REVIEW B. 91 (21).

Pilania, , and B. P. Uberuaga. Cation ordering and effect of biaxial strain in double perovskite CsRbCaZnCl6. 2015. JOURNAL OF APPLIED PHYSICS. 117 (11).

Pilania, , and Lookman. Electronic structure and biaxial strain in RbHgF3 perovskite and hybrid improper ferroelectricity in (Na,Rb)Hg2F6 and (K,Rb)Hg2F6 superlattices. 2014. PHYSICAL REVIEW B. 90 (11).

Pilania, G., J. E. Gubernatis, and T. Lookman. Classification of octet AB-type binary compounds using dynamical charges: a materials informatics perspective. Scientific Reports.

Pilania, G., P. V. Balachandran, J. E. Gubernatis, and T. Lookman. Predicting the formability of ABO3 perovskite solids: An initial machine learning study. 2015. Acta Crystallographica Section B. 71: 507.

Uberuaga, B. P., and Pilania. Effect of Cation Ordering on Oxygen Vacancy Diffusion Pathways in Double Perovskites. 2015. CHEMISTRY OF MATERIALS. 27 (14): 5020.

Studies on Functional Materials: Design and Optimization

Turab Lookman
20140682PRD4

Introduction

Accelerated materials discovery and design is the cornerstone of the US Materials Genome Initiative (MGI). Costly time-consuming trial and error methods have been the dominant approaches for searching for new materials with desired, target properties. However, computational material design based on data mining techniques and informatics tools are increasingly playing an important role in the discovery and design efforts. Very few examples exist and this work will provide specific examples for given materials classes that combine experiments, data and inference modeling. The implications for applications of finding materials with targeted properties are enormous. The focus will be on ferroic materials, which form an essential family of functional (or smart) materials, which combine polarization, magnetization and/or electronic properties to yield a nonlinear response to external stimuli such as temperature, pressure, electric, and magnetic fields. The huge demand to replace PZT (PbZrxTi1-xO3) containing Pb with Pb-free piezoelectrics, the attempts to minimize energy dissipation during thermo-mechanical energy conversion in shape memory alloys (SMAs), and the efforts to generate greater temperature differences in electrocaloric materials, are examples of intensive efforts involving functional materials design.

Benefit to National Security Missions

The work being proposed is at the interface of two of LANL's pillars, namely Materials for future and IS&T (Information Science and Technology) and is relevant to BES/DOE and the Office of Science initiatives under the "Materials Genome Initiative (MGI)". Ongoing LDRD-DR funded work at LANL is addressing how accelerated materials discovery might be realized. Several materials classes are under investigation, principally based on perovskites. The proposal complements these efforts in using the codesign strategy on materials such as electrocaloric materials, important in solid-state refrigeration, and energy harvesting materials such as ferroelectrics. Thus, it strengthens existing connections and will forge other connections, such as the use of coherent x-ray diffraction at LCLS/SLAC on functional materials, which connects to LANL's signature facility concept, MaRIE. This project goes beyond concurrent DR work in that its focus is on fundamental science governing optimal properties and the use of large scale facilities (such as CINT, LCLS) to probe mechanisms. In a more general sense, accelerated materials discovery, if we can demonstrate its effectiveness, is an approach to develop new materials for a broad range of missions including sensor and structural materials for nuclear nonproliferation, and replacement materials for stockpile stewardship.

Progress

Training and using state-of-art pulse laser deposition (PLD) equipment in the DOE facility, CINT, took up a substantial fraction of the year. Towards the latter part, a number of thin film systems have been fabricated and their properties measured. These included manganites on a number of substrates. The magnetization response was also characterized. Work on using novel substrates, such as the shape memory alloy, NiTi, has now begun. Having ensured that we are fabricating well controlled thin films, the set is stage for synthesizing functional materials and discovering systems with targeted properties, such as films with optimal dielectric tenability and new electrocalorics.

Another major effort that was completed over the course of the year was synthesizing and characterizing new NiTi based alloys with very low thermal dissipation. This effort was was synergistic with the LDRD-DR in materials informatics. The inference and machine learning models studied there predicted a number of alloys with anticipated targeted properties. Compounds were then synthesized based on these predictions and their properties measured. A number of new alloys (e.g. NiTiCuFePd) with better thermal dissipation properties than known previously in the literature have been synthesized and

the new discovery is now being prepared for publication. Such alloys are important as they minimize fatigue under thermal and mechanical cycling and have widespread use in industry.

Future Work

The focus in the second year will be on layered systems. Experiments will be developed using Pulsed Laser Deposition (PLD), which with existing data and statistical inference methods, will guide materials design. This work will complement other work using ab initio methods. I will first focus on dielectric systems to search for thin films (Barium Strontium based) deposited on specific substrates to find dielectrics with better tunable characteristics. I will also focus on developing a strategy for studying the electrocaloric effect in layered systems. The electrocaloric effect, the adiabatic temperature change that occurs in polar materials upon application of an electric field, is a promising route to solid-state refrigeration. My approach will be to optimize the large response of the polarization to electric field around the phase transition, as up to now the temperature window is too limited. I will therefore investigate bilayers of ferroelectrics with different transition temperatures (e.g. by doping with different amounts of Zr4+ into BaTiO3) in order to obtain a wider temperature range without sacrificing a large electrocaloric response (change in temperature induced by the electric field). The data will comprise thickness of layers, dopant concentrations and types and aspects of structure and chemistry, and will be assembled via a suite of experiments guided by statistical methods.

Conclusion

The research will focus on utilizing statistical methods to accelerate the discovery process with an emphasis on dielelectrics, ferroelectrics and shape memory alloys (SMAs). Augmented by well-established phenomenological approaches in the field, such as Landau theory, together with statistical and machine learning methods, as well as experiments in bulk and on layered systems, the work will demonstrate the essential components needed for finding materials with targeted properties.

Publications

Balachandran, P. V., D. Xue, J. E. Hogden, J. Theiler, and T. Lookman. Adaptive design strategies for materials design. Scientific Reports (2015).

Xue, D., O. V. Balachandran, H. Wu, R. Yuan, Y. Zhou, X. Ding, J. Sun, and T. Lookman. Designing vertical morphotropic phase boundaries in BaT iO3-based lead-free piezoelectrics. Science Reports (2015).

Xue, D., P. V. Balachandran, J. E. Hogden, and J. Theiler. Accelerated search for materials with targeted properties by adaptive design. Nature Communications.

Xue, D., R. Yuan, Y. Zhou, D. Xue, T. Lookman, X. Ding, and J. Sun. Design of High Temperature Ti-Pd-Cr Shape Memory Alloys with Small Thermal Hysteresis and High Reversibility. Scientific Reports (2015).

Probing and Controlling the Surface States of Topological Insulators

Scott A. Crooker
20140683PRD4

Introduction

Topological Insulators (TIs) are a recently discovered class of materials that have garnered significant attention in the last 5 years within the condensed matter physics community. They are bulk semiconductors such as Bi2Se3 and Bi2Te3 in which spin-orbit coupling gives rise to a topologically protected two-dimensional (2D) metallic surface, with a surface electronic structure similar to the Dirac cone spectrum of graphene. The surface states are protected from backscattering by time reversal symmetry, and therefore TIs have potential applications for spin logic devices and low-power electronics. Although there is tremendous excitement and interest in these novel materials within the physics and materials science community, the exploration of exotic spintronic properties in TIs such as spin photocurrent and current-induced spin-density properties are still at an early stage. The ability to control the topological surface states electrically or optically is the crucial key to the development of spin-based devices.

Luyi will probe, and ultimately manipulate, the spin degrees of freedom in TIs. A major part of this research will combine the unique optical and pulsed magnetic transport techniques at the National High Magnetic Field Laboratory at LANL to characterize spin structure and transport. In TIs it is possible to photoexcite currents whose charge, spin, and direction can be controlled by varying the helicity of the light. The subsequent spin currents and spin dynamics can be monitored and imaged via the magneto-optical Kerr effect. The unique nature of spin-momentum locking in the SSs suggests that the spin current in a TI can be generated with the same efficiency as charge photocurrent in a conventional insulator.

Benefit to National Security Missions

This project will build Laboratory capabilities in the areas of Materials Science, Emergent Phenomena, and Materials-by-Design, and also in novel measurement methods that enable new scientific discovery at LANL. It is based on the very recent discovery of a new class of so-called “topologically protected” materials, in which scattering and dissipative processes are prohibited from fundamental physics considerations. The experimental techniques that we will develop as part of this project will advance new Laboratory capabilities that underpin a wide variety of Laboratory missions related to Materials Science and Controlled Functionality in Materials. Beyond direct scientific impact, these studies have the potential to pave the pathways for new “topologically protected electronics”; that is, transport of charge and spin in new generations of lower-power and more efficient electronic devices, which has direct impacts on securing our energy future.

Progress

In FY16, Director’s-funded postdoc Luyi Yang built an experimental setup for measuring the dynamics of spin relaxation in the new atomically-thin semiconductors such as MoS2 and WSe2 (molybdenum disulphide and tungsten diselenide). This experimental capability is now fully functional, and involves the use of a tunable dye laser, and also an ultrafast optical parametric oscillator laser for time-resolved studies. She has successfully applied this technique to measure for the first time the very long spin relaxation in these new 2D materials. Her paper on this subject has been accepted at Nature Physics (July 2015); the first round of referee reports being quite favorable. In addition, Luyi published a paper in Scientific Reports in April 2015 (“Cross-correlation spin noise spectroscopy of heterogeneous interacting spin systems”).

Future Work

In FY16 we will focus primarily on constructing the infrared Magneto-Optical Kerr imaging microscope that will allow us to directly image the spin currents in these topological insulator materials. This will require the purchase and benchmarking of a variety of mid-infrared quantum cascade lasers. The first step will be to per-

form magneto-reflectivity and absorption studies, using these lasers, of a variety of TI materials, which will allow us to screen for the best ones.

Conclusion

The principal goal of this project is to image, via magneto-optical techniques pioneered at the NHMFL-Los Alamos, the spin currents that are predicted to form at the surface of TI materials. The results will allow direct visualization and spatial mapping of the topologically protected electronic states for the first time. Beyond direct scientific impact, these studies have the potential to pave the pathways for new “topologically protected electronics”; that is, transport of charge and spin in new generations of lower-power and more efficient electronic devices, which has direct impacts on securing our energy future.

Publications

Roy, D., L. Yang, N. A. Sinitsyn, and S. A. Crooker. Cross-correlation spin noise spectroscopy of heterogeneous interacting spin systems. 2015. Scientific Reports. 5: 9573.

Yang, L., N. A. Sinitsyn, J. Yuan, J. Zhang, J. Lou, and S. A. Crooker. Long-lived nanosecond spin relaxation and spin coherence of electrons in monolayer MoS2 and WS2. 2015. Nature Physics. 11: 830.

Three-Dimensional Nitrogen-Doped Porous Nanographene for High-Performance Supercapacitor

Hsing-Lin Wang
20140684PRD4

Introduction

For the past two decades, graphene has emerged as one of the most exciting carbon based materials due to its superior electrical conductivity, exceptional high surface area, and excellent structural stability. In recent years, graphene has revealed tremendous potential as an ideal electrode material in energy storage devices such as lithium ion battery and supercapacitor. However, graphene suffers from low processibility, difficult to scale up, and lack of tunability in structure and properties. In addition, as part of the anode materials in lithium ion battery and supercapacitors, graphene sheets often aggregate and restack with increasing operation time and charging/recharging cycles; this structure instability leads to a decrease in surface area and deter the electrolyte from accessing to graphene sheets surface. To mitigate the processibility, graphene are oxidized and then reduced to form the so called "reduced graphene oxide (RGO), which has limited solubility in certain organic solvents. However, this process also induced many structural defects that hamper the performance of in energy storage devices.

Our approach is to use three dimensional nanographenes synthesized in our laboratory and crosslinking these small nanographene moieties to form mesoporous nanographene which will have a well-defined molecular structure, high surface area and most importantly structural homogeneity. The design of this novel mesoproous nanographene is expected to exhibit very high capacitance and operational stability over a very long period of time. Our system is the first ever demonstrated to use mesoporous nanographene in energy storage devices. In addition, we will develop ways to dope these porous ographenes to render high conductivity to further improve their performances. Success of this project could have huge impact in the development of next generation energy storage devices .

This project is based on materials developed in our laboratory and technologies well established at LANL.

Benefit to National Security Missions

Controlled synthesis of 3D porous nitrogen-doped nanographene with defined flake sizes and doping (type, content, and location) will enhance graphene electron mobility and the as-prepared 3D porous structure, which is desired to overcome the restacking and defects observed in traditionally-reduced graphene oxides sheets.

We expect to design and synthesize novel and high-performance 3D porous nitrogen-doped nanographene supercapacitors with optimal chemical and structural properties to maximize specific capacitance, power density, energy density, and cycle life, relevant to LANL's Energy Security and Environment missions. If successful, this project will result in a deep understanding of the electrochemistry of 3D porous nanographene as well as the invention of the first 3D porous nitrogen-doped nanographene-based supercapacitor. The results will have wide-spread impact on the fabrication of high-performance supercapacitors.

Progress

In FY15, we developed a novel approach to synthesize a series of three-dimensional (3D) nanographenes (NGs) with well-defined molecular structures; in our synthesis, a variety of functional groups have been covalently attached to the NG flakes that enable fine-tuning of electron density on flakes and d-spacing between flakes. The multistep organic synthesis of 3D NG is designed to overcome the restacking observed in traditional rGO sheets and achieve graphene's intrinsically high Li storage capacity and diffusivity while simultaneously addressing the long-term stability issues.

We have carried out comprehensive structural characterization of the intermediate and NGs using MALDI-TOF, 1H NMR, and 13C NMR spectra. All the spectroscopic results are in perfect agreement with the proposed mo-

lecular structures, confirming the successful preparation of NGs. The thermal stability of NGs was examined by TGA . These NGs with various functional groups exhibit excellent thermal stability without significant mass loss up to 300oC under N2 atmosphere. The graphitized residue (char yield) of these NGs was more than 60% at 1000oC, which is attributed to their high aromatic (graphene-like) content.

Our 3D NGs reveal great promises for the fabrication of energy conversion and storage devices. We use NG as as anode for the Li ion battery, which was prepared for the first time to exhibit fantastic specific capacitance (> 900 mAh/g) - one of the highest ever reported for carbon based Lithium ion battery, and stability through hundreds of charging discharging cycles. Such performances are ranked the very top among all graphene based materials.

Future Work

There are two major tasks to be accomplished in FY16:

Electrochemistry and device tests

The electrodes prepared from the three-dimensional porous nitrogen-doped nanographene will be studied in supercapacitor and lithium-ion battery: In particular, the nanographene composite anode materials will be tested in thin-film and standard CR-2325-type coin cells for electrochemical and battery characterization, respectively, to study their lithium-ion diffusion coefficient, interfacial characteristics, reversible capacity, electrochemical resistance, and charge/discharge characteristics. We will study the charge transfer limitations (electronic and ionic) in various porous nanographene structures using experimental techniques such as chemical delithiation, galvanostatic charge and discharge, galvanostatic and potentiostatic intermittent titration techniques, cyclic voltammetry, and impedance measurements, to gain insights into the structure-property-synthesis correlations.

Physical characterization

Extensive physical characterization (high-resolution transmission electron microscope, scanning electron microscope, X-ray diffraction, X-ray photoelectron spectroscopy, Raman spectroscopy, Fourier transform infrared spectroscopy, Brunauer-Emmett-Teller surface area analysis, etc,) will be employed to determine the morphology, phase composition, heteroatom doping, surface area and porosity of the as-prepared porous nanographene materials.

Conclusion

We will synthesize the first porous nanographenes with a well defined molecular structure and surface area. We expect to demonstrate, for the first time, fabrication of supercapacitors based on a series of three dimensional nanographenes.

Photophysical Properties of Self-Assembled Nanoclusters

Jennifer Martinez
20150704PRD1

Introduction

Artists and scientists alike have made and studied metal nanoparticles for centuries. These early particles were the dichroic glass of the Lycurgus Cup (4th century), the lustrous ceramic glazes (> 9th century) of the Islamic world, and even the rich colors of stained glass (e.g. Rose Window of Notre Dame Catherdral, ca 1250). Those particles (hundreds of atoms) have been well studied, as has been the electronic phenomena, which allows their technological and artistic use. When we shrink the number of atoms from the hundreds or thousands of atoms to just a few atoms of gold or silver, we change the properties of the collection (i.e. they are now fluorescent). These new, very small collections are called "nanoclusters". Little is understood about their optical properties (e.g. origins of their photophysical properties), how to assemble those clusters into useful organizations (i.e. for solar harvesting or catalysis), nor how the clusters might electronically "talk" to one another. In this project we aim to produce these clusters within DNA and to assemble these clusters using the exacting nature of DNA-DNA interactions. It is only through the use of biological templation of materials that we can ultimately control their structure and thus their properties. While we have started to make progress in the controlled synthesis of these materials, we have little utilized the biological control of synthesis and assembly to understand and manipulate these new materials. If we are able to not only create, but understand these new materials we can create the next generation of optical devices (brighter and more touch sensitive phones), catalysts (energy for cars), and energy collecting devices (solar harvesting).

Benefit to National Security Missions

This project will answer long standing questions within the chemistry, materials and physics communities, by bringing a more thorough structure-function understanding of fluorescent silver and gold nanoclusters. Further, we will bring fundamental understanding of how to modulate nanocluster physics so that they can behave as molecules in one instance and particles in another instance. This basic research project has applications to many important needs including biosensors, catalysis, batteries and solar harvesting and thus supports laboratory missions in emerging threats (science of signatures), materials for the future and energy security.

The control of light energy and control of structure in self-assembled and biologically-assembled material architectures, as proposed here, is important for numerous applications of relevance to the Department of Energy. "From Quanta to the Continuum: Opportunities for Mesoscale Science", a BESAC report, identified a "grand challenge in materials science is to create multiscale functional structures that encode content; adaptively respond to their environment; and capture-transport, and utilize energy". Basic Research Needs for Solar Energy Utilization was the focus of a BES workshop. Here, one of five identified cross-cutting issues relevant to priority research directions was "... novel methods for self-assembly of molecular components into functionally integrated systems." Each of these areas is being addressed within this PD proposal.

Progress

Nanoclusters are collections of a few atoms of silver or gold that exhibit size dependent optical properties, such as strong fluorescence. Little is understood about their optical properties (e.g. origins of their photophysical properties), how to assemble clusters into useful organizations (i.e. for solar harvesting or catalysis), nor how the clusters might electronically "talk" to one another. In order to understand these questions we have developed strategies to self-assemble the clusters and study their photophysics (using a genetically engineered polymer and DNA) and to co-assemble the clusters with carbon nanotubes and enzymes to create a biocatalyst for alternative fuels.

To study how clusters talk to each other and how they

may transition to have more advanced properties we have created a cluster templated within a genetically engineered polymer. Genetically engineered polymers consist of repeating units of amino acid sequence yielding a polymer with defined stimuli response, biocompatibility and programed assembly (as a function of changes in temperature). For the first time we report the direct synthesis of pure, single sized, stimuli responsive, water-soluble and biocompatible elastin like polymer (ELP) templated Au nanoclusters. Optical absorption spectra and electron microscopy indicates that the particles synthesized were nanoclusters and their size was close to the boundary of plasmonic nanoparticles. From dynamic light scattering and electron microscopy we can observe that the clusters assemble with increase in temperature. We are now in the process of understanding how these clusters talk or change their electronic properties within these assemblies.

To more specifically assemble fluorescent clusters and study their photophysics we have used DNA. DNA is much like Velcro in that it can be designed to specifically bind its compliment and can serve as a molecular ruler by precisely spacing two materials away from each other to better understand at what distances the materials can communicate. We have created a highly fluorescent silver nanocluster templated within a piece of DNA. We observed that as the clusters were concentrated (effectively causing the clusters to assemble and touch each other) that we substantially red shifted the resultant fluorescence and absorbance of the material. This new "emergent" fluorescence was reversible with simple dilution of the clusters to reproduce the monomeric fluorescence. These initial results suggested that the clusters could electronically communicate. To better control this interaction we designed the cluster templating DNA to have a piece of overhanging DNA that could zipper together with its compliment (like Velcro). That compliment contained the identical type of fluorescent cluster with a complimentary overhanging DNA. We can control the separation of the two clusters with distances of 2, 4, and 6 nm. We find that the clusters communication (as seen by a substantial red shift in the fluorescence of 100 nm) decreases substantially with distance and drops off completely by 6 nm. Working with our theory colleagues we have indication that the clusters are coupling through dipole interactions that are as strong as strongly coupled (and touching) conjugated polymers, even though the clusters are far more separated than are polymers (suggesting that the clusters couple much more strongly than current materials in the literature).

Beyond organizing cluster-cluster interactions, we have organized clusters to assemble with nanomaterials (carbon nanotubes) and enzymes in the hope of creating an efficient electrode that can be used as a catalyst for alternative fuels. With sources of fossil fuels dwindling, there is an urgent need to find cheap, renewable, and alternate forms of energy using naturally abundant resources such as sunlight, air, and water. Nanostructured materials and enzymatic fuel cells are showing great promise in this respect, if only we can increase their efficiency. We have created a new DNA-templated gold nanocluster (AuNC) of ~1 nm in diameter. When integrated with bilirubin oxidase (BOD) and carbon nanotubes (CNTs), the AuNC acts as an enhancer of electron transfer (ET) and lowers the overpotential of electrocatalytic oxygen reduction reaction (ORR) by ~15 mV as compared to the enzyme alone (e.g. makes the electrode/alternative fuel more efficient). This unique role of the AuNC as enhancer of ET at the enzyme-electrode interface makes it a potential candidate for the development of cathodes in enzymatic fuel cells, which often suffer from poor electronic communication between the electrode surface and the enzyme.

Future Work

Goals and Tasks for FY16 include:

- Synthesize different cluster sizes, protected with either DNA or proteins.
- Design DNA clusters to produce self-assembled structures, utilizing the length of DNA as a molecular ruler to control the distance between clusters in the assembly.
- Use these created assemblies to understand distance dependent cluster-cluster interactions (energy transfer) and to address the nature of clusters interaction (plasmonic or nonplasmonic).
- Probe DNA protected nanoclusters with EXAFS (extended X-ray absorpotion spectroscopy) to understand the nanocluster size and bonding.
- Ustilize steady state and time resolved fluorescence spectroscopy and fluorescence microscopy to probe photophysical properties of clusters and their self assembly the combination of UV-Vis absorption spectroscopy

Conclusion

Overall technical goals: We will synthesize different cluster sizes, protected with either DNA or proteins; those clusters will be self-assembled utilizing the length of DNA as a molecular ruler to control the distance between clusters; these created assemblies will then be used to understand distance dependent cluster-cluster interactions (energy transfer) and to address the nature of clusters interaction (plasmonic or nonplasmonic).

Anticipated Impact: Residing directly between particles

and molecules, nanoclusters are the “missing link” in materials chemistry. Understanding how to create and control their properties not only solves an important mystery in science, but creates materials for new commercial technology.

Publications

Chakraborty, S., S. Babanova, R. C. Rocha, A. Desireddy, K. Artyushkova, P. Atanassov, and J. S. Martinez. A DNA-Hosted Gold Nanocluster Enhances Enzymatic Reduction of Oxygen by Facilitating Efficient Electron Transfer. 2015. Journal of the American Chemical Society. 137 (36): 11678.

Dynamic Strength and Phase Transition Kinetics in Geophysical Materials

Cynthia A. Bolme
20150707PRD2

Introduction

This project is performing cutting-edge science by using the most brilliant hard x-ray source available to examine the response of geophysical materials to strong shock waves. Only in the last few years has the ability to generate conditions of geophysical impacts been available at the same facility with a high brilliance x-ray source. This x-ray source is necessary to observe how materials like SiO2 and H2O change their structures from crystalline solids to disordered materials, like liquids or glasses. Understanding the changes in structure of these materials will provide new data about how these materials behave during geophysical impact events and about the properties of these materials when they exist at high pressures and high temperatures, such as inside planet Earth.

An experiment will be performed at the Linac Coherent Light Source (LCLS) to specifically examine the strength of iron at high temperatures and pressures. These pressure and temperature conditions will be similar to those found inside the earth.

Benefit to National Security Missions

This work contributes strongly to the basic understanding of materials by producing a new class of data that can be used to develop physically based models of dynamic materials response. This new class of data provides detailed information about the interatomic distances and the sizes and orientations of crystals in materials. Due to the specific materials being investigated (i.e. materials that are very common in geophysical bodies, such as asteroids, comets, and rocky planets), this work will also directly contribute to astrophysical areas of research.

The Laboratory's proposed Matter-Radiation Interactions in Extremes (MaRIE) Signature Facility includes a hard x-ray free electron laser, similar to the facility in which this work performs experiments, and the work in this project will help to define the characteristics of the MaRIE free electron laser and the details of the experimental stations for MaRIE. Understanding the behavior of matter during extreme shocks is directly relevant to the nuclear weapons program.

Progress

In FY15, we have gone through the journal review process for a journal article on the phase transition of amorphous fused silica to the crystalline stishovite phase during shock compression. The article is in the final stages of review, and we anticipate that it will be published in Nature Communication in the next few months. We also examined the structure of fused silica that was recovered after shock compression to learn about the phase reversion process to a high density amorphous phase.

We received x-ray beam time to perform an experiment at the LCLS to study the strength of shock compressed iron. We designed the iron experiment and prepared some of the samples that will be consumed during the shock experiment in December of FY16.

Future Work

In FY16, we will perform an experiment at the Linac Coherent Light Source (LCLS) to study the strength of iron under shock compression. The experiment will include polycrystalline and single crystal iron samples. The samples will be shock compressed to simulate the pressure and temperature conditions of iron inside the earth - from the crust to the molten iron core.

We will also complete the analysis of a previously acquired data set showing the fast dynamics of water freezing to the ice VII phase, and we will submit a journal article on these results.

Conclusion

This project will provide unique new data about how the atoms in geophysical materials (for example, water, SiO2, and iron) respond under conditions of high temperature

and pressure. This information will progress the current level of understanding about how these materials behave in geophysical events, such as asteroid impacts and the dynamics of the earth's molten iron core.

Publications

Gleason, A. E., C. A. Bolme, H. J. Lee, B. Nagler, E. Galtier, D. Milathianaki, J. Hawreliak, R. G. Kraus, J. H. Eggert, D. E. Fratanduono, G. W. Collins, R. Sandberg, W. Yang, and W. L. Mao. Ultrafast visualization of crystallization and grain growth in shock-compressed SiO2. 2015. Nature Communications. 6: 8191.

In-situ, 3D Characterization of Solidification in Metals

Amy J. Clarke
20150709PRD2

Introduction

The pRad facility at LANL provides the optimal size scale for doing solidification experiments with spatial resolution of ~20 µm and a field-of-view of several centimeters. This is superior to the more common x-ray experiments, because it allows for a sample size that is more representative of an actual casting, but the spatial resolution is still sufficient to capture the details of microstructural development. However, proton experiments have been limited by the relatively low image acquisition rate of 20 Hz, which results in an acquisition time of almost 30 seconds for a full 3D dataset.

Synchrotron x-rays, on the other hand, provide the temporal resolution needed to collect a 3D dataset in just a few seconds; however, x-rays are limited to about a millimeter of penetrating power. Furthermore, none of the in-situ x-ray experiments of metal solidification that have been done to date have used a well controlled furnace that can provide a given thermal gradient and cooling rate.

We propose to overcome the pRad temporal resolution limits by using the recently developed time-interlaced model-based iterative reconstruction (TIMBIR) method. This will provide temporal resolution that is on par with synchrotron x-ray experiments, but with the superior field-of-view provided by protons. Improvements on the scientific front will come from building and using a furnace that can provide controlled temperature profiles in space and time while also rotating, which is necessary for collecting a computed tomography dataset. This furnace will allow for a much better temperature control than has been achieved before, making it possible to do systematic studies of cooling rate, temperature gradient, and alloy composition on solidification behavior.

Benefit to National Security Missions

DOE/SC: This project is tied to science campaigns by generating datasets of microstructure evolution during solidification experiments in which the thermal gradient, cooling rate, and alloy composition are independently and systematically varied. These datasets will give us a better understanding of solidification and will be made available to validate simulation methods, including a microstructure prediction model that is currently being implemented in the advanced simulation and computing (ASC) code Truchas.

MaRIE: In this project, we will be using multiple beams (e.g. proton and x-ray) to interrogate samples during solidification. This data can be used to access multiple size scales, since proton imaging has a resolution of ~20 µm and x-ray imaging typically has a resolution of ~1 µm. As both methods have a field of view about 1000 times their resolution, protons can be used to see large volumes of material, while x-rays can give higher resolution views of smaller volumes. The multiple characterization methods also provide opportunities to examine the chemistry of samples in higher detail, due to the differing contrast mechanisms between the two beam types. This work is in alignment with MaRIE, as multiple beams are envisioned to simultaneously characterize samples in the future. This research will also help to define what is currently possible with existing characterization methods and outline what capabilities should be included in future instruments.

Progress

Since the fellowship started in April 2015, the main accomplishment has been the design of a furnace that will permit computed tomography (CT) during metal alloy solidification. The rotation and translation stages and the necessary controllers to perform CT experiments have been identified and quoted, and will be ordered and received by the end of the FY. The delivery timeframe for these parts is 8 to 12 weeks.

The furnace portion of the experimental setup has undergone a significant design change from our radiogra-

phy experiments, making it simpler and more capable. This design change permits the use of simpler resistive heating elements, rather than induction heating coils. The resistive heating elements have been specced out, and we are in the process of getting quotes.

On the scientific front, two papers have been published on the time-interlaced model-based iterative reconstruction (TIMBIR) methodology, which is one of the key enabling technologies of this project for achieving improved temporal resolution for the proposed dynamic solidification experiments. The first paper focuses on the mathematical formulation for TIMBIR, and the second paper showcases an application of TIMBIR to studying the morphology of free-growing metallic dendrites.

Future Work

During the remainder of FY15, the motion stages and furnace components will be specified, purchased, and delivered. Since there is a lead-time of several months between ordering and delivery of the components, the end of FY15 will also provide time to test the heavily revised TIMBIR code [1]. These tests will be used to determine if our 40-core computer cluster is sufficient for data processing, or if it will be necessary to request computing time on high performance computing machines.

With delivery of the experimental furnace and stage components by the end of FY15, assembly and testing of the system will start in early FY16. The testing will include programming the rotation stage for the particular motion that we want, and coordinating the rotation and heating control systems with the beamline/camera data acquisition system.

The first "in-beam" tests of the system should occur in the early part of FY16 with experiments at pRad, provided beam-time is received from a competitive, institutional proposal process. To our knowledge, this will be the first time that well-controlled, directional solidification experiments and 3D, in-situ characterization are combined. Initial experiments will look at void formation in castings, interfacial morphology and dynamics during solidification, and the evolution of solute distribution during solidification. The processing and analysis of these datasets will likely require most of FY16.

Conclusion

We will develop the capability to do controlled solidification experiments in any type of beamline, including the proton, neutron, and x-ray beamlines across the U.S. DOE complex. We will use this capability to probe solidifying metals with a variety of different diagnostic means to access a wide variety of spatial and chemical data. By using the new x7 magnifier at pRad and the recently developed time-interlaced, model-based iterative reconstruction (TIMBIR) methodology, we will be able to improve the spatial and temporal resolution from 50 µm to 20 µm and from 20 seconds to 1 second per 3D dataset.

Publications

K.A. Mohan, S.V. Venkatakrishnan, J.W. Gibbs, E.B. Gulsoy, X. Xiao, M. De Graef, P.W. Voorhees, C.A. Bouman. "TIMBIR: A Method for Time-Space Reconstruction from Interlaced Views." IEEE Transactions on Computational Imaging. DOI: 10.1109/TCI.2015.2431913 (2015).

J.W. Gibbs, K.A. Mohan, E.B. Gulsoy, A.J. Shahani, X. Xiao, C.A. Bouman, M. De Graef, P.W. Voorhees. The Three-Dimensional Morphology of Growing Dendrites. Scientific Reports. Accepted (2015).

Dendritic Microstructure Selection in Cast Metallic Alloys

Amy J. Clarke
20150713PRD2

Introduction

Complex – so-called dendritic – microstructures are most commonly observed in metallic alloys. Their morphological and compositional characteristics determine the mechanical properties and performance of cast parts.

From a theoretical standpoint, dendritic growth is a long-standing example of complex pattern formation, involving structural and chemical changes over multiple length and time scales. Most theoretical studies have focused on diffusive dendritic growth, neglecting convective solute transport in the liquid. Yet, gravity yields significant convection, resulting in detrimental microstructure inhomogeneities.

The first implementation of a novel, multi-scale dendritic needle network (DNN) model is orders-of-magnitude faster than simulation methods like phase-field and hence permits simulations at the mesoscale. In this project, liquid convection will be added into this model, enabling dendritic solidification simulations under realistic gravity conditions at length/time scales relevant to experiments and casting processes for the first time. Computationally intensive implementations of phase-field models will also be used as a validation tool, in support of the DNN model development.

Convection effects at the microscopic scale will be studied with phase-field and at the scale of experiments with multi-scale DNN simulations. The model developments will be validated by quantitative comparisons to experiments performed by Clarke's team at LANL. The simulations will guide the design of new experiments that will be executed at U.S. DOE User Facilities. By combining controlled experiments with intensive simulations, we will reveal the fundamental mechanisms of microstructure selection in the presence of unavoidable convection, which is essential to the properties and performance of cast materials.

The development of cutting-edge simulation techniques that predict realistic solidification scenarios will provide LANL with unique capabilities for the prediction and control of solidification microstructures.

Benefit to National Security Missions

DOE/SC: The development of a simulation capability for microstructure solidification at realistic time/length scales and gravity conditions, which is currently missing at LANL, will be a critical step toward predicting and controlling solidification structure evolution, which is key for LANL to support advanced manufacturing initiatives and the design of innovative processing studies.

MaRIE: This project is strongly motivated by the capability to quantitatively simulate solidification microstructures in realistic gravity conditions to support the design of solidification experiments with in situ imaging at LANL with high energy X-ray and proton beams. The multiscale modeling approach will not only guide multi-scale characterization experiments with MaRIE, but should also bring fundamental insight into the relevant physics that need to be included in our models.

Basic Understanding of Materials: Because dendritic solidification involves a broad range of length and time scales, it has only been approached theoretically at the scale of a few dendrites in idealized conditions, such as a purely diffusive regime. The current project will provide the first tool to quantitatively explore the crucial effect of gravity-induced convection on spatially extended dendritic arrays.

Climate and Energy Impact: The reduction of energy consumption, for instance in transportation, requires the development of innovative materials with tailored microstructures and properties. The ability to explore microstructure design through simulations will also accelerate the development and deployment of energy efficient processes.

Progress

Since the beginning of the project in May 2015, we are investigating which CFD numerical framework would be most suitable to a direct coupling with the multiscale Dendritic Needle Network (DNN) crystal growth model. The potential candidates for CFD approaches include Finite Volume, Finite Element, Finite Difference, and potential alternative approaches like Lattice-Boltzmann methods. The selection is based upon the potential of the approach to deal with fluid-structure and fluid-particle interactions in a quantitative way, as well as the potential to achieve highly scalable simulations. At this point, the two most promising approaches are the Finite Volume and Lattice-Boltzmann methods. The former benefits from broad expertise and various optimized tools already in place at LANL. The latter has recently shown great promise in the field of multiphase flows, and would provide an alternative approach that would be relatively simple to implement, be effective in handling microscopic fluid-particle interactions, and would offer a highly parallelizable framework. While no particular approach has been ruled out of the selection process yet, we are currently considering the feasibility of pursuing both Finite Volume and Lattice-Boltzmann methods and will benchmark them for DNN calculations.

Future Work

The main goal for FY16 is to design a two-dimensional model coupling the multi-scale Dendritic Needle Network (DNN) model for crystal growth to fluid dynamics in the liquid. Since Computational Fluid Dynamics (CFD) equations are harder to solve than the intentionally simplified DNN equations, it is more appropriate to incorporate the DNN model into a CFD code than vice-versa.

Toward that aim, in FY15 we will identify the CFD numerical framework most suitable to direct coupling with DNN crystal growth modeling. The potential candidates for CFD approaches include Finite Volume, Finite Element, Finite Difference, and potential alternative approaches like Lattice-Boltzmann methods. The choice will be based upon the potential of the approach to deal with fluid-structure and fluid-particle interactions in a quantitative way.

In FY16, we will develop and validate a new mathematical formulation of the DNN equations in the framework of the chosen CFD approach. This core step may require substantial DNN redesign, and a subsequent set of thorough validation tests to ensure that the crystal growth modeling provides reliable, quantitative predictions.

Finally, we will develop a fully coupled DNN-CFD implementation, which will be made computationally efficient by the use of advanced numerical techniques, such as intensive parallelization (e.g. using Graphic Processing Units).

The final goal at the end of the project in FY17 is an implementation in three dimensions (3D). Hence, each step will be toward this aim. Moreover, in the choice of the appropriate CFD approach, simulation tools already available at LANL (e.g. Truchas) will be strongly favored to ideally build a long-lasting, in-house capability for simulating dendritic solidification under realistic gravity and processing conditions.

While the anticipated lower budget allocation may affect the extent of the model deployment and coupling with other codes at LANL, the final goal remains a 3D coupled DNN-CFD implementation.

Conclusion

Cutting-edge, multi-scale simulations validated by in situ experiments will shed light on the poorly understood, yet crucial effects of gravity on microstructure selection in metallic alloys during metallurgical processing. Understanding crystal growth under gravity-induced liquid flow across length scales will enable the control of microstructure and defects in cast parts. This project will mark a transformational leap toward reaching predictive capability for advanced manufacturing at LANL, aimed at tailoring materials microstructures and properties relevant to national security and energy challenges. It will also provide new, predictive computational tools needed for future MaRIE studies.

Frustrated Materials

Cristian D. Batista
20120751PRD2

Abstract

Competing or conflicting interactions are ubiquitous in physical and biological systems that range from water ice and glass formation to neural networks and protein folding. Frustration in these many-body systems refers to the fact that local pairwise interactions cannot be satisfied simultaneously. Condensed matter systems with strong frustration exhibit a variety of fascinating features such as emergent gauge field, topological order, and fractionalized excitations. They are also hosts to various complex orders and exotic phases such as spin ice and topological insulators. The main goal of this project is to investigate various intriguing phenomena resulting from strongly frustrated interactions.

Background and Research Objectives

One of the most spectacular manifestations of geometrical frustration is the presence of the novel states of matter and associated phase transitions. These novel phases arise as a compromise between the opposite tendencies that are inherent to frustrated geometries. A triangular plaquette is an archetypal building block for lattices with geometrical frustration. Many unusual magnetic and orbital orderings in frustrated magnets are best understood from the viewpoint that the system is in the vicinity

of a metal-insulator transition. It is a challenging theoretical task to model these systems, which lie in the intermediate-coupling regime between deep Mott insulator and the metallic phase. To carry out such studies, we employed a combination of analytical and numerical techniques. We used mean field and semi-classical techniques for computing thermodynamic properties. For the numerical approach we implemented

a Mote Carlo algorithm for solving the problem of itinerant electrons interacting with localized classical spins. Since the action is quadratic in the fermion operators, the itinerant electrons can be integrated out exactly, leading to an effective non-local classical action for the local moments that will be solved by applying the Metropolis algorithm. All the thermodynamic properties could be computed under control because the statistical error can be made arbitrarily small by increasing the sample size. The temperature dependence of the thermodynamic quantities could thus be directly compared against the experiments.

Scientific Approach and Accomplishments

The research of Dr. Gia-Wei Chern has been focused on frustrated systems in general, and particularly in highly frustrated magnetism. The main goal here is to have a better understanding of these intriguing complex systems and to design and control their novel properties for applications to, e.g. magnetic storage, computing, and sensing.

Working with his collaborators at LANL, Dr. Chern has studied a novel magnetic field induced phase transition in vanadium spinels. The magnetic ions in these compounds form a highly frustrated pyrochlore lattice, which is a three-dimensional network of corner-sharing tetrahedron. The vanadium spinels have been a canonical system for studying frustrated spin-orbital interactions. Taking advantage of the high magnetic field facility at LANL, experimentalists have uncovered an interesting phase transition induced by magnetic field in these compounds. Gia-Wei and his colleagues have developed a theoretical model that successively explains the experimental results.

Another main area of his research is the study of artificially created frustrated systems, in particular the so-called artificial spin ice. Artificial spin ice is a booming field in condensed matter physics. Among the most exciting recent developments is the emergence of magnetic monopoles in these materials. Emergent phenomena, which until now have only been accessible at low-T, can thus be tailor-designed to manifest at room tem-

perature. In particular, the existence of mobile magnetic monopoles coupled to magnetic fields provides a promising approach to realize magnetricity, the control and manipulation of magnetic currents. With the rapid progress in nano-fabrications, it is now possible to realize artificial spin ice in various lattice geometries. One of the key advantages of these systems is that they allow direct experimental access to the microscopic degrees of freedom.

With collaborators in LANL, Dr. Chern has proposed the first feasible design of a three- dimensional artificial spin ice that has exactly the same lattice topology as the natural spin-ice compounds. Experimental realization of such systems will allow us to study the dynamics of magnetic monopoles in these novel materials taking advantage of the powerful tools of modern nanotechnology. In addition, the earlier proposal of composite monopole quasiparticles, namely an emergent monopole surrounded by background magnetic charges, has been experimentally confirmed; Dr. Chern was also involved in the theoretical analysis of this work.

Motivated by recent advances in thin-film growth technology, Dr. Chern also studied the triangular Ising antiferromagnetic thin films. He and his colleagues discovered unusual re-entrant phase transitions, which depend on the number of layers in the system. This study added a surprising chapter to this well studied canonical system of frustrated magnetism.

Collaborating with colleagues in the Theoretical Division (T-1), Dr. Chern has pioneered in applying the state-of-the-art large-scale Langevin dynamics simulations to investigating novel magnetic orders in metallic frustrated magnets. The Langevin dynamics method was developed at LANL for efficient simulations of electrons interacting with classical fields. One particular interest is the complex spin textures stabilized by electrons in the frustrated kagome lattice. In this study, Gia-Wei and his collaborators have uncovered several novel non-coplanar magnetic orders, some of which also support topological electron states.

The Langevin method can also be applied to improve the efficiency of quantum molecular dynamics (QMD) simulations, especially for metallic systems. With his collaborators, Dr. Chern has developed numerical schemes that integrate techniques for studying strongly correlated electrons with the efficient QMD simulations. More specifically, Dr. Chern worked on developing a quantum molecular dynamics simulations based on an efficient Gutzwiller method. He successfully developed a prototype Gutzwiller QMD code and discovered interesting new results based on this code. These works will contribute to our fundamental understanding of the dynamics of strongly correlated materials and are also important to the strategic mission of LANL.

Impact on National Missions

Given the complexity of correlated materials and the unlimited number of compounds, the discovery of new states of matter and functionalities must be organized around simple guiding principles. Our basic principle for discovering complex and collective forms of matter that exhibit novel properties and respond in new ways to environmental conditions is to make, characterize and model classes of materials with controllable degree of electronic localization. This is a necessary step towards the dream of “materials by design.”

With such tools, we can better understand the complexity of actinides and other correlated materials. Actinide based materials are of primary interest for energy security applications relevant for DOE/NNSA and DOE/SC. Moreover, our ability of predicting the behavior of correlated materials is crucial for optimizing response functions, such as magneto-electric susceptibility, which are necessary for sensing applications relevant for DoD basic defense applications (including detection), DHS basic homeland security (including detection) and Intelligence agencies. We are responding to the national need of predicting actinide, and more in general, correlated materials properties for energy security applications. Our work is a first step towards reaching the level where studies of actinide properties can be predicted from first principles computer-based simulations, thus avoiding costly experiments and contributing significantly to the reliability of the nuclear stockpile. The outcome of this project (new code for performing molecular dynamics of correlated materials) can also be used for studying the effects of matter and radiation in extremes, the mission of MARIE.

Publications

Chern, , Chien, and Di Ventra. Dynamically generated flat-band phases in optical kagome lattices. 2014. PHYSICAL REVIEW A. 90 (1).

Chern, , Maiti, R. M. Fernandes, and Woelfle. Electronic Transport in the Coulomb Phase of the Pyrochlore Spin Ice. 2013. PHYSICAL REVIEW LETTERS. 110 (14).

Chern, , Reichhardt, and C. J. O. Reichhardt. Avalanches and disorder-induced criticality in artificial spin ices. 2014. NEW JOURNAL OF PHYSICS. 16.

Chern, , Reichhardt, and Nisoli. Realizing three-dimensional artificial spin ice by stacking planar nano-arrays. 2014. APPLIED PHYSICS LETTERS. 104 (1).

Chern, , and Wu. Four-Coloring Model and Frustrated Superfluidity in the Diamond Lattice. 2014. PHYSICAL RE-

VIEW LETTERS. 112 (2).

Chern, G. W., C. Reichhardt, and C. J. O. Reichhardt. Frustrated colloidal ordering and fully packed loops in arrays of optical traps. 2013. PHYSICAL REVIEW E. 87 (6): -.

Chern, G. W., M. Morrison, and C. Nisoli. Degeneracy and criticality from emergent frustration in artificial spin ice. 2013. Physical Review Letters. 111: 177201.

Chern, G. W., R. M. Fernandes, R. Nandkishore, and A. V. Chubukov. Broken translational symmetry in an emergent paramagnetic phase of graphene. 2012. PHYSICAL REVIEW B. 86 (11): -.

Chern, G. W., and C. D. Batista. Spontaneous quantum Hall effect via a thermally induced quadratic Fermi point . 2012. Physical Review Letters. 109: 156801.

Chern, G. W., and O. Tchernyshyov. Magnetic charge and ordering in kagome spin ice. 2012. PHILOSOPHICAL TRANSACTIONS OF THE ROYAL SOCIETY A-MATHEMATICAL PHYSICAL AND ENGINEERING SCIENCES. 370 (1981): 5718.

Chern, G. W., and R. Moessner. Dipolar Order by Disorder in the Classical Heisenberg Antiferromagnet on the Kagome Lattice. 2013. PHYSICAL REVIEW LETTERS. 110 (7): -.

Choi, E. S., G. W. Chern, and N. B. Perkins. Chiral magnetism and helimagnons in a pyrochlore antiferromagnet. 2013. PHYSICAL REVIEW B. 87 (5): -.

Choi, E., G. W. Chern, and N. B. Perkins. Helimagnons in a chiral ground state of the pyrochlore antiferromagnets. 2013. EPL. 101 (3): -.

Gilbert, I. a. n., Chern, Zhang, O'Brien, Fore, Nisoli, and Schiffer. Emergent ice rule and magnetic charge screening from vertex frustration in artificial spin ice. 2014. NATURE PHYSICS. 10 (9): 671.

Knolle, J., G. -W. Chern, D. D. L. Kovrizhin, R. Moessner, and N. B. Perkins. Raman Scattering Signatures of Kitaev Spin Liquids in A2IrO3 Iridates. 2014. Physical Review Letters. 113: 187201.

Lin, , Kamiya, Chern, and C. D. Batista. Stiffness from Disorder in Triangular-Lattice Ising Thin Films. 2014. PHYSICAL REVIEW LETTERS. 112 (15).

Mun, E. D., Chern, Pardo, Rivadulla, Sinclair, H. D. Zhou, V. S. Zapf, and C. D. Batista. Magnetic Field Induced Transition in Vanadium Spinels. 2014. PHYSICAL REVIEW LETTERS. 112 (1).

Perkins, N. B., G. W. Chern, and W. Brenig. Raman scattering in a Heisenberg S=1/2 antiferromagnet on the anisotropic triangular lattice. 2013. PHYSICAL REVIEW B. 87 (17): -.

Rahmani, , and Chern. Universal Renyi mutual information in classical systems: The case of kagome ice. 2013. PHYSICAL REVIEW B. 88 (5).

Rahmani, A., and G. W. Chern. Universal Renyi mutual information in classical systems: The case of kagome ice. 2013. PHYSICAL REVIEW B. 88 (5): -.

Zhang, S., I. Gilbert, C. Nisoli, G. W. Chern, M. J. Erickson, L. O'Brien, C. Leighton, P. E. Lammert, V. H. Crespi, and P. Schiffer. Crystallites of magnetic charges in artificial spin ice. 2013. NATURE. 500 (7464): 553.

Designing and Probing Novel Materials by Pressure Tuning of Nanocrystals

Hongwu Xu
20120753PRD2

Abstract

Self-assembly of nanocrystals (NCs) into superlattices is an intriguing phenomenon that may lead to materials with novel collective properties, in addition to the unique properties of individual NCs compared with their bulk counterparts. Pressure tuning of nanocrystals (NCs) and their assembled superlattices is a novel approach to design, develop and probe new nanostructured materials. In this research, we have determined the structural evolution and stability relations of several NC superlattices (e.g. PbSe, PbTe and Pt) at high pressure (P) conditions. We started with controlled synthesis of nanoparticles with desired characteristics and then assembled them into ordered superlattices or supercrystals. We systematically investigated their high-pressure behavior using small-angle and wide-angle synchrotron X-ray scattering (SAXS and WAXS) coupled with diamond-anvil cell (DAC) techniques, and we determined the relative stabilities of different NC superlattice polymorphs using calorimetric techniques. Our results have provided important insights into the fundamental mechanisms underlying the formation of high-pressure nanocrystal phases and the coalesced superlattices potentially with enhanced or newly emerging properties.

Background and Research Objectives

Novel materials are often found by modifying the structures of existing materials without altering their compositions. As an important but underexplored thermodynamic variable, pressure can induce extreme changes in material structures, potentially leading to new physical properties. For example, soft, opaque graphite is the form of carbon stable at ambient conditions, but it can be turned into ultra-hard, transparent diamond at high pressures. To expand the range of available solid-state materials, it is important to find pathways leading to metastable, high-pressure phases that can be brought to ambient conditions for real-world applications.

Nanocrystals, which bridge single atoms to bulk solids and are structurally defect-free, possess unique properties compared to their bulk counterparts. Pressure tuning of nanocrystals is a unique method for designing and making novel nanostructured materials. Typically, NCs undergo structural transformations via single nucleation events at high pressures [1]. As the surface energy of NCs overwhelms their bulk energy, these phase transitions may be arrested at ambient conditions through surface stresses that are equivalent to external compressive pressures. Moreover, recent studies indicate that high pressure and deviatoric stress can be a more efficient way to tune NC superlattices and 1D/2D mesostructures [2]. These assembled NC architectures not only exhibit a single-crystal-like structure but also possess strong size-quantization effects and enhanced properties. Hence, studying nanoparticles and their assemblies under high pressures enables discovery and continuous synthesis of novel materials with potential applications in catalysis, solar cells and other areas [3].

Scientific Approach and Accomplishments

The general approaches of our research included: 1) synthesis of colloidal nanoparticles with desired characteristics (structure, size, shape etc.), 2) self-assembly of these nanoparticles into superlattices/supercrystals, 3) structural characterization of the nanoparticles and their assemblies at high pressures, and 4) determination of the stability relations among different NC superlattice polymorphs. The studied systems include PbTe, PbSe, Pt and NaYF4. We describe the specific results below.

Pressure-induced switching between amorphization and crystallization in PbTe nanoparticles

Combining in-situ high-P synchrotron X-ray scattering with transmission electron microscopy (TEM), we investigated P-induced structural switches between the rock salt and amorphous phases as well as the associated mechanisms of their formation in 6 nm PbTe nanocrystals [4]. To harvest the metastable phases of PbTe, we applied different maximum pressures on PbTe NCs and

selectively obtained the stable crystalline or metastable amorphous PbTe phases at ambient conditions. In addition, the conversion from the amorphous to crystalline PbTe phase was observed under electron beam irradiation with a TEM.

Synthesis of PbTe NCs and subsequent loading into a DAC. PbTe colloidal nanoparticles with an average size of 6 nm were synthesized as follows. 0.45 g of lead oxide (2 mmol), 4.2 mL of oleic acid and 12.0 mL of octadecene were loaded in a three-neck round-bottom flask under airless condition, heated to 170 °C for 30 min, and subsequently stabilized at 150 °C for 5 min under agitation and argon protection. Once the solution temperature was about 110 °C, 2 mL of Te-trioctyl phosphine (0.5 mol/L) was rapidly injected to initiate the formation of PbTe NCs, and was then ceased after 7 min with a cold water bath. Lastly, the PbTe NCs were dispersed in hexane, forming black transparent colloidal solutions.

The sample was loaded into a DAC by drop-casting a suspension of PbTe NCs into the gasket hole seated on the tip of one diamond anvil. This procedure was repeated 2-3 times to ensure that there were sufficient PbTe NCs in the DAC sample chamber. To determine pressure dependence of the phase transformation behavior of PbTe NCs, two separate runs were conducted to reach the maximum pressures of 15.6 and 19.7 GPa. Upon release of the pressure to ambient conditions, the sample was carefully transferred from the gasket hole to a Cu grid for later TEM observation.

High-P behavior of PbTe nanoparticles. Starting with the same rock salt PbTe NCs, depending on the maximum pressure, we harvested either rock salt or amorphous phase upon decompression (Fig. 1). When PbTe NCs were pressurized above 10 GPa, amorphization, rather than the rock salt to orthohombic transition observed in bulk PbTe, started to occur. When the maximum pressure reached 15.6 GPa, the amorphous phase transferred back to the starting rock salt phase after releasing the pressure. However, when the maximum pressure reached 19.7 GPa, the metastable amorphous phase could be kept at ambient conditions. The difference between these two recovered samples - crystalline phase from the 15.6 GPa run and amorphous phase from the 19.7 GPa run - can be readily discerned from their diffraction patterns. Hence, the metastable amorphous PbTe nanoparticles can be harvested by applying higher pressures on PbSe NCs.

Transition of PbTe nanoparticles from metastable amorphous to stable rock salt structure. We used TEM to investigate the effects of electron beam irradiation on the stability of amorphous PbTe nanoparticles (Fig. 1).

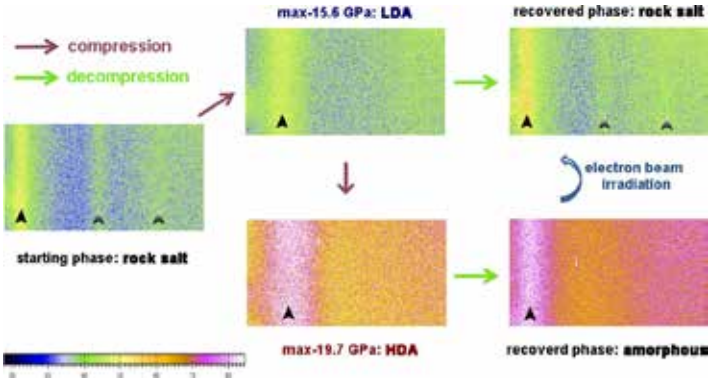

Figure 1. Several representative 2D WAXS images showing the two types of processes and their correlations.

Upon gradual increase of irradiation dose, there were more and more electron diffraction rings, and further, their intensities increased with irradiation time. These changes indicate that amorphous PbTe nanoparticles became crystallized upon electron irradiation, and the resulted NCs were confirmed to have the rock salt structure. Thus the recovered high-P amorphous PbTe nanoparticles can reverse back to the stable rock salt phase due to the thermal energy from electron beams.

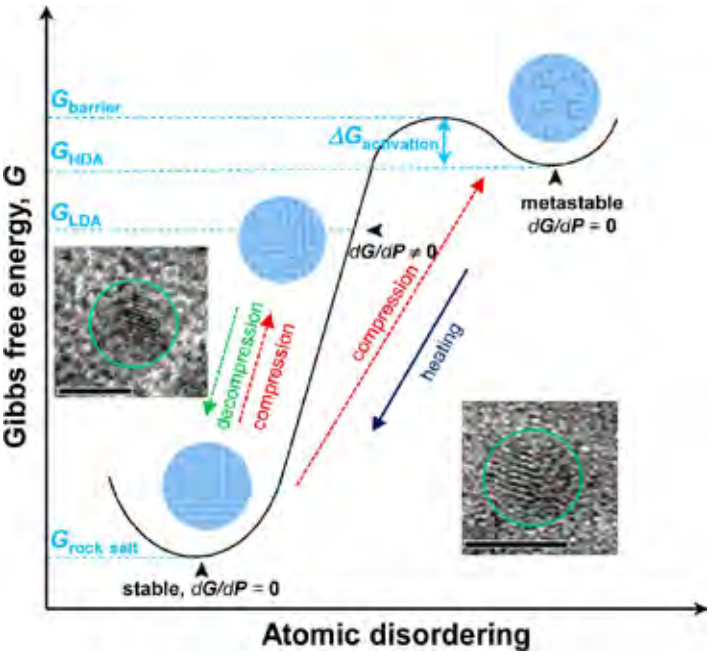

Figure 2. Schematic diagram showing the Gibbs free energy relation of the phase transitions observed in PbTe NPs and HRTEM images of the samples recovered from 15.6 GPa (left inset) and from 19.7 GPa at the initial stage of electron beam irradiation (right inset). The scale bars in both images represent 5 nm.

In summary, high pressure and thermal energy can be used to achieve multiple switching between stable rock-salt structure and metastable amorphous structure in

PbTe nanoparticles. Figure 2 shows the Gibbs free energy relations between the two structures, illustrating their switching mechanisms. The amorphous nanophase formed at 15.6 GPa has a lower density (LDA – low-density amorphous), is energetically unfavorable, and would revert back to the rock salt structure (memory effect). In contrast, the amorphous nanophase formed at 19.6 GPa possesses a higher density (HDA – high-density amorphous) and has a larger energy barrier, preventing it from reversion back to the rock salt structure. Nevertheless, the energy barrier between the recovered amorphous and rock salt structures of PbTe nanoparticles can be overcome by additional thermal energy under electron irradiation.

Controlled self-assembly of non-spherical Pt nanoparticles

Self-assembly of small building blocks such as atoms, molecules and nanocrystals into mesoscopic and macroscopic structures is an intriguing phenomenon and is an active research area in chemistry, biology and materials science [5]. Most of the earlier self-assembly preparations used spherical nanoparticles as their building blocks. Recently, progresses in colloid chemistry have made it feasible to prepare well-defined non-spherical nanocrystals, allowing design and fabrication of non-spherical NC-based supercrystals [6]. Through the delicate control over solvent-ligand interactions, we have shown that Pt nanocubes can be selectively assembled into two distinct types of superlattices in the form of 2D thin films: simple cubic and body-centered tetragonal [7], as described below.

Self-assembly of Pt nanocubes using a “home-built” setup. Uniform Pt nanocubes with an edge length of 10 nm and coated with oleic acid and oleylamine ligands were used as the building blocks. These nanocubes were separately dispersed in two solvents: hexane and toluene, forming colloidal solutions, and then these colloidal nanocubes were assembled in a controlled manner as follows. A two-layer substrate was used: the bottom layer is a square Si wafer, and the top layer is a TEM Cu grid placed on the Si wafer. Several drops of Pt nanocube solution were put onto the substrate, and, due to the surface tension of solvent on the Si wafer, the colloidal solution was constrained within the wafer. To slow down solvent evaporation, the substrate was immediately covered with a weighing dish and then sealed. After complete solvent evaporation, Pt nanocube assemblies formed on the substrates, which were later studied using TEM.

Controlling self-assembly of Pt nanocubes with different dispersion solvents. When toluene was used as the solvent, Pt nanocubes in different layers were stacked together with the face-to-face contact (Figs. 3a and 3b). From the TEM tomography results of the relative positions of nanocubes in different layers, it is clear that nanocubes in the top layer directly sit on the top surface of nanocubes in the bottom layer (Figs. 3d-g). Therefore, the formed Pt NC assembly has a simple cubic superstructure (Fig. 3h).

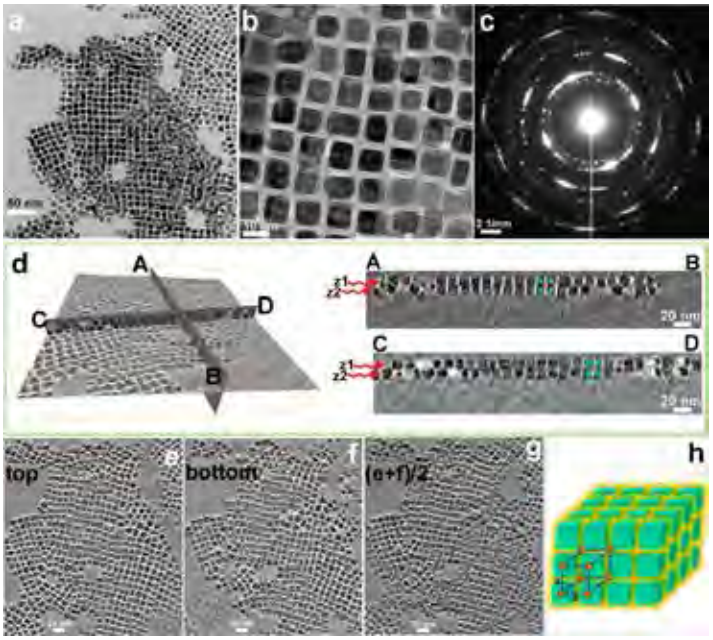

Figure 3. Self-assembly patterns of Pt nanocubes generated from a toluene solvent. (a) TEM image. (b) Magnified image from (a) and (c) SAED pattern from the same area. (d) 3D reconstruction (left) with two orthogonal views AB and CD (right). (e, f) Slice views of the top and bottom layers at the heights of z1 and z2, respectively, as indicated in (d). (g) Calculated image obtained by averaging (e) and (f). (h) Structure model of the sc superstructure assembly.

When hexane was used as the solvent (while other conditions were kept the same), a different assembly pattern resulted (Figs. 4a and 4b). Based on the TEM tomography results, Pt nanocubes in the top and bottom layers of a three-layer assembly occupy the same horizontal positions, while those in the middle layer situate in the interstices, each of which is produced by four nanocubes from the top and bottom layers (Figs. 4d-i). As a result, a body-centered-tetragonal superstructure is formed (Fig. 4h).

In summary, due to the presence of organic ligands outside Pt nanocubes, one can use different solvent types to modify the weak ligand-solvent and solvent-solvent interactions during the self-assembly process, thereby changing the relative positions of Pt nanocubes in different layers to produce different packing structures. Thus our developed method is an effective approach to synthesize different types of assemblies from the same non-spherical nanoparticles.

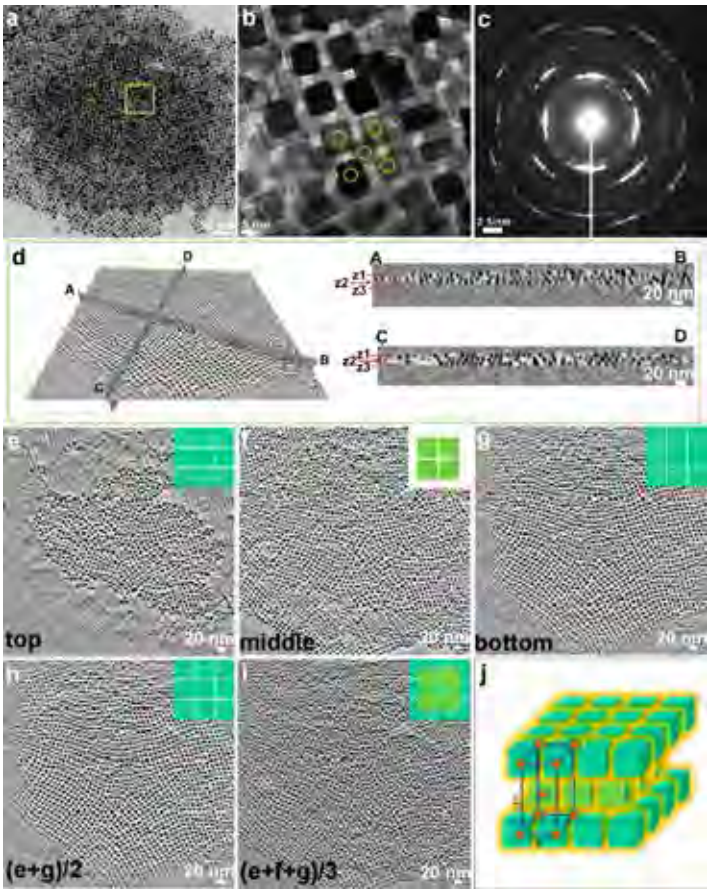

Figure 4. TEM and tomographic results of Pt nanocube self-assembly generated from hexane as the solvent. (a) TEM image. (b) Magnified image and (c) SAED pattern of the framed area in (a). (d) 3D reconstruction (left) with two orthogonal views AB and CD (right). (e–g) Slice views of the top, middle, and bottom layers at the heights of z1, z2, and z3, respectively, as indicated in (d). (h, i) Images obtained as the average of (e) and (g) and average of (e), (f) and (g), respectively. Unit cells are outlined. (j) Structure model of the bct assembly.

Energy Landscape of PbSe nanoparticle superlattice polymorphs

Different nanoparticle superlattice polymorphs with similar energetics can be made by slight changes in growth conditions. Using solution calorimetry with hexane as the solvent, we measured the enthalpies of disassembly of three PbSe NC superlattices and thus determined their stability relations [8].

Self-assembly of PbSe NCs into three superlattice polymorphs. Uniform PbSe nanoparticles with the shape of truncated ocathedron were used as the building blocks. Through controlling solvent type and substrate curvature, we assembled the PbSe NCs into three different supercrystals (Fig. 5a) - body-centered cubic (bcc), body-centered tetragonal (bct) and face-centered cubic (fcc). The nearest interparticle surface distance increases from bcc to bct and then to fcc supercrystals, and since they have the same NCs, ligand interactions were expected to decrease in this order.

Measurements of the disassembly enthalpies of superlattice polymorphs. The enthalpies of dissolution of the three supercrystals into well dispersed and separate NCs were measured using solution calorimetry with hexane as the solvent. Our results show that the dissolution enthalpies of all these polymorphs are on the order of 2 kJ per mol of PbSe, which is comparable to the energy of van der Waals interactions. Further calorimetric data analyses reveal that the bcc superlattice is the energetically most stable polymorph, with the bct being 0.32 and the fcc 0.55 kJ/mol higher in enthalpy. This stability sequence is consistent with the decreased packing efficiency of PbSe NCs from bcc (17.2%) to bct (16.0%) and to fcc (15.2%) (Fig. 5b). On the other hand, the enthalpy differences among the three polymorphs are small, confirming a closely spaced energy landscape and explain the ease of formation of different NC superlattices at slightly different synthesis conditions.

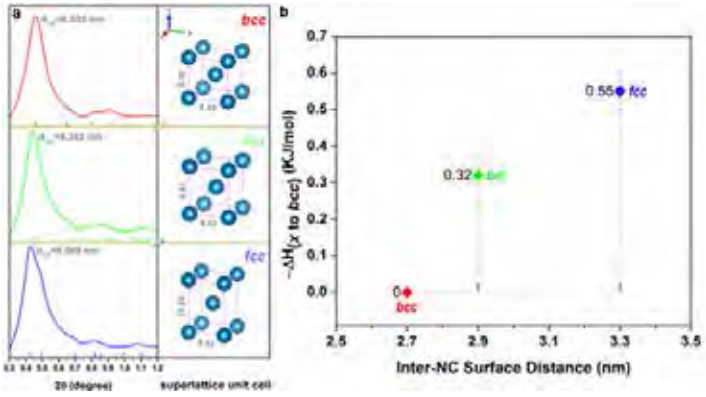

Figure 5. Three kinds of PbSe nanoparticle superstructures and their thermodynamic stability relations.

Other synchrotron X-ray scattering and calorimetry experiments

High-P SAXS/WAXS experiments of PbSe NC superlattices. We conducted in-situ high-P small-angle and wide-angle X-ray scattering experiments of PbSe nanoparticles with different sizes ranging from 3 to 10 nm and their assembled superlattices using DAC techniques. Depending on the size and/or shape of PbSe NCs, either a body-centered-cubic or face-centered-cubic superstructure is adopted. Two major results: First, we successfully prepared a series of nanostructures such as nanocube dimers and 1D nanorods/nanowires. Thus pressure tuning is an effective approach to produce novel types of nanoparticle mesostructures that are difficult to synthesize with conventional chemical methods. Second, the combined SXAS and WAXS measurements allowed examination of structural evolution, phase transformations and mechanical behavior of both PbSe nanocrystals (atomic-level) and their assembled architec-

tures (meso-scale) as a function of pressure.

SAXS/WAXS measurements of NaYF4 nanorod supercrystals. We successfully assembled NaYF4 nanorods into highly ordered supercrystals, in which both the atoms and nanoparticles have the same orientations. We have determined the 3D packing orientations and patterns of nanorods in the "single supercrystal" using synchrotron SAXS and WAXS with the goal of understanding the correlations between atoms and nanoparticles as well as resulting physical properties.

High-T calorimetric and SAXS/WAXS measurements of PbSe NC superlattices. Recently, we extended our calorimetric investigations of PbSe NC superlattices from room to elevated temperatures. Combined with high-T synchrotron X-ray scattering, the measurements revealed a thermally-induced phase transitions of PbSe NC superlattices from bcc to fcc. The combination of calorimetric with X-ray scattering measurements allowed correlation of the structural transition with its associated energetic change.

Impact on National Missions

The discovery of new materials that exhibit novel structures and emergent properties at high pressures provides a strong impetus for harvesting such materials at ambient conditions. Through the state-of-the-art synchrotron X-ray scattering and calorimetric measurements of series of lead chalcogenide, metal and other NC systems, we have determined the structural evolutions and transitions as a function of pressure or solvent type, and thermodynamic stability relations among various polymorphs for these nanoparticles and/or their assembled superlattices. More broadly, the obtained results have applications/implications for controlled nanoparticle synthesis and for design and fabrication of novel structured nanomaterials potentially with enhanced or newly emerging properties. In particular, the use of pressure enables systematic manipulation of the nanophases and their assembled architectures (e.g., interparticle spacing), thereby enabling tuning of their properties for specific applications. This research represents a new direction in high-pressure nanomaterials science with great potential for technological applications.

References

1. TOLBERT, S. H., and A. P. ALIVISATOS. HIGH-PRESSURE STRUCTURAL TRANSFORMATIONS IN SEMICONDUCTOR NANOCRYSTALS. 1995. ANNUAL REVIEW OF PHYSICAL CHEMISTRY. 46: 595.

2. Wu, , Bai, Sun, R. E. Haddad, D. M. Boye, Wang, and Fan. Pressure-Driven Assembly of Spherical Nanoparticles and Formation of 1D-Nanostructure Arrays. 2010. ANGEWANDTE CHEMIE-INTERNATIONAL EDITION. 49 (45): 8431.

3. Badding, J. V., J. F. Meng, and D. A. Polvani. Pressure tuning in the search for new and improved solid state materials. 1998. CHEMISTRY OF MATERIALS. 10 (10): 2889.

4. Quan, , Luo, Wang, Xu, Wang, Wang, and Fang. Pressure-Induced Switching between Amorphization and Crystallization in PbTe Nanoparticles. 2013. NANO LETTERS. 13 (8): 3729.

5. Whitesides, G. M., and B. Grzybowski. Self-assembly at all scales. 2002. SCIENCE. 295 (5564): 2418.

6. Quan, , and Fang. Superlattices with non-spherical building blocks. 2010. NANO TODAY. 5 (5): 390.

7. Quan, , Xu, Wang, Wen, Wang, Zhu, Li, C. J. Sheehan, Wang, Smilgies, Luo, and Fang. Solvent-Mediated Self-Assembly of Nanocube Superlattices. 2014. JOURNAL OF THE AMERICAN CHEMICAL SOCIETY. 136 (4): 1352.

8. Quan, , D. i. Wu, Zhu, W. H. Evers, J. M. Boncella, L. D. A. Siebbeles, Wang, Navrotsky, and Xu. Energy landscape of self-assembled superlattices of PbSe nanocrystals. 2014. In PROCEEDINGS OF THE NATIONAL ACADEMY OF SCIENCES OF THE UNITED STATES OF AMERICA. Vol. 111, 25 Edition, p. 9054.

Publications

Lu, , Yang, Quan, Lin, Bai, L. i. n. Wang, Huang, and Zhao. Enhanced Electron Transport in Nb-Doped TiO2 Nanoparticles via Pressure-Induced Phase Transitions. 2014. JOURNAL OF THE AMERICAN CHEMICAL SOCIETY. 136 (1): 419.

Quan, Z. W., Z. P. Luo, Y. X. Wang, H. W. Xu, C. Y. Wang, Z. W. Wang, and J. Y. Fang. Pressure-Induced Switching between Amorphization and Crystallization in PbTe Nanoparticles. 2013. NANO LETTERS. 13 (8): 3729.

Quan, Z., D. Wu, J. Zhu, W. H. Evers, J. M. Boncella, L. D. A. Siebbeles, Z. Wang, A. Navrotsky, and H. Xu. Energy landscape of self-assembled superlattices of PbSe nanocrystals. 2014. Proceedings of the National Academy of Sciences . 111 (25): 9054–9057.

Quan, Z., H. Xu, C. Wang, X. Wen, Y. Wang, J. Zhu, R. Li, C. Sheehan, Z. Wang, D. M. Smilgies, Z. Luo, and J. Fang. Solvent-mediated self-assembly of nanocube superlattices. 2014. J. Am. Chem. Soc.. 136 (4): 1352.

Wu, , T. M. McDonald, Quan, S. V. Ushakov, Zhang, J. R. Long, and Navrotsky. Thermodynamic complexity of carbon capture in alkylamine-functionalized metal-organic frameworks. 2015. JOURNAL OF MATERIALS

CHEMISTRY A. 3 (8): 4248.

Zhu, , Quan, Lin, Jiang, Wang, Zhang, Jin, Zhao, Liu, C. J. Brinker, and Xu. Porous Ice Phases with VI and Distorted VII Structures Constrained in Nanoporous Silica. 2014. NANO LETTERS. 14 (11): 6554.

NMR Study of Quantum States of Matter

Joe D. Thompson
20130780PRD1

Abstract

Quantum fluctuations that arise out of a zero-temperature magnetic transition, a magnetic quantum-critical point, are a promising candidate for the mechanism that creates unconventional superconductivity, one of the most intriguing of all quantum states of matter. Heavy-fermion materials, whose name comes from the heavy mass of their itinerant electrons, have emerged as prototypes for discovering new types of quantum-critical points and for exploring the relationship between quantum fluctuations and unconventional superconductivity that also is known to be hosted in materials based on plutonium. In this project, we have used nuclear magnetic resonance (NMR) to probe and understand quantum criticality in the heavy-fermion compound CeRhIn5, the nature of unconventional superconductivity in U2PtC2 and its possible relationship to quantum criticality, and the new heavy-fermion superconductor PuRhIn5, which is an isostructural Pu-analog of CeRhIn5. In addition, NMR studies have explored the effect of substituting Nd atoms for Ce in the quantum-critical heavy-fermion superconductor CeCoIn5 and to determine the magnetic ground state of (Me4N)2PuCl6. Progress in this project has advanced our understanding of the consequences of quantum fluctuations that emerge from a zero-temperature magnetic transition.

Background and Research Objectives

There are thousands of examples of a transition at finite temperature from a magnetically ordered state to a magnetically disordered state. At such a classical phase transition, thermal fluctuations due to the finite temperature environment drive the transition. But, it also is possible theoretically to have a transition from magnetically ordered to disordered states at absolute zero temperature where there are no thermal fluctuations. In this case the transition is driven solely by rules of quantum mechanics. There is a growing number of experiments suggesting that such a quantum-driven transition exists, but none of these examples can be explained completely with existing theory. Further, experiments during the last decade have found that an unconventional form of superconductivity tends to appear in the vicinity of a quantum-magnetic transition, but the possible relationship between quantum fluctuations at this zero-temperature transition and unconventional superconductivity remains an outstanding question. Nuclear magnetic resonance (NMR) is a particularly powerful microscopic probe of magnetism as well as of the nature of quantum fluctuations and their possible role in producing unconventional superconductivity.

Scientific Approach and Accomplishments

Nuclear magnetic resonance is most familiar in the context of magnetic resonance imaging (MRI) that is used to probe soft body tissue, but because the nuclei of atoms in a metal often have a spin like the nuclei of soft tissue, NMR also can be used to 'see what's inside' a metal and more importantly to determine at a microscopic level the nature of spins on electrons through their coupling to nuclear spins. Electrons and the spins that they carry are responsible for magnetic order that can be tuned by a non-thermal control parameter, such as an applied magnetic field, chemical composition or pressure, to absolute zero temperature. By analyzing NMR measurements it is possible to deduce microscopic properties of magnetic order, information about quantum-fluctuations of that order as its transition temperature is tuned to zero temperature and how electrons form superconductivity that appears in the vicinity of the zero-temperature magnetic boundary. Heavy-fermion materials, in which electron-electron interactions effectively increase the mass of electrons by a factor of 100 to 1000 times the mass of non-interacting electrons, are prototypes for discovering and understanding quantum states of matter, such as unconventional forms of superconductivity, and have been the focus of this research. In pursuing this research, this project has used the power of NMR to make new discoveries as well as to understand better the complex quantum states that can appear in heavy-

fermion materials, specifically U2PtC2, CeRhIn5, and PuRhIn5. In the following we highlight accomplishments from the study of these materials and more.

U2PtC2 has been known for nearly 30 years to be a superconductor below about 1.5K but the nature of the superconductivity has never been studied. NMR and NMR-Knight shift, a measure of the electron-spin response to a magnetic field, experiments were carried out on U2PtC2 at temperatures to 50 mK. The surprising conclusion from these experiments was that the superconductivity is highly unusual: superconducting electrons form with parallel spin alignment in contrast to the more typical antiparallel alignment. This discovery is one of the rare examples of equal spin-pairing superconductivity.[1] Additionally, analysis of the Knight shift showed that this unconventional superconductivity developed out of a state in which ferromagnetic correlations among electrons were particularly strong, raising the possibility that U2PtC2 is close to a ferromagnetic quantum-critical point. This possibility was supported by finding ferromagnetic order in samples of U2PtC2 where a small number of Pt (platinum) atoms were replaced by nickel (Ni).

During the course of this project, collaborators found evidence for two magnetic quantum-critical points in CeRhIn5 induced by magnetic fields of 35 and 50 T at atmospheric pressure. An interpretation of those discoveries requires assumptions about the nature of the magnetic order at these fields. Because NMR can detect the nature of the magnetic order, proposals were submitted to the National High Magnetic Field Laboratory in Tallahassee for NMR measurements to 30 T and at temperatures to as low as 300 mK. Those proposals were accepted and we carried out the proposed experiments under these very demanding conditions. The important conclusion is that a field of 30 T does not change the magnetic structure, but the ordered magnetic moment appears to have decreased by about 25 %. This result is consistent with the proposed interpretations that the field-induced quantum-critical states in CeRhIn5 involve both critical magnetic fluctuations and critical electronic degrees of freedom, a particularly interesting and unusual type of quantum criticality.

This unusual criticality also might be responsible for superconductivity that appears in CeRhIn5 as its antiferromagnetic transition temperature is tuned toward zero-temperature by applied pressure. Earlier experiments had suggested that magnetic order could be induced inside the superconducting state by an applied magnetic field. To test for this possibility, we used NMR measurements at pressures to 2 GPa (approximately 20,000 times atmospheric pressure), temperatures to 50 mK and magnetic fields to 12 T (approximately 200,000 times the earth's magnetic field) to search for field-induced magnetic order in the superconducting state of CeRhIn5. We found no evidence for the expected magnetic order, possibly because the coupling between nuclear and electronic spins changed from its value at atmospheric pressure and made NMR-detection of magnetic order impossible.

PuRhIn5 has exactly the same crystal structure as CeRhIn5 and also is a heavy-fermion material, but instead of ordering antiferromagnetically like CeRhIn5 at atmospheric pressure, it is superconducting near 1.5 K. Our NMR experiments on PuRhIn5 discovered that its superconductivity also is unconventional, so-called d-wave with zero net spin but finite orbital moment of superconducting electrons.[2] NMR measurements at temperatures above the superconducting transition were consistent with proximity of PuRhIn5 to an antiferromagnetic quantum-critical point. Indeed, similar measurements made on a sample in which a small number of In (indium) atoms were replaced by Cd (cadmium) found that superconductivity was replaced with antiferromagnetic order. It, therefore, seems likely that quantum fluctuations of antiferromagnetic order play an essential role in producing the unconventional superconductivity.

CeCoIn5 is an unconventional (d-wave) heavy-fermion superconductor at atmospheric pressure and its superconductivity is 'born' out of a quantum-critical state. Replacing 5% of the Ce (cerium) atoms by Nd (neodymium) to make Ce0.95Nd0.05CoIn5 induces magnetic order in the superconducting state; however, microscopic coexistence of the superconductivity and magnetism has yet to be determined. Alternating current (ac)-susceptibility measurements determined that the superconducting transition temperature is homogeneous throughout the material, indicating homogenously distributed Nd atoms. NMR measurements were performed on crystals of this compound at temperatures 1.5K to 295K and demonstrated that the normal state electrons behaved like local magnetic moments at sufficiently high temperatures. This is contrast to CeCoIn5 in which NMR indicated a quantum-critical state above the superconducting transition. This difference suggests that the Nd ions are removing some of the quantum fluctuations and in the process creating the unusual situation where magnetic order develops inside the superconducting state.

With interest in looking for an NMR signal from Pu (plutonium), we also pursued a search for this signal in the organic complex (Me4N)2PuCl6. Initial experiments in a sample with high abundance of the 239-isotope of Pu 239Pu, which is most desirable for NMR, showed several signals. To identify the nature of these signals, NMR was performed on a second sample with high 242Pu isotopic

abundance, an isotope that does not give an NMR signal. These experiments and simulation of NMR measurements identified the measured signals as coming from NMR of the Cl (chlorine) nuclei and not Pu. Once this was clarified, we could fully replicate the NMR data by theoretical calculations. These results, the first NMR experiments on this Pu-based material, will be published in the near future. [3]

Impact on National Missions

Unconventional superconductivity holds promise for exciting new energy and defense technologies, but how and where that superconductivity might appear cannot be predicted. Empirically, experiments have shown that this superconductivity frequently appears as a magnetic transition is tuned to zero temperature, but the nature of the quantum excitations and how they might induce superconductivity are major unanswered questions. Fundamentally new understanding of the mechanism of unconventional superconductivity and its possible relationship to quantum fluctuations is needed to be able to predict how and when superconductivity appears. With unconventional superconductivity also found recently in plutonium-based materials, superconductivity itself can be used to inform a much clearer perspective of states of matter than can arise from the electronic complexity of Pu. Using NMR to probe and understand novel quantum states of matter, this project has addressed DOE, Office of Science priorities called out in "Directing Matter and Energy: Five Challenges for Science and the Imagination," in particular addressed the the need for science that is required to discover, understand and control complex and collective forms of matter that exhibit novel properties and respond to environmental conditions, enabling the creation of materials with novel innate functionality.

References

1. Mounce, A. M., H. Yasuoka, G. Koutroulakis, N. Ni, E. D. Bauer, F. Ronning, and J. D. Thompson. Evidence for spin-triplet superconductivity in U2PtC2 from 195Pt NMR. 2015. Physical Review Letters. 144: 127001.

2. Koutroulakis, G., A. M. Mounce, H. Yasuoka, J. Mitchell, E. D. Bauer, and J. D. Thompson. Nuclear magnetic resonance study of unconventional superconductivity in PuRhIn5. Physical Review B.

3. Mounce, A. M., G. Koutroulakis, H. Yasuoka, J. Autschbach, K. A. Stosh, E. D. Bauer, J. D. Thompson, and D. L. Clark. Search for 239-Pu NMR in [(CH3)4N]2PuIVCl6. Physical Review B.

Publications

Koutroulakis, G., A. M. Mounce, H. Yasuoka, J. Mitchell, E. D. Bauer, and J. D. Thompson. A nuclear magnetic resonance study of the unconventional superconductor PuRhIn5. Physical Review B.

Mounce, A. M., G. Koutroulakis, H. Yasuoka, J. Autschbach, K. A. Stosh, E. D. Bauer, J. D. Thompson, and D. L. Clark. Search for 239-Pu NMR in [(CH3)4N]2PuIVCl6. Physical Review B.

Mounce, A. M., H. Yasuoka, G. Koutroulakis, N. Ni, E. D. Bauer, F. Ronning, and J. D. Thompson. Evidence for spin-triplet superconductivity in U2PtC2 from 195Pt NMR. 2015. Physical Review Letters. 144: 127001.

Electronic and Photonic Transport in Chiral Materials and Nanostructures

Diego A. Dalvit
20130781PRD1

Abstract

We have performed extensive studies of the spin physics and optical properties of 2D Dirac materials, which are atomically thin materials with elementary excitations governed by the Dirac equation. These include graphene, transition metal dichalcogenides, and topological insulators.

Background and Research Objectives

Chirality is prevalent in Nature. Certain molecules exhibit intrinsic optical chirality in which left-handed and right-handed circularly polarized light propagate differently. With the advent of metamaterials, optical chirality has been engineered in artificial systems allowing control of the photon polarization. Spin-orbit (SO) coupling in solids provides yet another important kind of chirality. In the last 20 years, research in SO coupling has been actively pursued in spintronics, and has recently led to the discovery of new classes of materials known as topological insulators and superconductors. Graphene and other newly identified 2D materials, on the other hand, also demonstrate a chiral property closely akin to SO coupling. Study of electronic and photonic chiral materials offers exciting opportunities for discovering interesting new physics and technologically important applications, including spintronics-based information processing, new material probe techniques, Casimir force repulsion, and tunable near-field radiative heat transfer.

Scientific Approach and Accomplishments

The Director funded postdoc associate Wang-Kong Tse has studied the spin dynamics and spin noise of 2D transition metal dichalcogenides in collaboration with T-4 staff members Nikolai Sinitsyn, Darryl Smith and Avadh Saxena. They derived the equations of motion for spin dynamics and spin noise, and developed a theory for optical observation of spin noise in these materials. A unique property that was discovered from our work is the emergence of valley noise due to the unique valley degrees of freedom in 2D Dirac materials. The work was published in the Physical Review Letters [1]. In connection with this work, they also collaborated with the experimental group of Scott Crooker at the High Magnetic Field Laboratory and expect continuing collaboration with theory and experiment. Wang-Kong has also initiated a study of excitonic effects on the optical properties of 2D transition metal dichalcogenides and work is in progress.

Wang-Kong studied the heat transfer in topological insulator systems in collaboration with T-4 staff member Diego Dalvit and external collaborator Pablo Rodriguez (U. Paris Sud, France). They developed a theory for the far field and near field radiative heat transfer between topological insulator surfaces, and discovered a simple power law for the near field heat transfer flux. The work was published as an invited article in the Special Issue on Casimir Physics of the Journal of Physics: Condensed Matter [2].

He has also collaborated with the experimental optics group of Prof. Peter Armitage at the Johns Hopkins University. He performed the theoretical analysis in conjunction with Armitage group's experimental Faraday effect measurements of topological insulators. They found an interesting magnetic field dependence on the transport scattering lifetime for electrons in topological insulators. The work was submitted to the Physical Review Letters [3] and review is in progress. Wang-Kong has also maintained an ongoing collaboration with Prof. Allan MacDonald at the University of Texas at Austin to study the D.C. Coulomb drag between graphene sheets in the quantum Hall regime. Preliminary results have been obtained and a draft of the manuscript for this work has been developed. This is a difficult problem because the interaction effects in quantum Hall systems are not easily amenable to precise quantitative description. Despite achieving considerable progress in this problem, there remain subtle issues that need further investigation and

understanding and work is ongoing in this problem. In addition, Wang-Kong has recently initiated a problem to study quantum friction and Coulomb drag with Diego Dalvit. He expects to maintain a collaboration with Diego to continue studying this problem after leaving from the lab.

Wang-Kong has mentored a Ph.D. student from University of Texas at Austin to study the renormalization of optical properties and plasmon properties in multilayer graphene systems due to electron-electron Coulomb interaction. They formulated a theory based on the quantum kinetic equation to take into account both the band-renormalization and excitonic effects on an equal footing. Their results show that there can be appreciable renormalization effects on the optical Drude weight and the plasmon frequencies in graphene systems, which was reported in the T-4 BLABS seminar.

He participated in grant proposal writing for one ER project and one DR project. The ER project proposal was written with Nikolai Sinitsyn and Scott Crooker, in which they proposed to expand the studies on spin and valley noise, the spin and valley dynamics of 2D transition metal dichalcogenides. The DR project was written with Houtong Chen, Diego Dalvit and Nikolai Sinitsyn in which they proposed to work on the optical properties of metamaterial heterostructures comprising metamolecules and Dirac materials. The DR project was finally funded.

Wang-Kong attended the 2014 and 2015 APS March meetings in which he delivered talks on “Spin and Valley Noise in Dirac materials” and “Nonlinear Optical and Excitonic Effects in Two-Dimensional Transition Metal Dichalcogenides”. In 2014, he visited the New York City College of Technology and delivered a talk on “Spintronics with Dirac electrons”. He delivered several internal talks at LANL: a CINT seminar on “Magneto-optical and Magneto-electric Effects in Topological Insulators”, a T-4 BLABS seminar “Many-body renormalization in Dirac Electronic Systems: Optical Properties”, and a T-4 BLABS seminar “Magneto-Coulomb drag in double-layer graphene”. He attended the LANL conferences “Information Science for Materials Discovery and Design” and “Mesoscale Science Frontiers”. In 2015, he visited and interviewed for faculty positions at the University of Delaware, Purdue University, University of Alabama, University of New Hampshire, and University of Massachusetts, where he delivered interview talks. He received an offer from the University of Alabama and gladly accepted the position. He will begin his new position in mid-August 2015.

Impact on National Missions

The research performed in this project made substantial progress in understanding the electronic and optical properties of chiral materials, and provided a strong theory support for the ongoing LANL programs at CINT on nanoscience and technology.

References

1. Tse, W. K., A. Saxena, D. L. Smith, and N. A. Sinitsyn. Spin and Valley Noise in Two-Dimensional Dirac Materials. 2014. Physical Review Letters. 113: 046602.

2. Rodriguez-Lopez, P., W. K. Tse, and D. A. R. Dalvit. Radiate Heat Transfer in 2D Dirac Materials. 2015. J. Phys.: Condens. Matter. 27: 214019.

3. Wu, L., W. K. Tse, M. Brahlek, C. M. Morris, R. Valdez Aguilar, N. Koirala, S. Oh, and N. P. Armitage. Observation of cyclotron resonance and electron-phonon coupling in surface states of bulk-insulating topological insulator Bi2Se3. Physical Review Letters.

Publications

Lopez, P. Rodriguez, W. K. Tse, and D. A. R. Dalvit. Radiate Heat Transfer in 2D Dirac Materials. 2015. Journal of Physics: Condensed Matter. 27: 214019.

Tse, W. K., A. Saxena, D. L. Smith, and N. A. Sinitsyn. Spin and Valley Noise in Two-Dimensional Dirac Materials. 2014. Physical Review Letters. 113: 046602.

Wu, L., W. K. Tse, M. Brahlek, C. M. Morris, R. Valdes Aguilar, N. Koirala, S. Oh, and N. P. Armitage. Observation of cyclotron resonance and electron-phonon coupling in surface states of bulk-insulating topological insulator Bi2Se3 . Physical Review Letters.

Alternating Positive-Negative Charge Systems: New Compounds and Synthetic Routes

David E. Chavez
20130788PRD2

Abstract

This report describes the preparation of 1-amino-1,2,3-triazole-3-oxide (DPX2) and its transformation to 1,2,3,4-Tetrazine-1-oxide. DPX-2 provides insight into a novel N-Oxide/N-Amino compounds, being the first energetic material in this class. The ability of this material to undergo a nitrene insertion forming 1,2,3,4-tetrazine-1-oxide was also studied, and evidence for this material, the first non-benzoannulated 1,2,3,4-tetrazine-1-oxide, is presented. The existence of both of these materials opens new strategies in energetic materials design. DPX2 was characterized chemically (Infrared, Raman, NMR, X-ray) and as a high explosive in terms of energetic performances (detonation velocity, pressure, etc.) and sensitivities (impact, friction, electrostatic). DPX-2 was found to possess good thermal stability and moderate sensitivities, indicating the viability of N-amino N-oxides as a strategy for the preparation of new energetic materials.

Background and Research Objectives

In the field of energetic materials chemistry a major challenge is to prepare extremely high performance materials while maintaining stability towards destructive stimuli such as heat or shock. These metastable materials offer unique insights into the factors affecting molecular stability [1,2] as a result of their lying on the borderline of existence and non-existence. Efforts such as these require a unique mix of theory and experimental work in order to fulfill practical requirements; how much energy can be packed into a molecule before it becomes too unstable for practical use [3]. Beyond this area, energetic materials research is also actively focused on novel energetic compounds and strategies for creating materials that possess reduced toxicological or environmental footprints.

At the forefront of energetics research are new synthetic strategies to impart unique energetic qualities to a molecule. Within energetic materials design, there are two broad categories of strategies to incorporate energetic properties in a molecule: conventional fuel/oxidizer strategies seen in explosives such as TNT (2,4,6-trinitrotoluene) or PETN (pentaerythritol tetranitrate) and high heat of formation compounds (ring strain, high-nitrogen content). While high heat of formation compounds display unique properties, increasing energy content by increasing nitrogen content can lead to explosive sensitivity and decrease in thermal stability. This can be seen when 1,1'-azobis(1,2,3-triazole) [4] and 1,1'-azobis(tetrazole) [3] are compared; the former can easily be handled, and the latter, despite only two CH groups being replaced by N, often spontaneously detonates during handling, and decomposes at a temperature over 100 oC lower. Additionally, highly strained compounds such as 1,3,3-trinitroazetidine or octanitrocubane have exceedingly long synthese times [5].

Strategies have been developed to stabilize high heats of formation compounds [6,7]. This can be achieved by tailoring both molecular shape as well as the addition of electron withdrawing substituents [8]. Perhaps the most striking effect of removal of electron density from a nitrogen system, thereby increasing stability, is through N-oxidation. 1,2,3,4-tetrazine-1,3-dioxide heterocycles are stable class of energetic compounds, often stable at temperatures above 200 oC [9], while only one, thermally labile, unoxidized 1,2,3,4-tetrazine ring system is known [10]. Beyond the stabilization of a nitrogen system by a N-oxide, the zwitterionic nature of this functional group leads to strong dipoles and intermolecular interactions which are known to stabilize energetic materials. 2,6-diamino-3,5-dinitro-1,4,-pyrazine-1-oxide is an example of such an explosive [11], and our recent work with nitrotetrazole, azidotetrazole, and bistetrazole oxides also confirm the ability of N-oxides to stabilize energetic nitrogen heterocycles [12-14].

Beyond N-oxides, N-amines have also demonstrated utility in energetic materials; the additional catenated

nitrogen atom increases the heat of formation and the NH2 unit is available for intermolecular interactions [15-16]. Molecules containing both N-oxides and N-amines on the same ring could be very high performing explosives [17-20]. Unfortunately the synthetic paths to N-amines and N-oxides often preclude them being on the same molecule, let alone the same heterocycle.

Scientific Approach and Accomplishments

In this work, we prepare the first energetic molecule containing both an N-oxide and N-amine on the same heterocyclic ring, by two distinct routes. The first route to the preparation of the new energetic material 1-amino-1,2,3-triazole-3-oxide (DPX2, 1) was via hypofluorous acid oxidation of 1-amino-1,2,3-triazole. An unoptimized procedure found that one equivalent of hypofluorous acid at -23 oC produced DPX2 (Figure 1). At higher temperatures the reaction of the hypofluorous acid appears to occur increasingly at the amine as opposed to the ring, resulting in loss of the amino group and formation of 1,2,3-triazole as identified by NMR and mass spectrometry. When increased equivalents of hypofluorous acid were used, oxidized and deaminated products were formed including triazole-1-oxide, as well as higher unknown oxidation products. Recrystallization of the desired material from nitromethane gave crystals suitable for diffraction. X-ray quality crystals of DPX2 were grown from nitromethane as the solvent. Single crystal X-ray analysis of DPX confirmed the molecular structure of the material and also showed that the compound has a density of 1.571 g cm-3 (Figure 2).

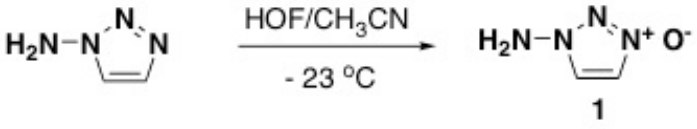

Figure 1. DPX-2 (1) was first synthesized through the use of the very powerful oxygen transfer reagent hypofluorous acid (HOF). The reaction proceeds to provide numerous oxidation products of 1,2,3-triazole, including (1). This product represents the first example of an energetic materials containing both N-oxide and N-amino moities in the same molecule. This combination of energetic functional groups may lead to novel explosive performance and safety properties and will serve as the basis for the study of future materials in this class of energetic materials

The thermal stability of DPX-2 was also determined using differential scanning calorimetry, which showed that the material was stable up to 210 oC, which is comparable to many existing conventional energetic materials. The heat of formation of DPX-2 was calculated to be 286.1 kJ/mol. With this data in hand, we next sought to determine how sensitive DPX-2 was towards destructive stimuli such as impact, electrostatic discharge, and friction. The experimental sensitivities are 8.5 Joules towards impact and 192 N towards friction,(slightly less sensitive than RDX) and insensitive toward electrostatic discharge. These results indicate that the novel energetic N-amino/N-oxide combination is capable of forming energetic materials that are not overly sensitive to mechanical or thermal stimuli, both important for the design of new explosives and thus confirming that this new energetic material strategy is viable and highly promising.

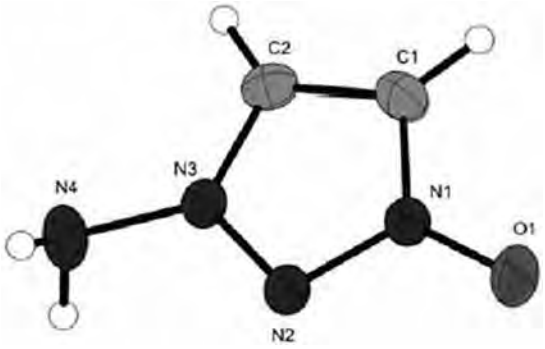

Figure 2. In order to confirm the molecular structure of , crystals suitable for x-ray crystallographic analysis were grown from nitromethane solvent. This figure confirms our proposed structure and displays the molecule as it appears in the crystal structure. Non-H atomic displacement ellipsoids are 50% probability.

With DPX-2 in hand we sought new routes to produce the material. In an alternate route, 1-(benzyloxy)-1,2,3-triazole was aminated with tosylhydroxylamine (THA) producing 1-amino-3-(benzyloxy)-1,2,3-triazolium tosylate. This molecule was then reduced without purification with hydrogen (Pd/C catalyst) giving the target compound (Figure 3).

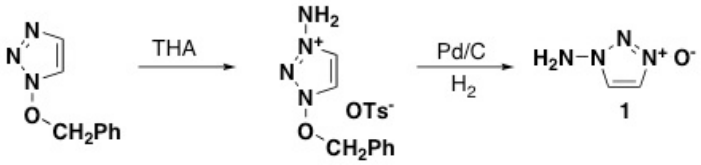

Figure 3. An alternate synthesis route to DPX-2 (1) was pursued as the original process was low yielding. In this alternate route, 1-(benzyloxy)-1,2,3-triazole was aminated with tosylhydroxylamine (THA), to provide the N-amino intermediate. This intermediate compound was converted to DPX-2 (1) using hydrogen gas in the presence of a palladium catalyst. Although this route requires two steps, it is more efficient than the original process to prepare DPX-2 (1).

In attempting to purify the 1-amino-3-(benzyloxy)-1,2,3-triazolium tosylate to obtain a crystal structure we observed loss of the NH¬2 protons by nuclear magnetic resonance, a shift in the remaining two protons and additional shifts in the carbon spectrum to 129.2 and 119.4 ppm. Mass spectrometry studies indicated that the produced material was two mass units lighter than the DPX-2. We suspected

spontaneous nitrene formation and ring expansion, forming the previously unknown 1,2,3,4-tetrazine-1-oxide (2). This result was verified by pursuing a deliberate route to produce 2 (Figure 4).

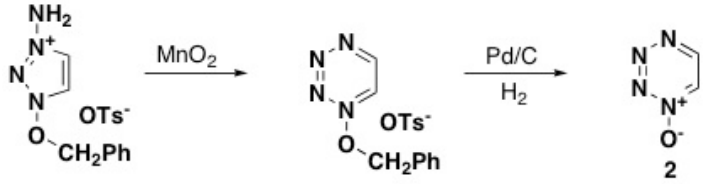

Figure 4. Our work proceeded toward the synthesis of the 1,2,3,4-tetrazine-1-oxide (2) using the route displayed in Figure 4. Synthesis route to 1,2,3,4-Tetrazine-1-Oxide (2). The first step involved a nitrogen insertion reaction using manganese dioxide as the oxidizing reagent to provide the desired 1,2,3,4-tetrazine oxide ring system. This intermediate has a protecting group on the N-oxide however and required removal to attain the desired compound (2). Removal of the protecting group using hydrogen gas in the presence of a palladium catalyst provided the desired compound, the first example of a non-fused 1,2,3,4-tetrazine-oxide compound.

This work is both the first non-annulated 1,2,3,4-tetrazine-1-oxide reported, as well as a new route to 1,2,3,4-tetrazine-1-oxides via the nitrene insertion of a 1-amino-1,2,3-triazole-3-oxide. Attempts to oxidize it to the 1,2,3,4-tetrazine-1,3-dioxide, providing a new route to this energetically-useful system have so far not been fruitful. We are currently attempting to obtain a crystal structure of the 1,2,3,4-tetrazine-1-oxide. Further attempts to convert 1 to 2 directly are currently ongoing.

In conclusion, we have prepared and characterized the first energetic N-amino-N-oxide-substituted heterocycle, using two routes to synthesize 1-amino-1,2,3-triazole-3-oxide from 1-amino-1,2,3-triazoles by hypofluorous acid oxidation, or from the amination of 1-(benzyloxy)-1,2,3-triazole followed by debenzylation. This unique energetic material possesses no undo sensitivities towards impact, friction, or thermal stimuli, and confirms the potential utility of our strategy in energetics design. Additionally, we have prepared 1,2,3,4-tetrazine-1-oxide, the first non-benzoannulated member of this class of compounds, using an approach that has not been utilized previously to reach this class of compounds.

Impact on National Missions

This work will have a direct impact on energetic materials for the future within the weapons program. The work has shown that the strategy of N-Amino/N-oxide functionalized molecules can lead to interesting new molecular structures and energetic materials that are stable and safe to work with. Additionally, our work has shown that, while still challenging, new routes to alternating positive and negative charge (ANPC) materials are possible, opening up new potential strategies to access these novel materials for use in numerous applications within the weapons program.

References

1. Klapoetke, T. M., and J. Stierstorfer. The CN7 Anion. 2009. Journal of the American Chemical Society. : 1122.

2. Huynh, M. H. V., M. A. Hiskey, D. E. Chavez, and R. D. Gilardi. Synthesis, Characterization and Energetic Properties of Diazido heteroaromatic High-Nitrogen C-N compound. 2005. Journal of the American Chemical Society. : 12537.

3. Klapoetke, T. M., and D. G. Piercey. 1,1'-Azobis(tetrazole): A Highly Energetic Nitrogen-Rich COmpound with a N10 Chain. 2011. Inorganic Chemistry. : 2732.

4. Li, Y. -C., C. Qi, S. -H. Li, H. -J. Zhang, C. -H. Sun, Y. -Z. Yu, and S. -P. Pang. 1,1'-Azobis-1,2,3-triazole: A High-Nitrogen Compound with Stable N8 STructure and Photochromism. 2010. Journal of the American Chemical Society. : 12172.

5. Zhang, M. -X., P. E. Eaton, and R. D. Gilardi. Hepta- and Octanitrocubanes. 2000. Angewandte Chemie International Edition. : 401.

6. Inagake, S., and N. Goto. Nature of Conjugation in Hydronitrogens and Fluoronitrogens. Excessive Flow of Unshared Electron Pairs Into Single Bonds. 1987. Journal of the American Chemical Society. : 3234.

7. Kalinin, A. V., E. T. Apasov, S. L. Ioffe, and V. A. Tartakovsky. N-nitrohydrazines and their Salts. 1991. Bulletin of the Academy of Science USSR Division of Chemical Science (English Translation). : 988.

8. Klapoetke, T. M., C. Petermayer, D. G. Piercey, and J. Stierstorfer. 1,3-Bis(nitroimido)-1,2,3-triazolate Anion, the N-Nitroimide Moiety, and the Strategy of Alternating Positive and Negative Charges in the Design of Energetic Materials. 2012. Journal of the American Chemical Society. : 20827.

9. Churakov, A. M., and V. A. Tartakovsky. Progess in 1,2,3,4-Tetrazine Chemistry. 2004. Chemical Reviews. : 2601.

10. Kaihoh, T., T. Itoh, T. K. Yamaguchi, and A. Ohsawa. First Synthesis of a 1,2,3,4-Tetrazine. 1988. Chemical Communications. : 1608.

11. Gokcinar, E., T. M. Klapoetke, and A. J. Bellamy. Computational Study on 2,6-Diamino-3,5-dinitropyrazine and its 1-Oxide and 1,4-Dioxide Derivatives. 2010. Journal of Molecular Structure: THEOCHEM. : 18.

12. Fischer, N., D. Fischer, T. M. Klapoetke, D. G. Piercey, and J. Stierstofer. Pushing the Limits of Energetic Materials - the Sythesis and Characterizations of Dihydroxylammonium 5,5'Bistetrazole-1,1'-diolate. 2012. Journal of Materials Chemistry. : 20418.

13. Gobel, M., K. Karaghiosoff, T. M. Klapoetke, D. G. Piercey, and J. Stierstorfer. Nitrotetrazolate-2N-oxides and the Strategy of N-Oxide Introduction. 2010. Journal of the American Chemical Society. : 17216.

14. Klapoetke, T. M., D. G. Piercey, and J. Stierstorfer. The Taming of CN7: The azidotetrazolate-2-oxide Anion. 2011. Chemistry a European Journal. : 13068.

15. Klapoetke, T. M., D. G. Piercey, and J. Stierstorfer. Amination of Energetic Anions: High-Performing Energetic Materials. 2012. Dalton Transactions. : 9451.

16. Klapoetke, T. M., D. G. Piercey, and J. Stierstorfer. The 1,3-Diamino-1,2,3-triazolium Cation: A Highly Energetic Moiety. 2013. European Journal of Inorganic Chemistry. : 1509.

Publications

Chavez, D. E., D. G. Piercey, S. Hemisch, C. Kirst, T. M. Klapoetke, and J. Stierstorfer. An energetic N-oxide and N-amino heterocycle and its transformation to 1,2,3,4-tetrazine-1-oxide. 2015. Propellants, Explosives, Pyrotechnics. : 491.

Chavez, D. E., T. M. Klapoetke, D. A. Parrish, D. G. Piercey, and J. Stierstorfer. The synthesis and energetic properties of 3,4-bis(2,2,2-trinitroethylamino)furazan. 2014. Propellants, Explosives, Pyrotechnics. : 641.

Microstructured Biohybrid Synthesis of Photosynthetic Assemblies

Gabriel A. Montano
20130796PRD2

Abstract

This project was focused on developing novel photonic materials that mimic the complex processes of light-harvesting and energy transfer in biological photosynthesis through materials self-assembly. Our approach was inspired by the most archaic of photosynthetic species, photosynthetic bacteria. First, we use solvent exchange strategies to generate amphiphilic polymer nanocomposites that demonstrate simple, two-component, light-harvesting assemblies that exhibit morphology-dependent energy transfer efficiency. We extended our solvent exchange process to generate polymer nanocomposites that structurally and functional mimic one of the most efficient biological light-harvesting complexes known, the chlorosome of green bacteria. Finally, we create a supramolecular energy landscape consisting of artificial chlorosome donors and planar, polymer membrane embedded acceptors. Our described results indicate the potential of amphiphilic polymers in generating modular, dynamic photonic materials using simple materials approaches.

Background and Research Objectives

Photosynthesis is the most prolific biological process on the planet with net primary production of biomass exceeding 100 Gt C yr-1. Photosynthetic organisms use complex and regulated multichromophore assemblies, called light-harvesting (LH) antennas, to capture, concentrate and direct solar radiation to reaction centers that then carry out concomitant chemistry. Nature's LH antennas are remarkable, operating with high efficiency in fluctuating environmental and photic conditions through nanoscale precision thus, serving as inspiration in material design. LH antennas are diverse in structure and chromophore composition, but have ubiquitous function: to provide a network of light-absorbing molecules that move electronic excitation energy to a "trap" that catalyzes endergonic electron transfer. Biological systems have accumulated structural complexity through evolution and natural selection necessary for biological systems that obfuscates the key design principles for optimizing solar light harvesting in artificial systems. Bio-inspired LH-materials should possess the desirable properties of biological systems such as efficiency without necessarily mimicking the atomic level details of most natural antenna systems. In this work, we proposed to replicate the function and efficiency of biological light-harvesting complexes using self-assembly approaches that are dictated by the natural propensities of amphiphilic copolymers to self-assemble in solution into membrane-like materials (micelles, bilayers, and monolyaers).

Our objectives were to 1)demonstrate efficient, modular light-harvesting and energy transfer in amphiphilic polymer nanocomposites through self-assembly, and 2) develop supramolecular photonic nanocomposites that rival biological light-harvesting structure/function relationships.

The goal of our work was to develop methods that allow for predicting and designing photonic nanocomposites that rival biological light-harvesting in function and efficiency, but completely through self-assembly of materials.

Scientific Approach and Accomplishments

Our approach in this effort was to build upon previous research in our laboratory that found short-chain amphiphilic block copolymers (Poly(ethylene oxide)-block-poly(butadiene) (PEO-b-PBD) are capable of forming micelles in solution and monolayer or bilayers on solid supports of thickness similar to biological membranes (~4-5 nm for bilayers) [1]. In this work, we exploit the thickness of these self-assembled polymer structures to induce the organization of chromophores in a manner that allows for efficient energy transfer between donor and acceptor molecules.

Polymer Nanocomposites for efficient light-harvesting

and energy transfer: Our initial strategy for developing photonic nanocomposites was based upon the self-assembly of PEO-b-PBD in solution to form micelles and subsequent bilayers. We introduced two chromophores, a donor (Bodipy-labeled lipid) and acceptor bacteriochlorin (BC-116), that have energy overlap favorable for Förster resonance energy transfer (FRET) and naturally self-assembled with the polymer micelles via solvent exchange. Since the bodipy dye is anchored to the lipid, it is expected to anchor close to the interface of the amphiphilic polymers. Similarly, the BC-116 is amphiphilic in nature, thus is also thought to anchor to the interface of the two polymer blocks. Thus, by intentional design using amphiphilic chromophores, we allow self-assembly to localize our molecules in proximity to one another for energy transfer (Figure 1). Thus, our resultant structures should exhibit the two necessary characteristics for FRET, being energetically matched to transfer energy and in close enough proximity to one another to transfer energy. We found that energy transfer efficiency was dependent upon the amount of quencher molecule (BC116) added to the sample and independent of donor, which is consistent with previous theories of energy transfer in photosynthesis. Micelles exhibiting a maximum energy transfer efficiency (ETE) of >65% were observed (Figure 1). In this result, the polymer plays two important roles: 1) it provides the nanoscale framework necessary to keep the chromophores in close enough proximity for energy transfer and, 2) the amphiphilic nature provides the chemical structure necessary to organize the amphiphilic chromophores without and secondary type of coordination.

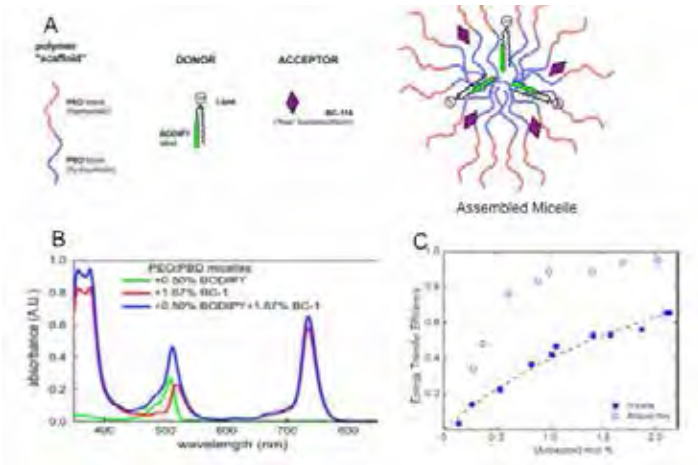

Figure 1. A. Components and structural assembly of photonic polymer micelle nanocomposites. B. Absorption spectrum showing micelles of the bodipy donor (green) and BC-116 acceptor (red) chromophores and micelles containing both species (blue). C. Plots of Energy transfer efficiencey in micelles (solid circles) and bilayer films (open circles) as a function of acceptor concentration. Dotted line is a theoretical fit of micelle data indicating an ability to predict and design photonic response.

In addition to miceller nanocomposites, we tested the propensity of PEO-b-PBD to spontaneously form monolayer/bilayer films on solid supports. Indeed, polymers containing our donor-acceptor chromophores formed monolayer/bilayer supports that exhibited ETE greater than 95% (Figure 1). These structures rival the ETE of natural photosynthetic light-harvesting complexes and do so completely through self-assembly of materials. Further, understanding the mechanisms that control ETE allows for design of photonic response and potential of modular behavior [2].

Polymer Chlorosome Nanocomposites (PCNs): Our work in this area was predicated upon the propensity for pEO-b-pBD to form micelles in solution. One of the most archaic yet efficient light-harvesting complexes known is the chlorosome of green photosynthetic bacteria. Chlorosomes are supramolecular structures containing 10-100's of thousands of bacteriochlorophyll (BChl) c (d,e, or f), which are self-assembled through H-bonding and π- π stacking interactions, and are bounded by a single membrane leaflet containing lipid and proteins (Figure 2).

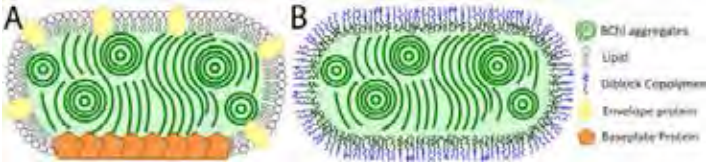

Figure 2. Model organization in natural and nanocomposite systems. In natural chlorosomes (A), a single membrane leaflet containing lipids and protein provides a hydrophobic environment for BChl c aggregation in the interior. Chlorosomes are attached to the cytoplasmic membrane through the baseplate protein that contains BChl a and serves as a mediator of energy transfer from BChl c in the chlorosome interior and BChl a in the membrane associated photosystem. The interior of the chlorosome also contains carotenoid molecules that aid light harvesting as well as photoprotection (not shown). (B) In the nanocomposite, the lipid and protein envelop of the natural system is replaced by an amphipathic diblock copolymer.

This organization scheme is starkly dissimilar to all other LH antennas where intricate protein coordination of chromophores is a requisite. Chlorosomes have considerable BChl concentration that results in effective harvesting of photonic energy while also being efficient at transferring energy to BChl a existing as a baseplate light-harvesting complex in the monolayer membrane of the chlorosome and to subsequent membrane-associated acceptors. From a biomaterials perspective, the spectroscopic and physical attributes of chlorosomes and the green bacteria LH system are very attractive, in particular the predominantly self-assembled nature of the system. Because pEO-b-pBD has a propensity to form micelles in solution, we attempted to use the micelle interior as a potential reservoir to

allow for organization of Bchl c to form functional mimics of chlorosome. Through our work, we found that we were capable of generating structural/functional mimics of chlorosomes of long-range order (Figure 3) [3].

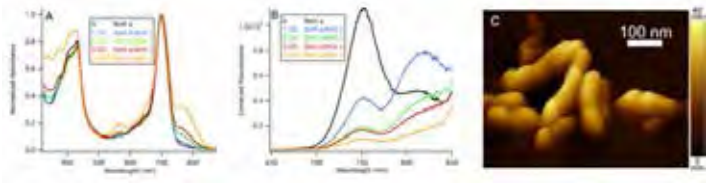

Figure 3. Spectral properties of PCNs containing additional chromophores. (A) Absorbance spectra of PCNs containing additional amounts of Bchl . Additions of Bchl result in a shoulder centered at ~790 nm. (B) Fluorescence emission spectra of samples containing Bchl . (C)- AFM topograph of PCNs. Data are displayed in 3D and demonstrate chlorosome-like morphology of PCNs.

Again, these nanocomposite structures were formed through solvent exchanged self-assembly allowing for modular control of composition in a scalable process. In addition, we were able to add additional chromophores such as Bchl a and carotenoid while retaining chlorosome function that resulted in supramolecular energy transfer. The generation of PCN's is significant for several reasons. Firstly, prior to these results, it had been speculated that some level of coordination via protein-interactions in native chlorosomes was necessary to generate the type of long-range order observed. Our results demonstrate that by providing a suitable environment, long-range order of the Bchl c molecules will happen spontaneously. Secondly, the Bchl a present in chlorosomes that serves as an energy acceptor from Bchl c is thought to do so in the form of a protein-pigment highly ordered structure called the baseplate. Our results suggest that protein is 1) unnecessary to induce the spectral properties observed by Bchl a in the baseplate and 2) self-assembly of Bchl a in PCNs is sufficient to obtain Bchl c-a ETEs observed in biological assemblies. This does not necessarily mean that the Bchl a observed in native chlorosomes is not in the form of a baseplate structure, but simply that such a structure is unnecessary to replicate similar function in PCNs.

Multimembrane Supramolecular Energy Transfer: In an attempt to mimic the type of complex to complex energy transfer observed in biological photosynthesis, we generated three-dimensional photonic-assemblies based upon the above described systems [3]. First, we adhered PCNs to a hydrophilic substrate. Next, we added a solution of pBD-b-pEO polymer micelles containing an energy acceptor (fluorescent dye 1,1'-Dioctadecyl-3,3,3',3'-Tetramethylindotricarbocyanine Iodide (DiR)) molecule to create polymer bilayers. This process results in multi-membrane assemblies capable of performing supramolecular energy transfer in a model that is structurally similar to biological assemblies, however again, is completely through self-assembly. A schematic representation of our assembly can be observed in Figure 4. We then utilized a technique called HyperSpectral Imaging (HSI) to determine ETE of our nanocomposite assemblies. HSI allows one to deconvolve the components contributing to fluorescence observed at any given pixel thus, in the case of our system, allowing us to determine if contribution from an energy donor (PCN) contributes to the fluorescence of an energy acceptor (membrane-DiR) (Figure 4). Our resultant nanocomposites exhibit ~55% energy transfer, [3] which is exceptional considering it is a proof of principle concept that has not been optimized for efficiency.

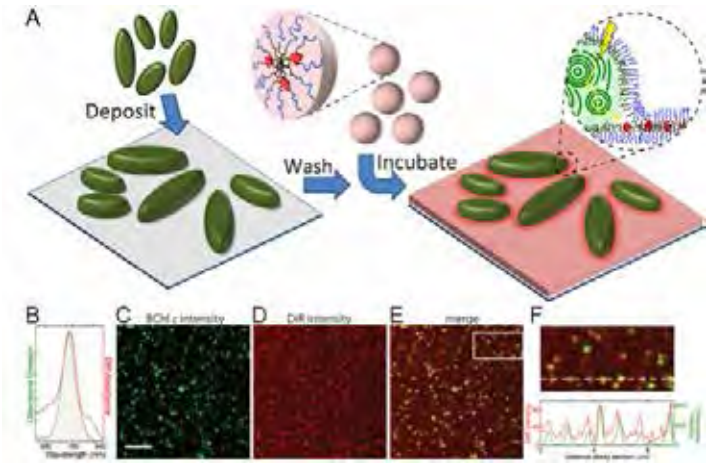

Figure 4. Three dimensional energy transfer in a spatial-energetic landscape. (A) Representation of the assembly process. PCNs are drop cast on hydrophilic glass and become immobilized on the substrate. The sample is then washed to remove loosely-bound PCNs and then backfilled with PEO-b-PBD micelles containing DiR acceptor chromophores. PEO-b-PBD forms a continuous bilayer film between and around the deposited PCNs. With selective excitation in to BChl c, emission from DiR is observed demonstrating energy transfer. (B) Spectral overlap of PCN emission (green) and DiR absorbance (red). The data have been normalized to the peak of each trace and the overlap region is shaded. (C-E) fluorescence images showing the distribution and location fluorescence intensity from PCNs (C) and DiR (D) and the merged image (E). The images are scaled from zero to maximum intensity within the image. (F) Zoomed in view of the boxed area in (E) along with the intensity profile of the PCN and DiR components along the indicated line. The scale bar in (C) represents 5 μm.

Ultimately, the results of this project demonstrate the potential of generating modular photonic assemblies based upon amphiphilic block copolymers. There are significant advantages to the systems described herein to natural systems: 1) all of our approaches are based upon self-assembly and thus overcome many of the limitations

of more synthetically arduous approaches: namely, our approach is quick and modular, scalable and inexpensive; 2) the use of amphiphilic polymers allows for functional/dynamic response as it is possible to include functional groups in polymer design that can be exploited by changes in the polymer environment. In addition, our designs have significantly added to the understanding of organization in chlorosomes, indicating that long-range order and morphology and coupling of energy donor/acceptors is not dependent on proteins of the chlorosome, but can instead be induced by providing the proper environment such as the pEO-pBD micelle. Together, the results of our project significantly advance the criteria for designing polymer membrane nanocomposites for photonic applications.

Impact on National Missions

The work performed in our project directly addresses laboratory missions in energy security and controlled functionality of materials. We have simplified the process of photosynthetic light-harvesting and energy transfer to its basic principles, removing the intricate coordination observed in most previous attempts and in nature itself. Our materials are simple, modular and efficient, all of which are goals of next-generation photonic materials. In addition, the information gained on polymer self-assembly and polymeric assembly of components can be utilized for other materials applications such as sensor design or responsive membrane systems allowing for design and control of emergent behavior of polymer nanocomposites.

References

1. Goertz, M. P., L. E. Marks, and G. A. Montano. Biomimetic Mono layer and Bilayer Membranes Made From Amphiphilic Block Copolymer Micelles. 2012. ACS NANO. 6 (2): 1532.

2. Adams, P. G., A. M. Collins, Sahin, Subramanian, V. S. Urban, Vairaprakash, Tian, D. G. Evans, A. P. Shreve, and G. A. Montano. Diblock Copolymer Micelles and Supported Films with Noncovalently Incorporated Chromophores: A Modular Platform for Efficient Energy Transfer. 2015. NANO LETTERS. 15 (4): 2422.

3. Collins, Aaron M., Jerilyn A. Timlin, Stephen M. Anthony, and Gabriel A. Montano. Polymer-dependent, self-assembled nanocomposites that structurally and functionally mimic green bacterial antenna complexes . Nature Communications.

Publications

Adams, P. G., A. M. Collins, Sahin, Subramanian, V. S. Urban, Vairaprakash, Tian, D. G. Evans, A. P. Shreve, and G. A. Montano. Diblock Copolymer Micelles and Supported Films with Noncovalently Incorporated Chromophores: A Modular Platform for Efficient Energy Transfer. 2015. NANO LETTERS. 15 (4): 2422.

Collins, A. M., G. A. Montano, Y. M. Tian, J. Duque, and T. Sahin. Block Copolymers for Responsive, Energetic Nanocomposite Membrane Assemblies. 2014. In 58th Annual Meeting of the Biophysical Society. (San Francisco, Feb. 15-19, 2014). , p. 420A. Cambridge, MA: Cell Press.

Broken Symmetries in Superconductors

Albert Migliori
20130813PRD4

Abstract

Broken symmetries lie at the heart of almost all modern physics problems — from the broken rotational and translational symmetries in magnets to the rather subtle gauge symmetry breaking in electro-weak theory (the Higgs mechanism) and superconductivity. Sometimes the symmetry breaking is known to exist, yet its form remains a mystery. Two good examples of this are the hidden-order in URu2Si2, and the pseudogap in high-temperature cuprate superconductors. Both problems are grand challenges in condensed-matter physics. We developed new high-field transport techniques, and improved the resonant ultrasound spectroscopy capabilities at LANL, to tackle these challanges.

Background and Research Objectives

The high temperature superconductor YBa2Cu3O6+x (YBCO) has been at the centre of many important results in condensed matter physics research, including measurement of the London penetration depth and determination of the Fermi surface by quantum oscillation measurements. Despite these and other achievements over the past 22 years, the fundamental nature of the physics in the pseudogap region of the cuprate (materials with copper-oxygen planes) phase diagram remains a mystery, even though it is now increasingly evident that it is paramount to understanding high temperature superconductivity (high-Tc) in these materials. While the breaking of both rotational and time reversal symmetry has been observed at the pseudogap onset temperature T* in neutron scattering experiments, thermodynamic evidence for a phase transition has yet to be measured. The experimental difficulty is that T* ranges from near 150 K to more than 300 K in underdoped YBCO: at these temperatures, signals from typical thermodynamic probes such as specific heat are dominated by phononic contributions. Another important question in the cuprates is how this pseudogap state and the small carrier pockets evolve with hole doping into the large Fermi surface seen in overdoped cuprates such as Tl2Ba2CuO6+x. Understanding high-Tc is closely linked to understanding how a strongly correlated Mott insulator evolves into a Fermi liquid.

In this research we employed resonant ultrasound spectroscopy (RUS), which measures the resonant vibrational frequencies in a crystal to better than part-per-million accuracy. Since the elastic moduli connect directly to the thermodynamics of the system, small changes in the state of the system can be detected, even at high temperatures4, allowing T* to be measured across the phase diagram. Further, the analysis of which elastic modes are coupled to the phase transition gives information about the symmetry breaking at T*.

A second research goal was to employ ultra-high magnetic field transport to map out the Fermi surface of the high-Tc superconductor YBa2Cu3O6+x. Using the unique capabilities at LANL, specifically the 100 T non-destructive magnet, we proposed to map out the Fermi surface in the underdoped pseudogap regime, providing complementary information to what was learned in the RUS experiments.

Scientific Approach and Accomplishments

Dr. Albert Migliori, a pioneer in the field of RUS, has a well-established group at Los Alamos National Labs (LANL). Prior to Dr. Ramshaw's arrival, preliminary measurements by his group on YBCO single crystals showed discontinuities in the sound propagation coefficients as a function of temperature, with features showing up at T*. One of the goals of this project was to complete these measurements and publish them.

Concurrent with the RUS experiments, Dr. Ramshaw worked with Dr. Neil Harrison, performing high field quantum oscillation measurements on YBCO. The recent development of the 100 Tesla pulsed field at LANL allowed them to measure quantum oscillations in YBCO at dopings higher than were previously possible, bridg-

ing the gap between the overdoped and the underdoped Fermi surface measurements. Quantum oscillation measurements of the electron effective mass and Fermi surface size nicely complemented the RUS projec.

We succeeded in publishing results on both of these main goals. Shekhter et al. Nature (2013) (see attached publication list) reports on a thermodynamic transition into the pseudogap state in both the underdoped and near-optimal doped regions of the phase diagram. Ramshaw et al. Science (2015) shows the evolution of the cyclotron effective mass and Fermi surface area in underdoped YBa2Cu3O6+x, and found a strongly enhanced electron effective mass—indicative of a quantum-critical point near optimal doping. In collaboration with other LANL scientists, we used our newly-enhanced RUS capabilities to measure the heavy-Fermion superconductor PuCoGa5 (see Ramshaw et al. Proceedings of the National Academy of Science (2015)). We discovered valence fluctuations in this material, and found that they are likely the driver of the unusually high superconducting transition in this material.

A number of other publications were completed as well, particularly relating to pulsed-field measurements on high-Tc superconductors (See publication list).

Impact on National Missions

The study of the cuprates and heavy Fermions has always pushed the envelope of experimental techniques–scanning tunnelling microscopy and angle resolved photoemission are but two examples with broad applications–Dr. Ramshaw's advancements during this project further our ability to perform RUS on small samples, and to perform high-precision transport in magnetic fields approaching 100 T. Mapping the effective mass of YBCO across phase diagram furthers our understanding of how these complicated materials become high-Tc superconductors. The study of PuCoGa5¬ provides insight into the unusual valence of plutonium—a material that is directly related to the core missions of LANL.

Publications

Doiron-Leyraud, , Badoux, S. R. de Cotret, Lepault, LeBoeuf, Laliberte, Hassinger, B. J. Ramshaw, D. A. Bonn, W. N. Hardy, Liang, J. -. Park, Vignolles, Vignolle, Taillefer, and Proust. Evidence for a small hole pocket in the Fermi surface of underdoped YBa2Cu3Oy. 2015. NATURE COMMUNICATIONS. 6.

Grissonnanche, , Cyr-Choiniere, Laliberte, S. R. de Cotret, Juneau-Fecteau, Dufour-Beausejour, M. -. Delage, LeBoeuf, Chang, B. J. Ramshaw, D. A. Bonn, W. N. Hardy, Liang, Adachi, N. E. Hussey, Vignolle, Proust, Sutherland, Kraemer, J. -. Park, Graf, Doiron-Leyraud, and Taillefer. Direct measurement of the upper critical field in cuprate superconductors. 2014. NATURE COMMUNICATIONS. 5.

Harrison, , B. J. Ramshaw, and Shekhter. Nodal bilayer-splitting controlled by spin-orbit interactions in underdoped high-T-c cuprates. 2015. SCIENTIFIC REPORTS. 5.

Ramshaw, B. J., Day, Vignolle, LeBoeuf, Dosanjh, Proust, Taillefer, Liang, W. N. Hardy, and D. A. Bonn. Vortex lattice melting and Hc2 in underdoped YBa(2)Cu(3)Oy. 2012. PHYSICAL REVIEW B. 86 (17).

Ramshaw, B. J., S. E. Sebastian, R. D. McDonald, Day, B. S. Tan, Zhu, J. B. Betts, Liang, D. A. Bonn, W. N. Hardy, and Harrison. Quasiparticle mass enhancement approaching optimal doping in a high-T-c superconductor. 2015. SCIENCE. 348 (6232): 317.

Ramshaw, B. J., Shekhter, R. D. McDonald, J. B. Betts, J. N. Mitchell, P. H. Tobash, C. H. Mielke, E. D. Bauer, and Migliori. Avoided valence transition in a plutonium superconductor. 2015. In PROCEEDINGS OF THE NATIONAL ACADEMY OF SCIENCES OF THE UNITED STATES OF AMERICA. Vol. 112, 11 Edition, p. 3285.

Shekhter, , B. J. Ramshaw, Liang, W. N. Hardy, D. A. Bonn, F. F. Balakirev, R. D. McDonald, J. B. Betts, S. C. Riggs, and Migliori. Bounding the pseudogap with a line of phase transitions in YBa2Cu3O6+delta. 2013. NATURE. 498 (7452): 75.

Hybrid Metal-Semiconductor Nanostructures for Optimized Photosynthetic Algal Growth

Jennifer A. Hollingsworth
20130816PRD4

Abstract

Our aim has been to develop approaches for increasing algal growth by way of a novel materials strategy. Namely, we sought to develop quantum dots (QDs) and hybrid nanoscale constructs that could efficiently color-shift solar light to the wavelengths most effectively utilized by algae for growth and algal-oil production. Moreover, we pursued QD materials that would be stable and would easily incorporate into a hydrogel framework, where the hydrogel beads would serve as the "vessels" in which algae would be grown (concept captured in patent application: 14/170,400). We further aimed to establish the nanomaterial-design principles for realizing high-performance QD and hybrid QD-metal or QD-antenna structures most useful for effective light-conversion processes.

Background and Research Objectives

Fuels derived from biomass are a promising source of energy. Cultivating aquatic microalgae in open ponds can generate large quantities of biomass, and recently, Sayre et al. showed a remarkable enhancement in algal growth inside hydrogel polymer beads. Further improvements in hydrogel-confined algae growth rely on efficient light utilization. Photosynthesis is facilitated by absorption of blue and red solar photons by chlorophyll, but green photons are transmitted. Our aim has been to develop approaches for increasing algal growth by way of "optically activating" hydrogel beads using fluorescent inorganic quantum dots (QDs) and, possibly, metal nanoparticles (MNPs) that exhibit surface plasmon resonance (SPR) peaks overlapped with QD absorption or emission. These nanoparticle inclusions would color-shift incident sunlight to wavelengths useful for photosynthesis (UV to blue, green to red), and, further, screen algal cells from damaging UV radiation.

The intrinsic optical properties of single-domain QD and MNP nanoparticles can be finely tuned by controlling particle size and shape. In addition, the controlled placement and connectivity of these functional nano-building blocks can give rise to synergistic "emergent" inter-particle interactions and properties. Thus, beyond addressing technical challenges facing algal fuels development, the proposed effort was also conceived to advance the development of functional materials-by-design, taking advantage of the postdoc's previous work in establishing a synthetic framework for constructing multi-domain hybrid nanoparticles. His, as well as other, synthetic strategies for nanoscale architectures-by-design were applied to the synthesis of novel, functional core/shell optical nanomaterials. Furthermore, in the context of creating truly hybrid, multi-component structures, strategies other than solution chemical synthesis were ultimately explored as more direct routes to "mixed-system" nanostructures. Specifically, we adapted scanning probe "direct-write" techniques to place QDs onto three-dimensional nanoscale antenna/plasmonic structures, where the resulting hybrid systems are anticipated to afford similar enhancement of QD photoluminescence properties as realized in QD-MNP couples.

Scientific Approach and Accomplishments

Early in the project, the postdoc became most interested in the "multi-domain" aspect of QD hetero-structures, i.e., how within nominally a single nanostructure, it is possible to incorporate complexity to evoke emergent behavior through effects brought about by internal nanoscale interfaces. He pursued novel chemistry and photophysical properties of multi-domain structures in the form of core/multi-shell QD systems. The emphasis was on new non-toxic compositions for best compatibility as color-converting phosphors in algae production. Specifically, he investigated indium phosphide (InP) QDs as core materials. Although not ideal for the algal-sensitization application, he determined that CdS-coated InP nanoparticles produced the unprecedented property of dual suppressed-blinking emission. As a result of its remarkable behavior, this system was explored in collaboration with researchers in MPA-CINT, C-IIAC and

Vanderbilt University. The approach aimed to understand the underlying mechanism for both dual emission and dual-color blinking suppression by combining results from time-resolved photoluminescence (ensemble and single-nanostructure), transient absorption, imaging and elemental mapping, and correlating these results with known synthetic experimental conditions. With respect to synthesis, numerous surface treatments were applied prior to addition of the outer layers of CdS that caused dual emission to either "turn on" or "turn off." From this correlated study, we were able to ascertain the design parameters for achieving dual emission and for obtaining the remarkable stability associated with non-blinking behavior for both emitted colors (red and infrared). In this way, the work as implications for the realization of other multi-domain nanostructures possessing designed properties.

The postdoc also explored a new approach to synthesis. As a first user of our custom automated-reactor system, he investigated our initial choice for the optically active nanoparticle for incorporation into hydrogel polymer beads -- the ultrastable CdSe/CdS core/thick-shell QD. His approach was to establish a better understanding of the colloidal growth conditions that support fabrication of high-performance hierarchical nanostructures. In so doing, he discovered that reproducibility in QD structure and performance could be significantly enhanced by controlling the quality of the core/shell interface, e.g., by careful handling of the cores prior to shell growth and by controlling precursor addition at the shell-solvent interface. The latter ultimately entailed manipulating QD-QD dipole-dipole interactions to minimize the impact of particle assembly on the shell growth process, controlling precursor rate of addition, optimizing the growth temperature for shell addition, and choosing a core QD that affords minimal interfacial defects upon epitaxial shell growth. These insights are proving invaluable as we move forward with applications of this material system in other light-conversion applications, including solid-state lighting.

Two approaches to creating QD-plasmonic/antenna assemblies were attempted -- self-assembly from solution and directed assembly using a scanning probe direct-write nanolithography system. The principal focus using the postdoc's novel non-blinking infrared QD building blocks was the latter, as the antenna structure was theoretically predicted to provide enhancement in the infrared, while metal-shell synthetic hybrids developed in our lab (to date) are better overlapped with visible-emitting QDs. Namely, the postdoc synthesized stable, non-blinking near-infrared emitting QDs with and without a silica spacer/protective layer. Through a collaboration and with the postdoc's guidance, these QDs were developed into liquid "inks." The inks were loaded onto atomic force microscopy tips and subsequently written onto pre-fabricated substrates, including 3D nanoscale dielectric antenna, for which enhancements in radiative rates and control of emission direction are expected.

In summary, the postdoc will be a co-author on two journal publications (down-conversion QDs for solid-state lighting and near-infrared non-blinking QDs for direct-placement on optical antenna) and first-author on one journal publication (novel dual-suppressed blinking QDs). Additional collaborative publications are also expected to result from his work. Also significantly, he made significant contributions to capabilities that will impact ongoing research in MPA-CINT, including in the area of advanced nanomaterial manufacturing, while the materials he explored are now well suited for application as down-conversion (color-converting) materials in optically enhanced algal production.

Impact on National Missions

DOE (basic and applied, EERE), DoD, NASA and NSF have all funded open or internal programs in algal biofuels, where NASA also aims to use the technology to treat wastewater. DHS has reported on the potential impact that a successful biofuels program could have on addressing both national economic and environmental/energy security needs. Thus, it is now broadly recognized that algal biofuels development will be a key component in our future energy profile. To this end, the project aimed to work with leading algal biofuels experts in further enhancing the efficacy of algal production. In doing so, it helped to establish a novel materials strategy for optimizing light utilization by algae, namely, an approach based on optically functionalizing a hydrogel algal growth matrix with QDs and MNPs. At the same time, the postdoc developed novel optical nanomaterials (see accomplishments) and worked with others on new approaches to creating hybrid semiconductor-nanoparticle/dielectric-antenna 3D constructs using direct-write techniques. In this way, the effort contributes directly to DOE Basic Science initiatives, relevant to Mesoscale Science, Additive (Advanced) Manufacturing, and the Scientific Discovery and Innovation Mission in the Basic Understanding of Materials. Importantly, the effort forges new expertise at the interface between materials chemistry/physics and bioscience.

Publications

Buck, M. R., A. M. Dennis, H. M. Nguyen, H. Htoon, and J. A. Hollingsworth. Simultaneous near-infrared and visible photoluminescence with suppressed blinking from type-II InP core/shell nanocrystal quantum dots. Presented at 248th American Chemical Society Meeting, Fall, 2014. (San Francisco, August 10-14, 2014).

Buck, M., A. M. Dennis, F. Wang, H. M. Nguyenm, J. L.

Casson, M. Sykora, H. Htoon, and J. A. Hollingsworth. Dual-color suppressed blinking in InP/CdSe/CdS core/shell/shell giant quantum dots. Nano Letters (in preparation).

Dawood, F., C. J. Sheehan, M. R. Buck, A. M. Dennis, N. Karan, I. Staude, J. Dominguez, G. S. Subramania, A. R. James, I. Brener, N. A. Amro, and J. A. Hollingsworth. Direct Placement of Colloidal Nanocrystal Quantum Dots on Three-Dimensional Nanostructured Dielectric Antenna by Dip-Pen Nanolithography. ACS Nano.

Hanson, C. J., M. R. Buck, K. Acharya, J. A. Torres, J. Kundu, X. Ma, S. Bouquin, C. E. Hamilton, H. Htoon, and J. A. Hollingsworth. Giant Quantum Dots: Matching Solid-State to Solution-Phase Photoluminescence Performance for Near-Unity Down-Conversion Efficiency. 2015. ACS Applied Materials and Interfaces . 7: 13125.

Ultrafast Measurements of Emergent Magnetism in New Complex Oxide Materials

Scott A. Crooker
20140657PRD1

Abstract

Strontium titanate (SrTiO3) is a foundational material in the emerging field of complex oxide electronics. While its electronic, optical, and lattice properties have been studied for decades, this non-magnetic semiconductor has recently become a renewed materials research focus catalyzed by the surprising discovery of magnetism and superconductivity at interfaces between SrTiO3 and other non-magnetic semiconducting oxides. The formation and distribution of oxygen vacancies, which donate two electrons for every one vacancy, is widely thought to play an essential but as-yet-incompletely understood role in these observations. Recent signatures of magnetization in gated bulk SrTiO3 have further galvanized interest in the emergent properties of this material.

Background and Research Objectives

To better understand how magnetization is created in these nominally non-magnetic complex oxide materials, we originally proposed to build and use an ultrafast pulsed pump-probe system in the National High Magnetic Field Laboratory (NHMFL) optics lab. In this experiment, wavelength-tunable light pumps the sample with circularly polarized pulses and probes it with linearly polarized light. In a Time-Resolved Faraday Rotation (TRFR) scheme, a magnetic field is applied to a semiconductor perpendicular to the direction of the light. The pump photo generates short-lived spins that are initially polarized along the direction of the pump beam, which then precess about the applied magnetic field. Because the spin precession, as well as the excited spin relaxation, alters the polarization of the linear probe light as a function of time between the pump and probe pulses, the spin relaxation dynamics can be measured by monitoring the probe polarization.

A consistent theme in this work was to establish a new, powerful, general-purpose ultrafast capability for elucidating the picosecond-timescale dynamics of magnetization in new magnetic materials of interest to materials science efforts at Los Alamos. We expected to develop experimental tools (based on ultrafast pulsed lasers) that allowed us to "watch" -- in real time -- how magnetization develops and decays in so-called new "complex oxide materials" such as strontium titanate (SrTiO3) and related compounds. Specifically, we planned to build and establish the technique of Time-Resolved Faraday Rotation (TRFR), which is an all-optical method using polarized pulsed of light that allows one to measure how magnetization develops on the timescale of atomic interactions: millionths of millionths of seconds.

Scientific Approach and Accomplishments

Director's-funded postdoc William Rice had a very successful postdoctoral appointment at the NHMFL in Los Alamos, with important papers published in high-impact scientific journals (see reference list). As originally proposed, he successfully established a fully-operational capability for measuring magnetization dynamics on picosecond timescales using the optical technique of Time-Resolved Faraday Rotation (TRFR). Bill used this new capability to measure the optically-induced magnetization in magnetically-doped semiconductor nanocrystals for the first time. He wrote a paper on his data that was accepted at the journal Nature Nanotechnology.

Prior to this, Bill's work on the static magnetic properties of strontium titanate was successfully published in Nature Materials.

Additionally, as part of these magneto-optical studies, Bill also published a paper in the Journal of Physical Chemistry Letters.

The TRFR capability established by Bill is now in constant use to study other material systems such as the new atomically-thin semiconductors as represented by MoS2, and is proving to be a valuable tool for materials science here at LANL.

Impact on National Missions

This project has established Laboratory capabilities in the areas of Materials Science, Emergent Phenomena, and Materials-by-Design, and also in novel measurement methods that enable new scientific discovery at LANL. It is based on the very recent discovery of a new Emergent Phenomena: optically induced magnetization in complex oxide materials. Our approach for developing ultrafast optical methods to time-resolve magnetization dynamics with sub-picosecond resolution goes well beyond the specific example of strontium titanate that were investigated here and is applicable to a wide range of new materials in general, such as semiconductor nanocrystals for optoelectronic applications (see results above). The experimental techniques (ultrafast optical studies based on Time-Resolved Faraday Rotation) that we developed as part of this project will advance new Laboratory capabilities that underpin a wide variety of Laboratory missions related to Materials Science and Controlled Functionality in Materials.

Publications

Rice, W. D., J. D. Thompson, P. Ambwani, C. Leighton, and S. A. Crooker. Revealing optically induced magnetization in SrTiO_3 using optically-coupled SQUID magnetometry and magnetic circular dichroism . 2014. Journal of Vacuum Science and Technology B. 32: 04E102.

Rice, W. D., McDaniel, V. I. Klimov, and S. A. Crooker. Magneto-Optical Properties of CuInS2 Nanocrystals. 2014. JOURNAL OF PHYSICAL CHEMISTRY LETTERS. 5 (23): 4105.

Rice, W. D., S. A. Crooker, P. Ambwani, C. Leighton, J. D. Thompson, G. Haugstad, and M. Bombeck. Persistent optically-induced magnetization in oxygen-deficient strontium titanate . 2014. Nature Materials. 13: 481.

Rice, W. D., W. Liu, T. A. Baker, N. Sinitsyn, V. Kilmov, and S. A. Crooker. Revealing giant internal magnetic fields due to spin fluctuations in magnetically-doped colloidal nanocrystals. To appear in Nature Nanotechnology.

Shock-Driven Material Dynamics Investigated by Ultrafast X-ray Diffraction

Cynthia A. Bolme
20140680PRD3

Abstract

The basic physical properties that dominate a material's behavior under dynamic compression are frequently governed by the material's response on the scale of the atomic lattice. Traditionally, shock compression research has relied upon measurements of the material's density and sound speed to deduce the lattice level response of the material. The recent advent of high brilliance x-ray sources (third generation synchrotrons and x-ray free electron lasers) has enabled the ability to directly probe the lattice level response of materials during shock compression. The Linac Coherent Light Source at SLAC National Laboratory was used to investigate the kinetics and mechanisms of deformation of shock compressed fused silica using x-ray diffraction. The fused silica underwent a transition from amorphous to the crystalline stishovite phase. This x-ray diffraction data was analyzed and a journal manuscript was submitted for publication.

Background and Research Objectives

Understanding the fundamental processes which dictate basic physical properties such as strength, elasticity, plasticity and the kinetics of phase transformations/ crystallization or recrystallization requires studies at the relevant length-scales (e.g., interatomic spacing and grain size) and time-scales (e.g., phonon period). Information about these processes is important for physics and chemistry, as well as applied sciences – geophysics and materials science as well as industry. Shock compression is an excellent platform for studying phase transformation kinetics and changes in microstructure (to see deformation mechanism) because the nearly instantaneous stress loading provides a fiducial from which to measure the material response. Until now, due to the challenges of performing destructive shock wave experiments, direct observation of the material structure during transformation has been difficult or impossible to resolve. The Linac Coherent Light Source (LCLS) at SLAC National Laboratory is unique in the world in that it has a dynamic compression driver (nanosecond optical laser) to generate high pressure-temperature conditions and the highest available x-ray flux, which can be used to probe the structure. We studied the shock driven process of crystallization from an amorphous phase in fused silica to gain new insight into crystallization processes on the scale of the atomic lattice.

Scientific Approach and Accomplishments

We analyzed laser shock driven experimental data that was collected in situ during the shock event on fused silica. The experimental data included laser velocimetry and x-ray diffraction using the x-ray free electron laser at the LCLS. By varying the laser pulse and peak power, the pressure and temperature conditions in the material were tuned to examine the change in the nucleation and growth kinetics of the stishovite grains. We completed data analysis of these crystallization kinetics, and we submitted a journal manuscript for review. We also applied for future LCLS beam time to examine strength in materials at high pressure.

Impact on National Missions

This project furthered our understanding about how to perform shock compression experiments with the unique x-ray characteristics provided by an x-ray free electron laser. Specifically, we improved our knowledge about x-ray diffraction experiments in the complicated regime involving non-crystalline (amorphous or liquid) states. Work like ours builds capability for the proposed MaRIE signature facility.

This project also yielded knowledge about the rate of crystalline grain growth in the transformation of amorphous fused silica into crystalline stishovite. This information is the subject of the journal manuscript resulting from this project and adds to our basic understanding of materials.

Publications

Gleason, A. E., C. A. Bolme, H. J. Lee, B. Nagler, E. Galtier, D. Milathianaki, J. Eggert, J. Hawreliak, D. Fratanduono, R. G. Kraus, G. W. Collins, W. Yang, and W. L. Mao. Ultrafast visualization of crystallization and grain growth in shock-compressed SiO2. Nature Communications.

Nuclear and Particle Futures

Illuminating the Origin of the Nucleon Spin

Ivan M. Vitev
20130019DR

Introduction

Nucleons (protons and neutrons) are not fundamental constituents of matter, but are instead made up of quarks and gluons, the elementary particles of the strong interaction. There is compelling experimental evidence that the sum of the quark and gluon intrinsic angular momenta only contributes ~1/3 of the total proton spin. Thus, the majority of the proton spin is unaccounted for, which has been referred to as the "proton spin crisis". The missing fraction of the spin is likely carried by the orbital angular momentum of the quarks and gluons. The long-term goal of this project is to develop the experimental capability to measure the spin of the proton in terms of contributions from the spins of the quarks, gluons and their orbital angular momentum. An equally important goal is to understand the relative significance of these spin contributions in the theory of strong interactions, Quantum Chromodynamics (QCD), and how they manifest them-selves in reactions with polarized proton beams and/or targets. To this end, we will determine the momentum distribution of quarks inside the proton, transverse to the proton momentum, from which one can deduce whether quark orbital motion contributes significantly to the proton spin.

To determine the distribution of quarks and gluons within a nucleon, we will construct a polarized target to install in Fermiab E906 experiment and carry out the world's first measurement of the production of two simultaneous leptons (electrons or muons) from a polarized proton target bombarded by a high-energy proton beam. From a detailed analysis of the azimuthal distribution of such di-leptons, one can deduce properties of the polarized nucleon structure. In particular, we will measure both the sign and magnitude of the quark Sivers distribution, which is expected to be zero if the quarks have no orbital angular momentum.

Benefit to National Security Missions

This work is central to the FY13, FY14 LDRD Strategic Investment Plan of Nuclear and Particle Futures. Building upon our existing strategic partnership with Fermilab (E906, MiniBoone and LBNE), this project will strengthen our fundamental science capabilities, bring new high-luminosity polarized target technology to LANL and provide a "major physics thrust to follow current commitments to RHIC". This project will maintain LANL's leadership position in the field of spin physics and produce the world's most accurate polarized Drell-Yan measure-ment in proton-proton reactions. Our project is a timely and direct response to the DOE Mile-stone (HP13) to "test unique QCD predictions for relations between single-spin phenomena in p-p scattering and those observed in deep-inelastic scattering". We anticipate that this LDRD project will result in DOE Office of Science funding for a LANL-lead spin physics program at Fermilab. Our integrated experimental and theoretical program will allow us to lead in a major advance in understanding the polarized nucleon structure through the only U.S.-based dedicated polarized DY experiment. Providing a polarized target to FNAL will greatly enhance Fermilab's capabilities and provide a much needed user facility for spin physics. Our target will also be able to polarize ND3, thus enabling one to extend the spin physics to polarized neutrons. Furthermore, developing and testing particle detector technology at high luminosity will directly benefit MaRIE, a LANL institutional priority. This detector development is also of fundamental importance to nuclear detection for applied missions like nuclear nonproliferation. Such detectors often operate in a high background environment.

Progress

Experimental: We presented an update of the experiment to the Fermilab Program Advisory Committee in January, with a new budget. We have started to collaborate with FNAL on the necessary changes to the experiment. We met with the FNAL leadership to discuss the support we will need from FNAL. Developed new beam line design with new optics. performed the acceptance

tests of the magnet at Oxford after reorientation of coils and refurbishing of the system. Magnet performed flawlessly, we took new field homogeneity data, and shipped the magnet to UVa. The refrigerator has been refurbished and leaks have been fixed. The refrigerator is ready for system tests in July. We had a high level meeting with the nuclear physics (NP) program manager from DOE office of science to discuss future funding needs, and collaboration between DOE NP and Fermilab.

We designed and manufactured first prototype of the target ladder and target cells. The nuclear magnetic resonance (NMR) VME-system first prototype is currently in testing mode and will go in production after it has been debugged. The large ROOTS pumping system has been setup and is in the process of being tested at the Lujan center before being shipped to Fermilab. The slow control system for the polarized target has been designed.

Theoretical: We investigated for the first time the role of gluons in generating the single transverse spin asymmetry. Through such a study, we understand better how gluon's transverse momentum is correlated with the proton's transverse spin. We derived the next-to-leading order transverse momentum-weighted Sivers asymmetry in semi-inclusive deep inelastic scattering (SIDIS) – those contributions from the so-called three-gluon correlation functions. Such a study provides a way to connect the quark and gluon's transverse motion, i.e., through QCD evolution of the relevant quark-gluon as well as three-gluon correlation functions. We will further generalize such a study to Drell-Yan production, which could help make more reliable prediction for spin asymmetry for our experiment.

Lee and collaborators D. Kang (LANL) and O.Z. Labun (Arizona) completed a paper on the first proof that the soft function for thrust distributions in Drell-Yan (DY), Deep Inelastic Scattering (DIS), and electron-positron (e+e-) collisions are equal up to two-loop order (second order in the strong coupling alpha_s). With existing known results on the two-loop e+e- soft function, this is the first two-loop result for the DIS and DY soft functions, and makes possible up to NNNLL accuracy in predictions for all three types of cross sections. This paper has been submitted to Physics Letters B and is under review. Labun will visit T-2 this summer to collaborate with Lee on the definition, computation, and evolution of TMDPDFs in SCET using the rapidity renormalization group.

Quasi-parton distribution functions (PDFs) are new theoretical objects, which could be computed directly on the lattice, and will approach the standard PDFs in the large proton momentum Pz. Since taking the $P_z \to \infty$ limit is not feasible in lattice simulations, it is essential to provide guidance for what values of Pz the quasi-PDFs are good approximations of standard PDFs. Within the framework of the spectator diquark model, we evaluate quark's quasi-PDFs and standard PDFs. We find that, for intermediate parton momentum fractions x, quasi-PDFs are good approximations to standard PDFs (within 20-30%) when $P_z \geq 1.5$-2 GeV. On the other hand, for large $x \sim 1$ much larger $P_z > 4$ GeV is necessary to obtain a satisfactory agreement between the two sets. This study provides useful guidance for our lattice team in simulating PDFs on the lattice.

The calculations of Sivers and Boer-Mulders functions have been completed on two ensembles with different lattice actions to study discretization errors. We find that both the domain wall and clover discretization schemes, which have very different chiral properties, give consistent results at pion masses of about 300 MeV. These results are being written up and will be presented at the Lattice 2015 International Conference. We are now developing and testing the all-mode-averaging technique to improve the statistical signal which is necessary to extend these calculations to lighter pion masses and higher momenta.

Future Work

Experiment: Following a successful test of the superconducting magnet at University of Virginia (UVa) in FY15, the magnet and power supply will be shipped to Fermilab (FNAL) and installed in the FNAL test area. The complete nuclear magnetic resonance (NMR) and microwave systems will be tested at UVa, then shipped to FNAL and installed. We will irradiate the frozen ammonium (NH3) target material, test a sample at UVa and transfer it to FNAL. The ROOTS He pumping system will be moved to FNAL, assembled, tested and installed. UVa will complete any remaining work on the two target ladders and test them in house. After testing, the liquid He refrigerator and target ladders will be sent to FNAL. A complete set of software for slow controls and data acquisition for the polarized target system will be developed and tested. In collaboration with FNAL we will design and build a cryogenic system, which will be installed in the Seaquest area.

Theory: We will perform a global analysis of the spin-averaged cross sections for both semi-inclusive deep inelastic scattering (SIDIS) and Drell-Yan (DY) production, as well as the spin-dependent cross sections (Sivers asymmetry) for SIDIS. We will promote our previous study to next-to-next-to-leading-log (NNLL) accuracy and make prediction of the DY Sivers asymmetry in the kinematics of our experimental set-up. In lattice QCD, we will develop and test the all-mode-averaging technique to improve the statistical signal which is necessary to extend calculations to lighter pion masses and higher momenta and carry out simulations

on a new set of clover configurations being generated at lighter pion mass and closer to the continuum limit. In on the one-loop computation of Transverse Momentum Distributions in Soft Collinear Effective Theory using the rapidity regulator and the rapidity renormalization group to compute their evolution to NLL accuracy and beyond.

Conclusion

Through a synergy between theory and experiment, we will make a fundamental advance in our understanding of the origin of the nucleon spin. In a strategic partnership with Fermilab, we will construct a polarized target to carry out the world's most accurate measurement of di-lepton production from a polarized proton target bombarded by a high-energy proton beam. We will develop state-of-the-art theoretical and computational tools necessary to interpret the experimental results that will directly lead to a major breakthrough in our understanding of the structure of matter and the theory of strong interactions.

Publications

Almeida, L., C. Lee, S. Ellis, I. Sung, G. Sterman, and J. Walsh. Comparing and counting logs in direct and effective methods of QCD resummation. 2014. Journal of High Energy Physics. 1404: 174.

Dai, L., Z. Kang, A. Prokudin, and I. Vitev. Next-to-leading order transverse momentum-weighted Sivers asymmetry in semi-inclusive deep inelastic scattering: the role of the three-gluon correlator . To appear in Physical Review D.

Echevarria, M.. QCD Evolution of the Sivers Asymmetry. 2015. In QCD Evolution Workshop 2014. (Santa Fe, NM, 12-16 May, 2014). , p. 1560025. Singapore: World Scientific.

Echevarria, M., A. Idilbi, Z. Kang, and I. Vitev. QCD Evolution of the Sivers Asymmetry . 2014. Physical Review D. 89: 074013.

Engelhardt, M., B. Musch, T. Bhattacharya, R. Gupta, P. Hagler, A. Schaefer, S. Syritsin, and B. Yoon. Nucleon transverse momentum-dependent parton distributions from domain wall fermion calculations at 297 MeV pion mass . 2015. In 32nd International Symposium on Lattice Field Theory (Lattice 2014). (Brookhaven, NY, June 23-28, 2014). , p. 23. Trieste23: SISSA.

Gamberg, L., Z. Kang, I. Vitev, and H. Xing. Quasi-parton distribution functions: a study in the diquark spectator model . 2015. Physics Letters B. : 112.

Jian, X.. Single Spin Asymmetries of Inclusive Hadrons Produced in Electron Scattering from a Transversely Polarized 3He Target. 2015. In QCD Evolution Workshop. (Santa Fe, NM, 12-16 May 2014). , p. 1560067. SIngapore: World Scientific.

Kang, D., O. Labun, and C. Lee. Equality of hemisphere soft functions for e+e-, DIS and pp collisions at O(alphas**2). 2015. Physics Letters B. 748: 45.

Kang, Z.. Single transverse spin asymmetries in polarized SIDIS and pp scattering. Invited presentation at The 5th Workshop of the APS Topical Group on Hadronic Physics. (Denver, 10-12 April 2013).

Kang, Z.. Nucleon spin: longitudinal, transverse, and evolution. Invited presentation at 2014 RHIC and AGS Annual Users Meeting. (Upton, NY, 17-20 Jun. 2014).

Kang, Z.. Advances in the determination of TMDs from global analysis. Invited presentation at E1039/E906 Collaboration Meeting. (Santa Fe, NM, February 11-13, 2015).

Kang, Z.. TMD evolution and global analysis. Invited presentation at The 6th Workshop of the APS Topical Group on Hadronic Physics. (Baltimore, MD, April 8-10, 2015).

Kang, Z.. Transverse single spin asymmetry of the W production at RHIC. Invited presentation at 2015 RHIC and AGS Annual Users Meeting. (Upton, NY, June 9-12, 2015).

Kang, Z. B., I. Vitev, and H. X. Xing. Transverse momentum-weighted Sivers asymmetry in semi-inclusive deep inelastic scattering at next-to-leading order. 2013. PHYSICAL REVIEW D. 87 (3): -.

Klein, A.. An Experiment to Measure the Sivers Asymmetry of the Sea Quarks. 2015. In QCD Evolution Workshop. (Santa Fe, NM, 12-16 May, 2014). , p. 1560064 . Singapore: World Scientific.

Klein, A.. Drell Yan at FNAL with a Polarized Target. Invited presentation at DNP Fall Meeting. (Waikoloa, HI, 6-11 Oct. 2014).

Klein, A.. The status of the polarized target and E1039. Invited presentation at Fermilab PAC Meeting. (Batavia, IL, January 2015).

Klein, A., P. McGaughey, and I. Vitev. Letter of Intent for a Drell-Yan experiment with a polarized proton target. 2013. Fermilab PAC .

Kleinjan, D.. A polarized Drell-Yan experiment at Fermilab. Invited presentation at CIPANP2015. (Vail, CO, 19-24 May 2015).

Kleinjan, D., and A. Klein. A Polarized Drell-Yan experiment to probe the dynamics of the nucleon sea. Invited presentation at Diffraction 2014. (Primošten (Croatia), 10-15 Sept. 2014).

Lee, C.. QCD Resummation: Comparing Direct and Effective Methods. Invited presentation at Boston Jet Workshop. (Boston, MA, 21-23 Jan. 2014).

Lee, C.. Comparing and Counting Logs in Direct and Effective Methods of Resummation. Invited presentation at SCET 2014. (Munich, Germany, 24-26 March, 2014).

Lee, C.. The Evolution of Soft-Collinear Effective Theory. 2015. In QCD Evolution Workshop. (Santa Fe, NM, 12-16 May, 2014). , p. 1560045. Singapore: World Scientific.

Lee, C.. Towards High Precision Resummation and Evolution Using SCET. Invited presentation at E1039/ E906 Collaboration Meeting. (Santa Fe, Feb. 2015).

Lee, C.. Direct and Effective Methods of QCD Resummation. Invited presentation at Loopfest XIII. (New York, 18-20 June, 2014).

Liu, M.. A new polarized solid proton target for Fermilab E1039 Drell-Yan experiment . Invited presentation at Spin2014. (Beijing, China, 20-24 Oct. 2014).

Liu, M.. A new NMR system for E1039 polarized target. Invited presentation at Spin2014 . (Beijing, October 2014).

Prokudin, A.. Transverse Spin Asymmetries and TMD Evolution. Invited presentation at POETIC V. (New Naven, CT, 22-26 Sep. 2014).

Vitev, I.. Transverse momentum-wighted Sivers asymmetry in semi-inclusive deep inelastic scattering at next-to-leading order . 2014. In QCD Evolution Workshop 2013. (Newport News, 14-17 May 2013). , p. 1460019. New York: International Journal of Modern Physics.

Vitev, I.. Theoretical Spin Effort at LANL. Invited presentation at E1039 Collaboration Workshop. (Batavia, IL, 18 March, 2014).

Vitev, I.. A study of quasi-parton distribution functions in the diquark spectator model . Invited presentation at CD Evolution 2015. (Newport News, VA, May 26-30, 2015).

Vitev, I., Z. Kang, and H. Xing. Transverse Momentum-weighted Sivers Asymmetry in Semi-inclusive Deep Inelastic Scattering at Next-to-leading Order . 2014. International Journal of Modern Physics Conference Series. 25: 1460019.

Yoon, B.. Disconnected Contributions to Nucleon Structure. Invited presentation at Lattice QCD 2014. (Upton, NY, 23-28 Jun. 2014).

Yoon, B.. Nucleon transverse momentum-dependent parton distributions: Comparing Clover and Domain wall fermion results at ~300 MeV pion mass. Invited presentation at The 33rd International Symposium on Lattice Field Theory. (Kobe, 14-18 July, 2015).

Probing New Sources of Time-Reversal Violation with Neutron EDM

Takeyasu Ito
20140015DR

Introduction

An electric dipole moment (EDM) measures the separation of positive and negative charges within a system and is an extremely sensitive probe of physics beyond the standard model, the accepted theory of elementary particles. The neutron EDM (nEDM) is said to have "killed more theories than any other single measurement."

This LDRD project is a joint experimental and theoretical project to probe new sources of time reversal violation (T violation) with the nEDM. Using the LANSCE (Los Alamos Neutron Science Center) Ultracold Neutron (UCN) source, we will develop a new nEDM experiment with a sensitivity goal of 3x10-27 e-cm, a 10-fold improvement over the current limit. More specifically, we will upgrade the existing UCN source which is expected to result in a 10-fold performance increase. In addition, we will build a prototype nEDM experimental apparatus. With the upgraded UCN source and prototype nEDM apparatus, we will demonstrate that it is possible to perform an nEDM experiment with a sensitivity of 3x10-27 e-cm. Note that the UCN density is the key parameter that is necessary for reaching the sensitivity goal.

At the same time, to match the anticipated experimental improvement, we will perform a comprehensive model-independent analysis of T violation beyond the standard model (BSM) and we will pioneer first-principles calculations of the matrix elements, essential in extracting and bounding the underlying BSM sources of T violation from EDM measurements.

The goal of this LDRD project is to reduce the technical risk of a full-fledged nEDM experiment at LANL with sensitivity of 3x10-27 e-cm.

Benefit to National Security Missions

The proposed research is central to both the LANL (Los Alamos National Laboratory) nuclear physics program and the future of the US (United States) program on fundamental symmetries in nuclear science. The proposed upgrade of the UCN (Ultracold Neutron) source is in line with the 2010 LANL NPAC (Nuclear, Particle, Cosmology, and Astrophysics) strategic plan that recommended development of a medium scale facility, and will benefit other experiments such as a neutron lifetime experiment, which received a strong community endorsement in a recent international workshop. Furthermore, completion of the proposed experimental tasks will provide a viable alternate approach to the high-risk SNS (Spallation Neutron Source) nEDM (neutron electric dipole moment) experiment, which has a large P division involvement. This will also lead to project funds coming to LANL if a decision is made to go forward with this new nEDM experiment.

In addition, this project will strengthen an already existing successful synergy of theory and experiment in fundamental neutron physics. This is a unique strength of LANL across US laboratories. This LDRD (Laboratory Directed Research and Development) will establish LANL T-division as one of the main US centers for nucleon matrix elements computations with lattice QCD (Quantum Chromodynamics). This will put a solid basis to seek additional external funding, through the channels of DOE (Department of Energy) Nuclear Theory topical collaboration centers as well as SciDAC grants in both High Energy and Nuclear Physics.

Additionally, the UCN source improvement will benefit fundamental neutron physics experiments, actinide sciences, and detection technology.

Progress

In FY15, the experimental effort has made a lot of progress in FY15, including:

(i) We tested the new guide coating material as well as the new guide coupling technology during the 2014-2015 LANSCE beam time. The results obtained for the

new UCN guide coating was very promising. For the new guide technology, while the results were encouraging we decided that further tests were necessary. We are planning further tests at Institut Laue Langevin in France in July-August 2015.

(ii) We have completed the UCN source design. The results were summarized in two documents, one describing the physics design the other describing the engineering design. We held reviews to review both the physics and engineering design and out design was supported by the review committees.

The theory effort has made progress on several fronts in FY15:

(i) We have performed a comprehensive analysis of the ultraviolet divergence structure of the dominant new operators that violate time-reversal (T) and parity (P) symmetries, thus inducing a neutron EDM. We have studied the off-shell mixing and renormalization of flavor-diagonal dimension-5 T- and P-odd operators These operators include quark electric dipole and chromo-electric dipole operators. In the process, we also provided a definition of the quark chromo-electric dipole operator in a regularization-independent momentum-subtraction scheme suitable for non-perturbative lattice calculations. We have also presented results on how to combine the non-perturbative numerical lattice QCD results and the perturbative analytic results to make consistent physical predictions. These results have appeared in a preprint ("Dimension-5 CP-odd operators: QCD mixing and renormalization", 1502.07325), submitted for publication in Physical Review D.

(ii) We have obtained Lattice QCD (LQCD) results on the nucleon tensor charges including for the first time an estimate of all systematic errors and a simultaneous extrapolation in the lattice spacing, volume, and light quark masses. We have included in the analysis both connected and disconnected diagrams, and find that the disconnected contribution is smaller than the statistical error in the connected contribution. We found an overall error of 10% on these matrix elements, a significant improvement over the previously estimated 50% uncertainty. Nucleon tensor charges are highly relevant to our project because they determine the size of the nucleon electric dipole moment (EDM) induced by quark EDMs, generated in many new scenarios of CP-violation beyond the Standard Model (BSM). We have used our results to derive model-independent bounds on the EDMs of light quarks and to update the EDM phenomenology in split Supersymmetry, a popular supersymmetric scenario that survives all the current constraints from collider searches. We are able to propose a stringent test that might be able to falsify this new physics scenario in the near future. We have written up our results in two manuscript, a long one with all the details to be submitted to Physical Review D, and a shorter one highlighting the results and impact, to be submitted to Physical Review Letter.

Future Work

In FY16, the main focus of the experimental part will be to 1) complete the construction of the ultracold neutron (UCN) source and the new UCN guides, 2) test them using UCN 3) install them, and 4) test their performance using UCN. During the LANSCE beam time in late 2015-early 2016, the new UCN source and the UCN guides will be tested using UCN from the existing UCN source. As soon as the beam time is over, the shielding blocks will be removed and the new UCN source and the UCN guides will be installed. Then when the LANSCE beam comes back in the fall of 2016, the performance of the new UCN source and the guide will be tested. At the same time we will make progress on the prototyping of the neutron electric dipole moment (nEDM) apparatus. This includes: a) continued testing of the high voltage, b) construction of the magnetic shielding and coils, c) construction of UCN detector and spin analyzer, and d) construction of the 199Hg comagnetometer system.

The theory effort will focus on two topics in FY16. (i) We will perform the first numerical implementation to determine the size of the neutron EDM induced by the so-called quark chromo-EDM operator, i.e. a CP-violating interaction of the quarks (that make up the neutron) with the electric field associated to the strong force. (ii) We will carry out a comprehensive phenomenological analysis of the CP-violating couplings of the newly discovered Higgs boson to quarks and gluons, the carriers of the strong force. The analysis will include a comparative study of the sensitivity to these new interactions from both EDM searches and high-energy collider processes.

Conclusion

By the end of the 3 year period, we expect to achieve the following:

1) Improved UCN source that increases flux by 20-fold

2) Demonstration of the feasibility of an nEDM experiment with a sensitivity of 3x10-27 e-cm, through demonstration of the necessary UCN density stored in the prototype nEDM chamber

3) First-principles calculation based determination of the relevant matrix elements, essential in extracting and bounding the underlying BSM sources of T violation from EDM measurements

Publications

Bhattacharya, T., V. Cirigliano, R. Gupta, E. Mereghetti, and B. Yoon. Dimension-5 CP-odd operators: QCD mixing and renormalization. To appear in arXiv:1502.07325 [hep-ph], submitted to Physical Review D.

Bhattacharya, T., V. Cirigliano, R. Gupta, H. W. Lin, and B. Yoon. Neutron Electric Dipole Moment and Tensor Charges from Lattice QCD. To appear in Physical Review Letters.

Bhattacharya, T., V. Cirigliano, S. Cohen, R. Gupta, A. Joseph, H. W. Lin, and B. Yoon. Iso-vector and Iso-scalar Tensor Charges of the Nucleon from Lattice QCD. To appear in Physical Review D.

Bhattacharya, T., V. Cirigliano, and R. Gupta. Neutron Electric Dipole Moments from Beyond the Standard Model Physics . 2014. In 31st International Symposium on Lattice Field Theory (Lattice 2013). (Mainz, Germany, July 29- Aug 3 2013). , p. 299. Trieste, Italy: PoS LATTICE2013 .

Ito, T.. Science program at lanl ucn source. Invited presentation at The 2nd International Symposium on Science at J-PARC (J-PARC 2014). (Tsukuba, 12-15 Jul. 2014).

Tang, Z., E. R. Adamek, A. Brandt, N. B. Callahan, S. M. Clayton, S. A. Currie, T. M. Ito, M. Makela, Y. Masuda, C. L. Morris, R. Pattie, Jr. , J. C. Ramsey, D. J. Salvat, A. Saunders, and A. R. Young. Measurement of spin-flip probabilities for ultracold neutrons interacting with nickel phosphorus coated surfaces . Nuclear Instruments and Methods in Physics Research Section A.

The Role of Short-lived Actinide Isomers in High Fluence Environments (U)

Marian Jandel
20140046DR

Introduction

In this project we will determine the nuclear physics properties of the actinide isomers, namely 236U and 239U, and quantify their role in explosive environments. Apart from the knowledge of their existence and half-lives, there are no available data on the quantitative population of these short-lived actinides isomeric states following neutron capture. Our preliminary experimental studies at LANSCE suggest there may be substantial population of high energy isomeric states in the neutron capture process on actinides. These new, unanticipated results may have significant implications on our understanding of nuclear reaction networks in high neutron fluence environments such as those occurring in nuclear explosions. New experiments will be staged and performed at LANSCE at the Detector for Advanced Neutron Capture Experiments facility (DANCE), that will provide new information about neutron-induced reactions on fissile actinides. With improved experimental capabilities, we will obtain new precision data on yields of isomers after neutron capture on 235U and information on prompt fission neutrons and gamma rays. Experimental and theoretical work on reaction rates leading to (and on) isomeric states is very complex and represents a high risk part of this proposal. Low risk objectives include neutron-induced fission studies, which must be performed very accurately in order to address the process of neutron capture in detail.Experimental work will include developments of a compact 4pi neutron detector array that will be installed in the central cavity of the DANCE detector array to detect prompt fission neutrons – NEUANCE (the NEUtron detector at dANCE). On the theoretical front we will develop models for calculation of neutron-induced reactions on excited states, neutron transport codes to populate excited isomeric states in actinides, and nuclear de-excitation models to interpret isomeric yields, and fission fragment de-excitation including prompt fission n-gamma-fission fragment correlations.

Benefit to National Security Missions

Recent and urgent interest of various governmental agencies, such as the Office of Non-Proliferation Research and Development (NNSA NA-22), in more precise and correlated data on neutron-induced reactions will put the capabilities developed during this project into a great position to support mission needs for systematic measurements of isomeric state production in neutron capture, correlated induced-fission data, predictive modeling of capture and fission and refinement of transport codes such as MCNP to include important details on correlated radiation from neutron-induced reactions. New signatures for special material detection, nuclear proliferation and forensics will be the objectives of the follow-up research, which is a core mission of this laboratory. Knowledge of the production and de-excitation properties of actinide isomers will provide constraints on our understanding of the performance of our well characterized US nuclear tests. Of equal importance it will provide insights to global security missions associated with nuclear forensics efforts where the ingoing properties of devices will be unknown and actinide observables such as 237U, 240U, are what will be available to diagnose the device characteristics. It is important that we understand how actinide isomeric population can influence the production of the actinide observables.

Progress

A prototype NEUANCE detector - NEUtron detector Array at DANCE (Detector for Advanced Neutron Capture Experiments) consisting of six, each 5 cm square by 10 cm long, EJ-309 liquid scintillators was tested in beam with the new data acquisition system at flight path 14 of the Lujan Center at Los Alamos Neutron Science Center (LANSCE). Data was taken using a 28 mg/cm2 thick 235U target as well as non-fissioning capture samples. Both photomultiplier and “silicon photomultiplier” sensors were tested. Properties of the detectors, such as neutron/gamma discrimination and pulse-height thresholds, were investigated. Although the details of the measure-

ment are still being investigated, some preliminary results are already driving design considerations for the full neutron detector array.

We were actively working on designing and testing a fission-fragment detector for DANCE. We built a prototype fission-fragment detector (FFD) based on thin scintillating films. The detector consisted of 10 films attached to light-guide rings and all rings glued together to a solid cylindrical body. We deposited a negligible amount (150 Bq) of Cf-252 at the last film. This prototype demonstrated that fission fragments can be detected with the thin scintillating films and the scintillation can be transported through the whole system of light-guide rings. The next step was to design a real FFD for DANCE that to be tested with a neutron beam. A FFD consisting five scintillating films was produced with three of the foils loaded with small amount of U-235, 0.9 mg in total. The detector was used in a test run in the Lujan Center in the middle of January 2015. A good time-of-flight spectrum of the U-235(n,f) reaction was obtained and efficiency of the FFD of 14(2)% was estimated. Currently we are working on production of a 10-film FFD loaded with 20 mg of U-235 for a production data measurement at DANCE planned early in October, 2015.

Measurements were carried out using a new data acquisition (DAQ) system. We received the DAQ hardware at the very end of FY14. In FY15 we installed, coded, and validated the operation of the new DAQ such that it meets or exceeds all the performance specifications imposed by the project. We demonstrated the integrated operation of different firmware types to handle the disparate detector types required for the project to succeed. Current capabilities include processing of signals from nearly any type of radiation detectors, including Germanium and Silicon detectors. In short, we demonstrated the DAQ's ability to perform the necessary experiments for the project to succeed.

On a theoretical side of the project, the CGMF (cascade gamma multiplicity for fission) code was developed to model the de-excitation of the fission fragments on an event-by-event basis, following the successive emissions of neutrons and photons. The emissions are treated in the Hauser-Feshbach statistical model. Part of the current proposal, we have improved the treatment of emission of electromagnetic radiation by taking into account the lifetimes of longer lives nuclear states (isomers), by implementing in CGMF a sampling procedure that correlate the measurement coincidence window with the lifetimes of the decaying nuclear states involved. We have made simulations of neutrons and gamma rays for several coincidence windows and provided the results to the experimental colleagues for detector analysis and design.

Finally, the reaction cross section calculation includes two parts, (1) the isomeric state production cross section by a neutron capture, and (2) the destruction of the isomers by neutron-induced fission. For the isomeric state production, we implemented a so-called discrete states embedded in the continuum in our Hauser-Feshbach code, which allows us to produced more discrete gamma-ray lines. This is particularly important to estimate the production of the isomeric states whose excitation energies are high. We performed cross section calculations for three different isomeric states. For the destruction of the isomers, the fission cross sections are calculated for the target in its ground and excited states, and an enhancement of the fission cross section for the isomers is confirmed. Calculation of the fission transmission coefficient including the Class-I and Class-II coupling is on-going, and preliminary implementation was done.

Future Work

- Carry out the measurement of neutron capture of U-235 with the thin film scintilator detector for fission fragments, at Lujan Center, LANSCE (October 2015) and analyze data.
- Carry out the measurement of neutron capture of U-235 using the NEUANCE detector at Lujan Center, LANSCE (January 2016) and analyze data.
- Implement the new DAQ using VME CAEN digitizers for experiment 1) and 2)
- Development of CGM: gamma-ray de-excitation model development using preliminary U236* data. Implement data from Task 1) and 2)
- Development of CGMF - fission event generator for NEUANCE design and optimization. Implement data from Task 1) and 2)
- Perform cross section calculations on the excited states calculations of U236*. Implement data from Task 1) and 2)
- Sensitivity studies in transport simulations including delayed gamma-ray emission. Implement data from Task 1) and 2)
- Develop a project continuation strategy and plan new measurements and attract sponsors.

Conclusion

New data on isomer production after neutron capture will help benchmark the theory of compound nucleus de-excitation and theory of the cross section on excited states. New capability will be created after completion of this project that will enable measurements of correlated data on fission relevant to applications of National Security, Nuclear Forensics and Energy.

Publications

Baramsai, B., M. Jandel, T. A. Bredeweg, A. Couture, S. Mosby, G. Rusev, J. L. Ullmann, and C. L. Walker. Characterization and testing of EJ-309 and Stilbene scintillation detectors . 2015. In Proc. SPIE 9593, Hard X-Ray, Gamma-Ray, and Neutron Detector Physics. (San Diego, Aug 9). , p. 1. San Diego: SPIE.

Jandel, , Baramsai, T. A. Bredeweg, Couture, Hayes, Kawano, Mosby, Rusev, Stetcu, T. N. Taddeucci, Talou, J. L. Ullmann, C. L. Walker, and J. B. Wilhelmy. Current and Future Research at DANCE. 2015. CGS15 - CAPTURE GAMMA-RAY SPECTROSCOPY AND RELATED TOPICS. 93.

Rusev, G., B. Baramsai, E. M. Bond, and M. Jandel. Fission-neutrons source with fast neutron-emission timing. Nuclear Instruments and Methods A.

Rusev, G., M. Jandel, B. Baramsai, A. R. Roman, J. K. Daum, R. K. Springs, E. M. Bond, T. A. Bredeweg, A. Couture, A. Favalli, K. D. Ianakiev, M. L. Iliev, S. Mosby, J. L. Ullmann, and C. L. Walker. Fission-fragment detector for DANCE based on thin scintillating films. To appear in Nuclear Instruments and Methods A, in print doi:10.1016/j.nima.2015.09.078.

Rusev, G., M. Jandel, B. Baramsai, E. M. Bond, T. A. Bredeweg, A. Couture, J. K. Daum, A. Favalli, K. D. Ianakiev, M. L. Iliev, S. Mosby, A. R. Roman, R. K. Springs, J. L. Ullmann, and C. L. Walker. Development of a thin scintillation films fission-fragment detector and a novel neutron source. 2015. In Proc. SPIE 9593, Hard X-Ray, Gamma-Ray, and Neutron Detector Physics XVII, 959314 (August 26, 2015); doi:10.1117/12.2192440. (San Diego, Aug 9). , p. 1. San Diego: SPIE.

al, A. Couture et. Enhancing the Detector for Advanced neutron Capture Experiments. 2015. EPJ Web of Conferences. 93: 07003.

al, I. Stetcu et. Properties of prompt-fission gamma rays. 2014. Phys Rev C. 90: 024617.

al, M. Jandel et. Current and Future Research at DANCE. 2015. In CGS15 – Capture Gamma-Ray Spectroscopy and Related Topics . (Dresden, August 25-29). , p. 1. Online: EPJ Web of Conferences.

al, M. Jandel et. Capture and fission with DANCE and NEUANCE. To appear in European Journal of Physics A.

al, S. Mosby et. A fission fragment detector for correlated fission output studies. 2014. Nuclear Instruments and Methods A. 757: 75.

Research Enabling a Next Generation Neutron Lifetime Measurement

Steven Clayton
20140568DR

Introduction

The lifetime of the free neutron is a fundamental input to the Standard Model of particle physics. At present the experimental situation with lifetime measurements shows a distribution of values for the lifetime that is outside the claimed accuracy of these measurements. Trapped ultra-cold neutrons (UCN) show great promise to both resolve existing discrepancies and to push the precision of lifetime measurements to the level of 0.1 sec . A major focus of this project will be the implementation of a new technique for in situ detection of UCN inside the trap. In the first year, we will test a proto-type system to do this. Subsequent years will make improvements to this system based on the experience in the first year. In the third year we expect to make extended running to make an initial lifetime measurement with well-characterized uncertainties controlled at the level of 1 second.

This project will develop and apply two major innovations to the study of neutron decay with UCN. We will make the first measurement of the UCN lifetime using an asymmetric trap that will serve to minimize systematic uncertainties caused by marginally trapped neutrons. Our measurement will also be the first to make an in situ measurement of the number of trapped UCN, which will eliminate uncertainties introduced in the alternate technique of measuring the surviving neutrons by draining them from the trap. Measurements at comparable accuracy to the present suite of experiments – but with fundamentally different and understood systematic uncertainties – will be key in understanding why earlier measurements underestimated their systematic uncertainties.

Benefit to National Security Missions

Better understanding the physical world - such as understanding the lifetime of the fundamental building blocks of matter, is central to the mission of the Office of science.

Nuclear physics experimental capability, specifically the ability to understand and make measurements with and about neutrons is a core capability of the nuclear weapons and nuclear nonproliferation programs which is sustained and advanced by this project.

Progress

In the past 12 months, we met all of our second-year goals, and furthermore developed a new detector for ultracold neutrons that is highly promising for the future of this experiment. The second year goals were to test and characterize improvements to the experiment:

- A new trap door system for improved loading. This was constructed and installed, and shows good loading efficiency consistent with the mock-up tested in the previous year.
- Improved system for detecting the decay products from the in situ vanadium detector, and a new vacuum jacket for the 52V decay products detector package. The new vacuum jacket was designed and installed, allowing the gamma detectors to be placed closer to the vanadium sheet for improved solid angle coverage, and improved shielding comprising lead bricks and borated plastic was installed that greatly reduced the background event rate.
- Measurements of the lifetime of ultracold neutrons in various gases were performed, setting detailed limits on the amount of residual gas permitted in the neutron lifetime apparatus to avoid a significant correction.

With the improvements to the experimental apparatus, we collected data for a ~3 second (statistical) precision measurement of the neutron lifetime, and performed several systematic studies, including tests of the normalization of the initial ultracold neutron population loaded into the trap, and tests of the time required to remove marginally-trapped ultracold neutrons from the trap (the neutrons that could slowly leak out from the trap dur-

ing the holding period, thus leading to a loss mechanism other than beta decay). Analysis of these data is ongoing and will result in either a physics result (if we have enough information to understand systematic errors at this level), or at least a measurement of the apparent holding time of the trap; we note that a physics result with ~3 second precision is already interesting in the context of the 6 second discrepancy between the world average neutron lifetime measured with the beam versus material bottle methods of previous workers.

We have also developed a new ultracold neutron detector technology based on a thin film of 10B on a ZnS scintillator medium. Ultracold neutrons capture on the 10B layer, and energetic reaction products create scintillation light in the underlying ZnS layer, which is viewed by a light sensor such as a photomultiplier tube. Unlike gas-phase detectors such as 3He-based technologies, the ultracold neutrons do not have to pass through a window, avoiding the potential barrier and losses in the window material. We demonstrated these detectors with ultracold neutrons from the LANSCE UCN facility, showing good efficiency and without the drop tube necessary for windowed detectors; a manuscript describing this work is near publication in the journal Nuclear Instruments and Methods A. We have begun development of upgrades to the UCNtau experiment based on this windowless detector technology, with plans to install them next year. The “cleaner” to remove superbarrier ultracold neutrons (those with energy greater than the trap potential), now a passive upscattering material, will be replaced with an active sheet that will enable a series of unprecedented systematics studies. Replacing the current in situ detector, based on absorption onto a vanadium sheet and subsequent counting of the decay of 52V, with a new active in situ detector that efficiently registers each neutron as it is absorbed, effectively improves the statistical reach of the experiment as well as enables systematic studies not possible with the current detector.

Future Work

In the third year of this project, we will take production data for a 1-second precision neutron lifetime measurement (i.e. comparable to the current world-average precision), study systematic effects, and implement a new idea for an active “cleaner” for marginally-trapped ultracold neutrons, as well as an active, in situ, ultracold neutron detector to replace the vanadium dagger. By counting superbarrier (above the trap potential) ultracold neutrons with good efficiency as they hit the cleaner, the active cleaner will allow us to perform unprecedented systematic studies, such as 1) cross-checks of the normalization of the initial ultracold neutron population in the trap; 2) observation of any marginally-trapped ultracold neutrons that take a long time to be cleaned; and 3) studies of any vibration induced heating of the trapped neutrons. The new, active detector to replace the vanadium dagger offers three distinct advantages. The first is improved statistics, due to higher detection efficiency of individual ultracold neutrons, and better beam utilization by eliminating the long period after every fill required to count decays from the vanadium detector. The second advantage of the active in situ detector is that, because we will count each ultracold neutron as it is absorbed in the detector, a possible systematic uncertainty due to changes in characteristic absorption time into the detector is eliminated. Finally, the active detector is expected to be much less sensitive to background events. Another goal for the third year of this project is detailed mapping of the magnetic field of the trap, following up on a rough mapping this year to search for any low-field regions on the trap surface, where neutrons could be lost, or zero-field regions in the trap volume, where neutrons could be depolarized and thus subsequently lost.

Conclusion

The overall goal of the project will be to characterize all systematic uncertainities involved in using this system to make a measurement of the neutron lifetime at the level of 1 second. A new measurement at the 1-second level will lower the uncertainty of the PDG evaluation of the lifetime. The neutron lifetime is one of its basic properties. It is an important input to the standard model of cosmology and understanding primordial nucleosynthesis. Combining neutron lifetime with the other parameters of neutron decay can be used to construct sensitive tests of the standard model of particle physics.

Publications

Salvat, D. J., E. R. Adamek, D. Barlow, J. D. Bowman, L. J. Broussard, N. B. Callahan, S. M. Clayton, C. Cude-Woods, S. Currie, E. B. Dees, W. Fox, P. Geltenbort, K. P. Hickerson, A. T. Holley, C. Y. Liu, M. Makela, J. Medina, D. J. Morley, C. L. Morris, S. I. Penttilä, J. Ramsey, A. Saunders, S. J. Seestrom, E. I. Sharapov, S. K. Sjue, B. A. Slaughter, J. Vanderwerp, B. VornDick, P. L. Walstrom, Z. Wang, T. L. Womack, and A. R. Young. Storage of ultracold neutrons in the magneto-gravitational trap of the <math xmlns=”http://www.w3.org/1998/Math/MathML”><mi>UCN</mi><mi>τ</mi></math> experiment. 2014. Physical Review C. 89 (5): 052501.

Wang, , M. A. Hoffbauer, C. L. Morris, N. B. Callahan, E. R. Adamek, J. D. Bacon, Blatnik, A. E. Brandt, L. J. Broussard, S. M. Clayton, Cude-Woods, Currie, E. B. Dees, Ding, Gao, F. E. Gray, K. P. Hickerson, A. T. Holley, T. M. Ito, C. -. Liu, Makela, J. C. Ramsey, R. W. Pattie Jr., D. J. Salvat, Saunders, D. W. Schmidt,

R. K. Schulze, S. J. Seestrom, E. I. Sharapov, Sprow, Tang, Wei, Wexler, T. L. Womack, A. R. Young, and B. A. Zeck. A multilayer surface detector for ultracold neutrons. 2015. NUCLEAR INSTRUMENTS & METHODS IN PHYSICS RESEARCH SECTION A-ACCELERATORS SPECTROMETERS DETECTORS AND ASSOCIATED EQUIPMENT. 798: 30.

k_effective: First Measurement of a Nanosecond-Pulsed Neutron Diagnosed Subcritical Assembly

Anemarie Deyoung
20150044DR

Introduction

Neutron generation is extremely sensitive to plutonium compressibility, and understanding the compressibility under the conditions encountered in a nuclear primary is key to Life-Extension Program (LEP) options (including pit reuse), guarding against untoward aging effects, and establishing the safety/surety characteristics for the future stockpile. These and other key drivers have been studied in a classified venue by our XTD Division advisors to the LDRD. In this project we will develop a precision measurement technique to determine the nuclear generation in a subcritical system, with an accuracy comparable to that obtained in nuclear testing. The Weapons Program requirement for an innovative alternative to nuclear testing is a dynamic pulsed measurement of neutron generation. The focus of this proposal is the feasibility of a subcritical static neutron generation experiment.

Previous subcritical experiments have not had the diagnostic capability to infer nuclear generation. Our project involving Neutron Diagnosed Subcritical Experiments (NDSE) provides neutron generation, which is an extremely sensitive integral constraint on both the distribution and nuclear properties of materials. Our proposed NDSE capability would enable inference of neutron generation or, more precisely, “alpha” (α), with the accuracy needed for weapons analysis. We will perform a high precision measurement of α using a static subcritical assembly. The challenge is to make the measurement under laboratory conditions with ~10 orders of magnitude fewer gammas than were available during nuclear testing.

We will develop a capability that includes (1) a pulsed neutron source and (2) a detector and data acquisition system with proper shielding and collimation to measure the gammas emitted from the package. The recent advances in pulsed neutron sources, detector technologies, fast electronics, and simulation-based analyses, have advanced the NDSE concept to a level that has a high chance of succeeding at a first ns-scale pulsed neutron generation measurement.

Benefit to National Security Missions

Success of this LDRD project would establish the technical feasibility of proceeding toward a large future weapons program in dynamic NDSE at the NNSS. Such a program would provide the first modern quantitative understanding of the neutronic properties of Pu at high pressures and thus provide experimental validation of weapons models which is key to Life-Extension Program (LEP) options (including pit reuse), guarding against untoward aging effects, and establishing the safety/surety characteristics for the future stockpile. This also has possible applications in the Global Security arena. The Nuclear Engineering and Non-proliferation (NEN) Division is expert in the use of passive and active diagnostic techniques for detection and characterization of configurations of special nuclear materials. The neutron generation measurement offers an opportunity to explore different techniques for simultaneously collecting, utilizing, and analyzing all the available time-dependent induced signatures.

Additionally, success of this project would advance the scientific state-of-the-art in gamma-ray detectors and DPF neutron sources. As well it would enable advanced criticality studies, e.g., study of fast pulse excitation of complex static critical assemblies. Measuring the alpha, using a fast neutron pulse, of a static but complex critical assembly, creates a new regime which permits advanced testing of simulation codes. Observation of alpha as it changes from an initial value (14 MeV excitation) to its equilibrium value, would allow separation of various contributions such as delayed neutrons, effects of cross section libraries for the unresolved resonance regions, and the time-dependence of complex moderation and reflection processes.

Progress

The safety and performance of the stockpile could benefit from a neutron-diagnosed subcritical experiment (NDSE) capability to challenge and inform our judgment in predicting the nuclear trigger's capability to generate enough neutrons to go supercritical. NDSEs quantify the generation of neutrons in a subcritical pit that is the fundamental mechanism generating energy in nuclear weapons. Neutron generation is extremely sensitive to plutonium compressibility, and understanding the compressibility of plutonium under the conditions encountered in a nuclear weapon primary will be a key factor in their developing life-extension program (LEP) options (including pit reuse), understanding aging, and establishing the safety/surety characteristics for the future stockpile.

To these ends, we are developing an NDSE capability comprising (1) a pulsed neutron source producing a neutron flash and (2) a detector and data acquisition system on a dedicated line of sight that will measure gamma-rays emitted from the dynamic package under interrogation. This capability would provide a unique ability to infer neutron generation and answer critical questions related to integral plutonium behavior. Here we describe our recent R&D advances in pulsed neutron sources, detector technologies, fast electronics, and simulation-based analyses.

Accomplishments to date are summarized as follows.

- DPF modeling – Hui Li, Anna Hayes /LANL
- Provided initial confirmation of physics behind reentrant tube capability to make single pulse; intent is to feed neutron output into MCNP modeling
- Gamma ray detector development – Vincent Yuan / LANL
- Detector lab testing of fast scintillators and Cerenkov media led to a downselect where we chose Liquid VI scintillator and manufactured a 2x2 array with each cell 15"x15"x8" for use on the gamma falloff experiment
- MCNP modeling of experiment – Tim Goorley /LANL
- Modeling of experiment design reduces background so that we can design the line of sight and make a good measurement; provides for prediction of gamma measurement
- Design of novel Boron 10 target – George Morgan / LANL
- Boron target avoids the large costs required for a Special Nuclear Material (SNM) target; and it enables validation - gamma falloff will be measured in the lab (future Pu sphere gamma measurement would have independent Rossi alpha measurement)
- DPF experiment – Scott Hsu, Robert Rundberg /LANL
- Use of optical spectrometer allowed first measurement of contaminants in the DD DPF pinch as well as electron density; use of shadowbar designed by George Morgan allowed for precision measurement of DT DPF neutron profile
- Boron target has been procured and testing has begun at LANL. The Laboratory is designing and procuring the iron and borated poly collimators to use as shielding for the static test. LANL is ready for the gamma measurement in September or October.

Future Work

Our goal is to perform an accelerated gamma measurement on a 10B target using concrete line of sight at NNSS by Oct 2015, and to perform an NDSE measurement on a static bare SNM assembly at the NNSS by September 2016.

Conclusion

We must develop novel gamma-ray detector technology to meet the requirements of the neutron generation measurement; this includes new materials to achieve a signal with large dynamic range and ultrafast few-ns scale time response. We must also develop a robust pulsed neutron source based on Dense Plasma Focus (DPF) technology; this lies at the forefront of plasma physics. The reduced funding of this project delays the first measurement on a static subcritical assembly to 20 months; reduced funding for criticality expertise increases our reliance on infrastructure support and generally increases the risk of a further delay in the experiment.

Publications

DeYoung, A., T. Goorley, A. Hayes, G. L. Morgan, V. W. C. Yuan, R. S. Rundberg, H. Li, G. Jungman, W. Myers, S. C. Hsu, T. J. Haines, E. Guardincerri, C. Hagen, D. Lowe, S. Molnar, P. O'Gara, I. Garza, E. Hunt, J. Tinsley, M. Kelley, J. Gatling, T. Waltman, R. Buckles, A. Luttman, N. Sipe, J. Friedman, N. Bennett, and E. Christensen. (U) Progress towards the NDSE LDRD gamma measurement on a static assembly. To appear in Nuclear Physics Design Physics Conference. (Los Alamos, NM, 19-23 Oct 2015).

DeYoung, A., V. Yuan, G. Morgan, C. Hagan, A. Obst, R. Rundberg, A. Hayes, T. Goorley, H. Li, G. Jungman, W. Myers, S. Hsu, T. Haines, J. Lestone, E. Guardincerri, M. Fowler, P. Koehler, J. Gatling, E. Hunt, M. Kelley, D.

Lowe, B. Davis, and J. Tinsley. New diagnostic: neutron diagnosed subcritical experiments (LA-CP-14-20196). Presented at Nuclear Explosive Code Development Conference 2014. (Los Alamos, NM, 20-24 October 2014).

Hsu, S.. DPF benchmarking diagnostics: present and future. Presented at DPF Workshop. (LLNL, Livermore, CA, 29 June 2015).

McKenzie, G. E., T. J. Grove, W. L. Myers, and R. G. Sanchez. Reactivity worth studies associated with a Rossi-Alpha measurement system (LA-UR-15-25941) . Presented at American Nuclear Society Winter Meeting. (Washington DC, November 2015).

Myers, W., J. Bounds, T. Cutler, J. Goda, J. Goettee, T. Goorley, S. Harbour, D. Hayes, R. Kimpland, S. Klein, D. Mayo, C. Moss, and S. Watson. Applications of fast burst reactors in support of data analysis tool development for the Neutron Diagnosed Subcritical Experiment (LA-UR-15-27621). To appear in Nuclear Explosives Design Physics Conference. (Los Alamos, NM, 19-23 Oct 2015).

Yuan, V., A. DeYoung, A. Obst, and G. Morgan. NDSE detectors development. Presented at 2015 Nevada working group meeting, LA-UR-15-22230 . (Las Vegas, Nevada, 31 March 2015).

Multi-Scale Kinetics of Self-Regulating Nuclear Reactors

Venkateswara R. Dasari
20150058DR

Introduction

Los Alamos is pioneering the development of self-regulating small compact nuclear reactors (SCRs). These reactors are of immense interest to the community of sponsors who have power needs in space, underwater and in remote areas. In this research, we propose to demonstrate the feasibility of self-regulation by developing and validating models for reactor behavior in tunable 'micro-engineered' materials specifically designed to achieve self- regulation. Reactors that self-regulate fission power to match varying operational needs and that protect the reactor core from exceeding thermal limits during accidents are ideal for unattended operations.

SCRs are significantly different in scale and design from conventional reactors. Making use of precisely engineered core and reflectors, SCRs can be designed to have relatively longer neutron life time, small excess reactivity in the core and low power density making them an ideal candidate for achieving self- regulation. The transformational goal of this DR is to precisely understand how novel SCRs can be designed to self-regulate with minimal control system or human intervention. In this research we are seeking a disruptive alternate based on the hypothesis that certain mesoscale properties of micro-engineered fuels can be 'tuned' so that emergent neutronic functionality maximizes SCR self-regulation. Building on this hypothesis, we have designed micro-engineered dispersed fuel composites that trigger and amplify negative reactivity feedback at different timescales and lengthen neutron lifetime by 'geometrically delaying' a significant portion of fissioning neutrons.

The focus of this research is to demonstrate the feasibility of our SCR concept by accomplishing three inter-related R&D objectives: to research and develop techniques to make limited quantities of tunable fuel composites that maximize self-regulation; to measure their neutronic and thermo-mechanical properties at different length-scales; and using this data to model the performance of the full-scale reactor to confirm self-regulation and quantify uncertainty.

Benefit to National Security Missions

Los Alamos is pioneering the design of self-regulating low-power small compact reactors. Such "fission batteries" are of immense interest to the community of sponsors who have power needs in space (NASA/DoD/IC), underwater (DoD/IC/DHS) and in remote areas coupled with renewable sources (DOE). Despite these transformative aspects, there is reluctance to adapt reactor technologies because they are perceived to be too financially risky and complex to operate. In this Directed Research, we propose to demonstrate feasibility of self-regulation and develop and validate constitutive models of neutron kinetic behavior in tunable 'micro-engineered' materials specifically designed to achieve self-regulation.

Los Alamos National Laboratory is singularly qualified to undertake this research because of our unique ability to bring together computational nuclear engineering, computational and experimental nuclear materials science, and criticality testing facilities at NCERC. Of particular importance are our capabilities (1) to precision design, engineer and fabricate nuclear components, (2) to build in proliferation resistance and (3) to test the system and its components relying upon methods developed as part of science-based stockpile stewardship. In addition to providing fundamental knowledge on nuclear materials, it also provides nuclear criticality data necessary for characterizing safety and non-proliferation implications of dispersed fuels and are likely to lead to fabrication of accident tolerant nuclear fuels. In summary we are leveraging specific capabilities being maintained at LANL for the purpose of carry out our primary nuclear security mission, to meet needs of other national security sponsors, and refining those actinide science skills for future weapons and nonproliferation missions.

Progress

The project has made progress in all key areas necessary to achieve the goal of improving the ability of a small reactor to self regulate using the physics of neutron reactions, in specially designed nuclear materials. Key areas include: 1) the ability to make a dispersed reactor fuel with properties that enhance the ability to provide negative reactor feedback; 2) Modeling the neutron and thermal physics of the reactor at a level that will allow for the physical effects to be predicted; and 3) determining the experiments that can be performed that will allow direct measurement of self-regulation.

A dispersed nuclear fuel is one in which uranium particle (kernels) are dispersed and compacted in robust materials, such as graphite and tungsten. The purpose of our research is to specially coat these fuel particles to enhance its neutronic performance. It has been shown theoretically that self-regulation can be significantly enhanced if the coatings are able to temporarily "trap" heat inside the fuel particle. This rapid heat up of the particle in relation to its surroundings produces the desired negative reactivity feedback necessary for self-regulation. Therefore thickness, conductivity and quality of the coatings is very important to this project. A key milestone for the first year is to design, make and characterize a limited amount of a dispersed fuel to demonstrate that such coatings can be fabricated and that they are robust enough to be extruded into a fuel compact. MST Division has developed the necessary hardware to coat fuel particles. Team has overcome numerous logistical and technical challenges to produce several batches of coated fuel-surrogates (Zr and Tungsten were instead of Uranium). The coatings produced to date have been very satisfactory in that they are uniform, robust and are of the required thickness. Coated particles have already been dispersed into graphite and extruded as fuel blocks to demonstrate that coatings are robust enough. A multitude of tests are being run at LANL and INL to exquisitely characterize their performance. We expect to repeat these activities using natural and low enriched uranium over the next two months. A contract has been signed with General Atomics to make UO2 and UC fuel particles from the feedstock obtained courtesy of the Y-12 plant. This positions us well to fabricate larger quantity of fuel next fiscal year which will ultimately be used in the neutronic experiments.

Simultaneously modeling tools are being developed or have been already developed to examine the reactivity feedback mechanisms for self-regulation. We have linked important LANL computer codes, e.g. MCNP, with the heat transfer and solid modeling codes that specialize in reactor scale modeling. We now have the capability to simultaneously evaluate neutronic, thermal and structural performance of real-scale reactor (a national first). This will enable us to quantify how a microscopic change, such as coating on a fuel particle, could impact the macroscopic self-regulation performance of a reactor. NEN and AET post-doctoral students are pushing this capability forward. We are already benchmarking these codes using past criticality experiments conducted by NEN division.

Another milestone relates to developing and refining experimental plans for neutronic experiments to be performed over the next two years; it was recognized that developing such a plan early on in the project and getting nuclear authorization will reduce project risk. Due to reduced funding received for the project and due to the fact that some of the nuclear specialists were pre-occupied with DAF restart, progress on this subtask is slightly behind the schedule, but will be completed as planned by the end of the fiscal year. We have already developed a list of experiments that will allow for the neutronic performance of the fuel described above to be verified and finalizing strategy for instrumenting them. The experiments will use COMET machine at DAF in the epithermal neutron flux configuration named "Zeus". First series of experiments, named "Helios", will be a variation of the "Zeus" experiment to accurately measure neutron flux and fuel temperatures induced by traditional fuel materials. The materials will be changed in a step-wise fashion to eventually arrive at a configuration that will use the fuel being developed by MST. By performing the experiments in a step-wise fashion, the uncertainty of each experiment can be better estimated which is essential for validating the aforementioned simulations.

The project to date is on track and meeting all proposed milestones. The early results have demonstrated the capabilities necessary to make this project successful.

Future Work

The project team will design, synthesize and characterize a limited quantity of fuel composite. Measurements of its materials and neutronic properties at various time and length-scales will provide data necessary to refine and validate models use in the design of small compact reactors.

As a first step, novel fuel materials will be designed, developed, fabricated and characterized. Candidate fuels will be manufactured at a specific micro-scale and then coated in a low thermal conductivity outer layer. The coated particles will then be added to a material material like graphite. The choice of fuel size, coating thickness, materials thermal conductivity will produce a thermal behavior that in turn will change the neutronic behavior of the material.

The second step is to perform nuclear reactor physics experiments on the fuel samples. In reactor physics, an integral property 'reactivity worth' is often used to represent aggregated effect of various nuclear reactions. Los Alamos maintains nuclear criticality benchmark machines for the explicit purpose of measuring reactivity worth of new materials. Samples will be placed in the benchmark machines to provide measurements of reactivity worth at various temperatures.

Finally, we will build refined models that will be used to perform an integrated assessment of self-regulation. We plan to model the experiments and parts of the core in explicit detail to capture the effects of the micro engineered materials.

Conclusion

We are seeking a disruptive solution based on the premise that dispersed fuel composites can be 'tuned' at the micro-scale such that emergent neutron behavior can be designed to self-regulate a reactor with minimal control system or human intervention. Operationally, the Defense Science Board identified small compact reactors to be "game-changers" whose demand cannot be underestimated for space exploration, for underwater vehicles, for assured arctic awareness and satellites that can operate on the dark side of the globe. This research will demonstrate feasibility and readiness of such a technology for near-term use by a community of sponsors.

Publications

Cummins, D. R., E. Luther, A. Telles, and P. Pappin. Low Temperature Sintering of Silicon Carbide for New Self Regulating Reactor Design. Presented at Rio Grande Fuels Conference. (Los Alamos/ Albuquerque, September 2015).

Luther, E., D. V. Rao, I. Usov, A. Telles, A. Nelson, and D. Hurley. Fabrication of Graphite Composite Fuel with Controlled Thermal Transport Properties . To appear in TMS 2016: the Materials and Fuels for the Current and Advanced Nuclear Reactors V symposium . (Nashville, TN, Feb 14-18).

Rao, D., A. Fallgren, and P. McClure. The Use of Moderation in Compact Fast Reactors to Improve Safety Performance and Reduce Proliferation Risks . To appear in Nuclear Technology.

Telles, A., E. Luther, P. Papin, and D. V. Rao. The Effect of Compositional Variations on the Fabrication of Extruded Graphite Composite Fuel. To appear in Rio Grande Fuels Conference. (Los Alamos/ Albuquerque, September 2015).

Next-Generation Double Beta Decay Experiment

Steven R. Elliott
20150088DR

Introduction

If neutrinos are their own antiparticles, technically referred to as Majorana particles, theories that explain the matter-antimatter asymmetry of the Universe and hence our presence become plausible. Neutrinoless double beta decay experiments are the only practical technique to establish that neutrinos are Majorana particles. A next generation experiment using approximately a tonne of source will have an exciting opportunity to make this determination. This is especially true given the knowledge we have regarding neutrino mass from other experiments. It is clear that this is an ideal time to begin planning such an experiment.

Some remaining R&D is required to eliminate risks associated with a next-generation experiment. This includes a number of technical and theoretical topics. This project intends to perform that R&D.

The Department of Energy is planning for a future large double beta decay experiment, but they haven't chosen the technology yet. With this R&D, we hope to improve the case for the use of Ge detectors.

Benefit to National Security Missions

This is a critical time for this R&D. The DOE-NP office is planning to fund a large-scale double beta decay experiment and is making plans for that eventuality. Presently, NSAC is doing an assessment of the possible techniques that can accomplish the goal and a sub-committee has posted its report. In April of this year, the committee submitted its initial report to NSAC indicating the importance of the science and the critical nature of the next 2-3 years in determining the final choice of technology. Therefore, the R&D accomplished in the next few years will greatly influence the final decision.

This research will also provide a significant improvement in HPGe detection limits, and the knowledge gained can be leveraged to lower backgrounds for operational (Global Security) relevant missions. The data acquisition and multiplexing will provide an excellent basis for better throughput in data collection and storage. The pulse shape discrimination (PSD) analysis work also may serve to improve detection sensitivities through recognition of background versus sample events. The PSD may also allow us to do better time coincidence measurements by looking for only coincidences with certain pulse shapes.

Low background gamma-ray detection has application to non-proliferation by lowering the limit of detection of radioactive effluent from reprocessing and other weapons production activity. This supports the Laboratories Science of Signatures Pillar.

Progress

This past year we made progress on all of the activities associated with our project. Our efforts are R&D aimed at improving the performance of a tonne-scale double beta decay experiment based on Ge detector technology (TSGe). Some of our efforts are dedicated experiments at LANL, whereas other efforts exploit data from the Majorana Demonstrator (MJD) presently operating at the Sanford Underground Research Facility (SURF) and critical theory for understanding the expected decay rate.

A stainless steel test cryostat has been fabricated and a gas handling system has been constructed. This system will be used to evaluate several aspects of the hybrid cryostat design. This system will evaluate the cooling efficiency of a gas filled cryostat, determine the proper operating pressure and purity for the gas, and a Ge detector will be cooled and operated in the cryostat. Other development work is ongoing for a second radio-pure test cryostat made of copper.

With the continued reliability issues for high voltage and signal connectors being uncovered by the operation of the MJD, we have begun pursuing more reliable connectors and working with several vendors on new radio-

pure options.

We have repaired our robot and are beginning studies of how to use robotics to reduce labor requirements for a large-scale double beta decay experiment.

A white-paper design was completed to form the basis of a design specification document for two signal-management concepts: radio-frequency domain multiplexing (FDM) and time-domain multiplexing (TDM). Both concepts are intended to reduce the required number of cables, and hence background, for TSGe. We are now working to down-select between these technologies.

A depth requirement concern is that of cosmic-ray muons. Double beta decay experiments are conducted deep underground to avoid these muons and any associated particles they may produce, such as neutrons, that may produce background. Hence, an important question for TSGe is how deep underground should the experiment be located to avoid this background. This is a key question for siting TSGe. We have begun preparing a simulation of muon propagation through the Earth and the subsequent particle production. This simulation framework combines particle reaction information and the experiment and the Earth-surface geometry. It is then possible to simulate the interaction of the particles with the experiment and the surrounding rock material. The current status of this analysis is that the experimental geometry has been implemented and the muon distributions at various depths have been simulated. These first results are promising, agreeing with other simulations and are being compared to data from the MJD.

Environmental neutrons can interact with materials and generate radioactive isotopes, which can then decay and produce background for TSGe. Many of these neutrons are produced by cosmic rays and hence the background is depth dependent. Some of these isotopes have a delayed-coincidence signature, allowing us to study and estimate the flux of neutrons in the deep underground environment. We have identified a number of such candidate isotopes and have begun searching for them within the MJD data. Placing constraints on the rate of such isotopes within MJD will permit us to define a depth requirement for TSGe.

The theory effort consists of two components, the calculations of nuclear physics matrix elements relevant to beta decay and double beta decay and the investigation of alternative Beyond-the-Standard-Model (BSM) mechanisms for neutrinoless double beta decay. For the matrix elements we have developed new algorithms to solve for the ground states in medium-mass and heavy nuclei. A paper has been published on this topic. We are presently studying operators relevant to beta decay and double beta decay. Some initial application of this work has been published this year. During the next year we plan to determine if these models adequately reproduce the decay-rate quenching found in essentially all nuclear beta decays, and start initial applications to double beta decay.

In BSM physics, we have investigated alternative new physics that could allow neutrinoless double beta decay. Some of these models are subject to tests in high-energy physics experiments at the LHC, where new particles could be produced directly.

Future Work

In the next fiscal year, we plan to make progress on several separate experimental R&D tasks. We plan to begin use of a new cryostat concept. We plan to make down-select choices within the various possible multiplexing schemes and then test a configuration. We plan to begin using a robot to perform some of the repetitive tasks in detector assessment and plan for future uses. We plan to study improvements in low-radioactivity connectors. We plan to begin analysis of data from a present underground experiment to assess the depth requirement for such experiments.

On the theory front, we will continue our studies on the influence of the axial vector coupling constants on the matrix element for double beta decay. We will also continue the study of other potential influences from particle physics on the double beta decay rate.

Conclusion

Our expected results include assessments of new cryostat designs for Ge detectors, use of robotics in assessing detectors, new data acquisition techniques, understanding the depth requirement for such experiments and key theoretical issues in nuclear and particles physics required to fully understand a measurement of double beta decay.

Cold Cathodes for Next Generation Electron Accelerators: Methodologies for Radically Improving Performance and Robustness

Nathan A. Moody
20150394DR

Introduction

Many grand challenges, including the quest for sustainable energy, continued scaling of computational power, detection and mitigation of pathogens, and study of the structure and dynamics of the building blocks of life require the ability to access, observe, and control matter on the frontier timescale of electronic motion and the spatial scale of atomic bonds. The only instruments with such capability are future coherent x-ray sources and advanced colliders, which demand increasingly high performance electron beams well beyond the present state-of-the-art. The purpose of this project is to address this technology gap and make parallel, transformational advances in the two critical performance areas of an electron source: lifetime and efficiency. Traditional approaches have failed because advances in one of these parameters have come at the expense of the other.

Transformational advance in electron source (cold cathode) performance requires that radical improvements in lifetime and efficiency be achieved simultaneously. Previous work has succeeded in delivering increases in one, but at considerable expense of the other because of the competing physical processes underlying traditional approaches to cathode design and optimization. The unique approach of this project is to decouple the competing mechanisms so that both lifetime and efficiency can be independently and substantially improved. The generalized hypothesis is that lifetime and efficiency of electron sources can be controlled by manipulating nano-scale structure of cathode materials, yielding emergent behavior which radically enhances performance. Our innovative approaches span three thrust areas and share a common theoretical framework: a.) Enhanced performance through nanostructure; b.) Enhanced lifetime through monolayer protective coatings, and c.) Integration of new physics in models, simulations, and technology demonstrations. Our progress to date has validated our research approach, which includes key risk mitigation and supporting engineering efforts.

Benefit to National Security Missions

DOE/DOD/SC/MaRIE

This project represents an enabling technology for existing and future light sources and particle accelerators, including MaRIE, which is intended as a tool to study weapons-relevant materials among others. Light sources and particle accelerators are key to the DOE/SC mission requiring state of the art electron beams for generation of coherent x-ray light as well as all electron-beam-based DOD missions, such a high power free electron lasers and radio frequency source technologies. Improved cold cathodes with controllable parameters allows for higher performance, reduced complexity, reduced cost, and reduced system maintenance in almost every relevant application area. It is directly enabling for all accelerator-based approaches to remote detection of chemicals, pathogens, and nuclear materials . It would benefit accelerator-based solutions for management of nuclear waste as well as the production of critical medical radioisotopes.

The monolayer coatings we employ can potentially be functionalized to act as detectors, of interest to DHS/DHHS, or as a key element in energetic neutral atom imaging for remote space sensing (NASA).

Basic Understanding of Materials

X-ray free electron lasers (X-FELs) are the ideal tool to interrogate, understand, and even control matter in extremes. To date, nineteen Nobel Prizes have been awarded for x-ray science using beam-based x-ray light sources, and we can expect more in the future as these tools open vast science frontiers to probe matter-in-extremes at unprecedented temporal, spatial, and energetic scales. The work represented in this project closes critical technology gaps in the fielding of X-FELs as instruments of discovery science.

Progress

This project is organized around 3 thrust areas, each

described below, and work has progressed on schedule relative to the goals and major milestones associated with each thrust area.

Thrust Area #1: "Controlling and enhancing cold cathode performance through nanostructure."

The unique control over electronic structure and optical dynamics in thin film nanomaterials suggests new methods for improving photoemission performance. We established a reference for comparing our methods and allowing systematic investigation of film composition, guided by our understanding of how composition relates to work function (or Fermi level), absorption cross section, carrier density, and other properties. We commissioned a dedicated electron gun chamber to conduct these studies and started investigating semiconductor nanocrystal quantum dot (QD) films by varying thickness (from 90 – 300nm) and using bare and gold-coated glass substrates. The QD diameter was ~7 nanometers (nm) and the films were made via sequential spin coating, followed by treatments rendering higher conductivity. Initial results using ~50 femtosecond pulsed laser excitation of 266 nm show a photoemission response with a power dependence suggesting that film thickness and charge mobility are important parameters. We began studying the role of ligand-removal, size, and composition variations of QDs, especially as they impact changes in mobility and Fermi levels.

Thrust Area #2: "Enhancing robustness and lifetime using monolayer barrier-shield coatings."

We established synthesis conditions for obtaining both defect-free graphene films (0.5 square cm) using single layer chemical vapor deposition (CVD) growth on Cu substrates and reduced graphene oxide (RGO) transferred and suspended on wire mesh. CVD graphene was grown directly on Cu with different crystal orientations: 100, 110 and 111. Measurements are underway to understand the influence of monoatomic graphene layers on the Cu photoemission processes and comparing to theoretical prediction. We demonstrated key results for multi-layer graphene growth (2-40 atomic layers) by utilizing nickel substrates. The resulting films were transferred to Cu and various wire meshes and the photoemission properties were correlated to thickness of the barrier film. Based on our initial evaluation, both routes (graphene and RGO) yield viable barrier membranes and need to be further optimized. We have focused on mesostructure control of graphene oxide precursors using different solvents, successfully identifying those which yield defect free films. Thin-films have begun gas barrier testing, and we have successfully incorporated monovalent ions (e.g. Na) into the graphitic sheets that impact their structural and photo-emission properties.

Thrust Area #3: "Integration of new physics in models, simulations, and technology demonstrations."

A strong theoretical framework enables understanding of photoexcitation and photoemission from nanostructured materials. Firstly, our density functional models generated exciting theoretical predictions of reduced work functions for specific copper crystal faces coated with monolayer(s) of graphene. These unexpected predictions may have significant impact on accelerators utilizing copper photocathodes. Secondly, we developed a preliminary photoemission simulation tool that assumes single photon excitation and predicts quantum efficiency (QE) for metal nanostructures including their power dependence and Schottky barriers. We used the tool to investigate the influence of plasmonic subwavelength gratings on QE in the low power limit. We found substantially improved QE, attributable primarily to increased photon absorption, but also impacted by surface structure. We began investigating plasmonic field enhancement in various laser and electric field regimes and extend these models to a variety of semiconductor photocathodes.

Regarding our technology demonstration, we have commissioned three separate experimental stations, with targeted experiments in progress on QDs, graphene, graphene oxide, reduced graphene oxide, and indium-gallium-nitride photocathode films. The project has identified key performance parameters specific to the film-on-barrier cathodes (e.g. barrier smoothness and porosity) and demonstrated the ability to simultaneously probe both sides of film-barrier cathode structures. We demonstrated reproducible growth of alkali antimonide photocathodes (QE ~2%), providing an ideal system to explore surface layer protection by nanometer-thick graphene shields (since these films respond to controlled gas contamination). We were able to quantitatively characterize the degradation process of an unprotected photocathode with data agreeing with an emerging surface degradation model, which predicts an exponential decay at a constant pressure. Our rapid design, fabrication and operational testing of the low-voltage DC cathode gun, and its accompanying femtosecond tunable laser source, has led to world-first measurements of electron beams launched from a quantum dot photocathode.

Future Work

Theoretical Framework: Establishing a validated understanding of photoexcitation and photoemission from nanostructured materials using first principles and experimental comparisons.

Goal 1: Understand applicability of existing models

Task: Comparison between families of density functionals

Goal 2: Down-select from among existing models and adapt to include nanostructure

Task: Determine and incrementally implement methods to account for effect of quantum dots, surface plasmonic structures, and monolayer protective coatings

Goal 3: Identify highest priority experimental parameters and measurements

Task: Direct validation of theoretical models using test-case scenario

Thrust Area #1: Controlling and enhancing cold cathode performance through nanostructure

Goal 1: Validation of methods for controlling surface cathode properties

Task: Fabrication and measurement of straightforward, first-generation plasmonic structures on photocathodes, allowing immediate comparison to theory.

Goal 2: Validation of methods for controlling bulk cathode properties

Task: Fabrication and measurement of straightforward, first-generation quantum dot (QD) photocathode samples, allowing immediate comparison to theory.

Thrust Area #2: Enhancing robustness and lifetime using monolayer barrier-shield coatings

Goal 1: Comparison between three primary methods for growing graphene

Task: Determine the advantages of each and degree of control over relevant parameters

Goal 2: Demonstrate transfer of large-area films

Task: Adapt existing glove-box transfer methods to vacuum environment and provide demonstration of prototype coatings

Thrust Area #3: Integration of new physics in technology demonstrations

Goal 1: Specify requirements, functionality, and design of multi-use cathode test environments

Task: Complete of engineering designs for all cathode test hardware, begin procurement/fabrication/assembly, and address any compatibility issues

Goal 2: Prepare existing rudimentary test hardware to scale to project needs

Task: Update/upgrade vacuum system to provide immediate photoemission data from first FY15 samples to accelerate model validation and overall interface between theory and experiment

Conclusion

We will develop and demonstrate 'designer' cold cathode electron sources with tunable parameters (bandgap, efficiency, optical absorption) that outperform present technologies in terms of efficiency and lifetime, where success in either of these is considered transformational. We introduce fundamentally new approaches to address decadal weaknesses in performance and enable cathode properties to be tuned or engineered for specific Department of Energy missions and related applications. This project will specifically yield new understanding of nanoscale structure on cathode performance, new fabrication methodologies, validation of simulation and modeling tools, and prototype demonstrations of novel cold cathodes incorporating these new features.

Publications

Alexander, A., N. A. Moody, and P. Bandaru. Enhanced quantum efficiency of photoelectron emission, through surface textured metal electrodes. Journal of Vacuum Science and Technology A (JVSTA-A-15-292).

Carlsten, B. E, S. J. Russell, J. W. Lewellen, D. C. Nguyen, P. M. Anisimov, C. E. Buechler, K. A. Bishofberger, L. D. Duffy, F. L. Krawczyk, Q. R. Marksteiner, N. A. Moody, N. Yampolsky, and R. L. Sheffield. MaRIE XFEL physics design risks and risk mitigation plans. 2015. Los Alamos National Lab. (LANL), Los Alamos, NM (United States); DOE Contract Number: AC52-06NA25396; LA-UR--15-22069.

Jensen, K. L., N. A. Moody, A. Shabaev, S. G. Lambrakos, D. Finkenstadt, A. Mohite, G. Gupta, and F. Liu. Photoemission from graphene on copper: theory and experiment. To appear in Journal of Applied Physics.

Nuclear Science for Signatures, Energy, Security, Environment

Albert Migliori
20150646DR

Introduction

This project, "Nuclear Science Fellowships for Signatures, Energy, Security, Environment" will support research in nuclear science relevant to Laboratory mission areas by attracting and funding projects of a future generation of scientists and engineers with a high expectation, based on results from previous actinide research projects, of exceptional science and of retaining them as permanent employees. Nuclear science areas include materials, material properties, signatures, modeling, predictions, fabrication, detection, disposal, global security implications, forensics, and the specialized science surrounding actinides and especially plutonium, uranium, and their surrogates as fuels for energy and nuclear weapons. The aim is to advance nuclear science in a comprehensive project that ties targeted research with Los Alamos mission imperatives. The mechanisms for this are support of the research arising from a multi-year broad-based postdoctoral fellows project, and a summer student fellows research project. The project will be administered by the Los Alamos G. T. Seaborg Institute, which is a center for actinide and transactinide science.

An internal cross-institutional LANL advisory committee meets to select Nuclear Science Fellows. Fellow selection is based on the excellence of the science in the proposed projects, the quality of the candidate, and the strategic value of the proposed science. The quality of a candidate is measured by the candidate's transcripts, publication and presentation record, educational background and relevance, and letters of reference. Successful proposals have a clearly defined research proposal that supports nuclear science at the single investigator or small-team level, described in a one-page abstract, and is written by the student and mentor. These research plans address nuclear science topics connected to the objectives of this project and span the strategic breadth of nuclear science at LANL. Postdoctoral fellows work on a project that connects directly to nuclear science and that is not otherwise funded.

Benefit to National Security Missions

Actinide and nuclear science continues to be essential to the U.S. and central to the missions of the DOE and its NNSA laboratories, including nuclear weapons, global security, energy security, nuclear safeguards, nonproliferation, environmental restoration, and radioactive waste management. With nuclear weapons technology continuing to play an enduring role in defense policy for the foreseeable future, knowledge and expertise in the production, processing, purification, characterization, analysis, and disposal of actinide series elements specifically and nuclear materials in general is essential to U.S. national security. Nuclear science and detection technology development is extremely important to nonproliferation and global security. Moreover, the risks of global warming, and the environmentally destructive effects of burning coal are such that nuclear energy is expected to assume a greater role in the nation's electrical energy production in the future.

Of the actinide elements, plutonium, uranium and neptunium are especially important to Los Alamos missions. These elements are of technological and scientific interest largely due to radioactivity and it is this property which makes their study particularly challenging. Special facilities, instrumentation, and training, existing in only a small number of locations worldwide, are required for safe and secure handling of these elements, distinguishing actinide science from most other research. Fundamental actinide and nuclear science provides the technical basis for process and separations chemistry, metallurgy, characterization, and detection related to the national security mission of the Laboratory and the national Integrated Plutonium Science and Research Strategy.

Progress

The scope of this project has been broadened in FY15 from actinide science and research to include nuclear science, research and technology.

There were several notable R&D accomplishments of post-doctoral fellows projects.

- Completed major-element and trace-element analyses of historic Trinity test samples. Developed method for improved measurement of U isotopes in fallout debris using the Los Alamos Cameca ins-1280 secondary ion mass spectrometer and measured U and Pu isotopes in Trinity test samples. Submitted an article for publication on the main formation mechanism of Trinity fallout debris.

- Developed new protocol and containment in order to analyze actinium at Stanford Synchrotron Radiation Lightsource (SSRL) for X-ray Absorption Spectroscopy (XAS) experiment. For the first time, actinium was measured using XAS technique and the first XANES and XAFS were collected for actinium acetate. In conjunction with DFT and molecular dynamics calculations (performed by Justin Wilson and Enrique Batista), EXAFS data analysis is underway. A manuscript is in preparation to communicate these new results.

- Commissioned a new beamline for parasitic data-taking without disturbing other experimental operations. We have explored methods for producing and characterizing actinide samples for optimal use in ultracold neutron experiments. We have built a new sample handling system which reduced contamination. We have placed first limits on the fission cross section at ultracold neutron energies.

- Pure iron and ferritic Fe-9Cr alloys with specific amount of carbon were received and metallurgically prepared. Microstructures were characterized by electron microscopy and electron backscattering diffraction techniques. Actinide-based nuclear fuel materials fabrication initiated.

- Preparation and measurement of 3 dimensional standards for evaluation of analytical capabilities, i.e., limit of detection for the XRF techniques. Publication of manuscript on determination of Pu in spent fuel with high resolution X-ray (McIntosh, et al., Spectrochimica Acta Part B, 2015, doi:10.1016/j.sab.2015.05.014). Publication of manuscript on characterization of Pu in soil samples with multiple XRF techniques (McIntosh, et al., Journal of Analytical Atomic Spectrometry, 2015, doi: 10.1039/C5JA00068H).

- Synthesized single crystals of the following systems: Ce1-xUxMAl4Si2 (M=Rh, Ir), La1-xUxMAl4Si2 (M=Rh, Ir), and U2RhIn8. In La1-xUxMAl4Si2 (M=Rh, Ir) materials, substituting 1, 3, and 5% U for La to characterize energy scale associated with the presence of hybridization between the 5f electron of uranium and the conduction electrons. In the Ce1-xUxMAl4Si2 (M=Rh, Ir), we substituted 5% U for Ce to characterize energy scale associated with removing Ce ions from the lattice, or “Kondo Holes”. Efforts are underway to perform similar measurements on U2-xThxRhIn8 to see how the magnetism changes with Th substitution into U2RhIn8.

- Development of a containment vessel for the study of radioactive materials under pressure in a safe manner has been developed and constructed and safety approval from the Health Physics group at the Argonne National Laboratory Advanced Photon Source has been completed. Demonstration that this system works on a non-hazardous material is complete and analysis of the data is proceeding.

- Designed and arranged the working environment for calorimetric experiment; Performed power-up procedures on the core equipment - calorimeter; set up and calibrated the calorimeter to its best status; worked with mentors on revising IWD for the calorimeter; collaborated on designing necessary parts for accomplishing Pu calorimetric experiments; Contacted potential collaborators in Advanced Photon Source for future material characterization (X-ray adsorption and diffraction).

- Developed a technique to exchange oxygen isotopes with uranium oxide ions by irradiating material dissolved in desired concentrations of isotope water. Multiple steps were used to ensure full exchange, each step replenishing the isotope water with the desired isotope concentration. NMR was used to track exchange of 17O while mass spectroscopy tracks 18O. Upon completion, the water is removed and the resultant powder is heated under nitrogen to produce UO2 powders for analysis.

Future Work

Future R&D tasks for this project include:

- Develop a portable, plasma-based, system for separating and detecting of actinides.

- Chemical and isotopic measurement to understand nuclear fallout formation for nuclear forensics tools

- Understand trivalent actinide chemistry from electronic structure and bonding.

- Utilize extremely low energy “ultracold” neutrons to induce fission in actinides near the material surface

and characterize sputtered materials.

- Explore the ternary U-Si-X, (X=Al and Ti) systems to assess oxidation resistance for accident tolerant fuels in nuclear reactor concepts.
- Investigate the effects of carbon on defects involved in hardening and void swelling in ferritic Fe-Cr alloys under irradiation.
- Enhance detection and characterization of actinides in complex matrices using multiple, complementary, nondestructive analytical methods based on X-ray fluorescence spectrometry.
- Enhance understanding of correlated electron behavior of U-based compounds, to elucidate their exotic ordered states, and to discover new U-based superconductors.
- Validate sole observation of magnetic resonance signature of the 239Pu nucleus.
- Demonstrate potential of magnetic resonance for nondestructive measurements of enrichment levels for nuclear forensics tools.
- Develop methods to understand how actinides form bonds with other elements.
- Observe elastic mechanical properties of actinide and lanthanide compounds at extremes of pressure and temperature.
- Measure thermodynamic parameters for Pu-bearing oxides and alloys, U nitride/carbide, and other related materials to better understand structure-stability relations and complex behavior of 5f electrons in transuranic compounds.
- Develop characterization methods to measure O isotope concentration in UO2, which will then be used to test the feasibility of O isotope forensics.
- Fabricate U and Th nitride nuclear fuels via a novel chemical process, in which the precursors contain a high percentage of nitrogen and undergo combustion to make the nitride material.
- Solution chemistry approaches to explore solid state chemistry of nuclear fuels.
- Observe the effect that Ga has on the oxidation state of δ-Pu with surface electronic studies.

Conclusion

This research aims to accomplish the following:

- Improve our understanding of the electronic structure, phase stability, thermodynamics and thermal properties of nuclear materials and the dynamic behavior of plutonium, uranium, and some of their compounds across pressure, temperature, time, phase space, surfaces and interfaces for nuclear materials.
- Develop advanced chemical separations and synthesis processes and determine their signatures.
- Expand capabilities in detection, measurement, and analysis of signatures of nuclear and radiological materials. Improve understanding of the environmental behavior and signatures of nuclear materials.
- Enhance our understanding of plutonium aging, electronic structure and chemistry with minimal impact from nuclear decay processes.

Publications

(McDonald), J. L. Brown, B. L. Davis, B. L. Scott, and A. J. Gaunt. Comparative structural studies of early lanthanide acetonitrile solvates. Inorganic Chemistry.

(McDonald), J. L. Brown, M. B. Jones, A. J. Gaunt, B. L. Scott, C. E. Macbeth, and J. C. Gordon. Lanthanide(III) di- and tetra-nuclear complexes supported by a chelating tripodal tris(amidate) ligand. 2015. Inorganic Chemistry. 54 (8): 4064.

(McDonald), J. L. Brown, and A. J. Gaunt. Non-aqueous and organometallic chemistry of plutonium. Plutonium handbook: a guide to technology. Edited by Clark, D. L..

Ardeljan, M., R. J. McCabe, I. J. Beyerlein, and M. Knezevic. Explicit incorporation of deformation twins into crystal plasticity finite element models. 2015. Computer Methods in Applied Mechanics and Engineering. 295 (1 Oct): 396.

Barker, B. J., J. Berg, and M. Wilkerson. Visible emission and low-lying LMCT states in Cs2NpO2Cl4. Journal of Chemical Physics.

Bonamici, C. E.. Formation of glassy nuclear fallout: An updated model. Geoghimica et Cosmochimica Acta.

Bonamici, C. E., W. S. Kinman, J. H. Fournelle, M. M. Zimmer, A. D. Pollington, and K. D. Rector. Formation of glassy nuclear fallout: An updated model. To appear in Geochimica et Cosmochimica Acta.

Bonamici, C. E., and W. S. Kinman. Tracking volatility and fractionation in the Trinity fireball through classgy fallout debris. Science.

Bonamici, C. E., and W. S. Kinman. Volatility in the Trinity

fireball as recorded in glass fallout debris. Actinide Research Quarterly.

Ellis, J. K., J. A. Leiding, W. M. Kerling, and A. P. Sattelberger. Novel metal-metal bonding in K[Tc8(μ-I)8I4]. Inorganic Chemistry.

Guo, X., A. Navrotsky, R. K. Kukkadapu, M. Engelhard, A. Lanzirotti, M. Newville, and S. R. Sutton. Structure and thermodynamics of uranium containing garnets. Energy and Environmental Science.

Guo, X., E. Tiferet, Q. Liang, A. Lanzirotti, M. Newville, M. Engelhard, R. K. Kukkadapu, D. Wu, S. R. Sutton, M. Asta, and A. Navrotsky. Structure characteristics and thermodynamic stability of metal monouranates MgUO4, CrUO4, and FeUO4: A combined experimental and theoretical study. Journal of the American Chemical Society.

Guo, X., R. K. Kukkadapu, A. Lanzirotti, M. Newville, S. R. Sutton, and A. Navrotsky. Charge-coupled substituted garnets (Y3-xCa0.5xM0.5x)Fe5O12 (M = Ce, Th): structure and stability as crystalline waste forms. 2015. Inorganic Chemistry. 54 (8): 4156.

Guo, X., S. Szenknect, A. Mesbah, S. Labs, N. Clavier, C. Poinssot, S. V. Ushakov, H. Curtius, D. Bosbach, R. C. Rodney, P. Burns, N. Dacheux, and A. Navrotsky. Thermodynamics of formation of coffinite, USiO4. 2015. Proceedings of the National Academy of Science, USA. 112 (21): 6551.

Hartig, K. C., J. Colgan, D. P. Kilcrease, J. E. Barefield II, and I. Jovanovic. Laser-induced breakdown spectroscopy using mid-infrared femtosecond pulse. 2015. Journal of Applied Physics. 118 (4): 043107.

Jacobsen, J. K., N. Velisavljevic, D. M. Dattelbaum, and R. S. Chellappa. High pressure and temperature equation of state and spectroscopic study of CeO2. Physical Review B.

Jacobsen, M. K., and N. Velisavljevic. Development of a containment setup for radioactive materials in the Paris-Edinburgh press. Review of Scientific Instruments.

Koutroulakis, G., T. Zhou, Y. Kamiya, J. D. Thompson, H. D. Zhou, C. D. Batista, and S. E. Brown. Quantum phase diagram of the S = 12 triangular-lattice antiferromagnet Ba3CoSb2O9. 2015. Physical Review B. 91: 024410.

Lichtscheidl, A. G., B. L. Scott, A. T. Nelson, and J. L. Kiplinger. Convenient and green synthetic methods to uranium(III) and uranium(IV) halide pyridyl starting materials. Green Chemistry.

Lichtscheidl, A. G., J. K. Pagano, B. L. Scott, A. T. Nelson, and J. L. Kiplinger. Expanding the chemistry of actinide metallocene bromides. Synthesis, properties and molecular structures of the tetravalent and trivalent uranium bromide complexes: (C5Me4R)2UBr2, (C5Me4R)2U(O-2,6-iPr2C6H3)(Br), and [K(THF)] [(C5Me4R)2UBr2] (R = Me, Et). Inorganics.

Lichtscheidl, A. G., K. P. Browne, M. J. Monreal, D. E. Morris, B. L. Scott, A. Nelson, and J. L. Kiplinger. Synthesis, reactivity, spectroscopic and electrochemical characterization of uranium(III) organometallic complexes. Organometallics.

Lichtscheidl, A. G., M. T. Janicke, B. L. Scott, A. T. Nelson, and J. L. Kiplinger. Syntheses, structures, and 1H, 13C{1H} and 119Sn{1H} NMR chemical shifts of a family of trimethyltin alkoxide, amide, halide and cyclopentadienyl compounds . 2015. Dalton Transactions. 44: 16156.

Loble, M., J. M. Keith, A. B. Altman, S. C. E. Stieber, E. R. Batista, K. S. Boland, S. Conradson, D. L. Clark, J. L. Pacheco, S. A. Kozimor, R. L. Martin, S. G. Minasian, A. C. Olson, B. L. Scott, D. K. Shuh, T. Tyliszczak, M. P. Wilkerson, and R. A. Zehnder. Covalency in lanthanides. An x-ray absorption spectroscopy and density functional theory study of LnCl6x-(x = 3,2). 2015. Journal of the American Chemical Society. 137: 2506.

Macor, J. A., J. L. Brown, J. N. Cross, S. R. Daly, A. J. Gaunt, G. S. Girolami, M. T. Janicke, S. A. Kozimor, M. P. Neu, A. C. Olson, S. D. Reilly, and B. L. Scott. Coordination chemistry of 2,2'-biphenylenedithiophosphinate and diphenyldithiophosphinate with U, Np, and Pu. To appear in Dalton Transactions.

McIntosh, K. G., N. L. Cordes, B. M. Patterson, and G. J. Havrilla. Laboratory-based characterization of plutonium in soil particles using micro-XRF and 3D confocal XRF. 2015. Journal of Analytical Atomic Spectrometry. 30: 1511.

McIntosh, K. G., N. L. Cordes, B. M. Patterson, and G. J. Havrilla. Laboratory-based characterization of plutonium in soil particles using micro-XRF and 3D confocal XRF. 2015. Journal of Analytical Atomic Spectroscopy. 30: 1511.

McIntosh, K. G., S. D. Reilly, and G. J. Havrilla. Determination of plutonium in spent nuclear fuel using high resolution X-ray. 2015. Spectrochimica Acta Part B: Atomic Spectroscopy. 110: 91.

McIntosh, K. G., S. D. Reilly, and G. J. Havrilla. Determination of plutonium in spent nuclear fuel using high resolution X-ray. 2015. Spectrochimica Acta Part B: Atomic Spectroscopy. 110: 91.

Radchenko, V., J. W. Engle, J. J. Wilson, J. R. Maasen, F. M. Nortier, W. A. Taylor, E. R. Birnbaum, L. A. Hudston, K. D. John, and M. E. Fassbender. Application of ion exchange and extraction chromatography to the separation of actinium from protron-irradiated thorium metal for analytical purposes. 2015. Journal of Chromatography A. 2015 (1380): 55.

Radchenko, V., J. W. Engle, J. J. Wilson, J. R. Maassen, F. M. Nortier, E. R. Birnbaum, K. D. John, and M. E. Fassbender. Production yields and chromatographic separation of protactinium isotopes formed in protron-irradiated thorium metal. Journal of Chromatography A.

Rusev, G., A. R. Roman, J. K. Daum, R. K. Springs, E. M. Bond, M. Jandel, B. Baramsai, T. A. Bredeweg, A. Couture, A. Favalli, K. D. Ianakiev, M. L. Illiev, S. Mosby, J. L. Ullmann, and C. L. Walker. Fission-fragment detector for DANCE based on thin scintillating films. To appear in Nuclear Instruments & Methods in Physics Research Section A: Accelerators, Spectrometers, Detectors and Associated Equipment.

Rusev, G., M. Jandel, B. Baramsai, E. M. Bond, T. A. Bredeweg, A. Couture, J. K. Daum, A. Favalli, K. D. Ianakiev, M. L. Iliev, S. Mosby, A. R. Roman, R. K. Springs, J. L. Ullmann, and C. L. Walker. Development of a thin scintillation films fission-fragment detector and a novel neutron source. 2015. SPIE ProceedingsSPIE Proceedings. 9593.

Sooby, E. S., A. T. Nelson, J. T. White, and P. M. McIntyre. Measurements of the liquidus surface and solidus transitions of the NaCl-UCl3 and NaCl-UCl3-CeCl3 phase diagrams. 2015. Journal of Nuclear Materials. 466 (November): 280.

Tamasi, A. L., K. S. Boland, K. Czerwinski, J. K. Ellis, S. A. Kozimor, R. L. Martin, A. L. Pugmire, D. Reilly, B. L. Scott, A. D. Sutton, G. L. Wagner, J. R. Walensky, and M. P. Wilkerson. Oxidation and hydration of U3O8 materials following controlled exposure to temperature and humidity. 2015. Analytical Chemistry. 87 (8): 4210.

Wilson, J. J., B. J. Barker, M. Ferrier, E. R. Batista, M. P. Wilkerson, J. M. Berg, S. A. Kozimor, K. D. John, J. W. Engle, and E. R. Birnbaum. Interactions of M3+ ions with Ds-DOTAM, a flouorescet macrocyclic ligand. Inorganica Chimica Acta.

Wilson, J. J., E. R. Birnbaum, E. R. Batista, R. L. Martin, and K. D. John. Synthesis and characterization of nitrogen-rich macrocyclic ligands and an investigation of their coordination chemistry with lanthanum(III). 2015. Inorganic ChemistryInorganic Chemistry. 54 (1): 97.

Wood, E. S., S. S. Parker, A. T. Nelson, and S. A. Maloy. MoSi2 oxidation in 670-1498 K water vapor. To appear in Journal of the American Ceramic SocietyJ.

Peta-scale Studies of Cosmic Explosions and Supernova Shock Breakout with Palomar Transient Factory

Przemyslaw R. Wozniak
20130030DR

Abstract

Time-domain astronomy and the science of cosmic explosions are currently at the forefront of modern astrophysics. The next generation Palomar Transient Factory (iPTF) and its successor project, the Zwicky Transient Facility (ZTF), are poised to revolutionize the field, but they require transformational advances in peta-scale data processing, as well as a comprehensive theory program. The main science goals of this multi-disciplinary LDRD project aimed to address the most pressing issues in modern data intensive sky surveys.

The most significant accomplishment of this project was the development and operation of the online transient selection system based on state of the art machine learning approach that relies on random forest and sparse representation algorithms. Our research and development program coupled observation, large-scale data processing, and computing technology with theory and simulation to uncover thousands of cosmic explosions. These discoveries and observations were used to explain the underlying physical mechanisms and contributed to more than three dozen refereed publications. The two most notable discoveries are: 1) observation of an early ultraviolet excess emission in supernova iPTF14atg that supports single degenerate scenario (with only one white dwarf object) in a least some type Ia supernovae; and 2) discovery of ASAS-SN-15lh, the most luminous supernova recorded in history.

We also carried out extensive radiation hydrodynamics calculations of transient emission from hot shocks over a wide range of astrophysical scenarios to help interpret observations, inform transient classifiers, and test physics code performance in a critically important range of physical conditions. The results of this project benefit two major areas of the national security mission through development and testing of advanced technologies for Global Security and simulation codes for the Weapons Program.

Background and Research Objectives

The next generation Palomar Transient Factory (iPTF) and its successor, the Zwicky Transient Facility (ZTF) are poised to revolutionize the field of time-domain astrophysics. PTF and ZTF have emerged as world leaders in the exploration of cosmic explosions such as supernovae (SN) and the most successful precursors to Large Synoptic Survey Telescope (LSST)---the first multi-Petabyte time-resolved sky survey scheduled to begin operations in 2022. iPTF is hosted on the 48-inch Schmidt telescope at Palomar (P48) and continuously surveys 8000 square degrees of sky on a 5-day cadence. In order to succeed, these data intensive surveys must promptly identify actionable information from the torrent of imaging data, classify emerging events, and obtain detailed follow-up observations using limited resources around the world and in space. They also require transformational advances in big data processing as well as a comprehensive theory program. In August 2013, under the leadership of our project team, LANL became a full institutional member of the iPTF Consortium of about half a dozen international partners led by California Institute of Technology.

Our multi-disciplinary LDRD project was conceived to address the needs of modern data intensive sky surveys and had three tightly interconnected major science goals: 1) conduct the first deep photometric search for supernova shock breakout events and other explosive phenomena on time-scales of less than a day; 2) perform extensive radiation hydrodynamics simulations and theoretical modeling to understand the physics of transients observed by time-domain surveys; 3) develop novel algorithms and computing capabilities that support real-time selection of astrophysical transients and optimization of follow-up observations based on machine learning algorithms.

The current-generation data intensive sky surveys searching for low probability explosive events produce data streams in which false positive detections due to

various artifacts and poorly controlled experimental factors outnumber real detections by several orders of magnitude. To address this challenge, we set out to develop an autonomous event broker that integrates cutting edge machine learning algorithms with high performance computing infrastructure. Given new iPTF capabilities we placed a major emphasis on studies of supernova shock breakout. After the initial collapse of the progenitor star, the shock wave that eventually disrupts the entire star and produces a core collapse supernova bounces off the dense core and propagates through outer layers of the star. As the shock breaks out of the stellar surface, it produces a bright flash prior to the main supernova event that can be detected as excess blue emission in visual band pass. Our plan was to observe up to half dozen such events in three years. We also anticipated discoveries of several thousand new transients from the comprehensive search.

We also planned to carry out extensive radiation hydrodynamics calculations of transient emission from hot shocks over a wide range of astrophysical scenarios to interpret observations from both iPTF and future experiments, inform transient classifiers, and test the performance of radiative transport simulation codes in a critically important range of physical conditions. Our goal was to build and publish a suite of approximately 100 explosion models with time-resolved spectra and synthetic light curves at about 100 epochs. A detailed comparison of these models with observed light curves provides valuable constraints on the structure of the supernova progenitor stars and lead to a better understanding stellar deaths and the physics of matter under extreme conditions.

Scientific Approach and Accomplishments

Drawing on unique capabilities across LANL, we conducted a comprehensive research and development program that coupled observation with theory, simulation, and computing technology to discover cosmic explosions and explain their mechanisms. Our project team contributed to a total of 41 refereed publications (32 published and 9 submitted) with about equal balance between theory/simulation and observations/data mining. This includes 3 papers in high impact journals Nature and Science (1 Nature paper published, 1 submitted to Nature and 1 to Science). We also co-authored nearly 200 short communications (Astronomers Telegrams a.k.a ATel). Senior investigators on the project delivered 16 presentations, about half of them were invited. In November 2013, in Santa Fe, NM we hosted a hugely successful 3rd edition of the "Hotwiring Transient Universe" workshop attended by over 80 participants representing leading forces in time-domain astrophysics. In recognition of our contributions to iPTF, our machine learning team was included in a prestigious "Builder's List" for iPTF, one of the key documents compiled for any major sky survey that codifies the most important credits. The remaining paragraphs of this section address the most important elements of our scientific approach and the corresponding results and accomplishments.

The most significant accomplishment of this project was the development and operation of the online transient selection system. We adopted a state of the art approach based on direct image differencing (Figure 1).

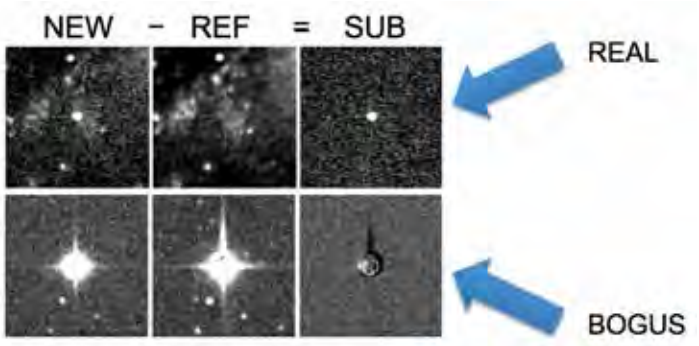

Figure 1. Selection of transient variability of astrophysical origin in optical images of the sky using direct pixel-by-pixel subtration. After a sophisticated preprocessing to match the point spread function of the new science image (left), the reference image (center) is subtracted to obtain the uncluttered difference image (right). A real transient (upper row) has the appearance consistent with the point spread function. However, candidate detections from data intensive sky surveys are dominated by a variety of false positives including saturation trails (bottom row).

The key innovation here was an automated classification engine for separating real transients from bogus detections based on the random forest algorithm in which a collection of randomized (and therefore de-correlated) decision trees is used in a voting scheme to label incoming candidate objects. Using sparse representations with learned dictionaries to provide additional image based features combined with the decision forest framework, we improved the figure of merit (missed detection rate at 1% false positives rate) by a factor of 2 compared to the system previously employed by PTF (Figure 2). This system also incorporates online learning, i.e. it autonomously adapts as more data becomes available. To our knowledge it is the first such system deployed on a live data stream in astronomy. LANL software has been deployed at NERSC supercomputing center since July 2013. As of September 2015 our transient selection software has been licensed to two different collaborations: iPTF and All Sky Automated Survey for Supernovae (ASAS-SN). We also developed automated classification algorithms for SN spectra with signal-to-noise ratio (SNR), sampling, and wavelength coverage corresponding to the specification of SEDMachine, a new iPTF instrument currently in commissioning. Tests on simulated

data achieved unprecedented 95% classification accuracy at SNR = 15 per pixel. The classifier can also be used to identify very young supernovae.

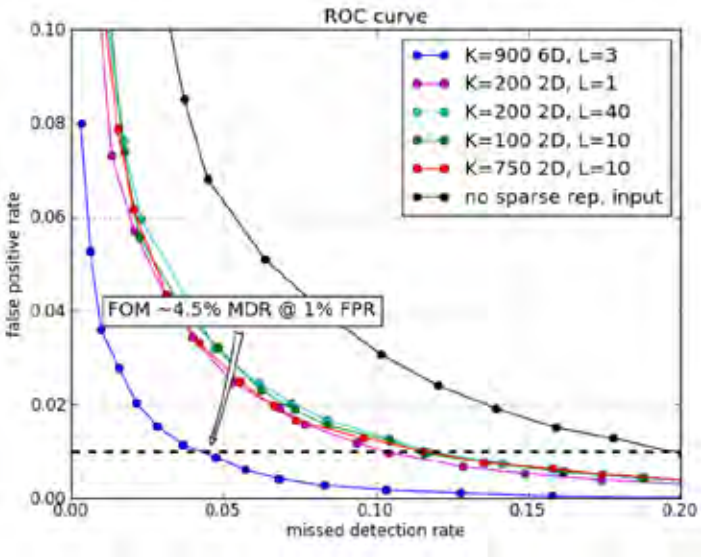

Figure 2. Performance of the LANL transient selection system in various configurations. The figure of merit (FOM) is defined as the rate of missed detections for a fixed false positive rate of 1%. This corresponds to the intersection between the receiver operating characteristic (ROC) curve for a given algorithm and a threshold at 0.01. The best performing LANL solution achieves FOM = 4.5%, more than a factor of 2 better than a competing algorithm that does not include machine learned features.

These decision support tools have enabled discovery of more than 10,000 named iPTF transients, including 851 confirmed supernovae (others awaiting confirmation), mostly type-Ia, but also 215 type-II and 80 type-Ibc. Many exotic transients have been identified, including 62 active galactic nuclei, 20 super-luminous supernovae, 3 tidal disruption flares, 15 cataclysmic variable outbursts, 8 GRB afterglows, and 1 calcium-rich transient that likely represents a new class. It is anticipated that ~1300 confirmed supernovae will be identified by the end of the project. Follow-up observations with the instruments onboard the Swift satellite were triggered for 35 transients, approximately 12 of which were detected in UV and resolved in time by the UVOT instrument. Six events have demonstrated some aspect of shock breakout and propagation with the corresponding analysis is presented in dedicated publications. Nearly 200 additional supernovae have been found by ASAS-SN collaboration using our software. Two of the above discoveries are having a particularly high scientific impact. The first is the observation of an early ultraviolet excess emission in supernova iPTF14atg that is best interpreted as the interaction of the material ejected by the explosion with a companion star. This provides evidence that at least some type Ia supernovae occur in binary systems with a single degenerate object (white dwarf), and against the competing double degenerate scenario [1]. The second is the discovery of ASAS-SN-15lh, the most luminous supernova recorded in history [2].

A distributed event broker architecture that supports automated inference of transient classifications has been developed and implemented (with the exception of the actual follow-up algorithm). The top level view of the system is shown in Figure 3. The system includes a selection of classification algorithms: Bayesian belief networks, support vector machines, random forest (decision trees), and sparse representations with learned dictionaries. The system can now be connected to data streams from Thinking Telescopes at LANL and high-energy transient localizations from Gamma-ray Burst Coordinates Network. Monte-Carlo simulations of real-time transient detections have demonstrated that the distributed event broker can accept input and process spatial and temporal cross correlations at a rate of 1 transient per second. This is more than sufficient for ZTF and we expect the system to be scalable to the LSST regime (10 times higher event rate).

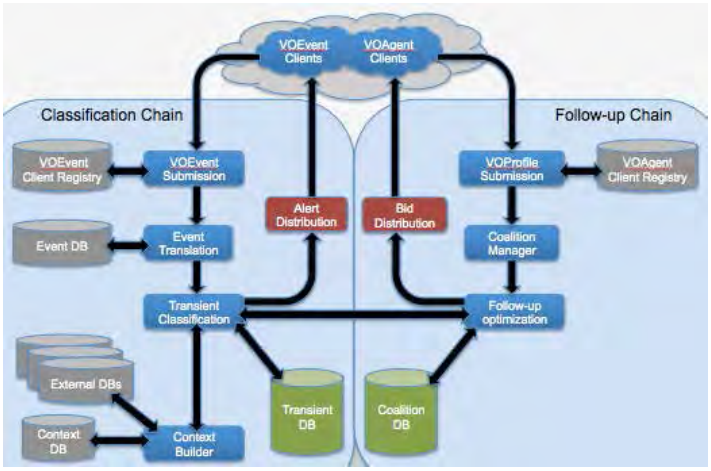

Figure 3. Top level architecture of the real time event broker. The role of the event classification engine (left) is to correlate new incoming observations with historical context, classify events, and alert subscribers about interesting changes. The role of the response optimization engine (right) is to coordinate follow-up observations given limited resources.

The project performed new opacity calculations and incorporated new physics into the simulation codes ([3] and Figure 4). The process of running grids of radiation hydrodynamics models and post-processing in the SPECTRUM framework has been automated. A new public user interface (supernova.lanl.gov) allows plotting multiple models and user data for a chosen scenario as well as tracking supernova emissions over time. Users can obtain publication quality plots and metadata of both time resolved spectra and light curves. 60 models are currently available.

Each model provides broad band spectra extending from radio frequency to gamma ray energies sampled at approximately 200 epochs. An important milestone was the study of the effects of the thickness of the hydrogen envelope on supernova shock breakout and observed light curves [4]. The timing and strength of the shock breakout flash relative to the main peak of the supernova emission turns out to be very sensitive to the mass of the envelope (Figure 5). As more and more mass is removed (plotted color moving from purple to red), the star becomes smaller, the breakout flash comes sooner, and the maximum brightness drops dramatically.

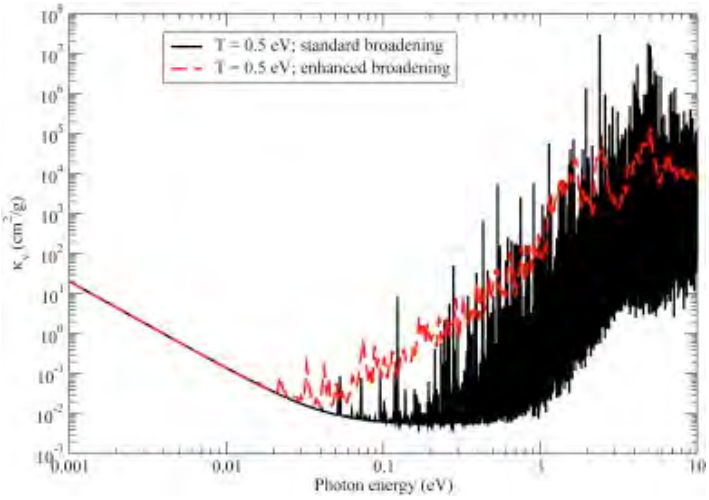

Figure 4. Monochromatic opacity of samarium (Sm, Z=62) over a broad range of photon energies. Our new local thermodynamic equilibrium (LTE) calculations show that line-rich spectra of heavier elements such as lanthanides increase the opacity in the visual and infra-red range by several orders of magnitude. The effect strongly impacts theoretical predictions of the electromagnetic emission from neutron star mergers widely anticipated to become the first directly detected gravitational wave (GW) sources. Early detection of optical counterparts to GW sources is currently a topic of intense interest both at LANL and across the astrophysics community.

The work on data intensive computing led to the development of a new distributed database architecture and working prototype for time-resolved photometric measurements from massive sky monitoring surveys. The data is partitioned according to the Quad Tree Cube (Q3C) indexing scheme that allows rapid storage and retrieval of measurements covering a random patch of sky. Physical storage is then mapped to a set of PostgreSQL database servers, each holding a fixed set of Q3C cells. The cells have fuzzy edges, i.e. measurements near their edges are replicated in neighboring cells, so that the data can be clustered and queried locally, without crossing server boundaries. This allows a linear scaling for the most time-consuming data manipulation tasks. We also invented a progressive hierarchical clustering algorithm for building long photometric time histories that does not require issuing unique object identifiers or frequent updates. This eliminates a very constraining performance bottleneck and the need for cumbersome book keeping. These results were presented at the Databases in Networked Information Systems 2014 workshop in Aizu, Japan.

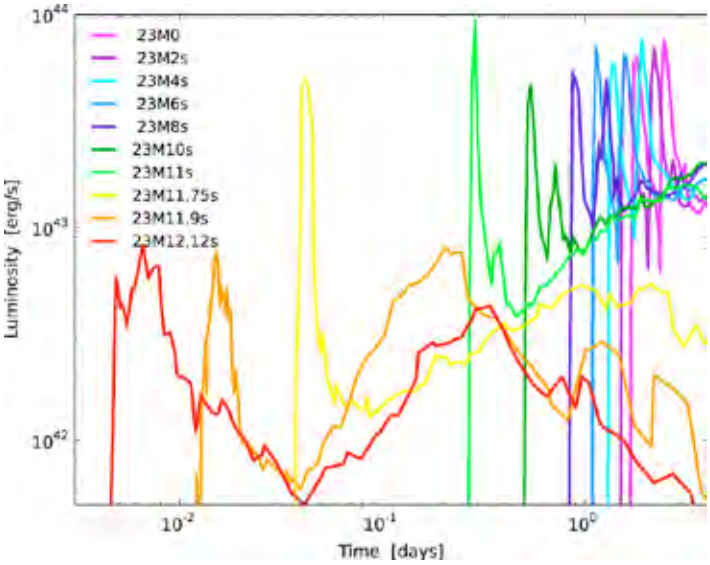

Figure 5. Time dependence of optical emission at shock breakout during a simulated supernova explosion. The progenitor is a massive star with the mass 23 times that of the Sun. Color coded lines correspond to different masses of the hydrogen-rich envelope material that was lost prior to the explosion. LANL simulations such as these allow observers to interpret the relative timing and strength of the shock breakout peak in relation to the main supernova light curve for transients detected by astrophysical time-domain surveys.

We also developed a new hierarchical pixel-level indexing scheme for sky monitoring images called Spherical-cube Quad-tree Unique ID (SQUID). SQUID maps patches of sky to integers in a way consistent with low level storage access patterns. Our reference implementation LibSQUID also supports very fast quad-cube map projections for resampling pixelated images to an efficient format and was released in public domain on GitHub (libsquid.github.io). Another technology product we expect to provide a lasting value is the distributed data storage and manipulation system (for both large-volume data and simulation outputs) based on web access protocols. The system currently supports online data access to Dark Sky Simulations (55 Terabytes of data), the first publicly released trillion particle cosmological N-body simulation.

Impact on National Missions

In the context of national security missions, the main focus of this project was to build new astro-informatics competency to address growing needs in Space Situational Awareness (SSA), develop new capabilities for the Weap-

ons Program, and test them using actual observations. In the process we also helped to facilitate hiring of three postdocs and five students, with one postdoc and one student converted to LANL staff members.

The image-based transient selection and spectral classification tools developed by our team will become a permanent addition to LANL SSA capabilities. To address the formidable complexity of optimizing the custody of resident space objects, we also developed a simulation toolbox for evaluating the relative merits of various observing strategies in detecting anomalous behaviors of Earth satellites. The software maintains a set of simulated orbits and predicts viewing conditions for satellites given the position of the Sun and a network of observatories placed around the globe. We used this framework to simulate interesting orbital anomalies and simple yet realistic collaborative and non-collaborative follow-up response scenarios. Our preliminary results indicate that our proposed coordinated observing approach (Dynamic Coalition Architecture) provides a substantial advantage over the un-coordinated approach with each telescope separately optimizing its own schedule. In the future, our statistical SSA simulation toolbox can be used to study a wide range of scenarios and telescope networking strategies.

Our detailed models of supernova shock breakout and other explosive transients were used to test Advanced Simulation and Computing (ASC) capabilities in the critically important regime at the transition between diffusion and free streaming using both flux diffusion and implicit Monte Carlo codes. New state of the art plasma opacity calculations for heavier elements such as lanthanides (Figure 4) completed over the course of this project will permanently enhance the physics simulation tools at the disposal of the Weapons Program at LANL.

Our novel SSA approach has been presented to numerous sponsors within the Department of Defense and other WFO organizations attracting significant attention each time. These program development efforts are already beginning to pay off with $250,000 of funding from a WFO sponsor in FY2015. This project also positioned us for a future role in the Zwicky Transient Facility (ZTF) and the Large Synoptic Survey Telescope (LSST) surveys as well as new opportunities for a major involvement in NASA missions and dark energy investigations identified in the strategic plan of the DOE Office of Science.

References

1. Cao, Y., S. R. Kulkarni, S. Valenti, D. A. Howell, I. Arcavi, J. Johansson, R. Amanullah, A. Goobar, J. Sollerman, F. Taddia, A. Gal-Yam, A. Horesh, I. Sagiv, S. B. Cenko, M. M. Kasliwal, P. E. Nugent, J. Surace, P. R. Wozniak, D. I. Moody, U. D. Rebbapragada, and B. D. Bue. Ultraviolet Radiation from Supernova-Companion Collision in a Type Ia Supernova . 2015. Nature. 521 (7552): 328.
2. Dong, S., B. J. Shappee, J. L. Prieto, S. W. Jha, K. Z. Stanek, T. W. Holoien, C. S. Kochanek, T. A. Thompson, N. Morrell, I. B. Thompson, U. Basu, J. F. Beacom, D. Bersier, J. Brimacombe, J. S. Brown, P. Chen, E. Conseil, A. B. Danilet, E. Falco, D. Grupe, S. Kiyota, G. Masi, B. Nicholls, F. Olivares, G. Pignata, G. Pojmanski, G. V. Simonian, D. M. Szczygiel, and P. R. Wozniak. ASASSN-15lh: The Most Luminous Supernova Ever Discovered. 2015. ArXiv e-prints.
3. Fontes, C. J., C. L. Fryer, A. L. Hungerford, P. Hakel, J. Colgan, D. P. Kilcrease, and M. E. Sherrill. Relativistic opacities for astrophysical applications. 2015. High Energy Density Physics. 16: 53.
4. Bayless, A. J., W. Even, L. H. Frey, C. L. Fyer, P. W. A. Roming, and P. A. Young. The Effects on Supernova Shock Breakout and Swift Light Curves Due to the Mass of the Hydrogen-Rich Envelope. 2015. The Astrophysical Journal. 805 (2): 98.

Publications

Barth, A. J., A. Voevodkin, D. J. Carson, and P. Wozniak. A Search for Optical Variability of Type 2 Quasars in SDSS Stripe 82. 2014. The Astronomical Journal. 147 (1): 12.

Bayless, A. J., T. A. Pritchard, P. W. A. Roming, P. Kuin, P. J. Brown, M. T. Botticella, M. Dall'Ora, L. H. Frey, W. Even, C. L. Fryer, J. R. Maund, and M. Fraser. The Long-lived UV "Plateau" of SN 2012aw. 2013. The Astrophysical Journal. 764: L13.

Bayless, A. J., W. Even, L. H. Frey, C. L. Fyer, P. W. A. Roming, and P. A. Young. The Effects on Supernova Shock Breakout and Swift Light Curves Due to the Mass of the Hydrogen-Rich Envelope. 2015. The Astrophysical Journal. 805 (2): 98.

Bellm, E. C., N. M. Barriere, Bhalerao, S. E. Boggs, S. B. Cenko, F. E. Christensen, W. W. Craig, Forster, C. L. Fryer, C. J. Hailey, F. A. Harrison, Horesh, Kouveliotou, K. K. Madsen, J. M. Miller, E. O. Ofek, D. A. Perley, V. R. Rana, S. P. Reynolds, Stern, J. A. Tomsick, and W. W. Zhang. X-RAY SPECTRAL COMPONENTS OBSERVED IN THE AFTERGLOW OF GRB 130925A. 2014. ASTROPHYSICAL JOURNAL LETTERS. 784 (2).

Cao, Y., S. R. Kulkarni, S. Valenti, D. A. Howell, I. Arcavi, J. Johansson, R. Amanullah, A. Goobar, J. Sollerman, F. Taddia, A. Gal-Yam, A. Horesh, I. Sagiv, S. B. Cenko, M. M. Kasliwal, P. E. Nugent, J. Surace, P. R. Wozniak, D. I. Moody, U. D. Rebbapragada, and B. D. Bue. Ultraviolet Radiation from Supernova-Companion Collision in a

Type Ia Supernova . 2015. Nature. 521 (7552): 328.

Dong, S., B. J. Shappee, J. L. Prieto, S. W. Jha, K. Z. Stanek, T. W. Holoien, C. S. Kochanek, T. A. Thompson, N. Morrell, I. B. Thompson, U. Basu, J. F. Beacom, D. Bersier, J. Brimacombe, J. S. Brown, P. Chen, E. Conseil, A. B. Danilet, E. Falco, D. Grupe, S. Kiyota, G. Masi, B. Nicholls, F. Olivares, G. Pignata, G. Pojmanski, G. V. Simonian, D. M. Szczygiel, and P. R. Wozniak. ASASSN-15lh: The Most Luminous Supernova Ever Discovered. 2015. ArXiv e-prints.

Fontes, C. J., C. L. Fryer, A. L. Hungerford, P. Hakel, J. Colgan, D. P. Kilcrease, and M. E. Sherrill. Relativistic opacities for astrophysical applications. 2015. High Energy Density Physics. 16: 53.

Frey, L. H., W. Even, D. J. Whalen, C. L. Fryer, A. L. Hungerford, and C. J. Fontes. The Los Alamos Supernova Lightcurve Project: Computational Methods. 2014. The Astrophysical Journal Supplement. 204: 16.

Frey, L., C. Fryer, and P. Young. Can Stellar Mixing Explain the Lack of Type Ib Supernovae in Long-duration Gamma-Ray Bursts?. 2013. The Astrophysical Journal Letters. 773: L7.

Fryer, C.. Compact Object Formation and the Supernova Explosion Engine. 2013. Classical and Quantum Gravity. 30 (24): 244002.

Fryer, C. L., W. Even, B. W. Grefenstette, and T. W. Wong. Observational constraints of stellar collapse: Diagnostic probes of nature's extreme matter experiment. 2014. AIP Advances. 4 (4): 041014.

Holoien, T. W., C. S. Kochanek, J. L. Prieto, K. Z. Stanek, S. Dong, B. J. Shappee, D. Grupe, J. S. Brown, U. Basu, J. F. Beacom, D. Bersier, J. Brimacombe, A. B. Danilet, E. Falco, Z. Guo, J. Jose, G. J. Herczeg, F. Long, G. Pojmanski, G. V. Simonian, D. M. Szczygiel, T. A. Thompson, J. R. Thorstensen, and P. R. Wozniak. Six Months of Multi-Wavelength Follow-up of the Tidal Disruption Candidate ASASSN-14li and Implied TDE Rates from ASAS-SN. 2015. ArXiv e-prints.

Hsiao, E. Y., M. A. Nyothers, P. W. Wozniak, and O. Yaron. Strong near-infrared carbon in the Type Ia supernova iPTF13ebh . 2015. Astronomy and Astrophysics. 578: A9.

Jin, Z. P., S. Covino, M. Della Valle, P. Ferrero, D. Fugazza, D. Malesani, A. Melandri, E. Pian, R. Salvaterra, D. Bersier, S. Campana, Z. Cano, A. J. Castro-Tirado, P. D'Avanzo, J. P. U. Fynbo, A. Gomboc, J. Gorosabel, C. Guidorzi, J. B. Haislip, J. Hjorth, S. Kobayashi, A. P. LaCluyze, G. Marconi, P. A. Mazzali, C. G. Mundell, S. Piranomonte, D. E. Reichart, R. Sanchez-Ramirez, R. J. Smith, I. A. Steele, G. Tagliaferri, N. R. Tanvir, S. Valenti, S. D. Vergani, T. Vestrand, E. S. Walker, and P. Wozniak. GRB 081007 and GRB 090424: The Surrounding Medium, Outflows, and Supernovae. 2013. The Astrophysical Journal. 774: 114.

Johnson, J., D. Whalen, W. Even, C. Fryer, A. Heger, J. Smidt, and K. J. Chen. The Biggest Explosions in the Universe. 2013. The Astrophysical Journal. 775: 107.

Khazov, D., O. Yaron, A. Gal-Yam, I. Manulis, A. Rubin, S. R. Kulkarni, I. Arcavi, M. M. Kasliwal, E. Ofek, Y. Cao, D. Perley, J. Sollerman, A. Horesh, M. Sullivan, A. V. Filippenko, P. E. Nugent, D. A. Howell, S. B. Cenko, J. M. Silverman, H. Ebeling, F. Taddia, J. Johansson, R. R. Laher, J. Surace, U. D. Rebbapragada, and P. R. Wozniak. Flash Spectroscopy: Emission Lines from the Ionized Circumstellar Material around < 10-Day-Old Type II Supernovae. The Astrophysical Journal.

Ofek, E., A. Zoglauer, S. Boggs, N. Barriere, S. Reynolds, C. Fryer, F. Harrison, S. Cenko, S. Kulkarni, A. Gal-Yam, I. Arcavi, E. Bellm, J. Bloom, F. Christensen, W. Craig, W. Even, A. Filippenko, B. Grefenstette, C. Hailey, R. Laher, K. Madsen, E. Nakar, P. Nugent, D. Stern, M. Sullivan, J. Surace, and W. Zhang. SN 2010jl: Optical to hard X-ray observations reveal an explosion embedded in a ten solar mass cocoon. 2014. The Astrophysical Journal. 781 (1): 420.

Palaversa, L., Z. Ivezic, L. Eyer, D. Ruzdjak, D. Sudar, M. Galin, A. Kroflin, M. Mesaric, P. Munk, D. Vrbanec, H. Bozic, S. Loebman, B. Sesar, L. Rimoldini, N. Hunt-Walker, J. VanderPlas, D. Westman, S. J. Stuart, A. Becker, G. Srdoc, P. Wozniak, and H. Olusei. Exploring the Variable Sky with LINEAR. III. Classification of Periodic Light Curves. 2013. The Astronomical Journal. 146: 101.

Panaitescu, A.. Optical Flashes from Internal Pairs Formed in Gamma-Ray Burst Afterglows. 2015. apj. 806: 64.

Panaitescu, A., W. T. Vestrand, and P. Wo'zniak. Peaks of optical and X-ray afterglow light curves. 2013. mnras. 433: 759.

Panaitescu, A., W. T. Vestrand, and P. Wo'zniak. ''Self-absorbed'' GeV Light Curves of Gamma-Ray Burst Afterglows. 2014. apj. 788: 70.

Panaitescu, A., and T. Vestrand. Synchrotron and Inverse-Compton Emissions from Pairs Formed in GRB Afterglows (Analytical Treatment). 2014. The Astrophysical Journal. 793: 104.

Pastorello, A., J. L. Prieto, N. Elias-Rosa, D. Bersier, G. Hosseinzadeh, A. Morales-Garoffolo, U. M. Noebauer, S. Taubenberger, L. Tomasella, C. S. Kochanek, E. Falco, U. Basu, J. F. Beacom, S. Benetti, J. Brimacombe, E. Cappellaro, A. B. Danilet, S. Dong, J. M. Fernandez, N. Goss, V. Granata, A. Harutyunyan, T. W. Holoien, E. E.

Ishida, S. Kiyota, G. Krannich, B. Nicholls, P. Ochner, G. Pojma'nski, B. J. Shappee, G. V. Simonian, K. Z. Stanek, S. Starrfield, D. Szczygiel, L. Tartaglia, G. Terreran, T. A. Thompson, M. Turatto, R. M. Wagner, W. S. Wiethoff, A. Wilber, and P. R. Wo'zniak. Massive stars exploding in a He-rich circumstellar medium - VII. The metamorphosis of ASASSN-15ed from a narrow line Type Ibn to a normal Type Ib Supernova. 2015. mnras. 453: 3649.

Rubin, A., A. Gal-Yam, A. De Cia, A. Horesh, D. Khazov, E. O. Ofek, I. Manulis, O. Yaron, P. Vreeswijk, S. Ben-Ami, S. R. Kulkarni, D. A. Perley, Y. Cao, M. M. Kasliwal, S. B. Cenko, D. Xu, A. V. Filippenko, J. S. Bloom, K. I. Clubb, P. Nugent, Y. C. Pan, J. M. Silverman, C. Badenes, I. Arcavi, D. A. Howell, S. Valenti, D. Sand, J. Sollerman, J. Johansson, D. C. Leonard, J. C. Horst, J. M. Fedrow, S. F. Armen, R. M. Quimby, A. Sternberg, T. Matheson, M. Sullivan, K. Maguire, J. Surace, U. D. Rebbapragada, and P. R. Wozniak. Early Type II Supernova Light Curves. The Astrophysical Journal.

Sesar, B., Z. Ivezic, S. J. Stuart, D. M. Morgan, A. Becker, S. Sharma, L. Palaversa, M. Juric, P. Wozniak, and H. Olusei. Exploring the Variable Sky with LINEAR. II. Halo Structure and Substructure Traced by RR Lyrae Stars to 30 kpc. 2013. The Astronomical Journal. 146: 21.

Shappee, B. J., A. L. Piro, T. W. Holoien, J. L. Prieto, C. Contreras, K. Itagaki, C. R. Burns, C. S. Kochanek, K. Z. Stanek, E. Alper, U. Basu, J. F. Beacom, D. Bersier, J. Brimacombe, E. Conseil, A. B. Danilet, S. Dong, E. Falco, D. Grupe, E. Y. Hsiao, S. Kiyota, N. Morrell, J. Nicolas, M. M. Phillips, G. Pojmanski, G. Simonian, M. Stritzinger, D. M. Szczygiel, T. A. Thompson, J. Thorstensen, M. Wagner, and P. R. Wo'zniak. The Young and Bright Type Ia Supernova ASASSN-14lp: Discovery, Early-Time Observations, First-Light Time, Distance to NGC 4666, and Progenitor Constraints. 2015. ArXiv e-prints.

Skillman, S. W., M. S. Warren, M. J. Turk, R. H. Wechsler, D. E. Holz, and P. M. Sutter. Dark Sky Simulations: Early Data Release. The Astrophysical Journal.

Smidt, J., D. J. Whalen, E. Chatzopoulos, B. K. Wiggins, K. J. Chen, A. Kozyreva, and W. Even. Finding the First Cosmic Explosions. IV. 90 - 140 M Pair-Instability Supernovae. 2015. The Astrophysical Journal. 805 (1): 44.

Smidt, J., D. J. Whalen, W. Even, B. Wiggins, J. L. Johnson, and C. L. Fryer. Population III Hypernovae. 2014. The Astrophysical Journal. 797: 97.

Ukwatta, T. N., and P. R. Wozniak. Investigation of Redshift- and Duration-Dependent Clustering of Gamma-ray Bursts. 2015. ArXiv e-prints.

Vreeswijk, P., A. Raassen, A. Smette, A. De Cia, P. Wozniak, A. Fox, W. Vestrand, and P. Jakobsson. Time-dependent excitation and ionization modelling of absorption-line variability due to GRB 080310. 2013. Astronomy and Astrophysics. 549: A22.

Whalen, D. J., J. Smidt, W. Even, S. E. Woosley, A. Heger, M. Stiavelli, and C. L. Fryer. Finding the First Cosmic Explosions. III. Pulsational Pair-instability Supernovae. 2014. apj. 781: 106.

Whalen, D. J., W. Even, J. Smidt, A. Heger, K. J. Chen, C. L. Fryer, M. Stiavelli, H. Xu, and C. C. Joggerst. Supermassive Population III Supernovae and the Birth of the First Quasars. 2013. apj. 778: 17.

Whalen, D. J., W. Even, J. Smidt, A. Heger, R. Hirschi, N. Yusof, M. Stiavelli, C. L. Fryer, K. J. Chen, and C. C. Joggerst. Pair-Instability Supernovae in the Local Universe. 2014. The Astrophysical Journal. 797: 9.

Whalen, D. J., W. Even, L. H. Frey, J. Smidt, J. L. Johnson, C. C. Lovekin, C. L. Fryer, M. Stiavelli, D. E. Holz, A. Heger, S. E. Woosley, and A. L. Hungerford. Finding the First Cosmic Explosions. I. Pair-instability Supernovae. 2013. apj. 777: 110.

Whalen, D., J. Johnson, J. Smidt, A. Heger, W. Even, and C. Fryer. The Biggest Explosions in the Universe. II. 2013. The Astrophysical Journal. 777 (2): 99.

Whalen, D., J. Johnson, J. Smidt, A. Meiksin, A. Heger, W. Even, and C. Fryer. The Supernova that Destroyed a Protogalaxy: Prompt Chemical Enrichment and Supermassive Black Hole Growth. 2013. The Astrophysical Journal. 774: 64.

Whalen, D., W. Even, C. Lovekin, C. Fryer, M. Stiavelli, P. Roming, J. Cooke, T. Pritchard, D. Holz, and C. Knight. Illuminating the Primeval Universe with Type IIn Supernovae. 2013. The Astrophysical Journal. 768: 195.

Wozniak, P. R., D. I. Moody, Z. Ji, S. P. Brumby, H. Brink, J. Richards, and J. S. Bloom. Automated Variability Selection in Time-domain Imaging Surveys Using Sparse Representations with Learned Dictionaries. 2013. In American Astronomical Society, AAS Meeting #221. (Long Beach, CA, 6-10 January 2013). , p. #431.05. Washington, DC: American Astronomical Society.

Yan, L., R. Quimby, E. Ofek, A. Gal-Yam, P. Mazzali, D. Perley, P. Vreeswijk, G. Leloudas, A. de Cia, F. Masci, S. B. Cenko, Y. Cao, S. R. Kulkarni, P. E. Nugent, U. D. Rebbapragada, P. R. Wo'zniak, and O. Yaron. Detection of Broad H$$backslash$alpha$ Emission Lines in the Late-time Spectra of a Hydrogen-poor Superluminous Supernova. 2015. ArXiv e-prints.

Yaron, O., D. A. Perley, A. Gal-Yam, J. H. Groh, A. Horesh, E. O. Ofek, S. R. Kulkarni, J. Sollerman, C. Fransson, A. Rubin, N. Sapir, P. Szabo, F. Taddia, S. B. Cenko, I. Arcavi, S. Valenti, M. M. Kasliwal, P. Vreeswijk, D. Khazov, O. D.

Fox, Y. Cao, O. Gnat, P. L. Kelley, P. E. Nugent, A. V. Filippenko, R. R. Laher, P. W. Wozniak, U. D. Rebbapragada, K. Maguire, and M. Sullivan. Confined Dense Circumstellar Material Surrounding a Regular Type II Supernova. Nature.

Microscopic Fission Model for Data Needs

Ionel Stetcu
20140581ECR

Introduction

The current project is motivated by both basic-science needs and applications to new signatures for material detection, proliferation and forensics. The development of new detection capabilities such as the time-projection chamber or SPIDER (Spectrometer for ion detection in fission research) is complemented by an equally important theoretical modeling effort, leading to updates in the state-of-the-art U.S. ENDF/B-VII.1 evaluated library that is used in applications. This project aims at complementing planned experiments at LANSCE (Los Alamos Neutron Science Center) by providing reliable modeling for relevant fission quantities (fission fragment yields, kinetic energy distribution). We will also obtain information about other quantities about which only indirect experimental information can be inferred (angular momentum of the fission fragments, excitation energy sharing between fragments). Hence, once implemented and tested, it will constitute a powerful tool in fission research.

For the execution of the project, we will make use of the latest-generation supercomputers to implement and study nuclear fission of actinides in the density functional theory (DFT) framework. DFT is the only microscopic approach currently feasible for heavy nuclei, and has the additional advantage of being able to treat on the same footing the isolated nuclear system and the interaction and response in time of a nucleus with external probes (e.g., incoming neutrons, photons, etc). In the current project, we will stretch the nucleus close to the breaking point, release it, and follow the dynamics of fission. Such calculations require extensive computational resources, as one has to solve tens to hundreds of thousands of time-dependent non-linear coupled three-dimensional partial differential equations and the developed software represents a true quantitative jump (it is at least a factor of a 1000 to 2000 more complex than that of the "nearest" competition). Because of its complexity, this software represents a first step toward exascale computing.

Benefit to National Security Missions

The successful completion of this project will contribute to our ability to provide reliable nuclear reaction data for both basic and applied physics need in direct support of the nuclear security mission. In particular, the principal investigator is working on fission simulations using the code CGMF (cascade gamma multiplicity for fission), which provides a description of the prompt neutron and gamma properties. This understanding is essential for developing new signatures for nuclear material detection, nuclear proliferation, forensics and energy generation, which are at the core mission of the laboratory and NNSA. More reliable input provided by this work will lead to more reliable predictions. Finally, given the planned experimental studies at the Los Alamos Neutron Science Center (LANSCE), a successful project will allow the development of an important capability at Los Alamos National Laboratory in both fundamental and applied nuclear physics, and it will complement the current experimental program.

Progress

In the last fiscal year, I have finished all the major computational implementation proposed. The code has been tested on titan at ORNL and moonlight at LANL, scales very well and makes efficient use of the GPUs (graphical processing units). Depending on the size of the problem, the GPU code is faster by factors of 15 to 25 with respect to the MPI (message passing interface) code from which it originated.

For a particular nucleus, the code starts with a set of self-consistent densities (obtained via another code). Different external perturbations can be applied in order to drive the system toward the point of breaking into two (or more fragments), process called fission. For applications of interest, this process happens at low excitation energies, and the goal of this project is to model this process and extract quantities of interest. However, applying external fields (which model real external probes

like photons and neutrons), has to be made with care because one needs to keep the system cool, that is as close as possible to the lowest energy surface. In order to achieve this, I have implemented the quantum friction (QF), which acts like an external field, designed to keep the energy low, while the system is deformed toward fission. QF has two components, one of them in the so called normal channel, and another one in the pairing channel. I have found that the cooling in the normal channel works very well, and reduces the final energy (when the external field is turned off) by about 10 MeV. However, in the pairing channel, the QF did not perform as expected, and the energy cannot be reduced by including QF. As a result, the evolution is not adiabatic, and the nucleus fission occurs only at high energies, of the order of a few tens to hundreds of MeV. This is not satisfactory, as the scope of the current project is obtaining fission at low energies. Hence, I was forced to look for other solutions that would allow a description of fission at low energies. For this, I have implemented modifications in the code that provides the initial conditions constraints that allow me to obtain the initial system already deformed at low energies. The initial conditions are used as input in the time-dependent code, where I release the constraint in a reasonably small amount of time, and follow the evolution in time. In this way, keeping the excitation energy very low, I was able to increase the deformation of the system by 30%, as a consequence of Coulomb interaction, which elongates the system, driving it toward fission. While the system did not break as of today, this result can be understood: in the solutions that I have, one needs to add another perturbation, that would make the system break asymmetrically, which is indeed observed (it is almost impossible to break the system at low energies in two identical fragments). I am exploring at the moment how one can produce two asymmetric fragments, without adding additional constraints in the initial conditions (the code that produces initial conditions is very demanding and can converge to the solutions slowly). If this is not possible with external probes, one can still implement additional conditions in the initial solutions.

Together with collaborators in Warsaw and Seattle, I have also implemented the required tools to calculate the total kinetic energy, once the two fragments separate. The code has been tested using fission at high energies, but it does not require any changes for low-energy processes. Thus, I am well positioned to calculate this very important observable, which is part of the goals of the current investigation, once the two fragments separate at low energies.

I have also worked to extend a calculation involving a photon interacting with a 238U nucleus. This is important and relevant for the current project as photo-fission is one of the processes that can be investigated with the current capabilities. This work was published in Phys. Rev. Lett. 114 (2015) 012701 and Acta Phys. Polonica B 46 (2015) 391 .

Future Work

In the period remaining until the end of the funding period, I will concentrate on obtaining, in a time-dependent approach, asymmetric fission at low energies. I will investigate several scenarios in which the asymmetry could be introduced via a perturbation in time. If this approach pumps too much energy into the system, I will have to revert to introducing the asymmetry directly into the initial conditions, that is the starting densities and wave functions which are evolved in time. This is possible, but I would like to avoid it because of the high cost in computing power. I will continue the investigations of 240Pu in smaller boxes, and once fission achieved, I would like to extract the total kinetic energy of the two fragments as a function of mass asymmetry, at least for a few light to heavy mass fragments. I also plan to investigate whether neutrons are emitted during the breakup in this approach.

Conclusion

The main goal of the current project is to provide a first fully quantum-mechanical description of nuclear fission, the physics process in which a heavy nucleus breaks apart. Our approach can provide a reliable method to extract fission properties that can be later used as input in simulations with applications to energy generation, global security, weapons, astrophysics. We plan to obtain fission yields in charge, mass, kinetic energy and angular momentum, and to study the properties of neutrons emitted during the breakup. Selected results will be tested against experimental data and predictions of other theoretical developments in our group.

Publications

Stetcu, . NUCLEAR STRUCTURE AND DYNAMICS WITH DENSITY FUNCTIONAL THEORY. 2015. ACTA PHYSICA POLONICA B. 46 (3): 391.

Stetcu, , C. A. Bertulani, Bulgac, Magierski, and K. J. Roche. Relativistic Coulomb Excitation within the Time Dependent Superfluid Local Density Approximation. 2015. PHYSICAL REVIEW LETTERS. 114 (1).

Relativistic Electrons in Magnetized Plasmas

Zehua Guo
20140605ECR

Introduction

This research project will develop a comprehensive physics model and the predictive capability for the generation and transport of relativistic electrons in magnetized plasmas with applications to tokamak fusion reactor, earth's radiation belt and solar corona. Runaway electrons (RE) during tokamak disruptions have been identified to be a potential showstopper for ITER tokamak reactor (ITER being built in France), because the projected tens of mega-ampere REs will cause intolerable materials damage when they intercept the reactor wall. To develop control and mitigation strategies, it is imperative to understand the physics underlying the generation and transport of these REs. We will upgrade our existing Fokker-Planck solver in the tokamak geometry to study the distribution functions of REs. Essential effects due to electron radial drift, radiation damping, Coulomb collisions and wave-particle interactions will be treated on the same footings for the first time. Stability analysis will be performed to identify unstable waves, and the subsequent wave-particle interaction will be incorporated into the Fokker-Planck model with quasi-linear theories. Since the collisional slowing down is ineffective for REs, we will explore the intriguing possibility of using waves, either self-excited or externally injected, to control the REs. We will focus on a novel mechanism that enhances the pitch angle scattering of REs and creates an energy exchange channel between thermal and REs through nonlinear wave-wave coupling between the whistler wave and the much slower electrostatic modes. This study will help establish the physics basis for reducing/removing relativistic electrons via wave injection or selective excitation.

Benefit to National Security Missions

This project aims to develop a one of a kind predictive modeling capability for runaway electrons in a magnetized plasma, commonly observed in space and astrophysical plasmas, and in the laboratory tokamak experiments. The immediate impact on the control and mitigation of disruption-induced runaway electrons is of great importance to overcome the plasma-wall interaction challenge on the ITER fusion reactor experiment, which is of high priority to the DOE Office of Science. The comprehensive Fokker-Planck solver developed in this project is also of interest to earth radiation belt modeling, a priority for our national security mission via LANL's Global Security program in space weather modeling and mitigation of intense relativistic electrons, which pose a threat to the satellites, spacecraft and astronauts. Other applications include high energy astrophysics and solar coronal heating.

Progress

We have derived the drift-kinetic equations for relativistic electrons in tokamaks and extended our existing Fokker-Planck code to be suitable for runaway electrons (RE). The relativistic collision operator for small-angle collisions has been implemented and the radial drift due to tokamak magnetic geometry is included. We have also studied the instabilities using analytical distribution functions of primary and secondary REs. The electrostatic Trivelpiece-Gould mode dominates for the primary RE distribution and the sonic-whistler type modes dominate for the secondary REs. A rather general tool for analyzing linear instabilities of arbitrary distribution functions has been developed and is ready to be verified against the analytical results. For the remaining four months of FY15, we will continue to benchmark our result with previous analytical and numerical solutions of the RE distributions and study the effects of radial transport on RE distribution.

Future Work

This project started in Oct 2014. For FY15, we focused on verifications against previous analytical and numerical results of the RE distributions, extension to include synchrotron radiation losses and analysis of their importance in determining the RE distribution. In the next fiscal year, our major tasks include: (1) understand the

radial losses of REs due to natural drift motion in tokamak geometry; (2) analyze the kinetic and fluid instabilities; (3) study the effects of wave-particle interactions on RE distributions. Using the steady-state (or transient) RE distribution functions, detailed stability analysis of the RE distribution function will be performed to understand the unstable waves. With the new distribution function, we will analyze the wave characteristics and compare to previous work where the radiation damping and radial transport physics were not accounted for. Furthermore, we will include the anomalous transport due to wave-particle interactions into the Fokker-Planck equation and study how RE distributions are modified. We will examine the idea that wave/turbulence induced transport can help to limit the growth rate of runaway electrons and quantity the effect together with the radial losses.

Conclusion

The project will produce a reliable model and code to simulate the relativistic electrons in magnetic fields for studying the runaway electron formation and control in a tokamak. The predictive capability will also be applicable to radiation belt dynamics and coronal flare physics. This work will help elucidate the role of nonlinear wave-wave coupling processes in the presence of relativistic electrons, and establish the physics bases for using wave-particle interaction to control runaway electron generation and radial transport in ITER.

Electron Transport in Warm and Hot Dense Matter

Charles E. Starrett
20150656ECR

Introduction

In this project we will develop a completely novel simulation capability for dense plasmas. Such plasmas exist in inertial confinement fusion plasmas (eg. at the national ignition facility (NIF)) as well as in astrophysics, for example, in the interiors of giant planets and in white dwarfs. Building on a existing computational tool developed by the PI, we will extend a method that has been very successful in condensed matter physics, into the dense plasma regime. This method, known as KKR-Green's function, will provide an description of these plasmas with unparalleled realism across the temperature and density regime of interest. We will apply the method to the calculation of electrical conductivity, which is of importance to the modeling of inertial confinement fusion experiments. In the lower temperature regime the new capability will complement current high accuracy tools, while for hot dense plasmas the method will provide a gold standard where none currently exists.

Benefit to National Security Missions

The project aims to greatly improve our understanding of electron transport in dense plasmas. As such, it will ultimately provide a tool that could be used to provide crucial input information into hydrodynamical simulations of implosion experiments of inertial confinement fusion. Such experiments, like those conducted at the national ignition facility and elsewhere, are essential for the stockpile stewardship mission of the DOE NNSA.

The new method that we aim to develop will provide simulations of of unparalleled physical realism across the temperature and density regime of interest to the inertial confinement fusion community. It will put LANL at the forefront of the rapidly evolving field of electron transport in warm and hot dense matter.

Progress

Since the beginning of this project at the end of January 2015, we have implemented the single center Green's function code. This has been tested against the PI's existing average atom code that uses the standard orbital based Kohn-Sham density functional theory. The Green's function code gives the same results to within numerical tolerance, as expected, but is a factor of 5 faster than the orbital based code.

The Green's function implementation also avoids two key numerical difficulties that are present in orbital based implementations - namely the search for weakly bound states and the tracking of resonance states. This numerical speed-up and fundamental new approach to the single center model have been accepted for publication in High Energy Density Physics.

Future Work

In this fiscal year we will develop the implementation of the single center solution. This will involve solving the Schrodinger equation for complex energies. The implementation will be tested against the PI's existing real-space implementation. Once this is completed we will begin the implementation of the so-called structure constants using the Ewald technique.

In FY16 we will complete the implementation of the so-called structure constants and combine this with the single center code that was completed in FY15. We will test this and implement the calculation of the conductivity.

Conclusion

The ultimate result of this work will be a completely new computational framework for calculating electrical conductivity in warm and hot dense plasmas. The method will compare favorably to the existing gold standard methods at low temperature, and provide the gold standard at higher temperatures, where none currently exists. The method will lead to a new understanding of electron transport in dense plasmas and the resulting calculations will of high relevance to the modeling of in-

ertial confinement fusion experiments (eg. at the National Ignition Facility).

Publications

Starrett, C. E.. A Green's function quantum average atom model. 2015. HIGH ENERGY DENSITY PHYSICS. 16: 18.

A Step toward Nuclear Reaction Studies for Applications at FRIB

Shea M. Mosby
20150683ECR

Introduction

The neutron capture reaction - in particular, the cross section - is of great importance for a variety of fields ranging from nuclear astrophysics to defense programs. This process must be understood across a whole host of elements and isotopes, with half-lives ranging from thousands of years to a fraction of a second. Current experimental access to this process is limited to stable and near-stable isotopes (half-lives ranging from months to years), and theoretical calculations are comparatively unreliable due to uncertainty in the nuclear structure inputs they require.

This project seeks to validate a potentially game-changing technique for measuring the necessary nuclear structure to accurately calculate the neutron capture cross section. Direct measurements using the Detector for Advanced Neutron Capture Experiments (DANCE) at Los Alamos National Laboratory will be made in parallel with indirect measurements using the Apollo instrument at Argonne National Laboratory. If successful, Apollo can be used to vastly improve our understanding of neutron capture on short-lived isotopes relevant for both nuclear astrophysics and defense programs.

Benefit to National Security Missions

Nuclear reaction rates (particularly neutron capture) on short-lived isotopes are known to have impact for basic science questions such as the origin of the elements heavier than iron, as well as radiochemical diagnostics used as part of our nuclear security mission. The current state of the art experimental methods for studying these reaction rates are limited to stable or long-lived isotopes. While several methods have been explored, no truly robust method of constraining neutron capture on short-lived isotopes has been demonstrated.

This project seeks to remedy that situation by performing the experimental work needed to validate a new method to constrain neutron capture rates on short-lived nuclei. The project will do this by performing two independent experiments on the same isotope - one using an established method for studying neutron capture, and one using the new method. By the end of the project, the two methods should provide consistent results for neutron capture, thus validating the new method and opening up hundreds of important isotopes for study.

Progress

The project start and end date was delayed until June to better match with facility run schedules. Nevertheless, there is significant progress in key areas needed to execute the experiments early next FY.

- The Argonne proposal was submitted and accepted such that all of our requested beam time is approved. We are communicating with them now to schedule the experiment.
- There has been no call for proposals for the Los Alamos aspect of the project. Nevertheless, we've performed rate calculations and analyzed some past data under similar conditions such that we understand what our beam time request will be.
- We've begun the analysis and simulation tool chain work such that we understand the scope of work needed. We believe that these tools will be ready prior to each experiment running.

Future Work

- Execute experiments at both Argonne National Laboratory (ANL) and the Los Alamos Neutron Science Center. Based on current information, we expect to run both experiments between November 2015 and January 2016. Both experiments will run at the behest of their respective facilities' operations schedule.
- Complete analysis software framework to move

from raw data to the relevant gamma-ray cascade spectra for comparison with theory.

- Complete the theory code / detector simulation integration so the experimental data can be connected to the relevant physics codes. The detector simulation output should be in the same data format as the experimental data so the same analysis toolchain can be used for consistency.

- Preliminary analysis of data performed such that rough results are in hand to guide the final stages on analysis. Detector calibrations (e.g. gain matching, time alignment) will be complete, and detector coincidence (e.g. particle / gamma-ray coincidences for the ANL experiment) spectra constructed.

Conclusion

The project will directly measure the 96Zr neutron capture cross section using DANCE, and constrain a theoretical calculation of the cross section using indirect techniques with Apollo. Furthermore, DANCE can make an independent measurement of the nuclear structure properties of 96Zr and independently constrain theoretical calculations of the capture cross section. It is expected that these three independent measurements will result in a consistent cross section prediction.

Optimization of Compton Source Performance through Electron Beam Shaping

Nikolai Yampolsky
20150690ECR

Introduction

The project aims to investigate a novel way for increasing brightness of light sources based on inverse Compton scattering (ICS). The key idea is to manipulate the electron beam phase space so that all the electrons emit photons of the same energy in some direction. During the course of the project we will study the feasibility of the scheme and determine how large an improvement can be achieved. Upon success of the project we will describe practical modifications to currently existing and future ICS light sources which should significantly improve their quality.

Benefit to National Security Missions

The proposed scheme may have a strong impact on MaRIE in its early stage. There is a possibility of reusing the planned MaRIE Injector Test Stand (MITS) as an ICS light source to enable early experiments. This project will also be beneficial for testing X-ray detectors planned for the MaRIE FEL.

Two ICS sources have been built and two future facilities are proposed to generate γ-rays through ICS for material science applications. Increasing the brightness of those sources will be beneficial for their host DOE facilities.

Recently, high-flux gamma rays have been proposed as approaches for detecting special nuclear materials and to address international nuclear proliferation concerns. Compact ICS source is an attractive option for generating these photons. The proposed method for conditioning the beam phase space will reduce the ICS bandwidth which will allow meeting the requirements. Moreover, increasing the brightness of such a source will allow reducing the power required to operate such a machine.

Progress

The equation of motion of an arbitrary relativistic electron in the fields of the plane electro-magnetic wave has been re-derived and the resulting radiation field has been found. This work resulted in the finding of the photon Wigner distribution function of a single-electron emission. The Wigner distribution function for the ensemble of electrons has been found and was reduced to the conventional form of a convolution between the electron distribution function in the bunch and a single-particle Wigner distribution function. The convolution has been calculated analytically for quasi-mono-energetic and low-divergence electron bunch and the result has been found in a compact form suitable for further analysis. The resulting form of the photon Wigner distribution function clearly shows the optimal beam conditioning resulting in the brightest inverse Compton scattering source.

Future Work

- Determine the required conditioning of the electron beam phase space
- Determine the beamline which is required to obtain the optimal beam distribution.
- Design and simulate beamline using standard accelerator code ELEGANT.
- Optimize beamline to minimize deleterious higher-order transport effects.

Conclusion

We expect to demonstrate that ICS brightness can be increased through appropriate conditioning of the electron beam phase space. We expect to eliminate the largest contribution to the brightness degradation, i.e. either due to the angular divergence or the energy spread of the electron beam. At the moment, it is an open question whether both effects can be suppressed simultaneously. We conservatively anticipate that only one of them can be compensated and the final source brightness will be defined by the smallest rather than the largest effect.

First Principle Study of Relativistic Beam and Plasma Physics Enabled by Enhanced Particle-In-Cell Capability

Chengkun Huang
20130744ECR

Abstract

Relativistic charged particles are commonly generated in nature and man-made experiments. They are accelerated/decelerated either naturally or deliberately for various purposes, e.g. 10s of GeV electron beams can be manipulated to produce intense coherent short-wavelength radiation in an X-ray Free Electron Laser (FEL) — an indispensible tool for material research at many scientific frontiers. Relativistic particles also play important roles in Inertial Confinement Fusion (ICF) energy generation employing laser-driven particle beams as ignitor and in various astrophysical phenomena such as jets and cosmic rays. The Particle-In-Cell (PIC) method has proven successful for kinetic simulations of weakly to mildly relativistic beams and plasmas, but its accuracy will decrease for highly relativistic particles due to the imprecise representation of the particles and their fields. In many cases, such inaccuracy can lead to numerical instabilities detrimental to the simulations. In this work, we systematically developed, validated and integrated recent improvements on the major components of the PIC method, enhancing its capability for the modeling of relativistic phenomena. A new high-order field solver with careful control of the dispersion properties is developed and benchmarked for the modeling of synchrotron radiation of highly relativistic charged particles. The benefits of high order particle shapes, digital filters and maintaining conservative properties are elucidated, especially with regard to the suppression of numerical instabilities. An unexplored attribute, the spectral fidelity, is found to have a critical role in the stability of the simulation model and used in the further development of a novel PIC method that is intrinsically stable. We already applied the enhanced capability for high fidelity self-consistent study of a class of accelerator and plasma physics problems involving such particles and the radiation they produced, including micro-bunching instability in FEL bunch compressor, particle acceleration in astrophysics and isochoric deposition of energetic particles in ICF capsule, thus establishing a numerical framework for investigating future light source development, astrophysical processes, kinetic high energy density laboratory plasma (HEDLP) and alterative ICF concepts.

Background and Research Objectives

The Particle-In-Cell (PIC) [1] method is a computationally efficient, fully kinetic ab-initio method widely used in plasma and particle beam modeling. Specifically, PIC models have been applied to a number of challenging problems involving relativistic particles: (1) understanding how the microbunching instability can arise from the interactions between a highly relativistic beam and its Coherent Synchrotron Radiation (CSR) in a FEL [2] bunch compressor and how it affects the beam quality and FEL performance; (2) investigation of the collisionless particle acceleration process in astrophysical shock and the deceleration process related to the collective wave-particle interaction in high-energy-density plasmas. The former application is directly relevant to the success of the MaRIE X-ray FEL signature facility at LANL, while the latter addresses fundamental science questions in both astrophysics and a high-risk yet high-potential Fast-Ignition (FI) [3] technology for inertial fusion energy. Although the standard PIC method with the second order accurate numerical algorithm is well suited for the study of beam and plasma dynamics at low speed, its application to relativistic phenomena is severely limited. The major limitations come from the dispersive and anisotropic propagation properties of the electromagnetic wave on the computation grid, the electrostatic and electromagnetic numerical instabilities associated with the use of a computation grid, and the undesirable noise due to the unphysical Cherenkov radiation of relativistic particles and under-resolved dynamics. These limitations necessitate a new computational framework based on the PIC method to compute and understand cutting-edge problems involving highly relativistic charged particles for applications such as FEL and FI-ICF. Our approach is to address the issues of the standard PIC method by identifying the key deficiencies in PIC components and

by carefully redesigning them. These include the lack of the spectral fidelity in the charge/current deposition and the accumulation of the phase error in the electromagnetic field solver. We will devise new numerical schemes to overcome these deficiencies. With this enhanced PIC capability, our ultimate goal is to provide accurate and self-consistent modeling and understanding to the relativistic beam/plasma problems of importance to LANL's mission and to the broader scientific community, particularly related to the coherent synchrotron radiation and collective particle acceleration/deceleration processes.

Scientific Approach and Accomplishments

In the PIC method, a fundamental incompatibility between the continuous particle model and the discrete field representation causes an aliasing effect. Under certain numerical conditions, the alias modes can interact with the other modes admitted in the electromagnetic PIC model, causing numerical instabilities that can render unphysical simulation results or even destroy the simulation. We found that alias modes can also be unstable by themselves, dependent on the deposition scheme employed. Such numerical instabilities will substantially affect the modeling of kinetic of the relativistic particles.

To thoroughly understand the characteristics and the origin of the grid type instabilities, we first reviewed the numerical dispersion relation of the standard electromagnetic PIC model based on the Yee Finite Difference Time Domain (FDTD) solver [4]. We abided by the following two guidelines that have been overlooked before:

(1) The eigenmodes in a PIC model consist of spatially continuous, temporally discrete particle eigen-distribution functions, and spatially and temporally discrete eigenfields. The sole cause of aliasing in PIC is the sampling of the continuous spatial variable onto the discrete one. As time and space are independent variables, this spatial aliasing effect will not introduce any temporal aliasing.

(2) Unnecessary algebraic approximations that may result in an approximation to the original model should be avoided.

Based on these guidelines, we rigorously derived the faithful numerical dispersion relation for the standard electromagnetic PIC model with a simple, direct current deposition scheme, which does not exactly conserve electric charge. We analyzed the numerical dispersion of the electrostatic-like mode in a 1-D electromagnetic PIC model with a drifting cold plasma and the Finite Grid Instability (FGI) [5] is predicted to be present. This instability in the electromagnetic PIC model has not been previously analyzed, nor has it been confirmed from simulation. We have obtained accurate numerical solutions and corresponding approximated growth rates. It has been shown that in the infinitesimal time step limit, and for sufficiently large grid size in the finite time step case, the dominant FGI is caused by the intersection of the finite grid plasma mode and the two lowest order alias modes. On the other hand, for relativistic cold plasma flow under the most relevant simulation parameters, an intersection of a stationary mode and alias modes, due to inexact charge conservation, can lead to the most dominant instability. The growth rate for this instability is obtained analytically and there is no threshold grid size or time step size below which this instability will not occur. This instability and associated growth rate have been confirmed in our simulations with excellent agreement with our predictions [6]. An investigation of charge conserving schemes commonly used in 1D electromagnetic codes indicates that each alias mode is unstable by itself, similar to the electrostatic case.

Next, the origin of the FGI is studied by resolving the dynamics in spectral domain at the single particle level and at the collective motion level [7]. The concept of spectral fidelity, i.e., how closely the PIC model resembles the underlying physical system in the spectral domain, is developed and used to contrast the PIC model with the gridless model. The systematic spectral phase and amplitude errors from the charge deposition and field interpolation are quantified for common particle shapes used in the PIC models for the first time. It is shown through such analysis and in simulations that the lack of spectral fidelity relative to the physical system due to the existence of aliased spatial modes is the major cause of the FGI in the PIC model. In this regard, the difference between the PIC model and the physical system (or gridless model) is technical, not fundamental — with a properly chosen particle shape such that its spectral content is band-limited to the maximum allowable wave-number in the simulation, the PIC models becomes effectively a gridless model. This opens the question of the optimal compact particle shapes for the PIC model. In addition, as with many physical instabilities which result from the constructive feedback of modes, it is understood that the systematic phase error plays a critical role in the development of FGI. This finding is verified in our simulation comparison with the gridless model. With this new understanding of how and where FGI arises in the PIC model, the optimal strategy/method to mitigate FGI has been devised and implemented [8]. As this improvement is readily extended to other particle mesh method, our work not only clarify and pave the way for the development of better PIC models which is used in plasma and beam physics, it is also applicable in a wide range of N-body type computation physics problem.

A third area of our improvement focuses on the need to improve the dispersive properties of the field solver, which is essential for modeling CSR from a relativistic beam. Although analytic solution of the CSR field exists in 1D, this problem is substantially complicated in realistic multiple dimension due to the lack of such understanding of the CSR field in multi-dimension thus there is no good known solution to benchmark the simulation. We approached this problem from both the semi-analytic and computation modeling aspects. For the synchrotron radiation near field, we extended the well-known 1D line charge model [9] to two spatial dimensions [10] in the bending plane and recently to full three dimensions [11]. These models overcome the diverging space charge potential and fields issues in the 1D line charge model for a coasting beam, therefore they are amenable to numerical integration even in the presence of the singularity from space charge field. Both our 2D and 3D models exhibit self-similar solution of the single particle synchrotron radiation field kernel through a rescaling of the spatial variables. This important property allows a convenient convolution procedure to replace the summation process for the CSR calculation of a smooth beam profile, which can be justified when the beam size is much smaller than the bending radius in the bunch compressor. We have built a 2D CSR numerical model based on this procedure. Our team has also successfully developed and tested a parallel high order finite volume field solver and validated its accuracy in the phase velocity. The solver has been implemented into a production parallel PIC code. We investigated the tunable dispersion property of this field solver and developed a tuning strategy optimized for the low (or high) frequencies for CSR (or numerical Cherenkov noise suppression). Another key component of the accurate electromagnetic solver for our relativistic beam and plasma modeling is the absorbing boundary condition that can correctly matched to the order of the filed solver. We have extended the state-of-the-art absorbing boundary condition -- Perfectly Matched Layer (PML), into a high order PML boundary condition, which proves to be critical for stable high order field solver. With this new high order field solver and absorbing boundary condition, we have benchmarked CSR of a coasting beam with our 2D model. In particular, our result indicated that (1) the velocity field from the Liénard–Wiechert formulation dominates in the CSR at beam energy below ~ 50MeV, and (2) the transient effect at the magnetic dipole entrance leads to smaller field at the front, opposite to the prediction from the 1D model.

Over the two-year project period, we have made technical presentations at the North America Particle Accelerator Conference in 2013, the APS Division of Plasma Physics annual meetings in 2013 & 2014, the Advanced Accelerator Concept workshop in 2014 and the International Conference on Numerical Simulation of Plasmas (ICNSP) in 2015. We have given one invited talk (ICNSP 2015) and received another invitation at the 8th International West Lake Symposium (not given). M. D. Meyers, a graduate student supported in the project, received a travel grant to the APS DPP annual meeting in 2014 for his work on the project. Two publications, one on the 3D synchrotron radiation near field [11] and another one on the numerical dispersion and finite grid instability [6] have resulted from the work in this project. One manuscript on the spectral fidelity of the PIC model is under peer-review [7] and another one on the mitigation method is in preparation [8].

Impact on National Missions

Our work has established a high-fidelity first-principle predictive modeling capability which resulted in improved understanding of how relativistic charge particles interact with the environment, including their own coherent radiation. Modeling of other plasma physics and beam physics problems, especially of kinetic plasma behavior under extreme conditions, will further demonstrate its potential. The enhanced modeling capability provides important impetus in many areas related to LANL's missions for the national security, e.g., high energy density plasma, accelerator beam dynamics, astrophysics and space applications, thus yielding many scientific and programmatic possibilities. It provided training to student/postdoc in these important fields and the experience gained can be used to enhance other state-of-the-art PIC codes used at many frontiers, including LANL's flagship VPIC code. The improved modeling capability and the new insights concerning coherent synchrotron radiation by a relativistic beam, the microbunching instability in XFEL as well as the particle acceleration/deceleration mechanisms in high energy density plasmas link directly into applications enhancing national security and energy security. The new simulation capability also supports future signature facilities at LANL, such as the Matter-Radiation Interactions in Extremes facility.

References

1. Birdsall, C. K., and B. A. Langdon. Plasma Physics via Computer Simulation. 1991.

2. Emma, P., R. Akre, J. Arthur, R. Bionta, C. Bostedt, J. Bozek, A. Brachmann, P. Bucksbaum, R. Coffee, F. J. Decker, Y. Ding, D. Dowell, S. Edstrom, A. Fisher, J. Frisch, S. Gilevich, J. Hastings, G. Hays, P. Hering, Z. Huang, R. Iverson, H. Loos, M. Messerschmidt, A. Miahnahri, S. Moeller, H. D. Nuhn, G. Pile, D. Ratner, J. Rzepiela, D. Schultz, T. Smith, P. Stefan, H. Tompkins, J. Turner, J. Welch, W. White, J. Wu, G. Yocky, and J.

Galayda. First lasing and operation of an aa ngstrom-wavelength free-electron laser. 2010. Nature Photonics. 4 (9): 641.

3. Fern'andez, J. C., J. J. Honrubia, B. J. Albright, K. A. Flippo, D. C. Gautier, B. M. Hegelich, M. J. Schmitt, M. Temporal, and L. Yin. Progress and prospects of ion-driven fast ignition. 2009. Nuclear Fusion. 49 (6): 065004.

4. Yee, K. S.. Numerical solution of initial boundary value problems involving maxwell's equations in isotropic media. 1966. IEEE Transactions on Antennas and Propagation. 14 (3): 302.

5. Langdon, B. A.. Effects of the spatial grid in simulation plasmas. 1970. Journal of Computational Physics. 6 (2): 247.

6. Meyers, M. D., C. K. Huang, Y. Zeng, S. A. Yi, and B. J. Albright. On the numerical dispersion of electromagnetic particle-in-cell code: Finite grid instability. 2015. Journal of Computational Physics. 297: 565.

7. Huang, C. K., Y. Zeng, Wang Y., M. D. Meyers, S. A. Yi, and B. J. Albright. Finite grid instability and spectral fidelity of the electrostatic Particle-In-Cell algorithm. 2015. submitted, arXiv:1508.03360.

8. Huang, C. K., Y. Zeng, Wang Y., M. D. Meyers, S. A. Yi, and B. J. Albright. A simple method to mitigate finite grid instability in the Particle-In-Cell algorithm. 2015. in preparation.

9. Saldin, E. L., E. A. Schneidmiller, and M. V. Yurkov. On the coherent radiation of an electron bunch moving in an arc of a circle. 1997. Nuclear Instruments and Methods in Physics Research Section A: Accelerators, Spectrometers, Detectors and Associated Equipment. 398 (2-3): 373.

10. Huang, C., T. Kwan, and B. Carlsten. Two dimensional model for coherent synchrotron radiation. 2013. Physical Review Special Topics - Accelerators and Beams. 16 (1): 010701.

11. Huang, C., T. J. T. Kwan, and B. E. Carlsten. Synchrotron Radiation Near Field In 3D. 2014. (Pasadena, 30 Sept. - 4 Oct. 2013). p. 487. Pasadena: JACoW.org.

Publications

Huang, C. K., Y. Zeng, Y. Wang, M. D. Meyers, S. Yi, and B. J. Albright. Finite grid instability and spectral fidelity of the electrostatic Particle-In-Cell algorithm. Computer Physics Communications.

Huang, C., T. J. T. Kwan, and B. E. Carlsten. Synchrotron Radiation Near Field In 3D. 2014. In 25th Particle Accelerator Conference. (Pasadena, 30 Sept. - 4 Oct. 2013). , p. 487. Pasadena: JACoW.org.

Meyers, M. D., C. K. Huang, Y. Zeng, S. A. Yi, and B. J. Albright. On the numerical dispersion of electromagnetic particle-in-cell code: Finite grid instability. 2015. JOURNAL OF COMPUTATIONAL PHYSICS. 297: 565.

Answer to Heavy Element Production Puzzle by Measuring Neutron-induced Charged Particles at LANSCE

Hye Young Lee
20130758ECR

Abstract

Despites decades of work on nuclear astrophysics, how heavy elements are produced remains an actively studied field. Above iron, heavy nuclei are produced via neutron capture, via either a s(low) process or r(apid) process. The 22Ne(alpha,n)25Mg reaction is thought to be the neutron source driving the synthesis of nuclides in the A = 60–90 mass range during the s process. Although many direct and indirect measurements were performed, the reaction rate still needs to be better determined due to poor resolution and limited sensitivity. With the WNR/LANSCE neutron beam upgrade and the advanced charged particle detection techniques, the goal of this research was to measure the time-inverse reaction as 25Mg(n,alpha)22Ne to answer the heavy element production puzzle [1]. As a commissioning of the detection system, the detectors were calibrated using an alpha-emitting radioactive source- 229Th and the in-beam measurement has been performed for 59Co(n,p) and 59Co(n,alpha) reactions.

Background and Research Objectives

The primary goal of this project is to extend our capability to measure neutron-induced reactions that produce and to further knowledge of these reaction that are a key to understanding of s-process nucleosynthesis. Due to the small reaction cross sections associated with neutron-induced charged particle reactions because of large Coulomb barriers and large signal-to-background ratios in detecting low energy alphas [2], building a very efficient detection system with the advanced technologies to achieve a large solid angle and good angular and timing resolutions was proposed. Once reliable experimental data are acquired, it was planned to compare them to verify theoretical predictions. Since heavy element production involves several thousands of nuclear reaction rates, the majority of rates heavily depend on model predictions that still hold rather large uncertainties. Detailed studies on these reactions over a much wider range of neutron energies and for previously unmeasured nuclides will certainly exceed present data quality.

Scientific Approach and Accomplishments

We have developed the instrumentation enabling the measurement of neutron-induced charged particle reactions. The LENZ (Low Energy n,z [3]) instrument is designed to precisely measure (n,p) and (n,alpha) reaction cross sections, using a time-of-flight method on the wide incident neutron energy range from thermal to several tens of MeV at LANSCE.

For better performance of detecting (n,alpha) cross sections for the energy range of astrophysical interest (below 3 MeV in neutron energy), we have enhanced the detection coverage and lowered the alpha detection threshold. LANSCE provides the continuous-in-energy neutrons from thermal to several hundreds MeVs using a spallation tungsten target; therefore it is necessary to identify different charged particles emitted from in-beam reactions. The collimators of the 0.71” opening size were inserted in the beam line in order to provide the beam spot of interest for the LENZ chamber.

The LENZ chamber (shown in Figure 1, 2, and 3) consisted of a Twin Frisch-grid Ionization Chamber as a “delta-E” detector (partial energy deposit) and a double-sided silicon strip detector (MICRON semiconductor product [4]) as an “E” detector (full energy deposit). Since charged-particle reactions often are suppressed from a large Coulomb barrier, this instrument is designed to enhance detection coverage. Initially, four different existing design concepts were reviewed for consideration; however, the twin Frisch-grid ionization chamber was the best suited for our purpose.

The dimensions of the ionization volume are set to be 63.5 mm of the anode radius and 37 mm of the distance between the cathode and anode, in order to cover about 120 degrees out of 180 degrees (66% coverage). Out-

side of the anode at a backward angle, there is an electric shield sheet for vetoing any beam-induced background charged particles outside of the ionization volume, which increases the signal-to-ratio and thereby lowers the detection threshold.

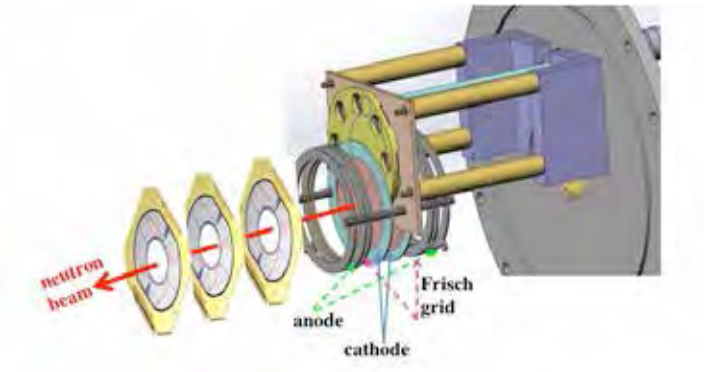

Figure 1. Diagram of the Frisch-grid twin ionization chamber and the double-sided silicon strip detectors

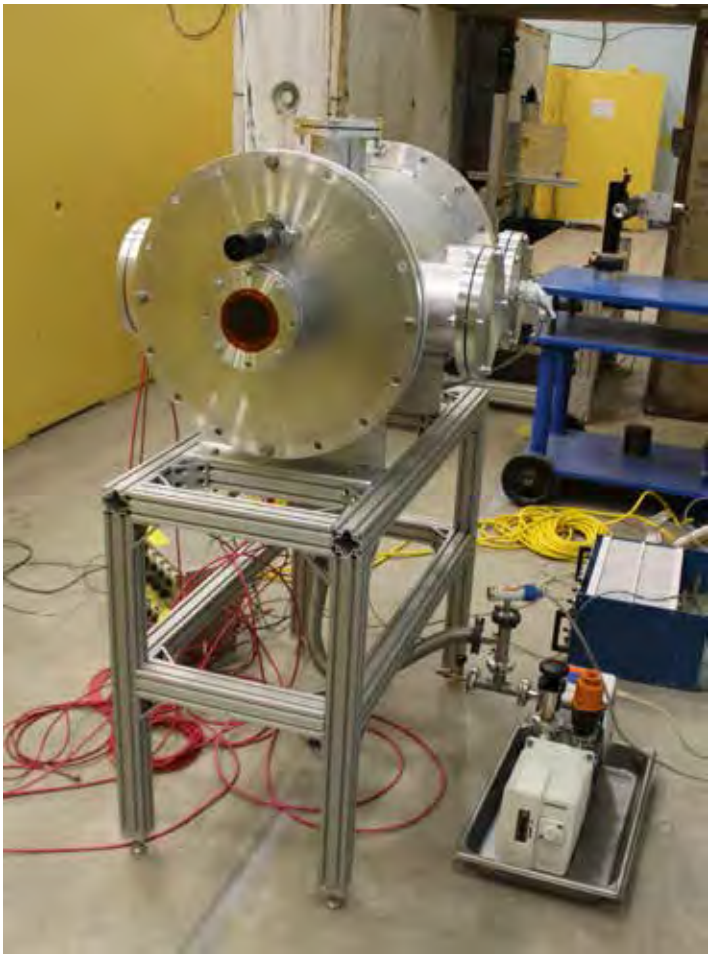

Figure 2. Pictures of the LENZ chamber located at the flight path during the in-beam commissioning runs.

For avoiding any alpha particle's energy degradation, the cathodes, grids, and anodes are made of thin tungsten wired grids instead of sheets or foils, so there is very minimum energy loss. Target thickness is also carefully determined by simulating Monte Carlo energy loss calculations TRIM [9] for minimizing any self-absorption of reaction alpha particles in a target medium.

Figure 3. Picture of the interior of the LENZ instrument.

The target wheel has 8 target locations, with one-inch openings. It is designed to readily accommodate multiple targets including a calibration target, such as 6LiF, an alpha source, reaction targets, and backing materials for background subtraction, without breaking vacuum system.

The ionization gas mixture was chosen to be a P10 gas – 90 % Argon gas and 10 % of CH4 gas, in order to reduce any beam-induced background from the counting gas. Often, neutron beams could create reactions with carbon, hydrogen, oxygen, and argon gases, so the type of gas is chosen for each reaction to minimize interference with peaks of interest. We used the P10 gas and the pressure of 550 Torr for optimizing the exit energy of low energy alphas and the ionization detector's performance. The pressure readout is well calibrated according to the manufacturer's manual. For future experiments, this type and pressure of gas mixture can be changed to different reactions.

Since LANSCE provides a white neutron energy spectrum, the beam energy information is deduced from a time of flight at a target, in this case cathode timing. Therefore,

the timing resolution has to be preserved as well as possible. We used waveform digitizers, which allowed us to store partial wavelet information to obtain the best timing and energy resolution, via post-processing using various digital filters. For the ionization chamber, the signals were fed into the low-noise charge-sensitive preamplifiers with fast rise time (CAEN product [10]), for obtaining the fast timing resolution. For the silicon strip detector, the signals were fed into the specially designed charge-sensitive preamplifiers (MESYTEC product [11]) for double-sided silicon detectors (DSSDs) whose output was captured by the digitizers directly. We have used x724 digitizers from CAEN with a 14-bit resolution and a 100 MHz sampling frequency, for achieving the best pulse height resolution. As shown in Figure 4, the energy resolution of DSSD using a digitizer was obtained as good as 55 keV for the alpha energy of 8.17 MeV. This LANL measured resolution is better than the specification from the Micron semiconductor manufacturer, which was 75 keV.

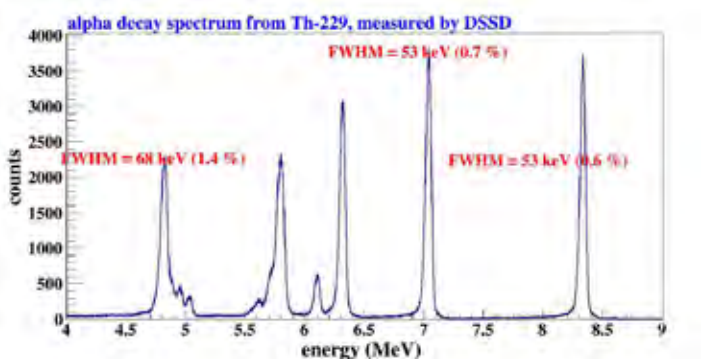

Figure 4. Double-sided silicon strip detector was calibrated for channel-to-energy and an energy resolution. Pulse height histogram was measured with a Th-229 radioactive source.

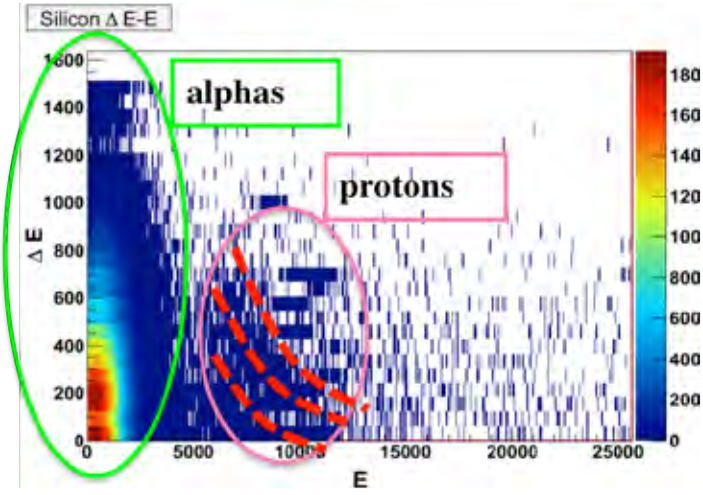

Figure 5. 2-dimensional plot of "delta-E" and "E" for demonstrating different charged particle identifications

The in-beam commissioning measurements were completed on a 59Co target in Nov. 2014 – Jan. 2015. Cobalt is one of the materials that are used widely in nuclear applications [12]. Since the radiation damage of materials is strongly related to the accumulation of helium gas produced by the (n,x-alpha) reaction, it is important to evaluate alpha-particle production cross sections. In this commissioning measurement, we intended to measure (n,p) and (n,alpha) cross sections in comparison to Hauser-Feshbach calculations [13]. The 59Co foil was installed in the target wheel; it ran for about three weeks of beam time at the flight path 15R in the WNR target 4. Figure 5. shows the particle identification measured from the "delta-E" signals from the gas detector and the "E" signals from DSSD detector. The proton and alpha groups are well separated without any beam energy gating. When the beam energy is gated into the data, the (n,p) and (n,alpha) reaction thresholds will be confirmed.

The data analysis is on going and the final results will be presented in the reaction cross sections of (n,p) and (n,alpha) on 59Co. The discussion with the nuclear reaction modeler (Kawano at T-2) on how to compare the measured cross sections to his Hauser-Feshbach calculations has been initiated and we expect we can improve the theoretical prediction through these fruitful data on LENZ measurements at LANL.

Impact on National Missions

The neutron-induced charged particle detection system enhances our capability to provide not only crucial nuclear information in astrophysics, but also high-quality nuclear data for nuclear applications. With this new capability, LANL is positioned to lead experimental efforts for detecting neutron-induced charged particles using the wide range of neutron energy.

Completion of this additional capability of measuring neutron–induced charged particle reactions allowed us to attract multiple funding agencies inside LANL. One of them is the precision measurement on the 16O(n,alpha) cross sections, which has critical impact on nuclear applications. Since water is used as moderator or cooling agent, this cross section has been of great interest for reactor designs and applications. However, the current status of evaluation still needs a new independent set of data to validate the normalization among different measurements [14]. LENZ measurement at LANSCE will be a perfect project to provide this invaluable data set to the community.

The other impact would be the continuous effort of improving the quality of nuclear physics input for better design of fusion reactors, nuclear fission reactors, accelerator-based advanced reactors, etc [15]. Estimating radiation

damage of structural materials by measuring neutron-induced hydrogen and helium gas production rates is a crucial part of new designs, in particular when associated with testing new materials. Therefore, new measurements on these test materials using LENZ at the relevant neutron energies available at LANSCE would be valuable.

References

1. M. Jaeger, R. Kunz, A. Mayer, J. Hammer, G. Staudt, K. Kratz, and B. Pfeiffer, Phys. Rev. Lett. 87, 202501 (2001)
2. H.Y. Lee, PhD Thesis, University of Notre Dame (2006), H.Y. Lee, et al., Proceedings of Science, PoS(NIC-IX)082, (2006)
3. R.C. Haight, Proceeding of Int. Conf. on Nuclear Data for Science and Technology, DOI: 10.1051/ nda-ta:07518 (2007)
4. http://www.micronsemiconductor.co.uk
5. N. Patel, The Colorado School of Mines, PhD Thesis (2010)
6. A. Goepfert et al., Nucl. Instr. Meth. A 441, 438 (2000)
7. G. Zhang et al., Nucl. Sci. and Eng. 156, 115 (2007)
8. N. Ito et al., Nucl. Instr. Meth. A 337, 474 (1994)
9. http://www.srim.org
10. http://www.caen.it
11. http://www.mesytec.com
12. S. Kunieda et al., Phys. Rev. C85, 054602 (2012)
13. T. Kawano, P. Talou, M.B. Chadwick and T. Watanabe, J. Nucl. Sci. Tech (2009)
14. G. Giorginis et al., Int. Conf. on Nuclear Data for Science and Technology, DOI:10.1051/ndata:07481 (2007), OECD discussion, CIELO project
15. INDC(NDS)-358.Status report of the final CRP Meeting, Japan, Ed. A.B. Pashchenko (1995)

Publications

Lee, H. Y.. Neuctron-induced Reactions Nuclear Astrophysics. Invited presentation at Joint DNP Town Meetings on Nuclear Structure and Nuclear Astrophysics. (Texas A&M University, 21-23 Aug. 2014).

Lee, H. Y., and R. C. Haight. Neutron-induced charged particle studies at LANSCE. Presented at The 4th Joint Meeting of the APS Division of Nuclear Physics and the Physical Society of Japan. (Waikoloa, Hawaii, 7-11 Oct. 2014).

Effects and Mitigation of Hot Electrons in Direct Drive Implosions

Natalia S. Vinyard
20140575ECR

Abstract

The National Igniftion Facilty (NIF) provides a unique experimental platform to support stockpile stewardship, study HEDP (high energy density physics), and advance our ultimate goal of inertial fusion energy (IFE). With NIF's current configuration, efficiently utilizing available power is of crucial importance for investigating strong-shock regimes. The laser direct drive (DD) concept, extensively employed by LANL at both the Omega Facility and NIF, can provide a superior experimental platform by allowing ~7 times more energy to be coupled directly to the capsule compared to ID. However, for DD experiments to be valuable to the Laboratory's primary mission, it is crucial to understand the subtleties of DD, such as the impact of kinetic effects, particularly if the modeling is done with rad-hydro codes. For example, recent defect induced mix experiments (DIME) on NIF show a bright band of self-emission around the capsule equator which was neither replicated in simulations nor seen at lower laser intensities (I0<1015 W/cm2). At the same time, hard x-rays emission (hot electrons' signature) occurred predominantly around the equator. Understanding these laser-driven kinetic effects have the potential to impact heat transport and burn models in Complex codes and have consequences for the DD intensity limit. Managing these issues requires a detailed knowledge of hot electron evolution under realistic DD conditions. While recently there have been great strides taken in understanding supra-thermal electron dynamics, to-date there has not been a detailed assessment of its impact nor means of mitigation for polar direct drive (PDD).

Therefore, the research objective is to investigate the generation, dynamics and impact of hot electrons on the heat transport under PDD with intent to develop a better heat conduction model and use it to explore possible mitigation schemes. We believe this research will advance the predictive capabilities of our hydro codes, thereby improving the effectiveness of future implosion physics experiments. Our collaborations with scientists from LANL, LLNL, and LLE will provide the required expertise.

Background and Research Objectives

Conducting high-profile cutting-edge experiments on the NIF dictates that we accurately predict each experiment's performance to quantitatively assess its scientific impact. Meanwhile, understanding the nuances of PDD allows us to develop experiments that are better aligned with the core mission of the Laboratory. For PDD, this requires detailed knowledge of energy transfer from the laser to the target as well as heat transport within the target which is comprised of thermal diffusion, dominated by the background material properties, and energy carried by the hot electrons.

Figure 1. Schematic diagram of targets for N130320(1)

It is well known that hot electrons play a significant role in laser-driven inertial fusion [1], both for ID [2] and DD [3],[4] configurations. For example, hot electrons produced by Two-Plasmon Decay (TPD) [5], are hypothesized to be the cause of a bright band of self-emission observed around the equator in recent DIME implosions on NIF [6]. Moreover, the growth rate of the TPD instability, which scales like which scales like LnI/Te, (where I is the overlapped laser intensity, Ln is the density scale-length and Te is the electron temperature) was in qualitative agreement with the observed data. However, to explain these observations it is imperative to understand the physical processes that drive hot electron evolution, from generation through transport to deposition under the direct-drive conditions.

Modeling this chain requires a detailed physical understanding of the dominate generation mechanisms, such as TPD, the resulting hot electron distribution function, and the details of energy transport that will occur in the target material. The implosion itself happens on a relatively slow, hydrodynamic time-scale and is modeled with rad-hydro codes. On the other hand, the part of the

heat transport, that is associated with the hot electrons dynamics, requires a much faster kinetic treatment. Since it would be computationally prohibitive to simulate the whole implosion with kinetic codes, certain approximations are usually employed to provide some improvement to the thermal transport accuracy. For example, when the temperature gradients become so steep that their characteristic scale length, , is surpassed by the electron mean free path, [7], the classical diffusion model for heat transport (where the heat flow is given by with Spitzer–Harm and Peltier thermal conductivities [8]) is no longer valid. In this case, a constant thermal flux limiter, f, is typically introduced to ensure that the heat flux never exceeds the free-streaming limit and whose value is set to provide a reasonable match to the experimental observations (e.g. f=0.03 [9]). However, the effects of additional heating, say from a kinetic hot electron population are not taken into account in this simple model. While some rad-hydro codes (e.g. HYDRA [10]) have an external energy source that can simulate hot electron behavior, it is up to the user to ensure the appropriateness of its spectral, spatial and temporal levels. Consequently, simulations have to be benchmarked against experimental data to ensure the correct flux limiter and hot electron behavior are used before one can have confidence in the modeling results. Our plan is to use TPD theoretical models, combined with kinetic VPIC [11] and rad-hydro HYDRA simulations, to enhance the understanding of hot electron dynamics and their effects on thermal transport during DD implosions. This work will have impact on burn and transport models in our radiation hydrodynamics codes as well as have possible implication on DD intensity limit. Our scientific collaborators have been chosen based on their expertise in PDD experiments, kinetic & TPD modeling and PDD rad-hydro modeling to maximize the probability of success for this proposed work.

Scientific Approach and Accomplishments

Our approach was to improve on a simulation technique by J. F. Myatt, et.al of LLE [3] by investigating the impact of the TPD-generated hot electron heating on the dynamics of the capsule implosion and incorporating 2D effects which are crucial under PDD conditions. This project had two main components. The objective of the first part was to study the creation and evolution of the hot electron population, particularly for realistic 2D geometry that has not been deeply explored. The second part of this work explored new scientific ground by determining how the presence of hot electrons influences the global parameters of the implosion.

Part 1: Production, evolution, and possible mitigation mechanisms of hot electrons

The first part of the project, which consisted of two phases, examined the processes that result in hot electron creation under the conditions relevant to PDD implosions, similar to the works of Myatt [3], Vu [12] and Yan [13], and assessed how global implosion parameters are affecting their evolution.

The first phase was to identify the relevant global laser and plasma parameters, such as laser intensity, density, pressure and temperature from 2D HYDRA simulations PDD design. Two shots from Defect Induced Mix Experiment (DIME) [6], N130320 and N130321 were taken as base-line scenarios to obtain the drive and plasma parameters for the follow up theoretical and PIC code initial conditions. These two shots were chosen in part due to the plethora of available experimental data, particularly pertaining to observation of the hot electrons. The targets imploded during these shots had plastic shells of 1100 µm nominal radius and 42 µm thickness. The inner 2 µm of the shell was doped with 2.1% of Ge, and a 2-µm layer, buried by 5 µm, was doped with 1.9% of Ga for spectroscopic measurements. The capsules were mounted on a glass fill tube and filled with 5 atm of deuterium at shot time. The capsules were driven by all 192 NIF beams in a PDD configuration and delivered 319kJ and 462kJ in about 2ns for N130320 and N130321, respectively. From prior experiments on NIF and Omega, it was known that uniform laser illumination, even with highly offset equatorial beams resulted in oblate implosion. To compensate for this, the PI developed a Cone Power Tuning illumination scheme that resulted in a very symmetric image for N130320. This was achieved by increasing the energy in the two equatorial beams, while simultaneously decreasing the energy in the two polar beams relative to the nominal setting.

Performing simulations of these two shots we were able to obtain the drive and plasma parameters. These were obtained from simulations of N130320 DIME's NIF shot. The experimental neutron bang time for this shot was 3.8±0.2 ns while the neutron yield was 7.2±0.2e+11, compared to simulated values of 4.19 ns and 6.14e+11, respectively. We plot simulated plasma and laser parameters at three different times: at the beginning of the pulse when the laser has reached its maximum power (t=0.15ns), in the middle of the pulse (t=1.20ns) and at the end of the pulse right before the laser is shut off (t=2.15ns).

N130320 simulated spatial profiles of the ions density, electron temperature, ion temperature, electron number density, and the laser energy absorbed per unit volume at three different times: at the beginning of the pulse when the laser has reached its maximum power (t=0.15ns), in the middle of the pulse (t=1.20ns) and at the end of the pulse right before the laser is shut off (t=2.15ns).

In the second phase, we examined the implosion conditions at a few polar points around the capsule, such as the equator and pole and extracted 1D radial profiles to be used as the initial value input parameters to VPIC simulations.

N130320 simulated equatorial and polar spatial profiles of the ions density, electron temperature, ion temperature, electron number density, and the laser energy absorbed per unit volume at three different times: at the beginning of the pulse when the laser has reached its maximum power (t=0.15ns), in the middle of the pulse (t=1.20ns) and at the end of the pulse right before the laser is shut off (t=2.15ns).

We can see that while some of the plasma parameters are very similar at the pole of the capsule as at the equator, others can differ by almost a factor of two.

Part 2: Effects of hot electrons on direct-drive implosions
The second part of the project investigated the effects of hot electrons on DD implosions. Their main impact comes in the form of preheat or deposited thermal energy into the shell and fuel, which, even in small quantities (<10%), can severely restrain the compression and degrade implosion performance. While we did not have time to input the obtained profiles into VPIC simulations, we did perform preliminary assessment of the hot electrons effects [14]. This was done with the non-local heat transport (NLET) model [15] in HYDRA, which takes into the account longer mean free paths of hot electrons.

Due to hotter temperatures and larger temperature gradients (by a factor of 1.8 at the beginning of the laser pulse) the hot electrons penetrate the capsule and deposit their energy deeper in the equatorial region than in the polar. As a result, the implosion exhibits a highly prolate symmetry, relative to the flux-limited case. This is a stark manifestation of hot electron effects on the capsule implosion.

Impact on National Missions

This work used theoretical and computational approaches to advance our understanding of heat transport during polar direct drive implosions. The accuracy of complex codes, i.e. HYDRA and RAGE, was improved, thereby enhancing its design capability for future laser-driven validation experiments. Moreover, this work can also impact stockpile stewardship. With ongoing science campaign experiments on OMEGA at LLE, in addition to planned direct drive ignition experiments on NIF within the next five years, it is crucial to address this issue now so our research results can be incorporated into these design efforts. Dr. Steven Batha, LANL ICF Program Manager, supports this work. He says, “Better understanding and modeling of hot electron transport is important for our ICF codes. This may clarify some aspects of the current indirect-drive target design, as well as improve the PDD ignition design. It is well known that the most serious impediment to PDD ignition is the production and transport of hot electrons arising from the TPD instability. The PDD platform is important for LANL and the National ICF Program because it may provide a high-yield, more robust platform than the current ID (indirect drive) platform.”

References

1. J. D. Lindl, Phys. Plasmas 2, 3933 (1995)
2. L. Yin, et al. Phys. Plasmas 20, 012702 (2013)
3. J. F. Myatt et al. Phys. Plasmas 19, 022707 (2012)
4. D. Shvarts, et al. Journal of Physics: Conference Series 112 (2008) 022005
5. B. Afeyan et al. Phys Rev. Lett. 75 (1995)
6. M. Schmitt et al. Phys. Plasmas 20, 056310 (2013)
7. D. R. Gray and J. D. Kilkenny Plasma Phys. 22 81 (1980)
8. L. Spitzer and R. Harm Phys. Rev. 89 977 (1953)
9. M. D. Rosen Comments Plasma Phys. Controlled Fusion 8 165 (1984)
10. M. Marinak, R. Tipton, O. Landen, et. al, Phys. Plasmas 3, 2070 (1996)
11. K. Bowers, B. Albright, L. Yin, B. Bergen, and T. Kwan, Phys. Plasmas 15, 055703 (2008)
12. H. X. Vu et al. Phys. Plasmas 17, 072701 (2010); Phys. Plasmas 19, 102703 (2012); Phys. Plasmas 19, 102708 (2012)
13. R. Yan et al. PRL 103, 175002 (2009)
14. T. J. Murphy, N. S. Krasheninnikova,G. A. Kyrala,et al. Phys. Plasmas, submitted 2014)
15. G.P. Schurtz, P.D. Nicolai and M. Busquet, Phys. Plasmas 7 4238 (2000)

Hybrid Shock Ignition as an Alternate Concept for Fusion Energy

Eric N. Loomis
20140180ER

Introduction

Achieving energy gain from thermonuclear reacting plasmas in a laboratory setting is a fundamental aim of researchers around the world since, in time, it would lead to a new and controllable energy source, as well as a much needed platform for supporting aspects of Stockpile Stewardship. Inertial Confinement Fusion (ICF) has remained at the forefront of this research for many years and its flagship, the National Ignition Facility (NIF), is currently performing the experiments towards ignition anticipated for well over a decade. In the past year, however, thermonuclear ignition on NIF using conventional indirect-drive ICF has proven more elusive than previously expected. Even if ignition is achieved, new high yield concepts are needed for useful energy production as well as future "Applications of Ignition" experiments. In this project we present a novel platform with the potential for high energy gain implosions, which integrates the existing advances made in Indirect-Drive Inertial Fusion with the promising new scheme of Shock Ignition (SI). If successful, our Hybrid SI concept will provide a new platform by which to study hohlraum-based implosion physics, but which accesses different conditions than current NIF ignition attempts and stresses different aspects of our predictive capabilities, which we expect will lead to improved physics models in numerical radiation hydrodynamics codes.

Hybrid SI will use spherical hohlraums with a novel arrangement of symmetric laser entrance holes that allow both indirect-drive beam access to the hohlraum walls followed by shock ignitor drive beams that directly illuminate and provide requisite heating to the compressed fuel. Our exploratory research into this concept will involve multi-dimensional radiation hydrodynamics design calculations that demonstrate adequate implosion and ignitor symmetry. These calculations will then be used to study new physics associated with instabilities generated by collisions of converging rippled shocks.

Benefit to National Security Missions

Alternate Inertial Confinement Fusion (ICF) concepts, such as Shock Ignition (SI), will stress different aspects of the ignition problem compared to conventional indirect-drive and will help elucidate shortcomings in our predictive capabilities. This platform is also a potential low convergence design that at ignition-scale could out-perform current NIF implosions or at least be more predictable. This work addresses a major gap: LANL is currently the only major ICF laboratory without an investment in SI and, furthermore, LANL is the only ICF laboratory without an investment in any alternative ignition platform. The intent of this project is to begin to build an innovative Hybrid SI program with potential experiments on NIF within four years.

Progress

In FY15 we completed 2-D design studies of our OMEGA scale targets, target fabrication of complex geometry gold hohlraums for experiments originally planned in FY16, began investigations into optimized laser pulse shapes for hybrid-driven implosions, and discovered the potential detrimental effects of perturbations on converging shocks for shock ignition. Since efficient transfer of energy during the collision of the ignitor shock with the rebounding initial compression shock is essential for reaching optimal conditions for thermonuclear ignition, this last accomplishment will likely prove to be of utmost importance. For this reason we plan to have it as our central focus for the remainder of FY15 and into FY16.

This issue revealed itself as we were studying the results of 2-D target simulations. These simulations studied the implosion physics of x-ray driven capsules with direct-drive ignitor shocks. Capsule diameters were maintained at 550 microns and contained deuterium-tritium gas. Capsules had either 50 or 25 micron thickness and 50 or 25 atmospheres of DT, respectively. Thinner capsules were expected to give greater neutron yield at the expense of diminished hydrodynamic stability.

Low-mode drive asymmetry on the capsule was imposed using spherical harmonic expansion of the radiation flux from the hohlraum wall plasma. Radiation from the hohlraum wall emission to the capsule was then transported using multi-radiation group implicit Monte Carlo photonics. Finite statistics of this radiation field imposed high spatial frequency roughness at the ablation surface of the capsule; seeding ablative Rayleigh-Taylor perturbations similar to what is imposed on real targets with finite surface roughness. The combination of this high frequency roughness and the low mode drive asymmetry allowed us to study near experimental conditions in two dimensions. The hohlraum and laser geometry suggested that our targets are most likely to have mode 4 drive asymmetries so these were imposed on both the thick and thin capsule simulations. Modulations at the inner surface of the capsule grew rapidly into the gas at the time of capsule deceleration after feeding through the shell from the ablation surface. Thinner shells were observed to reach higher DT ion temperatures and neutron yield, but suffered greater instability growth and mixing during deceleration. Prior to the formation of the instability growth at capsule stagnation, modulations in pressure were observed in the gas due to asymmetries carried by the initial shock convergence. These gas modulations reached their maximum at the time of shock bounce at the center of the capsule, but then reduced somewhat during the bounce and divergence stage of the shock. There is some theoretical evidence for this unstable/stable asymmetry transition in spherical shock problems, but it has not yet been studied in regards to shock ignition, which relies heavily on the strength and stability of converging shocks.

From 1-D simulations in the first year, we discovered a need for tailored pulse shapes that had features well-suited for the separate stages of fuel compression and ignitor shock heating. These features need to be contained within a single, shaped laser pulse due to the OMEGA facility restrictions. To accomplish this a pulse was used that had a high-intensity short prepulse followed by a roughly 2 ns duration square pulse of moderate intensity. In a real experiment, the beams creating the ignitor shock would be time such that the high-intensity prepulse would irradiate the capsule just prior to capsule stagnation, thus maximizing the strength of the ignitor shock. This pulse shape was simulated in a laser-hohlraum calculation using the code Lasnex to generate the radiation flux source used in the capsule simulations discussed above. Under OMEGA laser intensities the hohlraums are predicted to reach about 200 eV radiation temperatures during the peak of the main 2 ns pulse stage.

Following this set of 2-D OMEGA capsule simulations we decided to start exploring the effect of gas modulations on shocks in spherical geometry. Our first method for studying this effect was to use very thin (i.e., 5 micron) capsules known as Exploding Pushers because these types of targets due not suffer from deceleration Rayleigh-Taylor growth and may be a good platform for studying them experimentally. In Hydra we used radiation flux asymmetries to change the gas shock conditions, but can now also place single mode modulations at the inner surface.

Future Work

We were not awarded facility time under the OMEGA laser Laboratory Basic Sciences (LBS) program so experiments are not likely to occur in this project as originally planned. For this reason we will continue to focus our efforts on detailed 2- and 3-D simulations of new physics issues associated with Shock Ignition that we have discovered in this LDRD. One issue, specifically, is determining the loss in energy transfer from the ignitor shock to the compressed fuel when the fuel has a modulated density field or when the ignitor collides with a modulated rebounding shock. The modulations in these cases grow much more rapidly due to convergence of the ignitor shock reducing the amount of shock heating to the fuel. In FY16 we will study this behavior using the LANL Rage code and the LLNL Hydra code by applying inner surface perturbations to our OMEGA scale capsules. These perturbations will imprint themselves into the fuel, which will produce growing modulations in the converging ignitor shock. By varying the initial wavelength of the inner surface perturbation we can change the spatial and temporal distribution of fuel density modulations and thus the amount of shock heating to the fuel as well. This effect should be present in both the direct-drive and hybrid concepts and may set lower limits on required ignitor shock pressure to overcome the loss in energy transfer efficiency. Part of our FY16 efforts will go into designing actual experimental platforms to test this effect, which we will then propose to the Inertial Confinement Fusion Science Campaign to support in out years.

In FY16 a new postdoc will be joining XCP to work on designs at NIF-scale. These designs will be used primarily to study instabilities, such as converging modulated shock collisions, at ignition conditions.

Conclusion

Success of this project is based on demonstrating the novel integration and nuclear performance benefit of a hohlraum-driven implosion with direct-drive Shock Ignition of the fuel. Specifically, the outstanding questions that must be addressed to declare success regards the achievable symmetry of the hohlraum-driven capsule implosion and the symmetry that must be attained by the ignitor beams

to result in enhanced nuclear performance (neutron yield, ion temperature, and areal density) beyond standard implosion techniques. We will also produce ignition-scale design calculations in order to predict feasibility for NIF.

Quantum Kinetics of Neutrinos in the Early Universe and Supernovae

Vincenzo Cirigliano
20140252ER

Introduction

Neutrinos are perhaps the most mysterious and elusive of the known particles, and yet play a crucial role in the early universe and the life of stars. Neutrinos interact only very weakly and have tiny masses, the heaviest neutrino being at least a million times lighter than the electron, the lightest charged particle. Moreover, observations of solar, atmospheric, reactor, and accelerator neutrinos indicate that the neutrinos come in three different flavors, that can morph into one another as they evolve, through a genuine quantum mechanical interference effect. Despite their elusive nature, neutrinos play a special role in the dynamics of the early universe (EU) and supernovae (SN), because they come in huge numbers and because through their flavor-dependent weak interactions they can set the ratio of neutrons to proton in both the EU and in the heated ejecta of a supernova. Such ratio is a key ingredient in understanding quantitatively what atomic nuclei are synthesized in these two environment.

The overarching goal of this project is to set up the analytic and computational tools needed to describe neutrino kinetics in the EU and SN environments, simultaneously keeping track of the effect of quantum mechanical morphing and the role of inelastic collisions with the medium. The appropriate tool to describe neutrino evolution in a hot and dense medium are the so-called Quantum Kinetic Equations (QKEs). To date, no self-consistent derivation of the QKEs exists, let alone numerical solution. Our proposed research will improve on the current state-of-the-art in two important aspects: first, it will provide a first-principle derivation of the QKEs, based on non-equilibrium field theory and a controlled expansion in ratios of widely separated length scales.

Benefit to National Security Missions

Understanding how neutrinos have shaped the evolution of the cosmos and of stars, including the implications for the synthesis of atomic nuclei, is a major goal of both the Nuclear Physics and High Energy Physics Office of Science.

Moreover, our project will develop cutting edge capability in transport theory. While this will be applied to neutrinos in supernovae and early universe, in the future the very same tools could be applied to programmatic work supporting our national security mission.

Progress

Theory

The research team demonstrated that n anisotropic environments a coherent spin-flip term arises in the Quantum Kinetic Equations (QKEs) which govern the evolution of neutrino flavor and spin in hot and dense media. This term can mediate neutrino-antineutrino transformation for Majorana neutrinos and active-sterile transformation for Dirac neutrinos. In an article published in Physics Letters B (V. Cirigliano, G. Fuller, A. Vlasenko, "A new spin on neutrino quantum kinetics", Phys. Lett. B747 (2015) 27-35) we discuss the physical origin of the coherent spin-flip term: the spin of a massive neutrino can precess due to the interaction with an axial-vector field generated by other neutrinos or other matter particles, such as electrons and protons, carrying weak charge. This spin precession does not require the presence of a magnetic field nor a neutrino magnetic moments. In the same article we have provided explicit expressions for the QKEs in a two-flavor model with spherical geometry, the first step towards a computational implementation of the new effect. In the context of this two-flavor model, we have also demonstrated that coherent neutrino spin transformation depends on the absolute neutrino mass and the so-called Majorana phases, parameters that are very difficult to measure in laboratory experiments.

We obtained the analytic expression for the collision term of the QKEs, accounting for neutrino scattering on other neutrinios, electrons, protons, and nucleons. We have also included neutrino pair production and an-

nihilation, in summary all the processes that are relevant in the early universe and supernova environments. We are currently putting these results in a form that will be suitable for computational implementation (e.g. we are reducing some of the integrals from five-dimensional to two-dimensional, more amenable for an efficient numerical calculation). Within FY15 we expect to summarize our results in a publication.

Computation

On the computational/astrophysical front, we examined whether the newly derived neutrino spin coherence could lead to large-scale coherent neutrino-antineutrino conversion. We have done so in a simplified model of a supernova envelope, using the so-called single-angle approximation for the neutrinos emitted by the surface of the compact object. In a linear analysis we found that neutrino-antineutrino transformation is largely suppressed, but we have demonstrate that nonlinear feedback can enhance it. We have pointed out that conditions which favor this feedback may exist in core collapse supernovae and in binary neutron star mergers. Our results have appeared as a preprint (V. Cirigliano, G. Fuller, A. Vlasenko, "Prospects for neutrino-antineutrino transformations in astrophysical environments", 1406.6724) under review in Physical Review Letter.

Future Work

In the upcoming fiscal year, we will finish the analytic calculation of the collision terms, valid both for the early universe isotropic conditions and for anisotropic conditions relevant to compact astrophysical environments. Submit the results for publication in high impact journals

Our goals are summarized as follows:

- Perform numerical simulations of the full quantum kinetic equations (QKEs) describing the evolution and decoupling of neutrinos in the early universe. We plan to do this both for the case of three active neutrinos and for the case of active-sterile mixing.
- Perform exploratory numerical simulations of the QKEs in a spherically symmetric supernova geometry.

Conclusion

The proposed research will enable us to address two sets of outstanding questions:

1. What is the energy and flavor composition of neutrinos about 1 sec after the Big Bang, when the light nuclei are first synthesized? How does this knowledge constrain the existence of possible new neutrino states, so called "sterile" neutrinos?
2. How do inelastic collisions affect collective flavor transformation in a supernova envelope? What are the consequences for the synthesis of heavy elements in the neutrino-heated supernova ejecta? What are the consequences for the neutrino signal that can be potentially detected from galactic supernovae?

Publications

Blaschke, D., and V. Cirigliano. Neutrino quantum kinetics: the collision term. 2015. LA-UR-15-25029.

Cirigliano, V., G. M. Fuller, and A. Vlasenko. A new spin on neutrino quantum kinetics. 2015. Physics Letters B. 747: 27.

Vlasenko, A., G. M. Fuller, and V. Cirigliano. Prospects for neutrino-antineutrino transformation in astrophysical environments . . To appear in arXiv:1406.6724.

Vlasenko, A., V. Cirigliano, and G. M. Fuller. Neutrino quantum kinetics. 2014. Physical Review D. 89 (105): 004.

Designing the Next Generation Compton Light Source

Nikolai Yampolsky
20140269ER

Introduction

The ultimate goal is to prove the feasibility of the new technology for light sources based on inverse Compton scattering using microbunched electron beams. In this setup the scattered light will be coherently amplified since the radiation generated by each microbunch adds up in phase. The idea has never been explored since there was no recognized mechanism for creating very short wavelength density modulations in relativistic electrons beams with relatively low energy (~100 MeV). We propose to create the beam distribution consisting of several well separated energy bands through a series of manipulations with the bunch phase space using laser modulation and conventional electron beam optics. Such a distribution will drive the two-stream instability resulting in the plasma wave, i.e. density modulation. The proposed scheme can be split into three well separated stages, namely (1) creating required beam distribution, (2) development of the two-stream instability causing beam microbunching, and (3) scattering laser pulse off the microbunched beam to produce radiation with increased coherency. We will study each of these stages and analyze start-to-end performance of this novel scheme. We anticipate finding the parameters region for which the novel scheme results in 5-6 orders of magnitude increase in brightness over existing Compton light sources in 1-10nm wavelength range.

The largest challenge of this project is in mitigating various deleterious effects which may suppress the instability leading to beam microbunching. Preliminary analysis shows that they are negligible at large wavelengths (on the order of 1 micron) and dominant at small wavelengths (on the order of 1 nm). During the course of the project we will identify the precise limit of the novel technology.

Benefit to National Security Missions

If successful, the project will lead to development of a new generation soft X-ray Compton light source having significantly better beam quality over existing ones. This source will be compact (~100m) and relatively cheap (less than $100M), which makes it suitable to be widely distributed to multiple national laboratories and major research universities. The high brightness, tunability, and short duration of these sources will allow for many experiments which currently have to be conducted at the 3rd and 4th generation light source facilities which are severely overbooked. Development of a cheap, competitive, high-brightness soft X-ray light source will cover several national light source needs and will boost many research areas such as Biology, Chemistry, Physics, and Material Science.

AOT division is currently designing the Injector Test Stand (ITS) needed for testing novel ideas in Beam Physics required for successful commissioning of the MaRIE hard X-ray free electron laser (FEL). The ITS can potentially be used as a Compton source for enabling early MaRIE related experiments prior to construction of the FEL both for refining MaRIE FEL parameters and for providing additional FEL justification and motivation. The capability developed through this proposed work will allow a larger number and breadth of preliminary experiments to be done. This source can be used even after the commissioning of MaRIE FEL, adding a complementary soft X-ray capability to the facility.

Progress

Start-to-end simulations have started. The simulations include simulation of the electron optics beamline required to generate the unstable electron distribution (ELEGANT simulations) and further development of the multi-stream instability in the following focusing channel (CPIC simulations). The analysis of the results is underway.

Future Work

- 3D simulations of the instability.

- Detailed start-to-end simulations using output of ELEGANT as an input for CPIC.
- Include intra-beam scattering into CPIC.
- Optimize performance of the scheme resulting in the largest growth of the modulation.
- Estimate the limit of the technology in terms of the shortest wavelength modulation which can be produced.

Conclusion

Perform detailed study of the two-stream instability in relativistic beams driven by the multi-stream distribution. Support conclusions with detailed analytical estimates and numerical simulations including all relevant effects.

Determine whether this mechanism for the microbunching instability may be used for improving quality of the Compton light source. Provide reliable quantitative estimates of the resulting source parameters.

Determine whether this mechanism for microbunching may be significant in other applications in Accelerator Physics, e.g. seeding schemes for free electron lasers (FELs).

Publications

Yampolsky, N. A., G. L. Delzanno, C. Huang, and D. Shchegolkov. Two-stream Instability at Soft X-ray Wavelengths for Increasing Brightness of Compton Sources. Presented at 35th International Free-Electron Laser Conference. (New York, NY, 25-30 August, 2013).

Yampolsky, N. A., G. L. Delzanno, C. Huang, and D. Shchegolkov. Two-stream Instability at Soft X-ray Wavelengths for Increasing Brightness of Compton Sources. Presented at North American Particle Accelerator Conference. (Pasadena, CA, 29/09/ - 4/10, 2013).

Yampolsky, N. A., G. L. Delzanno, C. Huang, and D. Shchegolkov. Two-stream Instability at Soft X-ray Wavelengths for Increasing Brightness of Compton Sources. Presented at 55th Annual Meeting of the APS Division of Plasma Physics.

Combined Klystron and Linac (Klynac)

Bruce E. Carlsten
20140351ER

Introduction

We propose an engineering prototype demonstration (Technology Readiness Level (TRL) of 5) of a novel accelerator system architecture, where the accelerator's RF power source is integrated with the accelerator structure itself. Using a klystron as the RF power source, we have named this architecture "Klynac" to represent the functionalities of both the klystron and linear accelerator (linac) parts. To quantify its potential impact, the Klynac technology may lead to a reduction of a factor of 5 to 10 in over-all weight of portable radiography systems when used with an existing LANL TRL 6 capability, the resonant air-core transformer (compared to the 1900-lb, 3-MeV Varian Linatron M3, intended for fixed or truck-mounted applications). The reduced weight and size of the Klynac will allow man-portable radiographic missions, including emergency response, and provide a new technology to reduce the cost of medical radiography systems.

Benefit to National Security Missions

This project aims to develop technology that can be used to reduce the size of portable MeV-class radiography systems (including those use for medical cancer treatments) from ~ ton weights to a few hundred pounds. The NA-22 roadmap "Special Nuclear Materials Movement Detection Program Radiation Sensors and Sources Roadmap" calls for high-repetition-rate linacs (1–10 kHz) to increase photon flux compared to traditional linacs, allowing detection of both prompt and delayed signatures. The roadmap specifically calls for development of next-generation accelerator concepts and development of compact, mobile photon sources, which can be addressed with the technologies developed by the proposed work.

Progress

In FY15 we finished the stability analysis of the Klynac design, showing good operational stability (i.e., it will turn on and reach a stable operating point that is not highly sensitive to beam parameters. We also received our 50-kV electron gun and the final drawings for our Klynac structure. The first half of the klynac structure is currently being fabricated in a local machine shop, soon to be followed by the second half. After fabrication, there will be a fine-tuning process where we ensure all Klynac cavities have the correct resonant frequency. We anticipate the entire Klynac structure will be delivered before the end of the fiscal year. By the end of the fiscal year, we will also have completed the necessary modification to our test beamline where we will experimentally demonstrate our Klynac structure in FY16. These modifications include support structures, vacuum pumping, new solenoids with power supplies, and modification of the 50-kV CLIA pulse power supply.

Future Work

All hardware components were received by the end of FY15. Additionally, all modifications to our test beamline were completed at the end of the fiscal year. In FY16, we will test operation of this device. The key test, the proof-of-principle demonstration, will be to measure higher final electron beam energy than injected by the electron gun (50 kV). We will measure the final electron beam energy with an X-ray spectrometer.

Conclusion

The main technical goal of this project is to demonstrate that a portion of the bunched klystron beam can be accelerated in a linac. For this demonstration, a low voltage resonant klystron and linac will be built, driven at 50 kV and accelerating the electron beam to 1 MeV. The S-band linac design is standard, and will be identical to that used in the previous linacs. Likewise, the electron gun design and the 4-cavity klystron design will follow standard design practices.

Multi-GeV Electron Radiography

Frank E. Merrill
20140591ER

Introduction

This project will investigate the potential for multi-GeV electron radiography to provide high spatial and temporal resolution measurements of dynamic materials at the multi-probe diagnostic hall (MPDH) proposed at the Matter and Radiation in Extremes (MaRIE) facility. This technique has been proposed as one of the major diagnostics on the MPDH, but has not yet been experimentally demonstrated. We plan to design an imaging system to utilize the multi-GeV beams at Stanford Linear Accelerator Center to test the concepts and performance of high energy electron radiography. Although this type of imaging has been demonstrated with MeV-GeV protons, it has never been attempted with high energy electrons. The demonstration of this measurement capability would provide a new window into the dynamic process of opaque materials at unprecedented time and length scales. This new window would allow a more fundamental understanding of material response to extreme environments such as is experienced within a functioning nuclear weapon system.

Benefit to National Security Missions

This work will test the concept of using multi-GeV electrons for radiography of thin dynamic systems. This concept is a major pillar of the proposed Multi-Probe Diagnostic Hall at the Matter and Radiation in Extremes (MaRIE) facility. It is envisioned that these high energy electrons will be used to study materials relevant to the future weapons program, measuring fundamental materials properties with very high temporal and spatial resolution. The successful development of this technology will support the fundamental material research efforts within the DOE Office of Science and the fundamental and applied research in the nuclear weapons program for both inert as well as reactive materials such as high explosives. This capability to measure dynamic material response will also be applicable to DOD programs for military applications.

Progress

We have identified a location at SLAC to test eRad concepts. We developed the suite of simulation tools to simulate eRad performance and we have identified existing SLAC equipment for these measurements and have designed a system to utilize this equipment. The system is being installed and first measurements will be collected in late July, fully meeting our second year goals.

Future Work

In the third year of this project:

- The first data will be collected at the end of the second fiscal year.
- Analyzing the second year's data, we will assess the performance of the fielded imaging system.
- From the analysis of this data we will determine if further refinement of the system is needed. If so, we will design and implement these modifications.
- We will perform a second iteration of measurements at SLAC to determine the performance capability of multi-GeV electron radiography.

Conclusion

This project plans to design, assemble and test the first ever Multi-GeV electron radiography system. These measurements will focus on characterizing the performance of this type of radiography system. This effort will provide important information for the MaRIE project in determining the electron radiography capabilities as well as specifying the requirements for a future facility.

Publications

Merrill, F.. Imaging with penetrating radiation for the study of small dynamic physical processes. 2014. Laser and Particle Beams.

Photocathodes in Extremes: Understanding and Mitigating High Gradient Effects on Semiconductor Cathodes in X-FELs

Nathan A. Moody
20140616ER

Introduction

At the frontier of many scientific disciplines is the goal to understand, and even control matter, especially when it is subjected to extreme and dynamic conditions, such as those encountered in combustion, explosions, or other excursions in temperature and pressure. The ideal tool to probe matter in such extreme conditions is what has become known as an x-ray laser, or x-ray free electron laser (X-FEL). An X-FEL produces pulses of light (coherent hard x-rays) with a wavelength comparable to the distance separating atoms in solid materials and a pulse duration nearly as short as the changes which occur in materials, such as the formation and breakage of chemical bonds. Consecutive pulses of these hard x-rays would allow movies to be made of atoms or molecules, providing first-ever crucial information about how matter interacts under extraordinary environmental conditions. Any FEL relies upon a very strictly defined electron beam and what stands in the way of building an X-FEL light source like the one described above is the lack of sufficiently bright electron beam. Designs for such a beam exist but call for electron beam sources (cathodes) with performance that has never been proven or verified. These large scale X-FEL instruments are very costly and time consuming to construct, thus their design should be built on known facts regarding electron beam source performance and capability. The dominant question regarding most X-FEL designs relates to the maximum electric field strength it can be exposed to (and for how long) before the material breaks down due to the stress of the extreme electric field (> 100 MV/m). This project answers the question of whether present-day cathodes can survive high electric field gradient and it also presents methodologies for addressing and mitigating this risk.

Benefit to National Security Missions

MaRIE: This project addresses the highest risk element in Matter-Radiation Interacting in Extremes (MaRIE) x-ray free electron laser (X-FEL) design: the unknown effect of high field gradient on semiconductor photocathodes. Because these effects irreversibly damage the emitted electron beam, they impact nearly every other aspect of an X-FEL design and must therefore be rigorously and experimentally understood, quantified, and mitigated before such designs mature beyond the conceptual stages. This project accomplishes all these goals.

DOE/DOD/SC: all next-generation light sources require a high brightness electron beam source. This research will answer fundamental questions concerning the behavior of cathodes under extreme conditions. The results will include fundamental research validating the basic approach to electron beam source design, and demonstrations of the enabling technology required to successfully utilize those cathodes in next generation light sources, user facilities, or weapons systems. We identify key technical challenges and solutions which simplify FEL designs and/or reduce the commissioning and operatation costs significantly.

Basic Understanding of Materials: x-ray free electron lasers (X-FELs) are the ideal tool to interrogate, understand, and even control matter in extremes. To date, nineteen Nobel Prizes have been awarded for x-ray science using beam-based x-ray light sources, and we can expect more in the future as these tools open vast science frontiers to probe matter-in-extremes at unprecedented temporal, spatial, and energetic scales. The work represented in this project closes critical technology gaps in the fielding of X-FELs as instruments of discovery science.

Progress

RF cavity fabrication

The cavity proper has undergone its last fabrication step, high temperature brazing, and it passed leak rate, flatness, surface finish, and dimensional tolerance inspections at the manufacturer on 6/18. The next step is similar inspections at LANL upon its arrival toward

the end of June. Design considerations, preparation and machining of these cavity components, to accommodate the high temperature braze process at a temperature of 1700 Fahrenheit in hydrogen furnace, are similar to those which will be used during eventual fabrication of the MaRIE photoinjector structure. Thus, this LDRD project has significantly advanced this critical LANL capability by documenting and demonstrating best practices relating to: braze joint design (horizontal versus vertical), component modularity, braze alloy composition and temperature dependence, braze form factor (shim versus paste), braze temperature dependencies (melting, diffusion, and erosion), component cooling rates, pre- and post-braze stress release anneals, braze dependencies on surface finish, and mitigation of virtual leaks.

The power coupler assembly was updated and modified to reduce fabrication cost and time, to make the coupler more modular (for ease of later upgrade or, if necessary, repair). This further reduces project risk, enhances portability, and improves compatibility with our high-power testing host institution, the Argonne Wakefield Accelerator.

We are preparing for fabrication and brazing of the RF power coupler assembly, and expect to have all parts of the test cell in-house by mid- to late-August.

RF cavity testing
We are on-track to have essentially all of the test cell parts in-house and assembled and initial low-power RF tests performed by early September 2015.

Cathode fabrication
We have demonstrated in FY15 a LANL routine which allows us to reproducibly manufacture cesium antimonide protocathodes with quantum efficiency (the ratio of vacuum emitted electrons to surface incident photons) of about 2% at 405 nm wavelength on thick optically flat substrates like silicon, glass, and single crystal metals. Having demonstrated the requisite repeatability, we have also completed the required modifications to optimize cathode stoichiometry which will bring quantum efficiency (QE) up to greater than 10%. This complements our earlier demonstrations of utilizing encapsulated alkali-antimonide cathodes in long-term storage. The biggest advantage of the alkali antimonide photocathode family is very high, up to approximately 30%, quantum efficiency at the optimum wavelength which lies in the visible part of the spectrum. The photocathodes of this class can only be manufactured and operated under UHV conditions, which is why we have developed this LANL capability for the later stages of this project. Wide tunable bandgap semiconductors, comprised of InGaN are also being investigated for their potential as efficient and robust photocathode candidates. Several InGaN semiconducting thin films with bandgaps in the 2.0 to 2.5 eV range are being screened with and without surface Cs treatment for their photocathode response following illumination with 405nm light. Other InGaN films will be grown with optimized photocathode properties and characterized immediately following growth under ultra-high vacuum conditions using 405 nm light and a Faraday charge collection device recently installed on the LANL ENABLE growth system. None of these semiconductor cathode classes have been investigated at the high electric field gradients targeted in this project.

Future Work

Complete low power RF Cavity Testing
Having completed the fabrication of the RF cavity structure in FY15, we will repeat several of last year's measurements but this time as a fully-assembled structure: RF coupling, cavity resonance, coupling co-efficient, RF joint compatibility, initial cathode integration using instrumented metallic surrogate, and low power characterization of RF cavity. Milestone: report data on each of the metrics listed above.

High power RF testing
Transport assembled RF structure (on strong-back chassis) to RF testing station and integrate with the local control system, diagnostics, and drive laser. Dark current measurements using surrogate cathode first. Milestone: report data on each of the metrics listed above.

Design and fabrication of movable cathode seal
The above tasks use a non-removable cathode for simplicity but first introduction of semiconductor cathode and/or other metal samples into cavity test cell at high power RF require a mobile RF joint to allow cathodes to be removed and inserted. We will design, fabricate and test this seal, allowing us to gain first indications of cathode performance as a function of electric field gradient for both removable and non-removable cathodes. Milestone: first publication of results.

Begin full cathode characterization
Begin parametric testing at a variety of field gradients (starting with the lowest first), mitigation efforts of field breakdown, quantify electric field damage thresholds as a function of RF pulse duration, test multiple cathode samples involving more than one type of semiconductor film, scan surface area of cathode to provide a "map" of quantum efficiency across the surface. Milestone: second publication.

Conclusion

This research will answer fundamental questions concerning the behavior of electron beam sources (namely, upper limit of electric field) when subjected to the conditions

associated with an electron beam based x-ray free electron laser (X-FEL). The results will include both fundamental research validating the basic approach to designing electron beam sources, and/or demonstrating the enabling technology required to successfully utilize those cathodes in a specific X-FEL design. Key technical challenges and solutions, such as cathode seal geometry and high electric field surface treatment, will emerge and the data will allow future X-FEL designs to be based on validated test results.

Publications

Carlsten, B. E., S. J. Russell, J. W. Lewellen, D. C. Nguyen, P. M. Anisimov, C. E. Buechler, K. A. Bishofberger, L. D. Duffy, F. L. Krawczyk, Q. R. Marksteiner, N. A. Moody, N. Yampolsky, and R. L. Sheffield. MaRIE XFEL physics design risks and risk mitigation plans. 2015. Los Alamos National Lab. (LANL), Los Alamos, NM (United States); DOE Contract Number: AC52-06NA25396; LA-UR--15-22069.

Lewellen, J. W., and N. A. Moody. High gradient cathode testing for MaRIE. 2014. In FEL2014. (Basel, Switzerland). , p. THP024. Basel, Switzerland: JaCOW.

Moody, N., H. Yamaguchi, G. Gupta, and A. Mohite. Graphene shield-enhancement of photosensitive surfaces and devices. 2014. Micro- and Nanotechnology Sensors, Systems, and Applications VI. 9083 (6): 9083331.

Superconducting Nuclear Recoil Sensor for Directional Dark Matter Detection

Markus P. Hehlen
20150437ER

Introduction

The universe consists of 72% dark energy, 23% dark matter and only 5% of ordinary matter. One of the greatest challenges facing the scientific community today is to understand the nature of dark matter. Dark matter detection is shaping experimental work in astrophysics and particle physics, and it is widely recognized as the most important problem in 21st century cosmology. Current astrophysics and particle physics models suggest that dark matter is made up of slowly moving, weakly interacting massive particles (WIMPs). They pass through the solar system and should leave signals in detectors. However, their interaction with ordinary matter is exceedingly weak, making their direct detection in the presence of ubiquitous backgrounds a monumental task. Detectors that can sense the predicted sidereal variation of the WIMP flux direction hold the greatest promise to unambiguously prove the Galactic origin of WIMPs. The goal of this project is to explore a novel concept of a solid-state WIMP detector with direction sensitivity. The high density of a solid detector may overcome the background noise limitations of current large-volume gaseous detectors. The proposed detector consists of a layered structure comprising superconducting traces applied to ultra-thin glass sheets. The anisotropic structure is key to enabling the detector's direction sensitivity. WIMP interactions within the glass create nuclear recoils that migrate forward through the glass and deposit their energy in the adjacent superconductor. The respective heat can cause the superconductor to transition to an electrically resistive state and produce a measurable voltage spike. The results of this study will allow us to formulate a roadmap for the development of the first solid-state WIMP sensor that offers direction sensitivity and high density. Such a detector could usher in the next generation of dark-matter experiments looking to sense the unambiguous direction signature of WIMPs for the first time.

Benefit to National Security Missions

This work builds new capabilities for the LANL Nuclear and Particle Futures Science Pillar, specifically the Nuclear, Particle, Astrophysics, and Cosmology (NPAC) thrust area. Developing advanced detectors that may enhance our understanding of the physics beyond the current standard model is of particular importance and directly ties into national funding agencies such as DOE and NSF. In particular, the fundamental nature and the direct detection of dark matter is one of the key focus areas of the "Cosmic Frontier" research in DOE's High Energy Physics (HEP) program in the Office of Science as well as NSF's Division of Physics (PHY). The DOE Cosmic Frontier in particular focuses on new experimental concepts and dark matter detectors. Success in this project will allow us to develop new DOE-sponsored programs and will position LANL to assume the leading role in a next-generation directional dark matter experiment. The present work is also relevant to the Science of Signatures Science Pillar. It builds underlying science and technology in areas of interest to nuclear nonproliferation, treaty verification, and global security where directional detectors can play a critical role.

Progress

During an initial phase, we carefully studied various options of producing a multi-layer device consisting of alternating WIMP interaction layers and superconducting traces. Several device architectures were assessed based on material availability, ease of processing, scalability, and expected detector sensitivity. Practical considerations and model calculations informed each other. We concluded that the initial approach of stacking a large number of sub-micron thick polymer layers faces significant layer adhesion and surface roughness challenges. A new device architecture was developed that consists of superconducting Nb traces patterned onto commercial ultra-thin glass sheets. This design (1) is significantly more scalable, (2) maintains the directionality of the detector, (3) can be tuned via geometry to a desired recoil

energy range (enabling means for active background rejection), and (4) offers an attractive low-mass target (silica glass) that is suited for interaction with low-mass WIMPs. While previous dark matter searches have focused on the ~100 GeV/c^2 WIMP mass scale, the lower WIMP mass region (few GeV/c^2) has gained interest due to recent observational and experimental hints as well as motivations from theory. The low mass regime is challenging as it requires very low (few keV) energy thresholds, a region dominated by large backgrounds that are very difficult to discriminate. Due to these challenges, the current limits on dark matter in the <=10 GeV/c^2 region are quite poor. Therefore, the technology pursued by our experiment, with its potential low-keV energy sensitivity, could make a strong impact in this regime even with quite small target masses, particularly if background discrimination/mitigation and directional sensitivity can be achieved.

Work was focused on modeling (Task 1) as well as fabricating and characterizing (Task 2) the first single-layer prototype of the new device architecture. The key accomplishments are:

We identified two types of ultra-thin (25-30 µm) glass sheets that are commercially available as AF32 and D263 products in high quality and square-meter-scale areas from Schott Glass. Test samples were obtained from Schott, and their composition was measured using Secondary Ion Mass Spectrometry (SIMS). The compositional information served as input for the nuclear recoil modeling task.

Our University of New Mexico collaborators calculated the nuclear recoil energy distribution in the thin glass for interactions with WIMPs of different masses. This data was then used to perform SRIM (Stopping and Range of Ions in Matter) calculations to determine the recoil range and thus predict the required superconductor thickness. From the calculated 50-300 nm thickness range we then predicted the width of the Nb trace to be on the order of 2-30 µm in order to offer sensitivity to 5-50 keV nuclear recoils. These dimensions are routinely achieved with standard deposition and photolithographic processes.

Nb films were deposited on sapphire test substrates using both RF sputtering and e-beam evaporation at both room temperature and 800 oC and using two different LANL sputtering chambers. Superconductive film quality can be strongly influenced by deposition parameters. Evaluating different deposition techniques allows us to determine the optimal process. The films were analyzed by X-ray diffractometry to assess crystallinity and crystal phases. Test structures with Nb traces of various lengths and widths were fabricated from these films using standard photolithographic processes.

A new cryogenic test station was designed and fabricated to allow for electrical testing of superconducting devices between room temperature and 3.8 K using an existing closed-cycle helium refrigerator. A sensitive 4-wire resistance measurement setup was implemented to allow for the automated acquisition of resistance vs. temperature curves.

Superconductivity was observed at a critical temperature of 5.9 K in a device containing a meandering trace of 5 µm width, 1600 µm length, and 200 nm thickness deposited by RF sputtering at 800 oC. Characterization of the other films is currently in progress, and the results will allow us to downselect both the deposition chamber and the deposition process.

Work has started to measure the critical current density of the Nb traces and to record the fast superconducting-to-normal transients expected upon an interaction. This will initially be tested with an Americium-241 alpha source placed inside the cryostat. Once successful, the setup will be relocated to the LANL Ion Beam Materials Science Laboratory (IBML) for a systematic exploration of the detector's energy and flux dependence.

Future Work

The work in the second project year (FY16) will focus on assessing the performance of the superconducting nuclear recoil sensor (SNRS) (Task 3) and fabricating a multi-layer device prototype (Task 4). The device modeling (Task 1) will be refined and continue to guide the design and data analysis. Specifically, Task 3 will involve the fabrication of a range of single-layer devices with varying geometry in order to experimentally determine the energy response of the detector. Initial work will be performed with sealed sources on the existing instrumentation, followed by experiments on the beamline at IBML. If successful, we will discover a lower energy threshold where the SNRS begins to detect, and upper energy threshold where the SNRS latches (no self-recovery from normal to superconducting state), and possibly energy information in the pulse shape within the active energy region. This information will be critical (1) to designing the Nb trace geometry to match the desired nuclear recoil energy range and (2) to developing active and passive background rejection strategies. These experiments will also demonstrate the directionality of the SNRS. Work will then begin to fabricate a multilayer (e.g. 10 layers) device prototype. This will involve developing methods for mechanically stacking the individual patterned ultra-thin glass sheets, establishing electrical connections to each layer, providing means to cooling the structure below the critical temperature, and reading out the signals form all layers in parallel.

Conclusion

The overall technical goal of the project is to demonstrate the novel concept of a layered glass/superconducting sensor for directional dark matter detection. We will (1) comprehensively model the nuclear recoil properties in the detector materials, (2) fabricate a single layered detector structure, (3) assess the sensitivity and directionality of the device using ion beams, (4) fabricate a multilayer prototype to assess scalability, and (5) measure the detector background performance. We expect this work to produce numerous high-impact publications and to deliver the quantitative information needed to formulate a roadmap for the future development of a large-scale solid-state detector.

Neutrinos and Fundamental Symmetries in Nuclei

Stefano Gandolfi
20150476ER

Introduction

Nuclei are the testing ground for many measurements of neutrino physics and for tests of Physics Beyond the Standard Model. Experimental probes of neutrino physics and tests of fundamental symmetries have reached astounding precision with recent measurements of neutrino oscillations and limits on non-standard interactions in beta decays, for example. Commensurate theoretical advances in weak interactions in nuclei are within reach. In this project we will implement for the first time realistic treatments of two-nucleon correlations and currents to enable higher-precision studies of neutrino physics at high energy and momenta, and use these same methods to improve the calculation of nuclear beta decays and related probes of physics beyond the Standard Model.

It is already clear that improved models of the weak currents are required. Neutrino cross-sections on nuclei are 20-30% higher than predicted based upon simple models, it is likely that the energy dependence produced by these models is also incorrect as they only include simple single-nucleon kinematics. Similar discrepancies between theory and experiment in electron scattering have been understood in terms of realistic nuclear interactions and currents. We will implement these same models for weak interactions and neutrino scattering to enable much higher precision nuclear experiments.

Benefit to National Security Missions

This research is important for the DOE Office of Science, nuclear and high energy physics offices.

Understanding quantitatively the neutrino interaction with matter is relevant to experiments measuring neutrino oscillations, double beta decay, and beta decay studies of physics beyond the standard model. These experiments need high precision weak matrix elements in the nuclei.

Progress

During the first year of the project we have finalized the calculation of electroweak imaginary-time response functions of 4He and 12C. In the electromagnetic case, we found that the contribution of two-body operators is very large as expected. The results are in excellent agreement with the available experimental data, for both the longitudinal and the transverse response. We have also calculated the weak imaginary-time response functions, and we are working to extract information on the neutrino-nucleus cross sections.

The research team developed the code to calculate the charge-changing weak currents. The matrix elements for those operators are related to the beta decay. The subroutines have been incorporated in the variational Monte Carlo code that we will use for light nuclei We are currently testing the code and then we will work to optimize the subroutines and then proceed to the calculation in light nuclei.

We have made very important progresses through the extension of Auxiliary Field Diffusion Monte Carlo code to calculate properties of medium nuclei. The ground state of closed shell nuclei, including oxygen and calcium, can now be solved for realistic nuclear Hamiltonians that include two-body forces. We are now working to also include three-body forces in order to reproduce the binding energies of nuclei. These are essential to get a reasonable description of the nuclear states involved in the weak transition.

Future Work

Our goals for the next fiscal year can be summarize as follows:

- Calculate the imaginary-time responses that are relevant for electron and neutrino scattering for a variety of nuclei up to A=12.

- Develop a theory to extract the high energy and momentum part of response functions from two-nucleon propagators.
- Develop the relevant two-body currents needed to calculate beta decay rates in light nuclei.
- Extend existing Auxiliary Field Diffusion Monte Carlo codes to simulate the ground state of medium nuclei.

Conclusion

At the completion of this project we will have a vastly improved capability to predict weak interaction rates for nuclei, both at the low energy and momentum scales relevant for beta decays, the moderate momentum transfer relevant for neutrinoless double beta decay matrix elements, and an accurate two-nucleon model for quasielastic neutrino scattering.

Publications

Carlson, J., S. Gandolfi, F. Pederiva, S. C. Pieper, R. Schiavilla, K. E. Schmidt, and R. B. Wiringa. Quantum Monte Carlo methods for nuclear physics. 2015. Rev. Mod. Phys.. 87: 1067.

Gandolfi, S., A. Gezerlis, and J. Carlson. Neutron Matter from Low to High Density. 2015. Ann. Rev. Nucl. Part. Sci., in press.

Lovato, A., S. Gandolfi, J. Carlson, S. C. Pieper, and R. Schiavilla. Electromagnetic and neutral-weak response functions of $4mathrmHe$ and $12mathrmC$. 2015. Phys. Rev. C. 91: 062501.

Lynn, J. E., I. Tews, J. Carlson, S. Gandolfi, A. Gezerlis, K. E. Schmidt, and A. Schwenk. Chiral Three-Nucleon Interactions in Light Nuclei, Neutron-alpha Scattering, and Neutron Matter. 2015. Phys. Rev. Lett., submitted.

Tews, I., S. Gandolfi, A. Gezerlis, and A. Schwenk. Quantum Monte Carlo calculations of neutron matter with chiral three-body forces. 2015. Phys. Rev. C, submitted.

Assessing the Quantum Physics Impacts on Future X-ray Free-electron lasers

Mark J. Schmitt
20150508ER

Introduction

This project consists of theoretical and modeling efforts to develop a self-consistent model for the wave-electron interactions in x-ray free-electron lasers that includes quantum mechanical effects of the electrons. We conjecture that quantum mechanical spreading of the electron wave function down the wiggler, left out of current free-electron laser models, will degrade the extraction efficiency of these lasers. By including these effects in a new ab initio model, we hope to assess their impact for various laser configurations (e.g. fundamental and harmonic lasing) and determine the best way to optimize laser performance in their presence. The results of this new model will directly affect the design of future XFEL facilities and impact the capability for interrogating extreme states of matter.

Benefit to National Security Missions

This work directly impacts the design of the MaRIE 1.0 signature facility by providing an assessment of quantum effects potentially affecting the extraction of x-rays from energetic electron beams. This work will extend our current understanding of the generation of x-rays from high energy electrons relevant to astrophysics. The simulation models developed under this work will enhance the utility of MaRIE 1.0 and its ability to be used to interrogate materials in extreme states, directly impacting the validation of physics models used in weapons physics codes and for defense applications.

Progress

To accelerate the theoretical work of our research, Petr Anisimov spent the first three months of the ER in Wakoshi, Japan working with Dr. Franco Nori at RIKEN on the quantization of relativistic electrons in the magnetic field needed for a full quantum (QM) mechanical treatment of the FEL interaction. During this time Petr developed a QM mathematical formalism to describe the reduction in electron bunching and concomitant x-ray gain caused by the electron's QM phase uncertainty. Applying this theory to existing and planned x-ray FELs, the current model indicates that QM effects will cause electrons to spread by about 10% of the x-ray wavelength, resulting in a reduction in 3rd harmonic gain by a factor of about 2 for MaRIE-like parameters. A model for this reduced QM bunching has been added to the GENESIS code (the FEL code being used for the design of the MaRIE XFEL). Simulation results from the code show that degradation in gain increases with increasing x-ray harmonic wavelength, making operation at harmonic wavelengths more difficult that thought from a classical point of view. A presentation on the progress of this work is being prepared for presentation at the 2015 International Free Electron Laser Conference, organized by the Korea Atomic Energy Research Institute (KAERI), that will take place in August 2015 in Daejeon, Korea.

Future Work

Work for FY16 can be summarized as follows:

- Continue work on 3D quantum theory of XFEL operation incorporating feedback obtained from the scientific community. Milestone: Completion of 3D quantum theory.
- Implement the improved QM theory in a multi-electron Genesis code in conjunction with an existing classical radiation propagation model. Milestone: A numerical simulation code that describes quantum electrons and classical light in an XFEL.
- Conduct theoretical studies of the quantum startup regime where single photon light dynamics is important and compare results with the case where light is treated classically. Construct a fully QM startup module to be used in the main simulation code. Completed studies of the quantum startup regime and QM model.
- Submit publications/presentations of the work to refereed journals and scientific conferences and/or workshops.

Conclusion

As we construct our model, we will verify its predictions against conventional free-electron laser models in classical regimes, and validate its results against data generated at the LCLS facility. This new model will be used to predict the performance of future free-electron lasers including MaRIE 1.0.The successful execution of this high-leverage research would make a major advance in the XFEL field, placing LANL at the forefront of the design community for future XFELs

Publications

Anisimov, P. M.. Quantum Nature of Electrons in Classical X-ray FELs. To appear in International Free Electron Laser Conference - FEL 2015. (Daejeon, Korea, 23-28 Aug, 2015).

Transport Properties of Magnetized High-Energy Density Plasmas

Jerome O. Daligault
20150520ER

Introduction

There is a rapidly growing interest in exploring the application of magnetic fields to inertial confinement fusion systems in both laser and pulsed-power driven scenarios. The presence of magnetic fields change the fundamental properties of high energy density plasmas in ways that may bring significant rewards, but also present significant challenges for theory. Although decades of innovative research has led to a basic understanding of traditional inertial confinement fusion scenarios, the combination of high-energy density and strong magnetic fields requires extension of current physics models. In particular, understanding how strong magnetic fields, either induced or spontaneous, affect transport properties is a critical next step toward developing a theoretical understanding and modeling capability of these next-generation systems.

Combining numerical simulations and analytical modeling, we will enable a first-principles exploration of the transport properties of magnetized high energy density plasmas. We will develop a molecular dynamics simulation capability to account for both Coulomb interactions and magnetic fields over a wide range of Coulomb coupling and magnetic field strengths. This unique tool will be used to develop a fundamental physics understanding as to how the combined effects of many-body interactions and magnetic fields affect transport properties, and to validate new models of transport properties. We will augment our recent analytic transport theory for unmagnetized plasmas to include magnetic fields. Expressions for the transport coefficients will be cast in a form that is convenient for others to implement into the integrated simulation codes used to model ICF plasmas.

Benefit to National Security Missions

The results of this effort will introduce a new and unique simulation capability in modeling the influence of magnetic fields on high-energy density fusion plasmas at LANL. The capability will allow significant scope for exploration of non-equilibrium conditions in dense plasmas and materials under extreme conditions (e,g, radiation damage, ion slowing-down, non-equilibrium phase transitions). By enhancing our basic science capabilities, this project will help LANL meet its current and future applied missions and challenges, including the science campaigns, Advanced Scientific Computing (ASC) and national High Energy Density Laboratory Plasma (HEDLP) programs. This exploratory research has strong ties to the Nuclear and Particles Futures pillar.

Progress

The research team developed simulation capability to account for both Coulomb interactions and magnetic fields over a wide range of Coulomb coupling and magnetic field strengths. To this end, we added Lorentz forces in the Newton's equations for charged particles interacting through the Coulomb interaction in the presence of an external, homogeneous magnetic field. In the unmagnetized code developed by the PI in the past, the particle dynamics is integrated using the Verlet algorithm. The challenge was to develop an extension of the Verlet algorithm than can handle arbitrarily strong magnetic field. We first implemented existing velocity-dependent algorithms in the literature, including the Störmer-Verlet and the Boris algorithms, which are symplectic, stable, and arbitrarily accurate. However our numerical tests revealed that these algorithms were constrained to very small time steps (because the time step must be small compared to the Larmor cyclotron time, and therefore to short simulation time scales. This limitation prevents systematic studies over wide range of magnetic field strengths. We decided to design a new algorithm, where, unlike Störmer-Verlet and Boris, the choice of the time step is entirely independent of the strength of the magnetic field. The new scheme has been parallelized and incorporated successfully into our code.

We have begun a detailed study of the effect of magnet-

ic fields on the transport properties of high-energy density plasmas. After a long period of trial and error to determine the optimal simulation parameters, we have calculated for the first time the self-diffusion coefficients as well as the parallel-to-perpendicular temperature relaxation rates in one-component plasmas and in electron-ion plasmas, over a wide range of Coulomb couplings and magnetic field strengths. The analysis of the collected data and comparison with existing theoretical predictions are underway. Preliminary investigations reveal the limit of validity of the existing models and motivate the need for new theories. A paper on these results is in preparation.

We have derived and implemented the basic equations to include a magnetic field in our effective potential theory described in the proposal. Results from the effective potential theory will soon be compared to the molecular dynamics simulation results.

Our efforts this past year have been focused on the development of the new simulation capability, its testing, and the extension of the effective potential theory. We plan on publishing next year our numerical, analytical and physics results.

Future Work

The objective of this research is to develop a quantitative understanding of the dominant transport processes in magnetized high-energy density plasmas; including temperature relaxation, diffusion, electrical and thermal conductivity and viscosity. Models of transport properties will be developed and validated using molecular dynamics (MD) simulations. Our previous MD simulations and theoretical models have proven successful at capturing each of these transport properties in unmagnetized plasmas. The proposed work is a non-trivial extension to include an external magnetic field, which will contribute to individual particle equations of motion. Interaction forces will remain electrostatic. Extensive MD simulations will be carried out to unravel the microscopic particle dynamics in magnetized plasmas, and to develop a library of transport processes (diffusion, viscosity, resistivity, energy relaxation rate, dynamic structure factor, etc.) that will be used to validate the analytical models. Currently, our MD code allows for the simulation of classical systems of charges interacting through spherically symmetric potentials in a three-dimensional periodic domain containing up to several hundreds of thousands of particles and over long time scales. Currently, magnetic fields are not included. The inter-particle forces are obtained using the state-of-the-art particle-particle particle-mesh method, which combines high-resolution of close encounters and rapid, long-range force calculations. We will extend the present capability to account for magnetic fields, and apply it to explore a wide range of Coulomb coupling and magnetic field strengths. Two kinds of simulations will be done to explore the impact of magnetic fields: 1) We will develop our code to incorporate arbitrarily strong external magnetic fields. This requires adding velocity-dependent Lorentz forces in addition to the Coulomb forces in Newton's equations describing the particle evolution. 2) We will develop the effective potential to account for screened ion-ion interactions and then implement those effective potentials in our MD code and calculate ionic transport properties.

Conclusion

The primary result will be a microscopic-level understanding of the transport properties of magnetized plasmas across a broad range of coupling and magnetization strengths. Tangible products will be a numerical code and theory capable of describing these plasmas, and practical formulas that can be implemented into integrated simulation codes used to model ICF systems.

Publications

Baalrud, S., and J. Daligault. Modified Enskog kinetic theory for strongly coupled plasma. 2015. Phys. Rev. E. 91: 063107.

Daligault, J., and S. B. Baalrud. Plasma transport theory spanning weak to strong coupling. 2015. AIP Conf. Proc. . 1168: 040002.

Sjostrom, T., and J. Daligault. Ionic and electronic transport properties in dense plasmas by orbital-free density functional theory. Physical Review E Accessible at http://arxiv.org/abs/1510.00647.

Magnetic Rayleigh-Taylor Instability

Daniel Livescu
20150568ER

Introduction

While the goal of achieving economically viable controlled fusion remains remote in either the inertially (ICF) or magnetically confined configurations, it is generally believed that one of the main obstacles is the development of hydrodynamic instabilities. However, the complex physics associated with ICF makes such instabilities significantly more complicated than the classical Rayleigh-Taylor instability (RTI). The influence of magnetic fields, either self-generated or externally applied, has recently been an active research topic in the hope it may offer a way of controlling or inhibiting RTI and mixing in ICF. However, so far numerical investigations of this problem have been restricted to 2D, without realistic plasma transport properties, and the few existent studies investigating the coupling between magnetic fields and RTI seem to arrive at opposite conclusions.

In order to fill the gap in our knowledge of the coupling between RTI and magnetic fields, we will conduct a thorough study of the RTI in the variable-density (VD) magneto-hydrodynamics (MHD)-Hall limit using the first high-resolution 3D numerical experiments of plasma mixing with realistic plasma transport coefficients. In particular, we are aiming to address the following questions:

- Could a magnetic field suppress the late time growth of the RTI and, if yes, under what conditions and configurations?
- Could a robust lower limit on mixing exist in the Hall-magnetized plasma, similar to the bounds obtained earlier in the hydrodynamic limit? The existence of such a lower bound could impact the feasibility of obtaining ignition.

By examining a variety of configurations, we will not only answer the question regarding RTI growth in the presence of the MHD-Hall effect with realistic plasma transport properties, but also contribute to the understanding of the mix in ICF. In addition, the study will also address several astrophysical phenomena where the combined MHD-Hall effect and RTI occur.

Benefit to National Security Missions

Since one of the major sources of mix in Inertial Confinement Fusion (ICF) is Rayleigh-Taylor instability (RTI) development, controlling or suppressing this instability could have major implications in achieving ignition. In order to investigate this possibility, we will provide the first comprehensive studies using accurate numerical simulations of magneto-hydrodynamics (MHD)-Hall RTI with realistic plasma transport properties. The work will consider the role of external magnetic fields as well as various other effects (e.g. Biermann battery effect) on the development of RTI and electron thermal conductivity, at the conditions during the deceleration phase in ICF.

The results of the work could easily translate into future programmatic efforts. Thus, besides the importance of answering the central questions of the proposal, the mixing and turbulence characteristics we will identify may help address the physics of mix in ICF. For example, a recent DOE review regarding ICF concluded that the modeling of mix is likely inadequate and recommended "a program of scientific experiments and modeling focused on understanding the various physical effects, in isolation, that impact the integrated implosion experiments provides the best approach to eventually either achieve ignition, or to understand definitively why it may not be achievable." In addition, the extensive database we will generate of accurate simulations could be used to test and develop turbulence models and to test coarse mesh simulation codes of programmatic relevance. To this end, we are in contact with project leaders within several campaigns and the PEM program.

Progress

The project goals are to examine a variety of configurations, under late time ICF conditions, to understand the

role of the combined buoyancy, magnetic, and Hall effects on the Rayleigh-Taylor instability growth, turbulence, and mixing.

Work started by writing the full set of compressible equations describing the flow in a magnetized plasma: continuity, ion and electron momentum and energy, transport equations and Faraday's law. The heat and mass fluxes were derived, for the first time, using Onsager's relations for irreversible processes and Onsager's symmetry principle. The variable density density incompressible limit of these equations was derived assuming speed of sound much larger than any characteristic velocity, which is relevant to late time ICF conditions. The resulting equations have been implemented in the CFDNS code in both the Rayleigh-Taylor and homogeneous Rayleigh-Taylor configurations. Preliminary simulations have been started in both configurations. While the Rayleigh-Taylor set-up is directly relevant to ICF, the homogeneous set-up allows us to investigate the mixing problem under the ICF conditions, without the complications due to the presence of the edges.

In a related effort, we are finalizing a linear analysis of the compressible viscous Rayleigh-Taylor instability, with a background temperature gradient. The presence of a temperature gradient was never considered in such an analysis, yet in many problems (e.g. ICF or solar corona), there are strong temperature gradients. The results also address a recent controversy on the role of large plasma viscosity on the development of turbulence under ICF conditions. Thus, we show, for the first time, using realistic plasma viscosities, what are the likely perturbation wavelengths damped, in ICF, by the large increase in plasma viscosity and what is the range of wavelengths least affected.

Future Work

This is the first detailed study of the combined buoyancy, magnetic, and Hall effects on the Rayleigh-Taylor instability (RTI) growth, turbulence, and mixing. No previous study has been performed using realistic plasma transport properties and in 3D. The nominal case for the study addresses the conditions during the deceleration phase in Inertial Confinement Fusion (ICF). During this phase, the RTI development mixes hot and warm plasmas, which enhances thermal energy loss and produces a larger "warm-spot" instead of a hot spot. This undesirable effect could be mitigated by reducing the electron thermal conduction coefficient and/or the growth of RTI. As such, we aim to investigate the possibility of controlling the RTI development and electron thermal conductivity at the nominal conditions using external magnetic fields. We will also examine the turbulence and mix properties produced under these conditions. In order to be able to perform the study, during the second year we will focus on the following goals:

Theory

- Continue the analysis of the spectral range locality of the MHD-Hall equations, for the triply periodic case, following previous analysis of the pure MHD case.
- Examine the linear behavior of the MHD-Hall equations derived.
- Examine the structure of the MHD-Hall RT layer, in particular the verify the existence of an inner turbulent region and derive the scaling for the turbulent non-turbulent interface at the edges of the layer.

Computation

- Continue with the low resolution simulations to scope the parameter space, for the pure MHD and MHD-Hall cases in two configurations: triply periodic and classical RT.
- Start medium to high resolution simulations for the nominal cases.
- Start analyzing the data. In particular, examine the role of the increase of plasma viscosity with temperature on the turbulent evolution and/or suppression.

Conclusion

The central questions of the proposal, which we expect to answer, are related to the late time Rayleigh-Taylor (RTI) instability growth suppression using magnetic fields and the existence of a lower bound in the mix development. In seeking to address these questions, we will provide the first comprehensive studies using accurate numerical simulations of magneto-hydrodynamic (MHD)-Hall RTI with realistic plasma transport properties. We expect, along the way, to be able to address questions related to mix properties and the possibility of controlling mix in Inertial Confinement Fusion as well as many questions relevant to a multitude of astrophysical configurations.

Publications

Aslangil, D., D. Livescu, and A. Banerjee. Variable density mixing under variable mean pressure gradient. 2015. In 15th European Turbulence Conference. (Delft, The Netherlands, 25-28 Aug. 2015). , p. Paper number 122. Delft: TU Delft.

Aslangil, D., D. Livescu, and A. Banerjee. Reynolds and Atwood numbers effects on homogeneous Rayleigh-Taylor instability. To appear in 68th Annual Meeting of the American Physical Society Division of Fluid Dynamics . (Boston, 22-24 Nov. 2015).

Pulido, J., D. Livescu, J. Woodring, J. Ahrens, and B. Hamann. Survey and analysis of multi-resolution repre-

sentation methods using turbulence data. Computers and Fluids.

Reckinger, S. J., D. Livescu, and O. V. Vasilyev. Comprehensive numerical methodology for Direct Numerical Simulations of the compressible Rayleigh-Taylor instability. To appear in Journal of Computational Physics.

Wieland, S. A., D. Livescu, O. V. Vasilyev, and S. J. Reckinger. The compressible Rayleigh-Taylor instability and vortex dynamics in stratified media. To appear in 68th Annual Meeting of the American Physical Society Division of Fluid Dynamics . (Boston, 22-24 Nov. 2015).

Enhancing the Long-Baseline Neutrino Experiment Oscillation Sensitivities with Neutron Measurements

Keith R. Rielage
20150577ER

Introduction

The matter-anti-matter asymmetry of the universe is one of the key scientific questions of our time. In order to explain the asymmetry, a large violation of CP symmetry - particle vs. antiparticle behavior - is required. Of the two known types of matter particles - quarks and leptons - extensive studies of CP violation with quarks have been made and found to be too small to explain the asymmetry of matter and anti-matter in the universe. The discovery of neutrino oscillations gives us a mechanism to search for CP violation with leptons. The Long-Baseline Neutrino Experiment (LBNE), endeavors to make a comprehensive measurement of neutrino oscillation physics with a focus on measuring CP violation in the lepton sector for the first time. In addition, LBNE endeavors to over-constrain the leptonic mixing matrix giving unprecedented sensitivity to phenomena such as Non-Standard Interactions. LBNE will measure CP violation by making detailed studies of oscillation phenomena over a broad range of neutrino and anti-neutrino energies. They require an event-by-event reconstruction of the neutrino energy from the outgoing particles of the interaction - including neutrons. In this project, we will measure neutron interactions in a liquid argon time-projection chamber (TPC) in a well-understood neutron beam for the very first time.

Los Alamos has a unique neutron facility with a well-characterized, high-energy neutron beam. We will deploy a large liquid argon TPC in this beam in order to carry out the measurements. The theoretical part of the effort will be focused on determining the sensitivity of a variety of neutrino oscillation phenomena to the neutrino and anti-neutrino energy resolutions.

Benefit to National Security Missions

For neutrino oscillation experiments using liquid argon time-projection chambers, neutrons are a major challenge. Neutrino oscillation experiments employ neutrinos in the several hundred Mega-electron volts to several Giga-electron volt energies. At these energies, neutrons are often emitted in the neutrino interaction carrying away energy. Since the neutrino energy must be reconstructed using the outgoing particles, correlating neutron interactions in the detector with neutron kinetic energies is paramount. LANL has a unique high-energy neutron facility that enables these measurements.

The work will lead to a more robust approach to neutrino oscillation analysis that will be employed for searches of violation of CP symmetry (particle-anti-particle symmetry) as well as many other neutrino oscillation scenarios. CP violation in particular may be tied to the origin of the matter-anti-matter asymmetry of the universe.

This work contributes to the DOE Office of Science missions and directly supports the nuclear and particle futures pillar at LANL.

Progress

This three-year project aims to measure neutron interactions with argon and interpret the data in the context of neutrino oscillation analyses relevant to the international long-baseline neutrino effort currently being developed. The international long-baseline effort is being planned with the United States as the host country. The effort is currently called the Deep Underground Neutrino Experiment (DUNE). DUNE will employ an enormous liquid argon time-projection chamber (TPC) at a deep underground location in Western South Dakota. Our Laboratory Directed Research and Development (LDRD) project is designed to measure the response of a liquid argon TPC to neutron interactions at well-defined neutron kinetic energies up to 800 Mega-electron volts (MeV) using the Los Alamos Neutron Science Center's (LANSCE) Weapons Neutron Research (WNR) facility.

Since the beginning of the project in October, 2014, the team has carried out two liquid argon engineering runs

with the prototype detector for the Cryogenic Apparatus for Precision Tests of Argon Interactions with Neutrinos (CAPTAIN) program. The prototype, which we call Mini-CAPTAIN, consists of 1000 pounds of instrumented liquid argon. In our first test, we demonstrated our ability to achieve the very low electronics noise levels required for optimal operation. We then spent several months working on the purification system, conducting a variety of tests. We subsequently carried out the second engineering run and demonstrated good argon purity with respect to water. Our challenge now is to demonstrate good purity with respect to oxygen.

Since the second run, we have finished developing a gas-phase purification and condensing loop that will allow us to continuously purify the liquid argon and re-condense it. This system will allow us to obtain the optimal purity - especially with respect to oxygen. At the time of this writing, we have begun our third engineering run and begun operating the recirculation system. We will understand the performance of the recirculation system and determine if further modifications are necessary after this run. A neutron run is anticipated in fiscal year, 2016.

Several calculations and test effort has gone into the development of a neutron beam-flux monitoring system. Test data were taken in November and the system is now complete. The system will allow us to make flux and spectral measurements even at the low neutron rates we require to run the liquid argon TPC.

Future Work

During the first year, we have been working to commission the Mini-CAPTAIN detector. We are completing a second engineering run to demonstrate appropriate purity for the experiment. In tandem, we have put in a proposal to the LANSCE PAC to run at the WNR beamline 15R in the next run cycle. We expect to move the detector to the beam area in the beginning of FY16. The deployment and recommissioning of the detector requires significant set-up of cryogenic and electronics equipment. In addition, the detector will be filled with purified liquid argon that will be re-circulated to maintain optimum purity. The purity will be checked to assure high-quality data before taking beam. The detector will also be calibrated before taking beam.

Subsequently, the detector must be drained and removed from the beamline. The next experimental task will be to carry out a detailed data analysis as well as continued simulations.

The theoretical effort has stalled due to the departure of the T-division co-I. We are redirecting these resources into the commissioning of the detector. Detailed simulations will begin late this FY. The starting point is a detailed analysis of the energy resolutions of various charged particles and neutrons in liquid argon TPCs. The next step is to lay out what measurements will be made in the LBNE near neutrino detector. The final step is unifying the information from the near and far detectors in such a way that we can vary the resolutions of each piece of information in the oscillation analysis.

Conclusion

We will study neutron interactions on liquid argon in terms of their event signatures. We will use these results to test existing simulations of the interactions. We will then modify those simulations with our high statistics data-set. Ultimately, we will produce an oscillation analysis approach for LBNE that includes the impact of neutrons as well as a requirement to be sensitive to new physics. This analysis will create the near neutrino detector requirements essential for making the optimal design choices.

Direct Numerical Simulations of Magnetic Rayleigh-Taylor Instability

Daniel Livescu
20150732ER

Introduction

The development of hydrodynamic instabilities in the presence of complex plasma physics is one of the main obstacles in achieving ignition in both magnetic and inertial confinement fusion (ICF). Besides the important role of pure Rayleigh-Taylor instability (RTI) in many practical problems, magnetic RTI is very important for the compression (or lack thereof) efficiency in magnetic or inertial confinement fusion. Since the instability can limit the maximum compression achieved in the pinch or other inertial confinement fusion (ICF) implosions, controlling or, at least, understanding it is of critical importance.

At present, the role of a magnetic field on Rayleigh-Taylor Instability (RTI) growth is not well understood and the few existent studies seem to arrive at opposite conclusions. For example, recent numerical studies in 2D conclude that magnetic fields suppress instabilities and mixing while the only published study to explore the problem in 3D concludes that magnetic fields enhance the nonlinear growth of instabilities and mixing. Our recent simulations show that pure RTI growth is bounded from below by the growth of the inner turbulent region, which is independent of initial conditions or fluid properties at high enough Reynolds numbers. There is no systematic study examining the combined (magneto-hydrodynamics) MHD-Hall RTI turbulence and it is not known if such a lower growth bound exists for MHD-Hall RTI. It is also not known what effects the plasma transport properties could have on the growth of RTI. Moreover, there are many astrophysical systems which are not well understood, but where these effects likely play a role.

We propose to use Trinity Phase 1 to perform the first fully resolved 3D simulations, with realistic plasma transport properties, of the combined buoyancy, magnetic, and Hall effects on the RTI growth, turbulence, and mixing as well as electron thermal conduction, under realistic ICF conditions.

Benefit to National Security Missions

While the goal of achieving economically viable controlled fusion remains remote in either the inertially or magnetically confined configurations, it is generally believed that one of the main obstacles is the development of hydrodynamic instabilities. However, the complex physics associated with confined fusion makes such instabilities significantly more complicated than the classical Rayleigh-Taylor Instability (RTI). An example is the interaction between the confined plasma and magnetic fields. The influence of magnetic fields has recently been an active (experimental + numerical) research topic in the hope it may offer a way of controlling or inhibiting RTI and mixing or, more generally, understanding the role on the RTI development. For example, recent experiments on the Omega Laser facility resulted in the compression of an externally imposed magnetic field to around 20MG, which is dynamically important compared to characteristic RTI velocities.

Numerical investigations of this problem in the context of ICF have been limited to 2-dimensions (2D), and therefore are unable to capture the full 3-dimensional (3D) nature of magnetic RTI. It is well known that mixing and turbulence properties in 2D are completely different from 3D. We believe that conducting systematic investigations of magnetic field interaction with RTI in 3D would allow us to answer definitively whether or not magnetic fields can be used to control RTI.

This work will also benefit the stabilization of Trinity Phase 1 and further develop the CFDNS for efficient use on new and emerging architectures in support of our national security mission.

Progress

Our cycle on Trinity Phase 1 has not yet started. In preparation for the start date in mid July, the code has been ported to Haswell and small size simulations to test resolutions and parameter re=ranges are under way.

Future Work

This is a project for cycles on Trinity Phase 1 only. The simulations will be performed during the two month window for the stabilization process during the present fiscal year.

In order to study the instability growth and mixing characteristics due to the combined MHD-Hall RTI, we will conduct a series of numerical experiments, in the Hall-MHD limit that will cover typical conditions under the deceleration phase in ICF. Furthermore, we will compare the results with the MHD and hydrodynamic ($B \rightarrow 0$) limits to isolate the effects associated with magnetic fields and finite plasma skin depth. We are planning to use realistic plasma transport coefficients and fully resolve dissipation scales.

The project will use the OpenMP-MPI hybrid version of the CFDNS code. OpenMP is a library and API for shared memory multiprocessing, and is an industry standard for using threads within a code. It is expected that using MPI everywhere with upcoming many-core architectures, such as Trinity, will be too expensive. We plan on testing OpenMP by varying the number of threads used, and seeing if there are any performance increases. We have also made some changes to the code to increase the amount of vectorization to better utilize the more capable vector units found on Trinity. We will further test the implementation and use profilers such as Intel VTune and VampirTrace to identify potential bottlenecks.

Conclusion

In order to fill the gap in our knowledge of the coupling between instability development and magnetic fields in Inertial Confinement Fusion, we have proposed to conduct a thorough study of the Rayleigh-Taylor Instability (RTI) in the variable-density (magneto-hydrodynamics) MHD-Hall limit using high-resolution numerical experiments of plasma mixing with realistic plasma transport coefficients. In particular, we are aiming to address the following questions:

- Could a magnetic field suppress the late time growth of the RTI?
- Could a robust lower limit on mixing exist in the Hall-magnetized plasma, similar to the bounds obtained earlier in the hydrodynamic limit?

Publications

Srinath, A., R. Miller, and D. Livescu. OpenCL-based tridiagonal solvers for evaluation of compact finite differences on parallel architectures. 2015. Under preparation for a parallel computing conference.

Extreme-Scale Kinetic Plasma Modeling of Turbulence and Mix Using VPIC

Brian J. Albright
20150751ER

Introduction

VPIC is general-purpose, kinetic plasma modeling code that has been applied to and validated on a variety of problems, including laser-plasma instabilities in inertial fusion, dense plasma transport, thermonuclear burn, laser-driven particle acceleration, magnetic fusion, and applications in space and astrophysics. We propose to apply VPIC to three basic science problems central to our understanding of turbulence and mix in space and laboratory plasmas and particle acceleration arising in magnetized plasmas. To conduct this work, we will make several changes to the VPIC code base in order to enable its efficient use of the unique features of the Trinity supercomputer. Specifically, we will adapt the VPIC architecture to a four-tier structure that will enable exploitation of distributed-memory parallelism, task parallelism, data parallelism, and Trinity's specific single-instruction-multiple-data (SIMD) instructions. We will also examine the development of novel diagnostics taking advantage of the Burst Buffer capability Trinity has, a feature of the supercomputer enabling more extensive analysis of high data volumes than ever before possible, a potentially groundbreaking achievement. This modification to our flagship VPIC kinetic plasma modeling code will position the scientific community for effective use of Exaflop/s supercomputers in future years.

Benefit to National Security Missions

This work will vastly improve the state of the art in plasma kinetic modeling, a subject area with direct ties to many aspects of basic and applied science and national security.

The ability to resolve outstanding problems associated with plasma-phase mix ties directly to outstanding problems in high energy density science of direct importance to nuclear weapons programs.

Moreover, as noted in the research proposal, NASA missions rely heavily on large-scale simulations modeling magnetic reconnection and turbulence processes. Indeed, multiple active missions have been fielded specifically to advance our understanding of space science in these areas, which this project directly impacts.

Inertial fusion energy interests are also advanced by this project; not only is the VPIC computer code used to advance laser-plasma interaction science for direct- and indirect-drive inertial fusion energetics, but also plasma-phase mix of shell-fuel interfaces will be directly impacted by the atomic mixing studies we will conduct.

Finally, this work advances meaningfully the scientific community's ability to harness the power of modern and future supercomputers, making it of profound interest to the information science and technology communities. Also, the techniques developed to process large data volumes using the Trinity burst buffers may be of interest to information science applications involving similarly large data sets.

Progress

We have begun to assemble our team and issue work assignments for this project. No other progress yet to report.

Future Work

We will adapt VPIC to the Trinity architecture in a hierarchical way that reflects the physical characteristics of the system. As an overview, our approach will rely on asynchronous communication between compute nodes, task-parallel division across the intra-node single address space, data-parallel division within a task, and full vectorization within a thread of execution using AVX-512 intrinsics.

- Test performance of finer-grained MPI parallelism than employed previously. Assess performance tradeoffs when replacing MPI ranks with threads.
- Experiment with restricting task parallel threads to

optimize efficiency of the caches. Organize threads into user configurable groups such that each shares a replication of the field domain.
- Develop a hierarchical threading model combining atomic memory operations with stream reductions.
- Add support for AVX-512 intrinsics and find a suitable block size for processing particle data on Trinity. Explore new intrinsics available in AVX-512 and evaluate their effects on performance.
- Explore strategies for using Trinity high-bandwidth memory.
- Explore ways to use the new burst buffer capabilities of Trinity for checkpoint/restart and novel methods of high-data-volume postprocessing of simulation data
- Implement higher order particle weighting algorithm to VPIC to improve compute/data ratio
- Define key physics problems to be run “at scale” using Trinity during Phases 1 and 2 related to turbulence and mix of plasmas and particle acceleration
- Document and present results to the high performance computing and scientific communities.

Conclusion

At the culmination of this project, we will have made substantial progress toward resolving outstanding physics problems in plasma and high energy density science. Specifically, we will have revealed through large-scale calculations how dense plasmas mix with one another. We also will have advanced our understanding of the physics of magnetic reconnection and the acceleration of cosmic ray particles to very high energy. Another legacy of this project will be the development of our VPIC particle-in-cell kinetic plasma code for modern supercomputers such as Trinity and future multi-core platforms.

Publications

Huang, C. K., M. D. Meyers, Y. Zeng, S. Yi, and B. J. Albright. On the numerical dispersion and the spectral fidelity of the particle-in-cell method. To appear in 24th International Conference ont he Numerical Simulation of Plasmas . (Golden, Colorado, 12-14 Aug, 2015).

Huang, C. K., M. D. Meyers, Y. Zeng, S. Yi, and B. J. Albright. On the numerical dispersion and the spectral fidelity of the particle-in-cell method. To appear in Computer Physics Communications.

Nystrom, D.. Progress on optimizing VPIC for LLNL’s Sequoia Platform. To appear in 24th International Conference on the Numerical Simulation of Plasmas . (Golden, Colorado, 12-14 Aug, 2015).

Ultra-Bright Electron Beam Acceleration in Dielectric Wake Accelerators

Evgenya I. Simakov
20130463ER

Abstract

Debris from historic nuclear weapons test rests on the ground surface and within tunnels and underground cavities at all nuclear testing sites across the globe. This material could be used to determine device design and performance but is currently of limited diagnostic value because the short-lived fission products and key nuclear activation species have long decayed away. The goal of this project is to develop new measurement and assessment techniques necessary to reconstruct the diagnostic information still present in solid debris as the stable decay end-members. The original presence of short-lived radionuclides alters the ultimate isotopic composition measured in historic nuclear debris in a pattern that can be interpreted for detailed forensic and diagnostic evaluation. The success of the proposed effort will be a critical step towards a new capability with direct impact on nuclear forensics and on science based stockpile stewardship. The duration of this Exploratory Research project was one year. Based on the success of this initial "measurements focused" effort, a larger scale Directed Research project was begun under the leadership of Hugh D. Selby in 2016. The title of the follow-on project (20160011DR) is "Using extinct radionuclides for radiochemical diagnostics."

Background and Research Objectives

A nuclear explosion produces an intense burst of energy and associated radiation driven by the violent assembly of a critical mass of fissioning nuclear material. Details of the nuclear event have traditionally been inferred from measurements made during and immediately after the detonation. In the case of radiochemical measurements, many of the nuclear products that have been shown to be of most diagnostic value exist for but a moment in time, typically on timescales of hours to weeks. The key innovation of this proposal is the realization that short-lived fission products and key nuclear activation products that form the basis of modern technical evaluation can in fact be indirectly measured over vastly longer timescales from years to decades, and indeed centuries, after the detonation. We borrow a key insight in how to accomplish this task from similar approaches that have been successfully used in the field of cosmochemistry to measure extinct radionuclides in extraterrestrial samples like meteorites. Chemical fractionation between Pu and U that is known to occur during a nuclear event will cause systematic isotopic perturbation in 237Np and 239, 240Pu concentrations resulting from decay of short-lived U isotopes 237, 239, 240U. The proposed sampling and measurement techniques will be used to determine diagnostically sensitive and now extinct 237, 239, 240U isotopes in historic debris samples. A significant challenge of the proposed research will be to develop indirect methods to measure peak-yield fission products to determine total fissions in a given sample. In order to reconstruct this information we propose to measure perturbations in stable element isotopic composition to infer the original presence of short-lived fission products. This idea depends on the presence of stable multi-isotope elements for which one isotope is the end-point of a fission decay chain and another is blocked from fission decay by a different stable element.

Scientific Approach and Accomplishments

This research aims to develop analytical techniques to characterize the details of a nuclear detonation based on chemical analysis of aged nuclear debris. The analytes of interest are short-lived radionuclides that have decayed beyond detection, but leave signatures of their original presence in the isotopic composition in archived debris samples. We term these signatures, extinct radionuclides. The goals of the project are to recover two types of information, (1) short-lived uranium isotopes (237, 239, 240U) and (2) fissions. For each of these goals good progress has been accomplished. In order to determine the short-lived uranium isotopes, a collection of samples must span a suitable range of volatility as measured by sample specific 236U/238Pu ratios. Although only one unfractionated 236U/238Pu value is actually "true" of

the device, chemical distortion that occurs during debris condensation serves to generate a range of samples that can be relatively enriched (volatile) or depleted (refractory) in uranium compared to a reference 238Pu isotope. The proposed regression technique requires that 236U/238Pu span a sufficient range within the sample set to allow a robust linear fit. In the case of analyses of Trinitite, eight individual samples from archived LANL collections have been completed. The expected trends are observed, however the goodness of fit over a limited range in 236U/238Pu is not sufficient to obtain a high-quality measure of 237, 239, 240U. A new set of Trinitite samples obtained from a commercial rock and gem supplier has been procured. These samples appear as light green vesicular samples, distinctly different from the black glass found in the LANL collection. It is hypothesized that the light green vesicular samples will be more volatile compared to the black glass samples and will provide the range in 236U/238Pu that is needed. Initial analyses of archived core samples from an underground nuclear test have also been completed. For this test, archived samples that transit seven locations through the underground environment are available for analytical study. Duplicate analyses of the first two locations have been completed. Five more duplicate analyses will provide data to assess the 236U/238Pu volatility index and the feasibility of the technique to measure 237, 239, 240U in underground debris samples. Two independent approaches are being pursued to determine fissions in historical debris samples. These include direct measurements of 99Tc and indirect measurements of 95Zr and 97Zr through isotopic perturbation of stable molybdenum isotopic ratios (e.g. 95Mo/96Mo and 97Mo/96Mo). Each of these analytes is a peak yield fission product that can, in principle, be used to determine total fissions in the sample. The first phase of this project has focused on development of chemical methods used to isolate pure 99Tc and molybdenum concentrates that can be assayed using both single and multi-collector ICP-MS instrumentation. In the case of 99Tc determination, a method has been developed during the first year of this project to analyze for 99Tc in aged debris samples. Technetium is purified in high yields (80-100%) using extraction chromatography (TEVA resin) with good decontamination from both Mo and Ru. This decontamination is crucial to the success of the analysis because of potential isobaric interference from 98MoH+ and 99Ru. Standard addition experiments with solutions of Peruvian soil (NIST SRM 4355) and dissolved Trinitite suggest that accurate determinations of 99Tc can be obtained. The associated measurement uncertainty (20-30%) is higher than ideal and reflects inconsistencies in observed instrument count rates that are not yet fully understood. Additional work is needed to identify the source of the variation and improve measurement precision. In the case of 95, 97Zr determination, a novel technique using high precision isotopic measurements of stable molybdenum is being pursued. A sequential two-column ion-exchange protocol was developed and optimized. Purified Mo concentrates have been isolated with good decontamination against potential interferences from Zr, Ru, Cr, Mn, and Fe. The purification protocol performed well in an initial Mo analysis of a dissolved debris sample, which revealed significant deviation from the natural isotopic composition. An optimized measurement routine using the Neptune Plus multicollector ICP-MS is currently being developed. These high precision measurements will be used to quantitatively determine perturbations in 95Mo/96Mo and 97Mo/96Mo isotopic ratios. Future analyses using an isotopically enriched 96Mo spike will be interpreted for absolute fission concentration.

Impact on National Missions

A major limitation of current radiochemical diagnostics is the need to determine the concentration of key signature radionuclides with short half-lives. Within a month after a nuclear detonation, these radionuclides are largely extinct. If successful, the proposed work will be a critical step towards a new capability to extract this crucial information from nuclear debris at later times. Such a capability would have direct and lasting impact on two key DOE/NNSA missions: stockpile stewardship and post detonation nuclear forensics. A demonstrated capability to reanalyze archived debris samples from historic nuclear tests will improve the technical foundation that supports Stockpile Stewardship and will strengthen our Nation's commitment to deterrence without nuclear testing for decades to come. The limitations of historical measurements impacts nuclear forensics as well. Many of our earliest tests used simple designs that could be credibly replicated in a potential terrorist nuclear attack. Because many of these test were fielded in the late 1940's and early 1950's, the radiochemical data for these events is very sparse and/or of low quality. This leads to large uncertainties in evaluation of performance and yield, which in turn prevents proper calibration of LANL's computational design tools. A capability to obtain a complete radiochemical data set for early U.S. tests would significantly improve modeling and forensic capability envisioned for post-detonation nuclear forensics.

Publications

Gai, W., C. Jing, A. Kanareikin, C. Li, R. Lindberg, J. Power, D. Shchegolkov, E. Simakov, Y. Sun, C. X. Tang, and A. Zholents. Assesment of Opportunity for a Colinear Dielectric Wakefield Accelerator for a Soft X-Ray FEL Facility. 2014. In 36th International Free Electron Laser Conference FEL 2014. (Basel, Switzerland, 25-29 August, 2014). , p. FRB02. online: JACoW.

Huang, C., T. Kwan, D. Shchegolkov, and E. Simakov. Parti-

cle-In-Cell Modeling of Dielectric Wakefield Accelerator. 2013. In 2013 North American Particle Accelerator Conference. (Pasadena, CA, Sept. 29 - Oct. 4th, 2013). , p. MOPAC23. online: JACoW.

Shchegolkov, D. Y., and E. I. Simakov. Design of an emittance exchanger for production of special shapes of the electron beam current. 2014. PHYSICAL REVIEW SPECIAL TOPICS-ACCELERATORS AND BEAMS. 17 (4).

Shchegolkov, D. Yu., E. I. Simakov, C. Jing, C. Li, and A. A. Zholents. Suppressing Parasitic Effects in a Long Dielectric Wakefield Accelerator. 2015. In Advanced Accelerator Conference Workshop. (San Jose, CA, 13-18 July, 2014). , p. Still did not publish, ugh!!!. Melville, NY: American Institute of Physics.

Shchegolkov, D. Yu., E. I. Simakov, and A. A. Zholents. Towards a practical multi-meter long dielectric wakefield accelerator: problems and solutions. To appear in IEEE Transactions on Nuclear Science.

Shchegolkov, D., E. Simakov, S. Antipov, M. Fedurin, and C. Swinson. Beam Pulse Shaping Experiments for Uniform High Gradient Dielectric Wakefield Acceleration. 2013. In 2013th North American Particle Accelerator Conference. (Pasadena, CA, Sept.29-Oct.4th, 2013). , p. MOPAC24. online: JACoW.

Shchegolkov, D., E. Simakov, S. Antipov, and M. Fedurin. Dielectric wakefield accelerator experiments at ATF. 2015. In 2015 International Particle Accelerator Conference. (Richmond, VA, May 3-8, 2015). , p. WEPJE006. online: JACoW.

Shchegolkov, D., E. Simakov, and A. Zholents. Simulation studies of BBU suppression methods and acceptable tolerances in dielectric wakefield accelerators. 2015. In 2015 International Particle Accelerator Conference, Richmond. (Richmond, VA, May 3-8, 2015). , p. WEPJE007. online: JACoW.

Simakov, E., C. Huang, T. Kwan, and D. Shchegolkov. Shaping Electron Bunches for Ultra-bright Electron Beam Acceleration in Dielectric Loaded Waveguides. 2013. In 2013 North American Particle Accelerator Conference. (Pasadena, CA, Sept. 29 – Oct. 4th, 2013). , p. TUMPA13. online: JACoW.

Zholents, A., S. Doran, W. Gai, G. Ha, C. Li, J. Power, R. Lindberg, N. Strelnikov, Y. Sun, E. Trakhtenberg, C. Jing, A. Kanareykin, D. Shchegolkov, E. Simakov, P. Piot, and S. S. Baturin. A collinear dielectric wakefield accelerator for a soft X-ray FEL facility. To appear in 2nd European Advanced Accelerator Concepts Workshop. (Isola d'Elba, September 13-19).

Beyond the Standard Halo

Michael S. Warren
20130626ER

Abstract

We describe a project that culminated in the capability to do N-particle cosmological simulations for a record number of particles (N ~ 1012) in a record (short) amount of computer time. This capability was used to discover that dark matter distributions on galactic and larger scales in the Universe are not uniform "halos" as the standard approach predicts (or assumes), but are clumped in irregular structures. The complete results of the calculation have been released publically, and preliminary interpretations of them have been published.

However, a decision in 2015 by the PI of the ER project to take entrepreneurial leave changed the course of the research in its last year. The focus became LANL participation in the Large Synoptic Survey Telescope (LSST) consortium, which will probe four key areas: time-domain astrophysics, dark energy and weak gravitational lensing studies, Solar System science, and galactic structure and evolution.

Background and Research Objectives

This ER project addresses a crucial question in cosmology about the nature of the distribution of dark matter in the Universe on galactic and larger scales. This is necessary in order to interpret the results of dark matter searches, such as the data coming from the Planck Satellite. Investigating these distributions in both coordinate and momentum (velocity) space requires doing the largest N-body particle simulations ever attempted, with N now of the order of a trillion particles. Preliminary non-linear gravitational collapse calculations with 100 billion particles had revealed quite non- uniform structures in the dark-matter distributions in both spaces, in sharp contrast to the uniform distribution assumed for the "standard halo."

During the late spring of this year, Mike Warren, the PI of the project, decided to reduce substantially the time he spends at LANL, and on this ER project. Therefore, much of the funding for FY15 was transferred to Przemek Wozniak, of ISR-2, to finance LANL's continuing role as an institutional partner in the Large Synoptic Survey Telescope (LSST) consortium. Przemak provided the following motivation for continuing LANL's connection with the LSST:

Time-domain astronomy and the science of cosmic explosions are revolutionizing modern astrophysics with profound impact on fundamental physics, as evidenced by the 2011 Nobel Prize for supernova (SN) studies leading to the discovery of Dark Energy. The Large Synoptic Survey Telescope (LSST) selected as the top priority ground-based project by the Astro2010 Decadal Survey of National Academies will be the first multi-Petabyte time-domain survey. In 2014 NSF and DOE approved the $600 Million construction budget for LSST. The project gained new momentum and is poised to conduct a 10-year sky survey with unprecedented sensitivity, resolution, and coverage starting in 2022. LSST will open for exploration a parameter space that is three orders of magnitude larger than available today in four key areas: time-domain astrophysics, dark energy and weak gravitational lensing studies, Solar System science, and galactic structure and evolution.

Scientific Approach and Accomplishments

A major milestone achieved during the second year of the project was a complete trillion-particle simulation performed on the Titan supercomputer (ORNL), which ran continuously for about a day and a half with no failures. No other cosmological simulation code has achieved this level of resolution with such short run times. In the third year, the team focused on higher-resolution simulations on the galactic scale, which reveals more about baryonic properties of the early universe. They also performed calculations to assist in interpreting the possible dark matter signatures that will be coming out of new observational facilities such as the Dark Energy Spectroscopic Instrument (DESI) at the Kit Peak

Observatory. These calculations were done using a DOE INCITE proposal grant on the Titan supercomputer at Oak Ridge. These calculations and code (2HOT) clearly represent the state-of-the-art in N-body cosmological simulations.

Impact on National Missions

The dark matter project is a flagship of the NPAC component of the Nuclear and Particle Futures Pillar. It is also a prime example of the Data Science at Scale area of the Laboratory's Information, Science, and Technology Pillar. These calculations were used to push the limits of - and uncovered scaling issues with - the Mustang supercomputer Having a working code that can operate at the capability limits of any new computer system, yet is able to get answers in a reasonable length of time, not only is critical to national needs and emerging issues, but also is unique - not duplicative of capabilities at other national labs, esp. NNSA. It establishes enabling capabilities critical to Lab strategies for emerging technical endeavors, especially those related to "big data." There is ample potential for a two- way transfer of ideas, and technology to national security missions (e.g. nuclear, global, energy).

Wozniak summarizes the importance of the LSST connection as follows: Since 2006 LANL scientists (led by Przemek Wozniak, Thomas Vestrand, Chris Fryer, and Michael Warren) are members of LSST science working groups focusing on studies of explosive variability, supernovae, and structure formation in the Universe. We are recognized as intellectual and technical leaders in data intensive analysis and large-scale simulations. As a member institution of the LSST consortium, LANL is also represented by a voting member on the Board of Directors of the LSST Corporation. Supporting astrophysics and cosmology research at LANL and forging external collaborations with leaders in the field are both high priority areas for LDRD. Funding LANL participation in LSST is a great opportunity to advance these goals and reinforce LANL leadership in time-domain astrophysics and cosmology where LSST is expected to have a revolutionary impact.

Publications

Hamaus, N., B. D. Wandelt, P. Sutter, G. Lavaux, and M. S. Warren. Cosmology with Void-Galaxy Correlations. 2014. Physical review letters. 112 (4): 041304.

Johnston, R., D. Bacon, L. Teodoro, R. Nichol, M. Warren, and C. Cress. Reconstructing the velocity field beyond the local universe. 2014. General Relativity and Gravitation. 46 (11): 1.

Skillman, S. W., M. S. Warren, M. J. Turk, R. H. Wechsler, D. E. Holz, and P. Sutter. Dark Sky Simulations: Early Data Release. 2014. arXiv preprint arXiv:1407.2600.

Song, J., J. J. Mohr, W. A. Barkhouse, M. S. Warren, K. Dolag, and C. Rude. A Parameterized Galaxy Catalog Simulator for Testing Cluster Finding, Mass Estimation, and Photometric Redshift Estimation in Optical and Near-infrared Surveys. 2012. The Astrophysical Journal. 747 (1): 58.

Sutter, P., G. Lavaux, B. D. Wandelt, D. H. Weinberg, and M. S. Warren. Voids in the SDSS DR9: observations, simulations, and the impact of the survey mask. 2013. arXiv preprint arXiv:1310.7155.

Sutter, P., G. Lavaux, B. D. Wandelt, D. H. Weinberg, and M. S. Warren. The dark matter of galaxy voids. 2014. Monthly Notices of the Royal Astronomical Society. : stt2425.

Sutter, P., G. Lavaux, B. D. Wandelt, N. Hamaus, D. H. Weinberg, and M. S. Warren. Sparse sampling, galaxy bias, and voids. 2013. arXiv preprint arXiv:1309.5087.

Sutter, P., G. Lavaux, N. Hamaus, A. Pisani, B. D. Wandelt, M. S. Warren, F. Villaescusa-Navarro, P. Zivick, Q. Mao, and B. B. Thompson. VIDE: The Void IDentification and Examination toolkit. 2014. arXiv preprint arXiv:1406.1191.

Teodoro, L. F. A., D. G. Korycansky, M. S. Warren, C. L. Fryer, G. Rockefeller, K. Zahnle, and V. R. Eke. A new suite of hydrodynamical simulations of the origin of the obliquity of Uranus. Invited presentation at 46th Lunar and Planetary Science Conference. (The Woodlands, Texas, 16-20 March 2015).

Teodoro, L., D. Korycansky, M. Warren, C. Fryer, G. Rockefeller, and K. Zahnle. A Ten Million SPH Particle Simulation of the Origin of Obliquity of Uranus. 2014. In Lunar and Planetary Institute Science Conference Abstracts. Vol. 45, p. 2542.

Teodoro, L., M. Warren, C. Fryer, V. Eke, and K. Zahnle. A One Hundred Million SPH Particle Simulation of the Moon Forming Impact. 2014. In Lunar and Planetary Institute Science Conference Abstracts. Vol. 45, p. 2703.

Turk, M. J., M. S. Warren, and S. W. Skillman. Building a Community-Focused Data Platform. 2014. Urbana. 51: 61801.

Warren, M. S.. 2HOT: An Improved Parallel Hashed Oct-Tree N-Body Algorithm for Cosmological Simulation. 2014. Scientific Programming. 22 (2): 109.

Warren, M. S., and B. Bergen. Poster: The Hashed Oct-Tree N-Body Algorithm at a Petaflop. 2012. In High Performance Computing, Networking, Storage and Analysis (SCC), 2012 SC Companion:. , p. 1442.

Coherent Diffractive Imaging of Ultrafast Ejecta Processes

Cynthia A. Bolme
20130632ER

Abstract

The physical processes leading to the formation of particles ejected from a shocked rough surface (i.e. ejecta) is not well understood. The scientific challenge in studying the ejecta formation and evolution is obtaining high resolution structural information leading to an understanding of particle size and speed distributions. There are many factors affecting ejecta growth and production, especially when the pressure and temperature conditions of the shock wave causes the material to go through structural phase changes with the most significant changes occurring when the material transitions between solid and liquid phases. Not fully understanding the physics of ejecta leads to the inability to accurate predict ejecta formation. Diagnostics that are currently being used to probe the size and velocity distribution have produced incredibly useful data. However, these diagnostics have not been able to measure the small scale extent of the ejecta distribution due to the limited spatial resolution. This project sought to extend the spatial resolution of the measurement of ejecta particles to well below that which is currently achievable by performing coherent x-ray diffractive imaging with soft x-rays up to 100 eV (resolution < 100 nm) on a high repetition rate, in-house system laser system and down to a few nm resolution at X-ray free electron lasers. Here we summarize the background of the problem of imaging ejecta while it is developing and evolving at shock velocities (1-10 km/s), our efforts to develop single shot, nanometer scale X-ray imaging for ejecta, and the importance of this work to national missions.

Background and Research Objectives

When shock waves break out from a roughened surface, the interaction of the shock wave with the free surface causes material to be ejected from the surface in a process known as ejecta. Ejecta can form starting from an instability in the shock front caused by surface roughness that evolves into micro-jets and eventually into moving particulates. An important aspect of studying this challenging project that involves material phase transitions and plastic deformation processes is the dynamic evolution of the micro-jet that breaks up into particles ranging in size from 10s of microns to nanometers. These particles can be solid or liquid and can be reabsorbed, coalesce, or continue to break up depending upon the surface geometry, the surrounding environment, and the strength of the shock wave. Developing computational tools to understand and predict this process requires sophisticated material models and is of critical importance to the mission of the laboratory.

Ejecta have been studied using laser velocimetry, proton and X-ray radiography, and ultraviolet holography. The current techniques of proton radiography (pRAD) and ultraviolet (UV) holography have imaged late time ejecta dynamics with spatial resolutions down to 10 μm and to 800 nm, respectively. These techniques have been used to probe the particulate size and velocity distribution. However, due to the currently available resolution, the sizes, velocities, and shapes of the micro-jet and its subsequent particulates is unknown for features less than ~1 μm [1-5]. However, molecular dynamics (MD) models of singly and doubly shocked metals show a wealth of dynamic evolution on the sub-micron and sub-100 ps scale such as how and where bubbles (the region of material feeding the spike growth) form, break up, and eventually evolve into spike growth, spike break up and the constituent particle size distribution [6]. In a recent paper, molecular dynamics simulations of copper showed a power law decay in the particle size distribution with respect to number of aggregates [7]. The smallest particle volumes observed were about 40 cubic angstroms. For ejecta formation, molecular dynamics simulations have an advantage over other simulations in that they are more accurate in predicting surface tension – an important part of understanding liquid ejecta droplet evaporation and breakup. Thus we would expect that the molecular dynamics should produce a more realistic particle size and shape. In addition to the sizes and

shapes of the particles, molecular dynamics simulations also provide information about the structure (crystalline or liquid) and the crystalline grain sizes that are predicted for the ejected material, and those predictions can be compared to measurements made with wide angle x-ray scattering by hard x-rays. While very powerful, the information gleaned from molecular dynamics simulations have yet to be experimentally verified due to a lack of spatial and temporal resolution in previously available diagnostics.

To extend the available size and speed distribution measurements to capture the dynamics of smaller features and particulates, we proposed to develop new x-ray imaging capabilities with which we would probe ejecta dynamics for the first few ns with resolutions of sub-50 fs and sub-100 nm.

The main objectives of this project were to develop an ultrafast laser to create a shock wave at a metal sample surface and then to image dynamics with X-ray imaging. The samples have a periodically roughened surface, and the interaction of the shock wave with the structured surface creates instabilities in the material that will evolve in small jets of ejecta particles. This process was to be imaged using ultrafast x-rays either from a tabletop soft X-ray source or from an intense accelerator based X-ray Free Electron Laser (XFEL). In addition to ultrafast X-ray imaging, we also have performed molecular dynamic simulations of this ejecta forming process that are well matched in length and time scales to the experiments.

Scientific Approach and Accomplishments

This last year, our efforts were focused in three areas: 1) developing the single shot, tabletop soft X-ray source, 2) conducting the first dynamic ejecta imaging experiments at the LCLS, and 3) performing MD simulations of ejecta from Al surfaces using the best Al potential as determined in FY14's evaluation of the Al potentials. We continued to have problems with damaging the optical components in the laser system due to poor laser beam mode quality and high power. Team member Steve Gilbertson successfully incorporated a hollow-core spatial filter that improved the laser beam mode and enabled us to obtain much higher laser powers. With these changes, we have successfully compressed the amplified 10 Hz laser for the high harmonic generation drive and imaging to 38 fs, better than the 50 fs we were attempting. We currently have up to 100 mJ of pulse energy in this short pulse and have been able to generate intense soft X-ray pulses from argon filled gas cells. The soft X-ray photon energies have not been measured but are expected to be centered at 40 eV, and we have produced about 10 million photons in a single 10 fs long pulse. This soft x-ray photon production is about 3-4 orders of magnitude lower than expected, but at the time of this report, we have been scaling up the intensity of this soft X-ray system and expect soon to achieve enough flux for single shot imaging.

As mentioned before, the development of this unique system has been attracting interest from outside collaborators including Prof. Brian Abbey's group from La Trobe University in Melbourne, Australia who was a Physics Colloquium speaker last fall. Furthermore, a recent LANSCE hire, Prof. Edwin Fohtung, who is also a professor at New Mexico State University, has expressed interest in collaborating with us and using this unique single shot imaging system. These two groups bring strong expertise in coherent diffractive imaging techniques and algorithms and will greatly speed up the progress we can make on the imaging once the imaging experiments begin.

Computational progress has been made by performing many simulations of ejecta formation in Al with varying depths of sinusoidal roughness on the shocked free surface. The calculations have shown that there is a larger effect of material viscosity for more shallow surface roughness. The simulations have also shown that temperature does not strongly influence the ejecta production in Al.

The most significant progress has been the successful fielding of nanometer scale imaging of shocked materials at the world's first hard X-ray laser, the Linac Coherent Light Source (LCLS) at the SLAC National Accelerator Laboratory in May 2015. We obtained beamtime at the Materials in Extreme Conditions (MEC) endstation at the LCLS for approximately 12 hours of experimentation. Beamtime allocations for the LCLS are extremely competitive, so this was a great opportunity and it was the first time that ejecta experiments have been performed at LCLS. We fielded a low angle scattering detector for direct images of the ejecta process alongside wide angle scattering detectors for measuring changes to the ejecta material phase. The intense, sub-100 fs X-ray pulses from the LCLS capture the dynamic material motion in blur free images with approximately 500 nm resolution. Materials studied were tin, cerium, and titanium. Analysis of this data is ongoing. These results will not only lead to high impact publications but also to additional LCLS beamtime through strongly motivated user proposals.

Impact on National Missions

The development of nanometer scale dynamic imaging is addressing core mission problems and providing important validation of physics-based material models as the spatial and temporal resolutions achievable with these imaging diagnostics are an order of magnitude better than current dynamic diagnostic alternatives. This project's relevance

intersects the Nuclear Performance, IS&T, and Materials Grand Challenges, and it is directly linked with the proposed LANL Signature Science Facility MaRIE (Mater-Radiation Interactions in Extremes). The strategic impact of this project is the development of enabling capabilities in the following areas: in situ dynamics of materials in extremes with x-ray probes, intense next-generation laser sources of secondary radiation, and advanced research on real-time reconstruction of phase-coherent diffraction data into 3D images. Development of technologies like those in this project are crucial to providing otherwise unobtainable data for validation of codes on current materials problems of interest and will begin the decadal development of advanced coherent X-ray imaging at MaRIE.

Los Alamos is currently the world-expert in studying ejecta through both experiments and modeling. The majority of the ejecta research up to this point has been performed using codes and examining the material on the meso-scale. This work has expanded our expertise in ejecta into the nano-scale and will advance our basic physical understanding of the ejecta process by comparison with simulations that are based solely on atomic potentials.

References

1. Zellner, M. B., M. Grover, J. E. Hammerberg, R. S. Hixson, A. J. Iverson, G. S. Macrum, K. B. Morley, A. W. Obst, R. T. Olson, J. R. Payton, P. A. Rigg, N. Routley, G. D. Stevens, W. D. Turley, L. Veeser, and W. T. Buttler. Effects of shock-breakout pressure on ejection of micron-scale material from shocked tin surfaces. 2007. Journal of Applied Physics. 102 (1): -.

2. Grigsby, W., B. T. Bowes, D. A. Dalton, A. C. Bernstein, S. Bless, M. C. Downer, E. Taleff, J. Colvin, and T. Ditmire. Picosecond time scale dynamics of short pulse laser-driven shocks in tin. 2009. Journal of Applied Physics. 105 (9): -.

3. Rességuier, T. de, L. Signor, A. Dragon, M. Boustie, and L. Berthe. On the dynamic fragmentation of laser shock-melted tin. 2008. Applied Physics Letters. 92 (13): -.

4. Li, Z., Z. Luo, Z. Liu, Y. Ye, Z. Li, J. Zhong, and J. Li. High-speed microjet particles measurement using in-line pulsed holography. 2010. Journal of Applied Physics. 108 (11): -.

5. Sorenson, D. S., R. W. Minich, J. L. Romero, T. W. Tunnell, and R. M. Malone. Ejecta particle size distributions for shock loaded Sn and Al metals. 2002. Journal of Applied Physics. 92 (10): 5830.

6. Dimonte, G., G. Terrones, F. J. Cherne, T. C. Germann, V. Dupont, K. Kadau, W. T. Buttler, D. M. Oro, C. Morris, and D. L. Preston. Use of the Richtmyer-Meshkov Instability to Infer Yield Stress at High-Energy Densities. 2011. Phys. Rev. Lett.. 107: 264502.

7. Durand, O., and L. Soulard. Large-scale molecular dynamics study of jet breakup and ejecta production from shock-loaded copper with a hybrid method. 2012. Journal of Applied Physics. 111 (4): -.

In Search of Light WIMPs

Alexander Friedland
20130637ER

Abstract

Extremely low-background detectors designed for other experimental searches, for example neutrinoless double beta decay, can also be used to look for light (~1 GeV mass) dark matter. Theoretical possibilities for dark matter at this mass scale includes weakly-interacting massive particles (WIMPS), these can be searched for in experiments like MAJORANA. LANL has a substantial interest in the MAJORANA double-beta decay experiment looking for neutrinoless double beta decays. The same detector, and others like it, may be able to discover WIMPs in a mass and coupling range not accessible to other dark matter experiments. We also discuss possible new scenarios for light dark matter which include interactions with neutrinos to resolve problems with an overprediction of satellite galaxies if collisionless cold dark matter is assumed.

Background and Research Objectives

Dark Matter is known to compose about 25% of the energy density of the universe, as measured by Planck, and previously COBE and WMAP and other experiments including big-bang nucleosynthesis. However we do not know the particle content of this dark matter, what is it exactly? Various large experiments are searching for this matter, typically looking for recoils of large nuclei like Xenon to search for the presence of dark matter at the earth. Next generation experiments in the US include SuperCDMS at SNOLAB, the LUX-Zepelin (LZ) experiment, and the Axion Dark Matter experiment ADMX-Gen2. LZ and SuperCDMS will look for WIMPs, while ADMX-Gen2 will search for a different type of particle called axions.

To date, dark matter searches have not been very sensitive to light WIMPs, those of order 1 GeV or so. Also, they have not clearly detected dark matter particles in the heavier mass range. This project is aimed at studying how searches for lighter WIMPs might be undertaken, and searching for new theoretical models for cold dark matter that satisfy all experimental and observational constraints.

Scientific Approach and Accomplishments

The MAJORANA experiment is designed to search for neutrinoless double beta decay, a process in which two neutrons decay into protons inside a nucleus emitting two electrons but no neutrinos. This process is, in the standard picture, only possible for Majorana neutrinos, those that are there own anti-particle.

The current generation double-beta decay experiment is called the MAJORANA DEMONSTRATOR, it is a smaller scale experiment designed to understand what is required, in particular in the area of reducing backgrounds, to a full ton-scale detector that would be much more sensitive. Part of the strategy for improving these experiments is to reduce background and to reduce the energy threshold of the detectors. Achieving a sub-keV energy threshold would allow the MAJORANA demonstrator to also search for light WIMPs.[1]

Figure 1 shows the projected sensitivity to light mass WIMPs for 100 kg-years of exposure with a 0.3 keV energy threshold. As shown in the figure, at a mass of ~ 10 GeV present generation experiments are extremely sensitive. However below 1 GeV the cross sections have no stringent limits. The MAJORANA DEMONSTRATOR could be much more sensitive in this mass range, and of course the full MAJORANA would be even more sensitive, nicely complementing the higher-mass searches of other experiments. A modified low-background broad energy germaniam detector (MALBEK) has been deployed at the Kimballton Underground research facility in Virginia.

As part of this project, theoretical particle physics scenarios with light WIMPs were also investigated. Previously it had been thought that heavier WIMPs were more natural, and hence the concerted experimental ef-

fort to look in this regime where the recoil energy is larger. It has been suggested that collisionless cold dark matter over-predicts the number of satellite galaxies. This apparent lack of structure at small scales can be reconciled with theory by postulating interactions between neutrinos and dark matter with a force carrier of mass of order MeV. An important feature here is that the dark matter couples to normal matter only in the form of neutrinos. This scenario can be tested in the IceCube experiment.[2]

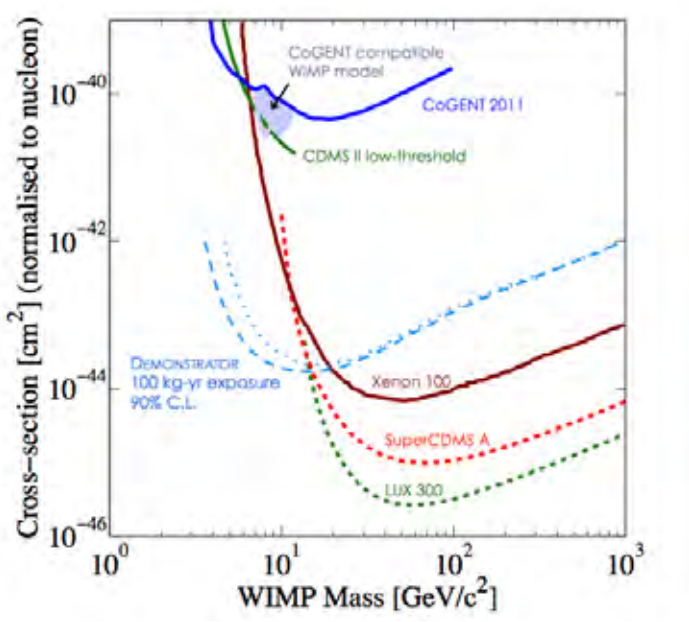

Figure 1. Sensitivity of the MAJORANA DEMONSTRATOR compared to other experiments to WIMPs as a function of the WIMP mass. Lower curves demonstrate increased sensitivity. The MAJORANA DEMONSTRATOR could be particularly sensitive to light-mass WIMPs.

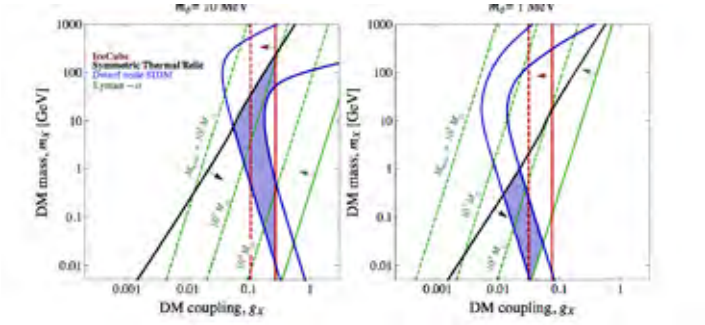

Figure 2. Allowed regions of mass and coupling for dark matter with the inclusion of neutrino-dark matter interactions. The shaded region is the allowed region. The left panel shows results for a 10 MeV force carrier, and the right for a 1 MeV force carrier. See text for further details.

Figure 2 shows the allowed regions of dark matter mass (vertical axis) versus coupling to neutrinos (horizontal axis) for two different mediator masses. In the left panel the force carrier for this new interaction has a mass of 10 MeV and in the right panel 1 MeV. The allowed parameters that fix the observational issues with small-scale structure are indicated by the filled blue regions. The other lines represent constraints from other observations, including the Lyman alpha forest (solid green curves) and the observed total amount of dark matter (black curves).

This investigation shows that new models of dark matter interacting with neutrinos are possible, resolve some discrepancies with observations of clustering at small scales, and are potentially testable at IceCube. The allowed regions of dark matter masses encompass the regions measured by traditional dark matter experiments and also the lighter masses that could be probed with MAJORANA.

Impact on National Missions

Dark Matter and neutrino physics are two of the highest priorities of the DOE Office of Science High Energy physics program. This LDRD-ER project materially advanced the prospects for searching for light WIMPs, an important experimental possibility for future experiments including those primarily designed for double beta decay searches. A small test experiment is already being performed, and future larger-scale efforts are being studied. This LDRD project also proposed new theories for dark matter that incorporate interactions between neutrinos and dark matter. These theories can experimentally tested in the future. The theories produced in this project can simultaneously solve some problems which result with comparing standard collisionless dark matter compared with astrophysical observations.

References

1. Giovanetti, G. K., and S. R. Elliott. A Dark Matter Search with MALBEK. 2014. Physics Procedia. 00: 1.

2. Friedland, A., and M. Shoemaker. Integrating In Dark Matter Astrophysics at Direct Detection Experiments. 2013. Physics Letters B. 724: 183.

Publications

Cherry, John Francis Jr., Alexander Friedland, and Ian M. Shoemaker. Neutrino Portal Dark Matter: From Dwarf Galaxies to IceCube. 2014. Physics Letters B.

Friedland, A., and M. Shoemaker. Integrating In Dark Matter Astrophysics at Direct Detection Experiments. 2013. Physics Letters B. 724: 183.

Friedland, Alexander, Annelise Malkus, and Gail C McLaughlin. Matter-Neutrino Resonance Above Merging Compact Objects. 2014. Physical Review Letters.

Giovanetti, G. K.. A Dark Matter Search with The MAJORANA Low-Background Broad Energy Germanium Detec-

tor. Invited presentation at TAUP 2013. (Asilomar, CA, USA, 9 Sep. 2013).

Giovanetti, G. K., and S. R. Elliott. A Dark Matter Search with MALBEK. 2014. Physics Procedia. 00: 1.

Gupta, Rajan, Alexander Friedland, Michael Lawrence Graesser, Tanmoy Bhattacharya, Michael S. Warren, and Emil Mottola. Los Alamos HEP Theory. 2014.

Emittance-Reduction System for Future Accelerator Solutions

Kip A. Bishofberger
20130688ER

Abstract

More than any other measure, the beam brightness has been the driving force for technological development in beam physics. The brightness refers to density of particles, both in physical space and phase space. The brighter the beam, the more structured the beam is to enable generation of X-rays, electromagnetic radiation, and unique particles. The opposite of brightness is called "emittance," representing the level of disorder and temperature within the beam. Until recently, the beam's emittances were considered constants of linear motion, and nonlinear forces only increased them, thereby reducing the beam brightness.

However, within the past couple of years, a breakthrough has developed, largely originating with scientists at LANL. The term "eigen-emittances" refers to the emittances that a beam would possess if there were no additional correlations. The new discovery is that, by generating a beam with specific initial correlations, the eigen-emittances can be substantially reduced, and through beam optics that unravel the correlations, the final, observed emittances will take on these improved values, thereby generating a significantly brighter beam for accelerator applications. This project successfully analyzed this technique and optimized an experimental setup to demonstrate this breakthrough eigen-emittance manipulation scheme.

The technology development capability supported by this project enhances our ability to design Engineered Systems. Additionally, compact, advanced accelerator technology supports a wide array of accelerator-based solutions to National Security missions. Two examples include Global Security, such as Warfighter Support (high-power Free-Electron Lasers) and Countering Weapons of Mass Effect (active interrogation).

Background and Research Objectives

Beam physics has been a useful tool for a variety of engineering and scientific goals. In every application, a demand is placed on the number of beam particles (electrons, protons, ions, etc.) that hit some target or pass through some structure. The "emittance" quantifies the amount of disorder within the beam (in each of three dimensions); a low-emittance beam, like a laser beam, can be focused very tightly or pass uniformly through a long distance. Beams with high emittance cannot be focused as tightly and are not nearly as efficient in their utility.

For decades, emittances were considered constants-of-motion through linear forces; in addition, nonlinear effects can raise emittances, but no simple technique could reduce them. Recently, unique beam systems were discovered that could reduce one or more emittances. These cases, led largely by LANL scientists, grew into a new framework upon which beam physics is based. A new term "eigen-emittance" was coined at LANL to describe intrinsic beam characteristics, and methods to reduce beam emittances were formalized.

This project used this new formalism to study a beamline device that converts transverse beam emittance into longitudinal. Similar to converting a flashlight into a laser, the beam is capable of being ten-times brighter through this conversion process, significantly increasing its utility in nearly all applications.

Scientific Approach and Accomplishments

The primary focus on the project was to study and optimize a unique beamline insertion device, known as an XZ-FBT (referring to a Flat-Beam Transformer between the x-plane and z-plane). The key piece of this device is an ultra-thin, wedge-shaped foil that the beam passes through. This tactic generates a unique spatial relationship on the particle distribution; a subsequent magnetic field profile converts this relationship into a lower-emittance beam that has significantly higher brightness than prior to the foil.

The majority of the project was devoted to a careful study of this manipulation system. In particular, the mechanism scales in a unique manner with beam energy and species. A model insertion device was optimized for protons and electrons at a variety of beam energies and initial emittances. Improvements in brightness were shown to be about than a factor of three in one dimension (a second insertion device would increase the brightness to nearly ten times total).

Multiple test facilities were analyzed to attempt a physical demonstration of the device. The Argonne Wakefield Accelerator (AWA) was selected as the ideal candidate to perform experiments, after they renovated their beamline to 75 MeV energy. An insertion device was constructed specifically for those beam parameters. At the end of the project, AWA was in the process of testing the critical foil experiments that underpin the success of the project. These tests indicate similar results to the simulations have indicated, but ongoing data analysis will provide the experimental verification to determine the system's viability.

Impact on National Missions

Major accelerator facilities at LANL include LANSCE and DARHT, and successful implementation of the proposed MaRIE signature science facility will require developing new accelerator capabilities. Additionally, several emerging major Global Security work- for-other missions require state-of-the-art accelerator technology.

The work in this project directly supports future light sources (such as that proposed for the MaRIE XFEL) and future linear colliders, which are major DOE Office of Science projects. In turn, light sources support the Materials: Discovery Science to Strategic Applications grand challenge and linear colliders support the Beyond the Standard Model grand challenge.

More directly, the technology development capability supported by this project enhances our ability to design Engineered Systems, another grand challenge. Additionally, compact, advanced accelerator technology supports a wide array of accelerator-based solutions to National Security missions. Two examples include Global Security, such as Warfighter Support (high-power FELs) and Countering Weapons of Mass Effect (active interrogation).

Reactor Power for Large Displacement Autonomous Underwater Vehicles

Patrick R. Mcclure
20150035ER

Abstract

This research project is an investigation into small reactors suitable for powering Autonomous Underwater Vehicles (AUVs.) The primary motivation was U.S. Navy moving toward a large fleet of AUVs. AUVs, much like drones in the U.S. Air Force, are envisioned taking over or supplementing a variety of missions, including: threat surveillance, situational awareness; anti-submarine warfare; information operations; wreckage recovery; and time critical strike.

However since beginning the research, the Navy has explicitly stated to LANL that they are not interested at this time in nuclear reactors for AUVs for political reasons. However, the general idea of a long-term power source for commercial AUVs is still viable and NASA has interest in AUVs for planetary exploration of the Saturn moon Titan, which has large methane seas.

The goal of this proposal is to design a small reactor suitable for AUVs. Nuclear power removes any time limitation on a mission, extending it from weeks to years (up to a decade.) A reactor is best suited for larger AUVs. This proposal targets development of a nuclear reactor capable of powering a large displacement (> 3 ft diameter, > 20,000 lbs) AUV. The reactor needs several key attributes including 1) self-regulation, 2) small volume dimensions and 3) it must be proliferation resistant. The last two attributes are the primary challenge for this concept. Proliferation resistant means that enrichment, fuel mass and fuel form must be managed carefully to address security concerns while keeping the reactor at an appropriate size. These issues are addressed in the research.

Background and Research Objectives

Several issues are important if a nuclear reactor were to be used for unattended operations in the ocean. The first issue is that the reactor needs to self-regulate and operate safely. The second would be that the reactor has to fit in the “as designed” vehicle or designed into the vehicle without rendering it non-functional. The final issue is the reactor must not present a proliferation concern given that it is unattended.

The reactor needs to be self-regulating since by definition AUVs have no personnel in attendance. The self-regulating feature is common to the small reactors designed by Los Alamos. Self-regulation is accomplished by using small highly reflected reactors (creating a large negative temperature feedback in the reactor) that allows the reactor to adjust to the power demands of the system. The physics of this system causes the reactor to load follow the power conversion system.

Fitting a reactor into a small diameter cylinder that is needed for the hydrodynamics of a sub is challenging. The core, its reflector, any reactivity make-up system and shielding has to fit into the AUV outer cylinder diameter. In addition, care must be used to maintain some key aspects of center of gravity of the AUV. Finally, how the heat is rejected from the reactor must be evaluated and designed.

LANL proliferation experts have provided guidance on how to lower the nuclear attractiveness of a reactor concept. The first is to keep the enrichment below the threshold for highly enriched uranium at 20% or at a value below 50% for highly enriched. The second is to keep the amount of U235 fuel low. In these concepts, ideal values are 6 kgs for 93% enriched or 50 kgs for 50% enriched and unlimited mass for 20% enrichments. These mass values favor a moderated reactor (slower neutrons and more uranium efficient) over a fast reactor (faster neutrons and less uranium efficient.) The third is to pick a form of fuel that is not a metal and preferably a ceramic to slow down the conversion to metal if the reactor were compromised. The final is to pick a fuel form where the fuel is dispersed in another material that makes conversion to metal even harder. A measure of

proliferation is the security category of the system using the DOE graded safeguards table.

These attributes were examined for a class of reactors spanning a power range from 1 kWe (electric) to 150 kWe (electric) for use either in a NASA AUV or a commercial AUV. The desired power level is in the low 10's of kWe.

Scientific Approach and Accomplishments

The research was performed using several LANL reactor design tools and commercial design tools. These tools included LANL developed tools MCNP-61, Monteburns2, Maggie, and the commercial software ANSYS3. LANL group NEN-5 has the capability to quickly model a reactor using pre-processers to quickly develop a set of radiation transport (MCNP-6) input decks that allow for a quick evaluation of the neutron physics of a particular design. Reactor burn-up (a measure of the fuel used) and shielding are done by the computer codes Monteburns and Maggie, respectively. LANL group AET-1 then uses ANSYS (a combination computer aided design, structural, heat transfer analysis software) to analyze the reactor fit and heat rejection of the proposed reactor concept.

LANL looked at multiple reactor designs ranging in power from 1 kWe to 150 kWe and using a fuel that spanned a range of attributes in order to achieve specific non-proliferation and size goals. All of these reactors are self-regulating due to a large negative reactivity coefficient. Small highly reflected cores that use heat pipes for cooling can be designed to have large negative reactivity coefficients. The physics of the design precludes inadvertently inserting positive reactivity into the core, thus making for a very safe reactor.

The factors that were traded included:

- Neutron Spectrum – Fast neutron spectrum versus a moderated neutron spectrum by adding a hydride (Yttrium Hydride or YH) to the reactor. Moderating (slowly down) the neutrons in a reactor core is one means of lowering the amount of uranium or lowering the enrichment of the uranium.
- Fuel Type – Conventional reactor fuel (uranium metal and uranium oxide) versus a uranium oxide fuel dispersed in graphite.
- Power Level – Varied over three power ranges.
- Peak Temperature – Some moderators and fuels do not perform in a high temperature environment (> 500 C) and thus have lower power conversion efficiency.

Constraints on design are based upon the upper diameter of the AUV, which is approximately 90 cm. The diameter has to accommodate the core, core reflector and any shielding needed in the radial direction.

Weight/size: For the higher power ranges (125 to 150 kWe), using a moderator makes about a 10% decrease in the weight of the reactor core regardless of fuel choice. Given the challenges of trying to engineer the moderator, moderating the reactor was not seen as a good engineering choice for this power range.

For the middle power cases (22 to 38 kWe) moderating the core can have some substantial benefit. The drop in weight is significant and more importantly the drop in Uranium in the core is about 75%. A single UZrH fuel (fuel and moderator combined) was examined. UZrH is a fuel with a long history and pedigree in TRIGA4 reactors. The downside to UZrH is that in order to limit hydrogen loss, the reactor core must operate at a lower temperature that, in turn, would limit efficiency. But the combined fuel-moderator is quite good in lowering overall weight, although reduction in U235 was about the same as fuel and moderator being separate.

For the very low power cases (1 kWe), the use of a moderator could approach the weight of an 93% enriched uranium system and lower the U235 mass by as much as 80%.

Proliferation: All of the 20% enriched cases are Security Category 4 (the lowest category.) But the use of 20% comes with substantial weight/size penalties. The metal core cases show the tradeoffs between weight/size and better security. The 93% enriched case is small and light, but would be burdened as Security Category 1 material (the highest category.) The 50% enriched case is a good example of getting the enrichment down and decreasing the U235 to a level that would be categorized as Security Category 3. The less than 50% enrichment and less than 50 kgs of U235 would drastically decrease the security requirements. The 20% enriched metal case is Security Category 4, but the size and weight would be unacceptable for many applications.

The moderated cases show that even the 93% enriched case can be lowered to a Security Category 3 by reducing the U235 to less than 6 kg. These cases have a total weight that is either better than or competitive with the HEU metal core cases. However, these designs do come with engineering issues. The moderated reactor cores have the following issues:

- Large temperature gradients between the fuel and moderator that require very robust means of insulating the moderator.

- The problem of hydrogen retention in the moderator during sequences that cause high temperatures in the moderator or over long periods of time (years.)
- Manufacturing some of the moderated designs would be difficult given the interleaved moderator and fuel configurations.

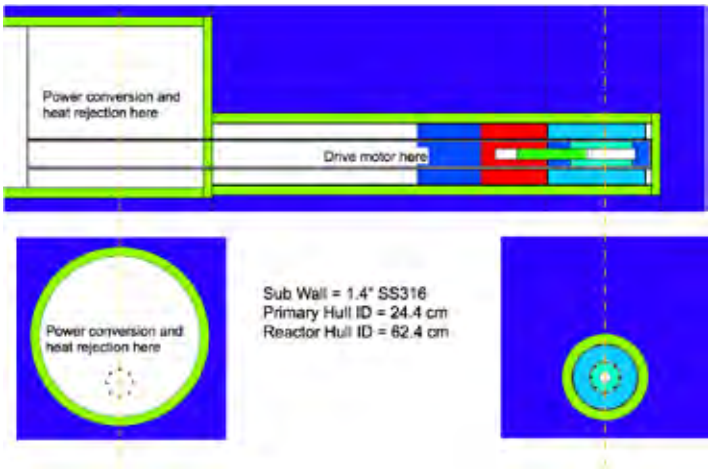

Figure 1. MCNP Model of Reactor for Titan Moon AUV

Packaging and Shielding: Fitting the reactor into a small long cylinder proved challenging. The AUV small diameter and long length is required to provide the appropriate hydrodynamics. The small diameters in AUV made shielding the reactor problematic. Shielding and packaging studies were done using the water (on earth) or methane (on the moon Titan) on the outside of the AUV with other internal shielding to get doses down to an acceptable level. This means the AUV would have to be shut down prior to surfacing, but it is an option over complete shielding of the reactor.

An example of the shielding model for an AUV for the moon Titan is shown in Figure 1. The results of the shielding study for neutrons dose for a surfaced AUV is shown in Figure 2. The study showed that using water or methane could achieve the required shielding while the AUV was submerged. Total shielding can be done for an AUV but is large and heavy in comparison.

An example of the packing of the reactor in the Titan moon AUV is shown in Figure 3. The packing of a reactor in a generic commercial AUV is shown in Figure 4. The results show that packing can be accomplished, but changes to the AUV outer structure are a possibility. Center of mass on the AUV could be impacted depending on reactor location. These issues are all solvable by traditional engineering methods.

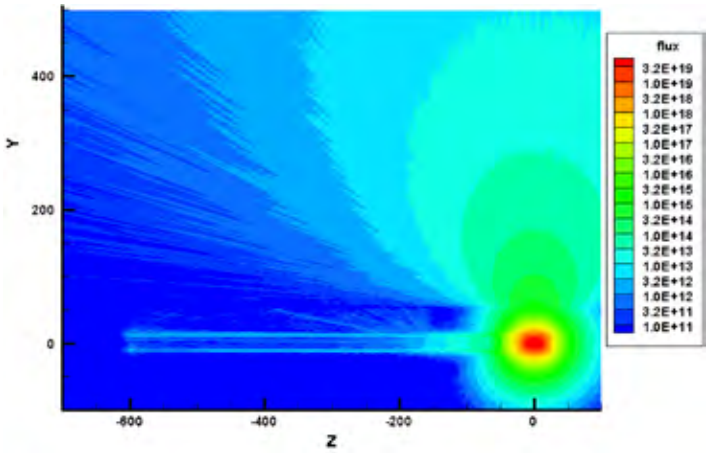

Figure 2. Shielding Study for Neutrons Dose for a Surfaced AUV.

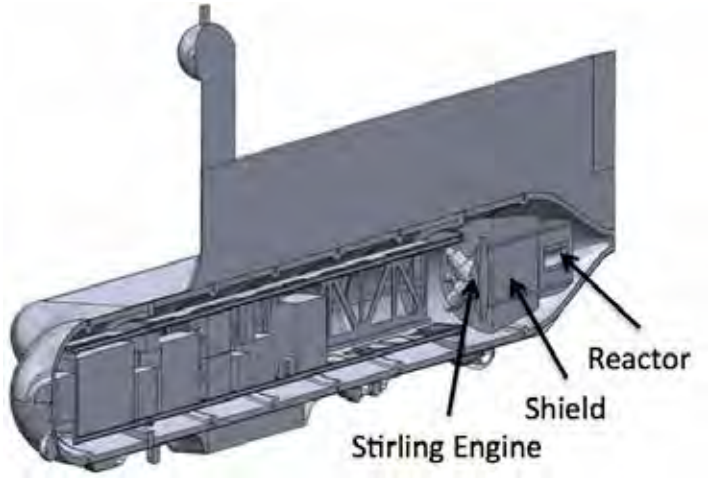

Figure 3. Titan Moon AUV Schematic of Reactor, Shielding and Power Conversion.

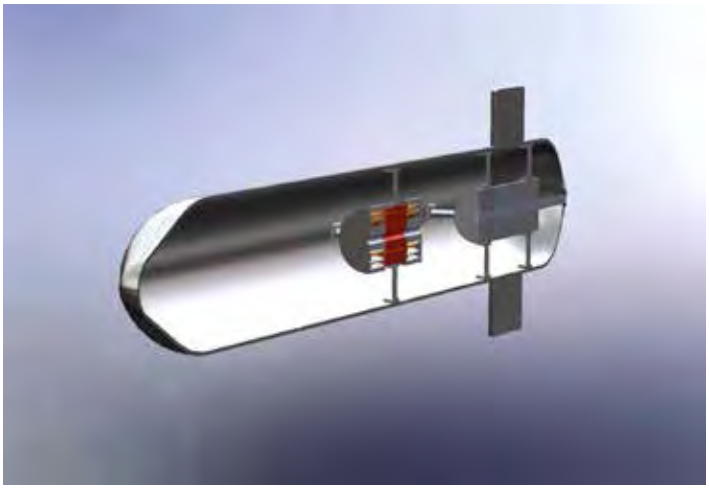

Figure 4. Generic AUV Schematic of Reactor and Power Conversion.

Impact on National Missions

Small, unattended reactors for missions that require self-regulation, small size and proliferation resistance can play a role in national missions. The U.S Navy may change its

stance on their use of nuclear power in AUVs. Agencies such as NASA and the NNSA have shown considerable interest in the use of reactors in AUVs. NASA is likely to purse the use of nuclear power in an AUV for its mission to the Saturn moon Titan. Fission power is an option over the use of traditional radioisotopes power sources.

Recent news reports have indicated that other foreign governments are also pursuing nuclear powered AUVs. The technology is very likely to be developed by the U.S if its adversaries continue to develop its use.

References

1. Pelowitz, D. B.. MCNP6 User's Manual. 2011. Los Alamos National Laboratory, LA-CP-11- 1708.

2. Poston, D. I., and H. R. Trellue. User's Manual, Version 2.0 for MONTEBURNS, Version 5B. 1999. Los Alamos National Laboratory, LA-UR-99-4999.

3. ANSYS Manual. 2003. ANSYS Inc..

4. TRIGA Reactor Fuel. 2015. General Atomic.

Publications

Fallgren, A., D. Poston, D. V. Rao, and P. McClure. The Use of Moderation in Small Reactors to Reduce Proliferation Concerns and Security Costs . Presented at To be determined. (TBD, TBD).

Towards Generating Laboratory Gigagauss Magnetic Fields and Their Impact on ICF Dynamics

Kirk A. Flippo
20150541ER

Abstract

This project aimed to build a basis for ultra-high magnetic field generation and use in the formation of a turbulent magnetic dynamo and develop a design for an experiment to produce one. Turbulent dynamos are believed to power the brightest light sources in the universe such as gamma ray bursts, black hole jets, and the most powerful cosmic rays and it also underlies the physics of the universe from the Earth's magnetic field to the formation of stars and galaxies [1-7]. In addition the ability to generate a dynamo and model it would have implications for Inertial Confinement Fusion if the models could be used to understand the spontaneous creation and evolution of these fields and show that they might impose significant changes to the physics of the implosion.

Background and Research Objectives

The magnetic dynamo is a fundamental process in plasma physics, taking kinetic energy and converting it to magnetic energy and is very important to planetary physics and astrophysics [8]. Yet, surprisingly, a first-principles understanding of turbulent dynamos and its saturation mechanism are missing and it has never been demonstrated experimentally [1].

It was shown by Ref. [9] that magnetic fields of up to 3000T could be generated using 1000 J of laser energy focused onto a specially designed magnetic field coil target. These measurements have not been confirmed independently yet, thus using this method is limited. We proposed to test the field generation and then design an experiment to use the applied field to produce amplification in a turbulent magnetic dynamo to study the process by which magnetic fields are amplified and can reconnect to produce energetic particles.

The current project was limited due to time to two experiments and to simulation studies to design a magnetic dynamo experiment which could be fielded at Omega EP in the near future. The two experiments performed developed and calibrated a Faraday rotation diagnostics and measured a laser generated ultra-high magnetic field using the Trident laser.

Scientific Approach and Accomplishments

We executed two experimental campaigns, one using the National High Magnetic Field Laboratory's (NHMFL) Single Turn Magnet, which can produce 100 T in a 1 micro second pulse, and another using the LANL Trident laser system. We used the NHMFL facility to test and calibrate a Faraday rotation diagnostic using an insulating hollow corundum tube with a polarizer/analyzer inside, which sits directly in the magnetic field. The polarizer/analyzer consists simply of two thin-film polarizers and a crystal between them. When a magnetic field is present the crystal will rotate any light passing through it due to the Faraday effect. The polarizers assure that the light entering the crystal is polarized in one direction and the second polarizer allows us to measure how much rotation of the initial polarization has occurred. The rotated light can be detected with either a fast diode or a streak camera to determine the amount of rotation and thus the field. We were able to measure the rotation from a 30T pulse at the NHFML, and on Trident we used the laser to produce a current to produce a high magnetic field, which was measured in the same fashion. Figure 1 shows the experiment as performed and the data from Trident experiment. The inset shows the measured 30 T field from the Trident shot using 200 J of laser energy to drive the coil. To our knowledge this is the first direct measurement of the field inside a laser driven coil. We designed at test four laser-driven coil targets during the Trident beam time, with several different laser pulse shapes and durations. Several coils produced ~10T and one produced ~30T. A publication on this work is in preparation [11].

In addition a suite of simulations have been performed using the LA-COMPASS MHD code to refine and coalesce

a turbulent dynamo design and to understand the evolution of a turbulent magnetic dynamo produced using a cylindrical target irradiated with 15kJ of laser energy. These simulations scoped out the required applied B-field strength and the expected plasma density and temperatures in our turbulent dynamo configuration. Figure 2 shows the simulations results of a designed experiment, which should be capable to amplify an applied magnetic field by a measurable factor of 3. A publication is in preparation [12].

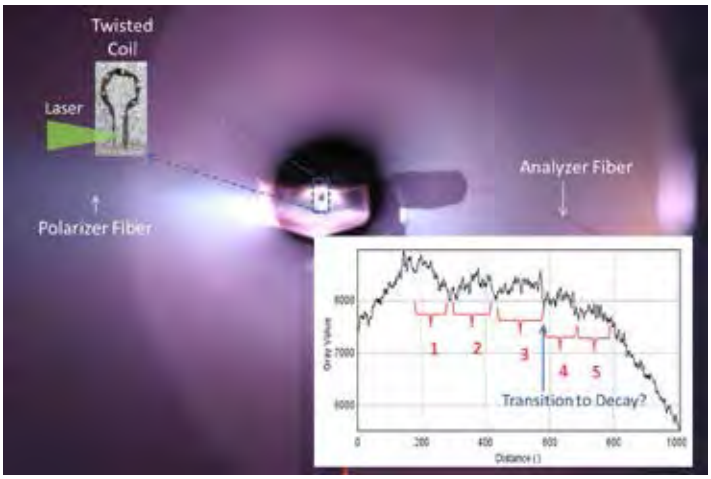

Figure 1. The experiment as performed and the data from Trident experiment. Inset: the measured 30 T field from the Trident shot using 200 J of laser energy to drive the coil.

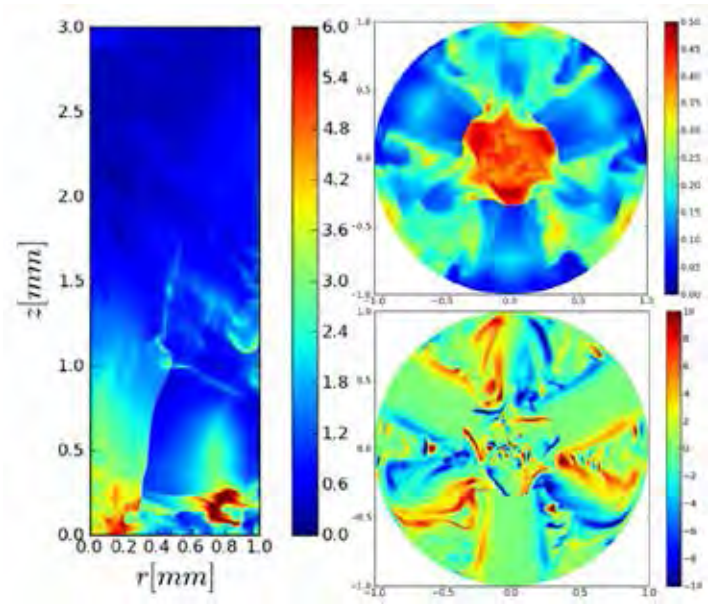

Figure 2. 3D simulation of the plasma flows inside a cylinder. (left) Density distribution (in 10 cm) in the [R,Z] plane showing the formation of a central column of plasma. (right) Temperature (in keV) and vorticity distributions in the [R,f] plane at z=0.5. The central hot plasmas are formed from three radial inflows colliding with each other and become turbulent around the central axis.

Impact on National Missions

The design of a platform to produce a turbulent magnetic dynamo provides a tool and a path forward for the C-10 program to consider a possible experiment to look into the feasibility that spontaneous magnetic fields are one of the potential reasons for the poor performance of ICF capsules, and magnetic fields can change the viscosity and the morphology of an ICF implosion well before the traditional thinking using the plasma beta equal to 1, where beta is the ratio of plasma pressure (temperature) to magnetic field pressure. What is possibly more important is the kinematic beta, which is the ratio of the fluid flow (possibly turbulent) energy density to the magnetic field energy density, which can reach unity at magnetic fields orders of magnitude smaller than those of the plasma beta, and cause deviation of the bulk flow and morphology inside the ICF implosion and may be responsible for the residual kinetic energy that does not go into heating of the hot spot and producing fusion energy. Such a discovery would have huge implications on ICF design and ICF code development.

References

1. Lathrop, D. P., and C. B. Forest. Magnetic dynamos in the lab. 2011. PHYSICS TODAY. 64 (7): 40.

2. Zhang, , R. E. Cohen, and Haule. Effects of electron correlations on transport properties of iron at Earth's core conditions. 2015. NATURE. 517 (7536): 605.

3. Li, , K. H. Yuen, Otto, P. K. Leung, T. K. Sridharan, Zhang, Liu, Tang, and Qiu. Self-similar fragmentation regulated by magnetic fields in a region forming massive stars. 2015. NATURE. 520 (7548): 518.

4. Balbus, S. A., and J. F. Hawley. Instability, turbulence, and enhanced transport in accretion disks. 1998. REVIEWS OF MODERN PHYSICS. 70 (1): 1.

5. Xu, H. a. o., H. u. i. Li, D. C. Collins, Li, and M. L. Norman. TURBULENCE AND DYNAMO IN GALAXY CLUSTER MEDIUM: IMPLICATIONS ON THE ORIGIN OF CLUSTER MAGNETIC FIELDS. 2009. ASTROPHYSICAL JOURNAL LETTERS. 698 (1): L14.

6. Xu, H. a. o., Govoni, Murgia, H. u. i. Li, D. C. Collins, M. L. Norman, Cen, Feretti, and Giovannini. COMPARISONS OF COSMOLOGICAL MAGNETOHYDRODYNAMIC GALAXY CLUSTER SIMULATIONS TO RADIO OBSERVATIONS. 2012. ASTROPHYSICAL JOURNAL. 759 (1).

7. Bell, A. R.. Turbulent amplification of magnetic field and diffusive shock acceleration of cosmic rays. 2004. MONTHLY NOTICES OF THE ROYAL ASTRONOMICAL

SOCIETY. 353 (2): 550.

8. KRAUSE, F., and K. H. RADLER. THEORY OF THE GEOMAGNETIC DYNAMO BASED ON MEAN FIELD ELECTRODYNAMICS. 1979. PHYSICS OF THE EARTH AND PLANETARY INTERIORS. 20 (2-4): 158.

9. Fujioka, , Z. h. e. Zhang, Ishihara, Shigemori, Hironaka, Johzaki, Sunahara, Yamamoto, Nakashima, Watanabe, Shiraga, Nishimura, and Azechi. Kilotesla Magnetic Field due to a Capacitor-Coil Target Driven by High Power Laser. 2013. SCIENTIFIC REPORTS. 3.

10. Rasmus, A., A. Stier, K. A. Flippo, H. Li, S. T. Li, and C. Mielke. Direct Faraday Measurements of a Laser-Driven Field Coil. Phys. Rev. Lett (in prep).

11. Li, H., S. T. Li, A. Rasmus, A. Stier, and K. A. Flippo. Design of a Laser-Driven Turbulent Magnetic Dynamo. Nature Physics (in prep).

Publications

Li, H., S. T. Li, A. Rasmus, A. Stier, and K. A. Flippo. Design of a Laser-Driven Turbulent Magnetic Dynamo. Nature Physics (in prep).

Rasmus, A., A. Stier, K. A. Flippo, H. Li, S. T. Li, and C. Mielke. Direct Faraday Measurements of a Laser-Driven Field Coil. Phys. Rev. Lett (in prep).

Theoretical Investigation of Nucleon and Nuclear Structure at Very High Energies

Zhongbo Kang
20130783PRD2

Introduction

The theoretical study and experimental exploration of the internal structure of nucleons (protons and neutrons) and nuclei are of fundamental importance to science and have recently entered a new exciting phase. In the past decades an understanding of nucleons in terms of quarks and gluons (partons) has successfully emerged. Progress has been made in constructing a "one-dimensional" picture of the nucleon, in the sense that we "only" know about the longitudinal motion of partons in fast moving protons and neutrons. However, the parton's motion that is perpendicular (transverse) to the proton momentum is still largely unknown and urgently needed in order to construct the 3-dimensional image of the proton. Since the transverse momentum component is usually much smaller than parton's longitudinal component, it is critical to develop accurate theoretical tools to extract this information. We propose two unique ways to attack this problem. One is through the transverse spin dependence of experimental observables, as transverse spin can correlate with the parton transverse momentum. The other way is through a discovery of a novel nuclear dependence, as the small transverse motion can be amplified by the nuclear size. We will develop the first solid theoretical framework that can utilize both methods to pinpoint the partons' transverse motion in both the proton and the big nucleus.

Benefit to National Security Missions

This project ties directly into the Laboratory mission in scientific innovation and discovery. Understanding the structure of the nucleon is central to the nuclear physics component of the National Science Foundation (NSF) and Department of Energy (DOE) Office of Science portfolios. Specifically, this project will provide new and unique 3 dimensional imaging information for the nucleon structure at the ~20% level. It will also give essential insights into how the quark and gluon dynamics are modified in a large nucleus. It will produce theoretical tools for the community to accurately and reliably extract such information from data collected in the US and abroad. It also provides much-needed theoretical guidance for and interpretation of the experimental results from the flagship nuclear physics program in US and abroad. This project will also help firm the scientific case for a future Electron Ion Collider.

Progress

In FY15 we made significant progress toward the ultimate goal of this project. We have written 9 papers, with six published already: one in Physical Review Letters, two in Physics Letters B, two in Physical Review D, and one in Nuclear Physics A. The rest three are submitted to Physical Review D, and we expect them to be published soon. We have delivered four invited talks at the international conferences. We have also helped organize three workshops, with Dr. Kang being the co-chair for QCD Evolution Workshop 2015, in which our research direction is one of the hot topics discussed. Dr. Kang has also been invited to give six one-hour lectures in the HUGS 2015 Summer School organized by Jefferson Lab, with the lecture topic on "QCD Structure of the Nucleon and Spin Physics'' -- one of the major research direction of our project.

In studying parton's transverse motion in the nucleon, most of the efforts in the community have been focused on quark transverse momentum, while gluon's transverse motion has to be further explored. With this in mind, in FY15 we investigated for the first time the role of gluons in generating the single transverse spin asymmetry. In this study, we understood better how the gluon's transverse momentum is correlated with the proton's transverse spin. We derived the next-to-leading order transverse momentum-weighted Sivers asymmetry in semi-inclusive deep inelastic scattering (SIDIS) - specifically contributions from the so-called three-gluon correlation functions. Such a study provides a way to connect the quark and gluon's transverse motion through the Quantum Chromodynamics (QCD) evolution

of the relevant quark-gluon and three-gluon correlation functions.

To further test QCD evolution and understand the spin correlation in the fragmentation process, In FY15 we performed global analysis of Collins spin asymmetry measured in both SIDIS at HERMES, COMPASS, and Jefferson Lab, as well as the e+ + e- experiments at BaBar and Belle. In this work we extracted the so-called quark transversity distribution and the Collins fragmentation function, both with proper QCD evolution taken into account.

In studying the parton's transverse motion in heavy nuclei, in FY15 we concentrate on the role of parton multiple scattering in various physical observables in p+A and e+A collisions. For example, we investigated the heavy meson production in p+A collisions at backward rapidity region, and found the parton multiple scattering in this region is mostly incoherent and led to the interesting nuclear enhancement compared to p+p collisions. Our predictions turned out to be consistent with experimental observations at both RHIC and LHC. We further extended such a study to e+A collisions, in which we performed a next-to-leading order computation of nuclear transverse momentum broadening for single hadron production in SIDIS.

Future Work

In FY16, we will continue to study the role of gluons in generating the spin asymmetries. In particular, we will generalize our current study on three-gluon correlation functions to Drell-Yan production and a color neutral scalar (for example the Higgs) production in transversely polarized proton-proton collisions. From this study, we will identify the complete Quantum Chromodynamics (QCD) evolution equations for both quark-gluon and three-gluon correlation functions. At the same time, we will study the QCD evolution in other important spin observables, such as the Boer-Mulders function in Drell-Yan production.

To further our understanding of parton multiple scattering, in FY16 we plan to concentrate on the so-called small-x region. In this region the parton's longitudinal momentum fraction is small and, thus, the transverse momentum component becomes the dominant degree of freedom. Furthermore, a new kind of divergence - so-called rapidity divergence - appears, which leads to the well-known small-x evolution of parton densities. We plan to use the newly developed rapidity regulator technique to regularize and isolate such a divergence, and perform the calculation for the cross sections of virtual/real photon and jet production to the next-to-leading order. The experimental data will be available in the near future from both RHIC and LHC. We will compare our theoretical formalisms with the experimental data, and extract the so-called unintegrated gluon distribution in the large nucleus, which contains important information on parton's transverse motion.

Conclusion

We will develop a new consistent theoretical formalism for evaluating the cross sections in polarized reactions with protons and nuclei. We will also investigate the novel nuclear dependence of experimental spin observables in both electron-nucleus and proton-nucleus collisions. We will use these theoretical formalisms to interpret the experimental data collected at the major experimental facilities in the US and abroad and extract the valuable information on the parton's transverse motion. This will provide unique 3-dimensional imaging information for the proton and nuclear structure at high energies.

Publications

Aschenauer, E. C., A. Bazilevsky, K. Boyle , R. Fatemi , C. Gagliardi, M. Grosse-Perdekamp, Z. B. Kang, Y. Kovchegov, and J. Lajoie. The RHIC Spin Program: Achievements and Future Opportunities . 2013. White Paper on RHIC spin physics to the Tribble Panel and Nuclear Science Advisory Committee.

Dai, L. Y., Z. B. Kang, A. Prokudin, and I. Vitev. Next-to-leading order transverse momentum-weighted Sivers asymmetry in semi-inclusive deep inelastic scattering: the role of the three-gluon correlator. PHYSICAL REVIEW D.

Echevarria, M. G., A. Idilbi, Z. B. Kang, and I. Vitev. QCD Evolution of the Sivers Asymmetry. 2014. PHYSICAL REVIEW D. 89: 074013.

Gamberg, L., Z. B. Kang, A. Metz, D. Pitonyak, and A. Prokudin. Left-right spin asymmetry in ℓN↑→hX. 2014. PHYSICAL REVIEW D. 90 (7): 074012.

Gamberg, L., Z. B. Kang, I. Vitev, and H. Xing. Quasi-parton distribution functions: a study in the diquark spectator model. 2015. PHYSICS LETTERS B. 743: 112.

Gamberg, L., Z. B. Kang, and A. Prokudin. Indication on the process-dependence of the Sivers effect. 2013. Physical Review Letters. 110 (23): 232301.

Gamberg, L., and Z. B. Kang. Single transverse spin asymmetry of prompt photon production. 2012. Physics Letters B. 718 (1): 181.

Huang, J., Z. B. Kang, and I. Vitev. Inclusive b-jet production in heavy ion collisions at the LHC . 2013. PHYSICS LETTERS B. 726: 251.

Kang, Z. B.. QCD and RHIC spin physics. Invited presentation at 2012 Fall Meeting of the APS Division of Nuclear Physics. (Newport Beach, CA, 24-27 Oct. 2012).

Kang, Z. B.. Polarized p+A, single spin asymmetries. Invited presentation at BNL-LANL-RBRC Joint Workshop on The Physics of p+A Collisions at RHIC. (Upton, NY, 7-9 Jan. 2013).

Kang, Z. B.. Single transverse spin asymmetries in polarized SIDIS and pp scattering. Invited presentation at The 5th Workshop of the APS Topical Group on Hadronic Physics. (Denver, CO, 10-12 Apr. 2013).

Kang, Z. B.. Forward physics from a theoretical perspective. Invited presentation at STAR Meeting on eSTAR Letter of Intent, Forward-Upgrades and Results from U+U Collisions. (Los Angeles, CA, 28-30 Aug. 2013).

Kang, Z. B.. Double parton fragmentation function and its evolution in quarkonium production . 2014. In QCD Evolution 2013. (Newport News, VA, 6-10 May 2014). Vol. 25, p. 1460040 . Singapore: International Journal of Modern Physics.

Kang, Z. B.. Unique opportunities in p+A collisions at RHIC and LHC. Invited presentation at APS Division of Nuclear Physics 2014 Long-range plan: Joint Town Meetings on QCD. (Philadelphia, PA, 13-15 Sept. 2014).

Kang, Z. B.. Nucleon spin: longitudinal, transverse, and evolution. Invited presentation at 2014 RHIC and AGS Annual Users Meeting. (Upton, NY, 17-20 June 2014).

Kang, Z. B.. TMD evolution of Sivers asymmetry. Invited presentation at Studies of 3D Structure of Nucleon. (Seattle, WA, 24-28 Feb. 2014).

Kang, Z. B.. QCD evolution of TMDs: what works?. Invited presentation at Indiana-Illinois Workshop on Fragmentation Functions. (Bloomington, IN, 12-14 Dec. 2013).

Kang, Z. B.. TMDs: Mechanisms/universality with ep and pp collisions. Invited presentation at QCD Frontier 2013. (Newport News, VA, 21-22 Oct. 2014).

Kang, Z. B.. TMD evolution and global analysis. Invited presentation at The 6th Workshop of the APS Topical Group on Hadronic Physics. (Baltimore, MD, 8-10 April 2015).

Kang, Z. B., A. Prokudin, P. Sun, and F. Yuan. Nucleon tensor charge from Collins azimuthal asymmetry measurements . 2015. PHYSICAL REVIEW D. 91: 071501.

Kang, Z. B., A. Prokudin, P. Sun, and F. Yuan. Extraction of Quark Transversity Distribution and Collins Fragmentation Functions with QCD Evolution. PHYSICAL REVIEW D.

Kang, Z. B., E. Wang, X. N. Wang, and H. Xing. Next-to-Leading QCD Factorization for Semi-Inclusive Deep Inelastic Scattering at Twist-4 . 2014. Physical Review Letters. 112: 102001 .

Kang, Z. B., E. Wang, X. N. Wang, and H. Xing. Transverse momentum broadening in semi-inclusive deep inelastic scattering at next-to-leading order. PHYSICAL REVIEW D.

Kang, Z. B., I. Vitev, E. Wang, H. Xing, and C. Zhang. Multiple scattering effects on heavy meson production in p+A collisions at backward rapidity . 2015. PHYSICS LETTERS B. 740: 23.

Kang, Z. B., I. Vitev, and H. Xing. Transverse momentum-weighted Sivers asymmetry in semi-inclusive deep inelastic scattering at next-to-leading order. 2013. Physical Review D. 87 (3): 034024.

Kang, Z. B., I. Vitev, and H. Xing. Next-to-leading order forward hadron production in the small-x regime: the role of rapidity factorization . 2014. PHYSICAL REVIEW LETTERS. 113: 062002.

Kang, Z. B., I. Vitev, and H. Xing. Multiple scattering effects on inclusive particle production in the large-x regime . 2013. PHYSICAL REVIEW D. 88: 054010.

Kang, Z. B., I. Vitev, and H. Xing. Initial-state cold nuclear matter energy loss effects on inclusive jet production in p+A collisions at RHIC and LHC. PHYSICAL REVIEW C.

Kang, Z. B., R. Lashof-Regas, G. Ovanesyan, P. Saad, and I. Vitev. Jet quenching phenomenology from soft-collinear effective theory with Glauber gluons. 2015. PHYSICAL REVIEW LETTERS. 114 (9): 092002.

Kang, Z. B., S. Mantry, and J. W. Qiu. Probing nuclear dynamics in jet production with a global event shape . 2013. Probing nuclear dynamics in jet production with a global event shape . 88: 074020.

Kang, Z. B., X. Liu, and S. Mantry. The 1-Jettiness DIS event shape: NNLL + NLO results. 2014. PHYSICAL REVIEW D. 90: 014041.

Kang, Z. B., Y. Q. Ma, J. W. Qiu, and G. Sterman. Heavy Quarkonium Production at Collider Energies (I): Factorization and Evolution. 2014. PHYSICAL REVIEW D. 90: 034006.

Kang, Z. B., Y. Q. Ma, J. W. Qiu, and G. Sterman. Heavy Quarkonium Production at Collider Energies: Partonic Cross Section and Polarization . 2015. PHYSICAL REVIEW D. 91 (1): 014030.

Kang, Z. B., Y. Q. Ma, and R. Venugopalan. Quarkonium production in high energy proton-nucleus collisions: CGC meets NRQCD. 2014. Journal of High Energy Physics. 01: 056.

Kang, Z. B., and B. Xiao. Sivers asymmetry of Drell-Yan production in the small-x regime. 2013. Physical Review D. 87 (3): 034038.

Vitev, I.. Transv. Invited presentation at Transverse momentum-weighted Sivers asymmetry in semi-inclusive deep inelastic scattering at next-to-leading order. (Newport News, VA, 6-10 May 2013).

Investigating Properties of Quark-Gluon Plasma Using Jets and Heavy Quark Production at RHIC

Michael P. Mccumber
20140665PRD2

Introduction

Jets measurements feature prominently in the current set of Large Hadron Collider (LHC) results. Measurements at Relativistic Heavy Ion Collider (RHIC) will provide insight into properties of the Quark Gluon Plasma (QGP) under different physical conditions than can be explored with the LHC alone. The 400 person PHENIX collaboration is planning to propose the construction of a new $30M detector, sPHENIX, to DOE to provide a comprehensive set of jet measurements at RHIC and to prepare for the construction of an electron-ion collider (EIC). These physics goals are much beyond the original design capabilities of the PHENIX experiment, which was designed two decades earlier. To achieve these measurements, this LDRD-PRD project proposes to spearhead the development and construction of a new RHIC detector needed to bring a world-class experimental jet physics program to LANL. The new detector is crucial to the full exploration and understanding of the Quark-Gluon Plasma.

This LDRD-PRD project is focused on a new research area of Heavy Ion Physics (using particle jet production as a probe to study the properties of Quark-Gluon Plasma). We propose to lead the development of the future upgrade of the PHENIX detector, opening up a new research direction for LANL's Nuclear Physics Program, which will go beyond the current capabilities of the DOE-funded program. The current DOE-funded Heavy Ion Physics program in P-25 has focused on higher energy muon detection through a magnetic spectrometer at the forward angle, and using a silicon vertex detector to separate primary muon from secondary decays. Our work in this project will go beyond this limitation by initiating a new set of detector systems (sPHENIX) which is designed specifically for high energy jet measurement. Therefore, technical schemes and scientific goals of this LDRD-PRD project are beyond existing DOE funded non-LDRD projects.

Benefit to National Security Missions

This project is highly relevant LANL's Scientific Discovery and Innovation mission, in the area of Nuclear, Particle, Cosmology, and Astrophysics. Quantum Chromodynamics (QCD), the Standard Model theory governing the behavior of quarks and gluons, predicts that a new phase of matter is present in the relativistic collisions of large nuclei. Matter generated by these collisions is at such high temperature and density that quarks and gluons are no longer imprisoned in hadronic states, but are instead free to interact with one another directly, a state of matter known as Quark-Gluon Plasma (QGP). The new phase of matter is being actively studied at hadron collider facilities such as the Relativistic Heavy Ion Collider (RHIC) at Brookhaven National Laboratory and the Large Hadron Collider (LHC) at CERN. Research work on the understanding of properties of Quark-Gluon Plasma will also contribute and lead to new resources of nuclear energy in the next generations.

Progress

FY15 has been a crucial period for progressing the proposal for a new detector at RHIC, sPHENIX, toward reality. Mike has been a leading physicist defending and advancing this case. At the beginning of FY14 sPHENIX had gone through an initial positive science review by the Department of Energy (DOE) and a committee of experts. In preparation for a final review, Mike and a small team of collaborators created a conceptual design for charged particle tracking device capable of precision Upsilon reconstruction, a mission need raised during the earlier DOE review process. He also developed additional particle jet observable projections and assisted with the development of a particle-flow jet algorithm for sPHENIX. The result of these efforts was a much improved sPHENIX proposal document (arXiv:1501.06197). This new proposal was reviewed by the DOE committee in April 2015, during which Mike defended the estimations of jet backgrounds and rejection techniques, features of the sPHENIX that are key to its ultimate suc-

cess for measuring modified jets in the collisions of large nuclei. The DOE review committee subsequently endorsed the sPHENIX project stating the science case as "clear and convincing" and that sPHENIX would "answer [science questions] of great significance not only to QCD and heavy ion physics, but to the larger nuclear and particle physics communities." This represents a major milestone for the project allowing the technical design phase of the experiment to fully begin.

Mike has continued to defend the sPHENIX program in scientific conferences, presenting the case at the APS Division of Nuclear Physics meeting, the APS Hadron Topical Group meeting. He was invited this year to present on sPHENIX bottom-quark jet observables at the RHIC & AGS Users meeting. He's been invited to present the sPHENIX science case at the International Conference for New Frontiers in Physics in August 2015. These presentations have been invaluable in creating broad community support for the program and bringing in new collaborators on the sPHENIX project. This wide spread support was recognized during the US Nuclear Physics Long Range Planning process where the sPHENIX program was unanimously voted to be the future direction at the Hot QCD town hall meeting in Fall 2014.

Mike is continuing the planning effort for the charged particle tracking for sPHENIX by developing a much detailed technical design. He is pursuing support to ensure a tracking system to be constructed that can fully exploit the opportunities for heavy flavor jet identification at RHIC. Mike is also participating in the technical design of the hadronic calorimeter detectors of sPHENIX by joining in detector workshops such a one held at Georgia State in December 2014. Associations with facilities and experimenters through the LANL will result in radiation testing of SiPM prototypes for the sPHENIX program later this year. Other ongoing activities include the organization and formation of an sPHENIX collaboration and additional sPHENIX simulation workshops to complete the tools need for the technical design effort.

In February 2015 Mike completed a 3-year term as PHENIX physics working group convener on hard-scattering in heavy ion collisions. In his role as convener he organized weekly physics working group meetings, prepared PHENIX results for presentation at APS, JPS, DNP, Hard Probes, Quark Matter, and many other conferences, and shepherded many analyses into publication in PRC, PRD and PRL. He now serves as on the PHENIX speakers bureau, which is responsible for selecting the speakers to represent the collaboration at conferences. He also continues to support PHENIX data taking and was responsible for successfully expanding the PHENIX data acquisition system for the new pre-shower detector installed this year.

Impact on National Missions:

Mike's scientific research efforts in LANL's P-25 group have put LANL in the forefront as one of the world's leading group in the field of Experimental High Energy Nuclear Physics. The research direction that Mike is currently leading clearly opens up several new fronts and new opportunities for US's Nuclear Physics program of the DOE's Office of Science, and especially for LANL to play leading roles in nuclear physics for many years to come, especially in the proposed future sPHENIX upgrade project. LANL is very fortunate to have Mike as a contributing and productive employee.

Future Work

This LDRD-PRD project focuses on a new research area of Heavy Ion Physics (using particle jet production as a probe to study the properties of Quark-Gluon Plasma) and leading the development of the future upgrade of the PHENIX detector. Our research will open up new and exciting research directions for LANL's Nuclear Physics Program, which is already striving to move beyond the existing capabilities of the currently funded DOE program. The current DOE-funded Heavy Ion Physics program in P-25 has been focusing on higher energy muon detection through a magnetic spectrometer at the forward angle and using a silicon vertex detector to separate primary muon from secondary decayed muons. During FY15, our work on this project surpassed this limitation by initiating a new set of detector systems (sPHENIX) which is designed specifically for high energy jet measurement. During FY16, our work will focus on providing a more sophisticated physics simulation package for bottom and charge quark jet physics, and making iterations on details of the hadron calorimeter and charge particle tracking detector designs. Therefore, the technical schemes and scientific goals of this LDRD-PRD project enable us to push the research boundaries beyond the existing DOE-funded non-LDRD projects.

During the development of the sPHENIX design, the PHENIX experiment gathered interesting data during FY15. As a physics working group convener in PHENIX for hard scattering physics, Mike will direct ongoing analysis and publication of the new research directions on topics including modified jet fragmentation, heavy quark energy loss, and quarkonia production. This part of the research effort is not on the original PHENIX experiment's physics plan approved by DOE, therefore, Mike's research work will push the physics frontier of PHENIX experiment much beyond the DOE funded projects.

sPHENIX detector at RHIC: in FY16, we will provide leader-

ship of the detector research and development needed for the construction of a jet-focused experiment at Relativistic Heavy Ion Collider (RHIC) covering both mid- and forward-rapidity in preparation for an Electron-Ion Collider (EIC) detector.

Conclusion

A key piece of physics necessary to obtain in the desired data is the energy loss of massive quarks in the Quark-Gluon Plasma (QGP). Mike will take a leadership role in the first direct analysis of heavy quarks at forward rapidity using the Forward Vertex (FVTX) detector (a LANL-led DOE project) from the heavy ion data to be collected in 2014. This work presents a pivotal test of the models describing the interaction of fast moving quarks with the QGP and thus will prepare the field for the suite of measurements to come using the sPHENIX detector.

Publications

Adare, A. M., M. P. McCumber, J. L. Nagle, and Romatschke. Examination whether heavy quarks carry information on the early-time coupling of the quark-gluon plasma. 2014. PHYSICAL REVIEW C. 90 (2).

McCumber, M.. PHENIX Future Plans and Prospects. To appear in International Conference on New Frontiers in Physics 2015. (Kolymbari, Greece, 23-30 Aug. 2015).

McCumber, M.. Future b-jet Measurements with sPHENIX. Invited presentation at RHIC and AGS Users Meeting 2015. (Upton, New York, 9-12 Aug. 2015).

McCumber, M.. Updated Jet Performance and Algorithm Approaches. Invited presentation at sPHENIX Department of Energy Science Review. (Upton, New York, 30 April 2015).

McCumber, M.. An Opportunity for Forward Jet Single Spin Asymmetry Measurements at RHIC. Presented at 6th Workshop on APS Topical Group on Hadron Physics. (Baltimore, Maryland, 8-10 April 2015).

McCumber, M.. fsPHENIX: Forward Jet and Drell-Yan Single Spin Asymmetries at RHIC. Presented at Joint Nuclear Physics Division Meeting of the APS and JPS. (Waikoloa, Hawaii, 7-10 Oct. 2014).

McCumber, M.. sPHENIX: An Upgrade Proposal from the PHENIX Collaboration. 2015. arXiv:1501.06197.

McCumber, M. P.. Back-to-back pair suppression at large transverse momentum in root s(NN)=200 GeV Au + Au collisions at PHENIX. 2011. NUCLEAR PHYSICS A. 855 (1): 408.

McCumber, M. P.. High p(T): Energy Loss Physics at PHENIX. 2013. NUCLEAR PHYSICS A. 904: 154C.

McCumber, M. P.. High p(T): Energy Loss Physics at PHENIX. 2013. NUCLEAR PHYSICS A. 904: 154C.

Nagle, J. L., Adare, Beckman, Koblesky, J. O. Koop, McGlinchey, Romatschke, Carlson, J. E. Lynn, and McCumber. Exploiting Intrinsic Triangular Geometry in Relativistic He-3 + Au Collisions to Disentangle Medium Properties. 2014. PHYSICAL REVIEW LETTERS. 113 (11).

New Tools to Probe Matter with an Electron-Ion Collider

Christopher Lee
20140671PRD2

Introduction

Protons and neutrons (hadrons) were once thought to be indivisible elementary constituents of ordinary matter. One of the greatest discoveries of the 20th Century, through electron-proton collisions, was that hadrons themselves are made of smaller "quarks." We also discovered that quarks are bound together by gluons, which transmit the force called the strong interaction. Now in the 21st Century, the focus of US nuclear physics is to map out the structure of this dynamic system in unprecedented detail at a new Electron Ion Collider (EIC), which will collide high-energy electrons and protons to probe their internal structure. Crucial measurements will include the strength of the interaction between quarks and gluons, called the strong coupling, and the 3-D momentum distribution of all the different kinds of quarks and gluons within the proton. One treasure trove of information in EIC collisions will be hadronic jets, collimated bunches of strongly interacting particles produced by the collisions. In the last decade, a powerful theoretical tool called soft-collinear effective theory (SCET) has led to unprecedentedly precise predictions for jet production, including determination of the strong coupling to incredible precision < 1% in electron-positron collisions. However, the value extracted this way disagrees with numerical simulations of strong interactions by more than three standard deviations, a puzzle urgently demanding resolution.

We will push the frontier of precision jet physics at the EIC using SCET. Together with the EIC, a concomitant effort to improve accuracy of theoretical predictions is essential. Our preliminary work on 2-jet production in electron-proton collisions has led to new methods to compute jet cross sections to any desired accuracy. We will use this power to compute EIC jet cross sections to the highest precision to date, allowing us to use future EIC data to resolve the existing discrepancies in determining the strong coupling.

Benefit to National Security Missions

The proposed research is directly aligned with LANL and national priorities in physics at a future electron-ion collider (EIC), a machine that would probe the structure of the proton and the nature of the strong interaction in unprecedented detail. The proton is a ubiquitous component of all ordinary matter in the universe, and the strong interaction is what binds the constituents of the proton (quarks and gluons) together and protons and neutrons to each other in nuclei. Understanding protons and the strong interaction is key to our fundamental understanding of Nature. Central to this proposal are development and application of Soft Collinear Effective Theory (SCET) to provide the high precision predictions necessary to interpret the unprecedentedly detailed data on nucleon structure that will come from EIC. The proposed calculations will allow us to use EIC data to resolve current disagreements in measurements of the strong coupling, a fundamental constant affecting all studies of nuclear matter (e.g. LHC, RHIC). EIC physics and SCET are high priorities under the LANL Nuclear & Particle Futures Pillar, under the research thrust "Advancing our understanding of QCD and the fundamental properties of nuclear matter." The 2007 NSAC Long-Range Plan for DOE identifies this research as highest priority: "The EIC embodies the vision of our field for reaching the next QCD frontier," further emphasizing, "It is essential that theoretical support for EIC-related physics is maintained at a healthy level." The proposed research will strengthen LANL and US leadership in this exciting international endeavor.

Progress

In November, together with Iain Stewart at MIT, Daekyoung and I published a paper in the Journal of High-Energy Physics on "Analytic Calculation of 1-Jettiness in DIS at O(alpha_s)" (JHEP 1411, 132) on the fixed-order computation in Quantum Chromodynamics (QCD) of the 1-jettiness distribution in Deep Inelastic Scattering (DIS) to first order in the strong coupling constant alpha_s).

This enables a more precise prediction of the 1-jettiness (tau_1) distribution at large values of tau_1, where fixed-order perturbation theory is more important that resummed perturbation theory. This is an important step towards predicting DIS jet cross sections to a precision sufficient to perform percent-level extractions of alpha_s from experimental measurements.

In April, together with PhD student O. Labun at Arizona, Daekyoung and I completed a paper preprint submitted to arXiv (1504.04006) which is being accepted by Physics Letters B for publication on "Equality of hemisphere soft functions for e+e-, DIS, and pp collisions at O(alpha_s^2)" on two-loop, or second order in the strong coupling alpha_s, soft functions that contribute to event shape distributions in the three types of collisions. These functions describe the effect of soft gluon radiation on jet cross sections in these collisions and are an essential ingredient to achieve next-to-next-to-leading logarithmic (NNLL) and NNNLL accuracy in resummed perturbation theory for event shape distributions. Since the e+e- (electron-positron) 2-loop soft function was already known, our proof of equality of the e+e-, DIS, and pp (proton-proton) soft functions immediately fills our previous gap in knowledge of the soft functions for DIS and pp.

Future Work

We plan to predict cross sections in Deep Inelastic Scattering (DIS) of electrons and protons, differential in one of several event shape variables known as "N-jettiness". These measure the degree of collimation of final state hadrons into N energetic "jets" in addition to radiation along the beam direction.

We will use our results obtained in the last fiscal year on two-loop soft functions together with progress in the literature on two-loop beam functions to complete our prediction of DIS 1-jettiness cross sections to unprecedented next-to-next-to-next-to-leading logarithmic (NNNLL) accuracy in resummed perturbation theory in Quantum Chromodynamics (QCD), a calculation which is already well under way. We will also compute numerically the fixed-order part of the distributions to two-loop order, going beyond the one-loop results we obtained last year.

We plan to explore generalization of our proof of equality of two-loop soft functions in electron-positron (e+e-) collisions, DIS, and proton-proton (pp) collisions to three loop order. We will also pursue the computation of multi-jet cross sections with N > 1.

With all these predictions in hand, we will begin to determine the best strategy to apply them to the extraction of the strong coupling at an Electron Ion Collider (EIC).

In parallel with the main thrust of his work on QCD predictions for EIC physics, Daekyoung is also pursuing applications of effective field theory to the physics of bound states in systems of particles with large scattering length, in particular in applications to dark matter physics. Daekyoung is seeking to answer the question of whether bound state effects need to be accounted for in dark matter detection experiments. This work is outside the direct scope of this proposal, but constitutes a broader, high-impact application of similar effective field theory methods used in both parts of Daekyoung's research.

Conclusion

The goals of this project include predicting cross sections to produce two hadronic jets at EIC to the highest precision to date, and so reduce theoretical uncertainty by up to an order of magnitude, and then to predict multi-jet production in EIC collisions, which exhibit even greater sensitivity to the strong coupling, alpha_s. These results will make possible the most precise extractions of alpha_s from DIS data and shed light on the current tension among different methods of extraction. alpha_s is a fundamental constant of nature and affects all predictions at colliders involving the strong interaction.

Publications

Kang, D.. DIS Event Shapes at N3LL. Invited presentation at DIS 2015: XXIII International Workshop on Deep-Inelastic Scattering and Related Subjects. (Dallas, TX, 27 Apr - 1 May 2015).

Kang, D., C. Lee, and I. W. Stewart. Analytic Calculation of 1-Jettiness in DIS at O(alpha_s). 2014. Journal of High-Energy Physics. 11: 132.

Kang, D., O. Z. Labun, and C. Lee. Equality of hemisphere soft functions for e+e−, DIS and pp collisions at O(alpha_s^2). Physics Letters B. 748.

Electric Dipole Moments of Hadrons from Lattice Quantum ChromoDynamics

Vincenzo Cirigliano
20140673PRD2

Introduction

The "Standard Models" of elementary particles and cosmology cannot account for a number of key features of our observed universe. Among these, most prominently the two standard models do not account for the excess of matter over antimatter in the universe (i.e. why there are stars and stardust instead of just radiation, i.e. photons).

An important clue towards the resolution of this puzzle would arise by the discovery and characterization of new physics that violates the symmetry exchanging particles and antiparticles (known as CP). A spectacular manifestation of this symmetry breakdown would be the existence of a permanent Electric Dipole Moment (EDM), i.e. a deviation from spherical symmetry, in certain atomic nuclei and their constituents, proton and neutron.

The overall goal of this theoretical project is to quantitatively improve the relation between the observation (or non observation) of a nuclear EDM and the mechanism and size of CP symmetry breakdown. The symmetry breakdown happens at the level of elementary constituents of neutron and proton, called quarks, that interact with each other very strongly. Therefore, in order to learn anything from EDM searches, one needs to perform complex calculations of how CP symmetry breaking interactions alter the neutron, proton, and their interactions in nuclei. We propose to perform such calculations using the only first-principle and improvable approach to deal with the theory of quark strong interactions, known as "lattice Quantum ChromoDynamics (QCD)". The key observation at the basis of this project is that the properties of QCD simplify the task of calculating these CP-breaking interactions by relating them to shifts in the masses of neutron and proton, that are relatively simpler to calculate. Our calculation will reach a precision of 20-30%, a considerable improvement over the current order-of-magnitude (factor of ten) uncertainties.

Benefit to National Security Missions

The experimental search for Electric Dipole Moments of the neutron and light nuclei is a recognized priority of the DOE/SC Office of Nuclear Physics. This theoretical project will elucidate the relationship between the experimental findings and the underlying interactions that break the so-called CP-symmetry, i.e. the symmetry that interchanges matter and antimatter. The relation between experimental results and underlying sources of CP-violation is characterized by a handful of coefficients (matrix elements), that are currently uncertain at the order-of magnitude level. Our theoretical calculations will reduce the current uncertainty to the level of 20-30%, thus greatly sharpening the interpretation of current experimental searches, in which DOE/SC is making considerable investments.

Progress

Electric dipole moments (EDMs) of elementary particles are an extremely sensitive probe of violation of time-reversal (T), or, equivalently, of the product of charge conjugation and parity (CP) beyond the Standard Model. An observation of an EDM in the next generation of experiments will be a clear indication of new physics, due either to a minute value of the QCD $\bar\theta$ angle, or to new particles and interactions appearing at very high scales, much larger than the electroweak scale. However, the interpretation of results of EDM experiments, and the connection to complementary probes at collider experiments, is hampered by the poor knowledge of the matrix elements of CP-odd operators between nucleon, and nucleon and pion states.

In the past year, this project has focused on improving the tools for the determination of these nucleon matrix elements. Their calculation from first principles involves physics at a scale at which QCD becomes strongly coupled, and is an inherently non-perturbative problem. Lattice QCD currently offers the most promising opportunity to perform systematically improvable evaluations

of the matrix elements. Operators induced by physics beyond the Standard Model (BSM), like the quark electric and chromo-electric dipole moments, are also starting to receive attention, with important contributions from the LANL lattice group. In order to make contact with phenomenology, and with possible manifestations of the effects of CP-odd operators at high energy, it is necessary to convert any results of lattice simulations to the same scheme that is used in perturbative calculations. This is a non-trivial task, which requires the definition of a renormalization scheme which can be implemented both in numerical lattice simulations, and in perturbation theory. We defined such a scheme, and studied the mixing and renormalization of flavor-diagonal dimension-5 T- and P-odd operators involving quarks, gluons, and photons, including quark electric dipole (qEDM) and chromo-electric dipole operators (qCEDM). Once the lattice matrix elements will become available, our result will immediately allow to bridge the gap between lattice and phenomenology. The results of this investigation have appeared as a preprint.

For systems more complicated than the nucleon, like deuteron, 3-He, or 199-Hg, a very important role is played by another class of couplings, T-odd pion-nucleon couplings, which mediate long-range T-violating nucleon-nucleon interactions. In this case, a direct lattice QCD calculation is more difficult, and has not been attempted yet. However, in many interesting cases the approximate symmetry of QCD under chiral transformations allows to relate the T-odd pion-nucleon couplings to modifications of the meson and baryon spectrum induced by the CP-even chiral partners of CP-odd operators. For example, the isoscalar T-odd coupling induced by the QCD theta term is related to the proton-neutron mass difference induced by the quark mass splitting. Lattice QCD is extremely well suited for the calculation of spectroscopic properties of meson and baryons, and indeed available lattice evaluations of the mass splitting allow to extract the pion-nucleon coupling with 10% uncertainties. Similar relations can be derived for the qCEDM, and offer a very promising route to determine couplings that at the moment are known with very large uncertainties. The relations between baryon spectrum and pion-nucleon couplings have been proven at leading order in the chiral expansion. With collaborators, we have started an investigation on the robustness of these relations, including subleading corrections in Chiral Perturbation Theory, the effects of the strange quark and of the decuplet baryons. We just completed the analysis for the QCD theta-term, in which case we showed that the corrections are small, and the relation robust. Next, we plan to extend our discussion to the qCEDM. The results have appeared in a preprint.

Future Work

In the next fiscal year, we plan to complete some of the steps that are necessary to express the pion-nucleon couplings induced by the qCEDM in terms of the coefficients of these operators at high energy. Currently, the lattice group at JLAB is pursuing the evaluation of the corrections to the nucleon and Goldstone boson masses induced by the quark chromo-magnetic dipole moment (qCMDM), the chiral partner of the qCEDM. In order to use these results, the careful definition of a renormalization scheme that does not violate the chiral Ward identity relating chromo-electric and chromo-magnetic operators is necessary, and this requires the extension of our recent work to include dimension-5 CP-even operators. In addition, it is extremely important to assess the robustness of the relation between spectroscopy and T-odd couplings in the case of the qCEDM,

Another interesting direction that we intend to pursue is the investigation of the complementarity of new physics searches at collider and low energy experiments. The CP-violating operators that induce EDMs at low energy also modify the interactions of the Higgs, Z and W bosons, in a way that can be directly tested at colliders. We have started to compare the bounds on CP-odd operators from EDMs to bounds coming from the Higgs and vector bosons production cross sections measured at the LHC. We plan to complete our analysis in the next few months, and to determine for which class of operators EDM and collider bounds are competitive, and how they can be improved in the next LHC runs.

Conclusion

In the next few years, several experiments with strong LANL involvement will significantly improve the sensitivity to Electric Dipole Moments (EDM) of the neutron and nuclei, and, hopefully, discover new physics. Our results will be essential in order to relate the experimental results to the underlying sources of charge conjugation and parity (CP) symmetry breaking (CP is the symmetry that relates matter and antimatter). This will allow a more robust interpretation of EDM signals, and a more direct connection to BSM models, with impacts in the fields of nuclear physics, particle physics, and cosmology.

Publications

Chien, Y. T., V. Cirigliano, W. Dekens, J. de Vries, and E. Mereghetti. Direct and indirect constraints on CP-violating Higgs-quark and Higgs-gluon interactions. Journal of High Energy Physics.

Vries, J. de, E. Mereghetti, and A. Walker-Loud. Baryon mass splittings and strong CP violation in SU(3) Chiral Perturbation Theory. 2015. Physical Review C. 92: 4.

Multi-wavelength Studies of Explosive Astrophysical Transients

Przemyslaw R. Wozniak
20140674PRD3

Introduction

High energy transients producing photons in the GeV-TeV energy range represent a largely unexplored phase space in transient phenomena. To study these extreme phenomena one needs a sensitive (large) detector, wide field-of-view and near continuous operations such as the High Altitude Water Cherenkov (HAWC) observatory. Astrophysical transients such as gamma-ray Bursts (GRBs), Active Galactic Nuclei (AGN), or high-mass X-ray binaries can emit across the entire electromagnetic spectrum from radio to high-energy gamma rays.

Rapid multi-wavelength observations are key to understanding the underlying mechanisms of particle acceleration and localizing emission regions. Swift is the only X-ray observatory that can respond quickly enough to HAWC transients and cover the HAWC error box to observe any contemporaneous lower-energy counterparts before they fade away. RAPTOR telescopes at LANL are uniquely equipped to rapidly (< 6 sec) cover the HAWC error box in the optical and catch the associated afterglow emission. Our approach is to automatically alert the most significant transients detected by RAPTOR, Swift, or HAWC, and immediately follow them up. For this purpose we will utilize our approved Swift Guest Investigator Target of Opportunity program and the RAPTOR network. The fast slewing capability of RAPTOR will enable follow-up of sub-threshold triggers from HAWC. In the case of a detection, we will use Swift to perform additional observations in X-rays.

To accomplish these goals we will develop new software and the instrument networking framework for real-time correlations of data arriving simultaneously from multiple instruments. Another important advance will be new transient search and classification algorithms for massive time-domain sky surveys such as the Palomar Transient Factory (PTF) and the Large Synoptic Survey Telescope (LSST). In the future, this technology will enable similar studies on much larger data sets.

Benefit to National Security Missions

Tilan Ukwatta will perform research to establish the origin of very high-energy photons in γ-ray bursts and explain the broad-band spectra of explosive astrophysical transients. To accomplish these goals, he will cross-correlate real-time data streams from the RAPTOR telescopes at LANL with data from the Swift satellite and HAWC (High Altitude Water Cherenkov) detector. For this purpose Tilan will utilize and extend LANL's unique capabilities in the area of telescope networking and continuous sky monitoring. He will also develop new transient search and classification algorithms and software for massive time-domain sky surveys.

This research is well aligned with the long-term vision for Global Security and Threat Identification and Response to develop cutting edge Information Science and Technology capability for national security. This include real-time, multi-source data fusion tools which have long-term implications for nuclear nonproliferation and other intelligence, surveillance, and reconnaissance missions, and wide-field sensor approaches relevant to space situational awareness.

Progress

In the first year of the project we developed a transient management system for High Altitude Water Cherenkov (HAWC) observatory that accepts gamma-ray burst (GRB) alert notices and sends them to the online data analysis system. The system stores GRB alerts and filters GRBs observable by HAWC. It also tracks transient search results from HAWC. This system provides an easy to use web interface allowing observers to view and respond to HAWC transients. HAWC started full detector operations in March 2015 and is in the process of verifying proper detector operations and data quality. HAWC transient searches have begun collecting transient alerts and we are developing real time alert distribution system for HAWC and RAPTOR based on live network socket connections implemented using zeromq software library.

Tilan Ukwatta is leading a research group investigating physical properties of evaporating primordial black holes (PBH). The group includes two high energy theorists, statistician, a postdoc and a graduate student (Michigan State University and University of North Florida). The main result in the past year is a detailed study of the sensitivity of HAWC to detect high-energy bursts from PBHs and new methods that can be used to detect those exotic transients. We have already published one paper in Astroparticle Physics journal titled "Milagro limits and HAWC sensitivity for the rate-density of evaporating Primordial Black Holes" (LA-UR-15-20829) and another paper is "Observational Characteristics of Evaporating Primordial Black Holes" (LA-UR-15-23058) is almost ready to be submitted for publication. In addition, we have presented our work at the "5th Fermi Symposium" and American Physical Society Meetings. We will also present our work at the 34th International Cosmic Ray Conference in July 2015.

We developed supernova.lanl.gov, an online database of time-resolved spectra and multi-color light curves from simulations of supernova explosions. This system allows users to compare their supernova data with supernova explosion models developed by the LANL supernova theory group. System has ability to analyze both spectra and light curves obtained with a variety of broad-band filters commonly used by modern sky surveys.

Tilan Ukwatta began a new collaboration with Kevin Hurley from University of California, Berkeley to develop a novel method to constrain distances of gamma-ray bursts (GRBs) using multi-satellite triangulation with the Interplanetary Network (IPN). So far we have constrained the minimum distances of 49 short duration GRBs that could in fact be PBH bursts. Our results indicate that using this technique we can set upper limits on the rate of PBH that are two orders of magnitude better than the current best limit. A corresponding paper titled "Investigation of Primordial Black Hole Evaporation Rates from a Sample of Interplanetary Network GRBs" will be submitted to the Astrophysical Journal in the following weeks.

A paper on redshift and duration dependent clustering in the GRB sky distribution is in the final stages. This investigation found that previous claims of clustering at redshift $z \sim 2$ are most likely due to statistical fluctuations and not a physical overdensity. However, we found more evidence for clustering of very short GRBs with duration less than 100 milliseconds. The title of the paper is "Investigation of Redshift and duration Dependent Clustering in the Gamma-ray Burst Sky Distribution" (LA-UR-15-24559) and we are planning to publish it in the Monthly Notices of the Royal Astronomical Society (MNRAS) journal.

We are developing machine learning techniques to identify high-redshift (or high-z) GRBs using promptly available multi-wavelength data from the Swift observatory. This work includes both classification and regression and in the accompanying paper we introduces the new term "machine-z" which is the redshift derived from machine learning techniques to complement two other redshift measurements: photo-z and spectroscopic z measurements. Unlike the alternative methods, our algorithm is capable of catching almost all high-z GRBs on average with limited follow-up resources.

Tilan Ukwatta is working with Intermediate Palomar Transient Factory (iPTF) team to discover and study supernovae. He already discovered three supernovae as a scanner. Tilan also performs regular shift duty as the Swift "Burst Advocate (BA)" and Swift "Burst Alert Telescope (BAT) Burst Scientist (BBS)".

For his work Tilan Ukwatta received The HAWC Excellence Award with the citation "Awarded in recognition of exceptional and sustained contributions to HAWC Remote Monitoring".

Future Work

The main goal for the project is to develop a preliminary version of the framework to cross-correlate transient events from RAPTOR, Swift, and HAWC. Triggering criteria for Target of Opportunity (ToO) observations of HAWC events must be designed, coded, and integrated with event messaging and database systems. New data ingest and event translation routines must be developed for anticipated transient events from all three instruments. We plan to perform cross-correlations of data streams from RAPTOR, Swift, and HAWC to provide enough triggers for executing ToO Swift observations. We will also develop a software pipeline to perform a blind search for intermediate duration HAWC transients lasting days to weeks.

Another goal is to perform iterative probabilistic classification of transients based on heterogeneous data such as time-resolved multi-color photometry, spectra, and possible X-ray/gamma-ray detections. We will develop a mathematical toolbox based on Bayesian networks that can go beyond classification problems constrained to a major class of transients such as Supernoave and instead handle a diverse set of transients.

Finally, we will model and interpret interesting transients observed over the course of the year. We will fit the observed light curves and time-resolved spectra with blast wave models to identify the relevant emission components and constrain their parameters. Using the relative strength and timing of those components we will constrain possible

emission sites and shock propagation scenarios.

We will finish developing and tuning our "machine-z" redshift (distance) estimator for gamma-ray bursts (GRBs). We plan to implement the technique in the Swift automated pipeline so machine-z values will be available to the GRB community for all GRBs newly discovered by the Swift satellite.

We will also search HAWC data for hypothetical TeV transients caused by Primordial Black Holes (PBH) that evaporate by Hawking radiation using techniques that we developed and published last year.

Conclusion

The overarching goal of this project is to perform state of the art real-time searches and joined follow-up campaigns of flaring GeV-TeV emitters using RAPTOR, Swift and HAWC instruments. For this purpose we must develop new software tools and the instrument networking framework for real-time cross-correlations of heterogeneous data streams. Our joined RAPTOR/Swift transient localizations and HAWC observations are likely to deliver the first ground-based detection of a GRB. Combined with follow-up studies and distance measurements, these observations will cover photon energies from eV to TeV, providing strong constraints on emission mechanisms that power these extraordinary objects.

Publications

Abdo, A. A., A. U. Abeysekara, Alfaro, B. T. Allen, Alvarez, J. D. Alvarez, Arceo, J. C. Arteaga-Velazquez, Aune, H. A. A. Solares, A. S. Barber, B. M. Baughman, Bautista-Elivar, J. B. Gonzalez, Belmont, S. Y. BenZvi, Berley, M. B. Rosales, Braun, R. A. Caballero-Lopez, K. S. Caballero-Mora, Carraminiana, Castillo, G. E. Christopher, Cotti, Cotzomi, De la Fuente, De Leon, DeYoung, R. D. Hernandez, K. L. Diaz-Cruz, J. C. Diaz-Velezi, B. L. Dingus, M. A. DuVernoisi, R. W. Ellsworth, D. W. Fiorinoi, Fraija, Galindo, Garfias, M. M. Gonzalez, J. A. Goodman, Grabski, Gussert, Hampel-Arias, J. P. Harding, Hays, C. M. Hoffman, C. M. Hui, Huintemeyer, Imrani, Iriarte, Kam, Kieda, B. E. Kolterman, Kunde, Lara, Lauer, W. H. Lee, Lennarz, H. L. Vargas, E. C. Linares, J. T. Linnemann, Longo, Luna-Garcla, J. H. MacGibbon, Marinelli, S. S. Marinelli, Martinez, Martinez, Martinez-Castro, J. A. J. Matthews, McEnery, E. M. Torres, A. I. Mincer, Miranda-Romagnoli, Moreno, Morgan, Mostafa, Nellen, Nemethy, Newbold, Noriega-Papaqui, Oceguera-Becerra, Patricelli, Pelayo, E. G. Perez-Perez, Pretz, Riviere, Rosa-Gonzalez, Ruiz-Velasco, Ryan, Salazar, Salesa, Sandoval, P. M. S. Parkinson, Schneider, Silich, Sinnis, A. J. Smith, Stump, K. S. Woodle, R. W. Springer, Taboada, P. A. Toale, Tollefson, Torres, T. N. Ukwatta, Vasileiou, Villasenor, Weisgarberi, Westerhoff, D. A. Williams, I. G. Wisher, Wood, G. B. Yodh, P. W. Younk, Zaborov, Zepeda, and Zhou. Milagro limits and HAWC sensitivity for the rate-density of evaporating Primordial Black Holes. 2015. ASTROPARTICLE PHYSICS. 64: 4.

Abeysekara, A. U., Alfaro, Alvarez, J. D. Alvarez, Angeles, Arceo, J. C. Arteaga-Velazquezd, Avila-Aroche, H. A. A. Solares, Badillo, A. S. Barber, B. M. Baughman, Bautista-Elivar, J. B. Gonzalez, Belmont, Benitez, S. Y. BenZvi, Berley, Bernal, M. B. Rosales, Braun, R. A. Caballero-Lopez, K. S. Caballero-More, Cabrera, Carraminana, Castaneda-Martinez, Castillo, Cotti, Cotzomi, de la Fuente, De Leon, DeYoung, Diaz-Azuara, Diaz-Cruz, R. D. Hernandez, J. C. Diaz-Velez, B. L. Dingus, Dultzin, M. A. DuVernois, R. W. Ellsworth, Fernandez, D. W. Fiorino, Fraija, Galindo, Garcia-Torales, Garfias, Gonzalez, L. X. Gonzalez, M. M. Gonzalez, J. A. Goodman, Grabski, Gussert, Guzman-Ceron, Hampel-Arias, J. P. Harding, Hernandez-Cervantes, C. M. Hui, Huentemeyer, Imran, Iriarte, Karn, Kieda, G. J. Kunde, Langarica, Lara, Lara, R. J. Lauer, W. H. Lee, Lennarz, H. L. Vargas, E. C. Linares, J. T. Linnemann, Longo, Luna-Garcia, Marinelli, L. A. Martinez, Martinez, Martinez, Martinez-Castro, Martos, J. A. J. Matthews, McEnery, E. M. Torres, Miranda-Romagnoli, Moreno, Mostafa, Nava, Nellen, Newbold, Noriega-Papaqui, Oceguera-Becerra, D. P. Page, Patricelli, Pelayo, E. G. Perez-Perez, Pretz, Ramirez, Renteria, Riviere, Rosa-Gonzalez, Ruiz-Sala, E. L. Ruiz-Velasco, Ryan, J. R. Sacahui, Salazar, Salesa, Sandoval, Santos, Schneider, Silich, Sinnis, A. J. Smith, K. S. Woodle, R. W. Springer, Suarez, Taboada, Tepe, P. A. Toale, Tollefson, Torres, Tinoco, T. N. Ukwatta, J. F. V. Galicia, Vanegas, Vazquez, Villasenor, Wall, Weisgarber, Westerhoff, I. G. Wisher, Wood, G. B. Yodh, P. W. Younk, Zaborov, Zepeda, and Zhou. VAMOS: A pathfinder for the HAWC gamma-ray observatory. 2015. ASTROPARTICLE PHYSICS. 62: 125.

Abeysekara, A. U., Alfaro, Alvarez, J. D. Alvarez, Arceo, J. C. Arteaga-Velazquez, H. A. A. Solares, A. S. Barber, B. M. Baughman, Bautista-Elivar, S. Y. BenZvi, Bonilla Rosales, Braun, K. S. Caballero-Mora, Carraminana, Castillo, Cotti, Cotzomi, de la Fuente, De Leon, DeYoung, Diaz Hernandez, B. L. Dingus, M. A. DuVernois, R. W. Ellsworth, D. W. Fiorino, Fraija, Galindo, Garfias, M. M. Gonzalez, J. A. Goodman, Gussert, Hampel-Arias, J. P. Harding, Huentemeyer, C. M. Hui, Imran, Iriarte, Karn, Kieda, G. J. Kunde, Lara, R. J. Lauer, W. H. Lee, Lennarz, Leon Vargas, J. T. Linnemann, Longo, Luna-Garcia, Malone, Marinelli, S. S. Marinelli, Martinez, Martinez, Martinez-Castro, J. A. J. Matthews, Mendoza Torres, Miranda-Romagnoli, Moreno, Mostafa, Nellen, Newbold, Noriega-Papaqui, T. O. Oceguera-Becerra, Patricelli, Pelayo, E. G. Perez-Perez, Pretz, Riviere, Rosa-Gonzalez, Salazar, F. S. Greus, Sandoval, Schneider, Sinnis, A. J. Smith, K. S. Woodle, R. W. Springer, Taboada, Tollefson, Torres, T. N. Ukwatta, Villasenor, Weisgarber, Westerhoff, I. G. Wisher, Wood, G. B. Yodh, P. W. Younk, Zaborov, Zepeda, and Zhou. SEARCH FOR GAMMA-RAYS FROM

THE UNUSUALLY BRIGHT GRB 130427A WITH THE HAWC GAMMA-RAY OBSERVATORY. 2015. ASTROPHYSICAL JOURNAL. 800 (2).

Sonbas, , G. A. MacLachlan, K. S. Dhuga, Veres, Shenoy, and T. N. Ukwatta. GAMMA-RAY BURSTS: TEMPORAL SCALES AND THE BULK LORENTZ FACTOR. 2015. ASTROPHYSICAL JOURNAL. 805 (2).

Ukwatta, T. N., D. Stump, J. H. MacGibbon, J. T. Linnemann, S. S. Marinelli, T. Yapici, and K. Tollefson. Observational Characteristics of the Final Stages of Evaporating Primordial Black Holes. To appear in The 34rd International Cosmic Ray Conference (ICRC2015) . (Hague, Netherlands, 30 Jul - 6 Aug 2015).

Ukwatta, T. N., D. Stump, J. H. MacGibbon, J. T. Linnemann, S. S. Marinelli, T. Yapici, and K. Tollefson. Sensitivity of HAWC to Primordial Black Hole Bursts. To appear in The 34rd International Cosmic Ray Conference (ICRC2015). (Hague, Netherlands, 30 Jul - 6 Aug 2015).

Ukwatta, T. N., D. Stump, J. T. Linnemann, J. H. MacGibbon, S. S. Marinelli, T. Yapici, and K. Tollefson. Primordial Black Holes: Observational Characteristics of The Final Evaporation. Astroparticle Physics Journal.

Ukwatta, T. N., and P. R. Wozniak. Investigation of Redshift- and Duration-Dependent Clustering of Gamma-ray Bursts. To appear in Monthly Notices of the Royal Astronomical Society.

3D Turbulent Magnetic Reconnection Experiments and Simulations

Scott C. Hsu
20120768PRD3

Abstract

The collective behavior, like transport, of strongly coupled plasma under various external fields is a key problem in studying plasma physics processes, although it has not been understood. In the past two decades, the collective behavior of strongly coupled dusty plasma without an external field has been studied well. Although external fields drastically change the motion of each individual particle, the effects of these external fields on the collective behavior of strongly coupled dusty plasma are still unknown. Using Langevin molecular dynamical simulations, we have been studying the collective behaviors of strongly coupled dusty plasma under various external fields. In our study, we focus on two types of external fields, which are (1) perpendicular magnetic fields, and (2) one-dimensional electric substrates. In the simulation with perpendicular magnetic fields, we discover that the motion of two-dimensional dusty plasma tends to be more superdiffusive under stronger magnetic fields. We also find that the shear viscosity changes when the perpendicular magnetic field changes, while the changing trend is different for different dusty plasma conditions. More simulations with different dusty plasma conditions are still needed to study this changing trend systematically. In the simulation with a one-dimensional periodic electric substrate with various widths, we find that the diffusion of two-dimensional dusty plasma oscillates periodically when the width of the electric substrate changes. We also investigate that the wave properties change dramatically with this one-dimensional electric substrate. Further simulations with more dusty plasma and electric substrate conditions are still needed to complete this project.

Background and Research Objectives

The plasma state of matter fills most of the universe, including the interstellar medium and stellar interiors. Because plasmas are strongly affected by electric and magnetic fields, they exhibit quite complex behavior. While the particles in most plasmas have modest charges, dusty plasmas are composed of particles (the dust grains) that can have very large charges – perhaps as high as tens of thousands. For this reason, dusty plasmas have further exotic behavior; for example, they can crystallize and form matter more similar to liquids and solids. Since 1990s, the collective behaviors of dusty plasma without external fields have been studied well, not only in theories but also in many experiments. However, the properties of such plasmas under external fields are currently not well understood yet.

Because of the properties of dusty plasmas, we cannot use standard plasma physics techniques, such as particle-in-cell or hydrodynamics methods. As such, we employ simulations that treat each dust grain explicitly. To compare and motivate experiments in the response of various fields, we simulate the behaviors of two dimensional dusty plasmas with different external fields. For example, we can add a force term corresponding to either a magnetic field or a periodic substrate. Here, we are interested in some basic properties of such plasmas and will focus primarily on diffusion and waves in these systems. We want to have a big picture of the effects of external fields on the collective behaviors of strongly coupled dusty plasmas.

Scientific Approach and Accomplishments

Our research performed here is primarily computational, with theoretical support. Since standard plasma physics techniques cannot be used in dusty plasmas, we employ simulations that treat each dust grain explicitly. We use the Langevin molecular dynamical simulation to mimic the motion of thousands of dust particles within the two dimensional plane. In the equation of motion of each simulated particle, we include various forces, like the particle interaction and gas frictional damping, which are the same in the dusty plasma experiments. We integrate the equations of motion for all particles, step by step, to obtained all particles' positions and velocities. With these particles' positions and velocities, we can do vari-

ous structural and dynamical analyses.

In the first project, we added an additional Lorentz force term corresponding to a perpendicular magnetic field in the equation of motion. From the particles' positions and velocity, we obtain many kinds of dynamics measures, like the mean-squared displacement, velocity autocorrelation function, vibrational density of states, phonon spectra of this system. These dynamics measures indicate that, the two dimensional strongly coupled dusty plasma tends to be more superdiffusive under stronger perpendicular magnetic fields. These results have been published [1].

Besides the diffusion, we have also calculated the shear viscosity of this system, which has never been studied before. We use the Green-Kubo relation to calculate the shear viscosity here. In the Green-Kubo relation, the viscosity is the integral of an autocorrelation function of the shear stress of the total system. We find that the external magnetic field changes the behavior of this autocorrelation function significantly, so that the integral of this function has also been changed due to this external magnetic field. As shown in Figure 1, the integral of this autocorrelation function with bigger magnetic fields (green and blue curves) is also bigger than those with smaller or zero magnetic fields (red and black curves). However, in other dusty plasma conditions, our simulation results indicate a different trend: bigger magnetic fields would reduce this integral. Further simulations with different dusty plasma conditions are still needed to systematically study this changing trend under external magnetic fields. Our current conclusion is that the magnetic field modifies the shear viscosity of this system significantly.

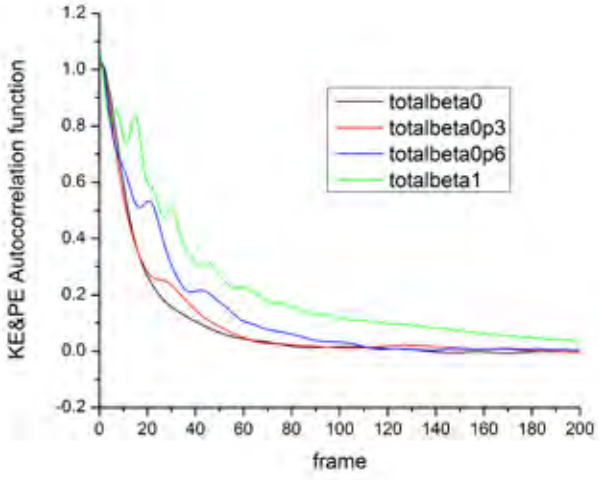

Figure 1. Autocorrelation functions of the shear stress, calculated from the two-dimensional dusty-plasma simulations with perpendicular magnetic fields. From the Green-Kubo relation, the time integral of this autocorrelation function corresponds to the shear viscosity of this system. Four curves of black, red, blue, and green correspond to the zero, smaller, bigger, and biggest perpendicular magnetic fields, respectively. For this dusty plasma condition, these curves indicate that the shear viscosity is increased as the perpendicular magnetic field increases.

In the second project, we add a force term corresponding to a periodic electric substrate in the equation of motion for all particles. A typical plot of trajectories of all dust particles is shown in Figure 2. To mimic the effects of different substrates, we change the width of this periodic electric substrate in our simulations. Then, to study the diffusion of dusty plasma under this one dimensional periodic electric substrate, we calculate the mean squared displacement due to the motion of all particles in the two directions. Figure 3 shows the obtained mean squared displacement under one dimensional electric substrate with different widths. From Figure 3, we find that the diffusion of this system oscillates periodically as the function of the substrate width. Although the electric substrate is aligned regularly in one direction, the diffusion in both directions shows the same general oscillation trend, which indicates that the motion in two directions is coupled with each other.

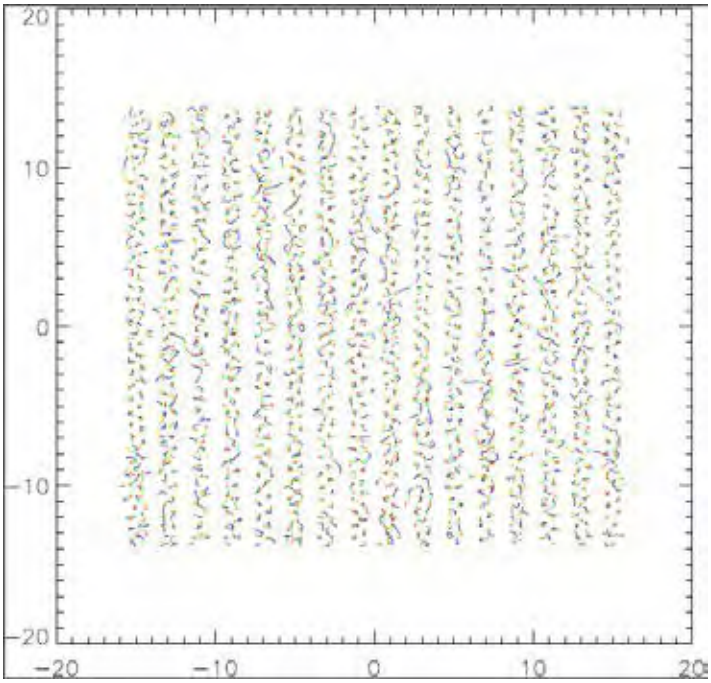

Figure 2. Trajectories of simulated dust particles within the two-dimensional plane with a one-dimensional periodic electric substrate. Different colors correspond to different times. Although most particles stay within the electric substrate potential well, a few of them can jump across the substrate.

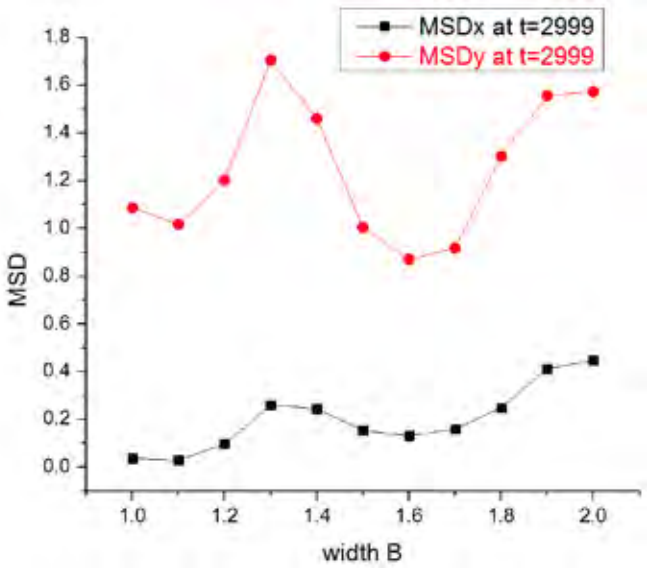

Figure 3. The mean square displacement of simulated dust particles in two directions as functions of the electric substrate width. The red symbols correspond to the diffusion along the substrate, while the black symbols correspond to the diffusion across the substrate. The diffusion in both directions oscillates periodically as the function of the substrate width, and they oscillate roughly in the same phase. This result indicates that the motion in the two directions is coupled with each other.

Besides the diffusion, we have also studied the wave spectra in this system. We find that the wave properties also change due to external force fields. Figure 4 shows the longitudinal wave spectra of 2D dusty plasma in this system without any electric substrate, while Figure 5 shows the modified longitudinal wave spectra, corresponding to the motion in the y direction, due to the applied electric substrate. From these plots, we can see that the one dimensional electric substrate modified the wave spectra significanly lot, causing the spectra to split to two branches, and one branch seems to show some optical mode feature. Similar features have also been observed in the transverse wave spectra. Further studies with more simulations, with various dusty plasma and electric substrate conditions, are still needed to confirm our conclusions.

Impact on National Missions

This work explores the cutting edge area of what is referred to as anomalous properties; that is, properties that are not well described by standard models. For example, standard model for diffusion is based on Fick's Law, which leads to the standard diffusion equation. However, here we discover that, in the two dimensional strongly coupled dusty plasma with very strong magnetic fields, the diffusion tends to be superdiffusive. Besides diffusion, the shear viscosity behavior is also unknown before our investigation. The study of the dusty plasma behavior under one dimensional electric substrate is a new topic. Understanding such novel transport processes is crucial for understanding diffusive mixing in a variety of applications, such as material mixing in experiments performed at a variety of Department of Energy facilities (e.g., Omega, Z, NIF, and LCLS).

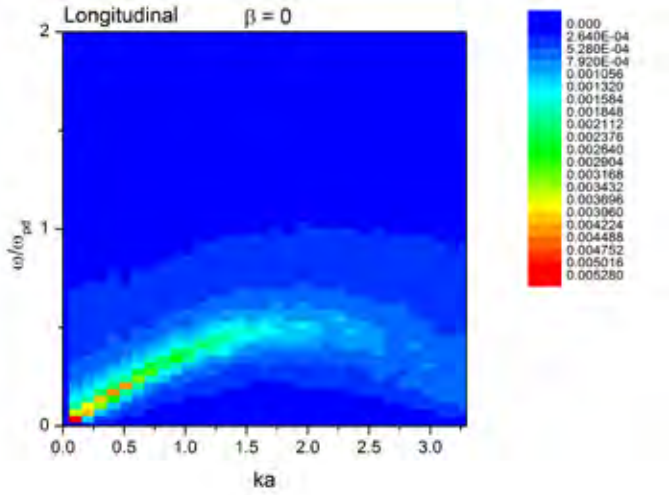

Figure 4. The longitudinal wave spectra of two-dimensional dusty plasma without electric substrate. These spectra and the related dispersion relation have been studied widely in the past in dusty plasmas, from both experiments and simulations.

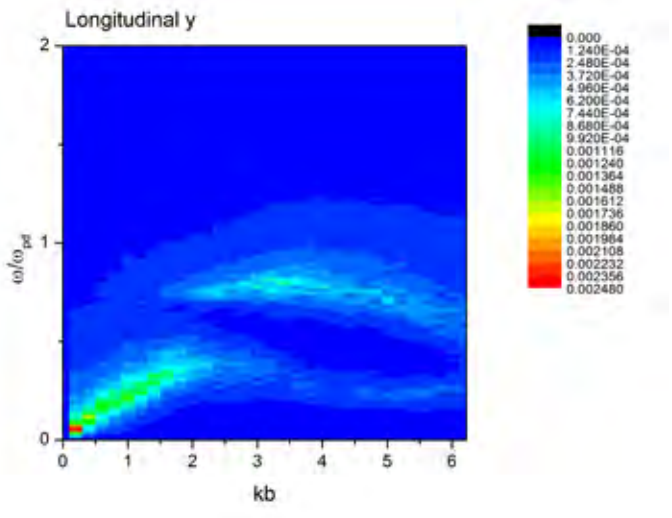

Figure 5. The longitudinal wave spectra of two-dimensional dusty plasma with a one-dimensional periodic electric substrate. This electric substrate causes the longitudinal spectra to slit to two branches. The fundamental reason for this split is still unknown. Further studies with more simulations, with various dusty plasma and electric substrate conditions, are still needed to confirm our conclusions.

References

Feng, Y., J. Goree, B. Liu, T. P. Intrator, and M. S. Murillo. Superdiffusion of two-dimensional Yukawa liquids due to a

perpendicular magnetic field. 2014. Physical Review E. 90: 013105.

Publications

Feng, Y. a. n., Goree, B. i. n. Liu, T. P. Intrator, and M. S. Murillo. Superdiffusion of two-dimensional Yukawa liquids due to a perpendicular magnetic field. 2014. PHYSICAL REVIEW E. 90 (1).

Feng, Y., J. Goree, and B. Liu. Longitudinal viscosity of two-dimensional Yukawa liquids. 2013. PHYSICAL REVIEW E. 87 (1): -.

Goree, , B. i. n. Liu, and Y. a. n. Feng. Diagnostics for transport phenomena in strongly coupled dusty plasmas. 2013. PLASMA PHYSICS AND CONTROLLED FUSION. 55 (12).

Intrator, T. P., Dorf, Sun, Feng, Sears, and Weber. Laboratory observation of magnetic field growth driven by shear flow. 2014. PHYSICS OF PLASMAS. 21 (4).

Intrator, T. P., Sun, Dorf, J. A. Sears, Feng, T. E. Weber, and H. O. Swan. Flux ropes and 3D dynamics in the relaxation scaling experiment. 2013. PLASMA PHYSICS AND CONTROLLED FUSION. 55 (12).

Sears, J., Y. Feng, T. P. Intrator, T. E. Weber, and H. O. Swan. Flux rope dynamics in three dimensions. 2014. Plasma Physics and Controlled Fusion. 56: 095022.

Boosting New Physics Discoveries with Jet Substructure

Christopher Lee
20130794PRD2

Abstract

High-energy physics is now in one of the most exciting eras in history as the Large Hadron Collider (LHC) collides protons at unprecedentedly high energies in an attempt to create new particles beyond the Standard Model (SM) that could help explain unsolved mysteries of Nature such as the composition of dark matter, the origin of mass, and the huge hierarchy of energy scales between gravity, electromagnetism, and nuclear forces. Many of these new particles decay to jets of hadrons, strongly interacting particles made up of confined quarks and gluons. These jets can thus contain signals of new physics beyond the SM. However, the SM itself produces an enormous background of jets that can swamp out the signals of new physics. This project has developed new measures and strategies to probe jet substructure that can help distinguish between signal and background jets. It has developed new, modern theoretical tools that can be applied to predict jet and subjet cross sections to the high precision and accuracy required to extract signals of new physics from LHC data. These new predictions will serve as input to Monte Carlo event generators that simulate large numbers of particles at the LHC and that are widely used in data analyses at the LHC. All together, these complementary tools and developments will serve as a comprehensive strategy to identify new particles produced at the LHC through their decays to hadronic jets.

Background and Research Objectives

The Standard Model (SM) of particle physics is the most precise and successful theory in the history of science, but it still cannot explain dark matter or the huge hierarchy of energy scales (from nuclear forces to gravity) found in nature. Much excitement today comes from predictions of new models of elementary particles that could help solve these mysteries and be detected at the Large Hadron Collider (LHC).

The LHC collides protons at high energies and records the resulting particles that are produced. The most common type of SM final state contains collimated streams of hadrons called jets, produced by radiation from high-energy quarks or gluons. On occasion, new, non-SM particles may be produced and decay into jets. A very difficult needle-in-the-haystack problem is to distinguish jets produced by new particles from the vastly larger number of jets produced by ordinary SM processes. This makes high-precision predictions of the SM jet background essential. Unfortunately, jet cross sections are among the least precisely understood due to the often prohibitively difficult nature of the calculations.

In this research we aimed to vastly increase the potential precision of theoretical jet cross section predictions. The theory of Quantum Chromodynamics (QCD) is highly successful in describing the strong interaction amongst quarks and gluons that make up jets, protons, and neutrons. Using the theory to predict properties of jets precisely, however, is still a formidable calculational challenge. In this project, we developed several new calculational and strategic tools to predict jet cross sections more precisely and mine the structure jets for maximal information about their origin.

Specifically, we developed strategies to characterize and probe the substructure of jets, which can serve as a discriminant between signal and background jets. We applied our expertise in theoretical methods to resum the effects of infinitely many quarks and gluons radiated from jets to predict jet cross sections to high precision and accuracy. We developed new methods to predict cross sections dependent on jet sizes or radii, never before accurately predicted. We improved the theoretical knowledge that can be put into Monte Carlo event generators that simulate large numbers of particles in high-energy collisions. All of these tools together greatly advance our ability to find evidence of new physics at the LHC inside hadronic jets.

Scientific Approach and Accomplishments

Our research accomplishments during the period of this project are in three categories: 1) advanced methods to mine more information from jets by considering multiple jet formation histories; 2) a new effective field theory that can predict the dependence of jet cross sections on the size or radius of jets; and 3) new predictions for a wide variety of jet shape variables in hadron collisions.

Qjets ("Quantum" Jets)

Postdoc A. Hornig has been developing a method called "QJets" that is designed to optimize the information one obtains when making jet measurements at particle colliders such as the Large Hadron Collider (LHC). He invented the method earlier with collaborators S. Ellis (Washington), D. Krohn and M. Schwartz (Harvard), and former LANL postdoc T. Roy [1]. Traditional methods rely on a single interpretation of how quarks and gluons shower from one to many particles (and eventually hadrons) to form the jets we measure. By utilizing the fundamentally quantum mechanical nature of this process and allowing for multiple such interpretations, much can be gained. For example, the spread in the masses one obtains, a measure of the ambiguity of a jet's mass (dubbed the Qjet "volatility"), can be used to distinguish background QCD jets from Standard Model and Beyond the Standard Model signal jets. In addition, the statistical nature of signal searches can be enhanced.

During the course of this project, Hornig worked with Ellis, Krohn, and Roy to perform detailed analysis of the statistics of QJets and evaluate its quantitative power to improve signal to background ratios. The improvement arises because assigning multiple interpretations to a jet done in a particular manner moves the QCD background to smaller mass, while only slightly distorting the signal distribution (negligible on the scale of a jet mass window typically used in experimental searches). This phenomenon is illustrated in Fig. 1. Hornig and collaborators showed that significant improvements in sensitivities to signals and more precise measurements of jet observables can be achieved by using QJets. This work was published in the Journal of High-Energy Physics [2].

Thanks to these demonstrated statistical improvements, QJets has now been incorporated into independent codes used by the wider theoretical and experimental communities analyzing LHC data for signals of new physics. The HEPTopTagger2 program codes an array of tools used to mine LHC data for signals of heavy top quark jets and BSM-produced jets. The latest version of the code now includes QJets and has demonstrated, as shown in Fig. 2, that it has the best performance of all observables and algorithms in improving signal-to-background ratios in searches for top quark jets, often an important component of signals for heavier BSM particles decaying to tops [3].

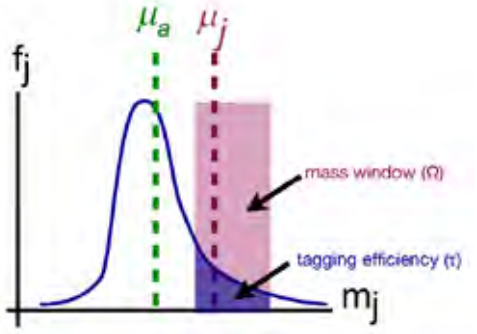

Figure 1. QJets moves the distribution of masses of QCD background jets from higher values mu_j to lower value mu_a. This removes much of the background from the mass window in which one is searching for jets constituting a signal (for heavy jets of SM or BSM origin). [2]

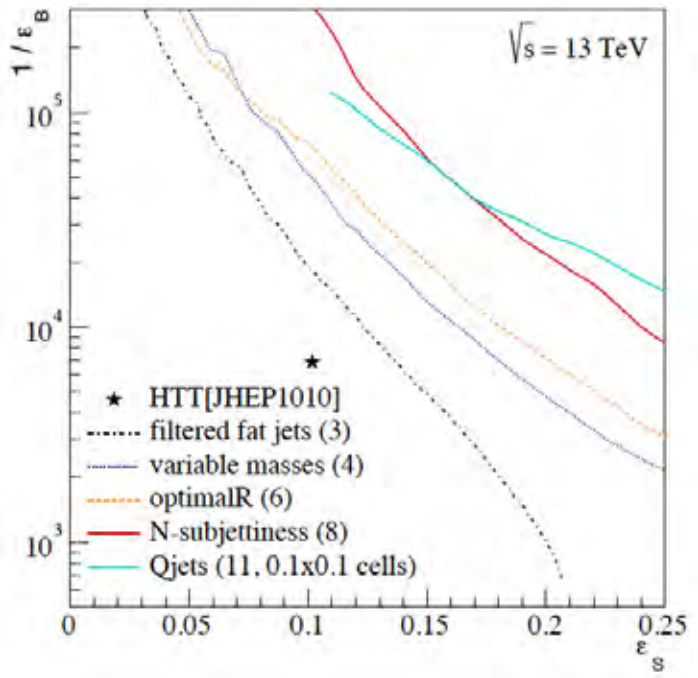

Figure 2. Performance of various algorithms and variables for tagging jets produced by top quarks at the LHC. The QJets algorithm (light blue solid line) performs the best of all methods in signal efficiency and reducing backgrounds. [3]

New Effective Theory for Jet Radii:

All searches for hadronic jets require the use of a jet algorithm to define which particles in the final state of a collision belong inside a jet or not. The simplest way is to define cones of radius R and define particles to be in a jet if they fit inside the cone. An event is a 2-jet event, for example, if most of the energetic particles fit inside two cones of radius R. A small amount E of the total energy Q in the final state can still lie outside the cones.

Predicting the dependence of jet cross sections in QCD on the parameters R and E/Q accurately has been a long-standing problem. For relatively large values, the problem is not so hard, but for smaller value, large logarithms of these parameters appear in perturbative predictions for cross sections dependent upon them, spoiling the convergence of the perturbative expansions in the strong coupling which is supposed to be small. In the past 15 years, Soft Collinear Effective Theory (SCET) has been developed and proven to be a powerful tool providing technology to resum such logarithms to all orders in the strong coupling for other jet observables, restoring convergence and reliability of the perturbative expansion. This had never been done beyond the leading accuracy, however, for jet radii R or the energy fraction E/Q outside jet cones.

In this project, A. Hornig and C. Lee together with LANL postdoc Y.-T. Chien succeeded in augmenting SCET with additional degrees of freedom that are able to probe the dependence of cross sections on the jet boundaries, isolate dependence on the scales of the soft radiation of energy E outside the jets, the hard energy Q inside the jets, and the scales ER and QR of soft and hard radiation, respectively, that probes the jet boundaries. Degrees of freedom probing ER had never been introduced into SCET before. We called this the new soft-collinear mode. We showed that introducing this mode allows resummation of all logarithms of R in jet cross sections, allowing for the vastly improved accuracy of predictions of the dependence of these cross sections on R. This is a major advance in the theory of jets in QCD and SCET, and opens the door to a wide array of improved predictions of many jet observables. This work has been submitted to the arXiv and has been accepted for publication in Phys. Rev. D [4].

In Fig. 3 we illustrate the improved convergence of resummed perturbation theory for the prediction of a jet cross section as a function of the "jet thrust," a measure of how collimated are the particles in a jet. With our new soft-collinear mode, the resummed perturbative prediction converges noticeably better from one order of accuracy (NLL, next-to-leading-log) to the next (NNLL, next-to-next-to-leading-log) than without it, in which case the theoretical uncertainties are considerably larger. This is because of uncontrolled dependence on the jet radius R in the latter case, which we have captured accurately in the first case.

Jet Shapes for the LHC:
While many jet cross sections simply look for the presence of jets, looking inside at their more detailed structure reveals much information about their origin and evolution, in particular, whether they are more likely to have come from the decay of a heavy particle in the SM or BSM, or from simple, standard, light quark/gluon dynamics in QCD. Finding ways to characterize this substructure in ways that are theoretically predictable to high accuracy is, however a challenge.

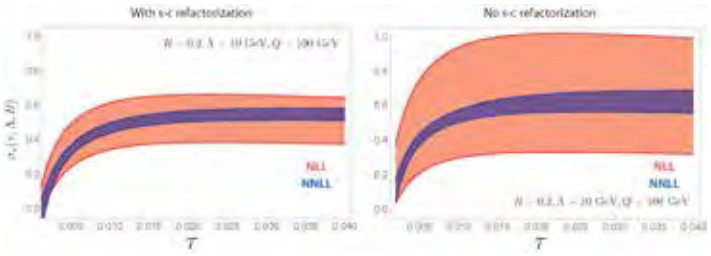

Figure 3. Impact of new effective theory with soft-collinear degree of freedom on jet thrust. The distribution in jet thrust in electron-positron collisions converges better from one order of accuracy to the next when the soft-collinear (s-c) mode is introduced into the theory and used to resum large logarithms of the jet radius (left). Without the mode, large unresummed logs of give a significantly larger theoretical uncertainty (right). [4]

A set of observables that smoothly probe the internal structure of a jet is the set of angularities. These sum over the particles in a jet with a particular weighting function of their energy and their angle from the jet axis. Smoothly varying this function gives an infinite set of different angularities. Comparing distributions of final states in different angularities reveals much about the structure of the jet. Angularities are also predictable to high precision in QCD perturbation theory. This was explicitly demonstrated for jets in electron-positron collisions by Hornig, Lee, and their collaborators in earlier work [5,6].

In this project, A. Hornig together with collaborators Y. Makris and T. Mehen (Duke) has modified definitions of the jet angularities to be appropriate for jets produced in proton-proton (pp) collisions such as at LHC. They extended the technology and computations in SCET to describe dependence on jet angularities and algorithms used in pp collisions. They demonstrated the ability to predict jet angularities at LHC to NLL and NNLL accuracy and provide the basis to go to higher accuracy and predict other jet shape observables at LHC. One of the first predictions for a jet angularity cross section in pp collisions to these orders of accuracy is shown in Fig. 4. This opens the door to precision jet and subjet studies at LHC that will be crucial in separating jets constituting signals for new physics and backgrounds from SM QCD. A publication on this work is very near completion and about to be submitted to JHEP [7].

BOOST Workshops on Jet Substructure
The study of jet substructure to mine more information about jet origins and distinguishing signals and backgrounds has been such promising, fruitful, and active endeavor in the past several years that a series of annual

workshops called BOOST bringing together theorists and experimentalists has been established. A. Hornig has been a leader in this endeavor. He is a co-author on a series of the very highly cited reports arising from these workshops, not only summarizing but also actively evaluating the new ideas and experimental results in this field each year and pointing towards the most promising avenues for research in the coming years. His leadership and expertise were called upon by the community to be a principal organizer and contributor of the report of the BOOST2013 workshop. This report is no simple proceedings of the workshop but rather an original synthesis and analysis of the ideas and results presented and discussed there and requiring significant new research time. The work was peer-reviewed and published in 2015 [8].

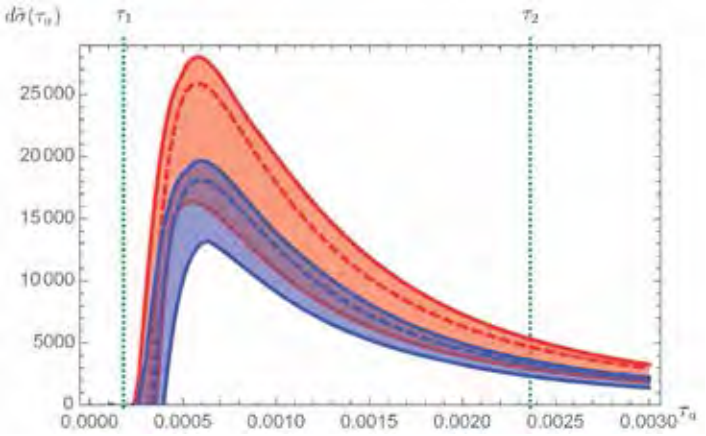

Figure 4. Angularity distribution for jets produced in hadron collisions at LHC to NLL (red) and NNLL (blue) accuracy. This is the first prediction of a jet angularity distribution at LHC to these orders of accuracy [7].

Impact on National Missions

Two key missions of the DOE Office of Science in High-Energy and Nuclear Physics are 1) to improve our understanding of Quantum Chromodynamics (QCD), the theory of the strong interactions between quarks and gluons, constituents of all ordinary matter; and 2) to search for new particles and forces beyond the Standard Model that will explain the origin of matter, dark matter, and masses of elementary particles.

Understanding properties of jets of hadrons produced by energetic quarks and gluons are key to achieving these objectives. They reveal the behavior of QCD itself and contain evidence of new particles that decay to jets.

This project has tackled problems at the forefront of QCD perturbation theory and strategies to search for signatures of new physics in the substructure of jets. Physically accurate predictions of jet cross sections require summing arbitrarily many soft and collinear quark and gluon emissions in and from jets. We have developed and applied tools for resummation that can make possible unprecedented precision in predicting jet cross sections for probing QCD and new physics at the Large Hadron Collider (LHC). In concert we invented and developed new strategies for finding and characterizing jet substructure and interpreting those characteristics as signatures for new physics. Many of the same tools we have developed can be applied to better predictions and understanding of physics at the Relativistic Heavy-Ion Collider (RHIC) and future Electron-Ion Collider (EIC), all high-priority facilities in US Nuclear Physics and in which LANL maintains extensive involvement and leadership.

The advances made by Dr. Hornig under this LDRD proposal open several new paths of research that support our goals in T-2 sponsored by DOE Office of Science, Offices of Nuclear Physics and High-Energy Physics, and also by the DOE Early Career Research Award given to Christopher Lee in 2015. We have extended Dr. Hornig's appointment here for a third year, through FY 2016, to continue his research under the aegis of DOE funding. His expertise is invaluable to the advancement of our research towards several of the highest priority goals of US Nuclear and High-Energy Physics efforts.

References

1. Ellis, S. D., Hornig, T. S. Roy, Krohn, and M. D. Schwartz. Nondeterministic Approach to Tree-Based Jet Substructure. 2012. PHYSICAL REVIEW LETTERS. 108 (18).

2. Ellis, S. D., A. Hornig, D. Krohn, and T. S. Roy. On Statistical Aspects of Qjets. 2015. Journal of High-Energy Physics. 01: 022.

3. Kasiecka, G., T. Plehn, T. Schell, T. Strebler, and G. P. Salam. Resonance searches with an updated top tagger. 2015. Journal of High-Energy Physics. 06: 203.

4. Chien, Y. T., A. Hornig, and C. Lee. A Soft-Collinear Mode for Jet Cross Sections in Soft Collinear Effective Theory. To appear in Physical Review D.

5. Hornig, A., C. Lee, and G. Ovanesyan. Effective predictions of event shapes: factorized, resummed and gapped angularity distributions. 2009. Journal of High-Energy Physics. 05: 122.

6. Ellis, S. D., A. Hornig, C. Lee, C. K. Vermilion, and J. R. Walsh. Jet shapes and jet algorithms in SCET. 2010. Journal of High-Energy Physics. 11: 101.

7. Hornig, A., Y. Makris, and T. Mehen. Jet shapes in SCET at the LHC for dijet events. Journal of High-Energy Physics, preprint LA-UR-27299.

8. Adams, D., A. Hornig, and others. Towards an Understanding of the Correlations in Jet Substructure. 2015. European Physical Journal. C75 (9): 409.

Publications

Adams, D., A. Hornig, and others. Towards an Understanding of the Correlations in Jet Substructure. 2015. European Physical Journal. C75 (9): 409.

Chien, Y. T., A. Hornig, and C. Lee. A Soft-Collinear Mode for Jet Cross Sections in Soft Collinear Effective Theory. To appear in Physical Review D.

Ellis, S. D., A. Hornig, D. Krohn, and T. S. Roy. On Statistical Aspects of Qjets. 2015. Journal of High-Energy Physics. 01: 022.

Hornig, A., Y. Makris, and T. Mehen. Jet shapes in SCET at the LHC for dijet events. Journal of High-Energy Physics, preprint LA-UR-15-27599.

Science of Signatures

Optical and Laser Spectroscopy of Th-229 Electronic and Nuclear Transitions for the Development of Solid State Nuclear Quantum Sensors

Xinxin Zhao
20140011DR

Introduction

Laser spectroscopy and atomic clocks are at the heart of several very important applications. For example, remote sensing and measurement techniques rely on converting an observable, such as the composition of a Martian rock or the position of a missile or smart phone, into frequency or time signatures that can be measured with the utmost precision and/or accuracy. All atomic clocks have a high quality atomic oscillator, but they differ in the type of oscillator that is used, how the atoms (ions) are isolated from the environment, and the way electronic transition frequencies are detected. Atomic clocks have led to many scientific and technological advances including the Global Positioning System (GPS) for navigation.

The Th-229 nucleus holds the promise of similarly profound impact by using nuclear rather than atomic states. Achieving laser interaction with a nucleus for the first time would dramatically advance the field of "nuclear quantum science and technology" and have transformational impact on fundamental science and sensing. This project builds on our recent breakthrough in Th-229 isomer research and aims for the first-ever demonstration of direct laser excitation of the nucleus. This project is high risk, but the potential payoff is very high because the demonstration of nuclear laser spectroscopy would literally be a "quantum" leap over Mössbauer spectroscopy and enable the realization of a nuclear clock with unmatched precision. If successful, this project would usher in a new era of nuclear quantum science with broad implications from fundamental science to important new applications. Scientists from four divisions (C, P, MST, and T) will contribute their diverse expertise and collaborate on these experiments.

Benefit to National Security Missions

This project lays the foundation for nuclear clock and nuclear quantum technology with transformational impact in navigation, quantum information, and threat reduction. It addresses LANL Science of Signatures goals: to revolutionize measurement and discovery signatures. It also supports the LANL Materials for the Future Science Pillar by creating novel materials with controlled functionality that advance our knowledge in intrinsic and engineered defects and enable observation of the emergent phenomena of laser-nuclear interactions. A global network of nuclear clocks and the related gravity sensors will be a powerful system for fundamental science, national defense, and threat reduction. LANL is one of only a few institutions worldwide that can assemble a tightly coupled effort combining experimental capabilities in actinides nuclear chemistry (relevant to the weapons program), precision laser spectroscopy, atomic, nuclear and material sciences. LANL has an opportunity to be a world leader in this groundbreaking field. Besides the advanced scientific applications mentioned above, thorium isotopes are also a nuclear "timer" for special nuclear materials. The ultra-sensitive detection of thorium isotopes developed under this DR will have important impact in nuclear forensic applications.

Progress

Some tasks were delayed due to funding cuts but we have made exciting progresses as summarized below and the project was rated outstanding at its midterm review.

We searched for the transition from 156nm-250nm by collecting thorium-229 recoils into MgF2 plate, and measuring the subsequent light emission using a monochromator. Results so far are very encouraging but additional measurements are required to confirm the discovery. A paper will be updated for resubmission to Nature or Physical Review Letters. The challenge for claiming the discovery is that the observed signal is very weak due to poor recoil efficiency of the U-233 sources. We have studied the source problem and plan to address it in

the next few months while taking more data with existing sources. A separate paper on preparing and charactering the U-233 sources is also in preparation.

The research team also performed absorption and laser induced fluorescence spectroscopy on MgF2 samples irradiated by thorium-229 and/or alpha particles with ~1011-12 atoms implanted into MgF2 crystals. The alpha radiated MgF2 plates serve as control disks to rule out spectroscopic features from color centers caused by radiation damage or other impurities. According to our theoretical predictions, the most likely charge state for the implanted thorium-229 atoms is +4. However, there may be some thorium atoms in lower charge states because the implantation is an equilibrium state. The lower charge states will have low-energy excited electronic states in the visible and near-IR portion of the electrometric spectrum, so they can be detected if exist. Experimental results so far support the theoretical prediction that the Th+4 are the most abundant in the crystal. We are finishing up these measurements and preparing a paper for publication.

Several options were examined to cover a wide range of laser wavelengths and we have constructed and characterized prototypes to generating the required light for laser excitation of the isomeric transition. For the shortest wavelengths, a possible scheme involves CW 5th harmonic generation of a Ti:Sapphire laser by mixing the 4th harmonic of a Ti:Sapphire laser with the unconverted fundamental wavelength using Sum-Frequency Generation. We have completed and optimized the first doubling stage with power output sufficient for the subsequent stages. For the long wavelength range, a two stage 4th harmonic generation can be used. First and second stage doubling cavities have been constructed using 920 nm Ti:Sapphire laser, with a first stage output of 200-300mW from a 1W input. We have also setup a new UHV and DAQ system that takes advantage of the high resolution of a new monochromator. We are characterizing a new PMT to reduce the background and improve the sensitivity for future measurement.

To maximize thorium-229 ion density in a crystal, we have partnered with the University of Pisa (Italy) who are leading experts in micro-pulling-down fluoride crystal growth. They have fabricated an exact copy of their high-performance growth furnace for delivery to LANL in the next few months. We have secured a new lab space for this equipment, completed the Radiological Engineering review, completed electrical/venting modifications, and installed a chiller system. In parallel to the high-quality crystal growth effort, we have explored a “quick and dirty” approach of growing a thorium-229 doped LiSrAlF6 crystal via spontaneous crystallization (SC) that performs slow cooling of a ~200 mg melt drop. An undoped crystal was successfully prepared this way, and we have tested its optical background at longer wavelengths (450 – 1800 nm). The SC growth system will now be moved into a radiological area for growth runs with thorium.

Finally, we have investigated the prospect of super-radiance in thorium-229-doped materials. Even at moderate doping concentration, thorium emitters can find themselves within the space that favors the cooperative emission of radiation called super-radiance. Super-radiant coupling may off-set the formidable challenges posed by the weak photon coupling for manipulating Th-299 nuclei. These calculations did not, however, take into account the inhomogeneous broadening resulted from environmental effects that would not affect the superradiant dynamics at early times but would degrade the coherence of the beam and require a higher concentration of thorium to observe super-radiance. Better understanding of these effects would guild the experiment for the laser search.

Future Work

- Improve the method to clean up U-233 solution chemically for molecular deposition of U-233 sources. Complete and publish the study and characterization of U-233 recoil sources.
- Complete and publish the ongoing nuclear optical spectroscopy measurement of thorium-229 isomeric transition. Continue to improve the measurement resolution and accuracy.
- Complete and publish optical absorption and laser induced fluorescence measurements of thorium electronic transitions.
- Build the lasers needed to drive thorium-229 nuclear isomeric transition. Setup the laser excitation/monochromator detection system. Minimize the PMT background and optimize the system.
- Setup and optimize crystal growth system with thorium-232, and make thorium-229 doped crystals.
- Perform theoretical study to better understanding of nuclear super-radiance effect.
- Calculate the charge state and the electronic transitions energies of thorium ions doped in LiCaAlF6.

Conclusion

We expect following results with the ultimate goal of achieving direct laser excitation of the nuclear transition:

- Improving the accuracy of direct optical spectroscopic measurements to within 0.01 nm or better. This is a prerequisite for the subsequent laser search to succeed.

- Identifying the electronic transitions of the Th ions in the host crystal. This is an unexplored area of research and will require close collaboration between theory and experiment.
- Preparing high-quality single crystals doped with Th-229.
- Developing a vacuum ultraviolet laser and demonstrating direct excitation of the Th-229 nuclear transition.

Publications

Ellis, J. K., Wen, and R. L. Martin. Investigation of Thorium Salts As Candidate Materials for Direct Observation of the Th-229m Nuclear Transition. 2014. INORGANIC CHEMISTRY. 53 (13): 6769.

Remote Raman-LIBS Spectroscopy (RLS) Signature Integration

Samuel M. Clegg
20140033DR

Introduction

Distinguishing man-made and natural sources of materials such as actinides can be accomplished from the detection of the molecular and elemental compositions. However, the detection of both molecular and elemental composition is a challenge for any analytical method and it is rarely possible remotely. An integrated Raman and Laser-Induced Breakdown Spectrometer (LIBS) instrument is uniquely capable of remote molecular and elemental quantitative analysis. This proposal will complete the fundamental physical studies required to realize the full potential of this novel integrated approach. The most significant scientific challenge of this project is the development of first principal molecular spectroscopy and plasma physics theoretical models to accurately assess and predict Raman and LIBS spectra, respectively. We will also integrate these theoretical and experimental spectra into a single multivariate matrix from which a self-consistent molecular and elemental quantitative description will be developed. In order to fully realize the potential of this integrated technique, we will prototype the first integrated Raman-LIBS remote sensing instrument capable of detecting actinides such as uranium. Finally, the theoretical models and integrated analysis methods will be validated against carefully designed remote sensing experiments under the most challenging environmental conditions. Consequently, this Science of Signatures project will satisfy all three themes: new signature detection, revolutionize measurement, and forward deployment.

Benefit to National Security Missions

This LDRD DR Science of Signatures project will focus on the detection of actinides which is an element of LANL's core mission. The team will use Raman and LIBS spectroscopy (RLS) to distinguish anthropogenic and natural actinides within complex geological materials as well as the advanced theoretical methods developed in this project. While the strategic focus of this proposal is to detect actinides, similar RLS instruments and theoretical methods could be used to remotely detect chemical and biological weapons as well as high explosives. RLS can be also used as an in situ analytical geochemical instrument to identify source of soil contamination (i.e. harmful metals) and terrestrially sequestered carbon. Finally, this RLS instrument will be the foundation for future planetary science mission. For the weapons program, we anticipate a new analytical tool for materials inspection.

Progress

The new transmission spectrometer that enables the collection of both Raman and Laser Induced Breakdown Spectroscopy (LIBS) spectra has been completed. This transmission spectrometer was designed by LANL and is now realized due to this LDRD program.

The ultraviolet (UV) and violet (VIO) spectrometers that record LIBS data over the 240 – 340 and 380 – 470 nm regions will be completed by the end of FY15.

All three spectrometers use miniaturized intensified charge coupled device (ICCD) detectors that were designed and built on this LDRD program. These miniature ICCD detectors enable the time-resolved LIBS and Raman analyses that are critical to understanding the underlying physics. They use components that make them more spectroscopically sensitive than commercially available ICCD detectors. Finally, these detectors are capable of many applications beyond the defined Raman and LIBS requirements including passive infrared spectroscopy.

These intensifiers used in the ICCD detectors require a 6 kV high voltage power supply (HVPS) that can operate under reduced pressures. Such a power supply is not commercially available. The engineering team on this project successfully designed a HVPS that meets these requirements.

The team successfully produced a theoretical LIBS spectrum of a complex basalt sample. The actual spectrum was reported in the 2012 ChemCam calibration paper by Wiens et al. because it reports the intensity in photons whereas most other published LIBS spectra report intensities in "arbitrary units." The theoretical and experimental spectra are in excellent agreement and theoretical compositions are proportional to the relative elemental abundance. This is the first major accomplishment towards the development of a quantitative theoretical interpretation of LIBS spectra. This work is in press in Spectrochimica Acta B (Colgan et al).

We recently identified experimentally observed oxygen emission lines that the theoretical calculations indicate are not energetically possible by standard LIBS ablation energies. We determined that these oxygen lines are actually produced from the breakdown of the atmosphere rather than the sample. This suggests that the breakdown of the atmospheric molecules produces atoms that are in highly excited states. This observation will be confirmed with the time-resolved RLS spectrometers early next FY.

We also completed an initial study on the Raman and LIBS detection of biological materials. This work was presented at an SPIE meeting and published (Anderson et al.).

In addition to the two published papers discussed above, we have submitted three papers and are preparing six manuscripts for submission before the end of the FY.

Future Work

The project will complete one task and continue to advance two tasks in FY16. The integrated Raman-Laser-Induced Breakdown Spectroscopy (LIBS) instrument will be constructed by the end of FY15.The integrated spectrometers will be fully characterized as soon as possible in FY16 such that it will be used to conduct experiments necessary to the theoretical calculations. This characterization will describe the component level throughput to produce a detailed end-to-end photon budget and intensities that are reported as photons. The LIBS plasma spectroscopy theoretical calculations will continue to integrated elements with higher atomic masses into the complex LIBS spectra. The Raman theoretical analyses will continue to develop the fundamental methods needed to accurately simulate Raman spectra of pure minerals and validate with the RLS instrument. Finally, we will continue experiments on complex actinide containing samples using standard laboratory hardware as an initial validation of the theoretical calculations.

Conclusion

The overall goal of this project is to develop the theoretical foundations that are capable of predicting and quantitative interpretation of Raman and LIBS spectra. These theoretical models will be tested and validated with the first fully integrated remote Raman – LIBS instrument used to probe actinides doped in complex geological samples. The theoretical methods will revolutionize the analysis of Raman and LIBS spectra within these communities and the instrument demonstration will lead to novel national security and planetary science capabilities.

Publications

Clegg, S. M., Wiens, A. K. Misra, S. K. Sharma, Lambert, Bender, Newell, Nowak-Lovato, S. u. e. Smrekar, M. D. Dyar, and Maurice. Planetary Geochemical Investigations Using Raman and Laser-Induced Breakdown Spectroscopy. 2014. APPLIED SPECTROSCOPY. 68 (9): 925.

Colgan, , E. J. Judge, D. P. Kilcrease, and J. E. Barefield II. Ab-initio modeling of an iron laser-induced plasma: Comparison between theoretical and experimental atomic emission spectra. 2014. SPECTROCHIMICA ACTA PART B-ATOMIC SPECTROSCOPY. 97: 65.

Colgan, , E. J. Judge, H. M. Johns, D. P. Kilcrease, J. E. Liarefield II, McInroy, Hakel, R. C. Wiens, and S. M. Clegg. Theoretical modeling and analysis of the emission spectra of a ChemCam standard: Basalt BIR-1A. 2015. SPECTROCHIMICA ACTA PART B-ATOMIC SPECTROSCOPY. 110: 20.

Hartig, K. C., Colgan, D. P. Kilcrease, J. E. Barefield II, and Jovanovic. Laser-induced breakdown spectroscopy using mid-infrared femtosecond pulses. 2015. JOURNAL OF APPLIED PHYSICS. 118 (4).

Explosives Signatures for Detection: Nonlinear GHz to THz Responses

David S. Moore
20140049DR

Introduction

This project aims to fill a major gap in our improvised explosive device (IED) detection arsenal, by detecting the explosive itself using penetrating but non-ionizing electromagnetic radiation. This project will develop new experimental and theoretical capabilities to exploit newly-discovered nonlinear coupling of GHz-to-THz electromagnetic radiation to bulk explosives and the detection of the alternative signatures that are generated. The characteristic that we exploit is the intrinsic property that defines an explosive - its metastable chemical energy that can be quickly released on command (by shock, friction, or spark). We will model the expected signatures across relevant length scales from molecular to bulk levels, quantify the complex permittivity versus temperature and amplitude, demonstrate piezoelectric and pyroelectric coupling to convert electromagnetic to ultrasonic energy in situ, and evaluate electro-mechano-chemistry effects. The measurements will be guided and interpreted using electromagnetic theory coupled to strain and heat diffusion, with the ultimate goal to develop fundamental principles that define the processes and signatures, leading the design of a prototype detection system with area-scanning capability from safe stand-off distances. The capability is not intended to be used in isolation, but rather as a tool in the toolset – a tool with drastically improved detection capabilities, viz. penetration through clothing, camouflage, or packaging by using GHz-to-THz frequency radiation, which is a unique electromagnetic spectral region with sparse application to explosives detection.

Benefit to National Security Missions

This project represents a transformational approach to uncovering the direct explosive signal type applicable to the Discover Signatures and Revolutionize Measurement components of the LANL Science of Signatures pillar. The overarching goal of the project directly supports LANL's long-term objective of discovery of the next generation of materials signatures of explosives within its global security mission. The deep fundamental understanding of energy absorption and subsequent responses are applicable to MaRIE's "Decadal Challenges for Predicting and Controlling Materials Performance in Extremes" for the design and control of energy release in explosives. Work under this proposal will develop a new framework for a unified description of explosives' hot spots coupled to the local mechanical, thermal and electromagnetic signatures. Understanding and controlling the material functionality of defects and crystalline interfaces is important for hot spots and their signatures and underpins the Materials for the Future pillar with the focus area Defects and Interfaces, as well as the priority area 2 for advanced (THz) spectroscopies. The explosive expertise developed in this project is of course highly relevant to the weapons program.

Progress

- Let a subcontract (Interagency Agreement) to NIST-Boulder for the measurement of complex permittivity from 220 to 500 GHz; samples sent to or are currently being prepared for this collaboration.
- Made THz measurements of pressed powder samples of TNT, HMX, PETN, RDX, and CompB as well as those materials in polytetrafluoroethylene (PTFE) at 10% and 70% concentration.
- Obtained micro-CT and THz spectra of the explosives simulants 1,3- and 1,4-dinitrobenzene (DNB); theory and modeling extended to calculate THz spectra of 1,3- and 1,4-DNB to compare to the experimental THz spectra (linear low power regime); theoretical methods used involve extending electronic structure methods to a supercell approach for calculations at the lower THz frequencies where possible motions are longer range and intermolecular rather than intramolecular; a paper on this work was submitted.
- Theory and modeling methods are being used to calculate THz spectra of the explosives and will be

compared to the experimental THz spectra; these models are being extended to include the nonlocal temperature fields caused by energy localization and/or chemical energy release.
- Methodology was established to input micro-CT image-derived FEA models into ABAQUS and COMSOL; code was developed to simulate RF electromagnetic field effects on the FEA models of PBX9501 and PBXN-110 and we have quantified the heterogeneous dissipation of energy (this is currently in 2-D, but is being extended to 3-D); code was also developed to extract the corresponding heterogeneous temperature fields (again currently in 2-D to be extended to 3-D).
- Developed a theory of explosions in solids where the parameters of the system exhibit frozen, sample specific spatial fluctuations. In this case, the crucial feature of the system is the existence of long tails in the distribution functions of the parameters of the system. We discovered the existence of a phase transition in the system. Above the critical temperature, an explosion of one spot induces an avalanche of explosions in which the total number of explosions diverges at the critical point. We confirmed existence of this phase transition performing numerical simulations. A paper is in preparation.
- Constructed a waveguide based system to measure upconverted non-harmonic RF emissions under RF stimulation; this effort is being replaced by task 1 in the technical description.
- Used a Raman spectroscopy system to measure the change in Raman spectrum induced by RF stimulation at 2.54 GHz, but the first results were negative.
- Used the Raman spectroscopy system to look for changes in Raman spectrum with static electric fields; in this case, the samples were held in a planar geometry double plate capacitor (1 mm sample thickness), capable of electric fields up to 2 MV/m, but no changes were observed.
- Measured THz spectra (low power linear response) of homemade explosive precursor oxidizers, again finding several with large absorbance at the 1 mm sample thickness; dilute samples in PTFE were pressed and their THz spectra are being obtained.
- We measured THz spectra of a TNT-CL20 co-crystal, and compared to the TNT THz spectra (new peaks in co-crystal), also as a function of temperature to beyond the TNT normal boiling point (showing co-crystal is not just a mixture of TNT and CL20). A paper is in preparation.
- Investigated masking of our modification of THz spectra of explosives and HME precursor oxidizers by fuels, matrix materials, and common interference materials; the first example of this kind of masking was demonstrated using KBr dilution. We can find no scientific literature with data on the variation of THz spectra in mixtures of neat explosives or HME precursors with common materials or fuels, which is of paramount importance for agencies investigating use of linear response THz spectral methods in screening applications.
- We (in collaboration with Mitchell Wood, Purdue University) adapted the molecular dynamics THz simulation methods pioneered by CalTech to investigate anharmonic frequency mixing and Raman processes in RDX and PETN in the THz spectral region. A paper is in preparation.

Future Work

Pursuant to the mid-project review, we have revised the tasks to the following:

The team will focus on the following explosive materials: PETN, AN (with and without fuel), HMX and/or RDX, single crystals of the above with engineered defects (micromachined void structures and deposited metamaterial structures).

Task 1: Elaborate and extend the 95 GH excitation up and down conversion emission experiments in the TA-35 anechoic chamber at MPA-CINT.

Task 2: Reproduce the time-dependent reflectivity experiments at or near 11 GHz with sugar and HMX, but with control of water content (by storage of samples in dessicators).

Task 3: Complete measurement of the complex permittivity in the 200-350 GHz regime using open Fabry-Perot resonator methods via collaboration with NIST Boulder (subcontract let June 30, 2014 for two years)

Task 4:Complete GHz and THz linear dielectric permittivity experiments, including 90/10 PTFE/material samples and 30/70 PTFE/material samples. Samples at these same ratios will also be sent to NIST Boulder (see task 3).

Task 5: Calculate heterogeneous dissipation of energy and conversion to heterogeneous thermal distributions using Abaqus and/or COMSOL through input of micro-CT derived FEA models of explosive/air systems.

Task 6: Continue MD simulation of nonlinear generation of new frequencies, extending towards lower frequencies by enlarging the simulation size and time, including geometric boundaries. We will also compute frequency conversion in reflection and transmission modes.

Task 7: Complete the THz and near IR studies on 1,3-DNB and submit a journal paper.

Task 8: Extend THz and NIR measurements and theory/ simulation to binder effects starting with measurements on HTPB.

Task 9: Manufacture samples (micromachined single crystals) for the Keith Nelson group at MIT for high power THz experiments. Samples include PETN and TATB.
Conclusion

The approach described in this project utilizes technologies in frequency regimes capable of penetrating non-metallic packaging, clothing, or camouflage to interrogate bulk explosives, filling a capability gap in the current suite of counter-IED technologies, which includes X-ray imaging, metal detection, trace analysis, intelligence, and persistent surveillance. It will jump-start new modeling capabilities at LANL enabling theory of elasto-electric coupling with chemical energy release at hot spots in explosives. The model development at multiple scales with the combination of coupled matter-energy interactions ranging from the nano to meso scale brings a fresh and new approach to this long-standing problem.

Publications

Chellappa, R., D. Dattelbaum, M. Graf, D. Moore, and Z. Liu. High pressure vibrational spectroscopy of dinitrobenzene isomers. Chemical Physics Letters.

Chellappa, R., D. Dattelbaum, N. Mack, T. Ahmed, M. Graf, A. Azad, D. Moore, and Z. Liu. Vibrational anharmonicity in 1,3-dinitrobenzene. To appear in Journal of Physical Chemistry A.

Chowdhury, D. R., X. Su, Y. Zeng, X. Chen, A. J. Taylor, and A. K. Azad. Excitation of dark plasmonic modes in symmetry broken terahertz metamaterials. 2014. Optics Express. 22: 19401.

Sorensen, C. J., and D. S. Moore. Radio-frequency electromagnetic emissions from materials under high-frequency mechanical excitation. To appear in American Physical Society Topical Conference on Shock Compression of Condensed Matter-2015. (Tampa, 14-19 Jun. 2015).

Wood, M. A., D. A. R. Dalvit, and D. S. Moore. Nonlinear electromagnetic interactions in energetic materials. Physical Review Applied.

Chemical Signatures of Detonation Born From Extreme Conditions (U)

David Podlesak
20150050DR

Introduction

The ability to infer information about high explosive (HE) type and design is of high value. Traditional nuclear forensic investigations provide little or no insight into the dynamics of HE detonation. Post-detonation and real-time signatures of explosive test programs and unique materials identifiers are needed, but can only come from a fundamental understanding of the physical processes that lead to their formation and evolution in time. Explosives detonation is an exothermic process whereby metastable, complex molecules are converted to simple, stable molecules and solid carbon, with the type of solid carbon formed depending on the type (composition) of explosive. Recovery studies indicate that several allotropes of solid carbon may form including amorphous graphite, "onion-like" carbon, and detonation nanodiamonds (DND). More recently, carbon graphite-to-diamond ratios have been correlated to explosive type, with high-performance, aromatic-ring based explosives producing the largest quantities of DNDs. We propose to establish an interdisciplinary effort to understand how solid carbon forms and evolves during detonation, develop new models to describe its evolution, and link in situ measurements of signature formation with post-detonation characteristics. A key feature of this effort will be discovery of signature formation in real-time behind the detonation front using in situ time-resolved x-ray scattering at the Advanced Photon Source and U.S. free electron laser beam lines. The formation and evolution of solid carbon (and fluids) will be modeled from formation through chemical equilibrium, and the concert of signatures from post-detonation residues will be analyzed in the context of statistical theories to glean requisite information pointing to intent.

Benefit to National Security Missions

We will establish detonation products as novel chemical signatures of explosive composition, performance, and state. Successful execution of this program will provide models critical to improved weapons simulation and results will be relevant to products Equation of States (EOS) used in DOE/NNSA defense and nuclear nonproliferation programs. As well, the integration and analysis of heterogeneous data to link detonation products with initial detonation conditions using modern data analytic techniques will provide a tool useful to multiple agencies involved in nuclear nonproliferation. The development of techniques to interpret heterogeneous data sets will also benefit other nuclear and non-nuclear forensic programs.

Progress

We continue to develop the capability to use detonation products as novel chemical signatures of explosive composition, performance, and state. Successful execution of this program will provide models critical to improved weapons simulation and results will be relevant to products Equation of States (EOS) used in DOE/NNSA defense and nuclear nonproliferation programs. As well, the integration and analysis of heterogeneous data to link detonation products with initial detonation conditions using modern data analytic techniques will provide a tool useful to multiple agencies involved in nuclear nonproliferation. The development of techniques to interpret heterogeneous data sets will also benefit other nuclear and non-nuclear forensic programs. We have made considerable progress to date. Please see specific notes on progress for each main task below.

Task 1: Continue in-house detonation experiments to obtain detonation product samples and use state-of-the-art analytical techniques to determine chemical compositions of detonation products including solids and gases. We have conducted >20 detonations, both steady and overdriven conditions, at LANL firing facilities with three HE formulations (Composition B, PBX 9501, PBX 9502) in ambient conditions and in an Ar atmosphere. Detonations and analyses are ongoing. Carbon

soot was collected from all detonations and analyzed with multiple techniques including electron microscopy, X-ray diffraction (XRD), X-ray photon spectroscopy (XPS), Raman spectroscopy, and isotope ratio mass spectrometry (IRMS). Initial results will be presented at the 19th Biennial Conference on Shock Compression of Condensed Matter (SCCM-2015) June 14-20, 2015. Results will also be published in the associated conference publication. Results will also be presented at the AVS 62nd International Symposium & Exhibition October 18-23, 2015.

Task 2: Continue to develop x-ray scattering techniques to record evolution of carbon (clustering, morphology, polydispersity) in high explosives in real time to provide a scientific basis of post-detonation signature formation. We continue to collaborate with LLNL on developing this capability including improving the design of the detonation vessel, vacuum system, and issues with timing. To date, we have collected some of the first X-ray scattering data in real-time for high explosive (HE: Composition B and PBX 9501) detonations in the United States. Early results that describes clustering characteristics of Composition B will be combined with static X-ray scattering measurements of soot collected from detonations at LANL for a time-line description of carbon clustering. Results will be presented at the 19th Biennial Conference on Shock Compression of Condensed Matter (SCCM-2015) June 14-20, 2015 and will also be published in the associated conference publication. We have added two postdocs, Rachel Huber and Bryan Ringstrand, to work on both Task 1 and Task 2.

Task 3: Continue development of carbon clustering physics capturing the fluid/solid mixture and carbon surface chemistry. This effort is critical in concert with the x-ray scattering data for defining how detonation products form and evolve; e.g. signature formation. We continue development of carbon clustering physics, specifically by combining theoretical models of X-ray scattering during detonation with empirical measurements.

Task 4: Continue to combine multi-phenomenological data such as the combination of pXRD analysis with XPS analysis of detonation soot to develop a methodology for abductive reasoning from the detonation products to the initial detonation conditions. This effort is ongoing with a collaboration established between LANL and North Carolina State University (NCSU), specially the Consortium for Nonproliferation Enabling Capabilities (CNEC). This collaboration includes sharing of an existing and open data set that can be used by an NCSU student so that progress on the combination of heterogeneous data sets moves forward more efficiently.

Task 5: Complete development of a new analytical methodology for pyrolysis-fluorination of actinide-oxides that can be used to quantify O and H isotope effects in these materials. We have innovated modifications to a pyrolysis reactor, and made proof of concept measurements of O-isotope ratios in surrogate oxides (Eu2O3) by high-temperature pyrolysis-fluorination using PTFE as the F source. This approach that will enable faster, safer and simpler analysis of actinide oxide samples as small as ~100μg. We continue to improve this system and will now carefully conduct experiments to demonstrate the robustness of the technique for actinide oxides, quantify any systematic fractionations induced by the methodology or impacts of analytical conditions and validate the new method by comparison with conventional laser-assisted fluorination analyses.

Future Work

Our goal is to continue to develop the capability to identify the intent/design of a detonation test using detonation products.

Task 1: Continue in-house detonation experiments to obtain detonation product samples and use state-of-the-art analytical techniques to determine chemical compositions of detonation products including solids and gases.

Task 2: Continue to develop x-ray scattering techniques to record evolution of carbon (clustering, morphology, polydispersity) in high explosives in real time to provide a scientific basis of post-detonation signature formation. This builds on ongoing and developing capabilities at the Dynamic Compression Sector (such as vessels, firesets, and x-ray optics).

Task 3: Continue development of carbon clustering physics capturing the fluid/solid mixture and carbon surface chemistry. This effort is critical in concert with the x-ray scattering data for defining how detonation products form and evolve; e.g. signature formation.

Task 4: Continue to combine multi-phenomenological data such as the combination of pXRD analysis with XPS analysis of detonation soot to develop a methodology for abductive reasoning from the detonation products to the initial detonation conditions.

Task 5: Complete development of a new analytical methodology for pyrolysis-fluorination of actinide-oxides that can be used to quantify O and H isotope effects in these materials.

Conclusion

We will establish detonation products as novel chemical signatures of explosive composition, performance, and state. To this end, we will combine novel methodologies to understand how solid carbon forms and evolves during detonation, develop new models to describe its evolution, and link in situ measurements of signature formation in real time behind the detonation front using time-resolved x-ray scattering at the Advanced Photon Source with state-of-the-art analysis of post-detonation gases and solids.

Publications

Firestone, M. A., D. M. Dattelbaum, D. W. Podlesak, R. L. Gustavsen, R. C. Huber, B. S. Ringstrand, E. Watkins, B. Jensen, T. Wiley, L. Lauderbauch, R. Hodgin, M. Bagge-Hansen, S. Seifert, and T. Graber. Structural evolution of detonation carbon in Composition B-3 by X-ray scattering. To appear in Proceedings of the 19th Biennial APS Conference on Shock Compression of Condensed Matter. (Tampa, FL, 14-19 Jun).

Podlesak, D. W., R. C. Huber, R. S. Amato, D. M. Dattelbaum, M. A. Firestone, R. L. Gustavsen, C. E. Johnson, J. T. Mang, and B. S. Ringstrand. Characterization of detonation soot produced during steady and overdriven conditions for three high explosive formulations. To appear in Proceedings of the 19th Biennial APS Conference on Shock Compression of Condensed Matter. (Tampa, FL, 14-19 Jun).

Willey, T. M., m. Bagge-Hansen, L. Lauderbach, R. Hodgin, D. Hansen, C. May, T. van Buuren, R. Gusavsen, E. Watkins, M. Firestone, D. Dattelbaum, B. Jensen, T. Graber, S. Bastea, and L. Fried. Measurement of carbon condensates using Small-Angle X-ray Scattering during detonation of high explosives. To appear in Proceedings of the 19th Biennial APS Conference on Shock Compression of Condensed Matter.. (Tampa, FL, 14-19 Jun).

Integrated Biosurveillance

Benjamin H. Mcmahon
20150090DR

Introduction

Our study will apply three state-of-the-art diagnostic technologies to a high disease burden population in western Kenya. We will perform multiple types of epidemiological analysis necessary to derive understanding from the novel data. The samples are derived from patients who frequently have co-infections (tuberculosis, Salmonella, Streptococcus, and Staphylococcus) and are associated with a 12 year longitudinal study performed in a pediatric malaria clinic in the Saiya District of Kenya by our collaborator, Prof. DJ Perkins of the University of New Mexico. The three diagnostic technologies are as follows.

Rapid Biomarker Detection
Approaches will be developed to detect proteins, lipids, and carbohydrates from human or animal samples. Reagents for tuberculosis, Staphylococcus, Streptococcus, and Salmonella will be applied and assessed.

Oligonucleotide-based diagnostics for pathogen characterization
This will include 48x or 96x multiplexed, PCR-based nucleic acid assays to species- strain- and antibiotic resistance- type for Streptococcus, Salmonella and Staphylococcus.

Sequencing of non-host RNA
Novel sample preparations will be developed and automated to provide 10 million pathogen RNA sequences from each sample. These data will be analyzed to observe unexpected pathogens, expression level of virulence factors, validity of nucleotide diagnostics from previous task, and strain-type relative database and other samples.

Our epidemiological model will predict outcomes for both individual patients and the population of Siaya (800,000 residents), as a function of investments, treatments, and mitigations. Our focus in the modeling will be to examine how the widespread co-morbidities of HIV, malaria, Salmonella, Streptococcus, Staphylococcus, and tuberculosis combine to cause 1) poor outcome for individuals and the community (30% mortality rate, at age 5), 2) emergence of antibiotic resistant forms, which spread across the globe, and 3) presence of novel pathogens.

This project will lay the foundations to achieve our long-term technical goals of situational awareness for global pathogen circulation and emergence.

Benefit to National Security Missions

This project directly addresses the National Security mission in the area of biological threat reduction by characterizing emerging diseases in the high-disease-burden region where they emerge. Providing this understanding impacts LANL's ability to respond to sponsor requests to predict the course of emerging diseases or bio-terrorism events or understand how climate change and demographic changes impact infectious diseases, which still cause the majority of deaths in developing countries. Furthermore, this project demonstrates how to systematically characterize these diseases as they emerge, in-situ, and how to integrate the resulting biosurveillance data. This capability is essential to accurately predict risk from novel engineered pathogens, as well as the risk to US personnel as they operate in the developing world.

Methodologically, this project integrates signature discovery with measurement in patients, and deployment of assays and models - an important template for the SoS strategy. Biosurveillance has been a key SoS endeavor at LANL, and senior lab leaders organized a biosurveillance deep dive in Sep 2013. At this event, external experts (programmatic, academic, industrial) critically reviewed LANL strategy and investment in BSV, and our proposed concept was extensively appreciated as innovative, challenging and critical. Our effort requires the

systematic integration of IS&T and experimental capabilities at LANL (Co-Design), which is not readily achieved in an academic setting. This integration is not limited to BSV, and can be applied to other threats (nuclear, chemical, environmental) in the future. Similar tools can be applied to nuclear non-proliferation or any other "big data" national security problem.

Progress

Overall, the project has made good progress towards its objectives. The following are technical highlights accomplished in each of the five tasks, in preparation for prospective data collection in Year 2.

Biomarker task, led by Mukundan: 1) Prepared antigens (proteins, lipids, sugars and DNA) for three of the focal pathogens (Salmonella, Staphylococcus, and Streptococcus) from patient isolates for assay development and screened them against all commercially available antibodies for detection assays. 2) Developed assays for two Salmonella signatures and one Staphylococcus biomarker.

PCR assays task, lead by Doggett: 1) Developed the experimental approach for testing blood spots, enabling hypothesis-testing on retrospective samples. 2) Designed PCR probes and begun validation assays on spiked samples of epidemiologically relevant questions on strains, virulence markers, and antibiotic resistance identified in combined genomic / clinical analysis.

Sequencing task, lead by Vuyisich: 1) Completed optimization and validation of depletion of host reads from blood samples, 2) Characterized, minimized, and mitigated cross-talk in RNASeq diagnostics due to bar-coding of samples. 3) Identified virulence markers, antibiotic resistance genes, and relevant strains from which PCR assays, above, should be derived.

Modeling task, lead by McMahon: 1) Worked closely with UNM collaborators to apply new statistical methods to longitudinal (across time) data from 18,000 patient visits, to accurately identify significant genetic, immunological, clinical, and demographic correlates for outcome in pediatric infectious disease patients. 2) Further developed and transitioned our (fairly complex) epidemiological model of nine co-circulating pathogens to an interactive web-based tool, enabling our UNM and Kenyan collaborators to relate the model to the clinical study design.

With the UNM/KEMRI subcontract, lead by DJ Perkins, we have: 1) Designed a prospective clinical study to provide diagnostic samples enriched in pathogens and characterize the burden of virulent pathogens in less-seriously-ill patients. This study will also demonstrate deployment of the tuberculosis, Salmonella, Staphylococcus, and Streptococcus assays, tailored PCR assays of these and other pathogens, and provide both metagenomic and diagnostic samples. 2) prepared a set of spiked samples of all sample type that can be related to the level of pathogen in the patient blood.

Public presentations of project work included two poster presentations at the Tropical Medicine meeting in New Orleans in November, 2014. Two posters were presented at DTRA's S&T meeting in St. Louis in May, 2015. Two invited talks were given at the Biosurveillance integration conference in Washington, DC, in June, 2015. Project work was featured in Mukundan's Frontier's in Science public lectures in March and April, 2015. The project was briefed to DHS's APEX program in biosurveillance in June, 2015.

Four follow-on projects were awarded in Year 1:

The DTRA projects awarded to Fenimore and Vuyisich on the basis of ideas and data developed in the pilot project were awarded supplemental projects. Fenimore's to provide epidemiological modeling support for CBEP-sponsored workshops in Africa and Asia, and Vuyisich's to apply RNAS-equencing as an infectious disease diagnostic in the US, in collaboration with the New Mexico Department of Health. DARPA awarded $150k to Mukundan and Hengartner to evaluate its 'Chikungunya Challenge' and provide 'lessons learned' report for use in developing US government biosurveillance capability. DHS awarded $100k to McMahon and Deshpande to articulate the case for global application of multiplexed antibody-based diagnostics in order to reduce the risk of $6Bn mitigations efforts such as the one required for the Ebola outbreak in West Africa over the past 1.5 years.

Collaborations were developed with DJ Perkins, Director of the Center for Global Health at UNM, Dr. Ravi Durvasula, Chief of Infectious Disease Medicine at UNM, and Richard Hatchett, Deputy Dir. of BARDA, Dylan George, currently at OSTP, and others involved in implementing the national biosurveillance strategy.

Future Work

Year two of our project will focus on collection of prospective clinical data in Siaya, Kenya, building off of a visit to Siaya by McMahon, Mukundan, and Noormohamed that should transpire at the end of Year 1. This visit will begin the process of translating the diagnostic assays and modeling capability to forward deployment, as well as facilitate the collection of samples to be shipped back to UNM and LANL for continued assay development and validation,

in keeping with our original project plan. Although we feel well-prepared for this effort, it will involve considerable logistical complexity, including international human subjects approvals, shipping of infectious disease samples, coordination with academics, clinicians, and goverment personnel in Kenya, data- and sample-tracking, and communication of results in publications and conference presentations. These logistical issues are formidable barriers to other US Government biosurveillance efforts, and our experience gained here should enable continued development of competitive proposals to several sponsors.

More specifically, our technical efforts will include:

- Validation of tuberculosis and Salmonella waveguide-based biomarker assays on clinical samples shipped back from Kenya, together with development of Staphylococcus and Streptococcus assays.
- Systematic application of PCR assays identified in Year 1.
- Application of RNASeq using end-to-end process developed in Year 1 on selected clinical samples, shipped back from Kenya, together with validation and development of analysis pipeline for RNASeq data.
- Transitioning of interactive epi-model to use by Kenyans in real-time interpretation of diagnostic results and further clinical study designs.

In addition, considerable effort will be required in bringing technical work from Year 1 to successful publication.

Conclusion

We will demonstrate integrative biosurveillance in the high disease-burden region of Siaya, Kenya. This will involve biomarker discovery, assay development, and assay deployment of three complementary infectious disease assays on a human population. Direct biomarker detection assays will provide results at the point of care, nucleic acid detection with PCR is a mature technology which will build on established reference laboratory techniques, and RNA sequencing will provide a broad range of genomic information of a variety of pathogens. Overall information integration and process optimization will result from both statistical analysis and development and application of realistic epidemiological models.

Publications

Brown, M., L. Moore, B. McMahon, D. Powell, M. LaBute, J. Hyman, A. Rivas, M. Jankowski, J. Berendzen, J. Loepky, C. Manore, and J. Fair. Constructing rigourous and broad biosurveillance networks for detecting emereging zoonotic outbreaks. 2015. PLoS ONE. : e0124037.

McMahon, B., P. Fenimore, S. Del Valle, N. Hengartner, R. Ribeiro, and J. Hyman. Modeling the impact of spatial heterogeneity, behavior change, and mitigations on the current Ebola epidemic. 2015. LAUR 14-27813.

Signatures of Change - Habitat Earth

Reinhard H. Friedel
20150647DR

Introduction

This DR proposes to expand the scientific understanding of fundamental physical processes that are critical to maintenance of habitat earth homeostasis with the long-term objective of achieving sufficiently detailed knowledge to identify the tipping points that can push habitat earth out of its homeostatic equilibrium. This scientific goal is achieved by promoting and coordinating basic research based on the science of signatures to gain understanding of the structure, and evolution of the earth, the solar system and the Universe in which habitat earth resides, ultimately relevant to understanding future changes as they might perturb habitat Earth homeostasis. Specifically, we propose to address the following scientific areas:

- Geoscience, with the goal of advancing our capabilities to measure and understand significant natural and human-induced changes within their background context using a portfolio of theoretical, modeling, and experimental methods;
- Climate with the goal of scientific advances that integrate theory, models, simulations, experiments, sensing and observations to push the frontiers of predictability to better prepare for impacts (extreme weather, tipping points, sea level rise), and plan for improved domestic, climate-friendly energy and resilient infrastructures for current and future climate states.
- Space Physics with the goal of advancing our understanding of the space environment from the Sun to the Earth and beyond – with the particular goal of understanding how the space environment affects space platforms that support security and quality of life in our increasingly technological society;
- Astrophysics which includes astro-biology, planetary studies, exo-planets, extinction events, other important astrophysical processes; and
- An emphasis on signature science and the overlap sciences between these fields.

Benefit to National Security Missions

The science of signature and the means to detect and interpret these signatures is directly applicable to the detection needs for nonproliferation and counter proliferation community, space weather and space events, remote sensing and detection of chemical, biological, nuclear, radiologic, or explosive threats, climate impact and treaty verification, and cosmology/astrophysics. Signature discovery and alternate signatures provide the new methods to detect and understand these areas of national need.

Progress

This project has been in effect about nine months. Four refereed publications have been published with more in progress. Also, 27 separate projects are underway in the disciplines of Geophysics, Climate, Space and Astrophysics. A call for proposals for new task starts in FY16 has been issued after ensuring alignment with Laboratory National Security strategies. A total of 38 proposals were received and are now under evaluation for scientific merit and alignment with Laboratory strategy.

Future Work

The scientific goal is to develop signatures or the means to measure signatures that provide insight into changes on earth and space. This goal is achieved by promoting and coordinating basic research on the understanding of the structure, and evolution of the earth, the solar system and relevant to understanding future changes as they might perturb habitat earth. The tasks will be to fund Los Alamos postdoctoral research associates and collaborative research between Los Alamos scientists and university researchers.

Conclusion

The impact is the enhancement of University-Laboratory relations by fostering collaborations between academic campus faculty, staff, students, and Los Alamos National

Laboratory staff; providing Los Alamos National Laboratory programs with systematic infusion of new ideas, people, and contact with the larger university community; direct support of Los Alamos postdocs; fostering top-quality research at Los Alamos National Laboratory in the more "basic" or "fundamental" aspects of fields that map into existing and/or emerging mission thrust areas of the Laboratory; and harnessing LANL's supercomputing and multiscale measurements and modeling capabilities.

Publications

Nonlinear elasticity and hysteresis: Fluid-solid coupling in porous media. 2015.

Anthony, R. E., R. C. Aster, Wiens, Nyblade, Anandakrishnan, Huerta, J. P. Winberry, Wilson, and Rowe. The Seismic Noise Environment of Antarctica. 2015. SEISMOLOGICAL RESEARCH LETTERS. 86 (1): 89.

Ferdowsi, , Griffa, R. A. Guyer, P. A. Johnson, Marone, and J. a. n. Carmeliet. Three-dimensional discrete element modeling of triggered slip in sheared granular media. 2014. PHYSICAL REVIEW E. 89 (4).

Harding, J. Patrick, C. L. Fryer, and S. Mendel. Explaining TeV Cosmic-Ray Anisotropies with Non-Diffusive Cosmic-Ray Propagation. 2015. High Energy Astrophysical Phenomena. 1: 26.

Hertzfeld, U. C., E. C. Hunke, B. McDonald, and B. Wallin. Sea ice deformation in Fram Strait— Comparison of CICE simulations with analysis and classification of airborne remote-sensing data. To appear in Cold Regions Science and Technology.

McDowell, N. G., N. C. Coops, P. S. A. Beck, J. Q. Chambers, Gangodagamage, J. A. Hicke, Huang, Kennedy, D. J. Krofcheck, Litvak, A. J. H. Meddens, Muss, Negron-Juarez, Peng, A. M. Schwantes, J. J. Swenson, L. J. Vernon, A. P. Williams, Xu, Zhao, S. W. Running, and C. D. Allen. Global satellite monitoring of climate-induced vegetation disturbances. 2015. TRENDS IN PLANT SCIENCE. 20 (2): 114.

Paris, M. W., E. B. Grohs, G. M. Fuller, and C. Kishimoto. Toward a Unitary and Self-Consistent Treatment of Big Bang Nucleosynthesis. 2015. Los Alamos National Laboratory for public release.

Ranasinghe, N. R., A. C. Gallegos, A. R. Trujillo, A. R. Blanchette, E. A. Sandvol, Ni, T. M. Hearn, Tang, S. P. Grand, Niu, Y. J. Chen, Ning, Kawakatsu, Tanaka, and Obayashi. Lg attenuation in northeast China using NECESSArray data. 2015. GEOPHYSICAL JOURNAL INTERNATIONAL. 200 (1): 67.

High Performance Atom-Based Sensors for Fields and Rotations

Malcolm G. Boshier
20130058DR

Abstract

The National Security community needs improved sensors for magnetic fields, gravity, acceleration, and rotations that advance the state of the art in performance, size/weight/power requirements, and ruggedness. To meet this challenge, we have used unique LANL technology for manipulating ultracold atoms to demonstrate two new types of sensor. The first, called a waveguide atom interferometer, is able to measure tiny energy differences and will be an extremely accurate device for gravimetry. The second sensor is called an Atom-SQUID. We have shown how to build an Atom-SQUID, and also provided the first demonstration that they can be sensitive detectors of rotation. In addition, we have taken atomic magnetometer technology from the laboratory to the field with the construction of a battery-powered, human-portable atomic magnetometer. Finally, we developed the theory of a new type of force sensor based on a circuit containing an Atom-SQUID. The results of this project have informed Defense Community science panels about the potential of cold atom sensors, been leveraged to start a Strategic Partnership project, and started a new research direction of using atomic magnetometers as compact low-frequency antennas.

Background and Research Objectives

The National Security community needs improved sensors for magnetic fields, gravity, acceleration, and rotations that advance the state of the art in performance, size/weight/power requirements, and ruggedness. The overarching goal of this project is to develop new atom-based sensors for these fields and motions. The gravity, acceleration, and rotation sensors exploit the quantum mechanical result that when atoms are made sufficiently cold they behave as waves. These "matter waves" can create interference patterns, somewhat like the colored fringes seen in a soap bubble, which are exquisitely sensitive to interactions or forces felt by the atoms, such as gravity or rotation. The magnetic field sensor uses a simpler technology demonstrated in the laboratory, but which has not been easy to use in the field. The four main research objectives and their outcomes are as follows.

1. To realize a waveguide atom interferometer, in which matter waves confined in a waveguide trap are split into two sections that use matter wave interference to measure acceleration or an energy difference. We were able to build this device with our atom manipulation technology and measure an energy difference equivalent to a change in temperature of a few billionths of a degree.

2. To realize a rotation sensor based on an atomic analog of the Superconducting Quantum Interference Device (SQUID). During this project we demonstrated the world's first DC Atom-SQUID, and we then showed that when it is rotated its properties change just as theory predicts.

3. To build a portable atomic magnetometer to enable this technology, which had previously only been applied in the laboratory, to be used in the field. During this project we developed a magnetic field sensor with the state of the art sensitivity, and then engineered it into a self-contained, human-portable, battery-powered instrument.

4. To investigate new theoretical approaches to sensing with quantum systems. In the course of developing the theory for our Atom-SQUID device, our team discovered a new approach to sensing forces with a variation of that device.

Scientific Approach and Accomplishments

The technical approach to the cold atom sensors applied a unique LANL atomic physics capability, the "Painted Potential", which allows for arbitrary manipulation of matter waves [1] (Figure 1). In this system, atoms in a vacuum cell are cooled to near absolute zero, forming a

so-called Bose-Einstein condensate (BEC), using standard techniques from the field of laser cooling and trapping. The cold atoms are attracted to the center of a focused laser beam, in much the same way that a sweater with a static charge attracts lint. The Painted Potential system moves the focused laser so fast that the atoms experience the time-averaged intensity distribution (exactly like a laser light show). With suitable computer programming we can trap the BEC atoms in any shape that could be drawn on a sheet of paper, and then move them around as we please.

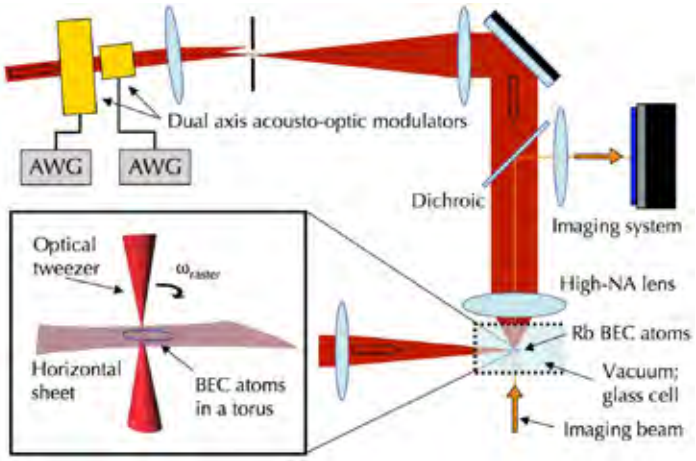

Figure 1. Schematic diagram of the Painted Potential system.

To realize the waveguide atom interferometer, one needs to start with a single BEC and then divide it into two pieces very gently, so as not to disrupt the matter waves in each half. Previous experiments have accomplished this by effectively moving apart two traps that were initially overlapped. This approach unavoidably disturbs the BEC, which in turn limits the measurement time and hence the sensitivity of the device. We used the flexibility of our Painted Potential system to demonstrate a much gentler approach to splitting the BEC (Figure 2). The BEC is first created in a U-shape (Figure 2a). We then slowly move the connecting arm in the U away from the two legs, which very gently turns a single BEC to two identical BECs (Figure 2b). The phase of each BEC then evolves at a rate which is proportional to its energy. After allowing this evolution for some time, the trapping laser beams are turned off. Freed from confinement, the two BECs expand to overlap with each other, where they form matter wave interference fringes. We record the density variation of the fringe pattern by taking an image with a video camera (Figure 2c). A difference in energy between the two BECs results in a difference in phase which shifts the fringe pattern. We imposed a known energy difference by changing the intensity of the painting laser when it illuminated one of the two BECs. Figure 2d shows our measurement of the expected shift in the fringe pattern as the energy difference is

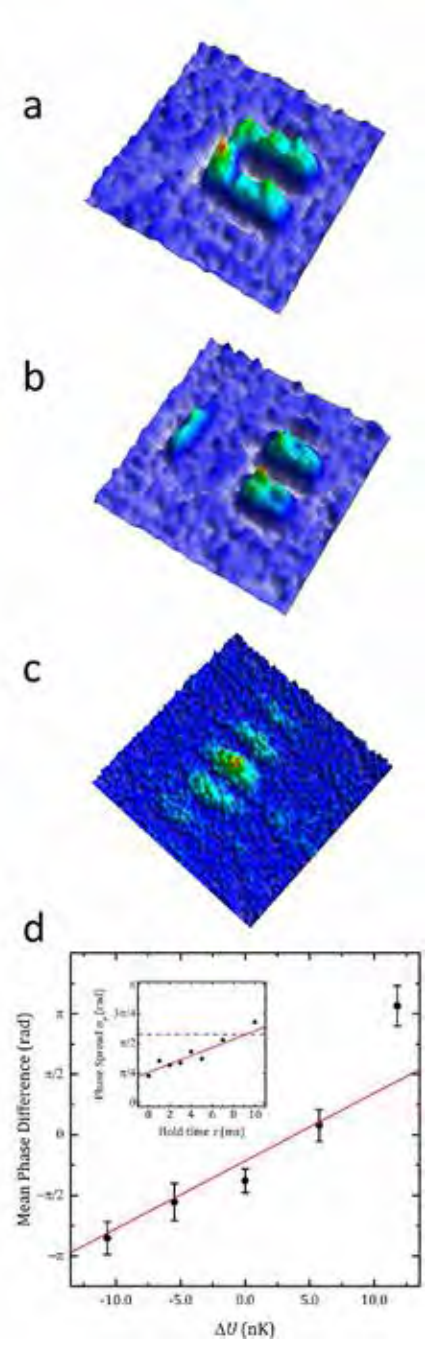

Figure 2.(b) Image of the BEC after the arm of the U has been moved away to leave two BECs. (c) Interference fringes formed when the Painted Potential is turned off and the BECs expand and overlap. (d) Data showing that the measured interferometer phase difference changes as expected when an energy difference is imposed on the two BECs. Inset shows how the spread in phases increases with the time between splitting and measurement. The blue dashed line indicates the point where it is no longer possible to determine the interferometer phase difference.

changed, showing that the device operates as an atom interferometer and that it is sensitive enough to measure an energy difference equivalent to a few billionths of a degree in temperature. The inset to Figure 2d shows how the spread in the phase difference measurements increases

as the time between splitting and interfering is increased. The increase is due to the combination of unavoidable random fluctuations in the number of atoms in each BEC with the fact that the rubidium-87 atoms we are currently using repel each other. That effect adds an additional random energy difference which currently limits the measurement time and hence the sensitivity. In a BEC of potassium-39 atoms, it turns out that applying a magnetic field with the right strength tunes the interactions to zero, which would remove this limitation on performance. A paper describing our new type of atom interferometer and its performance is in preparation.

The Atom-SQUID device is based on a BEC created in a toroidal Painted Potential. This toroidal BEC is very much a quantum mechanical object, as shown by our observation that it can only be made to rotate at certain discrete rates [2]. The toroidal BEC becomes a SQUID when two thin barriers are painted on the toroidal potential (that is easily accomplished by reducing the intensity of the attractive laser beam when it passes over the desired barrier locations) (Figure 3a). We performed experiments to demonstrate that our barriers behave as what are known as ideal Josephson Junctions (JJs) [3]. The JJ has the property that a small flow of atoms can pass through it (by quantum mechanical tunneling), but as the flow is increased a point is reached where the barrier becomes impenetrable. That flow rate corresponds to the so-called critical current. We were able to make an atomic current flow through the barriers by moving them towards each other. When they are moved slowly, atoms tunnel from one side to the other, keeping the density the same in both segments of the ring (Figure 3b). However, when the barriers are moved fast, the tunneling switches off and the atoms are compressed to high density in one side of the barriers and expanded to low density in the other (Figure 3c). Locating the transition point between these regimes measures the critical current. The critical current behavior that we measured was found to be in excellent agreement with our computer simulations of the system. The main reason for our interest in the Atom-SQUID is that theory predicts that the Atom-SQUID critical current should be a periodic function of rotation frequency. This is appealing because the analogous effect in the standard superconducting SQUID allows those devices to function as extremely sensitive magnetometers. We have just become the first group to observe the effect of rotation on an Atom-SQUID. We repeated the procedure to measure the critical current, but this time with the Painted Potential rotating about the center of the Atom-SQUID. Figure 4 shows the result. Here the critical point is located by measuring how many atoms must be added to the SQUID before it switches into the tunneling regime. The graph shows this critical atom number oscillating with rotation frequency, just as theory predicts. Refining our simulations of this behavior will allow us to design an optimal Atom-SQUID for rotating sensing and predict its performance. The observation of JJ behavior was published in Physical Review Letters [3]. A paper reporting our observation of the effect of rotation on the Atom-SQUID is in preparation.

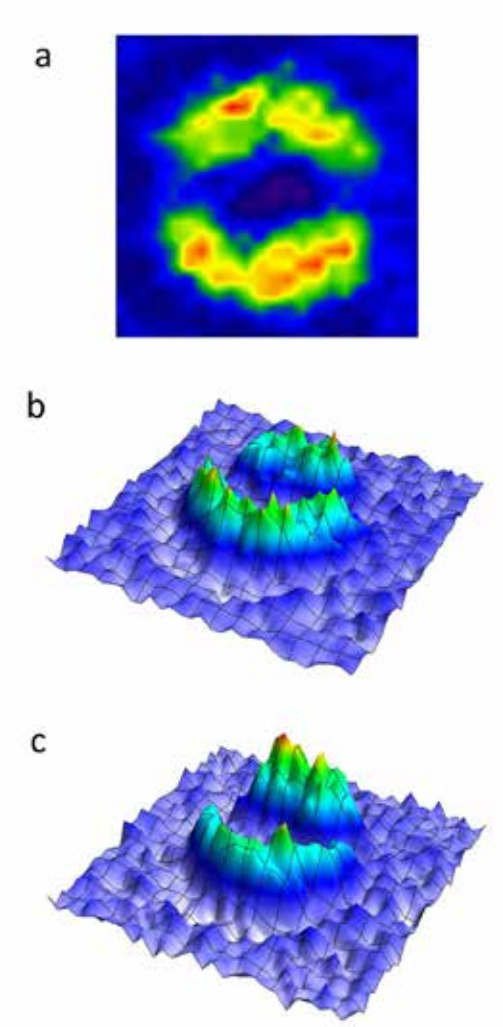

Figure 3. Images showing atoms in the Atom-SQUID. Red = high density, blue = low density. The diameter of the Atom-SQUID is 8μm. (a) The BEC initially formed in the Atom-SQUID, with the Josephson Junction (JJ) barriers opposite each other. (b) The final distribution of atoms when the JJs have been slower than the critical velocity, which allows atoms to tunnel through the JJs and maintain constant density on each side of the JJs. (c) The final distribution of atoms when the JJs have been moved faster than the critical velocity. No tunneling is possible, so the atoms in one side are compressed to higher density and those in the other side are expanded to lower density.

Work by a number of groups around the world has established the atomic magnetometer as the most sensitive instrument for measuring magnetic fields in the laboratory. Since there are mission-relevant applications of

magnetometers in the field (e.g. using the magnetic field emitted by power lines to determine the nature and status of equipment being powered by those lines), our third objective was to take this technology out of the laboratory. We first designed a magnetic field sensor head with state of the art sensitivity over a wide range of magnetic field frequencies. This work was reported in Applied Physics Letters [4]. Next, the engineers in our team designed and built a battery-powered portable control and data acquisition system for this head, using a combination of custom circuit boards and compact commercial data acquisition hardware. The resulting unit (Figure 5) is easily carried by one person and can operate off rechargeable batteries for several hours.

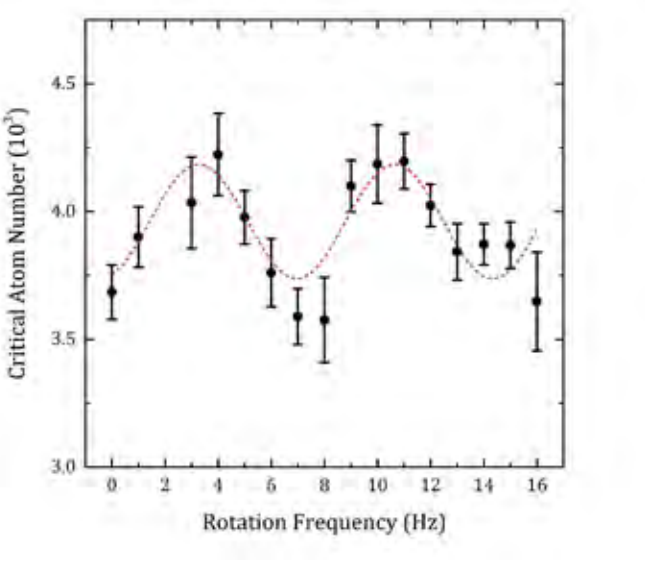

Figure 4. Measurements showing that the critical atom number in the Atom-SQUID varies periodically when the device is rotated. This demonstrates that the Atom-SQUID can act as a rotation sensor.

Figure 5. The battery-powered, human-portable atomic magnetometer constructed as part of this project.

Finally, members of our team developed theory for the devices described above and also performed numerical simulations. An unexpected discovery from this work was a new concept for a force sensor. The device would include an Atom-SQUID connected inside a larger loop (a geometry which is easily realized with the Painted Potential). If an atom current is established in the larger loop, quantum-mechanical constraints on the atom velocity mean that shrinking the dimensions of that loop will increase the current, until it reaches the critical current of the Atom-SQUID. We have found that the loop size at which the critical point is reached is very sensitive to any forces acting on the atoms in the Atom-SQUID. This work, along with supporting simulations, is being written up for publication.

Impact on National Missions

Improved rotation sensors, gravity sensors and magnetometers are of broad interest to many agencies in the Intelligence and Defense Communities. Device applications include respectively inertial navigation, detection of underground structures and of oil or mineral deposits, and the use of power lines for communication and for characterization of activities in inaccessible facilities. The devices based on quantum technologies that are the focus of this project offer potential gains in Size, Weight, and Power (SWaP) and in sensor performance.

The work performed in this project has been presented, at their invitation, to several science panels investigating future technology needs and opportunities for various parts of the Defense Community. Some of our work has already been leveraged to establish a new Work For Others program. The success of the portable atomic magnetometer component has enabled a new research direction to quantify the performance of atomic magnetometers as compact low-frequency antennas.

The project has also established Los Alamos National Laboratory as a world leader in the emerging field of Atomtronics, which seeks to build analogs of optical and electronic circuits based on matter waves flowing in waveguides. This new technology holds great promise for realizing better sensors and for providing new approaches to signal processing.

References

1. Henderson, , Ryu, MacCormick, and M. G. Boshier. Experimental demonstration of painting arbitrary and dynamic potentials for Bose-Einstein condensates. 2009. NEW JOURNAL OF PHYSICS. 11.

2. Ryu, , K. C. Henderson, and M. G. Boshier. Creation of matter wave Bessel beams and observation of quantized circulation in a Bose-Einstein condensate. 2014.

NEW JOURNAL OF PHYSICS. 16.

3. Ryu, , P. W. Blackburn, A. A. Blinova, and M. G. Boshier. Experimental Realization of Josephson Junctions for an Atom SQUID. 2013. PHYSICAL REVIEW LETTERS. 111 (20).

4. Savukov, , Karaulanov, and M. G. Boshier. Ultra-sensitive high-density Rb-87 radio-frequency magnetometer. 2014. APPLIED PHYSICS LETTERS. 104 (2).

Publications

Blinova, A. A., M. G. Boshier, and E. Timmermans. Two polaron flavors of the Bose-Einstein condensate impurity. 2013. Physical Review A. 88: 053610.

Campo, A. del. Shortcuts to adiabaticity by counter-diabatic driving. 2013. Physical Review Letters. 111: 100502.

Campo, A. del, I. L. Egusquiza, M. B. Plenio, and S. F. Huelga. Quantum Speed Limits in Open System Dynamics. 2013. Physical Review Letters. 110: 050403.

Ryu, C., K. C. Henderson, and M. G. Boshier. Creation of matter wave Bessel beams and observation of quantized circulation in a Bose–Einstein condensate. 2014. New Journal of Physics. 16: 103406.

Ryu, C., P. W. Blackburn, A. A. Blinova, and M. G. Boshier. Experimental realization of Josephson junctions for an atom SQUID. 2013. Physical Review Letters. 111: 205301.

Savukov, I., T. Karaulanov, and M. G. Boshier. Ultra-sensitive high-density Rb-87 radio-frequency magnetometer. 2014. Applied Physics Letters. 104: 023504.

Torrontegui, E., S. Ibanez, S. Martinez-Garaot, M. Modugno, A. del Campo, D. Guery-Odelin, A. Ruschhaupt, X. Chen, and J. G. Muga. Shortcuts to Adiabaticity. 2013. ADVANCES IN ATOMIC, MOLECULAR, AND OPTICAL PHYSICS, VOL 62. 62: 117.

Zurek, W. H.. Quantum Darwinism, classical reality, and the randomness of quantum jumps. 2014. Physics Today. 67 (10): 44.

Zurek, W. H.. Probabilities from entanglement and the origin of quantum jumps. 2013. In 25th Solvay Conference on Physics. (Brussels, October 2011). , p. 54. Singapore: World Scientific.

Zwolak, , C. J. Riedel, and W. H. Zurek. Amplification, Redundancy, and Quantum Chernoff Information. 2014. PHYSICAL REVIEW LETTERS. 112 (14).

Battlefield MRI

Michelle A. Espy
20130121DR

Abstract

Magnetic Resonance Imaging (MRI) is the best method for non-invasive imaging of soft tissue anatomy, saving countless lives each year. But conventional MRI relies on very high fixed strength magnetic fields > 1.5 T, with parts-per-million homogeneity, requiring large and expensive magnets. The overwhelming technological trend has been toward ever higher magnetic fields because the signal (sample magnetization), and the sensitivity of the Faraday detectors traditionally used scale with the applied magnetic field (readout frequency). Thus the benefit to signal-to-noise scales as the magnetic field squared. Thus, bigger fields have been widely accepted as the only way to obtain quality images. But there is a price: high field (HF) MRI is a first-world method that can only be used in highly controlled settings in well-funded medical centers where such large magnetic fields can be generated and do not pose a hazard. MRI machines weigh many tons, cost $3-5 million, and typically require 100-1000 liters of cryogens. The high magnetic fields restrict access other ways as well: HFMRI is not available in rural settings, and is not deployable to emergency situations or battlefield hospitals. The cost of a conventional HFMRI system is well beyond what can be afforded for billions of people in poor and developing countries. Subjects with unknown medical histories (e.g. unconscious, soldiers with possible shrapnel injuries, etc.) cannot be imaged due to the potential hazards of heating or moving of metal in the body. Even non-ferrous metal significantly distorts a HFMRI, precluding imaging of those with medical implants.

Recent demonstrations have shown that MRI can be performed at much lower magnetic fields (100 μT – 100 mT, the ULF or ultra-low field regime). Through the use of pulsed pre-polarization and SQUID detection, much of the signal loss can be mitigated. We and others have shown ULFMRI of the human hand, knee, arm, and brain, including imaging in the presence of (and even through) metal. The difficulties of operation outside of a highly shielded environment have also begun to be tackled. In the course of this project, we sought to accomplish the engineering to integrate these capabilities and move ULFMRI from a proof-of-concept in our laboratory to a functional prototype that will exploit the inherent advantages of the approach, and increase accessibility.

Background and Research Objectives

Magnetic Resonance Imaging (MRI) is the best method for non-invasive imaging of soft tissue anatomy, saving countless lives each year. But conventional MRI relies on very high fixed strength magnetic fields > 1.5 T, with parts-per-million homogeneity, requiring large and expensive magnets. The overwhelming technological trend has been toward ever higher magnetic fields because the signal (sample magnetization), and the sensitivity of the Faraday detectors traditionally used scale with the applied magnetic field (readout frequency) [1]. Thus, bigger fields have been widely accepted as the only way to obtain quality images. But there is a price: high field (HF) MRI is a first-world method [2, 3] that can only be used in highly controlled settings in well-funded medical centers where such large magnetic fields can be generated and do not pose a hazard. MRI machines weigh many tons, cost $3-5 million, and typically require 100-1000 liters of cryogens. The high magnetic fields restrict access other ways as well: HFMRI is not available in rural settings, and is not deployable to emergency situations or battlefield hospitals. The cost of a conventional HFMRI system is well beyond what can be afforded for billions of people in poor and developing countries. Subjects with unknown medical histories (e.g. unconscious, soldiers with possible shrapnel injuries, etc.) cannot be imaged due to the potential hazards of heating or moving of metal in the body. Even non-ferrous metal significantly distorts a HFMRI, precluding imaging of those with medical implants.

Recent demonstrations have shown that MRI can be performed at much lower magnetic fields (100 μT – 100

mT, the ULF regime). Through the use of pulsed pre-polarization [4] and SQUID detection [5], much of the signal loss can be mitigated. We and others have shown ULFMRI of the human hand [6], knee [7], arm [8, 9], and brain [10, 11, 12], including imaging in the presence of (and even through) metal. The large remaining challenges were to improve upon and integrate the existing methods into a functional prototype, while moving outside of the heavy magnetic and/or radio-frequency shields in which ULF MRI systems typically operate [13]. In the course of this project, we accomplished the engineering to demonstrate ULF MRI that exploits the inherent advantages of the approach, and shows true potential to increase accessibility of MRI outside of traditional settings.

Our research objectives were to develop a portable "Battlefield" MRI machine based on SQUID (superconducting quantum interference device) sensor technology and ULFMRI techniques developed at LANL. Our motivation was the lack of MRI technology available in any combat support hospital, despite of the promise of the method for early diagnosis of traumatic brain injury. The device was intended to provide a diagnostic quality image in a field deployable package. Specific objectives were to increase the pre-polarization field used to enhance the MRI signal, advance the SQUID detector tolerance to the changing magnetic field environment associated with MRI, without increasing the noise floor, and implement a novel "adaptive" open-coil shield to replace the tons of metal typically required in conventional MRI.

In the course of the project we believe we have demonstrated all these goals and shown the proof-of-concept for an imager that employs very low magnetic fields, which can be completely turned off during transport or when not in use. Most importantly, because the device operates in a fundamentally different regime than a high field MRI machine, it will be able to perform unique imaging tasks that traditional MRI cannot, such as imaging in the emergency room or in the presence of metal. Battlefield MRI will bring the power of MRI to settings where it is presently not possible

Scientific Approach and Accomplishments

Summary: Our scientific approach toward demonstration of a fieldable prototype was two-pronged. A first version (V1) system operating inside a magnetically shielded room (MSR) was engineered for the highest possible signal and lowest possible noise. The V1 system was also used to develop and demonstrate highly stable and low noise magnetic field generation; pre-polarization; SQUID feedback and noise reduction; and "fast" imaging, pulse sequences. Using this system we have demonstrated the highest quality ULF MRI images of the human brain recorded, over a very large (200 cm3) field of view. This result is summarized in the brain images shown in Figure 1, acquired in our V1 system. As our ultimate aim is unshielded operation, we also demonstrated a second-generation V2 system that performs ULF MRI outside of heavy magnetically-shielded enclosure, using field and adaptive noise cancellation methods. These results are summarized in Figure 2. The results from both V1 and V2 were validated against a comprehensive modeling capability that was developed for this project, and provides a quantitative method for designing and assessing the image quality from ULF MRI systems. This result is summarized in Figure 3, showing excellent agreement between our images (Figure 1) and the model (Figure 3). We also addressed the issue of flux trapping in the SQUID gradiometer coils after exposure to the large pre-polarization field. At the end of the project we have demonstrated two capable ULF MRI systems.

Figure 1. Horizontal (top down) image of the human brain acquired with the Los Alamos National Laboratory ULFMRI system developed with this project. The MRI was acquired at 100 uT (about twice the earth's magnetic field) and 10,000 times less than a conventional MRI.

The V1 shielded system: A photograph of the V1 system is shown in Figure 4. The sensor system in the V1 ULFMRI system consists of 7 second-order axial gradiometers with pick-up loop diameter and baseline ~90 mm. The gradiometer intrinsic field resolution is 0.5 fT/√Hz. Johnson noise from the RF shield increases this to ~1.3–1.5 fT/√Hz. To shield the SQUIDs from the high magnetic fields from the pre-polarization coil we use shields made of a eutectic lead bismuth alloy. Importantly for this project, we implemented a method of 2nd feedback [14] that was used to reduce low frequency transients and keep the SQUIDs within their dynamic range after pulsing the magnetic fields.

The polarization coil is a 510-turn copper coil. It typically operates at 100 A for a field at the center of 100 mT. The polarization field could ramp to 100 mT over a 200 cm3 volume and could be removed in < 50 ms. More importantly, the shape of the pre-polarization field (Bp) was optimized to minimize the effects of transients and magnetization of the MSR during and after the dynamic magnetic field changes associated with MRI. This reduced the "dead time" after Bp removal, which in turn provided higher signal-to-noise in the images. The coil is liquid nitrogen (LN) cooled and consumes 1.6 L/min of LN at 100 A. While this coil was used for the results presented below, we also completed development and testing of a water-cooled coil capable of achieving 250 mT.

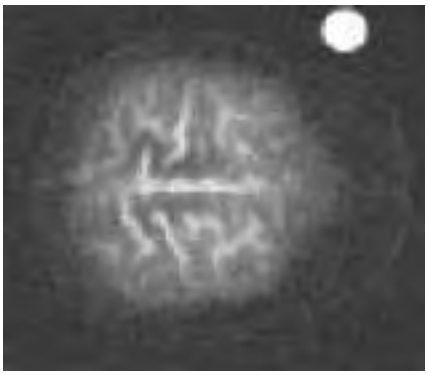

Figure 2. Simulated ULFMRI based on a model developed under this LDRD project. The parameters are the same as those in the experimentally acquired image shown in Figure 1. However, the brain used in the model is different. The similarities in signal-to-noise and image quality are quite similar, giving us confidence in the model's ability to predict diagnostic ability. Also shown is a spherical signal from water for reference.

The magnetic fields required for the remaining MRI sequence are provided by the coil set shown in Fig. 4. Parameters of the coils and amplifiers are provided in Table II. Our data acquisition (DAQ) was a commercial off-the-shelf a National Instruments (NI) 4497 PXI card. To galvanically isolate the DAQ reference path (zero volts, or ground) from that of the SQUIDs we used audio transformers. The SQUID electronics were grounded to a single point on the MSR where the RF shield on the cryostat and Bp coil were also grounded.

Critical to maintaining the SQUIDs within their dynamic range was the development of an adaptive field compensation coil set (Comp coils in Figure 4) which was able to dynamically cancel out the magnetic field transients associated with eddy currents in the MSR. Although the final goal is operation outside the MSR, compensation coils are still a critical demonstration because they can be implemented to maintain a stable magnetic field in the presence of dynamically varying fields present in an open environment.

When performing MRI, the noise rises to ~ 1.6–2 fT/√Hz near 8 kHz where the images are acquired. The 1/f nature of the noise even out to kHz is a phenomenon seen during pulsing, whereas the noise is flat if the system is not active. We infer that this noise is associated with flux trapping in the niobium wire. Flux trapping in the niobium wire traditionally used in SQUID gradiometers has been the primary limitation to increasing Bp beyond 100 mT in both our, and our colleagues approaches to ULFMRI. To address this issue we demonstrated a method of gradiometers made of tantalum, which can be easily and rapidly heated to expel flux. The noise from Bp pulsing was thus reduced. This approach will become increasingly important as Bp is raised from 100 mT to 250 mT, and the technique has resulted in a patent application presently under LANL legal review.

Figure 3. MRI for a gelatin brain phantom acquired in the unshielded MRI (V2). The small simulated stroke inclusion is noted by a circle.

The ULF MRI system described above operated inside a ~ 3×3×4 m3 magnetically shielded room (MSR) made of two pairs of alternating layers of aluminum and mu-metal. This room is in part a legacy of our combined ULF MRI and MEG efforts; such shielding is required in MEG to remove very low frequency noise. However, it is heavy and inhibits portable or inexpensive systems. Thus, one additional goal of our work was to reduce or eliminate the MSR entirely. To that end, we set up a second (greatly simplified) ULF MRI system operating outside of any MSR.

The V2 unshielded system: A photograph of the V2 system is shown in Figure 5. The ULF MRI working in unshielded environment consisted of gradient and measurement field coils as described in [15], and cryostat and 7-channel insert as used in [10, 11]. Three pairs of square Helmholtz coils, surrounding the gradient coil system, were added for cancellation of the Earth's magnetic field. The cancellation coils were powered by regular power supplies and adjusted until a fluxgate in the sample space showed zero

fields in three directions. The measurement field, which was on all the time, was generated by a power supply with a large capacitor across its terminals to reduce the noise. The gradients and spin-flip field were generated by battery-powered current generators receiving input voltages from an NI-6733 card. The pre-polarization coil was the same as used in the shielded system described above, with field generated by three sealed 12 V lead-acid batteries in series and ramped down through banks of solid-state switches both in parallel and series to handle both the required voltage and current. Using this system we were able to demonstrate MRI (Figure 3) of tissue phantoms taken unshielded and in noisy, active laboratory environment [13].

Figure 4. Photograph of the shielded (V1) ULFMRI system.

Developing the ULF MRI model: We have developed a predictive model of our ULFMRI systems. The excellent agreement between data and this model can be seen in the comparison between Figure 1 and 2. Using this model we have shown good contrast for a 1 cm inclusion with the relaxation properties of 50% blood and 50% brain tissue, indicating sensitivity to bleeding in the brain [13]. A more complete discussion can be found in [16]. To simulate the magnetic fields produced at the sample, the response of magnetization in the sample, and the signal detected in our sensor coils we use a simulation written in MATLAB, based on the Biot-Savart-LaPlace formulation of magnetostatics and the reciprocity principle. Spin evolution and NMR signals are computed using the Bloch equations. To simulate the signal and images from the brain we used the Montreal Neurological Institute digital brain model "Colin 27".

Figure 5. Photograph of the unshielded (V2) ULFMRI system.

Impact on National Missions

This proposal directly addresses the issue of improved accessibility to healthcare, the ability to provide care at the point of trauma (theaters of war, emergency or disaster response), our fundamental understanding of the human brain, and global health equality. All of these aspects are of specific concern to National security.

Customers from DoD, DARPA, and NIH continue to specifically request proposals in support of the issues listed above. The LDRD support for this effort represented a critical and timely "next step" in LANL's development of a world-leading capability in ULFMRI and applications. We arguably maintain at LANL the world's expertise in ULFMRI methods.

The work accomplished under this grant also enhances LANL's technical capability to serve the Nation in other areas of R&D including Science of Signatures and Bioscience. We anticipate a broad range of additional applications from basic research (NIH, e.g. ULFMRI combined with functional methods, fundamental understanding of brain, novel contrast at ULF for new diagnostics; global security, e.g. disaster response, non-invasive screening). We also anticipate significant potential for transition to industry partners. In fact, negotiations are actively in place at the time of this writing for follow-on work with a company to which two patents have already been licensed. Outside of the battlefield application, the most compelling need for this technology is in developing countries. Sharing

our prosperity in health care with the world is a national security interest as well as a humanitarian imperative [17]. This work belonged squarely within the National Laboratory where the fundamental groundwork could be done, decoupled from immediate need for a profit.

References

1. Clarke, John, Michael Hatridge, and Michael Mößle. SQUID-Detected Magnetic Resonance Imaging in Microtesla Fields. 2007. Annual Review of Biomedical Engineering. 9 (1): 389.

2. Ubelacker, S.. More MRI cash helping rich more than poor, study finds . 2009. The Globe and Mail.

3. Health Care Resources: Medical Technology. 2014. Organization for Economic Co-Operation and Development.

4. Macovski, A., and S. Conolly. Novel approaches to low-cost MRI. 1993. Magnetic Resonance in Medicine. 30 (2): 221.

5. Myers, W., D. Slichter, M. Hatridge, S. Busch, M. Mossle, R. McDermott, A. Trabesinger, and J. Clarke. Calculated signal-to-noise ratio of MRI detected with SQUIDs and Faraday detectors in fields from 10muT to 1.5 T. 2007. Journal of Magnetic Resonance. 186 (2): 182.

6. Zotev, V. S., P. L. Volegov, A. N. Matlashov, M. A. Espy, J. C. Mosher, and R. H. Kraus. Parallel MRI at microtesla fields. 2008. Journal of Magnetic Resonance. 192 (2): 197.

7. Espy, M., M. Flynn, J. Gomez, C. Hanson, R. Kraus, P. Magnelind, K. Maskaly, A. Matlashov, S. Newman, M. Peters, H. Sandin, I. Savukov, L. Schultz, A. Urbaitis, P. Volegov, and V. Zotev. Applications of Ultra-Low Field Magnetic Resonance for Imaging and Materials Studies. 2009. Applied Superconductivity, IEEE Transactions on. 19 (3): 835.

8. Seton, H C, J M S Hutchison, and D M Bussell. A 4.2 K receiver coil and SQUID amplifier used to improve the SNR of low-field magnetic resonance images of the human arm. 1997. Measurement Science and Technology. 8 (2): 198.

9. Mossle, M., W. R. Myers, S. K. Lee, N. Kelso, M. Hatridge, A. Pines, and J. Clarke. SQUID-detected in vivo MRI at microtesla magnetic fields. 2005. IEEE Transactions on Applied Superconductivity. 15 (2): 757.

10. Zotev, Vadim S., Andrei N. Matlashov, Petr L. Volegov, Igor M. Savukov, Michelle A. Espy, John C. Mosher, John J. Gomez, and Robert H. Kraus Jr.. Microtesla MRI of the human brain combined with MEG. 2008. Journal of Magnetic Resonance. 194 (1): 115 .

11. Magnelind, P. E., J. J. Gomez, A. N. Matlashov, T. Owens, J. H. Sandin, P. L. Volegov, and M. A. Espy. Co-Registration of Interleaved MEG and ULF MRI Using a 7 Channel Low-SQUID System. 2011. Applied Superconductivity, IEEE Transactions on. 21 (3): 456.

12. Vesanen, P. T., J. O. Nieminen, K. C. Zevenhoven, J. Dabek, L. T. Parkkonen, A. V. Zhdanov, J. Luomahaara, J. Hassel, J. Penttilä, J. Simola, A. I. Ahonen, J. P. Mäkelä, and R. J. Ilmoniemi. Hybrid ultra-low-field MRI and magnetoencephalography system based on a commercial whole-head neuromagnetometer. 2013. Magnetic Resonance in Medicine. 69 (6): spcone.

13. Espy, M., P. Magnelind, A. Matlashov, S. Newman, A. Urbaitis, and P. Volegov. Toward High Resolution Images With SQUID-Based Ultra-Low Field Magnetic Resonance Imaging. 2013. Applied Superconductivity, IEEE Transactions on. 23 (3): 1603107.

14. Matlashov, A. N., L. J. Schultz, M. A. Espy, R. H. Kraus, I. M. Savukov, P. L. Volegov, and C. J. Wurden. SQUIDs vs. Induction Coils for Ultra-Low Field Nuclear Magnetic Resonance: Experimental and Simulation Comparison. 2011. IEEE Transactions on Applied Superconductivity. 21 (3): 465.

15. Espy, M, M Flynn, J Gomez, C Hanson, R Kraus, P Magnelind, K Maskaly, A Matlashov, S Newman, T Owens, M Peters, H Sandin, I Savukov, L Schultz, A Urbaitis, P Volegov, and V Zotev. Ultra-low-field MRI for the detection of liquid explosives. 2010. Superconductor Science and Technology. 23 (3): 034023.

16. Espy, M., P. Volegov, and I. Savukov. Chapter 8 - Hardware Developments: Detection using Squids and Atomic Magnetometers. 2016. In Mobile NMR and MRI . Edited by Johns, M.. p. tbd. London: Royal Society of Chemistry.

17. Bonventre, E. V., K. H. Hicks, and S. M. Okutani. U.S. National Security and Global Health: An Analysis of Global Health Engagement by the U.S. Department of Defense-A Report of the CSIS Global Health Policy Center-Working Draft. 2009. ". Washington DC: Center for Strategic and International Studies.

Publications

Espy, M.. Applications of SQUID Detected MRI. Invited presentation at International Society for Magnetic

Resonance in Medicine. (Salt Lake City, Utah, 4-7 April, 2013).

Espy, M. A., P. E. Magnelind, A. N. Matlashov, S. G. Newman, H. J. Sandin, L. J. Schultz, R. Sedillo, A. V. Urbaitis, and P. L. Volegov. Progress toward a deployable SQUID-based ultra-low field MRI system for anatomical imaging. 2015. IEEE Transactions on Applied Superconductivity. 25 (3): pg 1601705.

Espy, M., P. Magnelind, A. Matlashov, S. Newman, A. Urbaitis, and P. Volegov. Toward High Resolution Images With SQUID-Based Ultra-Low Field Magnetic Resonance Imaging. 2013. Applied Superconductivity, IEEE Transactions on. 23 (3): 1603107.

Espy, M., P. Volegov, and I. Savukov. Chapter 8 - Hardware Developments: Detection using Squids and Atomic Magnetometers. 2016. In Mobile NMR and MRI . Edited by Johns, M.. , p. tbd. London: Royal Society of Chemistry.

Kraus, R. H., M. Espy, P. Magnelind, and P. Volegov. Ultra-Low Field Nuclear Magnetic Resonance: A New MRI Regime . 2014.

Magnelind, P E, Y J Kim, A N Matlashov, S G Newman, P L Volegov, and M A Espy. Toward early cancer detection using superparamagnetic relaxometry in a SQUID-based ULF-MRI system. 2014. Superconductor Science and Technology. 27 (4): 044031.

Matlashov, A., P. Magnelind, H. Sandin, M. Espy, A. Anderson, and H. Mukundan. SQUID instrumentation for early cancer diagnostics. 2013. In Superconductive Electronics Conference (ISEC), 2013 IEEE 14th International. , p. 1.

Matlashov, A., P. Magnelind, S. Newman, H. Sandin, A. Urbaitis, P. Volegov, and M. Espy. Multi-channel SQUID-based Ultra-Low Field Magnetic Resonance Imaging in Unshielded Environment. 2015. In International Superconducting Electronics Conference 2015. (Nagoya, Japan, 6-9 July 2015). , p. 1. IEEE/CSC & ESAS Superconductivity News Forum: IEEE Xplore.

Volegov, P. L., L. J. Schultz, and M. A. Espy. On a ghost artefact in ultra low field magnetic resonance relaxation imaging. 2014. Journal of Magnetic Resonance. 243: 98.

Laser-Driven Neutron Source for Detection of Nuclear Material

Andrea Favalli
20140580ECR

Introduction

Los Alamos National Laboratory has pioneered a new short duration yet extremely intense source of neutrons using laser-driven targets, with world record beating flux. This offers the potential for an entirely new way of nondestructively assaying (NDA) nuclear materials for safeguards and other purposes. Potential advantages of this neutron source include the tailoring of the neutron energy and angular distribution for particular applications.

The ultimate goal is to develop and optimize the process of neutron production for safeguards and homeland security applications. Pursuant to that goal, this project will perform the measurements needed to establish yield, temporal and energetic characteristics of the neutron beam for different configurations of target/converter (by changing converter/target distance as well different materials): this information is needed for Monte Carlo simulations of future instruments, and is required to address the detection of nuclear material by a laser-driven neutron source. Initially using depleted uranium (DU) this work will use induced fission signatures: specifically neutrons following neutron fission will be detected in a high efficiency neutron counter.

Benefit to National Security Missions

This research directly supports the nuclear security mission. The demonstration of this novel technology and capability will make Los Alamos a world leader in the active interrogation of nuclear materials using laser driven neutron sources. The existence and demonstration of this type of capability is expected to lead to work for existing and new sponsors in safeguards and homeland security. The assay of fuel debris following an accident, such as that at Fukushima, is one example where a bright source of this type combined with the measurement methods discussed might have important practical advantages. Another example could be a very high throughput interrogation of transportainers at ports, as well as in treaty verification. Many more applications and extension to other signatures can be expected, for example the replacement of nuclear reactors used for neutron production at universities.

Progress

Detecting shielded nuclear material in transport remains a challenging task. The need is for a fast, movable, and operationally safe neutron source featuring energy tunable and high directional neutron fluence, overcoming the limitations of present methods, which typically produce isotropic monoenergetic neutrons. Recent experiments show that a short-pulse laser-driven neutron source possesses these features, allowing for the interrogation of packages with variable shielding conditions and increased signal for the interrogation while improving operational safety.

The goal of this project is to develop a laser-based method of neutron production for active detection of special nuclear material.

During the past year the project has tackled, mainly through experimental activities, the following goals:

Target/converter study, improvement and optimization
The short-pulse high-power laser is focused on a foil of deuterated plastic, creating an accelerated deuteron beam directed towards a neutron converter. The neutrons produced from various nuclear reactions have an array of energies dependent on the source properties. Neutron production from beryllium and copper converters was investigated using MCNP Monte Carlo transport code. Based on such simulations, we redesigned a flexible, modular beryllium converter, composed of disks of different thickness, surrounded by a tungsten cylinder to enhance neutron production.

Diagnostics and methods for neutron-beam characterization

Neutron beam characterization during the past year showed a significant advance using our new diagnostics tools in development. We have been developing a new prototype of a neutron-time-of-flight detector (nTOF) system, necessary to measure the neutron energy spectrum produced. A nTOF measurement of an intense pulse of neutrons using photomultiplier and plastic scintillator presents several challenges related to PMT non-linearity when the intensity of the light pulse is too high. In our LDRD project, we have been able to develop a prototype with LANL custom-made components/devices, that was tested during our experimental campaign conducted at Trident, showing very good response linearity. We also worked on developing prototypes of an on-line monitor based on detecting source neutrons using a 3He proportional counter embedded in a high-density polyethylene moderator. We have developed front-end electronics to couple with the detectors. MCNP modelling was also used here for the study of the interaction of neutrons with the nTOF plastic detector, as well as in the design of the 3He based detectors.

Active interrogation of special nuclear materials

For the laser-driven interrogation, we explored an experimental setup where high efficiency well counters were used both in the so-called fast and thermal mode, where either fast neutrons or thermal neutrons interrogated the nuclear material, respectively. We developed a set of analysis codes to extract and analyze the data.

We conducted a three week experimental campaign at the Trident laser facility in the past year, where the innovations introduced above were tested. Here we report the highlight of the scientific results obtained:

- Record neutron beam intensity at the Trident laser facility, 1.1x1010 n/sr in one shot (surpassing the campaign in May 2012).
- Good reproducibility of shot-by-shot neutron yield, with an average yield of about 5x109 n/sr, a yield comparable with previous 2012 neutron record production in Trident. ptimized neutron flux diagnostics improved considerably the knowledge of the neutron energy spectrum, especially in the region around 1 MeV, not observed before. This should been seen as an important improvement allowing detailed characterization of the laser-driven neutron source we have been developing in Trident.
- First-time demonstration of detection of 235U in sample of enriched uranium by short laser-active neutron interrogation with only a single shot.

Future Work

The goal of our LDRD ECR project is to develop a laser-based method of neutron production for active detection of special nuclear material. The project will end on March 2016 (FY16) and for FY16 it will focus on the following tasks:

- Data analysis and modeling of the experimental campaigns conduct in the project. This is expected to bring a better understanding of the physics, and the technology challenge, of all the process from neutron production to interrogation.
- Analysis of deuteron angular and energy distribution after the target (inside the target chamber):
- Analysis of neutron angular distribution (outside the target chamber)
- Analysis of neutron spectrum from nTOF detector
- Analysis of prompt neutron signal (current measurement) for neutron interrogation
- Analysis of delayed neutron signals (high efficiency detectors) for neutron interrogation

Conclusion

The expected results are the knowledge of the key parameters for the performance of active neutron interrogation based on short-pulse-laser-driven neutron sources. A better understanding of the physics of all the processes from neutron production to interrogation will be a key benefit of the project. The results will be disseminated by presentations at international conferences and through peer-reviewed papers. The know-how developed will be the guidelines for the engineering of the approach proposed and will be used to write proposals to sponsors such as NA-22, NA-24, DHS and DoD for field applications.

Publications

Favalli, A., F. Aymond, J. Bridgewater, S. Croft, O. Deppert, M. Devlin, K. Falk, J. Fernandez, D. Gautier, M. Gonzales, A. Goodsell, N. Guler, C. Hamilton, B. Hegelich, D. Henzlova, K. Ianakiev, M. Iliev, R. Johnson, D. Jung, A. kleinchmidt, K. Koehler, E. McCary, S. Palaniyappan, I. Pomerantz, M. Roth, P. Santi, T. Shimada, M. Swinhoe, T. Taddeucci, and G. Wurden. Nuclear material detection by one-short-pulse-laser-driven neutron source. 2014. LA-UR-14-28697, IEEE Nuclear Symposium, 2014-11-09 (Seattle, Washington, United States).

Favalli, A., and M. Roth. Active interrogation of sensitive nuclear material using laser driven neutron beams. 2015. LA-UR-15-23312, International Workshop on Physics of High Energy Density in Matter, 2015-01-25

(Hirschegg, Austria).

Goodell, J. J., A. Favalli, M. T. Swinhoe, and J. S. Hendricks. Initial MCNP Simulations of Neutron Production at the Laser-Driven Neutron Source. 2014. Poster Presentation, LANL Student Symposium, 2014-08-05/2014-08-06, Los Alamos (NM, US).

Wurden, G., A. Kleinschmidt, A. Favalli, J. Fernandez, D. Cort, S. Frydrych, A. Tebartz, O. Deppert, J. Hornung, S. Jahn, D. Schaumann, V. Bagnoud, F. Wagner, B. Zielbauer, and M. Roth. Short-pulse thin-foil neutron generation experiments using the PHELIX laser. 2015. LA-UR-15-21249, 42nd European Physical Society Conference on Plasma Physics 2015, 2015-06-22/2015-06-26 (Lisbon, Portugal).

Deployment and Installation Technologies for Distributed Measurement Systems in Inconvenient/Hazardous Environments

David D. Mascarenas
20140629ECR

Introduction

This research aims to develop modular, scalable technologies/capabilities that allow us to deploy and install large-scale, distributed measurement systems in an automated, precise, reliable, cost effective manner while minimizing intrusion into the environment. This capability will be easy to employ from a variety of platforms including commonly available aerial robotics. Emplacing measurement systems in the appropriate environment is generally one of the most challenging and costly aspects of any experimental or field research program, but to date this aspect of technology development has been widely ignored. Manual installation of sensors is still the most common technique to deploy distributed measurement systems. This is particularly problematic when sensors must be located in inconvenient environments such as at heights, in rivers, or in Chem/Bio/Rad hazard areas.

The reason for the lack of work in this area is that the development of a lightweight, intelligent remote sensor placement capability that can place sensor nodes accurately and reliably without damaging them in the process is a challenging multi-disciplinary, cyber-physical system research effort. It requires taking into account dynamics, sensor measurement uncertainty, computer vision, projectile dynamics, and embedded systems.

This research effort intends to make Los Alamos a technology leader in this largely unexplored field by developing new engineering tools and capabilities that facilitate the large-scale deployment of wireless sensor networks in inconvenient environments. These techniques will be designed with discreetness in mind so that they minimally disturb the environment and avoid influencing the subjects we are trying to study as little as possible. We will develop the high-finesse engineering tools to enable a capability to intelligently, remotely deploy sensor nodes in such a way that when they arrive at their installation site they have enough energy to be installed correctly, but they have a low-enough energy to ensure the sensor itself is not damaged.

Benefit to National Security Missions

This work will strongly support LANL's mission in Global Security, Nonproliferation, and Environmental monitoring. It directly address the Science of Signatures pillar with respect to Forward deployment and it supports the IS&T pillar by providing new data streams for model validation and uncertainty quantification for global climate modeling and energy security. It is inspired by a crosscutting approach to global security mission needs. The work focuses on capability development for environmental sensing and nonproliferation. This work is in particular meant to address needs concerning the loose nuke problem. The team recognizes that in order for this effort to have a high impact we must engage with both the LANL community/customers and the broader sensor community to build useful deployment techniques. We will hold a mid-project workshop to get feedback from the LANL sensor community and global security program managers on how the work can interface with customer-driven sensor projects. The goal is that this will lead to follow-on collaborations and customer-driven work.

Progress

The 2015 fiscal year has resulted in many accomplishments for the remote sensor placement project. First, there has been some delays in getting testing approvals. So in order to ensure progress continued in spite of the delays, work has continued on technologies that will facilitate remote sensor placement. One of the main problems that needs to be explored going forward is navigating an aerial robot inside buildings in order to deploy sensor nodes. This is an important mission for first responders as well as for security professionals. In order to address this problem, the team has been developing techniques using emerging silicon retina technology to solve important problems such as rapidly detecting the presence of transparent barriers. This problem is impor-

tant because indoor areas where samples may need to be collected and sensor nodes may need to be deployed often feature windows that can hamper efforts to effectively navigate an aerial robot. To date a prototype intelligent transparent barrier sensor has been developed and undergone static testing. The results of this work have been written up and submitted to the IEEE sensors journal. The title of the paper is "A Multi-modal, Silicon Retina Technique for Detecting the Presence of Reflective and Transparent Barriers." In FY 2016 the team is planning to deploy the intelligent transparent barrier sensor onboard an aerial robot for dynamic testing once flight approval is obtained.

Technical staff in the ISR division have indicated to the team that there is a need for using aerial robots to perform environmental radiation surveys. The team has worked with Tyler Trombetta of the US Navy to develop a system that can fly onboard an aerial robot to collect radiation measurements and take photos of an environment for later analysis. This system is currently undergoing final integration and the hope is that it will be testing in FY2016 once flight approvals are obtained.

In FY2015 the team was made aware that there is interest both commercially, and in the Federal Highway Administration to use aerial robots for remote inspections. To date significant work has gone into using aerial robots for visual surveys, but this only addressed half of the procedure typically used to inspect structures. Structural inspectors will often perform tap tests and clean structures with brushes in order to remove debris and rust that inhibits the inspection. To date there is very little work concerned with using an aerial robot to physically interact with a structure to facilitate remote sample collaction. To fill this gap the PI is currently developing an instrumented tap-testing hammer that can be used to perform remote tap-tests. In addition work is currently underway to develop motorized tools that can be attached to an aerial robot. The research currently is focusing on outfitting the quadrotor with brushes, drills, and saws.

Another area that is important for facilitating remote sensor placement is developing human-machine interaction technologies to facilitate remote sensor deployment. The PI has spent the last four years developing a theory for synthesizing artificial personalities. Artificial personality synthesis is viewed as one tool that could have significant impact on human-robot teaming and human interfaces to a variety of cyber-physical systems. A paper on this theory has been submitted to the Neural Information Processing conference for review. The title is, "A Jungian Type-Based Framework for Artificial Personality Synthesis." Based on a recently (2014) publish literature review on artificial personality research, this is the only frame-work for artificial personality synthesis that does not use a trait-based approach. In this sense it is quite innovative.

Lastly, in order to mitigate any risk associated with not obtaining the ability to fly R&D aerial robots in FY 2016, the PI is considering developing a small, simple, ground robot that can demonstrate the concept. It is expected this would not take long given David's previous experience with ground robots. Such a robot may also be used as a platform to demonstrate the utility of ground robots in emerging applications.

Future Work

The main technical milestones for the 2016 fiscal year are as follows:

- Finalize approvals to test the remote sensor placement device.
- Document the work and write it up for peer-reviewed journals.
- Present our work at applicable robotics/wireless sensor networking conferences.

Conclusion

A successful completion of this project will result in solid first step towards a modular remote sensor deployment and installation capability that can be used by the wider sensor networking community. The most important output will be an intelligent, multi-shot, remote sensor placement device capable of being employed from commonly available aerial robotic platforms. We will work toward developing modular deployment packages and characterize a wide array of sensor package attachment mechanisms that can be used to connect sensor packages to a wide variety of materials. Finally, multiple demonstrations of the uses of this capability will be executed.

Publications

Green, A., K. Klein, I. Acevedo, D. Kraus, C. Farrar, and D. Mascarenas. A Multi-modal, Silicon Retina Technique for Detecting the Presence of Reflective and Transparent Barriers. To appear in IEEE Sensors Journal.

Mascarenas, D., A. Green, T. Trombetta, and C. Farrar. A Multirotor-based Approach For Tap-testing Difficult-to-access Structures. To appear in 10th International Workshop on Structural Health Monitoring. (Stanford, CA, Sept 1-3).

Mascarenas, D., L. Ott, A. Curtis, S. Brambilla, A. Larson, S. Brumby, and C. Farrar. Video: remote sensor placement. 2014. In MobiSys '14- Proceedings of

the 12th annual international conference on Mobile systems, applications, and services. (Bretton Woods, NH, 16-19 June 2014). , p. NA. Bretton Woods, New Hampshire: ACM.

Mascareñas, D., L. Ott, A. Curtis, S. Brambilla, A. Larson, S. Brumby, and C. Farrar. Demo: A remote sensor placement device for scalable and precise deployment of sensor networks . 2014. In MobiSys '14- Proceedings of the 12th annual international conference on Mobile systems, applications, and services. (Bretton Woods, NH, 16-19 June 2014). , p. NA. Bretton Woods, New Hampshire: NA.

Yang, Y., A. Cattaneo, and D. Mascarenas. Potential Structural Health Monitoring Tools to Mitigate Corruption in the Construction Industry Associated with Rapid Urbanization. To appear in 2015 International Conference on Sustainable Development (Winner of Best Paper Award). (New York, Sept 23-24).

Trojan Horse Drug Development Approach: Targeting Gene Dosage Control to Induce Bacterial Suicide

Sofiya N. Micheva-Viteva
20150664ECR

Introduction

Multi-drug resistant pathogens present an escalating threat to public health. In this project we seek to discover a novel class of antimicrobial therapies that can restrict the evolution of drug resistant pathogenic bacteria. To achieve this goal, we propose to elucidate a poorly understood mechanism for regulation of protein turnover in the bacterial cell. Messenger ribonucleic acids (RNA) translate the genetic information stored on deoxyribonucleic acid (DNA) molecules into amino acid sequence in the proteins. Gene expression is regulated both on transcriptional (DNA) and post-transcriptional (RNA) levels. We will address a fundamental science question of how bacteria use higher order molecular structures within RNA transcripts to control gene expression. Applying biochemical analytical tools and molecular dynamics simulation models we will identify two and three dimensional RNA structures with regulatory role in transcript stability. Furthermore, we will perform a high throughput screen of small molecule libraries to discover compounds that specifically bind to the RNA regulatory structural elements and alter macromolecular dynamics. We aim to identify chemical scaffolds that cause deregulation of protein dosage control. We will exploit a mechanism of gene regulation that is exclusively found in bacteria and lower eukaryotic cells to develop broad-spectrum antimicrobial drugs with minimum toxicity to the human host. Discovery of small molecules that specifically bind to higher order RNA structural elements is the grand challenge of this project.

Benefit to National Security Missions

This research directly supports LANL's mission in national security for biothreat reduction. Discovery of a novel class of antibiotic drugs that can restrict the evolution of drug resistant species directly addresses the "National Strategy for Combating Antibiotic-Resistant Bacteria" and is aligned with the LANL focus area in Complex Natural Systems and the new strategy for development of advanced therapeutics. DoD, DHS, and NIH are interested in discovery of novel antimicrobial therapies.

Progress

Our research is focused on the identification of structural elements that define the stability and function of bacterial ribonucleic acid (RNA) macromolecules. In our model highly conserved RNA structures regulate the activity of RNase E, an enzyme that is essential for the survival of bacterial cells. RNase E has a key role in the generation of mature ribosomal RNAs and regulates the stability of messenger transcripts (mRNA) encoding for proteins with potential cytotoxic activity. To test our model and to develop an assay for identification of small molecule inhibitors of RNase E function we generated an E.coli bacterial strain that produces high levels of recombinant RNaseE consisting of 400 amino acid polypeptide that harbor the enzyme catalytic and RNA substrate binding domains. We obtained 90% pure recombinant protein and verified its function using E.coli 9S RNA as substrate. In bacterial cells 5S RNA, a structural part of the larger (50S) ribosomal subunit, is synthesized as native transcript (9S) that is cleaved by RNase E to produce a mature ribosomal RNA. Due to the vital role of ribosomes in protein synthesis, inhibition of 5S maturation process will lead to cell death. We established an assay where in vitro synthesized 9S rRNA was cleaved by the recombinant RNase E peptide. Using Northern blot analysis we demonstrated that ofloxacin, a fluoroquinolone antibiotic, can inhibit 9S rRNA cleavage by RNaseE in vitro with half maximal inhibitory concentration IC50=60µM. This result has several key implications: 1) we have found an alternative molecular target for antimicrobial agent known to inhibit DNA gyrase activity; 2) to date, no drug has been reported to in vitro inhibit RNaseE activity in the µM range; 3) we have identified a small molecule inhibitor with well-established antimicrobial activity that can serve as a positive control for our high throughput drug screening assay.

To prove that RNase E activity is regulated by RNA elements with evolutionary conserved higher order molecular structures we tested the ability of E.coli-derived enzyme to process RNA substrate from genetically unrelated bacteria Burkholderia thailandensis. From our previous studies we have identified the RNA transcript encoding for soluble lytic transglycosylase (SLT) protein synthesis as a putative substrate for RNaseE. In the first six months of our project we developed both in vivo and in vitro assays to prove the role of E.coli-derived RNaseE in the catalytic cleavage of SLT RNA from B.thailandensis (B.th). We showed that high levels of full length B.th SLT RNA could accumulate in E.coli rne-3071 strain, producing temperature sensitive RNase E protein, only upon shift to 45°C of bacterial growth. At this temperature the RNaseE catalytic activity is suppressed and we registered that full length SLT RNA accumulation correlated with 2-fold increase in the percentage of dead cells at 3h post slt gene activation. SLT hydrolyzes peptidoglycan (PG) in the bacterial cell wall to facilitate the cell division however overproduction of a PG-degrading enzyme is known to induce cell lysis. We synthesized B.th SLT RNA in vitro and demonstrated that the E.coli-derived RNase E recombinant protein can induce cleavage of full length SLT RNA more efficiently than RNA with 300 nt truncation at the 3' end. Based on molecular modeling we have predicted that B.th SLT RNA has a complex secondary structure consisting of stem-loops and a very pronounced Rho-independent transcription terminator-like structure at the 3'end. Our biochemical assays indicate that there are several RNase E cleavage sites located closer to the 5' of SLT RNA, however the 300nt fragment at the 3' terminus appeared to be essential for efficient cleavage to occur. We are currently solving the SLT RNA structure via biochemical probing, known as SHAPE. Our results so far support a hypothesis that RNase E binding to the RNA substrates is regulated by structural elements located downstream of the cleavage site. Currently all molecular assays used to study the catalytic activity of RNase E employ short single stranded RNA oligonucleotides which we believe do not represent the in vivo substrates of the enzyme. We are developing a florescence resonance energy transfer (FRET) assay to screen drug library for identification of compounds that will specifically inhibit RNAse E cleavage of RNA with secondary structure found in the native substrates.

Future Work

During the Fiscal Year 2016 we will continue structure probing analysis to determine the nucleic acid architecture that regulates RNA stability through direct interaction with RNase E, an enzyme with endonuclease cleavage activity that plays a key role in bacterial RNA processing and stability. We will apply SHAPE, a chemical modification analysis that identifies structurally flexible regions in the backbone of RNA. We will perform foot-print analysis to identify RNA sequences that directly interact with the RNase E protein. We will use both well-established (5S rRNA) and newly discovered in our laboratory RNase E substrates, including B.thailandensis SLT transcript. The results from this assay will guide our work on structure probing analysis and will lay the groundwork for future 3D RNA structure analysis via nuclear magnetic resonance (NMR). Further, we will apply two analytical assays based on fluorescence anisotropy and Fluorescence Resonance Energy Transfer (FRET), to measure differences in the size and structure of the RNA molecule alone and in the presence of RNase E protein with small molecule inhibitor. We will use these analytical assays to screen a small molecule library consisting of 4,000 compounds in a high throughput mode to discover novel class antimicrobials that inhibit RNase E binding to RNA substrates. We will perform both in vitro and in vivo studies to validate the efficacy of compounds identified as leads from the high throughput assay (HTS) as drugs with antibacterial properties.

Conclusion

We will (1) elucidate a key mechanism of microbial cell survival driven by RNA instability, (2) complete a high throughput screen of small molecules in a fluorescence-based assay to find compounds that inhibit RNA degradation, and will (3) validate the small molecule antibiotic activity in live bacterial cells. We will pursue a thus far unexploited strategy for developing of an entirely new class of antibiotics. Discovery of therapeutics that can restrict the emergence of drug resistant pathogenic bacteria will have a high impact on drug development and national security.

Publications

Stubben, C. J., S. N. Micheva-Viteva, Y. Show, S. K. Buddenborg , J. M. Dunbar , and E. Hong-Geller . Differential expression of small RNAs from Burkholderia thailandensis in response to varying environmental and stress conditions. 2014. BMC Genomics. 19 (15:385): doi: 10.1186/1471.

Hand-held Laser-Ultrasound Two-Dimensional Scanner

Eric B. Flynn
20150673ECR

Introduction

Develop and demonstrate a hand-held laser ultrasound scanning device that provides rapid, convenient, stand-off inspection. The form-factor of this device will be similar to that of a hand-held barcode scanner. The device will be able scan at a rate of up to 250 scan lines per second. In this way, the device will generate a visibly continuous horizontal scan line that the operator can manually sweep over the inspection region.

The proposed hand-held scanner has only become realizable with our recent demonstration of a novel ultrasonic inspection technique based on spatial-frequency response, referred to as acoustic wavenumber spectroscopy (AWS). The premise of the technology is the measurement and analysis of a system's spatially-distributed response to a steady, single-tone excitation.

With AWS, we demonstrated the ability to scan the ultrasonic steady state response of a structure at up to five square meters per minute at a distance of three meters with a scan-line spacing of one mm. This is over 100 times faster than conventional ultrasound and translates to a linear speed of approximately 83 meters per second, which means a 30 mm long scan line can be recorded in 3.6 milliseconds, making a hand-held device possible.

AWS relies on the spatial frequencies, or wavenumbers, of the response. In a bounded medium, the wavenumber of a wave at a given frequency is a function of the geometry and material properties of that medium. By making direct estimates of local wavenumber on a pixel by pixel basis for a known excitation frequency, AWS can make estimates of local properties such as thickness or cracking. In AWS, the excitation source is fixed at an arbitrary location, and the location does not affect the imaging. This insensitivity to excitation source is also a key result for the proposed project.

Benefit to National Security Missions

Materials Storage: Rapid, standoff inspection of material storage containers for corrosion, cracking and the presence of material contents such as fluid build-up. A compact scanner could be mounted on robotic inspection systems (aerial or ground) and would enable inspection of hard-to-reach places, such as underground storage and between shielding and encasement layers.

Stockpile Stewardship: Provide a unique ability to detect interlayer disbonds and to map the transmission of acoustic/ultrasonic energy among assembled components. The latter may serve as a form of fingerprinting for identifying when something may have unexpectedly changed as a result of aging or exceeding environment specifications.

Nonproliferation: Ultrasonic fingerprinting (barcoding) of accountable systems and storage containers. In-the-field detection of tampering without the need for tamper evidence devices.

Manufacturing: Non-disruptive, layer-by-layer quality assurance of additive manufacturing processes (3D printing). A sufficiently small and fast scanning system could be built into assembly lines to provide quality control inspection of all manufactured parts (100% QC).

DoD and Aerospace: Maintenance of military air, ground, and naval assets accounts for the majority of system lifecycle cost. New, not well understood, lightweight composite materials magnify this problem. A rapid quick check capability could drastically improve the combat readiness and reduce the maintenance costs of systems utilizing these advanced materials.

Biomedical: Rapid assessment of the elasticity of diseased or burned tissue (far-reaching).

Progress

This project began in February, 2015. This progress report reflects the first four months of the project.

A single tone generation package that is smaller than 10 cm3 in size was designed, built, and tested. This is well within the desired specifications of "briefcase-sized". The maximum output is currently 20 Watts, and we do not anticipate pushing it to 50 Watts to be an issue. The package currently requires a warm-up time of about 20 seconds to allow for the frequency of the tone to stabilize. We are developing ways to decrease this time, and modifying the signal processing algorithms to compensate.

Also, we built and tested an initial prototype of the optics package. It can measure ultrasonic frequencies up to 100 KHz at a range of up to 50 cm without the need for a bulky Bragg cell. The prototype currently uses a HeNe laser, and we are in the process of designing a more compact photodiode as a replacement. The focusing optics are being incorporated to extend the range to the required one meter. Alternatives to the Bragg cell are being explored to achieve similar improvements in signal-to-noise ratio.

The electronics package has been designed and parts are currently being ordered. Testing will begin in July, 2015. Initial proof of concept work has been performed towards the co-registration algorithm. We have demonstrated the ability to automatically synchronize to an unknown excitation frequency, an important step towards full automated co-registration. Full testing and algorithm development will begin in June, 2015.

Future Work

Design, build, and test the ultrasonic generation package of the system. The ultrasonic generation package includes a compact ultrasound generator customized for the application and a resonant-tuned excitation transducer. The goal is to generate 50 watts of ultrasonic power with a device that can be carried over one shoulder.

Design, build, and test the optical breadboard prototype of the optics package. The optics package includes the laser source, the Doppler system, and the scanning mirrors.

Design, build, and test the working version of the electronics package. The role of the electronics package is to map the raw photo-diode signals into estimates of response amplitude and phase through analog and digital signal processing.

The goal with the optics and electronics package in the first fiscal year is to demonstrate the ability to make steady-state, single tone out-of-plane velocity response measurements from a range of 1 meter that are comparable to commercial off the shelf laser Doppler vibrometer systems.

Develop and demonstrate a first version of the coregistration algorithm. The goal is to demonstrate the ability to produce a spatially accurate 2D response map from a manual, hand-held scan. A laser Doppler vibrometer will be used in place of the final system for this demonstration in the first year.

Conclusion

Develop and demonstrate a scanner that is sufficiently compact to be carried by a person and operated by a single hand. The scanner will provide raw steady-state response measurements with more fidelity and at faster speeds that present commercial off the shelf laser Doppler vibrometry technology. It will seamlessly measure transitions between scanned components in an assembly and automatically map scan lines to physical space.

Enabled technologies would include mobile robotic inspection platforms, "ultrasonic fingerprint" readers, tamper-indicating scanners, inspection of hard-to-reach components, inspection of component assemblies, emergency and quick-check inspections, and in-line manufacturing quality control.

Publications

Flynn, Eric B., Anthony J. Haugh, and Sheri B. Lopez. Small defect detection through local analysis of acoustic spatial wavenumber. 2015. In International Workshop on Structural Health MOnitoring. (Palo Alto, 1-3 Sep. 2015). , p. 326. Lancaster: DEStech Publications, Inc.

Gannon, Adam M., Elizabeth M. Wheeler, Kyle J. Brown, Eric B. Flynn, and William J. Warren. A high-speed dual-stage ultrasonic guided wave system for localization and characterization of defects. 2015. In International Modal Analysis Conference. (Orlando, 2-5 Feb. 2015). , p. 123. New York: Springer International Publishing.

Lee, , C. M. Cho, C. Y. Park, Chung Thanh Truong, H. J. Shin, Jeong, and E. B. Flynn. Spar disbond visualization in in-service composite UAV with ultrasonic propagation imager. 2015. AEROSPACE SCIENCE AND TECHNOLOGY. 45: 180.

Remote Whispering Applying Time Reversal

Brian E. Anderson
20150688ECR

Abstract

The purpose of this project was to explore the use of time reversal technologies as a means for communication to a targeted individual or location. The idea is to have the privacy of whispering in one's ear, but to do this remotely from loudspeakers not located near the target. Applications of this work include communicating with hostages and survivors in rescue operations, communicating imaging and operational conditions in deep drilling operations, monitoring storage of spent nuclear fuel in storage casks without wires, or monitoring clandestine activities requiring signaling between specific points. This technology provides a solution in any application where wires and radio communications are not possible or not desired. It also may be configured to self calibrate on a regular basis to adjust for changing conditions. These communications allow two people to converse with one another in real time, converse in an inaudible frequency range or medium (i.e. using ultrasonic frequencies and/or sending vibrations through a structure), or send information for a system to interpret (even allowing remote control of a system using sound).

The time reversal process allows one to focus energy to a specific location in space and to send a clean transmission of a selected signal only to that location. In order for the time reversal process to work, a calibration signal must be obtained. This signal may be obtained experimentally using an impulsive sound, a known chirp signal, or other known signals. It may also be determined from a numerical model of a known environment in which the focusing is desired or from passive listening over time to ambient noise.

Background and Research Objectives

Time Reversal (TR) is a technique that provides spatially localized energy focusing and has been shown to provide secure, optimized underwater acoustic communication between two locations [1-3]. There have been a few studies that have explored the use of airborne TR communications in highly reverberant environments (i.e. racquet ball courts, parking garages) for Morse-code communications [4-5] and for imaging purposes [6-7], but these studies have not utilized typical room environments. This research aimed to develop covert extraction techniques of the calibration signal required for successful TR communications and to determine the range of applicability and limitations of using TR to communicate private, audible speech in various environments.

It was found that private communications are possible in a typical conference room. Speech-like sounds could be heard at all locations in the room but observers of a live demonstration of the focusing could not understand the speech unless they were at the target location. It was also found that several types of signal processing methods could be used to further mask the intelligibility of the speech without destroying the ability to communicate to the desired focal location. Proof of concept of communicating to a target inside a room with the equipment outside the room was also accomplished.

One major focus of this work was to develop covert means of extracting the calibration signal necessary for successful communications in clandestine operations. One of the methods proposed and studied was to record ambient noise present in the room of interest and record that noise at the location of both where the transmitting sources would be placed and at the intended, target location.

Scientific Approach and Accomplishments

A set of proof of principle demonstrations of private speech communications was conducted using four loudspeakers, a microphone, and a laser vibrometer setup in a conference room (see Figure 1). To start with, successful private communications were demonstrated by placing the loudspeakers inside the room along with using a microphone for the calibration. A demonstration of simultaneously focusing two speech signals to two

different locations was also done (see the first video demo at Ref. [8]). Further, we showed that a masking white noise could be added to the TR broadcast to mask the speech at most locations in the room but allow the target location to still understand the speech (see the second video demo at Ref. [8]). Private communications were also made with the loudspeakers placed outside the room (along a wall with several windows) and by using a microphone for calibration (see the third video demo of focused pulses at Ref. [8], listen for the pronounced pop at the microphone location). Then communications were demonstrated using loudspeakers and a laser vibrometer in the same room (see the fourth video demo at Ref. [8]). In this case the laser was used to remotely obtain the calibration signal to focus sound that one could hear at or near the location where the laser was shining.

Figure 1. Photographs of the conference room setup used for demonstrations of audible private communications. (a) Photo of two of the loudspeakers used and the microphone placed at a seat location. (b) Photo of a small laser spot shining on a white board above a chair with an outline of a hostage drawn on the board (note that the microphone was placed at the same location in order to record what one would hear at that location.

To explore the idea of using ambient noise to extract the calibration signal, measurements were conducted in the facilities at Brigham Young University (BYU) by the project's Principle Investigator (PI). Two microphones were setup in a large reverberation chamber to record 40 seconds of white noise that was broadcast from a loudspeaker (see Figure 2). The time-synchronized recordings of the noise were cross correlated. The cross correlation response has two halves which, according to ambient noise signal extraction theory, should be identical if the technique is performing well. These two halves were summed to provide the calibration signal. To determine the quality of the extracted calibration signal from ambient noise, a loudspeaker was placed at one of the microphone locations and the calibration signal between the two microphone positions could be obtained as a direct reference calibration signal. Figure 3 shows the comparison of these two results. One issue with obtaining the direct reference calibration signal is that the loudspeaker and microphone could not be co-located. Thus one might expect a delay in the reference calibration signal, which is indeed seen when comparing peaks in Figure 3 (arrows added to identify delays). The respective delays of each arrival of sound (peaks in the signal) will depend on the path orientation relative to the path distance between the loudspeaker and microphone that should be collocated. Qualitatively, the extracted calibration signal from ambient noise matches the direct reference measurement well, though the true quality of the ambient noise extraction cannot be determined due to the imperfect nature of the direct reference measurement (source and receiver could not be co-located).

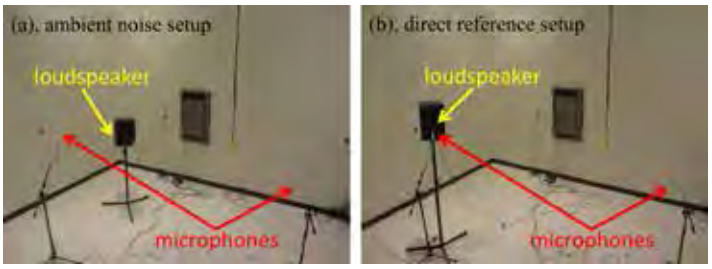

Figure 2. Photographs of the reverberation chamber used for ambient noise extraction of the calibration signal. (a) Setup used to extract the calibration signal from ambient noise. (b) Setup used to extract the calibrations signal directly between the microphones.

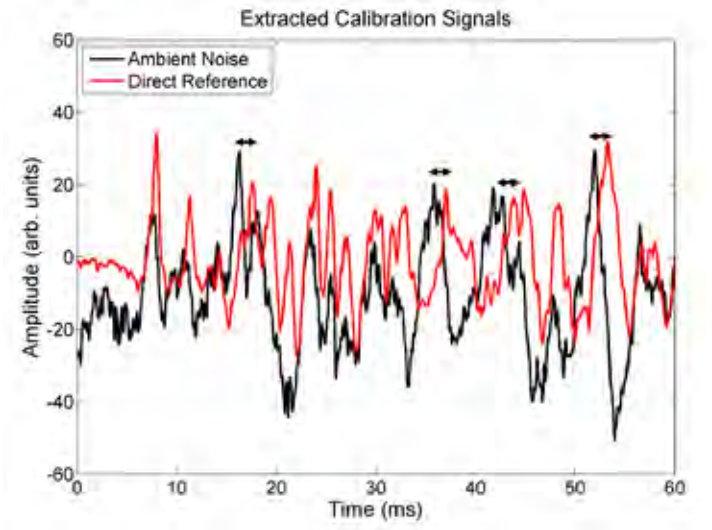

Figure 3. Sample calibration signals extracted from ambient noise and using a direct measurement setup. The ambient noise signal was extracted using the setup pictured in Figure 2(a), while the direct reference signal was extracted using the setup pictured in Figure 2(b).

The inability to co-locate the source and receiver does not only pose a problem with determining the quality of the proposed ambient noise signal extraction, but also for the practical implementation of the extracted signal in applica-

tions. Further work is needed to determine how the source and receiver may be co-located or whether a reversible source/receiver transducer may be used. Once this issue is resolved, one can explore the quality of the ambient noise signal extraction versus the length of recording time, the number of noise sources used, and/or the environmental conditions of the room (i.e. room size, and acoustical properties). While the ambient noise calibration signal extraction technique showed promise, it was not conclusive and further work needs to be done.

In FY13, the PI received LDRD Reserve Funding to study time reversal vibrational communications. The work completed provided proof of concept but it was not carried through to the point where a journal aricle could be published. The experiment utilized an 8.10 m long pipe system with 12 junctions and a 3 m portion encased in concrete. A single shaker source was mounted to one end of the pipe system with a triaxial accelerometer on the other end. In this project, the PI conducted improved measurements and presented the work at an Acoustical Society of America conference and submitted a journal article for peer review in the Journal of the Acoustical Society. Figure 4 shows how individual communication signals may be independently transmitted to any of the 3 channels of the accelerometer, allowing at least three channels of independent, simultaneous communications between a single source and a single receiver.

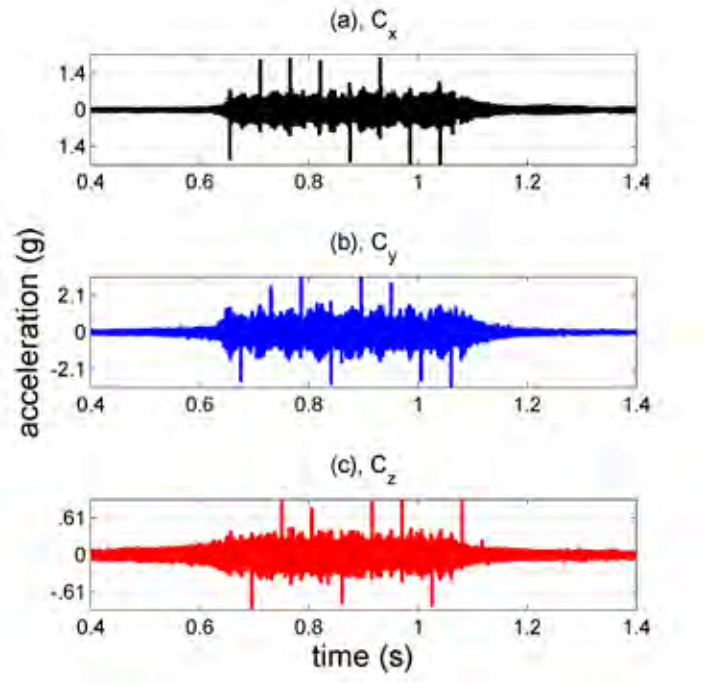

Figure 4. Sample signal transmissions from one source to one 3-axis receiver. Each subplot represents the signal transmitted to each axis of the 3-axis receiver. The transmitted signals are the ASCII representations of the letters "t", "l", and "m".

Impact on National Missions

Secure acoustic communications are important to global security (GS) needs and this work has generated discussions with GS program managers, as Dept. of Defense customers are looking for technologies to allow them to communicate with acoustic or vibration signals in situations where wires and radio communications are not feasible or not desired.

This work provides a significant research advance for energy resource extraction technologies. Our experiments on vibrational transmissions using time reversal have shown communication rates of at least 20 kbit/s and perhaps even 1 Mbit/s. Additionally, this research provides a means to communicate monitoring information through sealed nuclear reactor vessels and storage casks for safe operations and reliable storage of spent fuel.

References

1. Anderson, B. E., M. Griffa, C. Larmat, T. J. Ulrich, et.al. Time reversal. 2008. Acoustics Today. 4 (1): 5.

2. Parvulescu, A., and C. S. Clay. Reproducibility of signal transmission in the ocean. 1965. Radio and Electronic Engineers. 29: 223.

3. Song, , and Badiey. Time reversal acoustic communication for multiband transmission. 2012. JOURNAL OF THE ACOUSTICAL SOCIETY OF AMERICA. 131 (4): EL283.

4. Candy, J. V., A. W. Meyer, A. J. Poggio, and B. L. Guidry. Time-reversal processing for an acoustic communications experiment in a highly reverberant environment. 2004. JOURNAL OF THE ACOUSTICAL SOCIETY OF AMERICA. 115 (4): 1621.

5. Ribay, G., J. de Rosny, and M. Fink. Time reversal of noise sources in a reverberation room. 2005. JOURNAL OF THE ACOUSTICAL SOCIETY OF AMERICA. 117 (5): 2866.

6. Harker, B. M., and B. E. Anderson. Optimization of the array mirror for time reversal techniques used in a halfspace environment. 2013. Journal of the Acoustical Society of America. 133 (5): EL351.

7. Mimani, , C. J. Doolan, and P. R. Medwell. Multiple line arrays for the characterization of aeroacoustic sources using a time-reversal method. 2013. JOURNAL OF THE ACOUSTICAL SOCIETY OF AMERICA. 134 (4): EL327.

8. Anderson, B. E.. Video demonstrations of time reversal acoustic communications in a conference room. 2013. LAUR-13-27841.

Publications

Anderson, B. E., T. J. Ulrich, P. Le Bas, and J. A. Ten Cate. Three dimensional time reversal communications in elastic media. Journal of the Acoustical Society of America.

Time Resolved Phonon Spectroscopy for Cryogenic Bolometer Readout

John J. Goett III
20140200ER

Introduction

As the focus of experimental research moves to rare events beyond the scope of the standard model, it has become increasingly apparent that new technologies with improved background discrimination and reconstruction capabilities are needed to advance the field. Here we outline the first steps of an aggressive push into detector development that seeks to fill the gap that has left particle instrumentation largely divorced from advances in materials science and chemistry. Though bolometers have been successfully operated as sensitive thermometers, the physical phenomena underlying their effectiveness is heat propagation via phonon interactions within the bulk of the absorbing crystal. The details of phonon propagation have not been exploited in bolometric techniques. This proposal details the prerequisites for a program in phonon spectroscopy in radiation detectors with a fast readout device. Demonstrating our ability to measure these underlying processes will open the doors to a precision era in low-energy nuclear physics. In particular, as DOE-NP determines the best approach for a large-scale, double-beta decay experiment, the development of this technology will increase the LANL portfolio of capabilities applicable to that program.
Benefit to National Security Missions

A high resolution calorimeter with good discriminating ability and high throughput has applications that extend beyond a fundamental physics program. By constructing a well counter from high purity macro-bolometers with phonon readout one could perform non-destructive assay of materials extending beyond gamma spectroscopy. At present, a comprehensive assay of a material requires choosing between time consuming counting with a variety of techniques ranging from high purity germanium detectors and barrier silicon detectors which force a compromise between either small active area/long count times or high background; or destructive methods such as mass spectroscopy, neutron activation analysis or more comprehensive radio-chemical techniques. Developing the capability to monitor materials for all decay products in a single setup will streamline procedures for researchers working in environmental science and the non-proliferation/ treaty verification fields. Perhaps the greatest relevance to non-proliferation programs will lie in the separation of alpha peaks without resort to destructive assay. The detectors might also have higher efficiency but maintain the excellent low-energy x-ray resolution of smaller bolometers.

Progress

In year two we have made progress in each of our planned goals. We now have a laboratory space to support cryogenic work with an operating cryostat, along with the necessary electronics and control systems in place to take bolometric measurements. In collaboration with our colleagues at NIST, we have determined the formula for AlMn transition sensors, and have a clear path forward for growth on the crystal bulk. We believe we are on track to begin crystal measurements in late 2015 and early 2016.

We took delivery of the SQUID electronics and control hardware in the middle of the first quarter. Our initial effort was focused on operating the warm electronics in a ‘dummy-mode’ where a transistor array was set up to simulate a SQUID circuit. In this manner, we developed a slow control application for adjusting the voltage or current bias without risk of damaging the sensitive devices.

In tandem with the software development, we resumed commissioning and refurbishment of the dilution refrigerator unit. We ran extensive vacuum checks and eliminated a number of very small leaks discovered early in testing. In addition we designed and constructed a large anti-vibration stand suitable for small bolometric measurements. We produced an IWD for the recharge of the compressor and general cryostat operation and demonstrated a successful cool-down to 4K. Following the

cool down, we designed, fabricated and installed custom cable feedthroughs to route signals from the cold stage to the warm electronics. Following the installation we were again successful in cooling to 4K and demonstrated good temperature stability for an 11 day run. This alleviates concerns that the cable mass we were routing to support the multi-sensor measurement would introduce an unacceptably large heat load on the crystal.

In collaboration with our colleagues at NIST, we characterized a first run of AlMn transition edge sensors in a variety of geometries grown on a conventional silicon substrate. The initial tests indicated a slow superconducting transition at a higher than expected temperature. With discussion and a variety of tests, we concluded the difficulty was due to a thick shadow mask, which introduced thickness variations(and thus current irregularities) in the AlMn along the edge of the mask. This was simply solved by introducing a new shadow mask, which eliminated the variations. Initial measurements were completed in Boulder, and confirmatory measurements here at LANL are imminent.

The final two elements needed to operate the TESs and SQUIDS at base temperature here at LANL are superconducting shielding for the SQUIDS and a nitrogen cold trap to purify the helium mash before circulation. Designs for both these parts have been completed, and at the time of this report, are out for bid on fabrication.

Future Work

This work is planned to take place over three years. During years 1 and 2 we will prepare a facility where bolometric measurements can be made, and with our collaborators develop the necessary expertise to grow AlMn transition edge sensors directly onto a crystal bulk. In the 3rd and 4th quarter we will characterize initial runs of AlMn sensors and exercise our full DAQ and slow control chain.

In the third and final year of our program, funds will be allocated to a production run of AlMn transition sensors and a measurement campaign with multiple sensors deposited on the crystal bulk. These data will serve the dual purposes of demonstrating the utility of the focusing phenomenon in background discrimination and validating the simulation framework developed in years 1 and 2.

Conclusion

During the 3-year span of this proposed effort, we plan to determine the effectiveness of using multiple sensor readout of a bolometer for energy deposit localization and assess its utility for background reduction.

Measuring Winds in the Stratosphere Using Passive Acoustic Sensors

Omar E. Marcillo
20140237ER

Introduction

The fundamental goal of this project is to test the hypothesis that measurements of low-frequency sound from ocean surface wave collisions (microbaroms) recorded by multiple ground-based acoustic sensors at distances of several thousands of kilometers can be used to accurately measure winds in the stratosphere. In a pilot study we have already demonstrated that our methodology can estimate winds in the stratosphere using transient sources. Following these results we have identified a fundamental opportunity: to apply this inversion methodology to the continuous and ubiquitous acoustic background noise would allow us to measure the evolution of stratospheric winds everywhere without the need of an active source.

Three fundamental aspects are required to migrate from a transient to a continuous source for the inversion:

- infrasound noise from microbaroms is smaller in amplitude and peaks at lower frequencies than signals from discrete explosive sources; we need to refine our data analysis methodology,
- we need to validate our inversion results using an independent technique, and
- we need to formally quantify uncertainty of our measurements and predicted wind values. This project will develop and validate a stochastic method based on inverting low frequency acoustic signals from microbaroms, recorded on multiple ground sensors, to continuously track wind in the stratosphere. We will validate our technique by co-locating a specially-designed infrasound network with the only LIDAR system capable of reliably recovering wind and temperature from the stratosphere and mesosphere, which is located in Northern Norway.

Benefit to National Security Missions

The anticipated result from this project is a robust, validated method for measuring winds in the stratosphere using low frequency sound from ocean storms. If successful, we could measure the winds in the stratosphere anywhere over land at low cost with implications for a number of existing programs at LANL. The joint DOE/NSF Community Earth System Model (CESM) is one of three US IPCC-class climate models for which LANL personnel in T-3 and CCS-2 currently play an active research role. The CESM model includes an atmosphere configuration that extends to the thermosphere. Of particular interest for the stratosphere dynamics are effects of the ozone layer, which plays a key role in radiative interactions as well as gravity wave drag (a sub-grid scale phenomena that plays an important role in atmospheric dynamics). Furthermore, the availability of direct wind measurements in the tropics may be particularly important, due to the known inaccuracies of the thermal wind equation for the region. Our results also have implications for NASA programs and warfighter support and have potential implication for improving GPS accuracy through improved correction for stratospheric effects. Improved specifications for atmospheric winds also have an important implication for Global Security: because stratospheric winds influence the propagation of infrasound signals, our results can improve infrasonic location and yield estimation for nuclear tests as well as improve predicted dispersion of radioactive aerosols, which can reach the stratosphere.

Progress

The last 12 months of this project have been very successful as we finalized the deployment of the sensor arrays for the NORwegian StratospherE (NORSE) experiment in northern Norway during April, 2015. This successful deployment involved great logistical efforts from Los Alamos National Laboratory and the Alomar Observatory in Norway to install and maintain four infrasound arrays for 12 months in a very harsh environment. This deployment and data acquisition was the main task for year 2 of the project. We have been receiving data

from the network every three months and performed data preparation and quality control. Using data obtained during the initial phase of the Norway deployment (2 weeks in November, 2014), we have written and submitted a paper to the EOS Transactions AGU Journal focusing on the deployment of the network and its potential for atmospheric studies: "The NORwegian StratospherE (NORSE) experiment: Turning Low-Frequency Coherent Acoustic Noise into Signal" by Arrowsmith, Marcillo, et al. This article has helped us publicize our efforts so other institutions (e.g.: NORSAR, the Norwegian seismic center) are aware of our network design and preliminary results. Also, using the data from the initial phase of the Norway deployment we were able to identify and study acoustic signals generated by a rocket launched in close proximity to one of our network nodes. We studied the related infrasound, modeled its propagation, and submitted a scientific article that is currently under review at the Journal of Acoustical Society of America Express Letters. The article highlights the potential and implications of obtaining information about rockets (e.g.: trajectory, number of stages and type of engine) using acoustic observations: "Analysis and modeling of infrasound from a four-stage rocket launch" by Blom, Arrowmisth, and Marcillo. We have also refined the inversion framework in order to apply the method to both transient and continuous infrasound. An article discussing the extended framework and a theoretical evaluation of its stability is currently being revised for publication in the Geophysical Journal International: "A statistical framework for monitoring variations in the stratospheric winds using infrasonic signals" by Blom, Marcillo, and Arrowsmith.

We also completed the analysis of the data of our first network prototype deployed in Albuquerque, NM. With this dataset, we were able to identify and model infrasound produced by nearby wind farms in NM. We found that these infrasound signals can propagate several 10s of kilometers in the lower atmosphere under certain conditions. We wrote a scientific article for the Journal of Geophysical Research Atmospheres on the analysis of this source and its potential for applying the same methodology we are exploring to extract winds in the stratosphere to retrieve boundary layer and tropospheric winds and temperature: "On infrasound generated by wind farms and its propagation in low-altitude tropospheric waveguides" by Marcillo, Arrowsmith, et al. This result has very important implications for near-surface atmospheric interactions and boundary layer physics. This paper was accepted for publication and will be published in the next few months.

Future Work

In year three, we will complete the research for this project by finishing the data collection and analysis of our Norway network. By April 2016, we will complete the collection of one year of data from our Norway deployment. We will write a report on the quality of the data and the seasonal variability of the characteristics of the microbaroms signals. We also plan to complete a modeling study of the propagation of infrasound over long distances from microbaroms sources, using both geometric and full-wave methods, that was begun in year one.

The main goal for year three is to apply our inversion methodology to estimate winds in the stratosphere and validate the results against the measurements from the LIDAR facility. We will first apply a refined time-series analysis on each array and measure the inter-array coherency of microbaroms for multiple propagation distances. With the coherency results, we will apply our inversion methodology to estimate stratospheric winds. These estimations will be validated using the direct measurements of wind from the ALOMAR LIDAR facility. We expect at least one journal paper on the data analysis and the inversion. Also, Northern Norway features a variety of continuous (aurora) and discrete (rockets launches and mining explosions) acoustic sources that we expect to record with our network. We anticipate having at least one additional publication on the identification and characterization of these other sources.

Conclusion

The main expected result is a validated and operational ground-based technique that is capable of providing measurements of wind in the stratosphere from measurements of the continuous and ubiquitous acoustic background noise. This technique can be exported anywhere on Earth and does not require a known source, enabling us to track the wind continuously. We envisage this research to provide material for several peer-reviewed publications. As our main research result will be truly innovative and transformational, we expect our research to be suitable for a high-profile broad-audience journal, i.e., Nature or Science.

Publications

Arrowsmith, M., S. Arrowsmith , and O. Marcillo . The NORwegian StratospherE (NORSE) experiment: Turning Low-Frequency Coherent Acoustic Noise into Signal. To appear in EOS Transactions AGU.

Blom, P., S. Arrowsmith, and O. Marcillo. Analysis and modeling of infrasound from a four-stage rocket launch. Journal of acoustical society of America.

Marcillo, O., S. Arrowsmith, P. Blom, and K. Jones . On infrasound generated by wind farms and its propagation in low-altitude tropospheric waveguides. 2015. Journal of Geophysical Research: Atmospheres. : 1.

Matter Wave Circuits

Changhyun Ryu
20140362ER

Introduction

The goal of this project is to create the de Broglie wave analog of an integrated optical circuit, a device that might be called a matter wave circuit. In this technology, coherent atomic matter waves from an integrated source are guided and manipulated in confining potentials in much the same way that laser light propagation is controlled in a wave-guide photonic circuit. The push to develop matter wave circuits is motivated by several important differences between matter waves and light waves: atomic velocities can be controlled over a wide range; atoms can be brought to rest and trapped; atoms feel gravity and electromagnetic fields; atoms can interact strongly with each other; and atoms can be imaged with high efficiency. These characteristics enable matter wave circuit applications to sensing (particularly interferometry) as well as to quantum information processing, quantum atom optics, and emulation of transport problems in condensed matter systems.

This promise motivates our proposal to realize the first matter wave circuit. We will confine de Broglie waves from a Bose-Einstein condensate (BEC) in waveguides and manipulate them with optical elements, all created using LANL's unique "Painted Potential" capability. This technique creates arbitrary and dynamic time-averaged optical dipole potentials compatible with the very low energy of a BEC.

Benefit to National Security Missions

Atoms lie at the heart of some of the best technologies for measuring time, detecting rotations, and processing information on quantum computers. The atom optical technology that we will develop during this project supports Laboratory missions in Sensing, because the atom circuit technology is relevant to rotation sensing, and in Information Science and Technology, because matter wave technology in general is relevant to quantum information processing. These applications in sensing and quantum information processing are of interest to external sponsors in the intelligence and defense communities.

Progress

During the first year of the project, we realized various circuit elements for matter waves such as a straight waveguide, a circular bend, a closed stadium waveguide, and a Y-junction. In addition, a coherent splitting of matter waves through a Y-junction was demonstrated for the first time. To continue the success of the first year, we need to accomplish two tasks during the second year. First, a new Bose-Einstein condensate (BEC) setup for 39K needs to be built because many applications in matter wave circuits require varying interaction strengths, which can be achieved thorough magnetic field tuning with 39K. Second, simulation of matter waves in various waveguides is necessary to design complicated matter wave circuits and to find the right parameters for the experiment. During the last year, we have been working on these two main focuses.

To achieve a 39K BEC, we need several key elements: a vacuum chamber and pump capable of reaching the pressure of 10-11 torr, a laser system for cooling 39K atoms, and various electro magnets with magnetic field up to 500G. After careful design, the vacuum chamber was put together and sources for various alkali metal atoms were installed. After a few weeks of baking of the chamber, the vacuum inside is now 4×10-11 torr, low enough for the experiment. The lasers for the cooling of 39K atoms were purchased and tested, including coupling of various beams into single mode optical fibers to minimize fluctuation of the beam position. Several electro magnets were made and the magnetic field was measured to be in agreement with the calculation.

After successful completion of these steps, we started tests to achieve a 39K BEC. Because of the very low

pressure needed for a BEC production, the source chamber and the BEC chamber have to be separated to ensure large differential pressure. In the source chamber we achieved a magneto-optical trap (MOT) of 39K atoms, with the number of atoms as high as 3×109. From this MOT, atoms were pushed to the BEC chamber with a push beam. The MOT at the BEC chamber was also achieved. Currently both MOTs and transfer process are being optimized. We expect this process will be done within a month and the BEC of 39K atoms should be possible within the next 3 months.

Another major focus was the simulation of matter waves in various waveguides to determine experiment parameters for 39K atoms. One of the most interesting circuit elements is a cavity for matter waves. Although theoretical study was done before, there has been no experimental demonstration of a matter wave cavity. Since this is unexplored before, it is necessary to study the dynamics of matter waves with a cavity to understand the basic physics and to find the correct parameters for the experiment. The first problem we studied was the coupling of matter waves into a cavity. Here we found that without interaction, a high coupling efficiency is possible. Also by varying the length of the cavity, the variation in coupling which is clear signature of a cavity dynamics identical to optical cavity was shown. Another simulation study we did was the study of shortcuts to adiabaticity. Here the question is how fast we can change a trap for atoms without creating excitations compared to the adiabatic process. With this technique, it is possible to move and expand matter waves with much faster speed and the simulation was done to find the correct parameters for that. It was shown that with our set up various processes including expansion and movement of a BEC can be sped up.

The construction of a 39K BEC set up and simulation of a matter wave cavity and shortcuts to adiabaticity will be foundation for the work which will be done in the third and final year of the project. During the third year, we will focus on matter wave cavities. A 39K BEC with varying interaction strength will be used to study matter wave cavity dynamics. The demonstration of matter wave cavity will be a truly exciting development and our work will start a completely new research direction.

Future Work

In the first year of the project, we realized several basic matter wave circuit elements such as a straight guide, a circular bend, a stadium waveguide, and a Y-junction. Another important achievement is the coherent splitting of matter waves through a Y-junction. In the second year, we built a Bose-Einstein Condensate (BEC) set up for 39K atoms. This will make it possible to tune the interaction strengths for various matter wave circuit experiments. Simulation of various waveguides was done to design future experiments and find the right parameters for the experiment.

During the final year of the project, we plan to focus on studying physics of matter wave cavities. Here two mirrors for matter waves will be placed to form a cavity for atoms. Although there is some theoretical work, no experimental demonstration of matter wave cavity has been done. To study this, it is essential to be able to control interaction strength. From the simulation study, we found that the coupling efficiency gets much worse with interaction. To increase the coupling of atoms into a cavity, it is necessary to have zero interaction which is possible with 39K atoms through magnetic field tuning. Another interesting regime to study is the large interaction limit with a cavity. Here it is predicted that atoms leaving a cavity will have non classical distribution and we can reach this regime with the same magnetic tuning technique. With these studies, we will demonstrate the experimental realization of matter wave cavities for the first time and this will open the new research direction of matter wave cavity physics.

Conclusion

The overall goal is to demonstrate for the first time analogs of optical fibers and integrated laser sources with cold atoms. Specific technical goals include: (1) launching coherent matter waves into a single mode of a non-trivial waveguide geometry at controllable speed, (2) demonstrating the matter wave analog of a distributed Bragg reflector, and using two such optics to create a matter wave resonator, (3) demonstrating a “Y” beamsplitter by adiabatically deforming a single waveguide into two guides. Success will deliver new levels of control over atoms to important applications in sensing and information processing.

Publications

Campo, A. del, M. G. Boshier, and A. Saxena. Bent waveguides for matter-waves: supersymmetric potentials and reflectionless geometries. 2014. Scientific Reports. 4: 5274.

Ryu, C., and M. G. Boshier. Integrated coherent matter wave circuits. 2015. New Journal of Physics. 17 (9): 092002.

Chemical Shift Signatures of Nuclear Material: 235U and 239Pu NMR Spectroscopy

Michael T. Janicke
20140396ER

Introduction

The crux of this research is the development of low frequency Dynamic Nuclear Polarization Enhanced Nuclear Magnetic Resonance spectroscopy (DNP-NMR, imagine a MRI instrument for chemistry studies with 1000 times increase in signal to noise). DNP-NMR spectroscopy will be a tool for detection of 235U and 239Pu chemical shift signatures, monitoring the origin, fate and transport of these contaminants, and the bioavailability of such species in the environments. Much of this project will focus on 239Pu but work will be easily extended to the more challenging 235U in relation to using NMR as the most steadfast method for differentiating and quantifying molecular species.

This proposed research project will demonstrate that we can increase the sensitivity without increasing the sample size or experiment time and get the equivalent sensitivity to a commercial multi-million dollar instrument for a fraction of the cost. We will accomplish this by using DNP-NMR. At LANL we have demonstrated use of DNP at very low magnetic fields (10 mT) without cooling the samples to liquid helium temperatures via the Overhauser effect. In this approach, electrons spin transfer to nuclei is enhanced by microwave irradiation. Using this method we achieved ~ 100-fold polarization enhancement, followed by NMR signal readout at very low frequencies. A published system also based on relatively low magnetic field and without cooling the samples to liquid helium temperatures has been demonstrated for the relatively easy 1H isotope for roughly $100,000. However this system cannot measure low frequency nuclei such as 235U and 239Pu. With this low-cost instrument, the research group is achieving 1H enhancements of greater than ~ 100, as well. Combining the DNP with our demonstrated expertise at ultra-low field we anticipate for 235U and 239Pu the signal improvement will be >1000-fold compared to routine NMR techniques.

Benefit to National Security Missions

Plutonium has one of the most complex chemistries of any element. The shear diversity and unique chemical properties that Pu exhibits are ideally suited for Nuclear Magnetic Resonance (NMR) and for this reason this project aims to develop a new chemical signature, the 239Pu NMR chemical shift. Chemical shift is the change in NMR signal frequency from a known standard set at 0 ppm arising from local magnetic fields produced by the electron distribution. It is a direct measure of the bonding environment around specific nuclei and gives rise to the sensitivity of NMR chemical shift spectroscopy to chemical species. Analytical methods such as elemental analysis or detection of fission products (neutron, gamma, or beta) do not reveal the chemical species or its origin. Complex samples with multiple species cannot be analyzed using traditional methods, as they will inevitably have overlapping results that require precise use of model compounds and accurate computational methods for deconvolution. NMR presents us with the most accurate and quantitative method where differences in species will result in distinct chemical shifts. But due to the complexity of 239Pu NMR and plutonium chemistry, the NMR signature of 239Pu was only published in May of last year. This same basic technique can be expanded to include additional chemical, nuclear, and environmental threats that have chemical signatures and NMR active elements including 13C, 15N, 19F, and 31P and numerous heavy metals. Thus this project supports our national security mission from nuclear weapons to threat reduction and environmental monitoring/cleanup.

Progress

At the end of the first year, the ultra low field (ULF) dynamic nuclear polarization (DNP) nuclear magnetic resonance (NMR) platform had been commissioned with promising initial measurements of a water signal (task 1). Utilizing an air cored electromagnet, a DNP enhancement factor (that is, signal increase) of 20 was

seen with water, leading to signal to noise ratio (SNR) of 200, and a spectral resolution of 70 Hz. While promising for a prototype, higher SNR and better spectral resolution are needed to perform spectroscopic measurements on solutes. Improvements to the system were undertaken to achieve the year two goals. A conventional high field measurement was attempted on plutonium (IV) chloride sample, but no 239Pu NMR signal was observed in year 1. Continuing efforts on Pu (IV) and Pu (III) samples have also not been successful.

The two tasks for year 2 are as follows:

1. Validate a high field 239Pu NMR spectrum in the ULF system, developing chemical signatures
2. Develop the DNP protocols (polarizing agent optimization, probe refinements, etc)

In pursuit of these goals, we improved the performance of the ULF DNP NMR system substantially. We increased the spectral resolution by a factor of 70 by upgrading the electromagnet and through the addition of shimming coils to produced higher magnetic field uniformity, as well by reducing the size of the sample. In addition, we were able to increase the SNR from 200 to 500 for a water sample.

These improvements are critical for the accomplishment of the year 2 tasks. Although measurement of a 239Pu signal seems less likely in the absence of a result at high field, we are in the midst of measuring the NMR signal from a number of low sensitivity nuclei such as 199Hg and 125Te to fulfill task 2. This will pave the way for measurements of a wide variety of difficult, low sensitivity nuclei that are generally not accessible to a fieldable system that is available off the shelf.

As an intermediate step to task 1, we were able to explore if the current ULF DNP NMR instrument could be used to measure J coupled spectra as a possible novel signature for chemical threat agents. We have measured the ULF DNP NMR spectrum of isopropyl methylphosphonic acid (IMPA) in deuterated water, resolving the J couplings, which are field independent couplings that split the NMR spectrum according to the number of bonds between the nuclei. IMPA is of particular interest because it is a hydrolysis product of sarin gas; the potential to field this system makes such measurements especially interesting in the context of rapid diagnostics after a chemical weapons event. Discussions are ongoing with programmatic sponsors to build a program around this interesting method.

We are currently in the midst of a probe upgrade that will boost SNR enough to measure signals from dissolved metal species such as 75As or 199Hg. The new probe boosts signal by improving the filling factor of the NMR coil substantially, as well as the efficiency of the DNP process by optimizing the resonator design. Measurements with low sensitivity nuclei will commence following the completion of the upgrade. This work fulfills both task 1– acquiring signals from low sensitivity nuclei with adequate resolution for signature development, and task 2 – Improvement of the DNP process through refinement of the probe hardware.

Using the expertise we have gained in the optimization of the ULF system, we will begin to implement DNP at intermediate field with an iron-cored electromagnet and X-band (~10 GHz) cavity resonator for DNP. We possess the magnet and electronics necessary to perform NMR in this regime.

Future Work

In the first year we will have completed our first task, construction of our platform for detecting Nuclear Magnet Resonance (NMR) signature of chemical species (non-radioactive surrogates) with similar properties to 239Pu. We are on track for this.

In the second year of the project we will focus on Tasks 2 and 3 as defined in the proposal. Task 3 will extend into the third year of the project.

Task 2: Test and optimize our NMR instrument for 239Pu using a known PuO2 sample. We will validate and extend results with conventional high-field NMR (available at LANL or PNNL) and our new system (i.e. methods for handling short T1; methods for increasing temperature from 4K to room temperature). The advantage of this approach is significant reduction in magnet cost, complexity, and expense. Further, the compatibility with microfluidics means sample preparation and delivery can be done “on board” and without significant handling and sample minimization. High field NMR validation months: 1-6; Signature extension/ measurements in new system Months: 12-24.

Task 3: Develop protocol for dynamic nuclear polarization enhanced NMR (DNP-NMR) for sensitivity increase. This task includes instrument development and identification of free radical species for polarization transfer (ie. 2,2,6,6-Tetramethylpiperidin-1-yl)oxyl referred to as TEMPO, a water soluble, stable free radical benchmarked in many DNP-NMR studies) Months: 18-30.

Conclusion

The lower bounds of the frequency range for metals might

not be reached; however, there are other organic compounds containing 13C, 15N, 19F, and 31P that will be made accessible for DNP-NMR analysis that do not have these complications and have equal if not greater need for detection and forensics for chemical and biological agents. In other words, if we are not successful in analyzing metal speciation, the instrument will already have succeeded in measuring important organic compounds. Additionally, if we meet the challenges above, we will have an R&D 100 candidate, commercialization and licensing possibilities, and a portable instrument.

Solid-State Gamma-Ray Detectors Based on Quantum Dots

Jeffrey M. Pietryga
20140406ER

Introduction

The threat posed by the proliferation of illicit Special Nuclear Materials (SNM) is especially grave as they carry the potential for disaster in dangerously small packages. Hidden SNM can be found and identified by detection of the characteristic gamma radiation it emits, but this type of screening becomes quite complicated in real scenarios. Detectors at high-traffic border crossings, for example, must be able to distinguish SNM from a range of benign gamma-ray sources that are a part of ordinary commerce by determining the energy of gamma-rays with high precision, while sampling a large area at a very high rate of throughput. Unfortunately, current technologies cannot meet this need.

We propose to develop a new class of solid-state gamma-ray detectors based on cheap, solution-synthesized semiconductor nanocrystals that will offer a new standard in combined performance, low-cost and adaptability.

In this project, we will fabricate gamma-sensitive diodes based on semiconductor nanocrystals synthesized by low-cost, scalable chemical methods. Although these nanometer-sized bits of semiconductor materials exhibit extremely useful size-tunable electronic and optical properties, for most of their history nanocrystals had been considered ill-suited to applications in electronic devices (like diodes) because of the difficulty in achieving high electrical conductivity when they are assembled into thin films. Recent developments have cast that perception aside, and there are now numerous ways to make device-ready conductive films of nanocrystals that exploit their unique properties without sacrificing their advantages in cost and scalability. We propose to extrapolate this recent progress to an unprecedented degree to enable a new class of gamma-ray detectors. We will then probe their response to high-energy radiation, and optimize both the nanocrystals and the architecture to maximize energy resolution, with the ultimate goal of realizing performance on a par with current, much more expensive and less scalable technologies such as single-crystal gamma scintillators.

Benefit to National Security Missions

The guiding goal we have chosen for this work is to make gamma-radiation detectors that are comparable to gamma scintillators in energy-resolving performance, but much cheaper and easy to scale to portal-relevant detector sizes. The tie to nonproliferation-involved agencies, as well as to any other agencies (Defense or Intelligence) interested in detecting the presence of nuclear materials, is clear. The flexibility of our new detector class would easily make them adaptable to needs in nuclear reactor/facility monitoring, and radioactivity-related environmental remediation efforts. It is quite likely that specific needs of space science (gamma spectroscopy) and satellite surveillance could ultimately be met by the proposed class of detectors. Such sensors could also be of interest to materials scientists for use in various types of radiography, and to the medical field as cheap, superior replacements for current detectors used in x-ray, nuclear, and positron emission tomography (PET) imaging techniques. Finally, because this research will advance the understanding of achieving high conductivity in nanocrystal films, it will also likely have incidental benefits to current efforts in high-efficiency solar cells and solid-state lighting based on nanocrystals.

Progress

Our three-year goal is to create a new class of solid-state gamma-ray detectors based on colloidal semiconductor nanocrystals, or quantum dots (QDs). The principal activity of this project is leveraging and expanding upon the past decade of advances in the fabrication of highly conductive films based on colloidal QDs. Successful fabrication methods not only achieve continuous, crack- and pin-hole-free films, but also result in strong coupling of QDs by removal of native organic ligands. The ligand

shell surrounding the QDs are a byproduct of their colloidal synthesis allows for solution-processibility, but serves as a barrier to the QD-QD coupling necessary for charge transport. As described in previous reports, straightforward application of known film deposition methods, which are often iterative (i.e., require a sequence of thin depositions to build up to a final desired thickness), may not be appropriate for gamma detecting devices, which require film thicknesses orders of magnitude higher those used for, e.g., light-emitting diodes or solar photovoltaics.

Initial studies in the first year bore this out. Although response to X-ray excitation was observed in a simple photoconductive device based on a film ~3-5 microns thick, there were serious limitations to the "layer-by-layer" method used. The most important were that film production was extremely tedious and prone to error (requiring many 10s of sequential dip-coat or spin-coat steps to be performed manually), actual carrier mobility was less than that seen in thinner films, and physical stability (specifically resistance to flaking or crumbling during manipulation) prevented pressing to even thicker films. In addition, because this approach accomplishes QD layer deposition and ligand-removal in separate steps, it is incompatible with advanced methods like electrophoretic deposition.

Accordingly, this most recent year saw a concerted and ultimately successful effort at developing a single-step method for replacing QD ligands without sacrificing solution dispersibility, which had been accomplished in a handful of examples for other materials but never for lead chalcogenide QDs. The key breakthrough was to combine new methods for synthesizing lead chalcogenide QDs with greater amenability toward ligand exchange, and the identification of the perfect solvent for the process. The solvent needs to be polar enough to dissolve inorganic compounds that can displace ligands (e.g., potassium iodide) and to keep the QDs dispersed after exchange, coordinative enough to promote exchange chemistry without heating and yet aprotic and non-oxidative toward the frustratingly sensitive surfaces of lead chalcogenide QDs, and possessive of a boiling point low enough to allow dip- or spin-coating of QD films directly from solution. We found that exposure of lead chalcogenide QDs synthesized using lead chloride to a 2,6-dimethylpyridine solution of any of a wide range of ionic compounds results in quantitative ligand removal and transfer of the QDs to the polar phase, often within seconds. Moreover, unlike any previous method, the QDs in polar solutions retain their efficient fluorescence, demonstrating that the treatment does not create surface defects that will ultimately impact charge transport in films. Films deposited by spin-coating from these solutions show no detectable traces of the presence of the original organic ligands, and are smooth and crack/pin-hole free. Evaluations of these films for conductivity and radiation response are already underway. We also believe this achievement will be received very enthusiastically by the larger QD device community, and we will be submitting a manuscript on its development and use very soon.

Over the past year, this project also partially supported the development of a new technique for analyzing carrier transport in QD films, which we refer to as ultrafast transient photocurrent. In essence, it tracks the decay of conductivity of a thin film after excitation by a laser pulse with ~50 ps resolution. A manuscript describing the technique in detail, and its use to solar relevant phenomena in QD thin films, has been submitted for publication. Support from this project has also allowed us to revive our dormant capability in atomic-force microscopy, which allows us to evaluate film morphology and thickness in a relatively straightforward, non-destructive manner. Both methods are critical for relatively rapid analysis during our continuing film optimization efforts.

Future Work

The next year will see us pushing the envelope of achievable film thicknesses using our new one-step deposition approach, including in conjunction with electrophoretic deposition. This single method has been determined to be the most promising and flexible among all potential alternatives, so this will be the focus of the remainder of this project. A key part of studies going forward will be careful evaluation of the effect of ligand-removal on the stoichiometry of the QDs, that is, the atomic ratio of cations (lead) and anions (chalcogenides) in the QDs after deposition. Nominally, the ratio should be 1, but because of the flexibility of a material that is dominated by surface atoms, it can vary substantially from this ideal. This is known to impact not only carrier mobility, but also carrier density in QD films, both of which need to be optimized for use in a solid-state device. This will make use of our team-owned energy-dispersive x-ray spectroscopy (semi-quantitative) and inductively-coupled plasma emission spectroscopy (quantitative) instruments. By choosing different inorganic exchange compounds, it should be possible to control the stoichiometry. The precise effect of stoichiometry on carrier transport properties will be examined by conventional field-effect transistor device studies, as well as by using our new ultrafast transient photocurrent technique. Soon after, their response to alpha, beta, X- and gamma rays will be evaluated. As described in previous reports, this seeming departure from our motivation of gamma-ray sensing (which we maintain) is actually a good way to allow studies to take place before achieving optimized films thick enough to fully stop gamma rays (on the millimeter

scale). We believe that this approach will best enable us to advance the development of practical QD-based gamma-sensors, to the point of observing and quantifying energy resolution.

Conclusion

In order to create the first gamma-sensing diodes based on nanocrystals, we will need to make very thick conductive nanocrystal films in order to capture radiation effectively. Then, we will extensively characterize how simple devices based on these films respond to radiation of a range of energies, which would be a seminal accomplishment for this completely new category of sensing technology in itself. Finally, we will optimize the nanocrystals and the device structure with the goal of achieving performance comparable to common gamma scintillators, and potentially to other types of radiation detectors used in medical imaging or materials science.

Signatures of Reactor Operations from Plutonium Production samples (U)

Anna C. Hayes-Sterbenz
20140433ER

Introduction

This is a project is to quantify a novel scheme for using fission product ratios to determine detailed reactor operations used to irradiate nuclear material. We are proposing to analyze a very unique set of irradiated reactor samples and to use our measured fission product ratios to validate the scheme. The samples in question were part of a plutonium production-testing program. Our goal is to show how fission product ratios can be used to determine the reactor flux, the irradiation time, as well as the number of times the re-actor was shut off during irradiation. As detailed below, the key ratios of interest are the xenon isotopes and their decay products, 135Cs/137Cs, 103Ru/106Ru (and their decay products 103Rh/106Pd), and 85Kr/84Kr. The project is a joint experimental and theoretical one. The experiments will concentrate on measuring the relevant fission product ratios using analytic chemical techniques and mass spectroscopy. The theoretical program will derive semi-analytic prescriptions for extracting the signatures for the reactor operation parameters. The results will be com-pared with the reactor operations declared by the facility that provided the samples. The coupling of the two components (experimental and theoretical) of the project will provide the necessary quantitative validation that is needed for practical use of the scheme in scenarios ranging from pre-detonation forensics to monitoring of reprocessing facilities.

The ability to extract reactor flux, irradiation times, and shut downs from fission products would:

- Greatly narrow the possible reactors used to irradiated fuel, in the case of seized nuclear material.
- Determine the grade of plutonium and identify undeclared nuclear blankets, in the case that fission products were released in fuel reprocessing.
- Provide new signatures for verifying reactor operations, in the case of nuclear safeguards.

Benefit to National Security Missions

Nuclear non-proliferation represents a major component of LANL's mission, and is aimed at reducing the threat posed by nuclear weapons proliferation or the illicit trafficking of nuclear materials through the long-term development of new and novel technology. The new diagnostic signatures for reactor operations proposed here directly address several components of this mission. This work is of potential interest to non-proliferation programs.

Progress

This year we analyzed several samples from the reactor. Because the samples are old (over 20 years old), many of the short-lived fission products have decayed away, necessitating the use of long lived or stable isotopes for determining reactor conditions. Xenon isotopics and daughter cesium isotopes (136Xe/134Xe and 137Cs/135Cs) can provide information on the reactor flux, while ruthenium isotopics (106Ru/103Ru or their progeny 106Pd/103Rh) in conjunction with Pu isotopics can be used to infer irradiation time. Krypton isotopics (85Kr/84Kr) can be used to determine cooling time.

Historical methods for collecting these volatile fission products (VFPs) for isotopic determination are laborious and/or hazardous, thus we sought to streamline the collection and analytical process. Using simple extraction chromatography methods followed by Inductively coupled plasma mass spectrometry (ICP-MS) and thermal ionization mass specroscopy (TIMS) analysis we determined Cs, Ru (and daughter Rh/Pd), and Pu isotopics for a set of archived reactor targets that were subjected to low burn up irradiation. We compare our results to reactor models to evaluate the usefulness of VFPs for determining reactor operations at low burnup.

Separate aliquots from the primary dissolution were taken for U and Pu isotopic and assay determination.

Chemical separations were performed using a macroporous anion-exchange (60–150 mesh, chloride form) resin using a variety of mineral acids HCl and mixed HCl-HI to sequentially elute Am, Pu, and U, thus eliminating isobaric interferences between Pu and Am, and Pu and U The total U and Pu elemental contents and the blank were determined using standard isotopic dilution techniques with 233U and 244Pu enriched spikes. Following chemistry, elutions were dried, and loaded onto filaments for TIMS analysis.

Age corrected uranium and plutonium isotope compositions as well as total Pu content are shown in Table 2. The samples are slightly depleted in 235U relative to natural uranium. Total Pu contents are low (30 to 159ppm) and the Pu is almost entirely (>99%) 239Pu. There is a strong negative correlation between 235U/238U and 240Pu/239Pu and a positive correlation between Pu content and 240Pu/239Pu. Projecting the The U 235U/238U and 240Pu/239Pu correlation to 240Pu/239Pu = 0 yields a 235U/238U of 0.0724, very close to natural U (0.0725). These data indicate that the starting fuel was likely natural U which was subjected to very low burnup.

Results from ruthenium isotopic analysis are given in Table 3. The cumulative yields of 102Ru and 104Ru are vastly different between 235U fission and 239Pu fission. For the reactor targets, the 101Ru/104Ru and 102Ru/104Ru values are consistent with burnup of mostly 235U. Samples 3 and 4 plot close to pure 235U fission. Samples 1 and 2 have higher concentrations of 104Ru relative to 101Ru and 102Ru than samples 3 and 4, indicative of more fission contribution from 239Pu. Sample 2 plots off of the tie-line between 235U fission and 239Pu fission. This suggests that this sample contains some natural Ru.

The samples range from 137Cs/135Cs of 1.30 to 2.34. These suggest the samples experienced very low burnup. There is a positive correlation between 137Cs/135Cs and 240Pu/239Pu, which is consistent with increasing burnup. Record indicate that samples 1 and 2 were irradiated for 85 hours and samples 3 and 4 were irradiated for 80 hours. Thus, with the flux and irradiation time known (i.e. fluence) we can determine the number of reactor shutdowns from 137Cs/135Cs . It appears that the reactor was shut down 3 times during irradiation of sample 2. Sample 3 does not match this model, which could be due to it being in a different irradiation location within the reactor and receiving less fluence than recorded or obtained from the archives. Samples 3 and 4 were irradiated over the same time period. They appear to have experienced 5 reactor shutdowns during irradiation, with sample 4 potentially having experienced less fluence than records show.

Future Work

The goal of the project is to measure the ratios of fission products, as well as the uranium and plutonium content, of a number of reactor-irradiated samples that were part of a plutonium production program. In FY15 we analyzed 3 of the available samples, and found that all ratios that depend on the total neutron flounce agreed well with experiment. However, for those observables that are dependent on both the fluence and flux there was poor agreement between experiment and theory. To address this problem in FY16 we plan to extend our reactor burn code to include neutron production and depletion of all isotopes of interest and their precursors.

On the experimental side of the project we propose to develop a gas handling system that will allow us to measure the Kr and Xe fission fragment products in several samples. The system for this is designed to prevent (or at least minimize) noble gas losses. In addition, we plan to measure the daughters of the ruthenium isotopes, the rhodium and palladium isotopes. Analysis of the Rh and Pd isotopes will require correcting the measured yields in the samples for the direct fission held of these, as well as their production via the beta decay of the Ru isotopes.

In FY16, we also plan to finalize and publish our analysis of the first three samples studied to date.

Conclusion

We will analyze 15 reactor-irradiated samples that are representative of a range of reactor fluxes, irradiation times, and shutdown times. The grade of plutonium will be determined for each sample and the relationship between the fluence and the Pu grade mapped out. We will expand on our theoretical methods for deducing reactor fluxes from the 136/134Xe and 135/137Cs ratios to include burn scenarios in which isotopic ratios have not necessarily reached equilibrium because of frequent reactor shutdowns. We will develop new techniques for extracting irradiation times from the xenon, krypton and ruthenium ratios, and derive the necessary inversion algorithms.

Publications

Byerly, B., L. Tandon, A. Hayes, P. Martinez, N. Xu, F. Stanley, R. Keller, M. Schappert, M. Thomas, and K. Spencer. Determination of flux and irradiation time in archived low-burnup uranium ratgets. To appear in MARC (Methods and Aplications of Radioanalytical Chemistry) 2015. (Hawaii, 12-17 April, 2015).

Mapping Relativistic Electron Precipitation: Where and When?

Steven K. Morley
20150127ER

Introduction

Earth's upper atmosphere is a major sink for highly energetic electrons in the Van Allen radiation belts. Electron precipitation has been shown to affect telecommunications and atmospheric chemistry, and plays a critical role in determining radiation belt dynamics; it is therefore a key process to understand for space weather modeling. Current detection of electron precipitation into the atmosphere is limited to direct measurements at locations occupied by satellites. A major drawback is that for the large volume of space occupied by the Van Allen radiation belts we only measure this region sparsely and so directly measuring this precipitation is done with satellites at very low altitudes. Most satellite instrumentation on these low altitude missions cannot give sufficient information to describe the changes in the main Van Allen belt electron population, nor do they provide information about the processes driving the precipitation.

We propose a new approach that will allow the first specification of the spatial and temporal extents of electron precipitation from point measurements at high altitude. In essence, we propose to combine measurements from different points on the paths that electrons take when drifting around the Earth in the Van Allen belts (drift orbits) to provide a novel remote-sensing capability. Specifically, we will use the LANL particle instrumentation on the Global Positioning System (GPS) constellation, and at geosynchronous orbit, to identify differences in the electron population along a partial drift orbit, thus "remote sensing" the loss of energetic electrons. By using the measurements of the full electron population, and some modeling of the inner regions of geospace, we will also infer key properties of the waves believed to precipitate the electrons into the atmosphere.

This approach will overcome current sampling limitations to diagnose electron losses and answer the question: Where, and under what conditions, do highly energetic electrons precipitate into the atmosphere?

Benefit to National Security Missions

This project targets understanding where, when and why highly energetic electrons are lost from the Van Allen radiation belts. In order to answer these questions we will develop a new technique for combining point measurements from a constellation of satellites to give a remote sensing capability. From this we will map regions of electron precipitation and infer key properties of the waves driving the electron loss. The specific work proposed will enable future development of models of electron precipitation and EMIC wave activity and properties. Such a capability would directly address the goals of the NASA Living with a Star program: to improve our understanding of how the sun impacts the environment in which satellites operate. While this proposal does not directly address this, these models are known requirements for ongoing Space Weather and Space Situational Awareness modeling efforts. The datasets generated will enable further basic research and applied space weather research.

Progress

The magnetic ephemeris data required to identify the magnetic conjunctions have been calculated for a significant time span for many satellites. Software implementing the novel binary tree-based technique for efficiently identifying these conjunctions has been completed and tested for a small sample of satellites over a limited time range. This work is being presented at the International Association of Geomagnetism and Aeronomy (IAGA) general assembly - a major international conference.

Preparation of the data required for the "phase space density differencing" analysis has been performed for several satellite-years of LANL geosynchronous particle data and processing is ongoing. An improved method for calculating the phase space density data from the Van Allen Probes, using additional low-energy measurements to constrain the energy spectrum, has been implement-

ed and 4.5 satellite-years of data have been processed. Validation of these data is underway, including estimation of the uncertainties on the data (which will allow us to determine the sensitivity of our technique in detecting real loss of electrons from the Van Allen belts).

Cross-calibration efforts are underway between the primary data sets: LANL geosynchronous electron data are being validated against Van Allen Probes data; electron data from the LANL particle instruments on the Global Positioning System (GPS) are also being validated against Van Allen Probes. Preliminary on-orbit comparisons between GPS and Van Allen Probes show outstanding agreement and a manuscript is in preparation for submission to the Space Weather journal. Preliminary comparisons between geosynchronous satellite data and Van Allen Probes are generally encouraging but have shown a need to incorporate recent data, that better characterizes the Synchronous Orbit Particle Analyzer (SOPA) instrument response at different energies, so that the measured fluxes are consistent between both platforms.

As part of the National Science Foundation's Geospace Environment Modeling workshop, PI Morley is a focus group convener and has led efforts to define a number of candidate events for coordinated community modeling. One category of the candidate events provides ideal conditions for testing the proposed methodology and the community modeling will provide analysis against which the results can be validated. This gives the project a head start on the tasks for the second fiscal year, and provides specific intervals for which the remaining data processing and preparation can be targeted. The class of events is rapid depletions of the Van Allen radiation belt population that occur outside of geomagnetic storms – these events have rarely been reported in the literature and so a manuscript describing these events using data from many satellites is underway.

Future Work

The goals for the second fiscal year of this project are: to finalize the data and model preparation the underly the phase space density differencing technique; develop the PSD differencing technique and software to perform routine analysis; select key intervals for preliminary analysis; generate time-dependent maps of inferred non-adiabatic processes. Manuscripts on the cross-calibrations and preliminary analyses will be prepared and submitted for publication.

Conclusion

We will develop and test a new approach to locating regions in the Van Allen radiation belts from which electrons are being lost. Our primary objective is to demonstrate that point measurements from a constellation of satellites can be combined to remote sense, and hence map, regions of loss. Our secondary objective is to use these data to infer key properties of a type of electromagnetic wave responsible for driving some of the losses. This will produce new physical understanding, enable scientific studies not previously possible and provide critical inputs for radiation belt models.

Publications

Halford, A. J., B. J. Fraser, and S. K. Morley. EMIC waves and plasmaspheric and plume density: CRRES results. 2015. JOURNAL OF GEOPHYSICAL RESEARCH-SPACE PHYSICS. 120 (3): 1974.

Exploiting Cross-sensitivity by Bayesian Decoding of Mixed Potential Sensor Arrays

Rangachary Mukundan
20150236ER

Introduction

Finding specific chemical signatures amongst a background of ordinary substances – a trace explosive signature, an illegal narcotic, a chemical agent intended to kill our soldiers on the battlefield, or civilians in our cities – remains a daunting task. Dogs can seem to handle this proverbial "needle" quite well, but what man's best friend does so well has eluded the sensor industry. Science's best solution to date is devices that use large numbers of inexpensive sensor elements (typically resistive or polymer) in conjunction with pattern recognition methods: commercial instruments based on these principles are available. However, there are significant shortcomings with the performance and capabilities of these sensor constructs, as well as significant limitations to the pattern recognition methods used to extract a meaningful signal from the data because these devices target generic applications requiring significant calibration to obtain qualitative results. The sensors at the heart of these systems are prone to drift and irreversible poisoning, blocking their use in simple, yet harsh, energy-related tasks such as monitoring vehicle emissions or smokestack pollutants. We propose to use a special class of ceramic solid-state electrochemical sensors that are intrinsically inexpensive, durable, and stable. Nobody has ever attempted to create a sensor array using these devices before. Their robustness opens the possibility of detecting a great number of gas chemistries under conditions that would quickly destroy other types of electronic noses. Our highly innovative and original solution to the specificity problem is to create a new gas sensor technology that marries unique sensor design created at LANL with a recently--developed, advanced Bayesian inference treatment of the physical model of relevant sensor-analyte interactions. Our approach is designed to quantitatively decode complex mixtures with fidelity greater than present technology can deliver. Our methods will solve the major shortcomings of the electronic nose concept.

Benefit to National Security Missions

The concept described in this project has the potential to provide low-cost, robust, easily deployable gas-phase quantitative discriminatory sensing capabilities that do not exist today. The broad implications of this work directly support the Revolutionize Measurements aspect of the Science of Signature pillar, and the applications specifically targeted by the proposed work directly address key Energy and National Security concerns. There are presently no low-cost and durable sensors to control and monitor the vehicle emissions systems on today's Selective Catalytic Reduction (SCR) and Exhaust Gas Recirculation (EGR) pollution control technologies comparable to the automotive lambda sensor. Although exact details are understandably kept secret by the pertinent Federal Agencies, the explosives screening technologies employed at critical facilities and used on the battlefield are routinely rendered ineffective because of the presence of complex, natural and human-created background interferences. The proposed research has the ability to create a unique capability at Los Alamos National Laboratory (LANL) by supporting the development of inexpensive and portable systems for use both by civilian first responders and as dedicated screening systems at airports, federal buildings, cargo containers, etc. We will develop the program with collaborators in Materials Physics Applications (MPA-11) and Weapons (WX-9) and also work with Program Managers from Applied Energy (M. Fox) and Global Security- Emerging Threats (P. Knepper) to pursue additional funding from federal agencies interested in Energy Security (Vehicle Technologies (VT)), and explosives (e.g. the Defense Threat Reduction Agency (DTRA) and the Department of Homeland Security (DHS))

Progress

The first stage of this project involves the collection of a data set from LANL to feed into the proof of concept model development work at Rutgers University. A

subcontract was placed in March to Rutgers University to initiate the model development work. LANL performed extensive modification to an existing sensor test station to enable the collection of the appropriate volume and quality of data needed for the model development work. A multi-mass flow controller manifold was built and automated with a lab-view based control and data collection program. This system was successfully commissioned within the first 2 months of this project and is capable of automated data collection from multiple sensors in the presence of 4 distinct test gases.

LANL initiated the sensor testing with the low-risk activity of looking at the concentration of analyte species where background interferents are known and quantifiable — relevant to vehicle emissions monitoring (Energy Security). For this test Nitrogen oxide (NO) was chosen as the analyte species with Nitrogen dioxide (NO2), Ammonia (NH3) and Propane (C3H8) serving as the background interfering species. The first set of experiments involved the use of two distinct mixed-potential thin film sensors, one having a Lanthanum chromite (LSC) sensing electrode and the other using gold (Au) as the sensing electrode. Both sensors had a Platinum (Pt) reference electrode and yttria stabilized zirconia (YSZ) electrolyte. These sensors were specifically chosen as prior work had determined that the Au electrode had preferentially sensitivity to NH3 while the LSC electrode had preferentially selectivity to either C3H8 or NOx depending on the mode of operation. The two operational modes selected were “un-biased”: where the voltage was measured at zero current, and “biased”: where the voltage was measured at a fixed positive current bias.

The Au and LSC based sensors were tested in our newly modified test stand using various binary pairs of analyte/interferent gases at various mixing ratios (a). Five distinct as varying from 0 to 4 were selected for the 3 binary pairs (NO/C3H8, NO/NO2 and NO/NH3). A total of 125 combinations of these mixing ratios were measured for 12 distinct concentration of NO leading to 1500 distinct data points being recorded for the Bayesian model validation. The data was recorded simultaneously on both sensors at each gas compositions in order to accelerate data collection. This data was then analyzed by Dr. Morozov at Rutgers. Both linear and non-linear models were considered, with the non-linear model providing the best fit to the data. This is not surprising since the non-linear model accounts for the saturation of the sensor response at high analyte concentrations.

The preliminary model was trained with just the “un-biased” data set and was able to predict the as within 20% when using just the NO/C3H8 mixtures. However this data set was in sufficient to predict the NO/NO2 ratios with confidence. The model is currently being extended to use the “biased” data in order to provide further fidelity to the predictions. These initial results were presented in an invited talk titled “Quantitative Decoding of Complex Gas Mixtures for Environmental Monitoring Using Mixed Potential Sensor Arrays” at the 227th meeting of the Electrochemical society by Dr. Cortney Kreller.

The progress to date is on track to meet the first milestone of this project by the proposed deadline of December 2015. When the modeling and experiments are completed with the current sensor combination we expect the computational framework to provide feedback to the design of the physical mixed potential electrochemical Sensor (MPES) array by predicting optimal sensing characteristics and the number of sensor elements required for robust operation. We will then prepare that MPES configuration with the appropriate number and type of sensing element and evaluate it in the low risk application (Energy). We will then extend that work to low concentrations of analyte species belonging to a chemical signature of interest in the presence of a large and varying background (Homeland Security). We envision as our end goal a versatile, standalone device that after a single mission-specific calibration in a laboratory setting may be deployed in both remote and harsh conditions to provide quantitative analysis of chemical signatures against large and unknown environmental backgrounds.

Future Work

We will first demonstrate proof-of-concept of the mixed-potential electrochemical sensor (MPES) array by fabricating a prototype sensor array and developing/validating predictive algorithms for the quantitative assessment of individual constituent concentrations in a complex mixture under a laboratory setting.We will initially fabricate sensor arrays by sputtering working electrodes that are known to have widely different selectivity to Nitrogen oxides (NOx), ammonia (NH3), carbon monoxide (CO), and non-methane hydrocarbons (NMHCs). The electrode compositions to be used will include strontium doped lanthanum chromites and strontium doped lanthanum manganates along with platinum pseudo reference electrode onto the heater platform. The yttria stabilized zirconia (YSZ) electrolyte layer will be electron beam (e-beam) evaporated. We will measure the voltage response of each individual sensor element of this array to a wide range of ratios of target analytes, $\alpha=[Ca]/[Cb]$ (where [Ca] denotes the concentration of analyte a), as a function of operating temperature. We have at our disposal a number of variables to optimize the sensing characteristics of our array for a specific application. In addition to electrode composition and tem-

perature, if needed, we can also control electrolyte thickness and morphology (porosity), for each sensor element of the array. The dataset described above will be used to determine model parameters for our previously developed Bayesian algorithm that determines concentrations of all constituents in an unknown mixture from the output of a cross-specific sensor array. The Bayesian analysis will provide quantitative guidelines for designing optimal sets of sensors by enabling us to 1) identify the optimal dependence of individual sensor response on the relative amount of compounds in the mixture and 2) determine the number of sensors in the array required to successfully discriminate the target species from one another, as well as against additional background interferents.

Conclusion

Proof-of-concept will be demonstrated by fabricating a prototype sensor array and developing/validating predictive algorithms for the quantitative assessment of individual constituent concentrations in a complex gas mixture. After successful demonstration of proof-of-concept we will work closely with our partners at ElectroScience Laboratories (ESL) to fabricate for the very first time Mixed potential Electrochemical Sensor (MPES) array prototypes using their proven High temperature co-fired ceramic (HTCC) manufacturing methods. We will then demonstrate the ability of these sensor arrays and signal processing techniques to analyze individual gas components in two difference applications; viz: 1) vehicle emissions monitoring and high-explosive/energetic-materials detection.

Publications

Kreller, C. R, A. Nadiga, S. C. Brown, J. M. Reynolds, D. Spernjak, F. H. Garzon, E. L. Brosha, A. V. Morozov, and R. Mukundan. Quantitative Decoding of Complex Gas Mixtures for Environmental Monitoring Using Mixed-Potential Sensors. 2015. In 227th ECS Meeting. (Chicago, IL, 24-28 May. 2015). , p. Abstract MA2015. Chicago: ECS Meeting Abstracts.

Reynolds, J. M., S. C. Brown, E. L. Brosha, R. Mukundan, F. H. Garzon, and C. R. Kreller. Electrochemical Characterization of Electrode Materials for Mixed-Potential Sensors. 2015. In 227th ECS Meeting. (Chicago, IL, 24-28 May. 2015). , p. Abstract MA2015. Chicago: ECS Meeting Abstracts.

Measurement of Extinct Radionuclides in Historic Nuclear Debris (U)

Warren J. Oldham
20150298ER

Introduction

A nuclear explosion produces an intense burst of energy and associated radiation driven by the violent assembly of a critical mass of fissioning nuclear material. Details of the nuclear event have traditionally been inferred from measurements made during and immediately after the detonation. In the case of radiochemical measurements, many of the nuclear products that have been shown to be of most diagnostic value exist for but a moment in time, typically on timescales of hours to weeks.

The key innovation of this proposal is the realization that short-lived fission products and key nuclear activation products that form the basis of modern technical evaluation can in fact be indirectly measured over vastly longer timescales from years to decades, and indeed centuries, after the detonation. We borrow a key insight in how to accomplish this task from similar approaches that have been successfully used in the field of cosmochemistry to measure extinct radionuclides in extraterrestrial samples. Chemical fractionation between Pu and U that is known to occur during a nuclear event will cause isotopic perturbation in 237Np and 239, 240Pu concentrations resulting from decay of short-lived U isotopes 237, 239, 240U. The proposed sampling and measurement techniques will be used to determine diagnostically sensitive and now extinct 237, 239, 240U isotopes in historic debris samples.

A significant challenge of the proposed research will be to develop indirect methods to measure peak-yield fission products to determine total fissions in a given sample. In order to reconstruct this information we propose to measure perturbations in stable element isotopic composition to infer the original presence of short-lived fission products. This idea depends on the presence of stable multi-isotope elements for which one isotope is the end-point of a fission decay chain and another is blocked from fission decay by a different stable element.

Benefit to National Security Missions

A major limitation of current radiochemical diagnostics is the need to determine the concentration of key signature radionuclides with short halt-lives. Within a month after a nuclear detonation, these radionuclides are largely extinct. If successful, the proposed work will be a critical step towards a new capability to extract this crucial information from nuclear debris at later times. Such a capability would have direct and lasting impact on two key DOE/NNSA missions: stockpile stewardship and post detonation nuclear forensics. A demonstrated capability to reanalyze archived debris samples from historic nuclear tests will improve the technical foundation that supports Stockpile Stewardship and will strengthen our Nation's commitment to deterrence without nuclear testing for decades to come. The limitations of historical measurements impact nuclear forensics as well. Older U.S. tests have relevance to low-technology threat space. Because many of these tests were fielded in the late 1940's and early 1950's, the radiochemical data for these events is very sparse and/or of low quality. This leads to large uncertainties in evaluation of performance and yield, which in turn prevents proper calibration of LANL's computational design tools. A capability to obtain a complete radiochemical data set for early U.S. tests would significantly improve modeling and forensic capability envisioned for post-detonation nuclear forensics.

Progress

This research aims to develop analytical techniques to characterize the details of a nuclear detonation based on chemical analysis of aged nuclear debris. The analytes of interest are short-lived radionuclides that have decayed beyond detection, but leave signatures of their original presence in the isotopic composition in archived debris samples. We term these signatures, extinct radionuclides. The goals of the project are to recover two types of information, (1) short-lived uranium isotopes (237, 239, 240U) and (2) fissions. For each of these goals good

progress has been accomplished. In order to determine the short-lived uranium isotopes, a collection of samples must span a suitable range of volatility as measured by sample specific 236U/238Pu ratios. Although only one unfractionated 236U/238Pu value is actually "true" of the device, chemical distortion that occurs during debris condensation serves to generate a range of samples that can be relatively enriched (volatile) or depleted (refractory) in uranium compared to a reference 238Pu isotope. The proposed regression technique requires that 236U/238Pu span a sufficient range within the sample set to allow a robust linear fit.

In the case of analyses of Trinitite, eight individual samples from archived LANL collections have been completed. The expected trends are observed, however the goodness of fit over a limited range in 236U/238Pu is not sufficient to obtain a high-quality measure of 237, 239, 240U. A new set of Trinitite samples obtained from a commercial rock and gem supplier has been procured. These samples appear as light green vesicular samples, distinctly different from the black glass found in the LANL collection. It is hypothesized that the light green vesicular samples will be more volatile compared to the black glass samples and will provide the range in 236U/238Pu that is needed. Initial analyses of archived core samples from an underground nuclear test have also been completed. For this test, archived samples that transit seven locations through the underground environment are available for analytical study. Duplicate analyses of the first two locations have been completed. Five more duplicate analyses will provide data to assess the 236U/238Pu volatility index and the feasibility of the technique to measure 237, 239, 240U in underground debris samples.

Two independent approaches are being pursued to determine fissions in historical debris samples. These include direct measurements of 99Tc and indirect measurements of 95Zr and 97Zr through isotopic perturbation of stable molybdenum isotopic ratios (e.g. 95Mo/96Mo and 97Mo/96Mo). Each of these analytes is a peak yield fission product that can, in principle, be used to determine total fissions in the sample. The first phase of this project has focused on development of chemical methods used to isolate pure 99Tc and molybdenum concentrates that can be assayed using both single and multi-collector ICP-MS instrumentation. In the case of 99Tc determination, a method has been developed during the first year of this project to analyze for 99Tc in aged debris samples. Technetium is purified in high yields (80-100%) using extraction chromatography (TEVA resin) with good decontamination from both Mo and Ru. This decontamination is crucial to the success of the analysis because of potential isobaric interference from 98MoH+ and 99Ru. Standard addition experiments with solutions of Peruvian soil (NIST SRM 4355) and dissolved Trinitite suggest that accurate determinations of 99Tc can be obtained. The associated measurement uncertainty (20-30%) is higher than ideal and reflects inconsistencies in observed instrument count rates that are not yet fully understood. Additional work is needed to identify the source of the variation and improve measurement precision. In the case of 95, 97Zr determination, a novel technique using high precision isotopic measurements of stable molybdenum is being pursued. A sequential two-column ion-exchange protocol was developed and optimized. Purified Mo concentrates have been isolated with good decontamination against potential interferences from Zr, Ru, Cr, Mn, and Fe.

The purification protocol performed well in an initial Mo analysis of a dissolved debris sample, which revealed significant deviation from the natural isotopic composition. An optimized measurement routine using the Neptune Plus multicollector ICP-MS is currently being developed. These high precision measurements will be used to quantitatively determine perturbations in 95Mo/96Mo and 97Mo/96Mo isotopic ratios. Future analyses using an isotopically enriched 96Mo spike will be interpreted for absolute fission concentration.

Future Work

Chemical fractionation between Pu and U can be exploited to determine the original concentration of 237,239,240U produced in a nuclear explosion. The sampling requirements as well as the scope and limitations of the method need to be defined. This research will employ a case study approach to help determine these boundaries. During this FY, work will focus on analysis of archived debris samples from the Trinity test and from an underground nuclear test. The resulting data will be evaluated through a systematic uncertainty analysis to understand how uncertainty in both measurements and in linear regression techniques ultimately defines the analytical determination of extinct radionuclides. Final data will be evaluated in the context of nuclear debris diagnostics using the modern Isotope Production Code and compared to historic assessments. The second goal is to develop indirect methods to measure peak-yield fission products to determine total fissions in a given sample. Our first choice to accomplish this task is to determine the concentration of extinct 95, 97Zr isotopes through perturbations on stable molybdenum isotopic composition. The short-lived Zr isotopes decay to stable 95, 97Mo. Adjacent fission decay chains (mass 92, 94 and 96) are all blocked by stable Zr isotopes such that 92, 94, 96Mo are unperturbed by fission decay. A method to obtain high precision isotopic analysis of purified Mo samples

will be developed using multi-collector inductively-coupled plasma mass spectrometry (MC-ICP-MS). During this FY focused effort will be spent on developing and validating the chemical and instrumental methods. Beginning in the second year of this project we should be in a position to apply the Mo isotopic analysis approach to determine extinct 95, 97Zr fission product isotopes in archived debris samples. The same solutions used to determine actinide composition will be held until the extinct fission product measurement techniques are ready.

Conclusion

Debris from historic nuclear test rests on the ground surface and within underground cavities at all nuclear testing sites. This material could be used to determine device design and performance but is currently of limited diagnostic value because the short-lived fission products and nuclear activation species have long decayed away. The goal of this project is to develop new measurement and assessment techniques to reconstruct diagnostic information as the stable decay end-members. The success of the proposed effort will be a critical step towards a new capability with direct impact on nuclear forensics and on science based stockpile stewardship.

Publications

Hanson, S. K., C. R. Waidmann, J. L. Miller, H. D. Selby, and W. J. Oldham. Modern radiochemical measurement and evaluation of 1950's era debris from the Nevada Test Site (U). To appear in Defense Research Review.

Ultra-sensitive Parallel Micro-imaging with Atomic Magnetometer

Igor M. Savukov
20150300ER

Introduction

It is widely recognized that the next frontier for magnetometry is biological and neuroscience applications, where impact will result from improvements in both resolution and sensitivity. We propose to meet this need for higher resolution and higher sensitivity magnetometry with a novel approach: combining an ultra-sensitive atomic magnetometer (AM) with flux concentrators (FCs). The technological breakthrough will result from advances in atomic magnetometers and from the novel FC-AM concept. After developing the FC-AM device, we plan to demonstrate its performance by applying it to important problems in science, security, medicine, and industry.

The proposed research program will have two broad research goals. The first goal focuses on technology: (i) demonstrate the FC-AM principle, (ii) characterize its sensitivity and resolution, and (iii) demonstrate that FC-AM can operate in multi-channel configuration. The second goal focuses on applications in bio-security (detection of magnetic nano-particles, neuroscience, detection of bio-magnetic fields of a cluster of neurons), in energy research (fuel cell ion-transport imaging), and in industry (non-destructive evaluation, NDE).

Benefit to National Security Missions

The work directly addresses the need for sensitive magnetometers with high resolution. One class of NIH applications is based on detection of magnetic nano-particles with our micro-magnetometer: applications in detection cancer cells, infections and cancer therapy. The second class is based on detection of magnetic field of neurons.

Other potential applications include magnetometers, used for fuel cell diagnostics, which is relevant to reduction in CO2 emission and hence climate impact; pathogen detection based on magnetic nano-particles; checking for pathogens at our boarders; authentication of micro-chips; DNA detection and other applications of magnetic nano-particles; and brain science and cancer detection and studies.

Progress

A postdoc was hired and trained in safety, atomic magnetometers, magnetic field modeling, sensitive measurements, and some other fields.

The research team designed, modeled, and constructed a ferrite flux concentrator (FC). Its resolution and expected trade-off in sensitivity was verified. We found agreement between theory and experiment.

A small-size atomic magnetometer (AM) (1 cm outside dimension) was setup and tested. Its bandwidth, which is important parameter affecting the ultimate sensitivity, was measured and found to be within the expected range.

Atomic magnetometer was inserted into the flux concentrator and its sensitive operation was confirmed. We expected some effect of the flux concentrator on the operation of AM, namely the broadening of the AM magnetic resonance which could potentially substantially decrease the sensitivity. We solved the problem by adding compensation gradient coils. Now the AM operates inside the gap of the flux concentrator the same way as in the ideal shielded environment.

At this point, we are planning to replace the current AM with a new-generation AM from QuSpin company that will improve sensitivity by at least an order of magnitude. With this new AM, we planning to make demonstrations of sensitive detection of FC+AM single-channel system. This is our major milestone.

We also focused on improving the resolution of the tip of the FC. Initial ferrite FC was extended with mu-metal

tips, since ferrite material cannot be sharpened enough, and with this approach we are reaching our proposed target resolution of 0.1 mm. Various tests of resolution were conducted with micro-coils as the sources of magnetic field at small scale. Further improvements in resolution will require the use of micro-fabrication techniques and magnetic micro-particles.

Because we are now waiting for QuSpin company to manufacture for us a new-generation AM and we confirmed that FC-AM approach works, we started work on an AM multi-channel system. We are preparing 16-channel AM system that is based on a large pancake Rb cell, 16 fiber-coupled photo-diodes, and 16-channel DAQ interface.

We are preparing a paper for publication where we demonstrated a few fT/Hz1/2 sensitivity with a large Rb cell, which will be used later for multi-channel detection.

An additional postdoc was appointed as Director's Fellow, and will work in conjunction with this project. Although his project has many independent goals, there are many common goals, such as sensitive micro-imaging and its applications.

Detection of magnetic micro-particles with the system is in preparation stage and will be demonstrated after the new AM will be procured.

Overall, substantial progress was made. We were able to demonstrate a single channel FC-AM operation, although we continue the work to improve sensitivity to make our results even more exciting for the scientific community.

Future Work

A single-channel atomic-magnetometer and flux-concentrator system will be constructed to evaluate experimentally the resolution-sensitivity tradeoffs. A single-channel AM is already available for the project. The flux concentrator will be constructed from 500-micron ferrite rods sharpened to 100 micron, available from Ceramic Magnetic, Inc.

Characterization of the sensitivity and resolution will be conducted and work will start on developing new applications.

Conclusion

After the FC-AM devices have been tested and characterized, we will work on developing novel applications. We will demonstrate detection of magnetic nano-particles functionalized for specific molecules. Nano-particle applications are relevant to LANL missions in security, energy research, non-prolifiration. In addition, We will test non-destructive evaluation methods. Finally, if time permits, in collaboration we will work on detection of magnetic field of a single neuron or small clusters of neuron. The preliminary data will serve as the basis for proposals, for example within President Obama BRAIN initiative, or DHS (biosecurity), or DOE for fuel cell research.

Publications

Espy, M. A.. Hardware Developments: Detection using SQUIDs and Atomic Magnetometers, Mobile MRI/ Chapter 7. To appear in Mobile NMR and MRI: Developments and Applications. Edited by Price, B..

Karaulanov, T.. Spin-exchange relaxation-free magnetometer with nearly parallel pump and probe beams. To appear in Physical Review A.

Savukov, I. M.. SERF and derivative high-density alkali-metal magnetometers. To appear in Smart Sensing, Measurements of Instrumentation. Edited by Grosz, A..

Segregated Fuel-Oxidizer Propulsion for CubeSat Deployment

Bryce C. Tappan
20150323ER

Introduction

Small, utilitarian "cube satellites" (cubesat) that can be easily deployed into low-earth orbit and have high-functionality are increasingly more popular. These cubesats ride along with much larger expensive satellite launches on a "bus" and the customer is limited to a pre-determined orbit. As of yet, no propulsion system exists that has sufficient impulse for orbital plane adjustment as well as the required factors of safety necessary to piggyback on a launch that may surpass $1B in cost. Here we propose to develop a propulsion package based on the LANL segregated fuel-oxidizer rocket system, which could provide both the impulse and safety required for orbital plane adjustment for these small satellites. The main thrust of the research will be to design and test innovative form factors utilizing two different motor concepts that will provide sufficient impulse for orbital correction. Energetic fuels that provide copious amounts of high-temperature H2 gas can be incorporated into segregated systems that flows to a separate chamber that provides extremely high impulse by reaction with a solid oxidizer. Because the fuel and the oxidizer will remain separated until decomposition of the solid fuel, and both are relatively (or completely) insensitive to shock, the chance of accidental detonation or initiation of the rocket is dramatically reduced. Modifications of the system that will also be studied will incorporate a solid oxygen generator, much like those used for emergency oxygen on airplanes, to provide gaseous O2 that can react with fuel gases or solid fuels in a separate chamber, analogous to a liquid/liquid rocket chamber or hybrid rockets. Thus, three engineering concepts will be available to ensure success of the project.

Benefit to National Security Missions

The segregated fuel-oxidizer propellant system is a major break-through in solid rocket propulsion in terms of safety and energy. Because of the development of high-nitrogen/high hydrogen energetics at LANL that contain little or no oxygen, a segregated tandem system can be designed such that the energetic material will provide fuel from their decomposition that will be oxidized in a separate chamber by reaction with a solid oxidizer. Because the fuel and the oxidizer are separated until combustion of the fuel is initiated, and are both are relatively (or completely) insensitive to shock, the chance of accidental detonation or initiation of the rocket is dramatically reduced. These technologies will allow for both a higher energy and much safer solid propellant propulsion system than is currently offered the state-of-the-art. These aspects are particularly relevant to cubesat propulsion, as there are currently no high specific impulse (Isp) options that qualify as safe. Cubesats are a secondary payload and the orbit is dictated the primary payload, thus the ability to change orbitology from 300km to 500km is huge. Further points that are significant in cubesat propulsion include the ability to build/maintain a constellation, station keeping, the ability to extend the life of a very low orbit <300km and even interplanetary space travel to asteroids or the moon. This will greatly expand the functionality of existing cubesats. Also key in this development is the ability to deorbit, such that today's cubesat will not be tomorrows space junk.

Progress

Significant progress has been made in the primary goal of decreasing the thrust of the propulsion system. While high levels of thrust can be advantageous in atmospheric applications, in space applications only overall impulse is important, and lower thrust, while preserving overall energy, is desired for spacecraft stability during maneuvers. We were able to achieve this reduction by a two approaches; a modification in the fuel and oxidizer chemistry to provide a slower, but stable burning rate, as well as development of a new internal geometry in the fuel-oxidizer grains. With the change in fuel burning rate, and the level at which the oxidizer decomposition is catalyzed in this system, we were able to reduce the

thrust in core-burning geometries by ~3x. By producing an end-burning fuel grain (much like the regression of a cigarette) we were able to reduce the thrust further by ~10x. Furthermore, because of the inclusion of higher levels of aluminum powder in the fuel, this advantage of lower thrusts also comes with high specific impulse. Motors have been successfully tested at 1" diameter geometries, and we are currently scaling the system to 2" diameter. Initial observations, however, indicate that some formulation optimization will be necessary to obtain optimal system impulse as well as acceptable combustion stability. Further work this FY has also focused on scaling down the system to 12.7 mm, and development of an x-ray transparent motor casing at this size to dynamically analyze the motor performance during combustion.

Significant calculations have been performed using the thermal equilibrium codes Cheetah (LLNL) and NASA CEA, both provide important guidance in motor performance, although there is required effort to reconcile the data between the two models. Cheetah will always do the calculations by resizing the nozzle until the pressure of the combustion gasses in the nozzle is the same as the ambient conditions. The Cheetah program has the advantage of a containing a more advanced library of condensed phase species when considering aluminum reactions, but NASA CEA has a number of advantages. Both models converge on the overall fuel to oxidizer balance, but NASA CEA indicates that aluminum doesn't increase Isp or the characteristic exhaust velocity, indicating that the optimum Aluminum content is ~10 wt% in fuel (about 3 wt% in overall propellant), compared to the 30 wt% indicated by the Cheetah code. This combined modeling efforts was advantageous this FY in guidance to optimize the formulation while decreasing the number of expensive tests required. This is helpful as the high Al content is likely cause of the serious combustion instability we are observed in some of the rocket tests. Intermediate levels of aluminum additives have thus been developed and are expected to provide optimal impulse as well as combustion stability. Furthermore, alternative additives (aluminum hydride and aluminum-lithium alloy) have been investigated and show promise in modification of specific impulse, combustion stability as well as reduction in two-phase flow loss from the motor.

Future Work

Three different motor concepts will be considered, and the most practical will be selected and developed. The initial, and primary concept, will be arrays of right cylindrical motors with independent ignition control such that symmetrical sub-arrays can be fired at different times. The alternative designs will include the substitution of the flow through oxidizer with a solid pyrotechnic oxygen generator that provides gaseous oxygen to a mixing chamber with the fuel product gases, analogous to a liquid rocket engine. The same oxygen generator will be studied to provide oxygen to a solid fuel grain, analogous to a classic hybrid rocket engine, and the reverse of our primary concept. The primary approach motor array will be fixed to a cubic geometry, and the second two systems will be designed as back-up technologies in the event of insurmountable problems with the primary approach. The goal of all three systems is to provide consistent thrust, with a high-level of safety and better overall performance (specific impulse) than current proposed propulsion for cubesats.

Well timed, reliable ignition systems will be a key component to the success of the primary concept, so this will be one of the primary tasks for the first year. The goal will be to produce igniters that can function in less than one second from the sending of the electric pulse, as well as providing the sufficient heat to ignite the motor's fuel. Also key to the first year of the project will be the miniaturization of existing segregated fuel-oxidizer motors to fit the space demands of the LANL cubesats. The goal here is a 12.7 mm diameter motor.

A new spacecraft concept will be explored requiring a single, larger diameter motor.

Conclusion

The primary metric of success will be the measured system impulse of the propulsion system. These data will be used to calculate the different orbits achievable from the propulsion systems. Thrust and pressure measurements will be performed on individual motor sections as well. Independent, reliable, ignition control will be demonstrated so that motor arrays can be utilized to provide a constant predictable direction of flight. A thrust stand with at least four separate load cells will be developed to verify uniform thrust of the motor arrays.

Practical Antennas from Disruptive Technology

John Singleton
20150337ER

Introduction

The project will design and construct two practical, optimized, economical antennas to give improved performance compared to current state-of-the-art. The antennas to be built are called Superluminal Accelerated Polarization Current (SAPC) antennas, and are based on a new principle: moving a polarization current superluminally (faster than the speed of light in a vacuum) and accelerating it. The radio waves emitted by the polarization currents in SAPC antennas have properties analogous to the "sonic booms" of acoustics (emitted by accelerating supersonic airplanes) in that they can have relatively high intensities at large distances from the antenna. A technology-demonstrator SAPC antenna built at LANL has already shown advantages over conventional technology for transmission distances > 10 km; in the current project we hope to improve such antennas using the numerical technique of topology optimization. This technique varies the shape, size and configuration of a component to give the best possible performance; it tries out many more variables and variations than are possible for a human designer to achieve in a lifetime. Topology optimization has recently been used to give dramatic weight savings combined with improved drag and lift in aeronautical components; however, it has only had limited application in antenna design. Advances in computing mean that the time is ripe to apply topology optimization to electromagnetic problems; and that the novel SAPC antennas are suitable disruptive technology that could thus be brought to market.

SAPC antennas for two different applications will be optimized and built. The first will be for low-power, ultra-long-range communications. With optimization, we estimate that factor 10-100 power savings could be made for distances 1-100 km. The second SAPC antenna would focus radiation at a distance, demonstrating the feasibility of future medical, radar and directed-energy applications.

Benefit to National Security Missions

Work on SAPC antennas will lead to intellectual property relevant to radar (other federal agencies, DOT), remote sensing and surveillance (ultra-long-range transmitters running on very low power) and secure communications (relevant to other federal agencies), pivotal to LANL core missions. The current proposal represents a high-payoff quantum leap in the theory, computation and modeling of SAPC antennas (information techology). This work could give back to the US a lead in antenna technology, reducing dependence on imported components from e.g. China (relevant to DOC). With topology optimization applied to communications backhaul, we estimate that factor 10-100 power savings could be made for all distances 1-100 km. This could lead to the replacement of the world-wide telecommunications backhaul network (relevant to DOC, infrastructure etc.), with huge reductions in energy consumed; the lower transmitted powers needed ameliorate environmental concerns (relevant to environmental and Energy Impacts).

Accelerated superluminal polarization is thought to play a role in the emission of radiation by pulsars, quasars and gamma-ray bursts and in other astronomical phenomena. Therefore a deeper understanding of the electrodynamics of superluminal polarization currents is relevant to Cosmology and Astrophysics, as well as to DOE (SC) and NASA. Ultra-long-range, low-power communications are relevant to Space Science (communication with deep-space probes) and to NASA. Finally, the broadening of the application of topology optimization to antennas is relevant to information science and technology.

Progress

The first stage in optimizing the design of the SAPC antennas was to adapt numerical calculations of the emission from a superluminal polarization current to the various possible antenna geometries: (i) circular with radially applied electric field, (ii) linear with arbitrary

acceleration and (iii) arc with vertically applied electric field. These numerical models have all been coded and debugged, and the results compared with experimental data from earlier "proof-of-principle" SAPC antennas. To check the robustness of the numerical method, each type of calculation was coded in two independent ways using different computer languages and operating systems. Within each implementation, different methods of numerical integration and differentiation (finite element evaluation of the "curl" operation) were checked for accuracy, especially at the distances required to model communication performance: the phases of signals from an antenna measuring 1/3 of a metre across must be accurately evaluated at transmitter-to-receiver distances of up to 100 km. All of this was successfully accomplished.

The simple optimizations outlined in the proposal have taken the above results and used them to design a linear antenna (type (ii) above) for communications purposes. In contrast with previous "proof-of-principle" SAPC antennas, the volume of the dielectric is much larger compared to the emitted radiation's wavelength, and the elements are sparser (i.e. there are fewer elements per unit length). Both of these refinements have resulted in an additional benefit: a design that should be economical to mass-produce on a base made from standard 16 mil circuit board. Components for the new antenna are either already made, or are being fabricated and ordered; for flexibility, we are using mechanical phase shifters attached to each element to vary the antenna's emission pattern before fixing the design of the passive feed network that would animate the polarization current in a mass-produced device. The chassis, phase shifters, cables and several other components are presently under test in the TA-35 anechoic chamber. The design is modular, so that the current antenna elements can be replaced in future; refinements resulting from the more sophisticated optimization routines that will be applied to the proposed second antenna may result in further improvements.

All of these achievements form the basis of an invention disclosure for a future patent. Based on the encouraging results, a previous patent on SAPC antennas has also been extended to give further international coverage.

Extensive testing of dielectrics (including a novel metamaterial comprising micron-scale copper loops dispersed in a foam) has been, and is, also under way. Based on the need for a large volume polarization current suggested by the models, we have selected a plastic dielectric (rather than the alumina used in previous designs) for the preliminary design of the proposed second antenna. Data from the metamaterial have suggested a further possible application for SAPC antennas which is being studied for possible future patents.

During the optimization process, a completely new geometry of antenna (analogous to the synchrotron particle accelerator) was discovered; though not immediately applicable as a communications antenna (the beam is of an unusual form) this may have applications in radar (the device has a 360 degree view without mechanical scanning). The new design is being reserved for possible future improvement and patenting.

Coding associated with the proposed, more sophisticated topology optimization to be used with the second antenna design is under way and proceeding according to expectations. As part of this exercise, the numerical "algebra" necessary to deal with dielectric antenna elements of arbitrary shape has been developed.

Future Work

Optimization of the first antenna design will be carried out in three stages. (i) Starting with simple shapes, the dielectric parameters and shape, and the speed, acceleration and spatial modulation of the polarization current within will be optimized for directivity, and distance-dependent gain. This represents a relatively small number of design variables, so a genetic algorithm (GA) will be employed. The primary challenge is the computational cost in determining the antenna performance. This will be addressed using a multilevel radial basis function (mRBF) surrogate model, avoiding the need to analyze every candidate design. (ii) The means of animating the polarization current – electrodes on/in the dielectric driven by a passive feed network – will be included. We will employ a multiobjective GA, NSGA-II to explore optimization strategies. (iii) Having a coarsely optimized design, topology optimization will interrogate a wider design/shape space using the SLP level set method. Here, revolutionary improvement is expected; the previous stages are necessary to verify the method and the solutions. The number of variables will be ~1000 and the use of GA is no longer tractable. The optimum solutions from previous stages will provide benchmarks for verification of the level set optimization. Based on the analysis and experiment, we will select final optimum designs for the first antenna.

We demonstrated an economical SAPC concept employing passive feed networks and electrodes on commercial 30 mil circuit board, plus layers of easily shaped dielectric. Trial antennas, antenna elements and passive feed networks will be built on this principle and measured to validate numerical and optimization predictions using the anechoic chamber at TA-35. Optimization of dielec-

tric properties will be studied in the numerical work; to validate this, some trial antennas may employ metamaterials fabricated in MPA-CINT, tailored to fine tune dielectric properties. The first optimized antenna will be constructed based both on the outcome of the numerical optimization and fabrication/experimental experience with the trial antenna components.

Conclusion

The goal of the project is to build two antennas that combine and synthesize two recent developments: the novel Superluminal Accelerated Polarization Current (SAPC) antennas, developed at LANL and topology optimization, a numerical technique that has produced best possible designs for aeronautical components, but as yet has been little applied to antenna design. The first antenna, designed for communications, could lead to dramatic power savings for transmissions over distances of 1-100 km, leading to the replacement of the worldwide telecommunications backhaul network ($billions), with huge reductions in energy consumed. The second antenna will be used to demonstrate focusing of radio waves at a distance.

Next Generation Earth Models

Monica Maceira
20120047ER

Abstract

We address the fundamental problem of creating an accurate image of the Earth, currently a barrier to understanding the Earth's present state and evolution, as well as a limitation in our ability to monitor the globe for nuclear explosions and other seismic events of interest. Our prime goal was to develop an efficient method to derive the Earth's velocity structure from a combination of four geophysical data types - body waves travel times, surface wave dispersion, receiver functions, and gravity anomalies. Because of the complementary sensitivities of each of the data types employed, our multi-parameter inversion is able to produce more accurate Earth models than currently available and will form the basis for the next generation of Earth models. We applied our method to the western US, a perfect test bed for this effort, where unprecedented data sets are now available from the geophysics community. Our research effort has been a combination of code development, data gathering and processing, theory and method development, and extensive inversion of the multiple data types. This research has created unique expertise at the Laboratory and enhances the Laboratory's capability to address core missions in Nuclear Nonproliferation Programs.

Background and Research Objectives

When an earthquake or underground explosion occurs, seismic waves propagate from the source out through the Earth and can be recorded at a distance. Parameters derived from these waves, including their travel time, dispersion, and amplitude, are used to infer the structure of the Earth through which the waves have passed. When sufficient data are available, tomography can be used to invert seismic parameters for Earth's velocity structure.

The science behind creating images of the structure of the Earth is well developed. Current practice, however, is to perform tomography with a single data type (either travel time or surface wave dispersion, for example) and this results in incomplete retrieval of earth properties due to sensitivity limitations inherent in each of the data types. Under this project we have addressed this difficulty through simultaneous inversion of multiple datasets each of whose sensitivities fill the resolution gaps of one of the other data types, resulting in improved resolution. Prior efforts have primarily focused on integrating two, and in rare cases three - and focusing only on restricted locations-, parameters into the inversion procedure. We successfully developed a methodology and code to incorporate the simultaneous joint inversion of four consistent and complimentary datasets, and applied it to large data sets over a broad region.

Scientific Approach and Accomplishments

Data Gathering and Processing: The availability of Transportable Array (TA) data provided a tremendous opportunity, as data of this high a density over such a broad region had never before been available. The TA is a rolling array of 400 seismometers deployed on a 70-km-spacing semi-regular grid moving from the west coast of the US towards the east coast. When these stations are combined with other local networks in the west, the data coverage is exceptional. We gathered and processed body wave travel time data for all these stations. Initial body wave travel time tomography results were published in J. Geophys. Res.– Ref. [1].

Receiver functions (RFTNs), which can be thought of as the impulse response of a near-vertical wave beneath a seismic station, are available only from the TA and other selected stations through the Earthscope Automated Receiver Survey website [EARS]. We downloaded these RFTNs for about 1500 stations in the western US, sort them into bins by ray parameter and azimuth, and examine them for consistency and quality. Discarding the poor quality ones, we stacked receiver functions for the remaining 1400 stations across all azimuths to produce an average RFTN for each station in our region. This

careful processing of the EARS RFTNs was presented at the Seismological Society of America Annual meeting – Ref [2]. In the current implementation of our inversion algorithm, we can only use one station per cell, so we choose the best RFTN closest to the center of each cell, resulting in only 482 RFTNs for the inversion target area of western US. We then decided to compute our own RFTNs for the study region. We used all the TA stations for which stable receiver-function estimates were possible, and included several portable deployments in Canada. We began with all events (during station operation times) with magnitude mb > 5.7 recorded at epicentral distances from 30-100˚ and calculate receiver functions at 1096 stations using the time-domain iterative deconvolution algorithm. We obtained over a million RFTNs which, once interpolated (see below), provided us with the needed coverage.

As part of the systematic determination of earthquake moment tensors for North American earthquakes, collaborator Bob Herrmann (SLU) uses multiple filter analysis to obtain the fundamental mode Love and Rayleigh wave spectral amplitudes and group velocities. As of November 08, 2011, there were over 1227817 surface wave dispersion measurements available [NATOMO]. We used Bob's short-period observations and blended them with the intermediate and long-period observations from a global model from G. Ekström. We blended the data across the period range from 25 to 50 seconds, resulting in surface wave group velocities in the period range from 7 to 250 seconds.

Gravity data from several space and land missions provide high-resolution coverage of the western US and are freely available off the web [EGM2008]. These can be sampled at any regular or non-regular interval. To avoid mapping broad, possibly dynamically caused features in the western US gravity field into density and shear-wave speed variations, we high-pass wavenumber filtered the surface-gravity measurements with a simple box-car filter with a width of four cells (~440 km).

Method and Code Development: Throughout the extension of this project, we have improved several aspects of the inversion methodology and the associated software code. In order to process the millions of travel times available for the study area, we improved the efficiency of our body wave travel time predictions by replacing our finite difference travel time predictor with a ray bending approximation. Our ray bending is several orders of magnitude faster to compute than finite difference with only small losses in accuracy. Given the errors associated with our travel time data such losses are completely acceptable.

Body wave tomographic resolution increases with depth as a function of ray crossing, with shallow -crustal- regions suffering from a lack of resolution due to the scarcity of ray crossing there. In comparison, gravity surveys have traditionally offered optimal resolution at crustal depths. To increase the usefulness of gravity data and to avoid mapping broad, possibly dynamically caused features in the gravity field into seismic speed variations, we explored high-pass gravity filtering. Filtered gravity anomalies are expected to possess highest resolving power at short wavelengths and thus enhance resolution of lithospheric structure. We modified the joint inversion code to include the filtering of the gravity anomalies, as well as the corresponding gravity partial derivatives, which has made the computer code mathematically rigorous (Figure 1). Initial results with this newly developed technique were accepted for an oral presentation at AGU Fall meeting – Ref [3], the most important conference in geophysics.

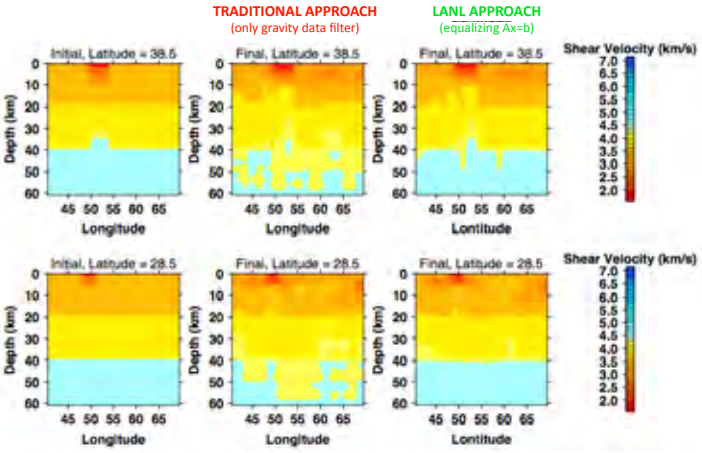

Figure 1. The effect on estimated shear velocity of filtering both the gravity and partial derivatives within the joint inversion code. Results for two E-W cross sections (at 38.5°N and 28.5°N) are shown. Left column is the initial model. Gravity data is filtered in both the center and right column, but gravity partial derivatives are not filtered in the center column; they are filtered in the right column. The results shown in the right column represent the preferred methodology

For data sets as large as those required for this project, combining data can require a laborious examination of the receiver functions or sophisticated stacking approaches that may or may not be effective, depending on the ray-parameter and azimuthal coverage in the receiver-function collection. Anyone who has examined receiver functions carefully is aware that the signals are often variable and at times it is difficult to be sure that an underlying simple component of the signal exists. Small additions to even a simple crust-mantle-transition-dominated receiver function can introduce vertical structural complexity that is as intriguing as it is difficult to validate. Another issue that has been difficult to address is the difference in spatial

sampling of the receiver-function and surface-wave data. Surface waves produce broad, low-wavenumber constraints on lateral variations in the structure but receiver functions are sensitive to the higher wavenumber features of the structure. For vertical resolution, the combination is ideal. However, when we look at how each signal averages the lateral structure, the sensitivity difference is not ideal. To explore and solve these issues, we used our computed TA RFTNs from the western US and constructed a receiver-function wavefield interpolation scheme that helps to equalize the lateral sensitivity of the receiver functions and the surface-wave dispersion, and that greatly simplifies the complexity in the receiver functions (Figure 2). Details of this novel technique were accepted for a presentation at SSA annual meeting – Ref [4], the most important conference in seismology, and it is under review for publication in GRL, a high-impact journal in geophysics – Ref [5].

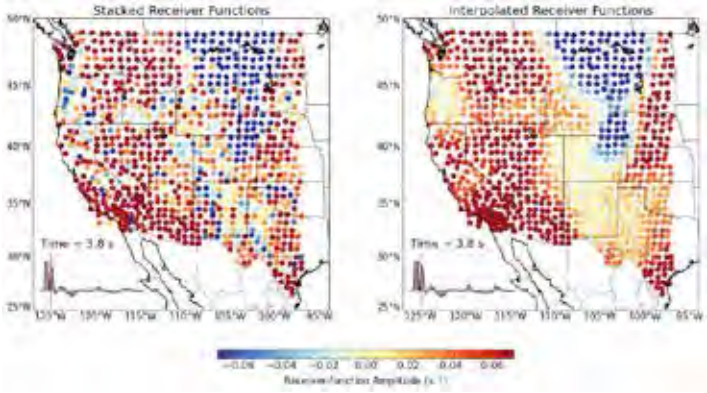

Figure 2. Time slices from the western TA receiver-function wavefield. Each circle represents a seismic station at which we have computed a stacked receiver function. The color indicates the amplitude of the receiver-function stack (left) or the interpolated value of the receiver function wavefield (right) at a time of 3.8 s. Inset shows the stack of all receiver functions and the red line shows the location of the time slice, which was chosen to show the structure near the time of the Ps converted phase arrival from the crust-mantle transition region.

Conventional seismic tomography methods typically produce smooth models, but these models may be inappropriate when subsurface structure contains discontinuous features such as faults or fractures indicating that tomographic models should contain sharp boundaries. For this reason, we developed a novel tomography method that uses a modified total-variation regularization scheme incorporated with a priori information on interfaces to preserve sharp property contrasts and obtain accurate inversion results. Our new approach was also accepted for a presentation at the SSA annual meeting – Ref [6], and it is under review for publication in GJI – Ref [7].

Application cases: We successfully applied the new and modified joint inversion technique to several regions at different scales. We first applied it to Parkfield, a small - 15km x 15km – region around the San Andreas Fault Observatory at Depth, California. The contributions of the different data types to the inversion were controlled by the relative weighting of the respective equations. We found that the trade-off between fitting the different data types, controlled by the weighting, defines a clear optimal solution. Preliminary results were accepted for an oral presentation at AGU Fall meeting – Ref [8], and the final model was published in Pure and Applied Geoph. – Ref [9].

We also jointly inverted 14 years of local earthquake body wave arrival times from the Alaska Volcano Observatory catalog and Rayleigh wave dispersion curves based upon ambient noise measurements for local seismic velocity models and hypocentral locations at Akutan and Makushin Volcanoes, an area of approximately 35km x 50km in Alaska. We found that the velocity structure and relocated seismicity of both volcanoes are significantly more complex than many other volcanoes. Seismicity is distributed among several areas beneath or beyond the flanks of both volcanoes, illuminating a variety of volcanic and tectonic features. The velocity structures of the two volcanoes are exemplified by the presence of narrow high-velocity features in the near surface, indicating likely current or remnant pathways of magma to the surface. A single broad low-velocity region beneath each volcano is slightly offset from each summit and centered at approximately 7 km depth, indicating a potential magma chamber, where magma is stored over longer time periods (Figure 3). These results were accepted for a presentation at SSA annual meeting – Ref [10], and are under review for publication in J. Geophys. Res. – Ref [11].

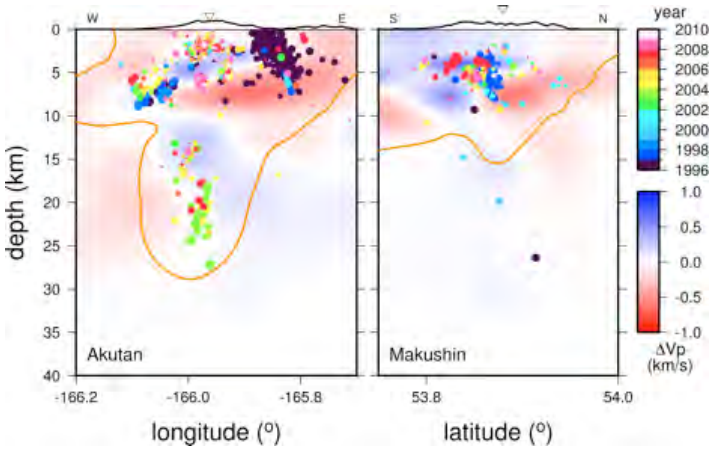

Figure 3. Cross sections of the V model and relocated seismicity through the caldera of Akutan Volcano and 5.5 km east of the caldera of Makushin Volcano. Seismicity color indicates the year in which the earthquake occurred. The inverted triangle indicates the center of each caldera. No vertical exaggeration.

The region of interest, western US, was our last application of the method due to the large amount of data and size of the area – 3000 km x 3000 km. Seismic wave speed variations in the resulting 3D model – Ref [5] - correlate strongly with expected geologic variations and illuminate broad scale features of the western US crust and upper mantle. The model is smooth, self-consistent and provides a good starting point for more detailed investigations (Figure 4).

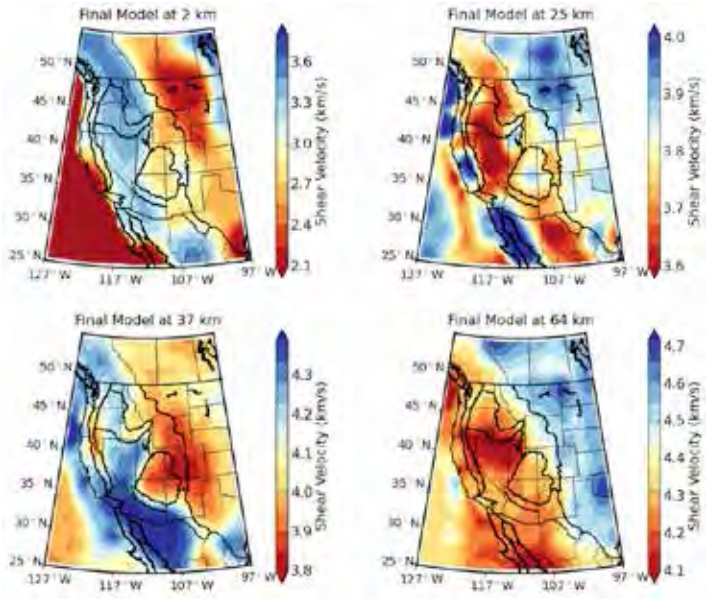

Figure 4. Shear-velocity slices through the 3D model. Dark lines show Fenneman's physiographic boundaries. Warm colors show relatively slower regions, cool colors indicate relatively faster regions. The anomalies show a combination of variations in sedimentary basin and crustal thickness with lateral variations in shear-wave speed within the crust and mantle.

Impact on National Missions

This research has enhanced the capability of the Laboratory through unique expertise in imaging Earth structure. This expertise has applications to Nonproliferation R&D under Nuclear Nonproliferation, where accurate Earth models are needed to locate, identify and determine yield for seismic events of interest such as underground nuclear explosions. In current operational practice, location accuracy has reached a bounding limit, due to a lack of detailed models of the Earth's crust. We are receiving additional funds from GNDD R&D program to prove the efficiency of our new methodology and contribute to reducing that bounding limit. We were also granted a new proposal through BAA jointly sponsored by DOE/NNSA/NA-22 to apply our new advanced multivariate technique to regions of interest for monitoring.

High-resolution Earth models are also required for characterization and monitoring within several other areas of LANL mission space including geothermal energy development, carbon sequestration, and used fuel disposition and salt repository. The expertise and methods developed here are transferable and DOE/Fossil Energy now funds us to use joint inversion techniques to model the state of stress around and away from the borehole.

References

1. Steck, L., M. Begnaud, W. S. Phillips, and R. Stead. Tomography of crustal P and S travel times across the western United States.

2. Steck, L., M. Maceira, R B. Herrmann, C. J. Ammon, and R. Stead. Crust and upper mantle structure of the western US from simultaneous inversion of surface wave dispersion, gravity, and receiver functions. 2012. In Seismological Society of America Annual Meeting. (San Diego, 17-19 April, 2012). , p. 380. El Cerrito: SSA.

3. Steck, L., M. Maceira, R. B. Herrmann, and C. Ammon. Structure of the lithosphere and asthenosphere beneath the western US from simultaneous multiparameter inversion. Presented at American Geophysical Union Fall Meeting. (San Francisco, 9-13 December, 2013).

4. Maceira, M., C. Ammon, C. Chai, and R. B. Herrmann. Application of advanced multivariate inversion techniques to the western U.S. 2014. In Seismological Society of America Annual Meeting. (Anchorage, 30 April - 2 May, 2014). Vol. 85, p. 502. El Cerrito: SSA.

5. Chai, C., C. Ammon, M. Maceira, and R. Herrmann. Inverting interpolated receiver functions with surface-wave dispersion and gravity - Application to the western US and adjacent Canada and Mexico. To appear in Geophysical Research Letters.

6. Lin, Y., E. Syracuse, M. Maceira, C. Larmat, and H. Zhang. Joint inversion for Kilauea volcano with an edge-preserving constraint. 2014. In Seismological Society of America Annual Meeting. (Anchorage, 30 April - 2 May, 2014). Vol. 85, p. 502. El Cerrito: SSA.

7. Lin, Y., E. Syracuse, M. Maceira, H. Zhang, and C. Larmat. Double-difference travel-time tomography with edge-preserving regularization and interface prior. To appear in Geophysical Journal International.

8. Zhang, H., C. Thurber, M. Maceira, and P. Roux. Joint inversion of body-wave arrival times and surface-wave dispersion data for three-dimensional seismic velocity structure around SAFOD. Presented at American Geophysical Union Fall Meeting. (San Francisco, 9-13 December, 2013).

9. Zhang, H., M. Maceira, P. Roux, and C. Thurber. Joint inversion of body-wave arrival times and surface-wave dispersion for three-dimensional seismic structure around SAFOD. 2014. Pure and Applied Geophysics. : DOI:10.1007/s00024.

10. Syracuse, E., M. Maceira, and H. Zhang. Joint inversion of seismic and gravity data for velocity structure and hypocentral locations at Akutan and Makushin volcanoes. 2014. In Seismological Society of America Annual Meeting. (Anchorage, 29 April - 2 May, 2014). , p. 500. El Cerrito: SSA.

11. Syracuse, E., M. Maceira, H. Zhang, and C. Thurber. Seismicity and structure of Akutan and Makushin Volcanoes, Alaska, using joint body- and surface-wave tomography. To appear in Journal of Geophysical Research.

Publications

Chai, C., C. Ammon, M. Maceira, and R. Herrmann. Inverting interpolated receiver functions with surface-wave dispersion and gravity - Application to the western US and adjacent Canada and Mexico. To appear in Geophysical Research Letters.

Lin, Y., E. Syracuse, M. Maceira, C. Larmat, and H. Zhang. Joint inversion for Kilauea volcano with an edge-preserving constraint. 2014. In Seismological Society of America Annual Meeting. (Anchorage, 30 April- 2 May, 2014). Vol. 85, p. 502. El Cerrito, California: SSA.

Lin, Y., E. Syracuse, M. Maceira, H. Zhang, and C. Larmat. Double-difference travel-time tomography with edge-preserving regularization and interface prior. To appear in Geophysical Journal International.

Maceira, M., C. Ammon, C. Chai, and R. B. Herrmann. Application of advanced multivariate inversion techniques to the western U.S. 2014. In Seismological Society of America Annual Meeting. (Anchorage, 30 April - 2 May, 2014). Vol. 85, p. 502. El Cerrito, California: SSA.

Steck, L., M. Begnaud, S. Phillips, and R. Stead. Tomography of crustal P and S travel times across the western United States. 2011. Journal of Geophysical Research. 116 (B11304): doi:10.1029/2011JB008260.

Steck, L., M. Maceira, R. B. Herrmann, and C. Ammon. Structure of the lithosphere and asthenosphere beneath the western US from simultaneous multi-parameter inversion. Presented at American Geophysical Union Fall Meeting. (San Francisco, 9-13 December, 2013).

Steck, L., M. Maceira, R. Herrmann, C. Ammon, and R. Stead. Crust and upper mantle structure of the western US from simultaneous inversion of surface wave dispersion, gravity, and receiver functions. 2012. In Seismological Society of America Annual Meeting. (San Diego, 17-19 April, 2012). Vol. 83, p. 380. El Cerrito, California: BSSA.

Steck, L., M. Maceira, R. Herrmann, and C. Ammon. Structure of the lithosphere and asthenosphere beneath the western US from simultaneous multi-parameter inversion. Presented at American Geophysical Union Fall Meeting. (San Francisco, 3 - 7 December, 2012).

Syracuse, E., M. Maceira, H. Zhang, and C. Thurber. Seismicity and structure of Akutan and Makushin Volcanoes, Alaska, using joint body- and surface-wave tomography. To appear in Journal of Geophysical Research.

Syracuse, E., M. Maceira, and H. Zhang. Joint inversion of seismic and gravity data for velocity structure and hypocentral locations at Akutan and Makushin volcanoes. 2014. In Seismological Society of America Annual Meeting. (Anchorage, 30 April - 2 May, 2014). Vol. 85, p. 500. El Cerrito, California: SSA.

Zhang, H., C. Thurber, M. Maceira, and P. Roux. Joint inversion of body-wave arrival times and surface-wave dispersion data for three-dimensional seismic velocity structure around SAFOD. Presented at American Geophysical Union Fall Meeting. (San Francisco , 9 -13, December, 2013).

Zhang, H., M. Maceira, P. Roux, and C. Thurber. Joint inversion of body-wave arrival times and surface-wave dispersion for three-dimensional seismic structure around SAFOD. 2014. Pure and Applied Geophysics. : DOI:10.1007/s00024.

Wide Field-of-View Plasma Spectrometer

Ruth M. Skoug
20130564ER

Abstract

For 50 years, Los Alamos has flown plasma spectrometers for national security payloads as well as NASA scientific missions. The space plasma environments measured by these payloads, such as the Earth's magnetosphere, are tremendously complex, with large spatial domains that can evolve within seconds or minutes. Since the dawn of the space age, researchers have sought to measure and understand these plasmas, the bulk of which lie in an energy range of several eV up to several tens of keV. Nevertheless, numerous questions concerning the nature and dynamics of space plasmas remain unresolved, and breakthrough understanding will require faster, higher accuracy plasma measurements.

To address these needs, we have, through the Wide Field-of-View Plasma Spectrometer LDRD-ER project, developed a fundamentally new type of space plasma spectrometer (named the 2PS Spectrometer, for its nearly 2-pi steradian field of view) with a wide field-of-view using fewer resources than traditional methods. The enabling component is analogous to a pinhole camera having an electrostatic energy-angle filter at the image plane. We have demonstrated the instrument concept through a combination of electro-optic simulations and laboratory measurements using a series of prototype instruments. We have begun studies to optimize the instrument for use in space plasma applications. In particular, we have found that appropriate energy and angle resolution can be obtained for very narrow filter plate channels, and that the required voltage can be reduced by appropriate shaping of the pinhole plate and filter plate. We have begun to explore fabrication techniques that will permit development of such devices.

We are exploring funding for continued development of the 2PS instrument, both for basic NASA science missions and for future national security payloads. We anticipate that the 2PS instrument concept will enable Los Alamos to continue to be a leader in space plasma and space environment measurements for both scientific and national security applications.

Background and Research Objectives

Throughout the space age, researchers have tried new ways to better measure and understand space plasmas [e.g. 1], the bulk of which lie in an energy range of several eV up to several 10s of keV with density ranging from 0.01 to 100 ions or electrons per cubic centimeter. One measurement technique employed for nearly 50 years in space is electrostatic energy analysis using nested spherical or cylindrical plates with different biases [e.g. 2; 3; 4]. The voltage difference between the two plates generates a radial electric field, such that a charged particle of the appropriate charge, energy, and incident direction can pass between the plates and be detected at the exit of the electrostatic analyzer. A full energy measurement of the plasma is derived by stepping the applied voltage over a range that matches the targeted plasma energies. We note that a typical detector is a channel electron multiplier (CEM) or microchannel plate (MCP), both of which are routinely flown on LANL space instruments. Los Alamos has flown this type of analyzer on both national security and NASA missions [e.g. 5; 6; 7].

A weakness of a cylindrical or spherical section electrostatic energy analyzer is its limited field-of-view (FOV). These instruments measure a narrow slice of the plasma distribution function at a given time. To fully characterize the plasma, such an instrument is typically mounted so that the fan is co-planar with the spacecraft spin vector, and the plasma is fully sampled over one spin. However, plasma dynamics and the physical processes that drive them can occur on time scales much faster than a typical spacecraft spin of 10-20 sec, making time resolution the primary limitation of this type of space plasma spectrometer.

The last high-impact innovation in plasma spectrometry

was the development of the "top hat" electrostatic analyzer [8]. The FOV of such an analyzer is circularly symmetric and the measurement sensitivity is independent of the incident angle of a charged particle around this circle. This innovation enabled acquiring a complete plasma distribution response function in half of a spin, i.e., in half the time of a traditional cylindrical or spherical section analyzer. However, the limited FOV is still intrinsically insufficient to measure a full plasma distribution function. Adding electrostatic deflection plates in front of the entrance to the top-hat [9] enables use of this instrument on a 3-axis-stabilized spacecraft, but requires substantial increases in power and mass. Los Alamos has used the top-hat geometry with scanning electrostatic deflection plates on our latest national security payloads.

To address these limitations of current instrumentation, the 2PS spectrometer measures incident ion or electron energies and incident angles over a >1.25π-steradian field of view. This design acquires a complete measurement in a single voltage sweep from a single stepped high voltage power supply without relying on spacecraft spin or additional deflection plates. The FOV is thus comparable to that of a top hat with deflector plates, but this FOV is obtained without the time or resources required to step deflectors over a range of angles. Therefore, a complete distribution function can be measured in less than 0.1 sec, enabling study of ultrafast dynamic processes of space plasma environments. The unique design enables a dramatic reduction of resources (mass, power, size, and cost) compared to the cylindrical and spherical section analyzers and top hat designs. This breakthrough concept will, for the first time, allow robust plasma measurements on 3-axis stabilized spacecraft, including smallsats and cubesats.

Scientific Approach and Accomplishments

The 2PS concept is shown schematically in Figure 1. An ion or electron enters the pinhole aperture at an angle α relative to the symmetry axis and an angle θ about the symmetry axis. It then encounters an electric field generated by the bias voltage Vf applied to the filter plate (the pinhole aperture plate is at ground). The incoming particle is deflected toward the filter plate, and enters the filter plate at an angle β and a distance r from the symmetry axis. The critical idea, and the innovative concept that underlies the 2PS concept, is that the angle β and the distance r are a unique and exclusive function of the particle incident angle α, incident energy E, and the applied voltage Vf. The angle θ of an incident particle is not affected by the electric field, so measurement of θ is trivial. In the figure, the bias voltage Vf is negative, for measurement of positive ions. By reversing the polarity to positive bias voltage Vf, electrons or negative ions can be measured with the same instrument. The filter plate consists of a series of circularly symmetric channels at a range of distances from the symmetry axis, where the bias angle β is a function of distance r from the symmetry axis. Particles from all incident angles are measured simultaneously, with the complete distribution function measured by scanning energy space by stepping the bias voltage Vf over the desired range. Following the filter plate, particles are detected using a microchannel plate detector with a position sensitive anode, allowing measurement of angle β and position r, and thus determination of the incident particle angle α and energy E. To prevent ultraviolet light and minimally deflected high energy particles from passing through to the detector, the channel angles β must be sufficiently large. This requirement precludes measurement of particles with angle α less than ~20°, as particles with smaller angles have direct access through the pinhole and the filter plate.

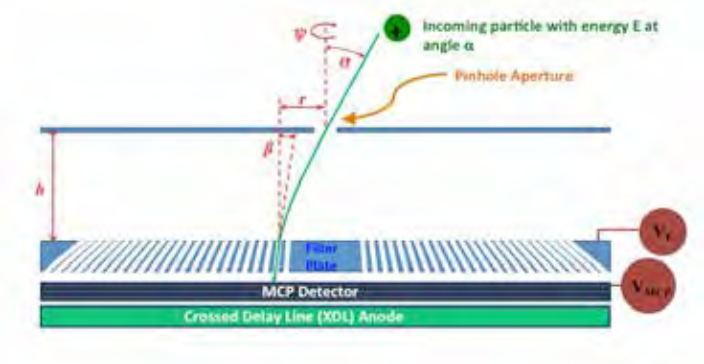

Figure 1. The 2PS spectrometer concept, including the pinhole aperture, electrostatic energy-angle filter plate, MCP detector, and position sensitive anode. Trajectories are shown for positive and negative particles in positive particle detection mode with negative bias voltage Vf.

The 2PS development effort involved two components: simulation of the instrument concept, and development and testing of prototype hardware in the laboratory. Both efforts focused on the filter plate concept, moving from proof of concept to optimization over the course of the project. Existing position sensitive detector systems are sufficient to meet the 2PS requirements. Thus further development in this area was not required and existing laboratory detectors and anodes were used for the 2PS development. This combination of laboratory measurements and simulations provides an efficient instrument design process, with laboratory measurements used to validate the simulation model, and the simulation then used to determine parameters that cannot be easily measured, such as the instrument geometric factor.

Electro-optic simulations were run using the SIMION software package [10]. These simulations included modeling of the full instrument concept as well as modeling of each

simplified prototype instrument. Most simulations were performed using SIMION in 2.5D mode, taking advantage of the cylindrical symmetry of the full instrument to design an instrument in 2 dimensions while particles are input in 3 dimensions. However, full 3D simulations were required for the original prototype due to lack of symmetry.

Multiple prototype designs were constructed and tested during the course of this project. The initial prototype filter plate was based on round holes. As drilling holes at angles is difficult, the design used appropriately sized counter-sunk holes at the filter plate entrance and exit, with each pair connected by a larger straight hole. While this instrument was relatively easy to fabricate, the lack of symmetry made it more difficult to simulate. The second prototype used a more realistic configuration, with cylindrically symmetric channels in the filter plate. This prototype demonstrated the feasibility of manufacturing such channels using wire electric discharge machining (EDM) in a single piece of metal. The symmetry of the instrument also facilitated electro-optic simulation. The combination of simulations and measurements from these prototype instruments validated the instrument concept. Figure 2 shows a comparison of the transmission as a function of energy for three channels (at different angles). The agreement between the measured and simulated distributions validates the simulation, allowing the model to be used for further optimization of the 2PS instrument. The main issue observed with these prototypes was the energy and angle resolution, which were found to be larger than desirable or typical for a current state-of-the-art instrument. Improvement of the resolution was addressed through optimization of the instrument parameters.

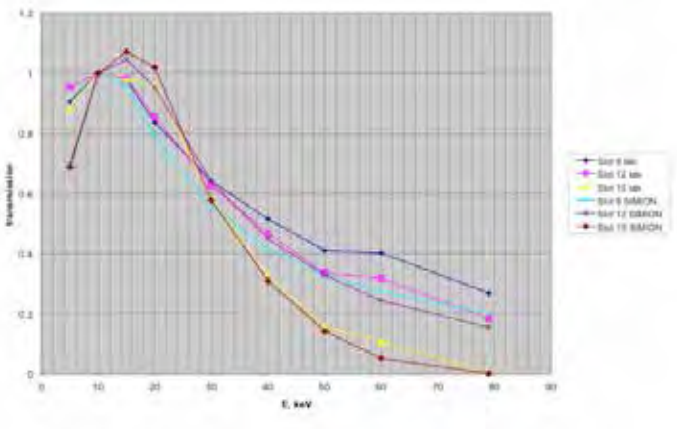

Figure 2. Comparison of simulated (cyan, purple, red) and measured (blue, magenta, yellow) energy distributions for three channels from the 2PS prototype for Vf = -5 kV. The agreement validates the simulation model.

Optimization of the instrument began with investigation of the instrument geometry, including pinhole plate and filter plate thicknesses, the distance between the two plates, and the dimensions of the filter plate channels. Simulations showed that resolution is most easily improved by reducing the width of the channels relative to the filter plate thickness. A third prototype was constructed, again using wire EDM construction, to explore the capabilities of this technique. This model had channels with ~0.5 mm diameter (compared with 0.7-2 mm diameters in the initial prototypes), and showed improved resolution, similar to current instruments. Figure 3 shows simulated 2PS energy resolution ΔE/E as a function of incoming angle α for three different channel widths. Uniform narrow widths are shown in blue and red, with wider, variable width channels in black. Allowing the channel width to increase with distance r from the symmetry axis gives more consistent resolution, but narrower channels are clearly required for resolution ΔE/E < 0.5, as in current instruments.

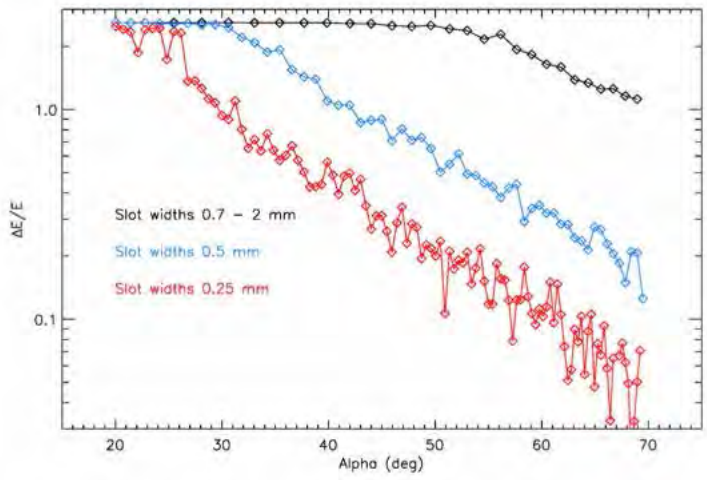

Figure 3. Energy resolution ΔE/E as a function of incoming angle α for three different channel geometries. Black: channel diameter varies with position on the filter plate from 0.7 mm near the center to 2.0 mm at the edge, blue: channel diameter of 0.5 mm at all locations, red: channel diameter of 0.25 mm at all locations.

Further optimization involved the introduction of 1) a spherical or conic structure in the center of the filter plate, and 2) a shaped pinhole plate. A model showing these structures is shown in Figure 4; these structures were also fabricated and added to the laboratory prototype. These structures add a radial component to the deflecting electric field, and the resulting increased deflection increases decreases the voltage required for measurement of particles of a given energy. For measurements at the same filter plate voltage Vf = -5000 V, Figure 5 shows the increase in energy for a laboratory prototype instrument without (red) and with (purple) the central cone and

shaped pinhole plate as shown in Figure 4. Note that this model allows measurement up to 40 keV with $\Delta E/E \approx 0.5$ for a potential of only 5 kV, and we anticipate that further reduction of voltage will be possible by optimizing the shapes of the cone and pinhole plate. The significantly reduced voltage required for measurements at a given energy will allow reduced size, weight, and complexity of the instrument electronics, making the instrument even more attractive for flight applications.

Figure 4. SIMION model showing a shaped pinhole plate and cone-like structure at the filter plate center. The pinhole is located above the center of the cone, and only a limited number of filter plate channels are shown.

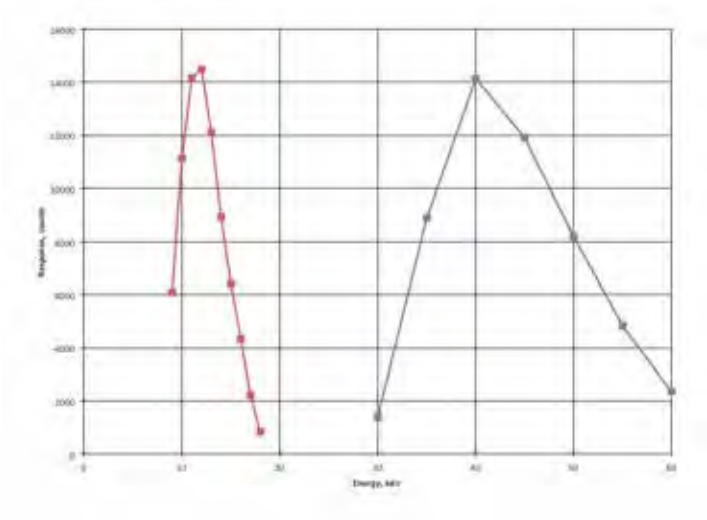

Figure 5. Comparison of measured energies for a model with 0.5 mm channels without (red) and with (purple) the cone structure and shaped pinhole plate shown in Figure 4.

Through this LDRD-ER project, we have demonstrated the 2PS instrument concept and shown that the instrument can be optimized for fast, high resolution measurements in space. The results discussed here were presented at the April 2015 Measurement Techniques in Solar and Space Physics conference, and will be submitted in late 2015 to a peer-reviewed journal as part of the proceedings of this conference.

Impact on National Missions

The 2PS Spectrometer represents a revolutionary advance for measurement of space plasmas and will realize improved performance with a reduction in required size, mass, and power resources. It will also, for the first time, enable ultra-fast measurements of plasmas to discover and test hypothesis about physical processes that induce dynamic plasma variations on short time scales.

Monitoring and understanding of the space plasma environment is a critical component of the LANL nuclear detonation detection nonproliferation mission. The Lab has also expanded its national security mission into space situational awareness, which entails understanding and predicting the space environment and its impact on the national space infrastructure. The 2PS Spectrometer will enable Los Alamos to continue to lead studies of space plasmas and the space environment, and it will position the Lab as an even stronger "go-to" institution for such measurements. We anticipate that this concept may also be the foundation for future generations of national security payloads.

We have presented the 2PS concept to the LANL national security payload program manager, and this concept will be explored further as part of a study to develop improved plasma measurement capabilities for the next generation nuclear detonation detection payloads. Additionally, a proposal for continued development of the 2PS instrument has been submitted to the 2015 NASA Heliophysics Technology and Instrument Development for Science call for proposals.

References

1. Stern, D. P.. A brief history of magnetospheric physics during the space age. 1996. REVIEWS OF GEOPHYSICS. 34 (1): 1.

2. Gosling, J. T., M. F. Thomsen, and R. C. Anderson. A cookbook for determining essential transmission characteristics of spherical section electrostatic analyzers. 2004. Los Alamos National Laboratory Report LA-10147-M.

3. Young, D. T.. Space plasma particle instrumentation and the New Paradigm: Faster, cheaper, better. 1998. AGU Monograph: Measurement Techniques for Space Plasmas (Particles) . 102: 1.

4. Funsten, H. O., and D. J. McComas. Limited resource plasma analyzers: Miniaturization concepts. 1998. AGU Monograph: Measurement Techniques for Space Plasmas (Particles). 102: 157.

5. BAME, S. J., J. R. ASBRIDGE, H. E. FELTHAUSER, J. P. GLORE, G. PASCHMANN, P. HEMMERICH, K. LEHMANN, and H. ROSENBAUER. ISEE-1 AND ISEE-2 FAST PLASMA EXPERIMENT AND ISEE-1 SOLAR-WIND EXPERIMENT. 1978. IEEE TRANSACTIONS ON GEOSCIENCE AND REMOTE SENSING. 16 (3): 216.

6. BAME, S. J., D. J. MCCOMAS, M. F. THOMSEN, B. L. BARRACLOUGH, R. C. ELPHIC, J. P. GLORE, J. T. GOSLING, J. C. CHAVEZ, E. P. EVANS, and F. J. WYMER. MAGNETOSPHERIC PLASMA ANALYZER FOR SPACECRAFT WITH CONSTRAINED RESOURCES. 1993. REVIEW OF SCIENTIFIC INSTRUMENTS. 64 (4): 1026.

7. Hahn, S., R. Elphic, T. Murphy, M. Hodgson, R. Byrd, J. Longmire, D. Lawrence, B. Barraclough, K. Fuller, T. Prettyman, M. Meier, E. Dors, H. Funsten, R. Belian, D. Patrick, T. Moore, M. Sweet, L. Burczyk, R. Williford, and C. Clanton. A validation payload for space and atmospheric nuclear event detection. 2003. IEEE TRANSACTIONS ON NUCLEAR SCIENCE. 50 (4): 1175.

8. Carlson, C. W., D. W. Curtis, G. Paschmann, and W. Michel. An instrument for rapidly measuring plasma distribution functions with high resolution. 1982. Advances in Space Research. 2 (7): 67.

9. Carlson, C. W., J. P. McFadden, P. Turin, D. W. Curtis, and A. Magoncelli. The electron and ion plasma experiment for FAST. 2001. SPACE SCIENCE REVIEWS. 98 (1-2): 33.

10. Dahl, D. A.. SIMION for the personal computer in reflection. 2000. INTERNATIONAL JOURNAL OF MASS SPECTROMETRY. 200 (1-3): 3.

Phase Transitions at Extremes: Emergence of Topological Defects

Vivien Zapf
20130601ER

Abstract

Topological states of matter are a current topic of intense scientific interest due to their potential utility in functional devices, and the intriguing challenge they pose to our scientific understanding. A key concept is "topological protection", which is the tendency of topological defects to be stable in otherwise complex and dynamic systems. Topological defects can have profound effects on the properties of materials, can potentially be used to store and manipulate information and create new couplings between materials properties. Here we explore topological effects in magnets and ferroelectrics. A long-standing theory from the 1980's, the Kibble-Zurek mechanism (KZM) [1,2], predicts that topological defects should form dynamically at phase transitions, due to freezing-in of fluctuations. Critical slowing down at the phase transition creates limitations on the speed of communication across a sample, and forces local choices of broken symmetry, creating topologically stable vortices and other defects.

We have succeeded in verifying the central prediction of the Kibble-Zurek mechanism at the ferroelectric phase transition of hexagonal manganites, and in ion coulomb crystals. (Figure 1) [3,4,5,6] In doing so, we not only verify an important theory of dynamic 2nd order phase transitions, but we also finally explain the origin of one of the first ferroelectric domain structures ever to be imaged in YMnO3 whose puzzling ferroelectric vortex structure has posed a long-standing puzzle. [7,8] We have also uncovered new examples of dynamic topological effects by using pulsed magnetic fields. Exploiting the unique capabilities of the National High Magnetic Field Lab at LANL, we have uncovered dynamic coherence effects that can be tuned with magnetic field sweep rate, as well as new topological domain structures that play a role in strong magnetoelectric coupling of ferromagnetic-like and ferroelectric-like hysteresis loops. [9,10] These topological effects go beyond KZM and enter the regime of high density defects with strong interactions, which is a new challenge to our understanding.

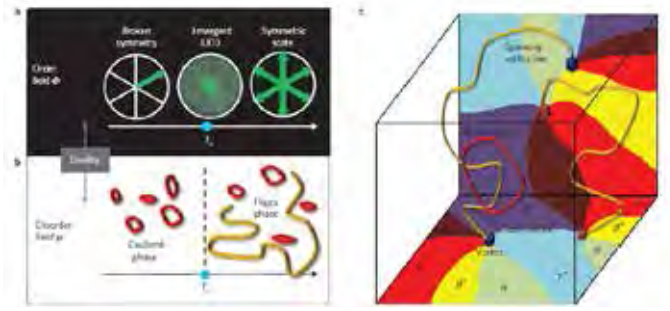

Figure 1. Topological vortices that emerge spontaneously at a dynamic second order phase transition. a) Transition from the low-temperature ordered state with broken axial symmetry to the symmetric state at high temperatures. b) Spontaneous vortex formation in the ordered and disordered state. c) Detailed simulation of vortices in the ferroelectric state of YMnO[3].

Background and Research Objectives

Phase transitions, such as the transformation from solid to liquid, or from paramagnetic to ferromagnetic, are of fundamental importance to chemistry, physics and engineering. Despite being complex many-body cooperate phenomena, they tend to obey universal rules and classifications. Landau's theory of 2nd order phase transitions has dominated our understanding of continuous phase transitions for nearly a century.[11] However, in the 1980's, Kibble and Zurek pointed out the phenomena of 'critical slowing down' and diverging coherence lengths ensure that dynamic effects will play important roles in 2nd order phase transitions even at relatively slow speeds. [1,2] Topological defects should form since limitations in the speed of communication across the sample can cause the choice of broken symmetry to be made locally. This results in domains and topological defects whose behavior is determined by the exponents of the universality class of the phase transition, and whose density increases with the speed at which the transition is traverse.

Despite their importance, characterizing these topological states to uncover their origin can be challenging. Many ferromagnets and ferroelectrics have long-range interactions that stabilize traditional domains that compete with topological defects formed due to KZM mechanisms. Moreover, imaging and counting individual topological states that have no magnetic or ferroelectric polarizations is a technical challenge.

We tackled our objective of uncovering dynamic formation of topological defects in three main ways. Firstly we used fast magnetic fields to quench magnetic spin systems to uncover new dynamic and topological effects. The magnets of the National High Magnetic Field Lab (NHMFL) at LANL span 11 orders of magnitude of magnetic field sweep rate and thus provide a unique opportunity to investigate dynamic phenomena. We discovered spontaneous non-equilibrium phase transition phenomena that occur at finite sweep rate. These frustrated antiferromagnets show characteristics of metastability and jamming, which requires another level of understanding beyond KZM because they lie in the strongly interacting regime. Specifically we investigated the problem of dynamically-induced metastable steps in frustrated Ca3Co2O6 and uncovered a new series of frustrated steps in Ca3CoMnO6 that occur five orders of magnitude faster. We used a combination of magnetic, structural, and ferroelectric measurements techniques in different pulsed magnetic field sweep rates. Moreover, another frustrated compound Lu2CoMnO6 exhibits dynamic and static jamming behavior that can be attributed to topological defect formation in frustrated quasi 1-D chains of magnetic ions. We observe unique coupling between magnetic and ferroelectric hysteresis loops.

A challenge of the magnetic field experiments is that the defect density and interaction strength falls outside of the regime where the Kibble-Zurek mechanism is predicted to be operative. Thus we also studied two systems where topological defects were generated at low densities to allow them to be counted and statistically analyzed. The ferroelectric vortices in hexagonal manganite compounds REMnO3 (RE = Y, Er, Yb) are generated with a density that depends on temperature sweep rates, and can be imaged and counted at room temperature using advanced spatially-resolved mapping techniques. The fortuitous fact that Zapf was collaborating with Sang-Wook Cheong's group at Rutgers, who was investigating vortex formation in ferroelectrics that exhibited unusual power-law scalings with quench rate, and also collaborating with Zurek who was predicting vortex formation with unusual power-law scalings with quench rate, allowed the two groups to find common ground.

Finally, we investigated topological defect formation in linear chains of ultra-cold ions. Upon rapid cooling, chains of ions undergo a phase transition from linear chain state to a zig-zag kink state that represents a topological defect. The ability to individually count the defects allows their statistics to be carefully investigated and compared to theoretical predictions.

We should mention here that a common theme in the experiments is 'multiferroic behavior' which is the coupling between magnetic and electric order in insulators. Magnetoelectric coupling in general has rather broad applications to every day machinery and devices. However, magnetoelectric coupling in insulators offers the possibility to couple magnetism to voltage, rather than current, which inherently lowers the power requirements by orders of magnitude. It is a current technological challenge to develop new multiferroic materials with strong coupling between net magnetic and ferroelectric polarizations in insulators. Achieving multiferroic behavior was not the central purpose of this ER, but topological behavior was uncovered nonetheless in several multiferroic compounds and contributes in a significant way to their functionality.

Scientific Approach and Accomplishments

Dynamic behavior in magnetic fields: We have discovered a series of systems where domains form below the phase transition that remain mobile at higher temperatures, before freezing at a second transition characterized by freezing and jamming. We have studied this phenomenology in Lu2CoMnO6, Ca3Co2O6 and Ca3CoMnO6. [9,10] In Lu2CoMnO6, in particular, we performed an extensive study of neutron diffraction, muon spin relaxation, and ac magnetic and electric susceptibility, which allowed us to characterize the material on widely different time scales. [9] Our results are consistent with topological defects in an axial next-nearest neighbor Ising model that remain mobile and highly fluctuating on the picosecond time scale of muons, yet allow for net magnetic and ferroelectric hysteresis, effectively preserving the topological domain structure. Thus defects are rapidly moving through the material without changing the overall topological configuration giving rise to a net magnetic and ferroelectric polarization. This material exhibits the unusual phenomenology of hysteresis loops of the net magnetization and ferroelectric polarization that are coupled to each other. This is rare, since most single-phase multiferroic materials exhibit little or no net magnetic hysteresis that is coupled to ferroelectricity. Coupled magnetic and electric hysteresis loops with net overall magnetic and electric polarization are a main goal of multiferroics research, due to the potential for new devices based on magnetoelectric coupling in insulators.

Meanwhile in the isostructural materials Ca3Co2O6 and

Ca3CoMnO6 we observe an additional effect, namely spontaneous coherence that is induced by finite magnetic field sweep rate (Figure 2). For certain intermediate ranges of magnetic field sweep rate (e.g. magnetic field-induced quenching), we measure sharp step-like behavior of the physical properties, while broad, continuous behavior occurs for faster, or slower sweep rates. Figure 3 shows steps in the magnetic, electric, and structural properties of the two compounds. Figure 3 shows that the steps occur for intermediate ranges of magnetic field sweep rate in Ca3CoMnO6. The ability to tune coherent phase transitions with magnetic field sweep rate is demonstrated here, and it persists across an incredibly wide range of dynamic sweep rates in two different isostructural magnets.

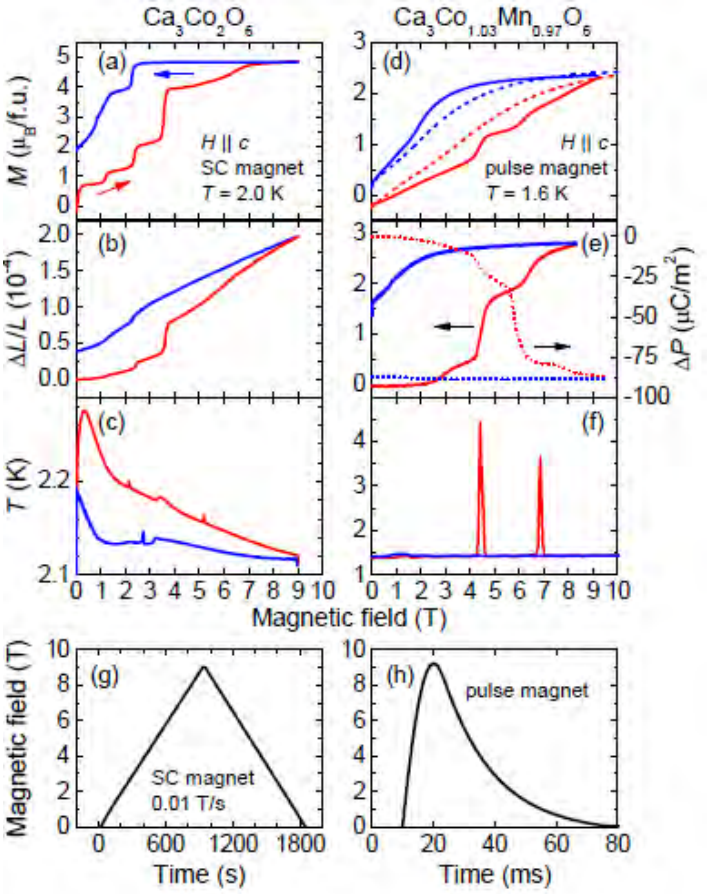

Figure 2. Steps in the magnetization M, relative length change DL/L, magnetocaloric effect (change in temperature T with magnetic field H) and electric polarization P of CaCoO and CaCoMnO, verified in multiple samples. The steps occur for sweep rates dH/dt above 1.6x10 T/s for CaCoO, and between 74 and 1,400 T/s for CaCoMnO. (g) and (h) show the magnetic field vs time profile for the SC (superconducting) and pulsed magnets used in this study. [10]

This work is being written up for publication in Physical Review Letters. [10]

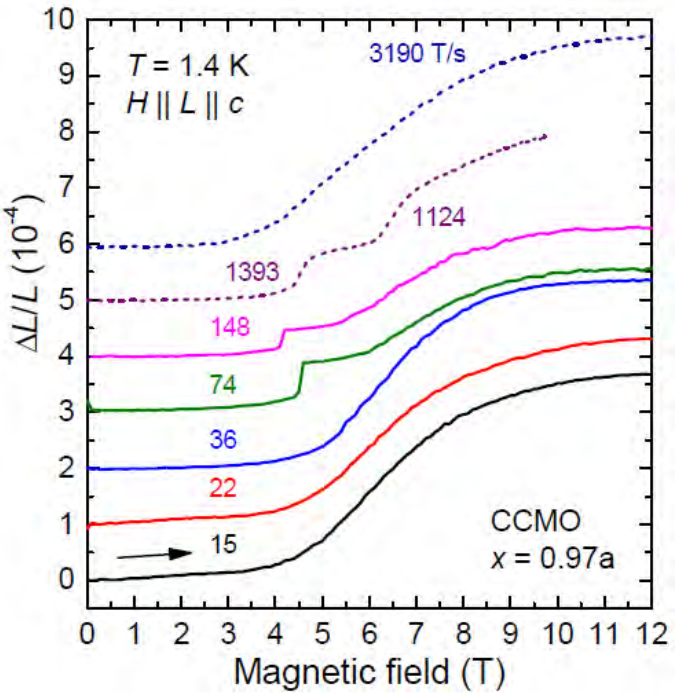

Figure 3. Magnetostriction (relative length change) of CaCoMnO (CCMO) as a function of pulsed magnetic field, where the speed is indicated in T/s. Sharp steps occur for intermediate speeds between 74 and 1393 T/s, similar to those observed at much slower speeds in CaCoO. This wide range of sweep rates is uniquely accessed by the magnets of the NHMFL at LANL. [10]

Static vortex freezing in hexagonal ferroelectrics

We have verified a central prediction of the Kibble-Zurek mechanism by investigating ferroelectric domains that form vortices at a structural phase transition well above room temperature in hexagonal manganites. This work is published in Nature Physics and summarized in Figures 1 and 4. [3] This ferroelectric/structural transition belongs to the discrete 3D XY model and chooses from among six different choices of broken symmetry. At room temperature, which is well below the phase transition temperature, the formation of ferroelectricity in these six different structural domains allows these domains to be imaged. Incidentally, at even lower temperatures the vortices pin magnetic domain boundaries and contribute to magnetoelectric coupling. Figure 4a shows calculated patterns of domains and vortices. Figure 4b shows the experimental results. G(r), the spatial correlation function between pairs of vortices is plotted as a function of their average distance, where Figure 4a shows the theoretical prediction and Figure 4b shows the experimental results for three different compounds. These ferroelectric domain structures were among the first ferroelectric domains ever to be imaged in the 1960's and have attracted extensive attention since then. [7,8] We model the origin of these defect patterns via detailed computational modeling of the dynamics of

different classes of vortices in the 3D XY model (extensive and localized loops). The predictions and experiments match to an extraordinary degree.

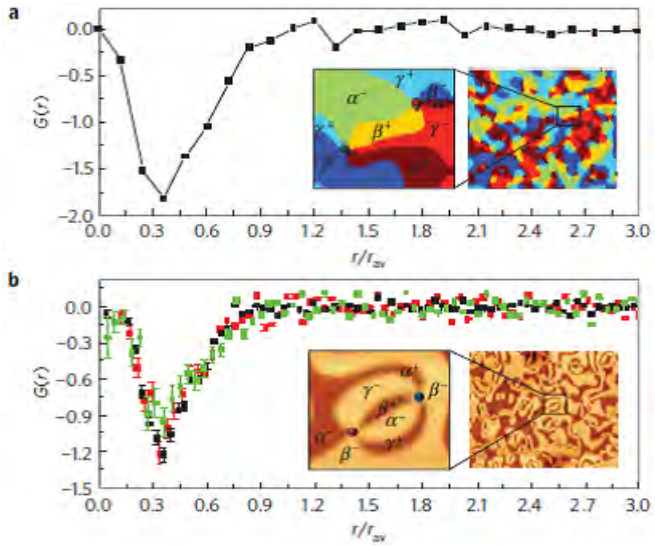

Figure 4. Statistics of vortex-vortex pair correlations in theory (a) and experiments (b) on YMnO, ErMnO and YbMnO (red, green, black data points) after dynamic quenching through a high-temperature phase transition. Images were taken at room temperature. The diagrams show patterns of six different structural/ferroelectric domains (labelled a,a, b,b,g,g) and the theoretical and experimental observation of vortex formation at finite sweep rate through the phase transition. [3]

Kibble-Zurek mechanism in Ion Columb Crystals

In the first section above detailing fast quenching in magnets, magnetic defects were created in effective 1-D chains of magnetic spins, with densities that exceeded our ability to image and count, and exhibited new kinds of collective behavior. Here we also studied defects in 1-D chains of laser-cooled ions that were rare, noninteracting and countable. [5,6] Thus we could compare the probability of topological defect formation to our theoretical models (Figure 5). We collaborated with the group of T. E. Mehlstäubler at TU Braunschweig, Germany, who studies ultra-cold ions such as those that undergo Bose-Einstein Condensation. 172Yb+ ions were confined to a three-dimensional segmented linear radio frequency Paul trap. After repeated quenching through a phase transition at sub-milliKelvin temperatures, the topological defects could be observed and their statistics counted. The ions form effective 1-D chains, spatially confined by a harmonic potential. Upon quenching, a structural phase transition occurred from a linear chain to a zig-zag chain. We were able to calculate the relationship between the defect formation probability and the speed of the quench, and compare to the predictions of our theoretical model. We found a regime of experimental parameters where friction and losses due to defect annihilation could be neglected, and so the theoretical predicted power-law relationship between topological defect formation and quench speed could be observed clearly in the experiments. This work is published in Nature Communications. [5]

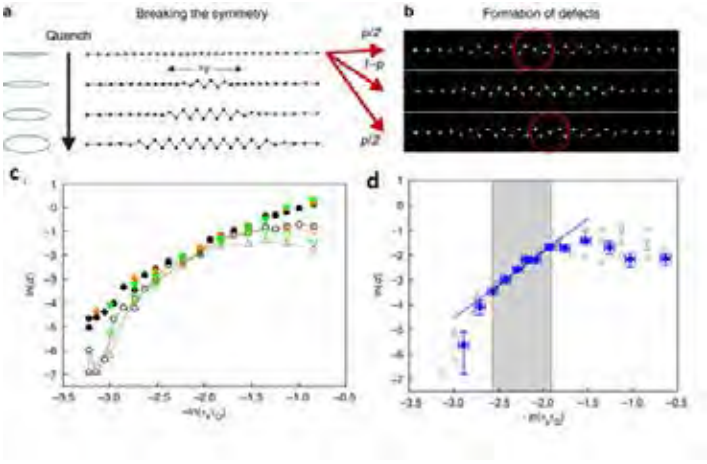

Figure 5. a) Formation of topological defects during a quench (rapid cooling), for chains of laser-cooled ultra-cold Yb ions confined to harmonic potentials. b) Zig-zag kink defects form in linear chains upon quenching. c) Theoretical prediction for the power-law behavior of kink density vs quench rate, and d) experimental results confirming the prediction. Deviations from power-law behavior (power-law behavior shown as a straight line) occur due to kink annihilation and friction effects. Here d is the defect density per quench, is the quench time at a fixed axial frequency /2=24.6±0.5 kHz, corresponding to the motion of defects. Data sets correspond to different experimental parameters described in the reference. [5]

Thus we verified a fundamental prediction of dynamic 2nd order phase transitions, in two different systems – ferroelectrics and trapped ultra-cold ions, with implications to superconductivity, magnetism, the Higgs mechanism and many other phenomena in the same universality class. Moreover, we uncovered a new set of dynamic coherence phenomena under millisecond magnetic field quenching, with practical implications to the performance of materials.

Besides our three main results, we have written several other related articles, and two invited review articles related to the topics in this ER. Our Rev. Mod. Phys. Paper was featured on the cover and on the main APS webpage for several months. [12,13]

Impact on National Missions

In our focus area of spin systems, topological defects have practical implications for performance of multifunctional materials. Topological defects are at present an international focus area due to the new multifunctional and unusual properties that arise from topological protection.

As improvements in magnetic storage densities, speeds, and power consumption approach saturation, ferroelectric storage offers a new next hope, with densities orders of magnitude above existing technology. To be feasible, ferroelectric bits must couple to magnetism to allow fast reading and writing. Such magneto-coupling mediated by spin textures and topological defects has been recently realized. Other applications include magnetic sensing, which can be achieved with record low power consumption in multiferroic materials. Topological objects by themselves can also be used to store and manipulate data in fundamentally new ways, such as by exploiting quantum entanglement. Understanding and controlling the origin of topological defects is critical.

However more generally, testing and refining general theories of non-equilibrium secon- order phase transitions has a truly broad impact, including diverse DOE agendas such as high energy physics and cosmology (universality of phase transitions means the four familiar forces of our Universe were born via this same mechanism). Condensed matter insights of the Kibble-Zurek mechanism were recognized on occasion of the 1996 3He Nobel Prize. Europe (EU) funded this research as COSLAB (COSmology in LABoratory) during 1996-2006. Capabilities that exist in NHMFL already overcome difficulties that hampered COSLAB (range of quench speeds, thermal gradients during quenching).

References

1. Zurek, W. H.. Cosmological experiments in superfluid helium. 1985. Nature. 317: 505.

2. Kibble, T.. Phase-transition dynamics in the lab and the universe. 2007. Physics Today. 60: 47.

3. Lin, S. Z., X. Wang, Y. Kamiya, G. W. Chern, G. Fan, D. Fan, B. Casas, V. Kiryukhin, W. H. Zurek, and C. Batista, S. W. Cheong. Topological defects as relics of emergent continuous symmetry and Higgs condensation of disorder in ferroelectrics. 2014. Nature Physics. 10: 970.

4. Zurek, W. H.. Topological relics of symmetry breaking: winding numbers and scaling tilts from random vortex–antivortex pairs. 2013. J. Phys.: Condens. Matter. 25: 404209.

5. Pyka, K., J. Keller, H. L. Partner, R. Nigmatullin, T. Burgermeister, D. M. Meier, K. Kuhlmann, A. Retzker, M. B. Plenio, W. H. Zurek, A. del Campo, and T. E. Mehlstaubler. Topological defect formation and spontaneous symmetry breaking in ion Coulomb crystals. 2013. Nature Communications. 4: 2291.

6. Partner, H. L., R. Nigmatullin, T. Burgermeister, J. Keller, K. Pyka, M. B. Plenio, A. Retzker, W. Zurek, A. Del Campo, and T. E. Mehlstaeubler. Structural phase transitions and topological defects in ion Coulomb crystals . 2015. Physica B. 460: 114.

7. Chae, S. C., N. Lee, Y. Horibe, M. Tanimura, S. Mori, B. Gao, S. Carr, and S. W. Cheong. Direct Observation of the Proliferation of Ferroelectric Loop Domains and Vortex-Antivortex Pairs. 2012. PHYSICAL REVIEW LETTERS. 108: 167603.

8. Safranokova, M., J. Fousek, and S. A. Kizaev . Domains in ferroelectric YMnO3. 1967. Czech Journal of Physics. 17: 559.

9. Zapf, V. S., B. G. Ueland, M. Laver, M. Lonsky, M. Pohlit, J. Muller, J. Mira, S. Yanez-Vilar, and M. A. Senaris-Rodriguez. Coupled magnetic and electric hysteresis in the multiferroic double perovskite Lu2MnCoO6 . Physical Review Letters.

10. Kim, J. W., E. D. Mun, M. Jaime, N. Harrison, J. D. Thompson, H. T. Yi, Y. S. Oh, S. W. Cheong, and V. S. Zapf. Metastable steps in the magnetic, electric and structural properties of multiferroic Ca3Co2-xMnxO6. . To appear in Physical Review Letters. It is IN REVISION. THAT DOES NOT MEAN 'TO APPEAR'!.

11. Landau, L. D.. Zh. Eksp. Teor. Fiz.. 1937. Zh. Eksp. Teor. Fiz.. 7: 19.

12. Campo, A. Del, and W. Zurek. Universality of phase transition dynamics: topological defects from symmetry breaking. 2014. In Symmetry and fundamental physics: Tom Kibble at 80. p. 31. Singapore: World Scientific.

Publications

Campo, A. Del, and W. Zurek. Universality of phase transition dynamics: topological defects from symmetry breaking. 2014. In Symmetry and fundamental physics: Tom Kibble at 80. , p. 31. Singapore: World Scientific.

Campo, A. del, T. Kibble, and W. Zurek. Causality and non-equilibrium second-order phase transitions in inhomogeneous systems. 2013. J. Phys. Condensed Matter. 25: 404210 .

Kim, J. W., E. D. Mun, M. Jaime, N. Harrison, J. D. Thompson, H. T. Yi, Y. S. Oh, S. W. Cheong, and V. S. Zapf. Metastable steps in the magnetic, electric and structural properties of multiferroic Ca3Co2-xMnxO6. . To appear in Physical Review Letters. It is IN REVISION. THAT DOES NOT MEAN 'TO APPEAR'!.

Lin, S. Z., X. Wang, Y. Kamiya, G. W. Chern, G. Fan, D. Fan, B. Casas, V. Kiryukhin, W. H. Zurek, and C. Batista, S. W. Cheong. Topological defects as relics of emergent continuous symmetry and Higgs condensation of disorder in ferroelectrics. 2014. Nature Physics. 10: 970.

Partner, H. L., R. Nigmatullin, T. Burgermeister, J. Keller, K. Pyka, M. B. Plenio, A. Retzker, W. Zurek, A. Del Campo, and T. E. Mehlstaeubler. Structural phase transitions and topological defects in ion Coulomb crystals . 2015. Physica B. 460: 114.

Pyka, K., J. Keller, H. L. Partner, R. Nigmatullin, T. Burgermeister, D. M. Meier, K. Kuhlmann, A. Retzker, M. B. Plenio, W. H. Zurek, A. del Campo, and T. E. Mehlstaubler. Topological defect formation and spontaneous symmetry breaking in ion Coulomb crystals. 2013. Nature Communications. 4: 2291.

Torrontegui, E., S. Ibanez, S. Martinez-Garaot, M. Modugno, A. del Campo, D. Guery-Odelin, A. Ruschhaupt, X. Chen, and J. G. Muga. Shortcuts to Adiabaticity. 2013. Advances in Atomic, Molecular and Optical Physics. 62: 117.

Tsyrulin, N., C. D. Batista, V. S. Zapf, M. Jaime, B. R. Hansen, C. Niedermayer, K. C. Rule, K. Habicht, K. Prokes, K. Kiefer, E. Ressouche, A. Paduan, and M. Kenzelmann. Neutron study of the magnetism in NiCl24SC(NH2)2. 2013. Journal of Physics - Condensed Matter. 25 (21): -.

Wulf, E., D. Huvonen, J. W. Kim, A. Paduan-Filho, E. Ressouche, S. Gvasaliya, V. S. Zapf, and A. Zheludev. Criticality in a disordered quantum antiferromagnet by neutron diffraction. 2013. Physical Review B. 88: 174418.

Zapf, V. S., B. G. Ueland, M. Laver, M. Lonsky, M. Pohlit, J. Muller, J. Mira, S. Yanez-Vilar, and M. A. Senaris-Rodriguez. Coupled magnetic and electric hysteresis in the multiferroic double perovskite Lu2MnCoO6 . Physical Review Letters.

Zurek, W. H.. Topological relics of symmetry breaking: winding numbers and scaling tilts from random vortex–antivortex pairs. 2013. J. Phys.: Condens. Matter. 25: 404209.

Magnetic Nanomarker Detection and Imaging with SQUIDs

Andrei N. Matlashov
20130624ER

Abstract

Despite the investment of billions of dollars over decades, many forms of cancer continue to pose a significant threat to public health. Early diagnosis of cancer, effective treatment with minimal toxicity is essential to decreasing the morbidity and mortality associated with cancer. Super-paramagnetic relaxometry (SPMR) using super-paramagnetic nano-markers (NM) is a revolutionary new technology for ultra-sensitive magnetic detection and imaging of cancerous tissue with detection limit less than 10 thousand cells. By comparison, conventional x-ray mammography requires over 10 million cancerous cells for detection. The SPMR method is based on the mapping of magnetic field generated by immobilized nano-markers. The magnetic field should be detected in many spatial positions, allowing localization of magnetic sources by solving an inverse problem. It is an ill-posed problem, i.e. a priori assumptions about magnetic sources are needed. At this point magnetic resonance imaging (MRI) can provide spatial information about sources as well as anatomical context and localization constraints. This provides realistic spatial bounds for the very accurate inverse problem solution. In this three-year project we have developed instrumentation and methods for detection (using SPMR) and imaging (using MRI) of super-paramagnetic nano-markers in phantoms and small animal models. We developed an MRI method at ultra-low magnetic field regime called ULF MRI that can detect extremely weak magnetic fields in unshielded environments in urban locations. Our instruments use highly sensitive Superconducting Quantum Interference Devices or SQUIDs. We developed highly balanced SQUID-based gradiometers with post-processing noise cancellation technique using external reference magnetometers. SPMR and ULF MRI have never been combined before in a single device. Our instruments have been tested in MD Anderson Cancer Center in Houston using small animal models in collaboration with Senior Scientific, LLC of Albuquerque.

Background and Research Objectives

Th super-paramagnetic relaxometry method includes targeting cells using antibody labeled single-core super-paramagnetic nanoparticles, followed by detection and imaging of the targeted area using high-resolution SQUID-based gradiometers. The first use of SQUIDs for detection of magnetic micro-markers in biological samples was proposed by Kötitz and colleagues in 1994 [1]. Only recently have advancements in biomarkers and nanotechnology, e.g. the production of very uniform and stable single core magnetic nanoparticles labeled with specific bio-agents, made this promising method practical as a cancer diagnostic [2]. Precise size and magnetic permeability allow researchers to pre-magnetize particles and measure the remnant magnetic moment during Néel relaxation of the particles [3]. Measurable magnetic signals featuring about one second relaxation time are generated only by bound particles of a specific size. Figure 1 illustrates schematically such a coated nanoparticle with a single-domain core [4]. It also shows a transmission electron microscope (TEM) image of a cancer cell with nanoparticles bound to the cell surface (small black dots). The particles were bound to this cell with a specific antibody – a large numbers of the NPs coat the surface with typically hundreds of thousands per cell. SPMR is used for detection of targeted cells with very high specificity: only bonded or immobilized nanoparticles will be detected via Néel relaxation. The bonding occurs only with cancer cells because of specific antibodies conjugated to the nanoparticle surface. Unbound nanoparticles will not contribute to the SPMR decay signal.

Tagging specific cells with superparamagnetic nano-markers with subsequent SQUID based relaxometry allows detection and localization of very small quantities of cells. Early detection of cancer cells is vital in minimizing the risk of entering a metastatic phase [5]. The detection limit of this technique is estimated to be as low as 10,000 cells or about 0.2 mm size tumor, which is 3

orders of magnitude lower number of cancerous cells than can be imaged by state of the art spiral X-ray Computer Tomography. Low-level cell detection can also be used for nonsurgical determination of organ transplant conditions using T-cell labeling [6] or for early diagnostic of Alzheimer's and other neurological diseases [7].

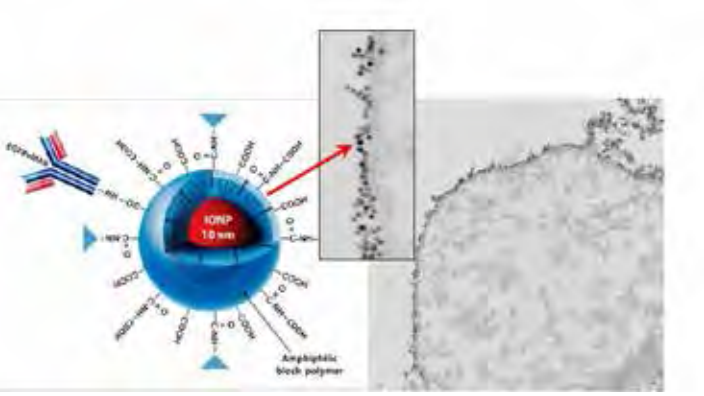

Figure 1. Illustration of super-paramagnetic Iron-Oxide Nano-Particle (IONP shown in red), it is coated with bio-compatible polymer (shown in blue) bio-conjugated to the antibody (EGFRvIIIAb) [4]. Right figure shows a transmission electron microscope image of a cancer cell covered with nano-markers (small black dots), the particles are bound to a cell with a specific antibody – a large numbers of the nanoparticles coat the surface with typically hundreds of thousands per cell.

The magnetic moment of the tagged tissue cannot be calculated from a single decay signal without knowing its exact spatial position. Thus, a multichannel system should be used that provides decay signals in many spatial positions, enabling the magnetic moment and its localization to be estimated using a multi-dipole source model fitting routine. Such a routine provides an estimated position and magnitude of the magnetized tagged volume using an ill-posed inverse problem solution. To obtain more accurate localization and spatial distribution for the tagged region MRI can be used. A conventional MRI can be used as a separate machine because of a presence of its high magnetic field [8]. Nevertheless, SPMR can be combined with ULF MRI using a single SQUID-based detection system. The spatial information obtained from ULF MRI can be used for dipole sources localization. At the same time ULF MRI cannot replace SPMR signals detection because magnetic imaging contrast is not linear function of magnetic dipole strength, so, it can provide a dipole localization but not its magnetic moment. Only a combination of ULF MRI and SPMR methods allows accurate dipoles localization and calculation their magnetic moments that are proportional to number of cancerous cells.

By combining SPMR with ULF MRI, using the same instrument, we image the targeted area that provides anatomical information. The same super-paramagnetic particles work as MRI contrast agents, as they change the relaxation rates of hydrogen nuclear spins, which are an abundant signal source due to the high water content of soft tissue. The combination of ULF MRI and SPMR provides both accurate localization and cell count of the targeted tissue. SQUIDs enable detection via gradiometers with unprecedented sensitivity. This approach provides a robust diagnostic tool for detection and localization of diseased (e.g., cancerous) tissue targeted with magnetic markers at a very early disease stage. This technique can be used as an in vivo (inside body) diagnostic. In this project ULF MRI and SPMR methods have been combined in a single device for the first time ever.

Scientific Approach and Accomplishments

During the first year the project development moved in three parallel directions. First, we significantly modified our existing 7-channel SQUID-based system that allowed using it both for ULF MRI and SPMR signals detection inside a 2-layer magnetically shielded room (MSR). Second, we have assembled and tested many different phantoms using commercially available 25-30 nm diameter super-paramagnetic nano-particles immobilized in agarose or on Q-tips. We used phantoms with different shapes and particles concentrations. Third, we started working on the development of a new instrument that could combine ULF MRI and SPMR measurements in unshielded environment.

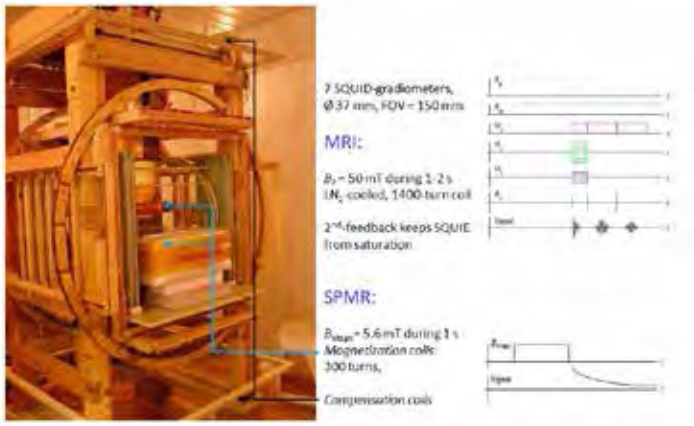

Figure 2. SQUID-based detection system for combined ULF MRI and SPMR installed inside the 2-layer magnetically shielded room (MSR). On the right panel shown shapes and timing of magnetic fields and gradients used for recording ULF MRI (upper graphs) and SPMR (bottom graphs).

Figure 2 shows the first version of our instrument. It consists of seven axial second-order gradiometers 37 mm diameter and 60 mm baseline placed inside a cryogenic vessel with liquid Helium. They are positioned in parallel one in the middle and six others surrounding it in a hexagonal pattern with 45 mm separation between the axes.

ULF MRI was performed using field-cycling and spin-echo protocol. A 3D Fourier imaging protocol was used with a frequency and phase encoding gradients. The resulting voxel size was 3×3×6 mm3 with 160 mm diameter field of view. The 1400-turn pre-polarization coil was cooled by liquid nitrogen. It was placed co-axial with the central gradiometer about 100 mm below its bottom pick-up coil. This coil generated a 50 mT pre-polarization field for ULF MRI measurements and 5.6 mT magnetizing field for SPMR measurements.

Figure 3 illustrates ULF MRI (upper panel) and SPMR (bottom panel) data recorded inside the MSR. ULF MRI was recorded using a water phantom. The phantoms were prepared using a small vial with nanoparticles inserted in a large dish of water, 140 mm ID and 45 mm deep. Agarose with uniformly embedded iron oxide nanoparticles was used to fill the vials. A small vial with 1 ml nanoparticles was used for both ULF MRI and SPMR measurements. This amount of nano-particles corresponds to about one million of tagged cells or a 1 mm size cancerous tumor. Agarose keeps NPs immobilized allowing only Néel relaxation in the case of magnetic relaxometry. In the case of ULF MRI, the same nanoparticles work as a contrast agent.

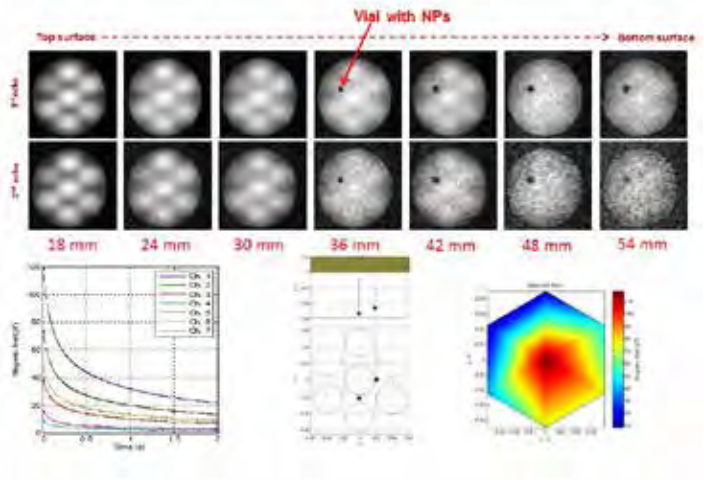

Figure 3. Upper panel: MRIs of a phantom with 1 cm NP volume (the black spot) recorded at 7 layers for 1 and 2 echoes. Bottom panel: SPMR signals, a phantom with two dipole localizations and the magnetic filed distribution.

A 3D Fourier imaging protocol was used to localize the vial. A four-echo imaging sequence was implemented (only the first and the second echoes are shown on Figure 3) that can be used to highlight the contrast caused by the nanoparticles. Magnetic relaxation was performed immediately after imaging with exactly the same phantom position (not shown). The position localized by the relaxation signals agrees with sub-millimeter accuracy with the physical location of the vial, as well as its location in the MRI [9]. The bottom panel in Figure 3 illustrates an example of SPMR signals and magnetic field distribution in the case of two closely placed dipoles (or tumors). One can see that the magnetic field distribution shows only one extrema. In this case ULF MR imaging results become very useful for two or more dipole accurate localization and magnetic moments calculations.

The SPMR signal from nanoparticles cannot be directly measured because of the presence of a large masking transient signals coming from surrounding equipment and walls. This problem was solved by recording a “baseline relaxation signal” without a phantom. Then it was subtracted from the signal recorded with a phantom in place. This difference reveals the relaxation signal primarily from the nanoparticles. Raw relaxation signals were fitted using logarithmic and polynomial functions for extrapolation to time zero. A dipole approximation can be used in the case of a single vial and an inverse problem solution allows accurate localization and the magnetic moment estimation. This approach works pretty well for a single dipole but its accuracy and trustworthiness become poor with a larger number of dipoles. It practically does not work for three and more dipoles.

The studies described here used Fe3O4 nanoparticles from two sources: from Ocean NanoTech (San Diego) and from Senior Scientific, LLC (Albuquerque). SHP and SPP series 25-nm and 30-nm diameter NPs from Ocean NanoTech showed not repeatable magnetic properties. Senior Scientific in cooperation with the Center of Integrated Nanotechnologies (CINT) developed a new manufacturing process that allowed making very uniform and stable 25 nm diameter NPs that received trade mark name PrecisionMRX™. Senior Scientific provided their new NPs for all phantoms which were built for SPMR and ULF MRI measurements at LANL.

We demonstrated, for the first time ever, the possibility of combining magnetic relaxometry and ULF MRI in a single instrument. Nanoparticles efficacy as a contrast agent was clearly demonstrated. MR images showing the influence of the nanoparticles as a contrast agent were obtained, and a plausible fit for the location and strength of magnetic dipoles were obtained by SPMR. These results have been reported at the 14th International Superconducting Electronics Conference (ISEC 2013) at the 11th European Applied Superconductivity Conference (EUCAS 2013) and at the 19th International Conference on Biomagnetism (Biomag 2014) and also published in [9, 10, 11].

During the second and the third years of the project we applied a lot of efforts toward development of new combined

ULF MRI and SPMR instruments for unshielded environments. A few versions of such instruments have been built and tested using phantoms and live animal models in cooperation with Senior Scientific, LLC, and MD Anderson Cancer Center. Figure 4 demonstrates a view of the unshielded SQUID-based detection system that allows performing both ULF MRI and SPMR signals detection in urban locations. This system has been used for demonstration ULF MR imaging capability using different phantoms. The right bottom image on Figure 4 illustrates how the human brain image may look. We used a phantom that consisted of a few volumes with different properties similar to the human brain tissue properties. A small white dot inside a red circle illustrates how a small blood inclusion will look like in such images. The results of these efforts have been reported at the 2014 Applied Superconductivity Conference (ASC'14) at the 15th International Superconducting Electronics Conference (ISEC 2015) and at the 12th European Applied Superconductivity Conference (EUCAS 2015) and also published in [12–19].

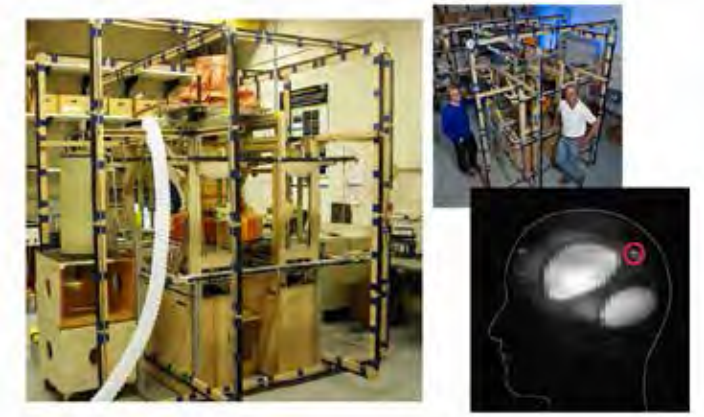

Figure 4. The unshielded SQUID-based detection system that allows performing both ULF MRI and SPMR signals detection in urban locations. The right bottom image shows ULF MR Image recorded using a phantom of the human brain with a small (1 cm) inclusion.

Figure 5 shows the multi-channel SQUID-based system that performs SPMR measurements in unshielded environment using live small animal models injected with the live human cancerous cells. This system was built and installed in Senior Scientific, LLC (Albuquerque), with LANL supervision and assistance under New Mexico Small Business Assistance Program 2013 and 2014 and under the Work for Others agreement in 2015 (NFE-15-0016). The second similar unshielded system was built and currently in use in MD Anderson Cancer Center (Houston). The most complete recent results accumulated during three years of collaboration with Senior Scientific, LLC have been published in [20].

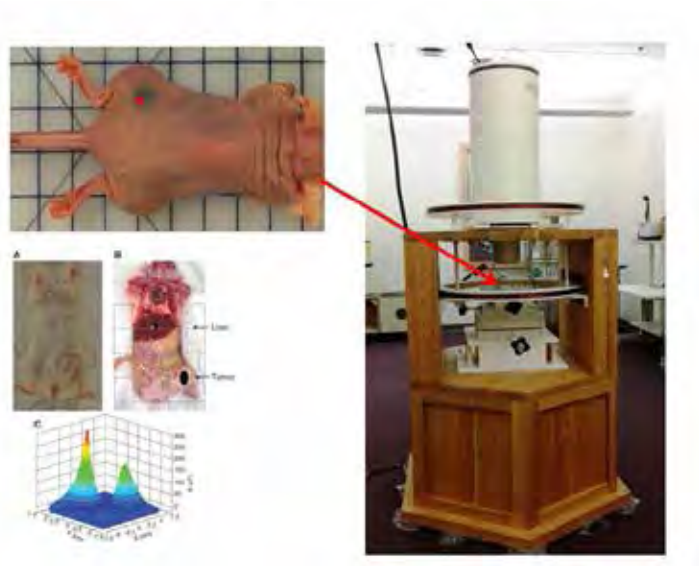

Figure 5. The unshielded SPMR system at Senior Scientific, LLC that was built with LANL supervision and assistance under New Mexico Small Business Assistance Program. The system is currently in use for investigation of the human cancerous cells behavior inserted in live small animals models [20].

Impact on National Missions

Super-paramagnetic relaxometry in combination with ultra-low field magnetic resonance imaging provide a revolutionary advance in the ability to detect and image very small numbers of labeled cells or other microscopic objects, with the resolution at least one order of magnitude better than any presently available methods suitable for routine and/or repetitive use. This project illustrates LANL's unique inter-disciplinary ability to develop new instrumentation and measurement technologies. Two key components are present at LANL – 1) Ultra-high resolution SQUID instrumentation; and 2) Magnetic nanoparticle synthesis and purification, surface modification, and specific bio-conjugation. The combination with imaging provides a truly unique approach to address both the presence and location of labels. The long-term relevance to national security science is in global health – as an early cancer diagnostic, but also in global security – the ability to rapidly detect exposure to pathogens for example, or small quantities of molecules in the environment, and in the capability to provide rare-molecule detection. The results of this work are of interest to NIH and DoD Congressionally Directed Medical Research Programs, such as the Breast Cancer Research Program.

References

1. Kötitz, R., L. Trahms, H. Koch, and W. Weitschies. Ferrofluid relaxation for biomagnetic imaging. 1995. In Biomagnetism: Fundamental Research and Clinical Applications. Edited by Baumgartner, C., L. Deecke,

G. Stroink, and S. J. Williamson. , p. 785. Amsterdam: Elsevier.

2. Adolphi, N. L., D. L. Huber, J. E. Jaetao, H. C. Bryant, D. M. Lovato, D. L. Fegan, E. L. Venturini, T. C. Monson, T. E. Tessier, H. J. Hathaway, Bergemann, R. S. Larson, and E. R. Flynn. Characterization of magnetite nanoparticles for SQUID-relaxometry and magnetic needle biopsy. 2009. JOURNAL OF MAGNETISM AND MAGNETIC MATERIALS. 321 (10): 1459.

3. Néel, L.. Some theoretical aspects of rock-magnetism. 1955. Advances in Physics. 4: 191.

4. Hadjipanayis, C. G.. EGFRvIII Antibody–Conjugated Iron Oxide Nanoparticles for Magnetic Resonance Imaging–Guided Convection-Enhanced Delivery and Targeted Therapy of Glioblastoma. 2010. Cancer Research. 70: 6303.

5. Hathaway, H. J.. Detection of breast cancer cells using targeted magnetic nanoparticles and ultrasensitive magnetic field sensors. 2010. Breast Cancer Research. 13: R108.

6. Flynn, E. R., H. C. Bryant, Bergemann, R. S. Larson, Lovato, and D. A. Sergatskov. Use of a SQUID array to detect T-cells with magnetic nanoparticles in determining transplant rejection. 2007. JOURNAL OF MAGNETISM AND MAGNETIC MATERIALS. 311 (1): 429.

7. Flynn, E.. Biomagnetic detection and treatment of Alzheimer's disease. 2011. US Patent 8,060,179 B1.

8. Adolphi, N. L.. Detection and Imaging of Her2-Targeted Magnetic Nanoparticles: Direct Comparison of SQUID-detected Magnetic Relaxometry and Magnetic Resonance. 2012. Contrast Media and Molecular Imaging. 7: 308.

9. Matlashov, A., P. Magnelind, Y. J. Kim, H. Sandin, M. Espy, A. Anderson , and H. Mukundan. SQUID-based ULF MRI and superparamagnetic relaxometry for early cancer diagnostics. 2013. Superconductivity News Forum (Global Edition). (25): ST 342.

10. Matlashov, A., P. Magnelind , H. Sandin, M. Espy , A. Anderson , and H. Mukundan. SQUID instrumentation for early cancer diagnostics: combining SQUID-based ultra-low field MRI and superparamagnetic relaxation . 2013. (Cambridge, 7 - 11 July 2013). p. 231 . Cambridge: IEEE Xplore.

11. Magnelind, P. E., Y. J. Kim, A. N. Matlashov, S. G. Newman, P. L. Volegov, and M. A. Espy. Toward early cancer detection using superparamagnetic relaxometry in a SQUID-based ULF-MRI system. 2014. SUPERCONDUCTOR SCIENCE & TECHNOLOGY. 27 (4).

12. Espy, M., A. Matlashov, and P. Volegov. SQUID-detected ultra-low field MRI. 2013. JOURNAL OF MAGNETIC RESONANCE. 228: 1.

13. Espy, M., P. Magnelind, A. Matlashov, A. Urbaitis, and P. Volegov. Toward high resolution images with SQUID-based ultra-low field magnetic resonance imaging. 2013. IEEE Transactions on Applied Superconductivity. 23 (3): 1603107.

14. Espy, M., P. Magnelind, A. Matlashov, S. Newman, H. Sandin, L. Schultz, R. Sedillo, A. Urbaitis, and P. Volegov. Progress toward a deployable SQUID-based ultra-low field MRI system for anatomical imaging. 2015. IEEE Transactions on Applied Superconductivity. 25 (3): 1601705.

15. Matlashov, A., P. Magnelind, S. Hewman, H. Sandin, A. Urbaitis, P. Volegov, and M. Espy. Multi-channel SQUID-based ultra-low field magnetic resonance imaging in unshielded environment. 2015. Superconductivity News Forum (SNF): Global Edition, STP 456.

16. Matlashov, A., P. Magnelind, P. Volegov, and M. Espy. Elimination of 1/f noise in gradiometers for SQUID-based ultra-low field nuclear magnetic resonance. (Nagoya, Japan, 6-9 July, 2015).

17. Matlashov, A., P. Magnelind, S. Newman, H. Sandin, A. Urbaitis, P. Volegov, and M. Espy. Multi-channel SQUID-based ultra-low field magnetic resonance imaging in unshielded environment. (Nagoya, Japan, 6-9 July, 2015).

18. Magnelind, P., A. Matlashov, P. Volegov, and M. Espy. Noise-reduction in wire-wound SQUID gradiometers used in ultra-low field magnetic resonance. (Lyon, France, 6-10 Sept. 2015).

19. Magnelind, P., A. Matlashov, S. Newman, H. Sandin, R. Sedillo, A. Urbaitis, and P. Volegov. Deployable SQUID-based magnetic resonance imaging systems. (Lyon, France, 6-10 Sept. 2015).

20. Haro, L. P. De, T. Karaulanov, E. Vreeland, B. Anderson, H. Hathaway, D. Huber, A. Matlashov, C. Nettles, A. Price, T. Monson, and E. Flynn. Magnetic relaxometry as applied to sensitive cancer detection and localization. 2015. Biomed. Engineering – Biomed. Technik by DE GRUYTER. : DOI 10.1515/bmt.

Publications

Espy, M., A. Matlashov, and P. Volegov. SQUID-detected ultra-low field MRI. 2013. JOURNAL OF MAGNETIC RESONANCE. 228: 1.

Espy, M., P. Magnelind, A. Matlashov, A. Urbaitis, and P. Volegov. Toward high resolution images with SQUID-based ultra-low field magnetic resonance imaging. 2013. IEEE Transactions on Applied Superconductivity. 23 (3): 1603107.

Espy, M., P. Magnelind, A. Matlashov, S. Newman, H. Sandin, L. Schultz, R. Sedillo, A. Urbaitis, and P. Volegov. Progress toward a deployable SQUID-based ultra-low field MRI system for anatomical imaging. 2015. IEEE Transactions on Applied Superconductivity. 25 (3): 1601705.

Haro, L. P. De, T. Karaulanov, E. Vreeland, B. Anderson, H. Hathaway, D. Huber, A. Matlashov, C. Nettles, A. Price, T. Monson, and E. Flynn. Magnetic relaxometry as applied to sensitive cancer detection and localization. 2015. Biomed. Engineering – Biomed. Technik by DE GRUYTER. : DOI 10.1515/bmt.

Magnelind, P. E., Y. J. Kim, A. N. Matlashov, S. G. Newman, P. L. Volegov, and M. A. Espy. Toward early cancer detection using superparamagnetic relaxometry in a SQUID-based ULF-MRI system. 2014. SUPERCONDUCTOR SCIENCE & TECHNOLOGY. 27 (4).

Magnelind, P., A. Matlashov, P. Volegov, and M. Espy. Noise-reduction in wire-wound SQUID gradiometers used in ultra-low field magnetic resonance. To appear in 12th EUropean Conference on Applied Superconductivity. (Lyon, France, 6-10 Sept. 2015).

Magnelind, P., A. Matlashov, S. Newman, H. Sandin, R. Sedillo, A. Urbaitis, and P. Volegov. Deployable SQUID-based magnetic resonance imaging systems. To appear in 12th EUropean Conference on Applied Superconductivity. (Lyon, France, 6-10 Sept. 2015).

Matlashov, A., P. Magnelind , H. Sandin, M. Espy , A. Anderson , and H. Mukundan. SQUID instrumentation for early cancer diagnostics: combining SQUID-based ultra-low field MRI and superparamagnetic relaxation . 2013. In Fourteenth International Superconducting Electronics Conference . (Cambridge, 7 - 11 July 2013). , p. 231 . Cambridge: IEEE Xplore.

Matlashov, A., P. Magnelind, P. Volegov, and M. Espy. Elimination of 1/f noise in gradiometers for SQUID-based ultra-low field nuclear magnetic resonance. To appear in 15th International Superconductive Electronics Conference. (Nagoya, Japan, 6-9 July, 2015).

Matlashov, A., P. Magnelind, S. Hewman, H. Sandin, A. Urbaitis, P. Volegov, and M. Espy. Multi-channel SQUID-based ultra-low field magnetic resonance imaging in unshielded environment. 2015. Superconductivity News Forum (SNF): Global Edition, STP 456.

Matlashov, A., P. Magnelind, S. Newman, H. Sandin, A. Urbaitis, P. Volegov, and M. Espy. Multi-channel SQUID-based ultra-low field magnetic resonance imaging in unshielded environment. To appear in 15th International Superconducting Electronics Conference. (Nagoya, Japan, 6-9 July, 2015).

Matlashov, A., P. Magnelind, Y. J. Kim, H. Sandin, M. Espy, A. Anderson , and H. Mukundan. SQUID-based ULF MRI and superparamagnetic relaxometry for early cancer diagnostics. 2013. Superconductivity News Forum (Global Edition). (25): ST 342.

Electron Capture Spectroscopy for Neutrino Mass: Isotopes, Science, and Technology Development

Michael W. Rabin
20130679ER

Abstract

The classic and traditional tritium-decay method for measuring neutrino mass will soon reach its performance limit. Alternative methods and isotopes are needed. We have conducted research developing and assessing an alternative technique for measuring the kinematic mass of the neutrino. This method is based on the electron-capture decay of 163Ho measured at high resolution with cryogenic microcalorimeter detectors. We have developed a complete process for proton-beam-based isotope production, isolation, and purification of 163Ho. About 145 micrograms of 163Ho have been produced, and about 13 nanograms of purified 163Ho are currently available for experimentation. We have developed methods for incorporating this isotope into high resolution microcalorimeters and successfully measured the electron-capture spectrum of 163Ho. These techniques have had a specific, technical impact with potential to open completely new areas of application in trace-level actinide analysis for environmental samples, nuclear nonproliferation, treaty verification, international safeguards, and nuclear forensics.

Background and Research Objectives

What is the mass of the neutrino? Answering this question is our long-term goal, a tremendous experimental challenge and a compelling world-physics problem. Not so long ago, the zero-mass neutrino was taken as a self-evident truth, but strong experimental evidence accumulated over the past fifteen years implies non-zero but very small mass. The best results to date suggest the neutrino mass scale is about ~0.05-0.5 electron volts, a million times smaller than the mass of the electron, making the neutrino the lightest of all the massive particles and making mass measurement extremely difficult. The neutrino has also moved to center stage in particle physics, displacing the Higgs boson, because neutrino mass has wide-ranging implications, significantly influencing the evolution of large-scale cosmic structure, the formation of atomic nuclei in the first few minutes after the Big Bang, stellar explosions, our understanding of basic symmetries and asymmetries of the universe, the use of neutrinos to probe the interior of both the sun and the earth, and the potential for antineutrino detector networks to monitor nuclear reactor operation and watch for nuclear explosions. Astonishingly, outcomes in all these areas, whether for science or nuclear security, depend on the mass of the neutrino.

The question posed above is a dramatic over simplification because neutrino physics is driven by hidden quantum masses. There are at least three of them, we have no direct experimental access to the individual masses, and experiments probing neutrino mass are sensitive, at best, to mathematical combinations of these quantum masses (technically called mass eigenvalues). There are four broad and complementary classes of relevant experiments, each sensitive to a different observable: neutrino oscillations, cosmology, double beta decay, and kinematics. Redundant results in each class are necessary to provide a complete picture of neutrino mass and determine each of the hidden quantum masses.

Our focus is on experiments measuring the kinematic mass, mkin, from radioactive decays that emit either a single neutrino or antineutrino. Fundamentally, kinematic experiments rely on the neutrino-mass-dependence of the shape of an energy spectrum of a decay product or products (electron, daughter atom or both) near the endpoint of that spectrum, Emax, the energy at which the spectrum reaches zero and above which the reaction is forbidden by energy conservation. These experiments are kinematic in the sense that the endpoint region of the spectrum corresponds to the neutrino momentum approaching zero and the energy of other decay products reaching a maximum. The classic and traditional method based on tritium decay will soon reach its technological zenith, with expected sensitivity of 0.2-0.3 eV. Recent cosmology and oscillation results suggest this will be insufficient for probing the neutrino mass scale, and

sensitivity of ~0.05 to 0.1 eV will be needed. Alternative methods and isotopes are under investigation to achieve this goal. The most promising alternative isotope is 163Ho, and development of a complete measurement method based on this isotope has been the primary objective of this project.

Scientific Approach and Accomplishments

Holmium-163 has become the center of attention for the determination of the kinematic mass of the electron neutrino using cryogenic microcalorimeters. Holmium-163 is a rare, unusual, synthetic isotope that decays purely by electron capture. The very low total nuclear decay energy (QEC<3 keV) and reasonable half life (4570 years) of 163Ho, make it attractive for high precision electron-capture spectroscopy (ECS) near the kinematic endpoint. In the ECS approach, an electron-capture-decaying isotope is embedded directly and completely inside a microcalorimeter designed to capture and measure the energy of all the decay radiation except that of the escaping neutrino. Future studies of the ECS endpoint region with large sensor arrays are planned to measure or put limits on the neutrino kinematic mass. The central challenges for this approach are: isotope production and purification; incorporation of 163Ho into sensors; high resolution spectroscopy of electron capture decays; scaling up to many thousands of pixels; independent measurement of QEC; and a complete understanding of the nuclear and atomic physics of the decay to determine the neutrino kinematic mass. We have developed 163Ho production using proton irradiation of isotopically natural dysprosium targets with both a low-beam-current cyclotron (University of Wisconsin, Madison) and a much higher current proton accelerator (Los Alamos National Laboratory Isotope Production Facility). We performed 163Ho purification with high performance liquid chromatography, producing 10-nanogram scale purified 163Ho isotope samples. Over the last two years we have successfully demonstrated the incorporation the 163Ho in absorbers attached to transition-edge-sensor microcalorimeters, and we have measured 163Ho spectra of the M and N spectral peaks.

Holmium-163 is not a naturally occurring isotope, and is not commercially available. We explored a variety of production options, described in [1]. Proton irradiation of natural Dy has advantages over other options, principally substantially higher isotopic purity of 163Ho and ease of obtaining the natural Dy target material. We have performed three proton irradiations of natural Dy, summarized in Figure 1. The first irradiation ("Foil 1") was a small-scale pathfinder, demonstrating all components of the process. The second irradiation was performed on a similar small-scale target ("Foil 2"), but with substantially improved starting chemical composition (about 2.8 ppm of natural 165Ho prior to irradiation). Combined with a longer irradiation, this led to a factor of 200 improvement in isotopic purity compared to Foil 1. A third, much larger target (IPF 1) was irradiated at the Los Alamos National Laboratory Isotope Production Facility, allowing us to increase beam current by a factor of over twenty. This target consists of 12.6 g of high purity natural Dy in an Inconel case. It was irradiated at a proton beam current of 230 μA with nominal incident energy 25 MeV and nominal exit energy 10 MeV, and a total cumulative charge of 33,645 μAh. It is estimated to contain approximately 145 μg of 163Ho corresponding to 2.48 MBq. A second, similar target (IPF 2) is available for a future irradiation.

Target	Proton irradiation	Dy mass	Initial ^{163}Ho mass	Estimated final ^{163}Ho mass
Foil 1	100 μAh, 16 MeV	377 mg	94 μg	60 ng
Foil 2	400 μAh, 16 MeV	677 mg	1.9 μg	170 ng
IPF 1	33,645 μAh, 10-25 MeV	12.6 g	35.3 μg	145 μg
IPF 2	Not yet irradiated	12.6 g	35.3 μg	N/A
Product	**Source**	**Residual Dy**	**^{165}Ho/^{163}Ho**	**^{163}Ho**
F1	Entire center of Foil 1 54.5 mg	401±15 ng	397±15	24.8±1.3 ng
F2C1	Wedge of Foil 2 (10%) 12 mg	40.5±1.3 ng	1.8±0.1	13.2±0.4 ng

Figure 1. Summary of targets and products for production, isolation, and purification of Ho using proton irradiation. Target materials are always isotopically natural Dy.

Holmium from portions of Foil 1 and Foil 2 was isolated by cation-exchange high performance liquid chromatography (HPLC) by a procedure described in [2]. Figure 1 summarizes properties of the separated 163Ho product solutions. The entire 54.5 mg center section of Foil 1, where most of the 163Ho was located, was used for product solution F1. The collected Ho fraction was processed in two steps by ion-exchange chromatography and extraction chromatography to remove the complexing agent (α-HIBA) and concentrate the Ho. The product solution was measured by inductively coupled plasma atomic emission spectroscopy (ICP-AES) and inductively coupled plasma mass spectrometry (ICP-MS) to contain 24.±1.3 ng 163Ho, 401 ±15 ng Dy, and a 165Ho/163Ho ratio of 397±15. Overall recovery of Ho from the center section of Foil 1 was 81.8±0.6%. A 12 mg portion of the center of Foil 2 was separated using a similar procedure to obtain product solution (Foil 2 Cut 1 or F2C1). An improved Ho-Dy separation factor was obtained by using lower Dy mass for this separation and a lower pH. The Foil 2 (F2C1) product solution contained 13.2±0.4 ng 163Ho, 40.5±1.3 ng Dy, and a 165Ho/163Ho ratio of 1.8±0.1. Approximately 90% of the center of Foil 2 (120 mg) remains available for future separations.

The unique requirements of 163Ho electron capture

spectroscopy motivated the development of a new style of transition-edge sensor. The primary concerns were low heat capacity so that the dynamic range of the sensor could be matched to the low Q value of 163Ho decay, and a mechanically robust design that would be compatible with a wide range of absorber attachment options during the prototyping phase of the project. The TES is conceptually similar to the larger devices made for Q spectroscopy of actinides, where the weak thermal conductance to the bath is provided by a silicon spring instead of the more typical silicon nitride membrane. The TESs for this project consist of a 350 µm square Mo-Cu bilayer with superconducting transition temperature near 110 mK, located on a 50 µm wide silicon beam for thermal isolation (Figure 2). The silicon beam is the full wafer thickness of 275 µm, and is defined by a deep reactive ion etch process. A pad at the end of the beam provides an absorber attachment point. During the first phase of the project, while 163Ho was being produced, testing of these transition edge sensors began with 55Fe. This isotope was immediately available, and provides energy peaks at 6539 eV, 769 eV, and 82 eV, corresponding to the electron binding energies of the Mn daughter atom (Figure 3, left). The best energy resolution from this type of detector, given by the Gaussian component of a Bortels function fit, was 7.6±0.6 eV FWHM at 6539 eV (Figure 3, right).

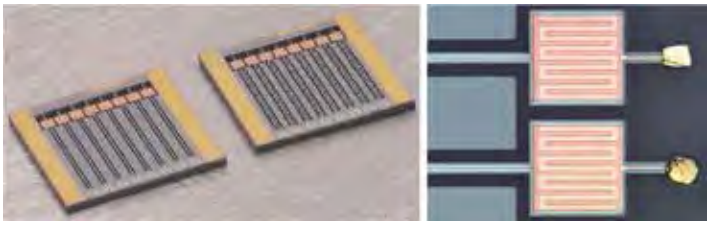

Figure 2. Transition edge sensors developed for Ho electron capture spectroscopy use a silicon beam thermal isolation to enable varied absorber attachments. Gold foil absorbers are attached to the end of the beam (right).

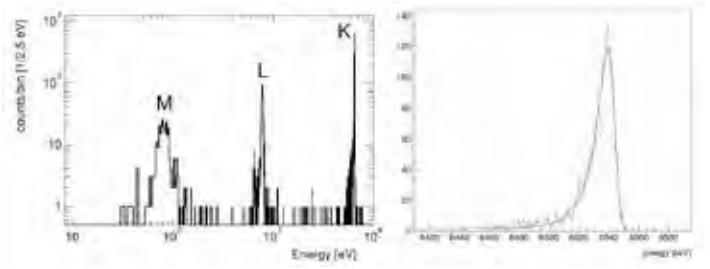

Figure 3. The isotope 55Fe is was immediately available.

Experiments with 55Fe, as well as our other work on Q spectroscopy of embedded actinides, suggested several important features for an optimal absorber with embedded radioactive material. First, purity of the embedded material is necessary. Additional material in the deposit, besides the radioactive isotope of interest, adds deleterious heat capacity and increases the potential for energy trapping in the deposit. Second, the radioactive material in the absorber matrix must be distributed in grains that are small compared to the relevant radiation path lengths in order to provide a uniform environment for energy deposition and thermalization [3-5].

We have focused on two methods of creating an absorber structure for electron capture spectroscopy of 163Ho: aqueous solution deposition in nanoporous gold and alloying techniques. To create nanoporous gold for absorbers, we used electron-beam evaporation to deposit a 1.5 µm thick layer of Au-Ag alloy on a 5 µm thick Au foil. The Ag was dealloyed by placing the foil in concentrated nitric acid for 48 hours. The resulting foil had a nanoporous gold layer with pore sizes in the 50-100 nm range (Figure 4).

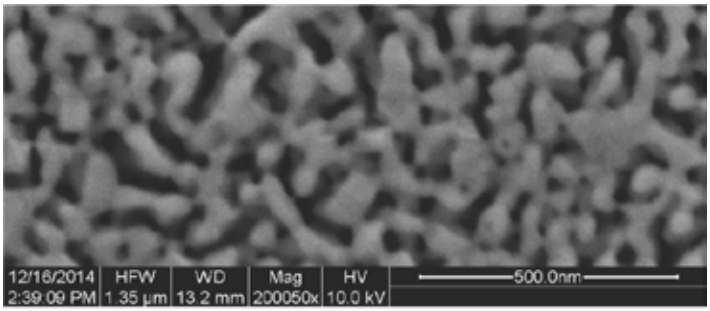

Figure 4. Nanoporous gold was used to constrain the crystal size in dried deposits of Ho product solution and create nanocomposite absorbers with embedded Ho.

Aqueous solutions are readily absorbed by the nanoporous gold layer. It acts like a sponge. When these solutions dry, the crystals in the deposit are constrained by the pore size to form a nanocomposite structure. Because of the foil backing, ~100 µm sections could be cut to form absorbers. F2C1 163Ho product in 0.1M HCl solution was deposited with a 30 µm diameter glass capillary onto ~50x100 µm sections of the foil-backed nanoporous gold. The foils were folded in half and pressed to encapsulate the deposits, then attached to TES die. Energy resolutions obtained for these detectors ranged from 50 to 60 eV. This method produced deposits with significant additional material besides the 163Ho. The composition of the deposits was measured by energy-dispersive x-ray spectroscopy (EDS) in a scanning electron microscope (SEM). The EDS spectrum indicated the presence of significant Na, Cl, and organic compounds. We have shown that most of these contaminants can be eliminated from the deposit by heating to 800°C in forming gas (<10% H2). EDS spectra of samples after this heating process no longer show measurable Na or Cl. Absorbers made by heating the foil-backed nanoporous gold after deposition show greatly improved energy resolution. The

best spectrum for this type of absorber is shown in Figure 5, with energy resolution of ~22 eV for the N line and ~40 eV for the M line, obtained from the Gaussian component of a Bortels function fit to the peaks. A single-point energy calibration is used, based on the binding energy of the M1 electron (n=3, l=0,j=1/2) of Dy. Key major peaks are observed, and these correspond to the M1, M2, N1, and N2 single-hole intermediate states of the 163Dy daughter atom.

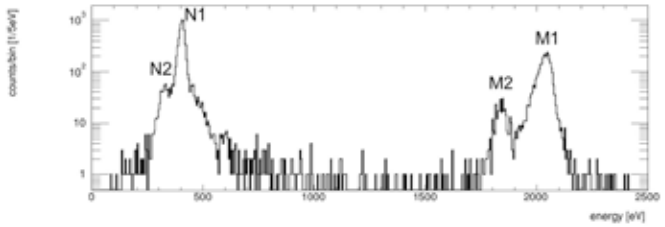

Figure 5. Measured electron-capture spectrum of 163Ho showing major peaks associated with the MI, M2, NI, and N2 single-hole intermediate states of the 163Dy daughter atom.

These results are extremely encouraging and scientifically timely. Only in the past few months have two independent experimental groups actively measuring 163Ho ECS spectra with sufficient data quality and two independent theorists actively making calculations been able to compare results closely. A detailed comparison is underway as of this writing.

Impact on National Missions

This project has had a specific, technical impact with potential to open completely new areas of application in trace-level actinide analysis for environmental samples, nuclear nonproliferation, treaty verification, international safeguards, and nuclear forensics. The simple methods discussed above for producing absorber nanostructure (mechanical alloying, gold nanofoam) and concepts in energy thermalization were developed first for neutrino science, and were then rapidly applied to the analysis of picogram-scale alpha-decaying actinides. We have recently published these astonishing results [5], which show the elimination of a pernicious double-peak structure that had been corrupting our measurements and to-the-baseline resolution between previously overlapping Pu peaks. We believe this creates substantial new opportunity for application to nondestructive isotopic assay of trace-level nuclear materials, especially particulate samples. These applications include (1) simultaneous analysis of multiple isotopes of multiple elements without standards, tracers, or time-consuming chemical separation, (2) determining the chemical age of trace-level Pu samples in a single measurement via the 241Am/241Pu chronometer, especially effective for young Pu (e.g. that from a new proliferator), and (3) direct analysis of as-received particles, the nuclear industrial dust of extraordinary value for IAEA safeguards and treaty verification.

References

1. Engle, J. W., E. R. Birnbaum, H. R. Trellue, K. D. John, M. W. Rabin, and F. M. Nortier. Evaluation of Ho-163 production options for neutrino mass measurements with microcalorimeter detectors. 2013. NUCLEAR INSTRUMENTS & METHODS IN PHYSICS RESEARCH SECTION B-BEAM INTERACTIONS WITH MATERIALS AND ATOMS. 311: 131.

2. Mocko, , W. A. Taylor, F. M. Nortier, J. W. Engle, T. E. Barnhart, R. J. Nickles, A. D. Pollington, G. J. Kunde, M. W. Rabin, and E. R. Birnbaum. Isolation of Ho-163 from dysprosium target material by HPLC for neutrino mass measurements. 2015. RADIOCHIMICA ACTA. 103 (8): 577.

3. Croce, M. P., E. M. Bond, A. S. Hoover, G. J. Kunde, Mocko, M. W. Rabin, N. R. Weisse-Bernstein, L. E. Wolfsberg, D. A. Bennett, Hays-Wehle, D. R. Schmidt, and J. N. Ullom. Microcalorimeter Q-spectroscopy for rapid isotopic analysis of trace actinide samples. 2015. NUCLEAR INSTRUMENTS & METHODS IN PHYSICS RESEARCH SECTION A-ACCELERATORS SPECTROMETERS DETECTORS AND ASSOCIATED EQUIPMENT. 784: 151.

4. Croce, M. P., E. M. Bond, A. S. Hoover, G. J. Kunde, W. A. Moody, M. W. Rabin, D. A. Bennett, Hayes-Wehle, Kotsubo, D. R. Schmidt, and J. N. Ullom. Integration of Radioactive Material with Microcalorimeter Detectors. 2014. JOURNAL OF LOW TEMPERATURE PHYSICS. 176 (5-6): 1009.

5. Hoover, A. S., E. M. Bond, M. P. Croce, T. G. Holesinger, G. J. Kunde, M. W. Rabin, L. E. Wolfsberg, D. A. Bennett, J. P. Hays-Wehle, D. R. Schmidt, Swetz, and J. N. Ullom. Measurement of the Pu-240/Pu-239 Mass Ratio Using a Transition-Edge-Sensor Microcalorimeter for Total Decay Energy Spectroscopy. 2015. ANALYTICAL CHEMISTRY. 87 (7): 3996.

Publications

Croce, M. P., E. M. Bond, A. S. Hoover, G. J. Kunde, Mocko, M. W. Rabin, N. R. Weisse-Bernstein, L. E. Wolfsberg, D. A. Bennett, Hays-Wehle, D. R. Schmidt, and J. N. Ullom. Microcalorimeter Q-spectroscopy for rapid isotopic analysis of trace actinide samples. 2015. NUCLEAR INSTRUMENTS & METHODS IN PHYSICS RESEARCH SECTION A-ACCELERATORS SPECTROMETERS DETECTORS AND ASSOCIATED EQUIPMENT. 784: 151.

Croce, M. P., E. M. Bond, A. S. Hoover, G. J. Kunde, W. A.

Moody, M. W. Rabin, D. A. Bennett, Hayes-Wehle, Kotsubo, D. R. Schmidt, and J. N. Ullom. Integration of Radioactive Material with Microcalorimeter Detectors. 2014. JOURNAL OF LOW TEMPERATURE PHYSICS. 176 (5-6): 1009.

Croce, M. P., K. E. Koehler, G. J. Kunde, M. W. Rabin, E. M. Bond, W. A. Moody, D. R. Schmidt, L. R. Vale, R. D. Horansky, Kotsubo, and J. N. Ullom. Eight-Channel TES Microcalorimeter System for Detector and Source Development. 2013. IEEE TRANSACTIONS ON APPLIED SUPERCONDUCTIVITY. 23 (3).

Engle, J. W., E. R. Birnbaum, H. R. Trellue, K. D. John, M. W. Rabin, and F. M. Nortier. Evaluation of Ho-163 production options for neutrino mass measurements with microcalorimeter detectors. 2013. NUCLEAR INSTRUMENTS & METHODS IN PHYSICS RESEARCH SECTION B-BEAM INTERACTIONS WITH MATERIALS AND ATOMS. 311: 131.

Hoover, A. S., E. M. Bond, M. P. Croce, T. G. Holesinger, G. J. Kunde, M. W. Rabin, L. E. Wolfsberg, D. A. Bennett, J. P. Hays-Wehle, D. R. Schmidt, Swetz, and J. N. Ullom. Measurement of the Pu-240/Pu-239 Mass Ratio Using a Transition-Edge-Sensor Microcalorimeter for Total Decay Energy Spectroscopy. 2015. ANALYTICAL CHEMISTRY. 87 (7): 3996.

Koehler, K. E., D. A. Bennett, E. M. Bond, M. P. Croce, D. E. Dry, R. D. Horansky, Kotsubo, W. A. Moody, M. W. Rabin, D. R. Schmidt, J. N. Ullom, and L. R. Vale. Q Spectroscopy With Superconducting Sensor Microcalorimeters. 2013. IEEE TRANSACTIONS ON NUCLEAR SCIENCE. 60 (2): 624.

Mocko, , W. A. Taylor, F. M. Nortier, J. W. Engle, T. E. Barnhart, R. J. Nickles, A. D. Pollington, G. J. Kunde, M. W. Rabin, and E. R. Birnbaum. Isolation of Ho-163 from dysprosium target material by HPLC for neutrino mass measurements. 2015. RADIOCHIMICA ACTA. 103 (8): 577.

Micro-Mirror Full-Frame Programmable Spectral Filters for the Long-wave Infrared

Steven P. Love
20140143ER

Abstract

This project has focused on developing application-specific micro-mirror arrays (MMAs) to improve the performance and extend the spectral range of our recently invented spectral imaging technology, the full-frame micromirror-based programmable spectral filter. This new approach to high-speed hyperspectral imaging performs spectral processing directly in the optical hardware to produce real-time video imaging of targeted chemicals. The throughput, sensitivity, and spectral range of the technology, however, have been limited by its reliance on commercial MMAs not designed for this application. These commercial arrays, because of their tilted-mirror design, suffer from grating-like spectral dispersion, which must be compensated at a major loss in throughput, and are limited by their small micromirror sizes to wavelengths shorter than 4 microns. The key requirements for our custom arrays are a programmable flat, array-plane configuration for the micromirrors, which eliminates the spectral dispersion problem, and substantially larger micromirror dimensions to enable operation in the application-rich long-wave infrared (LWIR, 8-12 microns). Beginning with single micromirror test devices and a functional macroscopic mirror array, the project explored various strategies for achieving the required characteristics, culminating in a 99-mirror array produced by our collaborators at Preciseley Microtechonolgy. In addition to the MMAs, this project also developed and implemented optical designs adapted for the new MMA configuration. While integration of all the components into a complete functioning LWIR instrument was not fully achieved before the project terminated, real-time LWIR imaging of a tetrafluoroethane gas plume was demonstrated using a manually-manipulated mirror installed in the LWIR optical system in place of the MMA.

Background and Research Objectives

Spectral imaging offers powerful capabilities for detecting and quantifying specific chemicals and materials, with applications ranging from medical imaging to proliferation detection. But traditional hyperspectral imaging (HSI) is intrinsically slow, typically involving "push-broom scanning" a line imager to build up a 2D image, a process that takes several seconds. It also generates huge data sets and requires computationally intensive post-processing to generate a useful final result. These issues limit HSI's usefulness for fast phenomena, broad-area searches, and wherever bandwidth and data volume are major concerns.

Under a previous LDRD project, and in a follow-on CRADA with an industrial partner (Chevron), we have developed a revolutionary new spectral imaging technology based on programmable MEMS (micro-electromechanical systems) micromirror arrays (MMAs), in which spectral processing takes place directly in the optical hardware. Now proven with working prototypes in the visible/near-infrared (VNIR) and short-wave infrared (SWIR) spectral regions, it implements background-suppressing matched-filter processing to pull out faint spectral signatures from complex backgrounds, and displays the already-processed results as real-time video-rate imagery. This speed increase does come at a cost: spectral information is thrown away, and one must specify in advance what chemical is being targeted. But where these limitations are acceptable, the new technology can be game-changing.

These prototypes, however, have thus far relied on commercial MMAs optimized for high-definition display applications, not spectroscopy. These MMAs are plagued by diffraction effects arising from the small size and tilted configurations of their micromirrors. The goal of this two-year engineering project has been to pave the way to improving the performance and extending the range of applications of our invention by developing much simpler, but spectroscopy-specific 1D arrays with two goals in mind: (1) To eliminate, at all wavelengths, the high-loss grating-like diffraction caused by the

commercial MMAs' always-tilted micromirrors, and (2) to extend the spectral range to the application-rich long-wave infrared (LWIR, 8-12µm) "chemical fingerprint" region.

Many MMA-based spectral imagers were proposed over the last decade [1-4]. But all these earlier devices were limited to 1D single-line imaging, necessitating a slow push-broom scan to acquire a full 2D image, negating the potential speed advantages that made MMAs attractive in the first place. Our patent-pending breakthrough [5-7] was the invention of optical systems that enable full 2D spatial images to be acquired at once, with the same MMA spectral processing applied simultaneously to the entire image. The key concept, illustrated in Figure 1 and described in detail in [6], is to create an image plane having the same angle of incidence throughout (i.e., a "telecentric" image), and to place the grating there, rather than collimating the light onto the grating as in standard spectrometers. This innovation results in light of each wavelength focusing to a unique location on the MMA, regardless of where in the image it originated, so that entire 2D images can be spectrally processed at once. Prototypes working in the VNIR and SWIR spectral regions have proven our optical concept, and demonstrated the ability to implement spectrally complex matched filters and produce high-quality video-rate imagery, as illustrated in Figure 1.

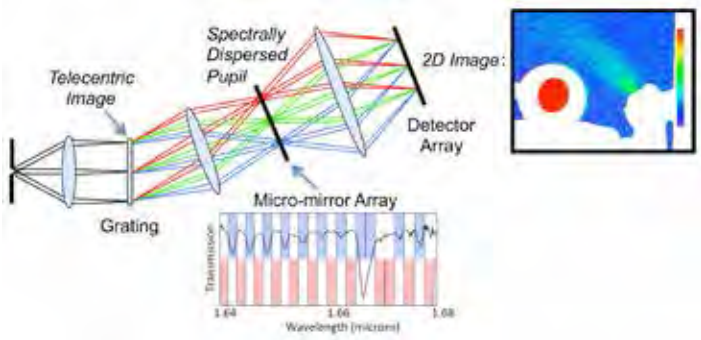

Figure 1. Principle of operation of a programmable micro-mirror spectral imager capable of simultaneous spectral manipulation of an entire 2D image. A telecentric image, in which light arrives at same angle of incidence throughout the image, is directed onto a diffraction grating, which disperses the light into its component wavelengths. Light of each wavelength, from all points in the 2D image, can then be focused to a unique location at a spectral plane, where a programmable micro-mirror array (MMA) can turn selected wavelengths "on" or "off" simultaneously for the entire image. The "on" wavelengths are chosen to correspond to the absorption features of a chemical of interest (methane in this example, selected wavelength bands shown in blue), or, to obtain a reference image for background suppression, to the non-absorbing regions in between the chemical features (shown in pink). A final imaging optic then collects the "on" wavelengths passed by this MMA selector and focuses this light to form a spectrally processed image at the detector array. (In this cartoon, the micro-mirror array is shown as transmitting instead of reflecting, so that the light path is unfolded for clarity). The result can be displayed as real-time video imagery showing the amount and location of the target chemical as it changes over time. The example image is an actual frame from one such video obtained with our short-wave infrared instrument, showing a methane gas plume in green (moderate concentration) and a methane reference cell in red (high concentration).

Being built around the Texas Instruments "DLP®" MMA, however, these prototypes are hampered by two features of that device. First, the DLP's micromirrors are settable to just two positions, tilted along the mirror diagonals by ±12˚ relative to the array plane. At either setting, the DLP is effectively a diffraction grating with a 12˚ blaze. This introduces spectral dispersion of its own, which must be compensated, at considerable cost to overall throughput (over 80% loss at certain wavelengths), with a second DLP. Secondly, the DLP micromirrors are simply too small (13.7µm square for the largest available), limiting instruments to wavelengths shorter than 4µm.

It has become clear that to move our technology forward to full practical fruition throughout the spectral regions of interest, particularly the challenging LWIR region, we must move beyond the off-the-shelf MMAs to arrays specifically designed for this application. Developing prototypes of such arrays, devising the optical systems to make use of them, and demonstrating actual spectral imaging in the LWIR region, were the primary goals of this project.

Scientific Approach and Accomplishments

The most troublesome feature of currently available commercial MMAs is their grating-like diffraction behavior, which occurs for both the "on" and "off" configurations of the micromirrors. If, instead of always being tilted either in one direction or the other, as they are in commercial DLP® micromirror arrays, the micromirrors could also be programmed to lie flat, in the plane of the array, the sections of the array programmed to this flat configuration would behave like a simple flat mirror rather than like a diffraction grating. This flat configuration could then be chosen as the "on" configuration, and light directed to the detector would no longer suffer from spectral dispersion introduced by the MMA. This would eliminate the need for dispersion compensation, resulting in greatly simplified optical systems and much-improved throughput. Developing MMAs having this flat micromirror orientation as a programmable configuration is a key project goal. The exact amount of micromirror tilt in the "off" configuration, and whether the rejected light exhibits spectral dispersion, is not important since that light is not used. It is important, however, that the tilt is sufficient to deflect the light be-

yond the optics that capture the “on” beam and send it to the detector. Therefore, one criterion in evaluating potential MEMS micromirror designs is that sufficient deflection of the “off” beam is achieved; in typical optical designs, deflections of several degrees are necessary. In addition, the individual micromirrors need to be much larger, in order to accommodate longer wavelengths without major diffraction losses, but the arrays only need be one-dimensional, consisting, for example, of long, thin micromirrors, since 1D selection is all that is needed for our spectral filtering application.

The project proceeded on two parallel tracks. First, for proof-of-principle purposes and as a backup, we will built a macroscopic version of a 1D LWIR-compatible mirror array, consisting of twenty “micro-” mirrors 2 mm wide and 30 mm long, mounted on hinged fingers and driven by conventional electro-mechanical actuators. Each mirror finger operates rather like a piano key, rotating about the short axis with the hinge near one end. While not a true MEMS device, this macroscopic system actually offers quite useful spectral capabilities, including the ability to distinguish a wide variety of gases in the LWIR, and it embodies the key features of a selectable flat configuration for the “micro-“ mirrors and negligible diffraction losses due to the large mirror size.

The primary focus of the project, however, was on developing true MEMS devices. We began by fabricating single-mirror prototypes of several designs using the economical PolyMUMPs wafer-sharing MEMS foundry service offered by Memscap Corporation. PolyMUMPs is a seven-layer process with three polysilicon layers, two sacrificial oxide layers, and one metal layer.

Two basic MEMS designs were fabricated using the PolyMUMPs process and evaluated for this effort. The first were square micromirrors capable of continuously variable tilt along the rectangular axis (as opposed to along the diagonal as with the DLP® arrays), the available tilts including, of course, the crucial plane-of-array mirror-like position as a settable option. These operate via an adjustable electrostatic force from an applied voltage, which works against the restoring force provided by a pair of zigzag-style silicon torsional springs. These devices were fabricated in various sizes (50, 100, and 150 microns square), and with varying designs for the size and strength of the springs. It was found that, although functional, the restrictions imposed by the wafer-sharing nature of the PolyMUMPs service, in particular the limited thickness and number of layers, resulted in devices with only a very small range of tilt angles (~1 degree compared to the several degrees required).

Much larger mirror tilts and beam deflections were achieved using the second MEMS design fabricated in this phase of the project. Emulating the “piano key” strategy of the macroscopic device, this second type of MEMS device consists of long thin micromirrors operated by zip actuators. In a zip actuator, the motion is controlled by a series of electrodes along the length of the structure. Although similar to a simple cantilever design, the zip actuator method is preferable to a simple cantilever because it provides greater motion control. Electron micrographs of several examples of these devices from our fabrication run are shown in Figure 2. Optical beam deflections of several degrees, as verified by reflecting a laser beam off the mirror surface, were achieved with these zip-actuator devices.

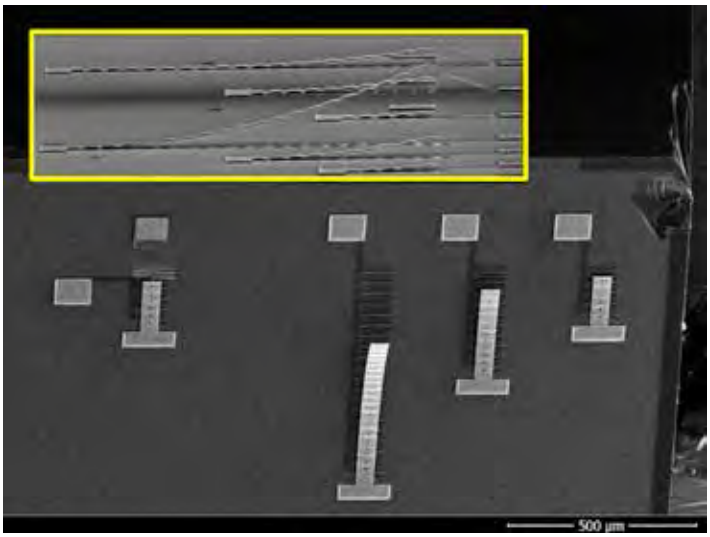

Figure 2. Electron microscope images showing several examples of zip-actuator-controlled micro-mirror devices fabricated using the PolyMUMPs MEMS fabrication process. At right are three simple zip-actuator mirror devices of various lengths, while on the left is an example incorporating a spring at the end of the mirror to limit the deflection and reduce the degree of curling. Inset shows a side view of both types of device, illustrating the large deflections of these devices, their strong tendency to curl, and the effect the addition of a spring has on reducing both effects.

Although more successful than the PolyMUMPs-based square mirrors, the first generation of zip-actuator micromirrors also exhibit some problematic behavior. In particular, near the flat, array-plane position that would be used as the crucial optical “on” position, the device becomes hard to control as the electrostatic attractive force between the micromirror and the actuator increases strongly and non-linearly as their separation decreases, eventually leading to an uncontrolled lock-down of the mirror. The locked-down device does not always release when the voltage is removed. This phenomenon is known as “stiction” and is a well-known problem in MEMS devices. The problem here is that the highest risk of stiction occurs

exactly where the device would need to be set most often.

These difficulties led us to move away from the zip actuator strategy and back to more conventional MEMS micromirror designs. But to achieve the needed mirror tilts and optical deflection, we needed more versatile MEMS fabrication capabilities than possible with PolyMUMPs. The search for sufficient fabrication capability within the limited budget of this project led us, eventually, into collaboration with Preciseley Microtechnology, a Canadian firm based in Edmonton. Preciseley had already been working on micromirror devices with similar requirements, for an entirely different application, and had made considerable progress. The prototype array Preciseley produced for LANL consists of 99 long, thin micromirrors, 100 µm wide and 900 µm long, arrayed much like a piano keyboard as we originally envisioned. Unlike a piano, however, each micromirror "key" is capable of rotating about either its long or its short dimension, and the rotation is continuously adjustable. This array is shown in Figure 3.

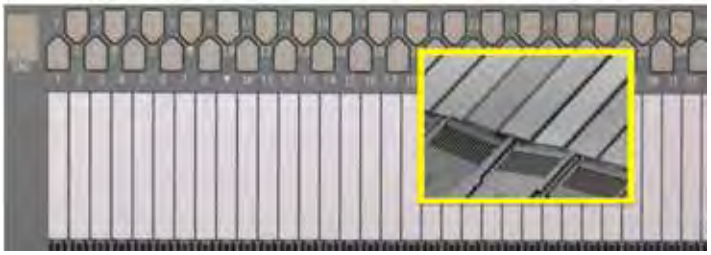

Figure 3. Photograph of the Preciseley Microtechnology micro-mirror array produced for LANL. The array consists of 99 micro-mirrors 0.1 mm wide by 0.9 mm long, each mirror capable of continuously variable rotation about either its long axis (inset) or short axis.

With this new array, together with its macroscopic analog, we are now in a position to produce a full working prototype of a programmable spectral filter for the LWIR. As of the time of writing this report, all the pieces are in hand – the macro- and micromirror arrays themselves, the controller electronics, and the LWIR optics for both the macroscopic and MEMS versions of the programmable filter. Final assembly, including interfacing the arrays to their controllers, is nearly, but not quite, complete as this project comes to a close.

To demonstrate the optical viability of the complete LWIR system in lieu of fully functioning micromirrors, we performed the following demonstration using the optical system designed for the macroscopic mirror array, which is illustrated in Figure 4. In place of a mirror array, a single strip of an ordinary mirror, 4mm in width, equivalent to two of the macroscopic mirror array's programmable mirrors, was set up on a translation stage at the spectral plane of the optical layout. This configuration allows for rudimentary "programming" of a single narrow spectral pass-band by simply translating the mirror across the spectral plane. In this manner, the spectral band can be varied across the entire 8-12 micron LWIR range.

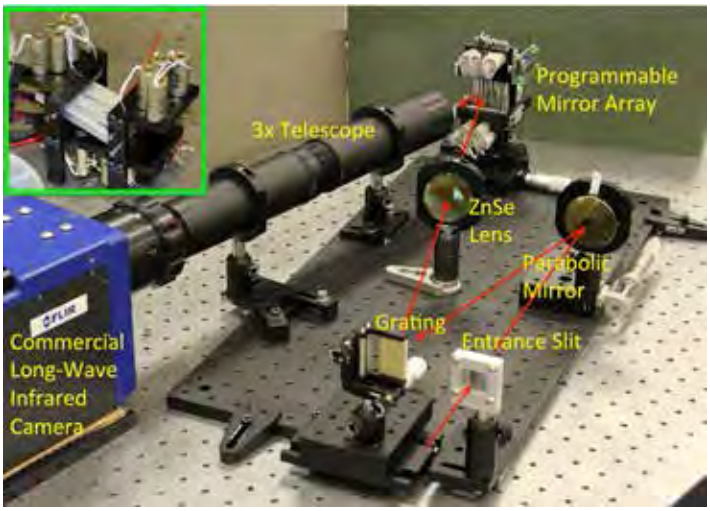

Figure 4. Photograph showing the optical layout of the first prototype long-wave infrared (LWIR) programmable spectral filter operating in the 8-12 micron spectral region, incorporating the macroscopic mirror array (inset shows a closer view of the device). As shown by the red arrows, light enters the system through an adjustable entrance slit, is focused by an off-axis parabolic mirror to form an image of the scene on the spectral dispersion grating. The mirror array, which consists of 2mm-wide by 30mm-high individually actuated mirrors, is located at the spectral plane. Selected wavelengths are then imaged by a commercial LWIR camera (a FLIR Systems HgCdTe array). In this first prototype, a 3x telescope is used to match the field of view of the programmable filter to that of the lens installed on the commercial camera; installing a longer focal length lens on the camera would make this unnecessary and simplify the optical system.

Results from this optical test are illustrated in Figure 5. 1,1,1,2 tetrafluoroethane, better known by its consumer trade names such as "Dust-Off" or "Aero-Duster," was chosen as the target gas, because its infrared spectrum is characterized by one particularly strong absorption band at roughly 8.8 microns, as shown in Figure 5. The "programmable" mirror was set to the 8.8 µm position, a plume of this gas was sprayed in front of a blackbody infrared light source, and the spectrally manipulated image was displayed in a real-time video output from a commercial LWIR camera placed behind the programmable filter. As can be seen in Figure 5, the gas plume is clearly visible in the filtered image, and is not visible in either a broad-band image or a filtered image at any other wavelength. (It should be acknowledged that, in a more realistic scenario, the thermal contrast would typically be much less than that provided by the hot blackbody used here. But compensat-

ing this, no effort was made in this first setup to limit the background interference from thermal IR emission by the instrument itself, normally accomplished by cooling key components, resulting in a major decrease in sensitivity compared to what could be achieved in a fully realized instrument.)

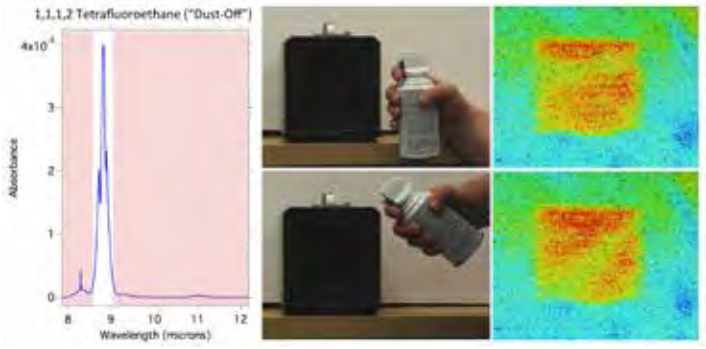

Figure 5. Real-time gas plume imaging results obtained using the LWIR optical system, shown in Figure 4, with a single 4-mm-wide mirror substituting for the mirror array. Translating this single mirror across the 8-12 µm spectral plane of the optical system provides a rudimentary "programmablility" in this mock-up test, which can be used to tune the filter to a particular spectral band. 1,1,1,2 tetrafluoroethane (a.k.a. "Dust-Off" aerosol dust remover) is used as the target gas. Its spectrum, together with the spectral pass (white) and rejection (pink) bands of the programmable filter are shown at left. At center are visible context images illustrating the aiming of the gas plume for two instances. The black box is a commercial blackbody infrared source. The resulting LWIR images at right, frames from a real-time video stream from the commercial LWIR camera, clearly show the gas plume as a green swath across the red face of the blackbody. The plume is only visible when the translating mirror is set to the 8.8 µm wavelength position; it is not visible at other wavelength settings or in broad-band images.

In summary, this project, while not fully realizing a complete, fully operational LWIR MEMS-based programmable filter, has put in place all the pieces necessary for doing so in the near term. With the partnership established with Preciseley Microtechnology, there is now a clear path forward for producing the advanced micromirror arrays needed to produce compact programmable imagers operable throughout the infrared.

Impact on National Missions

A low data volume, immediate-display spectral imaging capability for specific chemical targets, in the LWIR as well as in shorter-wavelength regions, is of potentially transformative usefulness anywhere limited bandwidth and a need for rapid turn-around as issues. Such applications encompass rapid ground-based surveys to search for specific chemicals (e.g. site inspections), tagging and tracking, DOE proliferation detection applications, and environmental and industrial monitoring (e.g. for the fossil fuel industry, as in our current CRADA with Chevron).

References

Love, S. P.. Programmable matched filter and Hadamard transform hyperspectral imagers based on micro-mirror arrays. 2009. Proceedings of SPIE. 7210: 721007.

Goldstein, N., P. Vujkovic-Cvijin, M. Fox, B. Gregor, J. Lee, J. Cline, and S. Adler-Golden. DMD-based adaptive spectral imagers for hyperspectral imagery and direct detection of spectral signatures. 2009. Proceedings of SPIE. 7210: 721008.

Wehlburg, C. M., J. C. Wehlburg, S. M. Gentry, and J. Smith. Optimization and characterization of an imaging Hadamard spectrometer. 2001. Proceedings of SPIE. 4381: 506.

Newman, J. D., B. V. Brower, P. P. K. Lee, A. D. Cropper, M. Gibney, and M. Pellechia. MEMS-based spectral-polarimetric imaging and target tracking architecture for airborne broad-area search. 2011. Proceedings of SPIE. 8053: 805302 .

Love, S. P., and D. L. Graff. Full-frame programmable spectral imager. 2012. International Patent Application PCT/US2012/000417.

Love, S. P., and D. L. Graff. Full-frame programmable spectral filters based on micromirror arrays. 2014. Journal of Micro/Nanolithography, MEMS and MOEMS. 13 (1): 011108 .

Graff, D. L., and S. P. Love. Toward real-time matched-filter imaging for chemical detection, using a DMD-based programmable filter. 2014. Journal of Micro/Nanolithography, MEMS and MOEMS. 13 (1): 011111 .

Cryogenic Laser Refrigerator for Infrared Imaging

Markus P. Hehlen
20140275ER

Abstract

This project has focused on the development of solid-state laser cooling as a new cryogenic refrigeration technology. Such optical cryocoolers have no moving parts and can therefore eliminate vibrations and increase reliability, two fundamental limitations intrinsic to current mechanical cryocoolers used in space-based infrared (IR) imaging. First, we have fabricated laser-cooling crystals with 5 times higher purity than any previously synthesized materials. This has resulted in the demonstration of a new world-record laser-cooling temperature of 91 K. In parallel, we have pursued the development of purification processes that target undesired transition-metal impurities present in the crystals. Our original approach of removing impurities by using chelating agents proved too complex and difficult to scale up. We developed a new method of removing impurities by electroplating. It showed excellent performance for the removal of copper, some reduction of iron, and little effect on nickel and cobalt. Further studies are needed to elucidate the exact reasons for this behavior and optimize the process. These results will pave the way to a scalable path to high-purity fluoride starting materials for the growth of laser-cooling crystals. Second, we have constructed an optical refrigerator device for cooling an IR sensor payload, an effort pursued in collaboration with the University of New Mexico. This first-ever reduction to practice of an optical refrigerator showed less than expected cooling. We have identified excess conduction of heat through the structure supporting the laser-cooling crystal as the main culprit. These results are informing subsequent efforts in the construction of a next-generation laser cooler. Third, we have developed a thermo-optical device model that allows us to predict laser-cooling temperatures and heat lifts. We predict that it will be possible to produce hundreds of milli-Watts of heat lift at 100 K, a performance suited to cool small IR sensor payloads for space applications.

Background and Research Objectives

Space-based infrared (IR) imaging is a critical asset that delivers essential information to important fields ranging from National security and nuclear non-proliferation to agriculture and climatology. IR sensors have to be cooled to cryogenic temperatures (below 123 Kelvin) so that thermal noise in the detector is sufficiently suppressed and maximum detector performance can be achieved. Space-based missions currently use mechanical cryocoolers for this purpose. However, these traditional and mature refrigerators contain moving parts which not only create vibrations and microphonic noise but also limit their reliability [1,2]. These drawbacks constrain the performance of the system and limit operational flexibility. Vibration-free and highly reliable cryocoolers have therefore been a recognized yet unmet need by numerous customers in this field for some time. This 2-year project has focused on optical refrigeration (aka solid-state laser cooling) as an alternative cryogenic cooling technology that has the potential to overcome the limitations of mechanical cryocoolers. Optical refrigeration was first discovered at Los Alamos National Laboratory (LANL) in 1995 [3]. It occurs when a solid material is excited by a laser and subsequently emits photons whose average energy is slightly greater than that of the pump laser (Figure 1).

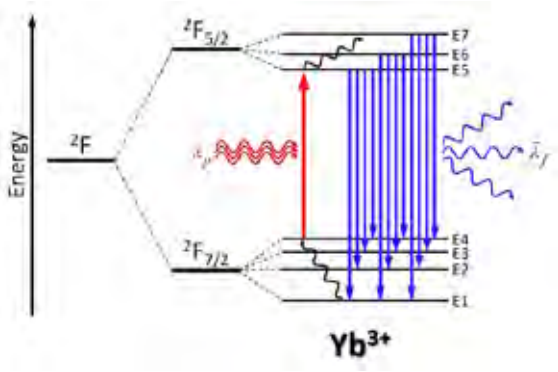

Figure 1. Energy level diagram of the ytterbium (Yb) laser cooling ion. The cooling cycle consists of absorption of laser

pump light (red arrow), absorption of phonons (vibrational energy) from the crystal (wiggly arrow), fluorescence (blue arrows), and finally absorption of phonons (vibrational energy) from the crystal (wiggly arrow). On average, the fluorescence occurs at slightly higher energy than the laser pump, thereby cooling the crystal in the process.

This effect is referred to as anti-Stokes luminescence, in which every excitation/emission event extracts a small amount of heat from the solid and carries it away as light. Optical refrigeration is the only refrigeration technology that offers vibration-free cooling of macroscopic payloads to cryogenic temperatures [4]. A long-standing successful collaboration between LANL and the University of New Mexico (UNM) has been the recognized leader in solid-state laser cooling and has, as part of the present project, experimentally demonstrated materials with new world-record performance and heat lifts that now enable cooling of actual sensor devices for the first time. Optical refrigeration is most successful when fluoride crystals doped with rare-earth (RE) ions (such as ytterbium-doped yttrium-lithium-fluoride, YLF:Yb) are used as the solid cooling medium [4]. Another approach is to use semiconductor materials as the cooling medium. Recently, a research group in Singapore has observed optical refrigeration in CdS semiconductor nanostructures for the first time [5,6]; however, semiconductor materials have not yet achieved any useful macroscopic heat lift. The primary engineering thrust and application focus is, therefore, on constructing optical refrigerators based on high-purity RE-doped fluoride crystals. One of the main limitations in optical refrigeration are impurities in the crystal that decrease the quantum efficiency and cause intrinsic heating, both effects that degrade the performance of the optical cryocooler. Furthermore, solid-state laser-cooling research up to this point had only focused on cooling the crystals themselves to the lowest-possible temperature, while no actual payload such as a sensor had ever been attached to and cooled by a laser-cooling crystal before. The ambitious research objectives of this project therefore were (1) to develop YLF:Yb crystals with a 10 times improved purity in order to realize laser cooling to 80 Kelvin, and (2) to cool an IR sensor to cryogenic temperatures using an optical refrigerator. Advances on either or both of these objectives would represent a significant breakthrough in this field and bring optical refrigeration closer to actual applications. First, in this project we have succeeded in improving the YLF:Yb crystal purity by approximately 5 times, which has allowed us to reduce the lowest achievable temperature from 115 K at the onset of the project to 91 K in the most recent materials (Figure 2) [7], a significant improvement that had been predicted by our initial model calculations. We have also measured heat lifts on the order of 100 mW at 100 K in these systems, a value that is adequate for cooling small IR sensors. We have discovered that the low impurity concentrations achieved in our best materials are pushing our state-of-the-art optical and analytical chemistry tools to their intrinsic limits and in some cases beyond, adding significant challenges in the development of purification processes. Second, we have for the first time constructed an optical refrigerator device designed to cool an IR sensor payload. The amount of cooling in this first reduction to practice of an integrated optical refrigerator was less than expected. We have identified the conduction of heat through the mechanical structure that supports the cooling crystal as the main culprit. These results have greatly advanced our knowledge of the optical cryocooler system, and they are currently being used to inform subsequent engineering efforts towards a next-generation device.

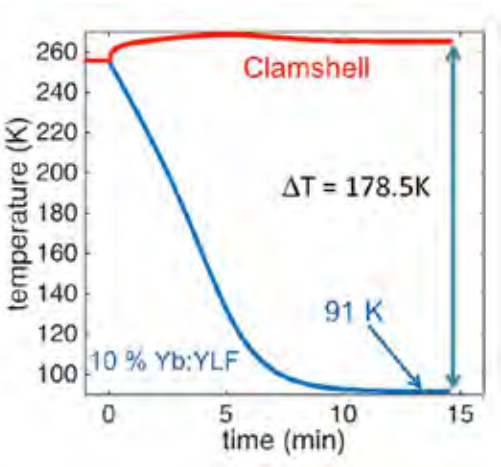

Figure 2. Latest world-record laser cooling experiment performed by the present project. A high-purity yttrium-lithium-fluoride crystal doped with 10% Yb3+ was used as the solid-state cooling medium. The 50 Watt pump laser was turned on at time = 0. Starting at 255 K, the crystal cooled to 91 K within about 10 minutes (blue curve). The crystal fluorescence and residual laser light was absorbed by the clamshell structure that surrounded the crystal, warming it to 265 K (red curve). The temperature difference achieved by this solid-state laser cooling experiment was a new record 178.5 K.

Scientific Approach and Accomplishments

The project has pursued three parallel development tracks: (1) the synthesis of high-purity precursors used for the subsequent growth of YLF:Yb single crystals, (2) optical experiments to achieve maximum laser cooling of the YLF:Yb single crystals and sensor payloads attached to them (collaboration with UNM), and (3) development of a thermo-optical device model to predict laser-cooling temperatures and heat lifts. The respective accomplishments are described in the following. (1) Commercial starting materials for crystal growth, such as yttrium fluoride (YF3), lithium fluoride (LiF), and ytterbium fluoride (YbF3), do not have the required purity to enable the ultimate perfor-

mance in a YLF:Yb laser-cooling crystal. The impurities of most concern are traces of ubiquitous transition metals such as copper, iron, cobalt, vanadium, and nickel. Initially, we have pursued the removal of these impurities by chemically binding them to a chelate (ammonium pyrrolidine dithiocarbamate) in a two-phase solvent extraction process repeated multiple times and carried out in a Class 100 clean room environment [8]. The changes in impurity concentrations were monitored throughout the process using inductively-coupled plasma mass spectrometry (ICP-MS). While some purification was achieved, we found that the process was difficult to scale up to the 50-200 gram quantities needed for the subsequent Czochralski crystal growth. Furthermore, the numerous additional chemicals required for this process themselves represented a source of impurities that proved difficult to control [9]. We therefore developed an alternative approach that targeted the removal of transition-metal impurities by electrochemically plating them out of a solution onto a reticulated vitreous carbon (RVC) electrode in a process carried out in a Class 100 clean room. Figure 3 shows the concentrations of select transition-metal impurities spiked into an yttrium chloride solution as a function of time of electroplating.

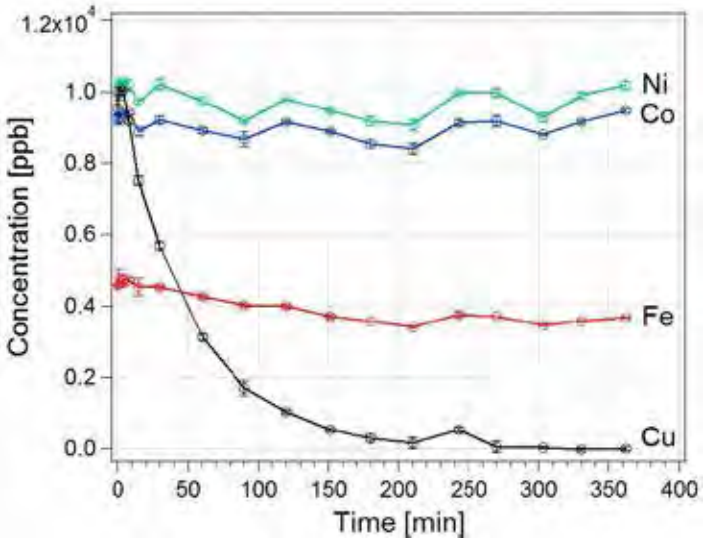

Figure 3. Concentration of copper (Cu), iron (Fe), nickel (Ni), and cobalt (Co) impurities in a solution of yttrium chloride as a function of time of electroplating at a potential of -1.0 Volts using reticulated vitreous carbon (RVC) as the working and counter electrodes.

We observed that the various metal impurities behaved differently: while copper (Cu) plated out rapidly as expected and the iron (Fe) concentration showed some reduction, nickel (Ni) and cobalt (Co) were unaffected. Further studies are needed to elucidate the exact reasons for this behavior. Nevertheless, these results will pave the way to a scalable path to high-purity fluoride starting materials for the growth of laser-cooling crystals. (2) The optical laser-cooling experiments carried out in parallel and in collaboration with UNM were performed using a YLF:Yb single crystal grown form high-purity commercial starting materials as well as a YLF:Yb single crystal grown from starting materials synthesized in the LANL Class 100 clean room facility. One of these crystals has shown a level of impurities so low that our highly sensitive optical characterization tools were only able to provide an upper impurity limit. This upper limit was 5 times lower than any previously tested crystal and therefore resulted, as predicted by our models, in a reduction of the lowest temperature from 115 K to 91 K when laser-cooling the crystal by itself in a custom chamber (Figure 2) [7]. The next step was to attach an IR sensor payload to the crystal. The engineering challenge herein was in providing a good thermal path between the payload and the crystal while preventing the intense laser and fluorescence light from the crystal to reach and thereby heat the payload. A double-kinked sapphire waveguide coated with a silver/gold mirror at the payload surface was designed using optical modeling, fabricated, and bonded to the YLF:Yb crystal (Figure 4).

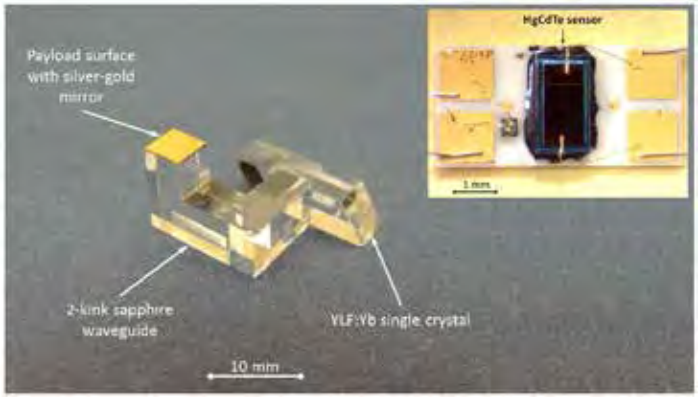

Figure 4. Picture of assembly consisting of a high-purity ytterbium-doped yttrium-lithium-fluoride (YLF:Yb) crystal and a two-kink sapphire waveguide. The YLF:Yb crystal input and output faces were cut at Brewster's angle in order to minimize reflection losses for the pump laser. The sapphire crystal was attached to the YLF:Yb crystal by a diffusion-bonding process that eliminated the use of adhesives, which could introduce parasitic heating. The two-kink sapphire waveguide provided a good thermal link between the crystal and the payload while preventing light from the crystal to reach the payload. A silver-gold mirror was deposited at the end of the sapphire waveguide for additional light rejection. The mercury-cadmium-telluride (MCT) infrared sensor (pictured in the inset) was mounted on top of the gold mirror.

A commercial mercury-cadmium-telluride (MCT) IR sensor chip was then attached as the payload (Figure 4). A new laser-cooling chamber was fabricated to accommodate this assembly, and the sensor payload temperature was measured as the YLF:Yb crystal was laser cooled. These first-ever experiments of optical refrigeration of a sensor payload

achieved less than expected cooling. Our latest time-resolved experiments indicate that the heat flow from the warm chamber walls through the structure that supports the crystal/waveguide assembly was greater than expected. This is valuable information that can now be used in the design of the next-generation laser-cooling device. (3) We have established a comprehensive thermo-optical model of an optical refrigerator [10]. The model includes the crystal inside the non-resonant optical cavity as well as convective, conductive, and radiative heat loads onto the crystal/waveguide assembly. The model parameters were informed by our extensive material characterization experiments. The calculations show that heat lifts of hundreds of milli-Watts at 100 K are possible (Figure 5).

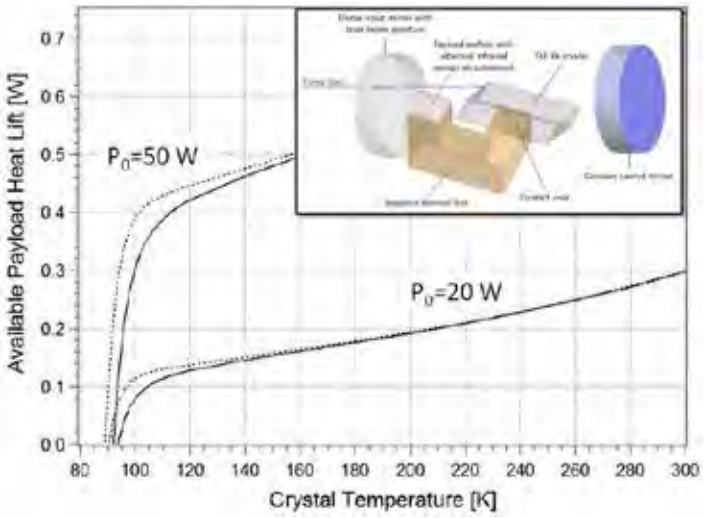

Figure 5. Calculations of available payload heat lift versus laser-cooling crystal temperature for two pump powers (20 and 50 Watt). The solid and dashed lines represent crystal purities at the beginning and end of the current project, respectively. Heat lifts of several hundred milli-Watts are possible in the 90-120 K cryogenic temperature range. The inset shows the optical raytracing model used to simulate the absorption of pump laser light in the non-resonant cavity and the propagation of the crystal fluorescence.

This potential performance is adequate to cool IR sensors in space-based instruments. In the course of this modeling work, we also discovered that maximum laser absorption and thus laser-cooling is achieved when the laser is trapped on a Lissajous-type path inside the non-resonant cavity [10]. This new finding is currently being implemented by the UNM in their latest laser-cooling setup. Finally, the project has produced one extensive book chapter, six peer-reviewed publications, and seven oral presentations (of which six were invited) at international conferences. It also provided opportunities for a graduate student and two postdoctoral researchers as they prepare for careers in material science and optical engineering.

Impact on National Missions

Cryogenic solid-state laser cooling has a direct and potentially substantial impact on a number of customers across several fields. A primary mission impact will be achieved by laser cooling of sensors used in electro-optical imaging. For instance, MCT and other advanced sensors require cooling to below 100 K to reach maximum performance. A solid-state optical refrigerator could be a key enabler for such revolutionary sensing capabilities. It would not only eliminate vibrations but its enhanced reliability would also allow for switching the refrigerator on and off on demand, an important capability that is not available from existing mechanical cryocoolers that run and consume precious power continuously. The National Reconnaissance Office (NRO) in particular has been apprised of our progress throughout the life of the project and has expressed interest in further developing this technology for their application needs. Furthermore, the National Institute of Standards and Technology (NIST) has expressed interest in using optical refrigerators to cool single-crystal silicon reference cavities. Such cavities are used to frequency-stabilize lasers that are used for precision measurements such as in atomic clocks. Laser linewidths of ~40 mHz have been achieved with traditional approaches which are, however, limited by vibrations. Silicon has a zero thermal expansion coefficient at 124 K, and realizing a silicon resonator cooled to this temperature without vibrations by an optical refrigerator would be a groundbreaking advance. Other high-impact applications of solid-state laser cooling include vibration-free cooling of samples in high-magnification electron microscopy where jitter is a major limitation.

References

1. Gilmore, G., and J. D. Hemingway. Practical Gamma-Ray Spectrometry. 1998.

2. Veprik, A. M., V. I. Babitsky, N. Pubdak , and S. V. Riabzev. Suppression of Cryocooler-Induced Microphonics in Infrared Imagers. 2009. Cryogenics. 49: 449.

3. EPSTEIN, R. I., M. I. BUCHWALD, B. C. EDWARDS, T. R. GOSNELL, and C. E. MUNGAN. OBSERVATION OF LASER-INDUCED FLUORESCENT COOLING OF A SOLID. 1995. NATURE. 377 (6549): 500.

4. Hehlen, M. P., Sheik-Bahae, R. I. Epstein, S. D. Melgaard, and D. V. Seletskiy. Materials for Optical Cryocoolers. 2013. JOURNAL OF MATERIALS CHEMISTRY C. 1 (45): 7471.

5. Li, , J. u. n. Zhang, and Xiong. Laser cooling of CdS nanobelts: Thickness matters. 2013. OPTICS EXPRESS. 21 (16): 19302.

6. Zhang, J. u. n., Li, Chen, and Xiong. Laser cooling of a semiconductor by 40 kelvin. 2013. NATURE. 493 (7433): 504.

7. Melgaard, S. D., A. R. Albrecht, M. P. Hehlen, and M. Sheik-Bahae. Solid-State Optical Refrigeration to sub-100 Kelvin Regime. Nature Communications.

8. Patterson, W. M., P. C. Stark, T. M. Yoshida, Sheik-Bahae, and M. P. Hehlen. Preparation and Characterization of High-Purity Metal Fluorides for Photonic Applications. 2011. JOURNAL OF THE AMERICAN CERAMIC SOCIETY. 94 (9): 2896.

9. Boncher, W. L., Judge, Sansinena, M. R. Dirmyer, and M. P. Hehlen. Purification of precursors of Yb3+-doped YLF crystals by solvent extraction and electrochemical processing. 2015. LASER REFRIGERATION OF SOLIDS VIII. 9380.

10. Hehlen, M. P., W. L. Boncher, and S. P. Love. Design study of a laser-cooled infrared sensor. 2015. LASER REFRIGERATION OF SOLIDS VIII. 9380.

Publications

Boncher, W. L., E. Judge, J. M. Sansinena, M. R. Dirmyer, and M. P. Hehlen. Purification of precursors of Yb3+-doped YLF crystals by solvent extraction and electrochemical processing. 2015. Proc. SPIE. 9380: 938004.

Epstein, R. I., M. P. Hehlen, M. Sheik-Bahae, and S. D. Melgaard. Optical cryocoolers for sensors and electronics. 2014. Proceedings of SPIE. 9070: 90702K.

Epstein, R. I., M. Sheik-Bahae, and M. P. Hehlen. Optical refrigerators outshine thermoelectric coolers. 2014. IEEE Photonics Society News. 28: 9.

Hehlen, M. P., M. Sheik-Bahae, R. I. Epstein, S. D. Melgaard, and D. V. Seletskiy. Materials for optical cryocoolers. 2013. Journal of Materials Chemistry C. 1 (45): 7471.

Hehlen, M. P., M. Sheik-Bahae, and R. I. Epstein. Solid-state optical refrigeration. 2014. In The Handbook on the Physics and Chemistry of Rare Earths. Edited by Buenzli, J. C.. Vol. 45, p. 179. Waltham, MA: Elsevier.

Hehlen, M. P., W. L. Boncher, S. D. Melgaard, M. W. Blair, R. A. Jackson, T. E. Littlewood, and S. P. Love. Preparation of high-purity LiF, YF3, and YbF3 for laser refrigeration. 2014. Proceedings of SPIE. 9000: 9000.

Hehlen, M. P., W. L. Boncher, and S. P. Love. Design study of a laser-cooled infrared sensor. 2015. Proceedings of SPIE. 9380: 938000I.

Agile Persistent SSA Surveillance Networks Using Mobile Platforms

W T. Vestrand
20140425ER

Abstract

The congested, contested, and competitive nature of Space in near earth orbit is driving an urgent National Security need for persistent surveillance of the full night sky. We developed an innovative approach that would fill this SSA knowledge gap through the use of an integrated, global, persistent surveillance network employing small, full-sky, optical/IR monitors deployed on mobile platforms. We designed, built, and tested inexpensive full sky optical monitors that can operate in harsh marine environments and be deployed on ocean-going ships. We also developed new simulation tools that demonstrate how a globally distributed network of these autonomous sky monitors can inexpensively provide custody of resident space objects.

Background and Research Objectives

In the 21st Century, with nearly 40 nations operating space missions, Space has become, in the words of former Deputy Defense Secretary William J. Lynn III, "congested, contested, and competitive". Traditional SSA monitoring has centered on catalog maintenance to conduct periodic checks on the locations of resident space objects. The existing system employs narrow field telescopes at a few, land-based, fixed locations constrained by Geopolitics. Furthermore, the current workhorse optical instruments have fields-of-view that only subtend a few square degrees. Since the full sky subtends 42,000 square degrees--- most of the sky is unwatched most of the time. This fact, and the growing need, is forcing significant re-evaluation of military Space Situational Awareness (SSA) community's practices.

LANL, with its successful Thinking Telescopes program, is a recognized champion of a radical new approach. This approach employs persistent surveillance of the full sky to recognize SSA threats and opportunities as they emerge and marshals real-time interrogating observations with autonomous robotic follow-up instruments. This new approach is receiving significant attention, but a key question remains: How do we achieve effective full sky persistent surveillance when faced with the reality of highly cost constrained budgets?

Scientific Approach and Accomplishments

The overarching goal of our project was to demonstrate how an inexpensive ecosystem of optical/IR telescopes can provide global persistent surveillance that would fundamentally enhance the capability of the Space Surveillance Network (SSN). This approach has the potential to cost only a few percent of traditional radar-based space fence systems and would provide global passive persistent surveillance of the entire sky.

Our key accomplishment is the development of the first full (night) sky optical monitors capable of autonomous custody of spaces objects from platforms on ships or moving platforms as well as stationary ground-based platforms. Since 2/3 of the Earth's surface is covered by oceans that are international waters, our success on this LDRD funded Engineering Project has opened up the possibility of building inexpensive, distributed, SSA monitoring networks at an unprecedented global scale. This accomplishment required the solution of three salient engineering challenges that posed a barrier to practical deployment: (1) Development of hardware and software modifications to enable accurate geo-registration and real-time onboard analysis on moving platforms; (2) Construction of environmentally hardened persistent SSA surveillance monitors that can be deployed in harsh conditions like those present on Ocean-going ships; and (3) Development of tools for determining optimal sensor placement to augment the existing SSN.

To enable dynamic deployment of our full sky monitors on moving platforms, we successfully developed new hardware and software that help enable our full sky monitors to recognize current geo-location and aspect. We deployed and demonstrated our prototype hardware on a truck-based mobile platform. This new capability

will allow autonomous real time operation from stabilized platforms on moving vehicles like ocean going ships.

We successfully developed and field tested the first full sky optical monitor for Space Situational Awareness that can be deployed in a harsh marine environments like those found on ocean faring ships. We started with our existing monitor designs that were optimized for the high altitude dry environments that are typically found at good astronomical sites. But the challenges posed by the corrosive marine environment meant that significant re-engineering of the design was required in order to ensure robust, reliable, operation on-board ships. Our engineering effort required the development of weather sealing, potting for sensitive electronics, sealed optical windows for the telescopes, and closed circuit temperature/humidity regulation systems. We also had to develop new environment and attitude sensors as well as new custom camera mounting platforms.

To test the new monitor design, we built, deployed, and operated one at remote marine location for six months. The cost for a six month deployment on an ocean going ship was beyond the financial scope of this project. So as a surrogate, we deployed a monitor for six month operational test at a location about 100 yards from the Pacific Ocean on Kwajalein in the Marshall Islands. That test was highly successful. This marine hardened monitor on Kwajalein has operated autonomously without fault for six months and collected very useful SSA observations. And, while operating in conjunction with three other autonomous full sky monitors located in Hawaii and New Mexico, our distributed sensor network functioned as a prototype autonomous space fence that spanned more than 6,000 miles. Figure 1 shows the marine-hardened system deployed on Kwajalein and Figure 2 shows a close-up of the monitor during leak testing.

We also developed a new suite of software tools that allows us to determine the optimal placement of sensors for addressing various SSA surveillance challenges. The coverage simulation suite includes object illumination conditions, sensor viewing frustum, and a tool that allows a satellite catalog (or subset) to be evaluated for optimization of sensor deployment. Figure 3 shows an example output from the visualization tool, depicting the viewing frustum for low earth orbiting satellites provided by our prototype space fence with monitors located at Kwajalein, Maui, and Los Alamos, New Mexico. Altogether, the new tools, when combined with our existing software, allow us to study and optimize ---all the way to the image level---global networks of dynamically distributed, heterogeneous, mobile sensors. These tools will be used to guide our future work for government sponsors on the number and location of sensors as well as latency tradeoffs for custody of resident space objects in LEO (Low-Earth Orbit), MEO (Medium-Earth Orbit), and GTO (Geostationary Transfer Orbits) orbits.

Figure 1. The marine-hardened full-sky optical monitor deployed on Kwajalein Atoll in the Pacific Ocean. This fully autonomous sky monitor was operated for six months without human intervention on Kwajalein. The system collected important Space Situational Awareness measurements and successfully passed it's marine environment testing.

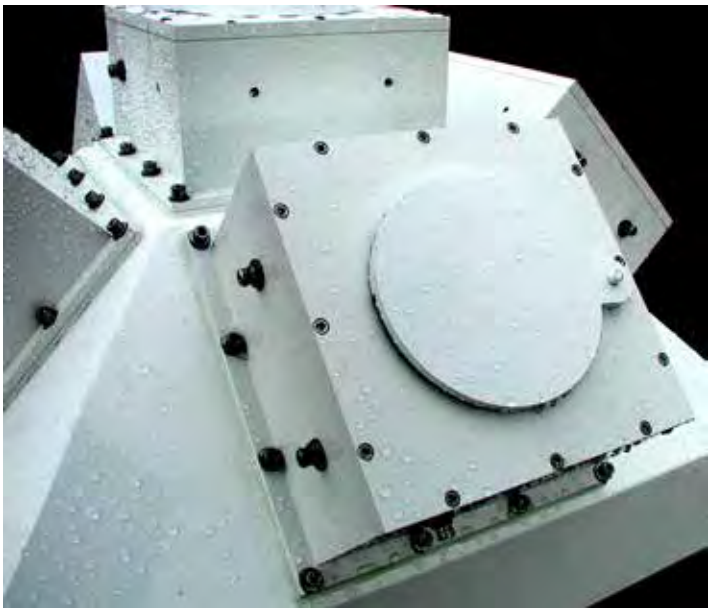

Figure 2. A close-up picture of the sky monitor with baffles removed during leak testing.

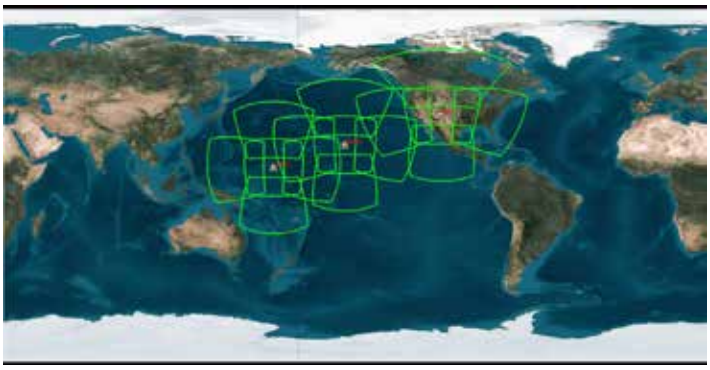

Figure 3. Three LANL full-sky optical surveillance systems, as currently deployed to Kwajalein, Maui, HI, and Los Alamos, NM. Each system consists of five sensors, capable of detecting resident space objects from Low Earth Orbit through Medium Earth Orbit. Here, the green lines depict coverage areas of each individual sensor for Low Earth Orbit objects. Together, these monitors form a surveillance network. The majority of the earth's surface (ocean) is accessible without geopolitical constraint. Our development of marine hardened mobile systems enables the deployment of this class of systems on sea faring mobile platforms. This capability paves the way for robust and economical continuous custody of resident space objects.

Impact on National Missions

Our ability to deploy inexpensive full-sky monitors in harsh marine environments is a fundamental enabling technology for the agile deployment of sensors to augment the existing Space Surveillance Network. And our full-sky monitoring capability provides a new approach for passive custody of operational satellites that can provide real-time recognition of spatial and photometric anomalies. As such, this work has garnered very significant high-level interest and endorsement from the US Air Force and other government agencies.

Ultrafast Nanocomposite Scintillators: Decay Rate Enhancement by Electromagnetic Coupling to Plasmon Resonances

Richard C. Schirato
20140655ER

Abstract

The phenomenon of electromagnetic coupling in the near field between excited states in a scintillator and plasmonic states in resonant noble metal nanoparticles was investigated to enhance the total light decay rate. Initially, the decay properties of fluorescent composite nanoparticle analogs were measured to verify the process and benchmark simulations in anticipation of nanoparticle scintillator fabrication. Using a technique including inert layers of silica to determine spacing between a silver metal core and a doped fluorescent layer, the general phenomenon of decay rate enhancement was demonstrated. Both semi-analytical Mie scattering calculations and Finite Domain Time Difference simulations were used to explore the relationship between nanoparticle (NP) sizes and distance relationships with respect to near-field quenching and photon emission stimulation on the one hand, and far-field absorption and scattering processes on the other. An important result demonstrated from those calculations is that the thickness of an electro- or radioluminescent conversion screen based upon plasmonic decay rate enhancement of approximately 10× would be limited to a few tens of microns or less based upon light transport issues. Furthermore, the process will be dominated by quenching effects limiting effective quantum yield. Several composite metal nanoparticle and scintillator material fabrication processes were explored with limited success, leading to a radiolytic seeded silver nanoparticle concept. To explore the initial scintillator growth process, a chemical reactor was modified to enhance structural integrity of the reaction vessel. Nanoparticle Cerium doped Yttrium Aluminum Garnet (YAG) was successfully fabricated. Before further fabrication processes could be fully explored, the project was brought to an early close due to the discrepancy between estimated bulk conversion screen thicknesses reasonably achievable and the MaRIE project X-ray conversion screen efficiency requirements. Leave-behind capability includes a Time-Correlated Single Photon Counting (TCSPC) emission lifetime measurement system capable of measuring decay lifetimes significantly less than a nanosecond.

Background and Research Objectives

Scintillators are materials which emit light when they absorb ionizing radiation, and enable a wide variety of radiation detection applications in basic science, medicine, and industry. How fast the light is emitted is dependent upon the material and the lifetime of its excited states. In certain applications, e.g. dynamic experimentation associated with Matter in Extremes, ultrafast image intensifiers, positron emission tomography (PET) neurological imaging, and X-ray Free Electron Laser (XFEL) diagnostics, researchers require light emission times on the order of or less than a nanosecond (one billionth of a second) to meet mission goals. Most currently available scintillators with good energy absorption and efficient light conversion properties do not emit light this quickly. The goal of this project was to produce scintillation materials with significantly reduced emission lifetimes as compared to their unmodified form. This goal was accomplished by fabricating nanocomposite structures that combine scintillator materials with noble metal nanoparticles. The metal nanoparticles will couple electromagnetically to the excited states in the scintillator. If the plasmon (charge density quantized state) resonant frequency of the nanoparticles equals that of the emitted light, then Quantum Electrodynamics (QED) predicts that the resulting resonant system will decay with a significantly higher light emission rate.

Figure 1 shows the simplified decay rate enhancement concept graphically. Shown as a yellow region, the bare scintillator is exposed to ionizing radiation which deposits energy into the material. Electrons are excited to higher energy states which decay either radiatively or nonradiatively, with respective decay rates ΓR and ΓNR. A spherical silver metal NP with a diameter of several 10's of microns will have plasmon resonances in the blue optical region, overlapping with the emission wave-

Spacer [nm]	τ1 [ns]	τ2 [ns]	τ3 [ns]	τ4 [ns]
0	*0.118±0.003 (34.78%)*	*0.466±0.009 (46.12%)*	*1.296±0.021 (16.77%)*	*8.098±0.268 (2.32%)*
5	*0.144±0.008 (22.18%)*	*0.469±0.008 (52.16%)*	*1.165±0.009 (24.47%)*	*6.602±0.349 (1.19%)*
10	*0.232±0.009 (28.80%)*	*0.628±0.012 (52.53%)*	*1.588±0.019 (17.00%)*	*8.472±0.476 (1.67%)*
20	*0.253±0.009 (33.60%)*	*0.670±0.016 (48.00%)*	*1.778±0.026 (16.41%)*	*8.732±0.455 (1.98%)*

Table1. Fit components of the non-exponential decay Ag core NP samples.

lengths and frequencies of relatively fast scintillators. If in the near field (significantly less than a wavelength of the light photons), such a NP can electromagnetically couple to an excited state, enabling two new decay pathways. The two additional decay paths are labeled ΓNPR and ΓMQ for radiative and nonradiative (quenching) decay rates, respectively. The resulting total decay rate is the sum of all four terms, thereby possibly increasing significantly depending upon the values of the new terms. An important characteristic is the quantum yield (QY) which gives the efficiency of photon emission, and is equal to the sum of the two radiative rate terms divided by the total decay rate.

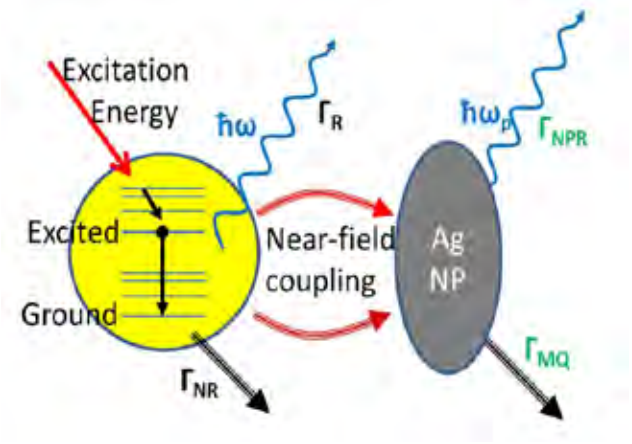

Figure 1. Near-field coupling between an excited state and a resonant nanoparticle allows new decay paths, thereby increasing total decay rate.

Challenges in this work include development of the nanocomposite scintillator fabrication process; tuning of the metal nanoparticles by shape, size, and material; and production of resultant macroscopic scintillators with good light transport properties.

Scientific Approach and Accomplishments

Simulation/Calculation The computational technique for simulation of time domain electromagnetics at the nanoscale was down-selected to the Finite Domain Time Difference (FDTD) technique, as compared to discrete dipole or "multi-multipole" techniques. Numerical techniques will allow simulation of a variety of nanoparticle (NP) shapes not achievable with analytical methods. A commercial FDTD software package from Lumerical Inc. was identified, acquired, and utilized to numerically simulate both near-field stimulated photon emission and quenching behaviors due to plasmonic interactions with coated spherical metallic nanoparticles. As an example of representative results, Figure 2 shows FDTD calculations of radiative and nonradiative relative decay rate enhancement terms as a function of distance from a silver NP with a radius of 35 nm.

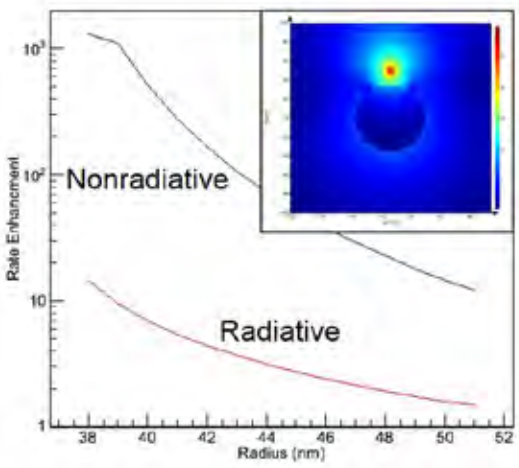

Figure 2. FDTD calculation results for decay rate enhancement at a wavelength of 400 nm as a function of dipole location for a 35 nm radius silver sphere clad with 17 nm of silica. Inset shows logarithm of average electric field for dipole at 15 nm from sphere surface.

These results and others show that the decay rate enhancement process will be limited to distances of tens of nanometers and will be dominated by the quenching process. In parallel for benchmarking and verification purposes, semi-analytic calculations based upon Mie scattering theory were performed. Whereas the Mie scattering method is limited to spheroidal shapes, the results from the two techniques for selected spherical symmetry test cases were in qualitative agreement. However, it was found that the accuracy of the specific FDTD software results was limited by calculational convergence issues at the size scales of interest. Future work may benefit from

investigation of discrete dipole methods to address these simulation limitations.

Semi- analytic Mie scattering calculations were performed to explore the relationship between NP sizes and distance relationships with respect to near-field quenching and photon emission stimulation on one hand, and far-field absorption and scattering processes on the other. An important result from those calculations is that the thickness of an electro- or radioluminescent conversion screen based upon plasmonic decay rate enhancement of approximately an order of magnitude will be limited to a few tens of microns or less based upon light transport issues, and will be dominated by quenching effects. This issue would appear to limit the applicability of plasmonic decay rate enhancement to electroluminescent phosphor plates, e.g. ultrafast image intensifiers or hybrid photomultipliers; or relatively low energy X-ray imaging conversion screens.

Materials Development and Measurements Experiments on a fluorescent analog of the scintillation application were performed to demonstrate decay rate enhancement from plasmonic interactions with metal nanoparticles, diagnostic instrumentation development, and for benchmarking purposes. Fabricated by NanoComposix, Inc. for this project, NP's with a solid metallic silver metal core were coated with an inert silica layer of varying thicknesses. Though different lots varied in size slightly, the average diameter of the silver NP cores was about 73 nm. These composite particles were subsequently coated with an additional silica layer doped with a fast-emission fluorescent dye. The intervening inert layer provides a well-known distance offset between the plasmon resonant core and the excited states in the doped layer. NP's similarly coated, but with a solid undoped silica core, were also fabricated for control purposes. The dopant dye was a form of fluorescein modified with an isothiocyanate functional group that covalently links the fluorophore with the silica so that the dye molecules do not diffuse out of the shell. The inset of Figure 3 schematically shows the geometry of the test NP's.

Diluted sample concentration was about 2×1010 particles per milliliter in ethyl or isopropyl alcohol. Using instrumentation developed on this project as described below, a significant decay rate enhancement was observed for this initial experimental demonstration, validating the general concept. Fluorescence light transients from these composite NP's are shown in Figure 3. Multiple exponential functions were fit to the experimental decay data, with three lifetime components found to be sufficient to describe ~98% of the emission. Table 1 includes the first four lifetime values for the four spacer thicknesses. (Lifetime is related inversely to decay rate.) For comparison, the first two fit lifetimes for the silica core control was 1.13 (40%) and 3.14 (60%), consistent with expectation for fluorescein. Since lifetime parameters generally went up with thicker spacer layers, the data can be interpreted as representing the integral over the separation of the excited states in the doped layers from the metal NP surface. Results from these test systems were used in benchmark validation of the numerical techniques described above.

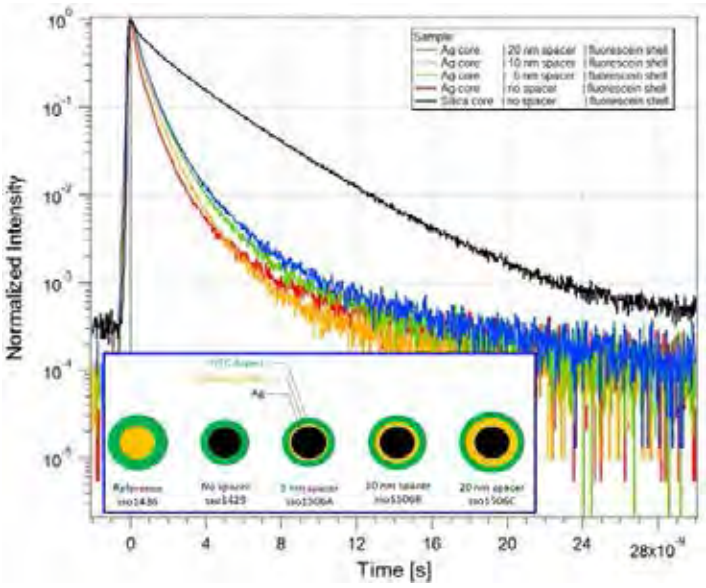

Figure 3. Fluorescence light transients from layered nanoparticles. Inset shows the nanoparticle geometries.

Several composite scintillator NP synthesis processes of possible applicability to production at a moderate scale were developed and tested. Significant challenges included synthesis of robust scintillating materials with well-defined size ranges, and controlled distances to metallic NP's of the order of nanometers. Initial experiments at LANL based upon coating of silver NP's, bulk mixtures, and infused mesoporous materials were not immediately successful at producing high quality material with uniform characteristics. After analysis, a concept for decoration of oxide scintillating NP's with silver NP's was developed. It is based upon a radiolytic process to seed in-situ silver NP growth on the surface of the scintillator particles.

In order to realize the seeded growth process, an improved bare scintillator NP fabrication methodology was required. An existing chemical reactor was modified with a new, more physically robust reaction vessel and re-certified for LANL pressure requirements. Cerium-doped Yttrium Aluminum Garnet (YAG) scintillating NP's were produced with this system using a high temperature, high pressure hydrothermal process. The NP's were found to be monodispersed; in other words, of a well-defined size range without excess agglomeration, as needed for this application. Fluorescence transient light output for YAG NP's produced from the revamped reactor are shown in Figure

4. While bare scintillator NP fabrication was successful with this method, further layered NP production was not performed due to the reduction in project schedule, funding, and scope.

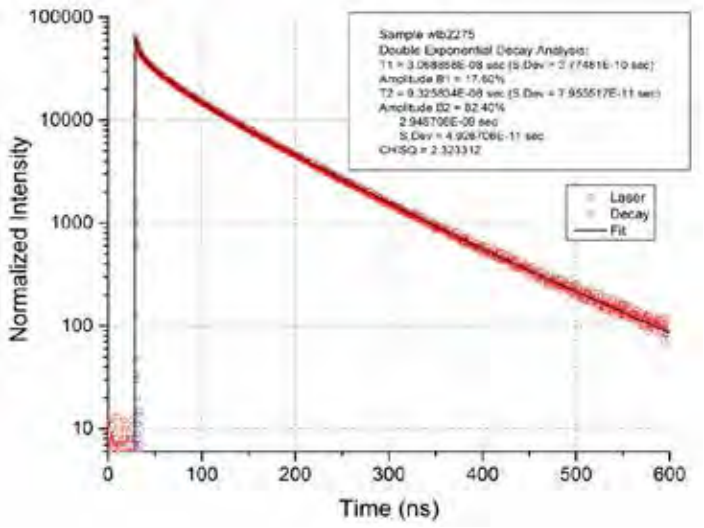

Figure 4. Fluorescence transient light output from Cerium doped YAG nanoparticles fabricated in chemical reactor modified according to project requirements. Parameters for functional fit are shown in legend.

Planar processing techniques for the deposition of metallic NP's were explored. Initial experiments included fabrication of silver nanoparticle arrays on sapphire substrates using electron photolithographic and/or self-assembly techniques. Whereas the processes were found to yield planar NP arrays with good characteristics, a decision was made to concentrate on bulk fabrication techniques due to limited resources and the ultimate application of making macroscopic X-ray conversion imaging screens.

Instrumentation/ Measurement Technique Development
Simplified instrument concepts and systems developed on this project are shown diagrammatically in Figure 5. A Time-Correlated Single Photon Counting (TCSPC) emission lifetime measurement system was assembled. Based upon commercial building blocks and design, the system provides the sub-nanosecond lifetime measurement capability needed for this project. By utilizing a high efficiency light transport path and high repetition rate light sources, instrument response function (IRF) temporal blurring is minimized and data acquisition time is reduced, while avoiding non-linear effects associated with excessive excitation power. A relatively large sample chamber was incorporated to allow measurement of various sample shapes, as compared to a cuvette-only system. The TCSPC system was utilized in the measurements of fluorescence lifetimes described here, and represents a significant leave-behind capability.

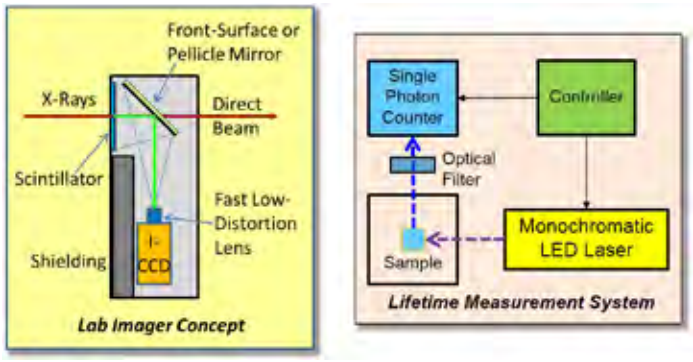

Figure 5. Instruments and measurement techniques developed on the project include a low light level imager and a high throughput fluorescence lifetime measurement system.

A low light level imager concept was developed to measure the Modulation Transfer Function (MTF) of any resulting bulk X-ray conversion screen. Derivatives of line spread functions measured from X-ray edge targets would yield MTF for the system as a whole. After measurement of MTF of the optical portion of the system using sinusoidal patterns, an estimate of screen MTF would be obtained. A high resolution cooled CCD camera system was identified and acquired on the project for measurements. While the early close of the project eliminated the need for such a system on this Matter in Extremes project, these concepts were incorporated into a gated time-of-flight high energy neutron imaging project being conducted in FY16.

Impact on National Missions

Matter in Extremes and stockpile stewardship dynamic experimentation imaging based upon X-ray Free Electron Laser, Time-of-Flight Neutron Imaging, or other accelerator fast pulse sources requires faster scintillator light emission speeds than are achievable now. The goal of this project was to produce scintillator technology applicable to radiation imaging conversion screens or image intensifier phosphors with significantly increased light emission rates. Whereas one result of the project was the realization of an effective thickness of resulting bulk conversion screens limited to tens of microns, the nanoparticle decay rate enhancement technology may find applications to low energy X-ray imaging and ultrafast image intensifiers. Leave-behind instrumentation technology includes a high throughput fluorescence lifetime measurement system applicable to a wide range of new scintillator technologies, and a low light imager and measurement concept already finding application to time-of-flight gated neutron imaging experimentation for stockpile stewardship and certification.

W-Band Synthetic Aperture Radar (SAR)

Bruce E. Carlsten
20150065ER

Abstract

This project evaluated a novel scheme for a synthetic aperture radar (SAR). Conventional SARs generate RF images with near-optical quality by coherently integrating the return of a frequency-chirped radar as it travels over some distance in order to form a synthetic aperture for the antenna. The radar return is mixed with the in-phase and out-of-phase transmit signal, which gives what is known as the in-phase return (I) and the quadrature return (Q). The magic of a SAR is that the complex sum (I+jQ) is the 2-dimensional Fourier transform of the actual image. In a conventional SAR, the return data is first interpolated onto a rectangular grid in Fourier space and then two numerical Fast Fourier Transforms (FFTs) are used to recover the image. The spacing required in the FFT numerical integration is proportional to the SAR's frequency bandwidth. Unfortunately, the SAR's resolution is also inversely proportional to the bandwidth, which means that very high resolution conventional SARs have significant computational loads. The original purpose of our SAR scheme was to greatly reduce the computation requirement for high resolution imaging. This is accomplished by using a spread-spectrum approach instead of a simple frequency chirp. A code division multiple access (CDMA) masking is used (just like in CDMA-based cell phone technology) which instantly provides one of the Fourier integrals. The single FFT that remains is computationally much quicker. Since we have begun work on this technology, we have shown how it also has broad applications past improving conventional SAR algorithms. This year, we have developed the image-recovery algorithm and a hardware implementation of this scheme. The CDMA SAR we built uses a 100 MHz bandwidth with a 1 GHz carrier.

Background and Research Objectives

To clarify how a SAR works, a plane-based SAR is shown in Figure 1. A target patch on the ground is interrogated at some distance orthogonal to a flight path. The direction away from the flight path is called "down-range" and the direction on the ground parallel to the flight path is called "cross-range". The SAR transmits at a frequency that chirps through a frequency bandwidth. This chirp occurs very fast, and for simplicity the plane can be considered stationary during the chirp. These chirps are repeated as the plane moves through discrete angular positions along the flight path relative to the target patch center, with a chirp and the associated reflected signal received at these specific angular locations. At each of these angular locations, in-phase and out-of-phase signals I and Q are found by mixing the returned signals with the carrier, as a function of the chirped frequency. Since the angular frequency divided by the speed of light, (2 pi f/c), is the wavenumber k, the Fourier transform of real space, the quantity (I+jQ) can be inverted to find the reflection function within the target patch.

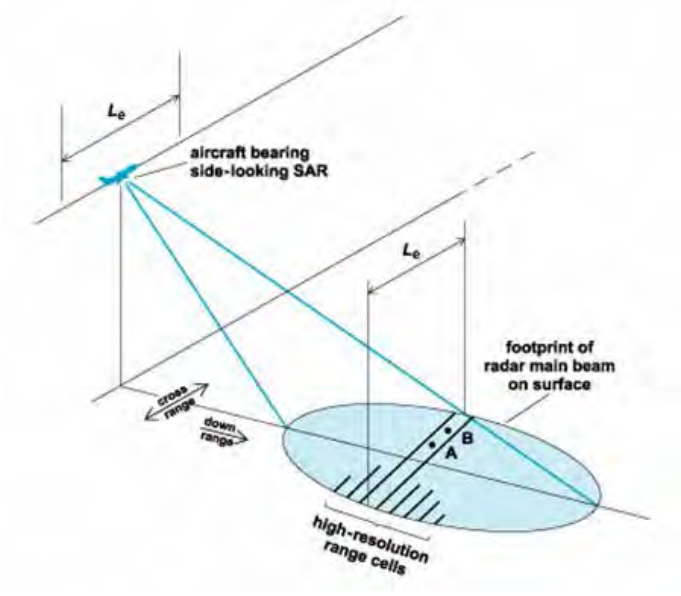

Figure 1. Definition of SAR parameters.

Importantly, this inversion can be thought of as first integrating along the direction of view (known as "de-ramping" because the Fourier integral is over the frequency

chirp) and then integrating along the angular spread of the wavenumber (which from a fundamental theory of Fourier transforms is the same angle as the physical viewing angle). The first de-ramping integral identifies the distance to the reflectors in the target patch but can not resolve their relative cross-range position. The de-ramping process bins down-range locations into "range cells", shown as lines along the target patch in Figure 1. These cells are the width of the SAR's range resolution For example, points A and B in Figure 1 would be indistinguishable from the de-ramping process. Importantly, each return signal from each range cell has a phase of I and Q associated with the offset of that position from the target patch center. The second Fourier integral is equivalent to an integral correlating these phases of each individual reflector, which change as the angular view changes.

The SAR image's resolution (i.e., the range cell size) in the down-range direction is 2B/c, where B is the SAR's frequency bandwidth and the resolution in the cross-range direction is the SAR's carrier wavelength divided by the total angular view on the target (in radians), (lambda/theta). To get fine down-range resolution, a very high bandwidth is needed. To get fine cross-range resolution, both a small carrier wavelength and a large angular view of the target patch is needed. Both increasing the bandwidth and the angular view lead to increasing numerical complexity in performing the Fast Fourier Transforms (FFTs) in inverting the quantity (I+jQ). In particular, the limited computing power of SARs on satellites tends to limit the ability to process large bandwidths.

This project's research objective is to evaluate a novel scheme to reduce a SAR's processing requirement. The scheme is based on transmitting a code division multiple access (CDMA) spread spectrum signal instead of a simple frequency chirp. If the spread spectrum bandwidth is the same, the SAR can return an equivalent down-range resolution. However, hardware masking is possible with the CDMA approach (that's how CDMA cell phones are distinguished from each other when talking to the cell tower) which allows us to essentially perform the first Fourier transform along the down-range direction in hardware, greatly reducing the overall computational load for generating an image. The project is focused on demonstrating this CDMA approach for a SAR with a 100-GHz carrier (W-band), with a 10-GHz bandwidth. This CDMA-SAR can theoretically have 1.5-cm resolution, better than any conventional SAR.

Scientific Approach and Accomplishments

The project's approach was to first demonstrate the CDMA-SAR principle using a 1 GHz carrier with a 100-MHz bandwidth in its first year (FY16) and then to extend this demonstration to a 100 GHz carrier with a 10-GHz bandwidth in its second year (FY17). The initial, lower frequency demonstration has allowed the project team to verify the basic principles of the CDMA-SAR at a frequency which can be directly measured with commercial RF diagnostics (e.g., oscilloscopes and network analyzers) and where required RF hardware like mixers and modulators work as expected. Importantly, this project's second year has been subsumed by a larger LDRD DR project, "W-Band Synthetic Aperture Radar Technology Development for Satellite Deployment", project 20160013DR, which runs from FY16 to FY18. About 80% of the DR's focus is on the development of a high-power, high-bandwidth W-band source. The other 20% of the DR project is to finish this CDMA-SAR demonstration at W-band and to integrate it with the high-power, high-bandwidth source for an outdoor demonstration. Because of the longer time scale of the DR project, the W-band CDMA-SAR development is extended through Q2 of FY17 with a low power W-band SAR demonstration scheduled at the end of FY17.

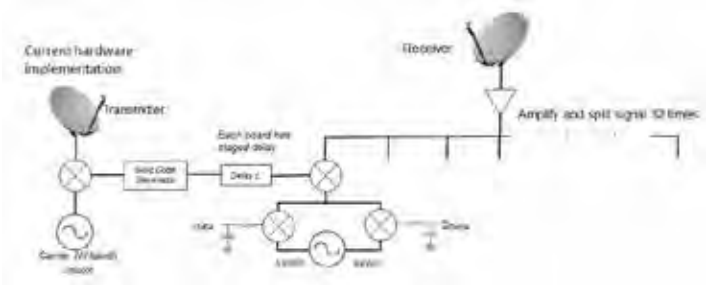

Figure 2. Concept of implementation of the CDMA SAR. Here the returned signal is multiplexed 32 times, each with a unique time delay of the Gold code modulation.

The CDMA approach is shown in Figure 2. In the following text, we will describe the functional parts of this implementation for our current 1-GHz demonstration hardware. A "Gold code" (also known as an M code) is generated at 100 MHz, where +1's and -1's are generated every 10 nsec. For our demonstration, the Gold code has 15 separate +1's and -1's (called "chips"), in a pseudo-random order. This sequence of chips (of length 150 nsec) is reproduced 10 times, for a total signal length of 1.5 microseconds. A Gold code has a delta function autocorrelation function, which means that a sequence of N identical 15-chip-long-Gold-code-sequence multiplied by itself equals 15N if the Gold code is in phase (i.e., the +1's and -1's line up) but is -N if it is not, as N become large. This gives us a mechanism to determine the distance a radar signal is reflected from by correlating the return of a transmitted signal with a delayed signal.

In Figure 2, the Gold code is multiplied in a mixer with the

carrier signal generated at 1 GHz. The Gold code changes the phase of the carrier by pi every time a -1 is generated. This phase modulated signal, known as binary phase-shift keying (BPSK) is transmitted and reflected from a target at a distance D. The received signal is amplified and split some number of times. For each split, the initial Gold code is delayed and mixed with the received signal. An I and a Q signal is generated from each split, by mixing in the in- and quadrature-phase modulations. For splits where the delay tau corresponds to a reflection distance (tau/2c) where there is no target I=Q=0. However, if the delay corresponds to a distance where there is a target, (tau=2D/c), I and Q are nonzero. Note that this configuration is best if the target distance is known (i.e., this configuration is not optimal as a search radar). But if the target distance is known and if the target range width of interest is say 10 to 100 down-range resolution cells, a very high resolution image can be generated very quickly.

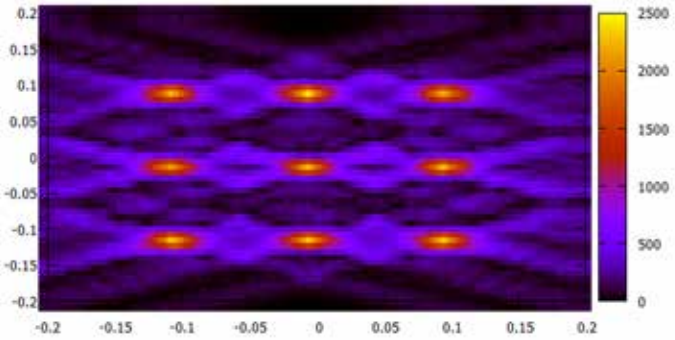

Figure 3. CDMA SAR reconstruction of nine 1-cm reflections spaced 10-cm apart 100-km from the radar.

A CDMA-SAR algorithm is similar to, but not exactly the same as a frequency chirped SAR algorithm. Specifically, the CDMA masking identifies the distance to the target reflectors along some angular look. To make the CDMA results mirror a conventional SAR, the I's and Q's found through the CDMA process are then modified to have the appropriate phase for the deviation of that reflector from the target patch center. Then the same Fourier correlation integral is used as in a conventional SAR inversion. Figure 3 shows the results of modeling the image of an array of nine reflectors using the CDMA-SAR algorithm we developed. In Figure 3, the nine reflectors spaced were spaced 10 cm apart, with a center distance of 100 km and a 60 degree total angular view (with 0.3 degree angular steps).

Our 1-GHz CDMA-SAR hardware implementation is shown in Figure 4. This hardware reproduces the schematic shown in Figure 1, but with only one receive channel (instead of multiplexing the received signal, we will use a single channel and vary the Gold code delay time to generate I and Q values for different reflection distances). The hardware has been placed on a mast with two horn antenna (one for transmit and one for receive). The entire assembly is on wheels to facilitate moving the radar along an equivalent "flight path" on the ground.

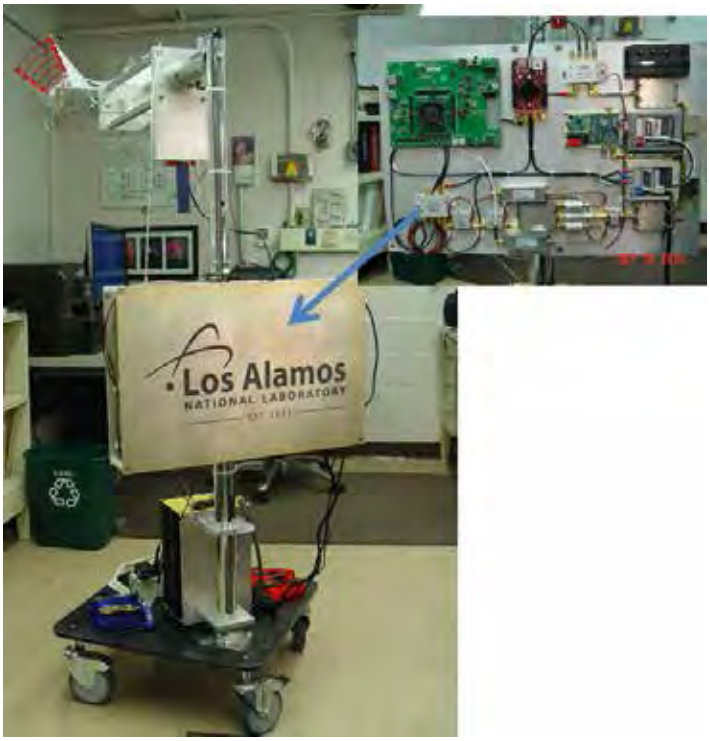

Figure 4. Our 1-GHz, 100-MHz bandwidth CDMA SAR hardware.

We have tested the CDMA-SAR by transmitting a signal down a long cable (equivalent to 150 feet) to the receive hardware. The received and the delayed signals are shown in Figure 5. The fast oscillations correspond to the 1 GHz carrier, with a period of 1 nsec. The zero or pi phase shift corresponding to the Gold code every 10 nsec is clearly shown (the phase shift is done quickly (~ nsec) because the system's actual bandwidth is ~ GHz). We use 15 "chips" in our implementation of the Gold code, for a total code length of 150 nsec. When the phase of the chips line up, the magnitude of I and Q in quadrature is a maximum, indicating there is a reflection at the distance corresponding to that delay. The signals shown are not in phase.

Impact on National Missions

This novel CDMA-SAR approach is a keystone technology that opens up broad national security missions. This is the first substantially different SAR approach in decades. Because the spread-spectrum approach reduces the computational load, this new approach will open up high resolution SAR applications on smaller, more autonomous platforms. Beyond that, there are basic science and treaty verification applications.

The successful results from this project were leveraged to expand this technology development to the larger LDRD DR project , “W-Band Synthetic Aperture Radar Technology Development for Satellite Deployment”, project 20160013DR, where this technology development is targeted for a specific, and urgent, national security need. Additionally, CDMA’s ability to generate range data (even without the angular integration) has motivated a conceptual new approach to measuring volume constrained atmospheric greenhouse gas concentrations for both climate science and future greenhouse gas treaty verification. This concept was awarded a FY16 LDRD ER project in Measurement Science, Instruments and Diagnostics (“Range-Resolved Measurement of Atmospheric Greenhouse Gases for Treaty Verification and Climate Science,” project 20160462ER) to perform a proof-of-concept demonstration. This work may lead to future NASA, DOE/Office of Science, or Department of State missions. The CDMA approach can also be applied to SARs with optical instead of W-band carriers. This has the potential for very long range imaging, and has led to a new project from the Department of State, “Hybrid Optical/X-Band SAR for GEO Imaging”, for developing verification technology for the DoS Bureau of Arms Control, Verification, and Compliance. Specifically, their unclassified (Official Use Only) need is to monitor satellite compliance with an international code of conduct for outer space activities. The optical SAR CDMA-based approach is to use 10-GHz BPSK modulation on an optical carrier (here +1’s and 0’s instead of +1’s and -1’s), transmitted from a moderate power laser on the earth. The signal is reflected from an object in geosynchronous earth orbit (GEO) and then imaged in the manner developed through this project by using a bistatic receiver with relative angular motion in low earth orbit.

Feasibility Study of Novel Fabrication of Dielectric Structures for W-Band Synthetic Aperture Radar for Satellite Deployment

Bruce E. Carlsten
20150714ER

Abstract

This project was a 4.5-month study funded at $150k to determine the feasibility of fabricating dielectric photonic-band gap (PBG) structures for high-frequency (~ 100 GHz) traveling-wave tubes (TWTs) using micro-drillling. The results from this reserve project are especially important because a follow-on project, 20160013DR, "W-band synthetic aperture radar (SAR) technology development for satellite deployment," was subsequently funded for FY16-FY18. A primary and a backup PBG architecture were identified by the follow-on project proposal. The results from this feasibility study will impact the down selection between these PBG structure options at a fabrication feasibility review towards the end of FY16 Q1. This review will also consider additional work funded by the new project that completes this fabrication study. For the primary PBG structure architecture, the RF properties are determined by a series of parallel, high aspect-ratio holes in the dielectric. These holes have to be held to a certain tolerance. This project and the upcoming feasibility review focus on the ability to accurately drill small holes in high-dielectric constant ceramics and to determine the tolerances required for these holes.

Three activities were completed by this project: (1) PBG RF structures were designed and relevant hole sizes were numerically determined; (2) holes were drilled in high-dielectric ceramic blanks and measured; and (3) the effect of hole size variations and misalignments on the RF mode propagation were simulated.

For the fabrication techniques used, the hole "wander" was larger than expected and appears to constitute the largest fabrication error. The wander was 33 +/- 13 micrometers for hole diameters of 400 and 640 micrometers, for ceramic slab thicknesses of 6.5 cm. We will continue this work with a two-month study under 20160013DR to determine if this wander can be reduced before the PBG-structure down selection. Specifically, this wander should depend on ceramic slab thickness and drill bit speed and can likely be reduced by a combination of slower bit speed and thinner slabs.

Background and Research Objectives

There is a need for a high-bandwidth, high output-power traveling-wave-tube (TWT) at relatively low electron-beam voltages (20 kV), for a high resolution synthetic aperture radar (SAR). The key advance needed for this technology is the development of a novel high-frequency TWT (operating in W-band between 90 and 100 GHz, and having an order of magnitude higher power and bandwidth than possible with current technology based on copper RF structures). The novel TWT would require the use of a sheet electron beam [1-6] in an elliptical, wide-bandwidth RF structure for the increase in power. A copper structure that is wide enough for the sheet electron beam would be overmoded and would lead to multi-mode competition, which is acerbated by high bandwidth (this is the basis for the fundamental limit of bandwidth and output power using conventional technology).

The key innovation of the TWT development is to use a dielectric PBG (photonic band gap) structure instead of a copper structure. Most importantly, PBG structures can be designed to be mode selective, thereby bypassing the entire multi-moding problem and enabling the required wide bandwidth and output power for the TWT. This work was motivated by the recent success of an LDRD ER which showed, for the first time, the use of a cylindrical PBG structure in a TWT (with the higher beam energy of 120 keV) [7-9].

Two possible PBG structure configurations are shown in Figures 1 and 2. Figure 1 shows an ideal PBG architecture, which is a uniform dielectric with holes drilled in it parallel to the electron beam flow (the sheet electron beam travels down the central slot). The purpose of the holes is to both capture the proper RF mode (a TM01 –

like mode centered along the central slot) and to reduce the average dielectric constant of the structure so the RF mode is slowed down to the speed of the electron beam (about 27.2% of the speed of light for a 20-keV electron beam; the effective dielectric constant needs to be about 13.7). These holes have high aspect ratios: for 100-GHz, the hole diameters are on the order of 200 to 600 micrometers, and the overall structure length is on the order of centimeters. Also, for a typical hole pattern, the dielectric constant of the ceramic needs to be ~ 20 for the effective constant to be 13.7 with the holes present. Figure 2 shows the leading backup RF structure architecture, which consists of a "folded-waveguide" PBG structure, with short dielectric rods sandwiched between metal plates. The RF mode is slowed down by making it meander back and forth across the electron beam along the transverse wide direction. This type of structure has been fabricated before [10,11] so its fabrication is considered to be low risk.

Figure 1. Ideal PBG architecture.

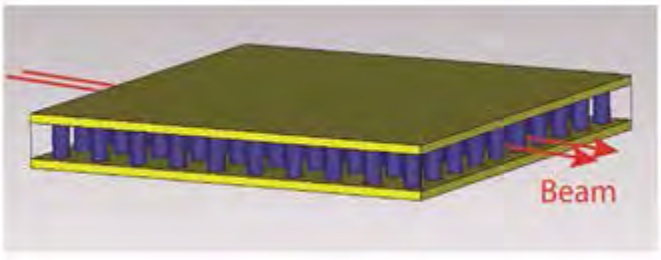

Figure 2. Leading backup RF structure architecture.

The geometry in Figure 1 is the simplest PBG configuration with the largest bandwidth and least RF complications. The purpose of this project was to determine if such as structure could be built with emerging micro-drilling technologies. Traditional high dielectric-constant ceramic materials have dielectric constants of only about 9 and cannot be used to slow electromagnetic waves below about 0.3 times the speed of light. Although low-loss, higher dielectric constant ceramics are now becoming available [10], the machining properties of these materials are unknown.

It is important to note that since the PBG bandwidth is so large (10%), the fabrication tolerances are expected to be rather broad. Quantifying what the maximum fabrication tolerances are and verifying they are consistent with the fabrication technique are key elements of this project and may significantly impact the feasibility of a high-bandwidth PBG TWT.

Scientific Approach and Accomplishments

This section is partitioned into approach and accomplishments in each of the following topical areas: PBG RF structure design, PBF structure fabrication and metrology, and error effect on the PBG RF mode. This section ends with a subsection on additional required fabrication tests to complete the feasibility study and subsequent feasibility review, and the PBG structure down selection.

Roughly 25% of the project's funding was spent on M&S (dielectric ceramics and drill bits), 25% on fabrication T&E, 20% on designing the PBG RF structure, 20% on gain simulations including fabrication errors, and 10% on project management including report writing, in agreement with the project's original plan.

PBG RF structure design

After comparing several alternative PBG designs, we settled on the geometry shown in Figure 3, referred to as SB_20-75. This geometry has an inner slot of size 7.5 mm by 0.75 mm, with small holes of diameter 400 micrometers and larger holes of diameter 640 micrometers, all separated by 770 micrometers.

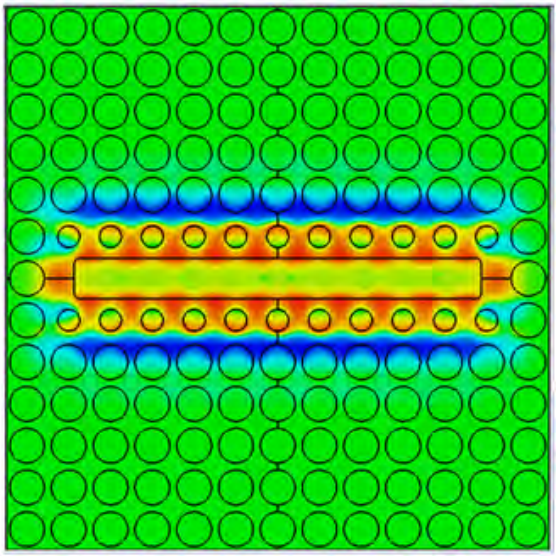

Figure 3. Geometry of alternative PBG design.

This structure assumes a ceramic with a dielectric constant of 20, and yields a phase velocity of 0.272c and a group velocity of 0.212c with a TM10 – like mode frequency of 94.00152 GHz. This structure does a good job being mode selective, with the nearest competing mode being a dipole mode at 94.04845 GHz. The structure mode impedance (a measure of how strongly it will couple to an electron beam) is 0.266 ohms, which is also good.

PBG structure fabrication and metrology

We ordered high-dielectric ceramic blanks from Euclid TechLabs, with dielectric constant of 15, 20, and 25. Euclid's ceramics are based on alumina (aluminum oxide, Al2O3), which has an intrinsic dielectric constant in the range of of 9 to 10. Euclid mixes in titanium to control the dielectric constant up to a maximum of 40. We also ordered special high-velocity drills (~ 60k rpm) from the German drill company G&G. The drills come both as diamond coated and regular. In principle, these drills can drill holes with 30:1 aspect ratios (so a 400 micrometer drill can make a 12-mm deep hole. These drills are very fine and are somewhat flexible.

Our original plan was to measure and compare fabrication errors using ceramics with different dielectric constants, but we had initially underestimated the time required to perfect the fabrication technique. By the end of the project we had spent about 200 hours of T&E fabricating 22 holes. Most of that time was spent in learning how to drill in these ceramics (e.g., speeds and other techniques to reduce drill bit breakage). We now estimate we require about ½ hour for drilling a 5-mm deep hole for future fabrication. We fabricated two pieces: (1) a 6.5-mm thick piece with eight 400-micrometer holes and twelve 640-micrometer holes (shown in Figures 4 and 5) and (2) a 3-mm thick piece with a single small and single large hole. The purpose of using two ceramic thicknesses was to compare hole wander. The hole diameters were chosen to be the same as the PBG RF structure design SB_20-75 and these ceramic thicknesses were considered representative.

The measured fabrication errors were surprising. For the first fabricated ceramic piece, the average wander was 33 +/- 13 micrometers and the average error in the hole diameter was 26 +/- 24 micrometers. Because it is reasonable to expect that the wander and perhaps the hole diameter error would scale as the ceramic thickness squared, we had hoped to get useful data on wander from the thinner second fabricated ceramic piece also. However, the statistics from the second piece were not adequate.

The registering offset turned out to be quite good, with an average error magnitude of 5 micrometers and a standard deviation of 8 micrometers. Since we would expect the accumulated registering errors to scale as the square root of the number of separate pieces used to assemble the PBG structure, it appears reasonable to expect that the total wander offsets can be decreased by increasing the number of segments in the PBG structure at the cost of increasing the accumulated registering errors. For example, we would expect the RMS registering error for a 5-cm PBG structure assembled from 25 separate 2-mm segments to be about 40 micrometers. Since the drilling time is mostly only dependent on the drill depth, this may be a practical approach.

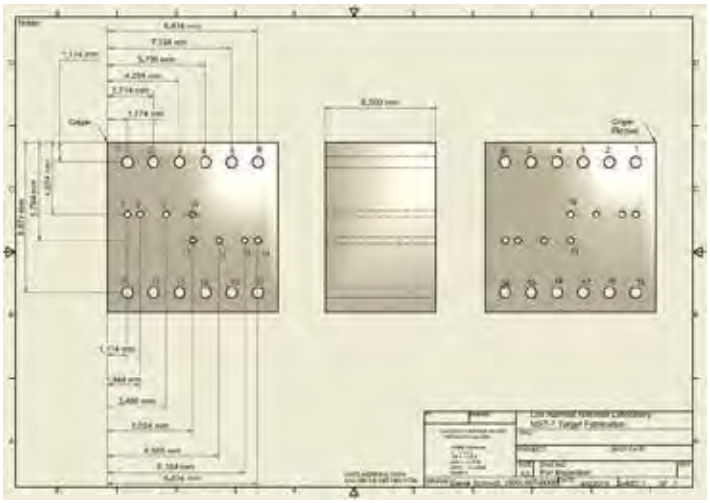

Figure 4. Fabricated pieces

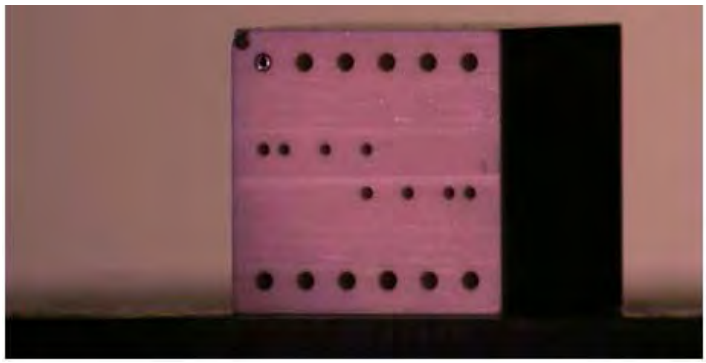

Figure 5. Fabricated pieces

These results indicate that additional fabrication testing should be conducted before the LDRD DR project 20160013DR feasibility review and PBG structure down selection. Our additional test plan which we will execute before the feasibility review will leverage the results from this project (including the learning curve to use the G&G drills) and will consist of these two core parts:

Test 1: Drill life and hole metrology versus drill speed (5 holes of each of three different speeds in 3 different ceramics; requiring 60 hours total drilling and inspection time)

Test 2: Accuracy of diameters and spacing using optimum drill speed (5 holes of each of three different drill sizes and three different ceramic thicknesses, for each of three different ceramics; requiring 90 hours total drilling and inspection time)

These additional tests will show if the drill size wander can be reduced through drill speed and using thinner ceramic thicknesses.

Error effect on RF mode
Initial studies on the effect of the PBG RF mode have been completed. Some changes in the RF mode structure have been seen using the RF simulation code CST Microwave Studio. Studies on the effect of gain (how the electron beam is used to increase the RF power) with CST Particle Studio are on-going and initial comparisons will still be completed in FY15.

Feasibility review criteria for project 20160013DR and PBG structure down selection

Successful evaluation of using micro-drilling to fabricate a PBG RF structure is based on the following steps:

1. Determination of fabrication tolerance errors due to the fabrication technique (hole position accuracy, hole diameter accuracy, angular accuracy, how much the hole tapers, and final alignment of the reassembled segmented pieces).

2. Determination of the degradation of the RF traveling-wave tube gain and efficiency due to these fabrication tolerance errors.

We have completed step 1 for a single drill speed and ceramic thickness. The FY16 tests indicated above must be completed to identify the fabrication parameters which will lead to the smallest fabrication errors. We are partially through step 2 – we have a simulation geometry generated and tested and will soon have a CST Particle Studio simulation result analyzing the effect on the structure gain. The CST Microwave Studio results show that the RF mode is deformed enough that we need to numerically verify the device's gain.

The criteria we will use at the feasibility review to determine if this specific fabrication technique is feasible are: (1) can 40 dB of gain still be obtained in 10-cm of PBG structure, (2) can the electronic conversion efficiency still be >=10%, and (3) can the 3-dB bandwidth still be >=10%.

Alternatively, if this fabrication technique is shown to be not sufficiently accurate, we can consider an alternative fabrication technique (e.g., using micro-waterjets instead of micro-drilling to fabricate the holes in the ceramic PBG RF structure), or depend on the backup acrylic folded-waveguide PBG RF structure described in the proposal for 20160013DR and shown in Figure 2. This backup architecture has no risk to fabricate (because we have successfully built channel drop filters with this design before) but has potential for field enhancement and breakdown at the interfaces of the dielectric and metallic plate.

Impact on National Missions

The high-power PBG traveling-wave tube development is specifically motivated by a space-situational awareness national security mission aligned with Sciences of Signatures (SoS) Priority Areas 2, 3, and 4 and which was described in the classified pre-proposal addendum for LDRD project 20160013DR. The broader impact of such a high power, high bandwidth W-band traveling-wave tube is large. TWTs generate RF power for military, commercial and science applications. There are about 2500 TWTs built per year, with about half going into space, and with an overall annual market of ~ $0.5B which is mostly for military use. Military applications include high-power amplifiers for high-bandwidth space and ground communications, surface-to-air and air-to-air missile fire radar control, remote spectroscopic sensing, and electronic countermeasures. Non-military examples include satellite TV and radio transmitters and terrain mapping for environmental science. This technology also enables a unique space-based atmospheric green-house gas monitoring mission for climate science. The basic principles behind that mission will be studied in another new LDRD ER, 20160462ER, "Range-resolved measurement of atmospheric greenhouse gases for treaty verification and climate science."

References

1. Carlsten, B. E.. Modal analysis and gain calculations for a sheet electron beam in a ridged waveguide slow-wave structure. 2002. Physics of Plasmas. 9: 5088.

2. Carlsten, B. E., S. J. Russell, L. M. Earley, F. L. Krawczyk, J. M. Potter, P. Ferguson, and S. Humphries. Technology development for a mm-wave sheet-beam traveling-wave tube. 2005. IEEE Transactions on Plasma Science. 33: 85.

3. Humphries, S., S. Russell, B. Carlsten, L. Earley, and P. Ferguson. Circular-to-planar transformations of high-perveance electron beams by asymmetric solenoids. 2004. Physical Review Special Topics - Accelerators and Beams. 7: 060401.

4. Carlsten, B. E., S. J. Russell, L. M. Earley, F. L. Krawczyk, J. M. Potter, P. Ferguson, and S. Humphries. Stability of an emittance-dominated sheet-electron beam in a pla-

nar wiggler and periodic permanent magnet structures with natural focusing. 2005. Physical Review Special Topics - Accelerators and Beams. 8: 062001.

5. Carlsten, B. E., S. J. Russell, L. M. Earley, F. L. Krawczyk, J. M. Potter, P. Ferguson, and S. Humphries. Stable two-plane focusing for emittance-dominated sheet-beam transport. 2005. Physical Review Special Topics - Accelerators and Beams. 8: 062002.

6. Russell, S. J., Z. F. Wang, W. B. Haynes, R. M. Wheat, B. E. Carlsten, L. M. Earley, S. Humphries, Jr., and P. Ferguson. First observation of elliptical sheet beam formation with an asymmetric solenoid lens. 2005. Physical Review Special Topics - Accelerators and Beams. 8: 080401.

7. Shchegolkov, D. Y., W. B. Haynes, R. M. Renneke, and E. I. Simakov. Millimeter-wave gain experiments with a wide-band omniguide traveling-wave tube. 2012. IEEE Conference Proceedings DOI: 10.1109/IVEC.2012.6262172. : 297.

8. Smirnova, E. I., B. E. Carlsten, and L. M. Earley. Design, fabrication, and low-power tests of a W-band omniguide traveling-wave tube structure. 2008. IEEE Transactions on Plasma Science. 36: 763.

9. Shchegolkov, D. Y., L. M. Earley, W. B. Haynes, R. M. Renneke, E. I. Simakov, and N. A. Yampolsky. Testing of the omniguide traveling-wave tube. 2010. Proceedings of the 11th IEEE International Vacuum Electronics Conference, IVEC 2010 DOI:10.1109/IVELEC.2010.5503475. : 497.

10. Shchegolkov, D. Y., C. E. Heath, and E. I Simakov. Low loss metal diplexer and combiner based on a photonic band gap channel-drop fileter at 100 GHz. 2011. Progress in Electromagnetic Research. 111: 197.

11. Simakov, E. I., L. M. Earley, C. E. Heath, D. Y. Shchegolkov, and B. D. Schultz. First experimental demonstration of a photonic band gap channel-drop filter at 240 GHz. 2010. Review of Scientific Instruments. 81: 104701.

Laboratory Directed Research & Development
Los Alamos National Laboratory
PO Box 1663, MS M708
Los Alamos, NM 87545
505-667-1235 (phone)